I. A. R. I. 6.
MGIPC—S1—6 AR/54—7-7-54—10,000.

THE

LONDON, EDINBURGH, AND DUBLIN

PHILOSOPHICAL MAGAZINE

AND

JOURNAL OF SCIENCE.

CONDUCTED BY

SIR OLIVER JOSEPH LODGE, D.Sc., LL.D., F.R.S.
SIR JOSEPH JOHN THOMSON, O.M., M.A., Sc.D., LL.D., F.R.S.
JOHN JOLY, M.A., D.Sc., F.R.S., F.G.S.
RICHARD TAUNTON FRANCIS, F.R.S.E.

AND

WILLIAM FRANCIS, F.L.S.

"Nec aranearum sane textus ideo melior quia ex se fila gignunt, nec noster vilior quia ex alienis libamus ut apes." JUST. LIPS. *Polit.* lib. i. cap. 1. Not.

VOL. VIII.—SEVENTH SERIES.

JULY—DECEMBER 1929.

LONDON:

TAYLOR AND FRANCIS, RED LION COURT, FLEET STREET.

SOLD BY SMITH AND SON, GLASGOW;—HODGES, FIGGIS, AND CO., DUBLIN;—AND VEUVE J. BOYVEAU, PARIS.

"Meditationis est perscrutari occulta; contemplationis est admirari perspicua .... Admiratio generat quæstionem, quæstio investigationem, investigatio inventionem."—*Hugo de S. Victore.*

——"Cur spirent venti, cur terra dehiscat,
Cur mare turgescat, pelago cur tantus amaror.
Cur caput obscura Phœbus ferrugine condat,
Quid toties diros cogat flagrare cometas,
Quid pariat nubes, veniant cur fulmina cœlo.
Quo micet igne Iris, superos quis conciat orbes
Tam vario motu."

J. B. Pinelli ad Mazonium.

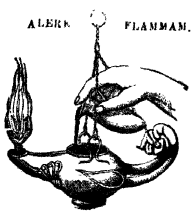

CONTENTS OF VOL. VIII.

(SEVENTH SERIES).

NUMBER XLVIII.—JULY 1929.

Page

NUMBER XLIX.—AUGUST.

NUMBER L.—SEPTEMBER.

NUMBER LI.—OCTOBER.

NUMBER LII.—NOVEMBER.

NUMBER LIII.—DECEMBER (SUPPLEMENT).

NUMBER LIV.—DECEMBER.

PLATES.

THE

LONDON, EDINBURGH, AND DUBLIN

PHILOSOPHICAL MAGAZINE

AND

JOURNAL OF SCIENCE.

[SEVENTH SERIES.]

JULY 1929.

I. *On Striations, the Cathode Dark Space, and the Negative Glow in the Electric Discharge.* By Sir J. J. Thomson, *O.M., F.R.S.**

SUMMARY.

When an electric discharge passes through a gas electrons are lost by combination with positive ions or uncharged molecules, or by diffusions to the walls of the vessel in which the gas is contained. In a steady discharge these losses must be balanced by the production of free electrons; if these are liberated by the collisions made by other electrons the latter must get from the electric field the energy required for the ionization. The stable form of the discharge will be that which produces the requisite number of electrons with the least expenditure of energy, for then the current through the gas will be maintained by a minimum difference of potential. When an electron ionizes by collision the whole of the energy given to it is not utilized in ionization. For besides the collisions which ionize it makes inelastic resonance collisions; these consume energy which, as far as ionization is concerned, is wasted. Thus in producing an electron by collision more energy than that measured by the ionizing potential of the gas must be expended. If for every ionizing collision made by an electron it makes, on the

* Communicated by the Author.

average, β inelastic resonance collisions, the average energy spent in producing an electron is

$$V_0 + \beta R,$$

where V_0 and R are the ionizing and resonance potentials respectively. The value of β will depend upon the velocity of the colliding electrons, for we know that the probability of an electron detaching an electron by collision with a molecule is very small when the energy of the electron is only just greater than the ionizing potential and increases to a maximum when the energy of the electron is between 150 and 200 volts. Little is known about the variation of the probability of an inelastic resonance collision with the energy of the electron, but what evidence we have points to the conclusion that the probability is a maximum at the resonance potential and diminishes as the energy of the electron increases. Each of these effects will make β diminish as the energy of the electron increases, so that electrons can be produced more economically by fast electrons than by slow ones. If this is so, then to produce electrons with the least expenditure of energy the electric force acting on the electron ought to be very large at the beginning of its path so as to raise its energy well above the ionizing potential. After this the force may drop to a small value and the energy already acquired by the electron be spent in producing ionization. This will absorb less energy than if the force is kept constant and the energy of the electron maintained at a uniform value just above the ionizing potential. The distribution of the force in the first of these cases is that in the striated discharge, in the second that in the uniform, positive column. To produce a given number of electrons the arrangement in the striated discharge is the most economical, but the striated arrangement may involve a greater loss of electrons by recombination and diffusion than the uniform column, and the theory of stratification advanced in this paper is that the discharge is stratified or not according as the economy in producing a single electron by the stratified arrangement is not or is overbalanced by the increased number of electrons which have to be produced.

The basis of this explanation is that whereas an increase in the energy of the electron increases, within certain limits, its chance of producing ionization by collision; the chance of its making a resonance collision has a sharp maximum at a particular energy and diminishes rapidly on either side

of this maximum. This principle has important applications to the theory of the cathode dark space and the negative glow as well as of the positive column. We may express it by saying that it is only when the energy of the electron is between R and $R+\Delta R$ that its collisions excite luminosity. Consider, first, the cathode dark space; the wide range in velocity of the positive rays coming from this space indicate that ionization is taking place throughout its length. There is a strong electric field in the dark space, and when an electron is liberated it will acquire energy rapidly. Regarded as a producer of resonance radiation the electron is active only when its energy is between R and $R+\Delta R$, the distance in which it is active is where it is acquiring the energy ΔR, and the length of this is $\Delta R/Xe$, where X is the electric force at the point in the dark space where the electron has acquired energy equal to R. Thus the length of its effective path, and therefore the probability that it makes a light-giving collision, is inversely proportional to X. According to Aston's measurements X is proportional to the distance from the boundary of the dark space; thus the brightness of the luminosity excited by these electrons will vary inversely as this distance, so that the luminosity will have a very well-marked maximum at the boundary. Those electrons which cross the boundary with energies between the given limits, will, since the electric force is exceedingly small in the negative glow, remain in the active state during the whole of their path through the negative glow, and thus a very large proportion of them will produce luminous radiation. They will not, however, ionize the gas. The ionization in the negative glow will be due to electrons which cross the boundary with energy greater than V_0, the ionizing potential. The energy of the electrons crossing the boundary will range from that corresponding to the full cathode fall of potential for those which have started from the cathode itself to very small values for those which come from near the boundary. All with energy greater than the ionizing potential will ionize and lose their energy as they pass through the gas. Those with energies in the neighbourhood of the maximum ionizing potential will do so most quickly, the electrons with these intermediate energies will be absorbed more rapidly than the very fast or very slow ones, and the ionizing power of the stream will diminish rapidly at first, more slowly afterwards as the distance from the boundary increases. The proportion of very fast and very slow electrons will increase with this distance, the slow group will lose more by diffusion to the sides of the discharge-tube

than the fast one, so that ultimately the stream will be reduced to high-speed cathode rays of small ionizing power. This agrees with observation, for these rays may often be seen passing not only through the negative glow but through the positive column and striations.

Though the energy of most of the electrons when they cross the boundary of the dark space is too large for resonance collision, yet, as they lose energy by ionizing collisions, they may reach a stage where their energy is between R and $R+\Delta R$, and then they will produce luminosity.

Since the electric force in the negative glow is exceedingly small, the electrons and positive ions liberated by ionization will accumulate until their density is great enough to carry the current by diffusion. The gradient in the negative glow both for electrons and positive ions will be a diminution in density as the distance from the boundary of the dark space increases. In addition to this gradient there will be an exceedingly steep one at the boundary itself. The diffusion of electrons into the dark space is prevented by the electric field, which stops them when they cross the boundary; the diffusion of positive ions into the dark space is, on the other hand, promoted by this field.

IN the steady state of the positive column work must be done by the electric field to

(1) Ionize the gas at a rate sufficient to replenish the loss of electrons due (α) to recombination with positive ions, (β) to their attachment to uncharged molecules, and (γ) to their diffusion to the walls of the discharge-tube.

(2) To supply the energy lost in those inelastic collisions which, though they put the molecule in an "excited" state and absorb energy proportional to the resonance potential, do not produce ionization. The energy absorbed in this way may under certain conditions be considerable in comparison with that spent on ionization. When an electron has acquired energy greater than that measured by V_0, the ionizing potential of the gas through which it is passing, it can produce ions by collision. The chance that it produces an ion in going through a distance dx may be written in the form $\phi(V)dx$, where V is the energy of the electron and ϕ a function which involves the pressure of the gas. In the same distance it is liable to make an inelastic collision, which will absorb an amount of energy R_1; the chance that it does this we shall denote by $\Psi(V)dx$. Thus in going through a

distance d the chance that the electron makes an ionizing collision is

$$\int_0^d \phi(V)dx.$$

The chance that it makes a resonance one is

$$\int_0^d \Psi(V)dx,$$

the energy absorbed is

$$V_0\int_0^d \phi(V)dx + R\int_0^d \Psi(V)dx,$$

and the number of ions produced

$$\int_0^d \phi(V)dx\,;$$

hence the energy absorbed in producing an ion is

$$V_0 + R\frac{\int_0^d \Psi(V)dx}{\int_0^d \phi(V)dx},$$

say

$$V_0 + \beta R.$$

The potential difference in the distance d will be proportional to the product of $V_0+\beta R$ and f the fraction of the electrons lost in travelling through a distance d.

There is evidence that in many cases the second term βR is larger than the first, and that the energy of electrons moving through a gas is to a large extent frittered away on non-ionizing effects, so that any saving in these would reduce considerably the energy required to produce an ion. Lehmann (Proc. Roy. Soc. cxv. p. 624, 1927) has shown that in nitrogen the ionization produced by electrons with energies of 200 volts or over only accounts for about 30 per cent. of the energy given up by the electrons to the gas, so that in this case the term βR must be more than twice V_0.

Energies corresponding to 200 volts are much larger than those we have to do with in ordinary striations, but we shall see that the slower electrons might be expected to convert a still smaller proportion of their energy into ionization.

It seems well established that the chance of an electron ionizing by collision is very small when its energy is but a little greater than the ionizing potential, and that the chance increases as the energy increases until the energy is of t

order of 150 or 200 volts, after which the probability of ionization diminishes as the energy increases (see Kossel, *Ann. der Phys.* xxxvii. p. 393, 1912). Thus $\phi(V)=0$ until $V=V_0$, it at first increases rapidly with $V-V_0$, attains a maximum when $V-V_0$ is between 150 or 200 volts, after which it diminishes.

The probability of an electron making an inelastic resonance collision seems (see K. T. Compton and F. L. Mohler, Bulletin of the National Research Council, vol. 9, p. 52, 1924) to be a maximum when the energy of the electron is equal to the resonance potential and to diminish as the energy increases.

The information we possess as to the way the probability of inelastic resonance and other non-ionizing collisions varies with the energy of the electron is exceedingly meagre; the experiments on resonance collisions seem to have been almost entirely confined to measurements of the resonance potentials and tell little, if anything, about their probability. That this diminishes as the energy of the electron diminishes is confirmed by the fact that, in some cases of the electrodeless discharge where the speed of the electrons is high, we get very intense ionization with little or no visible light. If we knew the form of the functions $\phi(V)$ and $\psi(V)$, we could calculate the value of

$$\frac{\int_0^d \Psi(V)dx}{\int_0^d \phi\,(V)dx}$$

for any assigned distribution of the electric force in a striation of length d and could compare it with that for the same length of the uniform positive column. Let f be the fraction of electron lost in passing through a distance d, then f is the number of electrons which an electron must produce in passing through a striation, and the energy required to produce this number of electrons is

$$f\left(V_0+R\frac{\int_0^d \Psi(V)dx}{\int_0^d \phi\,(V)dx}\right), \quad . \quad . \quad . \quad . \quad (1)$$

and this is the fall of potential in the striation required to give this energy to the electron. The criterion which determines the type of discharge is that the expression (1) should a minimum, for this would make the potential difference ired to maintain a given current a minimum.

In certain cases a correction which will be additive will be required for (1), for this expresses the condition that the energy given by the electric field to the electrons is sufficient to produce as many electrons as are lost. The electrons which are lost may, however, not only be abstracted from the gas, they may carry energy along with them. Thus, for example, if those which diffuse to the walls of the vessel have a finite amount of energy when they reach the walls their loss is not only a loss of electrons but a loss of energy as well, and this loss must be made good by the electric field, this will raise the potential difference in the striation beyond the value given by (1).

We have seen reasons for believing that β (p. 2) will be smaller for fast electrons than for slow, so that, in a sense, high-speed electrons (if their energy is not greater than 200 volts) are more economical ionizers than slower ones. We see from the form of expression (1) that its value will depend upon the value of V and the way V is distributed through the striation. The distribution of V would be known if we knew the distribution of the electric force along the striation. The theory of striation proposed in this paper is that, in consequence of the way the loss of energy by inelastic resonance collisions depends upon the energy of the electron, it is possible to have a non-uniform distribution of electric force through the striation which makes (1), and therefore the potential difference in the striation, less than it is for the uniform positive column. When this is the case the discharge will be striated. On this view stratification occurs because the distribution of force in the stratified discharge makes the energy wasted in non-ionizing collisions less than it would be if the electric force were uniform.

A gas which had no resonance potential less than the ionizing potential or, at any rate, no way of absorbing energy except by being ionized, would not on this view be striated.

In the uniform positive column the electric force is constant along the column, while in the striated discharge the force varies from point to point. The nature of this variation will be determined by the following considerations:— The positive column is on the anode side of the negative glow and is separated from it by the Faraday dark space. In the negative glow the electric force is exceedingly small, and, though there is intense ionization, the energy required for this comes mainly from cathode rays starting from the cathode and the dark space, and has not to be supplie

processes in the negative glow itself; this external energy is exhausted at the end of the negative glow. To produce ionization beyond this glow an electric field must be built up between the glow and the anode. The density of the electrons in the negative glow is very great, and from the anode end of it a slow stream of these sufficient to carry the current emerges. This will produce an excess of negative electricity in the region beyond the end of the glow, and this will make the electric force increase as the distance from the end increases. The rise of V with this distance x is given by the space-charge formula

$$V=\left(9\pi i\sqrt{\frac{m}{2e}}\right)^{\frac{2}{3}}x^{\frac{4}{3}}, \qquad \ldots \quad (2)$$

where i is the density of the current and m and e respectively the mass and charge of an electron. Until x is great enough to make V equal to the resonance potential the electron will not be able to excite luminosity and the discharge will be dark. This dark interval corresponds to the Faraday dark space. When x is greater than this value there will be luminosity but at first no ionization, and as no positive ions are produced to balance the negative charge carried by the electrons the electric force will go on increasing with x. In fact, the absorption of energy by the inelastic resonance collisions will make V increase more rapidly with x than it would if it continued to be represented by equation (2). When V reaches the value of the ionizing potential ionization will set in, and, though an electron is produced along with each positive ion, the electrons move away so much more rapidly from the place of ionization than the positive ions that the latter will accumulate, and the net result will be the production of a positive charge at the place of ionization. This will diminish the excess of negative electricity over positive and so slow down the rate of increase of X (the electric force) with x. X, however, will continue to increase for a time, and more and more positive ions will be produced as x increases until a point is reached when the positive charge balances the negative and the density of the electrification vanishes; beyond this the electrification will be positive and the electric force will diminish as x increases, the diminution may go on until there is not enough energy in the electric field to produce ionization. Then the ionization, as in the negative glow, will be produced by electrons which have acquired their ergy before they arrive at the place where they ionize. as in the negative glow these electrons will lose their

energy after going through a certain distance, the glow will then come to an end and a new Faraday dark space will begin and the cycle of changes we have just described

Fig. 1.

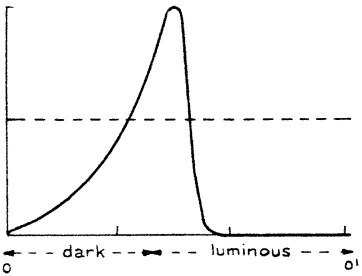

will recur. The changes in the electric force in this cycle are represented in fig. 1, where the ordinates represent the electric force at P and the abscissæ the distance of P from

Fig. 2.

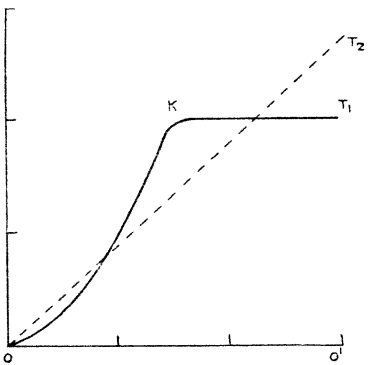

the beginning of the Faraday dark space. The potentia difference between O and P is represented in fig. 2 by th continuous lines for the striated discharge and by the dot

one for the uniform column. The column will be striated if T_1 is below T_2.

In the uniform column the electric force is constant throughout and just sufficient to supply at each point enough energy to balance the local loss of electrons. In the striated discharge the kinetic energy of an electron at the head of a striation (*i. e.*, the luminous part nearest the cathode) rises to a value much above that required to supply the local losses; in the tail of the striation, however, little or no work is done on the electron and its energy sinks to a very low value at the end of the tail.

The striated discharge we have been discussing is one of a special type where the electric force in part of the striation falls to negligible values. If with this distribution of electric force the ionization is accomplished with less expenditure of energy than in the uniform column the uniform column will be unstable and some form of striated discharge will occur. It does not follow, however, that the special form of striated discharge we have discussed is the most economical of all possible forms; there are many forms of striated discharge intermediate between the one we have considered and the uniform positive column. For example, we have supposed that the energy of the electron was increased to such an extent that the electric force fell to zero and no further work was done on the electron, so that the portion KT_1 of the potential curve was horizontal. The extent to which the electric force is reduced depends upon the number of positive ions produced by ionization. If the increase in the energy of the electrons had stopped at a stage earlier than K, say at L (fig. 3), then the ionization might not be able to reduce the electric force to zero, though it can reduce it below the value in the uniform positive column; in this case the graph for the potential distribution is that shown in fig. 3, while the graph for the electric force is that in fig. 4.

The form of striated discharge which would occur is that for which OT_3 is a minimum. Many observers have obtained graphs for the distribution of the electric form in the striated discharge similar to fig. 4. There is another form of distribution which has also been observed. Suppose that, instead of stopping the increase in the energy of the electron at an earlier stage than K, the increase is carried still further, so that the electron produces so much ionization that the electric force instead of vanishing becomes negative in the tail of the stria, the electron while moving against this force will store to the electric field some of the energy it had received

from it while passing through the head of the stria. The graph for the electric force in this case is of the type shown in fig. 5, while that for the potential is given in fig. 6.

In the Phil. Mag. (xviii. p. 441, 1909) I described experiments which showed that under certain conditions striations

Fig. 3.

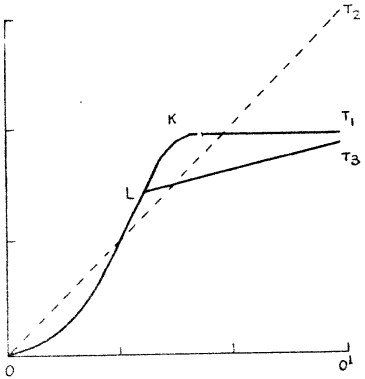

Fig. 4.

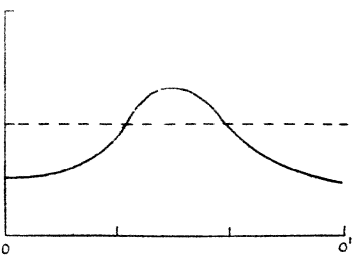

were produced in which the electric force near the tails of the striæ was in the opposite direction to that at the head.

The mathematical theory of the passage of electricity through a gas in which ionization is being produced by collisions between molecules and electrons is very complex, as the following discussion of the simplest case of all, that

of the uniform positive column, will show. In the steady state electrons have to be produced by collisions to replenish the losses due to combination of electrons with molecules and positive ions and by diffusion to the walls of the discharge-tube.

Fig. 5.

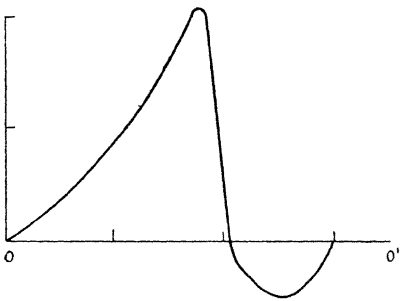

Fig. 6.

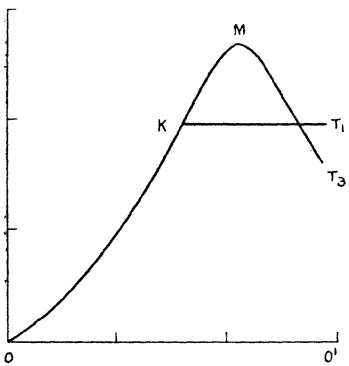

In most gases we should expect the losses due to the combination of electrons with uncharged molecules to be greater than that due to combination with positive ions. For unless the current density is very great, the number of uncharged molecules will be very large indeed compared with that of positive ions. Loeb has measured the number

of collisions an electron makes on an average with uncharged molecules before it is captured and forms a negative ion. This number is practically infinite for the inert gases, but falls to a few thousand for strongly electronegative elements; it does not depend upon the density of the gas.

Since the electron is deflected at each collision, its path through the gas is a zig-zag and not a straight line, and the distance measured in the direction of the electric force is only a small fraction of the whole distance travelled.

Very little is known about the direct combination of electrons and positive ions, or whether it takes place at all without the formation of a negative ion as an intermediate stage.

The number of electrons combining with molecules in a slab of unit area and thickness δx in the time δt will be proportional to $n\delta x\delta t \times$ (velocity of the electrons) ; n being the density of the electrons. If the velocity of the electron due to the applied force is greater compared with that due to thermal agitation, we may take the velocity of the electron as equal to u, the velocity due to the impressed force. And then the loss by union with uncharged molecules will be

$$g_1 nu \,.\, \delta x \,.\, \delta t,$$

where g_1 is a quantity proportional to the pressure of the gas. In addition to the loss by combination, the electrons will be deflected by the collision, and some of them may strike against the walls of the discharge-tube ; we shall suppose the loss from this cause to be $g_2 nu\, \delta x \,.\, \delta t$, where g_2 is a constant depending on the radius of the discharge-tube.

Then, if there is no ionization,

$$\frac{dn}{dt} = -\frac{d}{dx}(nu) - gnu,$$

where

$$g = g_1 + g_2,$$

when things are in a steady state,

$$\frac{d}{dx} nu = -gun,$$

or

$$nu = C\epsilon^{-gx}.$$

Thus a stream of electrons which has a flux equal to unity at its source will, after passing through a distance x, have a flux ϵ^{-gx}. Let us now consider a uniform column in which there is ionization; the electrons at any point in the discharge must have a wide range of velocities. Some

of them have been liberated close to the point and will only have acquired a small amount of energy from the electric field; others will have been liberated further away and will have had room to acquire a larger amount of energy. We proceed to find an expression for the number of electrons which possess energy between certain limits. We shall suppose that the collisions made by an electron are elastic, *i. e.*, do not involve an appreciable loss of energy, unless the energy of the electron is great enough either to put the molecule in an excited state or ionize it.

Suppose the rate of ionization throughout the positive column is q. Then the ionization between points distant ξ and $\xi + d\xi$ from P, the place of observation, will be $qd\xi$. The flux due to this will, when the electrons liberated reach P, be reduced to $qd\xi\epsilon^{-g\xi}$. This flux is equal to the number of electrons per unit volume moving in it multiplied by their velocity. If T is the kinetic energy of these electrons their velocity will be $\sqrt{2\mathrm{T}/m}$, where m is the mass of an electron. Hence the density of these electrons at P will be

$$qd\xi \frac{\epsilon^{-g\xi}}{\sqrt{2\mathrm{T}/m}}.$$

If X is the electric force, T the energy of an electron coming from a distance ξ is given by the equation

$$\mathrm{T} = \mathrm{X}e\xi;$$

hence $d\mathrm{T}$, the range of energy among the electrons, is equal to $\mathrm{X}ed\xi$.

Thus the density of the electrons at P is equal to

$$q\frac{d\mathrm{T}}{\mathrm{X}e}\frac{\epsilon^{-g\frac{\mathrm{T}}{\mathrm{X}e}}}{\sqrt{2\mathrm{T}/m}}.$$

This expresses the distribution of energy among the electrons whose energy is not so great as the first resonance potential. When the electrons before arriving at P acquire energy greater than this, they may lose energy by inelastic collisions and the equation

$$\mathrm{T} = \mathrm{X}e\xi$$

will no longer hold. When ξ is $> \mathrm{R}/\mathrm{X}$, where R is the resonance potential, the electron may lose energy as it moves through the distance $\xi - \mathrm{R}/\mathrm{X}$. The calculation of the probable loss of energy in this distance would require

a knowledge of how the probability of the collision varied with the energy; we have not this knowledge.

There are some indications that the frequency of the resonance collisions has a sharp maximum when the energy of the electrons is equal to the resonance potential, and falls away rapidly as the energy increases. As a working hypothesis, we shall suppose that the chance of an electron making a resonance collision is constant between the range of R*e* and R′*e* of the energy where R − R′ is small compared with R, and that outside this range there is no loss of energy by resonance collisions. The distance the electron would move through with energy between these limits is (R′ − R)/X; hence the probability of the electron making a resonance collision in its path will be equal to $\alpha(R'-R)/X$ when α is constant. The loss of energy at such a collision is R, hence we may put

$$T = Xe\xi - \frac{a}{X}, \quad . \quad . \quad . \quad . \quad . \quad . \quad (3)$$

where a is written for $\alpha(R'-R)R$.

The law of distribution is, when expressed in terms of ξ,

$$q\frac{d\xi\epsilon^{-\beta\xi}}{\sqrt{2\xi/m}}.$$

Substituting for ξ in terms of T from (3), the law where T > R becomes

$$q\epsilon^{-\frac{\beta a}{Xe}}\frac{\epsilon^{-\frac{\beta T}{Xe}}}{\sqrt{2T/m}}dT.$$

This, like the preceding, is of the form $A\frac{\epsilon^{-kT}}{\sqrt{T}}.dT$, but A has different values in the two cases.

This expression (3) will hold until the energy of the electrons reaching P equals that corresponding to the ionizing potential V; when the energy exceeds this value the electrons will lose energy by ionizing collisions. The experiments on this point show that the chance of such a collision increases with the excess of the energy over the ionizing potential, and attains a maximum when the energy of the electron is about that corresponding to a fall through 200 volts. When the energy is not much greater than the ionizing potential, the chance may be taken to be proportional to the excess of energy over the ionizing potential. When this is so, the chance of an ionizing collision in a distance $d\eta$

after the electron has moved through a distance η may be written as

$$\mu(\mathrm{T}-\mathrm{V}e)\,d\eta,$$

where T is the kinetic energy at the place η, and μ a constant proportional to the pressure of the gas.

The loss of energy at a collision is $\mathrm{V}e$; hence the probable loss of energy in $d\eta$ is

$$\mu(\mathrm{T}-\mathrm{V}e)\mathrm{V}e\,d\eta\ ;$$

thus

$$\frac{d\mathrm{T}}{d\eta}=\mathrm{X}e-\mu(\mathrm{T}-\mathrm{V}e)\mathrm{V}e,$$

or

$$\mathrm{T}-\mathrm{V}e=\frac{\mathrm{X}}{\mu\mathrm{V}}\,(1-\epsilon^{-\mu\mathrm{V}e\eta})$$

if $\eta=0$ when $\mathrm{T}-\mathrm{V}e=0$.

If x is the distance the electron has travelled before arriving at $\eta=0$,

$$\mathrm{V}e=\mathrm{X}ex-\frac{a}{\mathrm{X}};$$

hence, when the electron is produced at a distance ξ from P, when T is $>\mathrm{V}e$,

$$\mathrm{T}=\mathrm{V}e+\frac{\mathrm{X}}{\mu\mathrm{V}}\left(1-\epsilon^{-\mu\mathrm{V}e\left(\xi-\frac{(\mathrm{V}-a/\mathrm{X}e)}{\mathrm{X}}\right)}\right)\quad\ldots\quad(4)$$

and this expression holds from

$$\xi=\frac{\mathrm{V}+a/\mathrm{X}e}{\mathrm{X}}\quad\text{to}\quad\xi=\infty.$$

The law of distribution expressed in terms of ξ is

$$q\,d\xi\,\frac{\epsilon^{-\mu\xi}}{\sqrt{2\mathrm{T}/m}}.$$

Substituting the value of T in terms of ξ from (4), this expression gives the law of distribution in terms of ξ, and, knowing the value of ξ, we can get T from equation (4).

Thus in the positive column of gas there will, when there is only one resonance potential R, be three types of electrons, each with a special law of distribution :—

1. Slow electrons, whose energy is less than Re.
2. The intermediate electrons, whose energy is between Re and Ve.
3. The fast electrons, whose energy is greater than Ve.

The current sent through unit area by the electrons liberated between ξ and $\xi + d\xi$ is $q\epsilon^{-g\xi}d\xi$; hence the current density i is given by

$$i = \int_0^\infty q\epsilon^{-g\xi}d\xi,$$

$$= \frac{q}{g},$$

or $ig = q$; this is the condition that the number of electrons produced by ionization is equal to the number lost. We have supposed that the chance of an electron producing another electron in distance $d\xi$ is $\mu(\mathrm{T}-\mathrm{V}e)d\xi$. If there are $n_{\mathrm{T}}d\mathrm{T}$ electrons with energy between T and $\mathrm{T}+\delta\mathrm{T}$ the number of electrons they produce in unit volume per unit time $= \mu(\mathrm{T}-\mathrm{V}e)n_{\mathrm{T}}d\mathrm{T} \times v$, where $v = \sqrt{2\mathrm{T}/m}$, and therefore

$$q = \int \mu(\mathrm{T}-\mathrm{V}e)vn_{\mathrm{T}}d\mathrm{T}.$$

Changing the variable from T to ξ, this is equal to

$$\mu\int_{\mathrm{V}+\sigma\frac{\mathrm{X}e}{\mathrm{X}}}^{\infty} q\epsilon^{-g\xi}(\mathrm{T}-\mathrm{V}e)d\xi.$$

Substituting the value of $\mathrm{T}-\mathrm{V}e$ from equation (4) and integrating, we get

$$q = q\epsilon^{-g\frac{(\mathrm{V}+\sigma\frac{\mathrm{X}e}{\mathrm{X}})}{\mathrm{X}}}\frac{\mathrm{X}}{\mathrm{V}}\left(\frac{1}{g} - \frac{1}{g+\mu e\mathrm{V}}\right),$$

or

$$\mathrm{X}\epsilon^{-g\frac{(\mathrm{V}+\sigma\frac{\mathrm{X}e}{\mathrm{X}})}{\mathrm{X}}} = g\frac{(g+\mu e\mathrm{V})}{\mu e},$$

an equation to determine X, the force in the positive column.

Writing θ for $g\mathrm{V}/\mathrm{X}$, this equation may be written

$$\theta \cdot \epsilon^{\theta} = \frac{\mu\mathrm{V}e}{g+\mu e\mathrm{V}}\epsilon^{-\frac{a\theta^2}{g\mathrm{V}e}}. \quad . \quad . \quad . \quad . \quad (5)$$

Since $1/g$ measures the distance travelled by an electron before it unites with an uncharged molecule, and $1/\mu\mathrm{V}$ that passed over before its energy falls below the ionizing point, $\mu\mathrm{V}/g$ represents the odds in favour of the electron spending

its energy in ionization before being absorbed. When this quantity is large, the greater part of the energy given to the electrons is spent in ionization; when it is small this energy is wasted as far as ionization is concerned.

We see from equation (5) that $\theta\epsilon^{\theta}$ is always less than 1; hence θ must be less than ·56, and hence $X > 1{\cdot}78g\mathrm{V}$.

X will approximate closely to $1{\cdot}78g\mathrm{V}$ when $\mu\mathrm{V}/g$ is large and a so small that the factor $\epsilon^{-a6\pi^2 g\mathrm{V}^2 e}$ does not differ appreciably from unity.

When $\mu\mathrm{V}/g$ is small, an approximate value of θ is $\mu\mathrm{V}e/g$, and the corresponding value of X is given by

$$\mathrm{X} = \frac{g^2}{\mu e},$$

which is large compared with the previous values.

It is important, especially in connexion with the question of striation, to compare the expression for the force in the uniform column with that for other possible distributions of electric force. We will consider the potential difference required to maintain the discharge between two parallel plates at a distance l apart, when the fall of potential is supposed all to occur quite close to the cathode, and there is no force except in this region.

Let W be the fall of potential close to the cathode, i_0, the stream of electrons coming from the cathode. These electrons will acquire energy equal to We, and will ionize by collision on their way to the anode.

If T is the energy of an electron at a distance x from the cathode, using the same notation as before, we have

$$\frac{d\mathrm{T}}{dx} = -\mu(\mathrm{T} - \mathrm{V}e)\mathrm{V}e,$$

so that

$$\mathrm{T} - \mathrm{V}e = (\mathrm{W} - \mathrm{V})e\epsilon^{-\mu\mathrm{V}ex}.$$

The stream of electrons at x will be $i_0\epsilon^{-gx}$, and the production of ions between x and $x+dx$,

$$i_0\mu(\mathrm{W} - \mathrm{V})e\epsilon^{-\mu\mathrm{V}ex}\epsilon^{-gx}dx.$$

Of these only the fraction $\epsilon^{-g(l-x)}$ will reach the anode, so that the stream reaching the anode is

$$i_0\mu(\mathrm{W} - \mathrm{V})e\epsilon^{-gl}\int_0^l \epsilon^{-\mu\mathrm{V}ex}dx$$

$$= i_0\epsilon^{-gl}\frac{(\mathrm{W} - \mathrm{V})}{\mathrm{V}}(1 - \epsilon^{-\mu\mathrm{V}el}),$$

and as this must equal i_0, we have

$$W = V\frac{(\epsilon^{gl}+1-\epsilon^{-\mu Vel})}{1-\epsilon^{-\mu Vel}}.$$

Thus W is always greater than $V\epsilon^{gl}$.

Let us now compare W with Xl, the potential fall in the uniform positive column in the same distance. First take the case where μVe is large compared with g. Then when $a=0$ we have

$$Xl = 1{\cdot}78gVl\,;$$

hence

$$\frac{W}{Xl} > \frac{\epsilon^{gl}}{1{\cdot}78\,.\,gl}$$

As the minimum value of ϵ^{gl}/gl is equal to 2·71,

$$\frac{W}{Xl} > \frac{2{\cdot}71}{1{\cdot}78}\,;$$

thus W is greater than Xl, so that to maintain the discharge as a uniform positive column will require a smaller difference of potential than the one with the varying electric field.

Next take the case where μeV is small compared with g. Here

$$Xl = \frac{g^2 l}{\mu e}$$

and

$$W > \frac{V\epsilon^{gl}}{\mu Vel}\,;$$

hence

$$\frac{W}{Xl} > \frac{\epsilon^{gl}}{g^2 l^2}.$$

Now the minimum value of ϵ^x/x^2 is 1·84, so that

$$\frac{W}{Xl} > 1{\cdot}84\,;$$

thus W is again greater than Xl, so that again the discharge will take the form of the uniform positive column rather than that of the varying electric field. We have assumed $a=0$, *i. e.*, that there is no loss of energy by resonance or other non-ionizing collisions. This investigation indicates that in the absence of these the discharge will not be striated.

To find the connexion between X in the uniform positive column and the pressure of the gas we notice that μ is directly proportional to the pressure; g consists of two parts, one depending on the probability of the electron joining on to an uncharged molecule when it passes over unit distance

(this will be proportional to the pressure, and will not depend upon the cross-section of the tube); the other part, which measures the loss by diffusion, will depend upon the cross-section of the tube, and will increase as this diminishes. It will also tend to be greater at low pressures than at high. It will not be important in very large tubes, but when the free path of the electron is larger than, or even comparable with, the diameter of the tube, it may well be the predominant term. The quantity denoted by a is directly proportional to the pressure. Thus in tubes of large dimensions, g, μ, and a are all directly proportional to the pressure, and hence from equation (5) X will also be proportional to it. When the diameter of the tube is comparable with the free path of the electron, X will not increase so rapidly as the pressure and, indeed, may decrease as the pressure increases. It will increase as the cross-section of the tube diminishes.

With regard to the effect on X of the current density i, though i does not appear explicitly in equation (5), it may affect the value of the constants g, μ, and a, and thus produce an effect upon X. For example, with large current densities it may not be legitimate to neglect the recombination of the electrons with the positive ions; this recombination will increase the value of g and therefore of X. On the other hand, since the increase in current density increases the luminosity, it may tend to diminish the value of X, as exposure to radiation makes the gas more easily ionized (see J. J. Thomson, Proceedings of Physical Society, xl. p. 79, 1928), and thus diminishes the effective value of V.

When, as in the striated discharge, the electric field is not uniform, the differential equations for the various quantities involved are too complicated to be manageable. We have therefore to fall back on qualitative considerations. In the first place the distribution of electric force in the striations, viz., the very rapid increase in the electric force in front (*i.e.*, on the cathode side) of the luminous part of the striations, followed by the rapid fall to small values in the tail of the luminous portion and in the dark space between the end of this tail and the head of the next striation, is in striking agreement with the results of measurements of the electric force in the striations.

Many years ago (Phil. Mag. (6) xviii. p. 441, 1909) I made a series of experiments in which I used two methods for measuring the force, (1) by probes, (2) by the deflexion of a jet of cathode rays, starting from an electrode contained in a very narrow tube. I have lately made further measurements, using the very simple method represented in fig. 7.

AB is a straight cylindrical tube about 40 cm. long and 3 cm. in diameter. The cathode C and the anode D are flat aluminium disks stretching right across the tube so as to prevent discharges to the back of the electrodes. S is a magnetizing solenoid which serves to keep the cathode rays which start from C parallel to the axis of the tube. P is a platinum wire in a side tube; this is connected with one terminal of an electrometer, the other terminal of which is connected with the anode D; the discharge was produced by a high-tension dynamo which gave up to about 6000 volts. M is an electromagnet, which is used to deflect the cathode rays and shorten the negative glow.

Fig. 7.

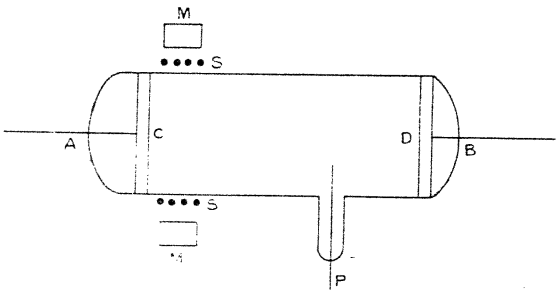

With the magnet off the pressure and current through the tube are adjusted until the negative glow reaches, as a uniform column, right up to the anode. A current is sent through the magnet and gradually increased. There is no appreciable change in the potential difference between D and P until the negative glow just fails to reach the anode, and there is a thin dark space between the end of the glow and the anode. Further increase in the current shortens the negative glow and increases the thickness of this dark space; for a time there is no visible luminosity beyond the end of the glow or on the anode itself, and there is a steady increase in the potential difference between P and D; then suddenly a thin sheet of luminous glow appears on the surface of the anode, and this glow gets thicker and thicker as the current through the magnet

increases. At first the increase in the thickness is accompanied by a very rapid increase in the potential difference between P and D, but after the thickness has reached a certain value d this increase practically ceases, and the potential difference remains constant until the thickness has become much greater than d; the glow then breaks away from the anode as a striation, and a dark space is formed between it and the anode. Now the potential difference between P and D begins again to increase, the same cycle is gone through as before, and a second striation is detached. Thus the distribution of potential difference in the striation is that represented by fig. 2.

Very interesting effects occur when a strong electromagnet is placed close to the anode so as to produce a strong magnetic force at right angles to the plane of the paper. This drives the current through the gas against the walls of the discharge-tube; this portion is full of fine striations very near together, the distance between them being only a small fraction of that when the magnetic field is not on: this is what we should expect. The magnetic field has produced a great concentration of the current, and therefore a great increase in the current density. We see from the space charge formula that the distance required to produce a given increase in potential is greatly diminished; the magnetic force produces a great increase in the potential difference between the probe and the anode; under very intense forces the difference of potential between the probe and anode may be greater than that between the probe and the cathode.

On the Length of the Striation.

A striation consists of several parts:—

1. The non-luminous part, where the energy of the electrons is less than the resonance potential.
2. The luminous part, which may be divided into two portions—the head; the part nearer the cathode, in which the electric force is large and the electrons acquire energy greater than the ionizing potential; and the tail, where the electric force is small and the ionization is produced by high-speed electrons coming from the head.

The tail of the striation may be compared with the negative glow, the head with the portion between the negative glow and the cathode, and the non-luminous part to the Faraday

dark space. The thickness of the dark layer may be got from the space-charge equation

$$V = \left(9\pi i\sqrt{\frac{m}{2e}}\right)^{\frac{2}{3}} x^{\frac{4}{3}}.$$

If we put in this formula $V = R_1$, where R_1 is the first resonance potential, then x will be the thickness of the dark space. We see from the equation that when V is given ix^2 is constant. Now, in the "normal discharge" i is proportional to p^2, where p is the pressure of the gas. When this is the case px will be constant, so that the thickness of the dark space varies inversely as the pressure. We should expect a similar law to hold for the thickness of the luminous portion at the head of the striation, in which there is no ionization, while in the luminous tail the length of the portion after the electrons have attained their maximum energy will also vary inversely as the pressure, as it will be proportional to the free path of the electron. Where the discharge is not normal the current does not vary as p^2, and the relation between the length of the striation and the pressure will be different.

Relation between the Length of a Striation and the Diameter of the Discharge Tube.

Let us now consider how the distance between striations will vary at different points of a tube of variable cross-section. If a is the radius of any section, i the current density at that section, $i\pi a^2 =$ constant. Substituting this value of i in the space-charge equation, we find x/a is constant; thus the thickness of the dark space and the length of the luminous head will be proportional to the radius of the cross-section; the length of the luminous tail will also increase with a, because in the smaller parts of the tube the electrons will strike against the walls of the tube sooner than they do in the broader, and hence their path through the gas will be curtailed.

On the view we have taken striations are produced because the waste of energy in non-ionizing collisions is less than it would be if the electric force were uniform. Thus anything which increases the probability of resonance collisions would tend to promote striation. Thus the presence of an impurity with a complicated molecule, or which, under the influence of the discharge, produced a compound with the gas in the tube, would tend to promote striations.

The presence of an electronegative gas would shorten the life of a free electron and thus increase the value of g, and

thereby, as equation (5) shows, the magnitude of the electric force required for the discharge. Whether this would favour striation or not would depend upon whether or not the chance of capture of an electron by a neutral molecule diminished as the energy of the electron increased. The energy of the electrons is greater in the striated than in the uniform discharge, and if the increase in energy were accompanied by a diminution in q it would promote striation. Nielsen (Phys. Review, xxvii. p. 716), who made experiments on the attachment of electrons to mercury atoms, found that the relation between the probability of attachment and the energy of the electron is somewhat complicated, for while in general the chance of attachment decreases as the energy increases, there are certain critical values at which the chance is a maximum.

The energy lost at resonance collisions might under certain circumstances be partially restored to the electrons, or it might increase the probability of ionization. For suppose that such a collision puts a molecule into an "excited" state, and that the current density is so great that before this state has disappeared the molecule is hit by another electron: it may, under these conditions, give up to the electron the energy it had absorbed, so that the production of this state would not in the end have absorbed any electronic energy. Again, since it is more easily ionized in the excited than in the normal state, it may be ionized by a collision which in the normal state would have absorbed energy without producing ionization, and thus compensate for the loss of energy incurred when the excited state was produced.

The average interval between two collisions of a molecule with an electron is

$$\frac{1}{N\pi a^2 v}.$$

where N is the number of electrons per c.c., v the velocity of an electron, and a the effective radius of the molecule.

Now $Nve=i$ if i is the density of the current, hence the interval between two collisions is

$$\frac{e}{\pi a^2 i}.$$

If i is a milliampere, $i=10^{-4}$, $e=1{\cdot}6\times10^{-20}$, so that the interval is $1{\cdot}6\times10^{-16}/\pi a^2$. If a is of molecular dimensions, and about 10^{-8}, the interval between the two collisions would be comparable with one second, whereas the duration of the excited state is in normal cases, according to Wien's experiments, of the order of 10^{-7} sec. Thus, though the effects we

have been discussing would tend to compensate for the loss of energy in non-ionizing collisions, the compensation with moderate-current densities would in normal gases be so small as to be negligible.

If the energy of a molecule in the excited state were emitted as radiation and then absorbed by an adjacent molecule, which was thereby put into the excited state, and if this process were repeated, the time with which we should have to compare the interval between the collisions of electrons with one molecule would not be the time any particular molecule was in the excited state, but the time which elapses before the process of emission and absorption of a particular quantum ceases. This time might well be greater than 10^{-7} sec., but it were comparable with one second, the quantum at the low pressures in the striated discharge would have travelled to distances from its source far greater than the dimensions of an ordinary discharge tube.

The Cathode Dark Space.

The theory of striation given above is based on the view that the power of an electron to excite resonance radiation by collision diminishes rapidly when the energy of the electron increases beyond the resonance potential. That, in fact, an electron only excites a particular radiation when its energy is within narrow limits. Though little has been done on this point by way of direct experiment, there are indications in the few experiments which have been made which point to this conclusion. A strong reason for thinking that it is true is that it would afford a simple explanation of the cathode dark space and the negative glow. For let us suppose that an electron only excites radiation when its energy is between R and $R+\Delta R$. The range in the velocity of the positive rays which come through the cathode shows that ionization is going on in the cathode dark space. The electrons produced by this will be accelerated in the strong field which exists in that region. Those which are produced near the cathode will acquire high velocities, those starting from near the other end of the dark space only small ones. On the view we are taking, the electron radiates only when its energy is between R and $R+\Delta R$, and thus is only luminous when describing the part of its path when its energy is between these limits. If it is moving in an electric field in which the electric force is X, the length of its path when in this state will be $\Delta R/Xe$, and will thus be inversely proportional to X. The probability of its making a collision

when in the active state will be proportional to the length of this path, and this probability is a measure of the intensity of the radiation it emits. Thus the luminosity emitted by an electron in an electric field will vary inversely as the electric force in the field. In the cathode dark space the electric force has been shown by Aston to be proportional to the distance from the boundary of that space, so that the light-producing power of an electron will be inversely proportional to its distance from the boundary, and there will thus be a very great increase in luminosity in that region. Again, consider the electrons which are liberated in the dark space near the boundary, and which, in falling from their place of origin to the boundary, acquire energy corresponding to the few volts which represents the resonance potential. These, when they cross, will have energy between the effective limits; after crossing they get into a region where the electric force is exceedingly small, so that their energy will not change appreciably. They will thus remain in the active state until they make a collision. Thus all the energy they possess will be spent in putting the molecules against which they collide into the excited state. Practically all the energy of these electrons will be spent in producing luminosity, so that in the region just beyond the boundary of the dark space—the negative glow—the luminosity will be very bright. The thickness of the region through which these molecules are active will be measured by the "collision free path" of the electrons. The collision free path is not the ordinary free path calculated from the size of the molecules, but the average distance an electron travels before making a resonance collision. If the gas is a mixture there will be more than one resonance potential—as, indeed, there may be in a pure gas. There may thus be several groups of electrons in the active state, each group being associated with a particular resonance potential. The collision paths of these different groups may be different, so that the thicknesses of the luminous belts just past the boundary of the dark space giving out a particular luminosity may be different, and thus the spectrum of the negative glow may vary with the distance from the boundary (Seeliger, *Ann. d. Phys.* lix. p. 589).

The bright belt of luminosity next the dark space is very conspicuous under suitable conditions. It can easily be shown by using a spherical ball for the cathode, the metal rod carrying the ball being fused into a glass tube, so that only the surface of the ball is exposed to the gas in the discharge tube and takes part in the discharge. When the pressure

in the tube is high the discharge starts from only a part of the ball; but on lowering the pressure the discharge will cover the ball, and the appearance will be like that shown in fig. 8. There is next the cathode dark space a belt of luminosity very sharply defined not only on the side abutting on the cathode dark space, but on the other side as well. Stretching beyond this there is fainter luminosity, which gets fainter and fainter as the distance from the ball increases.

In some gases—notably argon—the bright, sharply-defined ring shows different colours; in argon it is red on the outside and yellow on the inside. As the pressure is diminished and the dark space and the rings expand, the glow outside increases in intensity, and the outer boundary of the luminous shell is not so clearly marked; the luminosity outside this shell will, when the pressure is low, fill a large volume.

Since the chance of an electron emitting radiation is proportional to the length of path it has to travel before its

Fig. 8.

energy is increased by a definite amount ΔR, the luminosity due to an electron ought to be increased by a magnetic force at right angles to its path. For under this force the electron would no longer travel along the lines of electric force, but along paths inclined to them at a finite angle; thus the length of path it has to travel to fall through a given difference of electrostatic potential is increased by the magnetic force, and therewith the chance of the electron to excite luminosity. I have made some preliminary experiments on this point, which gave results in accordance with this view. When the pressure was such that with the ball cathode shown in fig. 8 the boundary of the dark space was a concentric sphere, on applying a transverse magnetic field it remained spherical until the force exceeded a certain value depending on the pressure, etc.; in my experiment it was from 50 to 60 gauss. The radius of the luminous boundary continually diminishes as the magnetic force increases; there is little change in the potential fall. This is what would happen if under the magnetic force electrons near the original boundary became luminiferous, while previously they had been dark.

The Negative Glow.

We have hitherto only considered the passage across the boundary of the dark space of electrons whose energy was in the neighbourhood of that corresponding to the resonance potential. We shall now consider the faster electrons, which have enough energy to ionize the gas through which they pass. Kossel's (*l. c.*) experiments show that the chance of an electron making an ionizing collision increases from zero when the energy is equal to the ionizing potential to a maximum when the energy is that corresponding to about 200 volts, and after that it decreases rapidly as the energy increases. The energy of the electrons crossing the boundary will range from that corresponding to the cathode fall of potential for those which have started from the cathode itself to very small values for those produced near the boundary. The electrons with energy greater than the ionizing potential will produce ionization and will lose their energy. Those whose energy is in the neighbourhood of the maximum for ionization will do so most quickly, so that the distribution of energy among the electrons will change as they travel through the negative glow. The electrons with intermediate energy will be more rapidly absorbed than either the very fast or the very slow ones, and the ionizing power of the stream will diminish, rapidly at first and more slowly afterwards, as the distance from the boundary increases. Thus the losses by collisions will cause the proportion of very fast or very slow electrons to increase as the stream moves through the gas. The slow ones are more likely to be driven against the walls of the tube by scattering than the fast ones, so that, after passing over a considerable distance, the original stream of electrons will be reduced to a stream of high-speed cathode rays of small ionizing power. This is in accordance with observation, for the high-speed cathode rays can be seen passing not only through the negative glow, but also through the positive column and the striations.

Though when the electrons whose energy when they crossed the boundary was greater than the ionizing potential, and they would therefore not make resonance collisions, yet as they lose their energy by ionizing collisions they may pass into a state in which their energy is between R and $R+dR$, and then they will produce luminosity.

Since the electric force in the negative glow is exceedingly small, the electrons and positive ions liberated by ionization will accumulate until their density is so great that their diffusion is sufficient to carry the current. The densities both of the electrons and positive ions in the negative glow

will diminish as the distance from the boundary of the dark space increases, so that their gradient will slope towards the anode. In addition to this there will be an exceedingly steep gradient at the junction of the negative glow and the dark space. The diffusion of electrons into this space is prevented by the electric field, which drives them back as soon as they pass the boundary. On the other hand, the diffusion of the positive ions into the dark space will be promoted by this field, which will move them away from the boundary and thus keep the gradient steep. There will thus be a considerable diffusion of positive ions into the dark space. The diffusion of electrons will be in the opposite direction; these will diffuse from the head of the negative glow—the part next the dark space, where their density is greatest—to the opposite end of the glow, where it is least. The electric current due to their diffusion will be in the same direction as that due to the diffusion of the positive ions.

II. *The Aluminium Electrolytic Condenser.* *By* R. E. W. Maddison, *B.Sc., Ph.D.(Lond.), of the European Installation Department, International Standard Electric Corporation* *.

Introduction.

Anodic Polarization.

If the voltage of an electrolytic cell or an electrode immersed in an electrolyte is altered by some cause from its equilibrium value, it is said to be polarized; anodically if it is made more positive than the equilibrium value; cathodically if more negative. Polarization may be produced by impressing an external voltage on the electrodes of the cell; it may result from concentration changes in the electrolyte, or from some interference with the main electrode reaction itself, as for example, the production of a non-conducting film on the electrode surface.

When a metal dissolves anodically, producing metal ions capable of combining with the ions of the electrolyte to give a sparingly soluble substance, further solution of the metal may be hindered as a result of the deposition of a film on the electrode surface. The presence of the film reduces the area of the electrode in contact with the electrolyte, and

* Communicated by Rollo Appleyard.

consequently increases the current density on the parts not affected. An increased polarization is then necessary to maintain a given current, and the electrode reaction may be modified. In those cases where the electrode surface is completely covered by such a film, exceedingly high polarizations may occur.

The physical properties of the film, such as its porosity, thickness, electrical conductivity, and so on, vary in different cases. It is upon the formation of badly conducting films at the surface of a metal anode, permitting the maintenance of high voltages between the electrode and the electrolyte, and preventing the discharge of anions (the passage of any appreciable current), and the relative stability of the anode film when made a cathode that the production of electrolytic condensers and rectifiers is rendered commercially possible.

The characteristic property of the anode film upon which its rectifying property depends is that of unidirectional current conductance. When the electrode is made positive, the current passing is very small after the film has formed; but on reversing polarity, current conduction is possible. The film, therefore, can act as a valve, and by suitable arrangements of electrodes bearing these films rectification of alternating currents is possible. The film also exhibits a very high electrostatic capacity, which property is utilized for the production of static condensers.

Although this valve action has been observed with most metals under suitable conditions, only two, namely aluminium and tantalum, have gained wide use commercially for rectifiers. For condensers, aluminium alone would appear to have found application.

Theories of Electrolytic Valve Action.

The various theories that have been advanced to explain the unidirectional current-flow characteristic and the dielectric properties of anode films may be divided into two classes:—

1. The Gas Film Theory,
2. The Solid Film Theory,

according as the active layer responsible for the phenomena is considered to be gaseous or solid. Although a visible oxide film is present on a formed anode (*e.g.* aluminium), it is certain that this visible layer is not the active one, but that another inner film is formed that is responsible for the behaviour of the electrode.

1. *The Gas Film Theory.*

K. E. Guthe[7] ascribed the high resistance of the aluminium anode to the presence of a thin film of oxygen gas covering the electrode, preventing the passage of negative ions from the electrolyte to the electrode. He likened the film produced on the electrode surface to a semipermeable membrane, allowing only certain ions to pass through it and to discharge. The behaviour of an ordinary copper ferrocyanide semipermeable membrane was compared with that of an aluminium anode, and found to be similar. It was observed that a high resistance was present when current was passed from a copper to a platinum electrode immersed in an electrolyte, the two electrodes being separated from each other by the semipermeable membrane; in the reverse direction the resistance was very low.

The gas-film theory has been supported in particular by A. Günther-Schulze[23, 24, 28], who considers that during the formation period of the valve metals there are produced simultaneously two films:

(*a*) an inactive solid oxide film,
(*b*) an active gas film.

The solid film is not responsible for the rectifying or condenser properties of the electrode, but serves to hold in position the oxygen gas film, which has the properties of a dielectric. The pores of the oxide layer, in so far as they are not occupied by gas, are filled by electrolyte. Electrons from the metal electrode can cross the gas film, but electrolytic ions from the electrolyte are unable to do so.

In extending Günther-Schulze's hypothesis, A. H. Taylor[33] considers the gas film to be held between an aluminium hydroxide layer and the aluminium electrode: the gas in contact with the aluminium surface combines partially with the metal to give a thin film of aluminium oxide.

2. *The Solid Film Theory.*

The rectifying and condenser properties of the aluminium anode have been ascribed by other workers[11, 14, 16, 34, 37, 38] to the presence of a solid film acting as

(*a*) a Wehnelt interrupter,
(*b*) an ohmic resistance,
(*c*) a true dielectric,
(*d*) a semipermeable membrane.

J. Slepian [30], in his contribution to the solid film theory, has applied the principle of thermionic rectification to explain the operation of thin films such as occur in electrolytic and other rectifiers.

He considers the gas film theory of rectification to be untenable on the following grounds. A gas film has a low dielectric constant (a little over unity), so that it is difficult to account for a sufficient lowering of the work function to permit electron emission from a metal surface at ordinary temperatures; the work function for the escape of electrolytic ions from an aqueous solution should be less than in the case of electrons escaping from a metal surface; lastly, electronic conduction may be imparted to the electrolyte without in any way destroying the rectifying properties of the film. He prefers to ascribe the behaviour of a valve anode to the solid film covering the electrode surface. In the case of aluminium the film is thought to consist of a transition or dehydration product of aluminium hydroxide produced during the forming period. This film has insulating properties in consequence of the almost complete lack of free electrons, exactly as in the case of a vacuum. Electron emission from the metal electrode into the insulating film is controlled by a work function as in the case from a metal to a vacuum. As a result of the definite time required for electrons to traverse the film from one electrode to the other, space-charge effects may arise, and thereby reduce the current flow to a very small value.

The dielectric constant of the film will also influence the work function. The extent of the attraction exerted by the dielectric on the electrons escaping from the metal surface will depend on whether the work function forces are operative within or without the dielectric layer. Assuming a dielectric constant of 13, the work function may be reduced to from 1/13 to 1/7 of its value for vacuum. In view of the fact that the electron emission is approximately proportional to the work function, it follows that it is possible for electron emission to take place at ordinary temperatures into a film of dielectric constant ca. 13, and that the electric field necessary to enable electrons to overcome the work function will be correspondingly reduced.

The above outline has assumed a uniform distribution of the dielectric film over the surface of the electrode. Seeing that the forces of the work function are operative through a distance of ca. 10^{-8} cm., which is of the order of atomic dimensions, this would mean that the film is discontinuous. It is possible that even in the case where the film is formed

or built up on the electrode itself, the work function is suppressed at some points and is operative at others: electrons will pass from the metal to the film only at certain discrete points. By combining a favourably polarizable junction surface with one that is non-polarizable, we obtain an asymmetric arrangement which will exhibit the unidirectional current flow characteristic upon which the production of electrolytic rectifiers and condensers is dependent.

F. M. Gentry [6] has established mathematically that the electronic conduction in unidirectional current conducting non-metallic films follows essentially the same law as that found for electronic conduction in an evacuated space. Satisfactory agreement was obtained between calculated and observed values for the current passed at various voltages by the film of an aluminium electrolytic condenser (see pp. 228 and 230 of discussion to [29]).

In connexion with the solid layer theory, it is interesting to note that a condenser with a solid dielectric (calcium fluoride), and analogous to the electrolytic type of condenser, has been prepared [18]. A metal filament covered with a layer of the salt is fused into a glass vessel, the walls of which are locally covered with a metal coating. The vessel is highly evacuated, the filament is heated to vaporize the salt layer, and finally the filament is heated to a higher temperature in order to volatilize it and deposit it on the salt layer. The dielectric is 100–150 molecules thick, and has a breakdown voltage of ca. 10^8 V./cm. Particulars of the capacity of this condenser, as well as other electrical properties, do not appear to be available.

W. W. Taylor and T. K. H. Inglis [34] found that the essential peculiarities of an aluminium anode could be reproduced by means of a platinum anode having a film of aluminium hydroxide deposited upon it. This film acts as a semipermeable membrane in permitting the diffusion through it of certain salts, but not others (*v. infra*). A. Rouban [22] followed up this work, using a copper ferrocyanide semipermeable membrane (*cf.* Guthe *supra*; see also [35]).

It may be mentioned that A. L. Fitch [5] proposed the theory of a double dielectric, consisting of a gas and a solid layer, to account for the behaviour of the aluminium anode.

Formation of the Anode Film.

In considering the various experimental data, reference will be made almost entirely to aluminium, and occasionally

to tantalum, as it is these metals that have been most studied in connexion with their use for rectifiers and condensers.

When one of the so-called valve metals is made an anode in an electrolyte, the voltage necessary to maintain a given current density increases almost proportionally with the time of closed circuit. At a certain voltage partial breakdown, and at a still higher voltage complete breakdown, of the film occurs. This period of polarization is referred to as the "formation" period.

Formation of the dielectric film can take place on D.C. or A.C. The film which first appears on aluminium is transparent and colourless, but as its thickness increases, interference colours become visible, and after usage it appears greyish, due to the increased thickness of the film. The current density at a given voltage and frequency has considerable influence on the time of formation of the film. The greater the current density (small surface area) the more rapid the formation. The following figures obtained by H. D. Holler and J. P. Schrodt[9] are of great interest in this connexion. The application of 25 V. D.C. to an area of 1 cm.^{2} of aluminium anode gave almost instant formation, the current being reduced nearly to zero in 3 seconds. With an area of 300 cm.^{2} the formation was so slow that even with an applied voltage of 120 V. D.C. several hours were necessary to effect complete formation. Using A.C. under similar conditions to those just described, the time required for formation was about five times as great. The formation is also influenced by the composition of the electrolyte and the temperature.

Anodically treated aluminium heated *in vacuo* to 1200° C. evolves a negligible amount of gas, from which it is concluded[32] that the anode film consists of aluminium oxide and not hydroxide. This is interesting in connexion with Slepian's theory (*v. supra*) regarding the nature of the active layer.

Thickness of the Active Layer.

It has been mentioned above that a distinction has to be made between the visible oxide layer and the inner active layer. The thickness of the active layer has been determined by measurements of electrostatic capacity (making the assumption that the dielectric constant is unity), by estimation from interference colours exhibited by the film, and by chemical analysis. The last two methods assume that the entire thickness of the film on the electrode is effective as a dielectric. Capacity measurements give results of a

different order of magnitude from other methods of determination. (For a summary of the various values see [1]). Capacity measurement gives values of the order of 10^{-6} cm. for aluminium formed at 100 V.: other methods give values of $20–100 \times 10^{-6}$ cm. This discrepancy, and the fact that the thickness determined by capacity measurements is practically independent of the electrolyte, suggests that the film produced on aluminium consists of two layers. According to Günther-Schulze [28], the thickness of the active layer is dependent on

(*a*) the metal employed,
(*b*) the applied voltage;

and is independent of

(*a*) the electrolyte for aqueous solutions,
(*b*) the temperature,
(*c*) the method of formation.

TABLE I.

Voltage.	Relative thickness δ/ϵ.	
	Aluminium.	Tantalum.
50	6·4	4·1
100	10·3	7·1
150	16·1	11·6
200	22·3	17·0
250	29·3	22·9
300	37·1	28·8
350	46·6	34·6
400	58·0	40·3
450	71·0	45·0
500	85·9	49·1

δ = absolute thickness.
ϵ = dielectric constant.

Table I. shows the relative thickness

$$\frac{\text{absolute thickness}}{\text{dielectric thickness}} = \frac{\delta}{\epsilon}$$

of the active layer formed on aluminium and tantalum at various voltages, assuming a dielectric constant of unity. Determinations of the thickness of the active layer depending

upon capacity measurements are subject to the effect of frequency (*v. infra*), though at a given frequency the electrostatic capacity is a function of the applied voltage; this capacity is taken as being a measure of the thickness of the active layer.

Resistance of the Active Layer.

The high resistance of the anode film has been ascribed to the development of a counter E.M.F., but the evidence

TABLE II.

Time.	Forming current. i mA.	Cell voltage. e volts.	Thickness of Solid layer. $\mu\mu$.	Thickness of Active layer, δ. $\mu\mu$.	$\frac{e}{i} = r$ ohms.	$\frac{r}{\delta}$ ohms/$\mu\mu$.
10".....	100	27	113	2·50		
30	100	73	160	3·53		
40	100	101·3	270	6·00	$1·01 \times 10^3$	$0·17 \times 10^3$
55	11	101·3	300	6·62	9·22	1·39
90	4·1	101·3	305	6·74	24·7	3·67
2'.....	3·1	101·3	307	6·78	32·7	4·82
10	1·16	101·3	325	7·17	87·2	12·2
60	0·54	101·3	335	7·39	188	25·5
260	0·37	101·3	350	7·72	278	36·0
450	0·25	101·3	355	7·82	413	52·8
2880	0·11	101·3	360	7·93	922	116
7340	0·07	101·3	390	8·60	1450	169
8780	0·06	101·3	395	8·72	1582	181

12·5 cm.² tantalum in 0·05 N. KNO_3. Formed at 100 V. D.C. Temperature 20° C.

mainly indicates that the resistance is of an ohmic nature. It depends not only on the thickness of the active layer, but also on the applied voltage [26]. From the figures given in Table II. it is seen that during the formation period the current flow decreases at a quicker rate than the thickness of the active layer increases, so that the resistance of the active layer at constant voltage with decreasing forming current very rapidly increases. Tantalum was chosen to obtain the results given in Table II., since with

2. Alloy 24·47 contained slight but definite traces of a second constituent under all conditions of annealing. There was a marked difference between the relative amounts of the second constituent in alloys 24·18 and 24·47, but the second constituent was always definitely present in the latter alloy, although in very small quantity, so that the composition is clearly very close to the boundary line of the solid solution, and we may therefore place this at approximately 24·5 atomic per cent. tin. The obtaining of this alloy was a fortunate coincidence, since it was clearly just on the boundary line.

3. Alloys 24·82, 24·93, and 24·96 were homogeneous after annealing and quenching from 400° and 500°, while at 625° C. alloys 24·82 and 24·93 were quite homogeneous, and alloy 24·96 may have contained traces of chilled liquid, but this could not be decided conclusively owing to the brittleness of the specimens. In the alloys annealed at 300° and then slowly cooled, alloys 24·93 and 24·96 were homogeneous, but alloy 24·82 contained slight traces of a second constituent. In order to see whether this was due to the fact that equilibrium had not really been reached, the whole series of alloys annealed and quenched from 500° was re-annealed at 300° for 7 days and quenched, when alloys 24·82, 24·93, and 24·96 were all homogeneous, showing that equilibrium had not been quite reached by the annealing at 300°; all other alloys were two-phase. These three alloys annealed at 200° for 32 days were nearly homogeneous, but definitely contained traces of a second constituent; but this again was because equilibrium had not really been obtained, for, in two separate series of experiments, alloys annealed at and quenched from 400° and 500° were re-annealed at 175° and 200°, but remained quite homogeneous, without precipitation of a second phase. These results indicate that a definite range of solid solubility exists.

4. Alloy 25·18, after all conditions of annealing and quenching, was definitely just outside the limits of the ε solid solution, the specimen quenched from 175°, 200°, 300°, and 400° containing traces of the η phase, whilst those quenched from 500° and 625° contained chilled liquid.

Discussion and Conclusions.

From the results of the present work it may be concluded that the ε bronze phase is a solid solution of which the limits vary from 24·5 to 25·1 atomic per cent. tin, any

variation of the solid solubility with temperature being within the limits of the experimental methods. This range of compositions includes the simple whole number ratio Cu_3Sn, and is thus in agreement with the X-ray crystal analysis of Bernal to which reference has been made, but amplifies the metallographic investigation to which the latter referred. In a recent private communication Mr. Bernal has kindly told the author that at a later date he considered that his X-ray data might agree with the formula $Cu_{50}Sn_{16}$, but that as the positions of all the atoms had not been worked out, a definite conclusion could not be made, so that the X-ray data are not conclusive ; but it is satisfactory to note that the present work is in agreement with Mr. Bernal's original conclusion, and that no conflict exists between the X-ray and metallographic results.

It is doubtful whether the microscopic method is accurate to more than 0·1 atomic per cent. with brittle compounds, so that it can hardly be said conclusively that the compound Cu_3Sn forms a solid solution with excess of tin, and it seems more than probable that the phase in equilibrium with the liquid is the pure compound Cu_3Sn. In this connexion it may be noted that the work of Matsuyama * indicates that the magnetic properties of molten copper-tin alloys show singularities in the neighbourhood of 25 atomic per cent. tin, indicating that a compound exists in the *liquid*, and hence, presumably, that there is a definite molecule of Cu_3Sn or some simple multiple of this formula.

On the other hand, the work seems to show conclusively that a solid solution exists on the copper side of the compound to an extent of about 0·5 atomic per cent., which is well outside the limits of experimental error. We seem, therefore, to have a real compound, in the chemist's sense of the word, corresponding to the existence of a definite molecule, but which can take up small amounts of one of its constituent elements into solid solution. It would be of great interest if a detailed examination of this very slight solid solution could be made by X-ray crystal analysis, since it is by no means clear that such a solution will be formed by the simple substitution process which is known to operate in the case of solid solutions of wide range. But if such an examination be made, the importance of a thorough annealing of the specimens cannot be overestimated, for it seems to be quite definitely established that in some alloy systems annealing may first produce a solid solution with the atoms

* Matsuyama, Sci. Rep. Tohôku Imp. Univ. xvi. p. 447 (1927).

arranged at random on a common lattice, whilst if the annealing be continued the atoms undergo further rearrangement, and in such cases it is clear that conflicting results will be obtained if the X-ray analysis be made before the final state is reached.

Acknowledgements.

The author must express his thanks to Professor W. H. Perkin, F.R.S., for having given laboratory accommodation for the present work, and to Sir Harold Hartley, F.R.S., for allowing the electrolytic analysis to be carried out in his laboratory. He must also acknowledge his indebtedness to Messrs. Brunner, Mond & Co. Ltd., for their assistance towards this and other research work, and to the President and Fellows of Magdalen College for a research grant.

Magdalen College, Oxford,
May 1929.

XI. *On Single Crystal Cathodes.* *By* K. G. Emeléus, *M.A., Ph.D., Lecturer in Physics, and* Jean W. Beck, *Queen's University of Belfast* *.

THE normal cathode fall in potential (V_n) of a glow-discharge has been found to be closely connected with the work function (ϕ) of the cathode for electrons. There is some evidence that in at least one instance the work function of a single crystal changes from one face to another [1], and it might therefore be anticipated that the discharge phenomena would be different if single crystal cathodes were used instead of ordinary polycrystalline pieces of metal. The fact that the latter present a mosaic of microcrystals to the ionized gas—unless they become fundamentally altered in their surface-layers under the influence of the discharge—might conceivably be responsible, through some averaging action, for the fundamental property of the normal discharge, viz., contraction of the discharging area at constant current density and constant cathode fall in potential (V_n) as the total current from the whole cathode is diminished. If this were so, a discharge should disappear from all parts of a surface of a single crystal simultaneously when the cathode

* Communicated by the Authors.

fall reached its normal value. In addition, the value of V_n should vary from one face to another proportionately with ϕ. Up to the present, we have been unable to obtain suitable metallic crystals to enable us to examine these points. We have, however, investigated the discharge from a crystal of pyrites (FeS_2) in various gases, and have found that continuous contraction of the discharging area occurs with this at normal cathode fall, as with ordinary material. The measurements of V_n also permit an estimate to be made of the work function of pyrites, and give some indication of its chemical behaviour in the discharge.

The crystal used was a cube, of side 1·4 cm. It had an electrical resistance of 62 ohms between opposite faces, but with the small currents that were passed through it in the discharge, of the order of 10^{-3} amp., the resulting fall in potential was almost negligible. The crystal was too hard to drill, and had to be supported by binding wire tightly round small notches in its edges. At intervals during the experiments the crystal was freed from possible impurities by lightly rubbing with emery paper; its behaviour was, in fact, unchanged by this treatment. All the main surfaces of this form of the crystal have identical surface lattices of atoms and behaved identically in the discharge.

The design of the discharge-tube used for the final measurements of V_n is shown in fig. 1. The whole of the crystal (C), except its lower face, was protected by a glass shield of square section. The anode (A) consisted of a cylinder built up of nickel and molybdenum wire, so that the cathode could be seen through it, and was degassed before mounting. The lower end of the tube was rounded off, and, whilst a discharge was passing, liquid air was kept round it up to the inlet-tube L. Pressures were measured by a McLeod gauge, without any allowance for fluctuations in temperature and density throughout the apparatus. The gases used were argon, freed from nitrogen by the calcium arc; nitrogen, prepared by exploding sodium azide (Kahlbaum), and stored over the resulting finely-divided sodium; oxygen, prepared by heating potassium permanganate (Kahlbaum); air, freed from carbon dioxide and water; and neon, containing some two per cent. of helium, but kept otherwise pure by means of charcoal cooled by liquid air. Before admitting each specimen of gas, the tube was baked, except for the part immediately adjacent to the crystal, and it was protected from tap-grease and mercury vapour by one or two liquid air-traps. On prolonged passage of the discharge the crystal tarnished somewhat in

all the gases, but the effect was pronounced for short times of passage of the current for oxygen alone.

The procedure consisted in measuring the least potential at which the discharge would pass at different gas-pressures, using for this purpose a potentiometer (1300 ohms) with a maximum of 450 volts. A typical series of results is given in Table I. To obtain a closer approximation to the cathode

Fig. 1.

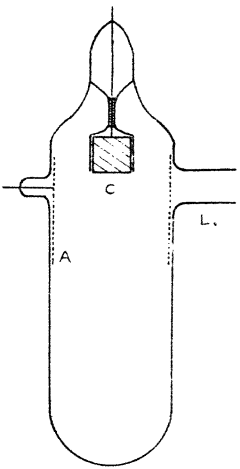

TABLE I.

Minimum glow-potential in oxygen at various pressures.

Glow-potential: volts	392	388	385	373	374	375	378	382	393	413
Pressure: mm. mercury	4·92	3·38	2·38	1·70	1·25	0·89	0·68	0·48	0·29	0·16
Anode glow ...	+	+	+	−	−	−	−	−	−	−

fall in potential, these numbers should be diminished by the ionization potential of the gas when an anode glow is present[2]; the corrected potential then becomes almost constant over a considerable range of pressures. There is

a slight tendency to increase at the higher pressures, probably due to an increase in the fall in potential in the non-luminous region between the negative glow, which was then closely contracted on to the cathode, and the anode glow. The more pronounced rise at lower pressures took place after the negative glow had expanded up to the anode, and is to be attributed partly to a true rise in the normal cathode fall [3], and partly to constriction of the discharge. The curve between pressure and minimum glow-potential is closely similar to that obtained when the minimum potential at which the discharge will run is measured for different positions of a movable anode [4], and the corrected applied potential, which is obtained immediately before the low-pressure rise, has been taken to be the normal cathode fall in potential.

The values of V_n obtained are collected in Table II. V_n' is Güntherschulze's value for the normal cathode fall in potential on an iron cathode at the pressure p at which the numbers

TABLE II.

Normal cathode fall in potential in various gases.

Gas	Ar.	Ne.	N_2.	O_2.	Air.
V_n: volts	222	168	288	373	314
V_n': volts	168	153	215	352	337
p: mm. mercury	(1·0)	(2·0)	0·76	1·70	0·50
ρ	1·32	1·09	1·34	1·06	0·93

The numbers in brackets are rough estimates made from the appearance of the discharge; the gauge was not in connexion, to avoid as completely as possible the presence of mercury vapour.

against V_n were determined [3]. Any error due to possible changes in the V's with pressure is only important in the case of nitrogen, and even then cannot be large. ρ is the ratio of V_n to V_n'. Accurate values of the thickness of the cathode dark space and of the normal current density could not be obtained with this apparatus, but they varied with pressure in the usual way.

The ratio ρ should measure approximately the ratio of the work functions for pyrites and for iron. Examination of Table II. shows that ρ is not far from unity for air and for oxygen; since the surface of an iron cathode is but little affected by a discharge through oxygen, this probably indicated that preferential oxidation and removal of sulphur were taking place. The value of V_n for neon was obtained from

a single measurement in a quartz tube, under conditions in which there was a slight access of carbon vapours from some picein rimmed glass to quartz joints, and rather less efficient liquid air cooling than in the glass tube of fig. 1. In the quartz tube the ultra-violet spectrum of the negative glow, in addition to showing the majority of the lines of Ne I [5], Ne II, and Ne III [6], included well-developed bands of carbon monosulphide [7]. The normal cathode fall in nitrogen was diminished by about 30 volts when liquid air was removed from the glass tube, so that it is probable that in the case of neon, when sulphur compounds were certainly present in the gas-phase, the value of V_n was also too small. V_n is also slightly less for neon when a little helium is present. It is concluded that the value of ρ for neon should be increased. The values of V_n for argon and nitrogen should be fairly reliable. Taking 1·3 as the most probable value of ρ, and 3·7 volts for the work function of iron, ϕ for pyrites is 4·8 volts. No direct determination of the work function of pyrites appears to have been made which could serve as a check upon this result, which is subject to all the uncertainties that arise in our measurements of V_n. These have been exaggerated by the use of a substance that is not an element as cathode, and we claim little more than to have pointed out the possible existence of a new effect in the normal discharge, and to have indicated an indirect method for obtaining the work functions for single crystals.

Summary.

A single crystal (pyrites) behaves like an ordinary piece of polycrystalline metal in the glow-discharge when used as a cathode. From the value of the normal cathode fall in potential in various gases, the work function of pyrites for electrons is calculated to be 4·8 volts.

We have to thank Prof. J. K. Charlesworth for providing the crystal, and for advising us on its structure.

References.

(1) Linder, Phys. Rev. xxx. p. 649 (1927).
(2) Emeléus and Brown, Phil. Mag. vii. p. 25 (1929).
(3) Güntherschulze, *Zeits. f. Physik*, xlix. p. 473 (1928).
(4) Güntherschulze, *Zeits. f. Physik*. xxx. p. 175 (1924).
(5) Paschen, *Ann. d. Physik*, lx. p. 405 (1919).
(6) L. Bloch, E. Bloch, and Déjardin, *Journ. d. Physique*, vii. p. 129 (1926).
(7) Jevons, Roy. Soc. Proc. A, cxvii. p. 351 (1928).

XII. *The Amount of Uniformly-diffused Light that will pass through Two Apertures in Series.*

To the Editors of the Philosophical Magazine.

GENTLEMEN,—

SOME time ago I made some calculations about the stationary flow of very rarefied gases through capillary tubes *. In accordance with Knudsen † these calculations are based on the validity of the "cosine-law" for the reflexion of the gas molecules by the walls of the tubes. This law is essentially the same as Lambert's law in optics. Now, my attention has been drawn to an article of Dr. L. F. Richardson ‡ in the November number of the Philosophical Magazine. Dr. Richardson there calculates the amount of uniformly-diffused light that will go in series through two apertures forming opposite faces of a cube. He starts with the general integral

$$F = \iiint\int \frac{\cos\zeta_1 \,.\, dA_1 \,.\, \cos\zeta_2 \,.\, dA_2}{r^2}, \quad . \quad . \quad (1)$$

in which dA_1, dA_2 are elements of the area of the apertures, r is the distance between the centres of dA_1, dA_2, and ζ_1, ζ_2 are the angles which the normals to dA_1, dA_2 make with the line joining the centre of dA_1 to that of dA_2. Coming to the special case of the cube, he derives an approximative value of F by replacing this integral by sums of respectively 1^4, 2^4, 3^4, and 4^4 terms and extrapolating to ∞^4 terms. In this way he obtains the value

$$F = (0{\cdot}6278 \pm 0{\cdot}0001)l^2, \quad . \quad . \quad . \quad . \quad (2)$$

in which l represents the length of the edge of the cube.

I wish to point out that this result may be obtained in a much more general form by direct integration of (1). Going back to my former publications, I found values of F for different forms of the apertures. Adding F for rectangular apertures and suppressing all values which may be easily derived from others, I obtain the following results:—

I assume that the apertures lie in two parallel planes, and that the line joining the centres is (1) a normal to these

* P. Clausing, *Versl. Afd. Nat. Kon. Akad. Wet. Amst.* xxxv. p. 1023 (1926); 'Over den verblijftijd van moleculen en de strooming van zeer verdunde gassen,' Dissertation Leiden, Chapter iii. (Amsterdam, 1928).

† M. Knudsen, *Ann. d. Physik*, xxviii. pp. 75, 999 (1909).

‡ L. F. Richardson, Phil. Mag. (7) vi. no. 39, p. 1019 (1928).

planes, and (2) the boundary of a movable plane which cuts the circumferences of the apertures in two corresponding points at a constant distance v apart.

Two circles with radii r and r':

$$F = \frac{\pi^2}{2}\{2rr' - v\sqrt{v^2+4rr'}+v^2\}. \quad . \quad . \quad . \quad (3)$$

Two equally orientated rectangles each with sides a and b:

$$\left.\begin{aligned} F = v^2\log_e\frac{(a^2+v^2)(b^2+v^2)}{v^2(a^2+b^2+v^2)} &+ 2av\,\mathrm{arc\,sin}\frac{a}{\sqrt{a^2+v^2}} \\ &+ 2bv\,\mathrm{arc\,sin}\frac{b}{\sqrt{b^2+v^2}} + 2a\sqrt{b^2+v^2}\,\mathrm{arc\,tan}\frac{a}{\sqrt{b^2+v^2}} \\ &+ 2b\sqrt{a^2+v^2}\,\mathrm{arc\,tan}\frac{b}{\sqrt{a^2+v^2}} - 4av\,\mathrm{arc\,tan}\frac{a}{v} \\ &- 4bv\,\mathrm{arc\,tan}\frac{b}{v}, \end{aligned}\right\} \quad (4)$$

in which now v is also the distance between the two parallel planes.

Formula (4) gives for $a=b=v=l$

$$F = 0{\cdot}6279\,l^2, \quad . \quad . \quad . \quad . \quad . \quad . \quad (5)$$

in excellent agreement with the value (2) of Dr. Richardson *.

Confining oneself to the cases of two apertures of identical form, one may easily obtain F in the following way. Join the corresponding points of the circumferences of the apertures by straight lines, forming a cylindrical tube. Move the plane of an aperture parallel to itself over a little distance dv. The two positions of the plane intersect an elementary ring on the wall of the tube. Next move the second plane over a distance δv, giving a second ring. Now first calculate F for these two rings, which only demands a double integration. Then integrate twice from v to ∞, and the F for the two planes is obtained, as is easily seen.

Yours faithfully,

Dr. P. CLAUSING.

Natuurkundig Laboratorium der
N. V. Philip's Gloeilampenfabrieken,
Eindhoven (Holland),
19 December, 1928.

Note at the correction.—Prof. Milne's result (Phil. Mag. (7) vii. no. 42, p. 273 (1929)) agrees with (3) (formula (272) in my dissertation) whilst (4) gives for $a=b=v=1$ the result obtained by A. Gerschun (Phil. Mag. (7) vii. no. 42, p. 419 (1929)).

XIII. *The Corona Discharge in Neon.*

To the Editors of the Philosophical Magazine.

GENTLEMEN,—

MR. PENNING, in a recent note (Phil. Mag., March 1928, p. 632) to your journal gives the result of a single experiment with a simplified apparatus, on the discharge in neon, between a wire and a cylinder. He remarks that his result differs from those which I obtained in the experiments described in my paper "The Corona Discharge in Helium and Neon" (Phil. Mag. v. no. 30, p. 721), and he concludes that the gas which I used was impure.

Mr. Penning finds that in neon at 40 mm. pressure the potential required to produce a discharge with the wire positively charged is greater than that with the wire negatively charged. He states that, after heating the electrodes and pumping out the apparatus, neon gas was admitted which was "*then* freed from traces of impurities by a glow discharge." This glow discharge was apparently passed between the wire and the cylinder. There is no mention of a spectroscopic method having been used to see whether the discharge introduces or removes impurities, but he assumes that this discharge removes impurities.

The changes in potentials which he finds are not inconsistent with the results which I obtained in the preliminary experiments which I made in order to remove impurities from the electrodes. My nickel apparatus was contained in a long quartz cylinder within which a space was left where an electrodeless discharge was produced, and the light from the discharge was examined spectroscopically. It was thus possible to observe directly the effect of the discharge between the electrodes on the purity of the gas. In all cases I admitted pure gas to the apparatus, and in the spectrum of the electrodeless discharge no lines due to impurity were found before a glow discharge was passed between the wire and the cylinder.

Before any measurements of potentials were made, the apparatus was heated and washed out with pure gas. Also large currents were passed in both directions between the wire and the cylinder. This was found to be very effective in driving impurities from the electrodes, as was seen from the spectrum of the electrodeless discharge. This process was repeated many times, and eventually a state was reached when slight heating of the apparatus or the passage of a

small current between the wire and the cylinder had no effect either on the spectrum of the electrodeless discharge or on the potentials required to maintain the currents.

It was found in the course of the experiments that the potentials required to maintain positive currents between the wire and the cylinder were increased when the gas became impure. The final results obtained with two different wires were in complete agreement, and were frequently repeated.

In the preliminary experiments before the apparatus was thoroughly washed out, the difference between the potentials required to start the positive and negative discharges was much less than that indicated by the potentials given in my paper. These preliminary experiments appear to be more consistent with Mr. Penning's observations.

On no occasion was it found possible to purify gas merely by the passage either of a direct or of a high-frequency discharge between the wire and the cylinder, or in similar experiments between parallel-plate electrodes.

Small traces of impurity may be removed from gas contained in a quartz or glass tube by an electrodeless discharge*, but this method of purifying a gas is not effective in removing large quantities of impurities which appear in the gas due to discharges between electrodes.

It would appear that in Mr. Penning's experiments impurities would tend to collect in the apparatus, and it would be impossible to estimate what effect they may have on the potentials required to produce discharges.

Yours faithfully,

The Electrical Laboratory.
Oxford.

L. G. H. Huxley.

XIV. *Notices respecting New Books.*

Flame and Combustion in Gases. By W. A. Bone, F.R.S., and D. T. A. Townend. (Longmans, Green & Co., Ltd., 39 Paternoster Row, London, E.C. 4.) Price 32*s.* net.

THIS volume, dedicated to Prof. H. B. Dixon, the "founder and doyen of the Manchester School of Combustion Research," covers the wide field of research on Flame and Combustion in Gases, especially the remarkable results obtained in France and England during the last forty or fifty years. The authors

* J. S. Townsend and S. P. MacCallum, Phil. Mag. (April 1928, p. 695).

give a detailed account of recent progress in this subject, not the least important the noteworthy researches carried out in the Imperial College by Prof. Bone and his co-workers.

With the exception of the historical review in the first chapter, the sections of the book on the initiation and development of flame and detonation in gaseous explosions, gaseous explosions in closed vessels, the mechanism of gaseous combustion and catalytic and incandescent surface combustion include a great part of Prof. Bone's researches, particularly the study of the combustion of mixtures of gases with oxygen and diluent gases under large initial pressures.

A very complete bibliography, setting out the names of authors and the titles of memoirs, is given at the end of each section. A number of beautiful plates, many from Prof. Bone's research records, photographs of flame movements, detonation waves and flame spectra, form a notable feature of this volume. Although almost daily advances are being made in the study of gaseous combustion, influenced to an increasing extent by the new ideas of atomic structure and radiation, 'Flame and Combustion in Gases' will long be recognized as the standard work on this branch of chemical science.

Matter, Electricity, Energy. By Prof. Walter Gerlach. Translated from the second German edition by Dr. F. T. Fuchs. (Chapman & Hall, Ltd., 11 Henrietta Street, London, W.C. 2.) Price 30*s.* net.

As the sub-title indicates, this work deals especially with the experimental results of atomic investigation, and is intended to meet the needs of advanced students of physics and other related subjects. Prof. Gerlach's researches in many branches of modern physics are well known, in particular the Gerlach-Stern experiment, described in some detail in the chapter on the magneton. In each chapter the author discusses a particular topic from the experimental side, and presents a review of recent investigations in a clear and readable form. The periodic system of the elements, isotopy, electron charge, photoelectric and Compton effects, X-ray spectra and super-conductivity, and other important phases of modern physics, have been chosen for discussion.

Dr. Fuchs has carried out his task of translation in a commendable manner, and helped the author in his desire to rouse the interest of the reader and to ground him in the modern views of matter, electricity, and energy.

Probability and its Engineering Uses. By Thornton C. Fry, Ph.D. [Pp. xiv + 476, with 49 figures.] (London: Macmillan & Co. 1928. Price 30*s.* net.)

This volume can be recommended without hesitation as one of the best introductions to the subject of probability. The treat-

ment of the subject is clear and logical, and difficulties are carefully explained. No extensive mathematical knowledge is assumed, and where mathematics is introduced any step which might prove a stumbling-block to a reader with slender mathematical equipment is explained in a footnote. The theory is illustrated by numerous examples, including many of the classical problems, worked out in detail. Additional examples to be solved by the reader are given. It is to be regretted that the answers to these are not included: the student has not the satisfaction of knowing whether his solution is the correct one.

It might be inferred from the title that the volume is suitable for engineering students only. Such is not the case. The engineering applications form only a small portion of the volume, and are in themselves of great interest; the chapter, for instance, dealing with the theory of probability as applied to problems of congestion is concerned with problems connected with automatic telephone exchanges. Such problems form excellent illustrations of the theory, and can be read with interest by any student, no engineering or technical knowledge being required.

The subjects dealt with include Bernouilli's and Bayes's theorems; distribution functions of various types; averages; curve-fitting, including tests of goodness of fit and fluctuation phenomena.

In a series of appendices are given valuable numerical data and tables, including factorials, logarithms of factorials, binomial coefficients; the normal error function; the normal law, its integral and derivatives up to the sixth; Poisson's formula; Pearson's criterion of goodness of fit.

The Physics of Crystals. By Dr. Abram F. Joffé. Edited by Prof. Leonard B. Loeb. [Pp. xi+198, with 61 figures.] (New York: McGraw-Hill Book Co., Inc.; London: McGraw-Hill Publishing Co., Ltd. 1928. Price 15*s.* net.)

An invitation to give a course of lectures in the University of California afforded Prof. Joffé an opportunity to collect together the results of a series of investigations, extending over twenty-five years, on the physics of crystals carried on by himself and his collaborators. The various problems brought under investigation are all discussed from the point of view of the electrical lattice theory of crystals.

The first six lectures are devoted to the elastic properties of crystals, and it is shown how these investigations checked the electrical theory not only qualitatively, but also quantitatively. By a series of well-devised experiments, involving a high degree of experimental technique, it is shown in a graphic manner how the various apparent contradictions to the theory were proved to be due to disturbing phenomena, such as the irregularities of heterogeneous bodies, interactions between crystalline grains, or rupture

inside small weak spaces within the body. The author and his collaborators were enabled, by investigating the phenomena which limited the scope of an experiment, to extend their experiments far beyond the limit of previous studies. They found it possible, for instance, that the scope of the elastic forces studied could be extended about five hundred times beyond the usual limit of rupture. Similarly, in the investigation of electrical properties, they found that in sufficiently thin sheets electric fields could be attained which reached three hundred times the value usually producing electrical breakdown.

The last eleven lectures deal with the electrical properties of both single crystals and solid dielectrics. Many new problems are suggested by the experiments described, and some of these are now under investigation.

It should be emphasized that the volume deals with only that portion of the field of the elastic and electrical properties of solids which has been investigated by Dr. Joffé and his colleagues. The title of the volume is therefore somewhat misleading. The original publication of much of the work described was in Russian, and this book will make these researches available to a wider circle of readers. The author hopes that his further experiments may throw some new light upon the origin and laws of the repelling forces between the atoms in solids.

The Symmetrical Optical System. By G. C. Steward, M.A., D.Sc. (Cambridge Tracts in Mathematics and Mathematical Physics, No. 25) [Pp. viii + 102, with figures.] (Cambridge: At the University Press. 1927. Price 7*s.* 6*d.* net.)

This is the second of the series of Cambridge Tracts in Mathematics and Mathematical Physics to deal with the symmetrical optical system. The tract under review is more advanced than the earlier tract by Dr. Leathem. It is essentially an exposition of the applications of the characteristic function of Hamilton or the allied function, the eikonal, to the theory of the symmetrical optical system, both from the purely geometrical and from the physical point of view. The various aberrations of optical systems are treated in some detail, and their geometrical meanings are explained. The diffraction patterns obtained with various shapes of aperture are investigated, and an account is given of the modifications of these due to the geometrical aberrations. One chapter is somewhat inappropriately named "The Computation of Optical Systems"; it would not be found of much assistance to the practical computer, although of theoretical interest. The mathematical treatment is somewhat compressed, and may offer difficulty to the reader of average mathematical attainments.

XV. *Proceedings of Learned Societies.*

GEOLOGICAL SOCIETY.

[Continued from vol. vii. p. 1206.]

April 24th, 1929.—Prof. J. W. Gregory, LL.D., D.Sc., F.R.S., President, in the Chair.

'The Geology of Part of North-Western Rhodesia.' By Robert Murray-Hughes, F.G.S., Assoc.I.M.M.

After defining the scope of the work, this paper goes on to describe the physical geography of the area, which lies approximately between lat. 14° and 17° S. and long. 24° and 30° E. The subject falls into three natural divisions, which follow each other roughly from west to east. The first is the flat, somewhat swampy country overlaid by the Karroo and Kalahari rocks; the second is the old peneplain-surface forming the plateau of Northern Rhodesia and underlaid by the Transvaal and Pretoria rocks, and those of the Swaziland System; and the third, a deeply dissected country overlaid mostly by the Swaziland rocks and drained by the Zambesi and Luangwa rivers.

The Swaziland rocks, composed of gneiss, chlorite-schists, and kyanite-schists with various hornblendic rocks, are described, and a short description is given of the Old Granite intrusive, and of the more recent dolerites. It is suggested that the last-named are of Karroo Age.

The following groups, named the Lusaka and Kafue Beds, and formed of calcareous, dolomitic, and quartzose rocks, are described, and a tentative correlation of them is made with the Transvaal and Pretoria Systems of the south. The Hook Granite forms one of the most important features in the geology of the country, and is shown to be intrusive into the Lusaka and Kafue Beds, which are strongly metamorphosed by it. It is normally a biotite-granite; but, in contact with the older sedimentaries, it takes on the form of syenite, gabbro, hornblendite, etc. Dykes of quartz-porphyry and minette are the later manifestations of this intrusion.

The discovery of flat-lying grits and sandstones in the west are correlated with similar beds found in the Luangwa Valley, and those in turn with the Karroo Beds described and mapped by A. J. C. Molyneux in the south-eastern portion of the area.

The covering of sand in the west, together with certain 'ancient laterites', is correlated with the Kalahari System.

A short attempt is made to indicate the principal structural features, these being divided into four groups :—

(1) The north-east and south-west foliation caused by the intrusion of the Older Granites.

(2) The north-west and south-east fracturing caused by the intrusion of the Hook Granite.

(3) The graben faulting, which forms a part of the Great Rift Valley.

(4) The folding of the Karroo Beds.

A few of the more important thermal springs are described, the widespread occurrence of laterite and its mode of development is indicated, and the paper concludes with a few brief remarks on the belts of alluvium.

May 8th, 1929.—Prof. J. W. Gregory, L.L.D., D.Sc., F.R.S., President, in the Chair.

The following communication was read :—

1. 'The Glaciation of Eastern Edenside, the Alston Block, and the Carlisle Plain.' By Frederick Murray Trotter, M.Sc., F.G.S.

Three glaciations separated by intervals within the glaciation have been recognized in Edenside.

The ice of the First or Scottish Glaciation deployed from the Southern Uplands, swept across the Carlisle Plain, one stream continuing eastwards, the other advancing up Edenside (where it was joined by a stream from the Lake District) in a manner similar to that described by J. G. Goodchild. Exposures of the ground-moraine of this glaciation are rare, and in Eastern Edenside the moraine is in places overlaid by a series of contorted laminated clays, etc., which are interpreted as indicating the departure of the ice from Edenside. These clays are in turn overlaid by the drifts of the Second or Main Glaciation. During that period Eastern Edenside was occupied by Lake-District ice and Cross-Fell ice. Because of the presence of Scottish ice on the north and ice from Howgill and Wild Boar Fells on the south, Edenside became congested with ice. The surface-level of the ice rose to 2200 feet at least, and probably higher. An ice-shed was established in Eastern Edenside and on the Alston Block, and from it ice flowed south-eastwards into the Stainmoor depression and northwards and north-westwards into the Tyne Gap area. Thus the Stainmore Glacier was fed from the north by ice from Edenside and Mickle Fell, and farther east was joined by a stream from Upper Teesdale (as proved by Dr. A. R. Dwerryhouse). The glacier in the Tyne Gap was fed by a powerful stream flowing down Edenside, and

by glaciers in the valleys of the South Tyne, West Allendale, and East Allendale. On the north the Tyne Gap Glacier was confluent with eastward flowing Galloway ice.

The retreat of the ice-front after the maximum of the Main Glaciation can be traced stage by stage, the following being the chief events in chronological order:—(1) Successive splitting-off, from east to west, of the East Allendale, West Allendale, and South Tyne glaciers from the ice in the Tyne Gap area; (2) Damming-up of glacier-lakes along the western slopes of the northern end of the Cross-Fell escarpment, and along the western slopes of the Bewcastle Fells, the drainage of both systems escaping into the Tyne; (3) Recession of the Edenside Glacier from the Galloway ice; and (4) Recession of the Cross-Fell ice from the Lake-District ice by successive splitting-off, from north to south, of six valley-glaciers of the Cross-Fell Inlier.

Several åsar-trains and kame-belts are recognized in the extensive deposits of outwash sand and gravel; of these the most noteworthy are the Tyne Gap åsar-train, which stretches westwards from Hexham for 26 miles, and the Brampton kame-belt, which is 12 miles long and 2 to 4 miles wide. It is shown that the outwash can be interpreted in terms of åsar, kames, outwash-fans, and outwash deltas, and by their aid and that of overflow-channels it has been possible to plot the position of the ice-front at twenty-four distinct halt-stages in the retreat.

The last glaciation of the area was the renewed advance of the Scottish ice across the Carlisle Plain, up to an altitude of 400 or 500 feet O.D. At its maximum extension, and during its retreat, this glacier dammed up glacier-lakes which drained south-westwards. Englacial or sub-glacial rivers of this glacier deposited three åsar-trains.

May 29th, 1929.—Prof. J. W. Gregory, LL.D., D.Sc., F.R.S., President, in the Chair.

The following communication was read:—

'The Pliocene and Pleistocene Deposits of Wadi Qena and of the Nile Valley between Luxor and Assiut (Qau).' By Kenneth Stuart Sandford, M.A., Ph.D., F.G.S.

Wadi Qena is a broad and deep valley which joins the Nile from the north at Qena, about 40 miles north of Luxor. The history of the two valleys is closely associated, and the former explains some of the problems of the latter. Like all the tributaries of the Nile (north of the Atbara), Wadi Qena is now a dry valley and a desert.

The oldest beds visible within the walls of the valley-system are of Pliocene age, deposited in a gulf of the Mediterranean. This

had been cut by river-erosion during the elevation of the Egyptian plateaux in Miocene and (in the south) partly in Oligocene times, and it was then flooded to a height of at least 550 feet above present sea-level. A non-fossiliferous series of strata was deposited in it: breccia and conglomerate at the valley-sides interdigitating with limestones, which, towards the centre, give place to clays and marls and, rarely, to sandy beds of quartz derived from the south. Great thicknesses of travertine are locally present in the series.

Re-elevation carried the flooded valley-system back to fluviatile conditions in Plio-Pleistocene times, accompanied by the irruption of enormous quantities of detritus from the Red Sea Hills. Some interesting relics of this early invasion are to be found throughout the area.

In Pleistocene times an ordered succession of river-terraces was laid down in the Nile valley and in all the major wadis, and by countless short tributaries rising in the Pliocene deposits which lined the sides of those valleys. A complicated series of local and non-local stages results, in which the meanders of the Nile (in particular) and their effects on the local stages may be traced. The gravels of each stage contain Palæolithic instruments, and on the surface of each may be found the working-floors of the next succeeding industry. The sequence is:—

100-foot terrace: Chellean.
50-foot terrace: Acheulean.
30-foot terrace: Early Mousterian.
15-foot terrace: Mousterian.'

Thereafter (in Upper Palæolithic times) desert conditions began to assert themselves, and the Nile alone survived, supplied from more favoured regions farther south.

At about the same time the Nile carved a deep channel of which we do not know the depth; it re-excavated the deeper parts of the Pliocene-filled Miocene gorge. The process of filling this up still continues.

There is good reason to suppose that certain fossil-bones found at Qau were derived from these now-hidden alluvial deposits. The fauna which they represent was not yet of desert type, and at the moment it can only be stated broadly, on external as well as on first-hand evidence, to be of Upper Palæolithic age.

[*The Editors do not hold themselves responsible for the views expressed by their correspondents.*]

THE

LONDON, EDINBURGH, AND DUBLIN

PHILOSOPHICAL MAGAZINE

AND

JOURNAL OF SCIENCE.

[SEVENTH SERIES.]

AUGUST 1929.

XVI. *The Magneto-Optical Dispersion of some Organic Liquids in the Ultra-Violet Region of the Spectrum.* By C. C. EVANS, *M.Sc.*, *and* Prof. E. J. EVANS, *D.Sc.**

INTRODUCTION.

THE magneto-optical rotations of a large number of substances have been determined by several observers. Perkin, in particular, has measured very accurately and compared the magneto-rotary powers of many substances at the wave-length of sodium light.

T. M. Lowry † has determined the magnetic rotations of many organic compounds in the visible spectrum, and others (especially Borel, Meyer, and Richardson) have also studied the problem of magneto-optical dispersion.

Our knowledge, however, of the magneto-rotary dispersion over an extended range of the spectrum (especially in the ultra-violet) is still very incomplete. The present work deals with the determination of the values of Verdet's constants at different wave-lengths in the ultra-violet for four organic liquids, and also embodies the results of an investigation of the refractive indices of three of these liquids. It is a continuation of work carried out by Stephens and Evans ‡, and by Jones and Evans §.

* Communicated by the Authors.
† J. C. S. i. p. 106 (1913).
‡ Phil. Mag., March 1927, p. 546.
§ Phil. Mag., March 1928, p. 593.

From measurements of the magneto-optical dispersion of any substance, it is possible, with a knowledge of its natural dispersion in the same region, to deduce important information with regard to the nature of the resonators in the atoms of the various substances. These resonators are responsible for the magneto-rotary effects, and from observations of the magneto-optical dispersion it is possible to calculate their free periods. The experimental results also afford a means of testing the various theories put forward to account for the magneto-optical properties of substances.

Reference has already been made to Richardson in this branch of work, and if we adopt here the same nomenclature as he used in his papers *, the following method of examining the experimental results in relation to theory will be employed.

Assuming that the natural dispersion of a substance can be represented by an equation of the Ketteler-Helmholtz type, we have

$$n^2-1=b_0+\frac{b_1}{\lambda^2-\lambda_1^2}+\frac{b_2}{\lambda^2-\lambda_2^2}+\ldots. \quad . \quad . \quad (1)$$

where n is the refractive index for wave-length λ ; b_0, b_1, b_2, etc., are constants ; and $\lambda_1, \lambda_2 \ldots$ are the wave-lengths of the absorption bands of the substance.

This equation represents the state of affairs accurately when not too near an absorption band. Now, the rotary power δ of any substance has been shown by Larmor† to be given by the equation

$$\delta=\frac{e}{2mc^2}\lambda\frac{dn}{d\lambda}. \quad . \quad . \quad . \quad . \quad . \quad . \quad (2)$$

c=vel. of light and $\frac{e}{m}$ the ratio of the charge to the mass for all the resonators.

If we suppose that the dispersion of the medium is controlled by a single absorption band, or by a number of such bands for all of which the Zeeman constant is the same, the formula should apply exactly. Assuming, however, that an equation of the same type as equation (2) still applies when $\frac{e}{m}$ has different values for the various reso-

* Phil. Mag. xxxi. pp. 232 & 454.

† 'Æther and Matter,' Appendix F, p. 352.

nators, and substituting the value of $\frac{dn}{d\lambda}$ from (1) in equation (2), it can be shown * that

$$\phi = n\delta\lambda^2 = k_1\left\{\frac{\lambda^2}{\lambda^2-\lambda_1^2}\right\}^2 + k_2\left\{\frac{\lambda^2}{\lambda^2-\lambda_2^2}\right\}^2 + \ldots, \quad (3)$$

where k_1, k_2, etc., are constants.

In the case of media transparent in the visible and infra-red regions $\lambda_1, \lambda_2 \ldots$ will represent ultra-violet free periods. If the substance possesses only one absorption band, which contributes to the magnetic rotation, the equation takes the form:

$$\phi = k_1\left\{\frac{\lambda^2}{\lambda^2-\lambda_1^2}\right\}^2. \quad . \quad . \quad . \quad . \quad . \quad . \quad (4)$$

From two values of the function ϕ corresponding to two values of λ, it is possible to determine the values of k_1 and λ_1 for the region of the spectrum between the two values of λ chosen. If it be found that the experimental results lead to different values of λ_1 depending on the values of λ chosen, and if these values increase progressively as the wave-lengths are taken in regions of shorter and shorter wave-lengths, it can be naturally inferred that the substance possesses more than one ultra-violet free period. In this case the magnetic-rotary dispersion equation assumes the form of equation (3), and as many terms appear on the right-hand side of (3) as there are absorption bands responsible for the rotary effect.

Apparatus.

The General Arrangement.

A detailed account of the apparatus used in this work has already been published †. It will therefore suffice to indicate briefly here the main features.

Light from a tungsten arc falls upon the polarizing unit of the apparatus and then traverses the liquid contained in the polarimeter tube, which is placed symmetrically inside the core of a solenoid. Between the tube and the solenoidal coil is a jacket through which water is passed, to enable constancy of temperature to be maintained.

The polarized beam, after emerging from the liquid, falls upon the analyser and afterwards upon a quartz-fluorite lens, which brings it to a focus at the slit of a quartz spectrograph.

* Richardson, *loc. cit.*

† Stephens and Evans, *loc. cit.*

The Polarimeter.

In these experiments the polarizer was of the Bellingham-Stanley type, suitable for ultra-violet work. It consisted of a quartz lens and a modified Jellet prism *. The beam of light, after emerging from the prism, consisted of two semicircular beams, the vibrations in one half being polarized at a slight angle with those in the other half, the line of demarcation between them being horizontal. The components of the analyser were assembled together with a thin film of glycerine between the faces in contact. The absorption of light in these experiments, due to this film of glycerine, was of no consequence, since the liquids used were themselves much more strongly absorbing. Both the analyser and the quartz-fluorite lens behind it were capable of being independently adjusted, so that the beam of light passed axially through the apparatus.

The Polarimeter Tube.

Throughout the whole investigation the same polarimeter tube was used. It was made of clear fused quartz, having an external diameter of 1 cm., and could contain a column of liquid 30·5 cm. long. The two ends of the tube were closed by fusing on disks of polished fused quartz. These disks rotate polarized light in a magnetic field, so that a correction has to be applied when measuring magnetic rotations of liquids. The values of the rotations of these disks at several wave-lengths were determined experimentally, and a curve drawn, so that the actual correction to be applied at any wave-length could be read off.

The Solenoid and its Magnetic Field.

At the commencement of this research the solenoid used was the identical one employed by Stephens and Evans †. These observers, by measuring the ballistic throw, determined the values of H at several points on the axis of the solenoid, and for the polarimeter tube 30·5 cm. long they deduced a value of 12,445 cm. gauss for ΣHl (where l is the length of the column of liquid over which H can be assumed to be constant).

Faulty insulation, however, necessitated the construction of a new coil after a few months' work. The new coil had the same number of layers of wire as the old one, but

* For details see 'Dictionary of Applied Physics,' iv. p. 476.

† *Loc. cit.*

improvements in the method of insulation altered the dimensions slightly, and therefore the field due to the same current was different.

A very careful series of determinations of the value of ΣHl was undertaken by measuring the magnetic rotations of conductivity water at several wave-lengths and using the known values of Verdet's constants at these points. The mean value thus found was 12,270 cm. gauss. The value calculated theoretically from the dimensions of the coil was 12,260 cm. gauss. Later, the values of H at various points along the axis of the coil were determined by observing the ballistic throws, and the above results were verified. The value finally adopted for ΣHl was 12,270 cm. gauss.

In series with the coil was a battery of 110 volts, a Weston volt-ammeter, and two variable resistances. One of these resistances served as a fine adjusting rheostat to keep the current steady. It is estimated that the current was kept steady at 2 amperes in these experiments to within 1 part in 700 on the average. The ammeter employed was periodically calibrated by comparing its readings with that of a large Weston Standard Ammeter. A reversing key was also introduced into the circuit, and the practical value of reversing the current in the coil will be referred to later.

To minimise difficulties and possible errors due to the heating of the liquid by the passage of the current through the coil, water was allowed to flow through the jacket during the experiments. It was found necessary to allow the current and water to flow for about an hour before taking a photograph, as this ensured a steady thermal state inside the core of the solenoid. The average variation of temperature during exposures was of the order of 0·1° C.

Source of Light and Spectrograph.

Throughout the whole investigation a tungsten arc was used as a source of light. Even with this powerful source of ultra-violet radiation, it was not found possible to work much below ·29 μ with the least absorbing of the liquids used in the present investigation.

The spectrograph employed was of the usual type and consisted of a Cornu quartz prism, together with quartz lenses.

The photographic plates used were either Imperial plates or Wellington Special Rapid plates, and the exposures, two of which were taken on each plate, varied from about 10 minutes at ·4 μ to about 40 minutes at ·29 μ.

Experimental Details.

The two beams of polarized light, after emerging from the polarimeter, appear as two superposed spectra after passing through the Cornu prism. These spectra appear at the camera end separated by a very fine horizontal gap.

In the absence of liquid in the polarimeter tube and the magnetic field, these spectra can be adjusted to be uniformly intense along the whole range. The intensities of the bottom and top halves, however, are not in general equal. They are only equally intense for four definite positions of the analyser with an angle of 90° separating one position from the next. Two of these positions separated from one another by 180° correspond to the maximum intensity, and the other two to positions of minimum intensity. In this latter position the instrument is extremely sensitive, and one of these positions is used as the zero reading of the analyser.

The actual position of the zero was determined by taking a series of photographs corresponding to different settings of the analyser near the position of minimum intensity, and carefully examining the plates. The zero having been fixed, a few photographs were taken in its neighbourhood with the liquid in the tube to ascertain whether or not the sample showed any natural rotation due to the presence of optically active impurities.

In the present work all four liquids were proved to be optically inactive.

When these preliminary observations had been performed, the magnetic rotary experiments were commenced. The analyser was rotated through a known angle θ_1 from the zero, the magnetic field applied, and a stream of water allowed to flow through the jacket. After an interval of about one hour, when temperature conditions were steady, a photograph was taken. During the exposure a constant watch was kept over the reading of the ammeter, the temperature of the water, and the position of the arc light. A second exposure was then taken on the same plate, corresponding to a rotation of θ_1 on the opposite side of the zero, with the magnetic field reversed.

On examining the plate, it is observed that, whilst the upper and lower halves of each spectrum are of very different intensities, there is a line of definite wave-length which has the same intensity in the upper and lower halves of each spectrum. The wave-length of this line is the same within a few Angström units for each direction of the magnetic field. The reversal of the magnetic field supplies a means

of eliminating certain sources of error, such as a slight mistake in the location of the zero position.

The experimental result that the wave-length for equality of intensity was the same for each direction of the field, also shows that the liquids employed did not contain any optically active substances as impurities.

If the mean wave-length as thus determined be denoted by λ, the rotation of the liquid at this wave-length $=\theta_1-\theta_2$, where θ_2 is the magnetic rotation of the quartz disks at wave-length λ. A series of determinations were then made, corresponding to increasing values of θ_1, until the point of equality had shifted to the limit in the ultra-violet.

The values of Verdet's constant δ were calculated from the formula: $\theta=\theta_1-\theta_2=\delta\Sigma Hl$.

Figs. 2, 3, 4, and 5 show the variation of δ with λ for the liquids investigated.

The Measurement of Natural Dispersion.

In the case of the four liquids experimented upon, namely isopropyl alcohol, allyl alcohol, methyl acetate, and ethyl acetate, values of the refractive indices in the ultra-violet could only be obtained for allyl alcohol*.

The values of the refractive indices in the ultra-violet for the other three substances were determined in the following manner:—

The same spectograph was used, with the Cornu prism replaced by a hollow prism closed by plates of polished fused quartz. A liquid whose refractive indices are known over a wide range of wave-lengths was placed in the prism, and a photograph taken with the top half of the slit illuminated by light from an iron arc. The liquid was then extracted from the prism, and the latter, which was rigidly fixed in position, was carefully cleaned and dried. A second photograph was then taken on the same plate, with the liquid whose refractive indices are required placed in the hollow prism. In this case the bottom half of the slit was illuminated by the light from the iron arc.

To find the refractive indices at various wave-lengths for the substances examined, it is only necessary to identify a line of wave-length λ_1, say, in the spectrum due to refraction through the standard liquid which is superimposed upon a line of wave-length λ_2 due to refraction through the substance.

* 'Etudes de Photochemie,' Victor Henri, p. 103.

The refractive index of the substance for wave-length λ_2 is then equal to the refractive index of the standard for wave-length λ_1.

In the present experiments pure ethyl alcohol was found to be a suitable standard liquid, and the refractive indices of isopropyl alcohol, methyl acetate, and ethyl acetate, over the ranges of wave-length required, have been determined with an accuracy of about 1 in 1000.

The values of the refractive indices of ethyl alcohol at various wave-lengths are due to Victor Henri *.

Experimental Results.

Table I. (*a*).

Natural Dispersion.

Isopropyl alcohol.		Methyl acetate.		Ethyl acetate.	
Wave-length.	Refractive Index.	Wave-length.	Refractive index.	Wave-length.	Refractive index.
·4384 μ	1·386$_5$	·3975 μ	1·372$_7$	·4384 μ	1·379$_0$
·3975 μ	1·391$_5$	·3813 μ	1·375	·4138 μ	1·381$_2$
·3720 μ	1·395$_3$	·3560 μ	1·377$_2$	·3930 μ	1·383$_6$
·3440 μ	1·400$_1$	·3491 μ	1·378$_2$	·3767 μ	1·385$_1$
·3189 μ	1·405	·3307 μ	1·381$_3$	·3625 μ	1·387$_1$
·3127 μ	1·407$_6$	·3195 μ	1·384$_3$	·3426 μ	1·391$_1$
·2973 μ	1·411$_1$	·3101 μ	1·386$_6$	·3227 μ	1·395$_1$
		·3025 μ	1·388$_7$	·3091 μ	1·398$_3$
		·2747 μ	1·398$_5$	·2973 μ	1·402$_1$
				·2880 μ	1·405
Mean Temperature 20° C.				·2830 μ	1·406$_3$

For the purpose of calculating the values of Verdet's constants from the magneto-rotary equations in the visible region of the spectrum, a few determinations of the refractive indices of each of the above three liquids were undertaken at well-known visible wave-lengths. These are collected and given in Table I. (*b*).

* 'Etudes de Photochemie,' Victor Henri, p. 61.

TABLE I. (*b*).

Refractive Index.

Wave-length.	Isopropyl alcohol.	Methyl acetate.	Ethyl acetate.
·6678 μ	$1{\cdot}375_3$	$1{\cdot}362_2$	$1{\cdot}371_6$
·6563 μ	$1{\cdot}375_7$	—	—
·5893 μ	$1{\cdot}377_1$	$1{\cdot}363_6$	$1{\cdot}373_7$
·5876 μ	$1{\cdot}377_7$	$1{\cdot}364_3$	1·374
·5461 μ	$1{\cdot}379_8$	$1{\cdot}366_3$	$1{\cdot}376_4$
·5016 μ	$1{\cdot}381_3$	$1{\cdot}367_8$	$1{\cdot}377_3$
·4713 μ	$1{\cdot}383_2$	$1{\cdot}368_7$	$1{\cdot}378_3$
·4472 μ	$1{\cdot}385_4$	1·370	—
	Mean Temp. 20° C.	Mean Temp. 16·8° C.	Mean Temp. 16·2° C.

Fig. 1.

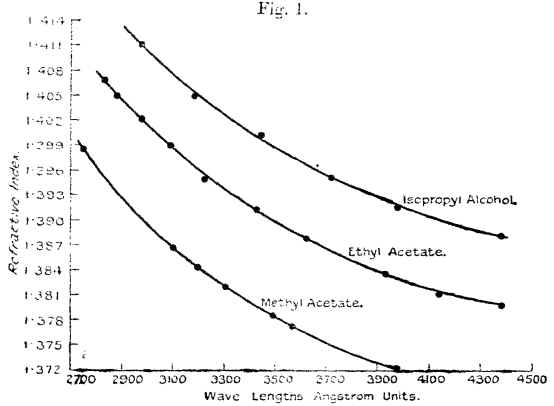

Magnetic Rotary Dispersion.

Isopropyl Alcohol.

Three sets of experiments were carried out on this liquid. The first two sets of results were obtained with the old solenoid, when the value of ΣHl for the polarimeter tube, 30·5 cm. long, was 12,445 cm. gauss. The third set was taken with the new solenoid, which gave for ΣHl the value 12,270 cm. gauss for the same tube. The experimental results are collected in Tables II. (*a*), II. (*b*), and II. (*c*).

The results tabulated in Table II. (*a*) were taken with a specimen of isopropyl alcohol from Poulenc Frères: those in Table II. (*b*) with a redistilled specimen from Dr. Schuchardt, of Görlitz. This latter specimen was also used in determining the results tabulated in Table II. (*c*).

TABLE II. (*a*).

Temp. in degrees Cent.	Wave-length in microns (10^{-4} cm.).	Verdet's Constant in min./cm. gauss.	Temp. in degrees Cent.	Wave-length in microns (10^{-4} cm.).	Verdet's Constant in min./cm. gauss.
16·0	·4400	·0238	15·7	·3586	·0377$_5$
15·7	·4008	·0293	15·5	·3504	·0402$_5$
16·2	·3913	·0309$_4$	15·4	·3415	·0429$_5$
15·5	·3866	·322$_5$	15·7	·3327	·0458$_3$
15·2	·3710	·0350$_5$	15·7	·3318	·0462
15·7	·3616	·0371$_5$			

TABLE II. (*b*).

Temp. in degrees Cent.	Wave-length in microns (10^{-4} cm.).	Verdet's Constant in min./cm. gauss.	Temp. in degrees Cent.	Wave-length in microns (10^{-4} cm.).	Verdet's Constant in min./cm. gauss.
15·0	·4400	·0238	14·9	·3730	·0347$_5$
13.6	·4010	·0293	15·0	·3710	·0350$_5$
13·7	·3940	·0304$_5$	15·0	·3590	·0377

TABLE II. (*c*).

Temp. in degrees Cent.	Wave-length in microns (10^{-4} cm.).	Verdet's Constant in min./cm. gauss.	Temp. in degrees Cent.	Wave-length in microns (10^{-4} cm.).	Verdet's Constant in min./cm. gauss.
10·9	·4380	·0240$_5$	11·0	·3730	·0347
10·9	·4193	·0266$_5$	11·0	·3590	·0377
11·1	·3995	·0295$_5$	11·1	·3564	·0387$_2$
11·0	·3973	·0299$_1$	11·0	·3495	·0409
11·1	·3877	·0321$_5$	10·8	·3417	·0429
10·9	·3840	·0329	10·8	·3356	·0447

From large-scale copies of the curves illustrated in figs. 1 and 2 a series of values of n, the refractive index, and δ Verdet's constant for isopropyl alcohol were read off; these are tabulated from Table II. (*d*), and were made use of in attempting to test the results in relation to Larmor's theory.

As a result of this, it was found that the experimental results fitted into a formula of the type :

$$\phi = n\delta\lambda^2 = k_1\left\{\frac{\lambda^2}{\lambda^2-\lambda_1^2}\right\}^2.$$

Fig. 2.

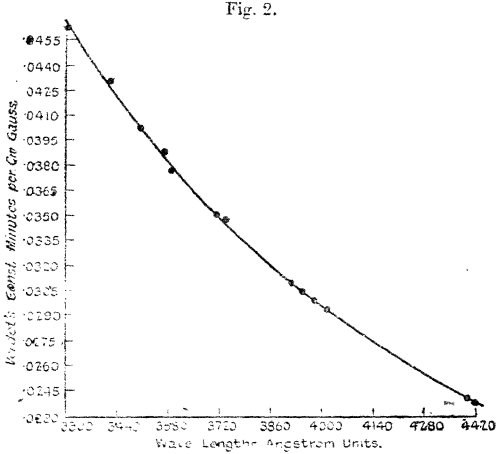

TABLE II. (*d*).

Isopropyl Alcohol.

	Wave-length in microns.	Refractive index.	Verdet's Constant, min./cm. gauss.		Wave-length in microns.	Refractive index.	Verdet's Constant, min./cm. gauss.
(*a*)	·4350 μ	1·3871	·0245$_5$	(*m*)	·3750 μ	1·3947	·0344
(*b*)	·4300 μ	1·3875	·0251	(*n*)	·3700 μ	1·3954	·0355$_2$
(*c*)	·4250 μ	1·3880	·0257$_2$	(*o*)	·3650 μ	1·3962	·0366$_4$
(*d*)	·4200 μ	1·3887	·0263$_5$	(*p*)	·3600 μ	1·3970	·0379$_4$
(*e*)	·4150 μ	1·3892	·0271$_1$	(*r*)	·3550 μ	1·3979	·0393$_3$
(*f*)	·4100 μ	1·3899	·0278$_4$	(*s*)	·3500 μ	1·3988	·0405$_5$
(*g*)	·4050 μ	1·3905	·0286$_4$	(*t*)	·3450 μ	1·3997	·0419$_7$
(*h*)	·4000 μ	1·3912	·0294$_5$	(*u*)	·3400 μ	1·4007	·0434$_4$
(*i*)	·3950 μ	1·3920	·0303$_7$	(*v*)	·3350 μ	1·4018	·0450
(*j*)	·3900 μ	1·3927	·0312$_5$	(*w*)	·3300 μ	1·4029	·0467
(*k*)	·3850 μ	1·3933	·0322$_2$	(*y*)	·3250 μ	1·4040	·0485
(*l*)	·3800 μ	1·3939	·0333$_2$				

The values of the function ϕ were calculated for each wave-length, and by eliminating k_1 from several pairs of these a set of values of λ_1 was obtained.

Eliminating k_1 from	λ_1 (microns).	Eliminating k_1 from	λ_1 (microns).	Eliminating k_1 from	λ_1 (microns).
(*c*) and (*o*)	·1134 μ	(*c*) and (*s*)	·1127 μ	(*c*) and (*w*)	·1139 μ
(*g*) and (*s*)	·1132 μ	(*j*) and (*w*)	·1136 μ	(*e*) and (*v*)	·1125 μ
(*e*) and (*t*)	·1137 μ	(*i*) and (*v*)	·1133 μ	(*i*) and (*w*)	·1132 μ
(*h*) and (*w*)	·1138 μ	(*b*) and (*n*)	·1160 μ	(*b*) and (*o*)	·1148 μ

The mean values of λ_1 from these $=$ ·1137 μ, and using this value of λ_1, the mean value of $k_1 = 5{\cdot}5526 \times 10^{-3}$ when δ is measured in minutes per cm. gauss and λ in microns. The equation therefore finally takes the form:

$$\phi = n\delta\lambda^2 = 5{\cdot}5526 \times 10^{-3} \left\{ \frac{\lambda^2}{\lambda^2 - (\cdot 1137)^2} \right\}^2 \quad . \quad . \quad (a)$$

This equation was used, together with values of n read off from fig. 1, to evaluate δ at a few wave-lengths where experimental determinations had been carried out. The result of such a comparison is shown in Table II. (*e*).

TABLE II. (*e*).

Isopropyl Alcohol.

λ.	δ (observed).	δ (calculated).	λ.	δ (observed).	δ (calculated).
·4400 μ	·0238	$\cdot 0237_5$	·3564 μ	$\cdot 0387_3$	$\cdot 0386_0$
·3866 μ	·0322	$\cdot 0319_6$	·3417 μ	·0429	$\cdot 0429_4$
·3730 μ	$\cdot 0347_3$	$\cdot 0347_7$	·3318 μ	·0462	$\cdot 0461_7$

Lowry and Dickson* have also determined the rotary dispersion of isopropyl alcohol at a few wave-lengths in the visible spectrum. These observers compare the rotary powers at various wave-lengths with that at $\lambda = \cdot 5461\ \mu$.

Using values of n obtained from a curve drawn from results tabulated in Table I. (*b*) and equation (*a*) above, δ was calculated for each of these wave-lengths, and the comparison is given below:

* J. C. S. l. p. 1072 (1913).

Wave-length, microns.	Rotary power relative to that at ·5461 μ.	
	Lowry & Dickson.	Present results.
·6708 μ	0·642	0·644
·6438 μ	0·702	0·703
·5893 μ	0·850	0·849
·5086 μ	1·163	1·167
·4800 μ	1·320	1·326
·4359 μ	1·634	1·646

Tho value of δ for the wave-length of sodium light was calculated from the formula (a), and found to be 0·01252 min. per cm. gauss.

Perkin * determined the rotation of isopropyl alcohol at this wave-length relative to water, and quotes the value 0·952. Using the value 0·0131 min. per cm. gauss for δ at ·5893 μ. in the case of water, this gives 0·01247 as the value for isopropyl at this wave-length.

The agreement between the value determined from the formula and the value obtained experimentally by Perkin is satisfactory.

It is interesting to point out that the equation connecting ϕ with λ in the case of normal propyl alcohol, as determined by Jones and Evans †, is given by

$$\phi = n\delta\lambda^2 = 5{\cdot}34 \times 10^{-5}\left\{\frac{\lambda^2}{\lambda^2-(\cdot1138)^2}\right\}^2.$$

On comparing the experimental results, it is seen that the absorption bands are situated almost exactly at the same point in the ultra-violet. The values of Verdet's constant for isopropyl alcohol are, on the average, 4 per cent. higher than the corresponding values for normal propyl alcohol: this is also the identical order of difference obtained by Perkin ‡ for these liquids at $\lambda = \cdot5893\ \mu$.

Allyl Alcohol.

In the present investigation the values of Verdet's constants for allyl alcohol have been determined from ·446 μ to ·2884 μ. The sample was experimented upon before and after a series of successive distillations. The results, in both cases, are identical, and are collected together in Tables III. (a) and III. (b).

* J. C. S. i. p. 468 (1884).
† *Loc. cit.*
‡ *Loc. cit.*

In Table III. (*c*) the values of Verdet's constants are those for which extremely accurate determinations had been carried out. The values of the refractive indices are those read off from a curve drawn from the results of Victor Henri *.

Here, again, the magnetic dispersion equation possesses only one term on the right-hand side, indicating that the magnetic rotation of allyl alcohol in the ultra-violet region investigated in this work is governed by a single absorption band.

TABLE III. (*a*).

Allyl Alcohol (before distillation).

Temp. in degrees Cent.	Wave-length in microns.	Verdet's Constant in min./cm. gauss.	Temp. in degrees Cent.	Wave-length in microns.	Verdet's Constant in min./cm. gauss.
11·1	·4460	·0311$_5$	11·2	·3689	·0500$_1$
10·9	·4282	·0344	11·2	·3649	·0516$_4$
10·8	·4229	·0354$_3$	11·2	·3593	·0532$_4$
10·8	·4145	·0371$_1$	11·1	·3560	·0548$_6$
11·0	·4136	·0374$_7$	11·2	·3520	·0546$_7$
10·8	·4073	·0387$_1$	11·2	·3472	·0584$_9$
11·0	·4012	·0403$_3$	11·1	·3416	·0605
11·0	·3985	·0411$_8$	11·0	·3382	·0625$_3$
10·9	·3940	·0419$_5$	11·0	·3346	·0645$_5$
11·0	·3890	·0435$_6$	11·0	·3299	·0671$_4$
11·0	·3828	·0451$_7$	11·0	·3240	·0702$_7$
11·2	·3783	·0467$_8$	10·8	·3181	·0751$_2$
11·2	·3736	·0483$_5$			

TABLE III. (*b*).

Allyl Alcohol (after distillation).

Temp. in degrees Cent.	Wave-length in microns.	Verdet's Constant in min./cm. gauss.	Temp. in degrees Cent.	Wave-length in microns.	Verdet's Constant in min./cm. gauss.
9·2	·3207	·0727	11·3	·2698	·0892$_3$
9·3	·3181	·0751$_2$	11·3	·2657	·0916$_4$
9·8	·3098	·0807$_3$	11·0	·2943	·0933$_7$
10·5	·3057	·0836	11·0	·2884	·0992$_6$

* *Loc. cit.* p. 103.

TABLE III. (*c*).

Allyl Alcohol.

	Wave-length in microns.	Refractive index. "*n*."	Verdet's Constant in min./cm. gauss.
(*a*)	·4282	1·4299	·0344
(*b*)	·3783	1·4366	$\cdot 0467_9$
(*c*)	·3299	1·4496	$\cdot 0671_4$
(*d*)	·2943	1·4658	$\cdot 0933_7$

Fig. 3.

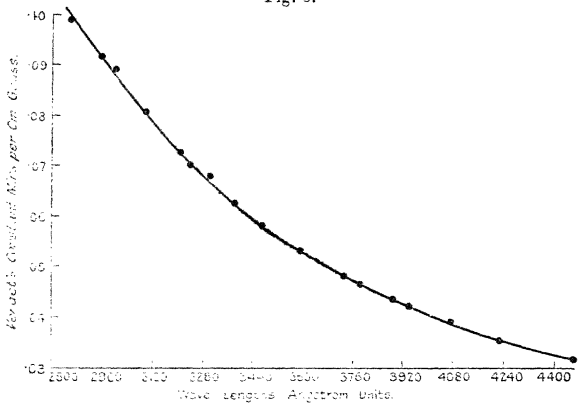

The following values of λ_1, the wave-length of the absorption band for allyl alcohol, were calculated by solving equation (4).

Eliminating k_1 from	λ_1 in microns.
(*a*) and (*b*)	·1365
(*b*) and (*c*)	·1363
(*c*) and (*d*)	·1384
(*b*) and (*d*)	·1375
(*a*) and (*d*)	·1372

These give for λ_1 a mean value $=\cdot 1372\,\mu$, and the mean value of $k_1 = 7\cdot 24 \times 10^{-3}$. These values of λ_1 and k_1 are also the identical values obtained from the mean of more than 20 solutions of equation (4), using values δ and n from the respective dispersion curves.

The final equation for this liquid, therefore, is

$$\phi = n\delta\lambda^2 = 7\cdot 24 \times 10^{-3}\left\{\frac{\lambda^2}{\lambda^2 - (\cdot 1372)^2}\right\}^2.$$

In Table III. (*d*) below, a comparison is given between the values of Verdet's constants as determined experimentally and those calculated from the above formula.

TABLE III. (*d*).

Wave-length.	δ (calculated).	δ (observed).	Wave-length.	δ (calculated).	δ (observed).
·4229 μ	·0353$_5$	·0354$_5$	·3593 μ	·0532$_5$	·0532$_4$
·4012 μ	·0402$_5$	·0403$_3$	·3472 μ	·0584$_1$	·0584$_0$
·3890 μ	·0435	·0435$_6$	·2957 μ	·0917$_\sim$	·0916$_\sim$
·3736 μ	·0482$_1$	·0483$_3$			

The above equation was used to calculate the values of Verdet's constant for the green and violet mercury lines at ·5461 μ and ·4359 μ. In this way it was found that the ratio

$$\frac{\delta_{\cdot 4359}}{\delta_{\cdot 5461}} = 1{\cdot}630.$$

Lowry *, who has determined the rotation of allyl alcohol for six wave-lengths in the visible spectrum (previously referred to), has found for this ratio the value 1·672. He expressed his results in the form of an empirical relation:

$$\alpha = \frac{k}{\lambda^2 - \lambda_0^2}$$

where α is the rotation for wave-length λ, k a constant, and λ_0 the wave-length of the absorption band. The absorption band from his value of λ_0^2 (·0293) is situated at ·1710 μ. According to the measurements of Victor Henri † on natural dispersion, the strong absorption band is calculated to be at ·1588 μ, whilst in the present experiments the absorption band is found to be at ·1372 μ.

The value of Verdet's constant at the wave-length of sodium light, according to the formula derived from the present work, = ·0165$_3$ minute per cm. gauss; the value given by Perkin's ‡ results at 13° C. = ·01639.

Methyl Acetate.

The magnetic rotations of methyl acetate have been examined in the present work from ·44 μ to ·2951 μ, and the experimental results appear in Table IV. (*a*). Combining these results with the data in Table I., according to Larmor's § theory, it was discovered that one absorption

* *Loc. cit.* † *Loc. cit.* ‡ *Loc. cit.* § *Loc. cit.*

band was responsible for the magneto-rotary effects of this liquid in the region of the spectrum investigated.

TABLE IV. (*a*).

Methyl Acetate.

Temp. in degrees Cent.	Wave-length (microns).	Verdet's Constant, min./cm. gauss.	Temp. in degrees Cent.	Wave-length (microns).	Verdet's Constant, min./cm. gauss.
11·7	·4386	·0260	11·7	·3465	·0346$_5$
11·7	·4238	·0216$_1$	11·7	·3423	·0356$_2$
11·7	·4050	·0240	11·7	·3340	·0376$_2$
11·6	·3992	·0247$_1$	11·7	·3277	·0396$_3$
11·7	·3908	·0256	11·6	·3248	·0404$_1$
11·6	·3806	·0275$_2$	11·7	·3230	·0410$_4$
11·7	·3754	·0284$_5$	11·8	·3170	·0428$_2$
11·7	·3675	·0300$_5$	11·7	·3109	·0449
11·7	·3654	·0304$_2$	11·7	·3079	·0461$_5$
11·7	·3620	·0310	11·6	·3064	·0467$_3$
11·6	·3568	·0323$_5$	11·7	·3020	·0484$_5$
11·7	·3507	·0339$_5$	11·6	970	·0506$_5$

Fig. 4.

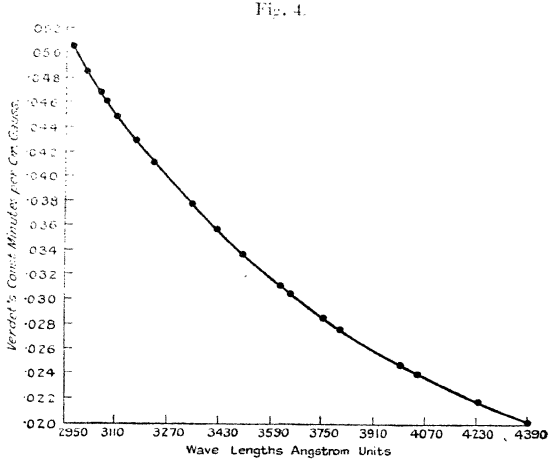

Table IV. (*b*) contains results read off from figs. 1 and 4.

TABLE IV. (*b*).

	Wave-length in microns.	Verdet's Constant, min./cm. gauss.	Refractive index.		Wave-length in microns.	Verdet's Constant, min./cm. gauss.	Refractive index.
(*a*)	·4000	$\cdot 0246_2$	1·3721	(*n*)	·3450	$\cdot 0349_8$	1·3792
(*b*)	·3950	·0253	1·3727	(*o*)	·3400	$\cdot 0362_2$	1·3801
(*c*)	·3900	$\cdot 0260_3$	1·3732	(*p*)	·3350	$\cdot 0375_2$	1·3811
(*d*)	·3850	$\cdot 0268_2$	1·3737	(*q*)	·3300	·0389	1·3821
(*e*)	·3800	$\cdot 0276_5$	1·3743	(*r*)	·3250	$\cdot 0403_5$	1·3833
(*f*)	·3750	$\cdot 0285_5$	1·3749	(*s*)	·3200	$\cdot 0419_2$	1·3845
(*g*)	·3700	$\cdot 0295_4$	1·3756	(*t*)	·3150	$\cdot 0435_6$	1·3858
(*h*)	·3650	·0305	1·3762	(*u*)	·3100	$\cdot 0452_6$	1·3871
(*k*)	·3600	$\cdot 0315_4$	1·3769	(*v*)	·3050	$\cdot 0472_5$	1·3885
(*l*)	·3550	$\cdot 0325_5$	1·3776	(*w*)	·3000	·0494	1·3900
(*m*)	·3500	$\cdot 0337_5$	1·3783	(*z*)	·2950	·0516	1·3916

Using the above results and solving the dispersion equation as before, we have the following values of λ_1 for the wave-length of the absorption band in the case of methyl acetate :—

Eliminating k_1 from	λ_1 (microns).	Eliminating k_1 from	λ_1 (microns).	Eliminating k from	λ_1 (microns).
(*a*) and (*w*)	·1109	(*b*) and (*q*)	·1121	(*g*) and (*z*)	·1108
(*b*) and (*p*)	·1129	(*g*) and (*n*)	·1117	(*k*) and (*s*)	·1091
(*a*) and (*p*)	·1116	(*f*) and (*v*)	·1103	(*a*) and (*o*)	·1139
(*a*) and (*r*)	·1109	(*d*) and (*t*)	·1114	(*d*) and (*r*)	·1113
(*a*) and (*m*)	·1129	(*c*) and (*r*)	·1139	(*c*) and (*s*)	·1119

These give ·1117 μ as a mean value of λ_1, and for k_1, the constant in the dispersion equation, the calculated mean is equal to $4{\cdot}587 \times 10^{-3}$.

The equation, therefore, finally takes the form

$$\phi = n\delta\lambda^2 = 4{\cdot}587 \times 10^{-3} \left\{ \frac{\lambda^2}{\lambda^2 - (\cdot 1117)^2} \right\} .$$

A comparison between the values of Verdet's constant calculated from this formula, and the values obtained experimentally, is given in Table IV. (*c*) below.

TABLE IV. (*c*).

Methyl Acetate.

λ.	δ (calculated).	δ (observed).	λ.	δ (calculated).	δ (observed).
·3026	$\cdot0484_2$	$\cdot0484_8$	·3423	$\cdot0355_4$	$\cdot0356_2$
·3170	$\cdot0429_5$	$\cdot0428_2$	·3675	$\cdot0299_7$	$\cdot0300_5$
·3230	·0410	$\cdot0410_2$	·4386	·0199	·0200

Unfortunately, no strict comparison can be made between the values of Verdet's constant as calculated from the formula derived from this work and that as determined by Perkin *, since the present determinations have been performed at 11·6° C. and Perkin † worked at 22° C. The value of δ, Perkin ‡ gives at $\cdot5893\,\mu = \cdot0102$ min. per cm. gauss at 22° C., whilst the value calculated from the present results = ·0104 min. per cm. gauss at 11·6° C.

Ethyl Acetate.

In the case of ethyl acetate the magnetic rotations were determined from $\cdot4404\,\mu$ to $\cdot3091\,\mu$; the results are collected together in Table V. (*a*).

As in the case of the other three organic liquids tested, it was found possible to account for these results on the assumption of one strong ultra-violet absorption band.

TABLE V. (*a*).

Ethyl Acetate.

Temp. in degrees Cent.	Wave-length in microns.	Verdet's Constant in min. cm. gauss.	Temp. in degrees Cent.	Wave-length in microns.	Verdet's Constant in min./cm. gauss.
11·6	·4406	$\cdot0207_2$	11·6	·3605	$\cdot0331_1$
11·6	·4305	$\cdot0219_1$	11·6	·3546	$\cdot0346_4$
11·6	·4075	$\cdot0246_1$	11·6	·3476	$\cdot0362_5$
11·6	·3995	$\cdot0258_1$	11·6	·3529	$\cdot0349_5$
11·6	·3920	$\cdot0270_3$	11·6	·3407	$\cdot0379_4$
11·6	·3850	·0283	11·6	·3346	$\cdot0397_8$
11·6	·3785	$\cdot0294_2$	11·7	·3270	$\cdot0417_8$
11·6	·3725	$\cdot0307_1$	11·6	·3206	$\cdot0439_5$
11·6	·3660	$\cdot0319_1$	11·6	·3152	$\cdot0459_3$
11·6	·3657	$\cdot0319_2$	11·6	·3103	$\cdot0477_6$

* *Loc. cit.* p. 494. † *Loc. cit.* ‡ *Loc. cit.*

Fig. 5.

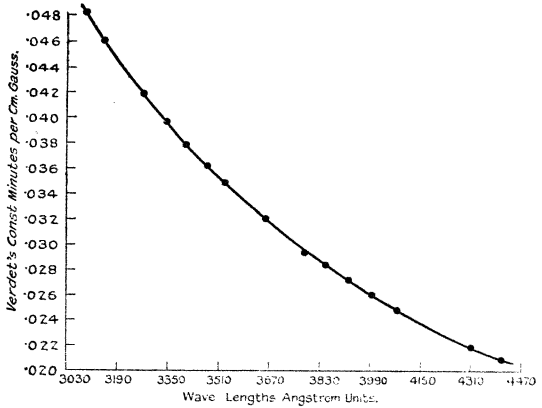

The results tabulated in Table V. (*b*) are those read off from figs. 1 and 5, and were made use of in calculating the value of λ_1 for ethyl acetate.

TABLE V. (*b*).

Ethyl Acetate.

	Wave-length in microns.	Verdet's Constant, min./cm. gauss.	Refractive index.		Wave-length in microns.	Verdet's Constant, min./cm. gauss.	Refractive index.
(*a*)	·4200	$·0231_5$	1·3808	(*m*)	·3600	$·0331_5$	1·3880
(*b*)	·4150	$·0237_4$	1·3812	(*n*)	·3550	$·0342_6$	1·3889
(*c*)	·4100	$·0243_6$	1·3817	(*o*)	·3500	$·0355_4$	1·3898
(*d*)	·4050	$·0250_4$	1·3821	(*p*)	·3450	$·0367_5$	1·3908
(*e*)	·4000	$·0257_4$	1·3826	(*q*)	·3400	$·0380_5$	1·3918
(*f*)	·3950	$·0264_8$	1·3832	(*r*)	·3350	$·0394_5$	1·3928
(*g*)	·3900	$·0273_6$	1·3837	(*s*)	·3300	$·0409_4$	1·3939
(*h*)	·3850	$·0282_5$	1·3843	(*t*)	·3250	·0425	1·3951
(*i*)	·3800	$·0291_2$	1·3850	(*u*)	·3200	$·0442_4$	1·3964
(*j*)	·3750	$·0300_6$	1·3857	(*v*)	·3150	$·0460_6$	1·3976
(*k*)	·3700	$·0310_3$	1·3864	(*w*)	·3100	$·0478_2$	1·3990
(*l*)	·3650	$·0320_9$	1·3872				

Eliminating k_1 from	λ_1 (microns).	Eliminating k_1 from	λ_1 (microns).	Eliminating k_1 from	λ_1 (microns).
(*e*) and (*q*)	·1164	(*a*) and (*w*)	·1113	(*c*) and (*n*)	·1153
(*p*) and (*b*)	·1146	(*c*) and (*w*)	·1134	(*g*) and (*r*)	·1153
(*j*) and (*u*)	·1136	(*b*) and (*t*)	·1127	(*o*) and (*v*)	·1119
(*b*) and (*q*)	·1134	(*g*) and (*u*)	·1147	(*e*) and (*k*)	·1156
(*c*) and (*s*)	·1143	(*g*) and (*v*)	·1147	(*k*) and (*w*)	·1113
(*e*) and (*s*)	·1156	(*b*) and (*l*)	·1143		

The mean value of λ_1 from the above $= \cdot1140\,\mu$, and the mean value of $k_1 = 4\cdot825 \times 10^{-3}$.

Thus the dispersion equation is.

$$\phi = n\delta\lambda^2 = 4\cdot825 \times 10^{-2} \left\{ \frac{\lambda^2}{\lambda^2 - (\cdot1140)^2} \right\}^2.$$

Table V. (*c*) shows a comparison between results calculated from the above equation and those determined experimentally.

TABLE V. (*c*).

Ethyl Acetate.

λ.	δ (calculated).	δ (observed).	λ.	δ (calculated).	δ (observed).
·4406 μ	·0207	·0206_5	·3476 μ	·0360_7	·0362_5
·4305 μ	·0218_3	·0219	·3529 μ	·0347_8	·0349_5
·4075 μ	·0247_5	·0246_9	·3270 μ	·0419_3	0417_8
·3725 μ	·0305_3	·0307_1			

Perkin's * values for the specific rotation at ·5893 μ, in the case of ethyl acetate, are 0·8315 at 10·5° C. and 0·8295 at 14·5° C. These give values of 0·01089 and 0·01087 respectively for δ in minutes per cm. gauss.

The value calculated from the formula derived here $=$ 0·01092 at 11·7° C.

SUMMARY.

(*a*) The magneto-optical rotations of isopropyl alcohol, allyl alcohol, methyl acetate, and ethyl acetate have been determined for various wave-lengths in the violet and near ultra-violet regions of the spectrum.

—The refractive indices of isopropyl alcohol and of methyl and ethyl acetates have also been determined in the visible and near ultra-violet regions of the spectrum.

(*b*) The magneto-rotary dispersion of isopropyl alcohol and of allyl alcohol for the ranges of wave-length investigated can be represented by the equations:

$$\phi = n\delta\lambda^2 = 5{\cdot}5526 \times 10^{-3} \left\{ \frac{\lambda^2}{\lambda^2 - (\cdot 1137)^2} \right\}^2$$

and

$$\phi = n\delta\lambda^2 = 7{\cdot}24 \times 10^{-3} \left\{ \frac{\lambda^2}{\lambda^2 - (\cdot 1372)^2} \right\}^2$$

respectively, where n is the refractive index and δ Verdet's constant in minutes per cm. gauss for wave-length λ. The strong ultra-violet absorption bands which control the magnetic rotation in the case of isopropyl alcohol and allyl alcohol have wave-lengths $\cdot 1137\,\mu$ and $\cdot 1372\,\mu$ respectively.

(*c*) The magnetic-rotary dispersion of methyl and ethyl acetates for the ranges of wave-lengths investigated can be represented by the equations:

$$\phi = n\delta\lambda^2 = 4{\cdot}587 \times 10^{-3} \left\{ \frac{\lambda^2}{\lambda^2 - (\cdot 1117)^2} \right\}^2$$

and

$$\phi = n\delta\lambda^2 = 4{\cdot}825 \times 10^{-3} \left\{ \frac{\lambda^2}{\lambda^2 - (\cdot 1140)^2} \right\}^2$$

respectively.

The wave-lengths of the absorption bands which control the magneto-optical rotation of methyl and ethyl acetates are $\cdot 1117\,\mu$ and $\cdot 1140\,\mu$ respectively.

Swansea,
January 1929.

XVII. *An Apparatus for the Measurement of Magnetic Susceptibility.* *By* W. Sucksmith, *B.Sc., Lecturer in Physics, University of Bristol* *.

IN connexion with another investigation the writer found it necessary to measure the magnetic susceptibilities of a number of paramagnetic substances. As the method employed embodies only very simple apparatus and is capable of measuring moderate susceptibilities with a fair degree of accuracy, it seemed worth while to deal with it in a separate communication.

* Communicated by the Author

Existing Apparatus and Methods.

The method most generally useful is that of Faraday, in which the force on a small specimen placed in a non-uniform field is measured. If an isotropic substance of mass m and susceptibility χ is placed in a non-uniform field H whose gradient perpendicular to the magnetic lines of force is $\frac{d\mathrm{H}}{dx}$, the force experienced along the x-axis is given by

$$\mathrm{F}_x = \chi m \mathrm{H} \frac{d\mathrm{H}}{dx}.$$

In the early experiments of Curie the substance was placed on the arm of a torsion-balance, and the force measured by the displacement experienced by the specimen. The displacement was kept small, otherwise the value of $\mathrm{H}\frac{d\mathrm{H}}{dx}$ varies considerably. The best position for the specimen is the point at which this is a maximum, so that errors due to accidental displacement from this position are reduced to a minimum. The susceptibility can be readily calculated from the constants of the system together with a knowledge of H and $\frac{d\mathrm{H}}{dx}$. The accurate determination of $\frac{d\mathrm{H}}{dx}$ is, however, rather difficult, and late experimenters have avoided it by comparing the susceptibility of the substance under examination with that of a standard substance placed in the same position, the susceptibility of which had been determined by other means (*e.g.* the Quincke ascension method for liquids, which has the advantage of employing a uniform field). With a torsion-balance the great sensitivity obtainable is offset by the difficulty of placing the comparison substance in exactly the same position as that occupied by the specimen, together with the unavoidably long period of oscillation of the system.

Weiss and his collaborators have developed an apparatus which is capable of considerable accuracy, the most recent form of which is due to Foex and Forrer*. The torsion-balance is replaced by a movable pendular system which carries the specimen. The moving system is suspended by fine threads so as to allow motion only in one direction. Thus, under the action of the magnetic field the system moves horizontally against the gravitational control of the

* *Journ. de Phys.* vol. vii. p. 180 (1926).

system in a direction perpendicular to the lines of force. A null method is used, and the magnetic force is compensated by the electro-dynamic force exerted between a coil carried on the moving system and a fixed permanent magnet. The latter force varied approximately linearly with the current carried by the coil. To indicate the zero of the system a Kelvin double-suspension mirror of special type was used, the supporting threads being 4 mm. apart. The authors claim an accuracy of 1 part in 750 in a measurement on 0·35 gram of a substance of susceptibility $0{\cdot}55\times10^{-6}$, the force being less than 3 dynes. The accuracy and sensitivity appear to be as great as is necessary, but these appear to be somewhat counterbalanced by the elaborate nature of the apparatus and the reliance placed on the relationship between restoring force and the current in the restoring coil. In addition, the apparatus is bulky, since the restoring coil should be well removed from the region of stray field of the magnet, though correction can be made for the residue of this. The suspensions are apparently of the order of 60 cm. in length.

For many purposes an accuracy of $\frac{1}{2}$ to 1 per cent. is quite sufficient, and it appeared possible to the writer to design an apparatus that would meet this requirement and at the same time eliminate the necessity of using restoring forces by making the displacements very small.

Description of Method.

The method depends on the deformation of a circular ring of strip phosphor-bronze fixed at the top and subjected to a force at the bottom. The applied force is due to the action of a magnetic field on a specimen under investigation. If such a ring is clamped in a vertical plane at its highest point, and a force P applied at the bottom of the ring vertically downwards, then the radial displacement u at any point is given by

$$u=\frac{Pr^3}{4EI}\left\{\theta\sin\theta+\cos\theta-\frac{4}{\pi}\right\},$$

where r = radius of the ring,

I = the moment of inertia of cross-section of the ring,

E = Young's Modulus,

and θ = angle between the radius through the point considered and the horizontal.

When $\theta=90°$, then the displacement of the lowest point relative to the point of support

$$=\frac{Pr^3}{2EI}\left\{\frac{\pi}{2}-\frac{4}{\pi}\right\}=\frac{0{\cdot}298\,Pr^3}{2EI}.$$

The angle turned through by the tangent to the ring is, to a first approximation, given by

$$\phi=\frac{1}{r}\cdot\frac{du}{d\theta}=\frac{Pr^2}{4EI}(\theta\cos\theta).$$

This is a maximum at about 49°, whence

$$\phi=\frac{0{\cdot}561\,Pr^2}{4EI}.$$

Two mirrors, facing each other, are placed at the points B and C (see figure), where the angular displacement is a

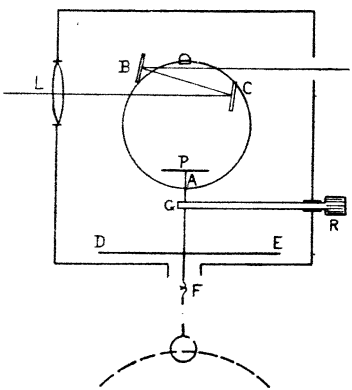

maximum. Light from a distant source passes through the lens L, and if, after reflexion at the two mirrors, it is focussed on a vertical scale D cm. away, then the scale-displacement corresponding to the force P is given by

$$v=\phi(4D+2d),$$

where d is the distance between the mirrors at B and C.

In terms of the constants of the system

$$v = \frac{(4D + 2d)0{\cdot}561 P r^2}{4EI}.$$

Hence

$$\frac{v}{u} = \frac{0{\cdot}943(4D + 2d)}{r}.$$

Since P is the magnetic force exerted on a body in a non-uniform magnetic field, u must be kept small, *i. e.* the ratio v/u should be as large as conveniently possible. The values chosen were $r = 2{\cdot}5$ cm., and D a distance of about 1 metre. This gives a scale-displacement about 150 times that of the body. For a source a lamp with a straight metal filament was found most satisfactory. With a distance D of 100 cm. the lens which gives best definition of the image is one of 50-cm. focus, so that the distance of the source is about 1 metre from the lens and the magnification of the image unity. Further, as the size of the mirrors governs the effective lens aperture, these should be as large as conveniently possible. These were made by chemically silvering selected plate-glass $10 \times 10 \times 1$ mm. In lieu of a scale, a microscope with vertical traverse is focussed on the image of the filament. Under these conditions it is easy with a little practice to read the position of the image to 0·01 mm., which corresponds to a displacement of the specimen of 0·000007 cm.

From the lower extremity of the ring hangs a copper wire carrying a light mica damping-vane D E. The specimen carrier for powdered material and liquids is a thin-walled glass phial at the end of an extension of thin glass tube. This hangs from the lower extremity of the copper wire at F. The joints at A and F are cemented rigid with shellac.

The whole apparatus is enclosed in a brass box $10 \times 10 \times 13$ cm. The support for the ring is a circular brass rod fitted into a friction-tight brass tube. This allows of approximately horizontal adjustment along or perpendicular to the lines of magnetic force. The dotted outline of pole-pieces is shown in the figure, so that for a paramagnetic substance the magnetic force is vertically downwards. In the tests to be described, plane pole-pieces of diameter 10 cm., 3 cm. apart, were used, thus ensuring a reasonable volume over which $H\frac{dH}{dx}$ is appreciably constant. The separation of 3 cm. is sufficient to allow the specimen to be enclosed in the usual apparatus

for high- or low-temperature work. The current used was 15 amperes, which gave a value of $H\frac{dH}{dx}$ of about 10^7.

Since the accuracy of the method depends on the linear relationship between force and displacement, tests were made to verify this. By putting weights on the small mica "scale-pan" P (see figure), this was shown to hold to within 1 part in 1000 for scale-displacements up to 3 cm. (3000 scale-divisions), which is more than adequate for the purposes of the apparatus. The setting of the specimen in the position of maximum $H\frac{dH}{dx}$ is carried out by levelling-screws on the electromagnet. If necessary more accurate setting can be made by slightly loading the scale-pan P. For subsequent measurements with different masses of materials for comparison, the same position of the image is maintained by loading or unloading the scale-pan. This is an accurate criterion of the setting of the phial in the same position. Independent settings of a specimen of paramagnetic material gave the same deflexion within 1 part in 500. The zero is extremely stable, and after a first preliminary deflexion due to the magnetic field, there is practically no sign of elastic fatigue. The times of oscillation of the systems used varied from 1/15 to 1/5 second, so that equilibrium is reached very quickly and a set of readings can be taken in a very short time.

To test the apparatus for accuracy in the actual measurement of magnetic susceptibility, the four substances shown in the table were chosen as being of various orders of susceptibility, about which different experimenters give results in good agreement. The first three materials, in the anhydrous state, were measured on a ring of phosphor-bronze 0·13 mm. thick by 3·0 mm. wide. One of these, $NiSO_4$, was measured on a weaker ring (0·10 × 2·0 mm.), as also was $NiSO_4 . 7H_2O$. On a third ring (0·065 × 2·0 mm.) pure water was used *. The second column gives the scale-deflexion for the weight used, the fourth column the scale-deflexion per gram of material. Column 5 gives the weight-calibration of the system, *i. e.* the scale-deflexion per gram weight of load placed in the pan P. This allows the results with different rings to be brought to a common basis

* In the case of this ring, the shape became somewhat elongated under the weight it had to carry. This was easily remedied by shaping the strip so that under a mean load it was approximately circular.

Substance.	v (cm.).	w (weight).	$v/w = V$.	W (cm.).	V/W.	$\chi' \times 10^6$.	$\chi \times 10^6$.
$MnCl_2$	1·304	0·1815	7·182	5·760	1·248	112·2	114·8 *, 111·8 †
,, ...	0·971	0·1355	7·167	5·760	1·244		
$CoCl_2$.....	1·165	0·1870	6·230	5·760	1·081	97·4	99·7 *, 95·0 †
$NiSO_4$	0·253	0·1515	1·670	5·760	0·290	26·1	26·5 ‡, 26·2 †
,, ...	0·812	0·1835	4·425	15·30	0·289	26·0	
$NiSO_4 . 7H_2O$ ...	0·659	0·2450	2·690	15·30	0·176	15·85	15·7 ‡, 15·5 §
H_2O	0·301	0·491	0·613	76·70	0·00799	0·720 ‖	

* Theodorides, *Arch. de Genève*, vol. iii. p. 161 (1921).

† Ishawara, Sci. Rep. Tohoku, vol. iii. p. 243 (1915).

‡ Jackson, Phil. Trans. A, vol. ccix. p. 1 (1924).

§ Onnes & Hof, see Jackson (*ibid.*).

‖ Taken as standard.

for comparison, which is expressed in column 6 as the force (in grams weight) per gram of specimen. In the seventh column the results are expressed as susceptibilities, the standard used being pure water ($\chi = 0{\cdot}72 \times 10^{-6}$). The most reliable results of experimenters are added for comparison in the last column, all results being reduced to 14° C., the temperature at which the measurements were made.

There is usually a field-gradient along the lines of force, such that $H\frac{dH}{dy}$ (where the y-axis is along the lines of force) is zero midway between the poles, with increasing positive values as the pole-pieces are approached. In other words, a paramagnetic specimen is in a position of unstable equilibrium as regards horizontal displacement, and may, if this force is sufficiently large, be drawn laterally to one or other of the pole-pieces. This fault is experienced for the largest deflexions (above about 500 scale-divisions), and is eliminated as follows:—Parallel to the lines of force a single cocoon silk fibre is fixed between the two adjustable rods R, which were each 5 cm. from the suspending ring. The rods are drawn towards the extension A F until the fibre just touches, where it is fixed by a speck of shellac. This addition neither alters the uniformity of deflexion with force nor is the sensitivity appreciably changed. With it the deflexions for four successive increments of 0·02 gram were 5·64, 5·66, 5·64, and 5·64 mm. respectively, whilst prior to the attachment of the fibre the mean deflexion was 5·67 mm.

Summary and Conclusions.

A simple apparatus admitting of rapid measurement of magnetic susceptibilities is described. An accuracy of $\frac{1}{2}$ per cent. is obtained on substances of moderate specific susceptibility, whilst for susceptibilities of the order 10^{-6}, measurements can be made to 1 per cent. on half a gram of material. The force experienced by a specimen in a non-homogeneous magnetic field produces a very small movement of the specimen, thus eliminating the necessity for a null method. The movement, which is directly proportional to the magnetic force, is magnified to a suitable value for observation. The method could be easily adapted to measurements of the large forces on paramagnetic substances at very low temperatures.

XVIII. *A Class of Artificial Lines containing a Class of Phase-shifting Networks.* *By* A. C. BARTLETT, B.A.* (Communication from the Staff of the Research Laboratories of the General Electric Co., Ltd., Wembley.)

THE class of artificial lines to be described is constructed of sections of which a typical half-section is shown in fig. 1. A complete artificial-line section is made by taking another identical half-section and connecting T_1' to T_1', T_2' to T_2', etc. The constants can be stated in terms of simple continuants. As a special case there occurs a class of phase-shifting artificial lines, *i.e.*, whose characteristic impedances

Fig. 1.

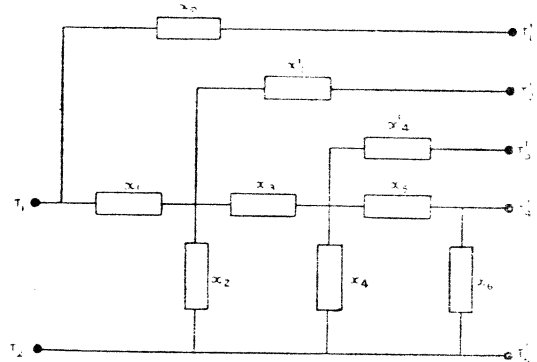

are pure resistances at all frequencies, whose attenuation constants are zero at all frequencies, and whose phase constants vary with frequency. Such networks are becoming of importance in long-distance telephony. The half-section of the artificial line to be considered consists of a series of impedances x_1, x_3, $x_5 \ldots x_{2n-1}$, of shunt impedances x_2, $x_4 \ldots x_{2n}$, and cross impedances x_0', $x_2' \ldots x'_{2(n-1)}$; fig. 1 illustrates the case $n=3$.

Applying a theorem previously given†, if Z_0 and θ are the constants of this section, then $Z_0 \coth \frac{\theta}{2}$ is the impedance

* Communicated by C. C. Paterson, Director.
† Phil. Mag., Nov. 1927.

of the half-section of fig. 1 measured at T_1T_2 with the terminal $T_1'T_2'$ ..... free, and so is the impedance of the ladder network

Fig. 2 *a*.

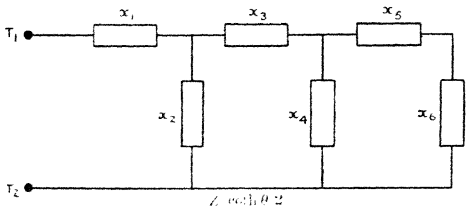

of fig. 2 *a*. Similarly, $Z_0 \tanh \theta/2$ is the impedance of the network of fig. 1 with the terminals $T_1'T_2'$, etc., connected together, which can be re-drawn as the ladder network shown in fig. 2 *b*.

Fig. 2 *b*.

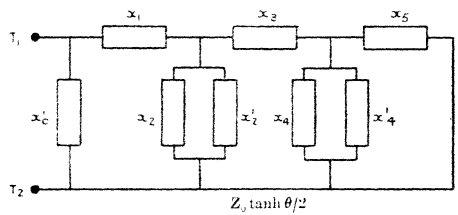

Let the impedances of x_1, x_2, x_5, etc., be a_1, a_3, a_5, etc., of x_0', x_2, x_2', x_4, x_4', etc., be $1/a_0'$, $1/a_2$, $1/a_2'$, $1/a_4$, $1/a_4'$, etc.; then the constants can be readily determined in terms of simple continuants *. $Z_0 \coth \theta/2$ is equal to the impedance of the network of fig. 2 *a*, which is

$$\frac{K(a_1, a_2, a_3 \ldots\ldots a_{2n})}{K(a_2, a_3 \ldots\ldots a_{2n})}, \quad \ldots\ldots \quad (1)$$

while in a similar way from fig. 2 *b*,

$$Z_0 \tanh \theta/2 = \frac{K(a_1, (a_2+a_2'), a_3, (a_4+a_4'), \ldots, a_{2n-1})}{K(a_0', a_1, (a_2+a_2'), a_3, \ldots\ldots, a_{2n-1})}. \quad (2)$$

These two equations determine Z_0 and θ for the general case.

* Post Office Electr. Eng. Journal, Jan. 1926.

Consider next the special case where x_1, x_3, x_5, ... x_{2-n1} are all numerical multiples of one type of impedance X, and are b_1X, b_2X, b_5X, etc., respectively. Let the other x's be all numerical multiples of another impedance Y, which is equal to Q^2/X, where Q is any impedance, so that a_0', a_2, a_2', a_4, etc., will be $b_0'X/Q^2$, b_2X/Q^2, $b_2'X/Q^2$, b_4X/Q^2, etc. Now let the b's be chosen so that

$$b_0' = b_1,$$
$$b_1 = b_2,$$
$$b_3 = b_2 + b_2',$$
$$b_3 = b_4,$$
$$b_5 = b_4 + b_4'.$$
$$b_5 = b_6,$$
etc., etc.

It will be seen, after inserting these values in (1) and (2), that with the b's so chosen the two networks of fig. 2*a* and fig. 2*b* are mutually reciprocal with respect to the impedance Q, *i.e.*, the product of their impedances is Q^2, and therefore, for this artificial line, $Z_0 = Q$. Now let Q be a resistance R and X any pure reactance ladder network, then $Y = \frac{R^2}{X}$ is a physically realizable pure reactance network.

The artificial-line section thus obtained therefore has a characteristic impedance R at all frequencies. Since $Z_0 \tanh \theta/2$ is the impedance of an entirely reactive network, it must be a pure imaginary, and thus, since $Z_0 = R$ and is real, $\tanh \theta/2$ and therefore θ must be pure imaginaries.

Thus the artificial line has zero attenuation at all frequencies, and is a pure phase-shifting network. The special case also leads to a class of artificial lines having the same characteristic impedance as a uniform line; for choosing the b's as before and choosing X and Y so that their product is

$$(R + jpL)/(S + jpC),$$

which can be done in an infinite number of ways, it is seen that the characteristic impedance of the artificial line is

$$\sqrt{\frac{R + jpL}{S + jpC}}.$$

XIX. *On the Modes of Vibration of a Quartz Crystal.* By J. W. Harding, *B.Sc., and* F. W. G. White, *B.Sc., Senior Scholar in Physics, Victoria University College, Wellington, N.Z.**

[Plates I.–V.]

Introduction.

THE existence of nodes and antinodes on the surface of an oscillating quartz crystal has been demonstrated by A. Crossley (P. I. R. E., April 1928), using ferro-ferricyanide solution as an indicator. It is stated that lycopodium powder was tried but was thrown off, leaving no trace on the crystal. Using a fairly thick crystal, the present writers have found lycopodium powder very effective, and a comprehensive study of the various patterns formed on the crystal surface for different modes of vibration has been carried out. Special care has been taken to trace the connexion between the modes of vibration of the faces and the air-currents which may issue from those faces.

Method of obtaining Figures.

The crystal was placed either between two vertical plane electrodes, in which case the top face was left clear, or, when it was necessary to use horizontal electrodes, the crystal was set oscillating, and then the electrode was gently pushed off the surface as far as possible and the lycopodium powder scattered in a fine layer by means of a small brush. Care had to be exercised that such patterns were not modified by air-streams issuing from beneath the electrode. The crystal was frequently cleaned by immersion in carbon tetrachloride, and it was noticed that vigorous oscillation was generally accompanied by a spark discharge between the electrodes and the quartz surface with consequent production of ozone. A large black film was sometimes placed between the brass plate acting as the lower electrode and the crystal in order to obtain better photographs of the wave-patterns. The electric field was applied parallel to the three different axes in turn, and the patterns, together with the corresponding frequencies, were recorded. The size of the crystal used throughout these investigations was 4 cm. × 3·5 cm. × 2·5 cm.

* Communicated by Sir W. H. Bragg, K.B.E., F.R.S.

At first the simple self-maintained circuit was used with the crystal in the grid circuit, and the plate circuit tuned to resonance with the crystal frequency. This circuit was afterwards modified to that shown (fig. 1). This circuit oscillated

Fig. 1.

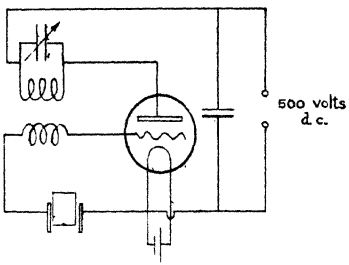

at definite frequencies only, corresponding to natural frequencies of the crystal, but, owing to the reactive effect of the grid coil, the oscillations were much stronger and much more easily maintained.

Fig. 2.

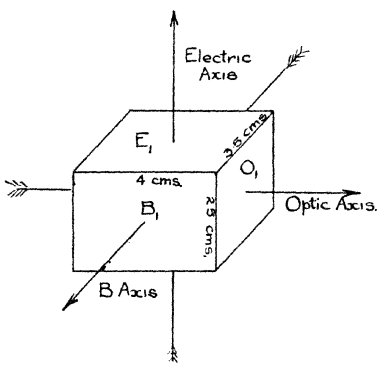

The method adopted of naming the faces in accordance with the three principal axes will be sufficiently clear from the diagram (fig. 2).

Description of Patterns.

1. *Field parallel to Electric Axis. Longitudinal Vibrations.*

The following faces are described with reference to figs. 3 and 5 :—

Face B_1.—The mode of vibration is very complicated. On the left the powder streams off in the direction shown, forming strong air-currents from the side faces. There are

Fig. 3.

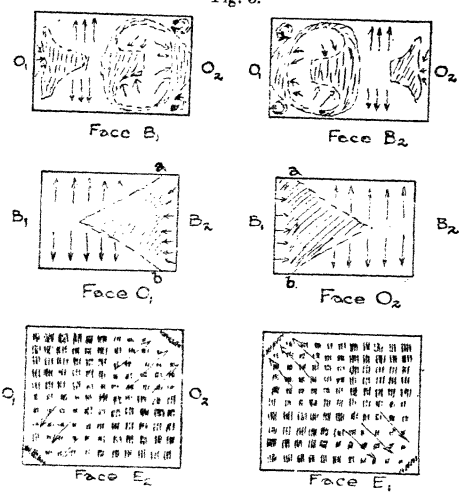

Field parallel to E axis.
Longitudinal mode.

other movements, as indicated by the arrows in the diagram, including the rotatory motion in the two right-hand corners. No air-currents issue from this face.

Face B_2.—Similar figure to above, with the orientation shown.

Face O_1.—The powder collects as shown on the right-hand side. There is a slight inward movement of powder on the right, while the powder streams off on the left in the direction of the arrows, forming strong air-currents from the side faces;

but there is no air-stream from this face itself. The nodes at *a* and *b* correspond to the two nodes across the corners of the E faces, as will be seen from the model. If a block of ebonite is supported a few millimetres from one of the side faces, the lycopodium powder can be seen suspended in the form of flat disks in mid-air at the nodes between the crystal and the block. It should be noted that this supports the assumption that the checker-board pattern of the E faces is maintained while the other faces are being examined, since the disks form along definite pencils in air above certain squares of the pattern.

Face O_2.—The pattern on this face is similar to the above, with the orientation shown.

Face E_1.—The powder collects in a checker-board pattern with two nodes across opposite corners. There is a small movement of the dust at these corners towards the two nodes, probably due to the presence of two strong air-streams issuing upwards most strongly from the regions indicated ; but there was no sign of an air-current from the sides in this case. As the condenser is turned the two nodes move inwards, and the rest of the powder moves outwards to form the ellipse of the other mode of vibration (see below).

Face E_2.—A similar figure, with the orientation shown.

Typical dust-figures are shown in the photographs of Pl. I.

2. *Field parallel to the Electric Axis. Transverse Vibrations.*

The following faces are described with reference to figs. 4 and 6 :—

Face B_1.—A general checker-board pattern. On the left-hand side the powder collects, but on the right it streams off in the direction of the arrows, and is also shot up into the air at a distance of several centimetres over this half of the crystal, since a current of air issues vertically from almost the whole of the right-hand side of this face. There is also an air-current from the side face, as shown, and a slight movement on the left-hand side along the edges is indicated by the arrows.

Face B_2.—The pattern is as described above, with the orientation indicated.

Face O_1.—On the right-hand side the powder collects in a checker-board pattern which moves in the direction of the arrows. This does not mean that the nodes change position, but that the powder is continually replaced by fresh supplies from the left. The powder flakes are shot into the air over

Fig. 4.

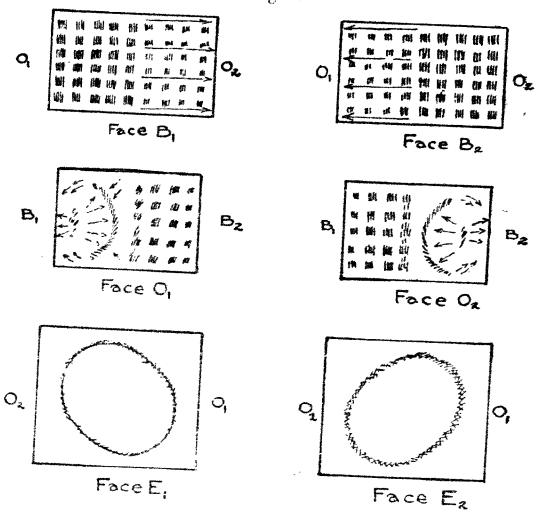

Field parallel to E axis.
Transverse mode.

Fig. 5.

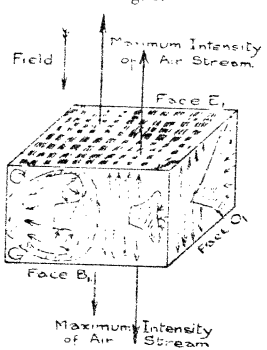

Longitudinal mode.

this face, the movement being most violent on the extreme right. Elsewhere the movement of the powder as it is sprinkled on is indicated as arrows, and there is an air-current from the right-hand B face.

Face O_2.—The figure is similar to that just described, orientated as shown.

Face E_1.—The powder moves in the direction of the arrows to form an ellipse of major axis 3 cm. and minor axis 2·5 cm. The major axis does not coincide with the diagonal of the rectangular face. This ellipse is very clearly defined if very little powder is used, and its dimensions may be accurately measured. Strong air-currents are produced from the side faces in the positions indicated.

Face E_2.—The same figure, orientated as shown.

Typical dust-figures are shown in photographs of Pl. II.

Fig. 6.

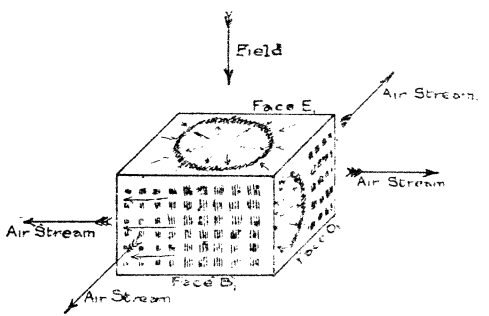

Transverse mode.

Photographs of Air-streams and Standing Waves.

In order to show the radiation of ultrasonic waves from certain sides of the crystal, several photographs were taken of the dust-pattern formed on a smooth horizontal surface round the crystal. If an obstacle is so placed as to reflect the waves, both the standing wave-pattern is obtained and also the air-streams noted by Meissner (P. I. R. E., April 1927). It is important to notice that the emission of ultrasonic waves and air-currents is always associated with the presence of the checker-board pattern on the radiating face.

In Pl. I., C and D show standing waves and air-streams

emitted from the E surfaces of the crystal. In these photographs the dust-figures surrounding the crystal are taken at a distance of about a centimetre below the upper surface, and show the air-stream emerging from the right-hand side. If the film is now moved down towards the lower face, the stronger air-current would now appear on the left side, corresponding to a reversal of the dust-pattern of the upper face on the lower surface.

When the crystal is oscillating longitudinally, air-streams and sound-waves emerge from the E surfaces only.

In Pl. II., A and C, ultrasonic waves are shown radiated from the B and O faces of the crystal. Photograph B shows the air-stream coming from the B face at about 5 mm. below the upper surface. Since the dust-pattern is reversed on the lower face, this air-stream will issue from the opposite B face at a similar distance from the lower face. These photographs, showing simultaneously both the pattern on a face and the air-streams issuing on adjacent sides, are particularly valuable in building up a model.

The various figures described above can be pieced together to form a model to illustrate the resultant pattern over all the faces simultaneously when the crystal is vibrating in the longitudinal or in the transverse mode, corresponding to two distinct vibration frequencies. This is shown in figs. 5 and 6.

Along certain nodes, such as the ellipse on face E, when the transverse mode is used, the powder tends to stick to the crystal face. Thus, if this particular surface is vertical, the powder running down the side will stick along the node-forming parts of the pattern on the side. This fact, as well as the existence of the air-streams, indicates that the same pattern is maintained when the crystal is turned on to a new side.

3. *Field parallel to the* B *Axis. Longitudinal Vibrations.*

The faces are described with reference to figs. 7and 9 :—

Face E_1.—There are nodes across the face and at the corners, as shown. Elsewhere the powder moves in the manner indicated by the arrows. There is a collection of powder at *a* and *b* corresponding to the collection of powder near *a* and *b* on the O faces, and there are air-streams from the side B faces, as indicated.

Face E_2.—The same pattern, with the orientation with respect to the O faces shown by the letters in brackets.

Face B_1.—On the lower half the powder forms into thick streams with a suggestion of the checker-board pattern, and

moves in the direction of the arrows. There is a small node at *a* which apparently extends up the middle of the face. At the top end the powder tends to collect, with a slow movement in the direction of the arrows. The whole pattern is difficult to obtain owing to the modifying effect of an air-current which comes mainly from the centre and lower half.

Face B_2.—The same figure, with similar orientation with respect to the E faces.

Face O_1.—The powder collects along O *a* and O *b*, corresponding to the position of the nodes on the E faces (see below), and there is a node up the middle of the face. The powder on the top half streams off rapidly in the direction of the arrows.

Fig. 7.

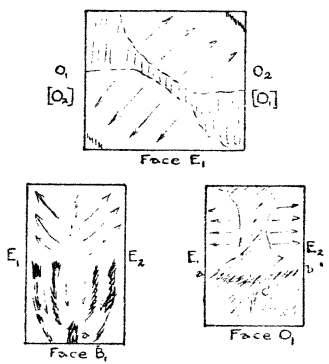

Field parallel to B axis.
Longitudinal mode.

Face O_2.—The same figure, with similar orientation with respect to the E faces.

Typical dust-figures are shown in the photographs of Pl. III.

4. *Field parallel to the B Axis. Transverse Vibrations.*

The faces are described with reference to figs. 8 and 10:—

Face E_1.—As the powder is scattered, it forms a checker pattern, and moves everywhere towards the distinct

nodal lines shown. Air-currents issue from this face, mainly from the corners.

Face E_2.—The same figure, orientated as shown by the letters in brackets.

Fig. 8.

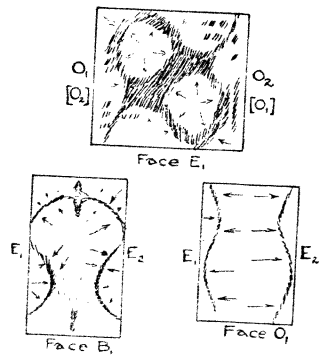

Field parallel to B axis.
Transverse mode.

Fig. 9.

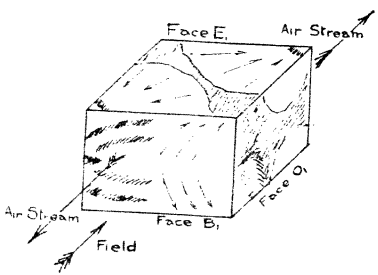

Longitudinal mode.

Face B_1.—The powder forms the nodal lines shown with a faint line up the centre, and dust moves everywhere towards the two outer lines. The nodes at the edges of the face join

up with corresponding nodal lines on the E faces, as can be seen from the model (fig. 10).

Face B_2.—The same figure, with similar orientation.

Face O_1.—If very little powder is applied, just the two outer lines are obtained. If more, the powder collects heavily in the centre, with a movement everywhere towards the nodal lines.

Face O_2.—The same figure, with similar orientation.

Typical dust-figures are shown in the photographs of Pl. IV.

Fig. 10.

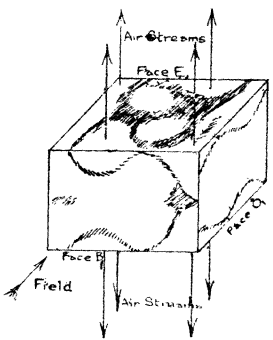

Transverse mode.

PHOTOGRAPHS OF AIR-STREAMS AND STANDING WAVES.

In Pl. V. are two photographs, showing simultaneously the patterns on the B faces with the air-streams emitted from the E sides. The apparent intensity of the emitted currents, as indicated by the dust-pattern, will depend on the position of the film on which the powder is scattered. In A the film has been placed over the brass electrode and the crystal has been removed. The pattern is seen to have formed underneath the crystal. B shows the pattern on top of the crystal for the same arrangement.

As in the preceding case, these patterns may be pieced together to form the two models given in figs. 9 and 10.

Vibrations with the Field parallel to the Optic Axis.

No vibrations could be induced in the crystal with the electric field parallel to this axis.

Summary.

Four models showing the possible normal modes of vibration of the crystal have been constructed—a longitudinal and a transverse mode for each of the two directions of the alternating field.

Two general features are evident from these models :—

(1) The presence of the checker-board pattern on a face indicates that an air-stream is issuing from that face.

(2) In all four models the pattern on the E faces has the same orientation on looking right through the crystal, while the patterns on opposite B and O faces are reversed.

The checker-board pattern is apparently the only one which has as yet received attention in the few publications on this subject. Crossley's experiments, using various solutions, cited in the Introduction, appear inconclusive in establishing the form of this pattern, but the general features are clearly indicated in the description of the "hillocks" over the crystal vibrating in transformer oil.

The modes of vibration are rather more complicated than one would expect, and the writers feel that it is rather premature to discuss this subject more fully until further research has been carried out, using crystals of different dimensions, and preferably employing independent methods as a confirmation of these results. Further work along these lines is now in progress.

In conclusion the authors wish to thank Prof. D. C. H. Florance for providing the facilities for carrying out this research, and the New Zealand Institute for a grant towards the cost of the necessary apparatus.

Victoria University College,
Dec. 1928.

XX. *Notes on Surface-Tension. By* ALFRED W. PORTER, *D.Sc., F.R.S., F.Inst.P., Emeritus Professor of Physics in the University of London* *.

IV. *The Mechanics of Drops Pendant from Cylindrical Tubes.*

IN Note II. (Phil. Mag. vii. p. 624, 1929) the method of dimensions was applied briefly to drops from cylindrical tubes. In the present note an examination will be made of the mechanics of a sustained drop for such a tube.

In practice it may be convenient to feed fresh fluid into the drop in such a way that there is no free surface in the fluid into the tube. If this is done the pressure cannot be observed directly. It is best in a theoretical inquiry to imagine it fed in through a capillary dipping into the tube but letting the free surface be observed. It will be assumed that the liquid wets the tube and that its angle of contact is zero.

The drop can be observed as it grows. Casual observation shows that two cases can arise. When the drop begins to grow it makes contact with the end face of the tube The outside edge is, of course, never a mathematical line, but is more or less rounded off, even in the case of a carefully ground "tip." The result is that the angle that the liquid makes with the *horizonal* at the point of contact is capable of varying between 0° and 90°. The more vertical the contact the greater the weight that can be sustained, though it must be borne in mind that the actual weight depends not only upon the tension, but also on the curvatures of the liquid surface where it touches. Meanwhile the point P (fig. 1) moves along the curved edge. In the case of a tube of several millimetres radius the drop falls just as it gets round the edge.

When a small tube is used the process does not stop there; but at a certain point—probably when P reaches the outer edge—the liquid *suddenly* leaps up so as to occupy a position such as Q, vibrating briskly before settling down: indicating that it has reached a stable position. With fresh accretion of liquid the point Q moves *downwards* until at last the drop breaks away when the edge is arrived at once more.

* Communicated by the Author.

We will consider this second case first, and assume that the contact is already made at such a point as Q. It will further be assumed, at first, that the tube-wall is infinitely thin. The external forces on the liquid (neglecting $a-r$)

Fig. 1.

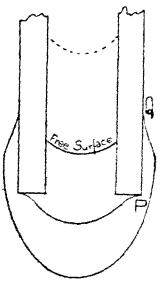

are $2\pi\sigma a$ at BB (fig. 2) and $2\pi\sigma a$ at AA, the atmospheric pressure cutting itself out on the whole. If W is the weight of the liquid below AA, and w that above AA, we have for equilibrium

$$W + w = 4\pi\sigma a.$$

Fig. 2.

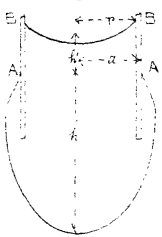

If h' is the "equivalent" height of the column w (*i. e.* the actual height $+\frac{1}{3}$ radius approximately), $w = h'\pi a^2 g\rho$ and

$$W = 4\pi\sigma a - h'\pi a^2 g\rho$$

or

$$\frac{W}{2\pi\sigma a} = 2 - \frac{h'a}{2\beta^2}, \quad \ldots\ldots \quad (1)$$

where $\beta^2=\sigma/g\rho$. Thus a determination of h' (as in Sentis's method) gives a connexion between W and β.

Again considering the level AA, the external forces are $2\pi a\sigma$ and $-\pi a^2\left(\frac{\sigma}{a}-\frac{\sigma}{c}\right)$, where c is the radius of the curvature at A in the plane of the diagram reckoned positive when concave outwards. Therefore

$$W=2\pi a\sigma-\pi a^2\left(\frac{\sigma}{a}-\frac{\sigma}{c}\right)$$

or

$$\frac{W}{\pi\sigma a}=1+\frac{a}{c}. \quad . \quad . \quad . \quad . \quad . \quad . \quad . \quad (2)$$

Hence a determination of c would give W for a liquid of known surface-tension.

No one of the approximate equations that have been given to the contour of a surface enables us to determine the value of c corresponding to a given value of a. Even Rayleigh's final equation (see Note I.) *, when the signs are adjusted to suit the case of the denser fluid being on the concave side, gives a contour asymptotic to the axis instead of to the outside of the tube. In order to obtain information in regard to contours which rigorously satisfy the differential equation, it is necessary to resort to a graphical method. Such a method was proposed by Lord Kelvin and placed in the hands of John Perry in 1874, and described before the Royal Institution, January 29th, 1886, together with diagrams drawn by Perry; reproductions of these drawings were first published in 'Nature' for 1886 (see also Kelvin, Popular Lectures and Addresses, vol. i.).

The method depends on the equation :

$$\frac{d\sin\theta}{dx}+\frac{\sin\theta}{x}=\frac{1}{a}-\frac{1}{c}+\frac{y}{\beta^2}$$

which expresses the fact that the total curvature increases at a uniform rate with increase in depth y. The curvature in the plane of the diagram is initially $\frac{1}{c}$; the curvature in the rectangular plane starts with the value $\frac{1}{a}$ and is at each point the reciprocal of the distance to the axis along the normal to the curve. Starting with the value $\frac{1}{c}$, a short

* *Loc. cit.*

length of the curve is drawn as a circular arc ; the normal distance of its end point from the axis is measured and also y ; whence the new value of c can be calculated and a further short length of the contour is drawn and so on.

In practice, in order to obtain diagrams holding for any value of β it is best to employ the reduced coordinates introduced by Bashforth and Adams. Each length is divided by B and taken as a new coordinate ; whence, representing those with a suffix r

$$\frac{d \sin \theta}{dx_r} + \frac{\sin \theta}{x_r} = \frac{1}{a_r} - \frac{1}{c_r} + y_r. \quad . \quad . \quad . \quad (3)$$

The suffixes can all be dropped until the end of the inquiry, when the lengths in the diagram can be transformed in the requisite ratio to suit any particular value of β.

By this graphical method the accompanying diagrams (fig. 3) have been constructed. They are for values of $a_r = 1,\ 0{\cdot}5,\ 0{\cdot}2,\ 0{\cdot}1,\ 0{\cdot}05$. In each case an initial value of c was assumed and the construction carried out from the top downwards*. The most characteristic (and unsuspected) result obtained was that unless a particular value of c, for a given a, happened to be selected, the contour refused to approach the axis normally at the bottom. If too small a value was selected, the curve turned upwards as the axis was approached, as in the dotted curve H ; if too large a value, it turned downwards, as in the dotted curve G, and then away from the axis. Hence the remarkable conclusion :— *In the assumed conditions and for a given outside radius of the tube one and one only initial curvature corresponds to a pendant-drop of a definite fluid in equilibrium.*

And in consequence : In the assumed conditions for a given material, one and only one weight of pendant-drop can be in equilibrium near the end of a tube of given outside radius of curvature, namely such that

$$\frac{W}{\pi \sigma a} = 1 + \frac{a}{c}, \quad . \quad . \quad . \quad . \quad . \quad . \quad . \quad (4)$$

where c is the unique value corresponding to a.

The foregoing account all refers to the case for which the tube has an infinitely thin wall. The solution obtained is correspondingly ideal. The assertion that there is one and only one weight of drop sustainable is so contrary to experimental experience (in which we examine a pendant-drop

* The reverse sense would have been much more convenient, but the construction then becomes "unstable"—any accidental departure from the correct line leads to still further departures.

Fig. 3.

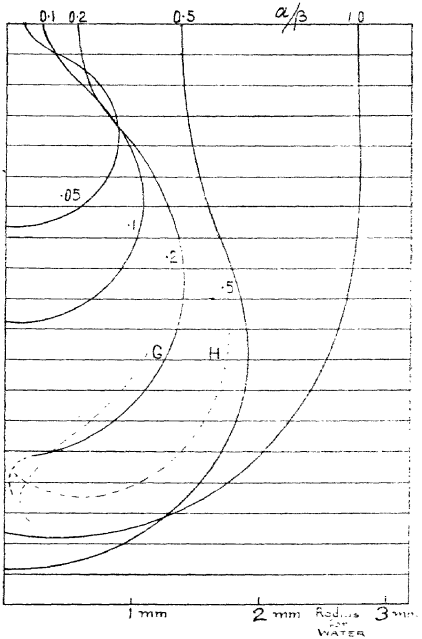

Fig. 4.

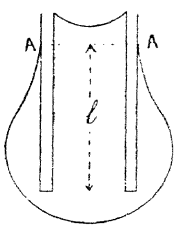

growing as fresh liquid is fed into it) that it is necessary to inquire into the way in which ideality is departed from in practice.

Experience shows that, when the sides of the tube are wetted, the drop extends some small distance along them, as shown in figure 4. In some cases, particularly for small drops, the wall reaches almost to the bottom of the drop. As fresh liquid is fed in, the level AA lowers. The force sustaining the drop is no longer $2\pi a\sigma$ together with the inside force at AA acting downwards, viz., $\pi r^2\left(\frac{\sigma}{a}-\frac{\sigma}{c}\right)$, because there is a downward force in the liquid at the bottom *horizontal* surface of the wall. Moreover, the weight of liquid sustained is no longer $g\rho V$, where V is the volume inside the contour of the drop, but V is less by the volume of wall immersed. If the sustained drop has a weight W',

$$W'=g\rho(V-\pi(a^2-r^2)l)$$

$$=2\pi a\sigma-\pi r^2\sigma\left(\frac{1}{a}-\frac{1}{c}\right)-\left(\sigma\left(\frac{1}{a}-\frac{1}{c}\right)+g\rho l\right)(\pi a^2-\pi r^2)$$

$$=\pi a\sigma\left(1+\frac{a}{c}-\frac{l}{\beta^2}\frac{a^2-r^2}{a}\right).$$

As fresh water is added the length l diminishes and the *greatest* weight sustainable is

$$W'=\pi a\sigma\left(1+\frac{a}{c}\right);$$

that is, it is the unique value sustainable for the given radius of curvature c corresponding to a in the case of an infinitely thin-walled tube.

These statements appear to be exact; but, of course, they must not be applied to the *fallen* drop because of uncertainty as to the exact position at which the drop nips off. In the case of a narrow tube this appears to be very close to the end of the tube; for a wide tube, however, it appears to be lower down, and there is a considerable remnant left behind when the fall occurs. It seems probable that this "remnant" consists in parts of fresh liquid which has moved downwards out of the tube during the process of rupture.

The non-dimensional term $W/(a\sigma)$ is the one considered by Rayleigh (see Note II., *loc. cit.*).

For fallen drops, its value for different reduced radii of tube (a/β) was determined by Rayleigh and extended values have been obtained by Harkins and Brown (J. Am. Ch.

Soc. xli. p. 499, 1919). It is interesting to compare these values with the corresponding values determined from equation (4), in which the values of c are obtained by the graphical method. In reality the graphical method can only give exact values with immense labour because the selection of values of c is made by trial and error ; each trial involves the construction of a complete curve. Only approximate values have yet been determined ; the direction in which they require correction is indicated by a + or − The accompanying table shows the results for the Rayleigh number divided by 2π.

Rayleigh number/2π.

$\frac{a}{\beta}$.	Static drop.	Fallen drop. H and B.
·025*	·92−*	·924
·05	·85−	—
·10	·78−	·805
·20	·745+	·741
·50	·65	·652
1·00	·58−	·599

* Not shown on fig. 3.

It is not suggested that the static values compete in accuracy with those for the fallen drop. The table is given as indicating for the first time the basis for an interpretation of these numbers. The link between the two sets must be concerned with the precise mode in which instability sets in and the changes of contour which ensue.

87 Parliament Hill Mansions, N.W. 5.
May 23, 1929.

XXI. *Simple Examples of Adiabatic Invariance.*

By W. B. Morton, *M.A., Queen's University, Belfast* †.

THE principle of adiabatic invariance of periodic systems plays an important part in the modern dynamics of the atom. In its simplest form, as applied to systems with one degree of freedom, it states that the action through a period remains the same when secular changes take place in the physical characteristics of the system. The meaning of

† Communicated by the Author.

this statement is easily understood, but the general proof of the theorem involves dynamical reasoning of a somewhat difficult kind. Under these circumstances there may be some advantage in multiplying illustrations of the theory which can be investigated by elementary methods. The classical example, and the only one treated in the accounts which I have read, is the small oscillation of a simple pendulum which is slowly pulled up through its point of support. This was the subject of a question put by Planck and answered by Einstein at the Solvay Conference in 1911. In the present note three cases are treated :—

(1) A simple pendulum swinging through an arc of any extent, and passing into complete revolutions. The bob is supposed to be constrained to move on the circle, so that in cases in which the string would become slack it is replaced by a weightless rod. Alternatively the particle may be supposed to move in a smooth circular tube, or as a bead on a wire, the tube or wire contracting slowly.

(2) A simple oscillator.

(3) A particle describing a planetary orbit.

In each case the slow changes are taken to affect all the magnitudes which enter as constants in the problem. The mass of the particle may be supposed to acquire additions by moving through a dusty or saturated atmosphere, and slow changes to take place in the values of gravity, the stiffness of the spring, and the strength of the centre of force.

(1) *Simple Pendulum.*

Let the thread, of length l, receive a small change of length δl when the inclination to the vertical is θ. The work done upon the system is

$$-\mathrm{T}\delta l = -(mg\cos\theta + mv^2/l)\delta l.$$

The first term is equal to the increase of the potential energy of the bob which is raised vertically through $-\delta l\cos\theta$, so the second term represents the addition to the kinetic energy, or

$$\delta(\tfrac{1}{2}mv^2) = -mv^2 \,.\, \delta l/l,$$

$$\delta v/v = -\delta l/l.$$

Next suppose that, in the same position, the bob picks up a small particle δm, previously at rest. Conservation of momentum gives

$$\delta(mv)=0, \quad \delta v/v=-\delta m/m.$$

Combining the two effects, we have

$$\delta v/v=-\delta l/l-\delta m/m.$$

Let h be the height of the level of no velocity above the lowest position of the bob. The motion is expressed by means of elliptic functions with $k^2=h/2l$ when the pendulum is oscillating, and $k^2=2l/h$ when it is making complete revolutions.

In order to include both types of motion we may use $h/2l$, instead of the angular amplitude of the oscillations, to characterize the extent of the motion In the critical case $h=2l$, although the period is infinite, the action is finite, and its value for the half-period of the oscillations passes continuously into that for the complete period of the rotations.

The connexion between θ and the time is given by the equation

$$\sin\tfrac{1}{2}\theta=k\,\mathrm{sn}\,nt$$

for oscillations, and

$$\sin\tfrac{1}{2}\theta=\mathrm{sn}\,(nt/k)$$

for revolutions, where $n=\sqrt{(g/l)}$. The half-period of the oscillations is $2\mathrm{K}/n$ and the whole period of the revolutions $2k\mathrm{K}/n$.

Taking first the oscillatory motion, we have

$$\begin{aligned} v^2&=2g(h-l+l\cos\theta)\\ &=4gl(k^2-\sin^2\tfrac{1}{2}\theta)\\ &=4glk^2\,\mathrm{cn}^2\,nt. \end{aligned}$$

The action taken through a half-period is

$$\int mv^2dt=8mgllk^2\int_0^{\mathrm{K}/n}\mathrm{cn}^2\,nt\,dt=8mg^{\frac{1}{2}}l^{\frac{3}{2}}(\mathrm{E}-k'^2\mathrm{K}).$$

If small changes in g and l are effected at position θ, we have

$$\begin{aligned} 2\delta v/v&=\delta g/g+\delta l/l+2k\,\delta k/(k^2-\sin^2\tfrac{1}{2}\theta)\\ &=\delta g/g+\delta l/l+8gl\,k\,\delta k/v^2. \end{aligned}$$

When the former expression for $\delta v/v$ is combined with this, we have

$$\delta m/m+\delta g/2g+3\delta l/2l+4gl\,k\,\delta k/v^2=0.$$

Now suppose the changes to be brought about so gradually that an increment, such as δl, which is a small fraction of the whole l, is spread over a large number of oscillations. We must then, before integrating the last equation, replace v^2 in its last term by the time-average. The expression for this is got at once from the action already obtained on removing the mass factor and dividing by the time; this gives

$$4gl(\mathrm{E}-k'^2\mathrm{K})/\mathrm{K}.$$

The last term becomes

$$k\,\mathrm{K}\,\delta k/(\mathrm{E}-k'^2\mathrm{K});$$

but

$$\frac{d}{dk}(\mathrm{E}-k'^2\mathrm{K})=k\mathrm{K}.$$

The last term, like the others, is thus a logarithmic differential, and the integral of the equation is

$$mg^{\frac{1}{2}}l^{\frac{3}{2}}(\mathrm{E}-k'^2\mathrm{K})=\text{const.},$$

or the action remains unchanged throughout the slow process of change in length, mass, and gravity.

For small oscillations $k=\frac{1}{4}\alpha^2$, where α is the amplitude,

$$\mathrm{K}=\tfrac{1}{2}\pi\left(1+\frac{1}{16}\alpha^2\right),$$

$$\mathrm{E}=\tfrac{1}{2}\pi\left(1-\frac{1}{16}\alpha^2\right),$$

$$\mathrm{E}-k'^2\,\mathrm{K}=\frac{1}{16}\pi\alpha^2.$$

The result is that $m^2gl^3\alpha^4=\text{const.}$ in adiabatic change.

When the pendulum is describing complete circles, we have

$$v^2=4gl(k^{-2}-\sin^2\tfrac{1}{2}\theta)$$
$$=4gl\,k^{-2}\,\mathrm{dn}^2(nt/k).$$

The action through a complete revolution is

$$8mg^{\frac{1}{2}}l^{\frac{3}{2}}\mathrm{E}/k;$$

the average value of v^2 is $4gl\mathrm{E}/k^2\mathrm{K}$.

$$2\delta v/v=\delta g/g+\delta l/l-2\delta k/k(1-k^2\sin^2\tfrac{1}{2}\theta)$$
$$=\delta g/g+\delta l/l-8gl\,\delta k/k^3v^2.$$
$$\delta m/m+\delta g/2g+3\delta l/2l-4gl\,\delta k/k^3v^2=0.$$

When the average value is substituted in the last term this has the form

$$-\mathrm{K}\delta k/k\mathrm{E}.$$

Now $$\frac{d}{dk}(\mathrm{E}/k)=-\mathrm{K}/k^2,$$

so $$-\mathrm{K}\delta k/k\mathrm{E}=\delta\log(\mathrm{E}/k).$$

The integral again expresses the invariance of the action.

In the earlier statements of quantum theory the constancy was ascribed to the energy of an oscillator divided by its

Fig. 1.

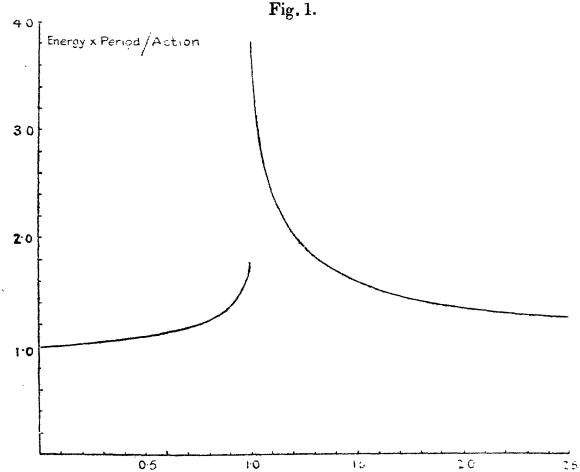

frequency, or energy multiplied by period. For a pendulum this is equivalent to constancy of the phase-integral only in the limit of small oscillations. In general, the magnitude, energy × period, bears to the action through the period the ratio

$$k^2\mathrm{K}/2(\mathrm{E}-k'^2\mathrm{K}),$$

which increases from unity to a logarithmic infinity with increasing amplitude, as shown on fig. 1. In complete revolutions it again approaches unity as the rate is increased.

The connexion between the amplitude and the length of a gradually shortening pendulum is shown on fig. 2, along with a continuation for the motion in complete circles. The

abscissa for both parts is the height of the level of no velocity above the lowest point expressed in terms of the diameter of the circle. Thus the first part is the graph of $(E-k'^2K)^{-\frac{1}{2}}$ against k^2, and the second that of $(E/k)^{-\frac{1}{2}}$ against $1/k^2$. Values of the amplitude $\alpha=\cos^{-1}(1-2k^2)$ are marked for the oscillatory portion. The vertical scale is such that unity is the length of the pendulum which just makes complete revolutions. A gap is left at the point corresponding to this length, where the curves should join, because both curves turn round rapidly to a vertical tangent close to this point, the tangent of the slope approaching infinity in a

Fig. 2.

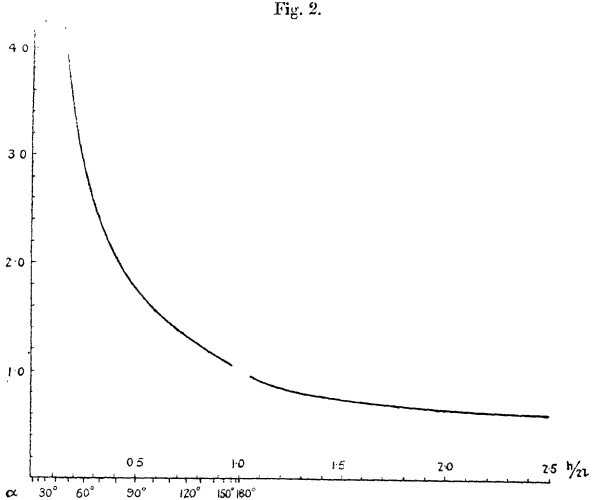

logarithmic manner. The left-hand curve has an inflexion in the neighbourhood of $\frac{1}{2}\alpha=75°$, $k^2=\cdot933$.

It is interesting to compare with the above theory the course of events when the small changes in length are always effected at the same angular position of the pendulum. We have, then, to integrate

$$\delta m/m+\delta g/2g+3\delta l/2l+k\delta k/(k^2-\sin^2\tfrac{1}{2}\theta)=0,$$

treating θ as a constant, which gives

$$m^2gl^3(k^2-\sin^2\tfrac{1}{2}\theta)=\text{const.}$$

or

$$m^2gl^3(\cos\theta-\cos\alpha)=\text{const.}$$

Thus a continual shortening applied at the end of the swing has no effect on the angular amplitude of the motion, while the most rapid increase is produced when the small pulls are made at the central position. General ideas regarding resonance would lead us to expect that in general the timed impulses would be more effective than those evenly distributed in the adiabatic mode. This is illustrated in fig. 3, in which is showed the connexion between length and angular amplitude for a pendulum which originally swings to 10° on each side. The upper curve gives the result when

Fig. 3.

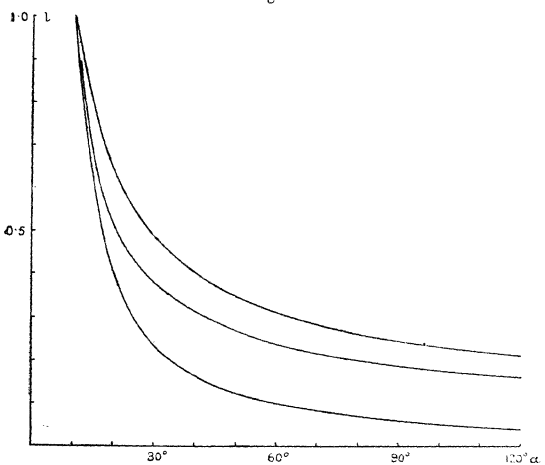

the impulses are applied at $\theta=0$, the middle one that for $\theta=7\frac{1}{2}°$, and the lowest for the adiabatic change.

Since the effect vanishes when θ is the amplitude, there must be some point near the end of the swing where the timed impulses are comparable in effect to the irregular ones. We may arbitrarily define the two cases as equivalent when the critical motion, of complete revolutions with zero velocity at the highest point, is reached with the same length of pendulum in both cases. This gives

$$\cos\theta=\{\cos\alpha+(\mathrm{E}-k'^2\mathrm{K})^2\}/\{1-(\mathrm{E}-k'^2\mathrm{K})^2\}.$$

This is shown on fig. 4, where θ is plotted against the angular amplitude α. The distance of the curve below the straight line shows how far from the end of the swing the timed impulses must be applied in order to be equivalent to the irregular. Incidentally this graph affords an extreme example of the slowness of approach to a logarithmic infinity. It is difficult to believe that when $\alpha=180^\circ$ is reached the curve runs up to the terminal point of the straight line.

Fig. 4.

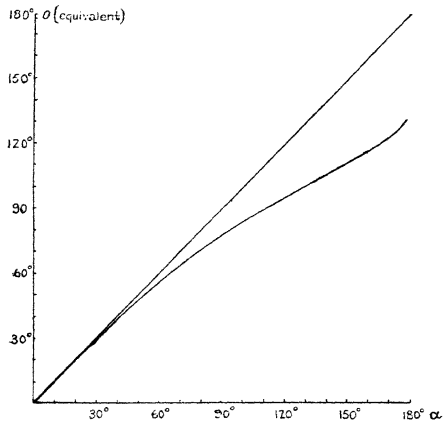

(2) *Simple Harmonic Oscillator.*

If the mass of the oscillating particle is m and the stiffness of the spring is k, so that the equation of motion is

$$m\ddot{x}+kx=0,$$

then the velocity is given by

$$v^2=k(a^2-x^2)/m,$$

where a is the amplitude.

If, at a given position x, the mass and spring and velocity are slightly changed, the resultant change of amplitude is given by

$$2a\,\delta a/(a^2-x^2)=2\delta v/v+\delta m/m-\delta k/k.$$

If the alteration in v is due to the picking up of a small mass δm, we have

$$\delta v/v = -\delta m/m.$$

The relation then becomes

$$2\delta a/(a^2-x^2)+\delta m/m+\delta k/k=0.$$

When the alterations of mass and stiffness are always made at the same position of the particle, this leads to

$$mk(a^2-x^2)=\text{const.};$$

but when they are distributed in a random manner through a long time, the time-average of (a^2-x^2) being $\frac{1}{2}a^2$, we have

$$mka^4=\text{const.}$$

In agreement with this the action through the period

$$2\pi\sqrt{(m/k)}$$

is $$\int mv^2dt=\int ka^2\cos^2(t\sqrt{k/m})dt=\pi\sqrt{(mk)}\,.\,a^2.$$

(3) *Planetary Orbit.*

The same analysis can be applied to the modification of a planetary orbit under slow accretion of mass and a gradual change in the strength of the centre of force. We have

$$v^2=\mu(2/r-1/a),$$

so $$\delta a/a^2=v^2(2\delta v/v-\delta\mu/\mu)/\mu=-(v^2/\mu)(2\delta m/m+\delta\mu/\mu).$$

It is easy to show that $\int r^{-1}dt$ round the orbit has the value $2\pi\sqrt{(a/\mu)}$, from which it follows that the action is $2\pi m\sqrt{(\mu a)}$, and that the average value of v^2 is μ/a. When this is inserted, the differential equation becomes

$$\delta a/a+\delta\mu/\mu+2\delta m/m=0,$$

expressing the adiabatic invariance.

This is a case of two degrees of freedom, and the theory requires the invariance of the two separate phase-integrals

$$\int m\dot{r}\,dr \quad\text{and}\quad \int mr^2\dot{\theta}\,d\theta,$$

which together make up the action. It is obvious that the alterations of μ and m do not affect the angular momentum round the centre, and so the θ-integral is unchanged; the invariance of the r-integral follows.

XXII. *Significance of X-Ray Analysis of Alkali Sulphates.* *By* A. E. H. Tutton, *M.A., D.Sc., F.R.S.**

THE X-ray analysis of the orthorhombic normal sulphates of potassium, rubidium, cæsium, and ammonium has proved to be of special interest from several points of view. It was first undertaken—in response to a request made to Sir William Bragg, early in the year 1916, when the value of the X-ray spectrometric method had proved itself—by Messrs. (now Professors) A. Ogg and F. Lloyd Hopwood †, then working in Sir William Bragg's laboratory. They used some of the same crystals as had been employed by the author in the detailed crystallographic and physical investigations of these salts.

So long ago as the year 1894 ‡ the relative dimensions and volumes of the unit cells of the space-lattices of the three alkali metallic salts had been determined by combining the crystal axial ratios with the densities of the crystals; and similar constants for ammonium sulphate were added in 1903 §. These strictly relative and truly comparable spatial constants, since known as "topic axial ratios," are rigidly valid when the crystalline substances compared are, as in the group in question, isomorphous in the strict sense known as "eutropic," the individual members of the series only differing by containing different elements of the same family group and type of series (odd or even) of the periodic classification, the system and class of symmetry and the structural space-group being identical. The actual values of these constants are given in the following table, χ, ψ, and ω representing the relative lengths of the edges of the rectangular unit cell of the orthorhombic space-lattice (No. 10 of Bravais), and V the relative volumes of the cells (the molecular volumes M/d). Two sets of the constants are given, the first set being the direct results of the use of the formulæ (given below) for the relative edge-lengths of the orthorhombic (rectangular) cell, a, b, and c being the crystal axial ratios.

$$\chi = \sqrt[3]{\frac{a^2 V}{c}}, \qquad \psi = \sqrt[3]{\frac{V}{ac}}, \qquad \omega = \sqrt[3]{\frac{c^2 V}{a}}.$$

* Communicated by the Author.
† Phil. Mag. xxxii. p. 518 (1916).
‡ Journ. Chem. Soc. lxv. p. 660 (1894).
§ *Idem*, lxxxiii. p. 1067 (1903).

Molecular Volumes and Topic Axial Ratios (Tutton).

Salt.	Mol. vol.	Direct results of formulæ.			ψ for $K_2SO_4=1$.		
		χ.	ψ.	ω.	χ.	ψ.	ω.
K_2SO_4.....	64·91	3·0617 : 5·3460 : 3·9657			0·5727 : 1·0000 : 0·7418		
Rb_2SO_4	73·34	3·1778 : 5·5528 : 4·1562			0·5944 : 1·0387 : 0·7774		
$(NH_4)_2SO_4$ ...	74·04	3·1788 : 5·6413 : 4·1289			0·5946 : 1·0552 : 0·7723		
Cs_2SO_4	84·58	3·3215 : 5·8149 : 4·3792			0·6213 : 1·0877 : 0·8191		

Absolute Dimensions of Space-lattice Cell (Ogg and Hopwood).

Salt.	Length of sides of unit cell in Å. U. (10^{-8} cm.).			Volume of unit cell.
K_2SO_4.....	5·731	10·008	7·424	$425·78\times10^{-24}$ c c.
Rb_2SO_4	5·949	10·394	7·780	$481·14\times10^{-24}$ „
$(NH_4)_2SO_4$	5·951	10·360	7·729	$485·71\times10^{-24}$ „
Cs_2SO_4	6·218	10·884	8·198	$554·88\times10^{-24}$ „

The second set is a simplified one, obtained from the first by dividing throughout by the value of ψ for potassium sulphate, and of course the numbers have precisely the same relations. Below these in the table are given the absolute dimensions and volumes of the unit cells, as determined in 1916 (*loc. cit.*) by Ogg and Hopwood as the result of their X-ray analysis, and confirmed and repeated by Prof. Ogg in his recent (1928) paper * in the Philosophical Magazine, describing further work in the Physics Department of the University of Cape Town. In this later memoir Prof. Ogg confirms the fact that the structure is based on a simple orthorhombic space-lattice, the rectangular one (No. 10), with four molecules of $R_2'SO_4$ to the cell, and decides that the space-group is V_h^{16}. The positions of the metallic atoms have been located, as also those of the tetrahedral SO_4 groups (the S atom at the centre of the tetrahedron and the four oxygen atoms at the corners in each case, as shown for other sulphates by Bradley, James and Wood, and Wasastjerna) in the cases of the sulphates of potassium, rubidium, and cæsium. The NH_4 groups in the case of ammonium sulphate are also shown to be tetrahedral, with the N atom at the centre of the tetrahedron and the four hydrogen atoms at the corners, the whole group NH_4 replacing the alkali metal.

* Phil. Mag. [7] v. p. 354 (1928).

Now, it is very satisfactory, and of great importance, that these facts have been independently confirmed by W. Taylor and T. Boyer, working in Prof. W. L. Bragg's laboratory at the University of Manchester, in a memoir * giving the results of an exhaustive X-ray analysis of cæsium and ammonium sulphates. They also find the space-group to be V_h^{16}, the space-lattice to be the orthorhombic (rectangular) one, and the cell to contain four molecules; and they indicate a similar allocation of metallic atoms or NH_4 groups, and of the SO_4 groups. They have redetermined the cell dimensions, and give them as under :—

Salt.	Length of sides of unit cell in Å.U.			Differences from Ogg and Hopwood.		
	a.	*b.*	*c.*	*a.*	*b.*	*c.*
Cs_2SO_4.....	6·24	10·92	8·22	0·02	0·04	0·02
$NH_4)_2SO_4$	5·98	10·62	7·78	0·03	0·06	0·05

The agreement between the results of these two independent investigations is thus very satisfactory, the maximum difference being only half a *per cent.*

Two further memoirs on the structure of the sulphates of potassium, rubidium, and cæsium by F. P. Goeder †, of the University of Chicago, were published in 1927 and 1928, giving some results obtained by the Laue spot-method. The same conclusion is arrived at that a rectangular orthorhombic space-lattice with four molecules to the unit cell is the basis of the structure, but the space-group is said to be V_h^{13}, while agreeing that the SO_4 group is tetrahedral, with the sulphur atom at the centre of the tetrahedron. No such detailed study by the X-ray spectrometer of the reflected spectra and their intensities, nor the use of the other available methods of investigation by X-rays, such as were carried out by Prof. Ogg and by Messrs. Taylor and Boyer, appear to have been made, so that the balance of evidence is so far in favour of the space-group V_h^{16}. Moreover, both Prof. Ogg and Messrs. Taylor and Boyer have made use of the results of Hartree ‡, and of those of James and Wood §, for the scattering functions of potassium and sulphur, in arriving at their conclusions.

* Mem. and Proc. Manchester Lit. and Phil. Soc. lxxii. p. 125 (1928).

† Proc. Nat. Acad. of Sci. of the U.S. America, xiii. p. 793 (1927) and xiv. p. 766 (1928).

‡ Phil. Mag. i. p. 289 (1925).

§ Proc. Roy. Soc. cxix. p. 598 (1925).

Two main facts which have been clearly proved by the detailed crystallographic and physical investigations of these anhydrous normal rhombic sulphates of the alkalies, and their selenate analogues, as well as of the monoclinic double sulphates and selenates with $6H_2O$, in which these salts are combined with one or other of eight dyad-acting metals (Mg, Zn, Fe, Ni, Co, Mn, Cu, or Cd), are clinched by these structure results of X-ray analysis. (1) There is a progression (increase) in the edge-dimensions and volumes of the unit cells of the space-lattice as one alkali metal of higher atomic weight or atomic number replaces the one below it in order, the rubidium salt in every case standing intermediate in regard to these structural constants, between the potassium and cæsium salts, usually somewhat nearer to the former, the progression being an accelerating one. (2) The crystals of the ammonium salt are very closely isostructural with those of the rubidium salt, the volumes and cell-edge dimensions being almost identical. That is, the ammonium group NH_4 replaces the alkali metallic atom so well that in the case of the middle member of the series of salts, the rubidium salt, the cell dimensions are scarcely changed at all. It is somewhat remarkable that this should be so, the ammonium salt not being entropically but only generally isomorphous with the metallic salts. It is obvious that the tetrahedral NH_4 group goes into the same space as a rubidium atom. That this is so Prof. Ogg now shows very clearly in his two models, illustrated in his 1928 memoir on plates v. and vi.

It was this fact of the isostructure of the ammonium and rubidium salts which had proved a stumbling block to the acceptance of the celebrated Valency Volume Theory of Crystal Structure, on the basis of which the ammonium salt cell should be twice as large as the rubidium one, the valency volumes of Rb_2SO_4 and $(NH_4)_2SO_4$ being 12 and 24. From quite other considerations, especially the ready formation of mixed crystals, it was not likely that the scale on which the metallic and ammonium salts were constructed was different, and consequently that the crystals were not strictly comparable, topic axial ratios being only valid for similar structures; but in any case the crucial test afforded by the new X-ray method, which gave us the absolute and not merely the relative cell dimensions, was of the greatest importance as being decisive on this point. The decision which it gave has, however, been so clear and unambiguous that there can be no doubt left that the structures are exactly analogous, and that the absolute as well as the

relative cell dimensions and volumes of the ammonium and rubidium salts are really practically identical.

But size of atom does come into the question, yet is not determined by the valency electrons chemically active outside the last complete shell of electrons, but by the size of that completed shell, which in turn depends on how many shells of electrons the atoms of that element possess. In the case of the alkali metals the outermost complete shell is that of the inert element of the argon group which immediately precedes it in the periodic table, namely, argon (atomic number 18) in the case of potassium (atomic number 19), krypton (36) in the case of rubidium (37), and xenon (54) in the case of cæsium (55). Now, krypton has either one or two (according to the particular version of the atomic structure theory we adopt) more shells of electrons than argon, and again xenon possesses one or two more than krypton, so that one or two complete shells are added each time we pass from potassium to rubidium and from the latter to cæsium, an addition in each case of 18 electrons. This progressive enlargement of the atom, with all its necessary consequences as regards chemical (particularly electro-positive) and physical properties, offers at once an explanation of the progressive increase in the cell dimensions of the crystal space-lattices of the salts of these alkali metals. Moreover, it is noteworthy that all the investigators who have been attempting to determine the sizes of the chemical atoms unite in showing that in a family group such as that of the alkali metals, and in compounds which are truly analogous in structure such as these sulphates and selenates, the atomic size is certainly progressive with the atomic number. This is true whether, for instance, we consider the atomic diameters for the alkali metals given by W. L. Bragg (and either his original or his modified ones), by Niggli in numerous recent memoirs, or most recently of all by V. M. Goldschmidt *, the atom (or "ion" if that term be preferred) of rubidium being invariably found to be of intermediate size and electropositive character as compared with the smaller atoms of potassium or the larger ones of cæsium, the most electropositive of all the elements.

It has also to be remembered that this property of the size of the structural unit cells is only one among many crystal properties, although one which has become very prominent owing to the new field of work opened up by the use of X-rays. The crystal angles, the refractive indices,

* *Ber. der deutsch. chem. Ges.* Jahrg. 60, Heft 5, p. 1263 (1997) and later papers.

the optic axial angles, the dimensions of the optical ellipsoid, and even its position when variable (in the monoclinic series), the thermal expansion, and in fact every detail of the physical properties of the crystals which have been studied, have all been shown to be progressive with the atomic number of the alkali metal. Moreover, this is not alone true for these rhombic sulphates and selenates, and for the monoclinic double salts which they form with the salts of the dyad-acting metals; it is true for all other series of compounds for which the structure has been proved to be strictly analogous and comparable throughout the series. The rhombic perchlorates of the alkalies are pre-eminently such a series, the crystal morphology of which has been determined by Barker *, and the physical properties of the crystals still more recently † by the author; and a similar progression of all properties and constants in the eutropic potassium, rubidium, and cæsium salts, and isostructure of the rubidium and ammonium salts, have been observed exactly as in the cases of the sulphates and selenates. A series of double chromates of the alkalies with magnesium chromate has likewise been studied in collaboration with Miss Mary Porter ‡, and Miss Porter has since § also investigated a series of ditartrates of the alkali metals, with analogous results in all cases.

Hence the fact is fully substantiated that whenever an unbroken strictly structurally comparable series of eutropically isomorphous compounds is investigated, the whole of the morphological and physical properties of their crystals are found to be functions of the atomic numbers and atomic weights of the interchangeable family-group elements which give rise to the series.

It was formerly supposed to throw doubt on this law that the alkali halides did not conform to it. But the advent of X-ray analysis has given a clear explanation of this fact by showing that the type of structure suddenly changes between rubidium and cæsium chlorides (or bromides or iodides). For whereas potassium and rubidium chloride possess the rock-salt structure, that of the centred-face cube, with four molecules of the salt to the unit cell, cæsium chloride possesses the structure of the centred cube, with only a single molecule to the cell. The discovery of this fact affords, indeed, only a further confirmation of the law, for

* *Zeitschr. für Kryst.* xliii. p. 529 (1907), and xlv. p. 17 (1908).
† Proc. Roy. Soc. A, cxi. p. 462 (1926).
‡ Min. Mag. xvi. p. 169 (1912).
§ *Zeitschr. für Kryst.* lxviii. p. 531 (1928).

this series of alkali halides is an exception because it is not structurally analogous throughout.

This beautiful law of progression with the atomic number of the interchangeable elements in a truly structurally analogous series of isomorphous substances, due fundamentally to the progressive change in atomic structure on the part of the interchangeable elements, receives also remarkable confirmation as regards crystal angles in the case of the hexagonal ethyl sulphates of the rare earths studied by F. M. Jaeger *, $R_2'''(SO_4 . C_2H_5)_6 . 18H_2O$, in which R''' may be any one of the rare-earth elements; for the angular differences between twelve of these salts proved to be so small as to lie within the limits of experimental error (a very few minutes), and the ratio of the axes $c : a$ was found to be identical within $\pm$ 0·0012. The reason is that in this remarkable group of rare-earth elements additions of electrons, as we proceed along the list of elements in order of atomic number, are not made as usual, to the outer shell, but to the interior of the atomic structure, causing the remarkable similarity of so many of the compounds of these elements, and the very great labour entailed in separating them from their natural ores and from each other.

Finally, it may with confidence be stated that this law of progression of the crystallographic properties with atomic number, in a eutropic isomorphous series, forms the ultimate proof of the law of Haüy, so long a matter of controversy, that to every definite chemical substance crystallizing in any but the cubic system of symmetry (in which the high symmetry itself fixes the invariable angles) there appertains a particular crystalline form (or forms, if polymorphous), peculiar to and characteristic of the substance. For even in these most closely of all related substances the crystal constants vary, and do so in accordance with the law of progression according to atomic number.

The full confirmation of the law, which is now afforded by X-ray analysis, is thus a matter for deep satisfaction, showing that the advances made in the last half century in pure crystallography are truly founded and may be received with every confidence.

* *Recueil des trav. chim. des Pays-Bas*, xxxiii. p. 343 (1914).

XXIII. *Linear Adsorption.* *By* R. S. Bradley *.

1. *The Three-phase Line.*

It is only comparatively recently that attention has been directed to an important boundary region, that between two interfaces. The number of molecules concerned, relatively to the number in the surface, is very small. The three-phase line becomes important, however, as a seat of reaction. Thus Volmer † assumes that reaction in the system solid surface-solid surface-gas occurs by adsorption of the gas on the solid surfaces, and by the motion of the adsorbed gas to the reaction line. Such a motion could be observed in the formation of iodine films on mercury. The normal solid reaction is, of course, primarily an interface phenomenon, in that it is concerned primarily with the advance of a reaction wall, and only secondarily with the conditions at the edge of that wall.

We have another experimental edge study in the observation of Estermann ‡ that the critical condensation temperature for a pointed trace of Cd atoms on glass is lower for the point than for the centre of the trace.

Schwab and Pietsch § have formulated equations for adsorption at a line analogous to those holding for the interaction of molecules between phases of three and of two dimensions. They assume a gas equation for the molecules in a line of the same form as for those in a surface. They also obtain the Langmuir adsorption isotherm and the corresponding equation for adsorption at a line by a thermodynamic cycle, involving calculations of ΔA.

In this paper adsorption at a line will be studied from the standpoint of surface thermodynamic activity, an expression for which is derived in section 2. In section 3 this will be applied to study Langmuir's adsorption isotherm. In section 4 a similar process will be used to obtain the adsorption isotherm for a line.

* Communicated by the Author.

† Volmer, *Zeit. Phys. Chem.* cxv. p. 253 (1925); cxix. p. 46 (1926).

‡ Estermann, *Zeit. f. Phys.* xxxiii. p. 320 (1925).

§ Schwab and Pietsch, *Zeit. Phys. Chem.* B. i. p. 385 (1928); B. ii. p. 262 (1929).

2. *The Thermodynamic Surface Activity.*

The free energy F′ per gm. mol. in the surface is $\int A\,dF$, where A is the area per gm. mol., F the two-dimensional pressure. Since

$$F(A-B) = RT,$$

where B is a constant,

$$RT \log a_s = F' - F_0' = RT \log \frac{RT}{A-B} + \frac{BRT}{A-B}$$

$$= RT \log F + BF. \quad . \quad . \quad . \quad (1)$$

Here a_s is the surface activity, and the standard state for F′ is defined by the limits $F' \to F_0'$ when $\frac{A-B}{A} \to 1$, $A \to \frac{RT}{F}$, $a_s \to F$.

H, the heat content per gm. mol., is easily derivable from the equation for a_s,

$$H = F' - T\frac{dF'}{dT}$$

$$= BF - BT\frac{dF}{dT} - RT^2\frac{d \log F}{dT}$$

$$= -RT.$$

3. *The Langmuir Adsorption Isotherm.*

The free energy per gm. mol. of a perfect gas is given by

$$(F' - F_0') \text{ 3-dimensional gas} = RT \log p,$$

where p is the pressure. For a two-dimensional gas we have equation (1). Hence for the partition of molecules between regions of two and of three dimensions,

$$RT \log \frac{RT}{A-B} + \frac{BRT}{A-B} = RT \log p + K_1,$$

where K_1 is the difference between the free energies in the standard states. Hence, writing $S = \frac{1}{A}$, the surface concentration in gm. mols. per cm.^{2},

$$\log p \left(\frac{1-SB}{S}\right) = \frac{SB}{1-SB} + K_2,$$

where K_2 is a constant, equal to $(F_{0_2}' - F_{0_3}')/RT + \log RT$. When $\frac{SB}{1-SB}$ is small compared with K_2, which will in general hold for S small compared with $\frac{1}{B}$, we get the Langmuir isotherm

$$\frac{\text{constant}}{p} = \frac{1}{S} - \text{constant},$$

i. e., the substance then distributes itself between the two regions according to the modified distribution law,

$$\frac{p}{S/1-SB} = \text{constant},$$

where $\frac{S}{1-SB} = S'$ appears as the effective surface concentration.

4. *Adsorption at a Line.*

A similar method may be applied to adsorption at a line. Here

$$RT \log a_l = RT \log RTL' + RTB^{\frac{1}{2}}L',$$

where a_l is the linear activity, L' the effective linear concentration in gm. mols. per cm., given by

$$L' = \frac{L}{1-LB^{\frac{1}{2}}},$$

L being the linear concentration. Hence

$$RT \log \frac{S'}{L'} = RTB^{\frac{1}{2}}L' - RTBS + K_3.$$

This reduces, as before, to the approximate distribution law

$$\frac{L'}{S'} = \text{constant} = e^{\frac{\Delta F_0}{RT}}.$$

ΔF_0 being the increase in free energy for the change line $\rightarrow$ surface in the standard states.

The University, Leeds.
May 1929.

XXIV. *Densitometer Curves of the Green Mercury Line.* *By* R. W. Wood, *Johns Hopkins University* *.

Metcalfe and Venkatesachar (Proc. Roy. Soc. cv. p. 520) found evidences of absorption by feebly-excited mercury vapour of the light of all of the satellites of the green mercury line with the exception of −0·237, which failed to confirm the claim of McLennan, Ainslie, and Miss Cale (Proc. Roy. Soc. cii. p. 33) that none of the satellites was absorbed with the exception of the unresolved ones −·008 and +·008, for which absorption was inferred from the circumstance that it was never possible to obliterate completely the main or central strong component, the unabsorbed edges being assumed to represent the satellites reported by Janicki and Nagaoka.

The observations of all these investigators were made with interference spectroscopes, and the spectra yielded by these instruments can be interpreted only after careful study. When modified by absorption they become still more confused, and in very few cases give any clear picture of the group of lines.

Having recently made densitometer curves with a new Moll registering photometer spectrograms of the green mercury line made some years ago with a large plane grating and a lens of very long focus, it has seemed worth while to put them on record, as I do not remember ever having seen a record of the structure of the line which shows such perfect resolution. These curves are reproduced on the figure in register, one above the other.

The lower curve was made from a photograph taken with the light of a glass Cooper-Hewitt mercury arc which emerged through the side of the tube; the upper was made with the tube "end-on," the light coming out through the negative electrode bulb.

The former gives the true structure of the line, the latter the structure as modified by absorption in the long column of luminous vapour. No trace of the satellite +0·124 appears in the lower photograph on account of its relative faintness. The small irregularities in the base line are due to the grain of the plate of course. In the upper photograph this satellite is well developed, which shows that it is absorbed to a much less degree than satellite +0·128, which

* Communicated by the Author.

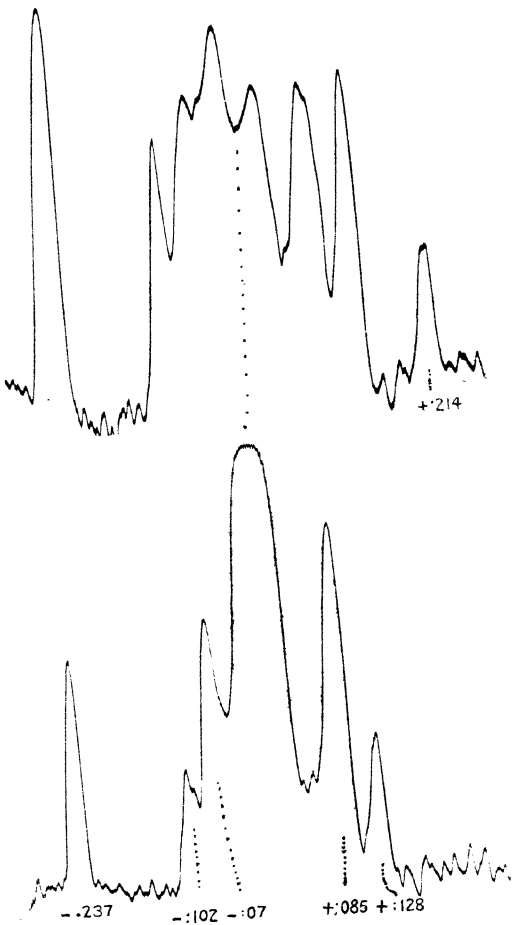
+·214
-·237
-·102
-·07
+·085
+·128

in turn is less absorbed than +0·085, the two latter having practically the same intensity when modified by absorption.

The satellites −0·102 and −0·07 are also very nearly equalized by the absorption, while −0·237 becomes the strongest component of all, which confirms Metcalfe and Venkatesachar's observation that this line was not absorbed at all.

The unsymmetrical reversal of the central or main component appears to be clearly indicated, but it must be remembered that this component is not single.

The photographs were made in the fifth order of a 7-inch plane grating ruled with 15,000 lines to the inch and an achromatic lens of 40-foot focus.

As is well known from the investigations of Nagaoka, recently confirmed most beautifully by Hansen with a Fabry and Perot interferometer and water-cooled arc of special construction (so I am informed), the central component consists of five lines sharp and well resolved.

XXV. *Spectra of High-frequency Discharge in O_2 and CO.*

By R. W. Wood, *Johns Hopkins University* *.

[Plate VI.]

A BRIEF account of some preliminary experiments, made in collaboration with A. L. Loomis, on high-frequency discharges in very highly exhausted tubes was published in 'Nature' in 1926. The tubes were exhausted at a high temperature with a molecular pump, until they were in the condition usually described as non-conducting, sealed from the pump, and excited through external electrodes by an oscillator giving a 3-metre wave.

References to earlier work in which this type of excitation had been employed were given in this note. The peculiar ruby-red fluorescence of the glass, which was observed by one of us many years ago during experiments with very long hydrogen tubes, when the hydrogen was replaced by oxygen, was found in the case of these high-frequency discharges, which showed the peculiar green colour characteristic of oxygen. This red fluorescence appeared in soft-glass, pyrex, and fused quartz tubes, and appeared to be due to the impact of cathode rays (*i.e.* electrons) in the presence of

* Communicated by the Author.

oxygen, as the fluorescent patches could be moved from one place to another by the approach of a magnet. The discharge is characterized by the appearance of luminous masses shaped like stream-lined bodies, *i. e.* with a blunt cone in front and tapering to a long pointed tail.

I have recently taken up the matter again, and find that the red fluorescence does not appear until the glass has been acted upon for some time by the discharge.

When the current is first applied to the tube through a single wire wrapped around it with one turn only, the discharge is bluish and exhibits the secondary spectrum of hydrogen. This is replaced in a few minutes by the greenish-yellow discharge of oxygen, and the spectroscope shows the four strong negative bands in the green-red region which are characteristic of the gas. The oxygen is evidently derived from the decomposition of SiO_2, as it appears in quartz tubes as well as in glass. After 4 or 5 minutes' operation the walls show a pink fluorescence, which presently becomes ruby-red, the oxygen pressure having risen in the meantime. If, now, the wire loop is moved to the other end of the tube, localizing the discharge in this region, no fluorescence is observed at first, though the pressure of the gas is the same.

A photograph of the discharge is reproduced on Pl. VI. fig. 1. In this case the luminous gas masses were spherical instead of stream-lined. The distribution of luminosity in the tube was very sensitive to the position of the electrode loop: moving it along the tube for a distance of a millimetre or two was sufficient to abolish the spheres, or cause their appearance in different regions.

The most interesting feature, however, and the one which forms the principal subject of this paper was revealed when a spectroscopic examination of the discharge was made. An image of one of the luminous spheres and the region above and below it was formed on the slit of a spectrograph with an achromatic lens, and the resulting spectrogram showed that the spectrum was made up of both lines and bands, the bands appearing enormously enhanced in the spectral images of the sphere. In other words, the sphere is delineated only by the light of the bands, and hence is a phenomenon associated with gas molecules and not with atoms. This indicated that the sphere would be invisible if viewed through a filter transmitting no light of the band spectrum. Glass coloured with nickel oxide and opaque to visible light was found to fulfil this condition, and a photograph of the discharge made with it is reproduced on Pl. VI.

fig. 2. As is apparent, the spheres have vanished. The same thing could be observed visually, though less perfectly, with a filter of a deep violet colour. The spectrum is reproduced in Pl. VI. fig. 3.

It was clear from visual observations that the light of the negative oxygen bands was concentrated in the sphere, while the atomic lines showed no such concentration. These bands do not show on the photograph reproduced, which was made on an ordinary photographic plate, non-sensitive in this region. The nature of the bands in the violet region was not immediately apparent. They were unfamiliar to me, but Professor A. Fowler, to whom I showed the plate, speedily identified them as the "comet-tail" bands, which he was the first to obtain with a terrestrial source. They are characteristic of discharges in carbon monoxide at very low pressure and are emitted by the singly-ionized molecule. Prof. Fowler very kindly measured one of the plates for me (on which there was an iron comparison spectrum) and identified most of the lines. The striking feature of the photograph is that the intensity distribution along the lines from top to bottom is not the same even for the lines due to O_{II}.

The upper of the two spheres was the one focussed on the slit (the electrode wire appears a little above the sphere in Pl. VI. figs. 1 and 2), and owing to the two inversions of the image, one by the lens and the other by the spectrograph, "above" and "below" correspond in the photographs and the spectrogram.

We see at once that the maximum intensity of the lines 4417, 4641, and 4650, all due to doubly-ionized oxygen O_{II}, is distinctly below the sphere, which is sharply defined in the comet-tail bands 4542 and 4273, while the line 4319, also due to O_{II}, has its region of maximum intensity much higher up, the distribution of intensity along the line being similar to that of the line 4368, due to O_I. In the case of the double line between 4474 (unidentified) and 4523 (probably O_I, but possibly a line of the Ångström band) the intensity maximum is still more elevated. These lines also appear to be due to O_{II}: that is, to the same type of atom as the one giving the line 4650, which has its intensity maximum at the bottom. Obviously we must study these differences in relation to the different spectral terms of O_{II}, but it is not worth while to do this until photographs have been made with higher dispersion, and of *both* of the spheres, to determine whether 4650 is brightest at the side of the sphere away from the electrode or on the side adjacent to the

portion of the discharge between the two spheres. It will be necessary also to study the effects with two electrodes.

The spheres are perfectly steady, no change in their appearance or position having been noticed during the half-hour exposure of the spectrogram.

If a magnet is brought up slowly the sphere gradually contracts to a point and vanishes, reappearing and increasing in diameter as the magnet is withdrawn. It will be interesting also to see the effects of obstacles such as thin glass rods or wire supported in various positions inside of the tube, and it seems highly probable that a further study of the spectra of these remarkable discharges will throw some light on their mechanism.

London.
June 8th, 1929.

XXVI. *Talbot's Law in connexion with Photo-electric Cells.* By G. H. Carruthers *.

[Plate VII.]

WITH reference to Dr. Campbell's comments † on the paper by Carruthers and Harrison on this subject ‡, and to the reply by Harrison and Stiles §, an account of some experiments on this subject with the aid of an oscillograph may be of interest, as they confirm that the "fatigue" effect discussed in these communications does not occur to any appreciable extent in any single exposure of a cell by a rotating sector.

The experiments were made with an oscillograph of the Wood type ‖. To obtain with this instrument a deflexion of the cathode stream of 10 mm., which is convenient for measuring purposes, a potential difference of about 10 volts must be applied to the electrostatic deflecting plates. To obtain this change with the photo-electric cells employed, which had a dark resistance of approximately infinity and a resistance when exposed to the illumination employed of the order of 10^{12} ohms, it was necessary to use a very high

* Communicated by the Author.
† Phil. Mag. viii. p. 63 (1929).
‡ Phil. Mag. vii. p. 792 (1929).
§ Phil. Mag. viii. p. 64 (1929).
‖ Journ. Institution of Electrical Engineers, lxiii. p. 1046 (1925).

resistance in series with the cell if subsequent amplification were to be avoided. Amplification by means of thermionic valves seemed undesirable in experiments of this nature owing to the possible introduction of distortion, and preliminary experiments were made by connecting a cell in series with a xylol-alcohol resistance of 10^{12} ohms. The ends of the liquid resistance were connected to the electrostatic deflecting plates of the oscillograph. The source of illumination was a 12–14-volt 48-watt gas-filled lamp. Between the lamp and the cell was arranged a small electric motor, to the shaft of which sectors of various angular apertures could be secured.

Figs. 1 and 2 (Pl. VII.) are records taken with a 60°-sector occulting the cell 100 times a second and 70 times a second respectively. The cell used was the cæsium cell used in the previous experiments, which exhibited distinct non-proportionality between photo-electric current and illumination. At the beginning of the records, which is on the left-hand side, the cell is in darkness. At A the cell is exposed to the illumination, and results in a deflexion of the cathode beam, shown downwards in the photographs, and at B the cell is occulted by the sector. Both records show a distinct lag of the apparatus in the recording of the photo-electric current. This lag was due to two causes: in the first place, the capacity of the leads and electrodes of the cell, amounting perhaps to 100 cm., that is 10^{-10} farad, discharging through the high resistance of 10^{10} or 10^{12} ohms will produce a time-lag of 1–100 seconds. In the second place, an apparent lag would be introduced by the light not being occulted instantaneously by the sector disk, but being gradually cut off as the sector moves between the light-source and the cell. To eliminate the latter effect a lens was introduced between the lamp and the sector to project an image of the single filament lamp on the sector disk. Thus, when the sector rotated, an almost instantaneous cut-off of the light was obtained. To eliminate the lag due to the high resistance, recourse was had to valve amplification. The first valve circuit employed is shown in the figure. The liquid resistance of 10^{12} ohms was replaced by a 5-megohm resistance, the junction point of the latter with the cell being connected to the grid of a thermionic valve. The other end of the resistance was connected through a biasing battery with a fine adjustment to the filament of the valve. A $\frac{1}{4}$ of a megohm resistance was placed in the anode circuit, and a micro-ammeter was also included to indicate when the grid bias was correctly adjusted for the valve to be working on

the straight part of its characteristic. The earthed plate of the oscillograph was connected through a biasing battery to one end of the $\frac{1}{4}$-megohm resistance, and the second plate to the junction of the $\frac{1}{4}$-megohm resistance and the anode. A separate biasing battery, which is not shown, was employed to avoid any disturbing effects due to the varying load on the valve high-tension supply.

Figs. 3 and 4 (Pl. VII.) are records taken with these modifications in the apparatus. Fig. 3 is a record of the non-proportional cell, and fig. 4 is a record of a cell for which the proportionality between photo-electric current and illumination strictly holds. At A the cell is exposed, and at B it is occulted by the sector. It will be noticed that

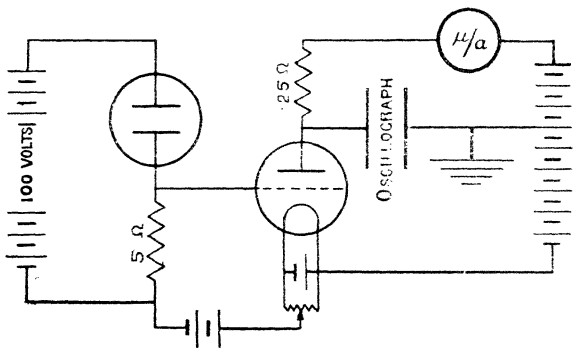

the deflexion when the cell is exposed is now in an upward direction in the photograph, this reversal being due to the introduction of the valve.

Employing one-valve amplification necessitated the use of a resistance, in series with the cell, sufficiently high to cause an appreciable lag, which is evident in the photograph. To eliminate this lag the 5-megohm resistance was replaced by a 2-megohm resistance, and two valves were used for the amplification. The type of record obtained with this arrangement is shown in fig. 5 (Pl. VII.), which is a record obtained with a non-proportional cell. As before, B indicates the point when the cell is occulted by the sector, and A the point when the cell is exposed. Superimposed on this record are two others showing the photo-electric current when the cell

is exposed to a steady illumination and when the cell is in the dark. The parallelism of the light and dark trammels thus obtained with the light and dark deflexions of the record when the cell was alternately illuminated and occulted by the sector-shutter indicates that there is no measurable fatigue in any one of these exposures, which were of the order of a fiftieth of a second. It follows that this "fatigue" or change of emission in non-proportional cells takes place over a number of such exposures corresponding to a period of exposure of $\frac{1}{2}$ to 5 seconds, as indicated by the galvanometer results mentioned in the last paragraph of the paper.

XXVII. *Notes on some Geometrical Radiation Problems.* *By* O. A. Saunders, *B.A., M.Sc., Fuel Research Division, Department of Scientific and Industrial Research* *.

Note I.

1. THE expressions obtained by Professor E. A. Milne in his recent paper † on the radiation transmitted through a pair of parallel circular apertures may be deduced more simply as particular cases of the following more general result :—

"If two apertures (not necessarily plane) are such that their bounding lines lie entirely on one and the same sphere, the radiation transmitted per second through both of them is given by

$$R = I\frac{S_1 S_2}{4\rho^2}, \quad \ldots\ldots\ldots \quad (1)$$

where S_1 and S_2 are the surface areas of the parts of the sphere cut off by the bounding lines of the apertures, and ρ is the radius of the sphere."

As in Professor Milne's paper, the radiation falling on the first aperture is supposed to be incident from all directions in which, according to the geometry of the system, it is possible for radiation to pass directly through both apertures ; I is the normal intensity at any point in the incident beam.

2. To prove this result, suppose that dS_1, dS_2 represent elements of area of a spherical surface at two points P_1, P_2.

* Communicated by Prof. E. A. Milne.

† Phil. Mag. [7] vii. p. 273 (Feb. 1929).

The radiant intensity transmitted through both elementary areas is given by

$$\frac{I \cos \zeta_1 . \cos \zeta_2 . dS_1 . dS_2}{P_1P_2^2},$$

where ζ_1 and ζ_2 denote the angles made with P_1P_2 by the normals to the surface at P_1 and P_2 respectively.

Since the surface is spherical, $\zeta_1 = \zeta_2$ and

$$\cos \zeta_1 = \cos \zeta_2 = \frac{P_1P_2}{2\rho},$$

whence the transmitted radiation is

$$\frac{I\, dS_1 dS_2}{4\rho^2}.$$

By integration, therefore, the intensity transmitted in series through two finite areas forming parts of a spherical surface is $IS_1S_2/4\rho^2$, where S_1, S_2 are the areas considered, measured upon the surface of the sphere.

Since the transmitted intensity depends only upon the bounding lines of the apertures, and not upon the shapes of the surfaces which are supposed to fill the apertures for the purpose of integration, the result is established.

3. In the particular case considered by Professor Milne, the two parallel circles clearly lie on a sphere whose centre is at O (see fig. 1), where OA = OC.

By the usual solid angle formula the surface areas of the caps cut off from this sphere by the planes of the apertures are given by

$$S_1 = 2\pi\rho^2(1-\cos\phi_1), \qquad S_2 = 2\pi\rho^2(1-\cos\phi_2),$$

where ϕ_1, ϕ_2 denote the angles marked in the figure. The transmitted radiation R is therefore, by (1), equal to

$$\pi^2\rho^2 I(1-\cos\phi_1)(1-\cos\phi_2) = 4\pi^2\rho^2 I \sin^2\tfrac{1}{2}\phi_1 . \sin^2\tfrac{1}{2}\phi_2.$$

The intensity transmitted through the aperture CD alone when the screen containing AB is absent is

$$\pi I . \pi\rho^2 \sin^2\phi_2.$$

Hence the fractional reduction in the radiation reaching CD, caused by the screen containing AB, is

$$\frac{\sin^2\tfrac{1}{2}\phi_1}{\cos^2\tfrac{1}{2}\phi_2} \quad \ldots\ldots\ldots \quad (2)$$

This is identical with expression (5) in Professor Milne's paper, for it is clear from the figure that, since A, B, C, D are concyclic,

$$\phi_1 = \hat{\mathrm{EOA}} = \tfrac{1}{2}\hat{\mathrm{BOA}} = \hat{\mathrm{BCA}} = \theta - \phi$$

and

$$\phi_2 = \hat{\mathrm{FOC}} = \tfrac{1}{2}\hat{\mathrm{DOC}} = \hat{\mathrm{DAC}} = \theta + \phi,$$

where θ and ϕ are the angles given in Professor Milne's trigonometrical interpretation, and are marked in fig. 1.

Fig. 1.

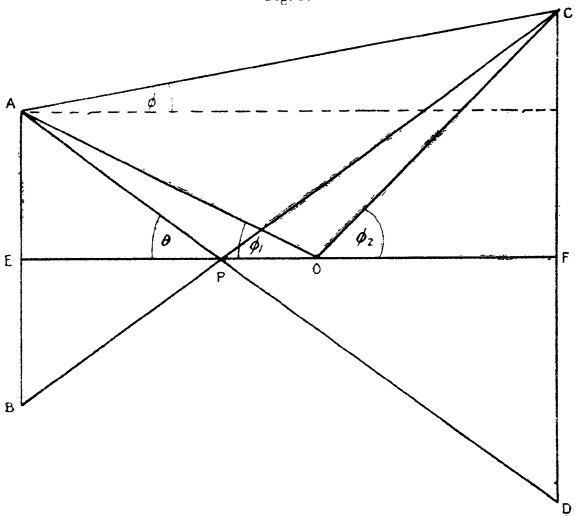

The other formulæ are, of course, easily deduced from (2). Equation (2) provides a very simple trigonometrical method of expressing the intensity transmitted through both apertures.

4. Several points of interest arise from the general result (1).

In the first place, it will be noted that the value of R is independent of the relative positions of the two apertures, provided, of course, that their bounding lines always remain on the same sphere. In other words, if a complete sphere

of thin material be taken and two apertures be cut in its surface at different positions, the intensity of the radiation transmitted through both apertures depends only on their spherical areas, and not upon their shapes and relative positions.

In the particular case when the apertures are circular and equal, a further result of some interest readily follows. The intensity transmitted through two equal parallel circular apertures with their planes at right angles to their line of centres is the same as that transmitted through the same two apertures when placed so that their circular boundaries have a common tangent, and with their planes at an angle $\pi - 2\theta$ to one another, where θ is the angle subtended by the radius of either aperture at the mid-point of the line joining their centres when the apertures are in the parallel position ; θ has the same meaning as in Professor Milne's paper.

Finally, if the distance apart of the apertures in the parallel position is equal to the diameter of either, $\theta = \pi/4$ and the transmitted intensity is the same as when the apertures are placed so as to have a common tangent and with planes at *right angles*.

5. The case of two square apertures considered by Dr. Richardson* cannot, of course, be solved in the above manner, since four lines forming a square cannot lie on a sphere.

The peculiar simplicity of the calculation of the transmitted radiation when the boundary lines of the apertures lie on a sphere might be utilized in practice when it is desired to limit a beam of radiation by means of a pair of apertures.

Note II.—*Radiation from a Concave Surface forming part of a Sphere.*

1. The properties of a spherical surface described in Note I. enable a simple expression to be given for the total rate of emission, including all multiple reflexions, of radiation from a diffusely reflecting concave surface of uniform curvature.

2. The fraction of the radiation from an elementary area dS_1 at P_1, which is intercepted by other parts of the surface and thus fails to escape directly, is equal to

$$\frac{1}{\pi}\int \frac{\cos\zeta_1 . \cos\zeta_2 . dS_2}{P_1P_2^2}, \quad \ldots\ldots \quad (3)$$

* Phil. Mag. [7] vi. p. 1019 (Nov. 1928).

where ζ_1 and ζ_2 represent, as before, the angles between P_1P_2 and the normals at P_1 and P_2 respectively, and the integral is taken over the whole surface.

As in Note I., since the surface is part of a sphere, this expression reduces to

$$\frac{S}{4\pi\rho^2}, \quad \ldots\ldots\ldots \quad (4)$$

where S = spherical area of whole surface,

ρ = radius of sphere.

This result is independent of the position of P_1; therefore the fraction of the total emission from the whole surface which *escapes* without striking other parts of the surface is

$$1-\frac{S}{4\pi\rho^2}.$$

Further, each element of area diffusely reflects a fraction $1-e$ of the radiation which is incident upon it from other parts of the surface, e being the uniform surface emissivity. Since the value of the integral (3) is independent of the position of P_1, it follows immediately that each element of area receives the same amount of radiation from the rest of the surface, and consequently the once-reflected radiation is uniformly distributed over the surface. Further, the distribution of intensity about the normal direction is the same for the diffusely-reflected radiation as for the original emission. Hence the fraction of the once-reflected radiation which escapes without striking other parts of the surface is also given by (4). Similarly for the multiply-reflected radiation.

The fraction of the emitted radiation finally escaping, including all multiple reflexions, is therefore

$$\left(1-\frac{S}{4\pi\rho^2}\right)\left[1-\frac{S(1-e)}{4\pi\rho^2}+\frac{S^2(1-e)^2}{16\pi^2\rho^4}+\ldots\right] = \frac{1-\frac{S}{4\pi\rho^2}}{1-\frac{S(1-e)}{4\pi\rho^2}}. \quad (5)$$

This result is independent of the shape of the surface, provided that it has uniform curvature (radius ρ) and total curved surface area S.

3. The "effective emissivity e'" of the concave surface may conveniently be defined as the ratio of the emitted

intensity to that which would be given out by a black surface ($e=1$) of the same shape and size. From (5), remembering that a grey surface only emits e times as much radiation as a black surface, it follows that

$$e' = \frac{e}{1-\frac{S(1-e)}{4\pi\rho^2}}. \quad \ldots\ldots \quad (6)$$

For a hemisphere this reduces to $2e/(1+e)$.

It will be noted that the effective emissivity is increased by reducing ρ, the radius of curvature. This is the principle underlying the well-known increase in radiating power which results from "pitting" or grooving a surface.

4. As $S \to 4\pi\rho^2$, the sphere tending to become complete, $e' \to 1$ whatever the value of e (provided $e \neq 0$), corresponding, of course, to the black-body enclosure. Expression (6) may be applied to determine the departure from the true black-body intensity in the case of the radiation escaping through an aperture of any shape cut in the side of a uniform temperature spherical enclosure whose internal surface is diffusely reflecting and has emissivity e.

For a circular aperture 2 in. in diameter in the side of a sphere of diameter 6 in. and emissivity 0·5, the emitted intensity is within 3 per cent. of that of a black body.

XXVIII. *Solute Molecular Volumes in Relation to Solvation and Ionization.* *By* Sir D. Orme Masson, *K.B.E., F.R.S.**

The Molecular Volume of a Solute Substance.

IT is a familiar fact that this is easily deduced from the composition and specific gravity of the solution if it be assumed that the solvent retains its original volume unchanged, *i.e.*, that the whole contraction (or expansion) on mixing belongs to the solute. On that assumption, if the solvent be water,

$$\phi = \frac{M}{d_w}\left(\frac{1}{ps} - \frac{1-p}{p}\right),$$

where M is the molecular weight of the solute, d_w the density

* Communicated by the Author.

of water at the temperature of observation, p the weight of solute per unit weight of solution, and s the specific gravity (d_4^t) of the solution. As, however, the above assumption is not necessarily true, ϕ is generally called the "apparent" molecular volume of the solute.

More than one way in which the water may suffer change of volume suggests itself. In the first place it may be diminished in quantity by solvate formation. If so, two possibilities have to be considered. Either (1) all the solute molecules will form some definite hydrate and thus destroy, as solvent, an amount of water strictly proportional to the concentration, from extreme dilution up to the point where the whole mixture has the composition of that hydrate, or (2) the average composition of the mixed hydrates present will vary continuously with the concentration. In the second place, apart from quantity, the solvent water may suffer physical changes as the result of admixtures. It has been proved that compressed gases do so, and it may well be argued that the effect should be greater in the liquid state. If so, every property of the water must alter with the concentration, including not only its specific volume but its degree of association and all related characters; and every study of aqueous solutions has, in fact, to deal with a new solvent at each concentration. Yet such a study may, though it neglects this possibility, be justified if it leads to a simple generalization; for in that event it would seem that the physical changes of solvent are relatively negligible in comparison with others that are taken into account.

In the present case evidence has been found to support the following statements. Where water is mixed with a soluble substance the change of volume that occurs is the sum of two changes. One is that due to the formation of a hydrate from its constituent molecules; the other is caused by the dilution of that hydrate with excess of water or with excess of the other component, *e.g.*, at the highest concentration of sulphuric acid. The former may be called the "chemical effect," as it is mainly that, though it also includes in most cases a volume change due to passage from the solid to the liquid state. The latter may provisionally be distinguished as the "physical effect." The chemical effect may be a contraction accompanied by heat evolution or an expansion accompanied by heat absorption; the physical effect is always a contraction, presumably with a corresponding heat evolution. The net effect may be either contraction with rise of temperature, as in the case of

sulphuric acid, or expansion with fall of temperature, as in that of ammonium chloride. The particular hydrate which forms the solute through a range of concentrations down to infinite dilution is, in some cases, the monohydrate; in others it is a higher hydrate. In most of the cases studied the substance is not sufficiently soluble to allow the point to be reached, which may be called the "hydrate point," at which the whole solution has the hydrate composition; but in some it is possible to find a range of higher concentrations through which that hydrate is mixed with a lower one, or a final stage in which the mixture contains mono-hydrate and anhydrous substance. Limits of solubility apart, therefore, there must be always two ranges, and there may be one or more intermediate ones.

In accordance with this view, it is easy to convert the apparent molecular volume (ϕ) of the anhydrous solute into what, if it be accepted, is the true molecular volume (ϕ') of the hydrate actually present. For, in estimating ϕ, it was assumed that a mixture of n molecules of anhydrous substance with n_w molecules of water contains all the latter with their unchanged original volume, viz., $\frac{18{\cdot}016}{d_w} . n_w$ c.c., whereas it really contains this number less xn and their volume is $\frac{18{\cdot}016}{d_w}(n_w - xn)$, where x is an integer indicated by the composition of the hydrate in question. It follows, of course, that $\phi' = \phi + \frac{18{\cdot}016}{d_w} x$. The "chemical effect" (contraction or expansion, as the case may be) is included in ϕ, which is thus never identical with the original anhydrous molecular volume. It includes also the "physical effect," which is always a contraction and the magnitude of which increases with dilution.

The complexity of the solute hydrate (*i. e.*, the value of x) can be definitely determined only in those cases where the solubility is great enough to enable the "hydrate point" to be reached and passed. Where this is not the case, however, the volume study does enable one to give a maximum possible value to x; and, of course, other considerations may help to decide its most probable value. But it will be shown that the interpretation of observed volume change—of the "physical effect" which follows the "chemical effect"—is less affected by any such uncertainty than might have been expected.

The Relation of Solute Molecular Volume to Concentration.

In all, twenty-eight cases have been studied, for which recorded density tables apparently offered suitable data. All but four of these belong to the class of good electrolytes; and twenty-two of them have been here found to conform to the rule that ϕ is a linear function of $n^{1/2}$, where n is the molar concentration (gram-molecules per litre). The two exceptions, magnesium nitrate and sodium acetate, seem to be abnormal, each in a different way, and may be set aside as requiring further investigation; and on the basis of the twenty-two other cases the generalization may be hazarded tentatively that, in the absence of unknown complicating conditions, the following equation holds for good electrolytes:

$$\phi=\left(\frac{1}{ps}-\frac{1-p}{p}\right)\cdot\frac{M}{d_w}=a+bn^{1/2},$$

where a and b are constants characteristic of the salt dissolved. The other four cases, viz., phosphoric acid, acetic acid, sucrose, and glycerol, are as yet too few to justify a similar generalization, even tentative, for poor electrolytes; but they will be discussed more fully later.

It follows from what has been stated already that the equation for the hydrated solute is

$$\phi'=\phi+\frac{18{\cdot}016}{d_w}x=a'+bn^{1/2},$$

where

$$a'=a+\frac{18{\cdot}016}{d_w}x,$$

and is therefore also a constant. When $n=0$, $\phi=a$, and $\phi'=a'$, which are the solute molecular volumes (apparent and real) at infinite dilution. As concentration increases, these minimum values are added to by an amount proportional to the square root of the concentration. The values of a and b are found from a graph in which ϕ is plotted against $n^{1/2}$; b from the slope of the straight line and a by its extrapolation downwards to $n^{1/2}=0$.

A maximum conceivable value of n and the corresponding value of ϕ may be calculated from the pair of equations,

$$\phi_m=a+bn_m^{1.2} \quad \text{and} \quad \phi_m=\frac{1000}{n_m},$$

whence $an_m+bn_m^{3.2}=1000$. The solution of this last gives the theoretical upper limit to the straight line. ϕ_m is not

the molecular volume of the undissolved anhydrous solvend in its usual state, but that which it would have if it could be contracted (or expanded) by the "chemical" effect in the entire absence of water, or conceivably by a sufficient change of pressure, to cause n_m molecules to fill exactly one litre. But, as a fact, this point is never reached, for the "hydrate point" at which $\frac{n_w}{n}=x$, puts an end to the straight line at a smaller n value. If the solubility is large enough to allow this point to be reached and passed, the value of x can be at once detected by the abrupt transition from the straight line to a curve in a new direction at an indicated value of $p_H=\frac{M}{M+18{\cdot}016x}$; and the corresponding ϕ and n values can be exactly determined by the solution of the equations

$$\phi'_H=1000 \quad \text{and} \quad a'n_H+bn_H^{3/2}=1000.$$

Even though the hydrate point be not reachable, the values of p_H, n_H, and ϕ_H, corresponding to any assumed value of x, can be determined in this way: but, if too large a value of x be assumed and it fall within the experimental range, it will be found that the straight line passes undeflected through the point. It is by this means that a maximum value of x can be calculated when its actual value is beyond reach.

The ϕ'_H value is already affected to some extent by a partial "physical effect" as well as by the complete "chemical effect"; for only the anhydrous substance at the higher n_m value could, even theoretically, be wholly free from the former.

The course of the volume change and the ideas already set forth are well illustrated by the H_2SO_4 graph (fig. 1), which shows the whole range from pure water to pure acid, and by those for NaOH, NaCl, and K_2CO_3 (figs. 2, 3 *a* and *b*), which all illustrate the case of limited solubility. The NaOH case is specially interesting: for it is one of two, among those studied, which give negative values of ϕ in the more dilute solutions. A negative volume, even at infinite dilution, is a contradiction in terms; but the difficulty vanishes when it is remembered that the true solute is a hydrate whose molecular volume is

$$\phi'=\phi+\frac{18{\cdot}016}{d_w}x.$$

In the NaOH case x is probably 1 (it cannot be greater

Fig. 1.

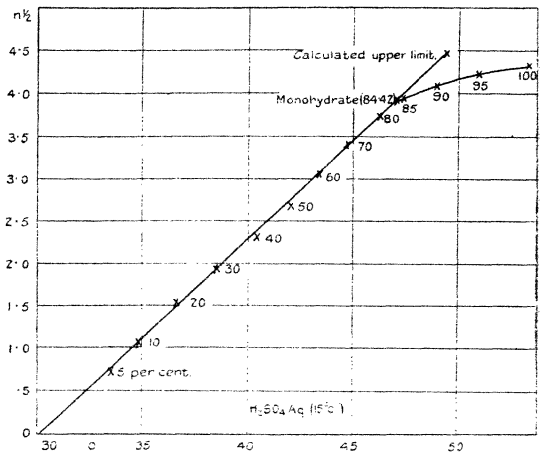
nϕ
4·5
4·0
3·5
3·0
2·5
2·0
1·5
1·0
·5
0
Calculated upper limit.
Monohydrate(84·4)
85
80
70
60
50
40
30
20
10
5 per cent.
90
95
100
H₂SO₄Aq. (15°C.)
30
0
35
40
45
50

Fig. 2.

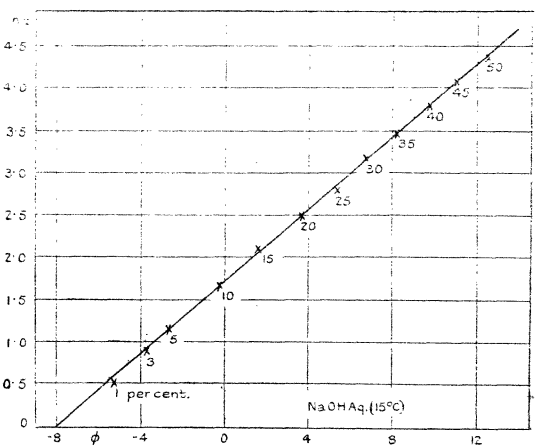
4·5
4·0
3·5
3·0
2·5
2·0
1·5
1·0
0·5
0
50
45
40
35
30
25
20
15
10
5
3
1 per cent.
NaOHAq.(15°C)
-8
ϕ
-4
0
4
8
12

than 2), and this is sufficient to convert the negative a into a positive a'.

The Nature of the "Physical Effect" : the Cause of the Change of Molecular Volume with Change of Concentration.

The large diminution of ϕ (or ϕ') in direct proportion to the fall of $n^{1/2}$ inevitably calls for some explanation of its cause ; and the suggestion is as inevitable that the hydrate exists in two forms, a greater and a smaller, and that ϕ', as measured, belongs always to a mixture of the two in a

Fig. 3.

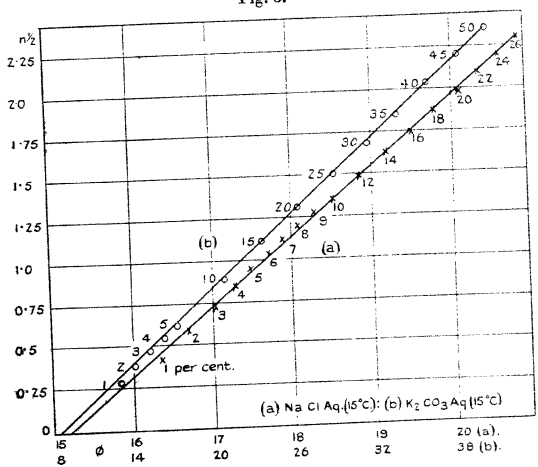

proportion determined by the concentration. The smaller form could exist by itself only if it were possible for the hydrate to exist at all in the complete absence of solute, *i. e.*, at infinite dilution. The larger form could exist by itself only if it were possible for the hydrate to exist at all in the complete absence of water, *i. e.*, at n_m (not at n_H), This puts the "physical" volume effect on a par with ionization, which is complete only at infinite dilution and may presumably be called nil only in the absence of water. Moreover, it is a generally accepted belief now that hydration of the solute is an accompaniment, or rather an

antecedent, of ionization. It seems quite probable, therefore, that the larger volume is that of the unionized molecule and the smaller one that of the molecule in its ionized state, *i. e.*, the sum of its ionic volumes. This hypothesis may or may not be true, but it at least calls for further examination.

The Ionic Theory of the Volume Change.

If α be the ionized fraction of the molecules at any given concentration, the theory may be put as follows:

$$\phi=(1-\alpha)\phi_m+\alpha\phi_i=\phi_m-\alpha(\phi_m-\phi_i)=\phi_i+(1-\alpha)(\phi_m-\phi_i).$$

When $n=0$,

$$\alpha=1 \quad \text{and} \quad \phi=\phi_i;$$

and when $n=n_m$,

$$\alpha=0 \quad \text{and} \quad \phi=\phi_m.$$

But

$$\phi=a+bn^{1.2};$$

hence

$$\phi_i=a, \quad \phi_m=a+bn_m^{1.2}, \quad \text{and} \quad b=\frac{\phi_m-\phi_i}{n_m^{1.2}}.$$

And, since

$$\phi=\phi_i+(1-\alpha)(\phi_m-\phi_i)=a+bn^{1.2},$$

it follows that

$$1-\alpha=\left(\frac{n}{n_m}\right)^{1.2}=kn^{1.2}, \quad \text{or} \quad \alpha=1-kn^{1.2}.$$

The fact that it is the hydrate which should be considered as the ionizing solute and that its x value is in most cases undetermined does not affect the conclusion as to the value of α; for, as already pointed out, the correction merely increases the constant term a (or ϕ_i) by $\frac{18{\cdot}016}{d_w}.x$ and leaves the equation otherwise unaffected.

We thus obtain (by hypothesis) a simple measure of the ionization factors at any concentration up to the hydrate point, if the solubility allows one to go so far; and it involves only one constant, $k=\frac{1}{n_m^{1.2}}$, which is easily evaluated in the manner already described. Beyond the hydrate point the formula can not apply; for, though there may still be some of the hydrate present and some ionization, as shown by conductivity, the solvent medium is a new one. But in the sulphuric acid case, if points on the curve beyond the hydrate point be recalculated as those of a solution of the

monohydrate in H_2SO_4, and the new $n^{1/2}$ and ϕ values so obtained be plotted, it is evident that here also the straight line rule obtains from infinite dilution (pure sulphuric acid) up to the monohydrate point. Confirmation has been obtained also in another case, which will be dealt with later. It seems likely, therefore, that further inquiry may show that ϕ and $n^{1/2}$ are rectilinearly related in solutions in other conducting solvents besides water, in which case the ionic interpretation will be applicable to them too.

The ionization fractions deduced from the volume study of aqueous solutions have to be compared with those obtained by the conductivity and other methods. To distinguish them, we may write β for $1-kn^{1/2}$, reserving α for the classic conductivity values. That they differ, especially at high concentrations, is not in itself a condemnation of β; for it is now generally recognized that $\lambda/\lambda\infty$ or α is in reality the product of the true ionization fraction and a mobility ratio. $\frac{u+v}{u_0+v_0}$ or $\frac{\mu}{\mu_0}$, and that the latter is not constant but changes with concentration in a manner related in some unknown way to the two ionic mobilities at infinite dilution. Should β make good the claim to represent the true ionization fraction, it should help to elucidate this mobility factor and its variation. The lack of any reliable method has led to the curious position that some investigators are claiming complete ionic dissociation for all good electrolytic solutions, while another school is inclined to dispute the truth of the fundamental principle of Arrhenius's theory—a theory that has done much for science and has certainly not been disproved.

Evidence based on published data of the Specific Gravity of Aqueous Solutions.

This is summarized in Table I., in which are given in consecutive columns (1) the formula of the anhydrous solute; (2) the temperature; (3) the highest concentration covered by the experimental work, in gram-mols. per litre; (4) $a=\phi_i$; (5) $b=\frac{\phi_m-\phi_i}{n_m^{1/2}}$; (6) ϕ_m; (7) n_m; (8) $n_m^{1/2}$; (9) $k=\frac{1}{n_m^{1/2}}$; (10) β when $n=1$; (11) β when $N=1$, which is $1-k$ when $N=n$ but $1-\frac{k}{2^{1/2}}$ when $N=2n$; (12) α when $N=1$; (13) the number of H_2O molecules (x) combined with one of the anhydrous substance in those cases where the composition

Table I.

Experimental :— $\phi_n = \frac{M}{d_w}\left(\frac{1}{p^s} - \frac{1-p}{p}\right) = a + bn^{1/2}$.

Theory :— $\phi_n = \phi_i + \frac{\phi_m - \phi_i}{n_m^{1/2}} n^{1/2}$; $\beta_n = 1 - \left(\frac{n}{n_m}\right)^{1/2}$.

Anhydrous Solute.	$t°$.	Highest concentration, mols. litre.	$a = \phi_i$.	$b = \frac{\phi_m - \phi_i}{n_m^{1/2}}$.	ϕ_m.	n_m.	$n_m^{1/2}$.	$k = \frac{1}{n_m^{1/2}}$.	β when $n=1$.	β when $N=1$.	$a = \lambda/\lambda\infty$ when $N=1$.	Hydrate Point. x.	Hydrate Point. n_H.
NaOH	15	19·12	−8·00	4·667	22·86	43·74	6·614	·1512	·8488	·8488	·736		
KOH	15	14·25	2·88	4·131	27·70	36·10	6·005	·1664	·8336	·8336	·770		
H_2SO_4	15	18·71	20·20	4·275	49·51	20·20	4·494	·2225	·7775	·8427	·517	1	15·36
$(NH_4)_2SO_4$	17·5	4·9	51·00	10·133	85·63	11·68	3·417	·2926	·7074	·7967			
$MgSO_4$	15	2·6	−4·96	11·118	46·75	21·39	4·625	·2162	·7838	·8471	·26		
$ZnSO_4$	15	3·2	1·20	10·71	49·64	20·14	4·488	·2228	·7772	·8425	·24		
HCl	15	14·28	16·60	1·260	24·63	40·60	6·372	·1569	·8431	·8431	·793	3·5	11·90
LiCl	18	12·5	17·20	1·385	25·82	38·73	6·223	·1607	·8393	·8393	·626	10	4·985
NaCl	15	5·34	15·24	2·425	29·39	34·03	5·834	·1714	·8286	·8286	·676		
KCl	15	3·86	25·75	2·650	39·14	25·55	5·054	·1978	·8022	·8022	·755		
NH_4Cl	15	5·22	35·30	1·633	43·16	23·17	4·814	·2078	·7922	·7922	·748		
$MgCl_2$	15	4·9	13·57	6·170	43·24	23·12	4·809	·2080	·7920	·8530	·552		
$CaCl_2$	15	5·05	15·10	7·100	47·67	20·98	4·580	2183	·7817	·8456	·584		
$CdCl_2$	18	4·6	22·77	5·715	48·67	20·54	4·533	·2206	·7794	·8440	...	11	4·385
HNO_3	15	23·5	27·80	0·925	32·90	30·40	5·513	·1814	·8186	·8186	·824	1	17·877
$NaNO_3$	20·2	8·32	28·90	2·105	39·49	25·32	5·03	·1987	·8013	·8013	·626		
KNO_3	15	2·37	35·75	3·270	50·25	19·90	4·46	·2242	·7758	·7758	·637		
NH_4NO_3	17·5	10·43	45·45	1·764	53·10	18·83	4·34	·2304	·7696	·7696	...	7	5·686
$AgNO_3$	18	6·77	26·25	3·148	41·67	24·00	4·90	·2041	·7959	·7959	·582		
$NaClO_3$	? 15	4·2	34·20	2·688	46·64	21·44	4·63	·2160	·7840	·7840			
$Na_2S_2O_3$	19	2·6	25·00	12·23	70·33	14·21	3·77	·2653	·7347	·8124			
K_2CO_3	15	5·6	8·80	13·60	62·99	15·88	3·984	·2510	·7490	·8228			

of the hydrated solute is indicated by termination of the straight line; (14) the n value at which this occurs.

In further illustration, reference may be made again to figs. 1–3, which represent typical cases. Various points of general or special significance are dealt with in the following notes.

Limits of accuracy.—Most of the data employed were taken from the tables of percentage composition and specific gravity given in the Comey-Hahn 'Dictionary of Solubilities.' They are quoted there from various authors and are not of equal accuracy. None were useful for the present purpose that give S to less than 4 decimal places. Some give it to 5, and in one case (Pickering's NaOH table) it is given to 6. Though most of the tables begin at $p=\cdot01$, it is only in exceptional cases that values below $p=\cdot05$ are accurate enough to give correct results. This is obvious when it is remembered that the calculated value of ϕ depends on the difference between $\frac{1}{ps}$ and $\frac{1-p}{p}$, and that this means the difference between 19 and a fraction and 19 at $p=\cdot05$, but between 99 and a fraction and 99 at $p=\cdot01$. At higher concentrations points are seen to deviate more or less on both sides of the straight line which represents the prevailing rule (see fig. 1); but such deviations are, at least partly, to be ascribed to erroneous data. Each table represents a curve in which interpolated values of s are plotted against p and thus involves errors inherent in the experimental determinations of p and s and also those due to the smoothing process. In the few cases examined from this point of view, it has been found that the points calculated from interpolated values deviate from the straight line considerably more than those derived from the experimental ones. But, of course, any errors in the data are magnified in the ϕ, $n^{1/2}$ graph. In the sulphuric acid case, p and s have been calculated back from points on the straight line where the graph shows maximum deviation, and this has been found to be covered by a difference of 2 or 3 units in the third decimal place of S. Such a difference is barely noticeable in a p, s curve drawn on any ordinary scale. Fig. 3 *b* (K_2CO_3) shows a case with deviations at a minimum. There are others in which they are somewhat greater than in the H_2SO_4 case.

The ϕ_i values.—The relation of these to the true molecular volumes of hydrated solute at infinite dilution has already been explained, and the significance of the negative ϕ_i of NaOH and of $MgSO_4$ has been pointed out in illustration

The ϕ_m and n_m values.—These were calculated from a and b as already described. Comparisons of the chlorides shows that ϕ_m increases, and n_m decreases correspondingly, in the order of, but not in proportion to, the molecular weights of HCl, LiCl, NaCl, KCl; that NH_4Cl has a greater ϕ_m than KCl; that it is almost the same for $MgCl_2$ as for NH_4Cl; and that $CaCl_2$ and $CdCl_2$ have larger values, in that order, but differ only slightly from each other. Closely similar relationship is shown by the nitrates of H, Na, K, NH_4, while $AgNO_3$ has a value between those of Na and K. The ϕ_m of $(NH_4)_2SO_4$ bears nearly the same ratio (1·77) to that of H_2SO_4 as NH_4Cl and HCl give (1·75), and in the case of the nitrates it is somewhat smaller (1·61). $MgCl_2$ and $MgSO_4$ occupy similar positions in their respective classes.

The β values.—Relations observed among the n_m values necessarily reappear in the comparison of $k=1/n_m^{1/2}$, and therefore also of $\beta=1=kn^{1/2}$ when $n=1$. It may be noted that H_2SO_4 has a considerably lower β than HCl when equimolar solutions are compared, but that they are practically equal in equivalent solutions.

Comparison with the corresponding α shows that β is uniformly higher. This is in accordance with the view that seems now to prevail, that the conductivity method puts the ionization fraction too low; but this matter will not be further discussed here.

The Indication of Definite Hydrates.

There are only five cases with entries in the last two columns of Table I., for the good reason that in those cases only does the rectilinear relation between ϕ and $n^{1/2}$ break down before the upper limit of the experimental range is reached—a range determined generally by the solubility of the substance. But they suffice to show that there is no uniform rule as to the complexity of the hydrate which forms the ionizing solute. They also show that it is not necessarily capable of separation as a crystalline solid, though some of those formed with contraction and heat production may be.

The first case is that of H_2SO_4, in which the rectilinear relation persists up to the monohydrate point. The p value here must be ·8442 and the other characteristics, calculated in the manner already indicated, are $n_H=15·36$, $n_H^{1/2}=3·920$, and $\phi'_H=65·087=47·086\times18·031$ (at 15°). The curve from this point to that of pure H_2SO_4 has been discussed already.

The monohydrate, which may be called ortho-sulphuric acid, is well known. It readily separates from super-saturated solution in H_2SO_4 at low winter temperatures when reagent bottles of "strong" sulphuric acid are shaken.

The case of HCl is somewhat uncertain. There is no doubt that the straight line which holds up to over $p=\cdot35$ gives place to a curve in the neighbourhood of ·37, but, unfortunately, the specific gravities at all higher concentrations up to ·43 (the highest) are recorded as less accurate than those below. It is most probable, however, that the break-away from the line occurs when $p=\cdot3664$ and the solution has the composition of $HCl.3\frac{1}{2}H_2O$. This requires $n_H=11\cdot897$, $n_H^{1/2}=3\cdot449$, and $\phi'_H=84\cdot055=20\cdot947+3\cdot5\times18\cdot031$ (at 15°). The curve from this point bends upwards in the direction that indicates it has been formed from its components with contraction, which accords with the marked exothermic reaction of hydrogen chloride and water. The only compound which has been isolated in the solid state is the monohydrate; but specific gravity data do not extend to such a high concentration ($p=\cdot6693$).

In the LiCl case the break-away from the straight line into a curve takes place at the point where the whole solution has the composition of $LiCl.10H_2O$, far below the saturation point, which extends to near $n=12\cdot5$. The characteristics of this hydrate point are $p=\cdot1908$, $n_H=4\cdot985$, $n_H^{1/2}=2\cdot2327$, and $\phi'_H=200\cdot60=20\cdot20+10\times18\cdot040$ at (18°). Both the line and the curve are accurately defined by points calculated from extensive experimental work done in the Melbourne laboratory (W. H. Green, Trans. Chem. Soc. 1908, p. 2036). The change from the line to the curve is fairly abrupt, so that there is small room for doubt as to the exact point at which it occurs. The case is very similar to that of H_2SO_4, except for the complexity of the hydrate indicated and for the fact that the curve bends away in the opposite direction, the hydrate in this case being formed from its components with expansion. $LiCl.10H_2O$ is not known in the solid state. Mono- and di-hydrates have been separated from more concentrated solutions, but the corresponding hydrate points are beyond the range of the experimental data.

The case of another very soluble salt is very similar. The straight line of NH_4NO_3 gives place to a curve at the hydrate point for $NH_4NO_3.7H_2O$, for which the p value is ·3884 and $n_H=5\cdot686$, $n_H^{1/2}=2\cdot3845$ and $\phi'_H=175\cdot87=49\cdot60+7\times18\cdot039$ (at 17·5°). Here also the curve tends in the direction which shows that expansion occurred on the formation of the

hydrate from its components. No hydrate of NH_4NO_3 has been separated in the solid state.

The straight line in the case of HNO_3 is relatively short, the acid being soluble in water in all proportions and the greater part of the ϕ, $n^{1/2}$ graph showing as a decided curve. The break-away from the line occurs at the $HNO_3 . 11H_2O$ hydrate point, *i. e.*, at (or close to) $p = \cdot 2413$, for which $n_H = 4 \cdot 385$, $n_H^{1/2} = 2 \cdot 094$, and $\phi_H = 228 \cdot 05 = 29 \cdot 71 + 11 \times 18 \cdot 031$ (at 15°). In this case the curve bends towards higher volume, showing that the hydrate has formed with contraction, like $H_2SO_4 . H_2O$. An attempt to straighten this curve by plotting ϕ against a higher power of n proved completely successful with $n^{3/2}$, for a straight line resulted which is defined by the equation $\phi = 28 \cdot 65 + \cdot 1225\, n^{3/2}$ and which, of course, does not include the points below the $11H_2O$ hydrate point. Again, however, there is a break-away from the line at a definite hydrate point; and this time it is the monohydrate, $HNO_3 . H_2O$, which requires $p = \cdot 7777$, $n_H = 17 \cdot 877$, $n_H^{1/2} = 75 \cdot 586$, and $\phi'_H = 55 \cdot 938 = 37 \cdot 907 + 18 \cdot 031$. Here another curve, itself nearly rectilinear, diverges in the direction of smaller volume. It is unbroken up to about $p = \cdot 93$, beyond which uncertainty attaches to the experimental data on account of the instability of very highly concentrated nitric acid. The whole range of concentrations is thus divisible into three stages, viz.: (1) from $n = 0$ to $n = 4 \cdot 385$, following the $n^{1/2}$ rule, with solutions of the $11H_2O$ hydrate in excess of water; (2) from $n = 4 \cdot 385$ to $n = 17 \cdot 877$, following the $n^{3/2}$ rule, with mixtures of the above hydrate and the monohydrate; (3) from $n = 17 \cdot 877$ to the end, with solutions of the monohydrate in the anhydrous acid. Pickering predicted and isolated as solids the monohydrate and trihydrate, but the present study of the solute volume has given no sign of the latter. The constitution of nitric acid in its higher concentrations has always been a problem. W. H. Hartley, from his study of the absorption spectra and other properties, was led to conjecture that it is a mixture of orthonitric acid (the monohydrate) and a polymerized anhydrous molecule, perhaps $H_2N_2O_6$, with oxidizing power but no acid characters. V. H. Veley, who did much work on the properties of nitric acid, held similar views. In the more dilute solutions, which, according to the theory given here, contain hydrates free from anhydrous acid, polymerized or otherwise, nitric acid closely resembles hydrochloric acid in its conductivity (α) values; but G. N. Lewis has shown that mobility considerations, based upon transport numbers, lead to somewhat lower

true ionization fractions for HNO_3 and the nitrates than for HCl and the corresponding chlorides. The β values given in Table I. accord well with this view.

Poor Electrolytes and Non-Electrolytes.

Of these, phosphoric acid, acetic acid, sucrose, and glycerol have been examined. Though conventionally distinguished as above, sucrose and glycerol have some small tendency to salt formation and should be classed in the same category with phosphoric and acetic acids. They all differ from the electrolytes already discussed, first in showing a much smaller percentage change of volume on dilution and, secondly and more radically, in not following the $n^{1/2}$ rule. All yield decided curves when ϕ is plotted against $n^{1/2}$. The

TABLE II.

Poor Electrolytes. $\phi = a + bn^{5/4}$.

Substance.	$t°$.	Highest concentration (mols per litre).	$a = \phi_0$.	$b = \frac{\phi_m - \phi_0}{n_m^{5/4}}$	$\phi_{m'}$	v_m.	$v_{m'}$.	At hydrate point. π.	u.
Phosphoric acid...	15°	8·8	45·16	·2024	55·10	18·833	39·233	—	—
Acetic acid	15°	17·58	50·91	·1385	55·99	17·86	36·713	1	13·77
Sucrose	17·5°	3·6	210·12	1·500	220·07	4·544	6·634	—	—

whole range in the case of glycerol, which is soluble in all proportions, yields a ϕ volume change of only about 4 per cent., and more exact p and s values than those available would be needed for any particular regularity to be disclosed. But the rather surprising fact has been ascertained that each of the others gives an undeniable straight line when ϕ is plotted against $n^{5/4}$. With lower powers (e. g., n itself) or higher powers (e. g., $n^{3/2}$) there is curvature one way or the other. Phosphoric acid, acetic acid, and sucrose, therefore, follow the rule that $\phi = a + bn^{5/4}$; but whether this is more generally true of the class to which they belong cannot be stated at present. The three cases are summarised in Table II.

In the case of phosphoric acid, the rule holds from $p = \cdot 15$ and $n = 1 \cdot 66$ to $p = \cdot 60$ and $n = 8 \cdot 8$, *i. e.*, through the whole range of available data, excluding those at the dilute end, where no certain conclusion can be drawn. In the sucrose

case the rule holds from $p=\cdot05$ and $n=0\cdot149$ to $p=\cdot85$ and $n=3\cdot6$ approximately,—again to the highest concentration for which data are available. But acetic acid, being soluble in water in all proportions, affords evidence up to $p=1$ and $n=17\cdot58$; and in its case the straight line runs from $p=\cdot10$, $n=1\cdot69$, to a point between $p=\cdot75$ and $p=\cdot80$, where regular curvature away from the line sets in. There is no doubt that this is the monohydrate (orthoacetic acid) point, for which the calculated characteristic values are $p=\cdot769$, $n_{\mathrm{H}}=13\cdot77$, $n_{\mathrm{H}}^{5/4}=26\cdot53$, $\phi'_{\mathrm{H}}=72\cdot622=54\cdot591+18\cdot031$ (at 15°) The case is like that of H_2SO_4 except for the different power of n. It is shown in fig. 4.

Fig. 4.

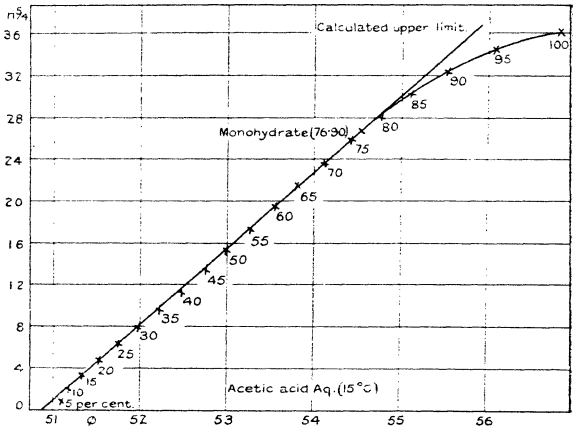

The curve between the monohydrate and anhydrous acid points has been examined as was done in the H_2SO_4 case, a few points being recalculated as solutions of $C_2H_4O_2 . H_2O$ in $C_2H_4O_2$; and again it was found that the new ϕ values when plotted against the new $n^{1/2}$ values give points lying on or close to a straight line, from $p=0$ at the anhydrous acid end to $p=1$ at the hydrate point. These two cases give some evidence, therefore, that the square root holds for electrolytic solutions in other solvents besides water, provided that complicating conditions be absent.

That there are some such complicating conditions in the cases of acetic acid, phosphoric acid, and sucrose in aqueous solution is suggested by their substitution of the $n^{5/4}$ rule for the other. That acetic acid is prone to form associated molecules offers a possible explanation in its case, for gradual depolymerization as dilution increases may well swamp a simultaneous but smaller volume change due to ionization. A similar complication may, perhaps, be at work in the more concentrated solutions of nitric acid: but, whatever the cause, acetic acid, phosphoric acid, and sucrose follow the same rule. Further investigation seems to be called for.

Summary.

1. It is shown that, in the great majority of instances, the apparent solute molecular volume of an electrolyte in aqueous solution is a rectilinear function of the square root of the volume concentration. In most cases of limited solubility the straight line representing this relation holds through the whole range of experimental data; but in those in which this range extends to sufficiently high concentration it is shown that curvature sets in, the change seeming always to originate at a point corresponding to the composition of some definite hydrate. In the case of sulphuric acid the monohydrate is thus indicated, while various higher hydrates are shown by nitric acid, hydrochloric acid, ammonium nitrate, and lithium chloride.

2. From these facts and other evidence the conclusion has been drawn that, below the point at which curvature originates, the solution is always that of a hydrate in excess of water, but that, above that point, it is not truly an aqueous solution but either a solution of a monohydrate in excess of anhydrous substance or an intermediate mixture of hydrates, as the case may be.

3. From this view it follows that the true solute molecular volume, below the hydrate point, is that of the characteristic hydrate and is the sum of the apparent molecular volume and a quantity determined by its degree of hydration. It includes the plus or minus volume change that accompanies its formation from its components and also a contraction, the extent of which depends on the dilution. This true molecular volume has a definite value at infinite dilution, which increases linearly with the square root of the concentration up to the hydrate point. The apparent solute molecular volume in a few instances is negative at low

concentrations; the true volume—that of the hydrate—is always positive.

4. It is suggested that the true solute molecular volume at infinite dilution is that of the completely ionized hydrate and that the larger measured value at any given concentration is the average value of a mixture of ionized and unionized molecules. It is shown, also, how the unreachable value of the completely unionized hydrate may be calculated from the two constants of the straight line.

5. It is shown, further, that, if this hypothesis be correct, it necessarily follows that the ionization fraction (β) at any given concentration (n) is expressed by the equation $\beta = 1 - kn^{1/2}$, where k is a constant readily calculated.

6. While the facts cited as to the apparent solute molecular volumes involve no assumptions, their interpretation in the manner explained assumes that any excess of water which remains as solvent after formation of the characteristic hydrate retains its original specific volume practically unchanged.

7. In the case of three poor electrolytes, viz., acetic acid, phosphoric acid, and sucrose, it is shown that the apparent solute molecular volume is a rectilinear function of the $\frac{5}{4}$ power of the volume concentration, the square root rule not holding. In the last two cases the straight line extends through the whole range of the experimental data, but in the acetic acid case it gives place to a curve above the monohydrate point. In both this case and that of sulphuric acid, points on the curve above this point have been recalculated as those of solutions of the monohydrate in anhydrous acid, and are found to lie on a straight line when plotted as solute molecular volumes against the square root of the concentration, thus supplying some evidence that this rule is not confined to aqueous solutions.

8. Twenty-two cases of alkalis, acids, and salts, and the above three cases of poor electrolytes, are summarized in tabular form and their more striking features are discussed in detail.

Melbourne,
October 1929.

XXIX. *On the Acoustics of Large Rooms**. *By* Dr. M. J. O. Strutt †.

Abstract.

The theoretical proofs hitherto given in literature of Sabine's experimental result, that the duration of residual sound in a large room does not depend upon the shape but only on the volume and the absorbing power, and is the same (generally) if measured in different points with the source at different places, may be said to be incomplete. They start from considerations of reflexion at the walls, but phase relations are left out.

Moreover, often a homogeneous distribution of sound-energy over space at the moment the source stops is assumed, which will not be true in various cases that, on the other hand, experimentally check Sabine's law very well.

The present treatment discusses the problem of forced oscillations in a continuous medium with arbitrarily distributed absorption, and shows Sabine's law to be a general asymptotic property of such oscillations, if the quotient of the forced frequency over the lowest free frequency of the system tends to infinity.

In addition, various special experimental features are discussed from this point of view.

The prevalence of Sabine's law in other departments of physics, *e.g.*, with the electromagnetic radiation in closed spaces, is predicted from its general character.

Introduction.

In a series of fundamental experiments W. C. Sabine has shown ‡ that the acoustical properties of large rooms may often be very well defined by the duration of residual sound. This duration is measured in the following way :—A source of sound (*e.g.*, organ pipes), of frequency generally large with respect to the lowest free frequency of the room, is operated constantly during a time sufficient

* The essential contents of this paper coincide with a lecture delivered by the Author before the Dutch Physical Society at Amsterdam, January 26th, 1929.

† Communicated by the Author.

‡ Collected papers on Acoustics.

to reach the stationary state of affairs. Then the source is stopped abruptly, and the time from this moment until the sound has fallen to the minimum audible intensity is measured. By a series of measurements this time is reduced to a value giving the duration of residual sound with an intensity at the moment the source stops which is a known multiple of the minimum audible intensity (*e. g.*, a million-fold).

Many experiments lead to the conclusion (hereafter referred to as Sabine's law) that in general *the duration of residual sound measured in this way is proportional to the volume of the room over the total absorbing power* (the meaning of this latter term will appear hereafter), *but does not depend on the shape of the room, the places of source and experimenter, while the frequency does not change much after the source has stopped,* this law being checked best in large rooms.

I must add that Sabine has also performed experiments which seem to contradict this law, but these experiments may in general be easily explained by special conditions, causing a deviation from the law, which, as will appear shortly, is only *exactly* followed in certain "ideal" conditions.

In general, experiments must be said to check the law with remarkable accuracy, as is illustrated by graph 1, which is taken from a paper by Sabine.

After this experimental discovery, which enabled rooms with improved acoustical properties to be constructed, many theoretical papers were devoted to proofs of the law. The first of such papers was by Sabine himself.

In most of them (including Sabine's) a homogeneous distribution of sound-energy over space at the moment the source stops is assumed, which leads to a proof of the law if certain elementary considerations of reflexion at the walls are followed.

It is easy to give simple cases in which this homogeneous distribution of energy cannot exist. This happens, *e. g.*, in a spherical room with the source at the centre. Another case is a cylindrical room with the source at the centre. All these cases are automatically excluded from the considerations mentioned above, and one might conclude (this point of view has indeed been supported by certain authors) that Sabine's law will not hold in such cases.

Now experiments are known in which a non-homogeneous distribution of energy certainly exists—*e. g.*, the Sanders' theatre, discussed by Sabine. However, the point (1) in

graph 1, belonging to this theatre, lies beautifully on the straight line. Hence this assumption of special energy distribution cannot be essential for the validity of Sabine's law.

In all of the papers mentioned above, considerations of reflexion are applied to the *intensity*, leaving out phase relations. It is difficult, if not impossible, to rate the error brought into the calculation by this neglect.

A Law similar to Sabine's holding in Physics.

In various departments of physics a law exists which bears some resemblance to Sabine's. It has first been

Graph 1.

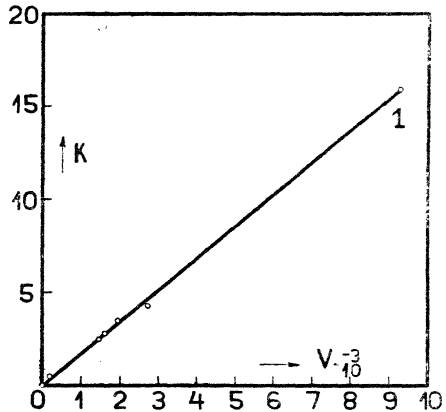

Vertical axis: Duration of residual Sound total absorbing Power.
Horizontal axis: Volume of room.

(Taken from a paper by Sabine.)

announced by H. A. Lorentz that the very high characteristic frequencies* (*i. e.*, the modes in which a system oscillates without outside forces acting constantly) of a continuous system *without* absorption will asymptotically depend only on the volume and the elastic properties, but be independent of the shape. This proposition has been proved mathematically by H. Weyl.

* Lorentz, 'Modern Physics,' p. 166 (1927).

Its physical plausibility is most easily seen by considering some applications.

J. H. Jeans and P. Debye have developed a theory of radiation in closed spaces, leading to Planck's experimental law. Herein the proposition must be supposed to hold, for otherwise Planck's law would not follow.

Similarly, in Debye's theory of specific heat * a cubic piece of metal would have a heat capacity different from a spherical piece of the same metal if Lorentz's proposition were not fulfilled.

A. Sommerfeld has pointed out that the proposition is also important for the acoustics of large rooms †.

In all of these theories systems without absorption were considered, and hence the angular frequencies in the notation

$$e^{j\omega}$$

$$(j = \sqrt{-1};\ t = \text{time})$$

are purely real. If we have absorption ω will have a real and an imaginary portion, the latter being of positive sign, so that any free oscillation once started in the system will die out after some time.

Lorentz's proposition, mentioned above, has been shown by Weyl ‡ to be an asymptotic property of the real characteristic values of the frequency ω belonging to systems *without* absorption.

In the present paper *Sabine's law will be shown to be an asymptotic property of the complex characteristic values of* ω *in systems with absorption.*

Once this analogy between Lorentz's and Sabine's laws has been formulated, the course which must be adopted in the analytical proof of the latter is quite clear. Firstly, it is necessary to calculate the complex characteristic values of ω in continuous systems with absorption distributed arbitrarily over space. As a special case we may then transport all absorbent matter to the walls, as is necessary for the acoustics of large rooms. In the second place, the forced and free oscillations of such systems must be studied in a general manner, for the process of residual sound involves a complete calculation of these oscillatory states. Combining the results of these two fundamental considerations, we shall be conducted to Sabine's law. Meantime we shall have

* Lorentz, *loc. cit.*

† *Physikalische Zeitschrift*, xi. p. 1057 (1910).

‡ *Mathematische Annalen*, lxxi. p. 441 (1912).

opportunity to define the exact conditions necessary for its validity. Also deviations from the law and special features, shown by experiments, must at once become clear from this point of view.

According to the general character of Sabine's law, indicated above, we shall be able to predict its existence in various other departments of physics, *e. g.*, with the electromagnetic radiation in closed rooms and with the oscillations of strings, bars, plates, etc.

Asymptotic Calculation of the Characteristic Frequencies in Continuous Systems with Absorption.

It is not my aim to go into mathematical details in the present paper. Of course, for a rigid proof these details become essential, but from a physical point of view they are quite unimportant. A special paper, entitled "Ueber das Daempfungsproblem der mathematischen Physik," which will appear in the *Mathematische Annalen*, is devoted to their discussion.

Improbable though it seems, I have found only one paper * in the mathematical and physical literature dealing with the problem of oscillating continuous systems with absorption distributed arbitrarily over the system. It gives the complete theory of such a system for *one dimension* (*e. g.*, string). The methods employed are such that no immediate generalization to more dimensions can be found. Moreover, the developments of Faber's do not permit us to prove Sabine's law for even one single dimension. On the contrary, they seem to indicate that no law such as Sabine's can exist in continuous systems with absorption.

For these two reasons it was necessary to start a completely new consideration, embodying the theory for more than one dimension and giving formulæ by which Sabine's law can be proved. Faber's development formula could be shown to be equivalent to the new one in the case of one dimension, its inability to prove Sabine's law being due to the special, and in this respect inefficient, form adopted by Faber.

As dependent variable in the analysis here given, I shall adopt a quantity u, referred to as "amplitude of oscillation." Afterwards this u may, in the acoustical case, be identified with the velocity potential or with the pressure at any one point.

* O. Faber, "Theorie der gedämpften Schwingungen," Dissertation Strassbourg (Referee: R. von Mises) (1914).

Let the amplitude of oscillation be given by the equation

$$\left(\frac{\partial^2}{\partial x^2}+\frac{\partial^2}{\partial y^2}+\frac{\partial^2}{\partial z^2}\right)u=\rho(xyz)\frac{\partial^2 u}{\partial t^2}+w(xyz)\frac{\partial u}{\partial t}, \quad . \quad (1)$$

which, by writing

$$u(xyzt)=v(xyz)e^{j\omega t},$$

yields

$$\left(\frac{\partial^2}{\partial x^2}+\frac{\partial^2}{\partial y^2}+\frac{\partial^2}{\partial z^2}\right)v+\omega^2\rho\left(1-j\frac{w}{\omega\rho}\right)v=0. \quad . \quad (2)$$

Here ρ is always supposed to be positive ($\rho > 0$), Equation (2) shows that for large values of ω the term between brackets reduces to 1, provided that w/ρ is nowhere infinite. By transferring (2) to an integral equation we may even see that the necessary condition is only that w/ρ integrated over the space considered does not become infinite, though w itself might be infinite at some points.

We require a solution of (2) which satisfies certain conditions at the boundary of the space considered, *e. g.*, the Newtonian condition

$$\sigma(xyz)u+\frac{\partial u}{\partial n}=0, \quad . \quad . \quad . \quad . \quad . \quad (3)$$

where n indicates the direction, normally outward, to the aforesaid boundary.

It is known that the problem (2), (3) can only be solved for certain values of ω, the characteristic frequencies. These values of ω will be complex, with positive imaginary part, so as to cause any free oscillation once started in the system to die out after some time :

$$\omega=\alpha+j\beta. \quad . \quad . \quad . \quad . \quad . \quad . \quad . \quad (4)$$

Now from (2) we may conclude that the imaginary part β of ω will be quite negligible in amount compared with α, if $\alpha\rightarrow\infty$:

$$\lim_{\alpha\rightarrow\infty}\frac{\beta}{\alpha}=0\left(\frac{1}{\alpha}\right), \quad . \quad . \quad . \quad . \quad . \quad . \quad (5)$$

where the symbol $0(1/\alpha)$ indicates that the right-hand side vanishes as a constant independent of α multiplied by α^{-1} for $\alpha\rightarrow\infty$.

This equation (5), in combination with (2) and a formula derived by Weyl in proving Lorentz's law, enables us to calculate α and β for large values of α.

Weyl's formula for the high characteristic frequencies

of (2) if the term within brackets is replaced by 1, *i. e.*, in the case of large values of α, is

$$\lim_{\alpha_n \to \infty} \alpha_n^3 = \frac{6\pi^2 n}{\iiint_v \rho^{\frac{3}{2}}\, dx\, dy\, dz} + 0(\alpha^2 \ln \alpha), \quad . \quad . \quad (6)$$

where the integral in the denominator is to be taken over the whole space V considered, n is a large integer, indicating the (according to our assumption large) order of the characteristic frequency α, and the symbol 0 has a meaning similar to that explained above.

From (5), replacing ρ in (6) by $1 - jw/\omega\rho$ according to (2), we find

$$\lim_{\alpha \to \infty} \beta = \tfrac{1}{2} \frac{\iiint w \sqrt{\rho}\, dx\, dy\, dz}{\iiint \rho^{\frac{3}{2}}\, dx\, dy\, dz} + 0\left(\frac{\ln \alpha}{\alpha}\right). \quad . \quad . \quad (7)$$

Hence the characteristic frequencies of very large order n have an imaginary part, which asymptotically tends to become independent of n (and hence of α) and depends only on w integrated over space divided by ρ times the volume considered, if we take ρ constant. This implies that the high free modes of oscillation in our system, once started, all die out at exactly the same rate, independent of the frequency α considered.

This, as we shall see, is one fundamental part in the proof of Sabine's law.

We now turn to the second part of this proof.

Proof of Sabine's Law.

In Sabine's experiments the system is operated by a force causing a stationary state of oscillation after some time. Hence, we proceed to consider the motion of our system under such a force, which differs from the equations above, as these only express the free motion without force. Let the force acting on the system be given by

$$\mathrm{F}(xyz)e^{j\omega t};$$

then the motion of our system is given by the equation

$$\left(\frac{\partial^2}{\partial x^2} + \frac{\partial^2}{\partial y^2} + \frac{\partial^2}{\partial z^2}\right) u = \rho \frac{\partial^2 u}{\partial t^2} + w \frac{\partial u}{\partial t} + \mathrm{F} e^{j\omega t}, \quad . \quad (1\,a)$$

the solution of which, in the stationary case here considered, can be shown to be

$$u = e^{j\omega t} \sum_{n=1}^{\infty} \frac{\iiint \mathrm{F} \cdot v_n \cdot dx\, dy\, dz}{\omega_n^2 - \omega^2} c_n v_n(xyz). \quad . \quad . \quad (8)$$

Here ω_n and v_n are the characteristic (complex) frequencies of (2) and the characteristic solutions of (2) respectively. The coefficients c_n do not contain ω, the *forced* frequency :

$$-\frac{1}{c_n}=\iiint \rho v_n^2\,dx\,dy\,dz+\frac{j}{2\omega_n}\iiint w v_n^2\,dx\,dy\,dz.$$

The derivation of (8) was carried out by application of a method, due to Poincaré, which is based on Cauchy's theory of residues. This rather lengthy method had to be adopted, as the ordinary method for the derivation of development formulæ of this type which is based on a property called orthogonality of the functions v_n could not be followed, the functions v_n in systems with arbitrarily distributed absorption being no longer orthogonal to each other, as may be proved from (2).

Faber, in his paper mentioned before, gives a formula equivalent to (8), but having in our notation $\omega_n-\omega$ in the denominator and, of course, somewhat different c_n which, as in our formula, does not contain ω. As will appear shortly, this formula of Faber's is unable to give Sabine's law.

Let us perform Sabine's experiment with our system, oscillating according to (8). We have to stop the source abruptly at an instant $t=t_0$ and see how the system behaves. From this instant onwards, as no force acts, the motion of our system can be described as an infinite sum of free motions, which are solutions of (2) and (3)

$$t>t_0 : \quad u=\sum_{n=1}^{\infty} A_n v_n e^{(-\beta_n+j\alpha_n)(t-t_0)} + \sum_{n=1}^{\infty} B_n \bar{v}_n e^{(-\beta_n-j\alpha_n)(t-t_0)}, \qquad (9)$$

where $\bar{v}_n$ is the conjugate complex function to v_n. The coefficients A_n and B_n have to be determined from the state of the system at the instant $t=t_0$, *i. e.*, by u and $\partial u/\partial t$ at this instant. These quantities may be found from (8)

$$\left.\begin{aligned}(u)_{t=t_0}&=e^{j\omega t_0}\sum_{n=1}^{\infty}\frac{\iiint \mathrm{F} v_n\,dx\,dy\,dz}{\omega_n^2-\omega^2}c_n v_n(xyz)\\ \left(\frac{\partial u}{\partial t}\right)_{t=t_0}&=j\omega e^{j\omega t_0}\sum_{n=1}^{\infty}\frac{\iiint \mathrm{F} v_n\,dx\,dy\,dz}{\omega_n^2-\omega^2}c_n v_n(xyz)\end{aligned}\right\}. \qquad (8a)$$

By differentiating (9) with respect to t, taking $t=t_0$, separating the real and imaginary parts of v_n and $\bar{v}_n$ and

comparing with (8 *a*), the coefficients A_n and B_n may be written down. We need not, however, write out this calculation, as we may at once see the result.

From (8 *a*) we see that the coefficients of v_n in both series differ from zero only by an arbitrarily small quantity up to a fixed but very large index n, if we take the forced frequency ω tending towards infinity $\omega \to \infty$. This implies the same property with the coefficients A_n and B_n of (9).

By combining this result with (7) we shall prove Sabine's law. Indeed, as the series (9) for $\omega \to \infty$ in (8 *a*) contains only terms of very large order n, these terms have all the same β by (7). In other words, we see that

$$e^{-\beta t}$$

may be placed before the sigmas in (9), so that the oscillation of the system dies out at a rate proportional to the volume over the total absorption independently of the shape, the places of the source and of the experimenter.

This is essentially what Sabine found.

Extension of the Theory.

Hitherto, for purposes of generality, I have considered a quantity u described as amplitude of oscillation. Before I proceed to show with exactly what quantity u has to be identified in the acoustical case, a slight extension of the considerations just exposed will be given.

In the first place, in the acoustical case the dissipation w is not distributed over the whole space, but is substantially localized at the walls. Hence we have to see how this will alter our formulæ.

From Weyl's derivation of (6) we may conclude that replacing the boundary condition (3) by any other condition will not alter this formula. The same may be said of (7).

If w vanishes everywhere except at the walls, the rate of decay β, however, remaining finite, the space integral in the numerator of (7) has simply to be replaced by a surface integral.

By going through the derivation of (7), as exposed above, it will be perceived that it is in no step essential to consider w as independent of ω. It may, indeed contain this frequency, but it may not become infinite if $\omega \to \infty$. In other words, it may be a *bounded function of the frequency*. As will appear shortly, this extension is of great importance for the acoustical problem, for now we are prepared to consider various hypotheses regarding the nature of the absorption.

It is at once clear that there will exist continuous systems with absorption in which w, in our notation, is no bounded function of the frequency. In such systems (7) is no longer true, and hence Sabine's law cannot exist. In the course of this paper an instance of such a system will be given.

Denoting the two series in (9) by Σ_1 and Σ_2 respectively and its differential quotients with respect to the time t by Σ_1' and Σ_2', whereas the expression (8) and its differential quotient with respect to t will be denoted by Σ_3 and Σ_3' respectively, the above derivation of Sabine's law can be written symbolically

$$\left.\begin{aligned} \Sigma_1 + \Sigma_2 &= \Sigma_3 \text{ for } t=t_0, \\ \Sigma_1' + \Sigma_2' &= \Sigma_3' \text{ for } t=t_0. \end{aligned}\right\} \quad . \quad . \quad . \quad . \quad (10)$$

Now consider the system at rest and a force F, defined as above, acting on it from $t=t_1$ onwards. If this force is not concentrated at a point, as real physical forces never are, we shall have for $t=t_1$

$$u=0 \quad \text{and} \quad \frac{\partial u}{\partial t}=0.$$

The state of our system for $t > t_1$ is described by

$$u=\Sigma_1+\Sigma_2+\Sigma_3. \quad . \quad . \quad . \quad . \quad . \quad (11)$$

Taking into account the conditions for $t=t_1$, we find

$$\left.\begin{aligned} \Sigma_1 + \Sigma_2 &= -\Sigma_3 \text{ for } t=t_1, \\ \Sigma_1' + \Sigma_2' &= -\Sigma_3' \text{ for } t=t_1. \end{aligned}\right\} \quad . \quad . \quad . \quad . \quad (12)$$

Comparing (12) with (10), it follows that in the present case the coefficients A_n and B_n of (9) are numerically the same as in Sabine's case, but of *reversed sign*.

Hence, in starting a system with absorption by an oscillatory source of high frequency, the rate of increase follows the same law as the rate of decay in Sabine's experiments. Moreover, from (11) we conclude that the increase of the oscillations in the system is *complementary* to the decay, *i.e.*, the sum of the amplitudes, taken at the same t, reckoned from the moment the source stops in one and the moment the source starts in the other case, equals the stationary amplitude as given by (8).

As will be shown in the following section, this theoretical conclusion has been borne out by experiments.

In applying the foregoing theory to the acoustics of large rooms (the condition "large" implies that the first free frequency of oscillation is very small with respect to the forced frequency), it is not clear from the start which quantity to take for our u.

From the theory of acoustics it is known that in systems *without* absorption the velocity potential and the pressure are given by equations as (1) with the term containing w left out. But in extending this to equation (1) *with* absorption w we should be forced to make very special hypotheses regarding the nature of the dissipation. This applies also to the boundary condition (3). Only very special walls would satisfy this condition.

Graph 2.

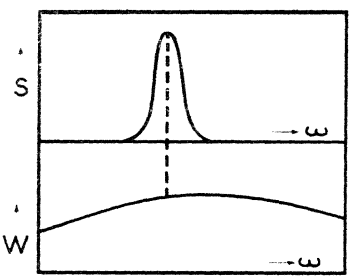

Upper part: magnitude of the terms in the series (9) as a function of ω.
Lower part: absorption w of eq. (1) as a function of ω for ω large.

In order to avoid these very narrowing and, in fact, for the present consideration not necessary restrictions, the theory has first to be extended in such way that a comparatively large degree of freedom is obtained regarding the boundary condition (3) and the function w in (1). This has been done in the foregoing section.

We may now take either the velocity potential or the pressure instead of our u, and can show from experiments that all remaining necessary conditions regarding w are fulfilled. This may be done in the following manner.

Let w be a function of ω, as in the lower part of graph 2. In the upper part of this graph, the magnitude of the terms in the series (9) is given as a function of ω. As we have

seen, all terms up to a certain ω_n in the neighbourhood of the forced frequency ω are very small. For ω_n about the same as ω they increase rapidly as a function of ω, but as the series converges they must decrease again if ω increases indefinitely. All that is required for our present consideration is that *w must be a slowly variable function of ω* as compared with the magnitude of the terms in (9) as a function of this ω. This is illustrated in graph 2. In this case, all β_n's in (9) are about of equal magnitude and our proof of Sabine's law holds.

On the other hand, if this is fulfilled we can, by measuring the rate of decay or of increase as a function of the forced frequency ω, find the absorption function w as a function of ω. Now Sabine has indeed performed such measurements, and we may see from his results that no experimental case is known where w is not a *bounded* function of ω. Reversing this reasoning, we conclude that, assuming the velocity potential or the pressure as our quantity u gives a satisfactory description of Sabine's results.

As the wave-length is in our considerations very small with respect to the dimensions of the room considered, we may treat the absorption by the walls in an elementary way, assuming an absorption coefficient A for the intensity of sound. In this way we find for w,

$$w = \frac{Ac\rho}{4},$$

where c is the velocity of sound and ρ is the same as in equation (1).

Considering the absorption of, *e. g.*, a porous wall in the way adopted by the late Lord Rayleigh, we find w to be a bounded function of ω with a maximum. Other kinds of absorption also lead to such bounded functions w, and here we have another more direct proof that the theory may immediately be applied to the acoustics of large rooms.

Special Experimental Features.

According to the formula (7), in reality Sabine's law will never be valid exactly. With given forced frequency it will be followed better if the volume increases, for then the second term on the right-hand side of (7) decreases.

It is, of course, always possible to dispose the absorbent material in such manner that Sabine's law is not followed. This occurs, *e. g.*, if the arrangement is such as to coincide with the loops and nodes of a free mode of oscillation of

frequency in the neighbourhood of the forced frequency ω. In this case the one special mode of free oscillation will decay faster than any other mode, as was shown in previous analysis *. Hence, in such a case Sabine's law cannot hold. We should always consider distributions of absorbing matter of a structure large as compared with the wave-length of the forced oscillations. From Sabine's experiments we conclude that this condition is often fulfilled in practice.

The proof given above of Sabine's law shows that the frequency remains substantially the same during the decay. This holds better, if w in graph 2 is a slower variable function of ω.

With the ear, and still better in oscillograms, we can perceive that in reality the intensity of sound at any place

Graph 3.

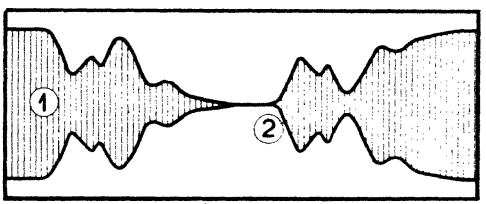

Oscillogram showing the decay of sound in a room to be exactly complementary to the increase.

does not die out in the simple exponential manner, as the above analysis seems to indicate. On the contrary, the intensity swells and decreases again more than once before it becomes inaudible. But this is exactly what equation (9) gives on a closer consideration. Although exp. $(-\beta t)$ may be placed before the sigma's, the terms under these signs are still oscillatory functions of the time. Hence their consonance, as the high free modes of oscillation lie very close together, will give large regions of interference, floating through space. What we perceive with the ear or the oscillograph is the passing of these regions.

This is illustrated in graph 3, drawn after such an oscillogram. At the point 1 the source stops, at 2 it starts again. We clearly see that the process of increase is

* *Annalen der Physik*, lxxxvii. p. 145 (1928).

complementary to the process of decrease, the duration of both being the same, as was described above *.

If we ask how to measure the duration of residual sound from an oscillogram, such as graph 3, the answer is that we have to take mean values over long intervals. The ear, recording the intensity logarithmically, is much more sensitive for small intensities than an oscillograph, and gives the ups and downs of intensity much less pronounced. Hence the process of taking mean values is much more easy to perform by the ear than from an oscillogram.

Sabine's Law in other Departments of Physics.

We have only proved Sabine's law to hold for systems the equations of which, by adopting a proper dependent variable, may be thrown in the form (1), with w a bounded function of the frequency.

In the first place, all closed electromagnetic systems belong to this type (even with w independent of the frequency). Here we may adopt any potential or field-strength function as dependent variable and always come to equation (1).

Hence the time of decay or of increase in a closed space, filled with electromagnetic radiation of frequencies all large with respect to the first characteristic frequency, is proportional to the volume over the total absorption and independent of the shape, the places of the sources and of the experimenter.

The oscillations of strings, membranes, etc. with dissipation proportional to the square of the velocity, are described by equations similar to (1). Sabine's law will be valid with these systems.

As an instance of a system which does not follow Sabine's law, we consider a column of liquid in a tube with dissipation by viscosity. Adopting Stokes's theory of viscous fluids, we have

$$\frac{\partial^2 u}{\partial t^2} = a\frac{\partial^2 u}{\partial x^2} + b\frac{\partial^3 u}{\partial x^2 \partial t},$$

where u is the velocity and a, b are constants, depending on the nature of the fluid.

* Oscillograms published by Trendelenburg (Siemens) and others do not show the exact complementary of decay and increase here described. This must, I think, be attributed to conditions not being *exactly* the same in oscillographing the decay and the increase. A series of oscillograms, taken in this laboratory by Dr. Zwikker, carefully observing the same conditions during the decay and the increase, all show the exact complementarity, which follows from the present theory.

With

$$u = v(x) \cdot e^{-j\omega t},$$

and

$$v(0) = v(l) = 0,$$

this equation yields

$$\omega = -j\frac{bn^2\pi^2}{2l^2} \pm \tfrac{1}{2}\sqrt{4a\frac{n^2\pi^2}{l^2} - \left(\frac{bn^2\pi^2}{l^2}\right)^2},$$

$$n = 1, 2, 3, 4 \ldots .$$

Hence we find that for large order n of the free oscillation considered, the imaginary part of ω increases proportional to n^2. As the asymptotic constancy (*i. e.*, independency of n) of the imaginary part of ω was necessary to prove Sabine's law (equation (7)), this law cannot hold in the present case.

Of course, other systems in which Sabine's law is not valid can be found.

The general importance of this law is, however, clear from the above considerations, showing its validity in the most common mechanic and electromagnetic systems.

Physical Laboratory of
Philips's Glowlampworks, Ltd.
Eindhoven, February 1929.

XXX. *Ionic Magnetic Moments.* *By* EDMUND C. STONER, *Ph.D.(Cambridge), Reader in Physics at the University of Leeds* *.

Introduction.

THE magnetic moment of an atom (or ion) may be calculated when its spectroscopic state is known. In many cases the normal spectroscopic state is not known from direct experiment, but it may be predicted with reasonable certainty. Of the *possible* states (determinable from the number of electrons), the deepest (corresponding to the normal state) is found with the aid of rules which were primarily suggested by the experimental facts, but which also have theoretical justification. Using this method,

* Communicated by Prof. R. Whiddington, F.R.S.

Hund calculated the magnetic moments of the rare earth ions, and obtained values which, with one exception, were in remarkable agreement with the values deduced from measurements of the susceptibility. For the ions of the first transition series, however, there was practically no agreement. This disagreement has not been removed by the more complete theory of Laporte and Sommerfeld.

A suggestion of Bose, that in the first transition series only the electron spin contributes towards the susceptibility, does give results which are in rather better agreement with experiment, but, as it stands, this suggestion cannot be regarded as completely satisfactory.

The problem arises as to why the behaviour of the ions of the first transition series and of the rare earths is different. The variability of magnetic moment is an associated problem. Although the magnetic moments of a particular ion (as deduced from susceptibility measurements on different salts, or even the same salt under different conditions) are grouped round a fairly definite value, the range in some cases is very much larger than can be accounted for by experimental errors.

These problems will be considered in this paper. Various theories which have been given will first be briefly reviewed in relation to the experimental results. A modified theory will then be put forward, which, although in some respects qualitative, does seem to remove a number of the present difficulties. The evidence for the view suggested, and some of its consequences, will be briefly discussed.

Theories.

For many "normal" paramagnetics the susceptibility varies with the temperature, over considerable ranges, according to the formula

$$\chi_M = \frac{C_M}{T-\theta}, \quad \ldots \ldots \quad (1)$$

where χ_M is the gram-molecular susceptibility and C_M the Curie constant per gram molecule. The classical Langevin-Weiss theory * then gives for the gram-molecular magnetic moment σ_M,

$$\sigma_M = \sqrt{3RC_M}.$$

* For further details see E. C. Stoner, 'Magnetism and Atomic Structure' (Methuen, 1926).

The calculated moment is usually expressed in terms of the Weiss magneton, M_W, as unit ($M_W = 1123{\cdot}5$), and is given as p Weiss magnetons:

$$p = \frac{\sigma_M}{1123{\cdot}5} = 14{\cdot}07\sqrt{C_M}. \quad . \quad . \quad . \quad . \quad (2)$$

On the quantum theory the average magnetic moment will depend on the quantum state of the atoms (or ions or molecules), and the most convenient procedure is to find an expression for p in terms of the quantum numbers defining the state. This theoretical value can then be compared with that found experimentally (or calculated directly from the experimental measurements on susceptibility by the standard method outlined above).

Following on earlier work of Pauli, Epstein, and Gerlach, Sommerfeld * calculated the p values corresponding to atoms or ions whose magnetic moments were integral multiples of the Bohr unit ($M_B = 5593$), assuming that the atoms orientated themselves in a magnetic field so that their resolved moments were the same as those of atoms in an S state, as revealed by the Zeeman effect. Let b be magnetic moment in Bohr units. (The resolved moments will be b, $b-2$, $b-4$ ... $-b$.) Then it may be readily shown that

$$p = \frac{M_B}{M_W}\sqrt{b(b+2)} = 4{\cdot}97\sqrt{b(b+2)}. \quad . \quad . \quad (3)$$

For $b = 1, 2, 3$ ... this gives $p = 8{\cdot}6$, $14{\cdot}1$, $19{\cdot}3$ ...

Assuming that for the ions with from 18 to 28 electrons b increased from 0 to 5 and then decreased to 0, the calculated values for p were found to be in rough agreement with the values found experimentally (except for the Co^{2} ion).

There was, however, no reason to suppose that the ions were always in an S state, and Hund † showed that in general the p value is given by

$$p = 4{\cdot}97g\sqrt{j(j+1)}. \quad . \quad . \quad . \quad . \quad . \quad (4)$$

where g is the Landé splitting factor and j the inner quantum number characterizing the state. This result was given before the advent of the spinning-electron theory, but it is simpler to discuss it in the light of this.

* A. Sommefeld, *Zeits. für Phys.* **xix.** p. 221 (1923).
† F. Hund, *Zeits. für Phys.* **xxxiii.** p. 855 (1925).

The total angular momentum—and magnetic moment—of an atom is a resultant of the orbital and spin moments of the electrons. In general the orbital moments may be regarded as combining to give a resultant characterized by the quantum number l ($l=0, 1, 2$ corresponding to S, P, D ... terms) and the spins to a resultant s ($s=0, \frac{1}{2}, 1, 1\frac{1}{2}$ ... corresponding to multiplicities $r=1, 2, 3, 4$ ...); j is the resultant of l and s, assuming values from $l+s$ to $|l-s|$. The spectroscopic symbol ${}^{r}\mathrm{L}j$ (*e. g.* ${}^{4}\mathrm{F}_{5/2}$) thus gives the spin moment s ($r=2s+1$), the orbital moment l (*e. g.* for F terms $l=3$), and the total moment j. The factor g may be expressed in terms of l, j, and s. An empirically correct expression for g, the ratio of the magnetic to the mechanical moment of the atom, was first given by Landé; with the assumption that the ratio of the magnetic to the mechanical spin moment is double that for the orbital moment, it has now been deduced theoretically, using the new mechanics. By Hund's method possible ${}^{r}\mathrm{L}$ states for an atom may be found by considering the resultant effect of the electrons in it, and making use of Pauli's exclusion principle. Experiment and theory * indicate that those with the highest r will be the deepest, and of these that with the highest l. In determining the j value corresponding to the deepest state (the ground state), it is taken to be the lowest j in the first half of a group and the highest in the second (corresponding to inverted multiplet intervals).

Following this procedure, and using the expression (4), Hund obtained p values which agreed closely with experiment for the rare earth ions. For the ions of the first transition group, however, the sequence of p values given by the theory was completely different from that observed.

Laporte and Sommerfeld † pointed out that if the multiplet intervals were small ($ch\Delta\nu_j$ comparable with $k\mathrm{T}$), the ions would not be all in the lower state, but that there would be a distribution of the ions among the different possible j states. They obtained the following general expression for p:

$$p=4{\cdot}97\sqrt{\left\{\Sigma(2j+1)g^2j(j+1)e^{-\frac{ch\Delta\nu_j}{k\mathrm{T}}}/\Sigma(2j+1)e^{-\frac{ch\Delta\nu_j}{k\mathrm{T}}}\right\}}. \quad (5)$$

* F. Hund, 'Linienspektren und periodisches System' (Springer, Berlin, 1927).

† O. Laporte and A. Sommerfeld, *Zeits. für Phys.* lx. p. 333 (1926).

Two limiting cases were considered:

(a) $\Delta\nu \gg kT$ ($\Delta\nu \to \infty$ or $T \to 0$)

$$p_\infty = 4{\cdot}97g\sqrt{j(j+1)}, \quad . \quad . \quad . \quad . \quad . \quad . \quad . \quad . \quad (5a)$$

(b) $\Delta\nu \ll kT$ ($\Delta\nu \to 0$ or $T \to \infty$)

$$p_0 = 4{\cdot}97\sqrt{\{\Sigma(2j+1)g^2j(j+1)/\Sigma(2j+1)\}}. \quad . \quad (5b)$$

The observed values of p should then lie between those given by ($5a$) and ($5b$). The limits are fairly wide, but some of the observed p values (for Ni^2 and Cu^2) still did not fall between them. More recently, by a process of extrapolation, Laporte * has estimated the multiplet intervals for the ions concerned and carried out a calculation of the p values, using the full expression (5). He finds that there is no agreement at all in the case of multiplet terms.

Van Vleck †, in his very complete treatment of paramagnetism on the basis of the new mechanics, obtains the same expression as ($5a$) for the case where the multiplet intervals are large. When the multiplet intervals are small ($ch\Delta\nu$ comparable with kT), he shows that the spin and orbital moments (l and s) are quantitized separately relative to the axis of the field—in small as well as large fields, by the principle of spectroscopic stability—and obtains, in place of ($5b$), the expression

$$p = 4{\cdot}97\sqrt{4s(s+1) + l(l+1)}. \quad . \quad . \quad . \quad (6)$$

The actual values differ little from those given by ($5b$).

Bose ‡ assumes that the paramagnetic susceptibility of the ions of the first transition series is due entirely to the spin moment of the electrons. The number of electrons N_l in a complete group is $2(2l+1)$. (For the first transition series the elections concerned are those for which $l=2$.) If there are Z electrons in an incomplete group in the atom, the maximum magnetic moment is $Z\mu_1$, for $Z \leqq 2l+1$; and for $Z \geqq 2l+1$ the maximum moment is $Z'\mu_1$, where $Z' = N_l - Z$. In a magnetic field Bose supposes that the possible moments for the atom with a maximum $Z\mu_1$ are $Z\mu_1$, $(Z-2)\mu_1 \ldots -Z\mu_1$, corresponding to $Z, Z-1 \ldots 0$, electrons having their spin moments parallel to the field, and the rest antiparallel; when $Z > 2l+1$ the moments range from Z' to $-Z'$ at

* O. Laporte, *Zeits. für Phys.* lxvii. p. 761 (1928).
† J. H. Van Vleck, Phys. Rev. xxxi. p. 587 (1928).
‡ D. M. Bose, *Zeits. für Phys.* lxiii. p. 864 (1927).

intervals of 2. This assumption of a variable moment of the atom due entirely to the electron spins gives the result

$$\left.\begin{aligned} p &= 4{\cdot}97\ \sqrt{Z(Z+2)} \\ \text{or} \qquad p &= 4{\cdot}97\ \sqrt{Z'(Z'+2)} \end{aligned}\right\} \quad . \quad . \quad . \quad . \quad . \quad (7)$$

If s is the resultant spin moment (corresponding to the multiplicity $r=2s+1$), this result may be written

$$p = 4{\cdot}97\ \sqrt{4s(s+1)} \quad . \quad . \quad . \quad . \quad . \quad (7a)$$

when the relation to Van Vleck's expression (6) becomes clear.

The actual result obtained is the same as that given originally by Sommerfeld (3), while the procedure followed is equivalent to stating that the ions behave magnetically as though they were in S states. It has been noted before that this is so for the ions with a smaller number of electrons*, but exceptions remain which indicate that the theory is by no means completely satisfactory empirically even for the first transition series, and no suggestion is given as to why the rare earth ions behave differently.

Comparison with Experiments.

The magnetic moments for the ions of the first transition series, calculated by the methods outlined above, are given in Table I. (The ions with 18 and 28 electrons, with a $^1S_0$ ground term, should have a zero moment, and are, in fact, diamagnetic). The observed values are also shown. (The index gives the positive charge on the ion.) It is not necessary to discuss these in detail †, but a few points may be mentioned.

With solutions, the apparent ionic susceptibility in many cases varies with the concentration. Thus with cobalt salts the p value for Co^2 varies between about 24 and 25; the addition of acid may cause the apparent p value to fall below 23. On the other hand nickel chloride, in concentrations ranging from ·62 to 22·69 per cent., gives a p value for Ni^2 constant to within about ·4 per cent., the value being practically the same for different salts. There are indications that in solutions θ (in eq. (1)) is not always zero. Birch ‡ has found for $CuCl_2$ in solution that from 0°–40°, $\theta = +10$ and $p = 9{\cdot}01$; from 40°–85° $\theta = -65$, $p = 9{\cdot}98$.

* E. C. Stoner, Phil. Mag. iii. p. 336 (1927).

† See P. Weiss, *Journ. de Phys.* v. p. 129 (1924); also 'Magnetism and Atomic Structure.' Chaps. vi. and vii.

‡ Birch, *Journ. de Phys.* ix. p. 137 (1928).

The solutions with different ions have not all been studied so thoroughly, but there can be no doubt that the apparent moment is not generally constant. The table gives a summary of the data so far available from the more precise experiments.

With solid salts the $1/\chi$, T curves are usually linear, at least over limited ranges; but where the investigations have been carried out over a large range of temperature, changes of slope or curvatures are frequently found. The procedure has usually been to consider linearity as a test for the validity of applying the Weiss-Langevin theory, or as a test for "magnetic purity"—the presence of a single carrier

TABLE I.

Calculated and Observed Magnetic Moments of Ions of the First Transition Series.

Number of electrons ...	19	20	21	22	23	24	25	26	27
Ground term	$^2D_{3/2}$	$^3F_2$	$^4F_{3/2}$	$^5D_0$	$^6S_{5/2}$	$^5D_4$	$^4F_{9/2}$	$^3F_4$	$^2D_{3/2}$
$4{\cdot}97\sqrt{4s(s+1)}$	8·6	14·1	19·3	24·4	29·4	24·4	19·3	14·1	8·6
$4{\cdot}97g\sqrt{j(j+1)}$	7·7	8·1	3·9	0	29·4	33·6	33·2	28·0	17·7
p from (5 b)	14·5	21·6	24·7	26·0	29·4	26·0	24·7	21·6	14·5
$4{\cdot}97\sqrt{4s(s+1)+l(l+1)}$.	14·9	22·2	25·8	27·2	29·4	27·2	25·8	22·2	14·9
Observed values of p. Solutions			Cr^3. 18·2–19·1	Cr^2. 23·8	Fe^3. 26–29·5 Mn^2. 29·4	Fe^2. 26·5	Co^2. 23–25	Ni^2. 16·0	Cu^2. 9–10
Solid salts.....	V^4. 8·9		Cr^3. 18·9 M^4. 19·8		Fe^3. 29 Mn^2. 27–30	Fe^2. 25–27·5	Co^2. 22–26	Ni^2. 14·5–17	Cu^2. 9–11

then being indicated. Attention has been directed more to finding linear parts of curves, and calculating p values from them, than to studying in detail divergences from the linear character. That there is definite variability of magnetic moment with different salts containing the same ion is shown by the careful experiments of Jackson*, who found, for example, the following p values for different salts of nickel, studied in the same manner :—

$NiSO_4$ $p=16{\cdot}9$,
$NiSO_4 . 7H_2O$ $p=14{\cdot}62$,
$NiSO_4 . (NH_4)_2SO_4 . 6H_2O$ $p=15{\cdot}9$.

* L. C. Jackson, Phil. Trans. A, ccxxiv. p. 1 (1923).

The apparent p value, calculated by the standard method, for the same ion in different salts may vary considerably; also the same salt may behave differently magnetically according to its thermal treatment, and give different p values over different ranges of temperature. The extensive investigation of Chantillon * on the cobaltous ion shows how widely the magnetic moment may vary (from 22 to 26).

The calculated and observed results are also shown in fig. 1. It will be seen at once that there is no question of the observed results falling even approximately on curve (2) —the Hund curve for large multiplet intervals. (It is the

Fig. 1.

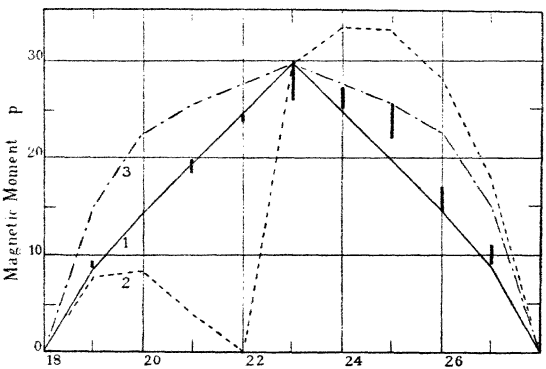

Calculated and observed magnetic moments.

Calculated { 1. ——— $p=4{\cdot}97\sqrt{4s(s+1)}$.
2. - - - - - - - $p=4{\cdot}97g\sqrt{j(j+1)}$.
3. — — — — $p=4{\cdot}97\sqrt{4s(s+1)+l(l+1)}$.

The thick vertical lines represent the range of observed values. (See Table I.)

corresponding curve which fits the results for the rare earth ions extremely well.) Moreover the observed values do not all fall between curves 2 and 3—notably Ni^2 26 and Cu^2 27. Curve 3 is that corresponding to small multiplet intervals (the Van Vleck expression is used). The suggestion

* A. Chantillon, *Annales de Phys.* ix. p. 187 (1928).

that the multiplets for the ions at the end of the series might be regular instead of inverted—so that the end part of curve (2) should be similar to the initial part—cannot be reconciled with the experimental spectroscopic facts, besides being at variance with the general theory. None of the suggestions put forward by Laporte seem adequate to explain the discrepancy.

The assumption of Bose, that only the electron spin contributes to the paramagnetism, leads to curve (1), which does agree fairly well with the experimental results; but the ions with 24 to 27 electrons certainly have moments greater than those indicated by the theory.

In short, none of the suggestions so far made seem adequate to account even qualitatively for some of the distinctive magnetic characteristics of the ions of the first transition series.

Modified Theory of Ionic Susceptibility.

Difference between ions of the two series.—For an ionic *gas* there can be little doubt that the treatment of Hund, as developed by Laporte and Sommerfeld, and by Van Vleck, is satisfactory, the p value, for large multiplet intervals, being given by

$$4{\cdot}97g\sqrt{j(j+1)},$$

and for small by

$$4{\cdot}97\sqrt{4s(s+1)+l(l+1)}.$$

That the first of these expressions gives results in agreement with experiment for the rare earth ions indicates not only that the multiplet intervals must be large, as is anticipated, but also that there is little disturbing interaction, and that the ions (in solids and solutions) behave in a magnetic field as though they were effectively independent.

In the ions of the first transition series it is the incomplete group of d electrons ($l=2$) which gives rise to the paramagnetism; in the rare earths the incomplete group of f electrons ($l=3$). The following numbers show the electronic constitution for two typical ions:—

n	1	2	3	4	5
l	0	0 1	0 1 2	0 1 2 3	0 1
Fe^3 23	2	8	8 5		
Gd^3 61	2	8	18	18 7	8

Numbers of electrons in groups in Fe^3 and Gd^3.

There is another difference besides that in the "orbital" character of the electrons in the incomplete groups. In the ions of the Fe^5 type the incomplete group of electrons belongs to the group with the highest total quantum number in the ion ($n=3$); in the ions of the Gd^3 type the incomplete group does not belong to the highest quantum number group. It is suggested that, just as it is the electrons of the highest total quantum number which are responsible for the ordinary valency properties (polar or homopolar) of atoms, so, in an ion, it is the group with the highest total quantum number which is primarily responsible for the interaction forces resulting in the formation of crystals or of aggregates in solutions.

The effect of interaction.—In an ion there is a strong interaction between the "orbital" moments of the different electrons, and also between the spin moments; these interactions between the l's of different electrons and the s's being much greater than the interaction between the l and s of a single electron. In a free ion the resultant l and s combine to give the total moment j, which is quantized with respect to an applied field. Where there is little interaction between an ion and its neighbours, in a solid or solution, the ion will still behave as "free." From a magnetic point of view an ion will behave as free if the group of electrons giving rise to the magnetic moment does not take part in the interaction. This is apparently the case in the rare earth ions.

If the magnetic group of electrons forms part of the "interacting" group, the ion will no longer behave as free. It may be anticipated that just as there is a strong l interaction between the electrons in a single atom, so there will be an l interaction between the different ions and atoms in a solid or solution. The ion may still behave as relatively free as far as the spin moment is concerned, for the "electrostatic" symmetry of an ion depends on the l moment, but not on the s moment. The suggestion is equivalent to supposing that the l moment of the ion (if this is due to electrons in the group of highest total quantum number) tends to assume a definite orientation with respect to neighbouring ions (or atoms or molecules). It would seem that this must be so in a crystal, where there is a definite arrangement of the centres of the electronic systems. Indeed, one of the main difficulties of the older theories of paramagnetic susceptibility was that they implied that the carriers of the magnetic moment were as free to change their orientation in a solid as in a gas. In a solution it might be thought that the ions had a greater

freedom for reorientation; but here the l moment of the ion may still tend to assume a different orientation with respect to the molecules or ions with which it is surrounded, even when these do not form a definite chemical complexion. In some cases there is very convincing evidence that similar associations are formed both in crystals and in solution. A study of the absorption spectra of cobalt compounds, for example, leads to the conclusion that both in solids and solutions the cobalt atom is associated with four groups in the blue compounds and with six in the red *.

It is suggested, then, that whereas in the rare earth ions there is a strong ls coupling, so that the resultant j is quantized with respect to an external field, in the ions of the transition series there may be a relatively weak ls coupling, while the l moment is subject to relatively strong interatomic coupling forces. With very strong interaction the s moment only may be quantized with respect to an external field H. The interaction field may be approximately regarded as a virtual magnetic field with direction distributed at random. The l quantization will then be with respect to the resultant of the external field and the random internal field. The limiting cases arise when the interaction field is very strong or very weak. For strong interaction

$$p=4{\cdot}97\sqrt{4s(s+1)}.$$

For weak interaction

$$p=4{\cdot}97\sqrt{4s(s+1)+l(l+1)}.$$

In general, it would be anticipated that, when there are no other disturbing factors, the observed magnetic moment would lie between these two values.

Comparison with experiment.—As may be seen from fig. 1, the observed moments generally fall between these not widely separated limits. For the ion 23, however, where there should be no variability for the reason under discussion (since $l=0$), the range is quite considerable. This is mainly due to the variation in the apparent moment of the Fe^3 ion in solution with concentration and amount of acid. The extraordinary variability in this case is probably due to chemical effects—possibly to the partial formation of complex ions of lower magnetic moment. It is noteworthy that Mn^2 23 has a remarkably constant moment. In a careful study of solutions of the chloride, sulphate, and nitrate Cabrera and his collaborators have found in each case a

* R. Hill and O. R. Howell, Phil. Mag. xlviii. p. 833 (1924).

value close to 29·35, independent of the concentration *. Bearing in mind the experimental difficulties and the uncertainty in the correction for the coexisting diamagnetism, the agreement between the observed and anticipated values is remarkably good.

Interaction equivalent to an initial virtual field.—The interaction between ions and surrounding ions and molecules is presumably of the same quantum type as that considered by Heitler and London in connexion with the formation of simple molecules. The general problem is a very complex one. It seems reasonable, however, to consider the initial interaction as similar to that resulting from an initial virtual magnetic field, with direction distributed at random. Such an assumption has proved remarkably fruitful in Kapitza's theory of the change of electrical conductivity in magnetic fields †. To see the general character of the effect of such initial field, the simplest possible case will be considered.

Consider a group of N ions, each a magnetic moment μ, and suppose that in a magnetic field the resolved moments are $\pm\mu$. Instead of supposing the initial field H_i to be distributed at random, it will be supposed to be parallel or anti-parallel to an external field H, the direction of which is taken as positive. The ions may be divided into two groups, N/2 in each, for one of which H_i is positive and for the other negative.

Let $$\mu H_i/kT = x, \qquad \mu H/kT = h.$$

The mean resolved moment may be obtained by the usual treatment:

(1) $H_i = 0$:

$$\frac{\mu}{\mu} = \frac{e^h - e^{-h}}{e^h + e^{-h}} = \tanh h \doteqdot h, \quad \mu = \frac{\mu^2 H}{kT} \quad . \quad . \quad . \quad (8)$$

(This is the well-known quantum-theory result for the case where μ is one Bohr unit. According to the classical theory,

$$\mu = \frac{\mu_c^2 H}{3kT}.$$

Thus

$$p = \frac{\mu_c}{M_W} = \frac{1}{M_W}\sqrt{\frac{3kT\mu}{H}} = \frac{1}{M_W}\sqrt{\frac{3kT\mu^2 H}{kTH}}$$

$$= \frac{M_B}{M_W}\sqrt{3} = 4{\cdot}97\sqrt{3} = 8{\cdot}6.$$

* See Weiss, *l. c.* p. 141.

† P. Kapitza, P. R. S. cxxiii. p. 342 (1929).

(2) $H=0$. Considering the two groups,

$$\frac{\bar{\mu}}{\mu}=\frac{e^{x}-e^{-x}}{e^{x}+e^{-x}}-\frac{e^{x}-e^{-x}}{e^{x}+e^{-x}}=0.$$

(3) Both H and H_i present:

$$\frac{\bar{\mu}}{\mu}=\frac{1}{N}\cdot\frac{N}{2}\left\{\frac{e^{x+h}-e^{-x-h}}{e^{x+h}+e^{-x-h}}-\frac{e^{x-h}-e^{-x+h}}{e^{x-h}+e^{-x+h}}\right\}$$

$$=\tfrac{1}{2}\{\tanh(x+h)-\tanh(x-h)\}. \quad . \quad . \quad . \quad (9)$$

For $h\ll x$ this gives

$$\frac{\bar{\mu}}{\mu}=\operatorname{sech}^2 x\times h. \quad . \quad . \quad . \quad . \quad . \quad (10)$$

For $\mu H_i<kT$, let $\phi=\mu H_i/k$. Approximately

$$\bar{\mu}\doteq\left\{1-\left(\frac{\phi}{T}\right)^2\right\}\frac{\mu^2 H}{kT}. \quad . \quad . \quad . \quad . \quad . \quad . \quad (11)$$

The expressions (9)–(11) indicate the general character of the effect of the initial field. The nature of the variation with temperature may be summarized by writing

$$\bar{\mu}=f\left(\frac{T}{\phi}\right)\bar{\mu}_0. \quad . \quad . \quad . \quad . \quad . \quad . \quad (12)$$

where $\bar{\mu}_0$ is the value when $H_i=0$. As T approaches zero, $\bar{\mu}$ approaches 0. In general $\bar{\mu}$ will be a fraction of $\bar{\mu}_0$, the fraction increasing as the temperature rises. In the limit it has the value 1. (For from (9), when x and h are both small, $\bar{\mu}/\mu\doteq\frac{1}{2}\{(x+h)-(x-h)\}=h$, as in (8)).

The general expression for the susceptibility must now be considered for the case where the ion has an s and l moment, the s moment being "free" and the l moment subject to the initial interaction field.

The Weiss-Langevin formula for the variation of the susceptibility with temperature is

$$\chi_M=\frac{C_M}{T-\theta}$$

$$=\frac{\mu_M^2}{3R(T-\theta)}=\frac{p^2 M_W^2}{3R(T-\theta)}. \quad . \quad . \quad . \quad (13)$$

Writing the quantum expression under consideration for p, this becomes

$$\chi_M=\frac{M_W^2(M_B/M_W)^2\{4s(s+1)+l(l+1)\}}{3R(T-\theta)}. \quad . \quad (14)$$

This requires modification in the light of the above view. The value of θ is not necessarily the same for the l and s moments. (θ arises from the Weiss "molecular field," which manifests itself when the substance is magnetized; that this field is a quantum interaction field has been shown by Heisenberg's treatment of ferromagnetism; it is probably related to the initial field, whose effect is represented by ϕ in (11).) Further, owing to the interaction field, the l moment may not be fully effective. The general expression may now be written:

$$\chi_M = \frac{M_B^2}{3R}\left[\frac{4s(s+1)}{T-\theta_s} + f\left(\frac{T}{\phi}\right)\frac{l(l+1)}{T-\theta_l}\right]. \quad . \quad . \quad (15)$$

If $\theta_l = \theta_s$, the expression is simplified, and p is given by

$$p = 4{\cdot}97\sqrt{\{4s(s+1) + f(T/\phi)\, l(l+1)\}}. \quad . \quad . \quad (16)$$

According to equation (15), the $\left(\frac{1}{\chi}, T\right)$ curves will not necessarily be linear, though the divergences from linearity may be relatively small if ϕ (corresponding to the l interaction field) is either very large or very small. In general the effective p value increases with the temperature, and the $\left(\frac{1}{\chi}, T\right)$ graph will show a curvature with the concave side towards the T axis. This type of variation is frequently found. As the results for the nickel and copper ions have not fitted in with previous theories, some of the results given by Weiss for these may be quoted. The measurements of Théodoridès on nickel chloride give $p = 16{\cdot}03$ between 15°·2 and 125°, and $p = 16{\cdot}92$ between 150° and 500°. Honda and Ishiwara find $p = 9{\cdot}2$ for $CuCl_2$ between $-140°$ to $+20°$, and $p = 10{\cdot}0$ from 20° to 500°. More recently Birch has found that $CuSO_4$ gives a non-linear curve between 10° and 537°—a curvature which is compatible with an s moment corresponding to $p = 8{\cdot}6$, and a partly effective l moment. The copper salts generally, with moments between 9 and 11, fit in well with the theory put forward, which gives 8·6 and 14·9 as the limits; moments from 14·5 to 17 are observed for nickel, the theory giving 14·1 and 22·2 as limits.

In the region of very low temperatures, the $\left(\frac{1}{\chi}, T\right)$ curves frequently show peculiar curvatures, indications of "cryomagnetic anomalies." A qualitative explanation of these has been given by Foëx * on a non-quantum theory which

* G. Foëx, *Ann. de Phys.* xvi. p. 174 (1921).

simply assumes the existence of a potential energy depending on the orientation of the magnetic carrier with respect to the crystal lattice. This theory may obviously be brought into relation with the assumption of an initial field.

It should, perhaps, be noted that the "initial" field has been taken to modify the effective l moment, having no effect on the s moment; this simply means that it has been assumed that there is a strong l interaction. As the s moment is a intrinsic property of the electron—in contradistinction to the l moment, which has reference to a nucleus or aggregate of nuclei—the s interaction will presumably be weak, though not necessarily non-existent. There may, therefore, be an initial field for the s moment, which, though small, may be effective at low temperatures in disturbing the susceptibility from its ideal value. This must be borne in mind in any more detailed consideration of cryomagnetic anomalies.

Complex salts.—Following Sidgwick, for a typical complex ion, it is possible to assign an effective atomic number to the central atom. The magnetic moment depends on the effective atomic number, which gives the number of electrons associated with the central atom. Let Z be the effective atomic number. When Z=36, the substance is diamagnetic (as in cobaltammines), 36 electrons presumably giving the argon configuration. The following p values have been found:

Z	32	33	34	35
p (obs.) ...	24	17–21	13–15	9–10

There is difficulty in interpreting these results, because it is not known how the Z electrons are distributed. The 33 configuration, for example, may consist of a closed group of 30, with $3p$ electrons ($n=4$, $l=1$) giving a $^4S_{3/2}$ ground term, or of a closed group of 18, an incomplete group of $7d$ electrons ($n=3$, $l=3$), and a closed group of 8 ($n=4$, $l=0, 1$), giving a $^4F_{9/2}$ ground term. For $[Fe(N_2H_4)_2]Cl_2$, with Z=32, Ray and Bhar * have found $p=24{\cdot}1$. If there are $2p$ electrons, in addition to closed groups, the corresponding ground term $^3P_0$ gives the limits as 14·1–15·8; with $6d$ electrons ($^5D_4$) the limits are 24·4–27·2. This suggests that it is the $n=3$ group which is incomplete. The experimental data available, however, are not sufficient to decide between the various possibilities, and, although the problem of the complex ions is an interesting one, it would not be profitable to discuss it further at present.

* See D. M. Bose, *Zeits. für Phys.* xliii. p. 878 (1927).

The gyromagnetic effect.—The theoretical ratio of the magnetic to the mechanical moment of a carrier is $\frac{e}{2mc}g$. The experimental ratio is found to be $\frac{e}{mc}$, so that $g=2$. It has been pointed out by Bose * that this is in agreement with the view that the electron spin is responsible for the magnetic effects. It is important to notice that the ratio has been measured only for ferromagnetic rods. If the ratio could be measured for paramagnetic salts, a different ratio would be anticipated for all those salts where the magnetic moment differs from that calculated, using the formula

$$p=4{\cdot}97\sqrt{4s(s+1)}.$$

It is of interest to consider the significance of the value $g=2$ found for ferromagnetics. It does not indicate, as has been stated, that the ratio measured is that for the free electrons in the metal—for these alone give rise to only a small, approximately constant paramagnetism, as has been shown by Pauli. It simply indicates that it is the electron-spin moment which is responsible for the magnetic properties. If this is so, the atomic moments must be integral multiples of the Bohr unit ($s=\frac{1}{2}$, 1, $1\frac{1}{2}$ ..., corresponding to $b=1$, 2, 3, ...). It has been shown by the writer † that the moments deduced from measurements of the low-temperature saturation intensity are compatible with this. As an example, in nickel, it is is supposed that in each group of 5 atoms there is one (Ni^0) with a moment of 2 Bohr units, one (Ni^1) with a moment 1, and three (Ni) with zero moment, the low-temperature p value (3) is accounted for

$$p=5\bar{b}=5\times\frac{1+2}{5}=3.$$

The paramagnetic susceptibility above the Curie point is accounted for by the same group of ions if Ni^2 and Ni^1 are assumed to have the same p values as those found for the ions with the same number of electrons in salts and solutions ($p=16$ for Ni^2, $p=9$ for Ni^1). This means that at the high temperatures the l moment is partly effective, but that at low temperatures—when the internal field exerts a greater effect—only the s moment is effective. This view as to the atomic moments of ferromagnetics thus fits in with

* Bose, *loc. cit.* p. 881.

† E. C. Stoner, Proc. Leeds Phil. Soc. i. p. 55 (1926).

the gyromagnetic effect, and also with the view here put forward as to the partial independence of the l and s moments; the s moment being primarily effective at low temperatures, and the l moment becoming increasingly effective at higher temperatures.

Summary.

Previous theories of ionic magnetic moments are briefly reviewed in relation to the experimental results.

The difference in the magnetic behaviour of the first transition series of ions and the rare earth series is attributed to the fact that in one the incomplete group of electrons belongs to the group of highest total quantum number, in the other to an "inner" group, and that interaction between an ion and its neighbours (in solids and solutions) affects mainly the electrons of highest quantum number.

Magnetically the rare earth ions behave as free, and have a moment, expressed in Weiss magnetons, given by

$$p=4{\cdot}97\,g\,\sqrt{j(j+1)}.$$

In the first transition series the orbital moment l and the spin moment s must be considered separately. The l moment is not fully effective, owing to the interaction field. This is treated as equivalent to an initial magnetic field, and the general character of its effect on the measured susceptibility is considered. It is shown that the p value should lie between

$$4{\cdot}97\,\sqrt{4s(s+1)} \quad \text{and} \quad 4{\cdot}97\,\sqrt{4s(s+1)+l(l+1)},$$

according to the interaction, tending to the former value at low and the latter at high temperatures. The scheme covers the experimental results very satisfactorily.

Complex ions are briefly discussed.

It is shown that, for ferromagnetics, the observed gyromagnetic ratio and the atomic moments deduced from measurements, both at low and high temperatures, are consistent with the scheme.

Physics Department
University of Leeds,
April 1929.

XXXI. *On the Derivation of the Law of Mass Action.*

To the Editors of the Philosophical Magazine.

GENTLEMEN,—

MAY I again point out, as I did in a previous letter *, that a fundamental condition of the van't Hoff cycle, which Mr. Goldstein entirely ignores in the first and the preceeding communication, is that, on removing a small quantity of matter from one of the reservoirs through a membrane, the pressure of the removed matter does not change during the process. It may be added that we are quite at liberty to have such an arrangement, and that we may assist in bringing it about, if we like, by the permanent addition of various substances in various states to the reservoirs. In that case, when a small quantity of matter is removed from a reservoir, the free energy of the system remains constant, while the work performed is of the form volume × pressure. The former result is used when the free energy is equated to zero in the van't Hoff cycle, while the latter result is used when the external work done is equated to zero.

Now Mr. Goldstein states, in the preceding communication than when "sepro-unstable" molecules are removed from a reservoir these undergo a change in free energy. Quite so, but since we have arranged that the free energy of the whole system is to remain constant, it follows that an equal and opposite change in free energy takes place in the reservoir from which the molecules were removed.

It may also be pointed out that, on simultaneously removing complex molecules from a reservoir and adding the equivalent simple molecules, and *vice versa*, the condition that the change in free energy shall be zero is satisfied in a simple manner.

Mr. Goldstein next proceeds to show how van't Hoff's law may be derived by means of imposed conditions contained in brackets under option (1). Now the law of mass action in the orthodox form has been obtained by means of a van't Hoff cycle supposing that the "sepro-unstable" molecules do not dissociate; but since there was no justification for this

* Phil. Mag. vii. p. 206 (1929).

assumption, some scientists supposed that the molecules are prevented from dissociating by some externally applied constraint. The two Mr. Goldstein mentions have already been used *; another that has been used consists of the introduction of a catalytic agent into the transferring chamber, where it is supposed to prevent dissociation taking place. Now the object of the paper I have published † was to see what result is obtained if no assumptions are introduced, or no constraints are applied to prevent molecular dissociation, keeping the conditions and process of the cycle otherwise the same; in other words, allowing the molecules to behave just as they please. It was found that these two different methods of procedure led to different results. There can be no question, however, about my procedure being the proper one. If it were permissible to prevent molecules dissociating by an applied external constraint, it would be equally permissible to induce the simple molecules to form various complex molecules by an external constraint while being transferred from one chamber to the other.

It is quite natural, therefore, that Mr. Goldstein should obtain the law of mass-action in the orthodox form on imposing the constraints or conditions he mentions. (It may be pointed out in passing that the first condition would not permit the process to be isothermal.) Furthermore, it is to be expected that since the two processes lead to different results, on using them together many apparent violations of the laws of thermodynamics would be obtained. They show that *it is not permissible to subject the chemical behaviour of molecules to an arbitrary constraint in an arbitrarily selected part of the van't Hoff cycle.*

Since κ_1 and κ_2, which control the chemical effectiveness of collisions, express the activation the colliding molecules have acquired through previous collisions, it surely follows simply enough that they may be functions of the independent variables of the system if all possibilities are taken into account. The activation imparted to a molecule by a collision may decrease before the next collision takes place, and the foregoing quantities are therefore functions of the temperature and the molecular free paths, or of the temperature and the molecular concentrations, where the form of the function depends on the rate of decrease of the activation. Since the concentrations are functions of the masses of the constituents

* 'Theoretische Chemische,' by W. Nernst, p. 677 (7th ed.).
† Phil. Mag. v. p. 263 (1928).

and the volume, it follows that, on taking all possibilities into account, κ_1 and κ_2 may be functions of these quantities and the temperature.

I have nowhere tried to disprove the equation following equation (12) in Mr. Goldstein's communication, as he states.

From the last but one of the equations developed by Mr. Goldstein it follows that

$$\frac{\kappa_1}{\kappa_2} = \frac{\alpha_{ce}^2}{\alpha_{e_2}\,\alpha_{e_2}}.$$

Now I fail to see that any simple relation exists between the κ's and the α's, whether we regard the latter as activities or activity coefficients. Evidently they cannot be identical. Without introducing any assumptions, we may write $\kappa_1 = \alpha_{ce}^2 . \phi$, $\kappa_2 = \alpha_{c_2}\alpha_{e_2} . \phi$, where ϕ is an arbitrary function of the coefficients, but these are far from being simple results.

Yours faithfully,

Schenectady, N.Y., U.S.A. R. D. KLEEMAN.

XXXII. *Notices respecting New Books.*

Heat and Thermodynamics. By J. K. ROBERTS, Ph.D. (Blackie and Son, Ltd., 50 Old Bailey, London. Price 30*s.* net.)

THE need of an advanced text-book for students taking higher University Courses in Physics has been met by the publication of this volume in the Student's Physics series. Dr. Roberts has paid particular attention to the experimental side of the subject and has incorporated many of the results of recent researches on gas thermometry, the specific heat and thermal conductivity of gases, the latent heat of fusion of metals, and the author's measurement of the expansion of bismuth crystals. Under radiation, the laws of Stefan and Wien and Planck's radiation formula are derived, with an account of the experiments verifying these theoretical results. The close agreement between experiment and the values calculated from Debye's law is shown in the case of aluminium in a table from a paper of Schrödinger's. Among the many references to the pages of this Magazine, the work of Millikan on the electron charge, of Brønsted and Hevesy on the isotopes of mercury, of Egerton on the vapour-pressures of metals, and the virial law of Clausius may be mentioned. In an appendix are set out the most important thermodynamic

relations, the properties of steam and, in connexion with refrigeration, the Mollier diagram for carbon dioxide. Dr. Roberts has given a clear and interesting presentation of the subject and has successfully accomplished the task of providing an excellent book for the guidance of those interested in this branch of physical science.

The Quantum and its Interpretation. By H. Stanley Allen, M.A., D.Sc. (Methuen and Co. Ltd., 36 Essex Street, London, W.C. 2. Price 13*s.* 6*d.* net.)

In this book, based largely upon lectures delivered to advanced students in the University of St. Andrews, Prof. Allen traces the growth and development of the quantum theory. The introductory section gives a review of the problems to which the theory has been applied and which has led to results of such importance. In addition to the quantum theory of line spectra, other applications are discussed in connexion with atomic magnetic properties, and the theory of spatial quantization of Sommerfeld and Debye confirmed by the experiments of Gerlach and later workers. Other investigations, not directly related to the Bohr theory, are described: Whittaker's four-dimensional tubes of force and their relation to the quantum theory and the character of the quantum; and the properties of magnetic tubes in rotation and the possible connexion between these rotating tubes and electrons, each quantum tube regarded as a potential atom. The final part of the book gives a survey of the recent developments of the quantum theory, with brief outlines of the new quantum mechanics and of the possible interpretations of the quantum. For more detailed information references are given to the works of Max Born, Jeans, Sommerfeld, Stoner, and others.

Infra-red Analysis of Molecular Structure. By F. I. G. Rawlins and A. M. Taylor. (Cambridge University Press. Price 10*s.* 6*d.* net.)

This, the first volume of the Cambridge Series of Physical Chemistry, is a welcome addition to the somewhat meagre literature of this branch of Physical Chemistry. The authors have placed investigators of molecular physics under an obligation by reviewing in detail the recent researches in this difficult field and bringing together a mass of information drawn very largely from papers contributed to German and American journals. No book in English deals with the applications of infra-red spectroscopy to the analysis of molecular structure. The contributions from English sources are almost entirely confined to the work carried out in the Cambridge Laboratory of Physical Chemistry by Mr. Rawlins and Dr. Taylor and by Dr. Rideal, who has written an introduction

to this book. In addition to the chapters dealing with the experimental researches on gases, liquids, and solids, and the all-important subject of technique, a section is devoted to the wave-mechanics of Schrödinger as applied to the special problems of infra-red spectroscopy. Attention is drawn to a number of outstanding problems which offer attractive fields of inquiry into crystalline and molecular structure.

Wave-Mechanics. By H. T. Flint, Ph.D., D.Sc. (Methuen and Co. Ltd., 36 Essex Street, W.C. 2. Price 3*s.* 6*d.* net.)

Dr. Flint has provided students of Modern Physics with a useful introduction to the Wave-Mechanics of de Broglie and Schrödinger. The analogy between the variation principles of Maupertius and Fermat suggested a method of describing mechanical processes by the theory of wave-motion, that a wave-motion is inseparable from the mechanical motion of a material particle. The Schrödinger equation is applied to the Planck oscillator, the rotator with fixed and with free axis and the hydrogen atom. The wave-equation for the determination of energy-levels in the hydrogen atom can be solved in terms of the confluent hypergeometric function.

In the chapter on the evidence for the existence of mechanical waves are described the remarkable experiments of Davisson and Kunsman on the scattering of electrons by metals, of Dymond on the scattering by helium, of G. P. Thomson on the behaviour of cathode rays after passage through thin metal films. The interpretations of the wave function due to Schrödinger and to Born and Heisenberg are given in the final chapter. The list of references to recent contributions, mathematical and experimental, will be of service for a deeper study of this subject.

XXXIII. *Proceedings of Learned Societies.*

GEOLOGICAL SOCIETY.

[Continued from p. 136.]

June 12th, 1929.—Prof. J. W. Gregory, LL.D., D.Sc., F.R.S., President, in the Chair.

Dr. E. Mackenzie Taylor (School of Agriculture, University of Cambridge) delivered a lecture on Base Exchange and its Bearing on the Formation of Coal and Petroleum.

The lecturer said that the discovery of a bed of vegetable débris containing both peat and fusain under a layer of alkaline soil in

Egypt led to the investigation of the effects of the presence of sodium-clay upon the decomposition of organic matter by bacteria. The alkaline soil was shown to be a sodium-clay produced by base exchange between the clay and solutions of sodium chloride. The properties of the sodium-clay were discussed, and it was shown that, as the result of hydrolysis, a continuously alkaline medium under anaërobic conditions was produced. In this medium continuous bacterial action is possible, as the acidic products of such action do not accumulate. The residue of such a decomposition is a reduced product. Lignocellulose decomposes under these conditions, yielding a material with fusain properties. The decomposition of proteins and fats takes place in the alkaline medium, and, in addition, it has been found possible to decompose free organic acids by bacteria under these conditions. The examination of coal-seam roofs showed that they had undergone base exchange and hydrolysis. The cap-rocks of petroliferous strata also contain sodium-clay as the main clay type. It was shown that the roofs of coal-seams, irrespective of geological age, have undergone base exchange, and could have supplied an alkaline medium under anaërobic conditions in which the continuous decomposition of organic matter by bacteria would have been possible. The materials classed as brown coals and lignites occur under a calcium-clay roof. Owing to the slow rate of hydrolysis of calcium-clay, the production of a continuously alkaline medium under a calcium-clay roof was impossible.

It was suggested that coal and petroleum have both resulted from the decomposition of organic matter by bacteria, under the alkaline anaërobic conditions provided by strata which have undergone base exchange with solutions of sodium salts and subsequent hydrolysis in fresh water. The conditions provided by such strata are favourable to continuous bacterial action, to the elimination of oxygen from the material, and to the accumulation of the decomposition-products as the result of the sealing of the organic deposit.

[*The Editors do not hold themselves responsible for the views expressed by their correspondents.*]

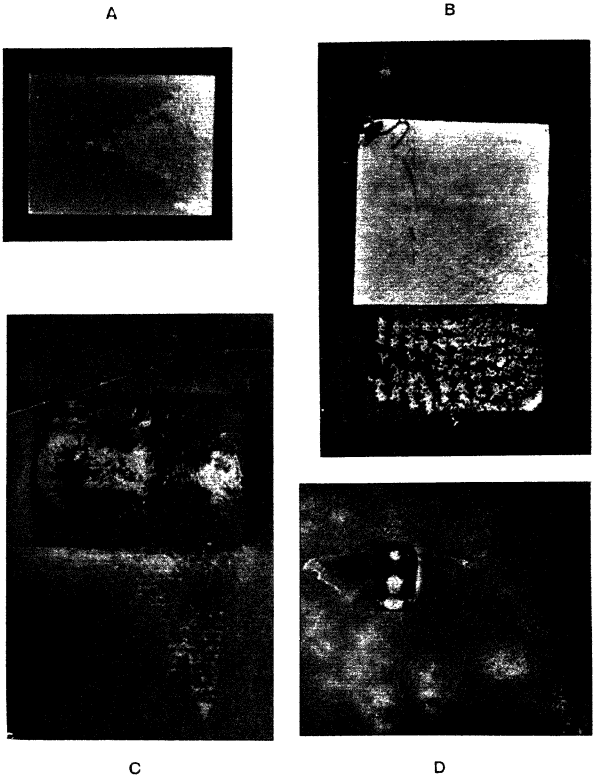

Dust-figures. Field parallel to E axis.
Longitudinal vibrations.

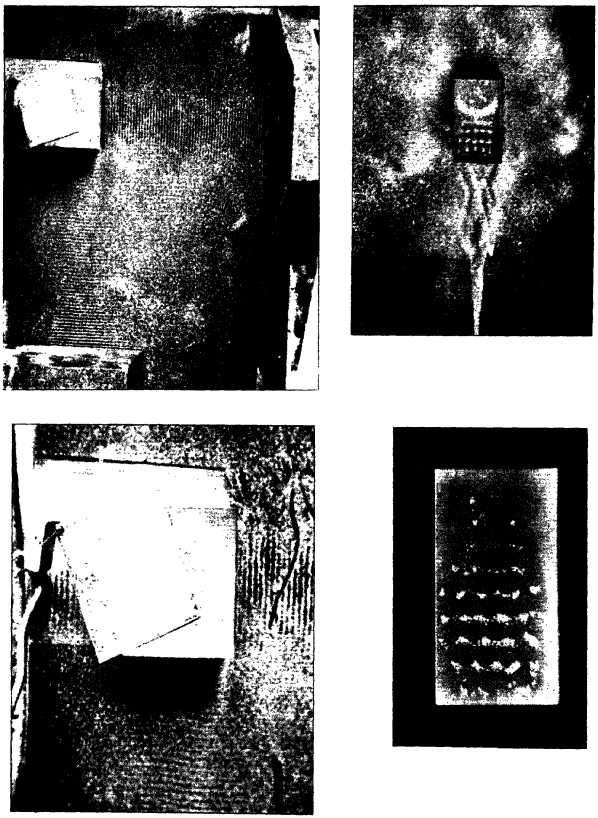

Dust-figures. Field parallel to E axis.
Transverse vibrations.

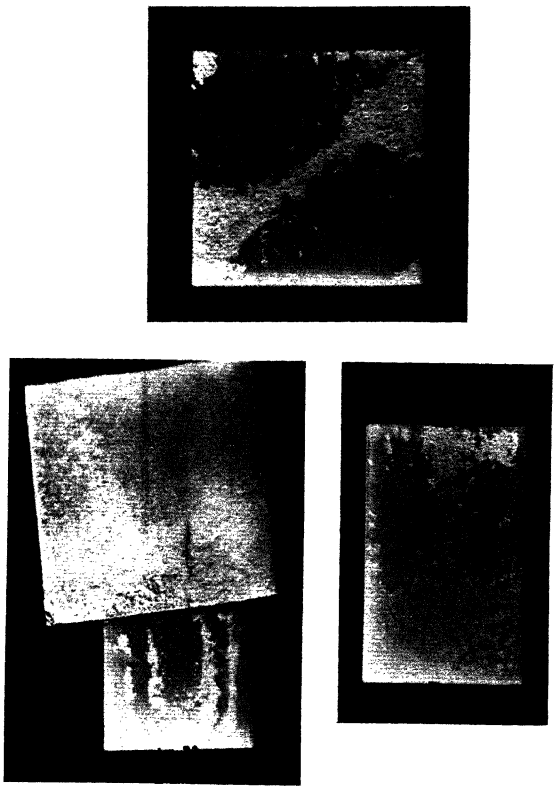

Dust-figures. Field parallel to B axis.
Longitudinal vibrations.

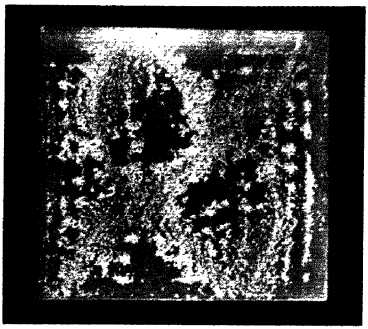

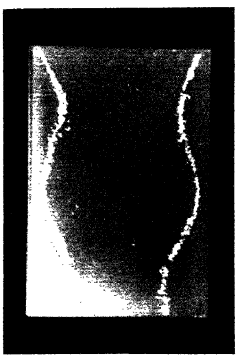

Dust-figures. Field parallel to B axis.
Transverse vibrations.

A

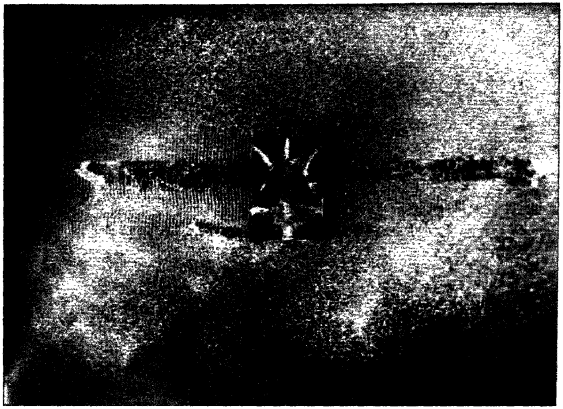

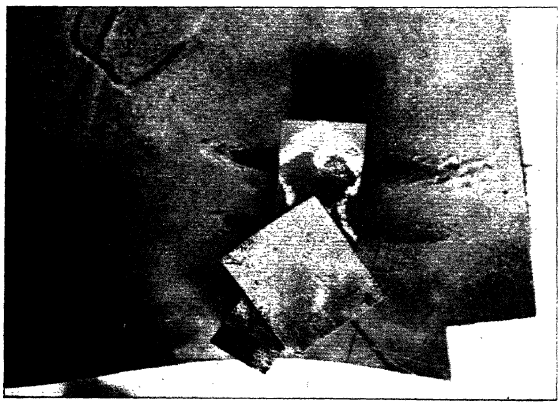

B

Dust-patterns showing air-streams and standing waves.

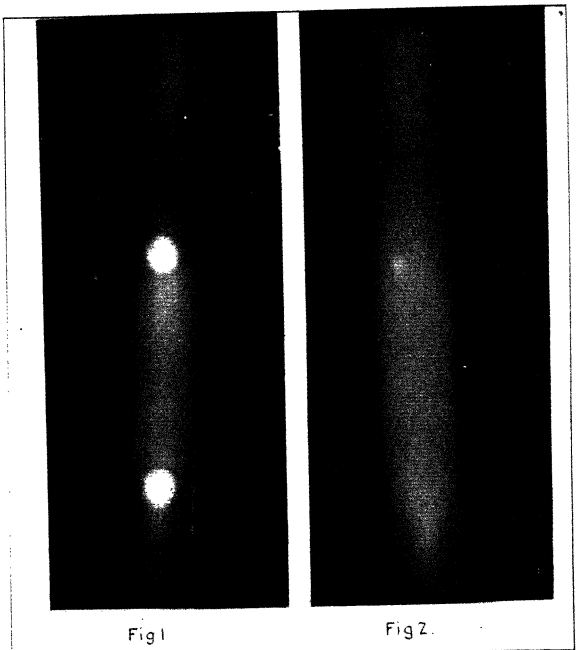
Fig 1
Fig 2.
4119
4138
Co 4273
O II 4319
O I 4368
O II 4417
? 4474
4523
Co 4542
Co 4587
4641
O II 4650
Co 4716

Fig 3.

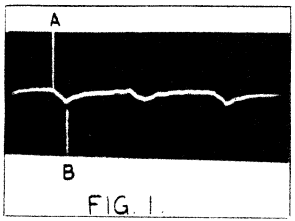

FIG. 1.

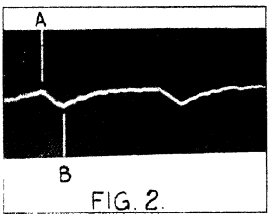

FIG. 2.

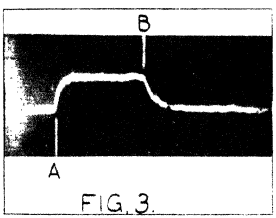

FIG. 3.

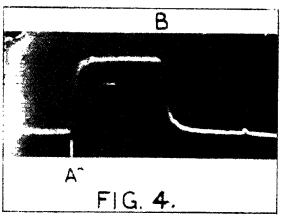

FIG. 4.

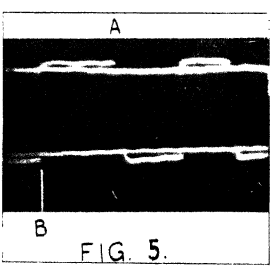

FIG. 5.

THE

LONDON, EDINBURGH, AND DUBLIN

PHILOSOPHICAL MAGAZINE

AND

JOURNAL OF SCIENCE.

[SEVENTH SERIES.]

SEPTEMBER 1929.

XXXIV. *The Hall Effect, Electrical Conductivity, and Thermoelectric Power of the Copper-Tin Series of Alloys.*

By EMLYN STEPHENS, *M.Sc., Physics Department, University College of Swansea* *.

Introduction.

THE Hall effect, electrical conductivity, and thermoelectric power of the copper-tin series of alloys have been determined with the object of comparing the curves showing the relation between these properties and composition of the alloy with the curves already obtained for the copper-antimony alloys †. The curves showing the relation between the electrical property and the composition of the alloy generally furnish singular points corresponding to compounds formed of the two metals. Two compounds, Cu_2Sb and Cu_3Sb, are formed of the two metals Cu and Sb, while Cu_3Sn and Cu_4Sn are considered to be the compounds formed of the metals Cu and Sn. The crystal structure of Cu_3Sn and Cu_4Sn has been examined by Westgren and Phragmén ‡. Cu_4Sn was found to have a face-centred cubic structure, with 416 atoms in the unit cell, while Cu_3Sn has an hexagonal

* Communicated by Prof. E. J. Evans, D.Sc., University College of Swansea.

† Stephens and Evans, Phil. Mag. vol. vii. Jan. 1929.

‡ *Zeits. für Metallkunde*, Sept. 1926.

close-packed structure. Jones and Evans * examined the structure of Cu_3Sn and Cu_3Sb, and their results for the Cu_3Sn were in very close agreement with the other workers. They found that the structure of both Cu_3Sn and Cu_3Sb was hexagonal close-packed, with the same axial ratio.

The electrical properties of metals and alloys depend on their physical state. In the present experiments the electrical resistivity was determined for the alloys after preparation, and was afterwards redetermined for each alloy after annealing at a suitable temperature. This was repeated until further annealing produced no change in the resistivity. The temperature coefficient of resistance, Hall effect, and thermoelectric power were then determined for the alloys in the final state.

The curve showing the variation of the electrical conductivity with the composition of the copper-tin series of alloys has been obtained by Lodge †, Matthiessen ‡, and Ledoux §, and singular points were obtained corresponding to Cu_3Sn and Cu_4Sn.

Experimental Work.

The copper used for making the alloys was of electrolytic origin, while the Chempur tin contained ·0115 per cent. impurities. The impurities were copper ·0005 per cent., lead ·003 per cent., bismuth ·0005 per cent., antimony ·0055 per cent., and iron ·0020 per cent. The alloys were chill cast in an iron mould in the form of plates, about 15 cm. long, 3·0 cm. wide, and ·4 cm. thick. The alloys near the compounds were very brittle, and plates were difficult to prepare, so that in most cases the mould was heated before pouring the alloy. All the alloys were approximately uniform, and the mean values of their dimensions, determined at regular intervals along them, were taken. The plates of alloys near the ends of the series could be machined, so that thin plates in a convenient form for determining the Hall coefficient could be obtained.

In these experiments plates were cast of the following percentage composition by weight :—(1) 90 per cent. Cu, 10 per cent. Sn ; (2) 80 per cent. Cu, 20 per cent. Sn ;

* Phil. Mag. vol. iv. Dec. 1927.
† Phil. Mag. vol. viii. p. 554 (1879).
‡ Landolt Bornstein, vol. ii. p. 1058.
§ *Comptes Rendus*, vol. clv. (1912).

(3) 72·8 per cent. Cu, 27·2 per cent. Sn (Cu_3Sn); (4) 68·1 per cent. Cu, 31·9 per cent. Sn (Cu_4Sn); (5) 65 per cent. Cu, 35 per cent. Sn; (6) 61·6 per cent. Cu, 38·4 per cent. Sn (Cu_3Sn); (7) 57·2 per cent. Cu, 42·8 per cent. Sn (Cu_3Sn_2); (8) 34·8 per cent. Cu, 65·2 per cent. Sn (CuSn); (9) 100 per cent. Sn.

The same plate of an alloy of given composition was used in the determination of all the electrical properties.

(1) *Electrical Resistivities and Temperature Coefficients of Resistance of the Alloys.*

The electrical resistivity was determined by fixing a plate of the alloy across two knife-edges, and determining

TABLE I.

Composition of alloy.	Resistivity before annealing, in microhms per cm.³ at 0° C.	Resistivity after annealing, in microhms per cm.³ at 0° C.	Annealing temperature in ° C.
100 % Sn ...	11·1	—	—
(*a*) $SnCu_4$ (34·8 % Cu) ...	11·3	10·95	155
(*a*) Sn_2Cu_3 (57·2 % Cu) ...	9·12	8·93	180
(*a*) $SnCu_3$ (61·6 % Cu) ...	10·5	8·72	565
(*b*) $SnCu_3$ (61·6 % Cu) ...	11·3	8·67	565
(*a*) 35 % Sn, 65 % Cu ...	10·2	26·0	565
(*a*) $SnCu_4$ (68·1 % Cu) ...	48·5	47·8	565
(*a*) $SnCu_3$ (72·8 % Cu) ...	37·5	35·8	500
(*a*) 20 % Sn, 80 % Cu ...	24·8	25·2	500
(*c*) 10 % Sn, 90 % Cu ...	13·1	15·0	750
100 % Cu ...	1·59	—	—

(*a*) Annealed in coal-gas.
(*b*) ,, ,, vacuum.
(*c*) ,, ,, nitrogen.

the resistance of a known length by means of the Kelvin Bridge. All determinations were made at 0° C., and the values of the resistivities in the initial and final states of the alloy are given in Table I. and Graph I.

The mean temperature coefficient of resistance over the range of temperature between 0° C. and 100° C. was determined for each alloy in its final state, and these results are

given in Table II. and Graph II. The resistivity determinations have been made with an accuracy of about $\frac{1}{3}$ per cent. The larger temperature coefficients of resis-

GRAPH I.

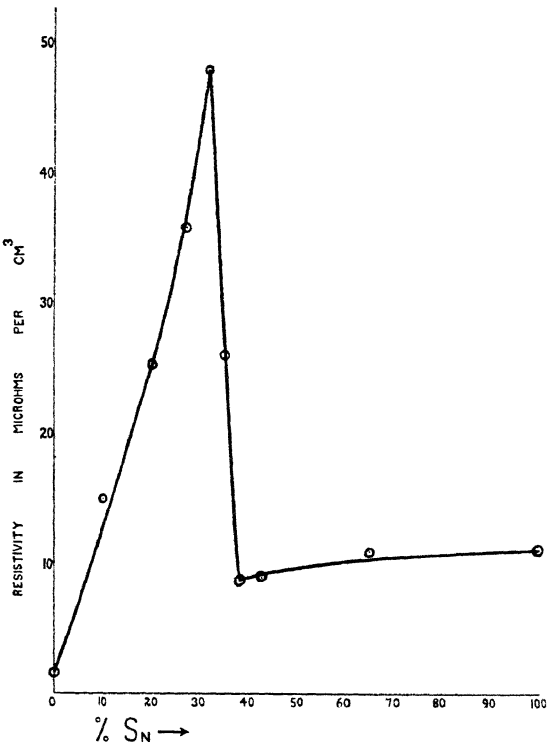

tance have been determined within approximately $\frac{1}{3}$ per cent., while the low values for the alloys in the region between Cu_3Sn and 90 per cent. Cu, 10 per cent. Sn are accurate to within 2 per cent.

TABLE II.

Composition of alloy.	Mean temperature coefficient of resistance between 0° C. and 100° C. × 10^4.
100 % Sn	43·3
SnCu (34·8 % Cu)...	36·3
Sn_2Cu_5 (57·2 % Cu).	34·3
$SnCu_3$ (61·6 % Cu) .	35·3
35 % Sn, 65 % Cu	13·0
$SnCu_4$ (68·1 % Cu) .	5·72
$SnCu_5$ (72·8 % Cu) .	5·88
20 % Sn, 80 % Cu	5·74
10 % Sn, 90 % Cu	6·25
100 % Cu	43·5

GRAPH II.

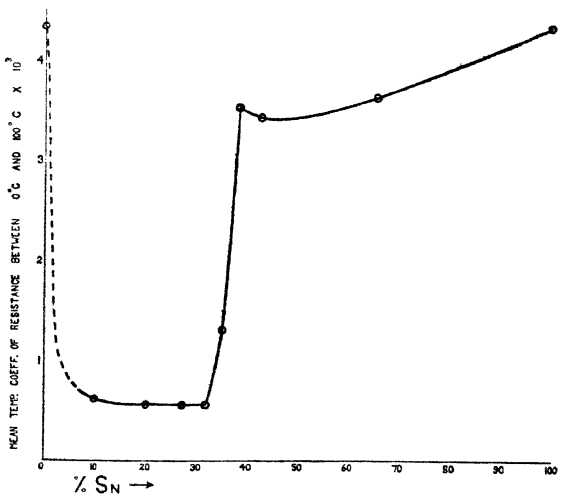

(2). *Thermoelectric Power of the Alloys.*

The thermoelectric properties of the alloys were examined with copper leads soldered to the ends of the plates. The copper-alloy junctions were enclosed in two jackets, by means of which one junction could be kept at the temperature of steam and the other at the temperature of running tap-water. Repeated determinations of the thermo-E.M.F. of the copper-alloy couples over this range of temperature were made by means of a Tinsley vernier potentiometer. The determinations of the thermo-electric power in micro-volts per degree centigrade when

TABLE III.

Composition of alloy.	Thermoelectric power with respect to Cu, in microvolts per degree centigrade.	Thermoelectric power with respect to Pb, in microvolts per degree centigrade.
100 % Sn	— 3·28	— ·12
SnCu (34·8 % Cu) ...	— ·75	+ 2·41
Sn_2Cu_5 (57·2 % Cu)...	— ·269	+ 2·89
$SnCu_3$ (61·6 % Cu) ...	+ ·06	+ 3·22
35 % Sn 65 % Cu	— ·612	+ 2·55
$SnCu_4$ (68·1 % Cu) ...	— 2·99	+ ·17
$SnCu_5$ (72·8 % Cu) ...	— 2·72	+ ·44
20 % Sn 80 % Cu	— 2·06	+ 1·10
100 % Cu ...	0	+ 3·16

The thermoelectric power is considered + ve if the potential of the cold copper-alloy junction is positive with respect to the hot junction.

the temperature of the cold junction was varied over a range of several degrees were in good agreement, so that the relation between E.M.F. and temperature was probably linear between room-temperature and 100° C.

The thermoelectric power of the alloys with respect to copper are given in Table III. and Graph III. The thermoelectric power of copper with respect to lead was also determined, and the calculated thermoelectric powers of the alloys with respect to lead are given in Table III. The determinations are made with an accuracy of about 1 per cent.

(3) *Hall Effect of the Alloys.*

When a metal plate conveying an electric current is placed in a magnetic field, so that the lines of force are normal to the conducting plate and to the direction of flow of the electric current, a transverse galvanomagnetic

GRAPH III.

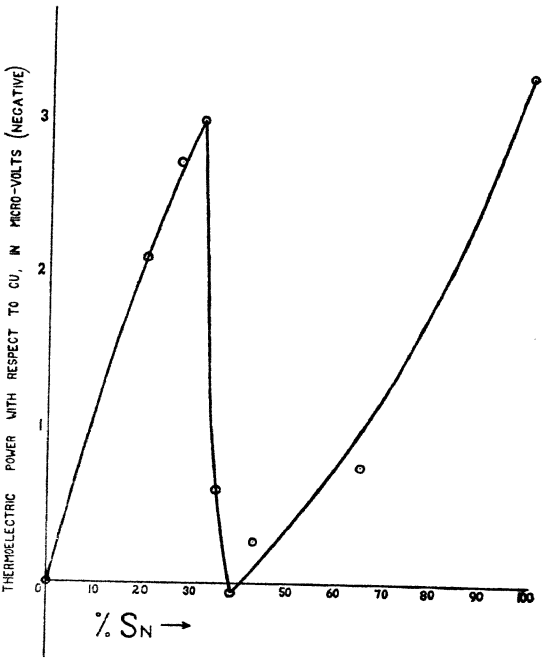

potential difference is set up between the edges of the plate.

It has been proved experimentally that for a given metal the Hall P.D. denoted by E is given in abs. units by the formula

$$E = \frac{RHI}{d},$$

where H is the magnetic field in gauss, I is the current in abs. units, d is the thickness of the plate in cm., and R is the Hall coefficient.

This coefficient R depends on the temperature, and, for some metals, on the intensity of the magnetic field as well.

It is of importance to note that the effect has different signs in various metals, and the convention with regard to sign can be readily understood by reference to fig. 1.

The rectangle X represents the plate, and the circle Y, with the arrowheads indicating the direction of current in the electromagnet. represents the magnetic field. The direction of the primary current is given by EF, the

Fig. 1.

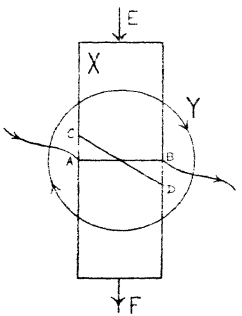

position of the equipotential line before the application of the field by AB, and the position of this equipotential line when the field is applied by CD. If the equipotential line CD is rotated in the direction of the current in the electromagnet the effect is said to be positive, and if the equipotential line is rotated in the opposite direction the effect is said to be negative. The Hall coefficient is negative for both copper and tin, the value for tin being about 4 per cent. that for copper.

The Hall effect for the copper-tin alloys is very small. Since the Hall P.D. is inversely proportional to the thickness of the plates, and very thin plates could not be prepared, a very sensitive galvanometer was required, and consequently a delicate Paschen galvanometer was used

in the present experiments. It was mounted on a stone pillar, at a distance of $7\frac{1}{2}$ metres from a large circular electromagnet which had been rotated into such a position that its effect on the galvanometer was a minimum. This electromagnet, excited by a current of 6 amperes, produced a field of 8500 gauss in the 1·5 cm. air-gap between the pole-pieces of circular section having a diameter of 9 cm.

The alloy plate under investigation was rigidly fixed in a vertical position in the magnetic field by two brass clamps which also served as leads for the primary current. These clamps were fixed to a wooden frame which also supported the secondary electrodes, consisting of spring copper contacts carried by bars of ebonite. These electrodes, which could be moved vertically along the edges of the plate by means of a screw arrangement, were connected to the galvanometer by long, well-insulated, flexible wires. These wires were pulled taut so as to eliminate the effects of vibration as far as possible.

In a determination of the Hall coefficient the secondary electrodes were adjusted on the equipotential line AB (fig. 1). Then, with the secondary circuit closed, no deflexion is produced in the galvanometer when the primary current is reversed. On applying the magnetic field and again reversing the primary current, with the secondary circuit closed, a deflexion due to the Hall P.D. between the edges of the plate is produced in the galvanometer. The Hall P.D. was determined for several values of the magnetic field up to 8000 gauss, and a graph drawn showing the relation between the P.D. and magnetic field. The value of $\frac{E}{H}$ could be determined from this graph, and the Hall coefficient calculated from the equation

$$R = \frac{Ed}{HI}.$$

The primary current (4 amperes) passing through the plate could be read on a Weston ammeter with an accuracy of about 1 in 1200. The magnetic fields corresponding to various currents passing through the electromagnet were determined by a search-coil and Grassot fluxmeter. The absolute value of the magnetic field when a current of 2 amperes passed through the magnet was determined by means of a delicate ballistic galvanometer and a search-coil of known mean area, and from this result corrections

could be applied to the fields as determined by the flux-meter. The magnetic field determinations are considered to be correct within about one-half per cent.

The Hall effect was determined at room-temperature, the exact temperature being observed by an accurate thermometer suspended with its bulb in contact with the plate.

The experimental results for the Hall coefficients are given in Table IV. and Graph IV.

TABLE IV.

Composition of alloy.	Thickness of plate in cm.	Hall coefficient.	Temperature of plate in ° C.
100 % Sn	—	—·000020*	—
SnCu (34·8 % Cu)...	·2370	+·000264	13·1
Sn_2Cu_5 (57·2 % Cu).	·4150	+·000775	18·9
$SnCu_3$ (61·6 % Cu)..	·4136	+·000935	13·1
35 % Sn, 65 % Cu	·4145	+·000713	15·6
$SnCu_4$ (68·1 % Cu)..	·4095	+·000802	17·7
$SnCu_3$ (72·8 % Cu)..	·4100	+·000139	14·4
20 % Sn 80, % Cu	·2562	—·000262	17·9
100 % Cu	—	—·000520*	—

* Campbell, 'Galvomagnetic and Thermomagnetic Effects.'

It is, however, important to point out that in addition to the Hall potential difference a transverse galvano-magnetic temperature difference is set up between the edges of the plate. This is the Ettingshausen effect, and is usually very small. The difference of temperature, ΔT, is given by

$$\Delta T = \frac{PHI}{d},$$

where H is the magnetic field in gauss, I the current in absolute units, d the thickness of the plate in cm., and P the Ettingshausen coefficient.

The Hall and Ettingshausen effects are superposed, and unless the secondary electrodes in the Hall-effect determinations are made of the same material as the plate itself, the Ettingshausen temperature difference ΔT set

up between the edges of the plate will result in a thermo-E.M.F. $\theta.\Delta T$ in the secondary circuit, where θ is the thermoelectric power of the electrode with respect to the

GRAPH IV.

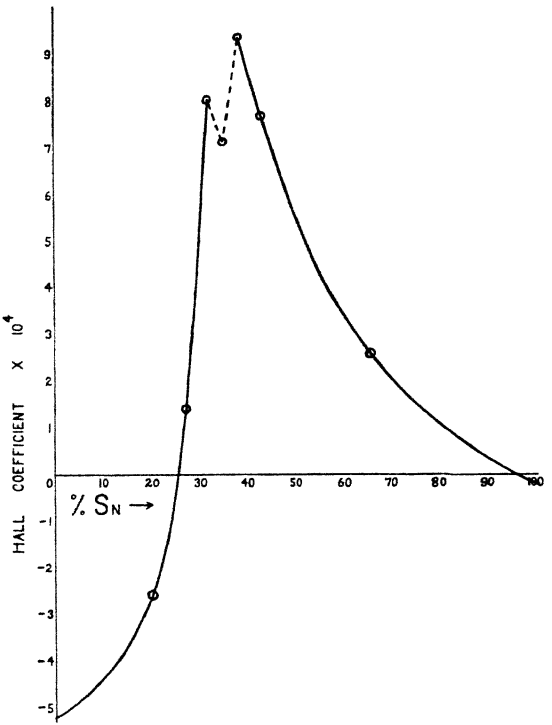

plate. Therefore the total potential difference as measured by the galvanometer in the Hall-effect determination is given by

$$E = E_H \pm \theta \,.\, \Delta T.$$

where E_H is the true Hall P.D.

Then R, the Hall coefficient, becomes

$$R = \frac{E \times d}{H \times I} \pm P.\ \theta.$$

Generally the Ettingshausen coefficient P is very small, but the factor θ also determines whether a correction to the Hall coefficient is necessary. In the Hall-effect determinations, when the primary current is reversed with the galvanometer circuit closed, the deflexion representing the Hall E.M.F. is taken up in a few seconds, while the Ettingshausen thermo-E.M.F., if appreciable, produces a secondary deflexion. In the present experiments the electrodes were made of copper and no secondary deflexion was observed, and thus no corrections for the Ettingshausen effect have been made. The Hall coefficients have been determined within 1 per cent.

The Annealing of the Alloys.

The annealing temperatures were obtained from the equilibrium diagram given in the International Critical Tables, vol. ii. The chill-cast alloys were annealed in an electric furnace in an atmosphere of coal-gas, to prevent oxidation. One plate was annealed in nitrogen owing to the high annealing temperature. The furnace was heated to the required temperatures very slowly, and could be kept at these temperatures within a few degrees for long intervals of time. The annealing was usually performed in periods of about 8 hours, and the furnace was allowed to cool to room-temperature before removing the alloy. The process was repeated several times for each alloy. The temperatures at which the various alloys were annealed are given below :—

65·2 per cent. Sn,	34·8 per cent. Cu	(SnCu) ...	155° C.
42·8 „ „ Sn,	57·2 „ „ Cu	(Sn_2Cu_5)...	180° C.
38·4 „ „ Sn,	61·6 „ „ Cu	($SnCu_3$)...	565° C.
35·0 „ „ Sn,	65·0 „ „ Cu	.....	
31·9 „ „ Sn,	68·1 „ „ Cu	($SnCu_4$) ...	500° C.
27·2 „ „ Sn,	72·8 „ „ Cu	($SnCu_5$)...	
20·0 „ „ Sn,	80·0 „ „ Cu	.....	
10·0 „ „ Sn,	90·0 „ „ Cu	.....	750° C.

The annealing of a plate of Cu_3Sn was also performed with the furnace evacuated to about 1/10 mm. pressure, and the result, as shown in Table I., is in good agreement with the plate annealed in coal-gas.

Discussion of Results.

The curves showing the relation between the electrical resistivity, temperature coefficient of electrical resistance, Hall effect, thermoelectric power, and the concentration of Sn in the alloy furnish singular points corresponding to both Cu_3Sn and Cu_4Sn. These curves differ greatly from the corresponding curves obtained for the copper-antimony alloys. The electrical resistivity, Hall effect, and thermoelectric power curves for the copper-antimony alloys * are similar in that the sign of the gradients of the curves is the same for corresponding compositions, but this is not the case with the curves for the copper-tin alloys.

The resistivity of the alloys of composition between 100 per cent. Sn and Cu_3Sn diminishes very gradually as the concentration of Sn is decreased. The resistivity of Cu_3Sn determined in the present experiments is $8{\cdot}72 \times 10^{-6}$ ohm. the value determined by Ledoux being $8{\cdot}75 \times 10^{-6}$ ohm. From Cu_3Sn to Cu_4Sn the resistivity increases rapidly to the value $47{\cdot}8 \times 10^{-6}$ ohm, while it diminishes in a regular manner as the composition is varied from Cu_4Sn to 100 per cent. Cu.

The curve showing the variation of the temperature coefficient of resistance with the concentration of Sn in the alloy is very sensitive to changes in composition of the alloy. The addition of tin to copper causes the temperature coefficient of resistance to diminish rapidly to a very low value. This low minimum value is constant over the range of composition from about 85 per cent. Cu, 15 per cent. Sn to Cu_4Sn. while between Cu_4Sn and Cu_3Sn the temperature coefficient of resistance increases very rapidly from the minimum value $5{\cdot}7 \times 10^{-4}$ to $35{\cdot}3 \times 10^{-4}$. As the composition of the alloy is varied from Cu_3Sn to 100 per cent. Sn. the temperature coefficient of resistance at first diminishes to a minimum value corresponding to an alloy of composition 54 per cent. Cu, 46 per cent. Sn, but afterwards increases uniformly. While singular points are obtained corresponding to the compounds Cu_3Sn and Cu_4Sn in the curve showing the variation of the temperature coefficient of resistance with the concentration of one metal in the alloy, no singular points are obtained corresponding to Cu_2Sb and Cu_3Sb † in the curve for the Cu-Sb system of alloys.

* Stephens and Evans, *loc. cit.*

† Stephens and Evans, *loc. cit.*

While the crystal structures of Cu_3Sb and Cu_3Sn are similar, and possibly identical, the presence of the Sb or Sn atoms produces a remarkable change in the electrical properties of the structure. The resistivity of Cu_3Sb is about eleven times that of Cu_3Sn, but the temperature coefficient of resistance of Cu_3Sb is only one-eighth that of Cu_3Sn. It is interesting to note that in both the Cu-Sn and Cu-Sb series of alloys the compound with the low resistance has a high temperature coefficient of resistance, and that the compound with the greater content of copper

TABLE V.

Compound.	Resistivity in microhms per cm.^{3} at 0° C.	Mean temp. coeff. of resistance between 0° and 100° C. $\times 10^4$.	Thermo-electric power with respect to Cu, in microvolts.	Hall coefficient.	Crystal structure.
Cu_2Sb.....	10·4	39·6	− ·09	+·0013	Tetragonal $a_0=4·029$ A.U. $C_0=6·140$ A.U. Cell contains two molecules *.
Cu_3Sb.....	98·5	4·33	+9·08	−·00176	Hexagonal close-packed, with the same axial ratio.
Cu_3Sn.....	8·72	35·3	+ ·06	+·000935	
Cu_4Sn.....	47·8	5·72	−2·99	+·000802	Face-centred cube, with 416 atoms in unit cell.

* Howells and Jones (not yet published).

has the greater resistance. Table V. gives the electrical properties of Cu_2Sb, Cu_3Sb, Cu_3Sn and Cu_4Sn.

In the copper-antimony series of alloys the Hall effect and thermoelectric power vary in a similar manner as the composition is changed. In the copper-tin system, however, there is no similarity in form between the curves showing the variation of the Hall effect and thermoelectric power with composition of the alloy, although both curves show well-defined singular points corresponding to the compounds Cu_3Sn and Cu_4Sn. The points corresponding to the thermoelectric power of the alloys 57·2 per cent. Cu,

42·8 per cent Sn. and 34·8 per cent. Cu, 65·2 per cent. Sn do not lie on the curve. This may be due to the first alloy consisting of the Cu_3Sn and ϵ' phases, and the second of the ϵ' and ζ' phases.

Although the Hall effect for both copper and tin is negative, it is positive for all the alloys in the range of composition from about 74 per cent. Cu, 26 per cent. Sn to about 4 per cent. Cu, 96 per cent. Sn. This change in sign of the Hall effect seems to indicate that while the sign and magnitude of the effect may to some extent depend on the atom itself, it also depends to a great degree on the crystal structure of the metal or alloy. Cu_3Sn has the maximum positive Hall effect, and is about one-half that of Cu_3Sb. The Hall effect, which was examined for each alloy for magnetic fields up to 8000 gauss, was found to be independent of the magnetic field for all the alloys.

The magnetic susceptibilities of the copper-tin alloys have been examined by Clifford *. Although tin is slightly paramagnetic and copper is diamagnetic, the alloys formed by the addition of a small percentage of tin to copper are more diamagnetic than copper. A maximum is obtained corresponding to an alloy of composition near Cu_4Sn, and with an increase in the tin content the alloys become less diamagnetic. Only the alloys in a small range of composition near the tin end of the series are paramagnetic. It should be noted that the susceptibilities of copper and tin, $-1{\cdot}22 \times 10^{-6}$ and $+{\cdot}31 \times 10^{-6}$ respectively, given in this paper are not in agreement with modern values. A complete analysis of the magnetic susceptibilities of many series of alloys has been made by Honda and Endo †. Determinations were made at room-temperature and at about 50° C. above the melting-points of the alloys. These investigators concluded that intermetallic compounds existing in the solid phase up to the liquidus points also persist in the liquid phase. The susceptibility-concentration curve at room-temperature for the Cu-Sn alloys has a singular point corresponding to Cu_4Sn, with breaks in the curve corresponding to Cu_3Sn and CuSn. In the susceptibility-concentration curve of the melt, however, a minimum is obtained near 40 per cent. Sn. Both tin and all the Cu-Sn alloys at the high temperature are

* Phys. Rev. vol. xxvi. no. 6 (1908).
† Journ. Inst. Metals, vol. xxxvii. p. 29 (1927).

diamagnetic. The susceptibility-concentration curve of the melt as obtained by Honda and Endo and the Hall coefficient-concentration curve obtained in the present experiments are similar in form, but the experimental results for the susceptibilities at room-temperature do not indicate any simple relation between magnetic susceptibility and Hall effect.

The effect of annealing on the resistivity of the alloys is shown in Table I. It is seen that the resistivity of one sample of the compound Cu_3Sn before annealing is approximately the same as that of pure Sn. The annealing of a plate of Cu_3Sn at 180° C. produced no appreciable change in the resistivity, but annealing at 565° C. diminished the resistivity by about 17 per cent. Annealing diminishes the resistivity of all the alloys of composition between Cu_3Sn and 100 per cent. Sn. The resistivity of the alloy 65 per cent. Cu, 35 per cent. Sn, which is between Cu_3Sn and Cu_4Sn, is increased by 35 per cent., and it seems that the alloys in the 6·5 per cent. range of composition from Cu_3Sn to Cu_4Sn are unstable. The resistivity of Cu_4Sn was only slightly diminished by annealing, but the resistivity of the 90 per cent. Cu, 10 per cent. Sn alloy, which consists of the α-phase, was increased by about 14·5 per cent. In the copper-antimony alloys, annealing increased the resistivity of the compound with the greater resistance, Cu_3Sb, while the resistivity of the other compound, Cu_2Sb, remained unchanged, but in the copper-tin alloys the compound with the greater resistance, Cu_4Sn, was not appreciably changed by annealing, while the resistivity of Cu_3Sn was diminished.

Summary.

1. The electrical resistivity, temperature coefficient of resistance, thermoelectric power, and Hall effect of the copper-tin series of alloys have been determined.

2. The alloys were chill cast in an iron mould in the form of plates, and the electrical resistivity at 0° C. was determined in this state. The resistivity was redetermined after the alloys were annealed at suitable temperatures, and the process of annealing was continued until the resistivity showed no further variation. The temperature coefficient of resistance, thermoelectric power, and Hall effect were then determined for the alloys in this final state.

3. Singular points corresponding to both Cu_3Sn and Cu_4Sn are obtained in each of the curves, showing the relation between electrical resistivity, temperature coefficient of electrical resistance, thermoelectric power, Hall effect, and the concentration of one metal in the alloy.

4. Although the Hall effect is negative for both copper and tin, it is positive for both the compounds Cu_3Sn and Cu_4Sn and the alloys of composition ranging between 74 per cent. Cu, 26 per cent. Sn and 4 per cent. Cu, 96 per cent. Sn. Cu_3Sn has the maximum positive Hall coefficient ·000935, which is approximately one-half the coefficient for Cu_3Sb.

5. Although the crystal structures of both Cu_3Sn and Cu_3Sb are hexagonal close-packed, with the same axial ratio, there is a remarkable difference in the electrical properties of these compounds. The resistivity of Cu_3Sb is about eleven times that of Cu_3Sn, but the temperature coefficient of resistance of Cu_3Sb is only one-eighth that of Cu_3Sn.

6. The effect of annealing on the resistivity of the alloys depends on their composition. A diminution is produced in the resistivity of Cu_3Cn, while the resistivity of Cu_4Sn remains practically unchanged.

In conclusion, I wish to express my warm thanks to Professor E. J. Evans, D.Sc., for his most valuable help and advice, and to Professor C. A. Edwards, D.Sc., who kindly granted facilities for preparing the alloys.

April 1929.

XXXV. *A New Conception of the Mechanism of Metallic Conduction.* *By* H. Monteagle Barlow, *Ph.D.**

THE introduction of quantum mechanics into mathematical investigations of the mechanism of metallic conduction was facilitated by the previous existence of the classical theory. The latest developments initiated by

* Communicated by the Author.

Sommerfeld * employ the idea of an electron gas interpenetrating the atoms of the metal as the basis of their argument.

In a recent paper † the author concluded that it is more accurate to regard the assembly of conduction electrons as forming what is equivalent to an incompressible fluid rather than a gas, and the following theory is put forward in an effort to provide a starting-point for future developments along these lines.

The Nature of the Conduction Process.

The atoms of the metal are regarded in the light of the Rutherford-Bohr model.

It is assumed that there are no "free" electrons in the sense that these are completely dissociated from the atoms. Every atom always has its normal complement of electrons, so that it can only give away one if at the same time it receives another.

Thus a current consists of a series of electrons passing simultaneously along a chain of atoms. In general the chain will have a zig-zag form, but with a resultant direction parallel with the electric force ‡.

The electrons concerned in the conduction process are supposed to reside in the outermost orbits of the atoms, and are recruited from the "valency" electrons employed in the theory of chemical action. It will be convenient to distinguish the particular electrons which lend themselves to the formation of an electric current by the name "fluid electrons."

If for any reason the outermost orbits of two neighbouring atoms were to come into contact, the nuclear attractions would exert opposing forces on a valency electron when situated between them, and such an electron would be equally ready to join the orbital system of either atom (fig. 1). A confluence of the outermost orbits is established at one point, and consequently no

* Sommerfeld, *Naturwissenschaften*, Oct. 14, 1927, p. 63; and *Zeits. für Phys.* xlvii. pp. 1 & 43 (1928).

† Barlow, Phil. Mag. vii. p. 459 (1929).

‡ This conception has been employed previously by (1) Fleming, 'The Interaction of Pure Scientific Research and Electrical Engineering Practice,' p. 38 (published by Constable, 1927); (2) Bridgman, Phys. Rev. xvii. p. 161 (1921), & xix. p. 114 (1922); and (3) Hall, Papers in Proc. Nat. Acad. Sci. and Phys. Rev.

energy would be required to effect the transference of an electron from one atom to the other, provided that there occurred a simultaneous ejection of another similar electron by the receiving atom and absorption by the emitting atom.

The path of the electrons through the atoms themselves is supposed to be perfectly resistanceless, as required by Bohr's theory of non-radiating quantum orbits. Hence, in a pure metal at the absolute zero of temperature, when the atoms are presumably at rest, and always in contact, a current, once started, will go on indefinitely. If there were any appreciable opposition to the motion of an electron through the atoms one would expect this to account for a large part of the resistance of a conductor, and it seems unlikely that there would be such a marked change when the temperature is reduced.

Fig. 1.

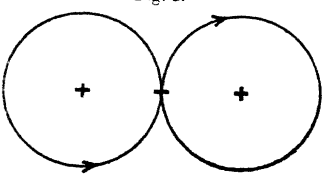

Under ordinary conditions the heat-motions make it impossible to have a chain of atoms with their outermost orbits all in contact at the same time, so that the production of a current must then involve an expenditure of energy. The shape and size of the orbit to which an electron settles down in assuming a stationary state depends upon the proximity of the positive nucleus and other negative charges. The stability of the rotating electron with regard to displacements in the plane of its orbit is then determined by the constancy of the angular momentum. Measurements of atomic diameter and the Avogadro constant prove that the distance between neighbouring atoms of a mass of metal is very small, even at high temperatures, and it is therefore reasonable to suppose that the configuration of the orbits belonging to one atom of such an aggregation is profoundly influenced by the relative position of adjacent atoms. In fact the shape of

the orbits must be continually changing to suit the conditions imposed at any instant by the heat-motions of the atoms.

Bohr assumes that the motions of the nuclei with respect to one another are so slow that the state of motion of the planetary electrons at any moment does not differ sensibly from that calculated on the assumption that the nuclei are at rest. This assumption is considered permissible on account of the large mass of the nuclei compared with that of the electrons, which means that vibrations resulting from a displacement of the nuclei are very slow compared with those resulting from a displacement of the electrons.

All available data point to the conclusion that at ordinary temperatures the valency electrons have an average velocity of vibration of about 10^6 or 10^7 cm. per sec., and consequently the orbits can scarcely be regarded as stationary states in the usual sense.

Energy must be expended to remove an electron from an atom, and, conversely, energy is radiated when a free electron is bound to an atom. In the process of transferring an electron from one atom to another not in absolute contact there must be a net absorption of energy. That energy ultimately appears as heat, and for the purpose of this discussion it is immaterial whether or not the energy takes some other form during the transition stage.

In order to get a mental picture of the mechanism adaptable to simple mathematical treatment we will suppose that the energy required to produce a current through a conductor is employed not in causing the electrons to jump through free space from one atom to another, but in distorting the outermost orbits until those belonging to adjacent atoms come together and allow an electron to pass across without opposition. This does not really involve any departure from the Bohr theory, because, as already pointed out, the shape of the orbits must be continually altering, and when an electron is transposed the change may be regarded as brought about either by a jump through free space from one stationary state to another or by a distortion of the orbits sufficient to bring them into contact at one point. The " fluid electrons " are therefore considered as always attached to one or other of the atoms which maintain electrical neutrality.

For a regular arrangement of the atoms there is obviously a relation between the spacing and the coefficient of expansion for the metal. As the temperature is raised from the absolute zero the atoms begin to execute heat-motions, and their average distance apart increases. Nevertheless there is generally one instant during each period of these heat-oscillations at which the outermost orbits of neighbouring atoms come together.

The application of an electromotive force to a metal bar is equivalent to an attempt to introduce some extraneous negative charges at one end and extract a similar number from the other end. As a result, the electron orbits belonging to the atoms at the two surfaces must suffer distortion, and that distortion will be propagated throughout the mass.

When a potential difference is maintained between two points on the conductor, it is known that a current will flow, no matter how small that potential difference, which is absorbed exactly by the forces opposing the flow of the current.

The outermost orbits of the atoms are assumed to be elongated in the direction of the pressure by an amount proportional to the pressure. This is in accordance with our knowledge of electric displacement in a dielectric, which we suppose only differs from a conductor in regard to the spacing of the atoms and the susceptibility of the atomic shell to distortion.

For a given potential difference between two points on a particular conductor there is a definite "total elongation" of the outermost electron orbits, remaining constant in time. That "total elongation" is really divided up between all the atoms separating the points considered, and is superposed on the heat-displacements. At one instant there may be no space between certain atoms, and therefore no distortion of their orbits is possible, but the remaining atoms in a particular chain will be allotted the elongation that the first-named are unable to accept.

In general the pressure is only sufficient to bridge a limited number of the gaps, so that the flow of "fluid electrons" is restricted to paths that are continually changing. The greater the applied pressure the larger the number of gaps included, and therefore the greater the average velocity of drift.

The distortion of an orbit is supposed to be perfectly elastic, the energy expended in producing a departure from the stationary state being completely returned if there is no interchange of electrons between different orbits. The linear relation between stress and strain for a metal bar subjected to a small tensile force indicates that an elastic deformation of the electron orbits is produced under such conditions.

A current in a conductor having a steady potential difference maintained between its ends is imagined to consist, therefore, of a number of rows of electrons periodically stepping forward along irregular chains of atoms. The electrons are always attempting to move towards the positive electrode, but they have to wait until an opportunity offers.

Fig. 2.

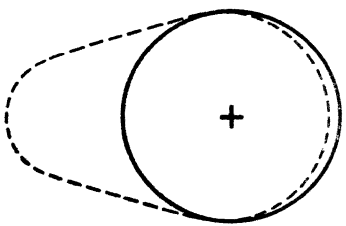

It might be argued that the compression of the orbit on one side of the atom counterbalances the extension on the opposite side, but when one considers that an inward displacement is opposed by the repulsion of all the electrons in the interior, whereas an outward displacement is only resisted by the comparatively weak residual attraction of the positive nucleus, it is apparent that there must be a net elongation of the atomic shell very nearly proportional to the applied force (fig. 2). This view is supported by the fact that the compression strength of a substance is invariably much greater than the tensile strength, although such a test is not altogether fair, on account of the accompanying lateral strain due to the molecules sliding over one another.

There is, of course, no reason to expect any change in the length of a conductor when a potential difference is

established between its ends. The equivalent pressure on the electrons is always just balanced, so that forces of this nature can never tend to separate the atoms.

The production of heat by a current is also consistent with the mechanism we have been considering. The energy employed in forcing an orbital electron to take a different path from the normal must be converted into heat when that electron is transferred to a neighbouring atom. The process is analogous to what happens when a force which has been stretching a helical spring is suddenly removed. Oscillations are set up corresponding to the heat-motions of the atom. If, on the other hand, the force extending the spring is reduced to zero gradually, there will be no oscillations, and. in the case of an atom which is perfectly elastic. no energy loss.

The heat-content of the atom is supposed to be a property of the orbital electrons. the contribution of the positive nucleus being relatively negligible. The positive nucleus is so massive that it remains practically at rest. while its satellites oscillate in their orbits relatively to it. The vibrations of the electrons are very rapid, and the nucleus to which they are comparatively loosely held will not respond to such vibrations. The conditions may be compared with those prevailing when the upper end of a spiral spring supporting a heavy weight is given a simple harmonic motion of high frequency. The periodic time of the applied oscillation is so much smaller than that natural to the system that the weight is almost unaffected by the vibration.

In a conductor at uniform temperature the average kinetic energy of the atoms is constant; but, if a temperature gradient is maintained, the atoms at the hot end try to get more elbow-room than those at the cold end, so that the average compression of the outermost electron orbits under the forces of cohesion would have to vary from one point to another unless the atoms with the greater energy were given more space. Thus the hot atom compresses its cooler neighbour, tending to distort the electron orbits. That distortion is cumulative, and builds up along the temperature gradient towards the cold end. A convection current is set up to equalize the distribution of the heat, because more energy must be employed transferring electrons from one atom to another where the average distortion is large than where it is small.

Since every atom always has its normal number of electrons, the flow across any section must be the same in both directions.

If the orbit of an electron belonging to one atom is distorted, there is always a tendency to share that distortion with all the other atoms in the assembly. This is one of the most fundamental properties of a conductor, and has its origin in the closeness of the atoms and the ease with which their outermost orbits can be distorted. It is significant to compare the rate at which the E.M.F. is built up along the length of a conductor and a dielectric substance when the two lie side by side with a magnetic field sweeping across them *.

No matter how small the E.M.F. induced in an insulated conductor, the total displacement of electricity is the same, whether the conductor is made of copper or lead. In fact the displacement is not limited in any way by the atoms of the metal. Dielectrics are quite different. They are made up of bulky polyatomic molecules separated from one another by comparatively large distances. If the potential gradient is increased sufficiently, breakdown ultimately occurs, due to the fact that the "total elongation" of the electron orbits belonging to a chain of atoms between the electrodes becomes sufficient to bridge all the gaps. The conductivity exhibited by insulators when subjected to potential gradients less than that required to produce breakdown is probably caused by an absorbed electrolyte.

Before proceeding to consider how these ideas can be interpreted mathematically, it will be convenient to discuss one other factor which is of importance in determining the conductivity of a metal.

The normal positive valency is given by the number of electrons in the outermost orbit of the atoms. Thus, copper has a positive valency of one, zinc of two, aluminium three, and so on. The mechanism of conduction which we have been discussing only allows one electron at a time to cross the bridge between two atoms. Hence, with regard to the number of electrons available for the production of a current, there is no particular advantage in having more than one in the outermost orbit of each atom. On the other hand, the larger the number of valency electrons the more

* H. A. Wilson, Phil. Trans. A, ccix. p. 121 (1905), and Proc. Roy. Soc. lxxiii. p. 490 (1904).

the work that has to be done to distort the orbit, and, consequently, the higher the resistance of the conductor. Moreover, a distortion of the outermost orbit involves a similar distortion of the inner orbits, so that the energy absorbed in this respect is also a function of the total number and distribution of planetary electrons in the atoms.

These deductions are confirmed by the periodic table of the elements. The electropositive metals with small atomic numbers are invariably the best conductors. Although the aluminium atom has three valency electrons, it only contains thirteen planetary electrons, and the resistance of this metal is therefore not very much greater than that of copper, with one valency electron and twenty-nine planetary electrons in the atom. Mercury and lead, with eighty and eighty-two planetary electrons in their atoms respectively, are relatively poor conductors.

Mathematical Interpretation.

(a) *Relation between potential and mechanical pressure on the "fluid" electrons.*

Consider a conductor of length x earthed at one end and raised to a potential V at the other (fig. 3). If the

Fig 3.

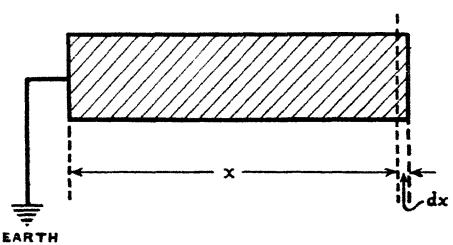

equivalent mechanical pressure per unit area on the electron fluid in the conductor is p, then the work done in producing a small displacement dx is given by

$p \, . \, dx$ per unit area,

and the corresponding quantity of electricity transferred from the end at potential V to earth is

$$N.e.dx \text{ per unit area,}$$

where N=number of "fluid" electrons per cubic cm. But by definition V=work done in moving unit charge from one end of the conductor to the other. Hence

$$V.N.e.dx=p.dx,$$

or
$$p=VNe \quad . \quad . \quad . \quad . \quad . \quad . \quad . \quad (1)$$

This relation is always applicable. It is equally true whether there is a flow of electricity or not. The pressure is exerted equally in all directions, as would be the case in an ordinary fluid.

(b) *Rate at which heat is developed in a conductor carrying current.*

Suppose that the average velocity of drift of the electron fluid through the conductor is w and the sectional area of the conductor is A, then the rate of doing work on the electron fluid is

$$pAw=VNeAw,$$

where V=P.D. between the ends of the conductor; but the current

$$I=NAew. \quad . \quad . \quad . \quad . \quad . \quad . \quad (2)$$

Hence power absorbed, producing heat in the conductor,

$$=VNeAw=IV,$$

as required.

(c) *Electrical conductivity and Ohm's Law.*

In considering the forces opposing the flow of the electron fluid through a conductor it is necessary to deal with time averages.

Let u=average velocity with which the distortion of an electron orbit is produced. This velocity is supposed to be practically constant over a wide range of temperature. Although the distortion of an orbit necessarily follows the heat-motion of the atomic shell, there are reasons to suppose that the fraction of the total mass of the atom in which the heat-energy is stored increases with the temperature. Thus at low temperatures (just above the point at

which supra-conduction begins) the inner rings of electrons to which the positive nucleus is more firmly attached are practically at rest, so that the heat-energy of the atom is confined to the electrons in the outermost orbits. As the temperature is raised, the inner rings of electrons begin to absorb part of the thermal energy, and start oscillating about the positive nucleus in much the same way as the valency electrons.

Assuming equipartition of energy between degrees of freedom for the atoms, we find that at atmospheric temperature u should be of the order 10^6 cm. per sec.

Let f_1=average force required to distort an electron orbit sufficiently to effect the transfer of a single electron from one atom to the next. This operation is carried out with average velocity u.

Then, if f_2=average force opposing the flow of a single electron, with average velocity w, through the conductor as a whole, we have

$$\frac{f_1}{f_2}=\frac{u}{w} \quad . \quad . \quad . \quad . \quad . \quad . \quad . \quad . \quad (3)$$

Again, if l=length of the conductor, the average pressure on the electron fluid per unit area is given by

$$p=\mathrm{N}lf_2=\frac{\mathrm{N}lwf_1}{u}, \quad . \quad . \quad . \quad . \quad . \quad . \quad (4)$$

N being the number of "fluid electrons" per cubic cm., as before.

Consider a simple cubic lattice arrangement of the atoms. Let s=average spacing between two adjacent atoms. This spacing must be directly related to the amplitude of the heat-vibrations, and may be assumed proportional to the absolute temperature T*.

Thus we have

$$s=y\mathrm{T}, \quad . \quad . \quad . \quad . \quad . \quad . \quad . \quad . \quad (5)$$

where y=increase in the linear dimensions of the average space occupied by a single atom per unit rise of temperature

Now let α=opposing force per unit outward displacement of the outermost electron orbit of an atom. This quantity is a function of the number and distribution of

* This hypothesis may not be strictly true, but the net result seems to be equivalent to it in most cases.

the electrons in the atom. It is quite independent of temperature. Hence

$$f_1 = \alpha s. \quad . \quad . \quad . \quad . \quad . \quad . \quad . \quad . \quad (6)$$

From the preceding equations we have

$$p = \frac{Nl\alpha sw}{u} = \frac{Nl\alpha wyT}{u}.$$

But $p = VNe$ (eq. (1)),

$$\therefore \quad V = \frac{p}{Ne} = \frac{l\alpha wyT}{eu}$$

and $V = IR = NAewR$,

where R = resistance of the conductor.

$$\therefore \quad R = \frac{V}{NAew} = \frac{l\alpha wyT}{eu}\left[\frac{1}{NAew}\right],$$

that is,

$$R = \frac{l\alpha yT}{NAe^2u}. \quad . \quad . \quad . \quad . \quad . \quad . \quad . \quad . \quad (7)$$

This equation gives R, the dimensions of a velocity, as required.

The specific electrical conductivity is given by

$$\sigma = \frac{e^2Nu}{\alpha yT}. \quad . \quad . \quad . \quad . \quad . \quad . \quad . \quad (8)$$

Thus, at constant temperature, σ is a constant, and Ohm's law is fulfilled. Moreover σ is inversely proportional to the absolute temperature, as required.

(d) *Thermal conductivity.*

When the temperature of a metal is increased it expands, because the atoms require more space in which to execute their heat-motions.

Let b = increase in the volume occupied by a single atom per degree rise in temperature.

Since an average of only one electron per atom is employed in producing a current in a conductor, we must have

$$N = \begin{cases} \text{number of "fluid electrons" per cubic cm.} \\ \text{number of atoms per cubic cm.} \end{cases}$$

Consider a cube of metal whose sides are 1 cm. long at the absolute zero of temperature. When the temperature

of this cube is raised to T degrees absolute, the volume increases by an amount

$$NbT,$$

N being in this case the number of atoms per cubic cm. If the cube were placed inside a box whose internal dimensions were 1 cm. each at all temperatures, the outward pressure which would be exerted on the sides of the box at the temperature T degrees absolute is given by

$$p' = GNbT, \quad . \quad . \quad . \quad . \quad . \quad . \quad . \quad (9)$$

where G = the bulk modulus of elasticity of the metal.

The kinetic theory gives a similar expression for the corresponding pressure exerted by a gas, that is,

$$p' = NKT.$$

K is a universal constant having the numerical value $1{\cdot}35 \times 10^{-16}$ ergs/degrees when p' is expressed in dynes per sq. cm. Thus the quantity K for a gas should be comparable with the quantity Gb for a solid.

Table I. shows that the quantity Gb is, in fact, very nearly constant for all metals, and has a value of about 10×10^{-16} ergs/degrees. The case of mercury is specially interesting because, when compared with the other metals, it has a small bulk modulus and a large coefficient of cubical expansion, but the value of Gb is about the same.

In a metal the pressure between the atoms due to their heat-motions is exerted for the most part on the electrons in the outermost orbits, because the inner orbits are relatively small *.

Thus it will not be far from the truth to take p' as the pressure on the " electron fluid " due to temperature, that is,

$$p' = p = GNbT \quad . \quad . \quad . \quad . \quad . \quad . \quad (10)$$

Now consider a section AB through a conductor in which a temperature gradient is maintained. Suppose that the section is taken between two layers of atoms, one of which is at temperature T_1 and the other at temperature T_2 (fig. 4.) The difference between the pressures exerted by the two layers is given by

$$p_1 - p_2 = GNb(T_1 - T_2),$$

* Frenkel, Phil. Mag. xxxiii. p. 297 (1917). Millikan, Phys. Rev. x. p. 194 (1917).

and since the velocity with which this resultant pressure causes the "fluid electrons" to flow across the section is u, the rate at which energy is transferred across the section is given by

$$(p_1-p_2)u=\mathrm{GN}bu(\mathrm{T}_1-\mathrm{T}_2).$$

If the diameter of an undistorted atom is d, the average temperature gradient is

$$\left[\frac{\mathrm{T}_1-\mathrm{T}_2}{d+s}\right] \quad \text{or} \quad \left[\frac{\mathrm{T}_1-\mathrm{T}_2}{d}\right] \quad \text{very nearly,}$$

since s is small compared with d. Hence for a thermal conductivity λ we have

$$\lambda\left[\frac{\mathrm{T}_1-\mathrm{T}_2}{d}\right]=\mathrm{GN}bu[\mathrm{T}_1-\mathrm{T}_2]$$

and

$$\lambda=\mathrm{GN}bud. \quad . \quad . \quad . \quad . \quad . \quad (11)$$

Fig. 4.

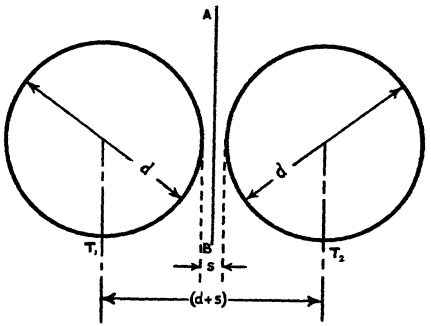

But the coefficient of cubical expansion for a metal is three times the coefficient of linear expansion, and therefore

$$\mathrm{N}b=3\left[\frac{y}{d}\right] \quad \text{or} \quad \mathrm{N}bd=3y. \quad . \quad . \quad . \quad (12)$$

Hence

$$\lambda=3\mathrm{G}yu. \quad . \quad . \quad . \quad . \quad . \quad . \quad . \quad . \quad . \quad (13)$$

(*e*) *Relation between thermal and electrical conductivity.*

We have now shown that the electrical conductivity

$$\sigma=\frac{e^2\mathrm{N}u}{\alpha y\mathrm{T}}. \text{ (eq. (8)),}$$

and the thermal conductivity

$$\lambda = 3Gyu \text{ (eq. (13))},$$

Thus

$$\frac{\lambda}{\sigma} = \left[\frac{3Gy^2\alpha}{e^2N}\right] T = \beta T \quad . \quad . \quad . \quad . \quad . \quad (14)$$

This ratio is directly proportional to the absolute temperature as required by experiment. In order to satisfy the law of Wiedemann and Franz the quantity

$$\beta = \left[\frac{3Gy^2\alpha}{e^2N}\right] \quad . \quad . \quad . \quad . \quad . \quad . \quad (15)$$

should have approximately the same numerical value for all metals. To prove this it is necessary first to determine α. The elastic constants of the metal provide some useful information regarding this quantity.

When a metal rod is subjected to a small longitudinal tensile force we may suppose that each atom undergoes an elastic extension. Taking two adjacent atoms, the force resisting such an extension is exerted presumably between the positive nucleus of the one and the planetary electrons of the other. A certain fraction z of the total interatomic force comes on the electrons in the outermost orbits, for which the restoring force per unit displacement is α.

Hence, if E = modulus of longitudinal elasticity of the metal, it is easy to show that

$$\alpha = z\left[\frac{E}{\sqrt[3]{N}}\right] \quad . \quad . \quad . \quad . \quad . \quad . \quad (16)$$

There are reasons to suppose that z is approximately the same for all common metals, having a value of about $\frac{1}{5}$, and in the subsequent calculations that assumption is made.

α has been calculated from the above formula, eq. (16), and the Wiedemann-Franz constant β deduced from eq. (15). The results are given in Table I., together with the corresponding values of the quantity u, which represents the average velocity of distortion of the outermost electron orbits. The agreement with experiment is remarkable considering the approximations introduced into the theory and the diverse sources from which the numerical values have been obtained.

There is, of course, no difficulty with the atomic heats, since there are no " free " electrons.

TABLE I.

Metal.	Values of Gb.	Values of a from $\frac{1}{5}\left[\frac{E}{\sqrt[3]{N}}\right]$ dynes per cm.	Values of the Wiedemann-Franz constant β. From experiment.	Values of the Wiedemann-Franz constant β. From $\frac{3Gy^2a}{e^2N}$	Values of u, cm. per sec.
Aluminium	$10{\cdot}0\times10^{-16}$	$3{\cdot}5\times10^{3}$	$2{\cdot}18\times10^{8}$	$2{\cdot}4\times10^{8}$	$13{\cdot}2\times10^{6}$
Iron	$10{\cdot}8\times10^{-16}$	$9{\cdot}7\times10^{3}$	$2{\cdot}78\times10^{8}$	$2{\cdot}5\times10^{8}$	$3{\cdot}2\times10^{6}$
Nickel.....	$11{\cdot}2\times10^{-16}$	$9{\cdot}0\times10^{3}$	$2{\cdot}4\times10^{8}$	$2{\cdot}3\times10^{8}$	$2{\cdot}6\times10^{6}$
Copper ...	$10{\cdot}9\times10^{-16}$	$7{\cdot}1\times10^{3}$	$2{\cdot}3\times10^{8}$	$2{\cdot}7\times10^{8}$	$17{\cdot}6\times10^{6}$
Zinc	$9{\cdot}1\times10^{-16}$	$6{\cdot}0\times10^{3}$	$2{\cdot}31\times10^{8}$	$3{\cdot}8\times10^{8}$	$7{\cdot}3\times10^{6}$
Silver.....	$11{\cdot}3\times10^{-16}$	$4{\cdot}1\times10^{3}$	$2{\cdot}35\times10^{8}$	$2{\cdot}3\times10^{8}$	23×10^{6}
Cadmium .	$10{\cdot}0\times10^{-16}$	$2{\cdot}8\times10^{3}$	$2{\cdot}43\times10^{8}$	$2{\cdot}5\times10^{8}$	$7{\cdot}1\times10^{6}$
Tin.....	$10{\cdot}2\times10^{-16}$	$3{\cdot}2\times10^{3}$	$2{\cdot}53\times10^{8}$	$2{\cdot}5\times10^{8}$	$5{\cdot}6\times10^{6}$
Platinum..	$11{\cdot}5\times10^{-16}$	$8{\cdot}5\times10^{3}$	$2{\cdot}59\times10^{8}$	$2{\cdot}1\times10^{8}$	$3{\cdot}5\times10^{6}$
Gold	$11{\cdot}5\times10^{-16}$	$4{\cdot}5\times10^{3}$	$2{\cdot}44\times10^{8}$	$2{\cdot}0\times10^{8}$	$16{\cdot}8\times10^{6}$
Lead	$11{\cdot}0\times10^{-16}$	$1{\cdot}2\times10^{3}$	$2{\cdot}46\times10^{8}$	$1{\cdot}3\times10^{8}$	$2{\cdot}9\times10^{6}$
Mercury ...	$11{\cdot}3\times10^{-16}$	—	—	—	—

In conclusion the author desires to thank Sir Ambrose Fleming, D.Sc., F.R.S., for the help he has given and the interest he has taken in the development of this work.

University College, London.
March 1929.

XXXVI. *An Experimental Method for the Determination of the Ballistic Demagnetization Factor.* By DONALD FOSTER *.

ABSTRACT.

A METHOD is described for experimentally determining the ballistic demagnetization factor. By means of a double search coil of novel design the magnetization and the magnetic field intensity are determined from ballistic galvanometer deflexions. While the discussion refers mainly to circular cylinders, the scheme is adaptable to specimens of other shapes. It is particularly designed to obtain

* Communicated by the Author.

accurate measurements of field intensity in cylinders of small diameter.

Details of a special design are given.

Curves are given which illustrate the variation of the demagnetization factor with the magnetization, as well as the dependence of this relation on the material and on the dimensional ratio.

---

1. *Introduction.*

THE magnetic field intensity in a substance is the resultant of the externally applied field and that due to the magnetization of the substance. The latter component is called the demagnetizing field because it is directed in the opposite sense to the polarization which causes it. If H is the resultant field, H_0 the applied uniform field, and h the demagnetizing field, the vector equation is

$$H = H_0 + h.$$

In order that the result of measurements of the relation between the magnetization and the field intensity may be independent of the exterior form of the specimen, it is necessary either to calculate or to measure the quantity h. The determination of the demagnetizing field has long been a problem of great urgency and practical difficulty.

It has been shown that the magnetization is uniform only when the bounding surface of the material is of the second degree *. The ellipsoid is the only such surface which is finite. For this case the demagnetizing field is calculable. The thin ring may also be mentioned as a shape for which the magnetization is approximately uniform, and for which the demagnetizing field vanishes. For ellipsoids h is proportional to the magnetization I. The ratio $N = -\frac{h}{I}$, which is known as the demagnetization factor, depends only on the axial ratio of the ellipsoid. Unfortunately, however, these shapes are often inconvenient or impossible to employ in magnetic measurements. For example, neither form is suitable for use with metallic single crystals.

The most convenient shape is usually the right circular cylinder. The problem of calculating its demagnetizing field is insoluble, except in special cases, because the distribution of magnetization in a cylinder is dependent upon the

* Neumann, J., Crelle's Journal, xxxvii. pp. 21–50 (1848). Maxwell, 'Electricity and Magnetism,' § 437.

magnetization curve of the material of which it is composed. A variety of apparatus has been developed for the purpose of obtaining uniform magnetization in cylinders in order to neutralize or render calculable the demagnetizing field. These devices are seriously limited in their accuracy and range of applicability. Permeameters of the yoke type have the additional disadvantage of putting the sample under constraint, and have been found unreliable when used with small stress-sensitive samples.

It has been commonly supposed that N is a constant for circular cylinders of given dimensions. Tables based on this assumption have been prepared by DuBois * and others †, and are still in general use for calculating the demagnetizing field, although the serious limitations of the data have been pointed out. Lamb ‡ and Holborn § measured the distribution of magnetization in cylinders and found that, in iron, the centroids of free magnetism move toward the middle of the rod and then outward again as the magnetization is increased. Searle and Bedford ‖ using a magnetometric method measured h at the middle of a long iron wire. The magnetization was measured ballistically at the middle of the wire. They found that h is a maximum at about the value of I for which $\mu=\mu_{max.}$. This result is in agreement with the data of Lamb and of Holborn. It was also found that h exhibited hysteresis toward H and I. This fact is invoked to explain the occurrence, with the method of reversals, of values of h less than that corresponding to uniform magnetization. Recently Dussler ¶, by a ballistic method, has demonstrated that N as a function of I is dependent upon the material of which the cylinder is composed.

The middle of the axis of a cylinder is a critical point at which I is a maximum and N a minimum. N for this point has been called the ballistic demagnetization factor, since in

* DuBois, H., 'Magnetische Kreise,' Berlin, p. 45 (1894); Wied. *Ann.* xlvi. p. 497 (1892).

† Ascoli, M. and Lori, F., *Atti della reale Accademia dei Lincei*, (5) iii. (2) p. 190 (1894). Mann, C. R., *Diss.* Berlin (1895); Phys. Rev. iii. pp. 359–369 (1896). Benedicks, C., *Ann. der Physik*, vi. p. 726 (1901). Schuddemagen, C. L. B., Phys. Rev. xxxi. p. 165 (1910).

‡ Lamb. C. G., Proc. Phys. Soc. Lond. xvi. pp. 509–518 (1899); Phil. Mag. (5) xlviii. pp. 262–271 (1899).

§ Holborn, L., *Sitz. der königl. preuss. Akad. der Wiss.* Berlin, i.–ii. pp. 159–168 (1898).

‖ Searle, G. F. C., and Bedford, T. G., Phil. Trans. Roy. Soc. Lond. A. cxcviii. pp. 33–104 (1902).

¶ Dussler, E., *Ann. der Physik*, lxxxvi. pp. 66–94 (1928).

ballistic measurements I is usually measured over a short segment at the middle of the sample.

Consideration of the facts shows that the ballistic demagnetization factor must be determined experimentally, point by point, along the magnetization or hysteresis curve of each specimen. It is the purpose of this paper to describe a convenient method whereby this may be accomplished.

2. *The Method of Measurement.*

The experimental arrangement is similar to that which is ordinarily used in making magnetic measurements ballistically. The sample is placed centrally in a magnetizing solenoid which provides a sufficiently uniform applied field. The double search coil is mounted inside the magnetizing coil and serves to measure both the magnetization and the field intensity. It consists of two coaxial solenoidal windings having equal numbers of turns. One coil is mounted inside the other, and the inner coil is wound on a radius just large enough to allow the pair of coils to be slipped over the specimen. When the coils are connected in series aiding to a ballistic galvanometer, the galvanometer deflexion can be made proportional to the magnetization I. When connected in series opposing, the effect due to magnetization is balanced out; and the galvanometer deflexion is proportional to the field H. By the use of an auxiliary air-core transformer, the double coil may be made to give deflexions proportional to the demagnetizing field h.

The method for measuring the field intensity is novel, chiefly in the design of the search-coil, which makes use of all the available area around the cylinder and introduces a minimum of electrical resistance, thus giving a sensitivity with rods of small diameter which has not been attained by other means.

The foundation of the method is the fact that the tangential component of magnetic intensity is continuous at the boundary between two media. The field intensity is measured in the region adjacent to the surface at the middle of the cylinder. While, in a uniform rod, the normal component vanishes at the middle, the method is independent of this condition because the measured quantities are the components of I and H parallel to the axis of the cylinder.

3. *Theory of the Double Secondary Coil.*

Let Φ be the flux linkage of the complete search-coil, and let a_1 be the effective area, and n_1 the number of turns on

the inner coil, and a_2, n_2 the corresponding quantities for the outer coil. Let a_s designate the cross-sectional area of the sample. Then for series opposing

$$\Phi=\{(\mu-1)\mathrm{H}a_s+\mathrm{H}a_1\}(-n_1)+\{(\mu-1)\mathrm{H}a_s+\mathrm{H}a_2\}n_2$$
$$=(\mu-1)\mathrm{H}a_s(n_2-n_1)+\mathrm{H}(a_2n_2-a_1n_1).$$

Putting $n_1=n_2\equiv n$, $a_2-a_1\equiv a$,

$$\Phi=\mathrm{H}n(a_2-a_1)=\mathrm{H}na \quad . \quad . \quad . \quad . \quad . \quad (1)$$

In series aiding connexion, we have

$$\Phi=(\mu-1)\mathrm{H}a_s(n_2+n_1)+\mathrm{H}(a_2n_2+a_1n_1).$$

If $n_1=n_2\equiv n$,

$$\Phi=2(\mu-1)\mathrm{H}a_sn+\mathrm{H}n(a_1+a_2)$$
$$=8\pi a_sn\mathrm{I}+\mathrm{H}n(a_1+a_2).$$

If the term $\mathrm{H}n(a_1+a_2)$ is balanced out by an air-core transformer whose primary is in series with the magnetizing solenoid,

$$\Phi=(8\pi a_sn)\mathrm{I}. \quad . \quad . \quad . \quad . \quad . \quad . \quad (2)$$

When it is desired to measure the demagnetizing field directly, instead of the resultant field (equation 1), the balancing circuit may be set to give no deflexion when there is no sample in the search-coil. The equation for the series opposing connexion then becomes in effect

$$\Phi=\mathrm{H}na-\mathrm{H}_0na$$

(the second term being due to the transformer). Putting $\mathrm{H}=\mathrm{H}_0-\mathrm{NI}$,

$$\left.\begin{aligned}\Phi&=(\mathrm{H}_0-\mathrm{NI})na-\mathrm{H}_0na,\\ \Phi&=-\mathrm{NI}na.\end{aligned}\right\} \quad . \quad . \quad . \quad . \quad (3)$$

It is important in making the coils to consider the relative error in measuring H which is contributed by a given error in making n_1 equal to n_2. We have for series opposition

$$\Phi=(\mu-1)\mathrm{H}a_s(n_2-n_1)+\mathrm{H}(a_2n_2-a_1n_1).$$

Putting $n_2-n_1\equiv\epsilon$; $\dfrac{a_2}{a_s}\equiv\alpha$; $\dfrac{a_1}{a_s}\equiv\beta$;

$$\Phi=a_s\mathrm{H}[\{(\mu-1)+\beta\}\epsilon+n_2(\alpha-\beta)].$$

When $\epsilon=0$,

$$\Phi=a_s\mathrm{H}n_2(\alpha-\beta).$$

The relative error in measuring H is therefore

$$\left\{\frac{\mu+\beta-1}{\alpha-\beta}\right\}\left(\frac{\epsilon}{n_2}\right);$$

and the factor $\frac{\epsilon}{n_2}$ is the relative error in making n_1 equal to n_2.

The quantity β is small, and μ is usually much greater than unity, so that the relative error reduces approximately to

$$\frac{\mu}{\alpha-\beta}\frac{\epsilon}{n_2}$$

which is proportional to the permeability. As a numerical example, suppose that

$$a_2=0{\cdot}922 \text{ cm.}^2 ; \quad a_1=0{\cdot}0697 \text{ cm.}^2 ;$$
$$\mu=10{,}600 ; \quad n_2=2761 ; \quad a_s=0{\cdot}0081 \text{ cm.}^2.$$

Then $$\frac{\mu}{\alpha-\beta}=100;$$

so that for an error in H of 1 per cent., the error in making the numbers of turns equal must be one-hundredth of 1 per cent. In this case, a tolerance of about one-third of a turn is allowed in matching the windings. It is necessary to avoid poor insulation or short-circuited turns in the coils. The existence of short circuits may be detected by means of an a.c. bridge, or by inserting into the search-coils a very long iron wire. As the magnetization approaches uniformity near saturation, the galvanometer deflexion due to the demagnetizing field becomes small in comparison with the effect of a single short-circuited turn, which may thus be readily detected.

4. *Design of the Coils and Measuring Circuit.*

Two facts determine the general design of the double search-coil. The polarization and the field intensity vary along the rod from the middle toward the ends; and the field intensity diminishes along the normal to the surface from the surface outward. These conditions are of such a nature as to limit the volume of the space in which the field is nearly uniform. The available winding volume is the quantity which determines the upper limit of sensitivity of the apparatus as a whole. When the winding volume of the search-coil is fixed, all sensitive moving-coil galvanometers give deflexions of about the same order of magnitude for a given change of flux. Using a given suspension fibre, the

sensitivity of the galvanometer to voltage impulses increases as the field magnet is weakened or the number of turns on the moving coil is diminished. At the same time, however, the critical damping resistance of the galvanometer is diminished, and it is necessary to use fewer turns (in the same volume) on the search-coil in order to keep the galvanometer critically damped. The sensitivity of the circuit may be increased a little by using a coil whose resistance is greater than the critical damping resistance of the galvanometer. Usually, however, it will be found more convenient to operate the galvanometer critically damped.

Consideration of these limitations of ballistic galvanometers, when used to measure voltage impulses in a closed circuit, shows the importance of using a coil design which makes the best use of all the space around the middle of the specimen. This type of coil is particularly desirable

Fig. 1.

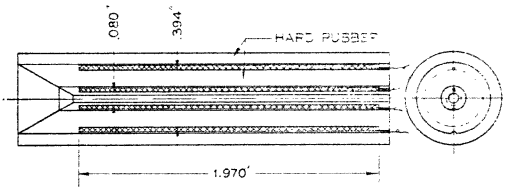

Double Secondary Coil.

for measurements on wires of diameter 0·1 cm. or less. If the cylinders to be measured have a small ratio of length to diameter, it will of course be necessary to use a short narrow coil. This does not imply a loss of accuracy in measuring the demagnetizing field because the field is much stronger for short specimens.

A double coil which has been used for measurements on single crystal specimens of 0·1 cm. diameter has the dimensions shown in fig. 1. The windings have 2761·5 turns in each of No. 40 single silk-covered copper-wire. The inner and outer spools have resistances of 100 ohms and 357 ohms respectively, and this device gives a galvanometer deflexion of 1 mm. at 1 metre upon reversing a field of 0·08 gauss. The effective volume between the coils is about 4·3 c.c., yet they are small enough to operate in a sufficiently uniform field. They were designed for use with

cylinders 60 cm. long and 0·05 cm. in radius. It is not possible to calculate the error due to the finite size of the coils except for the special case of uniform magnetization. In that case, it may be shown, for the example given above, that the extreme variation of the demagnetizing field within the coil is about 1 per cent. The average value, as measured by the coil, must therefore differ from the value at the middle of the sample by less than this amount.

5. *Some Examples of Measurements.*

Typical data for well-annealed iron and permalloy wires of approximately 0·1 cm diameter are given in the following

Fig. 2.

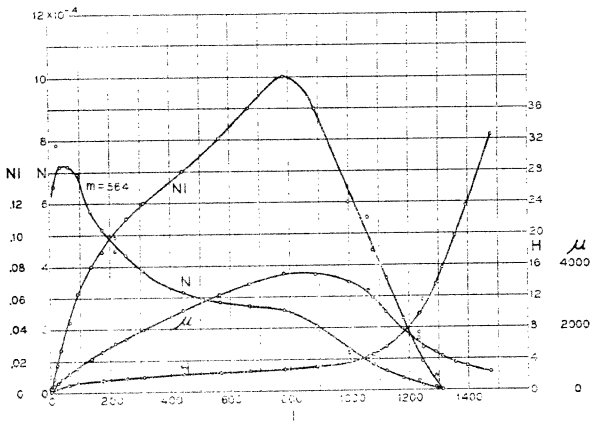

Electrolytic Iron.—Length=57 cm.; diameter=0·101 cm.

curves. The method of reversals was used, and the usual precautions were taken with regard to compensation of the earth's field, demagnetization of the sample, etc. In the figures m is the dimensional ratio (length/diam.). Fig. 2 shows the results for an electrolytic iron wire 57 cm. in length. Fig. 3 shows the same data for a permalloy (81 per cent. Ni, 19 per cent. Fe) wire of about the same dimensional ratio. The difference in the locations of the maxima of N is to be noted. It will be seen that for both materials the demagnetizing field is a maximum when the permeability is

Fig. 3.

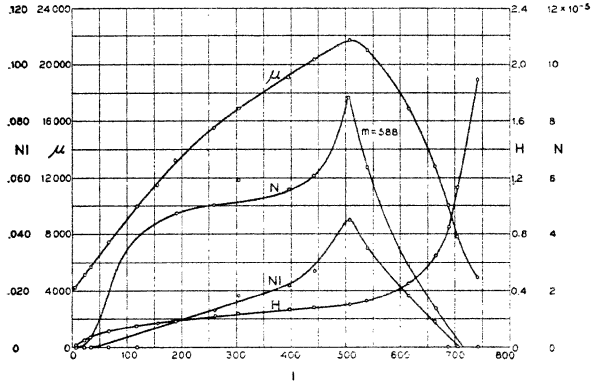

Permalloy.—Length = 60 cm.; diameter = 0·102 cm.

Fig. 4.

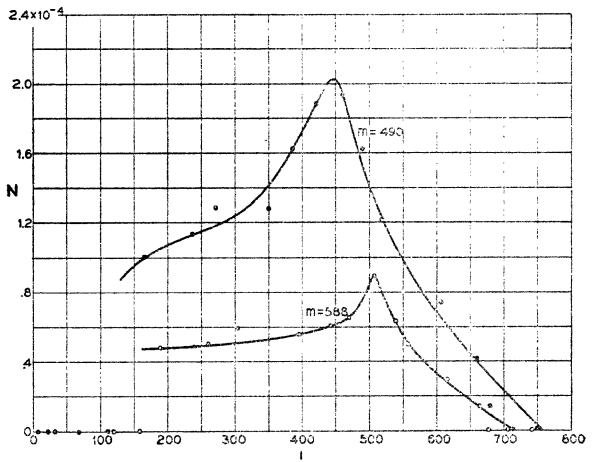

Permalloy.—Lengths 50 and 60 cm.; diameter 0·102 cm.

a maximum. For the permalloy samples N also has a maximum at the same point, although it occurs for a slightly lower value of I for the short permalloy specimen. Comparison of the demagnetization factors for two values of the dimensional ratio is given by fig. 4. The curves are taken on the same piece of permalloy.

In conclusion, it should perhaps be emphasized that the data given here apply only to the particular samples employed, and should not be used for the calculation of magnetic field intensities in other samples of the same dimensions.

I wish to express my thanks to Prof. L. W. McKeehan for stimulating my interest in this subject, and to Mr. Robert Bieling for assistance in preparing the data.

Bell Telephone Laboratories,
463 West St., New York, N.Y.,
October 1st, 1928.

XXXVII. *The Design of the Electron Collector for Retarding Voltage Analysis.* *By* H. W. B. Skinner *and* S. H. Piper, *University of Bristol**.

IN many experiments an electron collector (or Faraday Cylinder) is used to measure the current in an electron beam, and a velocity analysis of the beam is carried out by applying a variable retarding voltage so as to stop the slower electrons. If the slits which define the portion of the beam which is to be received are very narrow, probably there would be little difficulty in designing a suitable collector. We were requiring a collector with rather wide slits (2 by 6 mm.) and made one of the pattern shown in fig. 1. The outer case is a box of stainless steel sheet, $37 \times 19 \times 19$ mm. It was found on trial that this collector did not behave satisfactorily. The collector was mounted in a glass tube and a filament F (fig. 1) was placed in front of the first collector slit. The tube was exhausted, baked out at 420° C. for an hour, and sealed off from the pump. A charcoal tube, to be immersed in liquid air, was provided in order to absorb any gas given off.

A potential of 60 volts was applied between the filament F and the outer case C of the collector, and a variable

* Communicated by the Authors.

voltage V was applied between C and the inner box B of the collector. A potential V which tends to stop electrons is taken as positive. The current to B was read by a galvanometer. Under these conditions one might hope, as V is gradually increased, to get no change in the galvanometer reading until V is nearly equal to 60 volts. The voltage-fall across the effective portion of the filament was only about $\frac{1}{4}$ volt, and so would cause very little round-off of the curve. The actual curve obtained is shown in fig. 4. There is a very large fall in the observed current as V passes through the value zero. It seems fairly clear that the true electron current is measured by the dotted straight line shown, and that the remaining current is spurious. For the quantitative analysis of a beam which contains electrons of various velocities it is essential to

Fig. 1.

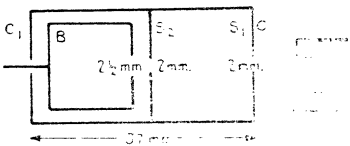

have a collector which, for each separate velocity, gives a flat retarding voltage curve. This condition is not satisfied by the collector described; an increase in the current for V negative would not matter, but the fall on the positive side of the zero is important.

The most obvious probable causes of spurious effects in collectors are as follows:—

1. The increase in the current may be due to the secondary emission of slow electrons from the slits.

2. The penetration of the field of the collecting box through the rather wide slits may (*a*) focus or spread the electrons in the main beam so that more or less are collected, or (*b*) draw the slow secondaries into the collecting box.

3. Certain anomalies may be due to the emission of secondary electrons from the box itself.

We call the collector of fig. 1 C_1. In order to try to find out the cause of the spurious behaviour, and to make a collector which works better, we made up three more—collectors C_2, C_3, C_4 (figs 2 and 3). These collectors all had defining slits 2 mm. × 6 mm., and the outer cases of all were of the same dimensions. The collectors C_2 and C_3 had open-fronted collecting boxes, and were the same except that a close gauze of 1 mm. mesh was placed over the slit S_2 of the collector C_2. The collector C_4 was, as will be seen, similar to C_1, except that a fourth slit (the "screen") was placed between S_2 and the collecting box and was insulated from the system so that any voltage could be applied to it.

Fig. 2.

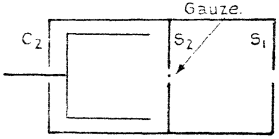

Fig. 3.

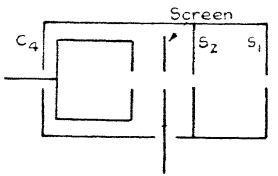

The slit on the screen was 2½ mm. wide, so that very few electrons from the main beam could hit it.

Let us consider first the behaviour of the collectors C_2 and C_3. Their curves for 60-volt electrons are shown in figs 5 and 6. (In these, and all subsequent curves, we have plotted the points on such a scale that the "true" current has a standard value.) The most noticeable feature is the dip in the curves in the neighbourhood of 30 volts. It is clear that this is due to the cause (3) mentioned above, namely, the ejection of secondaries from the box itself. This shows that a closed collecting box is imperative.

It will also be noted that C_2 and C_3 do not show so large an increase in the current in the neighbourhood of $V=0$

as C_1 does. Further, that C_2, which had the gauze, shows a smaller increase than C_3. It is clear that the field penetration will be less in open collectors of the type of C_2 and C_3 than in closed collectors of the type of C_1. It is therefore certain that interpenetration of field plays a part in causing the current to rise when V becomes negative. For practical purposes this is unimportant, as we have stated. The fact that the rise occurs in this neighbourhood shows that it is due to the collection of relatively slow electrons,

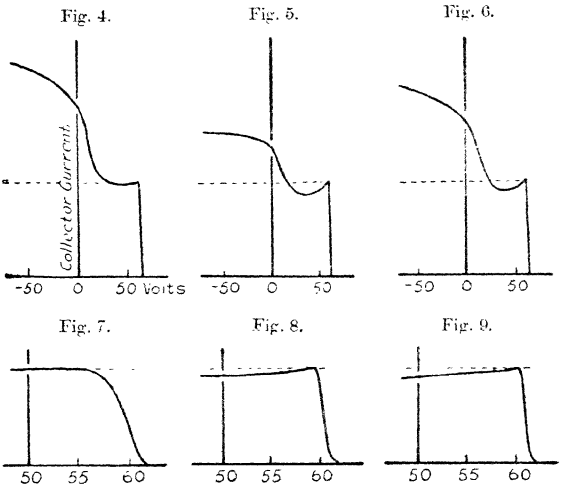

mostly ejected from the slit S_2. Some of these have sufficient energy to enter the box, even against a retarding voltage of 10–20 volts, and to this cause is due the practically important rise in the current as V is decreased from positive values to zero.

The feet of the curves for C_1, C_2, and C_3 are shown on a much larger voltage scale in figs. 7, 8 and 9. The zero of V was taken as the potential of the centre of the filament. The current into the collector came from a small part of the filament with a voltage drop across it of approximately $\frac{1}{4}$ volt. A slight spreading out of the feet of the curves will be caused by the finite velocity of emission of electrons

from the filament. It is seen that for C_2 and C_3 the drop at V=60 is very sharp; for C_1 less so. The explanation of this is that penetration of the field from the collecting box through the slit S_2 causes a slight spreading of the main electron beam, and some of the electrons which, geometrically, should go into the box do not do so when they are nearly reduced to rest by the retarding voltage V. In the cases of collectors C_2 and C_3, where the field interpenetration is less, this effect is much less than for C_1. If a sharp foot to the collector curve is required we must take care to avoid the field interpenetration.

Fig. 10.

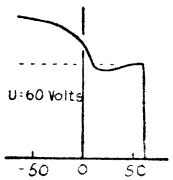

Fig. 11.

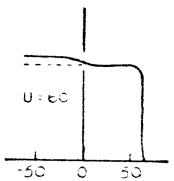

Fig. 12.

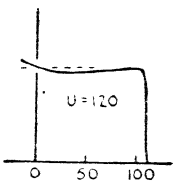

Fig. 13.

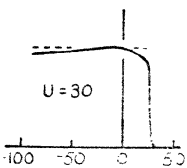

Fig. 14.

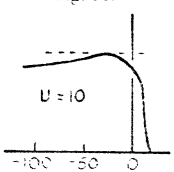

Fig. 15.

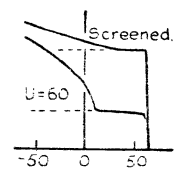

Actually in many cases this consideration is of little importance. An approximately flat curve from V=60 to V=0 may be required, and we hoped to obtain this by means of the screened collector C_4 (fig. 3). The screen can be used in a variety of ways, *e. g.*: (1) One may apply the retarding voltage to the screen and keep the box at a fixed potential. (This arrangment was a definite improvement, but the foot of the curve was excessively spread out on the voltage scale.) (2) One may place the screen at a high positive potential and hope that all the secondary electrons will be attracted to it, instead of going in the collecting box. Curves for this arrangement are shown in figs. 11, 12, 13, 14 (in which again the " true " current

has been arbitrarily taken as a constant). They are taken for various voltages U between the filament and the case, as marked. The screen voltage (420 volts) was chosen as being suitable for electrons of velocity about 50–100 volts, and it is seen that for this range the curves are fairly flat from V=0 to V=U, and the foot is reasonably sharp. For the analysis of slow-speed electrons the screen voltage is too high, and the screen robs the collector of some of the electrons when V approaches the value U. All the same, the curves of figs. 11 to 14 show that, working with the screen at 420 volts, we could obtain reasonably accurate information about the relative numbers of electrons of velocities between 10 and 120 volts in a mixed beam, and this could not be done with the unscreened collector. If there are no fast electrons in the beam the screen voltage could profitably be diminished. A curve for U=60 with the screen at 60 volts is also shown in fig. 10. This shows, as might be expected, a similarity to the curve of fig. 4 for the collector C_1, and the advantage of using the screen at a high potential is apparent.

The curves for the various voltages V were taken with a constant current of $\frac{1}{2}$ m.a. between the filament and the case. The actual number of electrons collected was nearly independent of the accelerating voltage U, except in the 10-volt case*. One has, however, no certainty that the number of electrons passing through the slit S_1 is independent of V. If we place the screen at the same potential as the outer case of the collector, and choose the retarding voltage so that no stray electrons are collected, then we may obtain a measurement of the current through S_2. This may be called using the collector "unscreened." It was found that the collector current with 420 volts on the screen was in all cases very nearly twice what it was with the collector unscreened. A special test showed that this ratio was independent of the precise screen potential provided it were greater than about 300 volts.

The obvious interpretation of this ratio 2 is that it is due to a "suck in" of electrons through S_2, caused by field interpenetration. Some of the electrons, which in the absence of the screen would not pass through S_2, are deflected between S_1 and S_2, and go through into the

* The greater spread in the foot of the curve for 10 volts may be due to the fact that a higher filament temperature was used.

collector. It was found, by experiments on the total filament emission, that the field penetration of the screen through S_1 was quite inappreciable. This "suck in" through the slit S_2 is a definite disadvantage of the screened collector. But the solid angle of the electron beam collected may be determined, and, as mentioned above, seems to be independent of the velocity, within wide limits.

When there is gas in the tube, *e. g.*, by allowing the charcoal to warm up, experiments showed that the advantage of the screened collector was fully maintained. The curves for $U=60$ are given in fig. 15.

A property of the screened collector which may be very valuable in some cases is that, owing to the strong retarding field between S_2 and the screen, the collector will not pick up any positive ions in a mixed beam of electrons and positives.

We do not intend to advocate the use of the screened collector in all cases. The chief disadvantage of the ordinary unscreened collector is the rise in the current when the retarding voltage is approaching zero. Thus, suppose we have a beam of electrons of various velocities up to 60 volts. We reduce the retarding voltage to 10 volts and the current rises. We deduce that there are a number of 10-volt electrons in the beam. This deduction may be quite erroneous. In cases of this sort the screened collector is a definite improvement; its only disadvantage, beside the extra complication, is the "suck in." In experiments where the beam of electrons is known to be practically homogeneous, the screen is of no use. In these cases, if we require a fine analysis of the beam, our tests have shown that considerable care should be paid to the question of field interpenetration through the slits. The chief value of these experiments is to show the kind of error into which it is possible to fall, and to emphasise the importance of trying the working of a collector with a beam of electrons of homogeneous velocity.

Summary.

Various types of errors into which it is possible to fall in using an electron collector of the ordinary type are discussed; and a screened collector is described which, for some purposes, is a definite improvement on the usual type.

XXXVIII. *Preliminary Determinations of Standard Electrode Potentials in Methyl Alcohol. By* PHILIP STRACHAN BUCKLEY, *B.A., B.Sc., and* Sir HAROLD HARTLEY, *M.A., F.R.S.* *

DETERMINATIONS of the standard electrode potentials of certain elements in methyl alcohol have been made by Neustadt and Abegg †, Isgarischew ‡, Neustadt §, and Carrara and Agostini ‖, but the values are known with much less certainty in this solvent than in water, as much of the experimental work has suffered from the following sources of error :—

(1) Insufficient attention was paid to preparing the solvent in a pure state.

(2) In the absence of any information as to the activities of the ions, the conductivity ratio $\frac{\lambda_c}{\lambda_0}$ was invariably used as a measure of their concentration.

(3) Calomel electrodes in water were used as reference standards. Besides the uncertainty of the liquid junction potential, this procedure introduces a risk of contaminating the solutions with water.

(4) Salts were used which do not behave as strong electrolytes in methyl alcohol, *e. g.*, the chlorides and nitrates of certain divalent metals.

(5) Sufficient care was not taken to prepare the metal electrodes in a reproducible and strainless condition.

(6) Liquid junction potentials were often ignored.

The values found by previous workers are given in Table I., referred in each case to silver, to which the value 0·76 volt is assigned, its approximate standard electrode potential in methyl alcohol referred to hydrogen as zero.

It will be seen that comparatively few elements have been investigated, and that the results of different investigators do not show satisfactory agreement.

* Communicated by the Authors.
† *Zeit. Phys. Chem.* lxix. p. 486 (1909).
‡ *Zeit. Elect.* xviii. p. 568 (1912), and xix. p. 491 (1913).
§ *Zeit. Elect.* xvi. p. 866 (1910).
‖ *Gazz. chim. ital.* xxxv. 1. p. 132 (1905).

The present communication contains an account of a new series of determinations of these constants for certain uni- and divalent elements in methyl alcohol. The measurements were planned so as to avoid as far as possible the above-mentioned sources of error.

TABLE I.

	Neustadt & Abegg.	Isgarischew.	Neustadt.	Carrara & Agostini.
Zn	−0·78	−0·65	...	−0·67
Cd	...	−0·30	...	−0·31
Pb	−0,21			
Cu	+0·33	+0·27	...	+0·43
Hg	+0·72			
Ag	+0·76	+0·76	+0·76	+0·76
I	...	...	+0·48	
Br	...	...	+0·90	
Cl	...	...	+1·19	

EXPERIMENTAL PROCEDURE.

The potentiometer, thermostats, and method of shielding were the same as those used by Nonhebel and Hartley *, and the cells were made of durosil glass in the form described by them. All measurements were carried out at $25{\cdot}0 \pm {\cdot}02°C$. The alcohol was prepared by the method described by Hartley and Raikes †. The salts used were pure specimens that had been prepared for conductivity work. The concentration of all solutions has been expressed in mols per 1000 grams of solvent, and accordingly molal activity coefficients have been used, referred to a standard state corresponding to the value of E_0^m defined by the equation

$$E_0^m = E + 0{\cdot}1183 \log m\gamma,$$

as explained by Woolcock and Hartley ‡.

The standard electrode potential, indicated by the symbol E.P., is taken as the potential of an element in contact with a solution containing its ions at unit activity defined as above, when measured against an electrode of hydrogen at atmospheric pressure, in a methyl alcohol solution containing hydrogen ions at unit activity. The sign of the electrode

* Phil. Mag. l. p. 729 (1925).
† J. Chem. Soc. cxxvii. p. 524 (1925).
‡ Phil. Mag. v. p. 1133 (1928).

potential is therefore in agreement with the usual custom adopted in Europe, but is the opposite of that used by G. N. Lewis. The values of the electromotive forces of the combinations described in this paper are written in accordance with the usual convention that the electrode on the right hand of the symbolic representation of the cell is positive.

Liquid Junction Potentials.

Nearly all the cells investigated included one or more liquid junctions, and it was essential that the potential differences at these junctions could be evaluated. Attempts were first made to eliminate the potentials at the liquid junctions by the use of a bridge consisting of a suitable saturated salt solution. The cell

$$\begin{array}{rc|l} & \text{HCl} & \text{NaCl} \\ \text{Ag, AgCl} & & \text{AgCl, Ag} \\ & 0{\cdot}1\text{ m.} & 0{\cdot}1\text{ m.} \end{array}$$

gave an electromotive force of 20·6 mv., and on the assumption that the activity coefficients of sodium chloride and of hydrogen chloride are the same at this dilution, and that therefore the potentials at the two electrodes are equal and opposite, this value represents the potential difference at the liquid junction. When the side-tubes of the two half-cells dipped into a saturated solution of ammonium nitrate, an electromotive force of 12·6 mv. was obtained. The theoretical boundary potential calculated by means of the formula of Lewis and Sargent* was 20·2 mv., which is in good agreement with the observed value. A similar cell containing hundredth molal solutions showed an electromotive force of 17·85 mv. when the junctions were kept flowing, but the value rose to 17·95 mv. as the boundary aged. When the liquid junction was made by means of a saturated solution of ammonium nitrate, the electromotive force was 12·45 mv., whilst a saturated solution of potassium iodide gave a value of 4·35 mv. The value of the electromotive force at the junction calculated by the Lewis and Sargent formula is 17·9 mv., which agrees well with the observed value 17·85 mv. These results justify the assumption of the equality of the activity coefficients of sodium and hydrogen chlorides in dilute solution, and show that it is impossible to eliminate completely the liquid junction potentials in methyl alcohol by the use of a

* J. Amer. Chem. Soc. xxxi. p. 363 (1909).

bridge of saturated salt solution. In addition, these two experiments show that the ordinary formulæ may be used to calculate liquid junction potentials in methyl alcohol with reasonable accuracy. In the present investigation the following formulæ have been employed for this purpose :—

1. For the general case in which the two solutions contain electrolytes at concentrations c_1 and c_2, whose cations have respectively mobilities u_1 and u_2 and valencies w_1 and w_2, and whose anions have mobilities v_1 and v_2 and valencies w_1' and w_2', Henderson's * formula is

$$E = \frac{RT}{F} \cdot \frac{(u_1 - v_1)c_1 - (u_2 - v_2)c_2}{(u_1 w_1 + v_1 w_1')c_1 - (u_2 w_2 + v_2 w_2')c_2} \log_e \frac{(u_1 w_1 + v_1 w_1')c_1}{(u_2 w_2 + v_2 w_2')c_2}.$$

The following special cases are of importance.

(*a*) When the solutions contain the same uni-univalent salt at concentrations c_1 and c_2,

$$E = \frac{u - v}{u + v} \cdot \frac{RT}{F} \log_e \frac{c_1}{c_2}.$$

(*b*) When the solutions are of equal concentration and all the ions are univalent,

$$E = \frac{RT}{F} \cdot \frac{(u_1 - u_2) - (v_1 - v_2)}{(u_1 - u_2) + (v_1 - v_2)} \log_e \frac{(u_1 + v_1)}{(u_2 + v_2)}.$$

(*c*) If, in addition, they have a common ion,

$$E = \frac{RT}{F} \log_e \frac{\lambda_v}{\lambda_v'},$$

where λ_v and λ_v' are the equivalent conductivities of the two solutions.

(*d*) For equally concentrated solutions of salts having a common univalent anion combined with univalent and divalent cations, Henderson's equation reduces to

$$E = \frac{RT}{F} \cdot \frac{(u_1 - u_2)}{(u_1 - 2u_2)} \log_e \frac{(u_1 + v)}{(2u_2 + v)}.$$

2. As a check on the results obtained for the potentials at liquid junctions comprising solutions of salts containing divalent ions, the independent formula of Pleijel † has also been employed. For the potential between equally concentrated solutions of salts $M'x$ and $M''x_2$ where M' has the

* *Zeit. Phys. Chem.* lix. p. 118 (1907), and lxiii. p. 325 (1908).
† *Zeit. Phys. Chem.* lxxii. p. 33 (1910).

mobility u_1, M'' has the mobility u_2, and x has the mobility v, this gives

$$E = \frac{RT}{F} \cdot \frac{4u_2 - 3u_1 + v}{8u_2 - 3u_1 + v} \log_e \frac{4}{3} \frac{2u_2 + v}{u_1 + v}.$$

In the application of this formula and of Henderson's the "mobility" of a divalent ion is taken as its mobility divided by its valency.

The data required for these calculations were obtained from the paper of Frazer and Hartley * and from unpublished figures for ionic mobilities available in this laboratory. In addition, certain conductivity measurements were made, the results of which are shown in Table II.

TABLE II.

Salt.	Concentration in gram equivalents per 1000 gms. MeOH.	Equivalent conductivity.
NaCNS	0·02	80·75
KI	0·054	76·2
NaBr	0·1	60·25
$TlClO_4$	0·00986	101·8
$AgClO_4$	0·01	96·76
$NaClO_4$	0·01	92·88
$AgNO_3$	0·00875	76·32
NaCl	0·01	78·3
NaCl	0·1	55·74

The values for the equivalent conductivity of sodium chloride calculated from the data of Goldschmidt and Dahl † at 0·01 m. and 0·1 m. are 79·2 and 56·0 respectively.

REFERENCE ELECTRODES.

Owing to the lack of a zero-electrode, constant and reproducible reference electrodes are indispensable to precise electromotive force measurements. In the present investigation, as is customary in water, the normal hydrogen electrode has been taken as the ultimate standard of reference. The hydrogen electrode in methyl alcohol is, however, unsuitable for use as a practical reference standard owing to the change of hydrion concentration due to esterification, to the considerable changes in the potential

* Proc. Roy. Soc. cix. p. 351 (1925).
† *Zeit. Phys. Chem.* cxiv. p. 3 (1924).

produced by small amounts of water with which the solutions may become contaminated, and to the fact that the iridized gold electrode is easily poisoned, and in methyl alcohol soon loses its activity, so that a fresh one is frequently required.

A secondary reference standard is needed whose potential is accurately known in terms of the normal hydrogen electrode, and for this purpose electrolytic silver-silver chloride electrodes appear to be most suitable. For prolonged measurements, however, these have the disadvantage that they can be relied on for only one or two days, and it was found in practice more convenient to employ reference electrodes of a type that could be used over long periods, and to check their potentials at intervals against freshly-prepared electrolytic silver-silver chloride electrodes. Calomel electrodes and electrodes of granular silver and precipitated silver chloride in both tenth and hundredth molal sodium chloride solution have been used for this purpose. Great care must be taken if the silver-silver chloride electrodes are to give reproducible values, whilst the calomel electrodes show a slow, continuous drift. Their potential, measured against a silver-silver chloride electrode in a solution of sodium chloride of the same concentration, was initially 46·5 mv., and rose to 49·9 mv. after three months and to 51·5 mv. after five months. This drift would be explained if slow oxidation of the calomel were taking place, as suggested by Gerke * and by Randall and Young †.

Activity Coefficients.

Electromotive force measurements are practically the only means available for the determination of activities in this solvent, and for this purpose it is necessary to use electrodes reversible to both the ions of the electrolyte. Wolfenden, Wright, Ross-Kane, and Buckley ‡ failed to obtain activity coefficients for sodium chloride solutions using electrodes of sodium amalgam, and hydrogen is the only electrode reversible to the cation whose behaviour has been studied in methyl alcohol and found satisfactory. The activity coefficients of hydrogen chloride in this solvent have been determined by Nonhebel and Hartley §. In the absence of values for the activity coefficients of other electrolytes, salts have been chosen which are known, from a study of their

* J. Amer. Chem. Soc. xliv. p. 1684 (1922).
† J. Amer. Chem. Soc. l. p. 989 (1928).
‡ Trans. Faraday Soc. xxiii. p. 491 (1927).
§ Phil. Mag. l. p. 729 (1925).

conductivities in methyl alcohol, to behave as strong electrolytes, and it has been assumed that the values of the activity coefficients of all uni-univalent electrolytes are the same as that of hydrogen chloride at the same concentration in dilute solution. This procedure is justified by the results of the two experiments described on p. 322, in which the assumption of similar activity coefficients for sodium chloride and hydrogen chloride led to values for the liquid junction potentials, which agreed closely with those calculated from the theoretical equation.

The activity coefficients of divalent ions were calculated by means of the equation of Debye and Hückel*,

$$-\log_e f_i = z_i^2 \frac{e^2}{2DkT} \cdot K;$$

where K is defined as

$$\sqrt{\frac{4\pi e^2}{DkT} \Sigma n_i z_i^2};$$

f_i is the activity coefficient of any ion, n_i the number of ions of the ith sort per c.c., and z_i their valency, e the charge on an electron, k the Boltzmann gas constant, T the absolute temperature, and D the dielectric constant of the solvent. Inserting the numerical values of these constants,

$$e = 4{\cdot}77 \,.\, 10^{-10} \text{ E.S.U.}, \quad k = 1{\cdot}371 \,.\, 10^{-16} \text{ erg/degree, and}$$
$$D_{MeOH} = 30{\cdot}3,$$

the expression becomes, for a divalent ion,

$$-\log f_i = 2{\cdot}427 \sqrt{\Sigma n_i z_i^2}.$$

If the concentration of the solution is c mols per litre, and the anion is univalent,

$$-\log f_i = 5{\cdot}975 \sqrt{6c}.$$

It is important to notice that the activity coefficients calculated from this formula refer to concentrations expressed in mols per litre. However, in dilute solutions whose density does not differ appreciably from that of the pure solvent, the numerical values of f and of the molal activity coefficient γ defined on p. 321 are identical.

* *Phys. Zeit.* xxi. p. 185 1923); xxv. p. 97 (1924).

Experimental Results.

Hydrogen.

The data of Nonhebel and Hartley* for the electromotive force of the cell,

$$H_2 - HCl \text{ in } MeOH - AgCl, Ag,$$

were used to calculate the potential of the electrode Ag, AgCl 0·1 m. HCl referred to the standard hydrogen electrode, giving a value of +0·0711 volt. On the assumption that the activity coefficients of hydrogen chloride and of sodium chloride are the same in tenth molal solutions, all potentials measured against the secondary reference electrode Ag, AgCl 0·1 m. NaCl have been referred to the standard hydrogen electrode by adding to them 0·0711 volt.

Sodium.

The standard electrode potential of sodium was obtained from the data of Wolfenden, Wright, Ross-Kane, and Buckley† for the electromotive force of the cell

$$\text{Sodium amalgam} - NaCl \text{ in } MeOH - AgCl, Ag.$$

The electromotive force of the equivalent cell with a metallic sodium electrode was first calculated from the data of Richards and Conant‡. Then if E is the electromotive force of the cell

$$Na - NaCl \text{ in } MeOH - AgCl, Ag$$

with a solution of sodium chloride of molality m and activity coefficient γ, the standard electrode potential of sodium ($E.P._{Na}$) can be calculated from the equation

$$E.P._{Na} - 0{\cdot}071 = -E + 0{\cdot}05915 \log (0{\cdot}1 \times 0{\cdot}461) - 0{\cdot}1183 \log m\gamma,$$

since the difference of potential between the electrodes Ag, AgCl 0·1 m. NaCl (in which solution sodium chloride has an activity coefficient of 0·461) and the standard hydrogen electrode is 0·071 volt.

Measurements in three of the more concentrated solutions,

* *Loc. cit.*
† *Loc. cit.*
‡ J. Amer. Chem. Soc. xliv. p. 601 (1922).

in which the behaviour of the amalgam electrode has not yet become abnormal, gave the following values :—

m.	γ.	E.	E.P.$_{Na}$.
0·01654	0·685	2·9490	−2·727
0·0568	0·525	2·9023	−2·730
0·0748	0·496	2·8886	−2·727

The mean value of E.P.$_{Na}$ is −2·728 volt.

Thallium.

The combination

Saturated thallium amalgam.	$TlClO_4$ 0·00987 m.	$NaClO_4$ 0·01 m.	NaCl 0·01 m.	NaCl Hg_2Cl_2, Hg 0·1 m.
	−	+ +	− −	+
		2·4 mv.	4·4 mv.	2·7 mv.

gave an electromotive force of 0·623 volt after subtracting 0·7 mv. to allow for the calculated potentials at the liquid junctions.

The thallium amalgam was made by warming small pieces of pure thallium metal with one and a half times their weight of distilled mercury. It was placed in a half-cell into which a platinum wire was sealed, and before being covered with the solution of thallium perchlorate it was washed repeatedly with oxygen-free alcohol to remove traces of oxide.

Assuming the activity coefficient of 0·00987 molal thallium perchlorate solution to be 0·746, and adding a correction of 2·6 mv. to allow for the difference of potential between thallium metal and its saturated amalgam (measured by Richards and Daniels*), the standard electrode potential becomes −0·499 volt referred to Hg, Hg_2Cl_2 0·1 m. NaCl, or −0·379 volt referred to the standard hydrogen electrode.

Silver.

The combination

Ag, AgCl	NaCl 0·01 m.	$NaClO_4$ 0·01 m.	$AgClO_4$ 0·01 m.	Ag
	−	+ +	−	
		4·4 mv.	1·1 mv.	

* J. Amer. Chem. Soc. xli. p. 1732 (1919)

gave an electromotive force of 0·5210 volt after subtracting a correction of 3·3 mv. to allow for the potentials at the liquid junctions.

A variety of silver electrodes were used to avoid errors due to mechanical strain in the metal. Silver wires coated electrolytically with silver from potassium silver cyanide solution were unsatisfactory. The best results were obtained using granular silver prepared by mixing boiling solutions of silver nitrate and ammonium formate. The silver perchlorate was prepared by dissolving pure silver oxide in perchloric acid, evaporating to dryness, and recrystallizing from benzene.

If the activity coefficient of 0·01 m. silver perchlorate solution is 0·745, the standard electrode potential of silver referred to Ag, AgCl 0·01 m. NaCl is +0·6465, or +0·7646 referred to the standard hydrogen electrode. A separate experiment, using silver wire electrodes, gave a value of +0·762 for the standard electrode potential of silver. The most probable figure is +0·764 volt.

Two experiments using 0·00875 m. silver nitrate solution gave values of 0·760 and 0·756 volt for the standard potential with different types of electrodes. Silver nitrate is known to be partially associated in methyl alcohol, and this would explain the lower values.

Cadmium.

As observed by Isgarischew *, it was found impossible to obtain a steady potential from a rod of cadmium dipping into the solution of a cadmium salt in methyl alcohol. The continuous fall of potential, which he attributed to passivity, occurs even with amalgamated electrodes, but can be prevented by bubbling hydrogen into the solution, and by this means the maximum uncertainty of measurement was reduced to 0·01 volt.

The combination

	$Cd(ClO_4)_2$		$NaClO_4$		NaCl	
Cd						AgCl, Ag
	0·01 m.		0·01 m.		0·01 m.	
		+	−	+	−	
		3·4 mv.		4·4 mv.		

* *Zeit. Elect.* xviii. p. 568 (1912) and xix. p. 491 (1913).

gave an electromotive force of 0·578 volt after adding a correction of 8 mv. to allow for the potentials at the liquid junctions.

The cadmium perchlorate solution was made by mixing equivalent amounts of methyl alcohol solutions of cadmium bromide and of silver perchlorate from a weight-burette. The hydrogen was generated by electrolysis of caustic soda solution saturated with baryta, and was freed from oxygen, dried, and saturated with methyl alcohol vapour before entering the cell. To obtain satisfactory results the rods of cadmium must be cleaned with 30 per cent. sulphuric acid, washed, and dried immediately before being used. When the electromotive force of the cell had become steady, the addition of a few drops of a solution of benzenesulphonic acid had only a very slight effect on the potential, showing that the cadmium rods were not acting as hydrogen electrodes, since in that case there would have been a considerable change in potential corresponding to the great change of hydrion concentration.

The activity coefficient of the cadmium ion in 0·01 molal cadmium perchlorate solution, calculated from the formula of Debye and Hückel, is 0·05, so that the standard electrode potential of cadmium is −0·376 volt referred to Ag, AgCl 0·01 m. NaCl, or −0·258 volt referred to the normal hydrogen electrode.

Copper.—The potential of a copper electrode, like cadmium, falls continuously when placed in contact with methyl alcohol solutions of its salts, but a steady electromotive force was obtained when a stream of hydrogen was bubbled through the solution. Various copper wires were used as electrodes, since the necessity for the hydrogen stream makes it inconvenient to use the metal in a finely divided state. When the electromotive force had become steady, addition of a small amount of acid showed that the copper was not acting as a hydrogen electrode, and, moreover, had this been so, the introduction of hydrogen would have produced a fall of potential and not a rise, as was invariably observed. To obtain a steady electromotive force it is essential that the copper should be cleaned immediately before putting it into the solution, and that the latter should be already saturated with hydrogen. The copper wires were cleaned most effectively with dilute sulphuric acid, followed by quick washing and drying. The copper perchlorate solutions were made by mixing equivalent amounts of methyl alcoholic solutions of copper chloride and of silver

perchlorate. The solution was almost colourless, and remained so when a steady potential was obtained as a result of cleaning the copper and passing hydrogen through the solution continuously. Without these precautions the solution became green during the measurements.

The combination

	NaCl	$NaClO_4$	$Cu(ClO_4)_2$	
Hg, Hg_2Cl_2				Cu
	0·01 m.	0·01 m.	0·0067 m.	
	−	+		
	4 mv.		negligible	

gave in three separate experiments electromotive forces of 0·480, 0·466, and 0·476 volt. The calomel reference electrode had a potential of 0·172 volt referred to the standard hydrogen electrode, and the calculated activity coefficient of copper perchlorate in the 0·0067 molal solution was 0·087. The corresponding values for the standard electrode potential of copper are 0·504, 0·490, and 0·500 volt.

In a fourth experiment, in which the solution was 0·00486 molal, the potential of the copper referred to the standard hydrogen electrode was 0·294 volt. At this concentration the calculated activity coefficient is 0·125, and hence the standard electrode potential of copper is 0·484 volt. The most probable value from the four experiments is +0·49 volt.

The Solubilities of the Silver Halides and the Calculation of the Standard Electrode Potentials of the Halogens.

Solubility product of Silver Chloride.

Since the electrode Ag, AgCl 0·1 m. HCl has a potential of 0·071 volt referred to the standard hydrogen electrode, the activity of silver ions in that solution can be found by substituting the values E = 0·071 and $E.P._{Ag} = 0·764$ in the equation

$$E = E.P._{Ag} + 0·05915 \log a_{Ag},$$

giving

$$E = E.P._{Ag} + 0·05915 \log a_{Ag},$$

giving a value of $1·94 . 10^{-12}$. Since the hydrogen chloride was 0·1 molal with an activity coefficient of 0·461, the solubility product of silver chloride is

$$1·94 . 10^{-12} \times 0·1 \times 0·461$$
$$= 8·93 . 10^{-14}$$

when the concentrations of the ions are expressed in gm. equivs. per 1000 grams of alcohol. The solubility of silver chloride is therefore $3{\cdot}0 \cdot 10^{-7}$ gm. equivs. per 1000 grams of alcohol, assuming that the activity coefficient is unity in so dilute a solution.

Solubility product of Silver Bromide.

The combination

	NaBr		NaCl	
Ag, AgBr				Hg_2Cl_2, Hg
	0·1 m.		0·1 m.	
	+		−	

2·0 mv.

gave an electromotive force of 0·1785 volt after adding 2·0 mv. to allow for the calculated potential at the liquid junction. The Hg, Hg_2Cl_2 0·1 m. NaCl electrode had a potential of 49·6 mv. positive to Ag, AgCl 0·1 m. NaCl, so that the potential of the silver-silver bromide electrode relative to the latter was −0·1290 volt or −0·058 relative to the standard hydrogen electrode. Substituting the values

$$E = -0{\cdot}058, \quad E.P._{Ag} = 0{\cdot}764$$

in the last equation, the activity of silver ions in the sodium bromide solution is found to be $1{\cdot}26 \cdot 10^{-14}$, and the solubility product of silver bromide

$$1{\cdot}26 \cdot 10^{-14} \times 0{\cdot}1 \times 0{\cdot}461 = 5{\cdot}8 \cdot 10^{-16}.$$

The solubility of silver bromide is therefore

$2{\cdot}41 \cdot 10^{-8}$ gm. equivs. per 1000 grams of alcohol.

Solubility product of Silver Iodide.

The combination

	KI		NaCl	
Ag, AgI				Hg_2Cl_2Hg,
	0·054 m.		0·1 m.	
	−		+	

0·6 mv.

using granular silver and precipitated silver iodide, gave an electromotive force of 0·3375 volt after correcting for the potential at the liquid junction. Silver-silver iodide electrodes prepared electrolytically gave an initial value agreeing approximately with this, but their potential fell rapidly, and

secondary reactions appeared to be taking place. The calomel reference electrode against which the measurement was made was 44·0 mv. positive to Ag, AgCl, 0·1 m. NaCl, so that the potential of the silver-silver iodide electrode referred to this was −0·2935 volt, and the silver ion activity in the potassium iodide solution was $2{\cdot}09 \cdot 10^{-17}$. Assuming that 0·054 m. potassium iodide solution has an activity coefficient 0·53, the solubility product of silver iodide is $6{\cdot}0 \cdot 10^{-19}$ and the solubility of silver iodide is

$7{\cdot}7 \cdot 10^{-10}$ gm. equivs. per 1000 grams of alcohol.

Solubility product of Silver Thiocyanate.

The combination

	NaCNS	NaCl	NaCl	
Ag, AgCNS				Hg_2Cl_2Hg,
	0·02 m.	0·02 m.	0·1 m.	
	+	−	− +	
	2·6 mv.	1·9 mv.		

using granular silver and precipitated silver thiocyanate, gave an electromotive force rising from an initial value of 0·023 to 0·055 volt, at which it became constant on the fourth day. Silver-silver thiocyanate electrodes prepared electrolytically were neither constant nor reproducible. Since the calomel electrode was 0·046 volt positive to Ag, AgCl 0·1 m. NaCl, the potential of the silver-silver thiocyanate electrode referred to this was −0·0009 volt, and hence the activity of silver ions in the thiocyanate solution was $1{\cdot}4 \cdot 10^{-12}$. If the activity coefficient of 0·02 m. sodium thiocyanate solution is 0·664, the solubility product of silver thiocyanate is

$$1{\cdot}4 \cdot 10^{-12} \times 0{\cdot}02 \times 0{\cdot}664$$
$$= 1{\cdot}8 \cdot 10^{-14},$$

and the solubility of silver thiocyanate is

$1{\cdot}3 \cdot 10^{-7}$ gm. equivs. per 1000 grams of alcohol.

Solubility product of Thallium Chloride.

The combination

Saturated thallium amalgam	NaCl 0·01 m. saturated with thallium chloride	NaCl 0·1 m.	Hg_2Cl_2, Hg
	−	+	
	2·7 mv.		

gave an electromotive force of 0·639 volt after correcting for the potential at the liquid junction. Adding 0·049 volt for the potential of the calomel electrode referred to Ag, AgCl 0·1 m. NaCl, and subtracting 0·0025 volt to allow for the difference of potential between thallium metal and its saturated amalgam, the activity of thallium ions in the 0·01 m. sodium chloride solution is found to be $3{\cdot}9 \cdot 10^{-3}$, and since the activity of chlorine ions is $0{\cdot}01 \cdot 0{\cdot}745$, the ionic product of thallium chloride is $2{\cdot}9 \cdot 10^{-5}$.

If the activity coefficient could be assumed to be unity, as with more insoluble salts, the solubility of thallium chloride would be $5{\cdot}4 \cdot 10^{-3}$ gm. equivs. per 1000 grams of alcohol.

The solubility data that have been obtained are shown in Table III., where they are compared with the figures for water.

TABLE III.

Salt.	Solubility product in methyl alcohol.	Solubility in methyl alcohol (gram equiv. per 1000 grams).	Solubility in water (gram equiv. per 1000 grams).	Solubility in water / Solubility in alcohol.
AgCl ...	$8{\cdot}9 \cdot 10^{-14}$	$3{\cdot}0 \cdot 10^{-7}$	$1{\cdot}3 \cdot 10^{-5}$	43
AgBr ...	$5{\cdot}8 \cdot 10^{-16}$	$2{\cdot}4 \cdot 10^{-8}$	$7{\cdot}8 \cdot 10^{-7}$	33
AgI	$6{\cdot}0 \cdot 10^{-19}$	$7{\cdot}7 \cdot 10^{-10}$	$1{\cdot}0 \cdot 10^{-8}$	13
AgCNS .	$1{\cdot}8 \cdot 10^{-14}$	$1{\cdot}3 \cdot 10^{-7}$	$1{\cdot}2 \cdot 10^{-6}$	9·2
TlCl ...	$2{\cdot}9 \cdot 10^{-5}$	$5{\cdot}4 \cdot 10^{-3}$	$1{\cdot}5 \cdot 10^{-2}$	2·8

The values for the solubility products of silver chloride, bromide, and iodide obtained by Neustadt*, when recalculated in terms of molal concentrations, are $9{\cdot}5 \cdot 10^{-14}$, $6{\cdot}4 \cdot 10^{-16}$ and $9{\cdot}5 \cdot 10^{-19}$, in fair agreement with the above results.

Standard Electrode Potential of Chlorine.

The standard electrode potential of chlorine was calculated from the solubility product of silver chloride by the following method :—

The electromotive force of the cell,

$$\mathrm{Ag}-\mathrm{AgCl}-\mathrm{Cl_2},$$

is a measure of the free-energy decrease in the reaction

$$\mathrm{Ag_{(solid)}} + \tfrac{1}{2}\mathrm{Cl_{2(gas)}} = \mathrm{AgCl_{(solid)}},$$

* *Loc. cit.*

and must be independent of the nature and concentration of the intermediate electrolyte. The electromotive force E of the above cell is given by the equation

$$-E = E.P._{Ag} - E.P._{Cl} + \frac{RT}{nF}(\log_e a_{Ag^+} + \log_e a_{Cl^-})$$

$$= E.P._{Ag} - E.P._{Cl} + 0{\cdot}05915 \log L_{AgCl},$$

where $E.P._{Ag}$ and $E.P._{Cl}$ are the standard electrode potentials and L_{AgCl} the solubility product of silver chloride in any particular solvent.

The value of E can be found by substituting in the equation the values for water, $E.P._{Ag} = 0{\cdot}7995$, $E.P._{Cl} = 1{\cdot}3594$, and $L_{AgCl} = 1{\cdot}8 \cdot 10^{-10}$. E is thus found to be 1·135 volt, agreeing well with the directly observed value of Gerke *, 1·1362 volt.

Substituting now in the equation the values for methyl alcohol, $E.P._{Ag} = 0{\cdot}764$ and $L_{AgCl} = 8{\cdot}93 \cdot 10^{-14}$,

$$E.P._{Cl} = +1{\cdot}128 \text{ volts.}$$

Standard Electrode Potential of Bromine.

The electromotive force of the cell,

$$Ag - AgBr - Br_2,$$

is given by the equation

$$-E = E.P._{Ag} - E.P._{Br} + 0{\cdot}05915 \log L_{AgBr}$$

By substituting the values for water, $E.P._{Ag} = 0{\cdot}7995$, $E.P._{Br} = 1{\cdot}0659$, and $L_{AgBr} = 6{\cdot}5 \cdot 10^{-13}$, E is found to be +0·986 volt.

Substituting now in the equation

$$-0{\cdot}986 = E.P._{Ag} - E.P._{Br} + 0{\cdot}05915 \log L_{AgBr}$$

the values for methyl alcohol, $E.P._{Ag} = 0{\cdot}764$ and $L_{AgBr} = 5{\cdot}8 \cdot 10^{-16}$,

$$E.P._{Br} = +0{\cdot}849 \text{ volt.}$$

Standard Electrode Potential of Iodine.

The electromotive force of the cell,

$$Ag - AgI - I_2,$$

is expressed by

$$-E = E.P._{Ag} - E.P._{I} + 0{\cdot}05915 \log L_{AgI}.$$

* *Loc. cit.*

Substituting the values for water, $E.P._{Ag} = 0\ 7995$, $E.P._{I} = 0{\cdot}5357$, and $L_{AgI} = 1{\cdot}0 \,.\, 10^{-16}$,

$$E = +0{\cdot}6802 \text{ volt},$$

which agrees fairly well with the directly-measured value 0·685 of Jones and Hartman *.

Substituting in the equation

$$-0{\cdot}683 = E.P._{Ag} - E.P._{I} + 0{\cdot}05915 \log L_{AgI}$$

the values for methyl alcohol, $E.P._{Ag} = 0{\cdot}764$ and $L_{AgI} = 6{\cdot}0 \,.\, 10^{-19}$,

$$E.P._{I} = +0{\cdot}369 \text{ volt}.$$

Discussion of Results.

Table IV.

Element.	E.P. in water.	E.P. in methyl alcohol.	$E.P._{H_2O} - E.P._{MeOH}$.
Na	−2·7125	−2·728	+0·015
Tl	−0·3363	−0·379	+0·043
Cd	−0·398	−0·258	−0·140
H	0	0	0
Cu	+0·345	+0·490	−0·145
Ag	+0·7995	+0·764	+0·036
I.....	+0·5357	+0·369	+0·167
Br	+1·0659	+0·849	+0·217
Cl	+1·3594	+1·128	+0·231

Table IV. gives the values which we have found for the standard electrode potentials of eight elements in methyl alcohol, together with the corresponding values in water. It will be seen that the relative positions of all the univalent elements are the same in both solvents, and that there is fairly close agreement between the two sets of values. All the univalent metals are rather more electropositive in methyl alcohol than in water by comparison with hydrogen, while the two divalent metals are considerably less electropositive. It must be remembered, however, that the activity coefficients are known with less certainty for the latter elements, as they have been calculated from the Debye-Hückel theory, whilst in the case of the univalent metals there is experimental support for taking them as equal to those of hydrogen chloride, which have been determined

* J. Amer. Chem. Soc. xxxvii. p. 756 (1915).

directly. The differences between the values of the electrode potentials in the two solvents are greatest for the halogens.

If the process of ionization were solely the separation of a charged atom from the electrode, as postulated in the original Nernst theory, it might be expected that the electrode potentials should be independent of the solvent. However, there is little doubt that the passage of an ion from the crystal lattice into solution is accompanied by its association with a certain number of solvent molecules. Hence the electrode potential of an element represents the difference in the free-energy content of the ions in the lattice and in a solvated condition. It is, therefore, not surprising that there should be individual differences between the electrode potentials in the two solvents corresponding to the varying affinities of the molecules of the two solvents for the same ion. But, as hydrogen has been chosen as the standard of reference in each solvent, without any knowledge of the energy of solvation of hydrogen ions in both, it is difficult to draw any conclusions as to the relative affinities of the two solvents for individual ions. It is possible, however, to calculate from the electrode potential data the free energy of transfer of one mol of various electrolytes from a solution in water to a solution of the same activity in methyl alcohol.

Thus the combination

$$Cl_2 - HCl \text{ in methyl alcohol} - H_2 \text{——} H_2 - HCl \text{ in water} - Cl_2$$

$$\xrightarrow[E_3]{a_3} \qquad \xleftarrow[E_4]{a_4}$$

$$\xleftarrow{\qquad E_5 \qquad}$$

has an electromotive force,

$$E_5 = E_4 - E_3$$

and $$E_3 = E.P._{Cl}^{alc.} - E.P._{H}^{alc.} - 0{\cdot}1183 \log a_3$$

and $$E_4 = E.P._{Cl}^{H_2O} - E.P._{H}^{H_2O} - 0{\cdot}1183 \log a_4.$$

Since $E.P._{H}^{alc.}$ and $E.P._{H}^{H_2O}$ are taken as zero,

$$E_5 = E_4 - E_3 = E.P._{Cl}^{H_2O} - E.P._{Cl}^{alc.} - 0{\cdot}1183 \log a_4/a_3,$$

and when the solute has the same activity in both solvents,

$$E_5^0 = E.P._{Cl}^{H_2O} - E.P._{Cl}^{alc.}$$

From the figures given in Table IV., the free energy of transfer of one mol of hydrogen chloride from its solution

of unit activity in water to that of unit activity in methyl alcohol is 5330 calories. Similar considerations for hydrogen bromide and hydrogen iodide lead to the values 5000 and 3850 calories respectively. These figures are inaccessible directly owing to rapid esterification making it impossible to measure the electromotive force of cells containing methyl alcohol solutions of these acids.

In addition, it is possible to calculate the free energy of transfer of thiocyanic acid from an aqueous to an alcoholic solution by making use of the data in Table III. to calculate the difference of standard potential between imaginary thiocyanogen electrodes in the two solvents.

Thus the combination

$$Ag-AgCNS-(CNS)_2$$

would have an electromotive force

$$-E=E.P._{Ag}^{H_2O}-E.P._{(CNS)_2}^{H_2O}+0{\cdot}05915 \log L_{AgCNS}^{H_2O}$$

when water is the solvent, and the same when methyl alcohol is the solvent, viz.,

$$-E=E.P._{Ag}^{alc.}-E.P._{(CNS)_2}^{alc.}+0{\cdot}05915 \log L_{AgCNS}^{alc.}.$$

Hence

$$\begin{aligned}E.P._{(CNS)_2}^{H_2O}-E.P._{(CNS)_2}^{alc.}&=E.P._{Ag}^{H_2O}-E.P._{Ag}^{alc.}+0{\cdot}05915 \log L_{AgCNS}^{H_2O}/L_{AgCNS}^{alc.}\\&=0{\cdot}036+0{\cdot}05915 \log 84\\&=0{\cdot}150 \text{ volt.}\end{aligned}$$

The free energy of transfer of one mol of thiocyanic acid from an aqueous to an alcoholic solution, both of unit activity, is thus 3460 calories.

The Quinhydrone Electrode.

The quinhydrone electrode has been studied in aqueous solutions by Biilman *, who obtained for the difference of potential between it and the hydrogen electrode the value 0·6990 volt. Using different preparations of quinhydrone and a variety of electrodes we have obtained for this potential difference the following results :—

Concentration of hydrogen chloride solution.	Concentration of quinhydrone.	E.M.F.
0·11 N.	0·006 m.	0·6989 volt.
0·01 N.	0·01 m.	$0{\cdot}6989_5$ volt.
0·01 N.	0·001 m.	0·6989 volt.
0·11 N.	0·005 m.	$0{\cdot}6990_7$ volt.

* *Annales de Chimie,* xv. p. 109 (1921). and xvi. p. 320 (1921).

The quinhydrone electrode has been used in methyl alcohol by Ebert *, who measured the hydrogen and quinhydrone electrodes successively in portions of the same solution against an aqueous calomel reference standard. For the difference between them he got concordant values of 0·724 volt at 18° C.

We have made many attempts to measure the potential of the quinhydrone electrode in methyl alcohol, but have not succeeded in obtaining a steady value. In general the potential was found to rise steadily for from one to six hours, at the rate of from one to three centivolts per hour, and then to fall steadily at the rate of one to two millivolts per hour. In six experiments extrapolation of the observed electromotive force back to zero time led to values for the potential difference between the quinhydrone and hydrogen electrodes of 0·716, 0·715, 0·710, 0·718, 0·719, and 0·716 volt. Considerable momentary rises of electromotive force were produced when the solution was stirred by moving the platinum electrode, which suggests that the cause of these irregularities was some reaction by which the quinhydrone was destroyed at the electrode surface. Addition of further quantities of quinhydrone to the solution produced a considerable rise of potential, which was not, however, reproducible. Removal of the platinum electrode, and heating it to redness in an alcohol flame produced a rise of potential of several centivolts, but the subsequent fall was rapid. In attempts to find the cause of these disturbances we have used different specimens of quinhydrone and electrodes of gold, of platinum gauze, and of bright platinum foil. Solutions of hydrogen chloride, of benzenesulphonic acid, and buffer solutions of succinic acid and guanidine succinate have given equally unsatisfactory results.

The Dissociation Constant of Methyl Alcohol.

The hydrogen electrode was used to measure the hydrion concentration in a solution of sodium methylate, and hence to calculate the dissociation constant of methyl alcohol.

Sodium methylate solution free from water and carbon dioxide was made by a method due to Mr. W. F. K. Wynne-Jones. Pieces of sodium as free as possible from oxide were melted under paraffin in a Pyrex flask, and drawn up into thin-walled glass tubing about 2 mm. in diameter. This was cut into convenient lengths, and the central portions dropped quickly into a flask containing methyl alcohol.

* *Berichte*, lviii. p. 175 (1925).

When the reaction was completed, the concentration of the solution was found by weight titration against standard acid.

The hydrogen was generated electrolytically from sodium hydroxide solution saturated with baryta, using nickel electrodes. It was freed from traces of oxygen by passing over a heated tungsten filament, dried with sulphuric acid, soda lime, and phosphorus pentoxide, and then saturated with alcohol vapour before entering the cell. It was found impossible to get a steady potential when using freshly iridized gold plates as hydrogen electrodes, and after several failures with platinum electrodes satisfactory results were obtained with one that had been freshly platinized.

The combination

$$\begin{array}{ccc} \text{MeONa} & & \text{NaCl} \\ \text{H}_2 & & \text{AgCl, Ag} \\ 0{\cdot}0217\ \text{m.} & & 0{\cdot}01\ \text{m.} \\ & + \quad - & \\ & 1{\cdot}7\ \text{mv.} & \end{array}$$

gave an electromotive force of 0·9930 volt. A correction of 1·7 mv. is to be added for the potential at the liquid junction and of 2·3 mv. to correct the hydrogen electrode to a partial pressure of hydrogen gas of one atmosphere. The secondary reference electrode had a potential of 0·047 volt referred to Ag, AgCl 0·1 m. NaCl, so that the potential of the hydrogen electrode in the sodium methylate solution referred to the standard hydrogen electrode was −0·879 volt.

Hence

$$\log a_{\text{H}} = -\frac{0{\cdot}879}{0{\cdot}05915} = \bar{1}5{\cdot}1395.$$

If the activity coefficient of 0·0217 m. sodium methylate solution is 0·652, the dissociation constant of methyl alcohol is calculated to be $1{\cdot}95 \cdot 10^{-17}$.

In a second experiment using a 0·0626 molal sodium methylate solution, the observed electromotive force was 1·0684 volt with a calomel reference electrode whose potential was −0·170 volt relative to the standard hydrogen electrode. Adding 2·3 mv. for the barometric correction, and 2·8 mv. for the liquid junction potential, the potential of the hydrogen electrode in the sodium methylate solution was −0·9035 volt referred to the standard hydrogen electrode. Hence

$$\log a_{\text{H}} = -\frac{0{\cdot}9035}{0{\cdot}05915} = \bar{1}6{\cdot}73.$$

If the activity coefficient of 0·0626 molal sodium methylate solution is 0·515, the dissociation constant of methyl alcohol is calculated to be $1{\cdot}73 \cdot 10^{-17}$. Less reliance is placed on this value than the first, as the electromotive force of the cell fell off after half an hour.

Previous determinations of this constant have yielded the following results:—

(i.) Carrara, by measurements of electromotive force at 10° C., got $4{\cdot}9 \cdot 10^{-17}$.

(ii.) Bjerrum, Unmack, and Zechmeister *, by a somewhat doubtful extrapolation to infinite dilution from two points, obtained $3{\cdot}6 \cdot 10^{-17}$.

(iii.) Wynne-Jones, in experiments (not yet published) on the alcoholysis of salts in methyl alcohol, found values varying from 3·0 to $2{\cdot}0 \times 10^{-17}$.

SUMMARY.

(1) A study has been made of reference electrodes, of liquid-junction potentials, and of activity coefficients in methyl alcohol.

(2) Measurements have been made of the standard electrode potentials of nine elements, and the results used for determining the solubilities of five sparingly soluble salts and the dissociation constant of methyl alcohol.

(3) The quinhydrone electrode has been studied in aqueous and alcoholic solutions.

Physical Chemical Laboratory,
Balliol College and Trinity College, Oxford.
February 1929.

XXXIX. *Unbalance in Circuits.* *By* M. REED, *M.Sc.* (*Lond.*), *A.C.G.I.*, *D.I.C.* (*Research Laboratories, International Standard Electric Corporation*) †.

1. *General.*

IN cases where accurate measurements have to be made, it is found that, in addition to the normal impedances, it is necessary to take into consideration the admittance to ground of various parts of the circuits under investigation. These admittances are generally very small, yet

* *Kgl. Danske Vid. Selsk. Mat.-fys. Medd.* V. ii (1924).
† Communicated by the Author.

under certain conditions their effect on the measurement can be quite appreciable. This paper considers how these admittances can influence the accuracy of a given measurement, and also how it is possible to avoid the errors that would result from their presence.

2. *Longitudinal Voltages.*

Suppose that it is required to measure the voltage between the terminals of a given piece of apparatus. Assume that this voltage is to be measured by means of a circuit which possesses a pair of input terminals, and which comprises a detector of some sort to indicate the value of the voltage which may be impressed across these input terminals.

It will be shown that it is necessary, in determining the behaviour of the circuit, to consider not only the impedance between the input terminals, but also the admittance to ground of each terminal. In the general case, when these admittances are unequal, it will be found that the voltage produced across the terminals of the apparatus under consideration will be measured incorrectly if the average voltage from these terminals to ground is not zero.

Consider the circuit of fig. 1.

Fig. 1.

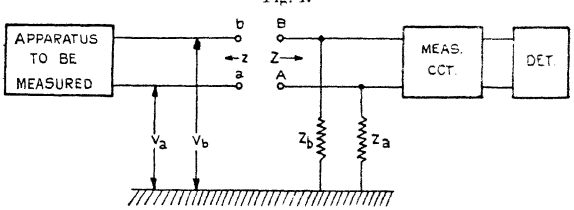

In this diagram assume that :—

z =impedance measured between terminals a and b.

V_a=magnitude of voltage between terminal a and ground.

V_b= ,, ,, ,, ,, ,, b ,, ,,

Z =impedance measured between terminals A and B.

Z_a= ,, ,, ,, terminal A and ground.

Z_b= ,, ,, ,, ,, B ,, ,,

If we assume that the physical mid-point of z is connected either directly or through an impedance Z_g to ground, then if V_a is not equal to V_b, the physical mid-point of z will not coincide with the electrical zero. The difference between V_a and V_b may be due to a number of causes, *e.g.*, unbalance in coils and transformers, interference from outside sources. The potential of the mid-point will therefore differ from that of ground by an amount given by $\frac{V_a \sim V_b}{2}$. Under these circumstances the circuit of fig. 1 can be regarded as equivalent to that of fig. 2.

In some cases the value of the impedance, as measured between the mid-point and terminals A and B, will not be

Fig. 2.

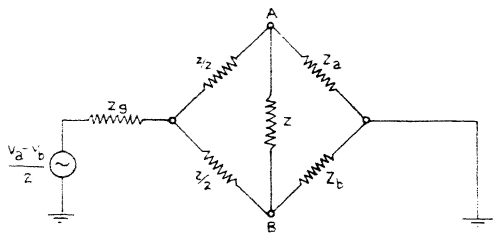

equal to $\frac{z}{2}$, but to some value which is less than half of the value of the impedance as measured between A and B. The value of the impedance between each terminal and the mid-point will, however, be the same; hence the diagram of fig. 2 will still be true in principle.

The voltages V_a and V_b are not shown, as they only give the voltage which would normally be measured across A and B.

Fig. 2 shows that the unbalance voltage $\frac{V_a \sim V_b}{2}$ acts across a circuit which is equivalent to a Wheatstone Bridge. It therefore follows that if Z_a is not equal to Z_b, then there will be a difference of potential set up across AB whose value will depend on the values of $\frac{1}{2}(V_a \sim V_b)$ and Z_g. The measuring circuit will record this voltage, in addition to the normal voltage, and hence there will be an error

introduced into the measurement. The unbalance current, and therefore the error, will be increased as the value of Z_g is reduced, the error being a maximum when $Z_g=0$. It is therefore undesirable that the mid-point of z should be connected directly to earth. If $Z_a=Z_b$, then there will be no unbalance current through Z, and the correct voltage will be measured. It is therefore necessary, in order that accurate and consistent results should be obtained, that the value of Z_a should be made equal to that of Z_b.

The above phenomenon, which is caused by the unbalance voltage $\frac{1}{2}(V_a \sim V_b)$, is said to be produced by a longitudinal voltage. This is to distinguish it from any voltage which acts across the terminals AB, and which is called a transverse voltage. A measure of the error introduced by the

Fig. 3.

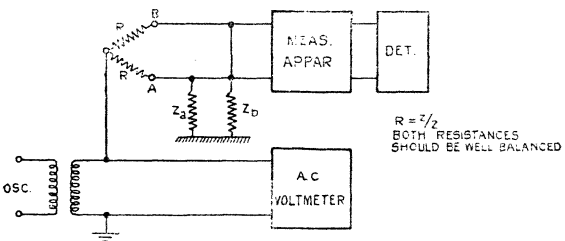

longitudinal voltage can be obtained in the following manner.

The circuit of fig. 3 is fitted up and the voltage V_1 produced by the oscillator is adjusted until some convenient reading is obtained on the detector. The value of this voltage is obtained from the a.c. voltmeter, which may consist of a suitable thermocouple with a series resistance. The voltage V_2 necessary to produce the same reading on the detector when the oscillator is applied to the terminals AB is then measured, care being taken that the oscillator used is well balanced to ground. The ratio V_2/V_1 will then give the value of the transverse voltage, which is equivalent to 1 volt of longitudinal voltage, and hence it will be a measure of the error that would be introduced into a given measurement.

When making this test care should be taken that the leads (if any) between the resistances R and the terminals AB do not introduce ground unbalances. If leads are used they should be short and unscreened. They can be tested for ground unbalances by reversing the connexions at A and B on the set. The value of V_1 should be unaltered by the reversal.

3. *The Balanced and Screened Transformer.*

It will be shown later that in the case of certain circuits it is desirable, in order to avoid the errors due to longitudinal voltages, to employ balanced and screened transformers. A brief description of this type of transformer is given below.

Each winding of the transformer consists of two sections, each section being wound to cover one-half of the core. The turns on the two sections, which comprise one winding,

Fig. 4.

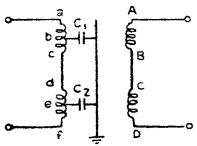

are adjusted until the sections are balanced. A shield is placed between the two windings, and the side of the transformer which is to be balanced is so wound that the capacities between the shield and each half of the winding are equal and symmetrically located with respect to the mid-point of the whole winding. This is accomplished by winding the sections *ab* and *de* and the sections *bc* and *ef*, each as twisted pairs. The total capacity of each section of the same winding will then be practically the same. Consider, for example, the transformer of fig. 4.

The windings *af* and AD would each consist of two sections. The sections *ac* and *df* of winding *af* would be balanced. Similarly the sections AB and CD of winding AD would be balanced. If it is required that the winding *af* should be balanced with respect to the shield, then this winding would be so arranged that the capacities C_1 and C_2 should act at points which are equidistant from the

mid-point *cd*. It would then be found that C_1 did not differ appreciably from C_2. A similar procedure would be adopted if it were desired to balance the winding AD to shield.

Further, owing to the presence of the shield, which is always earthed, there is no direct capacity between the windings *af* and AD. Hence any unbalance to earth which may occur on the right-hand side of the transformer will be completely cut off from the left-hand side.

The degree of unbalance between two sections of a winding can be very easily determined by the following method. The two sections are connected up with two resistance boxes to form a bridge of the form shown in fig. 5. The resistance boxes are then adjusted until the bridge is balanced, and the ratio of the values of the

Fig. 5.

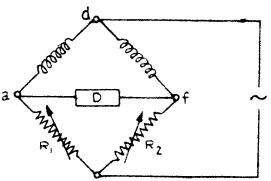

resistances gives a measure of the unbalance between the sections. The two sections can then be adjusted until the resistance ratio is unity, thus indicating zero unbalance.

4. *Unbalances in Practice.*

In practice unbalances are important because, as seen from fig. 2, they enable the longitudinal voltage to give rise to currents which are circulating, and which are therefore not attenuated by any apparatus that may be present in the circuit. In cases where this apparatus has high attenuation, the current due to the normal transverse voltage is greatly attenuated, whereas the currents due to the longitudinal voltage remain unattenuated. It is therefore quite possible, when the attentuation is very high, that the voltage produced at the far end by the circulating currents may be comparable with that produced by the normal current. The error introduced in this case would be fairly large.

It follows that if the unbalances in the circuit are such that they produce a transverse and not a longitudinal unbalance voltage, then the current which is derived from this voltage will suffer the same attenuation as the legitimate current, and hence the error introduced in a given measurement will be negligible.

In practice, measuring circuits are either of the balanced or of the unbalanced type. Each type will now be considered in detail, and it will be shown, in each case, how the accuracy of measurement is affected by unbalances in the circuit, and also how the errors can be avoided.

5. *The Balanced Circuit.*

In this type of measuring circuit the admittance to ground of all the terminals is assumed to be the same. Also the value of the impedance of each series arm is the same.

Fig. 6.

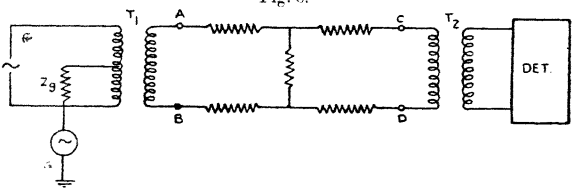

Consider, for example, the circuit of fig. 6, in which it is assumed that the balanced circuit is represented by the networks ABCD. This network is connected to an oscillator and a detector through transformers T_1 and T_2, respectively.

Assume that the terminals of the oscillator have different voltages to ground, so that we have in effect a potential difference between the mid-point of the primary winding of T_1 and ground. It is assumed that this mid-point has an impedance Z_g to ground. The following cases must now be considered.

5 (1). T_1 *and* T_2 *both without shields.*

If T_1 is without a shield, then the unbalance voltage will be transferred from the primary to the secondary side of T_1 through the stray capacity that will exist between the windings. Further, since T_2 has no shield,

it is very probable that the admittance to earth of terminal A will be different from that of terminal B. Hence we shall find, on replacing the circuit of fig. 6 by one similar to that of fig. 2, that there will be an unbalance current produced in winding CD. This current will give rise to a voltage across CD which will be transferred to the terminals of the detector, thus causing an error in the measurement. It will be noticed that the unbalance current is not attenuated by the network ABCD, and therefore it is quite possible, when the attenuation is high,

Fig. 7.

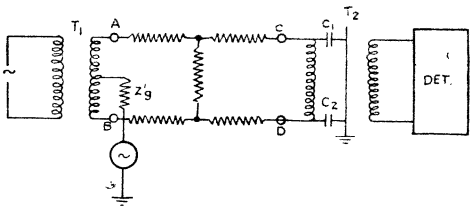

Fig. 8.

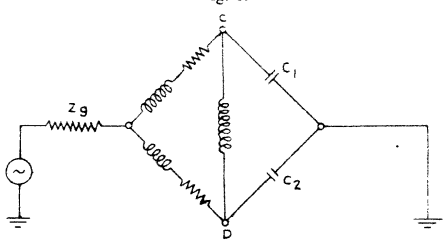

that the voltage across CD which is derived from the unbalance current may be comparable with that derived from the normal current.

5 (2). T_2 *has a shield, and winding* CD *is balanced to shield.*

Assuming that T_1 is still without a shield, then the conditions are as indicated in fig. 7.

This circuit can be reduced to that of fig. 8. It can be seen from this diagram that the longitudinal voltage will

produce no current in the winding CD, provided that $C_1=C_2$.

5(3). T_1 *and* T_2 *both shielded, and windings* AB *and* CD *balanced to their respective shields.*

T_1 now has an earthed shield, therefore it is impossible for the longitudinal voltage to be transferred from the primary to the secondary side of T_1. It is possible, however, for a longitudinal voltage to be obtained on the secondary side of T_1 under the following conditions. Consider fig. 9, and assume that the secondary of T_1 is not perfectly balanced to shield, that is, capacities C_a and C_b are not equal.

Fig. 9.

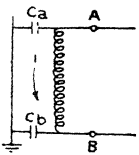

The voltage across AB will set up a current I, as shown in fig. 9. If C_a is not equal to C_b, then the voltage drop across these condensers will be different, and therefore the potential of the point A with respect to the shield (*i.e.*, to ground) will not be the same as that of point B. This condition is identical with that of fig. 1, and hence there will be a potential difference between the mid-point of the winding AB and earth. The problem will therefore reduce to that of case 5(2), and we shall obtain unbalance current in winding CD unless $C_1=C_2$.

5(4). *Unbalance between the two sections of the primary* T_1.

There is one further unbalance to be considered. Suppose that there is a slight unbalance between the two sections of the primary of T_1, and suppose further that we still have an unbalanced voltage to ground. The conditions will then be as indicated in fig. 10.

The currents I_1 and I_2 will be unequal, and the resultant current will set up an e.m.f. across the primary of T_1. This voltage will be transferred to the secondary side, but,

since it appears as a transverse voltage, the current resulting from it will be attenuated by the network ABCD. The final voltage across winding CD will therefore be extremely small, and the error introduced will be negligible. It is necessary, however, to maintain a fairly close balance between the sections, otherwise it will not be possible to obtain a high degree of balance between the primary winding and the shield in those cases where it is necessary to balance the primary side of T_1.

From 5(1), 5(2), and 5(3) we can deduce that, when dealing with a balanced measuring circuit, it is essential, in order to obtain accurate and consistent results, that both T_1 and T_2 should have shields. In addition, the secondary

Fig. 10.

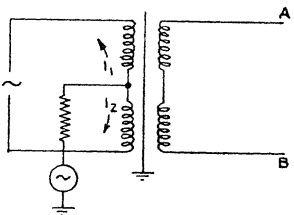

winding of T_1 and the primary winding of T_2 must be very closely balanced to their respective shields. If these precautions are not taken, then it is possible for conditions 5(1), 5(2), and 5(3) to occur either singly or together.

6. *The Unbalanced Circuit.*

In this type of circuit there is no assumption made with reference to the admittance to ground of the terminals. Also all the series impedances are contained in one side of the circuit.

In fig. 11 the network PQRS is meant to represent an unbalanced circuit. It is assumed that this network is connected to the oscillator and detector, respectively, by means of the transformers T_3 and T_4. Assume further that there is an unbalance voltage to ground on the primary side of T_3, and consider the following cases.

6 (1). T_3 *and* T_4 *have no shields.*

This case is identical with that of 5 (1), and we shall, in all probability, have an unbalance current in winding RS.

6 (2). T_4 *has a shield, and winding* RS *is balanced to shield.*

In this case, even though the balance of winding RS to shield may be perfect, yet there will probably be an unbalance current in this winding. If we reduce fig. 11 to a Wheatstone Bridge similar to that shown in fig. 8, it will be seen that one of the arms will contain the whole of the series impedance of the network; hence the bridge will be

Fig. 11.

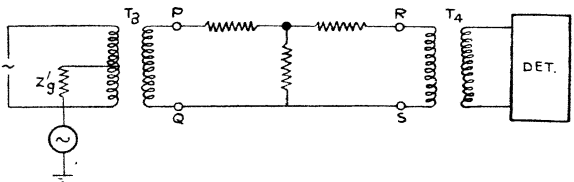

unbalanced, and we shall obtain an unbalance current in winding RS.

6(3). T_3 *and* T_4 *both have shields and windings* PQ *and* RS *are balanced to their respective shields.*

If T_3 has a shield, then the longitudinal voltage cannot be transferred from the primary to the secondary side of T_3. Since the terminals P and Q are not balanced to ground, it is extremely probable that the voltage to ground of terminal P will be different from that of terminal Q; hence the mid-point of winding PQ will have some potential to ground. This case will therefore reduce to the one dealt with under 6 (2).

Cases 6 (2) and 6 (3) indicate that, even if T_3 and T_4 both have shields and the appropriate windings balanced to these shields, it is still possible to obtain an unbalance current in winding RS.

6(4). *Capacity to earth of the network.*

In addition to the unbalances already considered, we have to consider the capacity to earth of the various members of the circuit. Assuming that there is no longitudinal voltage present, the circuit of fig. 11 can be replaced by that of fig. 12, where C_A, C_B, and C_D are capacities to earth of different components of the circuit. It is assumed that these capacities can be located at the mid-points of the respective elements.

From fig. 12 it is seen that the voltage across PQ acting in series with C_A and D_D will produce a current I_1 in MS. Similarly this voltage, acting in series with C_B and C_D, will produce a current I_2 in MR. In general these two currents

Fig. 12.

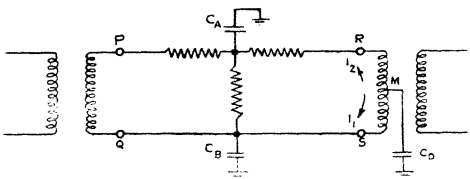

will be unequal, and the resultant current will set up a voltage across RS which will be transferred to the terminals of the detector and will cause an error in the measurement. It will be seen that the value of this unbalance current will not be influenced by the value of the attenuation in the network PQRS.

This source of error does not arise in the case of the balanced network, because it is assumed that in this type of circuit $C_A = C_B$; hence the currents I_1 and I_2 will be equal.

6(5). *One side of the network connected to earth.*

Suppose now that one side of the network PQRS is connected to earth. In this case C_B will be short circuited, C_A and C_B will be connected as shown in fig. 13, and any longitudinal voltage that may exist on the secondary side of T_3 will act across one-half of the winding PQ.

This voltage can therefore be replaced by a voltage acting across PQ, that is, a transverse voltage, and hence any current that it produces will be attenuated by PQRS. In addition, it is seen from fig. 13 that it is now impossible for the capacities C_B and C_D to produce a circulating current as in case 6 (4).

Hence by the above arrangement it is possible to avoid errors that would arise owing to unbalances in the circuits or the capacities to earth of various members of the circuits. If the side is not earthed as in fig. 13, then it is possible for all or any number of the conditions 6 (1), 6 (2), 6 (3), and 6 (4) to occur at the same time.

It will be seen from fig. 13 that it is unnecessary to balance to shield either the secondary side of T_3 or the primary side of T_4. It will only be necessary to shield T_3 and to balance the primary winding to shield if the oscillator output is balanced. The same applies to the

Fig. 13.

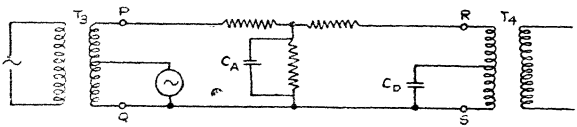

secondary winding of T_4 if the detector input is balanced.

In the foregoing it has been assumed that the frequency is not sufficiently high for the capacities C_B and C_D to offer paths of low impedance to the normal current.

7. *Conclusions.*

The above analysis indicates that, where possible, it is desirable to use an unbalanced measuring circuit with one side earthed. With this type of circuit it is possible to eliminate most of the errors that arise from unbalances. Where it is essential to use a balanced measuring circuit, it is necessary to employ shielded and well-balanced transformers in order to obtain consistent and accurate results.

When connecting a balanced to an unbalanced circuit, the circuits must be separated by a shielded transformer which is balanced on the side which is connected to the balanced circuit.

XL. *The Magnetic Susceptibility of Cæsium in the Solid and Liquid State.* *By* C. T. LANE, *M.Sc., National Research Student, Canada* *.

[Plate VIII.]

1. *Introduction.*

PAULI, in his notable contribution of 1927 †, was the first to give a satisfactory theory for the phenomenon of paramagnetism in metals. Very briefly he has considered the free electrons in a metal to constitute an ideal "gas" degenerate at all ordinary temperatures. Making use of the Fermi distribution function for such a gas, he has arrived at the result that the alkali metals should all be paramagnetic. Further, he has shown that the variation of susceptibility with temperature in these elements should be negligible. The theory, however, neglects the possible diamagnetic contribution to the susceptibility of the atom cores. Thus we are led to predict a paramagnetic value of the susceptibility in the case of copper, silver, and gold, whereas there seems little doubt but that these metals are diamagnetic.

If we calculate the diamagnetic contribution of the atom cores on purely classical principles, we are led to the conclusion that K, Rb, and Cs are actually diamagnetic ‡. In a recent article, however, Rosenfeld § has estimated the diamagnetic effect by making use of a calculation due to Bethe of the "lattice potential" in metals. He shows the diamagnetic contribution to be a function of the "lattice potential" (V_0) related by the expression

$$\chi_d = -\frac{eV_0}{4\pi mc^2},$$

where e, m, and c have their usual significance. The quantity V_0 of course can be determined from electron beam diffraction experiments, and applying this correction to the Pauli result, Rosenfeld arrives at a diamagnetic susceptibility for Cu, Ag, and Au. The correction has not been applied to the alkali metals owing to lack of information regarding V_0 for these elements.

* Communicated by Dr. A. S. Eve, F.R.S.
† W. Pauli, *Zeits. f. Physik*, xli. p. 81, Feb. 1927.
‡ *Cf.* E. S. Bieler, Journ. Frank. Inst. ccvi. p. 77 (July 1928).
§ L. Rosenfeld, *Naturwissenschaften*, xvii. p. 49 (Jan. 1929).

In the case of the alkali metals K, Na, and Rb, a number of independent experimental investigations have been made which are in good agreement with one another, and also in fairly good agreement with the values predicted by Pauli. In the case of cæsium, however, upon which, up to the present work, four investigations * have been made, the results are extremely divergent. Three observers find a diamagnetic value for the metal, whilst the fourth finds it paramagnetic. Again, two investigations on both the solid and liquid state have been made (by Owen and Sucksmith respectively). One observer finds no change in the susceptibility at the melting-point, while the other finds such a change.

In view of the theoretical interest involved in this subject, the author has reinvestigated cæsium in both the solid and the liquid state in the hope of definitely settling the value of the susceptibility. The results of this investigation are communicated in the following pages.

2. *Preparation of the Metal.*

The cæsium metal was obtained from Messrs. Einer and Amend, New York, and was guaranteed as "chemically pure." Nevertheless it was decided, in view of the importance of avoiding ferromagnetic impurity, to subject the metal to multiple distillation. The samples as obtained from the makers were in ½ gram lots, packed in oil. The problem of obtaining a suitable specimen, therefore, resolved itself into first separating the metal from the oil and, secondly, distilling it. The method finally adopted, after considerable preliminary trial, was that of fractional distillation of the metal from the oil, which has a considerably lower boiling-point than the cæsium. It was necessary, of course, that the whole operation should take place in a high vacuum.

Fig. 1 is a diagrammatic sketch showing the form of distilling apparatus finally adopted. A Langmuir mercury pump fitted with a liquid air-trap L, and backed by a "Hy-vac" pump, was the means of producing the required vacuum. The distilling apparatus proper consisted of a bulb B with a charging-tube F fitted with a ground-glass stopper W. The specimen tube into which the metal was

* These investigations are contained in the following papers:—M. Owen, *Ann. der Physik*, xxxvii. p. 657 (1912). L. Crow, Proc. Roy. Soc. Canada, III. xix. p. 63 (1925). W. Sucksmith, Phil. Mag. ii. p. 21 (1926). McLennan, Ruedy, and Cohen, Proc. Roy. Soc. A, p. 468 (Oct. 1927).

distilled is shown at S. The distilling apparatus connected into the vacuum system through an oil-trap O and a small discharge-tube T.

The apparatus is first pumped down and filled with nitrogen-gas through P. The metal and oil at about 30° C. are then introduced into B with a pipette. The apparatus is then re-evacuated and the charging-tube sealed off at the neck N. An electric furnace is now placed over the apparatus as indicated by the dotted lines, and a special heater (also shown dotted) is placed over the specimen-tube. These furnaces are both adjusted to about 200° C. and the oil distilled into the trap O. When all the oil has been

Fig. 1.

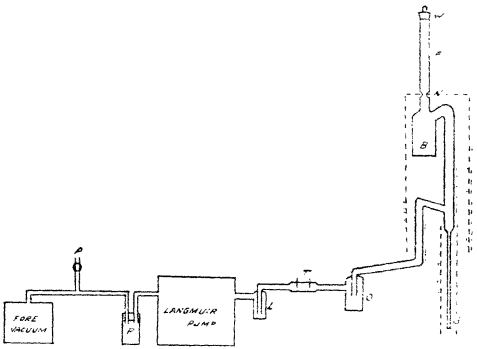

Distillation Apparatus.

distilled over a smaller electric furnace is placed over B, adjusted to 400° C., and the metal distilled into S.

In the present experiment this operation was done, in all, three times. In the first two cases all the metal and some protecting oil were distilled into S. In the final operation all the oil was removed and about three-quarters of the total metal in B was distilled over into S. A specimen of triply distilled cæsium completely free from oil was thus obtained.

Jena glass was employed in the construction of the apparatus as being the most suitable for the work in hand. The specimen-tube was of the same material, roughly 18 cm. long and 0·35 cm. in diameter.

3. *Method of Measurement.*

A modified form of the Gouy * method for measuring the susceptibility was employed wherein the specimen in the form of a long cylinder is suspended between the poles of an electromagnet, the cylinder having its axis perpendicular to the lines of force. The downward force on the cylinder is given by the relation

$$P = \tfrac{1}{2} \times A d (H_1^2 - H_0^2),$$

where P = force in dynes,

x = mass susceptibility,

A = cross sectional area of cylinder in cm.^{2},

d = density of cæsium,

H_1 = field in gauss in the magnet gap,

H_0 = field in gauss at the other extremity of the cylinder.

The force P was measured by means of a sensitive balance accurate to better than 1/50 mg. The magnetic field was produced by a large Weiss electromagnet with water-cooling arrangements. An aluminium housing was built around the magnet for the purpose of shielding the specimen from draughts. A mica window was provided in the housing so that the specimen could be observed at all times. A thermometer could also be observed through this window.

A certain degree of temperature control could be maintained inside the specimen-chamber by varying the rate of flow of water through the magnet-cooling coils. The measurements in the solid state were taken at about 15° C., and those in the liquid state at about 28° C.

The measurements on the solid state were done by the method similar to that employed by Také Soné † and McLennan, Ruedy, and Cohen ‡, wherein the effect of the glass tubing is automatically compensated for. Experiments on the empty tube showed the latter to be compensated to within less than 0·5 per cent. For the liquid state, on the other hand, it was feared that vapour in the upper part of the specimen-tube might affect the result. The unmodified Gouy method was therefore employed and a blank test was made for the glass container at the same temperature. In both cases the susceptibility was determined by a number of

* Stoner, 'Magnetism and Atomic Structure,' p. 40.
† Také Soné, Phil. Mag. xxxix. p. 305 (1920).
‡ *Loc. cit.* p. 472.

different field strengths. The magnetic field was measured by means of a null method originally due to Ellis and Skinner*, but discovered independently by the writer†. The method consists essentially in reducing a known current in the primary of a mutual inductance to zero, while the search-coil is cutting the lines of force. The mutual inductor secondary, the search-coil, and a ballistic galvanometer are connected in series. The instrument used in the present experiment is shown in the accompanying photograph (Pl. VIII.). The search-coil is wound on a long rectangular glass frame S, consisting of two turns of wire. One extremity of the search-coil moves wholly within the uniform field of the gap, whilst the other moves in a region where the field is negligible. The search-coil is mounted on a brass carriage M and can move a fixed distance in the horizontal direction. The carriage M carries a contact C (insulated from it) which slides over a wire resistance W connected to heavy brass plugs at each end. The function of this resistance is to provide approximately the same waveform in the mutual inductance secondary as that produced by the search-coil in cutting the lines of force. The binding posts are connected as shown, those marked HH being connected to the search-coil. In operation a 2-volt storage-cell is connected permanently across BB. Leads from the B terminal and P go to a mutual inductance primary *via* a control resistance. The search-coil, the secondary of the mutual inductance, and a ballistic galvanometer are connected in series. The current in the mutual inductance primary is then adjusted until the galvanometer is balanced, whence

$$H=\frac{MI}{NA},$$

where H = magnetic field in the gap,

M = coefficient of mutual induction,

I = steady current in mutual inductance primary,

A = area swept out by search-coil conductors,

N = number of search-coil turns.

Balance could be obtained with this instrument to better than 1 part in 2000. In the present work the field measurements are accurate to probably 0·25 per cent., a major portion of this error being due to fluctuations in the magnet-

* Ellis and Skinner, Proc. Roy. Soc. A, cv. p. 60 (1924).

† C. T. Lane, Journ. Sci. Inst. v. p. 214 (July 1928).

exciting current. A survey of the field in the vicinity of the magnet showed that H_0^2 was entirely negligible as compared to H_1^2.

Results.

The results for the solid and liquid states are given in Tables I. and II. respectively. In each case the results are

TABLE I.

Solid state (15° C.).

Current in magnet coils. Amps.	Force (P). Milligrams.	Magnetic field. Gauss.	Specific susceptibility.
1·4	$0·46_5$	4780	$+0·21_8\times10^{-6}$
2·0	0·95	6810	$0·22_0$
2·5	1·47	8440	$0·21_7$
3·0	2·08	10100	$0·21_9$
3·3	$2·49_4$	11100	$0·21_7$
3·6	3·01	12150	$0·21_9$
4·0	$3·74_7$	13520	$0·21_9$
4·3	4·21	14400	$0·21_8$
4·6	4·81	15370	$0·21_5$
5·0	5·64	16620	$0·22_5$
5·4	6·57	18000	$0·22_3$
5·8	7·51	19100	$0·22_0$
6·2	8·43	20300	$0·22_0$
6·6	9·41	22200	$0·22_1$
7·0	10·14	22200	$0·22_0$
7·5	10·82	22900	$0·22_1$
9·0	12·14	24200	$0·22_3$

Mean value $+0·22\times10^{-6}$.
Diam. spec. $0·0963_3$ sq. cm.
Density 1·90.

for the specific or mass susceptibility, the density of cæsium for the solid and liquid states (1·90 and 1·84 respectively) being taken from the International Critical Tables. In fig. 2 a curve is plotted showing the relation between susceptibility and magnetic field strength. As is seen, this curve does not depart from a straight line parallel to the field axis by more than approximately 1 per cent., which is within the experimental error. Further, Owen has shown * that if iron

* M. Owen, *loc. cit.*

TABLE II.

Liquid state (28° C.).

Current in magnet coils. Amps.	Force (P). Milligrams.	Magnetic field. Gauss.	Specific susceptibility.
3·0	1·80	10100	$+0{\cdot}19_0\times10^{-6}$
3·3	2·20	11100	$0{\cdot}19_3$
3·6	2·61	12150	$0{\cdot}19_6$
4·0	3·27	13520	$0{\cdot}19_-$
4·6	4·24	15370	$0{\cdot}19_9$
5·0	4·90	16620	$0{\cdot}19_6$
5·4	5·83	18000	$0{\cdot}20_0$
5·8	6·50	19100	$0{\cdot}19_7$
6·2	7·34	20300	$0{\cdot}19_3$
6·6	8·25	21400	$0{\cdot}20_0$
7·0	8·84	22200	$0{\cdot}19_3$
7·5	9·32	22900	$0{\cdot}19_7$
8·0	9·75	23400	$0{\cdot}19_-$
9·0	10·44	24200	$0{\cdot}19_-$

Mean value $+0{\cdot}20\times10^{-6}$.
Diam. spec. $0{\cdot}0963_3$ cm.
Density 1·84.

Fig. 2.

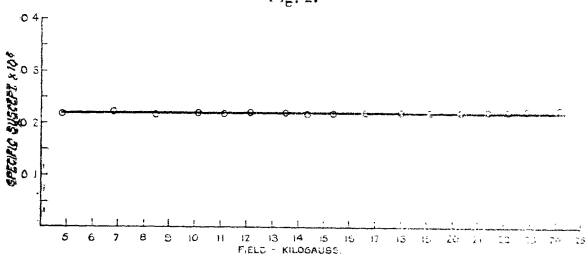

Curve showing relation between Susceptibility and Field Strength.

impurity be present in the specimen, we should have the following relation between susceptibility and field strength, viz. :

$$x = x_0 + \frac{\sigma}{H},$$

where x = measured susceptibility,

x_0 = "iron free" value of the susceptibility,

σ = saturation intensity of magnetization of the uncombined iron impurity,

H = magnetic field strength.

The susceptibility should therefore decrease with increasing field according to a hyperbolic law if any noticeable iron impurity be present.

In Table III. are collected together the four existing results on cæsium in the solid state, together with that found in the present experiment.

The agreement between the present results and that of McLennan, Ruedy, and Cohen appears to be quite good in the case of the solid state. As mentioned previously, the only results in the liquid state are those of Owen and Sucksmith.

TABLE III.

Cæsium (solid state).

Observer.	Owen. 18° C.	Crow. 20° C.	Sucksmith. 0° C.	McLennan, Ruedy, & Cohen. (None stated.)	Author. 15° C.
Specific suscept.	$-0{\cdot}10\times10^{-6}$	$-0{\cdot}06\times10^{-6}$	$-0{\cdot}05\times10^{-6}$	$+0{\cdot}18\times10^{-6}$ and $+0{\cdot}22\times10^{-6}$	$+0{\cdot}22\times10^{-6}$

The present work is in disagreement with Owen, who found no change in susceptibility between liquid and solid state. On the other hand, Sucksmith found a decrease in the diamagnetic susceptibility at the melting-point, whereas the writer finds a decrease in paramagnetic susceptibility in passing over into the liquid state.

The agreement with the value predicted by Pauli is reasonably good, as is here shown:

Calculated (Pauli) $+0{\cdot}24\times10^{-6}$.

Observed (Author) $+0{\cdot}22\times10^{-6}$ (solid state).

The probable error of the measurement of susceptibility in the solid state is about 1·5 per cent., while that in the liquid state is probably somewhat higher.

The present state of our knowledge of the susceptibility of the alkali metals is given in Table IV., which quotes the most trustworthy values of the metals Na, K, and Rb. So far as the author is aware this table contains all the recent results on these metals.

TABLE IV.

Observer.	Owen.	Sucksmith.	McLennan, Ruedy, & Cohen.	Author *.	Pauli (calculated).
Sodium	$+0.51\times10^{-6}$	$+0.59\times10^{-6}$	$+0.59\times10^{-6}$	$+0.65\times10^{-6}$	$+0.67\times10^{-6}$
Potassium ...	0·40	0·51	0·45	0·54	0·60
Rubidium	0·07	0·07	0·17	—	0·32

It is a pleasure to record my thanks to Dr. A. S. Eve, Director of the Physics Department, for his encouragement and advice, and also to Dr. L. V. King for many helpful discussions. I am indebted, further, to the National Research Council of Canada for a studentship during the tenure of which this work was done. Finally, I add to Dr. E. S. Bieler, whose death we deplore, a tribute for his enthusiastic guidance of my career in physics, and of my work in magnetism.

Macdonald Physics Laboratory,
McGill University,
March 1929.

XLI. *Cathode Phenomena in Geissler Discharges through Oxygen and Nitrogen.* *By* NORA M. CARMICHAEL, *M.Sc., Musgrave Student in Physics* (1928-29), *The Queen's University of Belfast* †.

[Plate IX.]

1. *Introduction.*

IN a recent communication ‡ a space-charge theory was developed for the primary dark space of a Geissler discharge, which although in accordance with the main experimental data, did not explain satisfactorily its apparent absence in oxygen and nitrogen. It is possible that the primary dark space does exist in these gases as an electrical unit of the discharge (although on any theory

* C. T. Lane and E. S. Bieler, Proc. Roy. Soc. Canada, III. xxii. p. 117 (1928).

† Communicated by Dr. K. G. Emeléus.

‡ Emeléus and Carmichael, Phil. Mag. v. p. 1039 (1928).

it would be extremely thin) but is masked by radiation. In the present investigation we have made a careful re-examination of the light on the immediate surface of the cathode under a variety of conditions. No evidence has been found for the existence of a primary dark space comparable with those present in the inert gases and in hydrogen, but a dark space has been noticed in oxygen at the negative edge of the negative glow maximum which does not appear to have been recorded previously.

2. *The Primary Dark Space.*

A cathode of the form shown in fig. 1 was used in the first part of the work. It consisted of two parts, A and B, cut from seamless steel tubing 2·9 cm. in diameter. B could be moved freely with a magnet along the two rods R, which were screwed to A, A having a fixed position in

Fig. 1.

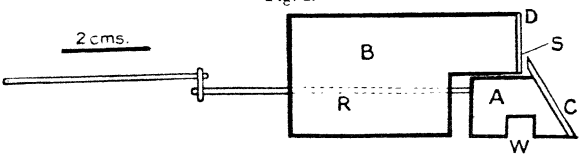

the discharge tube. The relative positions of A and B determined both the width of the slit S between the flat surfaces C and D, of polished silver, and the depth of discharge which could be viewed through the gap W. With this cathode, the feeble radiation from the surface of D could be exposed to a spectroscope or a camera for relatively long periods without disturbance due to stray light from the intense radiation from the negative glow. No soldering was used, and the complete electrode was degassed in a vacuum furnace before mounting, together with the anode, a plane disk of nickel.

The entire apparatus was baked out under vacuum with a hand blowpipe and allowed to cool. Pure finely divided potassium permanganate was then introduced into a series of small bulbs, liquid air put on to the traps, and the remaining parts baked again. Oxygen was then generated and collected in large glass cylinders. From these it was allowed to stream through one capillary to the discharge tube and was pumped out through a second

capillary; by suitable choice of capillaries and with the appropriate pressure in the cylinders a constant pressure was maintained in the discharge tube, a steady stream of pure oxygen being thus obtained. The pressure was measured by a McLeod gauge, protected by a liquid-air trap, and other traps were situated at the immediate entrance and exit of the discharge tube, and in the leads to the cylinders and the pump.

In the case of nitrogen the same baking process was carried out, and nitrogen generated from the explosion of sodium azide, the metallic sodium formed in the reaction assisting in its purification.

The applied potential had a maximum of 450 volts and could be varied by a wire potentiometer.

Pl. IX., *a*, is a typical example of some thirty photographs which were taken of discharges through nitrogen and oxygen. It shows the cathode glow distinctly (CG), but gives no indication of a primary dark space. L is light reflected from the cathode glow by the back surface of C inside S.

After running the tube for a short time a fine line of sputtering developed on the lower surface of the cathode along the line of separation of the parts exposed to and protected from the discharge, which was probably due to back sputtering from the fine edge of C. This may be associated with the observed strong development of the 1S–2P pair of lines of Ag I at 3281 and 3384 A., a result which would point to the above as a possible method for the investigation of the *raies ultimes* of small quantities of metals.

In view of the fact that this radiation from the cathode material was excited in the region we wished to study, the cathode was then replaced by one of simple type, a cylinder of seamless steel with a circle of platinum foil spun on to the plane face exposed to the discharge. The former precautions for purification were again observed. Examples of the resulting photographs are shown in Pl. IX., *c* and *d*, for nitrogen and oxygen respectively. These are deliberately over-exposed for the negative glow (NG), to bring out the cathode glow (CG) distinctly. There is again no indication of a primary dark space. Similar negative results were obtained with a cathode of iron, and have been obtained by Aston with aluminium *.

* Aston, Proc. Roy. Soc., lxxx. p. 45 (1908).

3. *A New Dark Space in Oxygen.*

A dark space which does not appear to have been described hitherto was observed in the discharge through oxygen, to the negative side of the curiously sharp edge of the negative glow that is characteristic of the Geissler discharge through this gas. It is intensely black and sharply bounded, features which it is difficult to reproduce in a photograph (Pl. IX., *b*) on account of the concavity of the negative glow surface towards the cathode. Its position is indicated in fig. 2. Its thickness (d) as estimated with a cathetometer appears to follow the law that $dV^{\frac{1}{2}}D$ is constant, which holds for the primary dark space where V is the cathode fall in potential and D the thickness of the cathode dark space. It is also thicker towards the periphery of the tube, where the current density is less

Fig. 2.

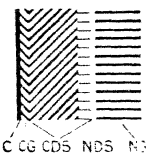

than at the axis. d is difficult to measure accurately, again because of the concavity of the negative glow, but some idea of its order of magnitude will be obtained from the following table :—

Thickness of new dark space. . . .	0·23 mm.
Thickness of cathode dark space . .	4·5 mm.
Cathode fall in potential	420 volts.
Gas pressure	1 mm. Hg.
Current density (average over cathode)	0·18 mA. cm.$^{-2}$

Cathode of platinum.

An attempt has been made to investigate this dark space by the Langmuir method of exploring electrodes in a simple tube of the type used by Emeléus and Harris *. The collector was a fine molybdenum wire of effective

* Emeléus and Harris, Phil. Mag. iv. p. 49 (1927).

length 0·3 cm. and 0·1 mm. diameter. The usual precautions were taken to ensure purity of the gas, and two large cylinders were put in connexion with the tube to minimize changes in pressure. Characteristic curves were taken in the usual way. There is some doubt as to the exact interpretation to be put upon collector characteristics for the more negative parts of this section of the discharge, but the usual curves were obtained to the positive side of the new dark space, and the anomalous cathode dark space type to its negative side. We can therefore regard the new dark space as a *region* in which the transition from the negative glow to the cathode dark space takes place, this conclusion being compatible with some measurements by W. L. Brown and E. E. Thomson made on the shadows thrown by collectors in the cathode dark space, details of which will be published shortly. The electron concentrations in the negative glow were of the usual order, but the electron temperatures were decidedly low, 0·5 volt and 1·8 volts being typical numbers for the two groups present in the middle of the negative glow in a 450 volt discharge at 0·5 mm. Hg.

Seeliger * has shown that it is necessary to proceed with great caution in interpreting the visual appearance presented by a discharge. In this particular instance the dark space remained unaltered in position, and lost none of its sharpness when viewed through a range of Wratten colour filters. The other possibility, that it is a contrast effect, is disposed of by its appearance on a photometric record of one of our less good plates.

The integrated colour of the light from each side of this dark space is the greenish white of the oxygen discharge, although it is naturally very feeble to its negative side, fading off rapidly into the violet of the cathode dark space proper. A study of the individual lines and bands in the discharge was made by the subjective method of Seeliger †. The discharge tube was mounted vertically and a fine black thread tied round it at the level of the new dark space. An image of the discharge was focussed on the slit of a Hilger constant deviation spectrometer, and the relative intensities in the spectrum on either side of the image of the thread noted. Several lines due to the excitation of sputtering metal atoms came up intensely

* Seeliger and Lindow, *Phys. Zeits.* xxvi. p. 393 (1925).

† *Loc. cit.*

at the cathode surface, and faded out towards the negative glow. The dark line of the image of the thread which marked the position of the new dark space coincided with the region of rapid fall in intensity of the ozone bands already recorded by Seeliger and Lindow *, and with the region of rapid fall in intensity of the green and red negative bands of oxygen, but some light due to both of these still persisted faintly to its negative side. The arc lines (O I) and spark lines (O II) of atomic oxygen showed a somewhat less rapid change in intensity, again in agreement with Seeliger's results.

Taking Seeliger's observations in conjunction with ours, particularly those made with an exploring electrode, we conclude that a very large number of the ions in the negative glow are probably molecular oxygen O_2^+ rather than atomic oxygen O^+. The positive ray analysis of Hogness and Lunn would suggest a ratio of the former to the latter of about seven to one †.

A search has again been made in other gases (nitrogen, oxygen, hydrogen, argon, neon) for this dark space, so far with negative results.

4. *Origin of the Dark Space.*

Our observations very strongly suggest that the new dark space is an ionic sheath, in this case separating two parts of the discharge instead of an electrode and the discharge. Other evidence for the existence of a sheath between different regions of an ionized gas would appear to be contained in some of the observations made by J. J. Thomson ‡ on the electrodeless discharge. The sheath is almost certainly one of positive ions, and its existence is compatible with Morse's theory of the cathode dark space §, which seems to allow of a rather abrupt transition from a moderately large field in the cathode dark space to practically zero field in the negative glow. Brown and Thomson (see above) have obtained experimental evidence for the existence of this fairly sharp transition. Interpreting it in terms of Poisson's relation, there should be present there a sheath of rather denser

* *Loc. cit.*
† Hogness and Lunn, Phys. Rev. xxvii. p. 732 (1926).
‡ J. J. Thomson, Phil. Mag. iv. p. 1128 (1927).
§ Morse, Phys. Rev. xxxi. p. 1003 (1928).

positive electricity than in neighbouring parts of the cathode dark space. In the case of argon there is independent evidence that there is an additional region of excess positive space charge in the negative side of the negative glow from the work of Emeléus and Harris *, who suggested that it existed to counteract the effects of diffusion from the intense ionization of the middle of the negative glow in this gas. No dark sheath has been observed in argon, but conversely our analysis with exploring electrodes has shown that the negative glow is much more nearly equipotential in oxygen than in argon (under the conditions mentioned in the last section it is equipotential to within 1·5 volts between the new dark space and the Faraday dark space), and has its maximum of ionization closer to its negative boundary, suggesting that the relative extents of the reversed field in the negative glow and the new dark space, if these can be associated with one another, are determined by the large mobility of electrons in argon, as compared with their small mobility in oxygen. If this is so, the dark space might be visible in the discharge through gases such as chlorine. A more detailed investigation of this part of the discharge in several gases has been planned, which it is hoped will decide these questions.

Summary.

A search has been made for a primary dark space in the Geissler discharges through oxygen and nitrogen, with negative results. A new dark space has been described in oxygen between the negative glow and cathode dark space, which appears to be a positive ion sheath between these two regions of the discharge.

I should like to thank Prof. J. Milroy for the loan of a Hilger constant deviation spectrometer; Mr. E. E. Thomson for assistance in some of the photography; Dr. S. W. J. Childs, of King's College, London, for photometring one of the plates; and Dr. Emeléus, for his help throughout the investigation and in the preparation of this paper.

* Emeléus and Harris, *loc. cit.*

XLII. *The Relation between Raman Lines and Infra-red Bands.* *By* C. P. Snow (*Keddey Fletcher-Warr Student*) *.

Introduction.

QUESTIONS of technique have hampered the growth of the theory of the Raman effect in a way which has not been fully realized. The discovery was made in liquids like carbon tetrachloride, toluene, and benzene; and, because the effect was observed most readily in such substances, attention was kept upon them. The result was that no comparison could be made between the Raman scattering due to a molecule and the detail of its infra-red absorption, for the bands of toluene or benzene are beyond the powers, both theoretical and practical, of present-day analysis.

Accordingly, the agreement of the position of known gross infra-red bands with the amount of scattering ($\delta\nu$) of some Raman lines was taken as proof of the simplest possible theory—that of Smekal, in which the molecule is supposed to absorb or emit a quantum $h\nu$, where ν is a characteristic infra-red frequency, usually of a vibration band. It was necessary to ignore the non-appearance of Raman lines corresponding to strong absorption bands, and the appearance of lines which had no corresponding bands at all.

These unexplained exceptions were soon reinforced by the results of experiments upon gases with well-known infra-red spectra; and it became clear that R. W. Wood's [1] work on hydrogen chloride and Rasetti's [2] on carbon dioxide made the existing theory inadequate. Langer [3] and Dieke [4] have now shown that the Kramers theory of dispersion includes, implicity, the theory of the Raman effect, and that these apparently anomalous results follow naturally from it. It predicts that the shifts of the Raman lines from the unmodified exciting line are equal to differences of excited levels of the molecule, where the excited levels themselves have a common ground-level. The intensity of any Raman line depends upon the transition coefficients from the common level of the two appropriate excited levels; Langer has derived the expression

$$\mathrm{A}_{kn}\,\mathrm{A}_{ln}\left[\frac{1}{\nu_2+\nu_{kn}}+\frac{1}{\nu\pm\nu_{ln}}\right](\nu\pm\nu_{kl})^2,$$

the square of which represents the intensity of the transition

* Communicated by Dr. Eric K. Rideal.

ν_{kl} *i.e.* $\nu_k - \nu_l$. A_{kn} describes the intensity of the transition of ν_{kn}, and is $\int r\psi_k\psi_n dx$.

Langer has shown the completeness with which this theory accounts for the Raman lines of carbon tetrachloride; and Dieke has given a convincing reason for the "missing line" of hydrogen chloride which was found by Wood. It is the writer's aim to make clear the application of the theory to some molecules for which there is considerable spectroscopic data, and to add a little lately acquired infra-red evidence.

I. Oxygen and Nitrogen.

Raman observations.

McLennan and McLeod [5] found that the Raman effect in liquid oxygen and nitrogen gives lines corresponding to the frequencies :—

for oxygen	1552	1551	3049
for nitrogen	2335	2322	4632

In their paper they mention that there are no infra-red bands due to O_2 or N_2, since the molecules are symmetrical and have no electric moment. Their suggestion is that in the liquid state there exists a mutual polarization, with the formation of weak dipoles (this must be the case in liquid sulphur, where the dipole $\overset{+}{S}-\overset{-}{S}$ is certainly present).

The actual process is likely to be the formation of quadripoles, which behave optically like dipoles to a first approximation.

Possible existence of infra-red bands of oxygen and nitrogen in the gaseous state.

Several considerations made it appear conceivable that gaseous oxygen and nitrogen might have vibration-rotation bands. They were

(i.) That the complete symmetry of O_2 and N_2 usually assumed is not proved, nor is there any other case (except perhaps I_2) known.

(ii.) That the emission curve of a Nernst glower or similar source shows irregularities, some of which are due to the absorption by carbon dioxide and water of the atmosphere; near to the carbon dioxide and water bands there are small dips at

frequencies much the same as McLennan and McLeod's. It must be borne in mind that these also may be caused by CO_2 and H_2O.

(iii.) That Coblentz [6] attributed absorption at $3{\cdot}2\,\mu$ (3100 cm.$^{-1}$) to oxygen, after considering the possibility of its being due to water.

(iv.) That Sleator [7], when determining the absorption of water at $2{\cdot}6\,\mu$, plotted bands which did not diminish when the amount of water in the absorbing system was lessened.

Hence (ii.) was investigated more fully. There was at hand a convenient instrument for the purpose, already described by A. M. Taylor and E. K. Rideal [8]. It is a small Hilger infra-red spectrometer, encased in a cast iron safe in order to protect the thermopile from disturbances caused by adiabatic expansion and contraction of the air. This made it easy to obtain a vacuum spectrometer, for a thorough covering of the outside with Chatterton's compound was all that was necessary. Inside the safe dishes containing sticks of potassium hydrate were placed; outside, the Nernst and mirrors were so arranged as to make the path of the radiation through air quite small. The air path was enclosed in a funnel made of sheet brass and lined with dishes of stick potassium hydrate.

The safe was evacuated, and the emission curve of the Nernst glower plotted. Two portions of the curve are shown in figs. 1 and 2; comparison with the ordinary emission curve in air emphasises the smoothing out of the dips due to absorption by carbon dioxide and water. The flatness in fig. 1 is probably caused by a little water vapour persisting in the system despite all precautions.

Oxygen was pumped in at an atmosphere's pressure, and the curve between $5{\cdot}9$ and $6{\cdot}8\,\mu$ plotted. The result is seen in fig. 1, and the curve in the neighbourhood of $4\,\mu$ with nitrogen at an atmosphere's pressure in the instrument is given in fig. 3. A rock-salt prism cannot profitably be used from 2–$3{\cdot}5\,\mu$, and so the curve at higher frequencies could not be obtained with any accuracy; it was obviously impossible to evacuate the high dispersion instrument recently described [10].

The curves suggest a small but definite absorption by oxygen and possibly by nitrogen. The effect was reproducible, qualitatively at least. However, it must be remembered that even for oxygen the effect is very small;

the complication introduced by the nearby bands of water and carbon dioxide is another factor which makes a definite claim unjustifiable. On the other hand, a precise and deciding test seems forbidden by the nature of the problem.

The frequencies of the possible bands are :—

oxygen ..... c. 1540 cm.$^{-1}$.
nitrogen ..... c. 2320 cm.$^{-1}$.

The conflict of their occurring with the inference from electric moment measurements is not serious, although the

Fig. 1.

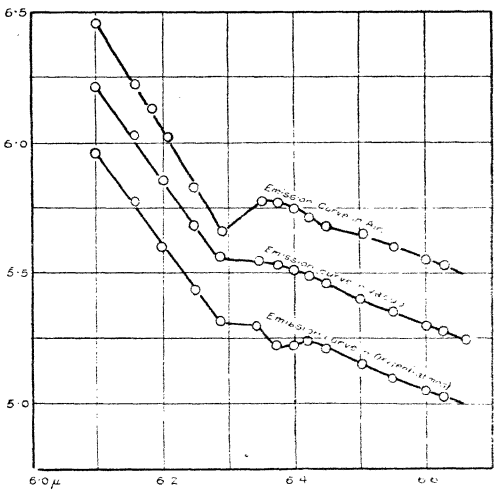

delicate method of Stuart [9] has confirmed previous work in giving a zero moment for both molecules. An effect of the magnitude observed would only require a moment of the order of $5 . 10^{-20}$ e. s. u.

Explanation of Raman lines of oxygen and nitrogen.

The general statement may be made, tentatively, that the Raman lines observed by McLennan and McLeod correspond to infra-red frequencies of the molecules both in the liquid

and in the gaseous state. The important result—which cannot be questioned—is that here the vibration frequency deduced from the Raman effect is not a difference frequency but a normal frequency of the molecule.

This must be the case if a diatomic molecule is to show any Raman shifts; Dieke has shown how the Kramers theory includes difference terms between rotational states. If (i, j)

Fig. 2.

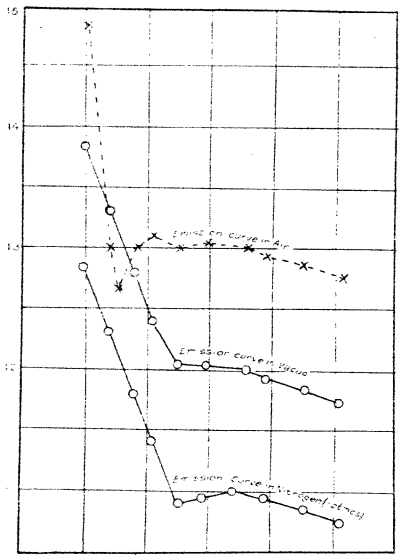

represents a molecule in its first excited vibrational state and its jth rotational state, then $(i, j-0, j_1)$ can under certain conditions be a Raman transition. The conditions obviously are $j=j_1$ or, alternatively, $j=j_1 \pm 2$. The predicted Raman lines are then a strong line corresponding to the centre or rotationless state of the infra-red vibration-rotation band, and weak lines at twice the separations of the infra-red bands (rotation bands). In Wood's case the dispersion was high enough to give this arrangement.

There is little doubt that the oxygen and nitrogen Raman lines would show a similar structure under high dispersion. It would be particularly interesting to see the convergence that can be prophesied on the low frequency side of the central line; and the intensity relationships of fundamental and overtone would be of value. The comparison of the ratio of the intensities of the Raman fundamental and overtone with the ratio of the intensities of the infra-red bands (they could be calculated for O_2 and N_2, and are known for CO) would act as a final proof of the correctness of the Lange-Dieke explanation.

There is some evidence already for this view. The position of the centre of an infra-red band can be calculated from electronic band spectra data. This has recently been shown to be true for both NO and CO (see later). To a close approximation, the centres of the infra-red band so calculated agree with McLennan and McLeod's figures for the Raman lines. Now, the oxygen and nitrogen bands in the infra-red, actual or hypothetical, must be very like the HCl or CO bands, and have no central line. That is, the Smekal theory would suggest two or more Raman lines arranged symmetrically about a missing central line. On the other hand, the new explanation would give, as a first effect, one central line.

	w_0 (electronic bands).	$w_0(1-x)$. Calculated centre of infra-red band.	Raman, Mc & McL.	Theoretical Raman, upon Smekal Theory.
O_2...	2165	2154	2152	Two lines, ca. 2151 and 2157
N_2...	2345	2331	2329	Two lines, ca. 2327 and 2335

II. Carbon Monoxide.

Rasetti observed a Raman line for carbon monoxide which shows a surprisingly close resemblance to the w_0 of the electronic bands of CO. This can scarcely be the case; with more accurate measurement, it is certain that the line corresponds to the centre of the infra-red band $w_0(1-x)$. Recent work [11] upon NO and CO has shown quite definitely that the centre of the infra-red band is described by this value: the relevant figures, together with Rasetti's Raman effect result, are given below:—

	w_0(electronic band spectra).	$w_0(1-x)$ [calculated].	Centre of infra-red band.	Raman.
NO.....	1892	1878	1883	—
CO.....	2155	2142	2144	2155

In every other way the Dieke explanation seems to hold ; it is significant from the point of view of intensity that the overtone has not yet been detected in the Raman effect.

III. Carbon Dioxide.

Rasetti's result for gaseous carbon dioxide is an interesting example of the truth of the Kramers prediction. The infra-red bands at $2{\cdot}74\,\mu(\nu_2)$ and $4{\cdot}25\,\mu(\nu_1)$ are drawn roughly in fig. 3.

ν_1 represents a vibration of the carbon atom perpendicular to the symmetry axis, and ν_2 one of the vibrations of the carbon atom parallel to it. Accordingly, they have a ground

Fig. 3.

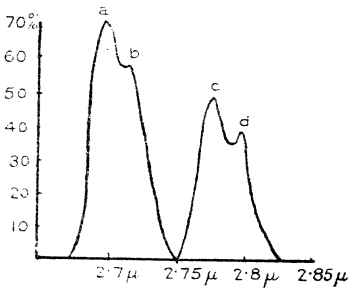

level, the unexcited state of the molecule ; and a transition between them is predicted by the Kramers theory. Actually, Rasetti observed two lines at $\partial\nu = 1392$ cm.$^{-1}$ and $\partial\nu = 1284$ cm.$^{-1}$. The difference between a and e is 1368 cm.$^{-1}$, between c and f 1295 cm.$^{-1}$.

The justification for this apparently arbitrary potentially, a number of Raman lines corresponding to the vibrational transition $\nu_2 - \nu_1$ and to various transitions in rotational quantum number. To a first approximation, the difference between the maxima of the R branches will be the strongest Raman line, with the difference between the maxima of the P branches of the same order of intensity. As Rasetti's photograph was taken under circumstances likely to give only the strongest lines, it was a qualitative test of intensity ; and the lines given by it may be looked upon as molecular "raies ultimes."

The correspondence of the frequency differences with the theoretical is fairly satisfactory. Rasetti himself, before the difference term was accepted as the normal Raman effect, noticed that the Raman lines were numerically very close to the differences of the maxima of the 4·25 μ band and the centres of the double doublet at 2·74 μ. His calculated differences are nearer to the observed fact than those taken as above; this seems to be due to the use of figures for the 4·25 μ band given by Schaefer and Phillips [12]. Their paper contains the misprint 4·255 (instead of 4·225) for the maximum of the R branch of the doublet. If the correct value is used, the differences taken in Rasetti's way do not agree with the Raman shifts as nearly as do the differences of the maxima.

It may be noticed that almost exact agreement with experiment can be obtained by subtracting the low frequency band of the 4·25 μ doublet from the two maxima *a* and *c*, of the double doublet. This does not seem legitimate, and it would involve, in any case, complicated selection rules. The difference of the maxima is the obvious course with the present data.

Some puzzling numerical relationships derived by C. R. Bailey [13] may be discussed briefly, as their acceptance as a representation of an unknown law would imply a more involved explanation of the Raman effect.

The energy expression for a rotator with two effective moments of inertia (the two large moments in CO_2 are nearly equal) is

$$E_r = \left[\frac{m(m+1)}{C} + \left(\frac{1}{A} - \frac{1}{C}\right)s^2\right]\frac{h^2}{8\pi^2}$$

(or, for simplicity, the older form)

$$E_r = \left[\frac{m^2}{C} + \left(\frac{1}{A} - \frac{1}{C}\right)s^2\right]\frac{h^2}{8\pi^2}$$

in ν_1, the selection rules apply

$$\Delta m = \pm 1,$$
$$\Delta s = 0.$$

Accordingly, the doublet shown in fig. 3 *a* is exactly like the band system of a diatomic molecule of moment of inertia C. The separation of the lines (at present unresolved) is $\frac{h}{4\pi^2 C}$. The separation of the doublet is described approximately

by the Bjerrum classical expression. It is of the order of 30 cm.$^{-1}$.

The band at 2·74 μ depends upon the selection rules

$$\Delta m = 0, \pm 1, \quad \Delta s = 1,$$

and can be divided into two systems of lines

Fig. 3*a*.

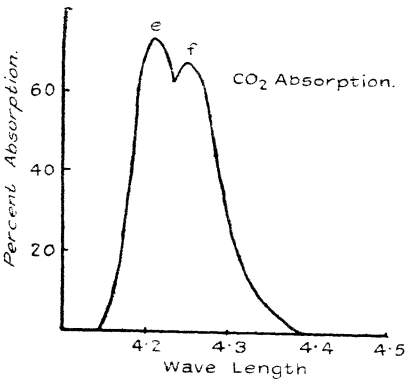

I. . . . . $\partial\nu = \left(\frac{1}{A} - \frac{1}{C}\right)\frac{h}{4\pi^2}$

(the four large bands of the double doublet belong to this system),

II. . . . . $\partial\nu = \frac{h}{4\pi^2 C}$

(these lines give a fine structure to the lines of I). The simplification happens that the maxima of the Bjerrum doublets coincide with the tops of the bands of I. *I. e.* the separation

$$\left(\frac{1}{A} - \frac{1}{C}\right)\frac{h}{4\pi^2} \doteq 30 \text{ cm.}^{-1}.$$

The separation

$$b - c = \left(\frac{1}{A} - \frac{1}{C}\right)\frac{h}{2\pi^2},$$

as, for example, in HCl, for there appears to be no Q branch. The numerical value of it is 70 cm.$^{-1}$; there is an irregularity which may vanish with more exact measurement.

Bailey's series depend upon the separation of the bands a and c in ν_2—the two more intense members of the doublets. He finds that half this separation is a constantly occurring frequency in CO_2 bands. As he says, it is difficult to see any reason for this. It is not surprising that the separation itself is common, for it is roughly three times the separation of the Bjerrum doublet where the fine structure is $\frac{h}{4\pi^2 C}$ (and, of course, three times the band separation $\partial\nu = \left(\frac{1}{A} - \frac{1}{C}\right).\frac{h}{4\pi^2}$). But half this separation would seem physically meaningless.

It is possible that the fine structure of the four large bands of the 2·74 μ band may show that the superposition of the band systems is not so perfect as has been assumed; the problem has, however, the experimental difficulty that the separations of the fine structure will be of the order of one wave number.

IV. Hydrogen.

The Raman lines of hydrogen at the moment have not been reconciled to the Langer-Dieke scheme. H. S. Allen[11], from a study of the "many lines" spectrum, found results which are not consistent with those of McLennan and McLeod, from the direct effect in liquid hydrogen; and neither of the sets of observations fits the theory well.

The adoption of Dieke's selection rule $j = j \pm 2$ means that the apparent beautiful confirmation in McLennan and McLeod's paper of the existence of symmetrical and antisymmetrical states of hydrogen cannot be retained, and the two lines detected by them should be of similar origin to the lines found by Wood on each side of the "missing line." If this were the case, it seems necessary that there should be a strongly marked difference in intensities between the two lines, as the alternation in intensity of the H_2 bands should persist. This does not appear to be verified by the experiment.

As hydrogen gives the most important difficulty, mention did not seem worthless, although the writer can offer no constructive suggestion.

Summary.

(i.) The Langer-Dieke account of the relation between Raman lines and infra-red bands is discussed.

(ii.) It is pointed out that for O_2, N_2, and CO a similar scheme to that proposed by Dieke for HCl must be used; and that, in all three cases, the position of the central Raman line should not coincide with the electronic vibration frequency.

(iii.) There is some experimental evidence for the existence of vibration-rotation bands of oxygen and nitrogen. Work with an infra-red vacuum spectrometer leads to the view that absorption by oxygen, while not definitely proved, is more than a possibility. The intensity of absorption for a metre path of oxygen has 5 per cent. as its upper limit.

(iv.) The agreement of the Raman effect for CO_2 with the Langer-Dieke account is stressed, and some suggestions are advanced upon the transitions to be expected.

(v.) The Raman effect for H_2 gives results which are not yet explained by the Langer-Dieke theory.

Acknowledgments.

I should like to give my thanks to Dr. A. M. Taylor, for advice and help, particularly in the use of the vacuum spectrometer; to Mr. F. I. G. Rawlins, who led me through the difficulties of the carbon dioxide question; to Mr. A. C. Menzies, of University College, Leicester, for many stimulating conversations; to Dr. E. K. Rideal, for interest and criticism, and for communicating the paper. Finally, I should like to state my continued gratitude to the Keddey Fletcher-Warr Studentship Board.

References.

(1) R. W. Wood, 'Nature,' No. 3095, p. 279 (1929); Phil. Mag. (7) xliv. p. 744.
(2) Rasetti, 'Nature,' No. 3093, p. 205 (1929).
(3) Langer, 'Nature,' No. 3097, p. 345 (1929).
(4) Dieke, 'Nature,' No. 3102, p. 564 (1929).
(5) McLennan and McLeod, 'Nature,' No. 3092, p. 160 (1929).
(6) Coblentz, Pub. Carneg. Inst. Wash. i. p. 49 (1905).
(7) Sleator, *Astrophys. J.* xlviii. p. 127 (1918).
(8) A. M. Taylor and E. K. Rideal, Proc. Roy. Soc., A.
(9) Stuart, *Zeits. f. Phys.* xlvii. p. 457 (1928).
(10) Snow and Taylor, Proc. Roy. Soc. In process of publication.
(11) From work about to be published.
(12) Schaefer and Phillips, *Zeits. f. Phys.* xxxvi. p. 641 (1926).
(13) C. R. Bailey, 'Nature,' No. 3098, p. 410 (1929).
(14) H. S. Allen, 'Nature,' No. 3091, p. 127 (1929).

XLIII. *Intensively Dried Liquids.*

By JOHN WILLIAM SMITH, *B.Sc., Ph.D.**

IT has been shown recently by Lenher † that the method used by Baker ‡ and by Smits § for the determination of the boiling-points of their intensively dried liquids may lead to superheating, yielding high values up to 27° above the normal boiling point even when ordinary pure, but undried, liquids are used. Hence it is claimed that such superheating may well account for Baker's boiling-point changes, which, therefore, are inconclusive in establishing a change in the internal state of the liquids. This discovery is extremely important, but it does not explain by any means all the phenomena observed with intensively dried liquids, and therefore must by no means be regarded as putting an end to this branch of chemistry.

The best established fact concerning intensively dried systems is their slowness in attaining the equilibrium state after any disturbance of the latter. For example, after a sudden change in temperature, dried liquids require a very considerably longer period than moist liquids in order to reach a steady vapour pressure ‖. The same phenomenon is observed after rapidly distilling a portion of the liquid away ¶. Dry sulphur trioxide exhibits these phenomena much more conspicuously even than dry liquids **. As has been pointed out by Smits ††, this slowness in behaviour may well be the cause of the very high vapour densities found by Baker for several liquids ‡‡, and for the abnormal latent heat found in the case of intensively dried benzene. Thus there is a good deal of fundamental evidence, mainly from the work of Baker, that there is some important change in the behaviour of liquids after intensive drying, though his view that there is a very large

* Communicated by Prof. F. G. Donnan, F.R.S.

† 'Nature,' cxxiii, p. 967 (1929).

‡ Journ. Chem. Soc. cxxi. p. 568 (1922).

§ Journ. Chem. Soc. cxxv. p. 1069 (1924).

‖ J. W. Smith, Journ. Chem. Soc. p. 857 (1927).

¶ Smits, de Liefde, Swart, and Claassen, Journ. Chem. Soc. p. 2657 (1926).

** Smits and Schoenmaker, Journ. Chem. Soc. cxxv. p. 2554 (1924); p. 1108 (1926).

†† Journ. Chem. Soc. p. 2399 (1928).

‡‡ Journ. Chem. Soc. p. 1051 (1928).

change in the molecular complexity does not seem to be supported on very firm grounds. Baker's measurements have always been made in what may be described as dynamic systems, in which the readings may have been taken before equilibrium has had time to establish itself, owing to the fear of rapid reversion to the normal state, the result being that large differences were found between the physical properties of the moist and dry liquids. On the other hand, other observers have measured static properties, *e. g.*, the change of the vapour pressure at the drying temperature, but the changes found have been small, in no way comparable with the large effects observed by Baker.

The slowing down of the rate of attainment of equilibrium in liquids seems to be quite parallel to the gradual slowing down of the velocity of many chemical reactions on the removal of water-vapour, and doubtless when a satisfactory explanation is found for the one it will apply to the other case also.

This slowness in the attainment of equilibrium may well account for the fact that Alex. Smith and Menzies* found that dry calomel exerted no vapour pressure at all, since during the brief period during which they heated the calomel (a quarter of an hour) before sealing off the large bulb containing the vapour, it is probable that the vaporization of the dry specimen would be very slight indeed, although the same period of heating may well have sufficed for the undried specimen under analogous conditions. Similar, but not so marked, effects have been observed recently by Rodebush and Michalek † in measurements of the vapour pressure and vapour density of ammonium chloride.

Having the criticism from Smits on the one hand ‡ that Baker's surface tension measurements are not true indications of a change in the inner complexity of the system, and from Lenher § on the other that the boiling-point determinations are inconclusive, there no longer remains any certain evidence in favour of perhaps the most surprising phenomenon indicated by Baker's experiments, that is, that liquids retained their abnormal "dry"

* *Zeits. phys. Chem.* lxxvi. p. 713 (1911).
† Journ. Amer. Chem. Soc. li. p. 748 (1929).
‡ Journ. Chem. Soc. cxxv. p. 2399 (1928).
§ 'Nature,' cxxiii. p. 907 (1929).

properties for some time after contact with moisture. This property, indeed, seems to have been relied upon by Lenher to enable him to complete his measurements before any considerable change in his "dry" liquids could occur. It now seems much more rational to suppose that, like the gaseous systems referred to above, the "dry" liquids will be extremely sensitive to very small traces of water-vapour and will revert to their normal behaviour almost immediately on contact with moist air or moist apparatus. Thus Lenher's experiments, using the boiling-point apparatus with a platinum wire heating element, do not prove conclusively that there was no abnormality in the liquid before the drying tube was opened, since no care was taken to avoid contact with moist air after opening the tubes.

The drying effect, if it is primarily a slowing down of the inner transformations, may well occur in quite the early stages of the usual long intensive drying process. Thus, in the author's experiments with nitrogen tetroxide, during the first few days after sealing the apparatus the liquid could be distilled over completely between two bulbs, one at 0° C. and the other at about 18° C., through a phosphorus pentoxide *U*-tube, in the course of about three hours. This period, however, increased gradually till over five hours were required for a complete distillation to be carried out under comparable conditions. The greater part of this slowing down of the rate of distillation occurred during the first month or two. The effect was not due to the compression of the phosphorus pentoxide column, since after moist air had been admitted to the apparatus and the latter re-evacuated and sealed off again with very little loss of the nitrogen tetroxide, the former three hour period was restored. Now, after a further two and a half years without any repeated distillation the time required is again much greater under the same conditions as before, being about six hours. It is proposed to carry out further experiments on the effect of drying on the rate of distillation of liquids.

Another recent communication which is of considerable interest in this connexion is that by Manley *, who has found that the specific volume of benzene in the presence of phosphorus pentoxide is dependent on the temperature

* 'Nature,' cxxiii. p. 907 (1929).

to which the benzene has been exposed before a determination is carried out, being diminished by previous cooling, and increased when the liquid has first been heated. He attributes the effect of cooling to the ejection of water from the benzene, and that of heating to the absorption of moisture from the metaphosphoric acid previously formed. It is quite possible, however, that this is only yet another example of the "slow" behaviour of dried liquids, some time being required for the inner equilibrium to be established after disturbance by temperature change.

In conclusion the author desires to express his indebtedness to Professor F. G. Donnan, F.R.S., for his helpful advice and criticism.

Sir William Ramsay Laboratories of
Inorganic and Physical Chemistry,
University College, London.
July, 1929.

XLIV. *The Spectrum of the Negative Glow in Oxygen.* *By* K. G. Emeléus, *M.A., Ph.D., and* Florence M. Emeléus, *M.Sc., Department of Physics, The Queen's University of Belfast* *.

1. *Introduction.*

MUCH work has been done lately on the interpretation of spectra associated with oxygen. In particular, the lines of the first spark spectrum of the atom (OII) have been catalogued and extensively analysed by A .Fowler †, H. N. Russell ‡, R. H. Fowler and Hartree §, and Mihul ‖, and the lines of O III have been examined by A. Fowler ¶ and others.

The negative glow in oxygen is a good source of band spectra, arc lines and the lower spark lines, affording, in fact, probably the most gentle method available for the production of the latter.

* Communicated by the Authors.
† A. Fowler, Proc. Roy. Soc. cx. p. 476 (1926).
‡ H. N. Russell, Phys. Rev. xxxi. p. 27 (1928).
§ R. H. Fowler and Hartree, Proc. Roy. Soc. cxi. p. 83 (1926).
‖ Mihul, *Annales de Physique*, ix. p. 261 (1928).
¶ A. Fowler, Proc. Roy. Soc. cxvii. p. 317 (1928).

A valuable partial photometric study of the negative glow for the visible region has been made by Seeliger and Lindow *. The present paper includes a more complete description of the spectrum of the negative glow, and an examination of the extent to which its production can be explained in the light of recent work upon the electrical conditions obtaining there.

2. *Apparatus and Results.*

The discharge tube used was originally designed for absorption work, and was similar to one referred to by Paschen †. It was 95 cm. long and 5·5 cm. in diameter, with the ends closed by metal caps, holding quartz windows, the leads to the electrodes, and a tube connecting with the pumping train. The electrodes consisted of rectangular sheets of degassed nickel, 65 cm. $\times 3{\cdot}5$ cm., supported in the tube on a framework of glass rods. The ends of the tube were sealed with picein. Oxygen was generated from potassium permanganate, and water and carbon vapours were removed by phosphorus pentoxide and caustic potash. The tube was protected by a pair of liquid air traps from tap-grease vapour, and from mercury vapour from the diffusion pump and McLeod gauge. The discharge was run off the 440 volt D.C. mains, at pressures of about 0·5 mm. Hg., and current densities of some 1-2 mA/cm.^{2} The negative glow occupied the middle of the tube, and there was present for part of the time a relatively feeble anode glow covering the whole of the anode.

The spectroscopes used were :—

(i) A glass prism instrument for the visible and infra-red, having a dispersion of 20 A per mm. at λ 4300, and 200 A per mm. at λ 8000.

(ii) A medium quartz prism instrument with a dispersion of 6 A per mm. at λ 2300, and 16 A per mm. at λ 3000.

(iii) A Hilger E 31 small quartz spectrometer for the ultraviolet below λ 2200.

Oiled plates were used for (iii), and Kodak special infra-red plates for the longer wave-lengths with (i).

The negative glow was viewed end-on through a quartz window, the times of exposure being usually 8 hrs. for

* Seeliger and Lindow, *Phys. Zeits.* xxvi. p. 393 (1925).

† Paschen, *Ann. d. Phys.* xlv. p. 625 (1914).

the visible, 25 hrs. for the ultraviolet and 50 hours for the infra-red. There was little radiation below λ 2200, except immediately after the tube was set up, when the carbon line at λ 1930 came up strongly. This had disappeared after running the tube continuously for a fortnight with repeated renewals of gas, and ultimately the only foreign spectra were the bands at λ 2882 and λ 2895 which have been attributed to carbon dioxide *, and these only appeared faintly.

The following spectra were present.—

(1) The visible and ultraviolet negative bands of oxygen, the latter being decidedly less intense relative to the line spectrum than on the plates obtained by R. C. Johnson, with a condensed discharge †.

(2) The violet ozone bands, again less intense than on Johnson's plates.

(3) All the strongest lines of nickel (Ni I) listed by Kayser ‡ between λ 4000 and λ 2900, without anomalies in relative intensity. These were due to the sputtering material of the electrode.

(4) The two lines of Ni II at λ 2546 ($a^2F_3'-a^2G_4'$) and λ 2511 ($a^2F_4'-a^2G_5'$) §, feebly.

(5) The O III lines at λ 3760 ($3s^3P_2-3p^3D_3$), λ 3754 ($3s^3P_1-3p^3D_2$) and λ 3299 ($3s^3P_0-3p^3S_1$), rather feebly ‖. Other may have been present in small intensity, but obscured by bands.

(6) All the strong lines of O I of wave-length less than λ 8000—the limit of our instruments—in about the relative intensities given by Kayser. λ 5577, if present, could not be resolved from the fine structure of the green oxygen band.

(7) The O II spectrum, to which special interest attaches. With a few exceptions most previously listed lines between λ 4674 and λ 2300 have been found on our plates. The missing lines are mainly those whose intensities have been previously given as (O) or (1), and, it is anticipated, these

* Fox, Duffendack, and Barker, Proc. Nat. Acad. Sci. xiii. p. 302 (1927).

† R. C. Johnson, Proc. Roy. Soc. cv. p. 683 (1924).

‡ Kayser, *Hauptlinien d. Linienpektra.*

§ Shenstone, Phys. Rev. xxx. p. 255 (1927).

‖ Fowler, Proc. Roy. Soc. cxvii. p. 317 (1928).

would have appeared on more prolonged exposure. The multiplets $(b, c)^2D'_{2,3} - (c, d)^2D_{2,3}$ were however definitely absent in all cases, and include strong lines which could not have been overlooked. Mr. E. M. Lindsay has verified for us that they appear in the spark between carbon poles in oxygen, so that it is unlikely that their absence is connected with the small trace of carbon present in our tube. We have also checked v. Wijk's observation of the visible lines with a silver spark in oxygen *. There is little room for doubt that they have been correctly assigned, particularly in view of Mihul's examination of the Zeeman effect of the strongest visible lines †. Moreover, Dingle finds corresponding lines in the second spark spectrum of Fluorine (F III)‡, although, as he points out, a number of expected combinations in O II and F III are absent. v. Wijk's investigation of the intensities of the multiplets missing on our plates is unfortunately incomplete. The lines comprise all possible transitions between the D and D′ terms arising from the s^2p^23p and s^2p^23d configurations of the oxygen ion. Apart from these, the relative intensities are about the same as described previously.

(8) A careful search has been made for the prominent lines of O IV. with negative results.

The arc and spark spectra O I and O II. and the negative bands are of comparable intensities. Although the light examined came from the whole of the negative glow, yet Seeliger and Lindow's work shows that it must have come preponderantly from its visually brightest part. which is also where the electrical analysis (below) has shown that the ionic concentrations are greatest.

3. *Correlation of Discharge and Spectroscopic Data.*

The properties of the oxygen atom and molecule are now sufficiently well known to permit of some correlation of the spectrum of the negative glow with the discharge conditions. The latter have been investigated by N. M.

* v. Wijk, *Zeits. f. Phys.* xlvii. p. 622 (1928).
† Mihul, *loc. cit.*
‡ Dingle, Proc, Roy. Soc. cxxii. p. 153 (1929).

Carmichael * in another connexion. Wrede † has shown that there is considerable dissociation into atoms in the oxygen discharge; from the ionic concentrations found in the work of Miss Carmichael, most of the atoms present must be neutral. We shall neglect their presence at first, and examine later the consequences of supposing that 10 per cent. of the gas content was atomic oxygen. Judging from Wrede's observations, fewer atoms would probably have been present. Atoms tend to accumulate in large numbers, because, unlike ions, they are not removed in the electric field.

The oxygen molecule (O_2) has a critical potential at about 8 volts, which probably corresponds to dissociation of the molecule into two neutral atoms ‡. The relevant data concerning ionization of the molecule are contained in the two equations §

$$O_2 = O_2^+ + e \quad -15 \text{ volts, and}$$
$$O_2 = O^+ + O + e - 21 \text{ volts.}$$

Oxygen atoms can thus be produced by at least two distinct processes.

The negative bands of oxygen originate in the ionized molecule O_2^+ ‖.

The resonance potential of atomic oxygen is 9·1 volts and its ionization potential 13·6 volts ¶. The ionization potential of singly ionized oxygen is 35 volts ** and that of doubly ionized oxygen 55 volts **.

The spectrophotometric analysis of Seeliger and Lindow has shown that the ozone bands fall off very abruptly in intensity in passing from the negative glow to the cathode dark space, the arc lines (O I) somewhat less abruptly, and the spark lines (O II) in general rather gradually. A visual study of the spectrum of the negative glow by the subjective method of Seeliger and Lindow showed that the green negative band behaved very much like the arc lines. No photometric study has been made for the ultraviolet

* Carmichael, see p. 362.

† Wrede, *Zeits. f. Phys.* liv. p. 53 (1929).

‡ Geiger-Scheele, *Handbuch d. Phys.* xxiii. p. 760.

§ Hogness and Lunn, Phys. Rev. xxvii. p. 732 (1926). The numbers have been slightly modified from those given by these authors.

‖ Lockrow and Duffendack, Phys. Rev. xxv. p. 110 (1925).

¶ Hopfield, Astrophys. Journ. lix. p. 114 (1924).

** According to previously mentioned spectroscopic data for O II and O III.

and infra-red, but there is not any reason to suppose that the behaviour of lines and bands in these regions should be any different from that of the corresponding visible spectra.

The Langmuir analysis * has shown that the ionization falls off very steeply from the negative glow to the cathode dark space, and more gradually towards the Faraday dark space, the negative glow being closely equipotential. Three groups of electrons are present, each with an approximately Maxwellian distribution of velocities, typical data concerning the brightest part of the negative glow in a 450 volt discharge in a tube essentially similar to that of § 2, with a gas pressure of 0·6 mm. Hg., being

Fast group	$3 \cdot 10^6$	per cc.	Average energy 17 electron-volts.
Secondary group	$3 \cdot 10^7$	,,	2·6 ,,
Ultimate group	$1 \cdot 2 \cdot 10^9$	,,	0·3 ,,

We will first calculate the number present in each group energetically able to effect ionization of the molecule at 15 volts in a single stage. This gives :—

Fast group	$3 \cdot 10^6 \varepsilon^{-15/17}$	or	$1 \cdot 3\ 10^6$ per cc.
Secondary group	$3 \cdot 10^7 \varepsilon^{-15\ 2 \cdot 6}$	or	$1 \cdot 0\ 10^5$,,
Ultimate group	$1 \cdot 2 . 10^9 \varepsilon^{-15\ 0 \cdot 3}$	or	$2 \cdot 3\ 10^{-13}$ per cc.

The contributions of the two slow groups can be neglected, and the same is true to an even greater extent of their action in producing combined ionization and dissociation at 21 volts. The ratio of the number of electrons able to effect the 21 volt process to the number able to effect the 15 volt process is $\varepsilon^{-21\ 17}$; $\varepsilon^{-15\ 17}$, or 0·9. The positive ray analysis of Hogness and Lunn†, in which conditions may have approximated very closely to those in the negative glow ‡, would suggest a ratio of the concentrations of O_2^+ ; O^+ of about 7·1. The above inferences from the results of the Langmuir analysis are consistent with this, and with Seeliger and Lindow's and our observation that the bands and spark lines (O II) are of comparable intensity. It is shown later that no essential modification of this conclusion is required when dissociation is taken into account.

The feeble intensity of the O III lines and the absence

* Carmichael, *loc. cit.*
† Hogness and Lunn, *loc. cit.*
‡ Morse and Gurney, Phys. Rev. xxxiii. p. 789 (1929).

of those of O IV is again consistent with the data for the electrons present.

No comment can be made upon the relatively feeble intensity of the ozone bands on our plates in absence of precise information as to how ozone is formed in the discharge.

A less satisfactory explanation can be given of the spectrophotometric results of Seeliger and Lindow, since only the critical potentials and not the excitation and ionization functions are known for oxygen. If these were known, however, they would have to be used in conjunction with the results of the Langmuir analysis for electrons moving in random directions, and not for any directed group of electrons supposed to be penetrating through the negative glow from the cathode dark space, since the work of Emeléus and Brown * has shown that the latter are practically absent under these conditions, except very close to the cathode dark space. Lack of knowledge of the excitation and ionization functions has also made it necessary to work in preceding paragraphs simply with the number of electrons energetically able to effect a process, irrespective of its probability. This is the best that can be done at present, but is unlikely to lead to serious error in the cases under consideration. In connexion with the results of Seeliger and Lindow, we may note however, that the form of the intensity-distance curves for the spectra is generally similar to that of the ionization-distance curves in such work as that of Emeléus and Brown. The maximum in the concentration-distance curve is also perhaps less sharp for the fast electrons than for the slow, as would be expected from the weak maximum in the intensity-distance curve for the spark lines (O II).

Another interesting point is that with certain exceptions the relative intensities of the spark lines (O II) in our tube correspond quite closely with their relative intensities in the positive column of a condensed discharge †. No analysis of the positive column has been made under these conditions with exploring electrodes, but we can predict with fair certainty that there must be present in the latter the fast group of electrons found in the negative glow of the more gentle discharge, with about the same energy, since otherwise production of the various excited states

* Emeléus & Brown, Phil. Mag. vii. p. 17 (1929).
† Mihul, *loc. cit.*

of the O^+ ion could hardly occur at the same rates in the two cases. We can offer no satisfactory explanation of the absence of certain important O II lines (§ 2). There is, as already stated, little room for doubt that they have been correctly assigned, and it does not seem worth while to carry out the rather elaborate investigation which would be required to find which of the discharge factors was responsible for their absence from our tube. Seeliger and Lindow mention that the behaviour of the O II lines is somewhat erratic, indicating that their excitation functions are not all similar.

The nickel lines are probably excited largely by the electrons of the secondary and fast groups. Their sharpness speaks against their being excited by collisions of the second kind, and is also in accord with the absence of a large field in the negative glow *.

Oxygen is not well suited for observation of the continuous and diffuse spectra which are characteristic of the recombination of ions and electrons.

We have neglected the possibility that cumulative processes might be responsible for the ionization and dissociation. Any theoretical discussion of this must be very uncertain, but we can proceed approximately in the following way.

Under the conditions mentioned at the beginning of this section there are some 10^{16} molecules per c.c. The number of collisions in which direct ionization at 15 volts and at 21 volts can occur will be the product of the molecular concentration by the number of electrons energetically able to effect the process in question, viz. :

$$10^{16}\,3{\cdot}10^{6}\,\varepsilon^{-15/17} \text{ or } 1{\cdot}3\ 10^{22}, \text{ at 15 volts} \quad . \quad . \quad . \quad (\alpha)$$

and $10^{16}\,3{\cdot}10^{6}\,\varepsilon^{-21/17}$ or $0{\cdot}9\ 10^{22}$, at 21 volts . . . (β)

again multiplied by factors depending on (*a*) the average energy of the electrons (17 volts in this case) and (*b*) the probability of ionization for different speeds of the electrons.

If there are x times as many excited molecules present as ions, or approximately $10^{9}x$ per c.c., each with an average energy of excitation of 10 volts, the number of collisions in which these can be ionized will be the product of another probability factor by

$$10^{9}x\ (3{\cdot}10^{6}\varepsilon^{-(15-10)/17}+3{\cdot}10^{7}\varepsilon^{-(15-10)/2{\cdot}6}) \quad \text{or} \quad 10^{16}\,x. \quad (\gamma)$$

* Frerichs, *Ann. d. Phys.* lxxxv. p. 362 (1928).

The ratio of this number to the number of direct ionizations at 15 volts is $5x10^{-7}$. The expression from which (γ) is derived contains two terms, each of which is arrived at in the same way as the single term above for direct ionization. The first represents the effect of the fast group, and the second that of the secondary group, which has now to be taken into account, although the slow group can still be ignored. 10 volts has been chosen as being between the 8 volt and 15 volt critical potentials for O_2, with a bias towards the lower of these. In view of the fact that the lower probably corresponds to dissociation, 10 volts is probably a considerable overestimate of the energy of excitation, which will make the subsequent calculations still more in favour of direct ionization at 15 volts.

Some measurements of anomalous dispersion made by Ladenburg * indicate that in the inert gases, under conditions similar to those in the negative glow, x is of the order 10^3. x would tend to be higher in the inert gases than in oxygen, since atoms can accumulate in metastable states in the former, but on the other hand the energies of excitation and ionization are more nearly equal in the inert gases than in oxygen. In the latter 10^4 seems a reasonable number to adopt, in which case the ratio becomes $5\,10^{-3}$. Even if the large target areas of excited molecules are taken into account, it is questionable if the differences in the probability factors could change this ratio to one of the order of unity or greater. K. T. Compton † has already suggested that it is ionization by single impact rather than by cumulative action which is of primary importance in Geissler tubes.

Returning to the effects of dissociation, we will consider a case when there are 10^{15} unexcited atoms per unit volume. The number of collisions in which they can be excited at 9·1 volts will be the product of a probability factor by

$$10^{15}(3\cdot10^6\varepsilon^{-9\cdot1\ 17}+3\cdot10^7\varepsilon^{-9\cdot1/2\cdot6}) \quad \text{or} \quad 3\cdot10^{21}. \quad . \quad (\delta)$$

and the number of direct ionizing collisions at 13·6 volts

$$10^{15}(3\cdot10^6\varepsilon^{-13\cdot6\ 17}), \quad \text{or} \quad 10^{21} \ . \ . \ . \ . \quad (\eta)$$

* Ladenburg, *Zeits. f. Phys.* xlviii. p. 15 (1928), etc.
† K. T. Compton, Phil. Mag. xliii. p. 534 (1922).

It is also readily seen from a calculation similar to that performed on p. 390, that cumulative ionization may now lead to the production of ions at a rate comparable with (η). Comparing (η) and (β), we see that they are of the same order, but there is no reason to suppose that ionization of the atom directly will disturb to any large extent the otherwise existing balance between O_2^+ and O^+.

The remaining part of the spectrum to be considered is that of the neutral atom (O I). In the case of oxygen, we can see in a general way that these lines will not be enormously strong relative to the spark lines, since atoms, before they can be excited, have to be produced by processes energetically comparable with those producing ions from the molecules. In the inert gases, however, the arc lines are found to be less prominent than the spark lines in many instances, and it thus appears that there is some other factor which we have not taken into account which tends to promote radiation from ions. One obvious agency would be interatomic fields, but we are not able to say anything definite on this point.

The great difficulty in making calculations of the type attempted in this paper, apart from very incomplete knowledge of the probability factors, is that although the negative glow is not a system in thermodynamical equilibrum, yet interchanges of energy occur within it too frequently to be treated other than statistically. However, as is shewn by the occurrence of several groups of electrons, each with an equivalent temperature, it is, so to speak, half-way towards thermal equilibrium, and we can thus hope to obtain some idea of what is taking place by the methods which we have adopted. Perhaps the most striking fact emerging is the important part played by the fast group of electrons, the main function of the other groups, particularly the ultimate group, being, as elsewhere in the discharge, to effect the transport of the current in the tube. There is some similarity between the properties of the equipotential negative glow and the properties of ionized stellar atmospheres; the one is receiving energy unilaterally from the cathode dark space, and the other from the interior of the star, and this analogy may prove fruitful in future developments of the theory of the negative glow.

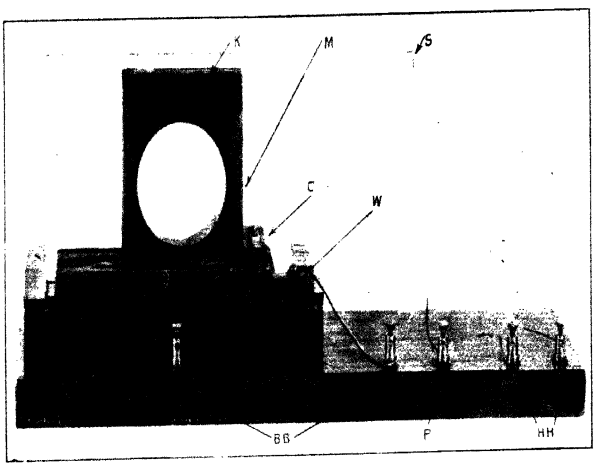

Instrument for measuring Magnetic Field Strength.

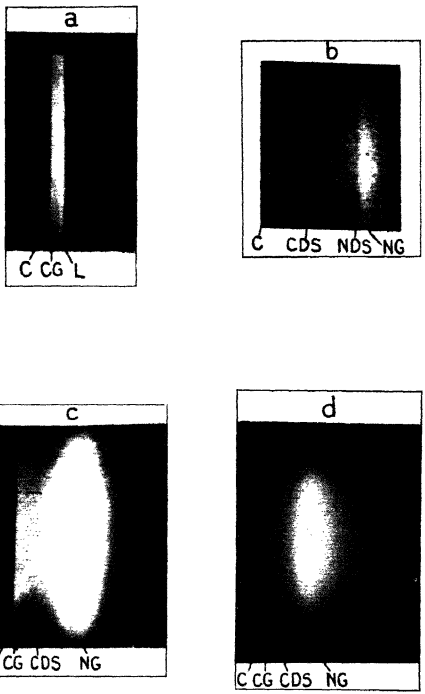

Cathode, C. Cathode glow, CG. Cathode dark space, CDS. Negative glow, NG. New dark space, NDS.

a. Discharge through nitrogen. Cathode fall in potenial 380 volts. Pressure 0·82 mm. Hg. Current density 0·07 mA/cm.^{2} Ilford special rapid panchromatic plate. Magnification 1·81.

b. Oxygen, 450 volts, 0·25 mm. Hg. 0·04 mA cm.^{2} Ilford special rapid panchromatic plate. Magnification 1·18.

c. Nitrogen, 400 volts, 0·53 mm. Hg. 0·05 mA cm.^{2} Ilford special rapid panchro matic plate. Magnification 1·37.

d. Oxygen, 420 volts, 0·33 mm. Hg. 0·09 mA cm.^{2} Imperial panchromatic plate. Magnification 1·04.

THE

LONDON, EDINBURGH, AND DUBLIN

PHILOSOPHICAL MAGAZINE

AND

JOURNAL OF SCIENCE.

[SEVENTH SERIES.]

OCTOBER 1929.

XLV. *On the Relation between the Cathode Fall of Potential, the Length of the Dark Space, and the Current in the Electric Discharge through Gases.* *By* Sir J. J. THOMSON, O.M., F.R.S.*

Summary.

THE relation between the thickness of the dark space, the cathode fall of potential, and the current is obtained both for the normal and abnormal discharge on the suppositions that

1. The number of ions produced by an electron per cm. is proportional to $kp(V-C)/\{(V-C)^2+M^2\}$, where V is the energy of the electron expressed in volts, C the ionization potential, p the pressure, k a constant, and M the value of $V-C$ when the ionization is a maximum.

2. That the electric force in the dark space at a point P is a linear function of the distance of P from the cathode (Aston's Law).

3. That the number of electrons liberated from the cathode by the impact on it of a positive ion is $\alpha+\beta V^2$, where V is the energy of the ion. This is suggested by the experiments of Bärwald and Oliphant.

* Communicated by the Author.

4. That the relation between the potential difference V, the current density i, and the thickness of the dark space d is

$$id^2 = (\text{constant})\, V^{\frac{3}{2}}.$$

On these suppositions it follows that in the abnormal discharge V varies very nearly as $(i/p^2)^{\frac{2}{3}}$ and pd as $(i/p^2)^{-\frac{1}{3}}$, where p is the pressure; thus V increases and d diminishes as the current increases.

Günther-Schulze, as the result of his experiments, gives the empirical formula V varies as $i^{\frac{1}{4}}$, so that the theory is in fair agreement with his result. The theory shows that a transverse magnetic force would diminish the thickness of the dark space, and also that it would diminish the potential difference required to produce a very short spark. The first result is well known to be true. An experiment is described which shows that the second is also true.

The result of the investigation is that the electronic collisions, though sufficient to account for the greater part of the ionization, require to be supplemented by other agents such as radiation, and an experiment is described showing the great effect on the discharge produced by radiation from the negative glow.

IN any self-sustained discharge two conditions must be satisfied; the first of these, which may be called the maintenance condition, is that there must be processes going on in the discharge which, for every electron taken from the gas by the discharge, produce another to take its place. This condition must apply whether the current passing through the gas is large or small.

The second condition is that the current density should correspond to that which the potential difference between the electrodes would send through the gas. Until the whole area of the electrodes is covered by the current, the current density may take any value within wide limits by adjustment of the area from which the current starts. Thus this condition, which is expressed as a relation between i the current density, V_0 the cathode fall of potential, and d the thickness of the dark space, will not put any limitations on the values of V_0 and d, but will determine the value of i corresponding to assigned values of these quantities. When, however, the current through the tube is so large that the discharge covers the whole of the electrode, the current density is now fixed by this current, and it is only values of

V_0 and d, which change as the current changes, which satisfy the condition. This case is often called the abnormal discharge; that when the current does not cover the electrode the normal one.

The maintenance condition will depend upon the types of ionization occurring in the discharge and the laws which they obey. There are many sources of ionization in the discharge, collisions of electrons, photoelectric effects at the cathode, and other effects due to the impact of positive ions on the cathode; the gas is also ionized by radiation excited by the discharge.

We shall begin by considering the ionization due to the collision of electrons. Experiments on the ionization produced by electrons moving with definite speeds have been made by several observers; the most recent are those by Kössel *, Hughes and Klein †, and Compton and van Voorhis ‡.

These, though they differ considerably in the numerical results, agree in their general features. The chance that an electron will produce other electrons by collisions with the molecules of the gas through which it is passing is zero until the energy of the electron reaches a definite value, which, when it is measured in volts, is called the ionization potential. After the energy passes this value the ionization is at first proportional to the difference between it and the ionization potential; it attains a maximum when the energy reaches a certain value, which, from Compton's curves, seems, for air, to be about 170 volts. Kössel gives it as 200 volts. The maximum is, however, so flat that it is very difficult to fix the exact spot at which it occurs. After the energy of the electron passes the value for maximum ionization, the ionization decreases, and is ultimately inversely proportional to the energy.

Compton's curves are in fair agreement with the formula, for which there are theoretical grounds, that the number of electrons produced per cm. of path by an electron whose energy is V, moving through a gas at pressure p, is equal to

$$\frac{kp(V-C)}{(V-C)^2+M^2},$$

where C is the ionization potential, M the value of $V-C$ when the ionization is a maximum, and k a constant. This constant can be determined for nitrogen, since Kössel and

* Kössel, *Ann. der Phys.* xxxvii. p. 393 (1912).

† Hughes and Klein, Phys. Rev. xxiii. p. 450 (1924).

‡ K. T. Compton and van Voorhis, Phys. Rev. xxvii. p. 724 (1926).

Compton agree that in this gas the maximum ionization is such that at a pressure of 1 mm. of Hg the electron produces 10 other electrons per cm. of path.

So that, if p is measured in mm.,

$$\frac{k}{2\mathrm{M}} = 10.$$

Taking Compton's value for M, *i. e.* 170 volts, $k = 3400$ for N_2.

For hydrogen the maximum ionization at a pressure of 1 mm. is 4 electrons per cm. Compton's value of M for hydrogen is 135, hence k for hydrogen is 1080.

The number of electrons produced when the moving electron goes from $x=a$ to $x=b$ is

$$\int_a^b \frac{kp(\mathrm{V}-\mathrm{C})}{(\mathrm{V}-\mathrm{C})^2+\mathrm{M}^2}dx.$$

If the electron is starting from the cathode and moving through the cathode dark space, the value of V at a distance x from the cathode would, since Aston's experiments show that the value of the electric force is a linear function of the distance from the cathode, be given by

$$\mathrm{V} = \mathrm{V}_0 \frac{x(2d-x)}{d^2},$$

where V_0 is the cathode fall of potential and d the thickness of the dark space.

We shall consider this case in detail later, but it may make things clearer if we take first a hypothetical case where the analysis is simpler and suppose

$$\mathrm{V} = \mathrm{V}_0 \frac{x}{d},$$

which corresponds to a uniform force in the dark space.

If this is the value of V, then

$$\int_0^d \frac{kp(\mathrm{V}-\mathrm{C})}{(\mathrm{V}-\mathrm{C})^2+\mathrm{M}^2}dx = \frac{kdp}{\mathrm{V}_0}\int_{\mathrm{C}}^{\mathrm{V}_0} \frac{(\mathrm{V}-\mathrm{C})d\mathrm{V}}{(\mathrm{V}-\mathrm{C})^2+\mathrm{M}^2}$$

$$= \frac{kpd}{2\mathrm{V}_0}\log\frac{(\mathrm{V}_0-\mathrm{C})^2+\mathrm{M}^2}{\mathrm{M}^2}.$$

When V_0 is small compared with M, this is equal to

$$\frac{kpd}{2\mathrm{V}_0}\cdot\frac{(\mathrm{V}_0-\mathrm{C})^2}{\mathrm{M}^2}$$

$$= \frac{kpd}{2}\cdot\frac{\mathrm{V}_0-\mathrm{C}}{\mathrm{M}^2},$$

when C is small compared with V_0.

When $V_0 - C$ is large compared with M, the number of electrons produced is

$$\frac{kpd}{2V_0} \log \frac{V_0^2}{M^2}.$$

The number of electrons produced is a maximum when

$$\frac{\partial}{\partial V_0}\left(\frac{1}{V_0} \log \frac{V_0^2 + M^2}{M^2}\right) = 0,$$

neglecting C in comparison with V_0. We find that $V_0 = 2M$ is a very close approximation to the solution of this equation. For this value of V_0 the number of electrons produced by an electron travelling over the dark space is equal to

$$\frac{kpd}{4M} \log 5 = \frac{\cdot 4kpd}{M}.$$

This is not very much less than $\cdot 5kpd/M$, which is the number which would have been produced if the moving electron had been ionizing at the maximum rate from start to finish.

Let us now consider the case where the distribution of V is that actually found in the dark space, *i. e.*, when

$$V = \frac{V_0}{d^2} x(2d - x)$$

or

$$1 - \frac{x}{d} = \sqrt{1 - \frac{V}{V_0}};$$

thus

$$\frac{dx}{d} = \frac{1}{2V_0} \frac{1}{\sqrt{1 - \frac{V}{V_0}}} dV.$$

Hence

$$\int_0^d \frac{kp(V-C)}{(V-C)^2 + M^2} dx = \frac{dkp}{2V_0} \int_C^{V_0} \frac{V-C}{(V-C)^2 + M^2} \cdot \frac{1}{\sqrt{1 - \frac{V}{V_0}}} dV;$$

or, putting

$$1 - \frac{V}{V_0} = y^2,$$

$$= dkp \int_0^{\sqrt{1 - \frac{C}{V_0}}} \frac{V_0(1-y^2) - C}{(V_0(1-y^2) - C)^2 + M^2} dy$$

$$= \frac{dkp}{2} \int \left(\frac{1}{V_0(1-y^2) - C + iM} + \frac{1}{V_0(1-y^2) - C - iM} \right) dy$$

$$= \frac{dkp}{4V_0} \left\{ \frac{1}{\sqrt{1 - \frac{C}{V_0} + \frac{iM}{V_0}}} \log \frac{\sqrt{1 - \frac{C}{V_0} + \frac{iM}{V_0}} + y}{\sqrt{1 - \frac{C}{V_0} + \frac{iM}{V_0}} - y} + \frac{1}{\sqrt{1 - \frac{C}{V_0} - \frac{iM}{V_0}}} \log \frac{\sqrt{1 - \frac{C}{V_0} - \frac{iM}{V_0}} + y}{\sqrt{1 - \frac{C}{V_0} - \frac{iM}{V_0}} - y} \right\}.$$

If $\frac{M}{V_0 - C} = \tan \phi$ and $\alpha = \sqrt{\frac{V_0}{V_0 - C}}$, this is equal to

$$\frac{1}{2} \frac{dkp}{V_0} \left\{ \frac{1}{2} \sqrt{\alpha \cos \phi} \cos \frac{\phi}{2} \log \frac{y^2 + \frac{2y \cos \frac{\phi}{2}}{\sqrt{\alpha \cos \phi}} + \frac{1}{\alpha \cos \phi}}{y^2 - \frac{2y \cos \frac{\phi}{2}}{\sqrt{\alpha \cos \phi}} + \frac{1}{\alpha \cos \phi}} - \sqrt{\alpha \cos \phi} \sin \frac{\phi}{2} \tan^{-1} \frac{\left(2y \sin \frac{\phi}{2} \sqrt{\alpha \cos \phi} \right)}{1 - y^2 \alpha \cos \phi} \right\}. \quad (1)$$

This represents the indefinite integral. When the electron travels through the dark space, *i. e.*, from $x = 0$ to $x = d$, the limits of integration when C/V is small are $y = 0$, $y = 1$, and between these limits the integral in this case is equal to

$$\frac{1}{2} \frac{dkp}{V_0} \left\{ \sqrt{\cos \phi} \cos \frac{\phi}{2} \log \frac{\cos \frac{\phi}{2} + \sqrt{\cos \phi}}{\sin \frac{\phi}{2}} - \sin \frac{\phi}{2} \sqrt{\cos \phi} \tan^{-1} \frac{\sqrt{\cos \phi}}{\sin \frac{\phi}{2}} \right\}. \quad (2)$$

From this equation the number of electrons produced by an electron starting from the cathode and travelling through

the dark space can be calculated for various potential falls V_0. The results are shown in the following table. The number of electrons produced is expressed as a fraction of $kdp/2M$, the number which would be produced if the electron from start to finish were moving with the velocity for maximum ionization.

$\frac{V_0}{M}$	·5	1	1·25	1·5	1·75	2	3	4	·6
Number of electrons...	·60	·81	·85	·86	·85	·83	·73	·62	·53

This table shows that the number of electrons produced is a maximum when $V_0=1{\cdot}5$ M. For some gases this value of V_0 seems to be not far from the truth; the values of M are, however, difficult to determine with accuracy. We see from this table that, though the velocity of the electron is changing throughout its passage through the dark space, there is a considerable range of cathode falls for which it produces more than 80 per cent. of the maximum number it is possible for an electron to produce.

It follows from the expression (2) that when V_0/M is very large, and therefore ϕ small, the number of electrons produced is equal to

$$\frac{1}{2}\frac{kpd}{V_0}\log\frac{4V_0}{M}. \quad . \quad . \quad . \quad . \quad . \quad . \quad . \quad (3)$$

Since the logarithm varies slowly, the number of electrons produced varies inversely as the fall of potential approximately.

The number when V_0/M is small is

$$\frac{4}{3}\cdot\frac{V_0-C}{M}\cdot\frac{kpd}{2M}.$$

From the expression (1) we can find the number of electrons produced by the moving electron between any two points in the dark space by taking as the limits of integration the values of y corresponding to these points. If the path under consideration starts from the cathode, the upper limit of y is 1; the lower limit when the path ends where the potential is V is given by $y^2=1-\frac{V}{V_0}$. By putting $y=1/\sqrt{2}$ we can find the number produced in the first half of the potential fall. When $V_0=3M/2$ the electrons produced in the first half of the potential fall are only 22 out of a total of 86 for the whole fall. Thus, in the normal discharge, about 75 per cent. of the electrons which cross the dark space have energies less than half that corresponding

to the cathode fall of potential. When, as in the abnormal discharge, the cathode fall is much greater than the normal value, the chance of an electron producing another in its passage across the dark space may be less than unity so that the majority of the electrons which cross the dark space will be those which started from the cathode, and which have the energy corresponding to the total cathode fall.

For large values of V_0 the number of electrons produced is, by equation (3),

$$\frac{kpd}{2V_0}\log\frac{4V_0}{M}.$$

pd is constant for the same gas; $kp/2M$ is the maximum number of electrons made per centimetre of path. In nitrogen at 1 mm. pressure this number is about 10, and the dark space in nitrogen at that pressure is ·3 cm., so that the number of electrons produced in the dark space is 3; hence $kpd/2M$ for nitrogen is about 3, and the number of electrons produced in the dark space

$$\frac{3M}{V_0}\log\frac{4V_0}{M}.$$

This is less than unity when V_0/M is greater than 11·5; hence, if we take the normal cathode fall as 1·5 M, the majority of the electrons leaving the dark space will have energies corresponding to the full fall of potential when the cathode fall is greater than about 8 times the cathode fall for the normal discharge.

We have hitherto considered only the electrons produced by primary electrons starting from the cathode; the secondary electrons these produce may, under the electric field in the dark space, acquire sufficient energy to ionize the gas and produce tertiary electrons, and these again may produce further electrons.

The number of electrons produced by the secondary rays can be determined by a slight modification of the preceding method. We must in equation (1) replace d by l (the length of the path of the secondary electron in the dark space), and V_0 (the cathode fall of potential) by V_0l^2/d^2, which is the potential through which the secondary electron falls.

The figures we have given show that when the potential difference is of the order of that corresponding to the normal discharge, the ionization is within a few per cent. of that which an electron would produce if it were ionizing at the maximum rate over the whole of its path. Under these

circumstances the ionization by secondary and tertiary electrons would be very important, and make the ionization proportional to $e^{kpd}-1$, rather than to kpd.

In the abnormal discharge, where the number of secondaries produced is small compared with the primaries, the subsidiary ionization would be insignificant and the ionization proportional to kpd.

The production of electrons in the gas by the collisions of electrons moving away from the cathode cannot by itself be sufficient to maintain the discharge; there must be some other process going on which will renew the supply of electrons coming from the cathode. The positive ions which are produced in the ionization by the electronic collisions will be driven on to the cathode by the electric force in the dark space. It is a well-established fact that the impact of positive ions against a metal plate causes it to emit electrons, the number emitted depending on the energy of the positive ions when they strike the plate, and increases rapidly as this energy increases. The graphs given by Bärwald (*Ann. Phys.* lx. p. 1, 1919) and Oliphant (Proc. Camb. Phil. Soc. xxiv. p. 451, 1928) for the relation between the number of electrons expelled from the plate by the impact of an ion and the energy of the ion, suggest that N, the number of electrons, is given by an equation of the form

$$N = \alpha + \beta V^2, \quad . \quad . \quad . \quad . \quad . \quad (4)$$

where V is the potential difference through which the ion striking the plate has fallen. There are some theoretical considerations in favour of this relation, since the depths to which the ions penetrate is proportional to the square of their energy. And even if the ions have no energy when they strike against the plate, when they get neutralized by receiving an electron, they will emit radiation, and this radiation, by its photoelectric effects on the cathode, will give rise to the emission of electrons. Oliphant (*loc. cit.*) has shown that the emission of electrons by the impact of positive ions is much influenced by layers of gas on the electrode. As in experiments on discharge through gases the electrodes are always in contact with gas at not infinitesimal pressures, there will always be layers of gas on the cathode, and its behaviour may depend more on the nature of these layers than on the metal of which it is made.

Assuming then that the expression holds for the electrons ejected by a positive ion, the number of positive ions produced by an electron in its passage through the dark space is equal to the number of electrons which it produces, and

for which we have found expressions. Let $F(kpd, V_0)$ be the number of positive ions produced; the number of electrons which these will expel when they strike against the cathode will be of the form

$$F(kpd, V_0)(\alpha+\beta V^2).$$

If this number is equal to 1, then every electron which starts from the cathode and passes through the dark space will automatically provide a successor, so that the discharge will be self-sustained; hence the maintenance equation is

$$F(kpd, V_0)(\alpha+\beta V_0^2) = 1.$$

The numbers given in the table on p. 399 for the number of electrons produced by a single electron moving through the dark space can be represented with considerable accuracy by the expression

$$\frac{kpd.V_0}{V_0^2+U^2},$$

where $U=1{\cdot}5$ M. To represent the effect of the ionization due to secondary, tertiary, and higher orders of electrons, we may replace this expression by

$$\epsilon^{\frac{kpd.V_0}{V_0^2+U^2}}-1,$$

and the maintenance equation is

$$\left(\epsilon^{\frac{kpd.V_0}{V_0^2+U^2}}-1\right)(\alpha+\beta V_0^2) = 1.$$

When $\frac{kpd.V_0}{V_0^2+U^2}$ is small, this becomes

$$\frac{kpd.V_0}{V_0^2+U^2}(\alpha+\beta V_0^2) = 1. \quad . \quad . \quad . \quad . \quad (5)$$

The function $\frac{V_0(\alpha+\beta V_0^2)}{V_0^2+U^2}$ is represented by graphs of the types (1), (2), (3), fig. 1, according as α/β is greater than, equal to, or less than U^2.

Thus, when the graph is of the type (1), there will, when *kpd* is within certain limits, be three values of V_0 for a given value of *pd*. The solutions corresponding to the points A and C, fig. 1, (1), are stable, while that corresponding to B is unstable. Thus, under certain conditions, two types of discharge with different potential falls and different current densities are possible at the same pressure and with the same length of dark space. When the graph is of type (2) or (3)

there is only one solution for any value of pd, and only one type of discharge is possible. It is not a very infrequent experience when working with discharge through gases to find the discharge changing backwards and forwards from one type to another.

We must now consider the second condition which must be fulfilled for the discharge to be possible. This is what may be called the characteristic equation, as it expresses the

Fig. 1.

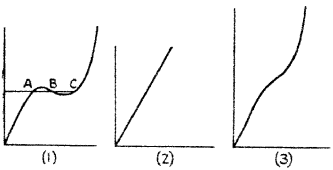

relation between the current density, the potential difference, and the distance between the electrodes. When, as in the normal discharge, the current does not cover the whole of the electrode, the current density, even when the total current is given, can have any value within wide limits; the characteristic equation determines the appropriate value of the current density, and does not put any restriction on the values of pd and V_0.

When, however, as in the abnormal discharge, the current covers the whole of the electrode, the current density, being the total current divided by the area of the electrode, is given, and we have to choose values of V_0 and pd which satisfy this equation, as well as the maintenance one.

One example of the characteristic equation is the well-known space-charge equation

$$id^2 = \left(\frac{1}{9\pi}\sqrt{\frac{2e}{m}}\right) V_0^{3/2}.$$

The space-charge equation is obtained on the assumption that there is no ionization between the electrodes, and so would not apply to our case. The result,

$$id^2 = \text{constant} \times V_0^{3/2},$$

is, however, not limited to the conditions postulated in the space-charge equation. It holds, for example, when there is uniform ionization throughout the dark space, a condition

which leads to Aston's Law for the distribution of electric force. It can be shown by the method of dimensions that

$$V_0^{3/2} = id^2\sqrt{\frac{M}{e}} \times f(w),$$

where $f(w)$ represents a function of w, and

$$w = e^4 m^{-1} i^{-2} d^{-7};$$

e is the atomic charge and m the mass of an electron. Under a considerable variety of conditions $f(w)$ seems to reduce to a constant.

We shall assume, then, that

$$id^2 = CV_0^{3/2}. \quad . \quad . \quad . \quad . \quad . \quad . \quad . \quad (6)$$

It is only in the abnormal discharge that the characteristic equation affects the relation between V_0 and pd, and in that case the ionization due to a single electron is small, so that the maintenance equation takes the form

$$\frac{kpd \,.\, V_0(\alpha + \beta V_0^2)}{V_0^2 + U^2} = 1.$$

The most interesting case is when V_0 is large compared with U; then the number of electrons produced by a single electron is, see (3), equal to

$$\frac{kpd}{2V_0}\log\frac{4V_0}{M},$$

and the maintenance equation reduces to

$$kpd\, V_0 \log\frac{4V_0}{M} = \text{constant}.$$

Substituting the value of d in terms of V_0 from

$$id^2 = C_1 V_0^{3/2},$$

we find

$$V_0^{7/4}\log\frac{4V_0}{M} = \text{constant} \times \left(\frac{i}{p^2}\right)^{1/2}. \quad . \quad . \quad . \quad . \quad (7)$$

Since the solution of the equation

$$x \log x = C,$$

when x is large, is approximately $x = C/\log C$, the approximate solution of (7) is

$$V_0 = \text{constant} \times \left(\frac{\left(\frac{i}{p^2}\right)}{\log \gamma\, i/p^2}\right)^{2/7},$$

and, corresponding to this,

$$pd = \text{constant} \times \left(\frac{i}{p^2}\right)^{-2/7} \times \{\log \gamma (i/p^2)\}^{-3/14},$$

where γ is a constant.

Thus V_0 increases and d decreases as the current increases; both these effects are well known. Günther-Schulze (*Zeit. f. Physik*, xxiii. p. 1, 1920), as the result of a long series of measurements, proposed the empirical formula

$$V_0 \text{ varies as } i^{1/4}.$$

The preceding theory indicates that V_0 varies a little less rapidly with the current than $i^{-1/3\cdot5}$, the logarithm in the denominator making the variation with i a little less rapid than the power law. The theory is thus in very fair agreement with Günther-Schulze's experiments.

When kpd is exceedingly small, we see from (5) that V_0 must be large and equal to $1/\beta\, kpd$. Thus the potential difference required to produce a very short spark will be inversely proportional to the length of the spark.

The quantity d, when it occurs in the maintenance equation, is primarily the length of path in the dark space or between the electrodes, and though this is equal to the thickness of the dark space or the distance between the electrodes when the path of the electron is along the line of electric force, it is not so when the electrons are exposed to a transverse magnetic force, which will make them describe curves whose length is greater than the distance between the electrodes. The maintenance equation gives the value of the length of the actual path, and requires this to have a definite value, whether the magnetic force acts or not. But if the curved path under the magnetic force is equal in length to the straight one when there is no magnetic force, the distance measured along the electric force, *i. e.*, normal to the electrodes, must be shorter when the magnetic force is on than when it is off; thus the thickness of the dark space must be diminished by the magnetic field. This is a well-marked and very striking phenomenon, the dark space under intense transverse magnetic fields shrinking to a fraction of its normal value.

If the distance between the electrodes is fixed, the magnetic force will increase the effective value of d, and this, by equation (5), will diminish the value of V_0, the potential difference required to produce a spark.

I find that this effect can be shown in a very marked way in the following manner. A and B (fig. 2) are two discharge-tubes placed in parallel and connected with the terminals of

an induction-coil. The electrodes in each tube are parallel plates near together; the distance between them in B was 1 mm., in A 2 mm. The backs of these electrodes and the wires inside the tube connecting them with the induction-coil were surrounded by glass tubes to prevent the discharge going from the backs of the electrodes. The space between the electrodes in B was between the poles M and N of a powerful electromagnet. The pressure in the tubes was adjusted within certain limits, and was such that it was far below the critical pressure for the tube B that the discharge only went through this tube with great difficulty. Then, when no current passed through the electromagnet, the discharge went entirely through A, and B was quite dark; when, however, a current passed through the electromagnet so that there was a strong transverse magnetic field across the spark-gap in B, all the discharge went through B, and A was quite dark.

Fig. 2.

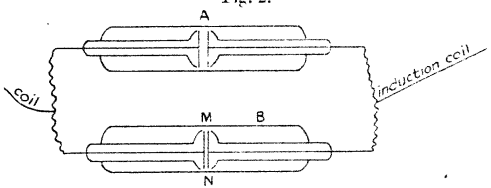

Though ionization by the collision of electrons and the ejection of electrons from the cathode by the bombardment of positive ions play a large part in maintaining the current, there are other agencies, such as the easily absorbable radiation which is produced by the discharge, which must take some part in the process. We can see by a simple calculation that it is probable that this radiation does produce an appreciable effect. We have seen that various experimenters have shown that the maximum ionization which can be produced by an electron moving through nitrogen is one electron per millimetre at a pressure of 1 mm. of Hg; at the pressure of n millimetres n electrons would be produced per millimetre. Now, suppose that the electrons in the dark space through the whole of their path are ionizing at the maximum rate, and that the secondary electrons they produce begin as soon as they are formed to ionize at the this rate, and that this holds for all the electrons produced in the dark space; then, when d is the thickness of the dark space, the number of electrons produced by one

electron will be ϵ^{nd}. Now nd is constant, so that this number will not vary with the pressure. When $n=1$, the thickness of the dark space is ·3 mm.; hence the number of electrons produced in the dark space is $\epsilon^3=20$. This is no doubt an overestimate, but the calculations we have given show that it is not so extravagant as might have been expected at first sight.

Along with these 20 electrons, 20 positive ions will be produced, and these will be driven against the cathode by the electric force in the dark space; thus, if the discharge is to be maintained, these 20 ions, when driven against the cathode, must liberate one electron. Thus the stream of electrons emerging from the cathode must be about 5 per cent. of the stream of positive ions impinging upon it.

The experiments of Oliphant and Bärwald (*loc. cit.*) show that when the energy of the positive ions is of the order of that due to a fall of potential of the order of the normal cathode fall, the number of electrons ejected from a metal plate by the impact of the ions is only about 1 per cent. of the number of ions striking the plate. In the case of the dark space there is a considerable electric force at the cathode in the direction tending to remove the ions from the plate. The presence of such a field increases the emission of electrons in the ordinary photoelectric effect unless the pressure of the gas is exceedingly low, much lower than is usual when the discharge is normal. This force would have to increaes the emission about five-fold to bring it up to the amount required to maintain the discharge. The numbers given seem to indicate that the electronic collisions may account for the greater part, but not for the whole, of the effect.

Another source of ionization we must consider is radiation emitted by the discharge itself. It is well known that the negative glow is especially active in emitting this radiation, so that if the help of this is required the presence of negative glow will be necessary for the discharge. To test this I tried the following experiment.

The discharge-tube (fig. 3) was cylindrical; the cathode C was a nickel disk nearly filling the cross-section of the tube; the anode A was a steel plate of the same diameter floating on the top of a column of mercury. The distance between the anode and cathode could be changed very gradually by moving the reservoir of mercury connected with the column. The discharge between A and C was produced by a battery of storage cells, and the current measured by a sensitive galvanometer. Starting from the position when A was sufficiently remote from C to allow of the development of both

the dark space and the negative glow, and making A gradually approach C, no appreciable change occurred in the current until the thickness of the negative glow was reduced to about a millimetre ; then the current diminished rapidly when the approach of A to C reduced the thickness of the glow. The appearance of the discharge changed altogether, and the current was reduced to a small percentage of its original value when the thickness of the glow fell to about one-third of a millimetre ; the abruptness with which the current stopped was very striking. The presence of at least a thin piece of the negative glow appears to be essential

Fig. 3.

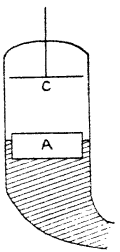

for the discharge. The fact that after the thickness of the dark space exceeds a millimetre or so the current is independent of the thickness is what we should expect if the glow rapidly absorbed the radiation it emits. A view that requires consideration is that the effect of the negative glow, a place where the density both of positive ions and electrons is very great, might be due not to radiation, but to the diffusion of positive ions from it into the dark space. These would be driven against the cathode by the electric field in the dark space, and there liberate electrons.

The calculation we have given above shows that if this were the explanation the number diffusing into the dark space from the negative glow would have to exceed the number of positive ions produced in the dark space itself, so that the majority of the positive ions reaching the cathode would have fallen through the whole of the cathode fall of potential, and would therefore have the maximum energy possible. The parabolas obtained in positive-ray photographs give an indication of the distribution of energy among the positive ions reaching the cathode. If the majority had the maximum energy these parabolas would have a bright

head and a faint tail. In most cases, however, the parabolas are of fairly uniform intensity, indicating that positive ions are produced pretty uniformly through the dark space.

The number of ions produced in the dark space by collisions diminishes rapidly as the cathode potential fall increases, while that due to radiation from the negative might be expected to be fairly constant, so that the radiation would be a more important factor in the abnormal discharge with large cathode falls of potential than in the normal discharge. In addition to the ionization it produces in the dark space, the radiation, when it strikes against the cathode, will, by the photoelectric effect, produce emission of electrons.

XLVI. *The Calibration of an Orifice.* *By* H. W. Swift, *M.A., D.Sc.**

IN two earlier papers the author has attempted to place upon a rational basis certain of the more important factors which produce systematic changes in the coefficient of discharge from an orifice. This work had for its ultimate object to determine how far the marked differences in published experimental results could be explained and systematised, and to what extent the orifice could be established as a reliable and consistent, as well as sensitive, meter for fluid discharge under varying conditions. In the present paper it is proposed to consider certain other of the factors which determine the coefficient of discharge, to apply the theories put forward in an examination of the discrepancies in earlier published results, and, in the light of these considerations, to suggest methods for the calibration of an orifice in order to ensure a satisfactory registration under the various conditions of service.

The volumetric rate of flow through an orifice is commonly expressed in the form $Q = C_d . a_0 \sqrt{2gH}$, where a_0 is the area of the orifice and C_d the coefficient of discharge. When conditions are such that the fluid in approach is sensibly at rest except in the immediate neighbourhood of the orifice, this expression is satisfactory, but in the more general case, when the velocity of approach is considerable, it seems better to adopt as a basis of comparison the flow

* Communicated by the Author.

of a " perfect " fluid (inviscid and incompressible) through an orifice mounted with similar conditions of approach to that under consideration and of the same size, but shaped so as to give no contraction of the jet. The quantity with which comparison is made is then $a\sqrt{2g\mathrm{H}}$, where

$$a=\frac{\mathrm{A}a_0}{\sqrt{\mathrm{A}^2-a_0^2}},$$

A being the area of the approach chamber, a_0 that of the orifice, and H the head of the fluid. Incidentally this generalized definition, which of course reduces to the common form when approach is unrestricted, accords with that accepted for the venturimeter, and has a certain empirical justification which will appear later. In general, therefore, we shall write

$$\mathrm{Q}=\mathrm{C}_d\,.\,a\sqrt{2g\mathrm{H}}=\mathrm{C}_d\,.\,a\sqrt{\frac{2\,.\,\Delta p}{\rho}},$$

where ρ is the density of the fluid approaching the orifice.

The coefficient of discharge is itself regarded as the product of the coefficient of velocity C_v, the coefficient of contraction C_c, and, in the case of compressible fluids, the attenuation factor C_a. The coefficients of velocity and contraction are well-established terms; the attenuation factor is introduced to allow for the fact that the volume of a compressible fluid, when measured at its initial density, is less than that of an incompressible liquid, owing to attenuation at reduced pressures.

The effect of the various factors controlling the value of the coefficient of discharge in the case of liquid flow has been considered in some detail in the papers referred to, and the mutual reactions of the coefficients of velocity and contraction are there discussed. Under the conditions of gaseous flow these factors will in most cases operate in a similar way, but there is an additional effect which must be taken into account—the effect of compressibility.

Compressibility.

The criterion which represents the effects of compressibility in orifice flow may most simply be written $\chi=\frac{r}{\gamma}$, where

r=ratio of pressure difference to initial pressure;
γ=ratio of specific heats.

In the case of a rounded orifice, or nozzle, the effect of compressibility is simple. Owing to the adiabatic expansion of the fluid during its passage through the orifice, the actual weight discharged is less than that calculated on the basis of the initial density, and may be determined * from this calculated quantity by the use of the "attenuation factor"

$$C_a = \frac{1}{r}\cdot\frac{\gamma}{\gamma-1}\cdot R^{2/\gamma}\left(1-R^{\frac{\gamma-1}{\gamma}}\right)\cdot\frac{n^2-1}{n-R^{2/\gamma}},$$

where $$R=\frac{p_2}{p_1}=1-r,$$

$$n=\frac{A}{a_0}.$$

When, as is commonly the case in the metering of steam and gases, the ratio r is small ($r=0{\cdot}1$ for atmospheric air corresponds to a water-gauge of over 40 inches), this factor, which for an inviscid fluid is the same as the coefficient of discharge, reduces to

$$C_a=\left(1-\frac{3}{4}\frac{r}{\gamma}\right)\sqrt{\frac{n^2-1}{n^2-R^{2/\gamma}}},$$

and when the orifice is small compared with the approach chamber or pipe,

$$C_a=1-\frac{3}{4}\frac{r}{\gamma}\text{ nearly.}$$

In the flow through an orifice where contraction of the jet occurs there will be introduced a secondary effect of elasticity—a reaction upon the area of the contracted jet. Comparing the conditions of effiux with those of an incompressible fluid, there will be a tendency, owing to the greater density of the fluid at the orifice section compared with that at the vena contracta, for the acceleration of the fluid to be less rapid when first passing the plane of the orifice and more rapid on approaching the vena contracta. Hence the curvature of this more slowly-moving fluid under the existing pressure across the streamlines will become sharper, and a larger jet will result.

As in the case of viscosity, therefore, we have in general two contrary effects of elasticity—a reduction in discharge due to attenuation, and an increase of the area of the

* Based on St. Venant's formula (*Comptes Rendus*, 1839).

contracted jet. As a rule, in practice, these effects will both be small, and can be treated by a simple approximation.

Since orifices for the measurement of gaseous flow are commonly mounted in a pipe or duct, it will be well to use the generalized definition of the coefficient of discharge:

$$Q=C_d \cdot a\sqrt{\frac{2\Delta p}{\rho}}, \quad \text{where} \quad a=\frac{Aa_0}{\sqrt{A^2-a_0^2}}.$$

If we neglect the effects of viscosity, we may also write

$$Q=C_a \cdot a'\sqrt{\frac{2\Delta p}{\rho}}, \quad \text{where} \quad a'=\frac{Aa_c}{\sqrt{A^2-a_c^2}}.$$

Hence $$C_d=C_c \cdot \frac{a'}{a}=\left(1-\frac{3}{4}\frac{r}{\gamma}\right)\sqrt{\frac{n^2-1}{n_c^2-R^{2\gamma}}} \text{ nearly,}$$

where $$n_c=\frac{A}{a_c}.$$

When $R=1$, compressibility has no effect, so that the theoretical coefficient $C=\frac{n^2-1}{n_1^2-1}$, n_1 being the value of n_c under ideal conditions, *i. e.*, when discharging an inviscid liquid. Hence, when r is small, the coefficient of discharge for an elastic fluid is given by

$$\frac{C_d}{C_0}=\left(1-\frac{3}{4}\frac{r}{\gamma}\right)\sqrt{\frac{n_1^3-1}{n_c^2-R^{2\gamma}}},$$

and, when n is large,

$$\frac{C_d}{C_0}=\left(1-\frac{3}{4}\frac{r}{\gamma}\right)\frac{a_c}{a_1},$$

where a_1 corresponds to n_1.

From a series of experiments the value of C_0 and the relation of C_d to r can be found, and the relation between a_c and a_1 deduced. The most complete and satisfactory experiments on gaseous discharge have been made by Hodgson *. Accepting his results for the discharge of air through a sharp-edged orifice, we find that,

when $n=5{\cdot}6$,

$$\frac{a_c}{a_1}=1+0{\cdot}41r \text{ up to a value of } r=0{\cdot}4,$$

and, when $n=1{\cdot}4$,

$$\frac{a_c}{a_1}=1+0{\cdot}42r \text{ over the same range.}$$

* Inst. C. E., Sel. Paper No. 31 (1925).

Hence, when viscosity is neglected, we are in a position to express the coefficient in the form

$$C_v = C_0\left(1 + 0{\cdot}585\frac{r}{\gamma}\right)$$

$$C_d = C_a \,.\, C_c = C_0\left(1 - \frac{1}{6}\frac{r}{\gamma}\right) \text{ very nearly.}$$

This factor may be applied with confidence to sharp orifices for values of r less than 0·2 and of n greater than 2, which covers generally the range of practical metering.

Returning now to a consideration of the joint effects of the various modifying factors, we find that for general purposes these are four in number, and may be denoted by the dimensionless criteria ξ for capillarity, η for viscosity, τ for turbulence, and χ for compressibility. The number of these factors in itself tends to complicate the problem of predicting the coefficient of discharge under assumed conditions, and this complication is further increased by the fact that they have each an effect upon, and are each affected by, the coefficient of contraction, and are therefore, to some extent, mutually reactive. Fortunately, however, the effect of each of these factors in ordinary metering practice is usually small; they are never all operative at the same time, and in those comparatively rare cases where one (either viscosity or elasticity) is important the rest, as a rule, are quite negligible.

When the effects are small, the size of the contracted jet is altered so slightly by each that the corrections due to the various component factors may be treated separately, and superposed with safety. Under such conditions a fairly simple expression can be found to cover changes in the coefficient:

$$C_d = C_0 - \kappa_1\xi + \kappa_2\eta + \kappa_3\tau - \kappa_4\chi,$$

where C_0 is the theoretical coefficient of discharge for an inviscid liquid, and ξ, η, τ, χ are the dimensionless criteria incorporating the effects of capillarity, viscosity, turbulence, and elasticity. κ_1, κ_2, κ_3, κ_4 are dimensionless constants sensibly independent of these criteria, but not independent of the value of C_0.

This simple form of expression has been based on a rational treatment of the conditions of flow, and confirmed, as far as possible, by experimental tests with circular orifices. For orifices of other shapes there are no tests

available from which the effect of factors other than viscosity can be checked; but since the controlling conditions are similar, and since the results of Bovey* and Hamilton Smith† may be shown to confirm for rectangular orifices of various proportions the linear increase of the coefficient with the viscosity criterion, it is reasonable to expect that the other results are similarly applicable in a descriptive way, with a reservation in the not important case of surface tension.

A consideration of the expression from the practical point of view shows that the terms are by no means of equal importance. The corrections for capillarity and for compressibility, when these are effective, are for practical purposes quite small, and, for circular orifices at least, may be computed with sufficient accuracy without special calibration. Turbulence introduces an element of inconstancy into the flow, and it is therefore necessary, for reliable registration, to take precautions to reduce its effects to a minimum. Where this cannot be done, the consistency will necessarily suffer. It would therefore seem that in the calibration of an orifice attention is mainly centred on the basic value of the coefficient C_0 and on the viscosity term $\kappa_2\eta$, which is always operative, and in liquid flow generally predominant.

It is now important to consider the theoretical value C_0 of the coefficient. This will depend upon two distinct circumstances—the form of orifice and the geometry of approach.

Form of Orifice.

Assuming unrestricted approach to an orifice in a plane wall as the standard condition, the value of C_0 is likely to be affected by the shape of the orifice both in and normal to this plane. There is no *a priori* reason why the coefficient should be the same for rectangular and circular orifices for example, and it is well known that a rounded orifice has a coefficient which may approach unity.

a. *Effect of Rounding.*

The theoretical treatment ‡ of the sharp slit orifice with

* 'Hydraulics,' p. 24.
† 'Hydraulics,' Chaps. III., XI.
‡ Kirchhoff, Crelle, lxx. (1869).

unrestricted approach shows that the free streamline is determined by the equations

$$x = 1 - \cos\theta \quad . \quad . \quad . \quad . \quad . \quad . \quad . \quad . \quad . \quad . \quad (\text{i.})$$

$$y = \sin\theta - \log\tan\left(\frac{\pi}{4} + \frac{\theta}{2}\right), \quad . \quad . \quad . \quad (\text{ii.})$$

when axes are taken as in fig. 1, and gives a value

$$\frac{\pi}{\pi+2} = 0{\cdot}611$$

for the coefficient of contraction. The development of

Fig. 1.

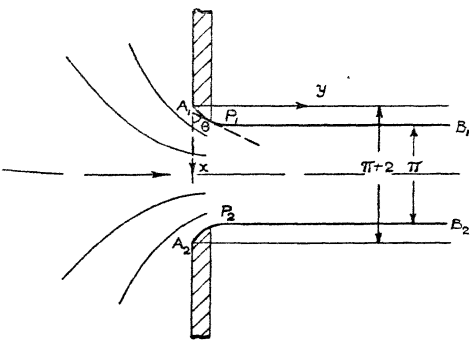

the theory leading to these results is such as to allow an identical configuration of efflux if the sharp orifice of width $\pi+2$ be fitted with a mouthpiece conforming to and following the surface of the escaping jet to any extent whatever. Hence the known equations of the free streamlines afford a theoretical value for the coefficient of contraction for such an orifice, provided only its shaping is consistent with the form of jet. For an orifice rounded in this way to the angle θ the ideal coefficient is given by

$$C_0 = \frac{B_1B_2}{P_1P_2} = \frac{\pi}{\pi+2\cos\theta}.$$

It appears, therefore, that rounding is always likely to increase the coefficient of contraction.

When the value of C_0 is correlated with the corresponding value of y from (ii.) we obtain some idea of the effect of

slight rounding. For a half-inch slit orifice corresponding values are

y.	x.	θ.	$\frac{C-C_0}{C_0}$.
·00017	·0015	10°	·0059
·00058	·0033	15°	·0132

A rounding of half a mil may therefore be sufficient to increase the coefficient of discharge by 1 per cent. This analysis is, of course, not applicable to forms of orifice other than the slit, but there are good reasons to expect that the general nature of the results will not be dissimilar, and the example cited will suffice to emphasize at once the importance and difficulty of obtaining true sharpness in such orifices. In one instance it is recorded * that a "hardly perceptible" rounding of the edge was sufficient to cause an increase of 20 per cent. in the delivery from a circular orifice, and it is probable that in the case of smaller orifices this is the largest systematic cause of disagreement in published results, and accounts for the serious discrepancies between the evidently careful work of such experimenters as Hamilton Smith, Unwin, Lesbros and others. For this reason, also, it would seem that theoretical values for the coefficient of discharge are not likely to have any great practical value for the engineer, who must in general rely on the experimental calibration of each individual orifice.

With an orifice which is "perfectly rounded" into the form of a nozzle (*e.g.*, a venturimeter) there occurs no contraction of the jet at all, and the value of C_0 is unity. It is sometimes assumed that contraction is completely suppressed in any orifice shaped so as to form a "smooth curve" finally parallel to the direction of the jet, and that an arbitrary value of the coefficient of velocity then enables the discharge to be calculated with sufficient accuracy. This has no rational or empirical foundation, and may lead to considerable errors. It is possible, for instance, with an orifice shaped in a "smooth curve," and having an axial length three-quarters of its diameter, to obtain a contraction of 10 per cent. in the jet. Moreover, the amount of this contraction is found to depend upon the exact

* Mair, Proc. Inst. C.E. lxxxiv. p. 428.

shaping of the orifice, and no simple relation between the value of C_0 and the axial length of the nozzle can safely be applied.

b. *Shape of Orifice.*

For the perfect slit orifice the value of C_0 as afforded by theory is ·611. In the absence of theoretical solutions for orifices of other shapes we shall have recourse to experimental results in forming an estimate of the corresponding values. In so doing it will be necessary to exercise some care in the acceptance of individual figures, for there are known to be marked discrepancies between published results, and the coefficients obtained empirically for other shapes have not been very different from those for slit orifices.

Apart from the accidental errors which are associated with hydraulic experiments in general, there are certain special errors of a more or less systematic nature which are peculiar to experiments in orifice flow. Of these the most fruitful source with smaller sizes is imperfect sharpness of the edge of the orifice. Differences in sharpness will introduce systematic errors which, in experiments with a single orifice, will be constant, tending to increase the coefficient of discharge, but not likely to affect the consistency of the results or the general law of systematic changes. With larger orifices and greater heads a more serious source of error is turbulence in approach. This again tends to increase the discharge from a sharp-edged orifice, but its effect is not constant, and it is liable to mask systematic changes. The size and shape of the approach chamber are effective factors in some tests with large orifices, and although an arbitrary correction has usually been applied, the results are of uncertain value. The tendency of any restriction in approach is, of course, to increase the apparent coefficient of discharge. The last common source of error to which attention is drawn is the method adopted for measuring the discharge; for many years the sharp-edged rectangular notch was in almost general use for this purpose. Apart from the fact that the formula used is now known to be merely an approximation applicable over a limited range, the notch itself is intrinsically less sensitive than the orifice as a means of measurement, and is therefore unsuited as a standard for its calibration.

Such errors as these, where the range of coefficients is so small—0·60 to 0·65 as a rule—make it difficult to interpret and reconcile the results of different workers, particularly in cases, not unfrequent, where the conditions of experiment are unrecorded. Further, it will be noted that these errors are mainly systematic, and tend to give high values for the coefficient, so that their effects cannot be eliminated by statistical methods.

Fig. 2.

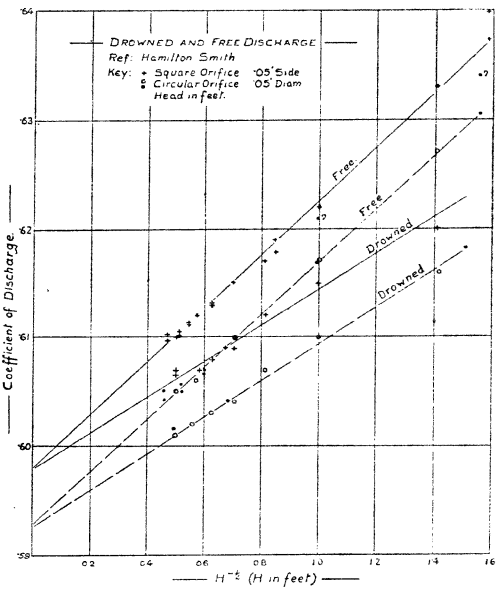

In interpreting the results of experiments we shall assume that in experiments with water the form of the law governing variations in the coefficient C_d with the head is not affected by the shape of the orifice, so that

$$C_d = C_0 + \kappa H^{-\frac{1}{2}}.$$

This assumption finds support in the results of Hamilton Smith and Bovey, under apparently satisfactory conditions, with the various shapes of orifice referred to in figs. 2

and 3. The limit C_0 determined by extrapolation from such results is the value with which we are concerned.

Recorded experiments with orifices approaching the slit form are rare. The experiments of Poncelet and Lesbros* were made with rectangular orifices of rather large size compared with the dimensions of the approach

Fig. 3 *a*.

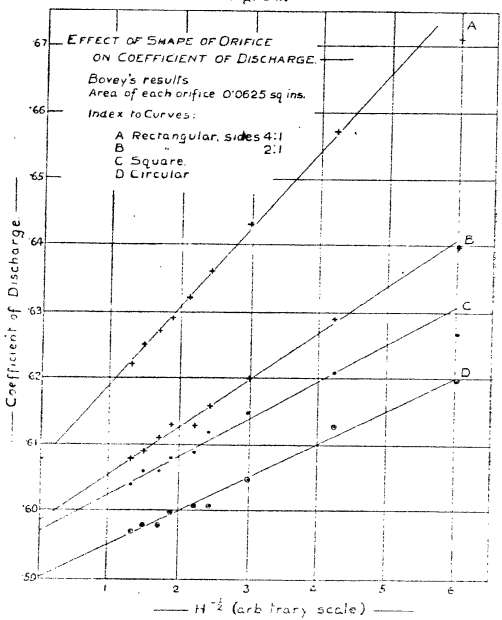

chamber, and since these orifices were in a vertical plane under low heads the value of the results for present purposes can only be regarded as qualitative. Bazin † made determinations with rectangular orifices fitted with side-cheeks to suppress end contraction, but employed a weir as standard of calibration, and did not obtain results sufficiently consistent for comparison. Hamilton Smith and Bovey

* Mem. Acad. Sci. iii. (1832); xiii. (1851).
† Mem. Acad. Sci. xxxii., tr. Trautwine, 1896.

used orifices of different shapes and proportions, and their results (figs. 2, 3) in the case of long, narrow, rectangular slits are seen to be consistent with anticipated variations, and to tend towards a limit which is in reasonable accord with Kirchhoff's ideal value of ·61. It is also worthy of note that for such an orifice no accredited value of the coefficient lower than this figure has been published.

Fig. 3 *b*.

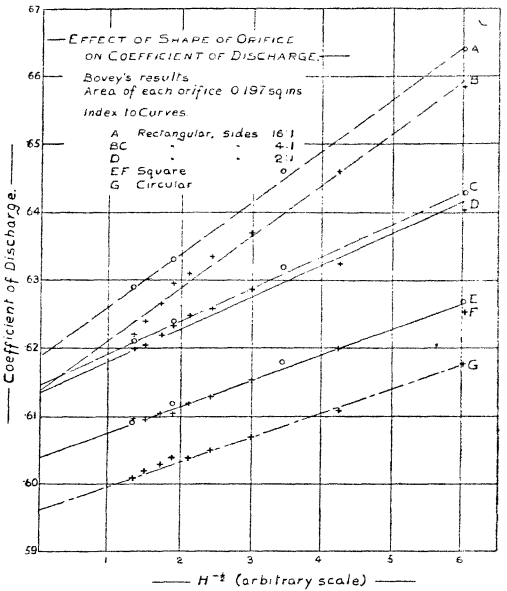

In the case of rectangular orifices of ordinary proportions, however, there is no general agreement with Kirchhoff's value, and there appears to be sufficient evidence that the theoretical coefficient of discharge is not independent of the shape. The closest practical approximation to the two-dimensional slit is found in the rectangular orifice with side-cheeks, and it is well established (Bidone, 1826; Bazin, 1890) that suppression of the end-contractions

increases the discharge. The analogous result is, of course, well known in the case of rectangular notches and weirs. Moreover, whereas coefficients lower than ·61 have not been recorded with orifices approaching to the slit, such lower values have been quite common with those more nearly square, and a coefficient as low as ·598 has been obtained with a large square orifice. In figs. 2 and 3 are plotted results obtained by Hamilton Smith and by Bovey and these afford rather striking evidence that the theoretical coefficient continually decreases as the orifice approaches

Fig. 4.

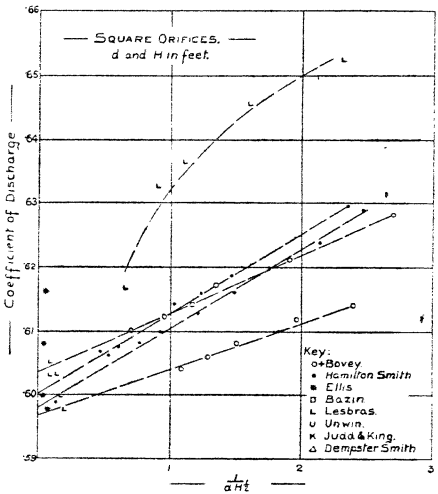

the square form from the slit, and suggest that its value for a square orifice should be about ·60. The results deduced by Fanning * for a series of orifices each one foot wide give qualitative support to this conclusion, and the determinations for square orifices from other sources, shown in fig. 4, when account is taken of the general tendency of systematic errors to give high results, show general agreement with a limiting value of ·60, or slightly less.

* 'Water Power Engineering' (1887).

For circular orifices a similar comparison of results indicates that the ideal coefficient is again different, and the value suggested by the numerous determinations shown in fig. 5 is close to ·59. It is interesting to note that this same limit is also indicated by the experiments of Watson and Schofield * with air through circular orifices.

It seems therefore reasonable to conclude that the value of C_0 for an ordinary " sharp " orifice with restricted approach will depend upon its shape, and will not be less than ·61 for

Fig. 5.

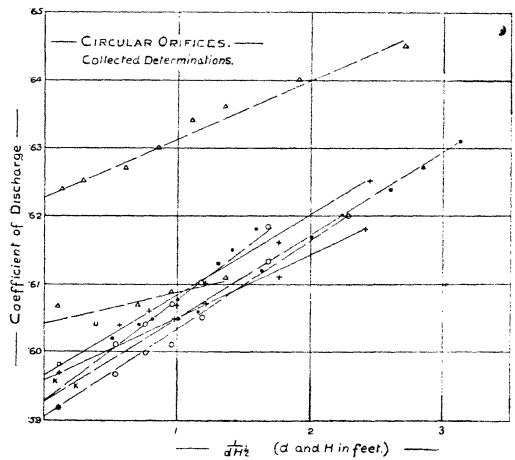

a slit, ·60 for a square, or ·59 for a circular orifice, its agreement with these values depending on its actual sharpness, and tending to improve as the size of orifice increases.

The values of C_0 derived by extrapolation from the results obtained by the author with orifices of various diameters up to one inch, shown in Table I., are reasonably consistent with this conclusion.

* Proc. I. Mech. E., May 1912.

TABLE I.

"Theoretical" Coefficient of Discharge, C_0.
Extrapolated from experimental results.

Orifice diameter, inches.	Value of C_0.
0·095	·617
0·302	·612
0·480	·603
0·499	·597
0·602	·593
0·701	·600
0·801	·594
0·907	·597
1·007	·594

Geometry of Approach.

Accepting as basis of comparison the coefficient C_0 for unrestricted approach, the geometry of the approach chamber will be likely to affect the discharge by

(*a*) reducing the depth normal to the plane of the orifice;

(*b*) restricting lateral approach.

For the slit orifice the effect of these factors is known.

(*a*) The dimension of the approach chamber normal to the plane of the orifice modifies the contraction according to the relation *

$$\frac{1}{C}=1+\frac{1}{\pi}\left(k_0+\frac{1}{k_0}\right)\log\frac{1+k_0}{1-k_0},$$

where $k_0=C\frac{a}{b_1}$, in fig. 6 *a*.

For small values of k_0 this shows that a reduction of depth will cause a decrease in the discharge by an amount given approximately by

$$C=C_0-0\cdot12k_1^2 \quad \text{when} \quad C_0=0\cdot61,$$

k_1 being the value of $\frac{a}{b_1}$.

* Math. Trip. ii. (1900).

(*b*) Restriction of lateral approach to a slit tends to increase the area of the contracted jet*, so that

$$\frac{1}{C} = 1 + \frac{2}{\pi}\left(\frac{1}{k_0'} - k_0'\right)\tan^{-1}k_0',$$

where $k_0' = C_0 \frac{a}{b_2}$, in fig. 6 *b*,

and for small values of k_0', when $C_0 = 0{\cdot}61$,

$$C = C_0 + 0{\cdot}12k_2^2, \quad \text{where} \quad k_2 = \frac{a}{b_2}.$$

Fig. 6 *a*.

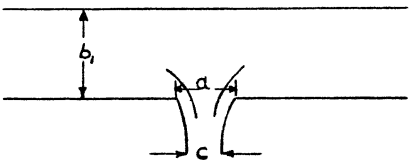

Fig. 6 *b*.

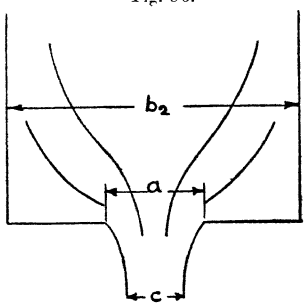

Effect of Restricted Approach.

It is not easy to point the analogies for a circular orifice, but there seems to be no physical reason why the general nature of the effects should be different. Experiment has shown that a reduction in depth of water over a horizontal orifice beyond a certain point does, in fact, tend to diminish the coefficient of discharge, but this fact has little practical significance. A matter of considerable

* L. H. Michell, Phil. Trans. p. 405 (1890).

importance, however, bearing on the registration of orifices in pipe-lines, is the effect of lateral restriction in approach.

This effect has been the subject of experimental investigation by several workers with water, steam, and air. In fig. 7 are plotted values of the coefficient of discharge for various ratios of pipe to orifice diameter, calculated on the basis defined on p. 410 from experiments by Müller *, Gaskell †, and Hodgson ‡. Müller's results were obtained with air, the others with water; Gaskell's refer to 8-inch and 6-inch pipes; Hodgson's to pipes $\frac{3}{4}$ inch diameter and less. Results given by Weisbach § have had to be rejected on account of uncertainty as to the basis on which his coefficients are calculated.

Fig. 7.

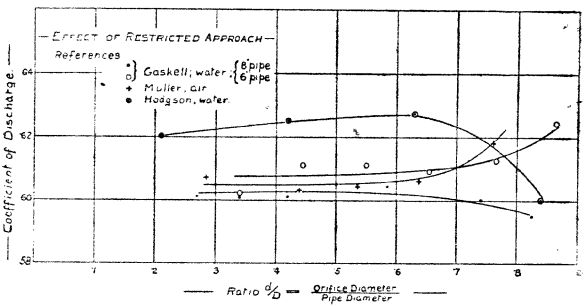

When due allowance has been made for the difficulties of experiment, the results plotted in fig. 7 give no evidence of any systematic change in the value of C_0 for values of $\frac{d}{D}$ less than about 0·7. Over this extensive range it would appear that, at any rate for purposes of commercial metering, the coefficient of discharge may be regarded as unaffected by restriction in approach, and this fact may be held to justify the basis on which the coefficient was defined. It is well to note that this constancy is confined to values of the coefficient C_0. When viscosity has an

* *Z. V. D. I.* lii. p. 285.
† Proc. Inst. C. E. cciv. p. 11.
‡ Proc Inst. C. E. excvii. p. 243.
§ 'Mechanics of Engineering,' p. 825 (tr. 1877).

important effect, the results of Hodgson show that the coefficient is by no means independent of the pipe to orifice ratio.

For values of $\frac{d}{D}$ greater than about 0·7 the tests quoted give divergent results; two give evidence of a rising coefficient, two a falling one, and there is more than a suggestion of increasing uncertainty in the coefficient. This uncertainty is not unexpected; the larger the orifice in a pipe of given diameter, the less the dead-water space on both sides of the diaphragm, the more unstable the conditions in this space and the greater the care required in locating the pressure-tube connexions. It would appear, in fact, that over this range the value of the coefficient is more affected by the exact setting of the diaphragm and arrangement of the pressure tubes than by changes in the ratio $\frac{d}{D}$, and that reliable registration can only be achieved after a careful calibration in which the most exact conditions of operation are reproduced. It is none the less a curious fact that the increase in the value of the coefficient with lateral restriction, which would occur with a slit orifice, should not be more certainly evident in experiments with the circular form.

Methods of Calibration.

Discussion of the various factors controlling orifice flow has led to the conclusion that the value of the coefficient of discharge under any given set of conditions depends upon a basic value C_0 and upon variations due to the physical properties of the fluid in use and to certain conditions of flow. It has been demonstrated that neither by improvement in theory nor by the accumulation of empirical results will it be possible in general to predict with certainty the value of the coefficient for an orifice without individual calibration by experiment. At the same time analysis of the effective factors has indicated the conditions which should be fulfilled in this calibration, and the simplest methods which will cover the required range of flow. These conditions and methods must clearly depend on circumstances.

So far as the constructional factors are concerned, these limit themselves in the case of any one orifice to the

conditions of approach and discharge, and the only satisfactory method of treatment is to ensure that the conditions under which calibration is made shall reproduce in effect the conditions under which the orifice will be required to operate in practice. The care with which these conditions should be reproduced is a matter for consideration in each case, having regard to the results discussed on page 425. It is hardly necessary to point out that an orifice to be employed under conditions of submerged discharge (*e. g.*, in the metering of gases or of pipe-flow) must be calibrated in the same way, and it is clearly important, for the sake of consistency, to reduce the effects of turbulence and pulsation as far as possible both in operation and calibration.

Variations in the coefficient of discharge arising from changes in the hydraulic conditions of flow can generally be covered satisfactorily by a suitable method of calibration. The choice of this calibration will be largely determined by the type of fluid with which the orifice is to be employed.

a. *Limpid Liquids.*

In the flow of any liquid through an orifice elasticity will, for practical purposes, be ineffective. Under the conditions of submerged discharge surface tension will also be inoperative, so that, in the absence of turbulence, viscosity is the only hydraulic factor which demands attention, and for limpid liquids the value of the coefficient of discharge C_d will follow closely the relation

$$C_d = C_0 + \kappa\eta.$$

For any single orifice the practical law of calibration may therefore be written

$$Q = C_0 a_0 \sqrt{2g}H + c\nu,$$

where $C_0 a_0$ and c are characteristic of the individual orifice. A comparison of published results, notably those of Hamilton Smith, Bovey, and the author, shows that in the common case of the free discharge of cold water through a sharp circular orifice the empirical formula which best agrees with experiment is

$$C_d = C_0 + \frac{\cdot 036}{d\sqrt{H}},$$

where d and H are measured in inches; but this figure is

a mean of rather a wide range of values, and cannot be relied upon for the calibration of any particular orifice. However, the value of the constant C_0a_0 has to be determined experimentally in any case, and only one further test is necessary to determine the other constant c. Thereafter the discharge under any other conditions may be computed from the differential pressure when the kinematic viscosity ν is known. This computation is a simple one, since the form of the expression given above shows that the effect of viscosity is virtually to increase the "theoretical" discharge by an amount which is proportional to the viscosity and independent of the rate of flow. This expression is clearly suited to cases in which the viscosity of the liquid in use is subject to variations, or where the liquid used in calibration is different from that to which the orifice is to be applied. An orifice for use with petrol or with an acid might, for example, be calibrated with water for convenience.

It frequently happens that the viscosity of a liquid flowing through an orifice maintains a reasonably constant value, and under these conditions the law of calibration assumes the still simpler form

$$Q = C_0a_0\sqrt{2gH} + q,$$

where q is characteristic of the orifice and liquid and independent of the rate of flow. Calibration at two different heads is still necessary to determine C_0a_0 and q, but the subsequent computation—consisting in the addition of the same small constant q to each "theoretical" discharge—is remarkably simple.

In the free discharge of a liquid to the atmosphere, surface tension also demands attention, and its effect may be estimated by means of the relation given in an earlier paper*. In those rare cases when the correction is considerable an additional test will be necessary in calibration in order to evaluate the three constants, q, C_0a_0, h_s in the relation

$$Q - q = C_0a_0\sqrt{2g(H - h_s)}$$

for a liquid where surface tension and viscosity remain sensibly constant. In computing subsequently the discharge corresponding to any observed head this head will first be

* Phil. Mag. p. 853, Oct. 1926.

"corrected" for surface tension by subtracting the constant h_s. From the head so corrected the "theoretical" discharge will be calculated, and this discharge corrected in turn for the effects of viscosity by adding the constant quantity q.

Although these corrections are simple in themselves, it is somewhat troublesome, from the practical point of view, to determine and apply them, particularly in the case of a sharp-edged orifice, for which the calibration is liable to become altered considerably by wear or contamination. The sharp-edged form of orifice is therefore at some disadvantage in the metering of liquids. On the other hand, a nozzle which entirely suppresses the contraction, and is not so liable to wear, is not so convenient to install and replace,

Fig. 8.

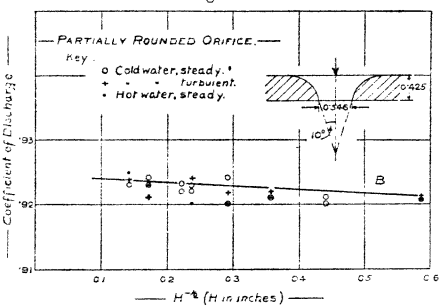

and is itself subject to some changes in coefficient at different rates of flow, the sign of q in the expression above in this case being negative. The most convenient form of orifice for practical metering when an accurate and permanent calibration is desired would appear to be one for which the value of q (or κ) vanishes; where, in fact, the suppression of contraction exactly balances the diminution in the velocity of discharge as the criterion varies. An orifice of this form should give a coefficient of discharge sensibly constant in value over a fair range of heads and viscosities for limpid liquids.

An attempt has been made by the author to produce an orifice of this kind, and, after several trials, the form shown in fig. 8 was constructed. When mounted in the base

of a large approach vessel, and discharging to the atmosphere, this orifice gave the results shown in fig. 8 and Table II. From this table it will be seen that the coefficient

TABLE II.

Special Rounded Orifice.

Diameter 0·546 inch.

A. Time for head to fall from 55 inches to 5 inches in tank about 2 ft. 6 in. diameter.

Conditions.	Temperature, ° C.	Time, seconds.
Quiescent	14	1149·8 1150·1
Turbulent	14	1150·2 1150·5
Quiescent	63	1151·4 1151·0

B. Determinations at constant heads.

Head, inches.	Value of C_d.
21·1	·923 ·922
5·15	·921 ·920

of discharge with water is practically independent not only of changes in head from 6 inches to 5 feet, but also of changes in viscosity due to temperature variations from 10° to 60° C. Furthermore, this orifice possesses another valuable characteristic from the practical point of view—its coefficient is practically unaffected by turbulence in approach. If, therefore, orifices of this form could be constructed without difficulty they would appear to be invaluable for metering purposes. Unfortunately, in the course of the trials which led eventually to this form it became clear that, even with rounded orifices, the details of curvature and construction exercise a considerable influence on the coefficient, so that special care would be required in the reproduction of orifices of other sizes.

Moreover, the form of orifice which gives this constancy of coefficient under conditions of free contraction does not do so when contraction is partially suppressed, as in a pipe, and a special shape would be necessary for each ratio of orifice to pipe-diameter. Once the labour of initial testing had been carried out, however, there seems to be no reason why a "constant coefficient" form of orifice should not be produced with suitable templates for conditions of either free or suppressed contraction.

b. *Viscous Liquids.*

The methods of calibration detailed above apply only to the range of flow over which the coefficients of velocity and contraction change in an approximately linear way with the value of the criterion η. This is true only for low values of this criterion such as are encountered in the flow of water and other liquids of low viscosity. As the value of the criterion η increases beyond this range, neither the coefficient of velocity nor (where effective) the coefficient of contraction follows such a simple law, and satisfactory calibration of a sharp-edged orifice under these conditions is a tedious matter. Furthermore, the actual curve connecting the coefficient of discharge with values of η has been found, at any rate for discharge to atmosphere, to be not independent of the liquid in use, so that changes in viscosity are liable to invalidate a calibration curve. On the other hand, the coefficient of velocity over the whole range of flow appears to follow fairly simple and systematic variations, and it would seem, therefore, that the most satisfactory course to follow in practice over the non-limpid range is to ensure that the shaping of the orifice is such as to suppress contraction, and so to confine consideration to changes in the coefficient of velocity. The extent to which an orifice would need rounding to satisfy this condition depends upon the liquid and size of orifice. For high values of η, contraction, even with a sharp-edged orifice, is practically entirely suppressed, and the more viscous the liquid and the smaller the orifice and rate of flow the less the amount of rounding required for the purpose. Assuming that this condition is fulfilled, the calibration is not difficult.

For a liquid of given viscosity the loss of head incurred during discharge from an orifice is proportional to the

velocity at the vena contracta. This fundamental assumption has been justified in the case of limpid flow, and fig. 9 furnishes experimental confirmation for very viscous flow where contraction is almost or entirely absent. It follows, by dimensional reasoning, that the loss of head may then be expressed as $H_{\iota}=c\eta\frac{V^2}{2g}$, and the velocity of discharge is related to the head according to the expression

$$H=\frac{V^2}{2g}+\frac{cv}{2gd}.V.$$

Fig. 9.

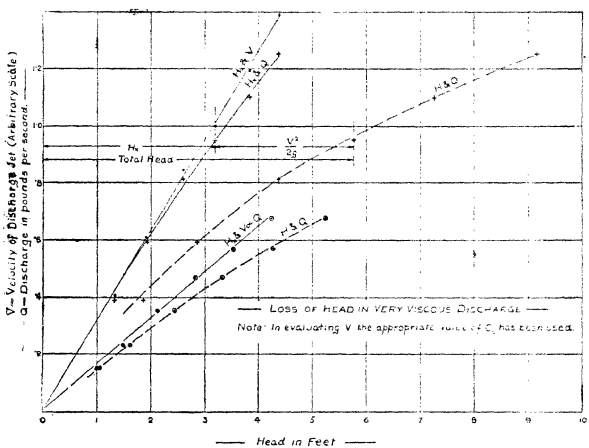

When contraction of the jet is entirely suppressed, the law of calibration is, therefore,

$$H=\frac{Q^2}{2ga_0^2}+bvQ,$$

where b is a dimensional quantity characteristic of and constant for any individual orifice. For a series of similar orifices the value of b should vary inversely with the diameter, and when there is no contraction of the jet this

relation is not likely to be very sensitive to small differences in workmanship. In fig. 10 are plotted values of b deduced from experiments with orifices from 0·48 to 1·0 inch diameter which confirm this relation, and thereby the reasoning on which it is based.

The calibration of an orifice under these conditions consists merely in the measurement of its area a_0 and in the determination of the constant b (or $b\nu$ if viscosity is invariable) by a single test which may best be made with a

Fig. 10.

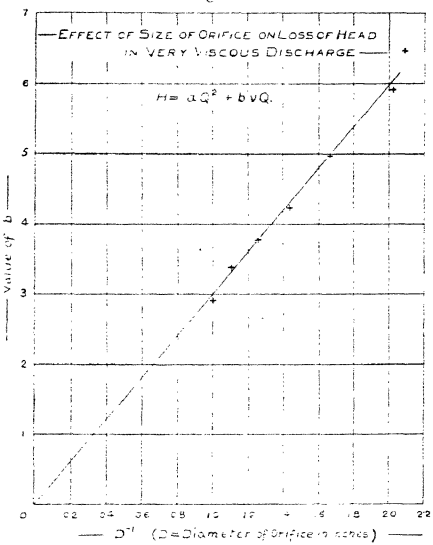

viscous liquid under a low head. Subsequently each computation of discharge corresponding to an observed value of the head would involve the solution of a quadratic equation in Q, but this may be avoided by the use of a simple calibration chart.

In applying this, or indeed any, method of calibration to an orifice for use with viscous liquids, it is important to realize that the more viscous the liquid the more sensitive

will the registration be to changes in viscosity, and as a rule, in practice, the viscosity of thick liquids is itself very sensitive to changes in temperature. Under such conditions, therefore, the accuracy of registration of an orifice or similar meter is limited not so much by errors of calibration as by uncertainty of the effective viscosity. A rise in temperature of 5° C., for example, might increase the coefficient of discharge for a thick oil by 50 per cent., and yet not affect the flow of water by ·2 per cent.

c. *Gases and Vapours.*

In gaseous discharge through an orifice, viscosity and elasticity are both effective, and the coefficient of discharge for conditions under which each effect is small is given by

$$C_d = C_0 + \alpha\eta - \beta\frac{r}{\gamma}$$

with the notation already adopted, and the flow may be expressed in the form

$$Q = q + C_0 a_0 \sqrt{2gH}\left(1 - c\frac{r}{\gamma}\right),$$

where q represents the effect of viscosity, as in the case of liquid flow, and the factor $\left(1 - c\frac{r}{\gamma}\right)$ represents the effect of compressibility.

In this case a complete calibration would involve three separate tests to determine q, $C_0 a_0$, and c, and the subsequent computation of Q would be made by correcting Ca, in the first place, for compressibility, and later adding to the calculated discharge the constant q for viscosity correction. In calibration the constants q and $C_0 a_0$ could be determined for convenience by means of tests made with water, but the third test, to determine the elastic effect, could only be made with a gas. This fact adds considerably to the trouble of calibration, and if one test has to be made with a gas there is little to be gained by using water in the other two. Fortunately, however, the correction for compressibility is generally so small that an approximate general formula can be employed without the possibility of a serious error, and in many cases it will be found that the correction itself is negligible.

For a rounded orifice, or nozzle, the correction can be calculated with confidence, and under normal conditions of metering $c = \frac{3}{4}$. For air at or near atmospheric pressure

the corresponding correction is less than 1 per cent. so long as the pressure difference across the orifice does not exceed $7\frac{1}{2}$ inches of water-gauge, and for saturated steam at a pressure of 200 lb. per sq. inch the corresponding pressure difference is about 6 inches of mercury. With a sharp-edged orifice partial suppression of the contraction has the effect of reducing the resultant correction, so that $c=\frac{1}{8}$ approximately, and the error involved by neglecting compressibility altogether is less than 1 per cent. with air at atmospheric pressure so long as the water-gauge is less than 34 inches, and with steam at 200 lb. per sq. inch pressure so long as the pressure difference does not exceed $27\frac{1}{2}$ inches of mercury. The fact that the correction for compressibility is so much smaller with a sharp-edged orifice places it at some advantage over rounded forms for use with gases ; it is true that the viscosity correction will usually be greater, but this is determinable by tests with water. It would appear that as a rule, with either form, the calibration of an orifice for use with a gas or vapour can be carried out satisfactorily by means of water, and if any correction for compressibility is necessary the values of c quoted above will give results sufficiently accurate for all ordinary purposes.

In arranging the calibration by means of water it is well that the tests should cover generally the same range of values of η as will obtain when the orifice is in use. For any one orifice corresponding heads are given by the formula

$$\frac{H_1}{H_2}=\left(\frac{\nu_1}{\nu_2}\right)^2.$$

If, for example, the orifice is required for air under approximately atmospheric conditions, the head under which it should be calibrated to correspond to a water-gauge p is approximately $5p$, which will normally be a reasonable head, and enable simple arrangements to be made. Unfortunately, the viscosity of steam under the conditions which prevail in practice does not seem to have been evaluated experimentally, so that it is not possible to give with confidence the corresponding heads of water for an orifice to be employed as a steam-meter.

XLVII. *The Nature of the General Polarization Effect in Aromatic Molecules.* *By* W. A. WATERS, *M.A., Ph.D., Lecturer in Chemistry, University of Durham (Durham Division)* *.

IN the following communication an attempt is made to correlate reaction velocity measurements, obtained with aromatic compounds, with electrical dipole moments, with the object of elucidating further these intramolecular forces which seem to be characteristic of aromatic ring systems.

Bradfield and Jones (J. Chem. Soc. pp. 1008, 3073, 1928), utilizing the equation

$$k = PSZe^{\frac{-E}{RT}} \quad . \quad . \quad . \quad . \quad . \quad . \quad . \quad (1)$$

for representing the velocity of any substitution reaction, have shown that it is the energy of activation (E) of any aromatic molecule which is primarily altered by the presence of a substituent group, so that in consequence the equation

$$RT \,.\, \log (K_{subs.}/K_{unsubs.}) = E_{unsubs.} - E_{subs.} \quad . \quad . \quad (2)$$

may be used for comparing the reaction velocities of substituted with those of unsubstituted compounds.

This equation is closely allied to that previously given by Shoesmith and Slater (J. Chem. Soc. p. 216, 1926):—

$$\log K_{subs.} = \log K_{unsubs.} + g + a + s \quad . \quad . \quad . \quad (3)$$

where g, a, and s, are arbitrary factors representing the magnitudes of the general, alternating, and steric effects respectively of the substituent group.

Of these factors, that representing the steric effect can only be observed when the substituent group is in the ortho position to the point of attack, and even then may be exerted only under certain special circumstances (*cf.* Olivier, *Rec. trav. chim.* xlviii. p. 227, 1929). It may perhaps be identified more closely with the steric factor (S) of equation (1). The alternating polarity effect (*a*) in contrast can be observed most decidedly with both ortho and para substituent groups. As, however, it has been characterized as a tautomeric (electromeric) transformation (Chemical Society, Annual Reports, p. 140, 1926, p. 151, 1927) it may not be noticed to any great extent in the case of a *meta*

* Communicated by Prof. Irvine Masson, D.Sc.

substituent group, as this would not be in a position conjugated to the point of attack.

The general polar effect, however, is an *inductive disturbance* (Chemical Society, Annual Reports, *loc. cit.*) which will influence the rate of any reaction, whatever the position of the modifying substituent group within the molecule. This effect can be correlated with the possession by the modifying substituent group of a dipole moment.

For, if μ be the dipole moment of the substituent group $-R$, then the induced potential at any other point P within the molecule will be $\mu \cos\theta/r^2$, and in consequence any moveable electron (or ion) at the point P will require for activation an energy

$$E_{subs.} = E_{unsubs.} + k \cdot \mu \cos\theta/r^2 \quad . \quad . \quad . \quad (4)$$

(according to the vector sign of the dipole moment).

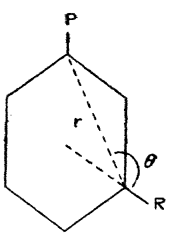

It follows that, for any fixed orientation relationship between P and $-R$, $\log\left(\frac{K_{subs.}}{K_{unsubs.}}\right) \propto \mu$, under conditions in which only the general polarization effect has an appreciable magnitude, whatever the nature of the substituent group $-R$. That the dipole moment has a magnitude approximately proportional to the change of energy of activation of aromatic molecules on substitution may be seen from the following typical tables of correlations of reaction velocity measurements with electrical dipole moments. Meta substituent groups have been examined in order to eliminate the alternating and steric influences as much as possible, following the hypothesis outlined above.

In considering the degree of correspondence between the functions $\log\frac{K_s}{K_u}$ and μ, it must be remembered not only that reaction velocity constants may be uncertain to a few

units per cent., but also that the recorded values of the dipole moments are at present of rather a tentative nature, especially with respect to groups with small dipole moments, as even the theoretical basis of the methods for their computations is still indeterminate (*cf.* Estermann, *Z. Physikal. Chem.* pp. 134–160, 1928 i.; Ebert, Eisenschitz, and von Hartel, *ibid.* pp. 94–114).

TABLE I.

Dissociation Constants of *m*— substituted Aromatic Acids at 25° C.

Substituent.	$K_{Ostwald}$.	$\log \frac{K_s}{K_u}$.	$\mu \times 10^{18}$ e.s.u.	$\frac{\log K_s/K_u}{\mu \times 10^{18}}$.
$-NO_2$	$3{\cdot}48 \times 10^{-4}$	+0·72	−3·75*	−0·21
−Cl	$1{\cdot}55 \times 10^{-4}$	+0·37	−1·58*	−0·24
−Br	$1{\cdot}45 \times 10^{-4}$	+0·32	−1·56*	−0·20
$-CH_3$	$5{\cdot}6 \times 10^{-5}$	−0·07	+0·43*	−0·17
$-COOCH_3$ ...	$1{\cdot}28 \times 10^{-4}$	+0·29	−1·8 °	−0·16
$-NH_2$	$1{\cdot}67 \times 10^{-5}$	−0·60	+1·6 °	−0·37
−COOH	$2{\cdot}9 \times 10^{-4}$	+0·64	?	(−0·36)
$-O{\cdot}COCH_3$ ..	$1{\cdot}31 \times 10^{-4}$	+0·30	?	(−0·16)

TABLE II.

Dissociation Constants of *m*— substituted Primary Aromatic Bases at 25° C.

Substituent.	$K_{Ostwald}$.	$\log \frac{K_s}{K_u}$.	$\mu \times 10^{18}$ e.s.u.	$\frac{\log K_s/K_u}{\mu \times 10^{18}}$.
$-NO_2$	$4{\cdot}1 \times 10^{-12}$	−2·05	−3·75*	+0·55
−Cl	$3{\cdot}45 \times 10^{-11}$	−1·12	−1·58*	+0·71
−Br	$3{\cdot}8 \times 10^{-11}$	−1·08	−1·56*	+0·69
$-COOCH_3$ ...	$4{\cdot}4 \times 10^{-11}$	−1·02	−1·8 °	+0·57
−COOH	$1{\cdot}2 \times 10^{-11}$	−1·58	?	(+0·88)
$-CH_3$	$5{\cdot}5 \times 10^{-10}$	−0·07	+0·43	−0·18

In the above tables the dissociation constants have been taken from Landolt-Börnstein's 'Tabellen.' The dipole moments marked * are taken from Höjendahl ('Nature,' cxvii. p. 892, 1926), and those marked ° from Estermann (*loc. cit.*). Where indicated by the query (?) no experimental measurement of the electrical dipole moment of the corresponding aromatic compound has yet been made,

but for the purposes of these computations it has been assumed provisionally that the dipole would be associated with the $=C=O$ group in each case, and that it would have the magnitude of about $1{\cdot}8 \times 10^{-18}$ e.s.u. as in the case of methyl benzoate.

A sign has been assigned to the dipole moment according to whether the electrical field produced at the point of reaction (P) corresponds with a positive or negative induced general polarity (I), following the standard nomenclature of Ingold (Chemical Society, Annual Reports, *loc. cit.*).

TABLE III.

Rate of Hydrolysis of *m*— substituted Benzyl Chlorides. (Olivier, *Rec. trav. chim.* xli. p. 646, 1922.)

Group.	$\mu \times 10^{18}$ e.s.u.	A..... 83° C.		B..... 30° C.	
		K_s/K_u.	$\frac{\log K_s/K_u}{\mu \times 10^{18}}$.	K_s/K_u.	$\frac{\log K_s/K_u}{\mu \times 10^{18}}$.
$-CH_3$	+0·43	1·39	+0·34	1·30	+0·27
$-Cl$	−1·58	0·237	+0·40	0·137	+0·55
$-Br$	−1·56	0·215	+0·43	0·132	+0·58
$-NO_2$	−3·75	0·09	+0·28	0·057	+0·33
$-COOH$ ...	?	0·235	(+0·35)	0·170	(+0·43)

TABLE IV.

Rate of Hydrolysis of *m*— substituted Benzyl Bromides. (From Shoesmith and Slater, J. Chem. Soc. p. 216, 1926.)

Temp.	Group.	$\mu \times 10^{18}$.	$(g-a)$.	$\frac{(g-a)}{\mu \times 10^{18}}$.
60° C.	$-OCH_3$	+0·8 °	>6·2	+0·78+
60° C.	$-CH_3$	+0·43	0·40	+0·92
76° C.	$-Cl$	−1·58	−0·82	+0·52
76° C.	$-Br$	−1·56	−0·82	+0·53
76° C.	$-NO_2$	−3·75	−1·72	+0·45
76° C.	$-COOH$	?	−1·12	+0·59

NOTE.—The value $(g-a)$ given by Shoesmith and Slater is equal to $\log K_s/K_u$ for the meta substituent groups.

In each of these widely differing sets of data the variation of the ratio $\frac{\log K_s/K_u}{\mu}$ is within the present limits of

accuracy of the experimental measurements. Both the reaction velocities and the dipole moments can vary widely, and not necessarily uniformly, with changes of physical conditions (*cf.* Estermann, *loc. cit.*, McCombie, Scarborough, and Smith, J. Chem. Soc. p. 803, 1927), and it must be remembered that the respective conditions chosen for the measurement of the reaction velocities and of the electrical dipole moments may not be strictly comparable.

In contrast to the above results, no such close relationship can be traced between the reaction velocity change on substitution and the dipole moment when the substituent group is in either the ortho or the para relationship to the point of reaction in the aromatic molecule. This may well be illustrated from the following table, which is typical of a wide range of experimental data that has been analysed in the same way.

TABLE V.

Dissociation Constants of Substituted Aromatic Acids at 25° C.

Group.	$\mu \times 10^{18}$.	Para Series.		Ortho Series.	
		$K_{Ost.}$	$\frac{\log K_s/K_u}{\mu \times 10^{18}}$.	$K_{Ost.}$	$\frac{\log K_s/K_u}{\mu \times 10^{18}}$
$-NO_2$	−3·75	$3{\cdot}93 \times 10^{-4}$	−0·21	$6{\cdot}5 \times 10^{-3}$	−0·53
−OH.....	+1·73	$2{\cdot}9 \times 10^{-5}$	−0·21	$1{\cdot}06 \times 10^{-3}$	+0·70
−COOH ...	?	$1{\cdot}5 \times 10^{-4}$	−0·20	$1{\cdot}26 \times 10^{-3}$	−0·70
$-CH_3$	+0·43	$4{\cdot}3 \times 10^{-5}$	−0·44	$1{\cdot}25 \times 10^{-4}$	+0·66
$-OCOCH_3$.	?	$8{\cdot}9 \times 10^{-5}$	−0·72	$3{\cdot}27 \times 10^{-4}$	−0·39
$-NH_2$	+1·6	$1{\cdot}2 \times 10^{-5}$	−0·46	$1{\cdot}06 \times 10^{-5}$	−0·50
$-OCH_3$.....	+0·8	$3{\cdot}2 \times 10^{-5}$	−0·39	—	—
−COPh.....	−2·5	—	—	$3{\cdot}7 \times 10^{-4}$	−0·19
−Cl	−1·58	$1{\cdot}3 \times 10^{-3}$	−0·82	$1{\cdot}32 \times 10^{-3}$	−0·82
−Br	−1·56	—	—	$1{\cdot}45 \times 10^{-3}$	−0·86
−COOMe...	−1·8	—	—	$6{\cdot}56 \times 10^{-4}$	−0·24

This would seem to support the supposition that the dipole moment can only be correlated with the *general* polarization effect.

The fact that a less pronounced, but detectable, correlation can be traced in several series of measurements of para substitution derivatives may perhaps be taken as evidence in support of the frequently expressed view that the general polarization effect is more powerful than the

alternating polarity effect (Berger, *Rec. trav. chim.* xlvi. p. 545, 1927) in modifying reaction velocities. In the case of ortho substitution compounds too many influences modify reaction velocity for any simple correlations to be observable.

From experimental evidence alone no estimate can be given for the magnitude of the general polarization effect in the ortho or the para position in comparison with that measurable in the meta position, though a rough theoretical conception of this relationship can be deduced from consideration of equations (3) and (4), from which it follows that :—

$$g_o : g_m : g_p = \cos\theta_o/r_o^2 : \cos\theta_m/r_m^2 : \cos\theta_p/_p r^2 \quad . \quad (5)$$

where θ and r are respectively the angles subtended, and the distances of the centres of the dipoles from the point of attack (P).

For the influence of dipolar groups attached directly to the aromatic ring upon other groups also attached directly to the ring this relationship simplifies down to :—

$$g_o : g_m : g_p = \frac{1}{2} : \frac{1}{2\sqrt{3}} : \frac{1}{4}.$$

In simple cases therefore the general polarization effect has a constant sign and diminishes regularly in magnitude with the distance of the substituent group from the point of reaction within the molecule. This is in complete agreement with the fundamental conception of the nature of the general polarization effect, as previously advanced by many authors from purely qualitative experimental evidence.

Summary.

The general polarization effect in aromatic molecules may be correlated with the dipole moment of the substituent group.

By utilizing the relationship $\log K_s/K_u \propto \mu$ the relative orders of magnitude of the reaction velocities of all meta substituted aromatic compounds can be predicted from a knowledge of the electrical dipole moments of the substituent groups and vice versa. With para substituted compounds the prediction is considerably less certain, and with ortho substituted compounds no such prediction can be made.

The hypothesis advanced is in complete harmony with earlier qualitative theories.

XLVIII. *On the Interpretation of X-Ray Crystal Photographs.*—Part II. *Complete Rotation Photographs.*

By Wm. H. George, *M.Sc., Ph.D., F. Inst. P., Assistant Lecturer in Physics in the University of Leeds* *.

[Plate X.]

Summary.

The paper describes a simple mathematical instrument which directly interprets principal-axis, complete rotation photographs of cubic, tetragonal, hexagonal, and trigonal crystals. A rotating cursor is clamped upon one scale, at a graduation depending upon the size of the unit-cell and the wave-length of the X-rays. The line of the cursor then intersects two other scales at a series of points, each pair of which corresponds to the crystal indices and the row-line reading upon the film where the "spot" of the photograph is to be sought.

In combination with the *grid-method* (Part I.) of measuring X-ray photographs, the method is entirely independent of the type and dimensions of the spectrometer, the wave-length of the X-rays, or the size of the unit-cell of the particular substance, and it involves no graphical construction or calculation.

Partial applications of the work are described, and some tables of constants are given for use in connexion with reciprocal lattice methods for interpretation of rotation photographs.

In the previous paper [1] a general method was described for measuring any kind of X-ray crystal photograph taken on any type of spectrometer. The next stage in the interpretation of the photograph is the identification, *i.e.*, determination of the Miller indices (*hkl*), of the sets of crystal planes which have caused the diffraction effects. For this purpose each type of photograph has to be treated separately. The procedure is of course to calculate all possible theoretical coordinates, using the known geometry of crystal structure, and to compare the results with the observed experimental values. In general the equations are complex [2]. For example, the Bragg angle θ_n for an nth order of reflexion of X-rays of wave-length λ from the (*hkl*) planes of any hexagonal crystal of cell dimensions a_0 and c_0 is given by :—

$$n\lambda = \frac{2a_0}{\sqrt{4/3(h^2+hk+k^2)+(la_0/c_0)^2}} \sin\theta_n. \quad . \quad (1)$$

Graphical methods of obtaining the theoretical values have been used, and an admirable summary of them has

* Communicated by Prof. R. Whiddington, F.R.S.

been given by Schiebold [3]. The objection to graphical methods is that they give results applicable to only one particular substance. In the present paper a simple mathematical instrument is described which directly interprets certain *types* of complete rotation photographs for all possible cases.

Complete Rotation Photographs.

The interpretation of rotation photographs is much facilitated by the use of the reciprocal lattice theory developed by Ewald [4], Polanyi [5], Schiebold [5], Weissenberg [5], Mauguin [6], and Bernal [7], and the instrument to be here described depends upon the use of this theory.

We will assume that the photograph has been taken by rotating a single crystal continuously through 360° about an axis perpendicular to the incident pencil of mono- (or di-) chromatic X-rays, the diffracted X-rays being recorded photographically on a coaxial cylindrical film or on a plane plate normal to the undiffracted X-ray pencil. We will assume further that, since reciprocal lattice theory is to be used in interpreting the photograph, one of the Bernal [7] charts (I. for a plane plate or II. for a cylindrical film) has been used to prepare the grid.

Notation.—Under these conditions, if cylindrical co-ordinates (ξ, ζ, ω) referred to the axis of rotation are used, the angular coordinate ω is indeterminate, since the orientation of the crystal when it is producing a given "spot" is incompletely known. The other two coordinates ξ and ζ are *either* coordidates of the point in the reciprocal lattice corresponding to the crystal plane which has produced the spot on the rotation photograph, *or* they are the coordinates of the spot read off from the photograph. In the latter case ξ is the reading of the *row-line* and ζ is the *layer-line* ("schichtlinie") reading. In the plate (fig. 3) of Part I. [1] the sets of curves are the row-lines and the vertical straight lines are layer-lines. These latter would have been hyperbolæ if a plane plate had been used.

a or c = length of an edge of the unit cell,

= primitive translation along the a or c axes in the crystal lattice.

$A = \lambda/a$ or $C = \lambda/c$ are the corresponding primitive translations of the reciprocal lattice.

λ = wave-length of the monochromatic X-rays used.

hkl = Miller indices of the sets of crystal planes.

We then have [7], [8] for a *cubic* or *tetragonal* crystal rotated about the principal axis (c) :—

$$\xi=\frac{\lambda}{c}\{h^2+k^2\}=\mathrm{C}\{h^2+k^2\}^{\frac{1}{2}} \quad . \quad . \quad . \quad . \quad (2)$$

and $$\zeta=l\mathrm{C}. \quad . \quad . \quad . \quad . \quad . \quad . \quad . \quad . \quad . \quad . \quad (3)$$

For a *trigonal* or *hexagonal* crystal referred to three orthohexagonal axes a, $b=a\sqrt{3}$, and c, and rotated about the c axis (c) :—

$$\xi=\mathrm{A}\left\{h^2+\frac{k^2}{3}\right\}^{\frac{1}{2}} \quad . \quad . \quad . \quad . \quad . \quad . \quad (4)$$

$$\zeta=l\mathrm{C}. \quad . \quad . \quad . \quad . \quad . \quad . \quad . \quad . \quad . \quad . \quad (5)$$

For the most general type of rotation of a *cubic* crystal about a $[uvw]$ zone-axis we have

$$\xi=\mathrm{C}\left\{h^2+k^2+l^2-\frac{hu+kv+lw}{u^2+v^2+w^2}\right\}^{\frac{1}{2}}, \quad . \quad . \quad . \quad (6)$$

$$\zeta=\frac{\mathrm{C}(hu+kv+lw)}{(u^2+v^2+w^2)^{\frac{1}{2}}} \quad . \quad . \quad . \quad . \quad . \quad . \quad . \quad . \quad . \quad (7)$$

Also under these conditions we have for all planes on the nth layer-line

$$hu+kv+lw=n. \quad . \quad . \quad . \quad . \quad . \quad . \quad (8)$$

The most commonly employed zone-axes are the [110] and the [111], when equations (6) (7) and (8) reduce to :—

For a *cubic* crystal rotated about the [110] zone axis,

$$\xi=\mathrm{C}\left\{l^2+\frac{(h-k)^2}{2}\right\}, \quad . \quad . \quad . \quad . \quad . \quad (9)$$

$$\zeta=\frac{\mathrm{C}}{\sqrt{2}}(h+k), \quad . \quad . \quad . \quad . \quad . \quad . \quad . \quad (10)$$

and $$h+k=n \text{ for all planes on the } n\text{th layer line} \quad . \quad . \quad . \quad . \quad . \quad . \quad (11)$$

For a *cubic* crystal rotated about the [111] zone-axis,

$$\xi=\mathrm{C}\left\{h^2+k^2+l^2-\frac{(h+k+l)^2}{3}\right\}^{\frac{1}{2}}, \quad . \quad . \quad (12)$$

$$\zeta=\frac{\mathrm{C}}{\sqrt{3}}(h+k+l), \quad . \quad . \quad . \quad . \quad . \quad . \quad . \quad (13)$$

and $$h+k+l=n \text{ for all planes on the } n\text{th layer-line.} \quad (14)$$

From an examination of these equations two features, of great importance from the present point of view, are apparent. Firstly, the quantities inside the brackets are quite independent of the wave-length of the monochromatic X-rays used, of the axial ratio or absolute dimensions of the unit cell of the particular substance, and of the distance from the crystal to the plane plate or cylindrical film. They represent, then, universal constants * for the particular crystal system or type of photograph. Secondly, if we assume that these constants have been worked out for all possible crystal planes (*i. e.*, integral values of *hkl*) which may occur in practice, then the equations are all of the very simple form $N = MK$. It is clear, then, that a machine which would solve this type of equation would directly interpret the types of photograph considered.

Theory of Instrument.

It would appear that where simplicity in the final result is desired, the best basis for such a machine is a nomographical solution of the equation. The principles of nomography are treated in standard works [9], and the solution (fig. 1) used here need only be described.

Three parallel straight lines of equal length are drawn perpendicular to a common base-line (not shown in fig. 1). The central line is midway between the other two, which may be *any* convenient distance apart. The left-hand line, marked ξ, is graduated logarithmically from 1 to 10, starting from unity at the *top*. The middle line is similarly graduated on a half-scale from 1 to 10 and 10 to 100, starting with unity at the *top*. The right-hand line is graduated according to the type of photograph to be interpreted. For example, for all cubic and tetragonal (*c*) axis rotation photographs it is graduated with the logarithms of the constants $\{h^2+k^2\}^{\frac{1}{2}}$ given in the third column of Table I. The scale of these graduations is the same as on the left-hand line, *i. e.*, from 1 to 10, but starting with unity at the *bottom*. The graduation is best done with a logarithmic ruler, so that graduations are made opposite the reading on the ruler

* Hull (Phys. Rev. x. pp. 661-696 (1917), has given tables of constants for the cubic system for the interpretation of powder photographs from spacing considerations. The spacing equations [2] for all other systems contain the axial ratios involved in terms together with with indices (*hkl*). Universal constants cannot therefore be calculated (*cf.* equations (1) and (4) of the present paper). The Hull constants for the cubic system differ from those given here, since the present ones are calculated for use with reciprocal lattice theory.

corresponding to each number in the third column of Table I., and each graduation is marked with the indices *hk* given in the first column.

The complete diagram (fig. 1) then represents all possible numerical solutions of equation (2), in that any straight line

Fig. 1.

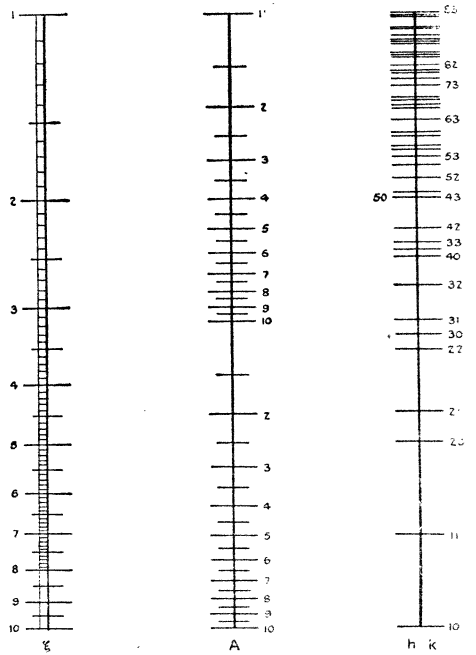

Tetragonal or cubic crystal rotated about principal axis.

passing through a graduation on the right-hand scale cuts the other two scales at points corresponding to some pair of possible values of ξ and A in equation (2). This type of nomographical solution of the equations forms the basis of the instrument shown in Pl. X.

Description of Instrument.

Three wooden scales with white xylonite facings carrying graduations, as described, were mounted on a drawing-board in the relative positions shown in fig. 1. On each scale the total length of graduations is 20 inches, so that the middle and left-hand scales can be ruled on a machine used to make 20-inch slide-rules. The right-hand scale, which can be changed according to the type of photograph, is ruled by hand according to the tables. On the centre scale, which is lower than the two outer ones, a brass fitting slides, and can be clamped by the lever shown on the right-hand side in Pl. X. at any desired position along the scale. This brass fitting carries a strip of transparent xylonite, ruled with a fine black line, to act as a cursor. The upper circular part of the brass fitting is held to the lower part by a spring, so that, although the cursor can be rotated about any point on the middle scale, it will also remain set in any desired position across the scales.

Use of Instrument.

For any type of complete-rotation photograph here discussed the left-hand and middle scales of the instrument (Pl. X.) are the same. The right-hand scale shown in the figure is the one used for photographs of cubic or tetragonal crystals rotated about the principal axis (c). For such photographs the brass fitting is clamped at the lower reading on the middle scale corresponding to the value of A ($=\lambda/a$), where λ is the wave-length of the monochromatic X-rays used, and a is the length on edge of the square base of the unit cell. Then for all spots on the zero layer-line the index l is zero, or in general l is the same as the number of the layer-line. The other two indices hk are got by merely rotating the cursor through the graduations on the right-hand scale. Then the intersection of the cursor with the left-hand scale gives for each pair of indices hk the row-line reading ξ, where the photograph must be examined for a possible crystal reflexion.

Great care must be taken in interpreting the zero layer-line, since the radiation used is often dichromatic, *i. e.*, the intensity of K_β radiation is quite great enough, compared with that of the K_α, to give spots from well-reflecting planes. For all except the zero layer-line the K_α and K_β reflexions lie on different layer-lines. Since in general the K_α and K_β reflexions lie on different row-lines, confusion can be

avoided by following the row-line of each spot on the zero layer-line, until it cuts some other layer-line. It is also easily possible to confuse the K_β reflexion of a plane with the K_α reflexion of some other plane. This coincidence of row-lines depends, of course, upon the particular values of λ and a, and all except the strongest spots on the zero layer-line must be re-examined, the second time with the cursor set at the reading $A' = \lambda K_\beta / a$. It is not safe to rely upon the detection of row-line coincidences by examination of layer-lines other than the zero layer-line.

Table I.

h, k indices of crystal planes which may produce spots on cubic or tetragonal (001) rotation photographs.

h	k	h^2+k^2	$\sqrt{h^2+k^2}$	h	k	h^2+k^2	$\sqrt{h^2+k^2}$
1	0	1	1·0	7	0	49	7·0
1	1	2	1·414	5	5	50	7·071
				7	1		
2	0	4	2·0	6	4	52	7·211
2	1	5	2·236	7	2	53	7·280
2	2	8	2·828	7	3	58	7·616
3	0	9	3·0	6	5	61	7·810
3	1	10	3·162	8	0	64	8·0
3	2	13	3·606	7	4	65	8·06
4	0	16	4·0	8	1		
4	1	17	4·123	8	2	68	8·246
3	3	18	4·243	6	6	72	8·485
4	2	20	4·472	8	3	73	8·544
4	3	25	5·0	7	5	74	8·602
5	0			8	4	80	8·944
5	1	26	5·099	9	0	81	9·0
5	2	29	5·385	9	1	82	9·055
4	4	32	5·657	7	6	85	9·219
5	3	34	5·831	9	2		
6	0	36	6·0	8	5	89	9·434
6	1	37	6·083	9	3	90	9·487
6	2	40	6·325	9	4	97	9·849
5	4	41	6·403	7	7	98	9·899
6	3	45	6·708	8	6	100	10·0

When, in the use of the instrument, the line of the cursor goes beyond the end of the graduations of the left-hand scale, the brass fitting is released and reclamped at the same A reading on the upper half of the middle scale, where it is used as before.

Partial Applications.

Fig. 1 can be very simply constructed by use of strips of semi-logarithmic paper pasted on cardboard. Instead of the rotating cursor of the instrument, a strip of glass or transparent xylonite having a black line ruled on it can then be used. Naturally this is not so convenient, as the reading on the middle scale has to be set each time.

The tables of constants given for the purpose of graduation of the right-hand scale of the instrument can be used for slide-rule calculation whenever reciprocal-lattice methods are to be used for interpretation of rotation photographs.

For example, in Table I. the constants of the middle column can be used to set the slide-rule cursor on the *top* scale of the slide-rule (when equation (2) is in use) or the constants in the third column can be set upon the *bottom* slide-rule scale.

Table II. gives the constants required for dealing with hexagonal or trigonal crystals. To get the equation (4) in suitable form for the present method, orthohexagonal axes are used, the crystals being referred to axes a, $b = a\sqrt{3}$, and c.

TABLE II.

Indices (h k l), referred to orthohexagonal axes a, $b = a\sqrt{3}$ and c, of crystal planes which may produce spots on c-axis rotation photographs of trigonal or hexagonal crystals.

h	k.	$h^2+k^2/3$.	$\{h^2+k^2.3\}^{\frac{1}{2}}$.	h	k.	$h^2+k^2/3$.	$\{h^2+k^2/3\}^{\frac{1}{2}}$.
0	1	0·33	0·577	2	1	4·33	2·082
1	0	1·0	1·0	0	4	5·33	2·309
0	2	1·33	1·155	2	2		
1	2	2·33	1·527	1	4	6·33	2·516
0	3	3·0	1·732	2	3	7·0	2·646
2	0	4·0	2·0	0	5	8·33	2·887
1	3			3	0	9·0	3·0

TABLE II. (*cont.*).

h	k.	$h^2+k^2/3$.	$\{h^2+k^2/3\}^{\frac{1}{2}}$.
1	5	9·33	3·055
2	4		
3	1		
3	2	10·33	3·214
0	6	12·0	3·464
3	3		
2	5	12·33	3·511
1	6	13·0	3·606
3	4	14·33	3·785
4	0	16·0	4·0
2	6		
0	7	16·33	4·031
4	1		
1	7	17·33	4·163
3	5		
4	2		
4	3	19·33	4·397
2	7	20·33	4·509
3	6	21·0	4·583
0	8	21·33	4·618
4	4		
1	8	22·33	4·726
4	5	24·33	4·933
5	0	25·0	5·0
2	8	25·3	5·033
3	7		
5	1		
5	2	26·33	5·131
0	9	27·0	5·196
1	9	28·0	5·292
4	6		
5	3	28·33	5·322
3	8	30·33	5·507
5	4		
2	9	31·0	5·568
4	7	32·33	5·686
0	10	33·33	5·773
5	5		
1	10	34·33	5·859
6	0	36·0	6·0
3	9		
6	1	36·33	6·027
5	6	37·0	6·083
2	10	37·33	6·110
4	8		
6	2		
6	3	39·0	6·245
0	11	40·33	6·351
1	11	41·33	6·429
5	7		
6	4		
3	10	42·33	6·506
4	9	43·0	6·557
6	5	44·33	6·658
2	11		
5	8	46·33	6·807
6	6	48·0	6·928
0	12		
7	0	49·0	7·0
1	12		
3	11	49·33	7·024
4	10		
7	1		
7	2	50·33	7·094
2	12	52·0	7·211
5	9		
7	3		
6	7	52·33	7·234
7	4	54·33	7·371
0	13	56·33	7·505
4	11		
3	12	57·0	7·550
1	13	57·33	7·572
6	8		
7	5		
5	10	58·33	7·637
2	13	60·33	7·767
7	6	61·0	7·810
6	9	63·0	7·937
8	0	64·0	8·0
4	12		
8	1	64·33	8·020

TABLE II. (*cont.*).

h	k.	$h^2+k^2/3$.	$\{h^2+k^2/3\}^{\frac{1}{2}}$.
0	14	65·33	8·082
3	13		
5	11		
7	7		
8	2		
1	14	66·33	8·144
8	3	67·0	8·185
2	14	69·33	8·326
6	10		
8	4		
7	8	70·33	8·386
4	13	72·33	8·504
8	5		
5	12	73·0	8·544
3	14	74·33	8·621
0	15	75·0	8·660
1	15	76·0	8·718
8	6		
7	9		
6	11	76·33	8·737
2	15	79·0	8·888
8	7	80·33	8·963
9	0	81·0	9·0
4	14	81·33	9·018
5	13		
9	1		
7	10	82·33	9·074
9	2		
3	15	84·0	9·165
6	12		
9	3		
0	16	85·33	9·237
8	8		
1	16	86·33	9·291
9	4		
2	16	89·33	9·452
9	5		
7	11		
5	14	90·33	9·504
4	15	91·0	9·0
8	9		
6	13	92·33	9·609
9	6	93·0	9·644
3	16	94·33	9·712
0	17	96·33	9·815
7	12	97·0	9·849
1	17	97·33	9·866
9	7		
8	10		
10	0	100·0	10·0
5	15		

Table III. gives the constants for cubic [110] rotation photographs. Here it is better to have a different scale for each layer-line if the instrument is to be of general use. For economy in printing, only the square of the constant K is given. In graduating the scales the *square roots* of the numbers in the second column must be set off with the aid of a logarithmic ruler. It should be remembered that for a *face-centred* lattice (F or $\Gamma r'$) X-ray reflexions can occur only from planes whose indices are all odd or all even (0 is even). That is, planes having mixed indices cannot produce spots on the rotation photograph. For the *body-centred* lattice (B or $\Gamma r''$) reflexions can occur only from those planes the sum of whose indices is an even number. It is therefore unnecessary to determine the theoretical

Table III.

Indices ($h\ k\ l$) of crystal planes which may produce spots upon cubic [110] rotation photographs.

Zero Layer-line. $h+k=0$.

h	k	l.	K.	Lattice.		h	k	l.	K.	Lattice.	
0	0	1	1			5	$\bar{5}$	0	50	B	
1	$\bar{1}$	0	2	B		5	$\bar{5}$	1	51		F
0	$\bar{1}$	1	3		F	1	$\bar{1}$	7			
0	0	2	4	B	F	5	$\bar{5}$	2			
1	$\bar{1}$	2	6	B		3	$\bar{3}$	6	54	B	
2	$\bar{2}$	0	8	B	F	4	$\bar{4}$	5	57		
2	$\bar{2}$	1	9			2	$\bar{2}$	7			
0	0	3				5	$\bar{5}$	3	59		F
1	$\bar{1}$	3	11		F	0	0	8	64	B	F
2	$\bar{2}$	2	12	B	F	5	$\bar{5}$	4	66	B	
0	0	4	16	B	F	1	$\bar{1}$	8			
2	$\bar{2}$	3	17			3	$\bar{3}$	7	67		F
3	$\bar{3}$	0	18	B		4	$\bar{4}$	6	68		F
1	$\bar{1}$	4				6	$\bar{6}$	0	72	B	F
3	$\bar{3}$	1	19		F	2	$\bar{2}$	8			
3	$\bar{3}$	2	22	B		6	$\bar{6}$	1	73		
2	$\bar{2}$	4	24	B	F	5	$\bar{5}$	5	75		F
0	0	5	25			6	$\bar{6}$	2	76	B	F
3	$\bar{3}$	3	27		F	0	0	9	81		
1	$\bar{1}$	5				4	$\bar{4}$	7			
4	$\bar{4}$	0	32	B	F	6	$\bar{6}$	3			
4	$\bar{4}$	1	33			3	$\bar{3}$	8	82	B	
2	$\bar{2}$	5				1	$\bar{1}$	9	83		F
3	$\bar{3}$	4	34	B		5	$\bar{5}$	6	86	B	
0	0	6	36	B	F	6	$\bar{6}$	4	88	B	F
4	$\bar{4}$	2				2	$\bar{2}$	9	89		
1	$\bar{1}$	6	38	B		4	$\bar{4}$	8	96	B	F
4	$\bar{4}$	3	41			6	$\bar{6}$	5	97		
3	$\bar{3}$	5	43		F	7	$\bar{7}$	0	98		
2	$\bar{2}$	6	44		F	7	$\bar{7}$	1	99		
4	$\bar{4}$	4	48	B	F	5	$\bar{5}$	7			
0	0	7	49			3	$\bar{3}$	9			
						0	0	10	100	B	F

TABLE III. (*cont.*).

First Layer-line. $h+k=1$. Absent for F.

h	k	l.	K.	Lattice.	h	k	l.	K.	Lattice.
1	0	0	0·5		2	$\bar{1}$	7	53·5	B
1	0	1	1·5	B	5	$\bar{4}$	4	56·5	
1	0	2	4·5		6	$\bar{5}$	0	60·5	
2	$\bar{1}$	1	5·5	B	4	$\bar{3}$	6		
2	$\bar{1}$	2	8·5		3	$\bar{2}$	7	61·5	B
1	0	3	9·5	B	6	$\bar{5}$	1		
3	$\bar{2}$	0	12·5		1	0	8	64·5	
3	$\bar{2}$	1	13·5	B	6	$\bar{5}$	2		
1	0	4	16·5		5	$\bar{4}$	5	65·5	B
3	$\bar{2}$	2			2	$\bar{1}$	8	68·5	
2	$\bar{1}$	4	20·5		6	$\bar{5}$	3	69·5	B
3	$\bar{2}$	3	21·5	B	4	$\bar{3}$	7	73·5	B
4	$\bar{3}$	0	24·5		6	$\bar{5}$	4	76·5	
1	0	5	25·5	B	3	$\bar{2}$	8		
4	$\bar{3}$	1			1	0	9	81·5	B
4	$\bar{3}$	2	28·5		7	$\bar{6}$	0	84·5	
2	$\bar{1}$	5	29·5	B	6	$\bar{5}$	5	85·5	B
4	$\bar{3}$	3	33·5	B	7	$\bar{6}$	1		
1	0	6	36·5		2	$\bar{1}$	9		
3	$\bar{2}$	5	37·5	B	7	$\bar{6}$	2	88·5	
2	$\bar{1}$	6	40·5		4	$\bar{3}$	8		
4	$\bar{3}$	4			5	$\bar{4}$	7	89·5	B
5	$\bar{4}$	0			3	$\bar{2}$	9	93·5	B
5	$\bar{4}$	1	41·5	B	7	$\bar{6}$	3		
5	$\bar{4}$	2	44·5		6	$\bar{5}$	6	96·5	
3	$\bar{2}$	6	48·5						
1	0	7	49·5	B					
4	$\bar{3}$	5							

Second Layer-line. $h+k=2$.

h	k	l.	K.	Lattice.		h	k	l.	K.	Lattice.	
1	1	1	1		F	2	0	3	11		
2	0	0	2	B	F	3	$\bar{1}$	2	12	B	
2	0	1	3			1	1	4	16	B	
1	1	2	4	B		3	$\bar{1}$	3	17		F
2	0	2	6	B	F	4	$\bar{2}$	0	18	B	F
3	$\bar{1}$	0	8	B		4	$\bar{2}$	1	19		
3	$\bar{1}$	1	9		F	4	$\bar{2}$	2	22	B	F

TABLE III. (*cont.*).

Second Layer-line. $h+k=2$. (*Cont.*)

h	k	l.	K.	Lattice.		h	k	l.	K.	Lattice.	
3	$\bar{1}$		24	B		2	0	8	66	B	F
1	1	5	25		F	6	$\bar{4}$	4			
2	0	5	27			4	$\bar{2}$	7	67		
4	$\bar{2}$	3				5	$\bar{3}$	6	68	B	
5	$\bar{3}$	0	32	B		3	$\bar{1}$	8	72	B	
5	$\bar{3}$	1	33		F	7	$\bar{5}$	0			
4	$\bar{2}$	4	34	B	F	7	$\bar{5}$	1	73		F
1	1	6	36	B		6	$\bar{4}$	5	75		
5	$\bar{3}$	2				7	$\bar{5}$	2	76	B	
2	0	6	38	B	F	7	$\bar{5}$	3	81		F
5	$\bar{3}$	3	41		F	1	1	9			
4	$\bar{2}$	5	43			4	$\bar{2}$	8	82	B	F
3	$\bar{1}$	6	44	B		2	0	9	83		
5	$\bar{3}$	4	48	B		6	$\bar{4}$	6	86	B	F
1	1	7	49		F	7	$\bar{5}$	4	88	B	
6	$\bar{4}$	0	50	B	F	3	$\bar{1}$	9	89		F
2	0	7	51			5	$\bar{3}$	8	96	B	
6	$\bar{4}$	1				7	$\bar{5}$	5	97		F
6	$\bar{4}$	2	54	B	F	8	$\bar{6}$	0	98	B	F
3	$\bar{1}$	7	57		F	4	$\bar{2}$	9	39		
5	$\bar{3}$	5				6	$\bar{4}$	7			
6	$\bar{4}$	3	59			8	6	1			
1	1	8	64	B							

Third Layer-line. $h+k=3$. Absent for F.

h	k	l.	K.	Lattice.	h	k	l.	K.	Lattice.
2	1	0	0·5	B	3	0	5	29·5	B
2	1	1	1·5	B	5	$\bar{2}$	3	33·5	B
2	1	2	4·5		2	1	6	36·5	
3	0	0			4	$\bar{1}$	6	37·5	B
3	0	1	5·5	B	6	$\bar{3}$	0	40·5	
3	0	2	8·5		5	$\bar{2}$	4		
2	1	3	9·5	B	6	$\bar{3}$	1	41·5	B
4	$\bar{1}$	0	12·5		6	$\bar{3}$	2	44·5	
3	0	3	13·5	B	4	$\bar{1}$	6	48·5	
4	$\bar{1}$	1			2	1	7	49·5	B
4	$\bar{1}$	2	16·5		5	$\bar{2}$	5		
3	0	4	20·5		6	$\bar{3}$	3		
4	$\bar{1}$	3	21·5	B	3	0	7	53·5	B
5	$\bar{2}$	0	24·5		6	$\bar{3}$	4	56·5	
5	$\bar{2}$	1	25·5	B	5	$\bar{2}$	6	60·5	
4	$\bar{1}$	4	28·5		7	$\bar{4}$	0		
5	$\bar{2}$	2							

TABLE III. (*cont.*)

Third Layer-line. $h+k=3$. Absent for F. (*Cont.*)

h	k	l.	K.	Lattice.
7	$\bar{4}$	1	61·5	B
2	1	8	64·5	
7	$\bar{4}$	2		
6	$\bar{3}$	5	65·5	B
3	0	8	68·5	
7	$\bar{4}$	3	69·5	B
5	$\bar{2}$	7	73·5	B
4	$\bar{1}$	8	76·5	
6	$\bar{3}$	6		
7	$\bar{4}$	4		
2	1	9	81·5	B
8	$\bar{5}$	0	84·5	
3	0	9	85·5	B
7	$\bar{4}$	5		
8	$\bar{5}$	1		
8	$\bar{5}$	2	88·5	
6	$\bar{3}$	7	89·5	B
4	$\bar{1}$	9	93·5	B
8	$\bar{5}$	3		
7	$\bar{4}$	6	6·5	

Fourth Layer-line. $h+k=4$.

h	k	l.	K.	Lattice.
2	$\bar{2}$	1	1	
3	1	0	2	B
3	1	1	3	F
2	2	2	4	B
3	1	2	6	B
4	0	0	8	B F
2	2	3	9	
4	0	1		
3	1	3	11	F
4	0	2	12	B F
2	2	4	16	B F
4	0	3	17	
3	1	4	18	B
5	1	0		
5	$\bar{1}$	1	19	F
5	$\bar{1}$	2	22	B
4	0	4	24	B F
2	2	5	25	
5	$\bar{1}$	3	27	F
6	$\bar{2}$	0	32	B F
4	0	5	33	
6	$\bar{2}$	1		
5	$\bar{1}$	4	34	B
6	$\bar{2}$	2	36	B F
3	1	6	38	B
6	$\bar{2}$	3	41	
5	$\bar{1}$	5	43	F
4	0	6	44	B F
6	$\bar{2}$	4	48	B F
2	2	7	49	
7	$\bar{3}$	0	50	B
7	$\bar{3}$	1	51	F
5	$\bar{1}$	6	54	B
7	$\bar{3}$	2		
4	0	7	57	
6	$\bar{2}$	5		
7	$\bar{3}$	3	59	F
2	2	8	64	B F
3	1	8	66	B
7	$\bar{3}$	4		
5	$\bar{1}$	7	67	F
6	$\bar{2}$	6	68	B F
8	$\bar{4}$	0	72	B F
8	$\bar{4}$	1	73	
7	$\bar{3}$	5	75	F
8	$\bar{4}$	2	76	B F
6	$\bar{2}$	7	81	
8	$\bar{4}$	3		
2	2	9		
5	$\bar{1}$	8	82	B
3	1	9	83	
7	$\bar{3}$	6	86	B
8	$\bar{4}$	4	88	B F
4	0	9	89	
6	$\bar{2}$	8	96	B F
8	$\bar{4}$	5	97	
9	$\bar{5}$	0	98	B
7	$\bar{3}$	7	99	F
9	$\bar{5}$	1		

values of ξ and ζ for such planes, as the lattice of a particular crystal can always be readily determined. Accordingly, in the third column of the table, the lattice is indicated. Reflexions may be observed from any of the planes if the lattice is simple cubic (Γr). In preparing the scales, the planes marked B may be indicated with a half graduation to the right, those marked F with half graduation to the left, the others with a full graduation right across the vertical line. This table should be of use, especially in metallurgical work. It will be noted that there is much less likelihood of spots being unresolvable in this type of rotation photograph than for the simple *c*-axis rotation (*cf.* Table I.).

In conclusion, it may be added that in actual practice the method here described, used in conjunction with that given in Part I., is so rapid that the film can be interpreted whilst it is undergoing fixation in the hypo-bath. It will, of course, be understood that unresolvable spots (especially those having high indices, *hkl*) may occur, but they are then unresolvable by any method of interpretation. It is then necessary to resort to oscillation or moving film or ionization spectrometer methods, which give additional information as to the position of the crystal when it is producing a particular reflexion. In Part III. it is hoped to deal with an instrument applicable to such cases.

The present instrument was made, with the help of a Royal Society Government Grant, in the workshops of the Physics Department of the University of Leeds by Mr. Ludbrook, to whom some of the details are due.

References.

(1) George, Phil. Mag. vii. pp. 373–384 (1929).
(2) Wyckoff, 'Structure of Crystals,' pp. 97–99 (1924).
(3) Schiebold, *ZS. f. Phys.* xxviii. pp. 355–370 (1924).
(4) Ewald, *Zs. f. Krist.* lvi. pp. 129–156 (1921).
(5) References are given in *ZS. f. Phys.* xxiii. pp. 337–340 (1924).
(6) *Bull. Soc. Française de Min.* xlix. pp. 5–32 (1926).
(7) Roy. Soc. Proc. A, cxiii. pp. 117–160 (1926).
(8) Polanyi and Weissenberg, *Zs. f. Phys.* x. p. 49 (1922).
(9) For example, D'Ocagne, 'Traité de Nomographie,' Paris, 1899, or Brodetsky, 'Nomography,' London, 1920.

XLIX. *The Effects of Magnetic Field on certain Chemical Reactions.* *By* S. S. Bhatnagar, *D.Sc.(Lond.)*, *F.Inst.P.*, R. N. Mathur, *M.Sc.*, *and* R. N. Kapur, *M.Sc.**

THE close relationship between electricity and chemical affinity on the one hand and that between electricity and magnetism on the other early raised the question whether magnetism would alter the character or degree of a chemical reaction. As early as 1881 Ramsen † observed that magnetism had a remarkable action on the deposition of copper from solution of its salts on an iron plate. In 1886 Nichols ‡ further investigated the action of acids on iron in a magnetic field, and in 1887 H. A. Rowland and Louis Bell read a paper at the Manchester Meeting of the British Association, September 1887, on "An Explanation of the Action of a Magnet on Chemical Action." They explained the protection of iron from the chemical action of hydrochloric acid in lines around the edge of the poles on the view that the force acting on the particle in any direction is proportional to the rate of variation of the square of the magnetic force in that direction. "This rate of variation is greatest near the edges and points of a magnetic pole, and more work will be required to tear away a particle of iron and steel from such an edge or point than from a hollow. This follows whether the tearing away is done mechanically or chemically."

Loeb § in 1891 and later Wolff ‖ tried the influence of magnetic field on the oxidation and reduction of iron salts, but obtained negative results. Jahr ¶ observed that a photographic plate immersed in a developer or even in distilled water is affected when brought near the pole of an electromagnet consisting of a bundle of steel wires.

Alexander De Hemptenine ** in 1900 published an interesting paper in which he showed that although theoretically there is an effect of the magnetic field, experimentally it is too small to be of much consequence. Among

* Communicated by the Authors.

† Ramsen, Amer. Chem. Journ. iii. p. 157 (1881).

‡ Nichols, Amer. Journ. Science, p. 372 (1886).

§ Loeb, Amer. Chem. Journ. xiii. pp. 145–53 (1891).

‖ F. A. Wolff, Amer. Chem. Journ. xvii. pp. 122–138 (1895).

¶ E. Jahr, *Electro-Chem. Zeitschr.* v. pp. 177–180 (1898).

** Alexander De Hemptenine, *Zeit. Physikal. Chem.* xxxiv. p. 669 (1900).

the later workers Berndt* found that the rate of solution of iron in hydrochloric acid in a magnetic field is smaller. With zinc no difference was observed. Recently Schukarew† performed a series of experiments to detect any possible effect on a number of chemical reactions by subjecting them to transverse and longitudinal magnetic fields ranging from 2000 to 7000 gauss. No general conclusions could be reached by him. According to Parker and Armes‡ the reduction of ferric chloride by iron and aluminium and the reduction of permanganate in acid solutions by metallic iron are accelerated by the field. Henglein§, however, found no difference in the combination of NO and Cl even with fields up to 20,000 gauss.

Theoretical.

For ferromagnetic bodies the reasons advanced by Rowland to explain the action of magnetic field on the dissolution of iron in hydrochloric acid and De Hemptenine's treatment of the subject on thermodynamic basis are worthy of mention. Taking, however, the more general case of para- and diamagnetic substances there are a number of theoretical reasons to expect an influence of an impressed magnetic field on chemical reactions.

Magnetism has been shown to have a profound influence on valence. G. N. Lewis‖ has discussed at length the magneto-chemical theory of valence. A chemical bond according to him is the pairing of two electrons and two isolated electronic orbits or magnets tend to couple with one another to eliminate their magnetic moment. E. H. Williams¶ has emphasized the scarcity of odd molecules, *i.e.* molecules having an odd number of electrons among the chemical compounds.

If, then, a chemical reaction involves change in valence of the reacting substances an external magnetic field must necessarily affect the reaction. Even in the case of double decomposition in which there is no actual change in the valence there may be a change in the magnetic moments of

* G. Berndt, *Physikal. Zeitschr.* ix. p. 512 (1908).

† A. Schukarew, *Zeit. Physikal. Chem.* cxiii. p. 441 (1924).

‡ M. A. Parker and H. P. Armes, Trans. Roy. Soc. Canada, xviii. III. p. 203 (1924).

§ F. A. Henglein, *Zeit. Electro-Chem.* xxxii. p. 213 (1926).

‖ G. N. Lewis, "Valence and Structure of Atoms and Molecules," Amer. Chem. Soc., Monographs (1923); also "The Magneto-Chemical Theory in Chemical Reviews," vol. i. no. 2 (1924).

¶ E. H. Williams, Phys. Rev. xxviii. p. 167 (1926).

the initial and final products. If during a reaction the magnetic moments tend to decrease then the presence of an external field will try to "conserve" the magnetism and so retard the rate of reaction. On the other hand, if the magnetic moment increases during the course of reaction, then the presence of a field will further help the increase and so accelerate the rate of reaction.

The idea is essentially of a system possessing inertia and by analogy may be called the "magnetic inertia" of the system.

We may consider the above in the light of the law of mass action. If A and B denote the concentrations of two reacting substances and C and D the concentrations of the reaction products, then for the equilibrium state we have

$$A \times B \times K_1 = C + D \times K_2$$

or

$$\frac{A \times B}{C \times D} = \frac{K_2}{K_1} = K$$

where K_1, K_2, and K are the usual constants. For any given concentration the velocities of the forward and backward reactions will then depend upon the constants K_1 and K_2. These constants while independent of concentrations may vary with the temperature, the nature of the medium, and other physical conditions.

On the basis of the kinetic theory a molecule (or an ion) A, when it collides with B, either unites with it to form a third substance C or rebounds elastically. The rate of formation of C will then depend upon the number of inelastic collisions per second between A and B. Any agency, whether internal or external, which affects the probability of inelastic conditions also affects the rate of reaction A + B. In a magnetic field the atoms (and presumably ions also) become spatially quantized, that is to say, they tend to assume certain definite positions relative to one another. And thus the collisions within the field are likely to take place in a more orderly and directed manner and the probability of inelastic collisions should change, and with it the velocity of the reaction also.

Thus, we conclude that a chemical transformation from diamagnetic to paramagnetic or less diamagnetic state should be accelerated, and that from a paramagnetic to diamagnetic or from a feebly diamagnetic to more strongly diamagnetic state should be retarded.

Considering again the above reacting system, it is evident

that if one of the reaction products possesses a different magnetic state from the rest, it would tend to localize itself in certain parts of the field and to withdraw itself from other parts. The reaction velocity A+B will then also vary accordingly. Following similar considerations Weigle* has obtained a mathematical relation between the concentrations inside and outside the magnetic field. This will be more fully discussed later.

Experimental.

A critical study of the previous work on the subject shows that in almost all cases where negative results were obtained, the reasons might be ascribed to the one or the other of the following causes:—

1. The reactions used proceeded with great velocity, *e.g.*, the oxidation of ferrous salts.
2. The analytical methods employed were incapable of measuring small changes in the amounts of reaction products.
3. There was no appreciable difference between the susceptibilities of the initial and the final reaction products.

Care was therefore taken in this investigation to select reactions with very small reaction velocity. Also reactions involving large changes in the susceptibilities of initial and final products were selected. The titration methods of analysis employed were found quite adequate.

The reactions were conducted in ordinary test-tubes which could be clamped within the pole-pieces of an electromagnet. In each case a control experiment was conducted side by side under identical conditions and temperatures were recorded. There was no appreciable temperature difference between the control and the reaction within the field. In order to be certain of any influence of the material of the test-tubes themselves on the reactions, the control and reaction tubes were interchanged each time. No difference due to tubes only was, however, detected. Only Merck's extra pure chemicals and reagents were used throughout.

A fairly large electromagnet provided the field. The strength varied from 600 to 1700 gauss with a gap of 1 cm. between the pole-pieces, which were conical and had a plane face of about 1 cm. diameter. A micrometric arrangement for adjustment of distance was provided. The current

* J. J. Weigle, Phys. Rev. xxxi. pp. 676-9 (1928).

passing through the electromagnet was kept constant by a variable rheostat and an ammeter.

The following reactions have been studied :—

1. Reduction of ferric chloride solution containing hydrochloric acid by metallic iron, aluminium, and zinc.
2. Dissolution of the metals iron, aluminium, and zinc in dilute hydrochloric acid.
3. The oxidation of oxalic acid by potassium permanganate.
4. Reduction of chromic acid by phosphorous acid.
5. Oxidation of potassium iodide by chromic acid.
6. Reduction of potassium permanganate by chloral hydrate.
7. The reaction :—

$$3FeSO_4 + 5KI + KIO_3 + 3H_2O \longrightarrow 3Fe(OH)_2 + 3K_2SO_4 + 3I_2.$$

8. The Reaction :—

$$3CoSO_4 + 5KI + KIO_3 + 3H_2O \longrightarrow 3Co(OH)_2 + 3K_2SO_4 + 3I_2.$$

9. Oxidation of hydriodic acid by hydrogen peroxide.
10. Esterification of acetic acid by hydrogen chloride.

We may now consider each of the reactions separately.

1. *Reduction of Ferric Chloride Solution containing Hydrochloric Acid by Metallic Iron, Aluminium, and Zinc.*— The velocity of reduction was measured by adding a weighed quantity of the metal to a known definite volume of the ferric chloride solution. After the reaction had proceeded for some time, a small quantity was pipetted out and titrated against a standard solution of potassium bichromate. From this the amount of Fe reduced was calculated.

The reaction mixture was stirred equally at intervals of 5 minutes during the course of reduction. It has been noted that stirring has a considerable influence on the rate of the reaction.

The reduction of ferric chloride in cases (1) and (3) in Table I. (p. 462) was also tried under different field strengths by varying the current in the electromagnet. The results obtained were similar to the above, and showed with iron a progressive increase and with zinc a progressive decrease in the velocity with increasing field strength.

The rate of reduction of ferric chloride solution is thus accelerated by iron and aluminium in magnetic field, while with zinc it is retarded.

TABLE I.

Strength of $FeCl_3$ solution = 162·50 gms. per litre.
Weight of the metal taken = 1·00 gm.
Temperature = 15·0° C.
Field strength = 1700 gauss.

Reaction.	Interval.	Titre value with N/50 potassium dichromate. Without field.	Titre value with N/50 potassium dichromate. Within field.	Change due to magnetic field calculated as amount of iron.	Remarks.
		c.c.	c.c.		
1. Ferric chloride and iron filings.	1/2 hr.	11·00	12·50	0·0017 gm.	Reaction accelerated by field.
	1 hr.	19·00	21·50	0·0028 ,,	
	1½ hr.	30·50	34·50	0·0045 ,,	
	2 hrs.	45·00	50·00	0·0056 ,,	
2. Ferric chloride and aluminium.	1/2 hr.	8·50	9·00	0·0006 ,,	Reaction accelerated by field.
	1 hr.	29·00	30·50	0·0017 ,,	
	1½ hrs.	38·25	40·00	0·0020 ,,	
	2 hrs.	47·00	49·00	0·0022 ,,	
3. Ferric chloride and zinc.	1/2 hr.	4·30	3·00	0·0014 ,,	Reaction retarded by field.
	1 hr.	14·60	12·80	0·0021 ,,	
	1½ hrs.	30·40	27·50	0·0032 ,,	
	2 hrs.	47·10	43·00	0·0046 ,,	

2. *The Dissolution of Metals in Dilute Hydrochloric Acid.*—According to Conroy *, who worked with iron, and Auren †, who used zinc, the reaction takes place in two periods. During the initial or "induction period" the reaction is slow. It then increases to a maximum and then finally falls down.

The rate of dissolution was determined in the following way :—

A definite volume of dilute hydrochloric acid was added to a known weight of metal cut into small pieces. After a definite time a small volume of reaction mixture was taken out and titrated for the amount of acid left against a standard solution of sodium hydroxide.

* James T. Conroy, *J. Soc. Chem. Ind.* xx. p. 316 (1901).
† T. Ericson Auren, *Zeits. anorg. Chem.* xxvii. p. 209 (1901).

The results are recorded below:

TABLE II.

Temperature = 16·0° C.
Field strength = 1700 gauss.

Reaction.	Interval.	Titre value with N/100 sodium hydroxide.		Change due to magnetic field.	Remarks.
		Without field.	Within field.		
		c.c.	c.c.	c.c.	
Iron in	1/2 hr.	336·00	337·00	1·00	Rate of dissolution retarded by field.
HCl (1·7N)	1 ,,	334·00	335·00	1·00	
1 gm. Fe in	1½ ,,	330·00	333·00	3·00	
10 c.c. acid.	2 ,,	326·00	331·00	5·00	
Zinc in	1/2 ,,	229·00	227·50	1·50	Rate of dissolution accelerated by field.
HCl (1·15N)	1 ,,	227·00	225·50	1·50	
2 gm. Zn. in	1½ ,,	225·00	223·00	2·00	
10 c.c. acid.	2 ,,	222·50	220·00	2·50	
Aluminium	1/2 hr.	155·00	155·00	No difference.	No appreciable difference.
in HCl (·78N)	1 ,,	154·00	154·00	,,	
1·5 gm. Al. in	1½ ,,	153·00	153·00	,,	
10 c.c. acid.	2 ,,	151·50	151·00	0·50	

The results shown above indicate that the rate of the dissolution of iron in dilute hydrochloric acid is slightly retarded by the magnetic field, while that of zinc is slightly accelerated. In the case of aluminium no appreciable difference is observed.

3. *The Oxidation of Oxalic Acid by Potassium Permanganate.*—According to Richard Ehrenfeld *, the reaction takes place quantitatively between potassium permanganate and oxalic acid in absence of mineral acids, according to the equation:

$$8C_2H_2O_4 + 2KMnO_4 = 2MnC_2O_4 + K_2C_2O_4 + 10CO_2 + 8H_2O.$$

The velocity of the reaction was measured by mixing the substances in solution both (*a*) outside magnetic field and (*b*) inside the magnetic field, and after a definite time a

* Richard Ehrenfeld, *Zeit. anorg. Chemie*, xxxiii. p. 117 (1902).

certain amount was taken out of the reaction mixture and added to a mixture of dilute sulphuric acid and potassium iodide. The liberated iodine was then estimated by titration against sodium thiosulphate. From the amount of iodine the amount of permanganate which had been decomposed was calculated.

TABLE III.

Strength of the potassium permanganate solution = 1·05 gms. per litre.
Strength of the oxalic acid solution = 6·0 gms. per litre.
Temperature = 17·5° C.
Field strength = 1700 gauss.

Interval.	Titre value with N/50 sodium thiosulphate. Without field.	Within field.	Change due to magnetic field calculated as the amount of $KMnO_4$ decomposed.	Remarks.
1/2 hr. ...	3·10 c.c.	2·85 c.c.	0·00016 gm.	The rate of oxidation is accelerated by the magnetic field.
3/4 ,, ...	2·40 ,,	2·05 ,,	0·00022 ,,	
1 ,, ...	1·70 ,,	1·20 ,,	0·00032 ,,	

It is clear from the results tabulated above that the rate of oxidation of oxalic acid by potassium permanganate is accelerated by the magnetic field. Further experiments showed that the difference in $KMnO_4$ decomposed within and without the magnetic field changes with the strength of the field.

4. *The Reduction of Chromic Acid by Phosphorous Acid.*— This was studied by Viard*. The velocity of the reduction was determined by mixing the two substances in solution, and after a definite time taking out a certain volume of the reaction mixture and adding to it dilute sulphuric acid and potassium iodide. The liberated iodine was estimated, and from it the amount of chromic acid which had been reduced was calculated.

Several test experiments had to be performed to find out whether the presence of phosphorous acid creates any difficulty in the accurate determination of chromic acid. No trouble, however, occurs due to this.

* G. Viard, *Comp. Rend.* cxxiv. p. 148 (1897).

TABLE IV.

Strength of the chromic acid solution = 49·6 gms. per litre.
Strength of phosphorous acid solution = 60 per cent.
Temperature = 24·0° C.
Field strength = 1700 gauss.

Interval.	Titre value with N/10 sodium thiosulphate. Without field.	Titre value with N/10 sodium thiosulphate. Within field.	Change due to magnetic field calculated as the amount of chromic acid reduced.	Remarks.
1/2 hr.	5·20 c.c.	4·45 c.c.	0·0029 gm.	The reduction
3/4 ,, ...	4·20 ,,	3·40 ,,	0·0031 ,,	is accelerated
1 ,, ...	3·70 ,,	2·80 ,,	0·0035 ,,	by the
1½ ,, ...	2·80 ,,	1·60 ,,	0·0047 ,,	field.

The above table shows that the rate of reduction of chromic acid by phosphorous acid is accelerated in magnetic field. Also, further experiments showed that the difference in reduction within and without the field decreases as the strength of the magnetic field is decreased.

5. *The Oxidation of Potassium Iodide by Chromic Acid.*—Delury *, who studied this reaction, found that the rate of the liberation of iodine is approximately proportional to the square of the concentration of the acid.

The rate of the reaction was measured by mixing the two substances in solution, and after some time putting the whole reaction mixture in a large volume of ice-cold water and titrating the iodine liberated. The results are recorded in the table below :—

TABLE V.

Strength of the potassium iodide solution = 40 gms. per litre.
Strength of the chromic acid solution = 12·87 gms. per litre.
Temperature = 25° C.
Field strength = 1700 gauss.

Interval.	Titre value with N/100 sodium thiosulphate. Without field.	Titre value with N/100 sodium thiosulphate. Within field.	Change due to field calculated as the weight of iodine liberated.	Remarks.
1 hr.	11·05 c.c.	11·60 c.c.	0·00007 gm.	The liberation of
2 ,, ...	11·90 ,,	12·70 ,,	0·00010 ,,	iodine is accelerated by the field.

* R. E. Delury, J. Phys. Chem. vii. p. 239 (1903).

The results given in Table V. (p. 465) show that the rate of the liberation of iodine by the action of the chromic acid on potassium iodide is accelerated to some extent. Also it was found that the difference in the amount of iodine liberated within and without magnetic field falls with decreasing strength of the magnetic field.

6. *The Reduction of Potassium Permanganate by Chloral Hydrate.*—It has been proved by Aladar Buzagh * that the reaction between potassium permanganate and chloral hydrate takes place quantitatively.

The velocity of the reaction was measured by the following method:—

A known volume of chloral hydrate (of known strength) was added to a measured volume of potassium permanganate. After a known interval of time the whole of the reaction mixture was added to dilute sulphuric acid and potassium iodide, and as before the liberated iodine was titrated.

TABLE VI.

Strength of potassium permanganate solution = 3·15 gms. per litre.
Strength of the chloral hydrate solution = 250 gms. per litre.
Temperature = 25·0° C.
Field strength = 1700 gauss.

Interval.	Titre value with N/100 sodium thiosulphate. Without field.	Within field.	Change due to magnetic field calculated as the amount of $KMnO_4$ reduced.	Remarks.
10 mts.	18·70 c.c.	18·30 c.c.	0·00013 gm.	The reduction is accelerated by the magnetic field.
45 „	15·50 „	14·60 „	0·00028 „	
2 hrs.	10·50 „	8·30 „	0·00070 „	

From the above results it appears that there is acceleration in the rate of the reduction of potassium permanganate by chloral hydrate in the magnetic field. Also it was found that the rate of reduction changes with the strength of the magnetic field.

In the reactions from Nos. 7 to 10, the magnetic field does not produce any difference in the velocity of reaction. The largest difference observed is 0·30 c.c. after

* Aladar Buzagh, *Matematikai es Termeszettudomanyi Ertesito* xl. p. 134 (1923).

an interval of 1½ hours, and this could be well within experimental error. The methods of estimation and some results are given below:—

7. The Reaction:

$$3FeSO_4 + 5KI + KIO_3 + 3H_2O = 3Fe(OH)_2 + 3K_2SO_4 + 3I_2.$$

8. The Reaction:

$$3CoSO_4 + 5KI + KIO_3 + 3H_2O = 3Co(HO)_2 + 3K_2SO_4 + 3I_2.$$

The velocities were determined by estimating the iodine liberated as in the reaction 5.

TABLE VII.

Field strength = 1300 gauss
Temperature = 21·0°.
Field strength = 1700 gauss.

Reaction.	Interval.	Titre value with N/100 sodium thiosulphate.		Change due to magnetic field.	Remarks.
		Without field.	Within field.		
7.	1/2 hr.	5·10 c.c.	5·10 c.c.	0·00 c.c.	No appre-
	1 „	6·55 „	6·80 „	0·25 „	ciable dif-
	1½ „	7·55 „	7·85 „	0·30 „	ference.
8.	1/4 hr.	5·70 „	5·75 „	0·05 „	No appre-
	1/2 „	6·70 „	6·80 „	0·10 „	ciable dif-
	1 „	7·40 „	7·50 „	0·10 „	ference.
	1½ „	7·90 „	7·90 „	0·00 „	

9. *Oxidation of Hydriodic Acid by Hydrogen Peroxide.*—According to Noyes and Scott *, the oxidation takes place quantitatively according to the equation:

$$2HI + H_2O_2 = I_2 + 2H_2O.$$

The liberated iodine was titrated as in the last reaction.

10. *The Esterification of Acetic Acid by Alcoholic Hydrogen Chloride.*—The course of the reaction was followed by mixing the two solutions, and after a definite time titrating against standard barium hydroxide solution, using phenolphthalein as an indicator.

* Arthur A. Noyes and Walter O. Scott, *Zeit. Phys. Chem.* xviii. p. 118 (1895).

We can now summarize the results obtained so far as below:—

Reaction 1. Reduction of ferric chloride solution containing hydrochloric acid ;

(*a*) with iron .... is accelerated by magnetic field.

(*b*) with aluminium is accelerated by magnetic field.

(*c*) with zinc .... is retarded by magnetic field.

Reaction 2. Dissolution of metals in dilute hydrochloric acid ;

(*a*) the dissolution of zinc is accelerated by magnetic field.

(*b*) the dissolution of iron is retarded by magnetic field.

(*c*) the dissolution of aluminium is not influenced by magnetic field.

Reaction 3. The oxidation of oxalic acid by potassium permanganate is accelerated by magnetic field.

Reaction 4. Reduction of chromic acid by phosphorous acid is accelerated by magnetic field.

Reaction 5. Oxidation of potassium iodide by chromic acid is accelerated by magnetic field.

Reaction 6. Reduction of potassium permanganate by chloral hydrate is accelerated by magnetic field.

Reaction 7. The reaction

$$3FeSO_4 + 5KI + KIO_3 + 3H_2O = 3Fe(OH)_2 + 3K_2SO_4 + 3I_2$$

is not influenced by magnetic field.

Reaction 8. The reaction

$$3CoSO_4 + 5KI + KIO_3 + 3H_2O = 3Co(OH)_2 + 3K_2SO_4 + 3I_2$$

is not influenced by magnetic field.

Reaction 9. Oxidation of hydriodic acid by hydrogen peroxide is not influenced by magnetic field.

Reaction 10. Esterification of acetic acid by alcoholic hydrogen chloride is not influenced by magnetic field.

A close study of the above with the magnetic properties of the reacting molecules enables us to draw some general conclusions. It is evident that the velocity of the reaction is increased in those homogeneous reactions in which the sum of the molecular susceptibilities of the reactants becomes greater as the reaction proceeds.

In Table VIII. we have put together the homogeneous reactions tried by us. Below each of the reactants we have given its molecular susceptibility. In column 2, $\Sigma\chi_{M_i}$ gives the sum of the molecular susceptibilities of the initial substances of the reaction, while in column 3, $\Sigma\chi_{M_f}$ gives the sum for the final products. We have here left out of consideration the case of heterogeneous reactions. The presence

TABLE VIII.

Reaction.	$\Sigma\chi M_i$	$\Sigma\chi M_f$.	Change in reaction.
3. $2KMnO_4+8C_2H_2O_4=2MnC_2O_4$ $+K_2C_2O_4+10CO_2+8H_2O$ $632{\cdot}0+(-482{\cdot}4)\rightarrow 44787{\cdot}6$ $+(-68{\cdot}06)+(+7{\cdot}48)+(102{\cdot}08)$	149·6	44624·96	Acceleration.
4. $2CrO_3+2H_3O+3H_3PO_3=Cr_2O_3$ $+2H_2O+3H_3PO_4$ $150+(-25{\cdot}52)+(-172{\cdot}2)\rightarrow 3800$ $+(-25{\cdot}52)$	−47·72	3774·48	Acceleration.
5. $2CrO_3+2H_2O+H_2O+6KI=Cr_2O_3$ $+3I_2+6KOH$ $150+(-25{\cdot}52)+(-12{\cdot}76)$ $+(448{\cdot}2)\rightarrow 3800+(-182{\cdot}7)$ $+(-117{\cdot}6)$	−336·48	3499·7	Acceleration.
6. $2KMnO_4+3CCl_3CH(OH)_2=2MnO_2$ $+2KOH+3CCl_3COOH$ $632{\cdot}0+(-302{\cdot}86)\rightarrow 4698$ $+(-39{\cdot}2)$	329·48	4658·8	Acceleration.
9. $2HI+H_2O_2=I_2+2H_2O$ $(-79{\cdot}36)+(-32{\cdot}30)\rightarrow(-88{\cdot}90)$ $+(-25{\cdot}52)$	−111·66	−114·42	No appreciable effects.
10. $CH_3COOH+CH_3OH$ $=CH_3.COOCH_3$ $+H_2O(-41{\cdot}4)+(-23{\cdot}68)\rightarrow(52{\cdot}54)$ $+(-12{\cdot}76)$	−65·08	−65·1	No appreciable effects.

NOTE. – In reaction 4 the value of H_3PO_4 is neglected. As it is diamagnetic its value will necessarily be very small and not likely to affect the result in the presence of the strongly paramagnetic substances. Similarly for CCl_3COOH in reaction 5.

of the solid phase in such reactions is a great disturbing factor. Moreover, the kinetics of some of these reactions are not clearly understood. The values of the molecular susceptibilities given in the above table are taken from Landolt and Börnstein's 'Physikalisch-Chemische Tabellen.' A few of the values not given in the tables had to be experimentally determined in the laboratory on a magnetic balance of the Wilson type, as set up in this laboratory for work on electronic isomers*.

It will be noticed that most of the values of the molecular susceptibilities given in the table refer to those of the

* S. S. Bhatnagar and C. L. Dhawan, Phil. Mag. v. p. 536 (1928); S. S. Bhatnagar and R. N. Mathur, Phil. Mag. vi. p. 217 (1928).

substances in the crystalline form and not in solution, which is the form in which the substances exist in the case of the chemical reactions. Epstein * and Gerlach † have shown that the susceptibility of the paramagnetic salts is independent of their being in solution or in the solid state, and that ions, whether in solution or in a space lattice, are arranged relatively to an external magnetic field in accordance with the quantum theory. Also from a study of the values of ionic moments given by Stoner ‡, it is evident that even experimentally determined values do not differ materially from the values deduced from the salts in the solid state.

In the reactions given in Table VIII, Nos. 3, 4, 5, and 6 are those in which the sum of the molecular susceptibilities of the final products is very much larger than that of the initial resultants. In the reactions 9 and 10 the summation values in the two cases are almost the same, and the very small change in the velocities within and without the magnetic field is obviously too small to show any detectable change in the velocity.

With heterogeneous reactions numerical evaluation is much complicated by the very incomplete knowledge we possess of the exact mechanism. In reaction 1 (*a*), for example, the molecular susceptibility of $FeCl_3$ is 14904×10^{-6} (taking mass susceptibility of $FeCl_3 = 91 \times 10^{-6}$ from Townsend's data), and that of $FeCl_2 = 11557 \times 10^{-6}$. In 1 (*a*) where iron is used for reduction the equation can be expressed as

$$2FeCl_3 + Fe \rightarrow 3FeCl_2$$
$$2 \times 14904 \rightarrow 3 \times 11557$$

as iron is used in metallic form, its ionic moment would be zero (or at any rate very small), and so the final product has a greater total susceptibility than the initial. The reaction is accordingly accelerated inside the magnetic field.

In the reaction 1 (*c*) where zinc is used, the final equation most probably is

$$2FeCl_3 + Zn \rightarrow 2FeCl_2 + ZnCl_2$$

as zinc chloride is diamagnetic, the total of the molecular susceptibilities of the final products is less than the initial,

* Epstein, 'Science,' lvii. p. 532 (1923).
† Gerlach, *Phys. Zeits.* xxiv. p. 275 (1923).
‡ Stoner Magnetism and Atomic Structure,' pp. 127–136.

and we find here a retardation in the velocity with the field.

We can now express the results obtained symbolically thus, when

$\Sigma\chi_{Mf} > \Sigma\chi_{Mi}$ the rate of reaction is accelerated by the field . . . . . (1)

and when

$\Sigma\chi_{Mf} < \Sigma\chi_{Mi}$ the rate of reaction is retarded by the field . . . . . (2)

while with

$\Sigma\chi_{Mf} = \Sigma\chi_{M}$ no change within and without the field . . . . . (3)

where

$\Sigma\chi_{Mf}$ = the sum of the molecular susceptibilities of the final products,

and

$\Sigma\chi_{Mi}$ = sum of the molecular susceptibilities of the initial substances

In all the experiments considered so far the case of reduction of ferric chloride with aluminium (1 *b*) stands out an apparent exception for in this case $AlCl_3$ is diamagnetic, and as in the case of zinc the reaction is expected to be retarded. Contrary to this, however, the reaction is accelerated. We can, however, say that in the cases where the metal itself is paramagnetic the reaction is accelerated. For both Fe and Al are paramagnetic. Zn is diamagnetic and the action is retarded. But the data at present are too meagre to say this. Moreover, the complexity of the reaction and the side reactions preclude any closer investigation. In the reactions 7 and 8, it has not been possible to evaluate the susceptibilities of the final products as the values for $Fe(OH)_2$ and $Co(OH)_2$ are still unknown. As, however, the rest of the reactants, except $Fe(SO_4)$ and $Fe(OH)_2$ in 7 and $CoSO_4$ and $Co(OH)_2$ in 8 are all diamagnetic, the values for $Fe(OH)_2$ and $Co(OH)_2$ or for the corresponding oxides should be very nearly equal to that of $FeSO_4$ and $CoSO_4$ respectively. In these cases the relation (3) above seems to hold good.

In the introductory part of this paper reference has been made to a recent paper of Weigle, who has shown mathematically that in the case of a solution placed in a magnetic

field, the concentration of the solution within and without the field is not the same, although the numerical value of this change is very small, being of the order of 10^{-5} for $NiSO_4$ in a field of 10,000 gauss. Yet, it is easily seen that in a mixture of two ions, say, Fe'' and Fe''', the numerical ratio of Fe'' to Fe''' will be quite appreciable and thus is likely to influence the velocity considerably.

Weigle's equation simplified for the case of a mixture of liquids is

$$\frac{n}{n^0} = e^{\frac{\sigma H^2}{2KT}},$$

where n^0 is the concentration when $H=0$ and n the concentration inside the field of strength H gauss σ is

$$\frac{\chi_M}{N};$$

χ_M being the molecular susceptibility and N Avogadro's number. k is Boltzmann's constant and T the absolute temperature.

We may now consider our reactions in the light of this equation. For this purpose the reaction 4 can be written in the skeleton form thus:

$$CrO_3 \rightarrow Cr_2O_3$$

$$\chi_M \text{ for } CrO_3 = 0{\cdot}75 \times 100 \times 10^{-6} = 75 \times 10^{-6}$$

therefore
$$\sigma_1 = \frac{75 \times 10^{-6}}{60{\cdot}6 \times 10^{22}} = 1{\cdot}25 \times 10^{-28}$$

$H=1300$ gauss, $T=297$ abs., $K=12{\cdot}5 \times 10^{-17}$

therefore
$$\frac{n_1}{n^0{}_1} = e^{28 \times 10^{-8}}$$
$$= 1{\cdot}000{,}000{,}003 \text{ nearly.}$$

Similarly for Cr_2O_3

$$\frac{n_2}{n^0{}_2} = e^{10{\cdot}52 \times 10^{-8}}$$
$$= 1{\cdot}000{,}000{,}1 \text{ nearly.}$$

If we assume that the concentrations outside the field are the same, *i.e.*, $n_1{}^0 = n_2{}^0 = n^0$ (say)
we have

$$\frac{n_1 - n_1{}^0}{n_2 - n_2{}^0} = \frac{3}{100}.$$

That is the final product of reaction Cr_2O_3 tends to concentrate about 33 times more in the field. As the field near the poles is strongest, it is probable that the largest concentration of the more paramagnetic ions will be found in their vicinity, leaving their concentration less in the rest of the space. As this space will in all probability be more extensive, the velocity of forward reaction in this space will certainly be greater, and we might reasonably expect a net increase in the forward velocity from this point of view alone. This increase in the forward reaction would always take place when molecular susceptibility of the final products is greater than that of the initial. In the reaction considered above, only the concentrations of the chief constituents have been considered. The presence of other ions is also likely to affect the results. But wherever large changes in the susceptibility of the chief constituents are involved and the other ions are either feebly para- or diamagnetic, we may be justified in neglecting them and considering only those having large paramagnetic values.

In the present investigation great care was taken to select only those reactions which involve large changes in susceptibility, for it is only in those cases that changes in the velocity would be large enough to be detected chemically

In the above consideration, based on Weigle's equation of changes in the concentration near the strongest parts, we find an explanation also for observations of Parker and Armes *, who noticed that in their reaction by keeping the liquid under constant stirring the change in velocity became much less. This was also noticed by us and so in our experiments particular care was taken to stir the solution only at fixed intervals, and only as much as was necessary to ensure a more or less homogeneous progress of reaction. It has also been noticed in confirmation of the above that in those strongly paramagnetic salts where precipitates are formed, the precipitate has a strongly marked tendency to concentrate near the poles.

* Parker and Armes, *loc. cit.*

University Chemical Laboratories,
University of the Punjab,
Lahore, India.
29th January, 1929.

L. *On the Variation with Temperature of Contact Electromotive Forces.* *By* J. J. McHenry, *M.A., M.Sc.**

IN a previous paper † experiments were described which suggested that the contact difference of potential between clean metals was proportional to the absolute temperature. In most of the work the metals used were copper and zinc, but experiments were also made with copper and aluminium and also with copper and tin, in which the contact potential differences were shown to obey approximately the above law. The metal surfaces experimented with were made as clean as possible by scraping with steel tools or emery paper, and were in contact with dry air at atmospheric pressure. The method used was the "null ionization method." This method, which had previously been used by Greinacher ‡

Fig. 1.

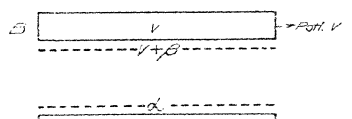

and Anderson & Bowen §, was used in some of the experiments described in this paper and the older condenser method was used also. A short description of both methods will now be given.

Consider two metals A and B (fig. 1). Let the interior of the metal A be at zero potential, and let it be insulated. Then a point just outside the metal is at a different potential α. This potential α is called by workers on photo-electricity the "intrinsic potential" of the metal A and is shown by them to be negative. Let the second metal B be maintained at a potential V and let its intrinsic potential be β. Just outside the metal B, the potential is then $V+\beta$. In general there is a difference of potential between the regions just outside the metals, or in other

* Communicated by the Author.
† Phil. Mag. iii. April Suppl. 1927.
‡ *Ann. der Physik*, xvi. p. 708 (1906).
§ Proc. Phys. Soc. Lond. xxiii. pt. 5 (1911).

words, there is an electric field in the space between the plates. If $V=0$, this potential difference is $\alpha-\beta$ and is called the contact potential difference between A and B. If $V=0$, the potential difference in the field between the plates is $\alpha-\beta-V$, and therefore vanishes when V is equal to $\alpha-\beta$, that is, when V is equal to the contact potential difference. In this case if there is ionized air between the plates no current flows, so that the insulated plate A remains at zero potential, and if joined to a quadrant electrometer in the usual way, no motion of the electrometer needle takes place.

In the condenser method, when $V=\alpha-\beta$, and there is no field between the plates, a relative motion of A and B produces no change in the potential of A, so that if V be

Fig. 2.

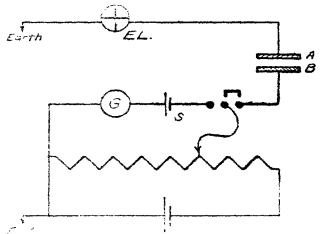

altered until this is so. V is equal to the contact potential difference. In our experiments V was varied by means of a potentiometer, the readings of which were checked against a standard cell. The electrical connexions for the "null ionization method" and the "condenser method" are shown in fig. 2, in which G is a sensitive galvanometer and S the standard cell.

In many of the experiments described in the previous paper (*loc. cit.*), the electromotive force of contact (E) varied in such a way with temperature that E was approximately equal to $T\frac{dE}{dT}$ where T is the absolute temperature. The graph of E against T was in general a straight line which if produced would pass through a temperature near absolute zero. In other experiments deviations from the above law were noticed and in particular it was

frequently observed, when the cell was warmed and cooled, that the graph of E against T instead of being straight was a closed loop, the values of E being smaller for ascending temperatures than for descending temperatures. This effect is shown in fig. 3 with the metals copper and nickel and in its most marked form in fig. 4 with the metals copper and tin. The arrows indicate the order in which the readings shown in the graphs were taken. In all these cases a copper vessel was the outer electrode and it was completely covered with water. The water was slowly heated by a Bunsen burner placed underneath, and

Fig. 3.

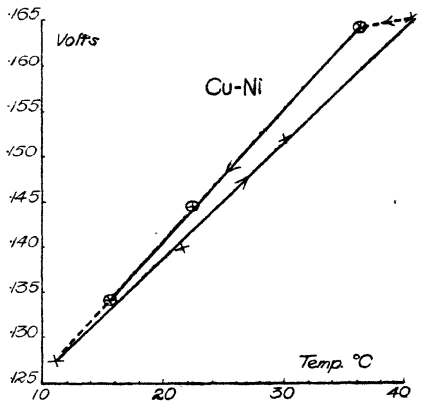

the temperature of the copper vessel and that of the inner electrode taken to be the same as that of a thermometer in the water. In general about eight readings were taken, at intervals of approximately one hour. It was thought that the "hysteresis" effect illustrated in figs. 3 and 4 might be due to a difference in temperature between the inner and outer electrodes, in spite of the time allowed for temperature equilibrium in the cell. If the inner electrode was appreciably cooler than the outer when the cell was being warmed and warmer when the cell was being cooled, the curved nature of the graphs shown could be explained. It was therefore thought advisable to change the mode of

experiment, and to alter the temperature of one electrode only. In this case $\frac{dE}{dT}$ is the rate of change of the intrinsic potential of one metal with temperature.

The new apparatus is shown in fig. 5, which is drawn to scale. The outer electrode is a stout copper vessel and lid, and the inner electrode is hollow so that its temperature could be varied by pouring in warm or cold water. A thermometer placed in this water and resting on the

Fig. 4.

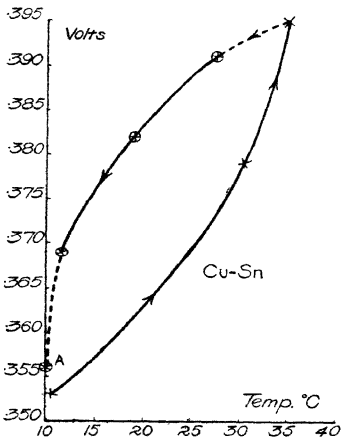

bottom of the inner electrode gave its temperature. The outer vessel was immersed in water, and its temperature taken with a second thermometer. The upper level of the water is shown dotted in the figure. A tube running from the copper vessel was connected with drying tubes containing metallic sodium and calcium chloride. Inner electrodes of copper, zinc, and aluminium were used. The air inside was ionized by a tube of radium bromide which was contained in a small jacket of copper. The inner electrode was joined by a soldered connexion to the screened electrometer leads. In the case of aluminium a platinum wire was welded to the aluminium vessel and

the wire soldered to the leads. The upper portion of the inner electrodes passed through an earthed copper tube, being insulated from the latter with sulphur which is marked S in fig. 5. Care was taken to fill up as much as possible of the space between the leads and the earthed tubes surrounding them with paraffin wax, so that

Fig. 5.

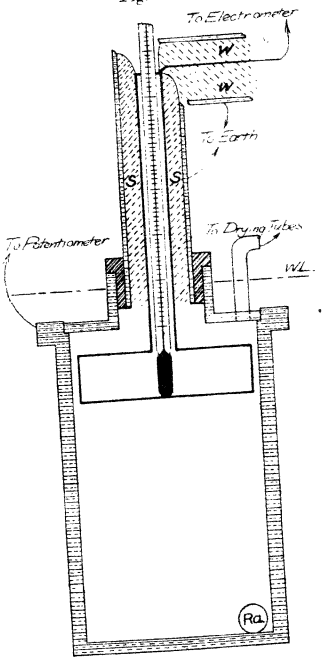

ionization of the air outside by the γ-rays which penetrated the copper vessel and lid might not affect the readings. The outer vessel was about 6 mm. thick, and the lid about 3 mm.

In experiments made with this new cell, when the inner electrode contained warm water, its temperature dropped slowly owing to loss of heat to the cold outer vessel, and

in consequence its temperature was taken before and after each reading and the mean of these temperatures, seldom differing by more than two degrees, was taken as the temperature of the inner electrode when the potential difference was being read.

Table I. and fig. 6 show the results of an experiment in which the inner electrode was made of zinc. The copper was kept at constant temperature, and the zinc was warmed and cooled. All temperatures are given in degrees centigrade.

TABLE I. (Fig. 6.)

Temp. of Copper.	Temp. of Zinc.		Mean temp. of Zinc.	E.M.F. (Volts).
	Before.	After.		
13·5	13·5	13·5	13·5	·518
13·4	24·5	23·4	24·0	·537
13·5	36·4	32·0	34·2	·568
13·5	33·5	32·1	32·8	·565
13·7	30·3	29·0	29·7	·562
13·4	26·6	25·5	26·1	·555
13·5	18·1	17·6	17·9	·533
13·8	13·5	13·5	13·5	·520

Fig. 6.

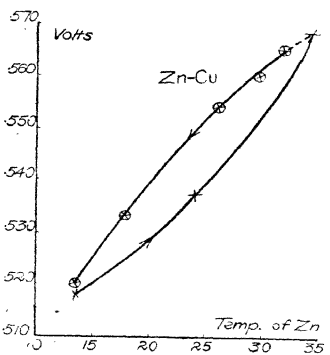

It will be seen from fig. 6 that the graph showing the relation between the e.m.f. and the temperature of the

zinc is a closed loop and not a straight line, so that the "hysteresis" noticed in the previous experiments is real, and cannot be explained by assuming an error in reading the temperature of the zinc electrode. The contact difference of potential, in these experiments where the

TABLE II. (Fig. 7.)

Temp. of Copper.	Temp. of Zinc before reading E.	Temp. of Zinc after reading E.	Mean Temp. of Zinc.	E.
12·1	12·1	12·1	12·1	·513
12·2	35·2	33·7	34·5	·565
12·2	34·5	32·4	33·5	·576
12·3	34·1	31·7	32·9	·569
12·4	34·6	32·1	33·4	·577
12·7	13·0	13·0	13·0	·526
12·7	13·2	13·2	13·2	·521
12·7	13·1	13·1	13·1	·519
12·8	13·0	13·0	13·0	·515
12·8	12·93	12·9	12·9	·515

Fig. 7.

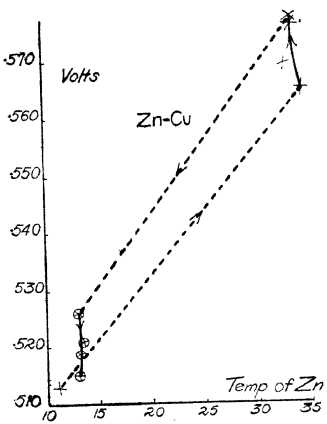

surfaces are in contact with air, depends not only on the temperature, but also on the previous treatment of the surfaces, and when the temperature of the metals is

altered the resulting change in the contact potential difference is not immediate but takes a very appreciable time to be complete. These facts are more clearly shown in other experiments, the results of which are given in Tables II. and III. and illustrated in figs. 7 and 8. In these readings the value of E, the contact potential difference between copper and zinc, was taken when both metals

TABLE III. (Fig. 8.)

Temp. of Copper.	(Mean) Temp. of Zinc.	E.	Time between Readings.
14·0	14·1	·682	5 minutes
14·0	37·5	·702	
14·3	37·6	·722	1 hour
14·8	38·2	·730	
14·9	25·0	·721	—
14·9	15·2	·709	—
13·2	13·2	·681	taken next day

Fig 8

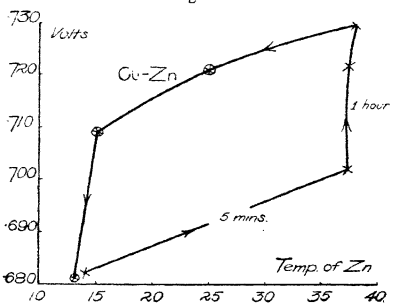

had been for some time at room temperature. Then the temperature of the zinc inner electrode was suddenly raised about 20 or 30 degrees, and maintained at this higher temperature for an hour or two. During this time the values of E were read, the first reading being taken about five minutes after the zinc was warmed. Cold water was then poured into the inner electrode to replace the warm

water, and with both electrodes at room temperature further readings of E were taken at intervals.

It is of interest to compare figs. 7 and 8. In the former the value of E is for all temperatures considerably lower than in the latter, so that in fig. 7 the zinc surface is somewhat "aged" or tarnished. In this case the response of E to a change of temperature is greater and quicker than for the cleaner metal of fig. 8. In fig. 7 the value of $\frac{dE}{dT}$ for a quick change is ·0023 volt/degree, and for a slow change ·003 volt/degree. In the experiment illustrated in fig. 8, and made with exactly the same apparatus as in fig. 7, the corresponding values of $\frac{dE}{dT}$ are ·00085 and ·0021 volt/degree.

Fig. 9.

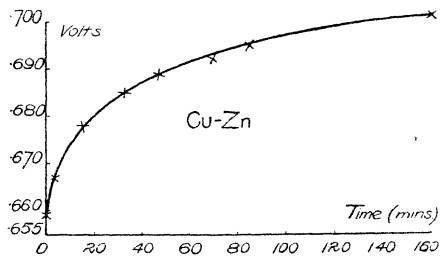

Fig. 9 shows how the contact potential difference between zinc and copper changes with time when the zinc has been suddenly warmed and kept at the higher temperature. E was read at room temperature. Then warm water was poured into the zinc electrode and the temperature raised to about 40° C. E was again read as quickly as possible, the first reading being completed about four minutes after the warm water was poured in. The temperature of the zinc was maintained at about 40° C. for nearly three hours and the e.m.f. measured every few minutes. The graph shows that complete equilibrium at the higher temperature is not attained even after 160 minutes.

In all the experiments, the cell returns after heating to its original state, the value of the e.m.f. at room temperature being the same at the end as at the beginning of the

experiment. The changes observed cannot, therefore, be explained by oxidation or reduction, as such chemical actions would hardly be reversible. On the other hand, since the value of E in all the experiments is less than the value obtained immediately after the metals are cleaned, it is possible that the effect of warming the metals is simply to drive out adsorbed gas or vapour, and that this change is reversed on cooling. This would agree with the result mentioned above that the change with temperature is smaller for clean metals than for metals which are more "aged." If this explanation is correct, heating would cause

Fig. 10.

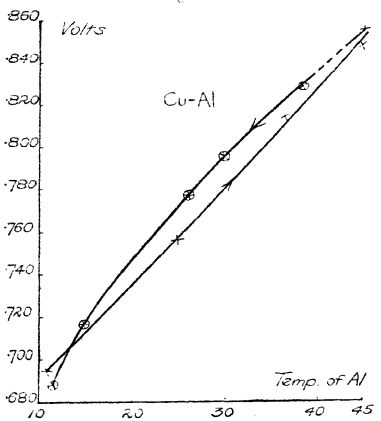

no appreciable change of the contact potential difference between copper and zinc if these could be experimented with immediately after being cleaned, and before the adsorbed layer of gas or vapour is formed. This point is referred to later in this paper.

The behaviour of aluminium is similar to that of zinc, and is illustrated in figs. 10 and 11. In the former the copper was kept at constant temperature, and the aluminium inner electrode warmed and cooled and readings of the e.m.f. taken at different temperatures between 11° C. and 46° C. The whole series of ten readings was

taken in about two hours so that approximately twelve minutes elapsed between one reading and the next. The points lie so nearly on a straight line that the hysteresis effect might easily escape detection, but it is shown to be present in the experiment illustrated in fig. 11, which gives the readings taken with exactly the same apparatus three days later. The time that passed between pouring of the warm water into the aluminium electrode and taking the first reading was about five minutes, and the readings between B and C in the graph took about fifty-two minutes.

Fig. 11.

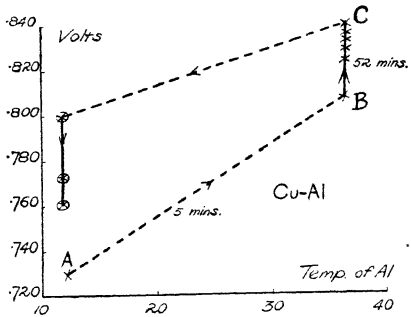

The value of $\frac{dE}{dT}$ from fig. 10 is ·0047 and in fig. 11 ·0045 volt/degree for a slow change. For a sudden change (AB) in fig. 11 $\frac{dE}{dT}$ is ·0032 volt/degree.

Zinc and aluminium become more electro-positive when heated, since the e.m.f. of the cell then increases. In other words, the absolute value of their intrinsic potentials diminishes as the temperature increases, by ·0045 volt/degree in the case of aluminium and by between ·0021 and ·003 volt/degree in the case of zinc. Experiments made with the hollow copper electrode showed that this metal became more electro-negative when heated, and by ·00074 volt/degree. In these experiments the inner electrode of copper was a few hundredths of a volt electro-positive to the outer copper vessel. Heating the inner vessel caused the e.m.f. to diminish, whereas in the

experiments with zinc and aluminium heating the inner electro-positive electrode caused the e.m.f. to increase. On the other hand, when the outer electro-negative electrode was heated the e.m.f. increased, so that the outer copper vessel also became more electro-negative when heated, and by ·00067 volt/degree. Heating the cell as a whole caused practically no change in the e.m.f., a rise of temperature from 15° C. to 39° C. causing the e.m.f. to increase from ·0297 volt to ·0305 volt.

The fact that copper becomes more electro-negative when heated, whereas aluminium and zinc become more electro-positive, is very striking, no matter to what causes we attribute the changes.

Surfaces under oil.—Condenser method.

We have mentioned as a possible explanation of the hysteresis effect noted with zinc and aluminium that the whole or part of the change of the contact effect with temperature which occurs with these metals, may be simply due to the removal of surface impurities such as adsorbed gas or water molecules. If this explanation is correct the contact potential difference between two metals should become independent of temperature when all the surface impurities are removed, and this constant value should be the same as that between two freshly cleaned metals. In our experiments the temperature could not be raised above about 50° C. owing to the use of wax in sealing the cell. It was, however, generally noted that the nearer the observed value of the e.m.f. was to that obtained with freshly cleaned metals, the smaller was the change on the e.m.f. with temperature. In illustrating this point we give the values of E and $\frac{dE}{dt}$ for zinc and copper in a number of experiments in which both metals were heated.

TABLE IV.

E.M.F. Zn—Cu at 12°C.	$\frac{dE}{dT}$
·565	·00213
·693	·00195
·716	·0014
·706	·0015
·703	·0011

In one experiment with copper and tin, a clean pair of surfaces seems to have been realised. The e.m.f. at 13·3° C. was ·471 volt and on warming the cell this value increased by about ·0012 volt per degree. When a temperature of 41° C. was reached the value of E was ·504 volt. On cooling the cell to 31° C. and further to 11·8° C., E remained practically unchanged at ·505 and ·503 volt. The next day, at 12° C., the e.m.f. was ·5015 volt, so that in the cooling part of the experiment the value of $\frac{dE}{dt}$ was practically zero, and the metals clean as indicated by the high value of the e.m.f.

We shall now give an account of attempts made to produce clean metal surfaces and to keep them from tarnishing. The metals were cleaned in air and then immediately placed under liquid paraffin. In some cases the metals were cleaned under the paraffin so that the new surfaces did not come into contact with air. The potential difference of contact was then measured by the condenser method. In an experiment where the electrodes were an aluminium plate and a copper vessel the potential difference at 17° C. was at first ·97 volt. On heating the apparatus to 41° C. this p.d. fell to ·94 volt, and fell further to ·80 volt when the cell was cooled to 16° C. At this stage further heating and cooling showed that the surfaces seemed to have become steady, as the graph of the contact p.d. against temperature became a straight line, the value of $\frac{dE}{dT}$ being ·0036 volt/degree.

The apparatus was then left standing for two days and when experimented with at the end of that time the surfaces were found to have changed considerably. The p.d. had decreased to ·58 volt at room temperature. At this stage the mere mechanical disturbance of the oil necessary in taking readings by the condenser method caused the measured value of the p.d. to increase from ·58 volt up to a final steady value of ·70 volt. On warming the apparatus the relation between the p.d. and the temperature again became nearly linear over the same values as were found in the experiment of two days before. The value of the p.d. at 62° C. was ·965 volt. Further heating made the oil conducting and at a temperature of 112° C., using a method similar to the ionization method,

the p.d. was found to be 1·074 volts, which is approximately the value obtained by other experimenters with newly cleaned aluminium and copper. The melting of the sulphur prevented us from warming the cell still further.

It will be seen, then, that the ageing or tarnishing of the metal surfaces takes place under the oil just as readily as in air, and the experiments gave no definite answer to the question whether the changes of the p.d. observed with changes of temperature were due to the removal of surface impurities or not. Drying the oil for a long time with sodium wire made no difference, the metals could not be made to keep their initial high value of the contact p.d.

Discussion of Results.

Before discussing the results, it is desirable to give an account of the work of other experimenters. In particular, we shall refer to papers by Erskine Murray *, Burbridge †, and Millikan and Winchester ‡.

In Erskine Murray's experiments the condenser method was used. The temperature of one plate of the condenser was varied, that of the other plate being kept constant. The following table gives some of his results.

Metal.	Treatment of Surface.	Range of Temp. used.	P.d. agst. Gold plate at 16° C. (volts).	Variation of p.d. for a rise of 1°C.
Al.	Polished on glass paper	16—50	1·10	+·0043
Al.	Waxed	16—40	·98	+·0032
Al.	Washed Alcohol... ...	—	1·30	+·0045
Zn.	Cleaned glass paper ...	—	·73	+·0013
Sn.	Cleaned glass paper ...	—	·52	—·0010
Ag.	Cleaned glass paper ...	—	·12	—·0007
Cu.	Cleaned emery	16—30	·04	Small
Cu.	Cleaned emery	30—60	—	+·0015
CuO.	—	—	—·11	—·0016

Erskine-Murray does not mention any hysteresis effect. The value of $\frac{dE}{dt}$ for aluminium, +·0045 volt/degree, is the same as that obtained by us for a slow change. The value ·0013 volt/degree given by him for zinc is intermediate

* Phil. Mag. xlv. p. 398 (1898).

† Burbridge, Phys. Rev. 2nd Series, ii. Sept. (1913).

‡ Millikan and Winchester, Phil. Mag. xiv. p. 201 (1907). Millikan, Phys. Rev. 2nd Series, vii. p. 18 (1916). Or "Atomes et Électrons" (Institut International de Physique Solvay (1923)).

between the values obtained by us for slow and rapid changes. He does not seem to have put the metals through a cycle of temperature. He states that the changes are not due to alteration in the amount of oxygen in the plates.

Burbridge (*loc. cit.*) also used a variable condenser method and the following table gives his results.

Metal.	Range of Temp.	Change of p.d. for 1° C.
Cu.	20—70	·00050
Ni.	20—90	·00086
Zn.	20—55	·0024
Sn.	20—45	·00096
Sn.	45—90	·0020
Al.	20—40	·0011
Al.	40—70	·0023
Al.	70—90	·0036

Burbridge states that oxidation effects were noticeable which have to be allowed for in estimating the changes due to rise of temperature. He does not mention any differences in sign between the temperature coefficients of the various metals, nor does he seem to have observed any "hysteresis" effect. It is possible that the latter may have been present in his experiments with tin and aluminium as the graph of temperature against potential difference given by him for these metals is curved.

Millikan (*loc. cit.*), who worked with metal surfaces in a vacuum, states that all photo-electric phenomena are independent of temperature, and in particular, that the "stopping potentials" are independent of temperature. The stopping potentials are the differences of potential which, maintained between the illuminated metal and the Faraday cylinder, are sufficient to prevent photo-electrons from reaching the cylinder. He deduces that the contact differences of potential are independent of temperature, but his experiments and those of Richardson & Compton * and Page † confirm the existence of a real contact or Volta effect between metals. It is of interest, also, that the values of the contact differences of potential obtained by these experimenters who worked with metal surfaces in a vacuum are practically the same as those got by experiments performed with metal surfaces in air.

* Phil. Mag. **xxiv.** p. 592 (1913).
† Amer. Jl. of Science, **xxxvi.** p. 501 (1913).

In connexion with Millikan's experiments, it may be pointed out that if the stopping potentials are independent of temperature, this merely proves that the intrinsic potential or voltaic character of the Faraday cylinder does not alter. The Faraday cylinder is made of oxidized copper. The "stopping potential" depends only on the frequency of the light used and on the nature of the Faraday cylinder or receiving electrode, and is independent of the nature of the illuminated metal. This was proved experimentally by Page (*loc. cit.*) and verified by Millikan. It would seem undesirable to assume that the result proved for a copper-oxide surface holds also for all pure metals.

Experiments were performed by us to determine the temperature coefficient of the intrinsic potential of a surface of copper oxide. It was found that a rise of temperature of 1° C. caused the surface to become more electro-negative, by between ·0012 and ·0008 volt. A rise of temperature of 100° C. should therefore cause a change of about one-tenth of a volt in the stopping-potentials in Millikan's experiments. The least change that could be detected in his experiments was a change of "some hundredths of a volt."

On the one side then, Millikan's experiments and the electronic theory of O. W. Richardson * demand that the intrinsic potentials of metals and the Volta effect are independent of temperature if changes of the order of those met with in thermo-electricity be neglected. On the other hand, the application of thermodynamics to the ionized air cell † and a more direct thermodynamical proof by Foa ‡ supported by the experiments of Erskine-Murray, Anderson, Burbridge and the author, indicate a much larger variation with temperature of the Volta effect. It must be emphasized that the latter experiments were all performed with metal surfaces in contact with air.

In connexion with the result obtained by us that the voltaic character of the metals zinc and aluminium takes an appreciable time to respond to temperature changes, some reference is relevant to the experiments of Perucca § and Bibesco ‖. From his experiments on the voltaic

* 'The Emission of Electricity from Hot Bodies.'
† Anderson, Proc. Phys. Soc. Lond. xxiv. pt. 2 (Feb. 1912).
‡ *Nuov. Cim.* iii. (1926) or *Journal de Physique*, Mars 1927, p. 152 D.
§ Phil. Mag. (Feb. 1928) or *C. R.* clxxv. p. 519 (1922).
‖ *Annales de Physique* (Mai–Juin, 1925).

character and surface tension of mercury, Perucca finds that a mercury surface, freshly formed in vacuo, attains immediately a stable state of least potential energy in which the surface tension and intrinsic potential have definite values. When the surface is formed in a gas the surface tension and intrinsic potential are initially very high, but change and reach the values of the vacuum-formed surface after the lapse of a time which increases with the gas pressure. He concludes that the bombardment of the surface by the gas retards the orientation of the mercury molecules necessary for the production of a stable condition of least surface potential energy. The presence of the gas, however, does not alter the final condition of the surface. A similar reason may explain the lag or "hysteresis" effect noted in this paper.

In conclusion, taking the values of the changes in the intrinsic potentials of aluminium, zinc and copper found in our experiments, we can deduce the changes in the contact potential difference between two of the metals when both are heated or cooled. The temperature coefficients of the intrinsic potentials of Al, Zn, and Cu were found to be (taking the maximum values) $+\cdot0047$, $+\cdot0030$, and $-\cdot0007$ volt per degree centigrade respectively. The contact potential difference between aluminium and copper should therefore increase by $\cdot0054$ volt per degree, and that of zinc and copper by $\cdot0037$ volt per degree. Consequently, calling the contact potential difference E, and the absolute temperature T, the value of $T\frac{dE}{dT}$ for Al—Cu at 17° C. would be 1·57 volts and the value for Zn—Cu ·97 volt. The value for $\frac{dE}{dT}$ obtained from these experiments does not, therefore, satisfy the equation $E=T\frac{dE}{dT}$, as the experimental values of E for Al—Cu and for Zn—Cu are generally found to be for new surfaces about 1·1 volts and ·7 volt respectively. The experimental value of $\frac{dE}{dT}$ is, however, of the same order of magnitude as that given by the equation.

The experiments performed with aluminium and copper under liquid paraffin are in better agreement with the equation, but the "ageing" of the surfaces which takes

place even under the oil renders the experiments unsatisfactory.

Summary.

The changes with temperature of the voltaic character of aluminium, zinc, and copper were examined, the metal surfaces being in dry air at atmospheric pressure. For a slow rise of temperature of 1° C. aluminium and zinc become more electro-positive by ·0047 and ·003 volt respectively. Copper, on the other hand, becomes more electro-negative by ·0007 volt/degree.

The changes with temperature of the voltaic character of the metals are not instantaneous, but take several hours to be complete.

It is found that $\frac{dE}{dT} > \frac{E}{T}$ where E is the contact difference of potential between a pair of the metals and T the absolute temperature. Taking the maximum values of $\frac{dE}{dT}$, it is found that they are roughly 40 or 50 per cent. higher than the values of $\frac{E}{T}$.

Experiments are described with metal surfaces under liquid paraffin in which the condenser method was used. The results are compared with those of other experimenters.

University College, Galway.

LI. *The Quantum Theory as a Problem in Lines of Force.* *By* C. D. Niven, *Ph.D., Toronto* *.

I. *General Introduction.*

THE tendency in physics at the present day is to make an assumption, and from that assumption to work out a mathematical theory. Following such a practice, Professor Planck discovered the Quantum Theory at the beginning of the present century; more recently the wave mechanics have been developed in a somewhat similar manner. Practically no attempt has been made to give a physical explanation of the Quantum Theory, and, although the

* Communicated by the Author.

wave mechanics have been strikingly successful in explaining facts, the mathematics are sufficiently involved to obscure the physics of the theory. In the following paragraphs an endeavour is made to express a point of view with regard to the Quantum Theory.

Suppose an electron be imagined as a point, having lines of force starting in all directions from it, and a proton or positive nucleus as a point on which these lines can terminate; such a picture is practically what Faraday visualised in his theory of lines of force. When an electron is at rest in free space, the lines of force extend to infinity in all directions; if we consider a proton brought near the electron, the lines of force will become "bunched" together around the line joining the electron and proton, with the result that fewer lines go out to infinity. Close to the electron the lines of force start in all directions, but farther out they are bent round so as to run parallel to the axis of the doublet—as the line may be termed which joins the proton and electron. The effect of bringing the electron closer up to the proton, on that part of a line of force which is near to the electron, is to make it swing round towards the direction of the axis, while the effect on the portion of the lines of force far out from the electron, and which is already running almost parallel to the axis, is to displace the line of force laterally towards the axis. When, therefore, an electron is brought near a proton, the lines of force tend to swing round and group around the axis; when the charges are separated the lines of force are released again. If now instead of bringing charges from infinity, two balls are taken at a distance "l" apart and positive and negative charges gradually piled on to them, the effect in the region midway between the balls is similar to the effect of bringing the balls fully charged from infinite distances in either direction.

Mathematically, two simple harmonic motions at right angles are equivalent to a circular motion; and therefore mathematical reasoning applied to the electric doublet of variable moment $el \sin nt$ was considered applicable also to the case in which the negative charge described a circle around the positive charge as centre. Although it would appear from our ideas of lines of force that there should be a similarity, yet the case of the hydrogen atom shows that an electron revolving about a nucleus does not emit

radiation. Furthermore, in the previous paragraph it has been pointed out that when positive and negative charges are piled on to two balls gradually, there is a gradual crowding together of lines of force in the region between them. In the case of the one charge revolving around the other, there is no such gradual crowding together. This crowding together seems therefore to have something to do with the emission of radiation, especially as the alternate crowding together and releasing of lines of force would resemble the condensation and rarefaction of air in the emission of sound.

In the treatment of the Hertzian oscillator the varying double $el \sin nt$ can be written in two ways $e \times l \sin nt$ and $l \times e \sin nt$. Although mathematically similar, they have different physical meanings; $e \times l \sin nt$ means that the charge remains constant throughout the motion but the length varies, and $l \times e \sin nt$ means that the length remains constant but the charge varies. If the expression $e \times l \sin nt$ be the correct way of writing the moment of the doublet then the circular motion of one charge about another might emit radiation; but if $l \times e \sin nt$ be right then the motion of one charge in a circle around another should not be connected to the motion in the Hertzian oscillator. In this communication it is to be taken that $l \times e \sin nt$ is the correct way of writing the expression for the moment of the electric doublet; the reason for this conclusion is drawn from what has been pointed out in the last paragraph, namely that the alternate crowding together and releasing of lines of force resembles the condensation and rarefaction of air in sound. Indeed, one might most easily visualise the process of radiation by imagining a "condensation" and "rarefaction" of lines of force; at the same time it must be pointed out that a "rarefaction" of lines of force simply means a condensation of lines of force in the opposite direction. Another important difference between the wave motion set up by the condensation of lines of electrical force and that set up by the condensation of air is that when the wave in the case of air passes a molecule of air, that molecule moves along with and against the direction of motion of the wave front; in the electrical case, if an electron is encountered by the wave, it moves along the direction of the lines of force, which are pointed first in one direction and

then in the opposite one, but are always perpendicular to the direction of motion of the wave front. As was pointed out when the problem of the Hertzian oscillator was treated many years ago, this transverse motion was demanded by the phenomenon of polarized light. What, however, was not pointed out at that time was that a wave of light was a true wave of condensation and rarefaction, not however of particles of æther but of lines of force. Before leaving the subject of the Hertzian oscillator, it may be of interest to quote from Hertz's own book*, where in explaining the Hertzian oscillator graphically, he writes, "But from the time $t=0$ onwards, such lines of force begin to shoot out from the poles"; and later, "At this time the electrostatic charge of the poles is at its greatest development; the number of lines of force which converge towards the poles is a maximum." From these remarks it would appear that Hertz had in view varying charge, not varying length. The two points of view are not the same, so far as the medium between the poles is concerned; for, in the case where the charge varies, when the doublet has its maximum value, the condensation of lines of force is a maximum; while, if the length varies, when the doublet has its maximum value the condensation of lines of force has its minimum value; in the latter case the maximum condensation of lines of force is reached when the doublet has moment zero; at that instant the condensation is theoretically infinite. The difference between the two cases could be illustrated by plotting density of lines of force against time. In the case where the charge varied, the curve would resemble a sine curve, but if the length varied, the curve would resemble a cosecant curve.

If the important part of the Hertzian oscillator be the condensation of lines of force between the poles, then it is clear that circular motion of one charge around another is a different type of problem, for in that case the density of lines of force remains the same but there is merely a change in direction of the lines of force; yet it would appear that if all the lines of force from the negative charge did not terminate on the positive charge, there might conceivably be some loss of energy; so in the treatment of the hydrogen atom it will be assumed that all lines of force from the electron are pulled round to terminate on the proton, when the atom is in its normal state.

* Hertz, 'Electric Waves,' chap. ix. pp. 146–147.

II. *The Bohr Model of the Atom and Emission of Light from Discharge Tubes.*

If it be assumed that the operation of the Hertzian oscillator is correctly described above, one must not apply any of the results obtained from the old theory of the Hertzian oscillator to the problem of an electron in an orbit. The case of an oscillator which has two simple harmonic motions at right angles, working similarly to a Hertzian oscillator having one simple harmonic motion, is somewhat like the case of an electron describing a rectangular hyperbola, and not like a hydrogen atom. The wave mechanics has solved most of the problems of orbits and at the present day little attention is paid to the classical methods; yet, in spite of the spectacular success of the wave mechanics, the theory has done very little towards explaining the meaning of the quantum theory. The wave mechanics method has introduced new hypotheses; working from these, results have been obtained agreeing excellently with experiment and the reality of the quantum theory has been more firmly established than ever. Unfortunately, the new hypotheses do little to elucidate the physical meaning of the quantum theory. In the following paragraphs an attempt is made to attach a physical meaning to the quantum theory, but this does not express a disbelief in the wave mechanics; the problem is approached from an entirely different standpoint, namely, to attach a physical meaning to a few of the most fundamental principles of the quantum theory.

The work of Wilson and Sommerfeld showed that the basic assumptions in dealing with the Bohr hydrogen atom should not be to quantize the energy and the angular momentum, but to put $\oint p_i dq_i = n_i h$. Working from the Wilson-Sommerfeld conditions, one could deduce the older ones. If the conception of lines of force is to be of any use whatever, we must make assumptions of such a nature that they will lead to some of the fundamental rules for quantization and to do this it seems reasonable to employ the Ehrenfest Adiabatic Principle at this point, and in the equation $2TE_{xin} = \text{const.}$ put the constant equal to "h," and endeavour therefrom to deduce some of the rules of quantization.

When the electron in the hydrogen atom is revolving in the orbit of lowest energy level, the lines of force can be supposed as all bunched together around the line joining the electron and proton; as the electron revolves in its orbit these lines move round too and there is an angular momentum. On the Bohr assumption, we have $mav = \frac{h}{2\pi}$. Again, the kinetic energy is equal to $\frac{mv^2}{2}$,

therefore $$E_{kin} = \frac{v}{2a} \cdot mav = \frac{v}{2a} \cdot \frac{h}{2\pi}.$$

But the time of revolution

$$(T) = \frac{2\pi a}{v},$$

therefore $$2TE_{kin} = 2 \cdot \frac{2\pi a}{v} \cdot \frac{v}{2a} \cdot \frac{h}{2\pi}$$
$$= h.$$

It seems as though with a given kinetic energy the lines can travel absolutely frictionlessly through the space around the nucleus, but cannot exceed a certain angular speed. The constant in Ehrenfest's equation for the case we have taken is "h." Let us now consider an electron at infinity brought to the proton and calculate the time the lines of force starting from the electron will take to move round so that all end on the proton, compared with the time taken for the revolution of an electron about a proton as in the problem just discussed. The lines of force near the line joining the electron and proton and directed towards the proton do not move at all, while the ones pointing away from the proton have to move through an angle "π." Therefore if it is permissible to consider all the lines taken on an average as starting at right angles to the line joining the electron and proton, for an electron to come up from infinity to the proton and then go back to infinity is like making the lines all turn through an angle "π." In the case of the electron in the orbit, the lines all travelled through "2π" during a complete oscillation. The energy to travel through "π" would be half that to travel through 2π and therefore if the two energies be denoted by E_π and $E_\odot$, we have $E_\pi = \frac{1}{2}E_\odot$. But from Ehrenfest's Adiabatic Principle:

$$\frac{E_\infty}{\nu_\infty} = \frac{h}{2} = \frac{E_\odot}{\nu_\odot}.$$

$$\therefore \quad \frac{1}{2\nu_\infty} = \frac{1}{\nu_\odot}.$$

$$\therefore \quad \nu_\odot = 2\nu_\infty,$$

that is to say, the frequency of revolution is twice the frequency of a jump from infinity; this is very well known and has been made the basis of Bohr's correspondence principle.

The method by which this result has been reached depends on the assumption that the two frequencies are the same type of thing, and in point of fact both depend on the movement of lines of force, although of course there is a very great difference so far as an observer at infinity is concerned, as he can only perceive the frequency caused by the jump from infinity. The result, however, which we have obtained gives a clue as to how the levels in the hydrogen atom are reached. When a jump is made between the second level and the first, the frequency $^1\nu^2$ is given by $^1\nu^2 = \frac{E_2 - E_1}{h}$. Now supposing in the second level half of the lines of force starting from the electron extended to infinity, and half terminated on the proton; the energy then in the region round about the proton would be $(\frac{1}{2})^2$ times what it would be when the electron had all its lines terminating on the proton, since the energy in a medium is proportional to the square of the electrical polarization. Therefore the difference of energy would be proportional to $[1^2 - (\frac{1}{2})^2]$. This energy comes from the kinetic energy of the lines of force as they sweep round to terminate on the proton. Then from the equation $2TE_{kin} = h$, $h\nu$ must be proportional to $[1^2 - (\frac{1}{2})^2]$. It is clear we could visualise the mechanism of the emission of light if we could just get a process whereby an electron could be compelled to extend a fraction of its lines to infinity and leave the remainder on the nucleus. At this point it might be of interest to refer to a paper by Professor Widdington on the discharge of electricity through vacuum tubes, as a remark is made which seems to support the mechanism of emission that is to be proposed below. Widdington remarked in his paper *: "It was inferred

* Widdington, 'Nature,' p. 503, Oct. 3, 1925.

that the main supply of electrons from the cathode arose somehow from the arrival there of positive ions originating at the edge of the negative glow." This remark therefore supports the idea that the mechanism of light emission is as follows :—An atom approaches the negative electrode to which electrons are clinging thickly ; one or more become attached to the gas atom, which is immediately repelled. On the average, after an atom has moved through the length of the mean free path, it hits another atom and becomes discharged. For example, a hydrogen atom comes, say, up to the electrode and receives one electron, and gets repelled immediately. After travelling the mean free path, say, it gets discharged. As soon as the electron it received became attached, half of the lines of force from the first electron at once extended to infinity. When the discharging takes place, the electron which remains with the proton has half of its lines extending to infinity and at once gets readjusted to its normal state by the lines sweeping round to terminate on the proton. There are obviously serious objections to the mechanism, because if lines of force came in from infinity, did not some go out in their place ? How this difficulty can be overcome is not clear to the writer, but if it can be the explanation of excitation in a discharge-tube would fit in with what is required to get a portion of the lines of force of an electron out to infinity. If three electrons became attached to the proton at the electrode and only one was removed by the colliding atom, then the energy change would be proportional to $\left\{\frac{1}{2^2}-\frac{1}{3^2}\right\}$ and so on.

This explanation of the process of light emission shows why a study of the hydrogen spectrum should give a clue as to how the other elements are constructed. The main difference is that with a normal unexcited element all the lines of force terminate on the nucleus, while an excited hydrogen atom having just the same number of electrons would have nearly all the lines of force extended to infinity.

We must now introduce the Azimuthal quantum number. It was suggested long ago that possibly when an electron revolved in a circle about a nucleus, no radiation was emitted ; when, however, it was discovered that ellipses gave energy levels of approximately the same energy as the circles, and that the eccentricity depended on the

azimuthal number, this theory was abandoned. We may, however, reconsider this theory, if we accept the proposed mechanism of electrons becoming attached and then suddenly detached. In that case we may account for the ellipses by assuming that in the case of two electrons, one of the electrons may give rise to a sort of linear motion while the other gives rise to a circular one. How the exact motion takes place is not clear, but what is meant is, that when there is only one electron, it must go in a circular orbit; when there are two both may go in circular orbits, giving an azimuthal quantum number 2, or else one may give rise to a sort of linear motion contributing nothing to the angular momentum, but merely upsetting the circular motion of the other one. On this conception the j_c quantum numbers would seem to be connected with the angular momentum, while the j_o quantum numbers would be connected with the "linear" oscillations. The j_s quantum number has been ascribed to the spin of the electrons, and it is unfortunate that this theory does not lead to that conclusion, since the application of the spinning electron theory to various problems has been very successful.

If there is any truth in the idea of electrons becoming attached and detached in the emission of light in a discharge-tube, something of the same nature should take place when band spectra are emitted; and it seems reasonable to suppose that, instead of electrons attaching themselves, charged atoms or groups of atoms attach themselves. In the case of homopolar molecules the two atoms are hard to separate and they consequently have to become attached in couples at a time.

III. *Thermal Radiation.*

The quantum theory was originally proposed by Professor Planck in order to get the energy distribution in the spectrum when light was emitted from a heated body. In Planck's treatment of the problem a number of oscillators are assumed, but it is not stated what these oscillators are; again, the reason why multiples of $h\nu$ should be taken is not clear either. It was this treatise of Planck's that originally started the idea of $h\nu$ being an entity like a corpuscle; in the first part of this communication an endeavour has been made to emphasize the fundamental

constancy of h. It appears to be the constant in the Ehrenfest's equation when one electron is considered. On the other hand, there seems to be absolutely nothing about $h\nu$ that justifies its being considered as an entity. On the contrary, $h\nu$ can have and has all values, theoretically, when we are dealing with the Planck radiation problem. The misleading part in Planck's treatise was that the equations were such that they had a summation prefix for all frequencies, and in solving, the summation could be neglected, since the solution for one frequency gave the solution for all frequencies. On the idea that when an electron is describing a circular or suitable elliptic orbit, no radiation is emitted, it is easy to see that if the electron got a blow to send it out of its path it would oscillate to and fro about that normal path and in doing so would radiate energy. Now, a solid differs from a gas in that the electrons are influenced by forces from other atoms. There must be lines of electrical or magnetic force holding the molecules together. When a solid is heated the electrons get, as it were, blows sending them out of their paths, and there are consequently changes not only in the lines of force from the nucleus of the atom but also in the lines from the neighbouring atoms to any particular electron. A reasonable way of picturing Planck's problem would be to imagine the number of electrons as the number of oscillators; if the electrons got blows displacing them—n_1 of them getting blows with energy $h\Delta\nu$, n_2 getting $2h\Delta\nu$, and so on, where $\Delta\nu$ is a small element of frequency, the first equation would then be:

$$n_0+n_1+n_2+n_3\ldots=\text{number of oscillators},$$

and second equation would be:

$$n_1 . h\Delta\nu+n_2 . 2h\Delta\nu+n_3 . 3h\Delta\nu+\ldots=\text{energy}.$$

The energy is given when the temperature is known. There would, of course, be an infinite number of ways of making the distribution—for instance, we might put all the energy into one oscillator. To get the actual distribution, Planck introduced the entropy equation

$$S=k\log W+C.$$

In this form the meaning of the equation is obscure; but if it be written $dS=k\frac{dW}{W}$, the constant is eliminated and

the meaning of the equation can be expressed as follows: "The increase in entropy is proportional to the percentage increase in the number of ways of making the distribution." The "stable" or resultant distribution of the energy is determined by making $d\mathrm{S}$ zero—that is, equivalent to picking the distribution that occurs most frequently when $(n_1+2n_2+3n_3+\ldots)$ packets of energy are divided among $(n_0+n_1+n_2+n_3+\ldots)$ oscillators. The reason for following up Planck's proof by the above method was because it seemed as though multiples of $h\Delta\nu$ might give some explanation why Planck needed multiples of $h\nu$, but this method does not lead anywhere. It appears hard to imagine that each oscillator has an infinite number of frequencies which Planck's original treatise seems to imply. On further consideration it appears very doubtful if we are justified in assuming the number of oscillators constant, especially as the only way multiple quanta of energy could occur like $3h\nu$ would be if three electrons and three positive charges acted as one oscillator. Yet any method in which the number of oscillators radiating $h\nu$ is counted should include this case automatically. A more reasonable method to approach the problem seems to be to take some function of ν as denoting the number of oscillators radiating with frequency ν. If we do this we can follow Professor Debye's mathematics so far, but the assumptions from which we start are different. Let $f(\nu)d\nu$ be the number of oscillators radiating with frequencies between ν and $\nu+d\nu$. Now the number of different frequencies between ν and $\nu+d\nu$ is $d\nu$. The number of different frequencies to be distributed is $d\nu$ and the number of oscillators is $f(\nu)d\nu$, and therefore the number of ways of making the distribution is

$$\frac{\lfloor f(\nu)d\nu + d\nu - 1}{\lfloor f(\nu)d\nu - 1 \quad \lfloor d\nu}.$$

The -1 can be neglected above and below and so we get

$$\mathrm{W} = \frac{\lfloor f(\nu)d\nu + d\nu}{\lfloor f(\nu)d\nu \quad \lfloor d\nu}.$$

This is practically Debye's expression. Our equations for entropy and energy can be written down, viz.:

$$\mathrm{S} = \int_0^\infty k \log \frac{\lfloor f(\nu)d\nu + d\nu}{\lfloor f(\nu)d\nu \quad \lfloor d\nu} \quad \text{and} \quad \mathrm{U} = \int_0^\infty h\nu f(\nu)d\nu.$$

If $\delta(S+\gamma U)$ be equated to zero as Debye did, then

$$\log\frac{(1+f)}{f} = -\gamma\frac{h\nu}{k} \quad \text{or} \quad f = \frac{1}{\epsilon^{-\gamma\frac{h\nu}{\kappa}} - 1}$$

Debye's proof cannot be followed farther, as the expressions here used are slightly different from Debye's; but the result so far as it goes seems interesting, as it is reached by making entirely different assumptions from those of Professor Debye, and because no reference is made to multiples of the quantum entity $h\nu$.

Before leaving the problem of heat radiation, it might be as well to point out why a gas should not radiate when heated. When an electron of a gas molecule receives a blow from another atom, instead of vibrating about its stable orbit, the molecule of gas moves as a whole, and so the speed of the molecules becomes increased. In the solid state this cannot occur, and the energy of the blow must be taken up by starting electrical oscillations.

IV. *The Photoelectric Effect.*

In the case of the photoelectric effect, the corpuscular view of the quantum theory has met with the greatest success. The size of the effect depends on the intensity of the light, while the wave-length of the light determines whether emission can occur or not. Now, if the period of the revolution of the electron be greater than the period of the motion of the lines of force of the exciting light, it is clear that the light would cause no effect, but if the frequency of the light were greater it would speed up the electrons and eventually throw them out. If the intensity were very weak the speeding up would be small. The fact that the effect starts at once can be explained by considering that all electrons may be at different positions in their orbits, and if the electron gets an acceleration at the time when it is traversing a certain part of the orbit, the force may be sufficient to throw the electron out.

V. *Conduction.*

If the view of thermal radiation described in this communication be correct, some light might be thrown on the process of electrical conduction. Kinetic energy of atoms, or heat, should be attributed not directly to the motion of

atoms but to oscillations in the lines of force starting from electrons. The writer's conception of a metal does not agree with the usual free electron theory ; for if some of the electrons in metals were really free they would flow to the surface and this seems unlikely ; and therefore, the opinion is favoured that all electrons stay by their atoms but travel in orbits composing uncompleted shells*. Seeing then the electronic system is not full, there is a tendency for another electron from a neighbouring atom becoming attached. If such a mechanism be correct, it fits in excellently with Benedicks' † theory of the atom of metal actually being the carrier of electricity. So far as the writer knows, Benedicks did not extend Drude's free electron gas theory to fit his model, but this can be very simply done.

If e be the charge on an electron, after adding an electron to an atom, the force repelling the atom from the negative source of potential (X) is $e\mathrm{X}$. An acceleration of f, say, is acquired ; so if M be the mass of the atom,

$$\mathrm{M} \times f = e\mathrm{X} \quad \text{or} \quad f = \frac{e\mathrm{X}}{\mathrm{M}}.$$

The time that this acceleration acts is $\frac{l}{u}$, where l is distance the atom can move in the metal and u is the mean velocity of approach of two atoms due to thermal agitation. So then, v, the velocity of drift, $= \frac{1}{2}ft = \frac{e\mathrm{X}l}{2\mathrm{M}u}$, provided that the velocity of drift is negligible compared with the velocity due to heat agitation—that is to say, the time is so short during which the force acts that practically no velocity is obtained. The current is equal to nev, and so the conduction is equal to

$$\frac{ne^2l}{2\mathrm{M}u} = \frac{ne^2lu}{2\mathrm{M}u^2}.$$

Now $\mathrm{M}u^2$ is simply twice the kinetic energy of the atom and the specific heat difficulty regarding the contribution from the free electrons is completely removed. The conduction

* See McLennan, McLay, and Smith, "Atomic States and Spectral Terms." Proc. Roy. Soc. A, vol. cxii. p. 76 (1926).

† Benedicks, "Beiträge zur Kenntnis der Elektrizitatsleitung in Metallen und Legierungen," *Jahrbuch der Radioactivitat*, xiii. p. 351 (1916).

can now be written $\frac{1}{4} \cdot \frac{ne^2lu}{\alpha T}$: since u is proportional to $\sqrt{T}$, l must diminish with temperature. It can easily be seen why this must be the case from what has been said in the first part of this communication, because when there is much thermal agitation the electrons get displaced from their orbits and the effective size of an atom is really larger than when the electrons are moving in their undisturbed orbits. When the temperature of the metal is very low, the speed of the atom of metal due to thermal agitation is no longer so large that the velocity of drift can be neglected in calculating the time during which the acceleration takes place and the expression obtained above for the resistance is wrong. In the limiting case where the velocity of drift is the only velocity to be considered, u could be neglected and the expression for the resistance would now be independent of temperature, which is what occurs with practically all non-superconducting metals.

In conclusion, the writer wishes to express his thanks to Professor J. C. McLennan, F.R.S., whose inspiring lectures were the source of many ideas contained in this communication, for his most helpful criticism and support.

LII. *The Polarization of Raman Lines.* *By* A. C. Menzies, M.A., *Lecturer in Charge, Physics Department, University College, Leicester* *.

Introduction.

In his first announcement of the discovery of the effect, Raman † stated that the scattered lines showed evidence of being polarized. That there is a difference between the various scattered lines in this respect was shown later by Raman and Krishnan ‡, and independently by Carelli, Pringsheim and Rosen §. For example, the second group of workers have investigated the effect in benzene, toluene, and carbon tetrachloride, and have shown that the lines scattered by benzene are all practically unpolarized, but

* Communicated by Prof. R. Whiddington, F.R.S.
† Ind. Journ. Phys. ii. p. 1 (1928).
‡ 'Nature,' cxxii. p. 169 (1928).
§ *Zeits. für Physik*, li. p. 511 (1928).

that in the other two substances some lines are definitely plane-polarized, and in the same direction as that of the ordinary Tyndall scattering. (This is with the observation at right-angles to the incident light.)

The above experiments were made by putting polarizing apparatus in the path of the emergent scattered light beam. The early announcement by Raman of the polarization of the scattered radiation led the writer to make experiments on the scattering of light already plane-polarized, using a double-image prism, and observing at various angles to the incident beam. The purpose of these experiments was to see if the polarization of the Raman lines was produced during the scattering process, or whether it occurred through molecules differently orientated being excited by incident light vibrating in the appropriate plane only.

In the meantime a preliminary announcement of a result of a similar experiment has been made by Lindemann, Keeley and Hall *, who therefore take priority in this respect. The result which they announced was that in the scattering of light by carbon tetrachloride, of four scattered lines observed, one was present only in the beam which privileged the ordinary Tyndall scattering, while the other three were present in approximately equal intensities in both beams. (Observations at right angles.)

In the present paper an account is given of the results obtained by the writer in the examination of the state of polarization of the lines scattered by carbon tetrachloride at different angles, and by quartz with its optic axis at different orientations. An attempt is made to explain the polarization which occurs, and a scheme of energy-levels is put forward to co-ordinate the infra-red and Raman data for quartz.

Apparatus and Method.

As the Raman effect is still new, it is felt justified to give an account of the methods employed in greater detail than they would otherwise warrant, since such details may be helpful to others taking up the work.

The source of light was a quartz "Atmospheric Pressure" mercury vapour lamp made by Messrs. Kelvin, Bottomley, and Baird; it took 2·6 amperes at 110 volts, and was worked from an accumulator battery employed exclusively for this purpose. This burner is automatically relit if it goes out, so that it can be left to burn without attention for days or

* 'Nature,' cxxii. p. 921 (1928).

weeks. The actual source of light is approximately L-shaped with the corner rounded off, but fortunately the vertical portion is by far the stronger. This particular lamp was selected because the small size of the source was very convenient for producing from it a narrow beam to pass through the polarizing apparatus.

It was found convenient to mount the lamp in a separate room, the light entering the dark-room through a condensing lens of 6 in. diameter let into the wall. In this way a real image of the source can be formed at the centre of a spherical flask when it is required to irradiate the liquid with ordinary unpolarized light. A device, which was found very useful when focussing an image of the centre of the flask on to the slit of the spectrograph, is to let down a long glass fibre into the liquid in the flask, in such a way that it reflects the incident light, and so appears from the side as a line of light. This may then be focussed on to the slit of the spectrograph, and the fibre withdrawn at the end of the initial setting-up. When the light is initially plane-polarized before entering the flask, having passed through a double-image prism, it is essential that the two images of the source should be as near to the centre of the flask as possible with the two beams just separated. This condition can be readily judged by letting down into the liquid a strip of opal glass or other diffusing material, and as before focussing can be carried out on these images. When the final adjustments have been completed, the liquid in the flask can be replaced by a clean sample.

For the mere observation of the effect, it is not at all necessary to employ only dust-free specimens of the scattering liquid. It is naturally preferable to do so, since the dust increases the intensity of the scattered unmodified lines.

The spectrograph was a constant deviation instrument made by Hilger, and Wellington "Xpress" plates were used (H. and D. 850, black backing). In order to bring up the faintest lines, the plates were developed with "maximum energy" developer, Eastman Kodak formula.

The number of surfaces in the optical train should be kept as low as possible. There seems no particular virtue in a large flask, and if the liquid is expensive, or tends to aborb the light, a small one is preferable.

Polarization of the Carbon Tetrachloride Lines.

(1) *Scattering of a plane-polarized beam observed at right-angles.*

The incident beam of light was horizontal, and composed

of two beams, polarized horizontally and vertically respectively.

With twelve hours' exposure a plate was obtained, showing that the scattered line $d\nu = 458$ cm.$^{-1}$ occurred only in the beam vibrating vertically, while the lines $d\nu = 215$, 314, were equally strong in each beam. This, as mentioned before, was the discovery of Lindemann, Keeley, and Hall. The two fainter lines at $d\nu = 758$, 788, seemed to be very slightly more intense in the beam vibrating vertically.

These results are similar to those of Carelli, Pringsheim and Rosen, who observed with the polarizer in the scattered beam. The simplest assumption to make then, is that the light vibrations in the incident and scattered beams and the oscillation of the CCl_4 molecule must all be parallel in the case of the 458-line. It was also observed that the polarization of 458 is more complete when the *incident* beam is polarized.

(2) *Forward-scattering of a plane-polarized beam.*

The foregoing experiment suggested that if the light scattered in a forward direction could be observed, the polarized line would be equally strong in each beam. This observation is obviously not possible, but it is possible to observe the light scattered obliquely.

By using a narrow diaphragm (an auxiliary spectrograph slit opened fully) and a condensing lens on to the slit, it was possible to observe the scattering at an angle of about 160°.

It was found that the lines were almost equally strong in each beam—both spectra presented the same appearance as that due to the beam vibrating vertically in the 90° experiment.

(3) *Forward Scattering of an Unpolarized Beam.*

It is clear from the foregoing experiment that in the forward scattering of an unpolarized beam, the line 458 will be twice as strong relatively to the other lines as in the scattering at right-angles. This was tried, and found to be the case. Two photographs were taken of the spectrum of the light scattered, under conditions as similar as possible, at 90° and at about 160°. The intensities of all the lines were considerably greater in the second case. This was thought to be due in part to the greater depth of the scattered beam. In the forward scattering the intensity of the line 458 is about twice as great as that of its near companion 315,

while in the 90° scattering it is only very slightly more intense.

It should be possible, then, to detect the polarized lines in any Raman spectrum, by the comparison of plates obtained by sideways and forward scattering, by the selection of the lines which are strengthened relatively in the forward scattering. This method may be applicable when the more direct method is not so readily applied.

Other liquids (such as paraldehyde, acetone, toluene, methylal, mesitylene, and nitromethane) were tried with similar results. (Mesitylene goes "milky" during the irradiation, with the result that the unmodified lines are greatly strengthened.)

Theory of the Raman Effect.

Two theories have as yet been proposed to account for the Raman lines. The first, proposed by Raman, is that the modified lines correspond to actual infra-red frequencies.

The second was deduced from the dispersion theory of Kramers by Langer* and Deike† independently. This theory has been applied successfully to the case of carbon tetrachloride by Langer. According to this theory the scattered lines originate in transfers from excited levels in one system to excited levels in another system of vibration of the molecule, provided that both systems have a common level. It is by no means intended to deny that some Raman lines may correspond to some infra-red frequencies, but these occur once more as differences between pairs of levels having a common-level—it can be provided by an added rotation or perhaps even a lattice vibration.

Theory of the Polarizations.

So far, the only attempt to account for the polarizations is one put forward by Raman and Krishnan‡ very recently. Briefly, the molecule is regarded as having three sets of axes, along each of which a vibration may be set up by the incident light beam. It is then postulated that for the different vibrations, corresponding to the different modified frequencies, the response along the three axes is different. Thus the observed different stages of polarization of the lines may be accounted for.

* 'Nature,' cxxiii. p. 345 (1929).
† 'Nature,' cxxiii. p. 564 (1929).
‡ Roy. Soc. Proc. A, cxxii. p. 23 (1929).

But, as has been mentioned in the previous paragraph, in the production of the Raman line, two vibrations are concerned rather than one, the energy of the Raman line corresponding to the difference between the energies of the two vibrations.

It is here suggested that a possible explanation (in the sense of a mechanical model) of the polarizations can be got by considering the different systems to correspond in fact to actual vibrations of the molecule. Any transition from a level in one system to a level in another system corresponds to a change in the mode of vibration of the molecule, *i.e.*, a transfer of energy of vibration from one mode of vibration to another. Now if these different directions of vibration are parallel to one another, we may expect the light scattered to be plane-polarized, while if they are mutually perpendicular, the light scattered will be unpolarized. Intermediately, the light scattered will be partially polarized. This parallelism of the directions of vibration may account for the greater intensity, as a rule, of the polarized lines, to which Raman has drawn attention.

It is clear that if this hypothesis can be established, considerable knowledge of the spatial distribution of groups in molecules can be gained by a study of the polarization of the Raman lines.

The Raman Spectrum of Quartz.

It was thought that considerable light might be thrown on the problem of the polarization of the Raman lines by a study of the modified lines scattered by crystalline quartz from this point of view, varying the inclination of the optic axis to the direction of the incident and scattered beams. Observation was made at right-angles to the incident beam in all cases.

Three cases were dealt with. First, the optic axis coincided with the direction of scattering, secondly with the direction of the incident beam, and lastly it was placed at right-angles to both. In all cases the incident light was unpolarized. These three cases will be distinguished in what follows as (1), (2) and (3).

Observations without the Interposition of Polarizing Apparatus.

There appeared to be no difference between the spectra in the three cases, except that lines appeared in case (3) for the first time with shifts of approximately 1293 and 1369 cm^{-1}. It is possible that a repetition of the experi-

ments with longer exposure may reveal this shift in all three cases. These lines are extremely faint. Measurements of all the shifts are tabulated in Table I.

Observations of the Polarizations.

When it is realized that the optical rotation of quartz in the region of the spectrum under investigation is of the order of 45° per mm., it will be clear that an attempt to observe the polarizations of the lines in case (1) is certain to fail. Consequently only the cases (2) and (3) were so investigated, where observation was made perpendicularly to the optic axis.

As was expected, in most cases the lines were plane-polarized, and moreover, the direction of polarization in some cases turned through 90° as the optic axis was turned similarly, showing that some of the vibrations involved were fixed in direction relative to the optic axis Other lines kept their direction of polarization fixed relative to the directions of the incident and scattered light, and independent of the direction of the optic axis, showing that the directions of the vibrations concerned were not fixed relative to the optic axis. In two cases ($d\nu = 265$ and 798 cm.$^{-1}$) the lines were polarized in a direction perpendicular to that of the unmodified lines in both cases (2) and (3). It is difficult to see simply how this can arise (a vibration parallel to the direction of the incident beam, independent of the direction of the optic axis) without the postulation of vibrators at right-angles, as has been suggested above.

In order to simplify the presentation of the results, the states of polarization are given in Table I., together with the values of the wave numbers found by other observers. The polarizations in the two cases are given in parallel columns; "π" means that the lines corresponding to the shift are plane-polarized parallel to the direction of the unmodified lines, "σ" that they are plane-polarized at right-angles to this, and "u" that they are unpolarized. The references are to Rao *, Krishnan †, Wood ‡, Pringsheim and Rosen §, and Landsberg & Mandelstam ‖. In the first case (Rao and Krishnan) the original papers were unavailable, so the reciprocals of the wave-lengths quoted in a paper by Czerny ¶ are given.

* Ind. Journ. Phys. iii. p. 123 (1928).
† 'Nature,' cxxii. p. 506 (1928).
‡ Phil. Mag. vi. p. 742 (1928).
§ *Zeits. für Physik*, l. p. 741 (1928).
‖ *Zeits. für Physik*, l. p. 769 (1928).
¶ *Zeits. für Physik*, liii. p. 317 (1929).

With regard to the actual values obtained for the shifts, the values obtained by the writer are probably not more accurate than about 1 per cent. The concordance is good; it seems likely that the values got by Landsberg and Mandelstam are in better agreement with the others than appears at first sight—it looks as if they had worked with a wide slit and so measured the mean of 694 and 798 as one line, and similarly for 1093 and 1157.

TABLE I.

Raman Frequencies.					Polarization.	
R. & K.	W.	P. & R.	L. & M.	Author.	Case 2.	Case 3.
85	—	—	—	85	u	u
128	125	125	123	126	u(π)	σ
206	204	—	211	209	π	π
267	—	262	—	265	σ	σ
—	—	(351)	—	(356)	(π)	π
—	—	(405)	—	(406)	(π)	u
463	462	465	465	464	π	π
—	—	—	—	(530)	(σ)	(π)
—	—	(706)	—	694	(π)	σ
—	—	802	743	798	σ	σ
—	—	—	—	1093	σ	π
1176	—	1157	1127	1157	π	σ
—	—	—	—	1240	(π)	(σ)
				1293	Absent.	(π)
				1369	Absent.	(π)

(Numbers within brackets are doubtful.)

Infra-red Data for Quartz.

It was next sought to frame a system of energy-levels which should represent the Raman lines as differences between levels having a level in common. Any such scheme must naturally satisfy the infra-red data also. The data available to the writer were those quoted in Lecomte, 'Le Spectre Infrarouge,' p. 145 (reflexion experiments by Nichols, Rubens & Nichols, and Reinkober) and p. 181 (absorption experiments by Merritt and Koenigsberger,

Dreisch, Coblentz, Nichols, and Rosenthal), together with the measurements of Coblentz, Schaefer, and Schubert. It appears that the strongest infra-red vibrations are in the neighbourhood of 9μ and 21μ, so that any successful scheme would presumably involve these as fundamental vibrations.

A scheme of energy-levels is set forth in fig. 1. Here it will be noted that the very strong infra-red vibrations just mentioned are represented on the left of the diagram, in two pairs of levels, having a difference in wave-number

Fig. 1.

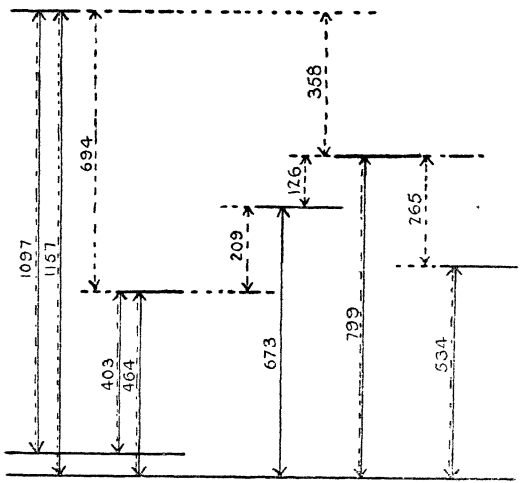

Energy-levels for Quartz.

of 61 cm.$^{-1}$. In the figure, a full line is drawn to represent a transition present in the infra-red spectrum, and a broken line to represent one present as a shift in the Raman spectrum. In addition to the lines indicated in the diagram, overtones of some of the fundamental frequencies shown occur in the infra-red spectrum. These are not shown in the diagram in order to keep it reasonably small. They are given in Table II. which follows. In the first column is given the wave-length in μ calculated from the frequencies in the diagram, in the second column the values obtained

by reflexion in the infra-red, and in the third column the values obtained by absorption in the infra-red. In the fourth column is an indication of the strength of the reflexion or absorption in the infra-red, in the fifth column "o" and "e" respectively indicates that the absorption or reflexion in the infra-red applies to the ordinary ray or to the extraordinary ray, and in the last column is given the origin of the vibration in terms of the present scheme.

TABLE II.

Wave-length.						
Calculated.	I. R. Refln.	I. R. Absptn.	I. R. Int.	I. R. Poln.		Origin.
2·98	3	2·97	Weak.			3×1096+61
3·04	„	3·02	„			3×1096
3·71	—	3·75	„			4×673
4·43	4·5	—	Weak.			2×1096+61
4·55	„					2×1096
4·95	—	5·02	„			3×673
6·26	—	6·26	„			2×799
8·64	8·50		V. strong.	o	e	Fundamental.
	8·70		„		e	
	8·90		„	o	e	
9·11	9·05		V. strong.	o	e	Fundamental.
12·5	12·52		Strong.	o		Fundamental.
	12·87		„		e	
14·9	14·55		„	o		Fundamental.
18·7	18·5		„			Fundamental.
	19·7		„		e	
21·6	21		V. strong.	o		Fundamental.
24·8	26		Strong.	o		Fundamental.
	27·5		„		e	

Still unaccounted for in this scheme are three weak infra-red observations, and the Raman lines at 85, 1240, 1293, and 1369, which are all weak.

It is difficult to draw any conclusions as to the connexion between the polarization of the infra-red vibrations and the polarization of the Raman lines, owing to the ambiguity in the infra-red observations.

A scheme of energy-levels which accords rather better with the Raman observations, but considerably less well with the infra-red data, can be built up with the following as fundamental frequencies :—700, 809, 1080, 1165, and 1291. This gives as differences :—85, 126, 211, 271, 356, and 465. The merit of the scheme is that it represents the strongest Raman lines (126, 211 and 465) as differences. Its drawback is that it does not involve the very strong infra-red wave-length at 21μ as a fundamental vibration, and does include as such the wave-number 1291, which has no counterpart in the infra-red.

More exact data in the infra-red region are required to settle this problem, and also more exact measurements of the Raman lines. The plates used in the course of the present work were obtained with an exposure of three days. These measurements will be repeated with the same specimen of quartz, using a still finer slit, and giving exposures of weeks in duration. It is worth while remarking that in the infra-red experiments the exact position of the band varies often from specimen to specimen.

I am indebted to my friend and former pupil Mr. C. P. Snow, of the Physical Chemical Laboratory, Cambridge, for helpful discussion.

Summary.

Using a small source and a double-image prism, observations have been made of the light scattered by carbon tetrachloride and other liquids at 90° and at an angle of about 160°.

It is suggested that the observed polarization of the line can be explained if it is supposed that the direction of the initial vibration is parallel to that of the final vibration in the case of the plane-polarized lines, and that they are perpendicular to one another in the case of the unpolarized lines. Lines partially polarized can be explained by the inclination of the directions of vibration to one another being intermediate between the two cases.

The Raman spectrum of quartz has been measured for three different orientations of the optic axis, and the state of polarization of the lines has been investigated. Some of the scattered lines change their direction of polarization through 90° as the direction of the optic axis is similarly turned. Two lines remain plane-polarized in the customary direction (parallel to that of the unmodified lines) in spite of the orientation of the optic axis being changed, and in the

case of two other lines the direction of polarization is invariable also, but is perpendicular to the usual direction (vibration parallel to the direction of propagation of the incident light).

An energy-level diagram is given which co-ordinates the Raman and infra-red observations, and may have some real significance.

(Since the above was written, I have seen a report by Cabannes in *Comptes Rendus*, clxxxviii. p. 249 (1929), in which he gives the results of experiments with quartz similar to those described in the present paper. The wave-numbers, measured by Daure, are 129, 208, 267, 357, 403, 467·5, 700, 796, 1062, 1165, 1287. They are represented as multiples of three small numbers.

The polarization observations are less complete than in the present paper, but are in agreement with those detailed here, except for a slight disagreement in the case of the weak line 1157. Cabannes suggests that the polarizations may arise through interference due to coherent scattering.)

Physics Department,
University College, Leicester.
June 27th, 1929.

LIII. *The Fine Structure of Spectral Lines.*

By J. C. McLennan, *F.R.S.*, *and* E. J. Allin, *M.A.**

(Holder of a National Research Council of Canada Studentship.)

[Plate XI.]

THE work described here is a continuation of experiments previously carried out by the authors†. The plan followed in this earlier work of studying lines in the first spark spectrum of an element and comparing the structures found for these lines with the structures found for lines in the homologous series of the corresponding arc spectrum has again been adhered to and the experimental method has not been changed except in the adoption of a means of spectrum excitation suitable to the

* Communicated by the Authors.
† Trans. Roy. Soc. Can. 3, xxiii. p. 7 (1929).

metal being studied. For this reason only the source of light used need be described in detail here.

To obtain the lines in the spectrum of zinc II. and of cadmium II. the hollow cathode discharge was used. Both electrodes were hollow cylinders made of the metal and enclosed in a pyrex glass tube which was exhausted and then filled with helium. The electrodes were carefully out-gassed and the helium purified as the presence of hydrogen and other impurities prevents the production of the spark lines. The pressure of helium in the tube also had an important effect on the character of the spectrum obtained. At a pressure of 2–2½ mm. of mercury with zinc electrodes and at a pressure of 5–1 mm. of mercury with electrodes of cadmium the lines of the spark spectrum possessed their greatest intensity. At higher pressures the helium spectrum alone was obtained and at lower pressures the arc spectrum of the metal became more prominent and the spark lines faded out. In most of the work a 30,000 volt alternating current transformer was used as a source of potential but the character of the spectrum remained unchanged when a 2000 volt direct current generator was substituted for the transformer.

For the study of lines in the spectrum of barium I. and of lanthanum II. it was the salts of the metals rather than the metals themselves that were available in quantity and it was necessary therefore to discard the method outlined above. It was decided to adopt that employed by Meggers and Burns * in the study of lanthanum I. and lanthanum II. A vacuum arc was constructed with carbon electrodes the lower of which was bored and filled with the salt of the metal under investigation. The electrodes led into the vacuum chamber through oil seals and the outside of the chamber was wound with brass tubing through which water flowed continuously to prevent the production of leaks due to the heating of the soldered metal joints. A pressure of considerably less than 1 mm. of mercury could be maintained while the arc was running. All salts of the metals were not found to be equally satisfactory. Of those obtainable barium oxide and lanthanum chloride gave the most intense spectra. A current of about 10 amperes at a potential of 220 volts was used throughout.

* J. O. S. A. (June 1927).

The results obtained are given in detail in Tables I., II., III., and IV.

TABLE I.

Results obtained for lines in the spectrum of Zn II.

Line.	Classification.	$\Delta\lambda$.	$\Delta\nu$.	Int.
6103 I.A.	$3^2P_2-4^2D_3$	Single		
6021 ,,	$3^2P_1-4^2D_2$	Single		
4924 ,,	$3^2D_3-4^2F_4$	0 −·071	0 +292	10 7
4912 ,,	$3^2D_2-4^2F_3$	Single		

TABLE II.

Results obtained for lines in the spectrum of Cd II.

Line.	Classification.	$\Delta\lambda$.	$\Delta\nu$.	Int.
6465 I.A.	$3^2P_1\ 4^2D_3$	0 −·075	0 +179	10 3
6360 ,,	$4^2F_4-6^2G$	0 −·055 −·131	0 +135 +323	10 1 10
530 ,,	$3^2D_3-4^2F_4$	+·053 0	−184 0	3 10
5337 ,,	$3^2D_2-4^2F_3$	Single		

TABLE III.

Results obtained for lines in the spectrum of Ba I.

Line.	Classification.	$\Delta\lambda$.	$\Delta\nu$.	Int.
6694 I.A.	$^3D_1{}^0-{}^3D_3$	Single		
6675 ,,	$^3D_1{}^0-{}^3D_2$	Single		
6595 ,,	$^3D_1{}^0-{}^3D_1$	0 −·099	0 +228	10 8
6527 ,,	$^3D_2{}^0-{}^3D_2$	+·131 0	−308 0	1 10
6499 ,,	$^3D_3{}^0-{}^3D_3$	Single		
6450 ,,	$^3D_2{}^0-{}^3D_1$	0 −·104	0 +250	10 1
6342 ,,	$^3D_3{}^0-{}^3D_2$	Single		
6063 ,,	$^3P_1{}^0-{}^3D_2$	+·181 ·066 0	−492 −181 0	1 10 9
6019 ,,	$^3P_0{}^0-{}^3D_1$	+·161 0 −·082	−444 0 +225	1 10 1
5997 ,,	$^3P_1{}^0-{}^3D_1$	0 −·066	0 +185	10 4

TABLE III. (*cont.*).

Results obtained for lines in the spectrum of Ba I.

Line.	Classification.	$\Delta\lambda$.	$\Delta\nu$.	Int.
5972 I.A.	$^3P_2^0-{}^3D_2$	+·137	−384	1
		0	0	10
		−·062	+173	1
		−·129	+362	5
5536 „	Unclassified	+·044	−144	1
		0	0	10
		−·041	+133	5
		−·065	+212	5
4934 „	Unclassified	+·043	−175	10
		0	0	10
		−·037	+152	9
4900 „	Unclassified	0	0	10
		−·060	+250	2
4554 „	Unclassified	0	0	10
		−·051	+246	9
		−·085	+411	8

TABLE IV.

Results obtained for lines in the spectrum of La II.

Line.	Classification.	$\Delta\lambda$.	$\Delta\nu$.	Int.
5304 I.A.	$^3D_1^0-{}^3D_2$	+·086	−307	2
		0	0	10
		−·065	+230	4
		−·129	+457	4
5183 „	$^3D_3^0-{}^3D_3$	Single		
5123 „	$^3D_2^0-{}^3D_2$	Single		
5115 „	$^3D_1^0-{}^3D_1$	Single		

The intensities quoted above give merely the relative intensities of the components of a line.

It is not felt that the results given for the spectrum of lanthanum II are as satisfactory as those given for the spectra of the other elements. This spectrum possessing as it does a great number of lines is extremely difficult to investigate particularly with a highly resolving echelon spectrograph.

Plate I is from enlarged photographs of some of the lines that showed fine-structure. (*a*) shows the line 5304 of lanthanum, (*b*), (*c*), (*d*), (*e*), (*f*), (*g*) the lines 4554, 4934, 5536, 5972, 6063, 6595 respectively of barium and (*h*), (*i*) the lines 5378 and 6360 of cadmium.

The structures obtained for the lines in the arc spectrum of barium may be represented by the energy diagram given

in fig. 1. It is interesting to note that by assigning the quantum numbers indicated in the figure and applying the exclusion principles which are found to hold in the analysis of line spectra we obtain the number of components experimentally observed for these lines except in the case of the line 5997, which has one component missing.

Table V. has been drawn up to allow a comparison to be made between lines in the spectrum of Zn II. and lines in the spectrum of Cu I., between lines in the spectrum of Cd II. and lines in the spectrum of Ag I. and between lines in the spectrum of La II. and lines in the spectrum of Ba I.

Fig. 1.

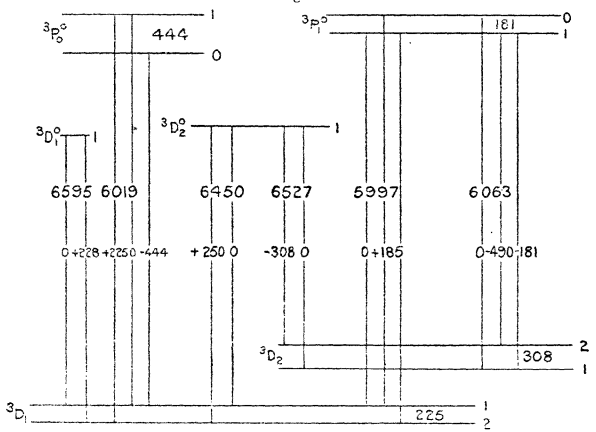

Energy levels, Barium I.

TABLE V.

$^2P_2$—$^2D_3$	Single in Zn II.	Single in Cu I.
$^2P_1$—$^2P_2$	Single in Zn II.	Single in Cu I.
$^2P_1$—$^2D_3$	Double in Cd II.	Single in Ag I.
$^3D_1^0$—$^3D_2$	Quartet in La II.	Single in Ba I.
$^3D_3^0$—$^3D_3$	Single in La II.	Single in Ba I.
$^3D_2^0$—$^3D_2$	Single in La II.	Double in Ba I.
$^3D_1^0$—$^3D_1$	Single in La II.	Double in Ba I.

Using fig. 1 we may also compare the results obtained by us for the spectrum of Ba I. with those obtained by

Meggers and Burns for the spectrum of La II. They state that in La II. the level $^3D_1$ is triple at least, the level $^3D_2$ is single and the level $^3D_3$ is quintuple at least. We find that in Ba I. the level $^3D_1$ is double as is the level $^3D_2$ while the level $^3D_3$ appears single.

These results, as well as those previously published, lead to the conclusion that there is no similarity between the structure of a line in an arc spectrum and the structure of a line in the homologous series of the corresponding first spark spectrum. This is in keeping with the view advanced on theoretical grounds that the fine structure of a spectral line originates in a property—the spin—of the nuclei of the atoms giving rise to it.

The Physical Laboratory,
University of Toronto.

LIV. *On Weber's Law and Visual Acuity.* *By* R. A. Houstoun, *D.Sc., Lecturer on Physical Optics in the University of Glasgow* *.

THE power to distinguish differences in the brightness of objects is one of the most important properties of the human eye. It has hitherto been specified by the ratio $\Delta I/I$ where ΔI is the smallest increase in brightness which can be detected, when the eye is adapted to brightness I. This ratio has been measured by different observers during a period extending now over a century and a half, and Fechner stated that

$$\frac{\Delta I}{I} \text{ is constant.}$$

This result he called Weber's law. If we write ΔS to denote the increase in sensation,

$$\Delta S = k\frac{\Delta I}{I}.$$

This gives on integration $S = k \log I + C$, a result known as Fechner's law. It was obvious to Fechner that Weber's law did not hold for high and low intensities. But he considered that these deviations were due to disturbing factors, to dazzle at high intensities and to the intrinsic

* Communicated by the Author.

light of the retina at low intensities, and regarded the ratio as constant for a wide interval between.

The most important investigation on the subject is that made by Koenig and Brodhun *, each of whom measured the ratio for white light and for six monochromatic regions of the spectrum over the whole range for which the eye can function.

Fig. 1 is a diagram representing their results taken from Helmholtz's 'Physiological Optics.' This diagram has now become classic. The ordinates represent the ratio. At high

Fig. 1.

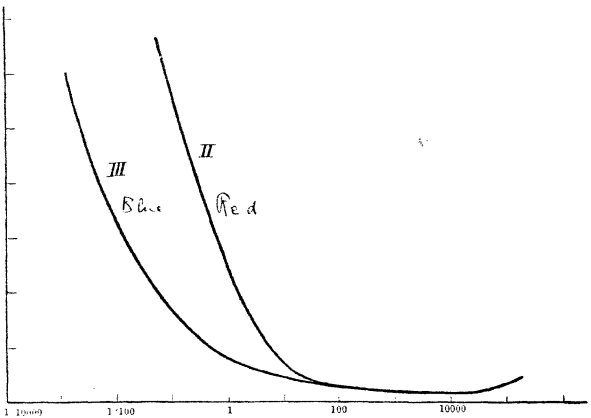

intensities it is represented by the same curve I. for all colours, and at low intensities by the curve II. for the red end, and by the curve III. for the blue end of the spectrum.

All the workers in the field have hitherto devoted their attention to the ratio $\Delta I/I$. In this it appears to me they have been wrong; it is not this quantity but its reciprocal that is important. What we are studying is the power of the eye to discriminate brightness; this should be measured by a number which is great when that power is great, and

* *Experimentelle Untersuchungen über die psychophysische Fundamentalformel in Bezug auf den Gesichtssinn. Sitzungsber. k. Akad. Wissensch.* 1888, p. 917; 1889, p. 641.

which should become zero, not infinite, in the case of a stone-blind man. I have consequently graphed in fig. 2 the mean of Koenig and Brodhun's values for $I/\Delta I$ for white light; the abscissæ are the logarithms of the intensity expressed in the arbitrary unit they used. The smooth curve is a probability curve $y=e^{-}$ adjusted by trial and error to fit the data. A better fit might have been obtained by more elaborate methods, but the accuracy of the data hardly appears to warrant the extra trouble.

The fit is a good one. It shows that there can be no question of the validity of Fechner's law, that there is no

Fig. 2.

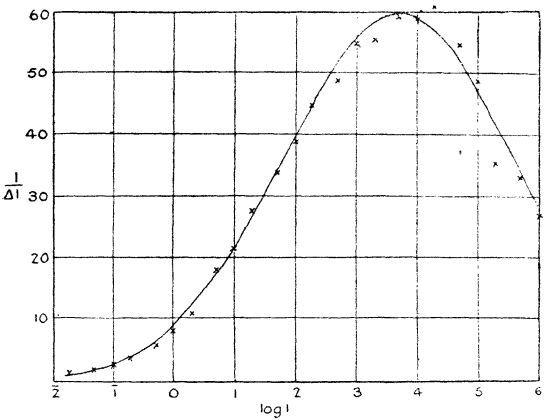

constant fractional increase, even for a limited interval. We are instead up against the laws of probability which always hold when there is a large number of objects grouped about a mean. In fig. 3 I have graphed the mean of Koenig and Brodhun's results for 605 $\mu\mu$, and in fig. 4 the mean of their results for 470 $\mu\mu$, in each case fitting a curve of the same type to the observations. In fig. 3 the fit is not so good as in fig. 2; the distribution is distinctly one-sided at the top. In fig. 4 there is a pronounced deviation at low intensities; it is this deviation that shows itself as the difference of the curves II. and III. in fig. 1.

Fig. 3.

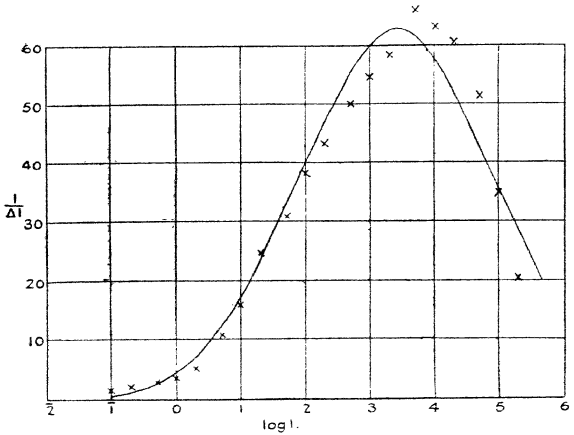
60
50
40
$\frac{I}{\Delta I}$ 30
20
10
$\bar{2}$ $\bar{1}$ 0 1 2 3 4 5 6
log I.

Fig. 4.

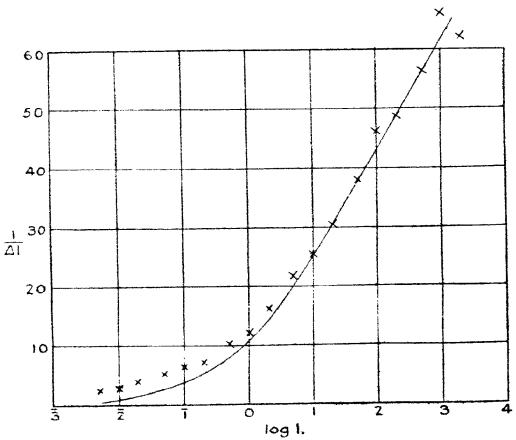
60
50
40
$\frac{I}{\Delta I}$ 30
20
10
$\bar{3}$ $\bar{2}$ $\bar{1}$ 0 1 2 3 4
log I.

To convert the brightness of the surface to absolute units Koenig and Brodhun's should be multiplied by 0·04. It is then expressed in millilamberts; when a perfectly diffusing surface is exposed normally to a point source of one candle-power intensity at a distance of 1 cm., it has a brightness of 1 lambert. Koenig and Brodhun did not correct their intensities for the variation in the aperture of the pupil. Their numbers are proportional consequently to the intensity of the light outside the pupil not to its intensity on the retina, and should be corrected by multiplying by the area of the pupil opening. I have not made the correction as I am not sure of the value of the correction under the conditions of the experiment, and in any case it is not large enough to affect the shape of the curves appreciably. Koenig, it should be noted, had normal colour vision, whereas Brodhun was a dichromat, but there was no appreciable difference between their results. Ten settings were made by each observer at every intensity; it is doubtless impossible to increase the range over which the observations were made, but it is desirable that the work on white light should be repeated with a greater number of observations, in order to see how closely the results fit the probability curve.

The question arises as to why the variation takes place with regard to log I, and not with regard to I? I think it possible to answer this question with a fair degree of certainty. The percipient elements in the retina are the rods and cones or the cones alone. There are the two views. According to the duplicity theory the rods are a separate system from the cones functioning at lower intensities than the latter; this view is the more widely held at present. According to the other view the rods are not percipient elements. On the first view the rods and cones are connected to the fibres of the optic nerve. Now we know as a consequence of the work of Adrian that the sensation is propagated along the nerve fibre by a series of impulses. The velocity of the impulses is constant, but their frequency increases with the intensity of the stimulus. R. S. Lillie has described a model which imitates very closely the propagation of the pulses. If an iron wire is dipped into a strong solution of nitric acid, its surface becomes "passive," *i. e.*, becomes covered by a sheath of oxide which protects it from the further action of the acid. If the wire is then immersed in a weaker solution of the acid and its surface touched with a zinc rod, the sheath is destroyed at the point of contact, and a pulse characterized by effervescence travels

rapidly along the wire. The sheath reforms behind the pulse, and after a short interval of time the wire is in a condition to transmit another pulse. By analogy the impulse in the fibre of the optic nerve should be started by applying a charge of electricity to the surface of the cone.

The light falls first on a photosensitive substance liberating electrons. These pass through an absorbing medium to the surface of the cone. Now a stream of electrons is absorbed according to the same law as a ray of light. If I denotes the initial and I_0 the final intensity of the stream,

$$I_0 = Ie^{-\mu x}$$

where μ is a constant and x denotes the length of the path in the medium. Consequently

$$\log I_0 = \log I - \mu x.$$

The length of the path will vary from cone to cone. One value will be most common and the others will be distributed around this. If we divide the cones into classes according to the value of x which they possess, and graph the number in each class against the value of x, we obtain a frequency distribution. Let us assume that the same intensity I_0 is required to start an impulse in each cone, then according to the above equation the distribution has the same shape, when it is graphed against log I instead of x.

When log I is small, all the cones are inactive. If log I is increased, each cone becomes active as its threshold is reached. Let us assume, that for a just perceptible increase in sensation the number of active cones always increases by the same amount. Then the ordinates in figs. 2, 3, and 4 represent the rate of increase of the number of active cones with the increase in log I where I denotes the intensity of the stream of electrons. Let us take the latter as proportional to the intensity of the incident light. The figs. then represent the distribution of the cones or other percipient elements in terms of the logarithms of their threshold intensities.

The photo-sensitive substance decomposes under the incident light and recombines again in the dark. The intensity of the stream of electrons is proportional to the incident light only if the quantity of substance decomposed is small. It is possible that there may be an effect due to the exhaustion of the photosensitive substance. Also, when a cone becomes active, its rate of activity increases with the increase in the intensity of the light until a stationary condition is reached, determined by the interval

necessary for the nerve to recover from the passage of the previous impulse. This stationary condition must, however, be reached very rapidly, otherwise the curves in figs. 2 and 3 would have no descending portions. Probably a satisfactory approximation to actual conditions will be obtained if we assume that all cones function at the same intensity once they are started, and if we place the threshold for each cone midway between its actual value and the intensity which produces the stationary condition. But the curves make it practically certain that the main consideration is a probability one which can be nothing else but the grouping of the percipient elements round a particular threshold intensity.

The question arises as to the nature of the percipient elements. According to the view most prevalent at present, the rods should function at low intensities, and there should be three different kinds of cones corresponding to the fundamental sensations of the Young-Helmholtz theory of colour vision. In fig. 2 I can see evidence only for one mechanism. In fig. 3 the one-sided distribution may be due to the overlapping of symmetrical distributions due to the different fundamental sensations of the Young-Helmholtz theory. It is, however, well to remember that most distributions which occur in nature due to the variation of one factor are one-sided; the Gaussian distribution is the exception rather than the rule. The deviation in fig. 4 may be due to a second system, presumably the rods; or it may be due to spherical aberration of the eye for blue light. We are compelled to suspend judgment, for there is not enough to form judgment upon.

According to the assumption of this paper, the sensation is proportional to the number of active percipient elements. If S denotes the sensation and the curve in fig. 2 is accurately represented by the probability expression, it follows that

$$\frac{dS}{d(\log I)} = ke^{-\frac{(\log I - \log I')^2}{2\sigma^2}}$$

where I' is the intensity at the maximum and σ is the "dispersion" or standard deviation. Hence we have

$$S = k\int_{-\infty}^{x} e^{-\frac{(\log I - \log I')^2}{2\sigma^2}}\, d(\log I)$$

instead of Fechner's law $S = k \log I + C$. This is an integral widely used in statistical work, and there are tables giving its value.

In 1897 Koenig* measured the resolving power of the eye for white, red, green, and blue light over as wide a range of intensities as possible. He used Snellen's test object E upon a background of the colour in question; this is turned left or right or up or down, and the measurement consists in finding at what intensity the direction of the open side can just be determined. If this can be done when the object subtends an angle of 5 minutes at the eye, the resolving power or acuity is said to have unit value. If the direction can be determined when the angle subtended is $2\frac{1}{2}$ minutes, the resolving power is 2. His results for white light are represented by the crosses in fig. 5 on the same

Fig. 5.

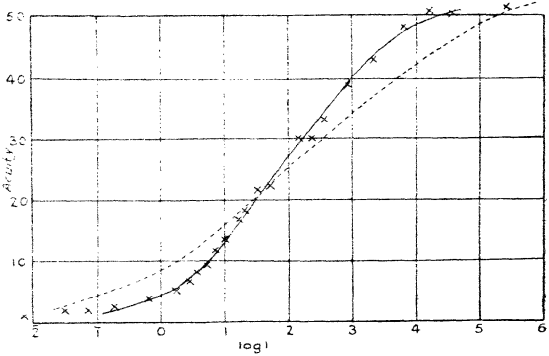

scale of intensity used for figs. 2, 3, and 4. The ordinates give acuity. The intensity is not corrected for variations in the aperture of the pupil. Koenig's observations were rather numerous, and have been averaged in groups of five consecutive readings by Hecht†; it is Hecht's averages that are represented in the fig. I have fitted a curve of the type

$$y = \int_{-\infty}^{x} e^{-x^2/2}\,dx$$

to the observations adjusting the origin and scale by trial and error. The agreement is within the experimental error.

* *Die Abhängigkeit der Sehschärfe von der Beleuchtungsintensität. Sitzungsber. k. Akad. Wissensch.* 1897, p. 559.

† "The Relation between Visual Acuity and Illumination." J. Gen. Physiol. 1928, xi. p. 255.

It will be noted that this curve is of the same type as has been used to represent S, and that there are no signs of two mechanisms.

On what should the variation of acuity with intensity depend? According to Hecht it depends only on the number of active percipient elements in unit area of the retina. The number of percipient elements is fixed anatomically. Hence we must assume that more become active as the intensity is increased, that is, we make the same assumption as before, namely, that the elements have different intensity thresholds. Let us suppose they are arranged in rows at equal distances from one another, and that there are N per cm. The number per unit area is consequently N^2, and this is proportional to S. The acuity as defined above is presumably inversely proportional to the distance between two percipient elements, *i.e.*, it is proportional to N. It is hence proportional to $\sqrt{S}$. I have calculated S from Brodhun's measurements on white light, and have plotted $\sqrt{S}$ as a broken line in fig. 5, choosing the scale of ordinates to give as good an agreement as possible. But $\sqrt{S}$ cannot be said to fit the observations, although the change takes place over the same range.

A little consideration shows that Hecht's assumption requires to be modified. If we consider the analogy with the photographic plate, the detail in the image certainly increases as the distance between the grains decreases. But it depends also on the degree of contrast in the plate. A plate with soft gradation which fogs slightly in the developer does not show up detail as well as a clean working plate. Something similar must happen in the retina. Let us suppose that the test object consists of two thin parallel white strips separated by a thin black strip. The black strip is not perfectly black, and we shall suppose that it reflects one-twentieth as much light as the white strip does. At low intensities the light reflected from the black strip is below the thresholds of all the percipient elements. As the intensity is raised, the light reflected from the black strip rises above the threshold of element after element; finally, when the intensity is very great, the light from the black strip is above the threshold of most of the elements. The degree of contrast consequently varies with the intensity of illumination. To obtain the acuity from $\sqrt{S}$ we must multiply the latter by a contrast factor. But the excellent agreement of the observations with the probability curve makes it certain that number of elements and contrast

should not be considered separately; the variation must depend on a single factor involving both these quantities.

It would be well in future determinations of the resolving power of the eye to use a series of equidistant parallel lines as test object, so as to eliminate disturbance due to end effects. Such a test object as Snellen's has the advantage that it eliminates dishonest work, and is valuable when examinations in visual acuity are a condition of admission to trades and professions. But in a scientific investigation the object should be geometrically as simple as possible.

Koenig found that the acuity was independent of the colour of the light. The readings for red, green, and blue agreed with the readings for white ight, whenever the intensities were reduced to the same unit.

If the percipient elements reach their thresholds gradually as the intensity increases, the question may be asked, why, when we look at a white sheet, does the image not show a grain at low intensities. It is possible that the brain interprets a particular kind of graininess as uniform intensity, just as it recognizes an inverted image on the retina as that of an erect walking man. But it is more probable that the threshold of each element changes frequently, as the supply of photosensitive substance varies, and that the uniformity is due to persistence of vision.

In order to explain the increase in sensation with intensity it might be suggested that the cones have all the same threshold, but that the molecules of the photosensitive substance have different thresholds, *i.e.*, some are decomposed more readily than others. But this will not explain the variation of acuity with intensity.

In measuring the resolving power of the eye for blue light, Koenig found that it increased more rapidly than it ought to increase, when he approached the the test object. Careful correction of the eye for myopia in the blue had no effect, and he concluded that the discrepancy was due to a large spherical aberration of the eye for blue light. He offers no explanation of the difference between curves II. and III. in fig. 1. It is possible that this is due to the same cause, for spherical aberration would blur the dividing edge of the comparison fields, and render the arrangement less sensitive. It would naturally come into play at low intensities when the full pupil was used.

In order to see how closely the results fit the probablity curve and settle some of the other points raised in this paper, we are at present preparing to repeat Koenig and Brodhun's entire investigation

LV. *The Effect of Boundary Distortion on the Surface Energy of a Crystal.* *By* BERYL M. DENT, *Department of Theoretical Physics, Bristol University* *.

§ 1. INTRODUCTION.

AS there is as yet no reliable experimental method of determining the surface energies of solids, and as a knowledge of the magnitude of the surface energy is essential to a proper understanding of many surface phenomena, any theoretical estimate of this quantity is of interest.

Hitherto it has only been possible to calculate the surface energy † on the assumption that the effect of the distortion or shrinking of the boundary of the crystal can be neglected, for the simple reason that no method existed of estimating the extent of this distortion. This has now been done. It has been shown ‡ that for a series of alkaline halide crystals it is the deformability of the surface ions which largely controls the distortion at the surface. If the ions were not deformable, the distortion would practically vanish. Actually the contraction in the interplanar spacing at the surface is about five per cent., and reasons have been given for supposing that this contraction is practically confined to the topmost layer.

The surface energy is found to be similarly sensitive to the deformability of the surface ions. Calculations for eight crystals of the rock-salt type show that the surface energy of the (100) plane is diminished by about 20 per cent., due to the deformability of the surface ions and the consequent contraction at the surface.

§ 2. METHOD.

In Born's notation § let the potential energy of the unbroken crystal be divided into three parts,

$$\phi = \phi_{11} + \phi_{22} + \phi_{12},$$

where ϕ_{11} and ϕ_{22} are the energies of the two parts which are separated by the net plane along which the crystal is broken, and ϕ_{12} is the mutual energy of these two parts.

* Communicated by Professor J. E. Lennard-Jones.

† Born, 'Atomtheorie des festen Zustandes,' 2nd ed., p. 538; Lennard-Jones and Taylor, Proc. Roy. Soc. cix. p. 476 (1925).

‡ Lennard-Jones and Dent, Proc. Roy. Soc. cxxi. p. 247 (1928).

§ Born, *loc. cit.*

The energy zero is assumed to correspond to a state of infinite dispersion of the ions, hence all the ϕ's are negative.

As the two parts of the crystal are separated, the two freshly-formed bounding surfaces will be slightly deformed, so that the energies ϕ_{11}^* and ϕ_{22}^*, after breaking, will be different from ϕ_{11} and ϕ_{22} respectively. The total energy after breaking

$$= \phi^* = \phi_{11}^* + \phi_{22}^*.$$

The surface energy σ is defined by the equation

$$\sigma = \frac{1}{2F}(\phi^* - \phi), \quad . \quad . \quad . \quad . \quad . \quad (2.1)$$

where F is the area of each new surface.

Hence

$$\sigma = \frac{1}{2F}\left\{ -\phi_{12} + (\phi_{11}^* - \phi_{11}) + (\phi_{22}^* - \phi_{22}) \right\}.$$

We suppose that the two parts are identical, so that

$$\phi_{11} = \phi_{22}; \quad \phi_{11}^* = \phi_{22}^*,$$

and therefore

$$\sigma = -\frac{\phi_{12}}{2F} + \frac{\phi_{11}^* - \phi_{11}}{F}. \quad . \quad . \quad . \quad . \quad (2.2)$$

Usually the difference $\phi_{11}^* - \phi_{11}$ is neglected, but we are now in a position to evaluate it.

Let

$$\sigma' = -\phi_{12}/2F, \quad . \quad . \quad . \quad . \quad . \quad . \quad (2.3)$$

and

$$\sigma'' = (\phi_{11}^* - \phi_{11})/F. \quad . \quad . \quad . \quad . \quad (2.4)$$

Then

$$\sigma = \sigma' + \sigma''. \quad . \quad . \quad . \quad . \quad . \quad . \quad (2.5)$$

Since ϕ_{12} is negative, σ' is positive. σ'', on the other hand, is negative because the energy tends to a minimum, and therefore $\phi_{11}^* < \phi_{11}$. Hence the effect of shrinking at the boundary is to decrease the surface energy.

§ 3. Calculation of σ'.

In order to calculate σ' a knowledge of the repulsive forces between the different ions occurring in the crystals is necessary. These repulsive forces have been investigated by Lennard-Jones in a series of papers on the assumption that they may be expressed by an inverse power law (λ/r^n), and a table of the repulsive force constants (λ) and indices (n) for many monovalent and divalent ions is given in the last of these papers †.

† Lennard-Jones and Dent, Proc. Roy. Soc. cxii. p. 230 (1926).

A method of calculating σ' has already been published, and numerical results have been obtained for four of the crystals dealt with in this paper, viz., NaF, NaCl, KF, KCl †. These values have been recalculated, using the slightly improved values of the force constants given in the table mentioned above, and the calculations for the remaining four crystals have been carried out. The results are given in Table I. ‡ The units are ergs per square cm.

TABLE I.

Values of σ' (Surface Energy, neglecting boundary distortion).

	F.	Cl.	Br.	I.
Na	307	93	90	88
K	178	75	73	72

§ 4. CALCULATION of σ''.

From equation (2.4)

$$\sigma'' = (\phi_{11}{}^* - \phi_{11})/\mathrm{F},$$

where ϕ_{11} is the energy of the semi-infinite crystal bounded by a (100) plane, and $\phi_{11}{}^*$ is the energy of the same crystal after breaking. Now it has been shown that the shrinking at the surface is practically confined to the top layer, and therefore the difference between $\phi_{11}{}^*$ and ϕ_{11} is mainly due to the ions in the surface layer. We therefore calculate the potential energy of a pair of unlike ions in the bounding plane, firstly in their original positions in the unbroken crystal, and, secondly, in their distorted positions. Let these energies be ϕ_s and $\phi_s{}^*$ respectively. Then

$$\phi_{11}{}^* - \phi_{11} = \phi_s{}^* - \phi_s, \quad \text{approx.},$$

and

$$\sigma'' = (\phi_s{}^* - \phi_s)/\mathrm{F}, \quad \text{approx.} \quad . \quad (4.01)$$

† Lennard-Jones and Taylor, *loc. cit.* p. 496.

‡ The calculations involve the size of the unit cell of each crystal. This quantity can be calculated by means of the force constants and indices mentioned above, and the results are found to agree very closely with those observed. See Proc. Roy. Soc. cxxi. p. 253, Table 4 (1928). For the sake of consistency, the calculated values have been used throughout.

(i.) *Calculation of* ϕ_s.

ϕ_s is made up of two parts, viz., ϕ_s^e, the energy due to electrostatic forces, and ϕ_s^r, the energy due to repulsive forces. We may neglect that due to polarization before the crystal is broken, since, in the interior of a crystal of symmetrical pattern, any displacement of the nucleus of an ion relative to the centre of the electronic structure is improbable. We also neglect the contribution of van der Waals's forces—this is negligible compared with the electrostatic potential. We therefore have

$$\phi_s = \phi_s^e + \phi_s^r. \quad . \quad . \quad . \quad . \quad . \quad (4.02)$$

In the notation of a former paper †

$$\phi_s^e = -\frac{8e^2}{a} \sum_{l,m}{}' (l^2+m^2)^{-\frac{1}{2}} c_{l,m} f_{l,m}(z) + \mathrm{A}(a/2), \quad (4.03)$$

where $\mathrm{A}(a/2)$ represents the effect of the remaining ions in the surface plane and is independent of z (the distance between the surface and the second plane), and the first term represents the effect of the rest of the crystal. The interatomic distance in the surface plane itself ($a/2$) is assumed to remain unaltered after breaking, and therefore the same quantity A will appear in the electrostatic potential energy ϕ_s^{*e}. A similar quantity B will appear in the expressions for ϕ_s^r and ϕ_s^{*r}. Both A and B will disappear on subtraction (see equation 4·01), and will be omitted in future.

It is convenient to write

$$\phi_s^e = -\frac{32e^2}{a} s_3(z/a), \quad . \quad . \quad . \quad . \quad (4.04)$$

where

$$s_3(z/a) = \tfrac{1}{4} \sum_{l,m}{}' (l^2+m^2)^{-\frac{1}{2}} c_{l,m} f_{l,m}(z), \quad . \quad (4.05)$$

in conformity with the notation of a recent paper ‡, where

$$s_1(z/a) = \tfrac{1}{4} \sum_{l,m}{}' c_{l,m} f_{l,m}(z)$$

and

$$s_2(z/a) = \tfrac{1}{4} \sum_{l,m}{}' (l^2+m^2)^{\frac{1}{2}} c_{l,m} f_{l,m}(z).$$

† Lennard-Jones and Dent, Trans. Faraday Soc. xxiv. p. 92 (1928).
‡ Lennard-Jones and Dent, Proc. Roy. Soc. cxxi. p. 250 (1928).

In the undistorted case $z/a = 0{\cdot}5$ and $s_3(z/a) = 0{\cdot}825 \cdot 10^{-2}$ (see Table IV.). The values of ϕ_s^e for the eight crystals are given in Table III. The contribution of the repulsive forces to the potential is easily seen to be

$$\phi_s^r = \frac{2\lambda_{12}k'(n_{12}, z/a)}{(n_{12}-1)(a/2)^{n_{12}-1}} + \frac{\lambda_{11}k''(n_{11}, z/a)}{(n_{11}-1)(a/2)^{n_{11}-1}} + \frac{\lambda_{22}k''(n_{22}, z/a)}{(n_{22}-1)(a/2)^{n_{22}-1}}, \quad . \quad (4.06)$$

where $\lambda_{12}/r^{n_{12}}$, $\lambda_{11}/r^{n_{11}}$, and $\lambda_{22}/r^{n_{22}}$ are the laws of force between a positive and a negative ion, between two positive, and between two negative ions respectively, and

$$\left.\begin{aligned} k'(s, z/a) &= \sum_{\substack{n \lessgtr 0 \\ l+m+n \text{ even}}} \{l^2+m^2+(2z/a+n)^2\}^{-(s-1)/2} \\ k''(s, z/a) &= \sum_{\substack{n \lessgtr 0 \\ l+m+n \text{ odd}}} \{l^2+m^2+(2z/a+n)^2\}^{-(s-1)/2} \end{aligned}\right\} . \quad (4.07)$$

A method of evaluating these summations has already been given *. It consists in calculating by direct summation the contribution of the ions within a certain spherical cap and in replacing the rest by a continuum, each volume element of which repels or attracts according to the appropriate law. The height of the spherical cap was taken to be $3a/2$ in each case.

Values of k' and k'' for $s = 9$, 10, 11, and for two typical values of $z/a = 0{\cdot}42$ and $0{\cdot}50$ are given in Table II. †

TABLE II.

	k'.			k''.		
s.	9.	10.	11.	9.	10.	11.
$z/a = 0{\cdot}42$	4·133	4·858	5·750	0·4966	0·3725	0·2820
$z/a = 0{\cdot}50$	1·065	1·035	1·019	0·2663	0·1834	0·1278

* Lennard-Jones and Dent, Trans. Faraday Soc. *loc. cit.*

I should like to thank Mr. F. E. L. Parsons, The University, Bristol, for his help in calculating a series of these summations.

Values of ϕ_s^r are given in Table III.

TABLE III.

Potential Energy of a Pair of Unlike Ions in the Undistorted Surface.

Crystal.	NaF.	NaCl.	NaBr.	NaI.	KF.	KCl.	KBr.	KI.
$\phi_s e 10^{12}$ ergs...	−1·310	−1·053	−1·010	−0·945	−1·137	−0·962	−0·928	−·868
ϕ_s^r ,, ...	+0·637	+0·716	+0·661	+0·564	+0·612	+0·639	+0·599	+0·501
ϕ_s ,, ...	−0·673	−0·337	−0·349	−0·381	−0·525	−0·323	−0·329	−0·367

(ii.) *Calculation of* ϕ_s^*.

The potential energy of a pair of ions in the distorted surface is made up of three parts :

$$\phi_s^* = \phi_s^{*e} + \phi_s^{*r} + \phi_s^{*p}, \quad . \quad . \quad . \quad (4.08)$$

where ϕ_s^{*p} is the energy due to the polarization of the surface ions.

The calculation of ϕ_s^{*e} and ϕ_s^{*r} is exactly similar to that of ϕ_s^e and ϕ_s^r, except that z/a, instead of being 0·5, must be given its appropriate value for each crystal, *i. e.*, the equilibrium distance between the two outermost layers. These values of z/a have been calculated in a previous paper†, and are reproduced in Table VI. (as $(z/a)_0$).

We require the values of the summations $s_3(z/a), k'(s, z/a)$, and $k''(s, z/a)$ for these equilibrium values of z/a. These were all obtained by graphical interpolation of a series of calculated values. Values of s_3 are given in Table IV.

TABLE IV.

Values of Certain Summations.

z/a	0·42	0·45	0·46	0·48	0·49	0·50
$s_1 . 10^2$	2·416	1·840	1·681	1·493	1·282	1·172
$s_3 . 10^2$	1·689	1·290	1·180	0·987	0·902	0·825

The values of ϕ_s^{*e} and ϕ_s^{*r} are given in Table VI.

† Lennard-Jones and Dent, Proc. Roy. Soc. cxxi. p. 247 (1928) (see Table VI.).

In order to calculate the effect of the polarizability of the ions, we assume, as usual, that in an electric field a dipole is produced in each ion whose strength is proportional to the field. The moment of the induced dipole is then

$$p = \alpha E,$$

where E is the electric field and α is an atomic constant called the coefficient of polarizability. This assumption is used in the theory of dielectrics, and, while it is probably justified for a weak homogeneous field, it is only a first approximation for an ion in the rapidly fluctuating field at the surface of a polar crystal. The electric field at any ion is due partly to the electrostatic charges in the remainder of the crystal and partly to the field set up by the array of dipoles in the surface. In the notation of a previous paper * we write the fields at a positive and negative ion respectively as

$$\left.\begin{aligned} E_1 &= E_1{}^c + E_1{}^d = \eta_1 E_1 \\ E_2 &= E_2{}^c + E_2{}^d = \eta_2 E_2{}^c \end{aligned}\right\}, \quad . \quad . \quad . \quad (4.09)$$

where η_1 and η_2 are functions of the coefficients of polarizability and the size of the unit cell. Values of η_1 and η_2 for the eight crystals here considered are given in Table V. The values of α, the coefficient of polarizability, were taken from a paper by Born and Heisenburg †.

TABLE V.

Values of η_1 and η_2

Crystal.	NaF.	NaCl.	NaBr.	NaI.	KF.	KCl.	KBr.	KI.
η_1.....	1·35	1·54	1·61	1·71	1·17	1·41	1·51	1·60
η_2.....	0·902	0·762	0·715	0·658	1·13	0·936	0·880	0·807

The potential energy of a dipole in an electric field is easily shown to be $-\frac{1}{2}\alpha E^2$, and therefore the potential energy of the two dipoles induced in a pair of unlike ions ‡

* *Ibid.* § 2.

† *Z. f. Physik*, xxiii. p. 388 (1924).

‡ Since the potential energy of a dipole at a point on a line bisecting it at right angles is zero, the presence of the dipoles will not affect the potential field at any point in the surface, and will, therefore, make no difference to the term $\phi_s{}^*{}_e$. The energy due to the dipoles is, therefore completely accounted for by the term $\phi_s{}^*{}_P$.

$$= -\phi_s^{*p} = -\tfrac{1}{2}\alpha_1 E_1^{\,2} - \tfrac{1}{2}\alpha_2 E_2^{\,2}$$
$$= -\tfrac{1}{2}\alpha_1\eta_1^{\,2}(E_1^{\,c})^2 - \tfrac{1}{2}\alpha_2\eta_2^{\,2}(E_2^{\,c})^2$$
$$= -\tfrac{1}{2}(E_1^{\,c})^2\{\alpha_1\eta_1^{\,2} + \alpha_2\eta_2^{\,2}\}, \quad . \quad . \quad . \quad (4.10)$$

since $E_1^{\,c} = -E_2^{\,c}$.

Now †

$$E_1^{\,c} = -(32\pi e/a^3)s_1(z/a). \quad . \quad . \quad . \quad (4.11)$$

The necessary values of the summation s_1 were found by graphical interpolation of the calculated values given in Table IV. Values of ϕ_s^{*p} are given in Table VI. For reasons given above (p. 536), no great accuracy is claimed for these values. They must be regarded as rough estimates only.

Table VI.

Potential Energy of a Pair of Unlike Ions in the Distorted Surface.

Crystal.	NaF.	NaCl.	NaBr.	NaI.	KF.	KCl.	KBr.	KI.
$z/a)_0$.....	0·483	0·475	0·469	0·472	0·476	0·465,	0·460	0·469
$\phi_s^{*e}10^{12}$ ergs...	−1·527	−1·316	−1·331	−1·213	−1·405	−1·311	−1·330	−1·148
ϕ_s^{*p} ,,	−0·057	−0·053	−0·058	−0·053	−0·076	−0·085	−0·096	−0·076
ψ_s^{*r} ,,	+0·866	+1·005	+1·015	+0·866	+0·915	+1·036	+1·058	+0·824
ϕ_s^{*} ,,	−0·718	−0·364	−0·374	−0·400	−0·566	−0·360	−0·368	−0·400

From equation (4.01) we have

$$\sigma'' = (\phi_s^{*} - \phi_s)/F,$$

where F is the area of a cell containing two unlike ions and $= \frac{1}{2}a^2$, $a/2$ being the smallest distance between the two ions. Values of σ'' are given in the second row of Table VII. The units are ergs per square cm.

§ 5. Results.

The total surface energy is given by $\sigma = \sigma' + \sigma''$ (equation 2.5), and is to be found in Table VII. The surface energy due to distortion is also given as a percentage correction to σ'.

† Lennard-Jones and Dent, Proc. Roy. Soc. cxxi. p. 250 (1928).

TABLE VII.

Surface Energy of Certain Salts (100 plane).

Crystal.	NaF.	NaCl.	NaBr.	NaI.	KF.	KCl.	KBr.	KI.
σ' ergs/cm.^{2}...	+307	+93	+90	+88	+178	+75	+73	+72
σ'' "	− 42	−16	−14	− 9	− 29	−19	−19	−14
σ "	+265	+77	+76	+79	+149	+56	+54	+58
Percent. Corr. $\frac{\sigma''}{\sigma'}$	14	17	16	10	16	25	26	19

It is sometimes useful to express the surface energy per pair of unlike ions, instead of per unit area. If ρ is the total surface energy per pair of unlike ions, then $\rho = \rho' + \rho''$, where $\rho' = -\phi_{12}/2$ and $\rho'' = \phi_{11}{}^* - \phi_{11} = \phi_s{}^* - \phi_s$. Values of ρ', ρ'', and ρ are given in Table VIII.

TABLE VIII.

Surface Energy per Pair of Unlike Ions.

Crystal.	NaF.	NaCl.	NaBr.	NaI.	KF.	KCl.	KBr.	KI.
ρ' 10^{12} ergs...	+0·325	+0·152	+0·161	+0·179	+0·230	+0·147	+0·153	+0·175
ρ'' "	−0·045	−0·027	−0·025	−0·019	−0·041	−0·037	−0·039	−0·033
ρ "	+0·280	+0·125	+0·136	+0·160	+0·209	+0·110	+0·114	+0·142

It is seen (Table VII.) that the correction due to distortion at the surface varies from 10 to 26 per cent.* This correction has hitherto been assumed negligible, but it now appears that the assumption is not justified. An accurate determination of the surface energy of an ionic crystal must take the distortion at the surface into account.

* Biemuller (*Z. f. Physik*, xxxviii. p. 759, 196) has investigated the effect of the polarizability of the ions on the surface energy of several alkaline halide crystals (100 and 110 planes). He assumes, however, that the positions of the ions in the surface are unchanged, which is contrary to the result obtained by Lennard-Jones and Dent, Proc. Roy. Soc. cxxi. p. 247 (1928).

§6. Summary.

1. A method of evaluating the effect of surface distortion on the surface energy of polar crystals is described.

2. The results for eight monovalent alkaline halides are given, and show that the distortion decreases the surface energy by about 20 per cent.

3. The effect is found to be due almost entirely to the polarization of the surface ions.

My thanks are due to Professor J. E. Lennard-Jones for suggesting this problem to me, and for his interest in the work.

LVI. *The Interpretation of the Temperature Coefficient of Surface Tension.* *By* N. K. Adam, *M.A.*, *Sc.D.* (*Royal Society Sorby Research Fellow*) *.

THE object of this paper is to suggest some kinetic considerations, which, although far from rigorous, indicate that many properties of the molecules of liquids, besides molecular association, must affect the value of the differential coefficient of the "molecular free surface energy"

$$k = -\frac{d}{dT}\left\{\gamma(Mv)^{2/3}\right\} \quad . \quad . \quad . \quad . \quad . \quad (1)$$

γ being the surface tension and Mv the molecular volume; k is often called the "Eötvös" constant. A few new data on the surface tension of long chain compounds are also presented.

Hunten and Maass † have recently considered the temperature coefficient of surface tension, and related functions, in the case of homologous series of aliphatic compounds. They point out that orientation of the surface molecules perpendicular to the surface will increase the number of molecules in the surface, and so the value of k. This paper suggests a new way of regarding the temperature coefficient, and shows that numerous other properties of the molecules, most of which cannot be allowed for in the present state of kinetic theory, will probably affect the value of k.

The inadequacy of the original theory of Eötvös ‡ and Ramsay and Shields §, as a means of determining the degree

* Communicated by the Author.
† J. Amer. Chem. Soc. p. 153 (1929).
‡ Wied. *Ann.* xxvii. p. 448 (1886).
§ Phil. Trans., A, p. 647 (1893).

of association in liquids, is now fairly generally recognized; they claimed that k has a value close to 2·1 for all liquids, if M is taken as the actual molecular weight of the liquid allowing for association. Jaeger's results* illustrate the enormous variations found in k, when a sufficiently extended range of compounds is taken; thus he found values from 0·67 up to 6·75 for ordinary organic liquids, k being not always constant even for a single substance. For liquid crystals the variations in k are much greater even than this.

It appears that the Eötvös constant k actually varies more than does the simple temperature coefficient of surface tension, $-\frac{d\gamma}{dT}$, for organic substances. In a table of over three hundred organic compounds, Harkins, Davies, and Clark† give no values greater than 0·18 or less than 0·05. Experience also shows that the value of k (see Hunten and Maass) rises steadily with the molecular weight, so that it appears that the plan of multiplying by a function of the molecular weight has not been altogether successful in bringing the physical quantity, $-\frac{d\gamma}{dT}$, to a common basis for different substances.

Ramsay and Shields stressed the analogy between the rise in surface tension as the temperature *falls* from the critical, and the rise in gaseous pressure as the temperature of a gas *rises*. The mechanism underlying this analogy is not easily seen in this statement, as the quantities considered move in opposite directions with temperature; and surface tension is not a tangible physical quantity in terms of molecules, like gaseous pressure, but is only the mathematical equivalent of free surface energy.

By considering the effect of the bombardment of a barrier in the surface by the molecules of the liquid, some idea may be obtained of the meaning of the temperature coefficient of surface tension. If a barrier separates two regions at different temperatures, the bombardment on the warm side of the barrier will be more intense than that on the cold side. Let the lateral pressure due to this bombardment be F and $F+dF$, at temperatures T and $T+dT$. The net lateral pressure per centimetre in the surface will be dF dynes, away from the warm side.

Suppose that this barrier is affected only by the molecules in the surface layer, which we will assume is n molecules

* *Z. anorg. Chem.* ci. p. 1 (1917).
† J. Amer. Chem. Soc. p. 556 (1917).

thick. It is thus purely ideal, as no barrier can be conceived which distinguishes between the molecules in the surface and those in the interior; nevertheless it enables calculations to be made which may illustrate the effect of the molecular motions. The net force on this barrier, $d\mathrm{F}$, is clearly equal to the decrease in surface tension, $-d\gamma$, with the rise in temperature $d\mathrm{T}$, for if the barrier is moved through a distance dx, the work done may be written either as $d\mathrm{F}/dx$, or as $-d\gamma/dx$.

With most substances, the decrease in surface tension is nearly linear as the temperature rises; therefore F, the lateral bombardment pressure, increases linearly with temperature. This is strictly analogous to the linear rise of the pressure of a gas, with rising temperature, and is due to the same cause, namely, the increased intensity of bombardment of the boundaries by the molecules; thus if we focus attention on the thermal pressure in the liquid surface, instead of on the surface tension, the comparison between the liquid and the gas is seen to be very close.

Factors Determining the "Eötvös Constant" on the preceding Theory.

The Eötvös constant (1) becomes

$$k = \frac{d}{d\mathrm{T}}\left\{\mathrm{F}(\mathrm{M}v)^{2/3}\right\} \quad . \quad . \quad . \quad . \quad . \quad (3)$$

If the molecules are symmetrical and may be taken as occupying cubical space, the number N_0 per square centimetre is

$$n\left(\frac{\mathrm{N}}{\mathrm{M}v}\right)^{2/3},$$

where N is the Avogadro number, and n the thickness of the surface layer in molecules.

(3) then becomes

$$\frac{d}{d\mathrm{T}}\left(\frac{\mathrm{F}}{\mathrm{N}_0}\right) = \frac{k}{n\mathrm{N}^{2/3}} = 1{\cdot}395 \times 10^{-16}\frac{k}{n} \quad . \quad . \quad . \quad (4)$$

But if A is the area per molecule, $\dfrac{\mathrm{F}}{\mathrm{N}_0} = \mathrm{FA}$,

and (4) is of the same form as the equation

$$\frac{d}{d\mathrm{T}}(\mathrm{FA}) = \mathrm{R} = 1{\cdot}372 \times 10^{-16} \quad . \quad . \quad . \quad . \quad (5)$$

obtained if we differentiate the equation of state of a two-dimensional gas, $\mathrm{FA} = \mathrm{RT}$.

It is interesting to compare the value of k with that which would be obtained, on the above theory, if the rate of variation of the horizontal bombardment pressure F with temperature were actually the same as that of a perfect gas. If this is the case, comparison of (4) and (5) shows that

$$k=0{\cdot}985n \quad . \quad . \quad . \quad . \quad . \quad . \quad . \quad (6)$$

It may be more than a coincidence that this value of k is of the same order of magnitude as the experimentally determined values; n, the number of molecules in the thickness of the surface layer, is certainly small.

Association of the molecules will on this theory cause k to vary inversely as the two-thirds power of the degree of association, as in Ramsay and Shields' theory, by diminishing the number of separate molecules in the surface layer in this ratio. Elongation of the molecules, and orientation perpendicular to the surface, will increase the number in the surface, and therefore increase k. If the molecules are x-times as long as thick, then the number in the surface is

$$nx^{2/3}\left(\frac{\mathrm{N}}{\mathrm{M}v}\right)^{2/3}$$

and the constant is increased in the ratio $x^{2/3}$. Thus molecules eight times as long as thick, if oriented perpendicular to the surface, will increase k four times.

It thus appears that the orientation of the molecules, if elongated, and the thickness of the surface layer, as well as simple molecular association, will affect the value of the Eötvös constant k. And perhaps more important still are the factors which may make the comparison between (4) and (5) invalid, by rendering the rate of increase of the thermal pressure in a horizontal direction, in the liquid, different from the rate of increase of gaseous pressure with temperature; these may include the chemical attractions laterally between the molecules, and details of their shape also.

Further developments are only likely to follow when the kinetic theory of liquids is more fully understood; but these considerations are advanced as showing perhaps which properties of surfaces may be useful in developing the kinetic theory of liquids by comparison with experiment. Born and Courant's discussion * of the theory of liquid surfaces gave a value of about 2·1 for k, when the number of degrees of freedom of the surface molecules was taken as

* *Physikal. Z.* xiv. p. 731 (1913).

three ; if the number of degrees of freedom had been n, the constant would be increased in the ratio $(n/3)^{2/3}$. One way in which additional degrees of freedom of the molecules might become important could occur with molecules like the triglycerides with long chains, where three flexible chains are united rigidly at one end but are free at the other. Each of these chains might produce a thermal bombardment pressure F, like that due to single molecules of long chain compounds.

The number of factors which may affect the value of the Eötvös constant k is so great, that it is not surprising that experience has shown it to be useless as a means of determining the degree of association in a liquid.

Variation of the Temperature Coefficient of Surface Tension in Homologous Series.

In 1924, guided by the kinetic considerations just outlined, and finding the data then available in the literature on the surface tension of long chain aliphatic compounds too meagre for a thorough examination of the effect of lengthening the chains, I determined the surface tension of several compounds by Sugden's maximum bubble pressure method, using the formula in his paper of 1924 *. The bubbler was immersed in a large beaker of mercury heated on gauze by a flame, and the temperature of the bath was recorded by a mercury thermometer reading to 250°, which was compared with a standard thermometer calibrated at the National Physical Laboratory, corrections being made for the exposed column. The temperatures were probably correct within one degree; no attempt was made to obtain high accuracy of temperature reading as it was desired to obtain a large number of readings as quickly as possible. Sugden's method is admirably adapted for this, as a determination of surface tension can be made well within a quarter of an hour, and the results are reproducible within 0·5 per cent. or less after very little practice, provided the apparatus is set strictly vertical. The density was determined by weighing a lump of glass suspended from a balance by a platinum hook and thread, in air and in the liquid at different temperatures ; this gave ample accuracy for the purpose, as the density only enters as a small correction. The compounds were purified or prepared here, and I have to thank Mr. J. W. W. Dyer for preparing several of them. In working with palmityl chloride, which is decomposed by

* J. Chem. Soc. p. 29 (1924

moisture, the air current necessary for forming the bubbles was dried by drawing over sulphuric acid.

Within the temperature range investigated, the variation of surface tension with temperature was linear within the accuracy of the data, for all the substances. The results follow :—

Surface Tension of Long Chain Compounds.

Substance.	Formula.	γ at 100° C. dynes per cm.	$-\frac{d\gamma}{dT}$	Temperature range.
Caprylic acid	$C_8H_{16}O_2$	22·5 (21·6)	·080 (·082)	20–140
Lauric acid.....	$C_{12}H_{24}O_2$	24·6 (24·2)	·075 (·079)	50–150
Palmitic acid	$C_{16}H_{32}O_2$	25·9 (25·9)	·075 (·075)	65–170
Eicosoic acid	$C_{20}H_{40}O_2$	26·7	·068	80–200
Hexadecyl alcohol.....	$C_{16}H_{34}O$	25·1	·078	·50–180
Palmityl chloride	$C_{16}H_{31}OCl$	25·0	·090	20–130
α Bromopalmitic acid ...	$C_{16}H_{33}BrO_2$	27·4	·072	60–150
Pentærythritol tetra-palmitate	*a*	26·6	·064	80–190
Tetradecane	$C_{14}H_{30}$	20·2	·085	20–150
Triacontane	$C_{30}H_{62}$	25·4	·070	75–175

a. $C(CH_2OOC.C_{15}H_{31})_4$. The Eötvös constant for this substance is 6·1.

The figures underneath mine for the first three acids, in brackets, are obtained by plotting Hunten and Maass' results. These were obtained by the method of capillary rise, and inspection of the plot shows that they lie rather less consistently on a smooth curve than mine; the discrepancy between my results and theirs is not serious except in the case of caprylic acid.

Conclusions from the behaviour of Long Chain Compounds.

The figure shows how the temperature coefficient of surface tension, $-\frac{d\gamma}{dT}$, varies with the length of the hydrocarbon chains in the case of the four homologous series, hydrocarbons, fatty acids, normal amines, and triglycerides. The data used are, in addition to the above determinations, those of Maass and Wright * and

* J. Amer. Chem. Soc. p. 1098 (1921).

Hunten and Maass on the acids and hydrocarbons ; and of Jaeger on the triglycerides and the normal amines, as well as a few data from the 'International Critical Tables,' iv.

The data gave practically constant values for $-\frac{d\gamma}{dT}$ over the whole experimental range of temperature, except for triacetin and tributyrin, for which the points plotted are the constant values between 65° and 200°; below 50° distinctly lower values were obtained.

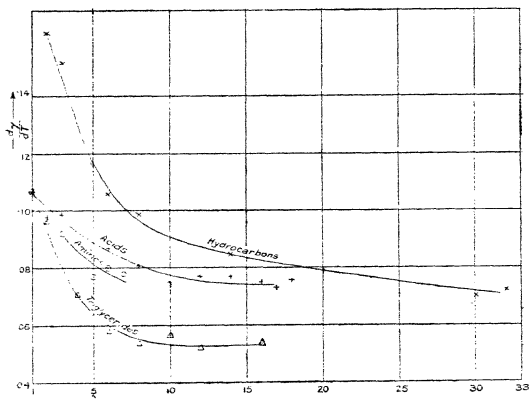

All the four series have high values of $-\frac{d\gamma}{dT}$ for the shorter chain compounds, which fall asymptotically to a nearly constant value as the chains are lengthened. The limiting value for the hydrocarbons, acids, and probably the amines also, is about 0·07; the triglycerides tend to a value about 0·053, decidedly lower. The acids, triglycerides, and probably the amines approach the limiting value within experimental error when the chains are about ten carbons long ; the hydrocarbons not till at least double this length of chain.

The results are most easily explained by an orientation of the molecules, which becomes nearly complete, and identical in the different series considered, when the chains are about

ten carbon atoms long, and the molecules have a polar group at one end. With the hydrocarbons, which are not loaded at one end, the orientation does not become complete until the chains are probably at least double this length. The orientation may be perpendicular to the surface, but the data indicate no more than that it is similar for all the series of single chain compounds. $-\frac{d\gamma}{d\mathrm{T}}$, or $\frac{d\mathrm{F}}{d\mathrm{T}}$, measures the change in the intensity of the horizontal bombardment pressure of the surface molecules on the ideal barrier of the preceding theory. This may be expected to be exerted mainly by the long chains singly, if they are long enough; the fact that the triglycerides tend to a rather lower limiting value of $\frac{d\mathrm{F}}{d\mathrm{T}}$ than the single chain compounds indicates that their thermal motions *per chain* (not per molecule) are somewhat more restricted than those of the single chain compounds. This may be due either to the polar ends of the molecules contributing less per chain to F than when these ends are separated, or to some restriction on the motions of the chains, due to their being united at their bases. But as the limiting value of $\frac{d\mathrm{F}}{d\mathrm{T}}$ is only about 25 per cent. less for the triglycerides than for the single chain compounds, it seems that there must be a considerable amount of separate transverse motion in the long chains of the triglycerides.

Certain knowledge along these lines must await a more accurate knowledge of the kinetic theory of liquids; but these considerations are advanced as showing that we may learn more from studying the simple quantity $-\frac{d\gamma}{d\mathrm{T}}$, in the light of the chemical constitution of the molecules, than by forming the Eötvös constant.

Summary.

The rate of decrease of surface tension with temperature, $-\frac{d\gamma}{d\mathrm{T}}$, may be quantatively regarded as the rate of increase, $\frac{d\mathrm{F}}{d\mathrm{T}}$, of the thermal bombardment pressure F, exerted by the surface molecules, parallel to the surface on a barrier in the surface. This point of view shows the

physical similarity between the rise in pressure of a gas and the fall in surface tension of a liquid, as the temperature rises.

The development of this theory shows that the following factors, besides molecular association, will probably affect the value of the "Eötvös constant"

$$\frac{d}{dT}\left\{\gamma(Mv)^{2/3}\right\} :$$

orientation of the surface molecules, the number of molecules in the thickness of the surface layer, the number of their degrees of freedom as regards motions which can produce thermal bombardment, and all properties which may cause the thermal bombardment pressure in the surface to differ from that of a perfect two-dimensional gas, which will include chemical attractions between the surface molecules and details of their shape and size. As these factors, particularly the last two, cannot be evaluated at present, it is not surprising that Eötvös' rule has been shown in practice to be quite untrustworthy for determining the molecular association of liquids.

The temperature coefficient of surface tension of four homologous series is considered, and some new data presented for long chain compounds. There appears to be nearly complete orientation of the surface molecules when the chains are ten carbons or more long, if the molecules have a polar group at one end: the hydrocarbons are probably not fully oriented till double this length of chain. The intensity of vibration of the molecules of the triglycerides appears to be somewhat less than that of three chains separately, although the chains clearly move independently to a large extent.

The University, Sheffield.

LVII. *The Heats of Dissociation of some Strong Electrolytes in Benzonitrile and their Calculation from Molecular Structure.* *By* A. R. Martin, *Ph.D.**

MEASUREMENTS of the dielectric constant of benzonitrile over the temperature range 0° to 70° C., for which the author is indebted to Dr. A. O. Ball, make it possible to calculate the dissociation constants of strong electrolytes in this solvent from conductivity data by the method and from the data published previously †, and from

* Communicated by Prof. J. C. Philip, F.R.S.

† Martin, J. Chem. Soc. p. 3270 (1928).

the variation of the dissociation constant with temperature to calculate the heats of dissociation by means of the van't Hoff Isochore.

The values of the dielectric constant of benzonitrile (D), determined by a bridge method at a frequency of 1000 cycles per second, are as follows :—

Temp.....	0°	25°	40°	50°	55°	70° C.
D.	27·58	25·22	24·04	23·31	22·96	21·98.

In Table I. are given the dissociation constants, corrected for activity, of the following electrolytes in benzonitrile

TABLE I.

Electrolyte and Temperature.	Dissociation Constant × 1,000. Dilution (litres). 5000.	2000.	1000.	500.	100.	Mean.
° C.						
LiI. 0.....	5	5	5	5	5	5
25.....	10	9	7	7	9	8
50.....		10	8	7	10	9
NaI. 0.....		8	10	12		10
25.....		15	15	13		14
50.....		13	10	10		11
70.....		15	10	7		10
KI 0.....		18	14			16
25.....	13	10	10			11
40.....	7·2	7·3	7·2			7·2
55.....	6·7	6·6	6·6			6·6
70.....	6·1	6·1	5·9			6·0
LiBr. 0.....	0·35	0·30	0·26	0·26		0·29
25.....	0·36	0·34	0·27	0·29		0·31
50.....	0·35	0·31	0·25	0·26		0·29
70.....	0·32	0·25	0·23	0·23		0·26
$AgNO_3$ 0.....	0·39	0·46	0·48	0·53	0·48	0·49
25.....	0·40	0·40	0·40	0·39	0·42	0·40
40.....	0·34	0·34	0·34	0·34	0·39	0·35
55.....	0·32	0·33	0·33	0·32	0·35	0·33

over the temperature range 0° to 70° C., the iodides of lithium, sodium, and potassium, lithium bromide, and silver nitrate.

The foregoing mean values of the dissociation constants yield the values of the heats of dissociation given below. The values of the dissociation constants at 0° C. are not as trustworthy as at the other temperatures, since the differences between the observed and theoretical values of the equivalent conductivity are smaller at this temperature than at

the others. For silver nitrate the heat of dissociation may be quoted to 0·1 k. cal., but for the other more strongly dissociated salts, where the values of the dissociation constants are less certain, the heats of dissociation may be quoted only to the nearest k. cal.

Electrolyte	LiI	NaI	KI	LiBr.	$AgNO_3$
Heat of dissociation in k. cals.	+2	−1	−3	0	−1·4

The heat of dissociation of an electrolyte in any solvent may be calculated from theoretical considerations in the following way. The dissociation may be imagined to be carried out in three stages, (1) removal of the undissociated molecule, which is an electrical dipole, from the solvent to a vacuum or air, (2) dissociation of the vapour molecule in a vacuum or air, and (3) solvation of the resulting ions.

The energy change in process (2) for certain atomic ions has been calculated by Born and Heisenberg *. Born and Heisenberg take into account the inverse square attraction, the inverse 9th power repulsion, and the attraction due to the dipoles set up by the mutual deformation of the ions. They show that the heats of formation of undissociated vapour molecules so calculated agree well (1 to 5 per cent.) with the difference between the lattice energy and the experimentally determined heat of sublimation of the salt. The effects of ionic deformation are responsible for 10 to 20 per cent. of the energy of formation of an undissociated vapour molecule.

The energy change in process (3) has been calculated by Born †, by considering the change in the energy in the medium resulting from the transfer of the ion, treated as a charged sphere, from a vacuum or air, that is from a medium of dielectric constant unity, to a medium of dielectric constant D. This energy change, in k. cals. per mol, is given by

$$\frac{z^2e^2}{2r}\left(1-\frac{1}{D}\right)\frac{N}{J} \quad . \quad . \quad . \quad . \quad . \quad . \quad (1)$$

where, e = the elementary charge of electricity;

N = the Avogadro number;

J = the mechanical equivalent of heat (ergs per k. cal.);

z = the valency of the ion;

r = the radius of the ion.

* Born and Heisenberg, *Z. f. Physik*, xxiii. p. 388 (1924).

† Born, *Z. f. Physik*, i. p. 45 (1920).

Born has shown that from the heats of hydration of ions obtained by the method of Fajans* values of r of the correct order of magnitude can be calculated by means of equation (1).

The energy change in process (1) may be calculated as follows. Consider a small electrical dipole in a medium of dielectric constant D. If the dipole is sufficiently small the electric field, E, at any point P is given by

$$E = \frac{M}{Dr^3}\sqrt{1+3\cos^2\theta}$$

where, M = the moment of the dipole;

r = the distance from P to the mid point of the dipole;

θ = the angle between r and the axis of the dipole.

The energy per c.c. of the medium is

$$\frac{DE^2}{8\pi} = \frac{M^2(1+3\cos^2\theta)}{8\pi Dr^6}.$$

The element of volume swept out by the element of area dS, in polar coordinates, at P in rotating about the axis of the dipole is

$$2\pi r^2 \sin\theta\, dr\, d\theta,$$

and since from symmetry every portion of this annulus is similarly situated with respect to the origin, the electric field at every point in it is the same, and the energy contained in the annulus is

$$\frac{M^2(1+3\cos^2\theta)}{4Dr^4}\sin\theta\, dr\, d\theta.$$

Therefore the total energy in the medium around the dipole is

$$\sum_{r=a}^{r=\infty}\sum_{\theta=0}^{\theta=\pi}\frac{M^2}{4Dr^4}(1+3\cos^2\theta)\sin\theta\, dr\, d\theta.$$

where a is some function of the size of the dipolar molecule,

$$=\frac{M^2}{4D}\int_{r=a}^{r=\infty}\int_{\theta=0}^{\theta=\pi}\frac{1}{r^4}(\sin\theta+3\cos^2\theta\sin\theta)\,dr\,d\theta.$$

* Fajans, *Verh. Deut. phys. Ges.* xxi. pp. 549, 709 (1919).

The evaluation of this integral is

$$\frac{M^2}{3Da^3}.$$

Therefore the energy change in removing the dipole from a medium of dielectric constant D to a vacuum or air is, in k. cals. per mol,

$$-\frac{M^2}{3a^3}\left(1-\frac{1}{D}\right)\frac{N}{J} \quad . \quad . \quad . \quad . \quad . \quad . \quad (2)$$

The lower limit of integration a, the distance from the origin at which the medium commences, has been taken equal to the radius of the sphere of volume equal to the volume of the dipolar molecule.

Owing to the uncertainty of the numerical values to be assigned both to a, which enters into the calculation cubed, and to the radii of the free ions, the following procedure has been adopted in applying these theoretical results to the present data. The values of M and of the heats of dissociation in a vacuum have been taken from Born and Heisenberg's paper. The volume of the undissociated molecule has been calculated by taking the distance apart of the nuclei of the ions given by Born and Heisenberg to be the sum of the ionic radii, and by assuming that the radii of the kation and anion bear the same ratio to each other in the dipole as in the crystal lattice. The heat of removing the undissociated molecule from the solvent and of dissociating it in a vacuum having thus been calculated, the value of the heat of solvation of the ions required in order that the calculated may equal the observed value of the heat of dissociation in the solvent was found. The free anion was assigned the radius given by Goldschmidt *, and its heat of solvation calculated. By subtracting this from the total heat of solvation required, the required heat of solvation, and hence, from equation (1) the radius, of the free kation was calculated. The dielectric constant of benzonitrile has been taken as 25.

In Table II. are given the results of these calculations for sodium and potassium iodides, together with the values of the ionic radii obtained from crystal data by Goldschmidt * (which are in close agreement with those calculated by Pauling † from the wave mechanics). It is impossible to perform the calculations for the other salts, since Born

* Goldschmidt, Trans. Faraday Soc. **xxv.** p. 253 (1929).
† Pauling, J. Amer. Chem. Soc. **xlix.** p. 765 (1927).

and Heisenberg's calculation cannot at present be carried out for polyatomic or for lithium ions.

TABLE II.

	Sodium Iodide.	Potassium Iodide.
Distance between the nuclei in the undissociated molecule (cms.)...	$2{\cdot}59\times10^{-8}$	$2{\cdot}86\times10^{-8}$
Radius of the anion in the undissociated molecule (cms.)	$1{\cdot}79\times10^{-8}$	$1{\cdot}79\times10^{-8}$
Radius of the kation in the undissociated molecule (cms.)	$0{\cdot}80\times10^{-8}$	$1{\cdot}07\times10^{-8}$
Radius of the sphere equal in volume to undissociated molecule (cms.).....	$1{\cdot}84\times10^{-8}$	$1{\cdot}92\times10^{-8}$
Dipole moment of the undissociated molecule (e.s.u. and cms.) .	$1{\cdot}24\times10^{-17}$	$1{\cdot}36\times10^{-17}$
Heat of removing the undissociated molecule from benzonitrile to a vacuum (k. cals. per mol)	−114	−123
Heat of dissociation in a vacuum (k. cals. per mol)	−126	−113
Heat of solvation of the ions required (k. cals. per mol)	+239	+233
Radius assigned to the free anion (cms.).....	$2{\cdot}20\times10^{-8}$	$2{\cdot}20\times10^{-8}$
Heat of solvation of the free anion (k. cals. per mol)	+ 72	+ 72
Heat of solvation of the free kation required (k. cals. per mol).	+167	+161
Radius of the free kation required (cms.)	$0{\cdot}95\times10^{-8}$	$0{\cdot}99\times10^{-8}$
Radius of the kation (Goldschmidt) (cms.)	$0{\cdot}98\times10^{-8}$	$1{\cdot}33\times10^{-8}$
Radius of the anion (Goldschmidt) (cms.).....	$2{\cdot}20\times10^{-8}$	$2{\cdot}20\times10^{-8}$

The agreement between the observed and calculated values of the ionic radii is satisfactory, considering the approximations which have been made in the calculations. It therefore appears probable that an undissociated molecule of a strong electrolyte in a solvent is the same as the undissociated vapour molecule, that is a pair of deformed ions in contact with each other, there being no intervening medium.

Imperial College of Science and Technology,
London, S.W. 7.
20th July, 1929.

LVIII. *Ionization Currents from Zinc Oxide Smokes.*

By H. P. WALMSLEY, M.Sc.*

THIS paper describes the ionization currents from clouds or smokes of zinc oxide particles and is supplementary to earlier work on the currents from clouds of cadmium oxide particles. A zinc oxide smoke is produced in a large cistern from say, an electric arc between zinc electrodes. The ionization initially and its time changes as the smoke ages are measured.

The general arrangement of the apparatus used and the manner of working have been described previously [1]. A steady flow of smoke from the cistern was passed through an ionization vessel consisting of two concentric cylinders. The outer cylinder was connected to one terminal of a battery giving up to 1,000 volts, to produce an electrostatic field within the vessel. The inner cylinder was connected to a Dolezalek electrometer. The currents were measured either by the time rates of the deflexions, or by shunting the inner cylinder to earth through a high resistance and measuring the differences in potential between the two ends of the resistance. The rate of flow of smoke through the ionization vessel was measured directly by the rate of efflux of water from the constant head aspirator producing the flow. It was found that flow-meters, particularly of the Venturi type, were unreliable, as constrictions in the circuit tend to get clogged with deposited particles.

Smokes dispersed from a Zinc Arc.

A series of smokes of increasing weight concentration produced from an arc between zinc electrodes was examined. The increases in the mass of material dispersed were obtained by keeping the conditions at the arc as nearly as possible constant throughout the series and allowing the current to flow for increasingly longer periods of time ranging from 10 seconds to 40 seconds. The absolute values of the concentrations are unknown. There is no simple and satisfactory method of measuring this quantity. To ensure homogeneity of the cloud, the fan in the cistern

* Communicated by the Author.

was kept running for some time after the smoke had been dispersed. Measurements of the ionization current were made from immediately after dispersal was complete until the currents became negligibly small. The rate of flow of

Fig. 1.

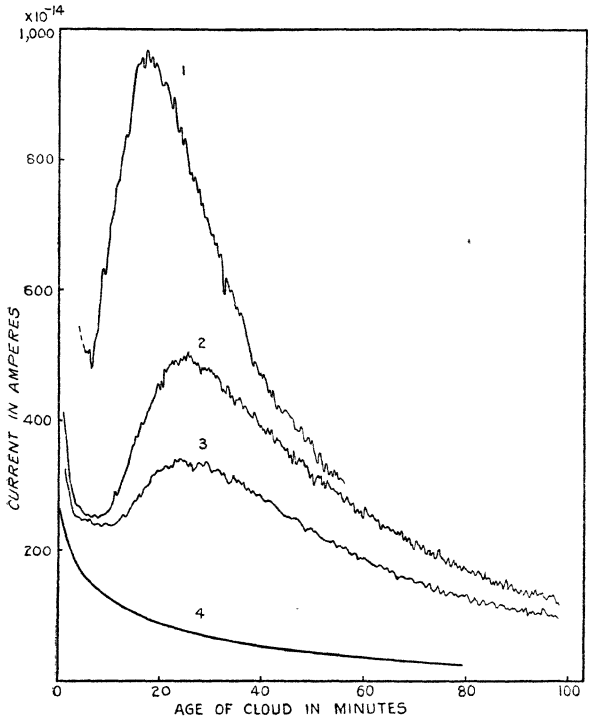

smoke through the ionization vessel was constant and the same in each run and the electric field was sufficient to give the saturation value of the current for all ions entering it of mobility greater than 1×10^{-4} cm^2./sec. volt.

The curves of fig. 1 show how, after dispersal, the ionization currents from negative carriers for four smokes of the series change with time. The currents were measured by the steady deflexion method and are represented by the ordinates, the unit being 10^{-14} ampere. Their numerical values are roughly equal to the deflexions observed in scale-divisions (mm.). Curve 1 was obtained from the smoke of greatest concentration. This filled the smoke chamber with a dense fog. Curve 4 was obtained from the smoke of least concentration. This was invisible in the smoke chamber. Curves 1, 2, 3 are oscillatory and show that at some time after the dispersal process has been completed, the current strength increases to a maximum before it ultimately diminishes. The fluctuations in curve 4, however, are only of the order of magnitude of the fortuitous movements of the electrometer needle about the zero, due to unsteadiness. In other words, the curve is indistinguishable experimentally from one which would be given by a smooth continuous process. The currents obtained from zinc oxide particles are therefore like the ones obtained from cadmium oxide particles produced under similar experimental conditions [2].

The behaviour of the ionization currents is closely associated with the behaviour of the particles which form the smokes. The primary particles of a smoke dispersed from a metallic arc diminish in number by a process of aggregation, whereby complex particles (aggregates) are produced. There is also a loss due to sedimentation of the heavier particles. Further, it is known both by direct observation with the ultramicroscope and from estimates of the mobilities of the ions, that the electrical charges are carried at least partially by the particles. Provided the particles are small enough, the charges carried can influence the rate of aggregation, but in most smokes a stage must ultimately be attained when their influence is negligible. There are reasons for supposing that the initial electrification of the primary particles is a secondary effect as regards the behaviour of the disperse system. The charges themselves are supposed to originate from thermal emissions at the high temperature of the arc and to combine afterwards with the primary particles formed simultaneously. This would account for the fact that the particles are not all charged and is supported by the observations of Erikson [3] and others on ions emitted

from hot metals. For example, it is found that although the initial positive ion emitted from hot platinum during an interval of the order of one-third of a second from birth usually changes over into a normal ion of mobility 1·36 cm.²/sec. volt, identical with the normal ion produced in air by the α rays from polonium, if the temperature of the platinum is very high and the ions are allowed to remain for a short time in the air which has left the platinum surface, they load up and form heavier ions. That is they unite with the particles which are known to be produced from a platinum surface under these conditions. The electrons and initial positive charges emitted by the arc during the dispersal process have the option of uniting with gas molecules to form normal ions and of uniting with primary particles. Their distribution as normal ions and charged particles depends upon the relative collision frequencies, the greater probability of a collision with a particle in the latter case being discounted on most occasions by the relatively much greater number of gas molecules. Thus we may consider that a smoke consists initially of a collection of charged and uncharged primary particles and of normal ions, which may disappear by uniting with particles subsequently and by recombination amongst themselves.

As the cloud ages, the process of aggregation of the particles, together with the loss of normal ions by combination with particles, produces carriers of varying and diminishing mobilities in the smoke. The loss of mobility of the charges of itself causes little diminution with time in the measured current strength, if the field in the ionization vessel is sufficiently intense to give continuously the saturation current from the stream passing through it; but a decrease begins of course, as soon as groups of charged particles are formed whose mobilities are so low that the velocity impressed upon a group by the field is insufficient to drive the whole of the carriers into the collecting electrode. Sedimentation and diffusion to the walls in the main body of the smoke also affect the currents measured, but the principal loss arises from the recombination of unlike charges on the normal ions and the particles. These effects account for the initial falls in current strength in the curves of fig. 1. Some of them are illustrated in more detail in what follows.

Recombination of the Initial Charges.

Fig. 2 shows how the reciprocal of the current varies with time for the smoke of curve 4, fig. 1. For a short period the curve is concave to the axis of time, but afterwards it is practically linear. The number N of negative charges per unit volume of the smoke at time t can therefore be represented by the equation

$$\frac{1}{N} - \frac{1}{N_0} = \beta t$$

Fig. 2.

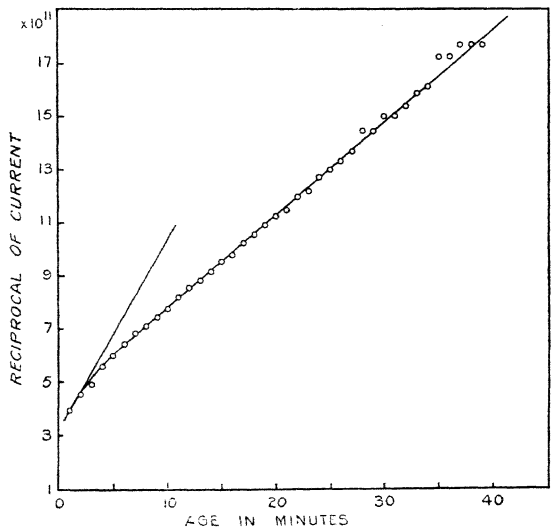

where N_0 is the initial number of negative charges. The value of β diminishes where the curve is concave, but it is constant over the linear portion. The most probable cause of the early curvature is that α, the coefficient of recombination of the charges, is diminishing in a similar way to the quantity β. This means that the mobilities of the carriers are diminishing as the smoke ages and/or that the ratio of the number of collisions which result in

recombination to the total number occurring between carriers of unlike charges decreases with time[1]. The quantity α is no longer a specific constant appropriate to a given type of ion, but is an average value which is changing with time. If the initial number of positive and negative carriers were unequal and α were constant, the curve of fig. 2 would be convex to the axis of time. It is probable from their origin that actually there is an initial excess of one kind of electricity, but it is not known with certainty whether an excess was present in this particular case. If there is a production of charges in the smoke after dispersal has ceased, and it will be seen later that this is the case, it is evident that a system which would otherwise obey the ordinary law of recombination and give a straight line when the reciprocal of the current is plotted against time, will now give a curve concave to the axis of time. The effects of sedimentation and diffusion, like inequality of the initial charges, tend to make the curve convex to the axis of time. As the observed curve is the resultant effect, it is obvious that β is a very complex physical quantity, although from fig. 2 it appears simple empirically. With denser smokes of course, *e. g.*, that of curve 3 (fig. 1), the curvature becomes increasingly noticeable. The numerical value of β in fig. 2 varies from $7{\cdot}0\times10^{-10}$ (the tangent) to $3{\cdot}6\times10^{-10}$ for the linear portion of the graph, where the second has been taken as the unit of time and the elementary charge as $4{\cdot}77\times10^{-10}$ E.S.U. The quantity β is therefore of much smaller magnitude than the coefficient of recombination for ions produced in air by X-rays. The value of the latter is $1{\cdot}6\times10^{-6}$. Therefore, if we assume that with clouds of very low concentration the order of magnitude of β is equal to that of α, the coefficient of recombination of the ions in the cloud, the mean mobility must be of the order of 10^{-4} cm.^{2}/sec. volt, since the coefficient of recombination is approximately proportional to the sum of the mobilities of the positive and negative carriers. Obviously the carriers of the charges in a smoke are large.

The close connexion between the particles and the charges makes a comparison of the rate of decay of the current with the rate of coagulation of a smoke of interest. The latter has been measured for smokes dispersed from various substances of low vapour-pressure by Green[4] who used a method based upon the Aitken effect, and by

Professor Whytlaw-Gray [5] and his collaborators, who used a modification of the Zsygmondy slit ultramicroscope to count the particles. It is found that the number n of particles per unit volume diminishes with the age t of a smoke according to the formula

$$\frac{1}{n} - \frac{1}{n_0} = \mathrm{K}t,$$

where n_0 is the initial number of particles per unit volume and K is a constant for a given cloud. As with β, it is found that K varies slightly from cloud to cloud. The mean of the values quoted by Green for ammonium chloride smokes is $9{\cdot}5 \times 10^{-10}$ and for cadmium oxide smokes it is $7{\cdot}7 \times 10^{-10}$, using the second as the unit of time. Whytlaw-Gray's values for a series of smokes from each of four substances, NH_4Cl, As_2O_3, antipyrin, and CdO range from $5{\cdot}0 \times 10^{-10}$ to $10{\cdot}0 \times 10^{-10}$ with a mean about $7{\cdot}3 \times 10^{-10}$. These quantities are of the same order of magnitude as the values for β in the smoke of fig. 2. It therefore seems that with clouds of low mass concentration, the rate of decay of the current is controlled mainly by the rate of aggregation of the particles. To a first approximation, the chance of a negatively charged particle uniting with a positively charged particle and thereby entailing the loss of a negative charge is equal to the chance of two uncharged particles colliding and uniting, causing the loss of a particle.

On theoretical grounds it is to be expected that, in the very early periods of the life of a smoke, the initial charges will disappear at a greater rate than the smoke particles, but that later, as they become attached to particles, the rate will approximate to that at which the particles disappear. This results from the size of the particles. An accurate comparison of the values of β and K would be of value but it requires two sets of observations upon the same cloud.

The concomitant disappearance of charges and particles according to the preceding formulæ has been observed by Kennedy [6] in the case of the large ions and condensation nuclei from a bunsen flame, where the particles are probably liquid. Kennedy's values for the quantities β and K were $6{\cdot}3 \times 10^{-10}$ and $14{\cdot}0 \times 10^{-10}$ respectively. Here the mobility of the large ions was found to be ·0003

cm.²/sec. volt, and the mobilities of all the ions were the same.

Ionization produced in the Smokes after dispersal.

When the mass of material dispersed is increased, fig. 1 shows that the ionization curves change their form. After the initial fall, the current rises again and passes through a maximum before settling down into a general decrease with time. It can be shown by the same methods which were used in the case of cadmium oxide smokes, that the rise in current strength is due to a production of ions in the smoke as it ages. To explain the curves the following theory was proposed [2]. It is supposed that the complex particles produced by the process of aggregation are not all stable and that the unstable complexes are liable to break up again, presumably under the influence of molecular bombardment by the gas molecules of the medium. When this occurs new charges appear. The intensity of the ionization so produced and the total number of complex particles in the smoke are assumed to change with time in a similar way. The intensity is therefore zero initially. It rises to a maximum and afterwards diminishes as the cloud ages. The total ionization at any moment in the life of a cloud thus consists of two parts, the charges remaining from the initial ionization which accompanied the formation of the primary particles and the charges produced by the disruption of unstable aggregates which have formed during the process of coagulation.

It has been shown with the smokes from many metals [7], and it is probably true for all, that the formation of the primary particles dispersed from an arc takes place at a high temperature. It has also been assumed that the initial charges are adventitious and arise from thermo-electric emissions at the high temperature of formation. The initial ionization ought to be eliminated therefore if we could disperse the same kind of particles at comparatively low temperatures, when we should obtain a system containing no ions initially, in which a spontaneous production of ions occurs as it ages. Such a system is obtained if the zinc oxide is dispersed by the decomposition of diluted zinc ethyl vapour in air. Fig. 3 shows two typical ionization curves for zinc oxide clouds produced in this way.

The zinc ethyl vapour was passed into the cloud chamber with a current of nitrogen. This was used so that the composition of the medium would be altered as little as possible from that of dry dust-free air. Nitrogen from a cylinder of the compressed gas, freed from oxygen and moisture in the usual way, passed through a flow

Fig. 3.

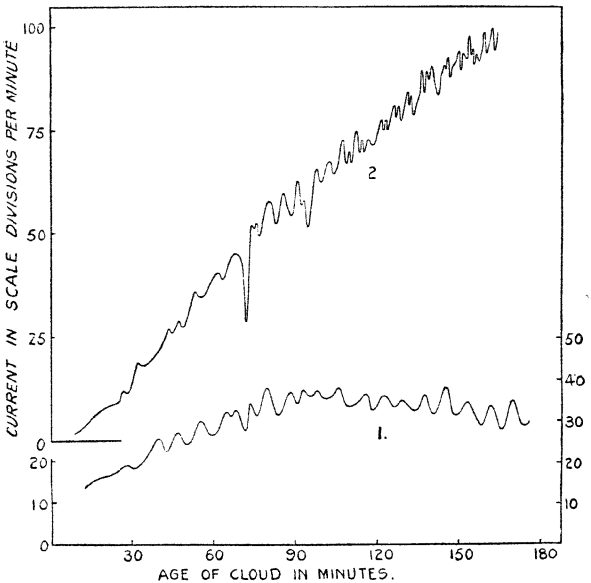

meter and dust filter along a tube which opened centrally in the cistern. A branch circuit was arranged between the flow meter and filter so that the gas stream could be deflected through a large bottle containing a little liquid zinc ethyl. The procedure adopted to disperse a series of clouds of increasing concentration was the following. Nitrogen was passed into the chamber at a fixed rate for a given period of, say, 10 minutes each run. During this period

the gas stream was diverted through the bottle containing the zinc ethyl for increasingly longer times up to 8 minutes. The nitrogen which passed into the chamber before the stream was deflected along the branch circuit swept the discharge tube free from air, and that which passed after the flow was redirected along the main circuit cleared the discharge tube from traces of zinc ethyl vapour. Equal quantities of nitrogen were used for the two operations in any given case so that the middle of the period of 10 minutes could be made the arbitrary zero of time for computing the age of the cloud. After dispersal, the currents were measured under precisely the same conditions as those in fig. 1. The currents obtained from all the smokes examined were very much weaker than those obtained from smokes dispersed from an arc, so they were measured by time rates of deflexion. To increase the number of observations on a given smoke, several measurements were made in succession each time the electrometer needle was set in motion. The measurements therefore occur in groups which can be fairly readily picked out on the graphs. These are drawn to include every observation.

Curve 1 (fig. 3) shows the results obtained from a smoke in which the zinc ethyl was at 15·5° C. during the dispersal process. The general trend of the current is from zero initially to a maximum at about 90 minutes, after which a slow diminution in current occurs. The curve is therefore of the form anticipated.

It was found that with the zinc ethyl at room temperatures, increasing the concentration of the smoke by the method already described did not cause any great changes in the currents measured. The ordinates of the curves which represented the smoothed out mean current at any age increased towards a maximum as the concentration increased but afterwards tended to diminish. The diminution occurred first where the age of the cloud was great and progressed gradually towards the origin of time, thus causing the current curves for larger concentrations to fall off more rapidly and intersect the curves from the weaker smokes. One would expect this effect if the masses of the particles rather than their number increased with increasing concentration and if the field strength employed was insufficient to ensure saturation. The same effect was observed in a series in which the nitrogen was replaced

by carbon dioxide, the general characteristics being similar. It is highly probable that this results from the relatively long time occupied in dispersing the cloud. The particles formed by the decomposition of the first portions of the zinc ethyl vapour as it comes in contact with the air in the chamber are distributed by the fan which is kept running to ensure homogeneity of the smoke. Hence, the later portions of the vapour decompose in a medium containing zinc oxide particles, which will undoubtedly act as centres of condensation and preferentially collect the molecules of zinc oxide which result from the reaction. This tends to increase the average mass of the particles rather than their number as the duration of the reaction is increased. It may be pointed out that cadmium oxide particles act in this way as nuclei for the condensation of cadmium oxide vapour [8]. The effect seems to have been observed more directly by Green [4]. He finds that the initial number of particles in an ammonium chloride smoke dispersed by volatilization in dust-free air increases very slowly with the concentration; *e. g.*, a tenfold increase in the latter gave an increase of about one third in the number of particles per unit volume. He explains this result on similar lines.

It was found that increasing the vapour pressure of the zinc ethyl leaving the discharge tube increased the ionization of the cloud. The bottle containing the zinc ethyl in the branch circuit was immersed in a bath of warm water and to prevent loss of vapour as it was carried through the filter by the nitrogen, the filter and the exposed parts of the discharge tube were raised to a higher temperature. Curve 2 of fig. 3 shows the currents obtained when the temperature of the bath was 35° C. and the time of flow of vapour was 2 mins., all other conditions being precisely the same as for curve 1, where the temperature was 15·5° C. and the time of flow 9 mins. The current rises as before and approaches a maximum nearly three times as great as the previous value, at about three hours after dispersal. Had measurements been continued longer the current would have been found to decrease.

If we assume von Weimarn's law of corresponding states to hold for the reaction with zinc ethyl in dust-free air, the increased vapour pressure in the case of the cloud of curve 2 will give a higher degree of dispersion than the reaction for the cloud of curve 1, that is, the particles

will be finer. The shorter time involved in dispersal will tend to enhance the difference in size since the particles first formed in the reaction are less likely to act as condensation nuclei for those formed later. The total mass of oxide produced will probably not differ much in the two cases, so there is a corresponding increase in the number of particles per unit volume in the cloud of curve 2. It is probable therefore that in this cloud the particles are both more numerous and smaller than in the cloud of curve 1 and it is tempting to ascribe to this the difference in intensity of the ionization.

The general shape of the two curves is the same and if we attribute the difference in quality to the degree of dispersion—the average size and distribution of sizes amongst the particles—we seem able to account for the failure at present to produce from zinc ethyl, clouds giving currents of the intensity of those attributed to the disruption of complexes in the clouds produced from a zinc arc. The supersaturation in the arc must be vastly higher than anything yet attained with zinc ethyl. The point established by the experiments is that there is a formation of ions in zinc oxide clouds as they age and that this is quite independent of whether the clouds are ionized on formation or not.

The Nature of the Zinc Oxide Particles.

The question whether the same kind of particles was produced by the decomposition of zinc ethyl and by the electric arc was decided by X-ray analysis. The dispersed particles were precipitated electrically by an intense field and a sample from each source was examined by the powder method using CuKα radiation. Each gave a spectrum characteristic of a crystalline powder, although the lines were rather diffuse on account of the small dimensions of the individual particles. Their positions and intensities were in close agreement with those recorded by Weber[9]. The closest agreement between the observed and calculated values for the spacings measured was obtained with an axial ratio of $\gamma = 1{\cdot}605$ which led to a mean value of $a = 3{\cdot}250$ Å. Thus the lattice constants are $a = 3{\cdot}250$ Å. $c = 5217$ Å., whence $\rho = 5{\cdot}62$ grams/cm.^{3} These agree with Weber's values, $a = 3{\cdot}251$ Å., $c = 5{\cdot}226$ Å., slightly better than with the more recent ones of Barth[10], $a = 3{\cdot}242$ Å., $c = 5{\cdot}176$ Å. The particles produced by both

reactions are therefore identical. They are minute crystals of the normal structure and density of zinc oxide in the crystalline form—zincite, and the complex particles are crystal aggregates, most probably dendritic in form.

Incidental Observations.

In the preceding experiments the currents were obtained from a portion of cloud in motion through a metal tube. Now it is well known that wet steam, that is steam containing liquid particles, impinging on a solid surface gives rise to electrification although dry steam or dry gases do not. This suggests that the motion of the cloud in the apparatus may have some effect on the currents measured. Again when fine dusts are dispersed by an air blast the particles become charged, the electrification being usually attributed to a frictional effect between the particles and the medium. We have to decide therefore whether the currents measured arise from the motion of the cloud or not. If they do, the charges in the case of a cloud produced from zinc ethyl may be attributable to a triboelectrical effect. If not, that cloud provides us with a system which has the novel property of ionizing itself spontaneously. Although it is probable that the ionization in smokes has a very close connexion with the electrification produced in dusts by an air blast, it is clear from the dependence of current strength upon the age of a cloud that more is involved in the production of cloud ionization than the mere rubbing of the medium against the surfaces of the particles. The following additional results on the cloud of curve 2 (fig. 3) seem to support the view that the ionization process is spontaneous.

(*a*) At 2 hr. 44 mins. the current from the smoke was 98 units. At 2 hr. 45 mins. a two-way tap immediately in front of the ionization chamber was turned and the flow of cloud was replaced by a flow of dry dust-free air entering at exactly the same rate as the cloud. The current immediately dropped and at 2 hr. 46·6 mins. was represented by 7·7 units. A later reading could not be obtained.

(*b*) At 2 hr. 48 mins. the tap was turned back again and the cloud allowed to pass into the ionization vessel. The following table shows the currents registered at times later.

0	$0^m\ 40^s$	$1^m\ 18^s$	$1^m\ 54^s$	$2^m\ 30^s$	$3^m\ 0^s$	
0	57·1	77·6	86·6	87·4	89·1	divs./min.

(*c*) At 2 hr. 52 mins. the flow was again stopped and the currents from the sample of cloud left behind in the ionization chamber were measured. Times are subsequent to 2 hr. 52 mins.

$1^m\ 0^s$	$2^m\ 14^s$	$6^m\ 12^s$	$13^m\ 7^s$	
83·4	78·3	75·0	73·2	divs./min.

On the hypothesis that the ionization was a frictional effect and provided we had a constant intensity of ionization and that all ions entering the electric field were driven to the electrodes, we should expect the currents (*a*) and (*c*) to be almost identical; for the ions present within the field at the moment the conditions are changed should be collected in the same time whether they possessed a component velocity at right angles to the field or not, and the total charge collected after the change should be the same in both cases. Further, the currents (*a*) and (*c*) should be complementary to (*b*). Since (*a*) and (*c*) are grossly dissimilar, we conclude that either the current is unsaturated, *i. e.*, we are collecting in (*c*) ions which pass completely through the field under the conditions in (*a*); or the cloud at rest in (*c*) produces ions as it ages.

Assume the current is unsaturated. Let E be the difference between the values of the total charge collected in (*a*) and (*c*) and let V be the volume of the ionization vessel. The ratio E/V measures the average charge per unit volume which passes completely through the field. This may be compared with the charge per unit volume actually collected from the steady flow. From the data available $\int idt$ can only be evaluated for 13 mins. in the case of (*c*) but this will be sufficient for our purpose. We find $E = 990 - 40 = 950$ units (divs./min. $\times$ mins.). The current from the steady flow was 90 divs./min. (limiting value in (*b*)) and the rate of flow was $3{\cdot}0 \times V$ c.c./min. The charge collected from V c.c. is 30 units, which is approximately 3 per cent. of the total charge in unit volume of the smoke. But the field gives the saturation current from all ions entering it whose mobilities are greater than 1×10^{-4} cm.^{2}/sec. volt, so the assumption leads to the result that over 97 per cent. of the charges are carried completely through the field on ions with mobilities less than 1×10^{-4} cm.^{2}/sec. volt. This is improbable.

On the same assumption, a lower limit to the mobility of the ions is given by the time taken for the current to disappear, for this is the time required for the slowest moving ions present, when the flow is stopped, to cross the field. The time may be very great. In fig. 4 of an earlier paper[1], a case is shown where this is at least 100 minutes, corresponding to a mobility of $1{\cdot}4 \times 10^{-8}$ cm.^{2}/sec. volt—the mobility of a spherical particle of radius $3{\cdot}4 \times 10^{-2}$ cm. charged with one electron. Since the ionization vessel is horizontal and the diameter of the outer cylinder less than two cm., particles of this size could not remain suspended in the field for 100 mins. We must conclude therefore that the slow decay of the current from a sample of cloud at rest in the electric field is due to ions produced in the field as the cloud ages. It is part of the process which gives the currents measured in fig. 3.

From this it appears that in the experiments of figs. 1 and 2, the zinc oxide clouds were actually producing ions in their passage through the ionization vessel. The corollary follows that we can never obtain "saturation" currents, for only a field of infinite intensity can collect all the ions from cloud in motion through it. This is a source of difficulty in the interpretation of experimental results.

Smokes of low mass concentration dispersed from a zinc arc give similar results. When the flow of smoke is replaced by dust-free air the current rapidly disappears. When the concentration is greater and the change is made after the current from the cloud has passed through the maximum, it is found that although the current falls rapidly at first, it often persists at an appreciable magnitude for a considerable time. It has been measured for as long as one hour after the change to dust-free air has taken place. If the cloud acted like a perfect fluid in its motion through the electric field, the cloud and the current due to ions received from it should disappear in the time (20 secs.) taken for V c.c. to pass through the field. Owing to viscosity the cloud is not swept out so quickly. The fraction remaining at any time can be calculated and it is found that the current disappears at a considerably slower rate. The excess current must arise from the zinc oxide particles deposited on the walls of the ionization vessel. Since the charges in the cloud are carried mainly by particles, the field collects particles when collecting charges. These form crystal growths on the electrodes

which apparently are able to produce ions in the cloud itself. Hence the currents measured in the experiments of figs. 1 and 3 are contributed partly by the cloud passing through the ionization chamber and partly by the deposit which is simultaneously accumulating on its walls.

Summary.

The ionization currents from clouds dispersed in air from a zinc arc and from the decomposition of zinc ethyl have been described. The cloud particles in both cases are crystalline, with the internal structure of zincite. The clouds from the arc are ionized on formation; those from zinc ethyl are not.

There seems to be a spontaneous production of ions in these clouds as they age. In the case of clouds from zinc ethyl the ionization increases from zero to a maximum intensity and then diminishes. Qualitatively the intensity increases with the amount of material dispersed and with the degree of dispersion.

The initial ionization in clouds from the arc is attributed to thermoelectric emission of charges at the high temperature of formation. With arc cloud of low concentration this diminishes with time and is the dominant effect. The coefficient of recombination of these ions is found to be of the same order of magnitude as the coagulation constant of similar clouds.

With increasing concentration of dispersion the two effects are superposed.

References.

(1) Walmsley, Phil. Mag. (7) i. p. 1266 (1926).
(2) Walmsley, Phil. Mag. (7) iii. p. 587 (1927).
(3) Erikson, Phys. Rev. xxi. p. 720 (1923).
(4) Green, Phil. Mag. (7) iv. p. 1046 (1927).
(5) Nonhebel, Colvin, Patterson, and Whytlaw-Gray, Proc. Roy. Soc. A, cxvi. p. 540 (1927).
(6) Kennedy, Proc. Roy. Irish Acad. xxxiii. A, p. 58 (1916).
(7) Walmsley, Phil. Mag. (7) vii. p. 1097 (1929).
(8) Walmsley, Proc. Phys. Soc. xl. p. 7 (1927).
(9) Weber, *Zeit. f. Kryst.* lvii. p. 398 (1922).
(10) Barth, *Norske Geol. Tid.* ix. p. 317 (1927).

The Physical Laboratories,
The University, Manchester.

LIX. *Forced Surface-Waves on Water.*

By T. H. Havelock, F.R.S.*

1. The following notes deal with some problems of forced waves on the surface of water, the waves being forced in that the normal fluid velocity has an assigned value at every point of a given vertical surface; the problems treated here are the elementary cases when the given surface is an infinite plane or a circular cylinder. The motion of the water surface consists in general of travelling waves together with a local disturbance, and the type of solution is one which may have possible application to the waves produced in water by the small oscillations of a solid body.

2. Consider first deep water, and take the origin in the free surface with Ox horizontally and Oz vertically downwards. The velocity potential satisfies

$$\frac{\partial^2\phi}{\partial x^2}+\frac{\partial^2\phi}{\partial z^2}=0. \quad . \quad . \quad . \quad . \quad . \quad . \quad (1)$$

Neglecting the square of the fluid velocity at the free surface, and omitting the effect of capillarity, the condition at the free surface is

$$\frac{\partial^2\phi}{\partial t^2}-g\frac{\partial\phi}{\partial z}=0, \quad . \quad . \quad . \quad . \quad . \quad . \quad (2)$$

and the surface elevation ζ is given by

$$\zeta=\frac{1}{g}\left(\frac{\partial\phi}{\partial t}\right)_{z=0} \quad . \quad . \quad . \quad . \quad . \quad . \quad (3)$$

For simple harmonic motion we assume a time-factor $e^{i\sigma t}$, and (2) gives

$$\kappa_0\phi+\frac{\partial\phi}{\partial z}=0, \text{ at } z=0, \quad . \quad . \quad . \quad . \quad (4)$$

with $\kappa_0=\sigma^2/g$.

Suppose now that we are also given

$$-\frac{\partial\phi}{\partial x}=f(z)\,e^{i\sigma t}, \text{ at } x=0, \quad . \quad . \quad . \quad . \quad (5)$$

where $f(z)$ is given for all positive values of z; and we require a solution of (1), (4) and (8) suitable for positive values of x.

* Communicated by the Author.

The solution can be obtained by various methods; for example, by combining suitable elementary solutions of (1) and (4). The usual solution for free progressive waves is found from

$$\phi = e^{-\kappa_0 z - i\kappa_0 x}. \quad . \quad . \quad . \quad . \quad . \quad . \quad . \quad (6)$$

There is also another elementary solution,

$$\phi = e^{-\kappa x}(\kappa \cos \kappa z - \kappa_0 \sin \kappa z), \quad . \quad . \quad . \quad . \quad (7)$$

where κ may have any real positive value.

We can generalize these solutions by means of th following integral theorem, which may easily be verified :

$$f(z) = \frac{2}{\pi}\int_0^\infty \int_0^\infty f(\alpha) \frac{(\kappa \cos \kappa z - \kappa_0 \sin \kappa z)(\kappa \cos \kappa\alpha - \kappa_0 \sin \kappa\alpha)}{\kappa^2 + \kappa_0^2} d\kappa\, d\alpha + 2\kappa_0 e^{-\kappa_0 z}\int_0^\infty f(\alpha) e^{-\kappa_0 \alpha} d\alpha. \quad . \quad . \quad . \quad . \quad (8)$$

Here $f(z)$ is given for all positive values of z, and it should be remarked that the proof involves the Fourier integral theorem, and that $f(z)$ is subject to suitable limitations.

We may now write down a solution which satisfies the condition (5). It is clear that, on the forced vibrations so obtained, we may superpose any free oscillations for which $\partial\phi/\partial x$ is zero over the plane $x=0$; we shall choose the latter so that the complete solution represents waves travelling outwards for large positive values of x. This solution is given by

$$\phi = 2e^{-\kappa_0 z} \sin(\sigma t - \kappa_0 x) \int_0^\infty f(\alpha) e^{-\kappa_0 \alpha} d\alpha + \frac{2}{\pi} \cos \sigma t \times \int_0^\infty \int_0^\infty f(\alpha) \frac{(\kappa \cos \kappa z - \kappa_0 \sin \kappa z)}{\kappa(\kappa^2 + \kappa_0^2)} \frac{(\kappa \cos \kappa\alpha - \kappa_0 \sin \kappa\alpha)}{} e^{-\kappa x} d\kappa\, d\alpha. \quad . \quad (9)$$

This gives a normal velocity $f(z)\cos \sigma t$ over the plane $x=0$, and reduces to a positive wave for large positive values of x. The corresponding surface elevation is

$$\zeta = \frac{2\sigma}{g} \cos(\sigma t - \kappa_0 x) \int_0^\infty f(\alpha) e^{-\kappa_0 \alpha} d\alpha - \frac{2\sigma}{\pi g} \sin \sigma t \int_0^\infty \int_0^\infty f(\alpha) \frac{\kappa \cos \kappa\alpha - \kappa_0 \sin \kappa\alpha}{\kappa^2 + \kappa_0^2} e^{-\kappa x} d\kappa\, d\alpha. \quad (10)$$

The first term of (10) is a plane progressive wave of the

same wave-length as the free wave of the same frequency, while the second term may be called the local oscillation.

If we take $f(z)=e^{-\kappa_0 z}$, the second term in (9) and (10) vanishes, and we regain the expressions for a simple progressive wave.

If we take, more generally,

$$f(z)=Ae^{-pz} \quad . \quad . \quad . \quad . \quad . \quad . \quad . \quad (11)$$

over the whole range for z, the second integral in (10) can be evaluated explicitly in terms of Cosine and Sine integrals, and we obtain

$$\zeta=\frac{2\sigma A}{\kappa_0+p}\cos(\sigma t-\kappa_0 x)-\frac{2\sigma A\sin\sigma t}{\pi g(\kappa_0+p)}$$
$$\times[Ci(px)\cos px-Ci(\kappa_0 x)\cos\kappa_0 x+Si(px)\sin px$$
$$-Si(\kappa_0 x)\sin\kappa_0 x-\frac{\pi}{2}(\sin px-\sin\kappa_0 x)]. \quad . \quad (12)$$

As we make p smaller we approach the limiting case of constant normal velocity over the whole of the plane $x=0$. It is of interest to note that the amplitude of the travelling wave remains finite in the limit, but that the amplitude of the local oscillation becomes logarithmically infinite at $x=0$.

3. A problem of some interest is the decay of the vertical oscillations of a floating body due to the propagation of waves outwards from it, but a direct attack upon the problem is difficult. We may perhaps obtain a rough estimate by applying the preceding analysis to a simplified form of the problem. Imagine a log of rectangular section floating in water with the sides vertical ; let b be the breadth and d the depth immersed. Now suppose the log made to execute small vertical oscillations of amplitude a and frequency σ. Let one of the sides of the log lie in the plane $x=0$; then the disturbance in the water on that side may be regarded as due to a certain oscillating distribution of normal fluid velocity over the plane $x=0$ from $z=d$ to $z=\infty$. If we make the assumption that this is of the form

$$f(z)\cos\sigma t, \quad . \quad . \quad . \quad . \quad . \quad . \quad (13)$$

then, from continuity of flow, we have

$$2\int_d^\infty f(z)dz=\sigma ab. \quad . \quad . \quad . \quad . \quad . \quad (14)$$

Without attempting to solve the actual problem, let us assume

$$f(z)=Ae^{-pz}; \quad . \quad . \quad . \quad . \quad . \quad (15)$$

then from (14) we have

$$A=\tfrac{1}{2}\sigma abpe^{pd}. \quad . \quad . \quad . \quad . \quad . \quad (16)$$

From (10) we find that the amplitude of the waves travelling out on either side of the log would be

$$\frac{\sigma^2abp}{g}e^{pd}\int_d^\infty e^{-(\kappa_0+p)\alpha}\,d\alpha$$

$$=\frac{\sigma^2abp}{g(\kappa_0+p)}e^{\kappa_0 d}. \quad . \quad . \quad . \quad . \quad . \quad (17)$$

A large value of p would correspond to a concentration of the outward flow round the lower edges of the log; hence this estimate gives, as an upper limit for the amplitude,

$$(\sigma^2ab/g)e^{-\sigma d/g}. \quad . \quad . \quad . \quad . \quad . \quad (18)$$

4. If, in the general problem of §2, the normal velocity at $x=0$ is a function of y as well as of z, the solution of the three-dimensional motion can be obtained by an additional Fourier synthesis.

Assume first that ϕ is proportional to $\cos\kappa'(y-\beta)$, then the potential equation is

$$\frac{\partial^2\phi}{\partial x^2}+\frac{\partial^2\phi}{\partial z^2}-\kappa'^2\phi=0. \quad . \quad . \quad . \quad . \quad (19)$$

The time entering as a simple harmonic factor, the boundary condition at $z=0$ is given by (4).

We have now the following elementary solutions, omitting the factors in y and t:

$$\phi=e^{-\kappa_0 z-ix(\kappa_0^2-\kappa'^2)^{\frac{1}{2}}}, \text{ for } \kappa'<\kappa_0;$$

$$\phi=e^{-\kappa_0 z-x(\kappa'^2-\kappa_0^2)^{\frac{1}{2}}} \text{ for } \kappa'>\kappa_0;$$

$$\phi=e^{-x(\kappa^2+\kappa'^2)^{\frac{1}{2}}}(\kappa\cos\kappa z-\kappa_0\sin\kappa z). \quad . \quad . \quad (20)$$

The theorem (8) may be generalized, with suitable limitations on the function $f(y, z)$, to

$$f(y,z)=$$

$$\frac{2\kappa_0}{\pi}e^{-\kappa_0 z}\int_0^\infty d\alpha\int_{-\infty}^\infty d\beta\int_0^\infty f(\alpha,\beta)e^{-\kappa_0\alpha}\cos\kappa'(y-\beta)d\kappa'$$

$$+\frac{2}{\pi^2}\int_0^\infty d\alpha\int_0^\infty d\kappa\int_{-\infty}^\infty d\beta\int_0^\infty f(\alpha,\beta)$$

$$(\kappa\cos\kappa z-\kappa_0\sin\kappa z)$$

$$\times\frac{(\kappa\cos\kappa\alpha-\kappa_0\sin\kappa\alpha)}{\kappa^2+\kappa_0^2}\cos\kappa'(y-\beta)d\kappa'. \quad (21)$$

Suppose that at $x=0$ we are given

$$-\frac{\partial\phi}{\partial x}=f(y,\,z)\cos\sigma t. \quad . \quad . \quad . \quad . \quad (22)$$

Then from (20) and (21) we obtain an expression for ϕ, valid for positive values of x, and adjusted so that it represents progressive waves at large values of x; we find

$$\phi=\frac{2\kappa_0}{\pi}e^{-\kappa_0 z}\int_0^\infty d\alpha\int_{-\infty}^{\infty}d\beta\int_0^{\kappa_0}f(\alpha,\,\beta)\sin(\sigma t-x\sqrt{\kappa_0^2-\kappa'^2})$$
$$\times\frac{e^{-\kappa_0 z}\cos\kappa'(y-\beta)}{(\kappa_0^2-\kappa'^2)^{\frac{1}{2}}}d\kappa'+\frac{2\kappa_0}{\pi}e^{-\kappa_0 z}\cos\sigma t\int_0^\infty d\alpha\int_{-\infty}^{\infty}d\beta\int_{\kappa_0}^{\infty}$$
$$\times f(\alpha,\,\beta)e^{-x(\kappa'^2-\kappa_0^2)^{\frac{1}{2}}-\kappa_0\alpha}\frac{\cos\kappa'(y-\beta)}{(\kappa'^2-\kappa_0^2)^{\frac{1}{2}}}d\kappa'+\frac{2}{\pi^2}\cos\sigma t$$
$$\times\int_0^\infty d\alpha\int_0^\infty d\kappa\int_{-\infty}^{\infty}d\beta\int_0^\infty f(\alpha,\,\beta)e^{-x(\kappa^2+\kappa'^2)^{\frac{1}{2}}}\cos\kappa'(y-\beta)$$
$$\times\frac{(\kappa\cos\kappa z-\kappa_0\sin\kappa z)(\kappa\cos\kappa\alpha-\kappa_0\sin\kappa\alpha)}{(\kappa^2+\kappa_0^2)(\kappa^2+\kappa'^2)^{\frac{1}{2}}}d\kappa'. \quad . \quad . \quad (23)$$

A particular case which would illustrate the spreading of plane waves emerging from a canal into an infinite sea is obtained by taking

$$f(y,\,z)=(ga\kappa_0\sigma)e^{-\kappa_0 z}\cos\sigma t, \quad . \quad . \quad . \quad (24)$$

over the whole range for z and between the limits $\pm b$ for y, the function being zero outside these limits for y. Substituting in (23), the third term disappears, and also the integrations with respect to β can be effected in the remaining terms. We find that the surface elevation for this case is given by

$$\zeta=\frac{2\kappa_0 a}{\pi}\int_0^{\kappa_0}\frac{\sin\kappa' b\cos\kappa' y\cos\{\sigma t-x(\kappa_0^2-\kappa'^2)^{\frac{1}{2}}\}}{\kappa'(\kappa_0^2-\kappa'^2)^{\frac{1}{2}}}d\kappa'$$
$$-\frac{2\kappa_0 a}{\pi}\cos\sigma t\int_{\kappa_0}^\infty\frac{\sin\kappa' b\cos\kappa' y e^{-x(\kappa'^2-\kappa_0^2)^{\frac{1}{2}}}}{\kappa'(\kappa'^2-\kappa_0^2)^{\frac{1}{2}}}d\kappa'. \quad . \quad (24)$$

The form of the surface could be studied by approximate evaluation of these integrals as in similar diffraction problems.

5. We return to plane waves, and suppose now that the water is of finite depth h. We have the additional condition

$$\frac{\partial\phi}{\partial z}=0, \text{ for } z=h. \quad . \quad . \quad . \quad . \quad . \quad (25)$$

The corresponding elementary solutions are

$$\phi = e^{i(\sigma t - \kappa_0 x)} \cosh \kappa_0 (z-h), \quad . \quad . \quad . \quad . \quad (26)$$

where κ_0 is the real positive root of

$$g\kappa_0 \tanh \kappa_0 h = \sigma^2; \quad . \quad . \quad . \quad . \quad . \quad (27)$$

and

$$\phi = e^{i\sigma t - \kappa x} \cos \kappa (z-h), \quad . \quad . \quad . \quad . \quad (28)$$

where κ is any real positive root of

$$g\kappa \tan \kappa h + \sigma^2 = 0. \quad . \quad . \quad . \quad . \quad . \quad (29)$$

This equation has an infinite sequence of real roots, together with an imaginary root $i\kappa_0$. We assume then the possibility of expanding a function $f(z)$ in the range $0 \leq z \leq h$, in the form

$$f(z) = \mathrm{A} \cosh \kappa_0 (z-h) + \Sigma \mathrm{B} \cos \kappa (z-h), \quad . \quad (30)$$

where the summation extends over the real positive roots of the equation (29). We find that the coefficients are given by

$$\mathrm{A} = \frac{4\kappa_0}{2\kappa_0 h + \sinh 2\kappa_0 h} \int_0^h f(\alpha) \cosh \kappa_0 (\alpha - h)\, d\alpha,$$

$$\mathrm{B} = \frac{4\kappa}{2\kappa h + \sin 2\kappa h} \int_0^h f(\alpha) \cos \kappa (\alpha - h)\, d\alpha. \quad . \quad . \quad (31)$$

If at $x=0$ we are given

$$-\frac{\partial \phi}{\partial x} = f(z) \cos \sigma t. \quad . \quad . \quad . \quad . \quad (32)$$

then the velocity potential for positive values of x, such that the motion at a distance is a plane progressive wave, is given by

$$\phi = \mathrm{A}\kappa_0^{-1} \cosh \kappa_0 (z-h) \sin (\sigma t - \kappa_0 x) + \Sigma \mathrm{B}\kappa^{-1} e^{-\kappa x} \cos \kappa (z-h) \cos \sigma t. \quad . \quad (33)$$

Suppose, for instance, that one end of a long tank is made to execute simple harmonic vibrations of small amplitude a, then we have $f(z) = \sigma a$. The values of A and B follow from (31), and from (33) we deduce the surface elevation in this case :

$$\zeta = \frac{2\sigma^2 a \sinh 2\kappa_0 h}{g\kappa_0 (2\kappa_0 h + \sinh 2\kappa_0 h)} \cos (\sigma t - \kappa_0 x) - \sin \sigma t \, \Sigma \frac{2\sigma^2 a e^{-\kappa x} \sin 2\kappa h}{g\kappa (2\kappa h + \sin 2\kappa h)}. \quad . \quad . \quad (34)$$

6. The same analysis may be applied to circular waves, and we limit consideration here to symmetry round the origin. The normal fluid velocity is supposed to be assigned over a vertical cylindrical surface; for example, we take

$$-\frac{\partial\phi}{\partial r}=f(z)\cos\sigma t, \text{ for } r=a. \quad . \quad . \quad . \quad (35)$$

The velocity potential satisfies

$$\frac{\partial^2\phi}{\partial r^2}+\frac{1}{r}\frac{\partial\phi}{\partial r}+\frac{\partial^2\phi}{\partial z^2}=0. \quad . \quad . \quad . \quad . \quad (36)$$

The condition at the free surface is the same as before, and we assume the water to be deep. Elementary solutions of the required form are found in terms of suitable Bessel functions. The solution

$$\phi=e^{i\sigma t-\kappa_0 z}\mathrm{H}_0^{(2)}(\kappa_0 r) \quad . \quad . \quad . \quad . \quad . \quad (37)$$

represents diverging waves for large values of r; while in the solution

$$\phi=e^{i\sigma t}(\kappa\cos\kappa z-\kappa_0\sin\kappa z)\,\mathrm{K}_0(\kappa r), \quad . \quad . \quad (38)$$

$\mathrm{K}_0(\kappa r)$ tends exponentially to zero for large distances from the origin.

Generalizing as before, we obtain the solution

$$\phi=2e^{i\sigma t-\kappa_0 z}\frac{\mathrm{H}_0^{(2)}(\kappa_0 r)}{\mathrm{H}_1^{(2)}(\kappa_0 a)}\int_0^\infty f(\alpha)e^{-\kappa_0\alpha}d\alpha-\frac{2}{\pi}e^{i\sigma t}$$

$$\times\int_0^\infty\int_0^\infty f(\alpha)\frac{\mathrm{K}_0(\kappa r)}{\kappa\mathrm{K}_0'(\kappa a)}\frac{(\kappa\cos\kappa z-\kappa_0\sin\kappa z)}{(\kappa\cos\kappa\alpha-\kappa_0\sin\kappa\alpha)}\frac{(\kappa\cos\kappa\alpha-\kappa_0\sin\kappa\alpha)}{\kappa^2+\kappa_0^2}d\kappa d\alpha, \quad (39)$$

where the real part is to be taken.

The surface elevation at a great distance from the origin is given by

$$\zeta\sim-\frac{2i\sigma}{g}\left(\frac{2}{\pi\kappa_0 r}\right)^{\frac{1}{2}}\frac{e^{i(\sigma t-\kappa_0 r+\frac{1}{4}\pi)}}{\mathrm{J}_0'(\kappa_0 a)-i\mathrm{Y}_0'(\kappa_0 a)}\int_0^\infty f(\alpha)e^{-\kappa_0\alpha}d\alpha, \quad (40)$$

or, in real terms, this gives

$$\zeta\sim-\frac{2\sigma}{g}\left(\frac{2}{\pi\kappa_0 r}\right)^{\frac{1}{2}}\int_0^\infty f(\alpha)e^{-\kappa_0\alpha}d\alpha$$

$$\times\frac{\mathrm{J}_0'(\kappa_0 a)\sin(\sigma t-\kappa_0 r+\frac{1}{4}\pi)+\mathrm{Y}_0'(\kappa_0 a)\cos(\sigma t-\kappa_0 r+\frac{1}{4}\pi)}{\mathrm{J}_0'^2(\kappa_0 a)+\mathrm{Y}_0'^2(\kappa_0 a)} \quad . \quad . \quad . \quad . \quad (41)$$

This expression might be used, as in §3, to give an estimate for the energy propagated outwards from a circular cylinder immersed to a given depth, and making small vertical oscillations of given frequency.

LX. *The Work of Sir Joseph Larmor* *. *By* Sir Oliver Lodge.

I DO not envy the historian who shall some day attempt to write the history of the development of modern physics, and shall attempt to assign due credit to the 19th century mathematicians for their contribution to whatever it is that shall survive out of the present 20th century turmoil. That great and surprising progress is being made is fairly evident, but what may be its quasi permanent form when the revolution has ended, and things have settled down again, who can say? The younger generation of mathematical physicists, absorbed in their brilliant abstractions, and vying with each other in the best mode of expressing them—sometimes without even attempting to form clear physical conceptions of the underlying realities which their equations must be supposed to represent—are apt to ignore the work of their predecessors, and to regard the old-fashioned methods as antiquated and superseded.

The historian, however, will, I anticipate, not take that view. He will, I hope, realise that the whole advance is a consistent evolution, and will be able to detect in the work of the leaders of the 19th century the germ of many ideas which by his time will have blossomed and borne fruit. To undertake such an historical survey at the present time would be hopelessly impossible, even for the best informed. Many theories are struggling for existence, and no one can tell in what form the fittest will survive. But one can safely say that whoever hereafter undertakes the work will find in these volumes of the Collected Papers of

* 'Mathematical and Physical Papers,' by Sir Joseph Larmor. In two volumes. £6 6*s*. net. Vol. i. pp. 679+xii; vol. ii. pp. 831+xxxii., with Prefaces, Notes, Index, and Appendices. (Cambridge University Press.)

Sir Joseph Larmor, a great mass of material, some of which must be discarded, but nearly all of which will be recognised as steps in the ladder of progress. And it is not unlikely that some of the ideas which now seem to be superseded by the modern points of view may revive and take their place in the ultimate coherent scheme, when the abstractions have once more become concrete, and when return to physical conceptions is possible.

Consequently, I think that Sir Joseph Larmor has performed a great service, not only in collecting his Papers into readily accessible form, but in editing them and as far as possible bringing them up to date by new footnotes and appendices and elucidatory remarks. He, himself, has done good work, as an incipient historian of the 19th century, by his Obituary Notices of some of the workers, and especially by his critical appreciation of the work of Lord Kelvin during those fruitful years of the 1840's before he was partially diverted from pure science by cable and other engineering developments, and while he was laying the foundation of thermodynamics and many another important subject, doing work which at that time no one else was competent to do. It seems a pity that these careful studies of early work should be excluded from the present volumes by pressure of other matter, and I venture to hope that the Cambridge University Press may contemplate the production of yet a third or supplementary volume, thinner than the other two, which shall include and make easily accessible all the present omissions, some of which are referred to in the Preface to vol. ii. For when we have been favoured with the life-work of a man of exceptional power and industry, it behoves us to make what use we can of it, and to make it available for the study of posterity, who by that time will doubtless have a criterion of value more serviceable than any we possess at present, and will not only find it of interest to recognise the intuitions of the great men of the past, but will be helped in their formulation of truth by the continuous thread of thought which runs through the labyrinth, and leads towards the ultimate, though even then still unreached, goal.

The time is as yet far distant for such a task to be undertaken even by a learned and leisurely historian. Anyone who has been trained in the methods of the 19th century must be liable to gasp when extracted from his habitual

medium into the rarefied atmosphere of the 20th century. Some will undoubtedly shine with undiminished lustre; such an one as Clerk Maxwell, for instance. The clarifying work of the late Lord Rayleigh cannot but be always useful. But what the verdict of history will be on the later work of Lord Kelvin, the less voluminous but brilliant intuitions of G. F. FitzGerald, the steady contributions of Poynting, and the contemporary work of Sir J. J. Thomson and Sir Joseph Larmor I do not presume to judge; though I may be permitted to guess that some of this work will be valued more highly than it is at present, and in the light of clearer knowledge will be better understood.

We, of this and future generations, surely ought to feel grateful for the strenuous labours of a mathematician who, living a secluded life in his rooms at St. John's College, Cambridge, has devotedly concentrated on problems of exceeding difficulty. Having put aside nearly all other interests, he must have laboured, ever since his Senior Wranglership, to absorb all the learning of his time in this department of knowledge, to subject it to critical examination, and to develop it further for his own satisfaction and for the benefit of his co-workers. Incidentally, he must have thus saved some pioneering work from destruction. Clerk Maxwell's and Rayleigh's, and I suppose Lorentz's, might be trusted to survive anyhow; but without Larmor I venture to think that Lord Kelvin's theoretical seeds might gradually sink into oblivion. Not in their original form will they continue to bear fruit; but the output of so great a genius, in spite of occasional narrownesses and mistakes, ought to exert a permanent and abiding influence, now that the clouds of which he complained are partially cleared away, and when the nature of fundamental reality is perhaps becoming better understood.

The Collected Papers of the great mathematical physicists are exceedingly useful to present and future students, and are of especial value when the author himself takes the trouble to collect and edit them with footnotes and appendices. The Collected Papers of Stokes, Kelvin, and Rayleigh constitute a monument of the end of the 19th century, as Thomas Young's Papers were for the beginning. And now Larmor's Papers link the two centuries together.

From another point of view these two volumes may be said to constitute the high-water mark of mathematical physics prior to the dawn of the 20th century.

To review these majestic volumes adequately is for any single writer impossible, even if he were qualified to understand the whole of their contents, which in the present instance is far from being the case. I can only pick out a few salient features on a few points of interest, and express admiration for the genius and learning displayed by them.

The whole question of rotational elasticity in space is not one to be lightly dealt with or criticised. I venture to think that more will be heard of it hereafter, and that Larmor is one of the pioneers. Absolute rotation is insisted on; and with regard to Newtonian absolute space and time, Larmor perceives that some of the philosophic or metaphysical complications introduced by Relativity are due to our practical dealing with space and time by means of light signalling. If light had happened to travel instantaneously, those difficulties would not have arisen. And even now absolute space and time are coherent as a logical scheme, because we can *imagine* instantaneous signalling: it is only impracticable when we have to depend on light. I have myself argued in the same direction, that we can *think* of simultaneity at a distance, though we cannot perceive it by any laboratory methods, and that accordingly undue philosophic emphasis ought not to be laid on considerations only made valid or plausible by the finite velocity of light.

On page 411 of vol. ii. there are some observations on the anthropomorphic nature of the dissipation of energy as expressed by Kelvin, and on Kelvin's treatment of the energy available to man for mechanical effect; an anthropomorphism which survived in modified form in Maxwell's demons.

A paper which really settled the question of why wireless waves can bend round the earth, a theory only partially anticipated by Dr. Eccles, will be found as Article 100.

Concerning metallic conduction, reasons are given for the number of electrons taking part in conveying a current. The argument makes the number of virtually free electrons in a molecule comparable with the number of

molecules, so that the mean free path is exceedingly short, and the velocity comparatively low.

There are some remarkable Appendices to vol. ii. beginning with Abstracts from Reports of the British Association, continuing with statistical methods in thermodynamics and limitations of equipartition, molecular scattering of radiation, time and space of astronomical observers, and concluding with such notable titles as "Mind, Nature and Atomism," and "Synoptic View of a Physical Universe as Optically Apprehended." There are also Appendices to vol. i. on Radiation from Accelerated Electrons, on Maxwell's Stress and Radiation Pressure, on the Repulsion of Bodies by Radiation, on the Inertia of Aggregation, and on Gyromagnetics.

I merely summarise these things briefly to show that in these volumes, in addition to mathematical analysis, there is a good deal that any educated reader might find of interest, some of it clearly, and all of it powerfully, presented.

On the whole I think the future historian will be most interested and most impressed by the content of vol. i., which carries the Papers up to the end of the 19th century. The beginnings of the electrical theory of matter and a theory of electrons are to be found in that comprehensive and masterly Phil. Trans. Memoir, dated 1894 and 1895, called "A Dynamical Theory of the Electric and Luminiferous Medium," covering over 200 pages in vol. i. and carried forward, in its application to material media, into vol. ii. where after another 100 pages it blends into the dynamics of a system of electrons or ions and the optical influence of a magnetic field. An attempt is here made at a rotational elastic fluid ether, and though such a medium has temporarily gone out of fashion, I fully expect its revival in some still more developed form hereafter. The famous Lorentz transformation to moving axes, called for by the nul result of the M.M. experiment made by moving observers, and utilised as an expression of the earliest Relativity theory, is here begun, and it is remarkable how much detailed knowledge about electrons is shown before the final discovery of those bodies.

There are some interesting remarks on the Poincarè pressure and its application to electron theory. Indeed, the whole treatment of electron theory will need careful

attention by the historian of the future. The author's dissatisfaction with the concealment or sophistication of the positive electron is manifest, and several times we find him exclaiming, in one form or another, "The problem of the positive electron remains."

The extremely general analysis introduced by Lagrange is the inevitable method of dealing with a medium whose physical properties and mechanism are absolutely unknown. Whether any real progress has been made towards an explanation of the universe in terms of a rotational fluid is a question that can only be answered by posterity. To me this idea seems more and more hopeful as time goes on, and it seems likely to be the ultimate elucidation of wave dynamics. At present this is little more than a pious opinion, and much further work is necessary before it can be consolidated into a comprehensive theory of physical existence. If ever it becomes possible to regard it in a still more inclusive manner as affording a physical basis for vital and mental phenomena, then philosophers of the future will owe a debt of gratitude to the pioneers who have groped their way through the present tangle into a brighter and more luminous region beyond.

The brief notes or summaries of the argument, which the author has been permitted by the Cambridge University Press to put in the margin of the pages, are a great help, not only to anyone looking through the book, but even as an elucidation of the text.

The author has prepared a comprehensive index to each of the volumes, but unfortunately both Indexes are printed at the end of the second volume. In a future edition this might be remedied, so that each volume might be self-contained.

But it may be said, Are there no other faults to be found with the production? Is there nothing that could have been put better? That I by no means claim. I find certain defects of style, which militate against a clear apprehension, or at any rate any rapid apprehension, of the meaning of the author. It is an unkindly act to criticise style, for style they say is the man. The author might well claim that his vagueness, whenever vagueness has to be admitted, is no more than is inevitable, and that attempted over-clearness would suggest a definiteness of knowledge which does not exist. He might also claim that

the involved parentheses, which sometimes spoil the run of his sentences, do not really confuse the meaning, but are necessary to its guarded presentation, and in this he could doubtless claim the example of Lord Kelvin. Still, I do venture to say that, apart from the mathematics, the style might be simpler. I sometimes think that even the mathematical expressions are not set forth with that clearness and efficiency which may be said to characterise the memoirs of H. A. Lorentz, for instance, and other Continental physicists: so that sometimes it unfortunately happens that fruitful expressions and valuable points of view are attributed to one or other of these writers, rather than to Larmor who was the first to state them, in rather a concealed and unemphasised manner. It may be the Cambridge method to write down results without emphasis, and without trying to elaborate their full meaning, trusting to disciples to do this spade work. Sometimes those disciples are forthcoming, but sometimes they are not, and so the work of the master gets overlooked, until rediscovered independently by others.

It may perhaps be said that I ought not to accuse my friend of an involved style without giving some example. Well, it is an ungrateful task, but here is an unfavourably chosen sentence taken from page xii. of vol. ii. He is referring to the problem of modes of vibration of a set of atomic singularities embedded in an isotropic elastic medium with certain properties, and seeking to assimilate the early methods of Stokes and Lamè with the recent equations of Schrödinger. But I find it difficult to understand what is meant by the following sentence:—

"For, pursuing the analogy, if the electric singular points of the æthereal vibrating system of the atom are not to be also singularities after the manner of the actual vesicles filled with compressed gas that occur in crystals, from or to which intense hydrostatic pressure radiates other than the intrinsic electrically sustained constant universal pressure aforesaid—and any such added source of pressure would probably spoil the type of model of a convected electron—we are invited to seek out forms of solution for disturbance superposed on this intrinsic æthereal pressure, adapted to the local field of the atom, of types which indeed converge radially on the positions of its electrons or other nuclei in a way prescribed by their electric field, but without tendency towards values there

increasing without limit; for stable modes of local vibration of the ambient æther could only occur around the definite configurations of the material atom permitting of such solutions of the pressure-equation, which alone could subsist."

There may bea lot of meaning in this, but it is not easy to disentangle.

Least Action methods are, of course, constantly employed, even in one of the earlier Papers dated 1884, and later on, in this same method, the beginnings of Schrödinger's wave theory can be traced. It may possibly come as a surprise to 20th century physicists, if they allow themselves to read these volumes, how much anticipation there is in these great 19th century Memoirs.

A treatment of the action of magnetism on light, and a correlation of optical theories, many of which though now discarded are full of interest, constitute Memoir 34 of vol. i. and of date 1893. The outstanding difficulty about radiation from a radially accelerated electron is discussed in an Appendix, page 650.

It is hopeless to go into details. I can only draw attention to a few salient features, of which others will find many more instances, some of fundamental and some of historical importance.

For instance, the mathematics of group waves and their treatment by Fourier's methods are usefully dealt with in a Paper on Harmonic Analysis dated 1916. Article 90. And it is noteworthy that even at that date there is an italic heading that energies of groups must be regarded atomically, and again that the energy of a group must be treated as an indivisible whole. He appears to say that travelling energy must come in atomically by group aggregates alone, like the energy of a vortex ring in hydro-dynamics or of a travelling electron. He recognzies that such groups are disentangled by dispersion, and that there can be an abrupt pulse in a dispersive medium, such as is suggested by the recent work of G. P. Thomson and others.

There is a good deal of discussion on group waves and their atomic character, and Fourier analysis is applied to sum up a large number of component waves. For the atomic energy of groups, page 551 may be referred to.

In an Address given to Section A at the Bradford Meeting of the British Association in 1900 the author, among other things, discusses the relative advantage of physical models

and mathematical abstractions (see page 213 of vol. ii.). He says :—

"The abstract standpoint is always attained through the concrete; and for purposes of instruction such models, properly guarded, do not perhaps ever lose their value: they are just as legitimate aids as geometrical diagrams, and they have the same kind of limitations."

"Gradual transition into abstract statement of physical relations amounts to retaining the essentials of our working models while eliminating the accidental elements involved in them . . . We cannot expect to mentally grasp all aspects of the content of even the simplest phenomena . . . In Maxwell's words, 'For the sake of persons of different types, scientific truth should be presented in different forms, and should be regarded as equally scientific whether it appear in the robust form and vivid colouring of a physical illustration, or in the tenuity and paleness of a symbolical expression.'"

And as illustrating the kind of desperation which seizes some investigators at the multiplicity and complexity and unsatisfactory character of present-day theories, the despairing opinion of Thomas Young is quoted, at the date 1817 when his faith in the undulatory theory of light had been eclipsed by Malus' discovery of polarisation by reflection, before the mystery had been solved (in so far as it was solved) by Fresnel. This difficulty, he says, "will probably long remain, to mortify the vanity of an ambitious philosophy, completely unresolved by any theory."

A feeling akin to despair must occasionally arise in the minds of all but the youngest when confronted with the amazing amount of still unresolved ignorance about existence in general, and it is comforting that even so great a man as Thomas Young could share that feeling.

These volumes constitute an amazing mass of information in almost every department of physics. They are a tribute to the insight and analytic power of the author, and they will probably long be referred to by investigators who are reaching what after all may be somewhat similar conclusions by other methods, and in a form susceptible of clearer and completer statement, by reason of the additional knowledge still constantly accruing.

LXI. *Precision Measurements of X-Ray Reflexions from Crystal Powders.*

To the Editors of the Philosophical Magazine.

GENTLEMEN,—

THE recent paper by J. Brentano and J. Adamson [1] on "Precision Measurements of X-ray Reflexions from Crystal Powders" has attracted my attention. These authors give the lattice parameter of cadmium oxide as 4·683 ± ·004 A. Pierre van Dyck, formerly of this laboratory, made precision measurements on cadmium oxide using the powder method and the standard X-ray diffraction apparatus by Davey [2] and manufactured by the General Electric Company. The value obtained was 4·681 ± ·002 A. This letter is written as an excellent check on the work of Brentano and Adamson and as an illustration of the comparative accuracies of the focusing method of Brentano [3], and the simpler but equally precise method of Davey [4]. The lack of agreement between the values obtained by Brentano and Adamson and by van Dyck, and those obtained by Davey and Hoffman [5], P. Scherrer [6], and H. P. Walmsley [7], which vary from 4·699 to 4·72, is probably due to differences in the purity of the specimens used.

P. van Dyck obtained the value 4·681 with a very pure sample of cadmium oxide which has been made by burning in air vacuum distilled cadmium metal, which was shown by spectrographic analysis to contain only very faint traces of zinc and lead. A pure grade of commercial cadmium oxide, which contained small amounts of carbon dioxide, zinc oxide and other foreign matter, was also measured. The value obtained was the same as that obtained with the extremely pure cadmium oxide. Cadmium oxide gives a powder pattern with unusually sharp diffraction maxima which lend themselves readily to precise measurement. This laboratory has often thought of using cadmium oxide as a reference standard for precision measurements by the powder method rather than sodium chloride. The diffraction maxima of cadmium oxide are much sharper than those of sodium chloride, and for the same exposure time a much wider range of accurately measurable lines is obtained.

The observed interplanar spacings for cadmium oxide, which were used in the calculations, are given below:—

Planar Indices.	Spacings.
110(2)	1·657
111(2)	1·351
100(4)	1·172
331	1·073
210(2)	1·046
511 } 111(3) }	0·901
110(4)	0·828

Bibliography.

(1) J. Brentano and J. Adamson. Phil. Mag. (7), pp. 507-517 (1929).
(2) W. P. Davey. General Electric Review, xxv. p. 565 (1922).
(3) J. Brentano. Proc. Phys. Soc. (London), xxxvii. p. 184 (1925).
(4) W. P. Davey. General Electric Review xxix p. 118 (1926).
(5) W. P. Davey and E. C. Hoffman. Phys. Rev. xv. p. 333 (1920).
(6) P. Scherrer. *Zeit. f. Kryst.* cvii. p. 196 (1922).
(7) H. P. Walmsley. Proc. Phys. Soc. xl. (1927).

The New Jersey Zinc Co., Pa., U.S.A.
July 1929.

Yours faithfully,
M. Luther Fuller,
Research Division.

LXII. *Notices respecting New Books.*

Astronomy and Cosmogony. Second edition. By Sir J. H. Jeans, F.R.S. (Cambridge University Press, Fetter Lane, London. Price 31*s.* 6*d.* net.)

THE first edition of this work appeared nine years after the author's 'Problems of Cosmogony and Stellar Dynamics,' and now the second edition has been called for within twelve months of the publication of the first, testimony that 'Astronomy and Cosmogony' has made a wide appeal not only to mathematicians and astronomers, but to the increasing number of educated laymen interested in modern scientific developments. The author's outstanding researches naturally play an important part in his review of the hypotheses put forward from the time of the earlier workers to the present day. The few pages of additional matter describe results obtained since the publication of the first edition, and in no way modify the general position taken up by Sir J. H. Jeans. A definite scheme of cosmogony is brought forward, but no claim is made that this is either complete

or even free from serious difficulties: the theories are set out "not in the belief that they will all prove to be true, but in the hope that the suggestions may in some degree help others ultimately to final the truth."

Introduction to Modern Physics. By F. K. RICHTMYER. (McGraw-Hill Publishing Co. Ltd., 6 & 8 Bouverie Street, London, E.C.4. Price 25*s.* net.)

PROF. RICHTMYER'S book is largely based on courses of lectures given by him at Cornell University on the origin and development of the more important physical concepts, and is intended to prepare the way for the effective study of the new physics. From his wide experience as a teacher, the author has written a clear and admirable account of some of the modern physical theories, including the quantum theory of specific heats, the structure of the atom and the origin of spectra, X-rays, and the Compton effect. The first three chapters are devoted to a brief historical survey of the subject from the time of the Greeks to that of Faraday and Maxwell. Although Prof. Richtmyer disclaims any intention of bringing his lectures strictly up to date, he has introduced a number of topics which have been the subject of recent research. Bibliographies have not been appended to the chapters, but references are given in the text to original papers for the latest investigations. An extensive index of authors and subjects is provided, and appendices give the data of atomic structure and important physical constants. In binding and printing this volume reaches a high standard, and from its able presentation of modern physical developments can be recommended as a helpful introduction to the study of present-day physics.

The Viscosity of Liquids. By EMIL HATSCHEK. (Geo. Bell & Sons, Ltd., York House, Portugal Street, London, W.C.2. Price 15*s.* net.)

'VISCOSITY of Liquids' is a welcome addition to the International Text-books of Exact Science. From the very extensive literature contributed to scientific journals the author has selected for inclusion in his book many important experimental researches, especially those on the viscosity of solutions of electrolytes, liquid mixtures, and colloidal solutions. The interesting historical chapter is followed by the elementary mathematical theory of flow in a capillary tube and the annulus of two vertical coaxial cylinders, and the description of various types of viscometers, their design and use. Recent work on the variation of viscosity with temperature and with pressure is set out in the form of graphs and tables of experimental results, whilst copious references to original papers are given at the end of the chapters.

The Principles of Mechanics. By H. C. PLUMMER, F.R.S. (Geo. Bell & Sons, Ltd., York House, Portugal Street, London, W.C. 2. Price 15*s.* net.)

THIS is an introductory course intended to prepare the reader for the further study of the advanced stages of the subject. The scope of the book may be indicated by noting that sections are devoted to the motion of a point in a plane, dynamics of translation, statics, including centres of gravity and friction, dynamics of a rigid body in two dimensions and in problems of elasticity, the torsion of cylinders, and the bending of rods. The notation of the differential and integral calculus is introduced and applied to the limited range of problems under discussion. Although the subject of the book is "Mechanics," not "Arithmetic," carefully chosen examples are given at the end of each chapter, with answers to the numerical exercises. A larger number of worked problems would have added to the value of the book and given the student experience in the application of principles and methods.

Polar Molecules. By P. DEBYE, Ph.D. (The Chemical Catalogue Co., 419 Fourth Avenue, at 29th Street, New York. Price $3.50.)

SOME seventeen years ago, Prof. Debye, from the study of the temperature variation of the dielectric constant, introduced the idea of molecular dipoles: he has now collected in this comprehensive volume the results of the numerous researches carried out during those years, and which have appeared largely in German scientific periodicals. Some experimental results are given here for the first time, and in all cases the author has been careful to give appropriate references. The author also makes suggestions for further experimental research in anomalous dispersion and electric saturation effects. In the study of the rotating diatomic molecule attention is drawn to the agreement between experiment and theory, that a molecular ray is partly attracted and partly repelled in a non-homogeneous electric field, the electric analogue of the Gerlach-Stern experiment. Prof. Debye has rendered good service in writing this monograph on the molecular interpretation of the dielectric constant, and in bringing together the widely-scattered contributions to recent theoretical and experimental research.

[*The Editors do not hold themselves responsible for the views expressed by their correspondents.*]

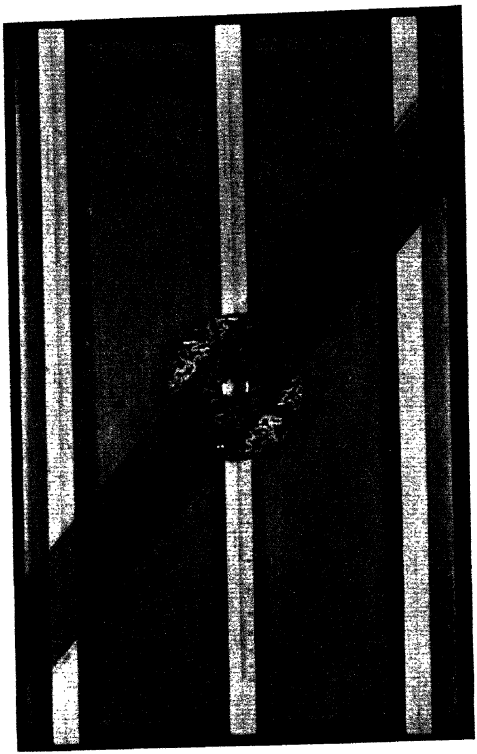

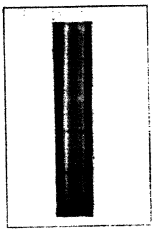

(a)

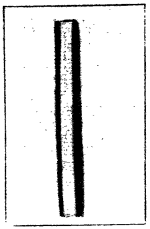

(b)

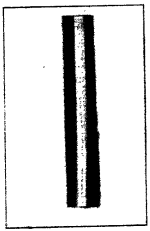

(c)

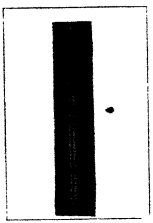

(d)

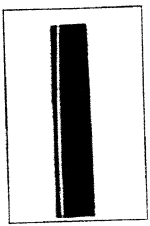

(e)

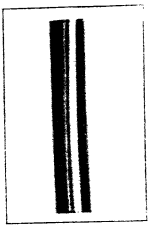

(f)

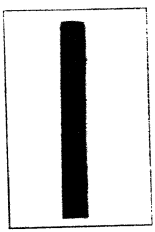

(g)

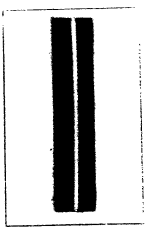

(h)

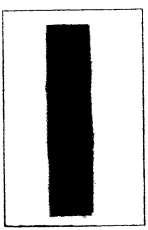

(i)

THE
LONDON EDINBURGH, AND DUBLIN
PHILOSOPHICAL MAGAZINE
AND
JOURNAL OF SCIENCE.

[SEVENTH SERIES.]

NOVEMBER 1929.

LXIII. *On Reactions in Solids.*

By JOHN HUME, *B.Sc.*, *and* JAMES COLVIN, *Ph.D.**

DESPITE the increased attention which has been paid to the study of solid reactions in recent years, no clear resolution of the factors governing the type of curve representing the course of the reaction has been attempted. In this paper we shall endeavour to investigate the importance of various factors in reactions of the type :—

$$\text{solid} \longrightarrow \text{solid}$$

$$\text{solid} \longrightarrow \text{solid} + \text{gas or liquid.}$$

An example of the former type is found in the change of monoclinic sulphur to rhombic sulphur [1] and of the latter in the decomposition of calcium carbonate hexahydrate [2].

These reactions, which consist essentially of the transformation of a metastable crystal lattice into one of greater stability, are characterized by the initiation of reaction at certain points where the formation of an element of the new lattice serves as a nucleus from which the decomposition spreads. From general considerations it appears that the most probable position for nucleus formation is the surface of the solid, particularly at points where deformation has occurred. By observation of the transformation of monoclinic sulphur into rhombic sulphur and of the dehydration

* Communicated by Prof. R. Whytlaw-Gray.

of potassium hydrogen oxalate hemihydrate [3], this view has been completely confirmed. Provided that solid solution formation does not occur between the reactant and the resultant, it has been shown by Langmuir [4] that reaction can take place only at the interface separating the two solid phases. The rate of advance of the interface, which we shall assume to be constant and the same in all directions, we shall call the linear rate of propagation.

The three factors governing the course of the reaction then are:

1. Rate of nucleus formation.
2. Linear rate of propagation.
3. Size of the reactant particles.

Observation of the course of such transformations shows that the formation of nuclei is invariably preceded by a more or less prolonged period of induction, the duration of which is markedly influenced by the previous history of the reactant. Despite this, once the formatien of nuclei begins, the velocity of the subsequent reaction appears to be characteristic of the particular preparation. This is clearly demonstrated in the reaction

$$MnC_2O_4.3H_2O \longrightarrow MnC_2O_4.2H_2O + H_2O,$$

which can be followed dilatometrically. One portion of a specimen of manganous oxalate trihydrate was placed in a dilatometer under its saturated solution and maintained at $25 \pm \cdot 01^\circ$ C. Under these conditions reaction was complete in about three hours. A second portion of the same specimen, washed thoroughly in ice-cold distilled water before placing in the dilatometer at the same temperature, showed an induction period lasting more than three days, although once the reaction started, decomposition proceeded as rapidly as before. In some reactions, especially those with a large rate of nucleus formation, this induction period is negligible. In this case, if the rate of nucleus formation is very great relative to the linear rate of propagation, the particles of the reactant will become covered instantaneously with a layer of resultant of approximately uniform thickness. Assuming the particles to be spherical, the volume of resultant v formed in the time t seconds after the beginning of the reaction will be given by the expression

$$v = \tfrac{4}{3}\pi a^3 - \tfrac{4}{3}\pi(a-ut)^3,$$

where u is the linear rate of propagation in cm./sec., and a is the radius of the particle in cm.

Hence the fraction α decomposed in this time will be given by the expression,

$$\alpha = 3\left(\frac{ut}{a}\right) - 3\left(\frac{ut}{a}\right)^2 + \left(\frac{ut}{a}\right)^3. \quad . \quad . \quad . \quad \text{(I.)}$$

Clearly the maximum velocity is attained at the beginning of the reaction, since the area of the interface then possesses its maximum value.

On the other hand, the rate of nucleus formation may be such that the particle develops only a small number of nuclei before its decomposition is complete, that is to say, before the interface has time to travel completely across the particle. By assuming that the reactant consists of spheres of uniform size and that each sphere develops only one nucleus, all the nuclei being formed simultaneously, Topley and Hume[2] have shown that the fraction α decomposed in time t is given by the expression,

$$\alpha = \frac{1}{2}\left(\frac{ut}{a}\right)^3 - \frac{3}{16}\left(\frac{ut}{a}\right)^4. \quad . \quad . \quad . \quad \text{(II.)}$$

By plotting α against t the sigmoid curve associated with autocatalytic reactions results. Hence by suitable choice of the size of particle used, either of the curves corresponding to expressions (I.) or (II.) might be produced. Whether this is possible in practice in a given case will depend on the relative velocities of nucleus formation and of linear propagation.

Finally, if the linear rate of propagation is so great that a particle may be regarded as completely decomposed as soon as it develops a nucleus, a new type of curve results. Provided that infection of the undecomposed particles by those already decomposed does not occur, the rate of decomposition will be simply proportional to the rate of nucleus formation, *i. e.*

$$\text{rate of decomposition} = k_0 N_t, \quad . \quad . \quad \text{(III.)}$$

where k_0 is the number of nuclei forming per second, and N_t the number of undecomposed particles present at time t. From this it follows that the reaction will be pseudo-monomolecular and should give a first-order velocity constant. Moreover, since the conditions for the applicability of equation (III.) will be best fulfilled by small particles, the course of all reactions of the type under consideration should tend to become pseudo-monomolecular by reducing the particle size. Naturally in many cases the

rates of nucleus formation and of propagation may not be consistent with the complete realization of the necessary conditions.

In order to test the views expressed in the preceding section, the following experiments were carried out. The reaction studied is the change

$$S_{\text{monoclinic}} \longrightarrow S_{\text{rhombic}}.$$

Experimental.

A quantity of rhombic sulphur was converted into monoclinic by heating to 150° C. for two hours. While molten it was poured into the bulb of a dilatometer of the type described by Hume and Topley [6] and allowed to cool very slowly. When the sulphur had solidified and cooled, air-free distilled water was introduced into the dilatometer. Complete filling of the bulb with water was ensured by repeated evacuation, after which the ground-glass stopper carrying the capillary tube was inserted. The bulb was then immersed in a thermostat maintained at a temperature of $20 \pm \cdot 02°$ C. The course of the reaction, which is accompanied by diminution in volume, was followed by reading the height of the water-column in the capillary tube.

Curve I. shows the result of plotting the decrease in height of the column calculated as a percentage of the total decrease against the time. The change was seen to begin on the free surface of the sulphur and to spread outwards across the surface. This gives rise to the initial autocatalytic portion of the curve. When spreading had occurred across the whole free surface the interface then travelled down the tube, giving rise to the long straight portion of the curve. When the rounded end of the bulb was reached, the reaction speed decreased as the interface diminished in area. The whole curve is a special case of the sigmoid curve, having an abnormally long straight portion, owing to the elongated cylindrical shape of the mass of reactant.

In another experiment about two grams of sulphur were fused and, while liquid, distributed in thirty-five approximately circular spots of equal radius on a small glass plate. The plate was then heated to 150° for two hours and cooled slowly. It was then placed in a dilatometer filled with water and immersed in a thermostat at $25 \pm \cdot 02°$, the reaction being followed as before. Curve II. gives the result of this experiment, plotted as before. It will be noted that the curve, more particularly at the start, is made up of small sigmoid portions, which represent the change of individual spots.

The curve up to 10 per cent. decomposition is typically sigmoid; but thereafter approximates to the type of which curve III. is an example.

In a third experiment, a mass of monoclinic sulphur was prepared as before and ground in an agate mortar to a very fine powder. The powder was then introduced into the bulb of a dilatometer, which was filled with water, and maintained at $20 \pm \cdot 02°$. The course of the reaction is shown in curve III.

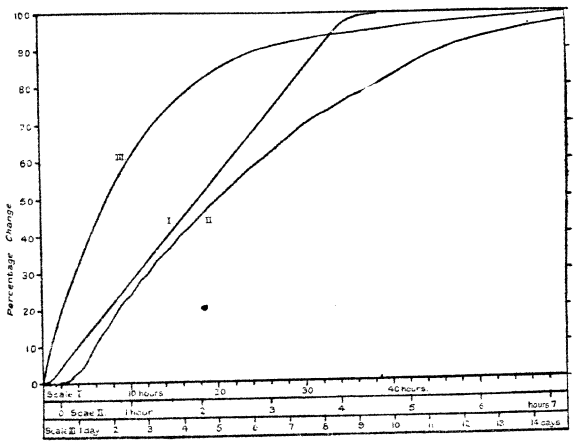

Proof that this is a truly monomolecular curve is afforded by the calculation of the velocity constant by the expression

$$k = \frac{1}{t} \log_{10} \frac{\Delta h_0}{\Delta h_0 - \Delta h_t},$$

where Δh_0 is the total contraction of the water column, and Δh_t is the contraction after time t. The results of the calculation are given in the third column of Table I.

The constancy of the values of k is satisfactory, excluding the two earliest points.

For this reaction, therefore, the predictions of the various forms of reaction curve obtainable by altering the size of the particles of the reactant are completely confirmed by an experimental study of the change.

The nature of the phenomena encountered in the investigation of the dissociation of the metallic carbonates, extensively studied by Centnerszwer and co-workers, may be interpreted in terms of the theory outlined. In the reaction,

$$CdCO_3 \longrightarrow CdO + CO_2,$$

in the neighbourhood of the dissociation temperature, Centnerszwer and Bružs[6] found that the velocity of decomposition of freshly prepared cadmium carbonate passed through a maximum after 380 minutes from the beginning of the reaction, and that after this period monomolecular velocity

TABLE I.

t in days.	Δh_t in cm.	$k = \frac{1}{t}\log\frac{\Delta h_0}{\Delta h_\infty - \Delta h_t}$.
0·0	0·0	
0·03	0·06	·2533
0·13	0·24	·2393
0·71	0·82	·1644
2·10	1·90	·1632
3·0	2·56	·1642
4·0	2·71	·1638
5·0	2·95	·1635
5·8	3·09	·1639
∞	3·48	—

constants were obtained. Samples of cadmium carbonate which had been previously partially decomposed did not show this induction period; but decomposed from the start according to the monomolecular law. From these observations Centnerszwer and Bružs suggested that cadmium carbonate exists in two forms; one of which, the α-form, existing at ordinary temperatures does not dissociate, but at the temperature of the experiment—376°—passes irreversibly into the β-form, which then dissociates into cadmium oxide and carbon dioxide. Comparison of results obtained when dealing with powdered cadmium carbonate with those obtained with the same material pressed into cylindrical form led the authors to conclude that the reaction is independent of the free surface and that reaction proceeds simultaneously throughout the whole mass of reactant, analogous to reaction in the homogeneous gaseous or liquid phases.

This last conclusion is of special interest in that it is in direct opposition to the views of Langmuir [4] on the analogous reaction, the dissociation of calcium carbonate. If we assume that the dissociation of cadmium carbonate occurs at the interface separating the two solid phases, $CdCO_3$ and CdO, and there does not appear to be any real evidence to show that such is not the case, an alternative explanation can be offered of the experimental results summarized above, without the necessity of postulating the existence of two forms of cadmium carbonate.

The sigmoid curve obtained for the course of the decomposition of fresh cadmium carbonate by plotting percentage decomposition against time, shows that the maximum velocity occurs when the reaction has proceeded to an extent of only 12 per cent. We conclude, therefore, that the rate of nucleus formation is high relative to the linear rate of propagation, and that consequently the particles become covered with a layer of cadmium oxide, the subsequent reaction proceeding according to equation (I.). This offers a satisfactory explanation of the observation of Centnerszwer and Bružs that partially decomposed cadmium carbonate showed no induction period, in that in the partial decomposition, the particles would develop a complete envelope of resultant.

Moreover, the constancy of the values of k, calculated by the expression

$$k = \frac{1}{t} \log \frac{V_\infty}{V_\infty - V_t},$$

after the induction period, is not sufficient to disprove the interfacial nature of the reaction. Since no data are given for the size of the particle employed, it is impossible to attempt any complete quantitative treatment of the results. By applying equation (I.), viz.,

$$100\,\alpha = \left\{ 3\left(\frac{ut}{a}\right) - 3\left(\frac{ut}{a}\right)^2 + \left(\frac{ut}{a}\right)^3 \right\} 100,$$

constant values for the ratio u/a should be obtained for any given run, provided that the reaction proceeds in the way suggested. Table II. contains the results of this calculation for the data of Centnerszwer and Bružs for the decomposition at 376° C.

The constancy of the ratio u/a is sufficient to justify the belief that the reaction is interfacial in nature. If the calculation of u/a is extended to the later stages of the run, it is found that the ratio shows a progressive diminution. This

is to be explained by the earlier extinction of the smaller particles present.

Finally, with reference to the effect of compressing the powdered cadmium carbonate into cylindrical masses, no great change in the behaviour is to be anticipated since mechanical compression would not result in the formation of larger aggregates possessing a continuous lattice.

TABLE II.

Time in min.	Vol of CO_2 in c.c.	$100\,x$.	$k = \frac{1}{t}\ln\frac{V_\infty}{V_\infty - V_t}$.	u/a.
0	0	0	—	—
40	4·80	3·13	0·000789	0·000262
80	9·59	6·25	0·000809	0·000262
120	14·45	9·42	0·000825	0·000265
160	18·95	12·36	0·000826	0·000262
200	23·44	15·28	0·000828	0·000267
∞	153·4	100·0	—	—

References.

(1) Fraenkel and Goez, *Zeitsch. für Anorgan. Chem.* cxliv. p. 45 (1925).
(2) Topley and Hume, Proc. Roy. Soc. A, cxx. p. 211 (1928).
(3) Hume and Colvin, unpublished.
(4) Langmuir, J. Amer. Chem. Soc. xxxviii. p. 2263 (1916).
(5) Centnerszwer and Bruzs, *Zeitschr. für Physikal. Chem.* cxix. p. 405 (1926).
(6) Hume and Topley, Proc. Leeds Phil. Soc. i. p. 169 (1927).

Department of Inorganic Chemistry,
The University, Leeds.

LXIV. *The Viscosity of Vapours.*—Part I. *Influence of Molecular Association on the Viscosity of Acetic Acid.* *By* A. G. NASINI, *Ph.D.**

SUTHERLAND'S formula, which in most cases agrees admirably with the experimental data for gaseous viscosity, almost always fails at low temperatures, and in particular in the range of temperatures below the critical, where the experimental values are usually higher than the

* Communicated by Prof. T. Martin Lowry, F.R.S.

calculated ones. It is natural to attribute this to the non-ideality of the gas, and to introduce corrections based on van der Waals's equation, or on modifications of this equation such as those of van Laar and of Trautz [1]; but these corrections would increase the viscosity values [2], thus giving still greater divergence from Sutherland's theoretical curve. Chapman [3] and others have attempted to improve the formula connecting viscosity with temperature, but these attempts always fail at low temperatures. Recently Hassé and Cook [4] have considered a gas composed of Sutherland molecules, in which the attractive force varies as the inverse fifth power of the distance from the centre of the molecule. Their more exact formula gives a calculated force-constant which in certain cases may differ considerably from that calculated by means of Sutherland's formula, but the two formulæ give equally good agreement in the calculation of the coefficient of viscosity; the authors therefore conclude that the agreement of the experimental data with a theoretical relationship is by no means a safe check on the formula.

In a paper by Condon and Amringe [5] a Maxwellian mean free path has been taken into consideration on classical lines, and some interesting remarks have been made upon Sutherland's constant, which in their viscosity formula would be about three-fourths of the ratio of the energy of two molecules at contact to the gas constant per molecule. Lennard Jones [6] has put forward an interesting theory, but it is not proposed to discuss this in the present paper. There are also many empirical formulæ, such as that of Nernst, which fit the low temperature data over a limited range of temperatures; but no general formulæ connecting viscosity and temperature has yet been found, and the problem is not yet solved.

Another method of attacking this problem is by considering the possibility of unequal molecular complexity of the gas at different temperatures, and applying the laws of chemical dynamics to the equilibrium between the simple and complex molecules. Some years ago Dr. E. K. Rideal expressed to me the opinion that gaseous viscosities can be considered as a chemical phenomenon; Trautz [7] and Duclaux [8] have recently advanced the same idea. The phenomena of molecular association and dissociation can indeed be regarded as the simplest type of chemical reaction, a transition term to the formation of stable compounds.

Since the diameter of a molecule is increased by increasing its complexity, the coefficient of viscosity will be decreased.

At low temperatures, therefore, the experimental values should be below the theoretical values for non-associated molecules; but this is not the case, and the correction is still in the opposite sense to that required in order to make the experimental values fit Sutherland's curve. Thus my recent experiments on the vapours of organic substances [9] always give high values for the viscosity-coefficient at low temperatures. If, however, we consider the viscosity values calculated by means of Meyer's formula of efflux, we see that the molecular weight enters the calculation as a vapour density, in such a way that an increase in its value leads to a higher calculated coefficient of viscosity. The value deduced for non-associated molecules must therefore be smaller than the real one whenever complex molecules are formed. The viscosity curve for a vapour undergoing association could then very nearly follow Sutherland's curve even at low temperatures, the normal increase of viscosity being compensated by the decrease due to larger molecular complexity.

In order to determine the real effect of molecular complexity on gaseous viscosity a series of experiments was made with acetic acid, since the anomalous behaviour of its vapour is well known, especially from the experiments of Ramsay and Young on its vapour densities. The acid (Schuchardt's acetic acid "puriss.") was purified by Orton and Bradfield's method [10], with acetic anhydride in stoichiometric quantity and chromic oxide: the product was then fractionally crystallized out of contact from moisture, and fractionally distilled; the fraction boiling at 118·1° under 760 mm. pressure was collected. The final product melted at 16·6° C.

The viscosimeter was of the same type as described [9] previously, with manometers on both sides of the capillary. It was quite suitable for this investigation, since it was possible to regulate the mean pressure and the temperature, and therefore to examine the substance at temperatures and pressures at which the substance is but little, if at all, associated. The dimensions of the capillary were

$$\Sigma \frac{l}{r^4} = 0{\cdot}972 \times 10^9 \text{ cm.}^{-3}.$$

The evaporation thermostat was kept at about 50° C., whilst the condensation temperature was kept some degrees above zero so as to give a condensation pressure of about 6 mm. The densities have been taken from the data of Jaeger [11]. The results of the experiments are collected in Table I. and

the mean values for a series of different temperatures are given in Table II.

The 93° values have not been corrected for slipping, in view of uncertainty as to the correct value of "R" to take, but they should not vary more than 2 or 3 per cent. The approximate value of the vicosity at that temperature can be taken as $0{\cdot}78 \times 10^4$ C.G.S. at a mean pressure of 31 mm. The observations at higher temperatures have been corrected on the assumption that the vapour consists of simple molecules. Table I. leads to the conclusion that, especially at the higher temperatures, substantial changes in the mean

TABLE I.—Viscosity of Acetic Acid.

No.	Temp. in C°.	p_1.	p_2.	Δ.	Mass transpired gr. hour^{-1}.	$\eta \times 10^4$ C.G.S.	$\eta \times 10^4$ C.G.S. corr.
1...	93·7	5·925	0·63	34·70	0·115	0·769	
2...	93·7	5·93	0·63	34·83	0·114	0·783	
3...	92·1	5·03	0·65	24·87	0·083	0·775	
4...	150·5	6·07	0·72	36·33	0·080	1·140	1·168
5...	150·1	5·15	0·62	25·66	0·049	1·150	1·184
6...	200·2	5·16	0·62	26·24	0·039	1·304	1·350
7...	201·9	5·746	0·66	32·58	0·0492	1·309	1·351
8...	250·8	5·736	0·62	32·53	0·040	1·458	1·514
9...	248·2	5·746	0·63	32·62	0·047	1·441	1·494

TABLE II.—Viscosity of Acetic Acid. (Mean values.)

Temperature in C°.	η corr. $\times 10^4$ C. G. S.
93·2	0·770
150·3	1·176
201	1·350
249·5	1·504

pressures produce no marked discrepancies in the final values of the viscosity, so that the vapour must be supposed to obey the gas laws.

Another point to be observed is that the viscosities at the lowest temperatures differ considerably from those at the three higher points. The 150° point already shows a downward tendency which is opposite to that usually seen in vapours, and the 93° value is quite remarkably lower, so that a downward concave curve can be drawn between the experimental values. This is of interest because it seems to confirm the view that the upward concavity of the experimental curve for other vapours is not due to molecular

complexity, which sharply reverses the shape of the curve. We may with a good approximation obtain provisional values for Sutherland's constant from the data for the two highest temperatures until other data for still higher temperatures are available *. Sutherland's constant would then be S = 725.

From a prolonged ideal line the viscosity at 0° has been extrapolated to $\eta_0 = 0{\cdot}724 \times 10$, giving as the value of the mean collision area

$$\overline{A} = 10{\cdot}00 \text{Å}.^2.$$

The mean area obtained seems to be of the right order of magnitude. Rankine found for methane a collision area of 7·7 Å.^{2}, and the dimensions of a COOH replacing an atom of hydrogen would be about 2·5 ångström square.

Using Meyer's formula to get the supposed molecular weight of the molecule at 93·7° from the extrapolated value of the viscosity, we get for the vapour density of the molecule 38·7 at a mean pressure of about 30 mm.: Ramsay and Young's value at 92° and at a pressure of 30·6 mm. is 39·8. The agreement is fair, although the values now given are considered to be only approximate, since exact quantitative results can only be derived from experiments made over a larger range of temperatures and with greater exactness, and in comparison with observations on analogous compounds which do not undergo association. On the other hand, it is reasonable to suppose that the values now obtained for acetic acid between 150° and 250° represent the viscosity of the simple molecule.

Another datum about the coefficient of internal friction of acetic acid vapour exists in the literature, namely Meyer's and Schumann's value[12]. This would give at 119° a viscosity of $1{\cdot}07 \times 10^4$ C.G.S., calculated on the basis of the theoretical vapour density, but, as the data are affected by an error of about 50 per cent., no useful purpose would be served by discussing them.

Summary.

1. The coefficient of internal friction of the vapour of acetic acid has been examined through a range of temperatures from 90° to 250° C.

2. The experiments have been made under reduced pressures, and the values from 150° to 250° are supposed to be those of the simple acetic acid molecule.

* Experiments are being set up for extending the range of temperatures to 500°.

3. The temperature-viscosity curve shows at lower temperatures an opposite shape to those of non-associated compounds.

4. The deviations from Sutherland's law are examined from different points of view and critically discussed.

References.

(1) M. Trautz and A. Narath, *Ann. d. Physik*, lxxix. pp. 637–672 (1926).
(2) *Ibid.*
(3) Chapman, Phil. Trans. A, ccxvi. p. 279 (1915).
(4) H. T. Hassé and W. R. Cook, Phil. Mag. p. 977 (1927).
(5) E. Condon and E. V. van Amringe, Phil. Mag. p. 604 (1927).
(6) Lennard-Jones, Proc. Roy. Soc. (a series of papers from 1924).
(7) *Loc. cit.*
(8) M. J. Duclaux, *Journ. de Phys.* viii. [vi.] p. 336.
(9) Proc. Roy. Soc. A. cxxiii. p. 692 (1929).
(10) K. J. P. Orton and A. Bradfield, J. C. S. p. 893 (1927).
(11) F. M. Jaeger, *Zeit. f. anorg. Chemie*, c. p. 1 (1917).
(12) *Wied. Ann.* vii. p 497 (1879).
(13) See my note upon benzene. (Proc. Roy. Soc. 1929.)

Istituto di Chimica Generale,
R. Università. Firenze, and
Istituto di Chimica Industriale,
R. Politecnico, Milano.

LXV. *The Viscosity of Vapours.*—Part II. *Relationships between Critical Constants and Gaseous Viscosity.* By A. G. Nasini, *Ph.D.**

FROM a consideration of the properties of systems which are mechanically and statistically similar, Kamerlingh Onnes [1] has deduced some relationships between the viscosity of liquids and the critical constants. Similar relationships ought to exist also for gases. Thus, from the simple kinetic formula for the viscosity of gases

$$\eta = \tfrac{1}{3} mnl\bar{c}$$

(where η is the viscosity, m is the mass of the molecule in grams, n the molecules per c.c., l the mean free path, and $\bar{c}$ the mean molecular velocity) we get by the substitution of suitable functions of the molecular radius, temperature, and critical density the following formula:

$$C = T^{\frac{1}{2}} m^{-\frac{1}{2}} \rho_c^{\frac{2}{3}},$$

where

$$C = \frac{1}{3} \frac{0{\cdot}7071}{\pi} \sqrt{3R}\, 2\pi^{\frac{2}{3}}.$$

* Communicated by Prof. T. Martin Lowry, F.R.S.

In this formula, T is the absolute temperature, ρ_c the critical density, and R the gas constant. Writing $M = mn \times 22414$, we obtain for the viscosity η_c at the critical temperature the relationship

$$\frac{\eta_c m^{\frac{1}{6}}}{T_c^{\frac{1}{2}} \rho_c^{\frac{2}{3}}} = C, \quad . \quad . \quad . \quad . \quad . \quad . \quad . \quad (1)$$

where T_c is the critical temperature in K° and M is the molecular weight. In a similar way the equation

$$\eta_c \sqrt[6]{\frac{T_c}{M^3 p_c^4}} = \text{const.} \quad . \quad . \quad . \quad . \quad . \quad (2)$$

may be obtained, which is Kamerlingh Onnes's relationship for liquids, where p_c is the critical pressure. Instead of the ratio M to ρ_c, we may insert the critical molecular volume.

In Table I. are collected the values necessary for calculations, together with those of the constant obtained from formulæ (1) and (2).

The viscosities used for the calculations are the most probable values selected from Landolt and Börnstein's Tables (1923 edition). The extrapolation and interpolation of the data for moderate and high temperatures have been made by Sutherland's formula, finding the constants where they had not been worked out previously.

The value of η_c for helium has been extrapolated from Günther's (2) values by means of Nernst's empirical formula. The exponent of the formula has been taken as unity, which is the maximum mean value found; this value is obviously rather uncertain, since experiments to show the behaviour of the viscosity curve 5° K have not yet been made. If Nernst's formula were right, the value of the exponent ought to reach 1·5. The data for hydrogen, which were interpolated by means of the same formula, are more certain, although it was not expected that the constants would be very accurate at low temperature, where the imperfection of the gas would be very obvious.

For benzene and acetic acid I have taken my own values, for ammonia and carbon dioxide the last values of Edwards & Worsick and of Smith [3].

The table shows that the agreement is quite good for the substances considered, and, indeed, the mean error of the calculated constants (6–7 per cent.) corresponds closely with the mean error of the experimental data. It is interesting to note that the constant of equation (1) gives divergent values for bromine, whilst it gives good values for water and acetic

acid, substances which usually show discrepancies in formulæ based upon the theory of corresponding states. The values calculated by equation (2), however, show an abnormal behaviour for the last two named substances, whilst chlorine also diverges from the mean values.

Taking $2{\cdot}80 \times 10^{-5}$ as the mean value for constant (1), the critical density of krypton ought to be 0·873; the value given by Goldhammer [4] is between 0·694 and 0·927.

TABLE I.

Substance.	M. weight.	Critical density.	η at critical temperature $\times 10^4$ C.G.S.	Critical temperature.	Critical pressure atm.	$\eta_c M^{1/6} \times 10^8$. $\rho_c{}^{2/3} T_c{}^{1/6}$	$\eta_c \sqrt{\frac{T_c}{M^3 p_c{}^4}} \times 10^8$.
Helium	4	0·065	0·086	5	2·3	3·01	3·23
Hydrogen	2	0·033	0·155	33	13	2·95	3·55
Nitrogen	28	0·311	0·867	126	33	2·93	3·54
Carbon monoxide ...	28	0·311	0·934	134	35	3·06	3·73
Argon	39·9	0·531	1·253	151	48	2·87	3·47
Oxygen	32	0·43	1·166	155	49·5	2·93	3·53
Methane	16	0·162	0·750	190	45·6	2·90	3·52
Ethylene	28	0·21	0·950	283	50·6	2·80	3·36
Xenon	130·2	1·15	2·266	288	58	2·74	3·40
Carbon dioxide	44	0·46	1·521	304	72·8	2·75	3·41
Ammonia	17	0·236	1·405	405	112	2·93	4·00
Chlorine	79·9	0·573	1·897	417	76	2·74	5·00
Isopentane	72·1	0·234	1·111	463	33	2·77	3·54
Ethyl acetate	88	0·307	1·384	523	38	2·81	3·70
Benzene	78	0·304	1·42	561	48	2·74	3·59
Bromine	159·8	1·18	2·874	575	—	2·50	—
Acetic acid	60·04	0·35	1·65	594	58·1	2·70	4·12
Water	18	0·329	2·315	647	217	3·09	4·44

The critical viscosity of neon by extrapolation to the critical temperature would be $0{\cdot}691 \times 10^{-4}$.

Several empirical rules connecting viscosity at the critical temperature with other constants have been found by Rankine. One of the rules is

$$\frac{\eta_c{}^2}{A} = \text{const.}, \quad . \quad . \quad . \quad . \quad . \quad . \quad (3)$$

where A is the atomic weight, valid for the rare gases and the halogens. The constant is not universal, but differs for

the two groups of the periodic system. If this relation were true for molecules, equation (1) would become

$$\frac{\eta_c^2}{M} = \frac{T_c \rho_c^{4/3}}{M^{4/3}} C^2 = \text{const.},$$

where C is the constant of equation (1). Since the molecular critical volume, v_c, is equal to M/ρ_c, the constant of equation (3) will have equal values when the ratio $\frac{T_c}{v_c^{4/3}}$ is also equal.

The molecular critical volume and temperature vary for the halogens and the rare gases with a certain regularity with increasing molecular weight; the gaseous viscosity at the critical temperature, which is connected intimately to these two quantities, may therefore be expected to show the same regularities.

Some values of $\frac{\eta_c^2}{M}$ are tabulated in Table II., where chlorine and bromine are seen to give similar values for this ratio.

TABLE II.—Viscosity at the Critical Point.

Substance.	$\frac{\eta_c^2}{M} 10^{-10}$.	Substance.	$\frac{\eta_c^2}{M}$.
Helium	0·185	Ethylene	3·22
Hydrogen	1·2	Xenon*	3·93
Nitrogen	2·68	Carbon dioxide.....	5·25
Carbon monoxide...	3·14	Ammonia	11·6
Argon *.....	3·93	Water.....	29·8
Oxygen	4·25	Chlorine	5·07
Methane	3·52	Bromine.....	5·17

* Rankine's values.

References.

(1) K. Onnes, Comm. Leiden Suppl. n. xxiii. p. 85.
(2) P. Günther, *Zeit. f. Phys. Chem.* cx. p. 626 (1924).
(3) C. J. Smith, Proc. Roy. Soc. xxxiv. p. 155 (1922) and R. S. Edwards and B. Worsick, Proc. Phys. Soc. xxxviii. p. 16 (1925).
(4) See J. W. Mellor's 'A Comprehensive Treatise of Inorganic and Theoretical Chemistry,' vii. p. 918 (1927).
(5) A. O. Rankine, Proc. Roy. Soc. lxxxiv. A, p. 190 (1910) and other papers.

Istituto di Chimica Generale,
R. Università, Firenze, and
Istituto di Chimica Industriale,
R. Politecnico, Milano.

LXVI. *On the Origin of the Electrodeless Discharge.*

By K. A. MacKinnon, *M.Sc.**

1. ALTHOUGH the electrodeless discharge was discovered as long ago as 1884, there are still conflicting views regarding its origin. Experimental evidence has been given by many writers (Lehrmann [1], Tesla [2], Lecher [3], Steiner [4], etc.) that the discharge is the result of the large alternating potential differences which exist between the ends of a coil carrying high-frequency currents, while according to Hittorf [5], its discoverer, and to J. J. Thomson [6] the discharge is due to electromagnetic induction. As recently as 1927, Thomson [7], using excitation by spark discharges, has given additional experimental evidence supporting the view which he has always held. This paper was followed by one by Townsend and Donaldson [8] criticizing the electromagnetic view. They point out that theoretically the electrostatic intensity (E_s) between the ends of a solenoidal coil of ordinary dimensions is more than thirty times the electromagnetic intensity (E_m) around a ring inside the coil. Thus they are led to conclude that the electrostatic forces are largely responsible for the electrodeless discharge. In support of this conclusion they give experimental evidence obtained with the use of continuous wave (c.w.) excitation.

In view of the apparent conflict between these two recent articles, the work of the present paper was undertaken.

2. At the outset it may be stated that Thomson's work has always been confined to the *ring* type of discharge which appears within a small range of pressures, while Townsend and Donaldson were dealing with a glow discharge obtainable over a much wider range. The work herein described indicates that the ring discharge is undoubtedly of electromagnetic origin, whilst the glow is largely or entirely electrostatic. In one sense, therefore, both are right. The failure of Townsend and Donaldson to recognize the difference between the two types of discharge seems to be the cause of the discrepancy.

* Communicated by Prof. J. K. Robertson. The writer undertook this work while a holder of a Bursary granted by the National Research Council of Canada, Ottawa.

Experiments with Damped Oscillations.

3. In this investigation, observations were made with both spark and c.w. excitation. The usual spark excitation circuit (fig. 1) was employed. S is a micrometer gap, C leyden-jars, and L a coil of a number of turns of heavy wire which fit around the cylindrical discharge bulb. The

Fig. 1.

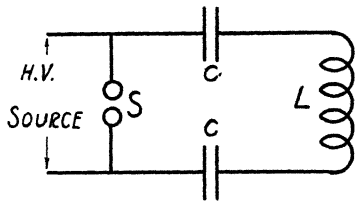

discharge bulbs used were 16 cm. long and 11 cm. in diameter (fig. 2, ignore copper band). The vapour in the bulb was either iodine or mercury. These substances were selected owing to the fact that each of them, on being subjected to a gradually increasing excitation, will change suddenly the colour of its discharge. Iodine breaks into

Fig. 2.

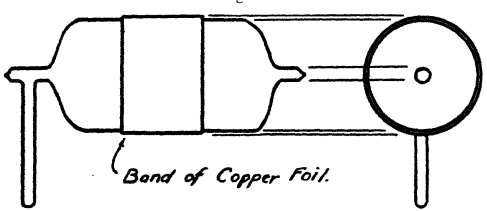

an intense green from a yellowish colour, whilst mercury jumps from a dull white into a dazzling white discharge. It is assumed that when this transition occurs, the forces acting on the exciting electrons have a definite value. These changes are obtained only if the pressure of the vapour be within a certain interval. In iodine the pressure was regulated by keeping the projecting stem of the bulb at a fixed temperature, generally 0° C. In the

case of mercury, as temperatures of between 50° and 100° C. were necessary, observations were made with the bulb in an electrically heated oven.

4. As the gap is gradually increased, many changes take place in the appearance of the discharge in iodine at 0° C. For very low excitations, there is a faint yellowish glow which extends from end to end of the bulb. This glow is weaker near the axis of the coil, but stronger in the central plane. As the excitation increases, the glow becomes brighter and brighter around the central plane, and finally breaks into a fitful green ring in that plane. This central ring is so bright that the glow formerly extending throughout the bulb is not noticeable. For still greater gaps several more green rings form near the central plane, until finally all these rings merge into one broad green annular band which extends nearly the length of the solenoid. The radial thickness, however, remains the same.

5. To ascertain the origin of the different types of discharges described above, the following experiments were performed :—

(*a*) The discharge bulb was held next to, but outside, the exciting coil. In this position the electrostatic forces have the same opportunity for ionizing as is the case when the bulb is inside the coil, but the electromagnetic forces are absent. The gap was adjusted so that, with the bulb inside the coil, the green ring was readily obtained. Then the bulb was placed outside, but next to, the coil. The discharge was merely a faint glow similar to that obtained with low excitation on the bulb inside the coil. This experiment demonstrates that, although the E_s between the ends of the exciting coil be high, the resulting electrostatic discharge is a relatively faint effect.

(*b*) In order to investigate the green ring discharge a loop of thin copper foil about 3 inches wide, closed on itself, was made to fit snugly over the discharge bulb (as in fig. 2). The gap was adjusted so that the iodine bulb (without the foil) gave a solid green annular band extending up and down the bulb. Then the bulb was removed from the coil, the foil slipped over it, and the bulb replaced. It was found that all green effects were absent inside the foil, but still remained at the exposed ends

of the bulb. Also the faint yellowish glow obtained by holding the bulb against the outside of the coil (as in 5 (*a*)) was obtained equally well with the copper foil in place. From this experiment it is concluded that the green ring is of electromagnetic origin.

(*c*) The effect of a peculiarly wound solenoid (fig. 3) similar to that used by Townsend and Donaldson [8] (coil G_2) was investigated. With this method of winding, the electrostatic field between the two ends is practically nil, but the electromagnetic field is about the same as in the case with an ordinary solenoid. Townsend and Donaldson found that, using this type of coil, the discharge obtained

Fig. 3.

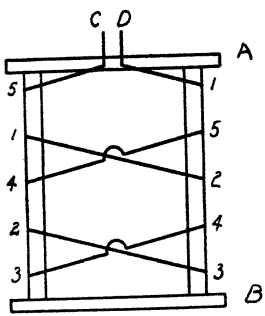

with c.w. started between the open ends CD, thus demonstrating the electrostatic origin of that discharge. With a solenoid of this kind, and spark excitation, observations were made by the writer with iodine. It was found that, for short gaps, there was a faint glow outlining the wires near the open end A of the coil, but no discharge at all at the closed end B. As the gap was increased, this glow also increased in intensity. As a certain gap length was reached however, there appeared *in the central plane of the coil* a yellowish ring, which suddenly broke into the ordinary green ring with any further increase in gap-length. The fact that the green ring occurred only at or near the central plane of the coil indicates that the ring is of electromagnetic origin.

(*d*) In order to make sure that the above results were not peculiar to iodine, the above experiments were repeated with mercury vapour, with similar results.

(*e*) In a spiral coil the electrostatic forces act radially outward from the inner turns so that the effect in an electrodeless bulb placed inside such a coil must be solely of electromagnetic origin. In the following experiment a spiral coil was made of such dimensions that it produced the same E_m in the bulb as the ordinary solenoid, when the frequency and the value of the currents through the coils were the same. To find the required dimensions of the spiral, a loop of wire of the same diameter as the inside surface of the discharge bulb (the green ring has this diameter) was shorted through a hot-wire ammeter (I_2 in fig. 4). This was placed in the central plane of the

Fig. 4.

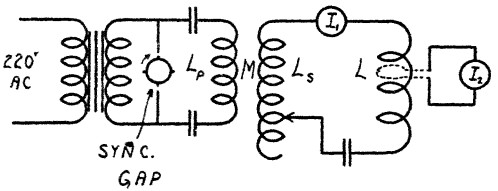

solenoid L. The coil L was in a tuned secondary circuit coupled to a fixed primary circuit excited by a synchronous rotary gap. The ratio of loop current (I_2) to secondary current (I_1) was determined for various values of current. Following this, solenoid L was replaced by the spiral, and the loop placed in its plane. The turns on the spiral were then adjusted to give the same ratio of I_1 to I_2. In the following test this length of spiral and this frequency were always used.

Observations were made of the gap-length just necessary to give the green ring during a flash, using the solenoid and then the spiral. The high voltage was applied to the gap only in short flashes with an interval of longer duration between the flashes. As the inductance of the spiral was greater than that of the solenoid, it was necessary to retune the circuit to the fixed frequency used whenever the coils were interchanged. This was done by varying either the

capacity of the oscillating circuit or the value of a separate tuning inductance. The results were slightly different, depending on which of these was altered during the retuning. In order to get steady conditions, an air-blast across the gap was used throughout. The values of the current given are for continuous discharge. The following results were obtained :—

	Spiral.	Solenoid.	Solenoid.
Wave-length.....	275 m.	275	275
Tuning inductance	1 turn.	1	4
Capacity	2 jars.	3	2
Current	4·6 amp.	5·2	4·5
Gap-length	8·5 mm.	6·3	8·5

If the electrostatic forces actually have an effect in forming the ring discharge, one would expect that the gap for the solenoid would be very much less than that for the spiral. Yet an examination of the results given in the above table indicates that *the critical gaps are of the same order of magnitude in the two cases.* Although, in the writer's opinion, little reliance can be placed in spark-gap readings for exact measurements, yet their accuracy here should be sufficient to demonstrate that the ring discharge is undoubtedly of electromagnetic origin.

The conclusions to be drawn from the above experiments are that with low excitations the discharge is electrostatic, but with higher excitations, when the bright ring appears, the discharge is of electromagnetic origin. Also, discharges of electrostatic origin are always of low luminosity, even though the electrostatic intensity be very high.

Experiments with Undamped Oscillations.

6. As Townsend and Donaldson had worked with c.w. only, the above experiments were repeated with this mode of excitation.

The generator used was a Hartley circuit as shown in fig. 5, involving a vacuum-tube oscillator of 250-watt rating fed by a 1500-volt d.c. generator. The discharge bulb was either inserted in the Hartley helix H, or in a coil connected in a tuned circuit magnetically coupled to H.

(*a*) The result, at first surprising, was that with the iodine bulb in coil H no green ring or ring of any kind could be obtained with undamped excitation. For certain adjustments the high-frequency current through th

Fig. 5.

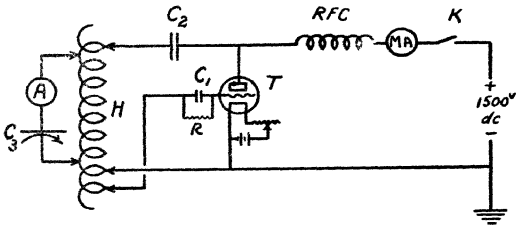

helix was more than 6 amperes, and yet with spark excitation the green ring appeared for currents of less than 3 amperes. The discharge actually obtained with c.w. was a solid glow throughout the bulb. The appearance was the same whether the bulb was held inside or outside next the coil. Also. the presence of the copper-foil loop around the bulb had no effect on this solid glow. These facts indicated that the discharge with c.w. excitation in iodine was of electrostatic origin.

Fig. 6.

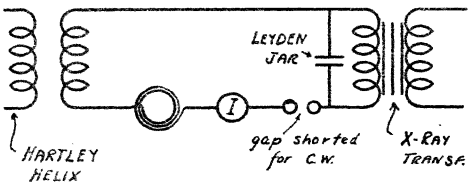

To eliminate the possibility that the difference in the capacities of the exciting circuits (air dielectric for c.w., glass for spark) might account for the failure to get the same discharge. the circuit of fig. 6 was tried. A pancake coil was used, as electromagnetic effects are more readily detected with it. It is seen that the identical exciting

circuit was used for both damped and undamped methods. The circuit was tuned to a wave-length of 171 metres. It was found that with a current of 5·5 amps. no discharge at all was obtained with c.w., but the spark gave a green ring with a current of 4·6 amps.

The probable explanation of the failure to obtain a ring discharge with c.w. is found in the difference between the graphs of "current *v.* time" for the two cases, (fig. 7 (*a*) spark, (*b*) c.w.). From these it is evident that, although the root-mean-square values (as indicated on hot-wire meters) of the currents in the two cases may be the same, the maximum value of the current during the first half-cycle of the spark current is enormously greater than that of

Fig. 7.

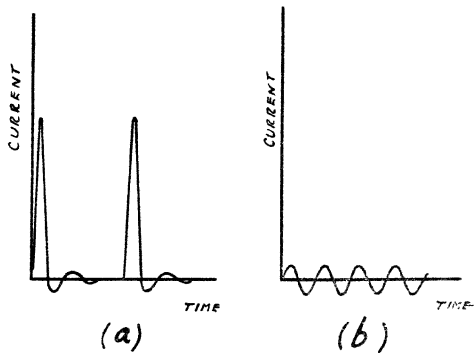

the c.w. current. As the maximum velocity acquired by an electron depends on the magnitude of the field intensity during the half-cycle, it follows that the excitation will be very much more intense in the spark case.

(*b*) From this explanation it is seen that, if the vapour were easily enough ionized, a ring discharge should occur even with c.w. excitation, and experiments with mercury vapour seemed to indicate the truth of this. With a constant current of about 6 amperes the discharge in mercury was examined as the bulb was gradually heated. At lower temperatures the glow was a dull white. After a temperature of 50° C. was attained a very bright white discharge filled the whole bulb and the solenoid current

dropped to 2 amperes, indicating the presence of heavy currents in the gas. As the temperature still rose the central part of the bulb became darker and darker, and finally at 140° C. the bright white discharge had dwindled to a bright white ring in the central plane of the solenoid—that is, it had the same appearance as the white ring obtained with spark. This ring disappeared suddenly at about 165° C., leaving an emerald-green glow filling the whole bulb. On cooling, the ring commenced again. It was found that the value of the wave-length had little effect on the change to the bright white discharge, but the capacity of the exciting circuit had to be kept low. For instance, if the air condensers were replaced by a leyden-jar, no bright white discharge could be obtained. But on replacing this jar by two tiny jars (1 in. diam., 3 in. high) in series the white discharge was readily obtained.

Using the three tests of 5 (*a*), (*b*), (*c*), it was readily shown that this bright white discharge in mercury was of electromagnetic origin, and also that the dull white discharge obtained with low excitations was of electrostatic origin.

Discussion.

7. It will be noticed that for low excitations the discharge was electrostatic, but as the excitation increased the electromagnetic discharge commenced suddenly, and was of much greater intensity than the previous electrostatic discharge. Now, Townsend and Donaldson showed (and experiments by the writer have confirmed their observations) that the ratio of E_s to E_m is greater than thirty for an ordinary solenoid. In the case of the solenoid of fig. 3, E between C and D is obviously very much greater than thirty times E_m around the inner surface of the bulb. On the other hand, the experiments presented in this paper indicate that, although *outside* the bulb E_s is so much greater than E_m, *inside* the bulb E_s must be either much less than E_m, or the exciting electrons in the electrostatic path cannot, for some reason, acquire as high a velocity as those in the electromagnetic path.

As regards the first suggestion, it was always noticed that when the electrostatic glow was taking place in any of the bulbs, the glass walls in the path of the electrostatic field got very hot quickly. This indicated great dielectric losses in the glass at the high frequencies used. The only

difference between the path of the electrostatic field and that of the electromagnetic field is that the former traverses two layers of glass before the gas is reached, while the path of the latter is entirely within the gas. The fact of the high dielectric losses in the glass suggests that the glass is acting appreciably as a very high resistance in the part of the electrostatic field which it occupies. For certain low excitations the value of E_m is almost neglibible, but that of E_s, since it is over thirty times greater than E_m, must be sufficient, after subtracting the potential drop through the glass walls, to cause weak ionization in the gas. This gives rise to the faint electrostatic glow one gets with low excitations. As the excitation is increased, the current tends to increase through the electrostatic path (glass to gas to glass). An increase in current through the gas means an increase in ionization of the gas, and thus a lowering of its effective resistance to the electrostatic voltage. Hence, although the total electrostatic voltage across the circuit is higher, the proportion of the voltage used up in the gas is less, because the resistance of it has dropped whilst the resistance of the glass has remained the same. Thus, even though E_s increases externally, it does not do so at the same rate internally. On the other hand, E_m increases directly with the excitation When ionization starts in the ring path, the resistance drops, but since the whole electromagnetic E.M.F. is always applied to the ring circuit, the current in the path must increase more quickly than E_m. Thus intense ionization sets in around the ring when E_m attains a certain value.

With reference to the second suggestion, it is noticed that the electrons moving in the electromagnetic field meet no obstruction, but those in the electrostatic field have a glass wall to strike at either end of the path. Any electrons striking the wall are lost so far as ionizing is concerned. Hence, if, for the pressure at which the electromagnetic ring discharge takes place most readily, the mean free path of the electrons be about equal to the distance between the glass walls in the electrostatic path, then no electrostatic discharge could be expected, even though E_s be greater than E_m inside the bulb.

8. In order to investigate the above possibilities experimentally, a tube fitted with tungsten electrodes, as illustrated in fig. 8, was used. At first it was filled with

iodine vapour in the ordinary way, but it was found that no ring discharge could be obtained, thus rendering the bulb useless for comparison with the bulbs without electrodes. It is possible that the presence of the tungsten electrodes prevented the formation of the ring, an effect

Fig. 8.

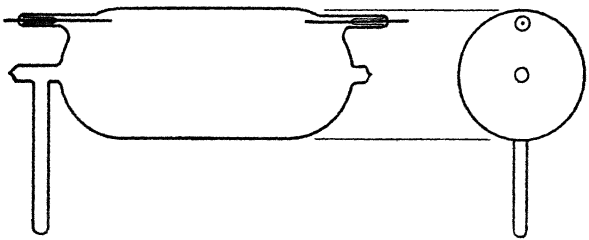

observed by Thomson [7] for certain impurities. It was thus necessary to use a continuous flow of gas through the bulb by connecting one tip of the bulb to a pump and letting the gas leak slowly into the other end of the bulb.

The gases tried were nitrogen, oxygen, and air, for all of which the general results were the same. The exciting circuit was arranged as in fig. 9 for the electrostatic effect, or with the bulb inside the solenoid in the ordinary manner

Fig. 9.

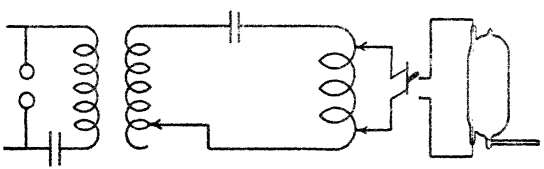

to get the electromagnetic effect. With the bulb inside the solenoid, and at the same time with the electrodes connected to the ends of the solenoid, the general effect in all three gases was the same. For instance, with nitrogen, from a high pressure of about 1·163 mm. down to about 0·0062 mm. there was no ring discharge, but there was a bright line discharge between the electrodes. At the pressure 0·0062 mm. this discharge ceased and the ring

discharge commenced. Around this pressure both discharges took place simultaneously. At 0·00017 mm. the ring discharge ceased and there was no discharge at all in the bulb.

These facts indicate that here the mean free path (pressure) is the predominating factor. For short free paths the high E_s between the electrodes causes intense ionization, but the E_m is too small to cause any ring discharge, as the electrons have collisions before acquiring enough velocity. When the pressure is so low that the mean free path is comparable to the distance between the electrodes, then the discharge between the electrodes ceases. But the electrons in the electromagnetic ring path have a sufficiently long free path to acquire enough velocity to cause ionization, thus causing the ring. It is at this low pressure that the iodine and mercury bulbs were used, because these bulbs were worked at a temperature which passed the electromagnetic ring discharge most readily. On the other hand, it should be noticed that at the high pressures where the *electrode* discharge passed readily there was no discharge whatever when the electrodes were disconnected from the ends of the exciting solenoid. Thus the electrostatic drop across the coil in the latter case must be reduced by the glass, as suggested previously. This explanation involving the mean free path fails to account for the weak electrostatic glow obtained in both iodine and mercury before the ring discharge commences.

The writer wishes to acknowledge his indebtedness to Prof. J. K. Robertson, at whose suggestion this work was undertaken, for his advice and criticism, and to Prof. D. M. Jemmett for the loan of apparatus and for suggestions regarding the work.

Bibliography.

(1) O. Lehrmann, Wied. *Ann.* xlvii. p. 427 (1892).
(2) N. Tesla, 'Electrical Engineer,' July 1891.
(3) E. Lecher, *Phys. Zeits.* v. p. 179 (1904).
(4) Steiner, *Wien. Ber.* cxiii.*a*, p. 403 (1904).
(5) W. Hittorf, Wied. *Ann.* lii. p. 473 (1884).
(6) J. J. Thomson, Phil. Mag. (5) xxxii. p. 321 (1891).
(7) J. J. Thomson, Phil. Mag., Nov. 1927.
(8) Townsend & Donaldson, Phil. Mag., Jan. 1928.

Department of Physics, Queen's University,
Kingston, Canada, July 1929.

LXVII. *On the Study of the Spectrum of Oxygen under Different Conditions of Excitation.*

By D. B. DEODHAR, *M.Sc., Ph.D., Reader in Physics, and* S. K. DUTT, *M.Sc., Lucknow University, Lucknow, India* *.

[Plate XII.]

RECENTLY a good deal of attention has been directed towards the investigation of the line as well as the band spectrum of oxygen. The important investigations on the atomic spectrum are by A. Fowler †, McLennan and others ‡, and Hopfield §. Among the workers on the molecular spectrum are Holland ||, Frerichs ¶, and Ellsworth and Hopfield **. Holland has observed a few groups of bands in the visible. Frerichs has measured the Q branches of five negative bands in the visible, namely, λλ 6856, 6419, 6026, 5632, and 5295. Ellsworth and Hopfield have made measurements of some bands of oxygen in the ultra-violet. Lockrow †† has mainly investigated the critical potentials of oxygen. Recently Johnson ‡‡ has measured the band lines of a group of bands in the ultra-violet.

However, it appears that even now the work of classification and measurement of lines and bands due to oxygen is not complete and that further experimental work is desirable in order to throw more light on the problem. It was with this view that we began the experimental study of the behaviour of the spectrum of oxygen under two different conditions of excitation, and the object of the present communication is to put forth the preliminary account of some interesting observations on a typical type of discharge compared to the usual Geissler tube discharge in oxygen.

* Communicated by the Authors.

† A. Fowler, Proc. Roy. Soc. vol. cx. pp. 476–501 (1926). A. Fowler, and Brooksbank, Roy. Astron. Soc. M. N. vol. lxxvii. pp. 511–517 (1917).

‡ McLennan, McLeod, and McQuarrie. Proc. Roy. Soc. vol. cxiv. pp. 1–22 (1927).

§ J. J. Hopfield, Astrophys. Journ. vol. lix. pp. 114–124 (1924).

|| F. Holland, *Zeits. Wiss. Phot.* vol. xxiii. pp. 342–363 (1925).

¶ R. Frerichs, *Zeits. f. Phys.* vol. xxxv 8–9, pp. 683–688 (1926).

** Ellsworth and Hopfield, Phys. Rev. vol. xxix. pp. 79–84 (1927).

†† L. L. Lockrow, Astrophys. Journ. vol. lxiii. pp. 205–217 (1926).

‡‡ R. C. Johnson, Proc. Roy. Soc. vol. cv. pp. 683–691 (1924).

Experimental Procedure and Observational Data.

The special discharge-tube (fig. 1), was made of transparent quartz made by the Thermal Syndicate Company of England. The anode A was made of thin nickel sheet rolled into the form of a cylinder. The length and diameter of this hollow cylinder were approximately 5 cm. and 2·5 cm. respectively. The bottom of the cylinder was closed with a plane nickel sheet. A small

Fig 1.

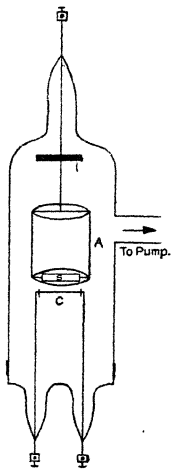

rectangular slit S about 2 mm. wide and 10 mm. long was cut in the central portion of the bottom of the cylinder; and a long vertical slit about 3 mm. in width was cut into the side of the cylinder. This cylindrical anode, to which a small piece of iron I was attached, was mounted on a long brass screw, and the anode could be moved backwards and forwards by means of a suitable electromagnet working from outside the discharge-tube. Such an arrangement was very useful in adjusting the distance between the filament and the anode without disturbing the discharge-tube. The cathode C was made of a thin

platinum strip 10 mm. long and 1·5 mm. wide. The middle portion of this strip was coated with barium oxide, and this oxide-coated filament when heated by an electric current served as a strong source of electrons. The filament was adjusted in such a way that it was parallel to the bottom slit of the nickel anode. The nickel chamber could be charged to a positive potential of any value lying between 2 volts and 150 volts by means of a slide-wire potentiometer arrangement. The stream of electrons shooting from the middle portion of the filament passed through the bottom of the anode into the anode chamber and collided with the gas molecules there. The luminous stream resulting from such a collision of electrons and gas molecules could be viewed through the window cut on the side of the cylindrical anode as mentioned above. As the anode is charged to a certain definite potential, the internal volume being enclosed by an equipotential surface is "field free," and such a kind of discharge may be conveniently called a "field free discharge."

Preparing the Oxycoated Filament.

After a number of trials we found a very effective method of coating the filament; and we should like to make a note of the procedure here, in view of the fact that the oxide usually rather falls off quickly from a coated filament. A small quantity of highly pure barium nitrate should be taken and its saturated solution should be made in distilled water in a test-tube which is first carefully cleaned and rinsed with boiling distilled water. A glass rod with a pointed end should be also well cleaned and rinsed in boiling distilled water just before use and put into the test-tube containing the saturated solution of the nitrate. The platinum filament should be electrically heated to redness before treatment and then the current should be switched off. A drop or two of the solution should then be put on the central portion of the filament with the help of the glass rod and the filament should be held above an extremely low bunsen flame to allow the drop to dry slowly. After the drop is dried up another drop of the liquid should be placed on the previously dried drop and the slow drying repeated. In this way a fair amount should be deposited at the required spot. After this the filament should be again electrically heated

to redness so that the nitrate melts and changes into oxide. The current should be kept on for a few seconds and then it should be gradually reduced to zero. In this way a very hard coating of barium oxide is formed on the filament. The process of putting more drops and drying and electrically heating may be repeated twice or thrice to get a good deposit. The deposit of oxide so obtained sticks very fast and its life is found to be 100 hours of actual use.

The discharge-tube with its anode and filament is shown in fig. 1, while the electrical circuit is shown in fig. 2. The

Fig. 2.

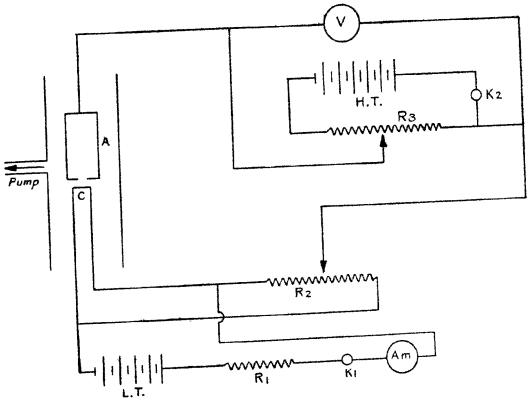

heating-current for the filament was taken from a low-tension battery of accumulators L.T. with an adjustable resistance R_1. The main source of the electrons was the central part of the filament, and in order to measure the voltage between the anode and the centre of the filament the following device was used. A large slide-wire resistance R_2 of 1300 ohms was placed in parallel with the filament, and the negative terminal of the high-tension battery H.T. was connected to the middle point of this resistance. The potential of the middle point of the filament is practically the same as the middle point of the high resistance, and so it could be safely accepted that the

applied voltage was between the anode and the middle point of the filament. The voltage was measured by the voltmeter V as shown in the figure. The filament could be taken out and sealed in at will.

The Vacuum System.

The vacuum system was composed of all glass joints except for the quartz discharge-tube, which was joined to the system by a sealing-wax joint. The rough vacuum was prepared by the Cenco Hyvac pump and the fine vacuum was obtained by Gaede's single stage diffusion pump backed by the Cenco pump. $CaCl_2$ and P_2O_5 were used in order to absorb water vapour, and NaOH was used as an absorbent of carbon as CO_2. The pressure was measured by a MacLeod gauge. With this arrangement a vacuum of the order of 10^{-3} mm. of mercury could be easily obtained. A Geissler tube was also attached to the side of the vacuum system so that its discharge could be viewed in the end-on position. The source of oxygen was a quantity of highly pure potassium permanganate crystals stored in a glass tube which was sealed to a spherical glass reservoir of about 150 c.c. capacity. This reservoir also formed a part of the vacuum system. The oxygen from the reservoir could be supplied to the system or shut off from it by means of a tap. Before entering the discharge-tube the oxygen had to pass over the drying agents and NaOH. Finally, the discharge-tube could be shut off from the system by means of taps.

After the whole of the apparatus was set up as described above, the Hyvac pump was started and when, with all the stopcocks open, the MacLeod gauge registered a pressure of about one-tenth of a millimetre, the diffusion pump was also started, and in about half an hour's time the pressure indicated by the gauge was 10^{-3} mm. The pumps were kept on and the glass tubes were baked as far as possible by means of a bunsen flame playing on them to take off the occluded gases. The permanganate was afterwards heated carefully. The oxygen thus given out was passed through the whole system and was pumped out. Several such washes of oxygen were given, and the observations were attempted when it was found that there was no detectable leakage eighteen hours after the pump was disconnected.

It was found by trials that at a pressure of about 0·2 to 0·3 mm. the spectrum of oxygen seen through the pocket spectroscope was fairly intense and that it contained a large number of lines and bands. The glow of the discharge of the Geissler tube was greenish yellow at this pressure. The Geissler tube was excited by an induction coil worked by a four-volt battery.

The colour and other spectral peculiarities in the low-voltage tube were dependent on the anode voltage and the pressure. The filament was kept at a distance of about one millimetre from the anode. For the same pressure the colour of the glow in the tube was yellowish, green, and pink at 30, 40, and 50 volts respectively. The change in colour is associated with a change in the spectrum, and thus we could obtain varieties of spectra observed for the same gas at different exciting voltages.

Our main object has been to look into the band spectrum of oxygen, and as at 50 volts the spectrum showed a number of band groups we restricted our observations to the discharge at 50 volts. The heating-current in the filament was kept at 4·5 amps. In the beginning of the work the green mercury line used to come up as an impurity, but repeated washes of oxygen made it very faint, and at a pressure of 0·2 to 0·3 mm. it was completely suppressed. It was curious that the hydrogen lines H_α and H_β appeared persistently in the discharge-tube and they could not be suppressed. When the visual observations through the pocket spectroscope showed that the character of the spectrum was the same for the same conditions of excitation and pressure, it was decided to photograph the spectra by means of a Hilger's constant deviation spectrograph. The Geissler tube was arranged in the end-on position, and its glow was focussed upon the slit of the spectrograph by means of a cylindrical lens. The exposure time was three and a half hours. In order to photograph the "field free" discharge the slit of the spectroscope was directed to the stream of light which appeared inside the cylindrical anode and an exposure of three and a half hours was given in this case also. An iron arc comparison spectrum was taken between the two spectrograms. Several plates were taken in this manner, and it was found that each plate showed a remarkable difference between the two spectra. Some lines and bands which were prominent in intensity in the Geissler tube appeared as weak in the "field free"

discharge and vice versa; and some lines which were not present in the one came out quite strong in the other. The accompanying plate (Pl. XII.) shows this behaviour in a striking manner. The low dispersion of the spectroscope could not allow the accurate measurement of the lines on the plate; but there was not much difficulty in identifying the prominent lines and bands with the help of the important iron arc lines on the plate and with the help of the oxygen lines given in the atlas prepared by Eder and Valenta. Certain lines were identified with the help of the list of wave-lengths given in Kayser's 'Handbook of Spectroscopy,' vol. vi. Some of the important observations from the plate are given below. For a quick reference the lines on the plate are numbered. The lines of the low-voltage discharge are given in dashed numbers to distinguish them from the Geissler tube lines.

Observations.

1 & 1′ represent the hydrogen line H_α.

2 & 2′ represent the oxygen line 6460, which is stronger in the low-voltage discharge than in the Geissler tube.

3 denotes a line 6276 which is absent in the low-voltage discharge.

3′ is a band head near λ 6430 which is absent in the Geissler tube.

4 is the oxygen line 6171 and it is fainter than 4′.

5 is a band head λ 6032 and it is much stronger than 5′.

6 is another band head λ 5630 which comes out stronger than 6′.

7 is a band head λ 5290 and it is also stronger than 7′.

8, 9, & 10 are lines 5130, 5020, & 4924, and these are not present in the low-voltage discharge.

11 & 8′ represent H_β.

12 is a band head λ 4830 which is much stronger than what comes out in 9′.

13 & 14 are oxygen lines 4710 & 4706 which are absent in the low-voltage discharge.

15 & 10′ denote the line 4699, where 10′ is very strong compared to 15.

16 & 11′ denote the line 4639, where 11′ is stronger than 16.

12′ & 13′ are lines 4609 and 4596. Both of these are absent in the Geissler tube.

17 & 14′ represent the line 4591, where 17 is stronger than 14′.

18 & 15′ denote the line 4540, 18 being stronger than 15′.

19 is λ4516, which is absent in the low-voltage discharge.

20 represents a strong band head whose value is about λ4500, and corresponding to this there is 16′, which is a faint indication of the same.

21 & 17′ represent the line 4417, and both of them are nearly equal in intensity.

22 is the line 4396 fainter than 18′.

23 & 24 is a pair of lines 4367 and 4352 which is better defined than 19′ and 20′.

25 is the line 4337, which is much weaker than 21′.

22′ & 23′ are lines λλ4320 and 4303, and both of them are absent in the Geissler tube discharge.

24′ is the line 4275, which is much stronger than 26.

27 & 25′ denote a faint band head 4260, 25′ being a little stronger than 27.

26′ is the line 4233, which is stronger than 28.

29′ is the line 4191 much stronger than 27′.

28′ is λ4154, which is absent in the Geissler tube.

29′ is λ4137, which is stronger than 30.

31′ is λ4122, which is absent in the Geissler tube discharge.

Concluding Remarks.

The selective behaviour of the two spectra becomes evident from the above comparison. Among these observations a new band head in the neighbourhood of λ4500 not mentioned by the previous observers has persistently appeared in our plates; as we could not detect any impurity excepting a trace of hydrogen, it appears that this band is due to the oxygen molecule. The band heads in the visible mentioned by other experimenters have also appeared on our plate. This matter is being investigated with the help of the Hilger Interchangeable Quartz Spectrograph of ten feet focus, and it is hoped to deal with that investigation in another communication.

Summary.

The spectrum of oxygen has been studied at a pressure of 0·2 to 0·3 mm. in a Geissler tube and in a special type of quartz discharge-tube. A striking differential behaviour in the nature of the two spectra was observed and a few striking differences are summarised above. In addition to this a new band head is observed in the neighbourhood of λ 4500. The structure of this band is being investigated with the help of the Hilger Interchangeable Quartz Spectroscope of ten feet focus.

Physics Department,
Lucknow University,
Lucknow, India.

LXVIII. *Scattering of Thorium C'' γ-radiation by Radium G and Ordinary Lead.* By W. KUHN, *Ph.D.* (*Heidelberg*) *.

Introduction.

THE question was put forward some time ago whether, corresponding to an emission of monochromatic γ-rays by atomic nuclei, there should also exist a selective absorption of these rays. This would be in close analogy, *e. g.*, with the absorption of the D-lines by non-luminous sodium vapour. If one carries this analogy somewhat further, it is easy, with the aid of thermodynamical considerations †, to obtain an estimate of the order of magnitude of the absorption coefficients which might be found when atomic nuclei are irradiated with γ-rays of the proper frequencies. If N_0 be the number of atoms in unit volume, λ the wave-length of the radiation in question, g_0 and g_1 the statistical weights of the normal and excited states of the nucleus, the maximum value of the absorption coefficient in an undisturbed line would be expected to be

$$\frac{1}{d}\log_e \frac{I_0}{I} = \epsilon = \frac{g_1}{g_0}\frac{N}{2\pi}\lambda^2. \quad . \quad . \quad . \quad . \quad (1)$$

By introducing for N the value 3×10^{22}, which corresponds to the density of solid lead, and taking λ equal to 10 X-units, ϵ will come out about 50. This would be about one

* Communicated by Dr. J. Chadwick, F.R.S.

† W. Kuhn, *Zeits. f. Phys.* xliii. p. 56 (1927).

hundred times as large as the absorption coefficient due to the scattering of γ-rays by the electrons in the optical and X-ray levels of the same substance.

It will be seen, however, that the assumption of an undisturbed line is not satisfied under experimental conditions which can be attained in the laboratory. The observable absorption will then depend on the natural half-width of the line and the magnitude of the disturbing factors. As the half-width depends mainly on the charge and mass of the emitting particle, it is clear that a measurement of nuclear absorption might give us some information about the origin of the γ-rays and the circumstances accompanying their emission.

Instead of measuring the absorption, the scattering of thorium C'' γ-radiation by radium G and by ordinary lead has been compared. According to Aston * ordinary lead contains about 50 per cent. of isotope 208. The latter may be identified with thorium D, the end-product of the radioactive disintegration of thorium. Thorium D is formed from thorium C in two ways: two-thirds of the atoms of thorium C are transferred into thorium C' by a β-transformation and into thorium D by subsequent α-emission, while the remaining third of the thorium C-atoms emit an α-particle first, a transformation which leads to thorium C''. The thorium C'' nuclei finally transform into thorium D by a β-transformation followed by γ-ray emission. This γ-emission is thus the last step in this branch of the radioactive processes. It is therefore possible that some γ-lines of thorium C'', namely, those which are combinations of excited states with the normal state of thorium D, are resonance lines. Assuming that the nuclei of thorium D formed from thorium C in the two ways mentioned are all identical, and identical with the isotope 208 of ordinary lead, we would expect that 50 per cent. of the atoms present in ordinary lead are capable of resonance in such a way that a part of the γ-radiation of thorium C'' would be absorbed by the nuclei of thorium D, and re-emitted afterwards. The secondary radiation from ordinary lead would be increased, both electrons and nuclei taking part in producing the scattering. In the case of the lead isotope radium G, however, no nuclear scattering of thorium C'' radiation should be expected.

* F. W. Aston, 'Nature,' cxx. p. 224 (1927).

Experimental Arrangement.

The arrangement chosen was the following. T_1 and T_2 (see fig. 1) are two ionization chambers, rectangular boxes (about $10 \times 10 \times 25$ cm.), covered on the outside with 2 mm. of lead except for the top, which is a plate of brass 2 mm. thick. To these chambers voltages of equal magnitude (40 v.) and opposite sign were applied, so that the currents balanced one another. An initial difference

Fig. 1.

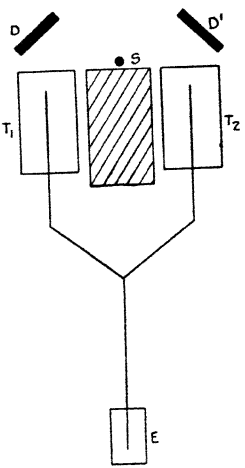

in the natural leak was corrected with the aid of a small subsidiary radioactive source. placed near one of the chambers. Thus the Compton electrometer E did not acquire a charge. A radioactive source S, *e. g.*, a tube containing radiothorium, is then placed near the top between the ionization chambers. The latter are screened from direct radiation by about 5 cm. of lead. In front of each ionization chamber glass dishes D and D' (diameter 8 cm.) could be placed. They had exactly the same size, and could be interchanged. Their position is reproducible with great accuracy, it being determined by a wooden

frame fastened with wax to the ionization chambers T_1 and T_2. One of the dishes contained 126 g. of ordinary lead chloride, the other the same amount of radium G chloride *. The chloride was firmly pressed down into the dish and fixed in position by a plain wooden disk.

The γ-radiation from the radiothorium source falls through the bottom of the dishes on the layer of $RaG\,Cl_2$ or $PbCl_2$. The secondary radiation produced there will fall into the ionization chambers. By shifting the source by means of a screw, a position can be obtained where the currents through the chambers again very nearly cancel. The dishes with the ordinary lead chloride and the radium G chloride are then interchanged. A current different from the previous one will now flow to the electrometer. This difference can be due (1) to a real difference in the scattering power of the isotopes of lead; (2) to a geometrical irregularity in the arrangement of the substance inside the dish; (3) to differences concerning the dishes or the quantity of material used; (4) to the radioactivity of the uranium lead preparation, due to radioactive products separated with it.

The disturbing points (2) to (4) can most easily be eliminated by substituting for the radiothorium source a radium source of equal strength. In fact a nuclear resonance should not be expected at all with a radium source, either in radium G or in ordinary lead, while the factors (2) to (4) should remain unchanged. Therefore, if *a nuclear resonance of thorium D for the γ-radiation of thorium C'' were present, we should find the difference in current observed for the two positions of the scatterers more in favour of the ordinary lead when a radiothorium source is used than when a radium source is used.*

* The author wishes to express his thanks to the Union minière du Haut Katanga, Brussels, from which he has obtained a preparation of $RaG\,CO_3$. The atomic weight of the RaG has been determined by Prof. W. Hieber, Chemical Institute, University of Heidelberg, with the assistance of Messrs. Ries, Martin, and Eichel. The method consisted in recrystallizing the chloride, following the prescriptions of Hönigschmidt, and comparing the density with the density of ordinary lead chloride, purified in a similar way. The density of our $RaG\,Cl_2$ was, at 25°, $5{\cdot}8788 \pm 0{\cdot}0007$, while the density of $PbCl_2$ was $5{\cdot}9034 \pm 0{\cdot}001$. Hence it follows that the atomic weight of our uranium lead was 206·04. Our preparation was thus practically pure isotope, 206·0. The author wishes to express his thanks, too, for the careful carrying out of this determination.

Experimental Result.

No such effect could be found, although about 100 curves (time against electrometer deflexion) were obtained and studied. In more detail the results were the following :—

(*a*) The current produced in one ionization chamber by the adjacent scattering dish (*e. g.*, in chamber T_1 by dish D, fig. 1) gave an electrometer deflexion of 570 mm./min. It was the same whether the radium or the radiothorium source was used.

(*b*) The current produced by the radioactivity of the uranium lead itself corresponded to 10 mm./min., or about 2 per cent. of the current due to the secondary radiation in the experiment.

(*c*) The current produced by the scattered radiation from ordinary lead exceeded the current produced by the scattered radiation from radium G by

$17{\cdot}6 \pm 1{\cdot}5$ mm./min. in the case of a RdTh source, and by
$18{\cdot}3 \pm 1{\cdot}5$ mm./min. ,, ,, Ra ,,

The ordinary lead thus apparently scattered both the thorium C'' γ-radiation and the radium γ-radiation more than did uranium lead. This is probably due to a different distribution of the chlorides inside the dishes (point (2) of the above-mentioned possibilities). The difference between the results with radiothorium and radium sources ($18{\cdot}3 - 17{\cdot}6 = 0{\cdot}7$ mm./min.) is certainly less than the sum of the possible errors (3 mm./min. $= 0{\cdot}5$ per cent. of the total current). It can therefore be considered as proved that *the scattering of the γ-radiation of radiothorium* (*in equilibrium with thorium C''*) *by the thorium D nuclei present in ordinary lead is at least* 200 *times smaller than the electronic scattering in lead.*

Discussion.

We shall now discuss the possible theoretical meaning of this result. As the effect was a negative one, we shall be able only to exclude certain posibilities ; but even this may have some interest.

Assumption.—In order to make the problem more definite, we shall assume that one " resonance line " in

origin and mechanism of the γ-ray emission. If the natural half-width is very narrow, the disturbances will be able to change the absorption effect completely. A small natural width ν' means a long duration τ of the emission process, since these two magnitudes are connected by the relation $\tau = \frac{1}{2\pi\nu'}$, which is a simple geometrical consequence of the wave-theory of light. A long duration of the emission process again means a small energy emission in unit time, and therefore a small electric moment connected with the motion inside the nucleus which gives rise to the γ-emission. In classical theory and in wave mechanics the mean time of duration of an emission process is determined in the same way (formulæ (2) and (3)) if the charge, frequency, and (reduced) mass of the system is given. If we therefore construct any model of a γ-emitting nucleus, and assume that the model may be described by the help of quantum mechanics (some successful attempts have been made recently), we should be able to predict, as far as the order of magnitude is concerned, the width of the γ-lines.

If we seek to devise a model which will provide the fluctuating electric moment to which we attribute the emission of the γ-rays, we must suppose that some constituents of the nucleus are in relative motion to other constituents which have a different specific charge. Three especially simple possibilities present themselves. The electric moment might be due (*a*) to an electron ; (*b*) to a proton ; (*c*) to a helium nucleus moving as an individuum inside the heavy nucleus. For these cases the width of the γ-lines will be estimated and its effect on the observable absorption discussed.

(a) *Case of γ-rays due to an electron.*—In the case where the γ-rays were due to electrons bound inside the heavy nucleus, we should expect a half-width ν', given in order of magnitude by

$$\nu' = \frac{4\pi e^2 \nu^2}{mc^3} f, \quad \ldots \ldots \quad (2)$$

where f is a number somewhat smaller than unity. By introducing for e^2 and m the values characteristic for the electron, we get $\nu' \simeq 10^{18}$ sec.$^{-1}$. The natural width would be about 1000 times larger than the disturbances. The absorption phenomenon would be that of an undisturbed

line. This possibility, and thereby the electronic origin of the γ-rays, must consequently be excluded. The argument is in agreement with conclusions drawn from the polarizability * of nuclei and, according to Ellis, from the homogeneity † of the γ-rays.

(b) *Case of γ-rays due to protons.* The half-width to be expected if the γ-rays are emitted by protons can, in a rough approximation, be calculated from (2). It is not quite correct, because in the emission process we have neglected the contribution to the total electric moment which is due to the motion of the heavily-charged residual nucleus. This contribution (quite negligible for intensity questions in the Bohr hydrogen atom) becomes important because it is of the same order of magnitude as the moment due to the motion of the proton or α-particle which we suppose to be responsible for the γ-radiation. The correction will be particularly important in the case where the α-particle emits the γ-radiation.

If a particle of mass m and charge ze performs a harmonic motion together with another particle of mass M and charge Ze, the energy emission $\frac{dE}{dt}$ corresponding to the component of motion along the x-axis will depend on the acceleration of the electric moment $\mathfrak{m}$, namely,

$$\frac{dE}{dt} = \frac{2}{3}\frac{\ddot{\mathfrak{m}}^2}{c^3} = \frac{2}{3}\frac{e^2}{c^3}\left(z\ddot{x}_m + Z\ddot{x}_M\right)^2 = \frac{2}{3}\frac{e^2}{c^3}z^2\ddot{x}_m^2\left(1-\frac{Z}{z}\frac{m}{M}\right)^2.$$

From this we see that the true emission is smaller by the factor $\left(1-\frac{Z}{z}\frac{m}{M}\right)^2$ than the emission present if the motion of the residual nucleus were neglected. For that reason the half-width of the line will be reduced by the same factor, and consequently will be

$$\nu' = \frac{4\pi e^2\nu^2 z^2}{mc^3}\left(1-\frac{Z}{z}\frac{m}{M}\right)^2 \cdot f. \quad . \quad . \quad . \quad . \quad (3)$$

If we take m equal to the mass of the hydrogen atom, $z=1$, we find $\nu' = 2\times10^{14}\times f$. As f is rather smaller than unity, we may say $\nu' = 10^{14}$ sec.$^{-1}$.

The influences of the three disturbances on the absorption

* W. Kuhn, *Zeits. f. Phys.* xliv. p. 32 (1927).

† *Cf.* W. Kuhn, *Naturwissenschaften*, xvii. p. 431 (1929).

have now to be discussed. The temperature agitation broadens the line about three times and reduces the maximum absorption coefficient from 250 to 80. The β-recoil broadens the emission line further from 3×10^{14} to 3×10^{15} sec.$^{-1}$. We have mentioned that only a part of the emission line will now be absorbed. We shall therefore make an estimate of the value to which the absorption coefficient really falls at the edge of our emission line. As far as the temperature agitation is concerned, the absorption of the edge of the emission line will be negligible ; it would be of the order $\varepsilon_{\max.}=e^{-\frac{3.10^{15}}{3.10^{14}}}$. But it is well known that the decrease in intensity of an absorption or an emission line due to the " natural frequency-intensity distribution " of the line is, at large distances from the centre, much slower than the decrease due to the temperature agitation. We have now to find the absorption coefficient of a line at a distance $\nu_0-\nu=1{\cdot}5\times10^{15}$ from the middle of the line, the maximum absorption coefficient of the undisturbed line being 250 and the natural half-width $\nu'=10^{14}$. The value is to be obtained from the relation

$$\varepsilon=\varepsilon_{\max.}\cdot\frac{\nu'^2}{4(\nu_0-\nu)^2+\nu'^2}=250\,\frac{1}{4\,.\,1{\cdot}5^2+1}\doteq0{\cdot}28\,. \quad (4)$$

We see that even the edge of the emission line will be absorbed considerably.

The γ-shift will be smaller than the β-recoil broadening, namely, $\delta\nu_\gamma=2{\cdot}2\times10^{14}$. The greater part of the emission line will therefore be absorbed, and we should expect with our resonance line and our nine non-resonance lines a resultant nuclear effect about 50 per cent. as strong as the electronic scattering.

This result would even be true if we neglect the β-recoil broadening. According to Jacobsen*, it seems quite possible that a considerable time (about 10^{-5} sec.) elapses between the emission of the β-particle and the γ-radiation. In this case the γ-emitting atom would have lost the β-recoil velocity. The γ-recoil alone would now provide us with an emission line (temperature plus natural width) shifted relative to the absorption line by $2{\cdot}2\times10^{14}$ sec.$^{-1}$. Disregarding the temperature agitation, we find the absorption coefficient at the centre of the shifted line $\varepsilon\doteq250\,\frac{1}{4\,.\,2^2}\doteq16$.

* J. C. Jacobsen, 'Nature,' cxx. p. 870 (1927).

The γ-shift brings the emission line away from the maximum absorption, but still leaves it in a region where it will be completely absorbed. *Thus in all cases which can be considered under the assumption that a proton emits the γ-radiation, we expect a nuclear effect which is much stronger than is allowed by the experiments.*

(c) *Case of γ-rays due to helium nuclei.*—In order to find the half-width of the emission line when a helium nucleus is supposed to emit the γ-rays, we have in formula (3) to put $z=2$ and to take $m=4$, the mass of the helium atom. The half-width then becomes $\nu' \mathrel{\hat{=}} 2 \times 10^{13} \times f$. Taking again for f a value about 0·5, we have $\nu' = 10^{13}$sec.$^{-1}$. This value is ten times smaller than the value obtained for a proton as emitter of the radiation.

The reduction is due to the fact that the specific charge for the α-particle is nearly equal to that of the residual nucleus. If the two were exactly equal, the half-width would be infinitely small, the duration of the emission process infinitely long, because there would then, to a first approximation, be no change in the electric moment of the system, and therefore no radiation emission.

Quite in analogy to the previous treatment, we find that the temperature agitation brings the maximum absorption coefficient down to 8, while the β-recoil broadens the emission line. The edge of the emission line will no longer be absorbed; only the centre of the line (about 30 per cent.) remains absorbable. In fact, for the edge of the line we find the absorption coefficient $\varepsilon \mathrel{\hat{=}} 250 \dfrac{1}{4.150^2} \mathrel{\hat{=}} 0{\cdot}003$. As the γ-shift is smaller than the β-broadening, we expect in this case an apparent nuclear scattering only 30 per cent. of the electronic scattering.

If we, on the other hand, assume that the γ-emission follows the β-emission after more than 10^{-11} sec., the β-recoil broadening will be missing, and the emission line will fall to a place of the absorption curve where the absorption coefficient would be $\varepsilon \mathrel{\hat{=}} 0{\cdot}16 = \dfrac{250}{4 \times 20^2}$. The energy absorbed and scattered by a layer of 3 mm. will be $1 - e^{-0{\cdot}3 \times 0{\cdot}16} \mathrel{\hat{=}} 0{\cdot}05$, or about 5 per cent. of the electronic scattering of the lines. This amount reduces to 1 per cent. if we assume that the resonance line has a wave-length of

only 10 X.U., and would reduce to 0·25 per cent. if we had taken for f the value 0·25 instead of 0·5.

Summary.

We might expect a nuclear resonance of thorium D nuclei for some γ-lines of thorium C″. In order to test its existence, the scattering of thorium C″ γ-radiation by the lead isotope radium G and by ordinary lead has been compared.

It was found that the nuclear effect produced in ordinary lead by the γ-radiation of radiothorium in equilibrium with thorium C″ is at least 200 times smaller than the electronic scattering.

In explaining this negative result we should get into serious difficulties if we assumed that the γ-rays were emitted by electrons or by protons. The difficulties are smaller, and the expected effect falls within the limit of our experimental error, if we assume that :

1. The γ-rays are emitted by helium nuclei.

2. A time-interval of about 10^{-10} sec. or more elapses between the emission of the β-rays and the emission of the γ-rays. Some evidence of such a time-interval has previously been given by Jacobsen.

3. The resonance line must, in the case of thorium D, have a rather short wave-length (ca. 10 X.U. or less).

4. The movements of the α-particle cause the residual nucleus to move in such a way that the centre of gravity is at rest.

It is hardly necessary to emphasize that these conclusions have been drawn on the basis of a negative experimental statement. It is, of course, also possible that entirely new points of view are valid in the case of the nucleus ; but it may be interesting to see that the present state of the experiments does not yet make a fundamental change in our aspects necessary.

The experiment has been carried out in the Cavendish Laboratory, Cambridge. I wish to thank Prof. Sir E. Rutherford and Dr. J. Chadwick for the opportunity they gave me, and to Mr. G. T. P. Tarrant for experimental help during the investigation.

Chemical Institute,
University of Heidelberg.

LXIX. *Classical and Modern Electromagnetic Theories.* By A. Press *.

Summary.

A number of outstanding formulæ characterize the Restricted Relativity Theory of Prof. Albert Einstein. Notably a set of formulæ made use of by him is that of the Lorentz Transformation, according to which

$$T = \beta\left(t - \frac{vx}{c^2}\right); \quad X = \beta(x - vt).$$

It is shown that if account is taken of the two Fresnelian types of ætheric media, the one condensed after the manner of Stokes near atomic nuclei and forming the atomic diameters, the other being the normal æther between atoms, then the following Classical Formulæ obtain, viz. :—

$$T_1 = t - \frac{vx}{c^2}; \quad X_1 = \frac{1}{\beta}x - vt.$$

Again there is the formula according to which the non-Newtonian composition of velocities for electromagnetic (*i. e.*, light) waves is given by

$$w = \frac{u+v}{1+\frac{uv}{c^2}}.$$

This also is shown to follow from the nature of the atomic atmospheres already outlined and discussed in the author's previous paper, published in the Phil. Mag., Oct. 1925, p. 809. The reconciliation then appears to be practically complete.

Later it is shown that for moving material dielectrics, using the above ideas of condensed and normal æthers, Heaviside's Wave-speed Mathematics, given in his 'Electromagnetic Theory,' iii. p. 45, can be clearly pictured. Thus the electromagnetic equations for moving dielectrics become

$$\frac{d\mathbf{D}}{dt} = \mathrm{curl}\,\{\mathbf{h} - \kappa V \mathbf{D} v\},$$

$$\frac{d\mathbf{h}}{dt} = -\frac{c^2}{\mu k}\cdot\mathrm{curl}\left\{\mathbf{D} - \frac{\kappa(k\mu)}{c^2}V\mathbf{h}\right\}.$$

* Communicated by the Author.

As against the latter, using the Heaviside methods of analysis, these are equivalently expressed by the equations

$$\text{curl}\,(\mathbf{h}-\mathrm{V}\mathbf{Dq}) = \dot{\mathbf{D}} = \text{curl}\,(\mathbf{h}-\kappa\mathrm{V}\mathbf{Du})$$
$$-\text{curl}\,(\mathbf{E}-\mathrm{V}\mathbf{wB}) = \dot{\mathbf{B}} = -\text{curl}\,(\mathbf{E}-\mathrm{V}\mathbf{wB}).$$

These equations lead at once to the Fresnelian drag coefficient and to the non-Newtonian composition of velocities required by the Einstein relativistic ideas.

Turning next to an independent derivation of the fundamental equations of Lorentz, it is shown that the Trouton-Noble experiment falls into line because of the important limitation due to the divergence operator employed. Incidentally it also follows that the Wilson effect and the Röntgen current accord with the above equations.

In the last section is discussed the Michelson-Morley experiments. The formulæ derived indicate that for air, at least, the effect should be null.

Effective Optical Times and Distances in Classical and Relativity Theories.

ON the theory of æther-condensation atmospheres produced by the presence of atomic nuclei in the æther, two time-periods T_0 and T_v are indicated. An electromagnetic disturbance travelling through a material dielectric of length

$$x = \mathrm{AB}, \quad . \quad . \quad . \quad . \quad . \quad . \quad . \quad (1)$$

Fig. 1.

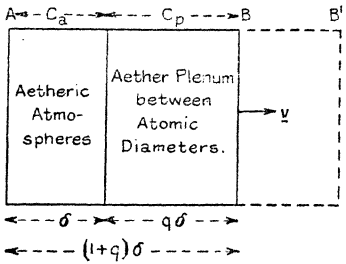

with regard to A as the origin, requires a time T_0 if the body is at rest relative to the normal uncondensed æther. It, however, requires a different time T_v if the material of

length $x = AB$ is moving forward with velocity $\mathbf{v}$ in the same direction as the propagated electromagnetic wave. This is because, in travelling forward, the end-point B in the meantime reaches a point B′ in the normal æther. The time T_0 is given by the expression

$$T_0 = \frac{\delta}{c_a} + q\frac{\delta}{c_p} = \frac{\delta}{c_a c_p}\{c_p + qc_a\}, \quad . \quad . \quad . \quad (2)$$

where we have that

c_a = velocity of light through the ætheric condensation atmospheres,

c_p = velocity through the normal interatomic æther plenum.

On the other hand, for the T_v time the expression obtained is

$$T_v = \frac{\delta}{c_a} + \frac{q\delta + vT_v}{c_p + v} = \frac{\delta}{c_a c_p}\{c_p + qc_a + v\}, \quad . \quad (3)$$

The ratio of the two time-periods is therefore given by

$$\left.\begin{aligned} T_v/T_0 &= 1 + \frac{v}{c_p + qc_a} \\ \text{and} \qquad T_v &= T_0 + \frac{v}{c_p + qc_a}\cdot T_0. \end{aligned}\right\} \quad . \quad . \quad . \quad . \quad (4)$$

Yet from the figure we have that

$$x = AB = (1+q)\delta. \quad . \quad . \quad . \quad . \quad (5)$$

The definitions of the two times can also be taken as follows:—

$T_0 = t$ = optical time with body at rest;

$T_v = T'$ = effective optical time with body in motion arising from differential motions due to the Fresnelian æthers.

Thus we can write

$$\left.\begin{aligned} t = T_0 &= \frac{x}{1+q}\cdot\frac{c_p + c_a q}{c_a c_p}, \\ T' &= t + \frac{vx}{(1+q)c_a c_p}. \end{aligned}\right\} \quad . \quad . \quad . \quad . \quad (6)$$

For the bodily velocity $\mathbf{v}$, therefore, taken negatively or opposite to the propagational direction of the electromagnetic disturbance, we have

$$T' = t - \frac{vx}{(1+q)c_a c_p}, \quad . \quad . \quad . \quad . \quad . \quad (7)$$

which, of course, bears a distinct resemblance to the Lorentz Transformation T in Relativity Theory.

Calling c' the average velocity of propagation through the distance $(1+q)\delta$, with the body at rest relative to the æther, we can write

$$(1+q)\frac{\delta}{c'}=\frac{\delta}{c_a}+q\frac{\delta}{c_p},$$

$$1+q=\frac{c'}{c_a}+q\frac{c'}{c_p}. \quad . \quad . \quad . \quad . \quad . \quad . \quad (8)$$

Introducing n_a as the refractive index of the atomic diameters, we have practically that

$$n_a=\frac{c}{c_a}\equiv\frac{c_p}{c_a}. \quad . \quad . \quad . \quad . \quad . \quad . \quad . \quad (9)$$

It will be noticed that a possible distinction can be made between the c_p of the interatomic æther and the c of free space. Again, if n is the mean refractive index of the material medium as a whole (when the body is at rest relative to the æther) it will follow that

$$n=\frac{c}{c'}\equiv\frac{c_p}{c'}. \quad . \quad . \quad . \quad . \quad . \quad . \quad . \quad (10)$$

The equation therefore becomes

$$1+q=\frac{n_a}{n}+q\frac{1}{n}\ ; \qquad n_a-n=(n-1)q\ ;$$

$$1+q=\frac{n_a-1}{n-1}. \quad . \quad . \quad . \quad . \quad . \quad . \quad (11)$$

The denominator of T′ is transformable, as a consequence of the above, into the form

$$(1+q)c_a c_p\equiv\frac{n_a-1}{n-1}\cdot\frac{1}{n_a}\cdot c^2. \quad . \quad . \quad . \quad . \quad (12)$$

This means, with the understanding "at rest," we can assume for the respective refractive indices that

$$\left.\begin{aligned}\frac{n_a-1}{n-1}\cdot\frac{1}{n_a}&\equiv 1,\\ n_a\equiv n&\equiv 1.\end{aligned}\right\} \quad . \quad . \quad . \quad . \quad . \quad (13)$$

We have, as a result, that

$$\mathrm{T}'=t-\frac{vx}{c^2}. \quad . \quad . \quad . \quad . \quad . \quad . \quad . \quad (14)$$

The Lorentz Transformation and the Relativity Theory require that we write

$$T = \beta\left(t - \frac{vx}{c^2}\right). \quad . \quad . \quad . \quad . \quad . \quad . \quad . \quad (15)$$

Thus the difference between T′ on the Classical Theory and the T of Relativity Theory is a factor β, where

$$\beta^2 = \frac{1}{1 - \frac{v^2}{c^2}}. \quad . \quad . \quad . \quad . \quad . \quad . \quad . \quad (16)$$

The latter involves terms of the second order only.

Treating now optical distances in the same manner, we have from the figure that the effective optical distance X is given by

$$X' = (1+q)\delta + BB' = x + BB'. \quad . \quad . \quad . \quad (17)$$

The same reasoning as before has to be advanced. A light disturbance generated at A in the moving body not only has to pass through the sum total of ætheric atmospheres indicated by the length δ with respect to the actual (at rest) length AB, but, by virtue of the body moving forward with velocity v, traverses a normal æther distance $q\delta + BB'$, because the real end of the body B reaches the point B′ in the meantime.

The addition BB′ due to the motion of the body through the normal æther medium is given by

$$BB' = vT_v. \quad . \quad . \quad . \quad . \quad . \quad . \quad . \quad (18)$$

Thus it follows that

$$X' = x + vT_v = x + v\left(t - \frac{vx}{c^2}\right). \quad . \quad . \quad . \quad (19)$$

That is to say, on rearrangement of terms, we have

$$X' = \left(1 - \frac{v^2}{c^2}\right)x + vt. \quad . \quad . \quad . \quad . \quad . \quad (20)$$

Taking, therefore, v negatively, as before, we have as a consequence

$$X' = \frac{1}{\beta}x - vt. \quad . \quad . \quad . \quad . \quad . \quad . \quad (21)$$

The Relativity Theory gives, however,

$$X = \beta(x - vt). \quad . \quad . \quad . \quad . \quad . \quad (22)$$

The difference between the optically effective value of X in the two systems is therefore of the second order.

Part II.

The Differential Equations of Electromagnetic Theory.

Let the electrical displacement of Maxwell be represented by

$$\mathbf{d} = D + \mathbf{D}, \quad . \quad . \quad . \quad . \quad . \quad . \quad (23)$$

where $\mathbf{D}$ represents a circuital displacement for all space due to electrization as defined by Heaviside, and D represents a polar displacement due to electrification as defined by Heaviside. If, then, we operate with div and curl, it follows that

$$\operatorname{div} \mathbf{d} = \operatorname{div} D = \rho, \quad . \quad . \quad . \quad . \quad . \quad (24)$$

$$\operatorname{curl} \mathbf{d} = \operatorname{curl} \mathbf{D}. \quad . \quad . \quad . \quad . \quad . \quad . \quad (25)$$

Differentiating with respect to time, we have from (24)

$$\frac{d\rho}{dt} = \operatorname{div} \frac{dD}{dt}. \quad . \quad . \quad . \quad . \quad . \quad (26)$$

Consider, on the other hand, the divergence of a vector $\rho\mathbf{u}'$, where $\mathbf{u}'$ is the translational velocity of a charge density ρ across free space. We have

$$\operatorname{div} \rho\mathbf{u}' = \nabla\rho\mathbf{u}' = \left(\mathbf{i}\frac{\partial}{\partial x} + \mathbf{j}\frac{\partial}{\partial y} + \mathbf{k}\frac{\partial}{\partial z}\right)(\rho u_x \mathbf{i} + \rho u_y \mathbf{j} + \rho u_z \mathbf{k})$$

$$= \frac{\partial}{\partial x}(\rho u_x) + \frac{\partial}{\partial y}(\rho u_y) + \frac{\partial}{\partial z}(\rho u_z). \quad . \quad . \quad . \quad . \quad . \quad (27)$$

Ordinarily, however, we shall also have (for the general case, mathematically)

$$\frac{d\rho}{dt} = \frac{\partial\rho}{\partial t} + \frac{\partial\rho}{\partial x}\cdot\frac{dx}{dt} + \frac{\partial\rho}{\partial y}\cdot\frac{dy}{dt} + \frac{\partial\rho}{\partial z}\cdot\frac{dz}{dt}. \quad . \quad (28)$$

If, then, there is no change in the ionization occurring, we shall have

$$\frac{\partial\rho}{\partial t} = 0. \quad . \quad . \quad . \quad . \quad . \quad . \quad . \quad (29)$$

Thus, with the electrification constant,

$$\frac{d\rho}{dt} = \frac{\partial\rho}{\partial x}\cdot\frac{dx}{dt} + \frac{\partial\rho}{\partial y}\cdot\frac{dy}{dt} + \frac{\partial\rho}{\partial z}\cdot\frac{dz}{dt}. \quad . \quad . \quad . \quad (30)$$

Given that the coordinates (x, y, z) pertaining to the location of a charge density ρ change with respect to time

relative to a fixed frame of reference (x', y', z'), we shall have

$$\left.\begin{aligned} u_x' &= \frac{dx}{dt}, \\ u_y' &= \frac{dy}{dt}, \\ u_z' &= \frac{dz}{dt}. \end{aligned}\right\} \quad . \quad . \quad . \quad . \quad . \quad (31)$$

Thus, by means of (31) it follows that

$$\frac{d\rho}{dt} = u_x' \cdot \frac{\partial \rho}{\partial x} + u_y' \cdot \frac{\partial \rho}{\partial y} + u_z' \cdot \frac{\partial \rho}{\partial z} \cdot \quad . \quad . \quad . \quad (32)$$

Equation (32) has now to be correlated with (27). Yet in order that (27) and (32) should be equivalent, we must specify

$$\left.\begin{aligned} u_x' &= f_x(y, z, t) \text{ and independent of } x, \\ u_y' &= f_y(x, z, t) \quad ,, \quad\quad ,, \quad\quad ,, \ y, \\ u_z' &= f_z(x, y, t) \quad ,, \quad\quad ,, \quad\quad ,, \ z. \end{aligned}\right\} \quad . \quad . \quad (33)$$

These are very serious limitations. Only when (33) are satisfied can we write (32) in the form

$$\frac{d\rho}{dt} = \frac{\partial}{\partial x}(\rho u_x') + \frac{\partial}{\partial y}(\rho u_y') + \frac{\partial}{\partial z}(\rho u_z'). \quad . \quad . \quad (27')$$

Thus, if we are considering a given distribution of ρ in space, then the velocity component u_x' of the charges plus and minus for the whole field must be independent of x, etc. Surely this is equivalent to regarding the movement of the whole aggregation of charges + and − as partaking of a rigid body movement. Thus the distance between neighbouring charges becomes invariable. The equation

$$\frac{d\rho}{dt} = \operatorname{div} \rho \mathbf{u}' \quad . \quad . \quad . \quad . \quad . \quad . \quad (27'')$$

constitutes one of the "derived equations" of Lorentz (see Cunningham, 'Relativity,' p. 23). The limitations (33), however, are ignored, and would not permit of a Lorentzian type of "polarization," which is polar, and never circuital, in its displacement flux distribution. *It also explains the Trouton-Noble negative result.*

Equation (27''), with changed sign of $\mathbf{u}'$, is equivalent to

$$\operatorname{div}\left\{\frac{d\mathbf{d}}{dt} + \rho \mathbf{u}'\right\} = 0, \quad . \quad . \quad . \quad . \quad (28')$$

so that for the general case we can assume a circuital vector $\mathbf{h}$ such that

$$\operatorname{div}\operatorname{curl}\mathbf{h} = 0, \quad . \quad . \quad . \quad . \quad . \quad (34)$$

and, combined with (28′), we have

$$\frac{d}{dt}\mathbf{d} + \rho\mathbf{u}' = \operatorname{curl}\mathbf{h}. \quad . \quad . \quad . \quad . \quad . \quad (35)$$

The latter constitutes one of the "fundamental equations" of Lorentz. Here, however, it is made a derived equation (Cunningham, *l. c.* p. 23).

Lemma.

Postulating now that in an electromagnetic field the velocity with which a lateral disturbance can be propagated forwardly is represented by c, we have for the magnetic effect $\mathbf{h}$ in an x-direction

$$\mathbf{h} = \mathbf{h}_0 . \mathrm{F}(x - ct) = \mathbf{h}_0 \mathrm{F}(\xi). \quad . \quad . \quad . \quad (36)$$

It would then follow, by differentiating,

$$\left.\begin{aligned} \frac{\partial \mathbf{h}}{\partial t} &= \mathbf{h}_0 . \frac{d\mathrm{F}}{d\xi} . \frac{\partial \xi}{\partial t} = \mathbf{h}_0 \frac{d\mathrm{F}}{d\xi}(-c), \\ \frac{\partial \mathbf{h}}{\partial x} &= \mathbf{h}_0 \frac{d\mathrm{F}}{d\xi} . \frac{\partial \xi}{\partial x} = \mathbf{h}_0 \frac{d\mathrm{F}}{d\xi}, \\ \frac{\partial \mathbf{h}}{\partial t} &= -c \frac{\partial \mathbf{h}}{\partial x}, \\ \frac{\partial^2}{\partial t^2} &= c^2 \frac{\partial^2}{\partial x^2}. \end{aligned}\right\} \quad . \quad . \quad . \quad . \quad . \quad (37)$$

Operating now on (35), with curl, we have

$$\operatorname{curl}\frac{d}{dt}\mathbf{d} + \operatorname{curl} . \rho\mathbf{u}' = \operatorname{curl}^2\mathbf{h}. \quad . \quad . \quad . \quad (38)$$

Yet from (27″) $\rho\mathbf{u}'$ cannot have curl, since it already has divergence, and then note must be taken of (33). Thus, by (23), (38) reduces to

$$\operatorname{curl}\frac{d\mathbf{D}}{dt} = \operatorname{curl}^2\mathbf{h}. \quad . \quad . \quad . \quad . \quad . \quad (39)$$

Vectorially, however, if $\mathbf{h}$ is wholly a circuital vector, then the operator curl^2 reduces to $-\nabla^2$. That is, in this instance,

$$\operatorname{curl}^2 = -\nabla^2 = -\left(\mathbf{N}\frac{d}{d\mathrm{N}}\right)^2 = -\frac{d^2}{d\mathrm{N}^2} = -\frac{\partial^2}{\partial x^2}.$$

The equation (39) therefore becomes

$$\operatorname{curl}\frac{d\mathbf{D}}{dt} = -\frac{\partial^2}{\partial x^2}\mathbf{h}. \quad . \quad . \quad . \quad . \quad . \quad (40)$$

For a progressive wave possibility in $\mathbf{h}$, therefore, according to (36) and (37), we have

$$\left.\begin{aligned} \nabla^2\mathbf{h} &= \frac{1}{c^2}\frac{d^2\mathbf{h}}{dt^2}, \\ \operatorname{curl}\frac{d\mathbf{D}}{dt} &= -\frac{1}{c^2}\frac{d^2\mathbf{h}}{dt^2}, \\ \operatorname{curl}\mathbf{D} &= -\frac{1}{c^2}\frac{d\mathbf{h}}{dt}. \end{aligned}\right\} \quad . \quad . \quad . \quad . \quad . \quad (41)$$

The two equations fundamental to electrodynamics, namely,

$$\left.\begin{aligned} \frac{d\mathbf{d}}{dt} + \rho\mathbf{u}' &= \operatorname{curl}\mathbf{h}, \\ -\frac{1}{c^2}\frac{d\mathbf{h}}{dt} &= \operatorname{curl}\mathbf{d}, \end{aligned}\right\} \quad . \quad . \quad . \quad . \quad . \quad (42)$$

have been derived without requiring the introduction of the ideas of the electrical intensity $\mathbf{E}$ and magnetic density $\mathbf{B}$.

Laws of Moving Dielectrics with Fresnel Correction.

Consider, in the first instance, a material dielectric system S of refractive index n at rest relative to the ætherial medium. A progressive wave of displacement is set up, and the equations to be satisfied are still the following:

$$\left.\begin{aligned} \frac{d\mathbf{D}}{dt} &= \operatorname{curl}\mathbf{h}, \\ \operatorname{curl}\mathbf{D} &= -\frac{1}{c^2}\frac{d\mathbf{h}}{dt}. \end{aligned}\right\} \quad . \quad . \quad . \quad . \quad . \quad (43)$$

The term $\rho\mathbf{u}'$ is ignored, since progressive waves are in question.

Suddenly let a relative motion $\mathbf{v}$ be produced of the material dielectric relative to the æther. Then will equations (43) need to be modified if ætheric reactions are assumed to take place by virtue of the relative motion between the æther and the material dielectric. Maxwell had already introduced a motional electric force $\mathbf{e}$ given by

$$\mathbf{e} = \mathrm{V}\mathbf{v}\mathbf{B}. \quad . \quad . \quad . \quad . \quad . \quad . \quad (44)$$

Yet the circumstances are not quite the same; whereas Maxwell imagined the **e** is set up by a conductor cutting across a magnetic field **B** fixed in the æther, in the present case the **B** (as well as the **D**) were already travelling as progressive waves in the material dielectric when the latter was at rest with respect to the æther. It is the additional effect that is sought as the æther moves with respect to the dielectric, in which latter the progressive waves of **D** and **h** (or **B**) already happen to find themselves.

Thus, with Fresnel (see Silberstein, 'Theory of Relativity,' p. 37), let the refractive index, or optical "density," of a material dielectric be explainable on the basis of a denser ætherial medium within the matter. In the writer's paper (*l. c.*) it was brought out that the atoms were to be conceived as atomic nuclei producing by their presence, in a gravitational or Stokesian sense, a condensed ætheric system of atmospheres about the nuclei wherever they may happen to be, whether at rest or in motion.

In reality, if δ_0 is the normal density of the free æther outside, then, with Fresnel, it is the excess density

$$\delta - \delta_0$$

that moves, or appears to move, with velocity **v**, since it is this amount that is continually being produced by the presence of the atomic nuclei. The actual "quantity of movement" is therefore

$$(\delta - \delta_0)\mathbf{v}.$$

However, in terms of the over-all density δ we shall need to introduce a coefficient κ, since the waves will partly travel through the denser ætheric medium, and only in between times through the otherwise æther medium itself, filling the spaces between atoms. Thus, as explained in the paper above mentioned, if the nuclei carry their condensing power with them as they travel through space, then the only transport through the æther is that due to the travelling nuclei and not the atomic atmospheres which they produce as they move along. This suggests, of course, Dr. C. V. Burton's strain-figure theory already discussed by Heaviside in his 'Electromagnetic Theory,' i. Thus we need to write for the statistical or average effect

$$\left.\begin{aligned}(\delta - \delta_0)v &= \kappa\delta v,\\ \kappa &= 1 - \frac{\delta_0}{\delta}.\end{aligned}\right\} \quad . \quad . \quad . \quad . \quad . \quad (45)$$

But Fresnel assumed that the elasticities of the free and condensed æthers are the same. Thus we have that

$$n = \frac{\sqrt{\epsilon_0/\delta_0}}{\sqrt{\epsilon/\delta}},$$

$$\kappa = 1 - \frac{1}{n^2}. \quad . \quad . \quad . \quad . \quad . \quad . \quad . \quad (46)$$

From this point of view it is the condensed æther only that can be said to travel with respect to the free æther.

Provisionally, therefore, we can write, with κ as the slippage coefficient,

$$\mathbf{e} = \frac{\mathbf{D}e}{k_e} = \kappa \mathrm{V}\mathbf{v}\mathbf{B} = \left(1 - \frac{1}{n^2}\right)\mathrm{V}\mathbf{v}\mathbf{B}. \quad . \quad . \quad . \quad (47)$$

Similarly, for the electrical effect of moving media we may write

$$\mathbf{h}_1 = \kappa \mathrm{V}\mathbf{D}\mathbf{v}. \quad . \quad . \quad . \quad . \quad . \quad . \quad . \quad (48)$$

The latter formula, by the way, agrees exactly with the requirements of the experimentally-determined Röntgen current, as given by Eichenwald (see Silberstein, *l. c.* p. 275). Given then that $\mathbf{u}$ is the velocity of propagation in the material medium when at rest relative to the æther, we have

$$u^2 = \frac{c^2}{\mu k}, \quad . \quad . \quad . \quad . \quad . \quad . \quad . \quad (49)$$

and the equations become

$$\left.\begin{aligned} \frac{d\mathbf{D}}{dt} &= \mathrm{curl}\{\mathbf{h} - \kappa \mathrm{V}\mathbf{D}\mathbf{v}\}, \\ \frac{d\mathbf{h}}{dt} &= -\frac{c^2}{\mu k}\mathrm{curl}\left\{\mathbf{D} - \frac{\kappa(k\mu)}{c^2}\mathrm{V}\mathbf{v}\mathbf{h}\right\}. \end{aligned}\right\} \quad . \quad . \quad (50)$$

The above, when checked, will be found to give the Fresnel dragging coefficient κ, where

$$\frac{w-u}{v} = \kappa = 1 - \frac{1}{n^2},$$

and w is the resultant velocity of the $\mathbf{D}$ or $\mathbf{h}$ wave in the material dielectric of the form

$$\mathbf{D} = \mathbf{D}' \sin(x - wt).$$

This will be gone into a little later. One thing is very clear, that where

$$n \equiv 1,$$

as in air, in which medium the Michelson-Morley-Miller experiments were conducted, practically no evidence of a difference in the moving-medium wave-velocity **w** as against the stationary-medium wave-velocity **u** should be found.

Alternative Fresnel Correction Derivation.

The two motional equations given by Heaviside in his 'Electromagnetic Theory,' i. p. 43, are as follows:

$$\mathbf{e} = \mathbf{Vq}\mathbf{B}; \quad \mathbf{h} = \mathbf{VDq}, \quad . \quad . \quad . \quad . \quad (51)$$

with **q** as the velocity. (*The Heaviside notation will be used exclusively in this section.*)

In treating of the æther drag Heaviside (*l. c.* iii. p. 45) considers the case where two parallel and distinct electrical displacements are assumed, set up as a consequence of a single impressed force. Thus for the more general case, which can include the so-called "polarization" of Lorentz (in reality the latter's "polarization" is but a separation of charges), let

$\mathbf{D}_0$ = Maxwellian ætheric displacement,

$\mathbf{D}_1$ = second (including that of Lorentz), but always associated with the presence of matter.

Then can we write

$$\mathbf{D} = \mathbf{D}_0 + \mathbf{D}_1 = c\mathbf{E}. \quad . \quad . \quad . \quad . \quad . \quad (52)$$

(Note c is here the dielectric constant, and not the former velocity of light. The **E** is the impressed electrical force.)

It is then assumed that we have

$$\mathbf{D}_0 = c_0\mathbf{E}; \quad \mathbf{D}_1 = c_1\mathbf{E};$$
$$\mathbf{D} = \mathbf{D}_0 + \mathbf{D}_1 = (c_0 + c_1)\mathbf{E} = c\mathbf{E}. \quad . \quad . \quad . \quad (53)$$

Similarly we have for the magnetic case

$$\mathbf{B} = \mathbf{B}_0 + \mathbf{B}_1 = \mu\mathbf{H} = \mu_0\mathbf{H} + \mu_1\mathbf{H}. \quad . \quad . \quad . \quad (54)$$

Thus does it follow that

$\mathbf{B}_0$ = magnetic density set up in free space.

$\mathbf{B}_1$ = magnetic density set up as a consequence of the presence of matter (ferromagnetic effect).

Now in order to give tangibility to Heaviside's otherwise very obscure reasoning regarding his velocities **q** and **w**, the Ætheric Atmosphere Theory of Atoms (*l. c.*) lends a

helping hand. Thus the propagational velocity in the matter as a whole will be influenced by the velocity through the atomic diameters as against the different velocity through the free æther between atoms. Thus, assuming

$$\left.\begin{aligned} \mathbf{u} &= \text{bodily velocity of the matter concerned, then} \\ \mathbf{u}+\mathbf{v}_a &= \text{resultant propagational velocity through the atomic atmospheres, where} \\ \mathbf{v}_a &= \text{the propagational velocity with the matter at rest relative to the æther.} \end{aligned}\right\} \quad (55)$$

In the free æther of the intervening spaces we have

$$\mathbf{v} = \text{velocity of propagation in the æther itself.}$$

A wave travelling through the matter, therefore, would thus have a velocity intermediate between $\mathbf{v}$ and $\mathbf{u}+\mathbf{v}_a$.

With the above visualization, let

$$\left.\begin{aligned} \mathbf{q}_0 &= \text{effective velocity linked with the dielectric displacement } \mathbf{D}_0, \text{ and giving} \\ V\mathbf{D}_0\mathbf{q}_0 = \mathbf{h}_0 &= \text{motional magnetic intensity set up. The } \mathbf{q}_0 \text{ would then correspond to a space averaging for the inter- and intra-atomic spaces.} \\ \mathbf{q}_1 &= \text{effective velocity linked with the displacement } \mathbf{D}_1, \text{ and giving} \\ V\mathbf{D}_1\mathbf{q}_1 = \mathbf{h}_1 &= \text{motional magnetic intensity set up. The } \mathbf{q}_1 \text{ here corresponds to the space averaging necessary due to the localization of the } \mathbf{D}_1 \text{ displacement itself.} \end{aligned}\right\} \quad (56)$$

Thus both the $\mathbf{q}_0$ and $\mathbf{q}_1$ are really functions of the translational velocity $\mathbf{u}$ with which the matter moves relative to the æther. Similar equations will therefore follow for the magnetic motionals.

If, then, $\mathbf{H}$ and $\mathbf{E}$ are the respective forces set up by a wave when the body is at rest, then correspondingly the forces when the body moves with velocity $\mathbf{u}$ will be

$$\left.\begin{aligned} \mathbf{H}-(\mathbf{h}_0+\mathbf{h}_1), \\ \mathbf{E}-(\mathbf{e}_0+\mathbf{e}_1). \end{aligned}\right\} \quad \ldots\ldots \quad (57)$$

The equations for a moving dielectric should then be

$$\left.\begin{aligned}\operatorname{curl}\{\mathbf{H}-(\nabla\mathbf{D}_0\mathbf{q}_0+\nabla\mathbf{D}_1\mathbf{q}_1)\}&=\dot{\mathbf{D}},\\ -\operatorname{curl}\{\mathbf{E}-(\nabla\mathbf{w}_0\mathbf{B}_0+\nabla\mathbf{w}_1\mathbf{B}_1)\}&=\dot{\mathbf{B}}.\end{aligned}\right\} \quad . \quad . \quad (58)$$

It is the latter equations that will be shown not only to give the Fresnel drag coefficient, but actually to lead to the equations (50).

The Fresnel Wave-speed and Final Form of Electromagnetic Equations.

To investigate for a plane wave travelling in the moving body with a velocity U relative to the stationary æther, the

Fig. 2.

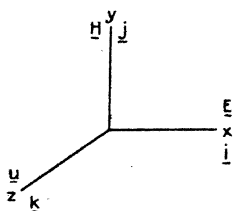

form of the function would depend on the expression

$$\left.\begin{aligned}&f(z+\mathrm{U}t),\\ \text{giving}\qquad&\frac{\partial}{\partial z}=\frac{1}{\mathrm{U}}\frac{\partial}{\partial t}.\end{aligned}\right\} \quad . \quad . \quad . \quad . \quad . \quad (59)$$

Thus we can set **E** in the direction of the unit vector **i** (axis of x), with **H** along **j**, and the wave itself travelling parallel to **u** or the axis of **k**.

The curl equations become, with

$$\nabla\nabla=\operatorname{curl}=\frac{\partial}{\partial z}.\mathbf{k},.$$

$$\frac{\partial}{\partial z}\{\mathrm{H}+q_0\mathrm{D}_0+q_1\mathrm{D}_1\}=\mathrm{U}\frac{\partial \mathrm{D}}{\partial z},$$

$$\frac{\partial}{\partial z}\{\mathrm{E}+w_0\mathrm{B}_0+w_1\mathrm{B}_1\}=\mathrm{U}\frac{\partial \mathrm{B}}{\partial z}.$$

That is, we have the equations of condition,

$$\left.\begin{aligned} \mathrm{H}+q_0\mathrm{D}_0+q_1\mathrm{D}_1 &= \mathrm{UD}, \\ \mathrm{E}+w_0\mathrm{B}_0+w_1\mathrm{B}_1 &= \mathrm{UB}. \end{aligned}\right\} \quad . \quad . \quad . \quad . \quad (60)$$

However, it is easy to see that the latter can be greatly simplified, for we note that

$$q_0\mathrm{D}_0+q_1\mathrm{D}_1 = (q_0c_0+q_1c_1)\mathrm{E}.$$

Since we can also write, for convenience, that

$$q_0c_0+q_1c_1 = qc,$$

and already by (53) we have

$$c = c_0+c_1,$$

the definition of q is therefore

$$q = \frac{q_0c_0+q_1c_1}{c} = \frac{c_0}{c}q_0+\frac{c_1}{c}q_1. \quad . \quad . \quad . \quad (61)$$

The velocities q, q_0, q_1 are then so related that we can write

$$\mathbf{q}\mathbf{D} = (c_0\mathbf{q}_0+c_1\mathbf{q}_1)\frac{\mathbf{D}}{c} = (c_0\mathbf{q}_0+c_1\mathbf{q}_1)\mathbf{E}. \quad . \quad . \quad (62)$$

Thus but one effective velocity $\mathbf{q}$ need be considered in conjunction with but a single displacement $\mathbf{D}$ instead of the two before employed.

Similarly therefore we have

$$\mathbf{w}\mathbf{B} = (\mu_0\mathbf{w}_0+\mu_1\mathbf{w}_1)\frac{\mathbf{B}}{\mu} = (\mu_0\mathbf{w}_0+\mu_1\mathbf{w}_1)\mathbf{H}. \quad . \quad (63)$$

The corresponding equations in w are therefore

$$w = \frac{w_0\mu_0+w_1\mu_1}{\mu}; \qquad \mu = \mu_0+\mu_1. \quad . \quad . \quad (64)$$

The curl equations become considerably simplified, for we have equivalently that

$$\left.\begin{aligned} \mathrm{curl}(\mathbf{H}+\mathrm{V}\mathbf{D}\mathbf{q}) &= \dot{\mathbf{D}} = \mathrm{curl}(\mathbf{H}-\mathbf{h}), \\ \mathrm{curl}(\mathbf{E}-\mathrm{V}\mathbf{w}\mathbf{B}) &= -\dot{\mathbf{B}} = \mathrm{curl}(\mathbf{E}-\mathbf{e}). \end{aligned}\right\} \quad . \quad . \quad (65)$$

These, however, are not in the final form required.

Turning to the relation of wave-speed U in terms of $\mathbf{q}$ and $\mathbf{w}$ we have from (60) that

$$\mathbf{H}+q\mathbf{D} = \mathrm{U}\mathbf{D}; \qquad \mathbf{H} = (\mathrm{U}-q)\mathbf{D};$$
$$\mathbf{E}+w\mathbf{B} = \mathrm{U}\mathbf{B}; \qquad \mathbf{E} = (\mathrm{U}-w)\mathbf{B}.$$

Eliminating $\mathbf{E}$, it follows that

$$\mathbf{H} = (\mathrm{U}-q)c\mathbf{E} = (\mathrm{U}-\mathfrak{q})c(\mathrm{U}-w)\mu\mathbf{H} = \mu c(\mathrm{U}-q)(\mathrm{U}-w)\mathbf{H}.$$

It follows in consequence that

$$1 = \mu c(\mathrm{U}-q)(\mathrm{U}-w). \quad . \quad . \quad . \quad . \quad (66)$$

Since, now, the velocity of propagation $\mathfrak{v}$ with the medium at rest relative to the æther is given by

$$\frac{1}{\mu c} = v^2. \quad . \quad . \quad . \quad . \quad . \quad . \quad (67)$$

we have, solving for U in (66), that

$$\mathrm{U}^2-(w+q)\mathrm{U} = v^2-wq,$$

$$\mathrm{U} = \tfrac{1}{2}(w+q) + \sqrt{v^2+\tfrac{1}{4}(w-q)^2}$$

$$\equiv v+\tfrac{1}{2}(w+q). \quad . \quad . \quad . \quad . \quad . \quad . \quad (68)$$

If, then, w and q are both zero (medium at rest), then U_0 equals v. *Thus* U *is the velocity of propagation for a moving dielectric as against the rest value* U_0.

The change of wave-speed from what it would be with a material dielectric stationary is therefore

$$\mathrm{U}-v \equiv \tfrac{1}{2}(w+q). \quad . \quad . \quad . \quad . \quad (69)$$

Noting, however, that both w and q are functions of the translatory velocity $\mathfrak{u}$, we can write

$$\left.\begin{aligned} \mathfrak{w} &= \kappa_w.\mathfrak{u}, \\ \mathfrak{q} &= \kappa_q.\mathfrak{u}. \end{aligned}\right\} \quad . \quad . \quad . \quad . \quad . \quad . \quad (70)$$

We then have that

$$\frac{\mathrm{U}-v}{u} = \kappa = \tfrac{1}{2}(\kappa_w+\kappa_q), \quad . \quad . \quad . \quad . \quad (71)$$

where κ is Fresnel's dragging coefficient. If, then, we set

$$\left.\begin{aligned} w = q\ ; \quad \kappa_w = \kappa_q = \kappa\ ; \\ \frac{\mathrm{U}-v}{u} = \kappa = 1-\frac{1}{n^2}; \end{aligned}\right\} \quad . \quad . \quad . \quad . \quad (72)$$

where n is the refractive index. Making, therefore, use of (70) and (72), it follows that (65) becomes

$$\left.\begin{aligned} \dot{\mathbf{D}} &= \mathrm{curl}\{\mathbf{H}-\kappa\mathrm{V}\mathbf{D}\mathfrak{u}\}, \\ \dot{\mathbf{B}} &= -\mathrm{curl}\{\mathbf{E}-\kappa\mathrm{V}\mathfrak{w}\mathbf{B}\}, \end{aligned}\right\} \quad . \quad . \quad . \quad . \quad (50')$$

which are really equations (50)!

Classical Non-Newtonian Composition of Velocities for Moving Dielectric Media.

The two equations previously developed for moving media were as follows :

$$\left.\begin{aligned}\frac{d\mathbf{D}}{dt} &= \operatorname{curl}\{\mathbf{h}-\kappa\mathrm{V}\mathbf{D}\mathbf{v}\},\\ \frac{d\mathbf{h}}{dt} &= -\frac{c^2}{\mu k}\operatorname{curl}\{\mathbf{D}-\frac{\kappa k\mu}{c^2}\mathrm{V}\mathbf{v}\mathbf{h}\},\end{aligned}\right\} \quad . \quad . \quad . \quad (50)$$

in which the slippage coefficient κ is given by

$$\kappa = 1-\frac{1}{n^2} = \frac{w-u}{v} \quad . \quad . \quad . \quad . \quad . \quad . \quad (73)$$

In the latter formula we have

n = refractive index,

w = wave-propagational velocity in moving dielectric,

$\mathbf{u}$ = wave-propagation velocity in the same dielectric at rest with respect to the æther, and

$\mathbf{v}$ = translational velocity of the dielectric.

In the Michelson-Morley experiment, where for air we have

$$n \equiv 1,$$

it was shown that

$$\kappa \equiv 0,$$

and therefore, quite irrespective of the direction of $\mathbf{v}$ with respect to the direction of light propagation, we have

$$\kappa = 0 \; ; \quad \mathbf{w} = \mathbf{u}. \quad . \quad . \quad . \quad . \quad . \quad (74)$$

In other words, the velocity of light $\mathbf{w}$ in the material medium, moving with velocity $\mathbf{v}$ with respect to the æther, has the same velocity of propagation $\mathbf{u}$ as it would have were the material medium at rest. This is the Einstein condition, at least for air, whereas for media in which

$$n > 1$$

the resultant velocity $\mathbf{w}$ in the moving medium depends on $\mathbf{v}$, according to the formula

$$\mathbf{w} = \mathbf{u}+\kappa\mathbf{v}. \quad . \quad . \quad . \quad . \quad . \quad . \quad (75)$$

It will be noted that only when we take in (75),

$$\kappa = 1,$$

making the slippage coefficient exactly unity, does the Newtonian compounding of velocities take place. Equations (50) above for moving dielectrics do not, therefore, follow the simple rule of Newtonian Mechanics.

To compare the Einstein addition formula of velocity vectors, namely,

$$\mathbf{w} = \frac{\mathbf{u}+\mathbf{v}}{1+\frac{\mathbf{uv}}{c^2}}, \quad . \quad . \quad . \quad . \quad . \quad . \quad (76)$$

we have substantially that

$$\mathbf{w} \equiv (\mathbf{u}+\mathbf{v})\left(1-\frac{\mathbf{uv}}{c^2}\right)$$

$$\equiv \mathbf{u}+\mathbf{v}-\frac{u^2\mathbf{v}}{c^2}-\frac{\mathbf{u}v^2}{c^2}$$

$$\equiv \mathbf{u}\left(1-\frac{v^2}{c^2}\right)+\mathbf{v}\left(1+\frac{u^2}{v^2}\right). \quad . \quad . \quad . \quad (77)$$

Since $\mathbf{v}$ is the translational velocity of the dielectric, $\left(1-\frac{v^2}{c^2}\right)$ is substantially equal to unity. Writing, however, κ for $1-(u/c)^2$ in (77), we have, then, that

$$\mathbf{w} = \mathbf{u}+\kappa\mathbf{v}, \quad . \quad . \quad . \quad . \quad . \quad . \quad . \quad (75)$$

showing that under these circumstances there is accord between the Einstein relativity formula (76) and that of Classical Mechanics leading to (75).

Thus, writing according to (75) and (77) that

$$\kappa = 1-\frac{u^2}{c^2}, \quad . \quad . \quad . \quad . \quad . \quad . \quad . \quad (78)$$

we need to have, according to the Fresnel formula

$$\kappa = 1-\frac{1}{n^2}, \quad . \quad . \quad . \quad . \quad . \quad . \quad . \quad (79)$$

that

$$1-\frac{u^2}{c^2} = \kappa = 1-\frac{1}{n^2}. \quad . \quad . \quad . \quad . \quad (80)$$

This requires that the refractive index n be given by

$$n = c/u. \quad . \quad . \quad . \quad . \quad . \quad . \quad . \quad (81)$$

Part III.

The Michelson-Morley Experiment in an Optically Dense Medium.

Light from a source S reaches a mirror a, b, and is partly reflected to B and partly transmitted to A. At the points

Fig. 3.

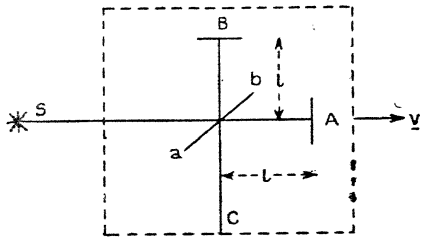

A and B the light is reflected back, meeting the eye at C According to equation (72) we have

$\mathbf{v}$ = translational velocity of the medium,

$\mathbf{u}$ = velocity of light in the material medium when at rest relative to the æther,

$\mathbf{w}$ = resultant velocity of light in the material medium when in motion,

with the equation for the drag coefficient given by

$$\left.\begin{aligned} \mathbf{w} &= \kappa\mathbf{v} + \mathbf{u}\,; \qquad \kappa = \frac{w-u}{v}\,; \\ \kappa &= 1 - \frac{1}{n^2}\,; \end{aligned}\right\} \quad . \quad . \quad . \quad (72)$$

In the latter n is the refractive index of the medium.

The light, in going from O to A, will have an actual velocity

$$w_{OA} = \kappa\mathbf{v} + \mathbf{u},$$

and for the return journey it will be

$$\mathbf{w}_{AO} = -\kappa\mathbf{v} + \mathbf{u}.$$

Thus, for the total time t_{0A0}, going from O to A and return, we have

$$t_{0A0} = \frac{l}{u+\kappa v} + \frac{l}{u-\kappa v} = 2l \cdot \frac{u}{u^2-\kappa^2 v^2} \cdot \quad . \quad . \quad (82)$$

To obtain the number m of wave-lengths λ laid down, the formula gives

$$\lambda = w\mathrm{T},$$

where we have w as the actual velocity and

T = time taken to lay down one wave-length λ.

Thus it follows by (82) that

$$m = \frac{t_{0A0}}{\mathrm{T}} = \frac{t_{0A0}}{\lambda} w = 2l \frac{w}{u} \cdot \frac{1}{1-\kappa^2 v^2/u^2}$$

$$\equiv 2l \cdot \frac{w}{u}\left(1+\frac{\kappa^2 v^2}{u^2}\right). \quad . \quad . \quad . \quad . \quad . \quad . \quad . \quad (83)$$

Similarly, for the light reflected at O and travelling toward B, the velocity formula becomes

$$\mathbf{w}' = \mathbf{u}' + \kappa \mathbf{v}, \quad . \quad . \quad . \quad . \quad . \quad . \quad . \quad (84)$$

where $\mathbf{u}'$ is now pendicular to $\mathbf{v}$, but whose tensor is still u. The reflected ray in consequence suffers a slightly oblique reflexion toward B′ instead of toward B, making the resultant path traversed slightly longer. This means that instead of l we have

$$\mathrm{OB}' = \mathrm{OB} \cdot \frac{w}{u} = l \sqrt{1+\kappa^2 v^2/u^2}$$

$$\equiv l\left(1+\tfrac{1}{2}\frac{\kappa^2 v^2}{u^2}\right). \quad . \quad . \quad . \quad . \quad . \quad . \quad . \quad (85)$$

Fig. 4.

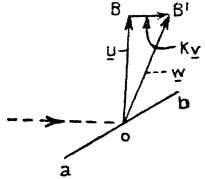

On the reverse path the same elongation is produced, so that in effect the path traversed is

$$2\mathrm{OB}' \equiv 2l\left(1+\tfrac{1}{2}\frac{\kappa^2 v^2}{u^2}\right).$$

However, the wave-length λ is similarly elongated, so that, so far as the number of wave-lengths set up is concerned,

Fig. 5.

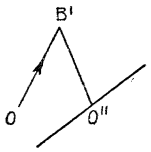

the result is the same as if the light ray had only traversed the path

$$2OB = 2l.$$

Thus the number of wave-lengths really becomes

$$m' = \frac{2l}{\lambda}. \quad . \quad . \quad . \quad . \quad . \quad . \quad . \quad (86)$$

The difference Δ of the number of wave-lengths laid down by the light traversing the two types of paths is therefore

$$\Delta = (m-m') = \frac{2l}{\lambda}\left[\frac{w}{u}\left(1+\frac{\kappa^2v^2}{u^2}\right)-1\right]$$
$$= \frac{2l}{\lambda}\left[\left(\frac{w}{u}-1\right)+\left(\frac{w}{u}-1\right)\frac{\kappa^2v^2}{u^2}+\frac{\kappa^2v^2}{u^2}\right]. \quad (87)$$

We note, however, that

$$\frac{w}{u}-1 = \frac{w-u}{u} = \frac{w-u}{v}.\frac{v}{u} = \kappa\frac{v}{u}, \quad . \quad . \quad (88)$$

whence (87) transforms to

$$\Delta = \frac{2l}{\lambda}\left[\frac{\kappa v}{u}+\frac{\kappa^3v^3}{u^3}+\frac{\kappa^2v^2}{u^2}\right]$$
$$= \frac{2l}{\lambda}\left[1+\frac{\kappa v}{u}+\frac{\kappa^2v^2}{u^2}\right]\kappa.\frac{v}{u}. \quad . \quad . \quad . \quad (89)$$

To a first approximation, therefore, with

$$\frac{v}{u} << 1,$$

$$\Delta \equiv \frac{2l}{\lambda}.\frac{v}{u}.\kappa \equiv \frac{2l}{\lambda}.\frac{v}{u}\left(1-\frac{1}{n^2}\right). \quad . \quad . \quad . \quad (90)$$

The formula usually employed for the Michelson-Morley experiment gives

$$\Delta_x = \frac{2l}{\lambda}\left(\frac{v}{c}\right)^2.$$

The above, (90), gives practically zero for air! The true effect with water or carbon disulphide should therefore be quite large, even for a span of $l=11$ cm. Turning the apparatus through 90° the value of Δ for the same l should be doubled, giving

$$\Delta_{90^\circ} = \frac{4l}{\lambda}\,\frac{v}{c}\left(\frac{c}{u}\cdot\kappa\right) = \frac{4l}{\lambda}\cdot\frac{v}{c}\cdot n\kappa. \quad . \quad . \quad . \quad (91)$$

The residual effect of Miller would thus seem to be accounted for.

August 1928.

LXX. *The Crystal Structure of Wurtzite.* *By* M. Luther Fuller *.

Abstract.

A method of preparing wurtzite quite free from cubic zinc sulphide by heating cubic zinc sulphide with 10 per cent. of sodium chloride at 1100° C. is described.

The observed intensities on powder patterns are in good agreement with those calculated for space group $6e-4$ with $V=\frac{5}{8}$.

The unit-cell dimensions of wurtzite are found to be:

$a_0=3{\cdot}811\pm{\cdot}004$ A, $c_0=6{\cdot}234\pm{\cdot}006$ A, and $c/a=1{\cdot}636$.

W. L. Bragg [1], from a basal plane reflexion of a crystal of wurtzite, predicted the zinc oxide grouping to be the correct arrangement for wurtzite, the hexagonal form of zinc sulphide.

Aminoff [2] and Ulrich and Zachariasen [3], from powder patterns of wurtzite, confirmed the prediction of W. L. Bragg. The relative intensities of the diffraction maxima on the powder patterns obtained by these workers are not in

* Communicated by Prof. W. L. Bragg, F.R.S.

good agreement with those calculated from the assumed structure. This lack of agreement is considered by Aminoff, Ulrich and Zachariasen to be due to an admixture of crystals of sphalerite, the cubic form of zinc sulphide.

The tendency for wurtzite to revert partially to sphalerite, at room temperature, is well known. This change is easily brought about if the crystals are subjected to a mechanical strain such as grinding or crushing. It is difficult, however, to detect sphalerite in the presence of wurtzite, since all the strong diffraction lines of sphalerite are coincident with wurtzite lines. It seems reasonable to explain the discrepancies noted above, between the observed and calculated intensities of the lines, by assuming that the wurtzite reported in the literature [2, 3] contained considerable sphalerite. Taking advantage of the published data on the properties of wurtzite, noted above, a small quantity of wurtzite was made and put into form suitable for crystal structure analysis in such a way as to produce the minimum sphalerite content. The diffraction patterns of this specimen gave good agreement between the observed and calculated intensities. It is the purpose of this paper to give the results in detail together with a precision measurement of the wurtzite lattice constants.

Experimental.

The specimen of wurtzite was prepared as follows: pure precipitated cubic zinc sulphide with ten per cent. of sodium chloride mixed with it, was heated at a temperature of 1100° C. for one hour. After the heating the sample was cooled to room temperature in about ten minutes. An atmosphere of hydrogen was maintained around the sample during the heating and the cooling. Without putting any mechanical strain on the crystals the sample was screened on a 325 mesh screen and the fine portion used for the X-ray specimen. When zinc sulphide is heated without sodium chloride, the product is not as free from cubic zinc sulphide as when sodium chloride is used. There is no evidence of sodium chloride crystals in the final product heated at 1100° C.

The General Electric X-ray diffraction apparatus described by Davey [4] was used to obtain the patterns. Molybdenum K alpha radiation is used in this apparatus. Three films were made. In two of these exposures the

small glass specimen tube had the wurtzite in the one end of the tube and the calibrating substance, sodium chloride, in the other end [5]. In each case the wurtzite and the sodium chloride were diluted with flour to reduce their opacity to about the same amount [6]. In the third of these exposures the sodium chloride and wurtzite were mixed throughout the specimen tube [7].

The wurtzite crystals were too large to furnish sufficient orientations of the crystals to give continuous lines on the film. It was, therefore, necessary to slowly rotate the specimen tube during the exposure by means of a small clock the shaft of which was connected to an end of the specimen tube by a small rubber tube.

Calculation of the Results.

The interplanar spacings measured on the three films were corrected by means of a calibration made in terms of the sodium chloride spacings. The corrected spacings were in good agreement with each other and an average was taken from which the final calculations of the unit cell dimensions were made.

Thirteen interplanar spacings from 1·904 A to 0·912 A were used in the calculations. These spacings correspond to planes of Miller indices, 11·0, 10·3, 10·0(2), 11·2, 20·1, 10·1(2), 20·3, 21·0, 21·1, 10·0(3), 21·3, 11·0(2) and 11·6, Nine of these are the average of measurements on the three films and four are from two films, omitting the third because of the masking effect of the superimposed sodium chloride lines. The axial ratio was found graphically [8] to be between 1·634 and 1·640. A set of values of a_0 was calculated from the observed interplanar spacings and a given axial ratio for each value in this range. The results were plotted on probability paper [9], one curve for each value of the axial ratio. The curve plotted for axial ratio 0·636 is the closest to a true probability curve and gives $a_0=3{\cdot}811$ A from which $c_0=6{\cdot}234$ A. This method of calculating axial ratio is more completely described by the author in a previous paper [10].

The nature of the lines on the pattern was such that their position could be read with an accuracy of 0·1 per cent. over the range given above. The method of finding the axial ratio is more sensitive than 0·1 per cent. Hence the values of the unit cell dimensions are: $a_0=3{\cdot}811 \pm {\cdot}004$ A and $c_0=6{\cdot}234 \pm {\cdot}006$ A. The density calculated

from these data is 4·10 ±·01. The density [11] of the naturally occurring mineral wurtzite is given as 3·98. The density [12] of artificially prepared wurtzite is reported to be 4·087.

Table I. shows the average observed spacings of the three films and the observed intensities for two of the films. The observed intensities are estimated by eye and range from 10, very black, to 0+, extremely faint. The calculated intensities were calculated on the basis of the zinc oxide type of structure, space group $6e-4$ ($C^4 6V$) with $V=\frac{5}{8}$, according to the formula given by Wyckoff [13].

The empirical formulas used by various investigators for calculating the intensities of lines to be expected for a given crystal structure differ primarily in the value assigned to an exponent [14]. Values for this exponent may be found in the literature varying from 2·00 to 3·00. It is better, instead of comparing actual values of observed and calculated intensities, to number the lines on the diffraction pattern in the order of their intensity, designating the most intense line as 1, the next most intense as 2, etc.[15]. In this way the final result is relatively independent of the value chosen for the exponent in the formula. The difference between the numbers expressing the calculated and observed orders of intensity is then a measure of the agreement between theory and experiment. Of several attempted solutions, the one giving the smallest total error is the one to be taken as most probably correct.

Table II. gives, for comparison, the observed intensities of Aminoff and of Ulrich and Zachariasen. The order of the observed intensities is also given, as well as can be deduced from the published observed intensities. The total error in these two cases is much greater than that found in the evaluation of the patterns made by the present author.

The wurtzite lines corresponding to the planes 00·1(2), 11·0, 11·2, 00·1(4), 11·4, 10·0(3), 11·5, 00·1(6), 11·0(2), and 11·6 are coincident with lines on the pattern of sphalerite.

This investigation completely confirms the prediction of W. L. Bragg as to the structure of wurtzite, and indicates that the specimen used was quite free from cubic zinc sulphide.

It is a pleasure to thank Dr. W. P. Davey of Pennsylvania State College and Messrs. C. C. Nitchie and

Table I.

Planar Indices.	Average observed spacings.	Obs. Intensities, Film No. 1177.			Obs. Intensities, Film No. 1189.			Calc. Intensities.	
		Int.	Order.	Error.	Int.	Order.	Error.	Int.	Order.
10·0	3·29A	2	3	0	2	3	0	2·12	3
00·1(2)	3·11	0·6	7	1	1	5	3	1·29	8
10·1	2·91	1·9	4	0	1·9	4	0	1·77	4
10·2	2·27	0·5	9	1	0·5	10	0	0·91	10
11·0	1·904	2·5	2	0	2·3	2	0	2·31	2
10·3	1·759	2·5	1	0	2·5	1	0	2·48	1
10·0(2)	1·651	0+	19	2	0+	20	3	0·41	17
11·2	1·628	0·8	5	0	0·9	6	1	1·75	5
20·1	1·593	0·2	12	3	0·1	16	1	0·43	15
10·1(2)	1·458	0·1	17	2	0·1	18	1	0·32	19
20·3	1·292	0·5	8	1	0·6	8	1	1·20	9
21·0	1·249	0·1	14	3	0·1	13	2	0·90	11
21·1	1·224	0·1	16	2	0·1	15	1	0·46	14
10·5 21·2	1·166	0·3	10	3	0·5	9	2	1·03 0·40	7
10·0(3)	1·099	0·2	11	2	0·2	11	2	0·64	13
21·3	1·068	0·6	6	0	0·7	7	1	1·54	6
11·5 00·1(6)	1·038	0·1	18	2	0·1	19	1	0·00 0·10	20
20·5 10·6	0·995	0·1	15	3	0·1	14	2	0·75 0·09	12
11·0(2)	0·955	0+	20	2	0·1	17	1	0·40	18
11·6	0·912	0·2	13	3	0·2	12	4	0·42	16
			Total error ...	30		Total error ...	26		

TABLE II.

Comparison of Observed Intensities.

Planar Indices.	Film No. 1177*.			Film No. 1189*,			Aminoff.			Ulrich and Zachariasen.			Calc. Intensities.	
	Int.	Order.	Error.	Int.	Order.	Error.	Int.	Order.	Error.	Int.	Order.	Error.	Int.	Order.
10·0	2·0	3	0	2·0	3	0	2	6	3	2	10	7	2·12	3
00·1(2)	0·6	7	1	1·0	5	3	3	4	4	4	3	5	1·29	8
10·1	1·9	4	0	1·9	4	0	1	8	4	2	11	7	1·77	4
11·0	2·5	2	0	2·3	2	0	4	1	1	5	1	1	2·31	2
10·3	2·5	1	0	2·5	1	0	1	7	6	3	7	6	2·48	1
11·2	0·8	5	0	0·9	6	1	4	2	3	4·5	2	3	1·75	5
20·3	0·5	8	1	0·6	8	1	½—1	13	4	2	12	3	1·20	9
21·0	0·1	11	1	0·1	11	1	1	11	1	2·5	9	1	0·90	10
10·5 } 21·2 }	0·3	9	2	0·5	9	2	1	10	3	3	8	1	1·03 } 0·40 }	7
10·0(3)	0·2	10	2	0·2	10	2	3	5	7	4	4	8	0·64	12
21·3	0·6	6	0	0·7	7	1	1	9	3	3·5	6	0	1·54	
11·5 } 00·1(6) } ...	0·1	13	0	0·1	13	0	4	3	10	4	5	8	0·00 } 0·10 }	13
20·5 } 10·6 }	0·1	12	1	0·1	12	1	1	12	1	2	13	2	0·75 } 0·09 }	11
	Total error ...		8	Total error ...		12	Total error ...		50	Total error ...		52		

* These data differ from those of Table I. in that only those lines are included which are given in the published data of Aminoff and Ulrich and Zachariasen. This makes possible a direct comparison of the data.

H. M. Cyr of this laboratory for their helpful advice during the course of this investigation.

Bibliography.

(1) Bragg, W. L., Phil. Mag. xxxix. p. 647 (1920).
(2) Aminoff, *Zeit. f. Kristall.* lviii. p. 203 (1923).
(3) Ulrich and Zachariasen, *Zeit. f. Kristall.* lxii. p. 260 (1925).
(4) Davey, Gen. Elec. Rev. xxv. p. 565 (1922).
(5) Davey, Phys. Rev. xix. p. 538 (1922).
(6) Davey, Gen. Elec. Rev. xxviii. p. 586 (1925).
(7) Havighurst, Mack, and Blake, J. Am. Soc. xlvi. p. 2368 (1924).
(8) Hull and Davey, Phys. Rev. xvii. p. 549 (1921).
(9) Whipple, Jour. Frank. Inst. clxxxii. p. 37 (1916).
(10) Fuller, M. L., 'Science,' lxx. p. 196 (1929).
(11) Dana, 'A System of Mineralogy,' p. 70.
(12) Allen and Crenshaw, Am. J. Sci. xxxiv. p. 341 (1912).
(13) Wyckoff, 'The Structure of Crystals,' p. 201.
(14) Wyckoff, 'The Structure of Crystals,' p. 102.
(15) Bradley, A. J., Phil. Mag. xlvii. p. 657 (1924).

LXXI. *Electron Scattering and High Frequency Radiation.*

By J. A. C. Teegan, *M.Sc., Lecturer in Physics, University College, Rangoon* *.

1. M. De Broglie has introduced a new system of mechanics according to which a moving particle behaves as a group of waves of velocity and frequency governed by the mass and speed of the particle. If m_0 is the mass, and v the velocity, the frequency is given by

$$\nu = \frac{m_0 c v}{h\sqrt{1-\frac{v^2}{c^2}}}. \quad . \quad . \quad . \quad . \quad . \quad (1)$$

The waves are considered as possessing no energy, being simply geometrical phase waves, so that the fact of their velocity $V\left(=\frac{c^2}{v}\right)$, being greater than the velocity of light is not impossible.

Considering such waves associated with an electron, their frequency will depend on the velocity v, and for a value of the velocity equal to $\frac{c}{10}$ will be about the same as that of moderately hard gamma-rays.

* Communicated by Prof. W. L. Bragg, F.R.S.

2. G. P. Thomson (Proc. Roy. Soc. A, clxii. p. 600 (1928)) has examined the diffraction of homogeneous beams of cathode rays in passing through thin metal films. These metal films consist of a number of minute crystals arranged at random, and the photographic diffraction patterns obtained in all cases are identical with those obtained in the Hull-Debye-Scherrer apparatus, employed for the diffraction of X-rays. Calculation from the diffraction patterns is in excellent agreement with the "De Broglie" conception of electron waves.

3. If the wave hypothesis of the electron be extended to the absorption of high speed electrons in matter, some interesting conclusions regarding the nature of the so-called "cosmic-rays" may be derived. The view that these penetrating radiations consist of short "gamma-rays" has been prevalent because their large penetrating power is associated with radiation of the gamma-ray type. Millikan, from an analysis of his "depth-ionization" curve, singled out three homogenous groups of penetrating cosmic radiation, with absorption coefficients in matter equal to ·35, ·08, and ·04 metre^{-1}. Assuming the radiation of the γ-ray type, the wave-lengths of these radiations were calculated from the absorption formula of Dirac * :—

$$S=\frac{2\pi Ne^4}{m^2c^4}\frac{1+\alpha}{\alpha^2}\left\{\frac{2(1+\alpha)}{1+2\alpha}-\frac{1}{\alpha}\log(1+2\alpha)\right\}$$

$$\text{where } \alpha=\frac{h\nu}{mc^2}. \quad . \quad . \quad . \quad . \quad . \quad . \quad . \quad . \quad . \quad (2)$$

The wave-lengths came out to be ($\cdot 35\times10^{-11}$ cm, $\cdot 117\times10^{-11}$ cm., and $\cdot 059\times10^{-11}$ cm.), which were in excellent agreement with the attractive supposition that these penetrating radiations have their origin in the formation of the most abundant atoms.

Subsequently the Dirac formula has been modified by Klein and Nishina ('Nature,' September 15th, 1928) as follows :—

$$S=\frac{2\pi Ne^4}{m^2c^4}\left\{\frac{1+\alpha}{\alpha^2}\left[\frac{2(1+\alpha)}{1+2\alpha}-\frac{1}{\alpha}\log(1+2\alpha)\right]+\frac{1}{2\alpha}\log(1+2\alpha)-\frac{1+3\alpha}{(1+2\alpha)^2}\right\}. \quad . \quad . \quad . \quad (3)$$

The introduction of the last term in this formula leads

* Dirac, Proc. Roy. Soc. A, cxi. p. 423 (1926).

to a deviation from the Dirac formula of the order $\left(\frac{h\nu}{mc^2}\right)$, and the wave-lengths of the cosmic-rays come out lower when calculated on the Klein and Nishina theory. Thus the most penetrating cosmic-rays observed by Millikan have a wave-length equal to $\cdot 013 \times 10^{-11}$ cm., corresponding to a quantum of energy of 940 million volts. The origin of this radiation is traced to the annihilation of matter by the coalescence of protons and electrons, which Eddington assumes is taking place in the interior of the hot stars.

4. Denoting the frequency of a radiation by ν_1,

$$h\nu_1 = m_0c^2\left(\frac{1}{\sqrt{1-\frac{v^2}{c^2}}}-1\right). \quad . \quad . \quad . \quad . \quad (4)$$

where v is the velocity of an electron whose energy corresponds to that of the radiation.

Such an electron will be accompanied by "De Broglie" waves of frequency ν_2 given by :—

$$\nu_2 = \frac{m_0vc}{h\sqrt{1-\frac{v^2}{c^2}}}. \quad . \quad . \quad . \quad . \quad . \quad . \quad . \quad (5)$$

Obviously, when v is approximately equal to c, the two frequencies ν_1 and ν_2 are almost identical, so that the frequency of a very penetrating gamma radiation will differ only very slightly from that of the "De Broglie" waves of an electron, whose energy corresponds to that of the gamma-ray quantum.

5. Assuming that high speed electrons are scattered by matter in the same manner as gamma-rays, of the same frequency as that of their accompanying electron waves, the Klein–Nishina formula may be applied to their absorption by substituting for the mass of the gamma-ray quantum $\frac{h\nu}{c^2}$ the electronic mass

$$(m) = \frac{m_0}{\sqrt{1-\frac{c^2}{v^2}}}.$$

The "mass" of a very high frequency gamma-ray quantum

$\frac{h\nu}{c^2}$ is, however, almost identical with that of an electron (m) of corresponding energy. Actually

$$\frac{h\nu}{c^2} = \left(1 - \sqrt{1 - \frac{v^2}{c^2}}\right) m, \quad . \quad . \quad . \quad . \quad (6)$$

which for values of $\frac{v}{c}$ close to unity reduces approximately to $\frac{h\nu}{c^2} = m$.

6. A very slight difference in the absorption coefficients will therefore result if m is substituted for $\frac{h\nu}{c^2}$ in the Klein and Nishina expression, and we have the interesting result that the absorption coefficient of electrons (or electron waves) of very high velocity should differ only very slightly from that of a gamma radiation of the same energy. Thus electrons corresponding to 940 million volts might be expected to behave in their absorption by matter in a manner almost identical with that of a gamma radiation of corresponding wave-length ($\cdot 013 \times 10^{-11}$ cm.), and it would not appear possible to predict, from a study of its absorption, whether the most penetrating of the cosmic radiations is of a corpuscular or gamma-ray nature.

LXXII. *Photoelectric Thresholds of the Alkali Metals.* By N. R. Campbell. (Communication from the Research Laboratories of the General Electric Company, Limited, Wembley.) *

H. E. Ives and A. R. Olpin † have recently described experiments indicating that the photoelectric thresholds of thin films of the alkali metals are identical with the resonance potentials of their neutral atoms; on this identity they have founded a tenatative theory of the photoelectric effect. This theory is not easily reconciled with Sommerfeld's theory

* Communicated by the Director.

† H. E. Ives and A. R. Olpin, Phys. Rev. xxxiv. p. 117 (1929).

of the metallic state, which has been applied to the photoelectric effect with some success by Fowler *. It may be well, therefore, to point out that their conclusions, though doubtless perfectly valid for the instances that they examined, may not have the generality that they are inclined to attribute to them.

It seems to be a consequence of their theory that the threshold of a thin film of the alkali metals should be independent of the surface upon which it is deposited. This is proved by their experiments, when this surface is gas-free platinum or silver; it may possibly be true, as they suggest, whenever the surface is gas-free. Some experiments conducted in these laboratories suggest that the threshold is displaced towards longer wave-length when other metals, and in particular gold, are used as the support for the thin film; but there is some uncertainty whether the gold surfaces that were employed were truly gas-free.

However, it is certain that, if the support for the thin film is not a gas-free metal surface, but a metal surface deliberately oxidized, the threshold is not identical with the resonance potential of the alkali metal. Thus thin films of potassium deposited on oxidized surfaces of copper † have thresholds that certainly lie on the long wave-length side of $0{\cdot}85\,\mu$, while thin films of cæsium deposited on oxidized silver ‡ have thresholds that lie on the long wave-length side of $1\,\mu$. The resonance potentials of potassium and cæsium are given by Ives and Olpin as $0{\cdot}79\,\mu$ and $0{\cdot}89\,\mu$.

It should be observed that it is much easier to establish experimentally that the threshold lies on the long wave-length side of some limit than that it lies on the short wave-length side. For since the emission falls towards the threshold from the short wave-length side, a failure to find emission on the short wave-length side may indicate merely that the method of detecting a photoelectric current was not sufficiently sensitive. If, however, a photoelectric current is detected on the long wave-length side of the limit, there can be no doubt that the threshold lies on that side.

* R. H. Fowler, Proc. Roy. Soc. A, cxviii. p. 229 (1928).
† N. R. Campbell, Phil. Mag. vii. p. 633 (1928).
‡ L. R. Koller, Gen. Elec. Rev. xxxi. p. 476 (1928).

LXXIII. *Freezing-point Measurements in Very Dilute Solutions of Strong Electrolytes in Cyclohexanol.* *By* Professor E. SCHREINER *, *Ph.D.*, O.E. FRIVOLD, *M.Sc.*, *Ph.D.*, *and* F. ENDER, *M.A.*†

Introduction.

IN an earlier paper ‡ we have given some results of freezing-point measurements in very dilute solutions of uni-univalent salts in a solvent with a small dielectric constant, viz., cyclohexanol D = 15·0.

It appears plainly from these measurements that the electric properties of the solvent have a great influence on the osmotic behaviour of a solution. The results obtained from these freezing-point measurements also indicate good agreement with the Debye-Hückel theory, according to which the relative deviations of the freezing-point depression from the values to be found in an ideal solution are inversely proportional to $D^{3/2}$.

This is in many respects quite remarkable, as, according to the theory, one may expect deviations in solvents with a small dielectric constant. For in Debye-Hückel's theory certain approximations have been made by deduction of the laws found, the influence of which will be the stronger the less the dielectric constant, viz., the greater the inter-ionic forces. It seemed to us of importance, therefore, to extend the freezing-point measurements also to uni-bivalent and uni-trivalent salts in the same solvent, as the influence of the greater charges must be expected to be stronger than those of uni-univalent salts.

For the same reason measurements were made with mixtures of one uni-univalent and one uni-trivalent salt.

Besides this solvent having a dielectric constant of the right magnitude, cyclohexanol is also adapted for this purpose by having a great freezing-point constant—about 20 times that of water. It was therefore possible to make freezing-point measurements with a Beckmann thermometer divided in $\frac{1}{1000}$ degree centigrade. The pure solvent has a freezing-point at about 24° C., which makes it suitable for freezing-point measurements. The only disadvantage is that

* We regret to record that Professor E. Schreiner, with whom we have co-operated in the preparation of this paper, passed away shortly before its completion. His passing leaves us with a deep sense of personal bereavement.—O. E. F., F. E.

† Communicated by Prof. Sem Sæland.

‡ *Zeits. f. phys. Chem.* cxxiv. p. 1 (1926).

cyclohexanol is very hygroscopic. It was therefore necessary to carry out the measurements in a closed apparatus.

Apparatus.

The same apparatus previously described for freezing-point measurements of uni-univalent salts was used for these measurements also, viz., a modified Beckmann apparatus. The stirrer consisted of pure silver (*loc. cit.*). The Beckmann apparatus was closed in order to keep out the humidity of the air. The stirrer was therefore equipped with a mercury fitting (see Ostwald-Luther, 'Physiko-Chemische Messungen,' 3rd ed., p. 276).

Precautions against Errors.

In the former paper reference has been made to many errors which may have an influence upon the measurements, especially on account of the hygroscopity of the solvent and errors by the Beckmann thermometer. Special care was taken in order to calibrate the thermometers used.

Solvent and Salts.

Cyclohexanol (from Poulenc Frères, Paris) was twice distilled in a vacuum at about 2–3 mm. mercury pressure. The first fraction contained small quantities of water. The freezing-point of the main fraction in the second distillation varied between 23·3 and 23·9 degrees centigrade in the different cases, and could not be raised appreciably more. This fraction was used for the measurements, and the mean value, 23°·6 C., was used for the calculation of the results obtained.

The following three salts were employed in the measurements:—

LiCl, from Poulenc Frères, was dissolved in alcohol (absolute), and to the solution was added Li_2CO_3. After being filtered, the solution was evaporated on a water-bath and then heated in a platinum vessel until the salt was thoroughly melted. After cooling, the same procedure was repeated. The pulverized salt was at last heated about 12 hours in a drying-oven, at about 160°, until the weight was constant.

Pure uranyl acetate, from Kahlbaum, was used. The salt was freed from water of crystallization and dried until it showed constant weight.

$La(NO_3)_3$, from Merck, was heated about 12 hours at 120°. It was then heated for about the same time at the same

temperature in vacuum, and lastly about 24 hours at 150° to 155°. After being pulverized it was heated about 12 hours at 150° until the weight was constant.

Results of Measurements.

In the following pages the freezing-point depression of an ideal solution is indicated by $\bar{\Delta}$. This can be calculated when the freezing-point constant is known. $\bar{\Delta}=\nu k\gamma$, where ν is the number of ions in a molecule, k is the freezing-point constant, and γ is the concentration of the solution in mols per litre.

If the freezing-point depression measured is indicated by Δ, then

$$\frac{\bar{\Delta}-\Delta}{\bar{\Delta}} = 1-\frac{\Delta}{\bar{\Delta}} = 1-g$$

gives us the relative deviation of the measured freezing-point from the classical value. g is the osmotic coefficient according to Bjerrum, and $1-g$ therefore the deviation of the osmotic coefficient from its limiting value. The magnitude $1-g$, in the tables as well as in the figures, has been given in its dependence of the square root of the ionic concentration.

The freezing-point constant was found before :

$$k = 38{\cdot}2 \pm 0{\cdot}1.$$

As the salts used are very hygroscopic, it was necessary to work with a standard solution of the salt in cyclohexanol. From this it was added to the Beckmann apparatus, which originally contained the pure solvent.

The experiments with mixtures containing LiCl and $La(NO_3)_3$ were performed in the following way. In the bottle where the standard solution was made, weighed quantities of the two salts were dissolved in cyclohexanol in such a way that the ratio p between the two molalities δ (of $La(NO_3)_3$) and γ (of LiCl) was very near $\frac{1}{8}$, $\frac{1}{2}$, and 1 in the different cases.

From such a standard solution a portion was added to the Beckmann apparatus by aid of a pipette, and freezing-point measurements were made (*loc. cit.*).

If we use the following notations, $p=\frac{\delta}{\gamma}$; ϕ and ν=number of ions in a molecule of $La(NO_3)_3$ and LiCl, we get

$$\bar{\Delta} = k(\nu\gamma+\phi\delta) = k(\nu+p\phi)\gamma.$$

The results of the measurements will be found in the following tables.

In Tables I., II., III., IV., and V., under γ will be found the concentration expressed in mole salt in 1000 c.c. solution (in the case of the mixtures γ indicates the concentration of LiCl); in the second column will be found the square root of the ionic concentration; $\bar{\Delta}$ is the calculated freezing-point depression for an ideal solution; Δ is the depression actually observed; $1-g=\frac{\bar{\Delta}-\Delta}{\bar{\Delta}}$; $(1-g)_{\text{corr.}}$ are the values of $1-g$ corrected for the humidity (*loc. cit.*).

TABLE I.—$La(NO_3)_3$.

$$1-g=\frac{\bar{\Delta}-\Delta}{\bar{\Delta}};\quad \bar{\Delta}=k.4\gamma;\quad k=38{\cdot}22.$$

γ.	$\sqrt{4\gamma}$.	$\bar{\Delta}$.	Δ.	$1-g$.
0·000223	0·030	0·034	0·012	0·64
0·000500	0·045	0·076	0·027	0·65
0·000934	0·061	0·143	0·044	0·69
0·002919	0·108	0·446	0·086	0·81
0·004933	0·141	0·754	0·143	0·81
0·008037	0·179	1·229	0·269	0·78
0·01105	0·210	1·689	0·387	0·77
0·01279	0·226	1·956	0·450	0·77
		Second Series.		
0·000618	0·050	0·094	0·034	0·64
0·000808	0·057	0·124	0·052	0·58
0·001310	0·072	0·200	0·058	0·71
0·002462	0·099	0·376	0·103	0·73
0·00	0·128	0·629	0·183	0·71
0·006217	0·158	0·951	0·257	0·73
0·008109	0·180	1·240	0·334	0·73
0·01131	0·213	1·728	1·448	0·74
0·01215	0·221	1·858	0·482	0·74

TABLE II.—$UO_2(C_2H_3O_2)_2$.

$$1-g=\frac{\overline{\Delta}-\Delta}{\overline{\Delta}}\ ;\ \overline{\Delta}=k.3\gamma\ ;\ k=38{\cdot}22.$$

γ.	$\sqrt{3\gamma}$.	$\overline{\Delta}$.	Δ.	$1-g$. Measured.	$1-g$. Corrected.
0·00118	0·060	0·135	0·081	0·40	0·39
0·002236	0·082	0·2564	0·1206	0·530	0·516
0·003828	0·107	0·4389	0·2103	0·521	0·507
0·005913	0·140	0·6780	0·3134	0·538	0·524
		Second Series *.			
0·000589	0·042	0·067	0·053	0·22	
0·001233	0·061	0·141	0·072	0·49	
0·002343	0·084	0·2686	0·1286	0·521	
0·004029	0·110	0·4620	0·2179	0·528	
0·005593	0·130	0·6413	0·3056	0·524	
0·007123	0·146	0·8167	0·3634	0·556	
		Third Series.			
0·001656	0·071	0·190	0·086	0·55	0·51
0·002612	0·089	0·300	0·1340	0·553	0·517
0·004690	0·119	0·5377	0·2221	0·587	0·552
0·006620	0·141	0·7590	0·3493	0·540	0·504
		Fourth Series.			
0·001436	0·066	0·165	0·084	0·49	0·48
0·002630	0·089	0·3015	0·1504	0·501	0·491
0·005137	0·124	0·5891	0·2487	0·578	0·568
0·006545	0·140	0·7504	0·3194	0·574	0·565
0·007427	0·149	0·8516	0·3795	0·554	0·544

* For this and other cases the correction for the humidity was withou influence.

TABLE III.—$LiCl + La(NO_3)_3$.

$1-g = \frac{\bar{\Delta}-\Delta}{\bar{\Delta}}$; $\bar{\Delta} = k(\nu + p\phi)\gamma$; $k = 38{\cdot}22$; $\nu = 2$; $\phi = 4$; $p = 0{\cdot}126 \cong \frac{1}{8}$.

γ.	$\sqrt{(\nu+p\phi)\gamma}$.	$\bar{\Delta}$.	Δ.	$1-g$. Measured.	$1-g$. Corrected.
0·000695	0·042	0·067	0·049	0·26	0·26
0·001731	0·066	0·1657	0·1077	0·350	0·345
0·003146	0·089	0·3008	0·1828	0·392	0·387
0·006025	0·123	0·5760	0·3399	0·410	0·405
0·0109	0·165	1·043	0·5650	0·458	0·453
0·01365	0·185	1·306	0·7071	0·458	0·453
		Second Series. $p = 0{\cdot}125$.			
0·001840	0·068	0·1757	0·1127	0·359	
0·003466	0·093	0·3311	0·1953	0·410	
0·006395	0·126	0·6108	0·3540	0·420	
0·008790	0·148	0·8395	0·4357	0·481	
0·01272	0·178	1·2149	0·6306	0·481	
0·02682	0·259	2·562	1·295	0·495	
0·04720	0·343	4·508	2·209	0·510	
0·06570	0·406	6·275	3·043	0·515	
0·07641	0·437	7·298	3·494	0·521	

TABLE IV.—$LiCl + La(NO_3)_3$.

$1-g = \frac{\bar{\Delta}-\Delta}{\bar{\Delta}}$; $\bar{\Delta} = k(\nu + p\phi)\gamma$; $k = 38{\cdot}22$; $\nu = 2$; $\phi = 4$; $p = 0{\cdot}505$.

γ.	$\sqrt{(\nu+p\phi)\gamma}$.	$\bar{\Delta}$.	Δ.	$1-g$. Measured.	$1-g$. Corrected.
0·000590	0·049	0·0907	0·0459	0·49	
0·001800	0·085	0·2766	0·1279	0·538	
0·002882	0·108	0·4429	0·1835	0·586	
0·004418	0·133	0·6791	0·2813	0·586	
0·007571	0·175	1·1637	0·4709	0·595	

TABLE IV.—$LiCl + La(NO_3)_3$ (*cont.*).

$1-g=\frac{\bar{\Delta}-\Delta}{\bar{\Delta}}$; $\bar{\Delta}=k(\nu+p\phi)\gamma$; $k=38{\cdot}22$; $\nu=2$; $\phi=4$; $p=0{\cdot}505$.

Second Series. $p=0{\cdot}5005$.

γ.	$\sqrt{(\nu+p\phi)\gamma}$.	$\bar{\Delta}$.	Δ.	$1-g$. Measured.	$1-g$. Corrected.
0·000582	0·048	0·0891	0·0476	0·47	0·45
0·001193	0·069	0·1828	0·0897	0·509	0·493
0·001788	0·085	0·2740	0·1346	0·508	0·492
0·002884	0·0108	0·4415	0·1907	0·569	0·554
0·003870	0·0124	0·5935	0·2580	0·566	0·551
0·00666	0·0164	1·020	0·4290	0·580	0·565
		Third Series. $p=0{\cdot}504$.			
0·000623	0·050	0·0956	0·0472	0·51	0·50
0·001011	0·064	0·1553	0·0799	0·486	0·481
0·001680	0·082	0·2579	0·1183	0·541	0·536
0·003518	0·119	0·5401	0·2382	0·559	0·553
0·006229	0·158	0·9563	0·4067	0·575	0·569
0·008151	0·181	1·2513	0·5157	0·588	0·583

TABLE V.—$LiCl + La(NO_3)_3$.

$1-g=\frac{\bar{\Delta}-\Delta}{\bar{\Delta}}$; $\bar{\Delta}=k(\nu+p\phi)\gamma$; $k=38{\cdot}22$; $\nu=2$; $\phi=4$. $p=1{\cdot}01$.

γ.	$\sqrt{(\nu+p\phi)\gamma}$.	$\bar{\Delta}$.	Δ.	$1-g$.
0·0002689	0·040	0·0621	0·0315	0·49
0·0003628	0·072	0·1992	0·0828	0·58
0·001357	0·091	0·3132	0·1362	0·565
0·003197	0·139	0·7381	0·2749	0·628
0·006012	0·191	1·3878	0·4900	0·647
0·006957	0·205	1·6060	0·5394	0·664
		Second Series. $p=1{\cdot}01$.		
0·001082	0·081	0·2498	0·0905	0·64
0·001837	0·105	0·4241	0·1585	0·626
0·005398	0·181	1·2461	0·4215	0·662

Testing of the Debye-Hückel Osmotic Theory.

According to Debye-Hückel's theory, the relative deviation of the freezing-point depression from the classical value is

$$1-g=\frac{\epsilon^2}{6\mathrm{D}k\mathrm{T}}\sqrt{\frac{4\pi\epsilon^2\mathrm{N}}{1000\mathrm{D}k\mathrm{T}}}\cdot\omega\sqrt{\nu\gamma}\cdot\sigma(\kappa a), \quad . \quad (1)$$

where

$$\omega=\left(\Sigma\frac{\nu_i z_i^2}{\nu}\right)^{3/2},$$

$\epsilon = 4{\cdot}77\,.\,10^{-10}$ e.s.u.,

k (Boltzmann's constant) $= 1{\cdot}37\,.\,10^{-16}$ erg.,

$\mathrm{N} = 6{\cdot}06\,.\,10^{23}$,

D = Dielectric constant,

T = Temperature abs.,

γ = Concentration in mole/litre.

The salt molecules are split in $\nu_1, \nu_2, \ldots \nu_i$ ions of the kind $1, 2, \ldots i$, $\nu=\Sigma\nu_i$. The valencies of the different ions are indicated by $z_1, z_2, \ldots z_i$. $\sigma(\kappa a)$ is a function whose value is less than one, and is dependent on the ratio between the ionic diameter a, and the dimension of the ionic atmosphere $\frac{1}{\kappa}$ gives us a measure for this atmosphere. By infinite dilution $\sigma(\kappa a)=1$.

For a solution of infinite dilution the function tends towards 1, viz., in such solutions the influence of the dimensions of the ions disappears in comparison with the influence of the ionic atmosphere. In this case it will be seen from formula (1) that $1-g$ is proportional to the square root of the ionic concentration, viz., if we plot $1-g$ in relation to $\sqrt{\nu\gamma}$, it must be expected that curves through the points experimentally found and point of origin in small concentrations will coincide with the tangents theoretically calculated. The slopes of these tangents are, according to the theory, determined by the known quantities ϵ, k, T, N, of the dielectric constant D, and the valency factor ω.

Mixtures of Electrolytes.

For mixtures of electrolytes we get an expression for $1-g$ quite similar to formula (1).

We dissolve γ mole per litre of a salt (LiCl) whose molecules are split in $\nu_1, \nu_2, \ldots \nu_i$ ions of the kind $1, 2, 3, \ldots i$. The valencies of the ions we indicate by $z_1, z_2 \ldots z_i$, $\Sigma\nu_i=\nu$.

We dissolve also δ mole per litre of another salt, $La(NO_3)_3$, whose molecules are split in $\phi_1, \phi_2, \ldots \phi_i$ ions of the kind $1, 2, 3, \ldots i$. The valencies of the ions we indicate by x_1, $x_2, \ldots x_i$, $\Sigma\phi_i = \phi$.

For this mixture of two electrolytes we have, denoting $\frac{\delta}{\gamma}$ by p,

$$1-g = \frac{\epsilon^2}{6Dk\overline{T}}\sqrt{\frac{4\pi\epsilon^2 N}{1000.Dk\overline{T}}}\,\omega\,\sqrt{(\nu+p\phi)\gamma},$$

$$\omega = \left(\frac{\gamma\Sigma\nu_i z_i^2 + \delta\Sigma\phi_i x_i^2}{\nu\gamma+\phi\delta}\right)^{3/2} = \left(\frac{\Sigma\nu_i z_i^2 + p\Sigma\phi_i x_i^2}{\nu+p\phi}\right)^{3/2}.$$

Measurements were made with solutions where p is very nearly equal to $\frac{1}{8}$, $\frac{1}{2}$, and 1. For these values of p it will be found that $\omega_{1/8}=5{\cdot}47$, $\omega_{1/2}=9{\cdot}34$, and $\omega_1=11{\cdot}77$.

Fig. 1.

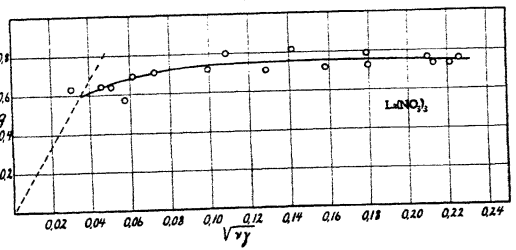

Discussion of the Results obtained.

In figs. 1, 2, 3, and 4 are plotted the relative deviations of the freezing-point depression from the classical values in relation to the square root of the ionic concentration. The results obtained for LiCl, $La(NO_3)_3$ for mixtures of these two salts and for uranyl acetate will be found. In the same figures the theoretically calculated tangents are plotted.

It will be seen from the graphical representation that it will be necessary to perform sufficiently accurate freezing-point measurements at considerable lower concentrations for $La(NO_3)_3$ than for LiCl in order to be able to test the limiting law. On account of this it has been impossible by these experiments to test the limiting law to the same extent as has been the case with the uni-univalent salts.

The graphical representations show, however, especially as regards the mixtures, that the curves experimentally found do not coincide with the tangents theoretically calculated, as was the case with the uni-univalent salts, in very small concentrations. The results obtained by the uni-bivalent uranyl acetate do not seem to conflict with the theory.

Fig. 2.

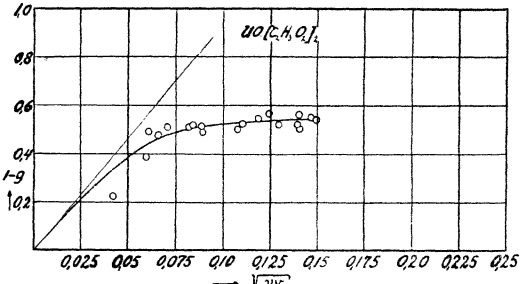

Fig. 3.

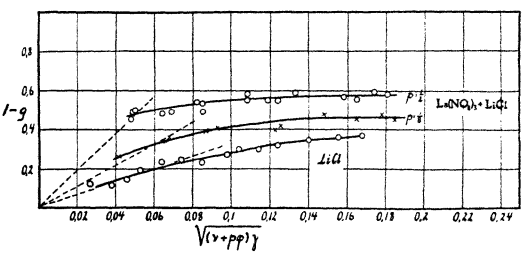

Deviations from the theory of the same nature as found by the mixtures have also been found by Brönsted and Petterson, and later on by La Mer and Mason * in aqueous solutions by solubility measurements. This is the case at small concentrations, when the solution contains saturating salts with high-valence cations in the presence of solvent salts with high-valence anions.

* Journ. Amer. Chem. Soc. xlix. p. 410 (1927).

At the same time it appears that the mean ionic diameter calculated according to theory varies in many cases to a great extent with the concentration—the calculated values for the ionic diameters are improbably small or negative. These discrepancies with the theory have caused Müller *, Gronwall, La Mer and Sandved † to examine the influence of the approximation made in the Debye-Hückel theory introduced by the calculation of the distribution of the potential round a particular ion.

These investigators have solved this problem with a greater approximation than Debye and Hückel, and also found that more of the deviations mentioned above of the aqueous solutions will disappear under these circumstances.

Fig. 4.

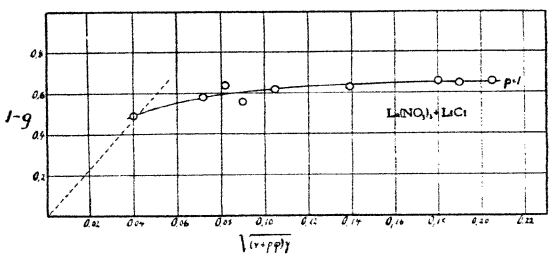

The improved theory shows that the discrepancies from the Debye-Hückel's theory will be greater the less the ionic diameter, and the greater the valencies of the ions. According to the improved theory for small ionic diameters, the curves, indicating the connexion between $1-g$ and $\sqrt{\nu\gamma}$, will cut the theoretically-calculated tangents in the same way as found by us experimentally with the mixtures (figs. 3 and 4), and by infinite dilution will join the theoretical tangent, according to Debye-Hückel's theory.

Otherwise it is to be observed that the result found by Gronwall, La Mer and Sandved by the calculation of the activity coefficient only can be applied to salts of the symmetrical type, as KCl and $CuSO_4$; on the contrary, not on asymmetrical salts, like $La(NO_3)_3$, or mixtures of two salts.

* Müller, *Phys. Zeits.* 1927, p. 324; 1928, p. 78.

† T. H. Gronwall, La Mer and K. Sandved, *Phys. Zeits.* Bd. xxix. p. 358 (1928).

Nor are there measurements accurate enough for non-aqueous solutions which make a comparison possible between the improved theory and the experiments. But so much can be said—that the greater the valencies of the dissolved ions are, and the less the dielectric constant of the solvent, the greater the deviations that can be expected from the original Debye-Hückel theory.

Owing to lack of room the above measurements were carried out in the Pharmacological Institute, thanks to the courtesy of the professor, Dr. E. Poulsson.

We also wish to express our thanks to the directors of the "A/S Norsk Varekrigsforsikrings Fond," who have granted the funds necessary to carry out this work.

Physical Department,
University, Oslo,
March 1929.

LXXIV. *Double-Valued Characteristic of a Direct Current Feed-Back Amplifier.* *By* PRESTON B. CARWILE, *Ph.D.*, *and* FREDERIC A. SCOTT, *M.S.*, *Lehigh University, U.S.A.* *.

A MODIFIED Hartley † direct current feed-back amplifying circuit with connexions as shown in fig. 1, exhibits an anomalous static characteristic under certain feed-back conditions. It is the purpose of the present paper to describe and explain this effect.

Let m be the voltage amplification of the two ‡ tube circuit due to thermionic action alone, M the *total* voltage amplification due to thermionic and feed-back action combined, R the external resistance in the plate circuit of tube 2, r that portion of R between the filament and the feed-back tap T, I_p the current through R, E_g' the grid potential of tube 1, and E_g the portion of E_g' furnished *externally* (as by potentiometer P), exclusive of the potential due to feed-back action.

* Communicated by the Authors.

† R. V. L. Hartley, 'U.S. Letters Patent,' No. 1, 218, 650. See also van der Bijl, 'The Thermionic Vacuum Tube and its Applications,' p. 257.

‡ It is necessary to use at least two tubes in a direct current feed-back amplifier in order that the feed-back and input potentials may be in phase.

Assuming that there is no grid current through tube 1 it can easily be shown * that

$$M = m\left[1 + \left(\frac{r}{R}m\right) + \left(\frac{r}{R}m\right)^2 + \left(\frac{r}{R}m\right)^3 \cdots\right]$$

$$= \frac{m}{1 - \frac{r}{R}m}, \quad \ldots \ldots \ldots \ldots \quad (1)$$

provided $\frac{r}{R}m < 1$. Thus the total amplification M approaches infinity as $\frac{r}{R}m$ approaches unity.

Fig. 1.

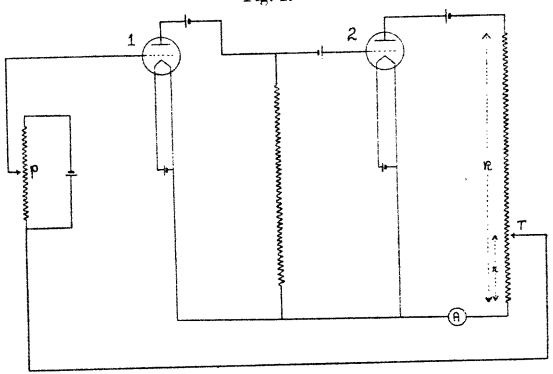

First let us consider a "base" characteristic, *i. e.* one obtained by pure thermionic action with no feed-back ($r = 0$). If we plot I_p as ordinates and E_g' as abscissæ (plotting negative values, however, towards the right) we shall have a curve of the form shown in fig. 2. It is readily seen that the slope of this curve is proportional to the voltage amplification. Hence, in terms of arbitrary units we may say that the slope *is* the amplification m.

This base characteristic still applies, even with feed-back action taking place, since E_g' is the *actual* grid potential whether obtained from an external source or from the feed-back tap or partly from both.

* *Loc. cit.*

Suppose we set r at some fixed value such that on the steepest part of the base characteristic $\frac{r}{R}m > 1$. Evidently there will be some point A on the lower bend of the curve

Fig. 2.

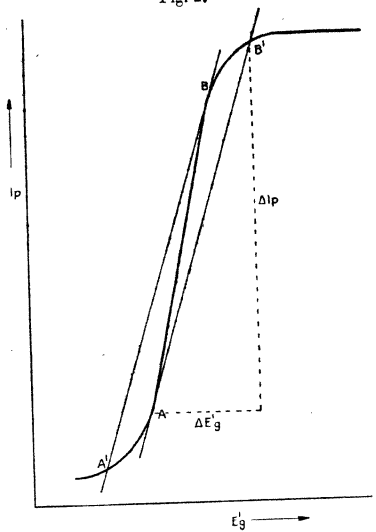

and another point B on the upper bend where $\frac{r}{R}m$ will be unity, or

$$\frac{r}{R}m_A = \frac{r}{R}m_B = 1, \quad . \quad . \quad . \quad . \quad . \quad (2)$$

and

$$\frac{r}{R} = \frac{1}{m_A} = \frac{1}{m_B}. \quad . \quad . \quad . \quad . \quad . \quad . \quad (3)$$

At points A and B the *total* amplification M is infinitely large, as shown by equations (1) and (2). Thus at point A an infinitesimal increment of E_g' toward the right (fig. 2) causes an increase in I_p. Feed-back action supplies an additional increment to E_g' and this causes a further increase in I_p, and so on. This rise in I_p does not stop at point B as

one might suspect at first, but continues to the point B′ where the tangent from A intersects the upper part of the curve, since over this whole range

$$\frac{\Delta E_g'}{\Delta I_p} = \frac{1}{m_A} = \frac{r}{R},$$

or

$$\frac{r}{R}\Delta I_p = \Delta E_g',$$

so that the feed-back action alone supplies the requisite grid increment corresponding to the current increment.

Fig. 3.

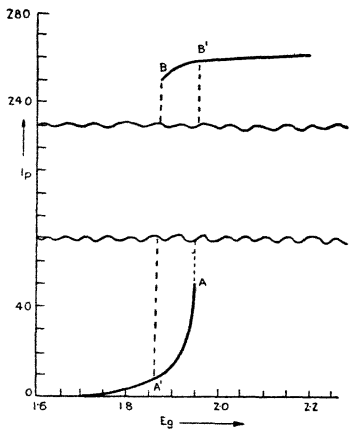

The plate current I_p becomes stable, however, after reaching B′, and remains stable over the whole upper part of the curve as far down as B, since over this region the slope is smaller than at B, so that $\frac{r}{R}m < 1$, and hence according to equation (1) the total amplification is finite. If the current is brought an infinitesimal amount below its value at B it suddenly drops to its value at A′ where the tangent from B intersects the lower bend.

If, under the same circuit conditions, we plot the plate current I_p as ordinates and *externally* applied grid (negative) potential E_g as abscissæ, the characteristic takes the form shown in fig. 3, which was drawn from experimental data.

The slope of this curve, in arbitrary units, is the total amplification M. The points A, B′, B, and A′ represent approximately the same respective plate currents in both fig. 2 and fig. 3. Thus at point A in fig. 2 the slope is m_A such that $\frac{r}{R} m_A = 1$. By substituting this value of m in equation (1) we see that the total amplification M_A should be infinite. In fig. 3 it is seen that the slope does approach infinity at A.

The loop A B′ B A′ A in fig. 3 may be traversed counter-clockwise, but not clockwise since the transitions from A to B′ and from B to A′ are sudden and irreversible. The other portions of the curve A′ A and B B′ are stable and reversible. It will be seen that for every externally applied grid potential between A′ and A the plate current may have either its value on the lower bend between A′ and A or its value on the upper bend between B and B′. Thus previous history determines which value of plate current obtains at any particular value of externally applied grid potential.

LXXV. *On the "Flash" in the After-glow of the Electrodeless Discharge with Change of Pressure.* *By* CHAS. T. KNIPP, *Ph.D., Professor of Experimental Electricity, University of Illinois, and* LEE N. SCHEUERMAN, *M.A.**

PHENOMENA attending the electrodeless discharge in gases were described many years ago by Sir J. J. Thomson †, who at the time called attention to the phosphorescent glow produced in certain gases and the absence of this glow in others, notably "in a single gas (as distinct from a mixture), unless that gas was one which formed polymeric modifications." This requirement of a mixture, or the trace of another gas as an impurity, was also observed by later investigators. Quite recently Lewis ‡ has shown by experiment that absolutely pure oxygen or nitrogen in an uncontaminated out-gassed tube will yield no after-glow. However, if there is a little

* Communicated by the Authors.

† Phil. Mag. ser. 5, xxxii. pp. 321, 445 (1891). 'Recent Researches,' p. 184 (1893).

‡ Journ. Amer. Chem. Soc. li. pp. 654, 665 (1929).

water-vapour present, or if the walls of the tube are contaminated with another gas, an after-glow is formed. Adding a little oxygen to pure nitrogen, or *vice versa*, will give an after-glow. This would indicate the correctness of Thomson's theory referred to above, and extended recently*, in which he states that the after-glow is caused by the formation of systems more easily ionized than the normal gas, rather than by simple recombination of the ionized gas-molecules.

This note has to do with the "flash" that may be made to appear, when the conditions are favourable, in the after-glow on the sudden compression of the glowing gas. It was suggested to one of the writers two years ago, while at the Cavendish Laboratory, by the researches of Sir J. J. Thomson. One of the experiments performed by Sir J. J. Thomson on the lecture table was that, on admitting suddenly a small quantity of gas into the discharge chamber, the after-glow appeared to "flash" momentarily and then faded quickly away. The question naturally arose: What are the conditions that obtain within the tube to produce this flash? Are they brought about in part by the introduction of fresh gas, or may the same flash be obtained by merely compressing the residual gas in the tube, other conditions being favourable?

As a simple initial test the discharge tube was made long, with the exciting high-frequency coil placed at the far end from the gas inlet (this form may also have been used by Sir. J. J. Thomson). Under this arrangement the compression at the exciting end was as by an "air piston." This method of procedure gave quite consistent "flashes."

A more comprehensive test, based on compression only, was planned. The apparatus as ultimately constructed is shown in the figure. C is the discharge chamber, about which is placed the exciting solenoid S of the high-frequency circuit. D is a rubber diaphragm held between the two ground ends of the divided tube, thus separating the compression chamber C from the expansion chamber B. Rubber dental dam was used for D. At the lower end of B is a large-throated valve V for permitting the gas to be introduced quickly into B, and thus causing a sudden

* Phil. Mag. ser. 7, iv. p. 1128 (1927). Proc. Phys. Soc. xl. p. 79 (1928).

compression in C. This large-throated valve consists simply of a rubber stopper mounted on a central rod held firmly against the ground-lip of the tube, extending down from B, by a stiff spring, as shown. Guides are provided to keep the valve central. To the lower end of the valve-stem is attached a winch W which permits opening the valve V quickly. The small manometer gives an indication of the pressure in the system, while the large manometer is used as a means of measuring and regulating the amount of gas being introduced to bring about the

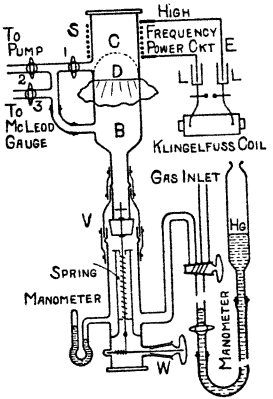

desired compression. The action of this arrangement is apparent from the figure.

The method of operation is to open stopcocks 1, 2, and 3, then lower the valve V by the winch W, and pump the whole system out to the pressure desired. This pressure is read on the gauge. Next stop-cocks 1, 2, and 3, and also the valve V, are closed. The pressures in C and B are the same, and the diaphragm D occupies the unstretched position shown. Gas is now introduced in "doses" through the three-way valve by means of the large manometer until the desired pressure, as indicated by the small manometer, is reached. Everything is now ready for the test. The gas in C is excited by the high-frequency discharge. After

a few moments the exciting current in the solenoid is cut off and the after-glow alone remains. This glow gradually fades; however, before it ceases to be visible, the large-throated valve V is quickly opened and the excited gas in C is suddenly compressed, owing to the excess of pressure in B over that in C. The rubber diaphragm now occupies the position indicated by the dotted line. It is at the end of this sequence that the "flash" in C occurs.

Carrying out the experiment was not at first so simple. Thomson * had observed that some metals, mercury, and, apparently, some non-conductors, seem to kill the after-glow. With the introduction of the rubber diaphragm it was hoped that this difficulty would be eliminated. However, this was not the case; the sulphur in the processed rubber, being electropositive, killed the after-glow. This difficulty was overcome by dipping the dam in pure latex, which contains no sulphur. The coating formed when dry was smooth, and interfered but little with the flexibility of the dam. This covering proved entirely satisfactory—the after-glow seemed to be in no way diminished. That this was the case was thoroughly tested by introducing latex-covered rubber dam into an electrodeless discharge tube specially constructed for testing different substances.

With this annoyance removed, an exhaustive series of experiments was undertaken to determine under what conditions a given gas could be made to "flash." Air, oxygen, and nitrogen were successively worked with. In air the "flash" was noticeable over the whole range of pressures for which the after-glow was visible. In oxygen the "flash" showed the same characteristics. Nitrogen was in marked contrast to oxygen and air. The after-glow in nitrogen, as shown by Thomson, has a maximum life of about 125 seconds. It was very bright, and diminished gradually. The "flash" in nitrogen could be obtained at any time while the after-glow was visible. Its brilliancy seemed to be in direct proportion to the brilliancy of the after-glow. At no time in air, oxygen, or nitrogen, the three gases studied, was a "flash" formed if the compression took place after the after-glow had completely disappeared. An interesting phenomenon in

* Phil. Mag. ser. 7, iv. p. 1128 (1927). Proc. Phys. Soc. xl. p. 79 (1928).

the case of nitrogen was that, following the "flash," the after-glow was still visible, and continued to die out gradually instead of disappearing completely with the flash, as in the case of oxygen. Other interesting results were observed that seemed to be wholly lacking in the case of oxygen; these, however, may have been due to the greater intensity of the after-glow and flash in nitrogen.

A question may be raised as to whether the "flash" here described is really a flash; but, instead, may it not be the uniform illumination of the after-glow compressed into a smaller volume, and thus made to appear brighter? The writers think not. The two cases can readily be distinguished. The "flash" of the after-glow occurs, as seen by the eye, in the form of a flat disk which travels upward from the diaphragm when the gas is suddenly compressed. It seems to accompany a pressure-pulse in the gas. Granting that the after-glow is due to the illumination which accompanies recombination in an ionized gas, we find a plausible explanation of the "flash" in that, on compression, the ions are pushed closer together, which in turn facilitates recombination. On this view no "flash" should result on sudden expansion of the excited gas. Although the effect of expansion has not been exhaustively investigated by the writers, simple preliminary tests indicate that expansion of an ionized gas does not cause a "flash."

Addendum *.

H. F. Newall † investigated pressure conditions in the electrodeless discharge many years ago, and found that in a mixture of two gases (oxygen and nitrogen) the phosphorescence reaches a maximum at about 0·4 mm. Hg, and fades away as the pressure is either increased or decreased from this value. He produced a striking effect by initially adjusting the gas-pressure slightly higher than that for maximum phosphorescence; then, while the gas was glowing, the electrodeless discharge having been cut off, the pressure was suddenly reduced, and he observed a wave of increased brightness travel along the tube toward the

* Newall's experiment, and also Sir J. J. Thomson's account of it, escaped the writers' notice during the progress of this investigation. These were kindly brought to our attention by the Editors after the authors had submitted the MS. for publication.

† Proc. Camb. Phil. Soc. ix. p. 295 (1897).

remote end from the pump. Reasoning from the above, it follows that there should result a wave of diminished brightness if the pressure is suddenly slightly increased. Again, if the pressure is accurately adjusted for maximum brightness, then a wave of diminished brightness should result for *either* a decrease or an increase in pressure. And further, if the pressure is adjusted to a value lower than for maximum brightness, then a reduction in pressure should result in a wave of diminished brightness. In Newall's article mention is made of performing the experiment by causing a reduction in pressure only, his apparatus evidently lending itself better to that case; however, no reference is made to having observed a wave of diminished brightness.

An account of Newall's experiment was given recently by Sir J. J. Thomson* in a lecture before the Société Française des Electriciens in Paris, in which it was shown that there are many cases of luminosity which could not be explained by compression.

In the light of the foregoing, and also of our own results, it seems probable that the alteration in phosphorescence due to change in pressure has two sources: (*a*) that described by Newall, and later by Thomson, in which the original grouping of the atoms or molecules is no longer stable, and the gas passes into a new state of grouping with the evolution of energy, part of which would account for the " pressure-glow," and which persists for some time; (*b*) that designated by the term " flash " in this article, whose appearance is only momentary, accompanying a pressure pulse of the residual gas, but not an expansion; it assumes the gas to be ionized, and, granting that compression facilitates recombination, there results an increased illumination. The two types or kinds of phosphorescence are shown in the case of nitrogen, the former continuing for many seconds, the latter for but a moment.

The apparatus sketched in the figure, with slight modifications in the design of chambers C and B, will work equally well on compression or expansion.

* *Supplément au Bulletin de la Société Française des Electriciens*, no. 77, 4th sér., tome 8 (1927).

LXXVI. *The Rotating Electron in a Beam of Light.*

By B. M. Sen, *Professor, Presidency College, Calcutta* *.

THE theory of Compton effect was investigated by Dirac † using the methods of Heisenberg's matrix mechanics and by Gordon ‡ with Schrödinger's Wave mechanics, with frequent reference to the light-quantum hypothesis and the Correspondence Principle.

It is proposed in the present paper to find a solution of the Wave equation of a rotating electron under a plane polarized beam of light, and indicate the effects.

In 'Nature' of Sept. 15, 1928, Klein and Nishina have given a formula for the intensity of Compton scattering calculated from Dirac's equation. Presumably the method is an extension of that used by Klein in *Zs. f. Phys.* xli. (1927), but the details have not yet been published.

1. Dirac has shown that the Wave equation of a free electron can be written in the form

$$(p_0+\alpha_1 p_1+\alpha_2 p_2+\alpha_3 p_3+\alpha_4 mc)\psi = 0,$$

where the α's are certain four-rowed matrices. p_1, p_2, p_3 are the components of momentum, and are to be replaced by

$$p_1 = \frac{h}{2\pi i}\frac{\partial}{\partial x}, \quad p_2 = \frac{h}{2\pi i}\frac{\partial}{\partial y}, \quad p_3 = \frac{h}{2\pi i}\frac{\partial}{\partial z},$$

and

$$p_0 = \frac{\mathrm{E}}{c} = -\frac{h}{2\pi i}\frac{1}{c}\frac{\partial}{\partial t}.$$

For an electromagnetic field p_0 is to be replaced by $p_0+\frac{e}{c}\mathrm{V}$, p_1 by $p_1+\frac{e}{c}\mathrm{A}_1$, p_2 by $p_2+\frac{e}{c}\mathrm{A}_2$, p_3 by $p_3+\frac{e}{c}\mathrm{A}_3$, where V is the scalar potential and $(\mathrm{A}_1, \mathrm{A}_2, \mathrm{A}_3)$ is the vector potential.

We take

$$\mathrm{V} = 0, \quad \mathrm{A}_1 = \mathrm{A}_3 = 0, \quad \mathrm{A} = a\cos\omega(t-x/c).$$

Taking the values of α_1, α_2, α_3, α_4 given by Dirac, we get Darwin's form § of the Wave equations:

* Communicated by the Author.
† Proc. Roy Soc. cxi. p. 405.
‡ *Zs. f. Phys.* xl. p. 117.
§ Proc. Roy. Soc. cxviii. p. 655.

$$(p_0+mc)\psi_1+(p_1-ip_2')\psi_4+p_3\psi_3=0, \quad . \quad . \quad (1)$$

$$(p_0+mc)\psi_2+(p_1+ip_2')\psi_3-p_3\psi_4=0, \quad . \quad . \quad (2)$$

$$(p_0-mc)\psi_3+(p_1-ip_2')\psi_2+p_3\psi_1=0, \quad . \quad . \quad (3)$$

$$(p_0-mc)\psi_4+(p_1+ip_2')\psi_1-p_3\psi_2=0, \quad . \quad . \quad (4)$$

where $p_2'=p_2+e'A_2$ and $e'=e/c$.

These, then, are the appropriate Wave equations for a moving electron under a ray of light incident along the x-axis. We note that p_0, p_1, p_2, p_3, regarded as differential operators, commute with one another. p_2, p_3 commute with A_2, but p_0 and p_1 do not commute with A_2.

We shall require the following relations, which are easily verified :—

$$\left.\begin{aligned}&\{(p_1+ip_2')(p_0+mc)-(p_0+mc)(p_1+ip_2')\}\psi\\&\quad=\{(p_1+ip_2')(p_0-mc)-(p_0-mc)(p_1+ip_2')\}\psi\\&\quad=-ie'\psi p_0A_2,\\&\{(p_1-ip_2')(p_0+mc)-(p_0-mc)(p_1-ip_2')\}\psi\\&\quad=\{(p_1-ip_2')(p_0-mc)-(p_0-mc)(p_1-ip_2')\}\psi\\&\quad=ie'\psi p_0A_2.\end{aligned}\right\} \quad (5)$$

$$\left.\begin{aligned}(p_1+ip_2')(p_1-ip_2')\psi&=(p_1^2+p_2'^2)\psi-ie'\psi p_1A_2.\\(p_1-ip_2')(p_1+ip_2')\psi&=(p_1^2+p_2'^2)\psi+ie'\psi p_1A_2.\end{aligned}\right\} \quad (6)$$

2. Multiplying (1) by p_1+ip_2', (2) by $-p_3$, (4) by $-(p_0+mc)$, and adding, we have

$$\{p_1^2+p_2'^2+p_3^2-(p_0^2-m^2c^2)\}\psi_4-ie'\psi_1p_0A_2-ie'\psi_4p_1A_2=0.$$
$$\quad . \quad . \quad . \quad (7)$$

Similarly from (3), (4), (1) we get

$$\{p_1^2+p_2'^2+p_3^2-(p_0^2-m^2c^2)\}\psi_1+ie'\psi_1p_1A_2+ie'\psi_4p_0A_2=0.$$
$$\quad . \quad . \quad . \quad (8)$$

Also from (1), (3), (2) we get

$$\{p_1^2+p_2'^2+p_3^2-(p_0^2-m^2c^2)\}\psi_3+ie'\psi_3p_1A_2+ie'\psi_2p_0A_2=0.$$
$$\quad . \quad . \quad . \quad (9)$$

Lastly, from (3), (4), (2) we get

$$\{p_1^2+p_2'^2+p_3^2-(p_0^2-m^2c^2)\}\psi_2-ie'\psi_3p_0A_2-ie'\psi_2p_1A_2=0.$$
$$\quad . \quad . \quad . \quad (10)$$

These are equivalent to the differential equations

$$-\frac{h^2}{4\pi^2}\left[\frac{\partial^2}{\partial x^2}+\frac{\partial^2}{\partial y^2}+\frac{\partial^2}{\partial z^2}-\frac{\partial^2}{c^2\partial t^2}\right]\psi_4+m^2c^2\psi_4$$
$$+\frac{h}{2\pi i}\left[2e'a\cos\theta\frac{\partial\psi_4}{\partial y}+ie'a\psi_1\frac{\partial}{c\partial t}\cos\theta-ie'a\psi_4\frac{\partial}{\partial x}\cos\theta\right]$$
$$=0, \quad . \quad . \quad (7')$$

$$-\frac{h^2}{4\pi^2}\left[\frac{\partial^2}{\partial x^2}+\frac{\partial^2}{\partial y^2}+\frac{\partial^2}{\partial z^2}-\frac{\partial^2}{c^2\partial t^2}\right]\psi_1+m^2c^2\psi_1$$
$$+\frac{h}{2\pi i}\left[2e'a\cos\theta\frac{\partial\psi_1}{\partial y}+ie'\psi_1\frac{\partial}{\partial x}\cos\theta-ie'a\psi_4\frac{\partial}{c\partial t}\cos\theta\right]$$
$$=0, \quad . \quad . \quad (8')$$

where $\theta=\omega(t-x/c)$.

ψ_2 satisfies the same equation as ψ_4, and ψ_3 as ψ_1.

3. Since $(p_1-p_0)A_2=0$, it is obvious that $\psi_1+\psi_4$ and $\psi_2+\psi_3$ also satisfy the differential equation

$$\left(-\frac{h^2}{4\pi^2}\right)\left[\frac{\partial^2}{\partial x^2}+\frac{\partial^2}{\partial y^2}+\frac{\partial^2}{\partial z^2}-\frac{\partial^2}{c^2\partial t^2}\right]u$$
$$+m^2c^2u+\frac{h}{2\pi i}2e'a\cos\theta\frac{\partial u}{\partial u}=0, \quad (11)$$

neglecting the square of a.

Assume as a solution

$$u\propto e^{\frac{2\pi i}{h}(k_1x+k_2y+k_3z+\lambda ct)+B\sin\theta}, \quad . \quad . \quad . \quad . \quad (12)$$

where θ has been put for $\omega(t-x/c)$.

The equation (11) will be satisfied if

$$k_1^2+k_2^2+k_3^2-\lambda^2+m^2c^2=0 \quad . \quad . \quad . \quad . \quad (13)$$

and

$$\frac{h}{\pi i}(k_1+\lambda)\frac{B\omega}{c}=2e'ak_2,$$

which gives

$$B=\frac{2\pi i}{h}\frac{e'ack_2}{\omega(k_1+\lambda)}. \quad . \quad . \quad . \quad . \quad . \quad . \quad (14)$$

B is, therefore, a pure imaginary, and is of the same order as a. We can, therefore, write down the solution of (11) in the form

$$u\propto e^{\frac{2\pi i}{h}(k_1x+k_2y+k_3z+\lambda ct)}(1+B\sin\theta),$$

neglecting the square of a.

4. To find expressions for ψ_1 and ψ_4 separately, we take the equations (7), (8). Assume as a solution

$$\psi_1 = \mathrm{P}_1 e^{\frac{2\pi i}{h}(k_1x+k_2y+k_3z+\lambda ct)}(1+\mathrm{B}\sin\theta+\mathrm{C}_1\cos\theta), \quad (15)$$

$$\psi_4 = \mathrm{P}_4 e^{\frac{2\pi i}{h}(k_1x+k_2y+k_3z+\lambda ct)}(1+\mathrm{B}\sin\theta+\mathrm{C}_4\cos\theta), \quad (16)$$

where B and the C's are small, and

$$\mathrm{P}_1\mathrm{C}_1+\mathrm{P}_4\mathrm{C}_4=0.$$

Then

$$\frac{\partial^2\psi}{\partial x^2} = \mathrm{P}_1\frac{2\pi i}{h}k_1\Big[\frac{2\pi i k_1}{h}(1+\mathrm{B}\sin\theta+\mathrm{C}_1\cos\theta) - \frac{\omega}{c}\mathrm{B}\cos\theta+\frac{\omega}{c}\mathrm{C}_1\sin\theta\Big]e^{\frac{2\pi i}{h}(k_1x+\ldots+\lambda ct)}$$
$$+\mathrm{P}_1\Big[\Big(\frac{2\pi i}{h}k_1\mathrm{B}+\frac{\omega}{c}\mathrm{C}_1\Big)\Big(-\frac{\omega}{c}\cos\theta\Big) + \Big(\frac{2\pi i}{h}k_1\mathrm{C}_1-\frac{\omega}{c}\mathrm{B}\Big)\frac{\omega}{c}\sin\theta\Big]e^{\frac{2\pi i}{h}(k_1x+\ldots+\lambda ct)},$$

$$\frac{\partial^2\psi_1}{\partial y^2} = \mathrm{P}_1\Big(\frac{2\pi i k_2}{h}\Big)^2(1+\mathrm{B}\sin\theta+\mathrm{C}_1\cos\theta)e^{\frac{2\pi i}{h}(k_1x+\ldots+\lambda ct)},$$

$$\frac{\partial^2\psi_1}{\partial z^2} = \mathrm{P}_1\Big(\frac{2\pi i k_3}{h}\Big)^2(1+\mathrm{B}\sin\theta+\mathrm{C}_1\cos\theta)e^{\frac{2\pi i}{h}(k_1x+\ldots+\lambda ct)},$$

$$\frac{\partial^2\psi_1}{c^2\partial t^2} = \mathrm{P}_1\Big(\frac{2\pi i\lambda}{h}\Big)\Big[\frac{2\pi i\lambda}{h}(1+\mathrm{B}\sin\theta+\mathrm{C}_1\cos\theta) + \frac{\omega}{c}\mathrm{B}\cos\theta-\frac{\omega}{c}\mathrm{C}_1\sin\theta\Big]e^{\frac{2\pi i}{h}(k_1x+\ldots+\lambda ct)}$$
$$+\mathrm{P}_1\Big[\Big(\frac{2\pi i}{h}\lambda\mathrm{B}-\frac{\omega}{c}\mathrm{C}_1\Big)\frac{\omega}{c}\cos\theta + \Big(\frac{2\pi i\lambda}{h}\mathrm{C}_1+\frac{\omega}{c}\mathrm{B}\Big)\Big(-\frac{\omega}{c}\sin\theta\Big)\Big]e^{\frac{2\pi i}{h}(k_1x+\ldots+\lambda ct)},$$

$$2e'a\cos\theta\cdot\frac{h}{2\pi i}\frac{\partial\psi_1}{\partial y} = 2e'ak_2\cos\theta\,\mathrm{P}_1 e^{\frac{2\pi i}{h}(k_1x+\ldots+\lambda ct)},$$

$$\frac{h}{2\pi i}\Big[ie'a\psi\frac{\partial}{\partial x}\cos\theta-ie'a\psi_4\frac{\partial}{c\partial t}\cos\theta\Big] = \frac{he'\omega a}{2\pi c}(\mathrm{P}_1+\mathrm{P}_4)\sin\theta.$$

Substituting in equation (8′), and putting the finite terms and the coefficients of $\cos\theta$ and $\sin\theta$ separately to zero, we have the relation (13), the value of B found before (14), and

$$P_1C_1 = -\frac{ie'a(P_1+P_4)}{2(k_1+\lambda)} \quad . \quad . \quad . \quad . \quad . \quad (17)$$

We have, therefore,

$$P_4C_4 = \frac{ie'a(P_1+P_4)}{2(k_1+\lambda)} \quad . \quad . \quad . \quad . \quad . \quad . \quad (17')$$

And similarly,

$$P_2C_2 = -P_3C_3 = \frac{ie'a(P_2+P_3)}{2(k_1+\lambda)} \quad . \quad . \quad . \quad . \quad . \quad (18)$$

5. The relations between P_1, P_2, P_3, P_4 are obtained by substituting the values of ψ_1 and ψ_4 given by (15), (16) and two similar expressions for ψ_2, ψ_3 in equations (1)–(4). We thus obtain

$$(-\lambda+mc)P_1+(k_1-ik_2)P_2+k_3P_3=0, \quad . \quad . \quad (19)$$

$$(-\lambda+mc)P_2+(k_1+ik_2)P_3-k_3P_4=0, \quad . \quad . \quad (20)$$

$$(-\lambda-mc)P_3+(k_1-ik_2)P_4+k_3P_1=0, \quad . \quad . \quad (21)$$

$$(-\lambda-mc)P_4+(k_1+ik_2)P_1-k_3P_2=0. \quad . \quad . \quad (22)$$

Also, the first approximation terms give

$$P_1C_1\{(-\lambda+mc)-(k_1-ik_2)\}+k_3P_3C_3 = \frac{h}{2\pi i}(P_1+P_4)\frac{B\omega}{c}+\frac{ie'}{a}P_4, \quad (23)$$

$$P_2C_2\{(-\lambda+mc)-(k_1+ik_2)\}+k_3P_4C_4 = \frac{h}{2\pi i}(P_2+P_3)\frac{B\omega}{c}-\frac{ie'}{a}P_3, \quad (24)$$

with

$$P_1C_1+P_4C_4=0, \qquad P_2C_2+P_3C_3=0,$$

and

$$k_1^2+k_2^2+k_3^3-\lambda^2+m^2c^2=0.$$

These relations are not all independent. It is easily verified that if we substitute the values of P_1C_1 and P_3C_3 in (23) we get

$$(P_1+P_4)\{(-\lambda+mc)-(k_1+ik_2)\}+k_3(P_2+P_3)-2P_4(k_1+\lambda),$$

which is an identity by virtue of equations (19), (23). We may take for the independent relations the equations (13), (14), (17), (17′), (18) and two out of the four equations (19)–(22).

We proceed to find expressions for the components of the stream-vector.

6. The stream vector * is given by the equations

$$\rho = -e\{\psi_1'\psi_1 + \psi_2'\psi_2 + \psi_3'\psi_3 + \psi_4'\psi_4\}, \quad . \quad . \quad (25)$$

$$j_1 = ce\{\psi_1'\psi_4 + \psi_2'\psi_3 + \psi_3'\psi_2 + \psi_4'\psi_1\}, \quad . \quad . \quad (26)$$

$$j_2 = ce\{-i\psi_1'\psi_4 + i\psi_2'\psi_3 - i\psi_3'\psi_2 + i\psi_4'\psi_1\}, \quad . \quad (27)$$

$$j_3 = ce\{\psi_1'\psi_3 - \psi_2'\psi_4 + \psi_3'\psi_1 - \psi_4'\psi_2\}. \quad . \quad . \quad (28)$$

ψ_1' being the imaginary conjugate to ψ_1, the Wave functions being so normalized that

$$\int (\psi_1'\psi_1 + \psi_2'\psi_2 + \psi_3'\psi_3 + \psi_4'\psi_4)\, dx\, dy\, dz = 1.$$

For the plane Wave solution, which has been taken as the basis, normalizing has no significance. For a plane de Broglie wave the density must be supposed to be distributed uniformly over the whole space †.

7. Denoting by $(\rho)_0$ the value of ρ when a is put equal to zero, *i. e.* the finite terms of ρ, and by $(\rho)_1$ the small terms of the first order, we have

$$\left(-\frac{\rho}{e}\right)_0 = \{P_1'P_1 + P_2'P_2 + P_3'P_3 + P_4'P_4\}.$$

From (19), (20),

$$P_1 = \frac{k_1 - ik_2}{\lambda - mc} P_4 + \frac{k_3}{\lambda - mc} P_3, \qquad P_1' = \frac{k_1 + ik_2}{\lambda - mc} P_4' + \frac{k_3}{\lambda - mc} P_3',$$

. . . (29)

$$P_2 = \frac{k_1 + ik_2}{\lambda - mc} P_3 - \frac{k_3}{\lambda - mc} P_4, \qquad P_2' = \frac{k_1 - ik_2}{\lambda - mc} P_3' - \frac{k_3}{\lambda - mc} P_4'.$$

. . . (30)

Substituting these values, and simplifying,

$$\left(-\frac{\rho}{e}\right)_0 = \frac{2\lambda}{\lambda - mc}(P_3P_3' + P_4P_4'). \quad . \quad . \quad . \quad (31)$$

* Darwin, Proc. Roy. Soc. cxviii. p. 660 (1928).

† *Cf.* Sommerfeld, 'Atombau und Spektrallinien, Wellenmechanischer Ergänzungsband,' p. 287.

Remembering that B is a pure imaginary, we have from (25)

$$\left(-\frac{\rho}{e}\right)_1 = [P_1P_1'(C_1+C_1') + P_2P_2'(C_2+C_2') + P_3P_3'(C_3+C_3') + P_4P_4'(C_4+C_4')]\cos\theta$$
$$= 2iQ[P_1P_4' - P_1'P_4 + P_2'P_3 - P_3'P_2]\cos\theta$$
$$= \frac{4k_2Q}{\lambda - mc}(P_3P_3' + P_4P_4')\cos\theta, \quad . \quad . \quad . \quad . \quad (32)$$

where $Q = e'a/2(k_1+\lambda)$.

Similarly,

$$\left(\frac{j_1}{ce}\right)_0 = \frac{2k_1}{\lambda - mc}(P_3P_3' + P_4P_4'), \quad . \quad . \quad . \quad (33)$$

$$\left(\frac{j_2}{ce}\right)_0 = \frac{2k_2}{\lambda - mc}(P_3P_3' + P_4P_4'), \quad . \quad . \quad . \quad (34)$$

$$\left(\frac{j_3}{ce}\right)_0 = \frac{2k_3}{\lambda - mc}(P_3P_3' + P_4P_4'), \quad . \quad . \quad . \quad (35)$$

which have the obvious meaning that in the absence of the electromagnetic field the current at any point is in the direction of the plane wave. Proceeding to the first approximation, we have

$$\left(\frac{j_1}{ce}\right)_1 = [P_1'P_4(C_1'+C_4) + P_4'P_1(C_4'+C_1) + P_2'P_3(C_2'+C_3) + P_3'P_2(C_3'+C_2)]\cos\theta$$
$$= 2iQ[P_1'P_4 - P_4'P_1 + P_2P_3' - P_2'P_3]\cos\theta$$
$$= -\frac{4Qk_2}{\lambda - mc}(P_3P_3' + P_4P_4')\cos\theta, \quad . \quad . \quad . \quad . \quad . \quad . \quad (36)$$

$$\left(\frac{j_2}{ce}\right)_1 = [-iP_1'P_4(C_1'+C_4) + iP_4'P_1(C_4'+C_1) + iP_2'P_3(C_2'+C_3) - iP_3'P_2(C_3'+C_2)]\cos\theta$$
$$= 2Q[(P_1+P_4)(P_1'+P_4') + (P_2+P_3)(P_2'+P_3')]\cos\theta$$
$$= \frac{4Q(\lambda+k_1)}{\lambda - mc}(P_3P_3' + P_4P_4')\cos\theta, \quad . \quad . \quad . \quad . \quad . \quad (37)$$

$$\left(\frac{j_3}{ce}\right)_1 = [P_1'P_3(C_1'+C_3) + P_3'P_1(C_3'+C_1) - P_2'P_4(C_2'+C_4) - P_4'P_2(C_4'+C_2)]\cos\theta$$

$$= iQ[P_3(P_1'+P_4')-P_1'(P_2+P_3)+P_1(P_2'+P_3')$$
$$-P_3'(P_1+P_4)+P_4(P_2'+P_3')-P_2'(P_1+P_4)$$
$$+P_2(P_1'+P_4)-P_4'(P_2+P_3)]\cos\theta$$
$$= 0. \quad . \quad . \quad . \quad . \quad . \quad . \quad . \quad . \quad . \quad . \quad . \quad . \quad . \quad . \quad . \quad . \quad . \quad . \quad (38)$$

We get, therefore,

$$j_1 : j_2 : j_3 = 2k_1 - 4Qk_2\cos\theta : 2k_2 + 4Q(\lambda+k_1)\cos\theta : 2k_3$$
$$= 2k_1 - \frac{2k_2e'a}{\lambda+k_1}\cos\theta : 2k_2 + 2e'a\cos\theta : 2k_3. \quad . \quad (39)$$

Thus there is an impulse not only in the direction of the ray, as in the light-quantum hypothesis, but also in the direction of the electrical force, but none in the direction of the magnetic force. If we generalize the solution (15), (16) after Fourier, we get expressions for the stream-vector in the same form as Gordon's.

8. It would be interesting to compare these expressions with those of Gordon. His expression * for the stream-vector runs as

$$S_\alpha = \frac{2\pi}{h}\int\{\sigma p_\alpha + (\pi_\alpha\sigma k - 2b_\alpha)\cos\phi\}$$
$$e^{\frac{2\pi i}{h}\delta W} z(p)z(p')C(p)C(p')\,dp\,dp', \quad (40)$$

with his own notation. The expression within the curly brackets reduces to the following, if we allow for the difference in the notation :—

$$\left.\begin{array}{ll} j_1 & 2k_1 + \dfrac{2k_2e'a}{\lambda+k}\cos\theta, \\ j_2 & 2k_2 - 2e'a\cos\theta, \\ j_3 & 2k_3. \end{array}\right\} \quad . \quad . \quad . \quad . \quad (41)$$

The factors $z(p)$, $C(p)$ are the Fourier generalizing factors. These expressions differ from (39) in having opposite signs in the effective terms.

These relations may give interesting comparisons with Klein and Nishin's work when the details are available

March 17, 1927.

* Gordon, *Zs. f. Phys.* xl. p. 126 (1927).

LXXVII. *On the Structure of Serial Relations.* *By* D. M. Wrinch, *M.A.*, *D.Sc.*†

IN some papers in the *Berichte der mathematisch physischen Klasse der Königlich Sächsischen Gesellschaft der Wissenschaften zu Leipzig* ‡, Hausdorff has introduced the notion of the element and gap characters of a series of terms. By means of it interesting facts about the nature of the more complicated serial types can be obtained. The theory of series, in general, deals only with Dedekindian series, with series having Cantorian continuity as a subclass of these, with well-ordered series, and with rational series. Dedekindian series, it may be recalled, are defined as series which are compact and Dedekindian: a series is compact if between every two terms there is another term, and a series is Dedekindian if every segment has a sequent. Rational series are defined as series which are compact, have no beginning or end, and consist of an enumerable infinity of terms: they are ordinally similar to the series of rational proper fractions arranged in order of magnitude. Series are said, further, to have Cantorian continuity if they are Dedekindian series and contain a rational series in such a way that there are terms of the rational series between any two terms; they are ordinally similar to the series of real numbers in order of magnitude, including 0 and ∞. Well-ordered series are defined as those series in which every existent class contained in them has a first term: the series of integers in order of magnitude provides an example of a well-ordered series.

The theory of the element and gap characters of series deals, however, not only with these well-known types of series: it suggests innumerable further serial types, and indeed directs attention to the fact that, so far, only the simplest kinds of serial types have received any attention in technical mathematics and that the nature of serial types in general is a practically untouched field.

A term x of a series P is said to be a (ν, μ) element, where ν and μ are less than ω, if there is an ω_μ series contained in P having x as its upper limit, and an $*\omega_\nu$ series contained in P having x as its lower limit. Thus the term $\frac{1}{2}$ in the series of fractions arranged in order of magnitude has

† Communicated by the Author.

‡ "Untersuchungen über Ordnungstypen," 1906 and 1907.

the character (0, 0), since there is an ω_0 (generally written ω) contained in the series, *e. g.*,

$$3/8,\ 7/16,\ \ldots\ (2^{n+1}-1)/2^{n+2},\ \ldots,$$

which has $\frac{1}{2}$ as its upper limit, and an ${}^*\omega_0$ (generally written ${}^*\omega$) contained in the series, *e. g.*,

$$\ldots\ (2^{n+1}+1)/2^{n+2},\ \ldots\ 9/16,\ 5/8,$$

which has $\frac{1}{2}$ as its lower limit. If it is assumed that the same term cannot be the upper limit of an ω_m and an ω_n in the same series unless $m=n$, it would follow that the element character of any term is unambiguously defined. It should, however, be recorded that this assumption, though it is almost universally adopted, has not yet been proved without the Multiplicative Axiom †.

For convenience we can bring the notion of a term of a series being the limit of an ω_μ and being also the last term of a series under the notion of a (ν, μ) term. For we have the convention that the last term of a series is the lower limit of the null class with respect to the series; so introducing the *ad hoc* definition of ω_z as the ordinal type of a series whose field is the null class Λ, we are able to systematize such a term as being a (z, μ) element. Similarly, we systematize the first term of a series which is the lower limit of an ${}^*\omega_\nu$ as a (ν, z) element.

Thus we have, adopting throughout the notation of 'Principia Mathematica,'

$$x\epsilon(\nu,\mu)_{\mathrm{P}} : = : (\exists \mathrm{R}, \mathrm{S}) . \mathrm{R}, \mathrm{S}\epsilon Rl`\mathrm{P} . \mathrm{R}\epsilon\omega_\mu . \mathrm{S}\epsilon{}^*\omega_\nu . \mathrm{seq}_{\mathrm{P}}`\mathrm{C}`\mathrm{R}$$
$$= x = \mathrm{prec}_{\mathrm{P}}`\mathrm{C}`\mathrm{S} \quad . \quad . \quad (\mathrm{Df})$$

as the definition of what is meant by saying that a term x in a series P has the element character (ν, μ). Then, since the last term of a series is the lower limit of the null class with respect to the series ‡,

$$\mathrm{B}`\breve{\mathrm{P}} = \mathrm{prec}_{\mathrm{P}}`\Lambda .$$

Introducing the definition of ω_z in the form suggested, namely,

$$\omega_z = 0_r,$$

we deduce that

$${}^*\omega_z = 0_r$$

† See 'Principia Mathematica,' *265.
‡ See 'Principia Mathematica,' *207.17.

also. It follows, then, that

$$x\epsilon(z,\mu)_P = (\exists R, S).R, S\epsilon Rl'P.R\epsilon\omega_\mu.S\epsilon 0_\nu.\mathrm{seq}_P'C'R = x \ \mathrm{prec}'C'S,$$

which implies, since a 0_ν has $\wedge$ as its field, that

$$x\epsilon(z,\mu)_P = (\exists R).R\subset P.R\epsilon\omega_\mu.\mathrm{seq}_P'C'R = x = \mathrm{prec}'\wedge,$$

and consequently that

$$x\epsilon(z,\mu)_P = x = B'\breve{P}.(\exists R).R\subset P.R\epsilon\omega_\mu.x = \mathrm{seq}_P'R.$$

The interpretation of a (z,μ) element and a (ν,z) element is therefore achieved.

It will, further, be convenient to systematize the cases which arise when a term in a series has an immediate successor or predecessor. Since Hausdorff deals only with compact series, the case of consecutive terms does not arise in his work.

Let us call a term which is the upper limit of an ω_μ and has an immediate successor a $(-1,\mu)$ element, and a term which is the lower limit of an ${}^*\omega_\nu$ and has an immediate predecessor a $(\nu,-1)$ element. A term which has an immediate predecessor and an immediate successor would be called a $(-1,-1)$ element. These definitions are convenient, as they enable us in specifying the element characters of the terms of a series to specify not only the kinds of well-ordered series and converses of well-ordered series of which terms of the series are limits, but also the existence of consecutive terms. The use of the index -1 in such cases can be legitimized by the introduction of the convention that

$$\omega_{-1} = s'\mathrm{NO}\,\mathrm{fin},$$

which involves also that

$${}^*\omega_{-1} = s'\mathrm{NO}\,\mathrm{fin}.$$

From this definition the interpretation of the index as denoting an immediate predecessor or successor easily follows.

For suppose that x is an ω_μ limit, but has an immediate successor. Then

$$(\exists R).R\epsilon\omega_\mu.x\ \mathrm{prec}_P C'R.(\exists y).xP_y.R\epsilon Rl'P,$$

so that

$$(\exists R, S).R, S\epsilon Rl'P.R\epsilon\omega_\mu.S\epsilon 1.\mathrm{prec}_P'C'R = x = \mathrm{prec}_P'C'S.$$

It then follows that

$$x\epsilon(-1,\mu)_P.$$

It will be convenient also to introduce the definition

$$(\nu, \mu) \epsilon \operatorname{elt}' P = (\exists x) . x \epsilon (\nu, \mu)_P . \quad . \quad . \quad . \quad (\mathrm{Df})$$

To illustrate the ideas here defined, we may consider the element characters of various well-known serial types. An ω_1 series has a $(-1, z)$ element, since it has a first term which has an immediate successor. It also has $(-1, 1)$ elements, and, since it has a term which is an ω limit and has an immediate successor, a $(-1, 0)$ element. The fact that the left-hand member in each case is -1 expresses the fact that each term in the series has an immediate successor: this is one of the marks of a well-ordered series. Finally, the fact that the right-hand members are -1 or 0, shows that the series contains no series greater than an ω, and the non-occurrence of z on the left denotes that the series has no end. An ω_2 would have as element characters

$$(-1, 1), \ (-1, 0), \ (-1, -1), \ (-1, z),$$

and an ω_3 the element characters

$$(-1, 2), \ (-1, 1), \ (-1, 0), \ (-1, -1), \ (-1, z),$$

and so on. A rational series with ends has element characters

$$(z, 0), \ (0, 0), \ (0. z).$$

An interesting point emerges when we consider the element characters of a series which possesses Cantorian continuity. Evidently its only element characters are

$$(z, 0), \ (0, 0), \ (0, z),$$

and these are those possessed by a rational series.

The specification of the element characters of a series takes no account of whether or not there are series of ascending or descending ordinal types which are not limited, *i. e.*, which do not possess limits among the terms of the series; and this is where a rational series with Cantorian continuity differs: for a rational series contains ω and ${}^*\omega$ series without limits, whereas in a series with Cantorian continuity all ω and ${}^*\omega$ series have limits. We therefore make use of Hausdorff's concept of the gap characters of a series.

A series P will be said to have a (ν, μ) gap, if there is an ω_μ and an ${}^*\omega_\nu$ contained in P such that any term of the series following the whole of the ω_μ follows at least one member of the ${}^*\omega_\nu$, and any term of the series preceding the whole of the ${}^*\omega_\nu$ precedes at least one member of the ω_μ. Just as we had the case of a term of a series being an ω_μ limit, and being the last term of a series, so now we have the case of there being in a series P, a series which is an ω_μ

and which is such that no term of the series follows all the ω_μ series. And using the definition already introduced for ω_z, we can bring this case under the case of a (ν, μ) gap. For we have

$$(\nu, \mu) \epsilon \operatorname{gap}`P := : (\exists R, S) . R \epsilon \omega_\mu . S \epsilon {}^*\omega_\nu . R . S \epsilon Rl`P$$
$$. p`\overrightarrow{P}``C`S \subset P``C`R . p`\overleftarrow{P}``C`R \subset \breve{P}``C`S. \quad . \quad (Df)$$

P is then "confinal" with an ω_μ if

$$(\exists R) . R \epsilon Rl`P . R \epsilon \omega_\mu . p`\overleftarrow{P}``C`R \subset \wedge . C`P \subset P``C`R,$$

that is, if

$$(\exists R, S) . R \epsilon Rl`P . R \epsilon \omega_\mu . C`S = \wedge . p`\overleftarrow{P}``C`R \subset C`S$$
$$. p`\overrightarrow{P}``C`S \subset P``C`R,$$

that is, if

$$(\exists R, S) . R, S \epsilon Rl`P . R \epsilon \omega_\mu . S \epsilon \omega_z . p`\overleftarrow{P}``C`R \subset C`S$$
$$. p`\overrightarrow{P}``C`S \subset P``C`R,$$

that is, if

$$(z, \mu) \epsilon \operatorname{gap}`P.$$

In the same way, P is "co-initial" with an ${}^*\omega_\nu$ if

$$(\nu, z) \epsilon \operatorname{gap}`P.$$

We may therefore follow Hausdorff and introduce the following definitions:—

$$P \operatorname{conf} \omega_\mu = (z, \mu) \epsilon \operatorname{gap}`P, \quad . \quad . \quad . \quad (Df)$$
$$P \text{ co-in } {}^*\omega_\nu = (\nu, z) \epsilon \operatorname{gap}`P. \quad . \quad . \quad . \quad . \quad (Df)$$

It will be remarked that rational and continuous series which share a trio of element characters may be differentiated by means of their gap characters.

On the basis of the definitions it proves feasible to analyse the nature of serial types in general. It is noteworthy that the series usually discussed can be so conveniently specified by means of element and gap characters. But the importance of the ideas resides in the fact that they afford a method of continuity and of generalizing it, and indeed suggest various lines of investigation which yield results belonging to the theory of serial structure. These will be given in other communications.

Lady Margaret Hall,
Oxford,
October 3, 1929.

LXXVIII. *Changes in the Dimensions of Metallic Wires produced by Torsion.—*I. *Soft Drawn Copper.* By THOMAS LONSDALE, *M.Sc.* (*London*), *F.Inst.P.*, *British Silk Research Association* *.

Summary.

THE paper gives measurements of the changes in length of "high conductivity" soft drawn copper wire which occur while the wire is being twisted at room temperature, the wire being under a constant load which is small in comparison with the load necessary to produce permanent set. Considerable elongations are produced even under very small tensions; for somewhat larger tensions much greater elongations are produced for the same degree of twist.

If e is the elongation as a percentage of the initial length, T the twist put in in turns per cm., t the initial tension in kg. per sq. cm., D the diameter in cm., then the expression $e = 4{\cdot}9\ \mathrm{DT}(1+0{\cdot}0065\ t)$ roughly gives the relationship existing within the limits of 0–1·05 for DT, and 10–500 for t, for values of D of 0·071, 0·037, 0·023 and 0·012 cm. The wire is apt to break when an elongation of 3–4 per cent. is reached, but elongations of 1–012 per cent. have been observed. For insufficiently annealed wire the elongations are rather smaller, while hard drawn copper wire contracts as much as 1 per cent. on twisting under small tensions.

IN 1906 Ercolini[1] found that cycles of torsion applied to a loaded copper wire caused the wire to elongate.

Later, Poynting[2] showed mathematically that a perfectly elastic solid of cylindrical form when subjected to a pure torsional shear experiences a small elongation which is proportional to the square of the twist. Working within the torsional elastic limit, he verified this prediction for hard drawn copper and steel wires[3], and for one turn of twist in a length of 160·5 cm. found the elongation to be $6{\cdot}81 \times 10^{-4}$ cm. for a copper wire of diameter 0·1219 cm. and $4{\cdot}66 \times 10^{-4}$ cm. for a steel wire of diameter 0·1210 cm.;

* Communicated by the Author.

he found the permanent set in these wires to be very considerable for three turns of twist.

In the experiments now described the changes in length were measured which occur when "high conductivity" soft drawn copper wire under various tensions is twisted until the breaking-point is reached.

The tensions applied were too small to produce measurable elongations when acting alone in the absence of torsion, and as the elongations within the torsional elastic limit studied by Poynting are less than can be measured by the apparatus employed, the considerable elongations observed (5–10 per cent.) are those produced in the post elastic state of the material by the combined action of the torsion and the tension. The measurements were made at room temperatures.

Apparatus and Method.

The apparatus is shown diagrammatically in fig. 1. The wire under observation is mounted vertically between an upper clamp K and a lower clamp K'. The upper clamp K hangs from a thread which, passing over a pulley, sustains at its other end the weights W to balance the weight of the clamp and exert any desired tension on the wire; the clamp can move freely up and down, but is prevented from rotating by an attached horizontal brass bar, the ends of which lie in "key ways" milled in two cylindrical shafts B which are mounted vertically in a fixed position. The lower clamp K′ is mounted so that it can experience only a rotational movement round a vertical axis. The wire is twisted by rotating this lower clamp, which is fitted with a revolution counter R to record the number of turns of twist introduced into the wire. In order to ascertain whether the wire turns in either clamp during twisting, the wire is passed right through the clamp and then bent at right angles. No movement of the bent end relative to the clamp was observed in any experiment.

The jaws of the clamps are faced with cardboard for the finer wires, and with leather for the thicker ones; if the jaws are not faced, the wires tend to break at the clamps at abnormally low values of the twist and extension. Even with the faced jaws the wire may break at one or other of the clamps, but when this happens with the faced jaws the twist and extension at break are not much less than when the wire happens to break in the middle.

The initial length of wire between the clamps was usually 1·75 metres. The changes in length corresponding to successive equal increments of twist as recorded on the revolution counter were read off in terms of the movement of the upper clamp by means of a vertical scale fixed to the steel shafts.

Fig. 1.

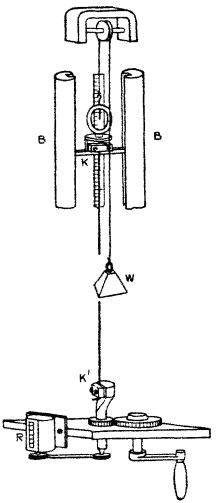

Tensions employed.

In these experiments the tensions employed ranged from 9–515 kg. per sq. cm. They were less than those required to produce a measurable extension in the absence of torsion during the time occupied by the experiment.

In the absence of torsion a tension of 515 kg. per sq. cm. acting for 24 hours produced no measurable elongation of the copper wires. The elastic limit of annealed copper is given by Tammann [4] as 203 kg. per sq. cm., but measurements made by Andrade [5] show that the elongation of soft drawn copper wire is extremely small for tensions

considerably greater than this. This was confirmed for the material used in the present experiments. Thus a length of copper wire of diameter 0·0375 cm., under a tension of 1020 kg. per sq. cm. but not subjected to torsion, showed an initial elongation of 0·14 per cent. and a further elongation of 0·05 per cent. after 24 hours. The tensile strength of annealed copper wire is about 3000 kg. per sq. cm.

The considerable extensions produced by twisting under tensions far below the elastic limit recorded by Tammann are indicated in Table I., in which a few of the results obtained are summarized.

TABLE I.

Extension of Copper Wires on twisting.

D = diameter of the wire in cm.

L = load in grams.

t = initial tension in kg. per sq. cm.

T = twist in turns per cm. of the initial length.

e = the corresponding elongation per cent. of the initial length.

D=0·0715 (22 S.W.G.).

L	40	260	510
t	10	65	127

T.	e.	e.	e.
2	0·69	1·10	1·54
4	1·81	2·38	3·01
6	2·92	3·74	4·58
8	3·99	4·97	6·05
10	4·85	6·00	7·29
12	5·50		8·30
14	5·99		9·13

D=0·0375 (28 S.W.G.).

L	10	70	140
t	9	64	127

T.	e.	e.	e.
4	0·59	0·88	1·27
8	1·31	1·83	2·46
12	2·08	2·78	3·66
16	2·76	3·68	4·75
20	3·31	4·42	5·70
24	3·72	5·00	6·49
28		5·46	

D=0·0230 (34 S.W.G.).

L	4	26	53
t	10	63	128

T.	e.	e.	e.
6	0·50	0·77	1·07
12	1·21	1·67	2·23
18	1·93	2·54	3·32
24	2·55	3·33	4·29
30		4·01	5·15
36		4·57	

D=0·012 (40 S.W.G.).

L	1	7	14
t	9	62	124

T.	e.	e.	e.
10	0·48	0·66	0·95
20	1·21	1·57	2·10
30	2·01	2·53	3·26
40	2·73	3·39	4·31
50	3·33	4·13	5·23
60	3·80		5·97

The results in Table I. show that the dependence of the extension upon the tension is quite large, even for small tensions. In Table I. the lowest tension employed (9–10 kg. per sq. cm.) is only just enough to give the wire an approach to straightness before twist is introduced. The first few turns of twist in the 1·75-metre lengths (not turns per cm.) have the effect of straightening the wire, thus enabling measurements to be obtained, yet even for this very small tension the elongations produced by further twisting are quite large.

In Table II. the extension obtained by the action of tension alone is compared with that obtained by tension and torsion.

TABLE II.

Comparison of Tension alone and of Tension + Torsion required to produce a given Elongation (Annealed Copper Wire).

	Diameter 0·0444 cm. Without twist. (Andrade.)	Diameter 0·0375 cm. Twist 24 turns per cm. (from Table I.).
Tension (kg./sq. cm.).....	1696	9
Elongation (per cent. of initial length).	3·7 immediate; 5·9 after ½ hour.	3·7

Discussion of the Results.

Some of the results obtained are shown graphically in fig. 2, which gives the twist-extension curves for approximately the same range of tensions for wires of four diameters.

These curves show some remarkable features. The general appearance of the four sets suggests that they belong to the same family, and that the phenomenon under consideration is therefore a definite physical effect; the elongation produced by a given amount of twist is strikingly dependent upon the diameter of the wire and its tension. These factors are discussed separately.

Effect of Diameter of Wire.

The diameters of the four wires employed are in the ratio of (approximately) 6 : 3 : 2 : 1. In the curves the scales of "twist" have been adjusted to be in the same ratio, that is, the scale of the first set is twice that of the second, three times that of the third, and six times that of

the fourth. It will be seen that in this way the four sets of curves are made comparable; they occupy approximately the same space. In other words, the elongation

Fig. 2.

Twist-extension Curves for Soft Drawn Copper Wire of various Diameters under various Tensions.

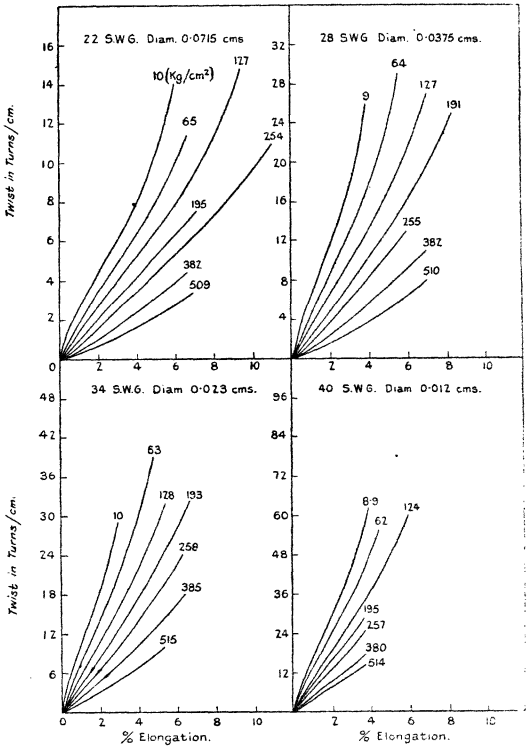

(The number at the top of each curve is the initial tension on the wire in kg./sq. cm.)

for a given twist and a given tension is roughly proportional to the diameter of the wire. The mean percentage

elongations at which break takes place for the four sets of curves, namely 7·7, 6·4, 5·5, 4·2, show that the thinner wires tend to break at a less extension than the thicker ones, but that the tendency to break is by no means proportional to the diameter of the wire.

Effect of Tension applied to Wire.

As the wire elongates, its diameter decreases slightly and the tension corresponding to a given load therefore increases. This increase, however, is only a matter of a few parts per cent. and has been neglected.

With increasing tension the elongation increases, but the proportionality is by no means direct. The curves also change their shape in each of the four sets of curves. For low tensions (such that initial twist is required to straighten out the wires) the curves are slightly S-shaped, the rate of extension per unit twist being greatest towards the middle of the curve. For the highest tensions employed, the lower part of the S has disappeared and the rate of extension per unit twist is greatest at the origin. In the case of the thinner wires the high-tension curves are practically straight lines. No attempt to express these facts by means of a definite family formula has met with any great success. Neglecting the sinuosity of the curves, it may be stated empirically that the percentage elongation e varies approximately as $(1+0{\cdot}0065\ t)$, where t is the initial tension in kg./sq. cm.

Effect of Twist applied to Wire.

For a given diameter and applied tension the percentage elongation increases almost directly with the amount of twist. This again neglects the sinuous character of the curves, which are assumed to be nearly linear, as indeed they are for low diameters and high tensions.

An approximate formula covering the whole family of curves is :—

$$e = k\,.\,\mathrm{DT}\,(1+0{\cdot}0065\ t), \quad . \quad . \quad . \quad . \quad (\mathrm{A})$$

where e is the elongation expressed as a percentage of the initial length of the wire,

D is the diameter in cm.,

T the twist in turns per cm.,

t the initial tension in kg. per sq. cm.

A more complex expression:

$$e=k\{1+aF(t)DT-bF'(t)D^2T^2\}(1+ct)DT, \quad . \quad (B)$$

where $F(t)$ and $F'(t)$ are such that they are equal to 1 when $t=0$ and decrease very rapidly to zero as t increases, partly allows for the sinuosity of the curves, but does not fit the whole series of experimental results very well.

For the simpler expression A, Table III. shows the value of the constant k obtained by substituting representative experimental values of e, D, T, and t.

TABLE III.

Experimental Values of the Constant k in the Expression $e=k\,DT(1+0{\cdot}0065\,t)$.

(Notation as in Table I.)

L	...	40	...	260	...	510	...	780	...	1020	...	1530	...	2040
t	...	10	...	65	...	127	...	195	...	254	...	382	...	509
DT.		k.		k.		k.		k.		k.		k.		k.
0·150		4·6		5·3		5·7		5·7		6·1		6·5		6·8
0·300		5·9		5·8		5·7		5·9		6·0		6·2		
0·450		6·5		6·1		5·8		5·8		5·8				
0·600		6·5		6·0		5·7				5·6				
0·750		6·3		5·8		5·5				5·4				
0·900		5·9				5·2								
1·050						4·9								

D=0·0375 cm. 28 S.W.G.

L	...	10	...	70	...	40	...	210	...	280	...	420	...	560
t	...	9	...	64	...	127	...	191	...	255	...	382	...	510
DT.		k.		k.		k.		k.		k.		k.		k.
0·150		3·6		4·1		4·6		5·1		5·5		5·9		6·5
0·300		4·1		4·3		4·5		4·7		4·9		5·1		5·4
0·540		4·3		4·4		4·4		4·6		4·7				
0·600		4·3		4·3		4·3		4·4						
0·750		4·2		4·2		4·2		4·2						
0·900		3·9		3·9		3·9		4·0						
1·050				3·7										

D=0·023 cm. 34 S.W.G.

L	...	4	...	26	...	53	...	80	...	107	...	160	...	214
t	...	10	...	63	...	128	...	193	...	258	...	385	...	515
DT.		k.		k.		k.		k.		k.		k.		k.
0·150		3·5		4·0		4·3		4·6		4·9		5·0		5·7
0·300		4·1		4·2		4·4		4·4		4·6		4·8		
0·450		4·3		4·3		4·3		4·3		4·4				
0·600		4·2		4·2		4·2								
0·750				4·0										
0·900				3·8										

TABLE III. (*cont.*).

Experimental Values of the Constant k in the Expression $e = k\,\mathrm{DT}(1 + 0{\cdot}0065\,t)$.

D=0·012 cm. 40 S.W.G.

L	1	7	14	22	29	43	58
t	9	62	124	195	257	380	514
DT.	k.	k.	k.	k.	k.	k.	k.
0·150	4·0	4·1	4·5	4·4	4·5	5·0	5·0
0·300	5·1	4·9	4·9	4·7			
0·450	5·4	5·0	5·0				
0·600	5·4	4·9	4·8				
0·750	4·9						

The mean value of k computed from this table is 4·9. The approximate expression is thus

$$e = 4{\cdot}9\ \mathrm{DT}(1 + 0{\cdot}0065\ t)$$

within the limits of 0–1·05 for DT, and 10–500 kg. per sq. cm. for t, for values of D of 0·071, 0·037, 0·023, and 0·012 cm.

The wires are apt to break for values of e greater than 3–4 per cent., though elongations of as much as 12 per cent. have been obtained.

Changes in Diameter.

Concurrently with the elongation of the wires that occurs on twisting, a decrease occurs in the diameter as measured by a screw gauge; but this decrease of diameter is less than would be required to maintain constancy of volume, and the density calculated from these measurements therefore shows a decrease which may be as much as 1 per cent. after severe twisting. The decrease of density actually observed, using a density bottle, with six specimens of wire on twisting severely, was only one-third per cent. (mean relative density at 25°/4° C. of the untwisted wire 8·93; of the twisted wire 8·90). This discrepancy finds a ready explanation in the regular distortion of the surface of the wire that occurs on twisting into fine parallel spiral ridges and depressions; the diameter measured by the gauge is, of course, that of the ridges. An examination of these spirals, which present a beautiful effect when viewed microscopically, shows that the twist distributes itself fairly uniformly along the wire.

Annealing.

In the case of fine wires of soft drawn copper, the necessary winding after the wire leaves the annealing furnace is known to harden the wire. In order to see if the wire to be used was quite soft, a skeleton series of twist-extension experiments was made on each "gauge" of wire used, first as purchased, and then after annealing in oil for 15 minutes at 300° C. and cooling slowly[6]. No differences were found in the results, except in the case of the finest wire used (diameter 0·012 cm.), which for the same twist showed increased elongations after annealing. Hard drawn copper wire under small tensions shows a contraction in length on torsion which may be as much as 1 per cent. As a check on the efficacy of the annealing, a length of hard drawn copper wire annealed with the soft drawn copper gave subsequent results on twisting identical with those of the soft drawn copper. In the main series of experiments the wires were used as purchased, with the exception of the finest wire, which was annealed as described above before use.

Accuracy of the Results.

Repetition of some of the measurements showed that the elongations of different portions of wire from the same coil, under the same tension for a given twist, did not vary by more than one part in twenty; the variation was usually much less than this.

Preliminary Experiments made to detect some possible Causes of Error.

Andrade (*loc. cit.*), referring to wires of lead and soft drawn copper, remarks: "Large preliminary strain whether of extension or rotation puts the wire in a state to flow viscously" (under tension). In order to see if the highly-twisted wire commences to flow viscously at a rate that would affect the elongation sensibly, a soft drawn copper wire of diameter 0·0375 cm. was loaded to 1·020 kg. per sq. cm. and twisted to 2·5 turns over cm. (nearly to its breaking-point). The extension produced by this twist was 6·45 per cent., whereas the subsequent extension observed under this tension without further twisting was only 0·01 per cent. after 1 hour and less than 0·02 per cent. after a further 12 hours.

Experiments were also made to ascertain whether within the range of rates of twist employed the elongation is a function of the *rate* of twisting. Some of the results obtained are given in Table IV. (using the notation of the previous tables).

TABLE IV.

Twist—Elongation Measurements for different Rates of twisting.

L=780 grams, t=195 kg. per sq. cm., D=0·0715 cm. Length of wire 1·75 metres.

Rate of twisting (turns per cm. per second).	0·038	0·0038	0·00038
T.	*e.*	*e.*	*e.*
1	1·06	1·10	0·98
2	1·97	2·00	1·89
3	2·86	2·90	2·76
4	3·80	3·84	3·65
4·9.....	4·64	4·69	4·47

These differences are barely significant.

These experiments seem to show that (at room temperatures), within the range of tension and rate of twist employed, the elongation is a function merely of the torsion and the tension applied to a given wire.

This work is being continued, and extended to include the study of twist similarly in other materials under various conditions, with, among other objects, that of ascertaining whether definite family relationships reveal themselves between metals of which the structures are known from X-ray analysis to be similar.

The experiments which initiated this work were carried out at the suggestion of W. S. Denham, D.Sc., F.I.C., Director of Research of the British Silk Research Association, to whom I am greatly indebted for helpful advice.

References.

(1) Ercolini, *N. Cimento*, xi. p. 43 (1906).
(2) Poynting, Proc. Roy. Soc. A, lxxxii. p. 546 (1909).
(3) Poynting, Proc. Roy. Soc. A, lxxxvi. p. 534 (1912); or 'Collected Papers,' Cambridge University Press, 1920.
(4) Tammann, 'Text-Book of Metallography,' p. 81. Chemical Catalogue Co., New York, 1925.
(5) Andrade, Proc. Roy. Soc. A, xc. p. 336 (1914).
(6) Beilby, Phil. Mag. ser. 6, vol. viii. p. 262 (1904).

LXXIX. *The Magnetic Properties of some Compounds of Manganese.* *By* L. F. Bates, *B.Sc., Ph.D., Senior Lecturer in Physics, University College, London* *.

FERROMAGNETIC materials have recently assumed great importance from the point of view of theory and of practical application, and it is desirable to have full information on all such substances which may be artificially prepared. It is intended in this paper to report further upon the properties of two simple compounds of manganese, namely a compound of manganese and phosphorus and a compound of manganese and arsenic, whose compositions may be respectively taken as MnP and MnAs to a very close degree of approximation. Experiments with the arsenic compound (Bates, Proc. Roy. Soc. cxvii. p. 680, 1927) have shown that it is ferromagnetic with a magnetic critical point at 45° C. It is characterized by very pronounced thermal changes in the region between 38° and 45° C. It also exhibits a temperature hysteresis, for, although it loses its ferromagnetic properties at 45° C., these properties do not reappear until a temperature of 34° C. is reached. The phosphorus compound has been investigated by B. G. Whitmore (Phil. Mag. vii. p. 125, 1929). It possesses a magnetic critical point, not so sharply defined as that of the arsenide, below 40° C., but its thermal changes are very much less pronounced and it does not exhibit a temperature hysteresis. Both substances have been prepared in the form of powders, but the arsenic compound possesses very definite crystalline characteristics.

Ferromagnetic Properties.

For the measurement of the magnetic properties of the substance in fields of various magnitudes the usual magnetometer method was employed. The substance was placed in a copper tube 22 cm. long and 0·508 cm. in diameter. The tube was fitted with copper plugs, so that the length of tube occupied by the magnetic specimen was 20 cm. Brass rods could be attached to these plugs, so that the specimen could readily be mounted axially in a

* Communicated by Prof. E. N. da C. Andrade.

vertical water-cooled solenoid. In order to facilitate the maintenance of a steady temperature around the specimen, a glass tube 3·5 cm. in diameter was mounted inside the solenoid. Guide rings were provided so that the specimen could be accurately placed in position at any time. The solenoid consisted of eight layers of No. 18 S.W.G. double cotton-covered wire ; its internal diameter was 4·15 cm., its external diameter 5·99 cm., and in all 2415 turns were wound on a length of 40 cm. The field acting on the specimen was calculated from the formula given by Adelsberger (*Ann. der. Phys.* lxxxiii. p. 186, 1927).

The magnetometer was adapted from an excellently made piece of apparatus designed by Carey Foster for his projected determination of the standard ohm. It was provided with two vertical coils each of 20 layers of 20 turns per layer, the mean radius of the inner layer being 17·58 cm., the mean radius of the outer layer 18·91 cm., and the centres of the coils 18·28 cm. apart. The magnetic system and mirror were suspended by a fine silk fibre. The whole possessed considerable moment of inertia to counteract the effects of small stray fields of a temporary nature. The effect of the field of the solenoid on the system was neutralized by the suitable adjustment of three circular coils wound with the same wire as, and in series with, the solenoid. Two of the coils were about a foot in diameter, and the other 4 inches in diameter. On placing a demagnetized specimen in the solenoid, the magnetizing current was switched on and the resulting magnetometer deflexion was immediately neutralized by sending an appropriate current through the magnetometer coils. This current was measured on a calibrated millivoltmeter shunted by a suitable resistance. With practice, a complete series of measurements could be taken very quickly without appreciable heating of the solenoid, even when a maximum current of 10 amperes was used.

Fig. 1 shows one-half of a typical hysteresis cycle obtained with a specimen of the arsenide when surrounded by melting ice. It will be observed that even with a field strength of 760 gauss, saturation is by no means attained. In this experiment the powder was tightly packed, so that the density of the packing was 3·68 gm. per c.c. The maximum value of the intensity of magnetization attained was 203·2 c.g.s. units. Hence the value of the maximum magnetic moment per gm. of arsenide in this experiment

was 55·1 units. Hysteresis curves were also obtained when the specimen was at room temperature and when at the temperature of liquid air, the latter condition being obtained by mounting the specimen inside an elongated Dewar flask, containing liquid air, placed inside the solenoid. In the latter case the magnetization for the same maximum field was increased to 220·2 units, the curve being of almost identical shape, with a trifle less hysteresis.

The magnetic properties of the phosphide were not so pronounced as those of the arsenide; the hysteresis was

Fig. 1.

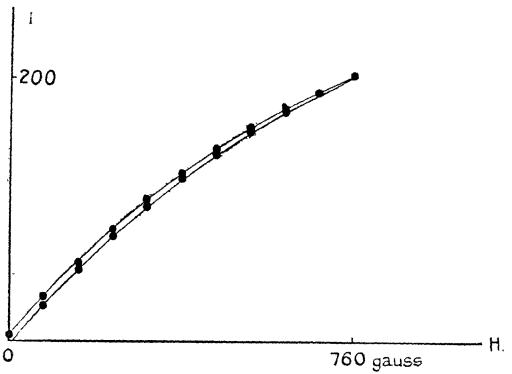

very small, and, as shown in fig. 2, the maximum intensity of magnetization for a field of 760 gauss and a packing of 2·24 gm. per c.c. was 24·0 c.g.s. units; *i. e.* under these conditions the maximum magnetic moment was 10·7 units per gm.

Properties above the Critical Temperature.

All previous work on the magnetic properties of these compounds has been confined to temperatures below or only slightly above the magnetic critical point. Above this point the compounds are strongly paramagnetic, and

a preliminary investigation, kindly carried out for me by Mr. B. G. Whitmore, showed that the chemical balance method would be the most satisfactory with the apparatus at our disposal. The arrangement of the apparatus is shown in fig. 3.

An outer copper vessel of the shape depicted in section in fig. 3 was placed with the lower portion between the poles of a Du Bois electromagnet, whose circular pole pieces were 8 cm. in diameter. The diagram is approximately drawn to scale, the vessel being 7 cm. wide and 12 cm. long. It was suitably lagged with cotton-wool and

Fig. 2.

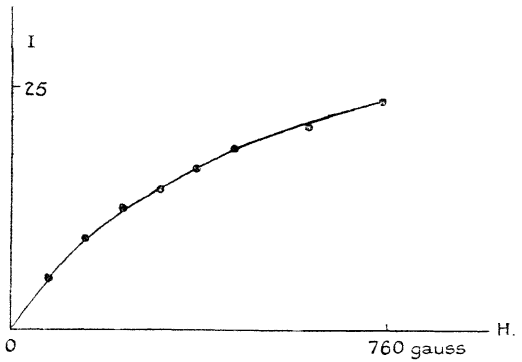

cardboard, and provided with a wooden cover. A rectangular copper tube, soldered in a vertical position in the middle of the vessel, provided a chamber in which the specimen could be suspended. The material was packed inside a uniform copper tube, the lower end of the tube being closed by a thin copper disk, and the upper end by a small copper plug. Copper has obvious disadvantages for such work, but it was felt that uniformity of temperature and easy passage of heat were so important that copper was used. Preliminary experiments showed that the magnetic effect of the copper tube in air was quite negligible compared with the magnetic effect of the material it

contained at all temperatures at which measurements were made. To the upper end of the tube was soldered a loop of copper wire with a stiff wire ending in a hook, so that it could be attached to the lower end of a long

Fig. 3.

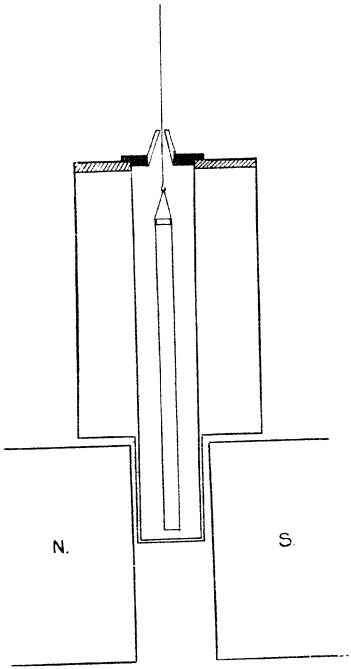

straight brass wire suspended from one arm of a sensitive balance. The hooked wire passed through a soapstone guide, consisting of a suitably bored gas-burner fitting, mounted in a cork plug fitted to the top of the copper chamber. When powerful magnetic fields were used, there was some tendency of the specimen to lateral motion,

and the guide served occasionally to maintain it in its undisplaced position with a minimum of frictional resistance to vertical motion. The outer vessel was filled with B.P. paraffin, which was electrically heated and very efficiently stirred with a centrifugal stirrer. The temperature was measured by a mercury thermometer, placed inside the chamber with its bulb close to the lower end of the specimen. For purposes of temperature control a similar thermometer was placed in the oil. The copper vessel of fig. 3 was used only for measurements up to 163° C. For higher temperatures an electric furnace was used; it consisted of a copper tube 15 cm. high, whose internal and external diameters were 2·5 and 4·5 cm. respectively. The temperature was measured as before and could easily be kept constant to 0·1° C.

We have seen that it was not necessary to apply a correction for the magnetic effects of the copper tube. Experiment also showed that the magnetic effect of the air displaced by the specimen might also be neglected. Hence, as the substance is paramagnetic, on exciting the electromagnet so that a field H is established at the lower end of the specimen and a very much weaker field H_0 at the upper end of the specimen, the specimen experiences a downward force given by

$$W = \tfrac{1}{2} . K . \alpha . (H^2 - H_0^2),$$

where K is the susceptibility per c.c. of material, and α the area of cross-section of the specimen. For our purposes it is more satisfactory to express the force in terms of the susceptibility per gm. of the substance. If, then, there are m gm. of the substance in 1 c.c. and the length of the tube occupied by the substance is l, we may write

$$W = \frac{1}{2} . K . \frac{m . \alpha . l}{m . l} (H^2 - H_0^2) = \frac{1}{2} . K_m . \frac{M}{l} . (H^2 - H_0^2),$$

where K_m is the susceptibility per gm. and M is the total mass of the substance. The weights used in the determination of W were calibrated by the method of Pienkowsky (Bur. of Standards Comm. xxi. p. 65, 1916). The magnetic fields were measured by a Grassot fluxmeter, which was usually shunted so that one division on the fluxmeter scale was equivalent to a change of 38·43 lines of force per sq. cm. Corrections were, of course, applied

for the residual fields when the electromagnet was not excited.

Results for Manganese Arsenide.

In the experiments on the arsenide a copper tube of internal diameter 0·506 cm. was used, the length of tube

Fig. 4.

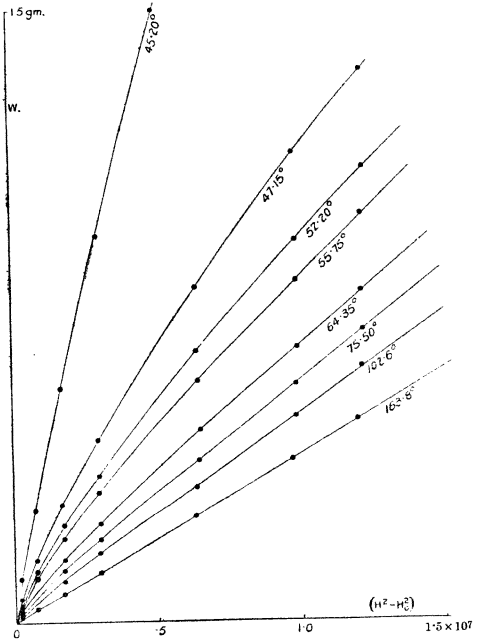

occupied by 8·535 gm. of the substance being 10·95 cm. The behaviour of the material is shown by figs. 4, 5, and 6, in which each curve represents the values of W plotted against $(H^2-H_0^2)$ at a given temperature, *i. e.* each curve is an isothermal. It will be noted that the curves are all

concave towards the axis of $(H^2 - H_0^2)$ until a temperature in the neighbourhood of 92° C. is attained, after which all isothermals, up to the highest temperature investigated, are straight lines passing through the origin. For the sake of clearness, the isothermals in figs. 5 and 6 have been

Fig. 5.

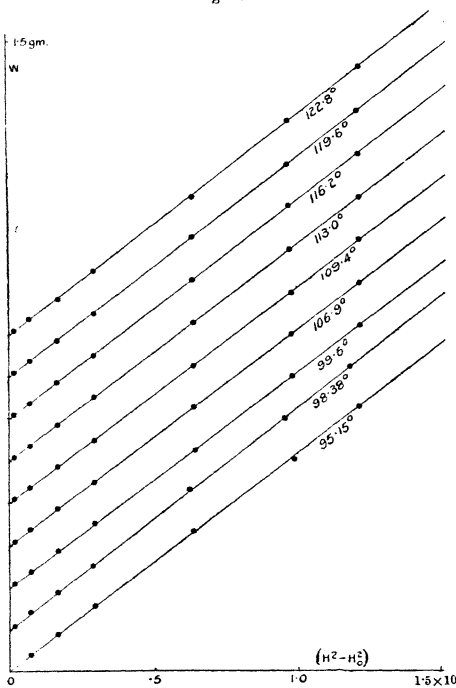

drawn with ordinates displaced upwards. It is clear from fig. 6 that a transition is occurring in the temperature region between 90° and 130° C., for here the isothermals have practically the same slope. Their behaviour is perhaps rendered more clear by reference to fig. 7, where

the force for a value of $(H^2 - H_0^2)$ equal to $1{\cdot}195 \times 10^7$ units is plotted against the temperature. It will be observed that the force is practically constant over the temperature range from 92° to 130° C., and it is rather surprising that the isothermals in this region should be straight lines.

Fig. 6.

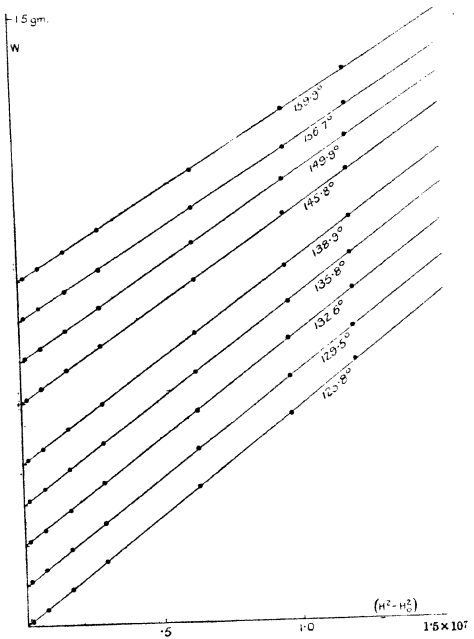

Curves similar to fig. 7 could, of course, be given for other values of $(H^2 - H_0^2)$, but no further point of interest has been noted to justify their inclusion here. It should be stated that the points plotted in fig. 7 were obtained in a definite sequence. Each point, of course, represents a value obtained from a separate isothermal. Only a few

such isothermals could be obtained on one day, and as it was thought that the preliminary experiments indicated the occurrence of some permanent change, in addition to the temperature hysteresis already described, when the substance was heated above about 70° C., the isothermal for the temperature nearest the critical point was first obtained, after which the isothermals for successive higher

Fig. 7.

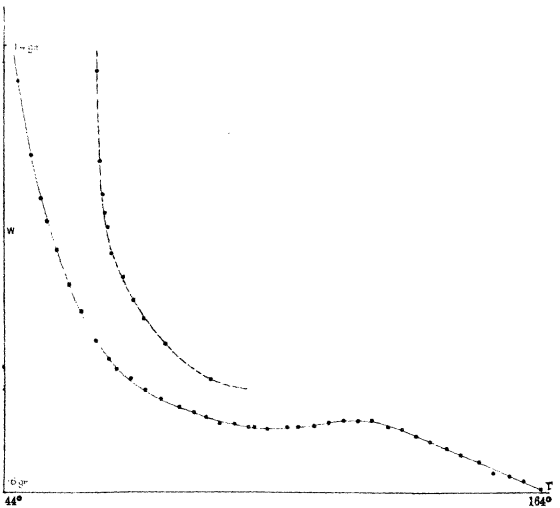

temperatures were obtained. The danger of permanent change, however, seems to have been somewhat overestimated. This is, perhaps, sufficiently clear from the orderly arrangement of the points in fig. 7, for some of the consecutive points were obtained from isothermals recorded at different times separated by intervals of some days. In addition, a series of experiments was carried out at the close of the above series of experiments to test directly for permanent changes. The specimen was heated to 55° C. and the force for a known field was obtained. It was then

heated to 100° C., cooled to room temperature and again heated to 55°, when the force was again recorded. This process was repeated several times. The first reading was always a very little greater than subsequent readings, but the latter were always the same within the limits of experimental error and on different days.

In view of the temperature hysteresis, it was considered of interest to obtain a set of isothermals for the substance when it was first heated to 100° C. and then allowed to cool to temperatures down to 34° C. Between 58° and 34° C. eleven such isothermals were obtained. They are not reproduced here, it being sufficient to mention that they showed a marked similarity to the isothermals for temperatures below 92° C., shown in fig. 4. For the sake of comparison the force is plotted against temperature for the same value of $(H^2-H_0^2)=1{\cdot}195\times10^7$ units, in the broken curve of fig. 7, the abscissæ of the curve being displaced by 30° for convenience in plotting. It is seen that as the point at which ferromagnetism is regained is approached, the rate of increase of the force is rather greater than the rate of decrease shown by the smooth curve of fig. 7. This is the more noteworthy as experimental error would tend to cause a reverse state of affairs.

For assistance in the discussion of results, the reciprocals of the forces shown in the initial portion of the smooth curve in fig. 7 have been plotted against temperature in fig. 8. It is clear from the isothermals and from fig. 8 that below 92° C. the substance does not possess a paramagnetic susceptibility independent of the field, and between 92° and 130° C. we have a susceptibility which is practically independent of the temperature and independent of the field. In fig. 9 are plotted the values of $1/K_m$ for temperatures between 130° and 370° C. We see that the graph is approximately a straight line. In other words, in this region the substance obeys the Weiss law, which may be written

$$K_m=\frac{M^2\,.\,z^2\,.\,\mu^2}{3\,.\,M\,.\,R}\cdot\frac{1}{T-\theta}=\frac{C}{T-\theta},$$

where M is the molecular weight of the substance, μ the magnetic moment per molecule, θ a temperature characteristic of the material, R the gas constant, and T the absolute temperature. This may be rewritten

$$M\,.\,z\,.\,\mu\,.=\sqrt{3\,.\,M\,.\,R\,.\,K_m}\;\sqrt{T-\theta}.$$

Fig. 8.

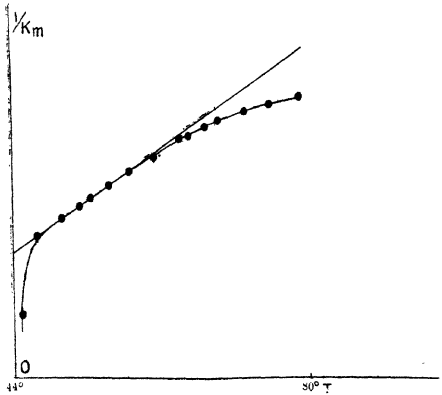

Fig 9.

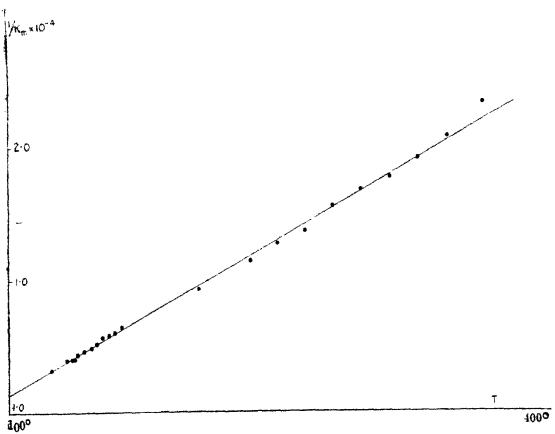

From fig. 9, θ was found to be 274·5° abs., and the value of K_m at 636° abs. was taken as $4{\cdot}675 \times 10^{-5}$ c.g.s. unit per gm., whence $M{\cdot}z{\cdot}\mu = 2{\cdot}34 \times 10^4$ c.g.s. units or 20·83 Weiss magnetons, or 4·2 Bohr magnetons, per gm. mol.

A tangent was also drawn as shown in fig. 8, and θ here was found to be 294·1° abs. and $M.z.\mu$ was 3·87 Bohr magnetons per gm. mol. Of course these particular values are unreliable, and are only included here for the sake of completeness. It is interesting that the two results for $M.z.\mu$ are so close. We are singularly reminded of the behaviour of Feβ and Feδ, which have the same structure, but it would be unwise to attach too much importance to this resemblance.

It now remains to calculate the value of the factor ν by which the intensity of magnetization of the specimen must be multiplied in order to obtain the value of the Weiss internal field. This may be obtained from the expression $C = \theta/\nu\rho$, where C and θ have the same meanings as before, and ρ is the density of the substance, which at room temperature is 6·02 gm. per c.c. From fig. 8 the value of ν is 3390 and from fig. 9, 2700. It must be emphasized that we have used the value of the density at room temperature in both calculations, so that the results, particularly the second, must be regarded as approximate only. Their order of magnitude is, however, quite in accord with the values of ν obtained for other ferromagnetic substances.

Results for Manganese Phosphide.

In the experiments on the phosphide a similar copper tube was used, the length of the tube occupied by 5·884 gm. of the powder being 11·7 cm. Once again the preliminary experiments showed the magnetic effect of the copper tube to be negligible, and again the magnetic effect of the air could be neglected. Isothermals up to 140° C. were obtained with the apparatus of fig. 3, and up to 265° C. with the electric furnace. The isothermals for 36·1° C. and for all higher temperatures were straight lines, within the limits of experimental error, and the isothermals for 31·95° and for 34·05° C. were not very markedly curved. There was no sign of permanent change or of temperature hysteresis. Fig. 10 shows some of these isothermals.

Fig. 11 shows the behaviour of the reciprocal of the susceptibility with temperature. There appears to be a

slight discontinuity about 135° C., but it is doubtful if it has any real significance, for, as we have seen, the experimental arrangements were completely changed at this juncture and the magnetic field completely altered, so that

Fig. 10.

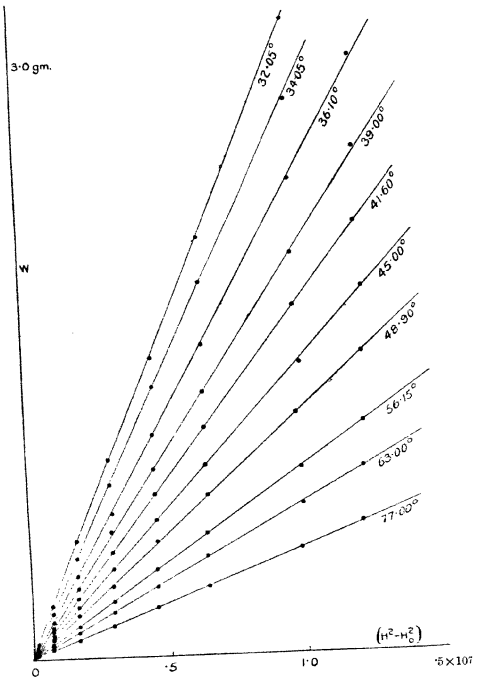

there is a distinct possibility that a slight discontinuity may enter into the work here. From fig. 11 it was found that for $(H^2-H_0^2)=1{\cdot}477\times10^7$ units the downward force when the temperature was 300°C. was 0·1188 gm., and θ was found to be 42° C. Hence, at 300°, $K_m=3{\cdot}137\times10^{-5}$ c.g.s.

unit, so that $M.z.\mu$ is equal to 11·83 Weiss magnetons or 3·69 Bohr magnetons per gm. mol. The factor ν for the Weiss internal field is found to be 8080, the density of the substance at room temperature being 4·82 gm. per c.c. The value of the factor is in good accord with the values for the arsenide, when the properties of the two substances are remembered.

Discussion of Results.

A considerable amount of attention has recently been paid to the theoretical aspect of ferromagnetism; in

Fig. 11.

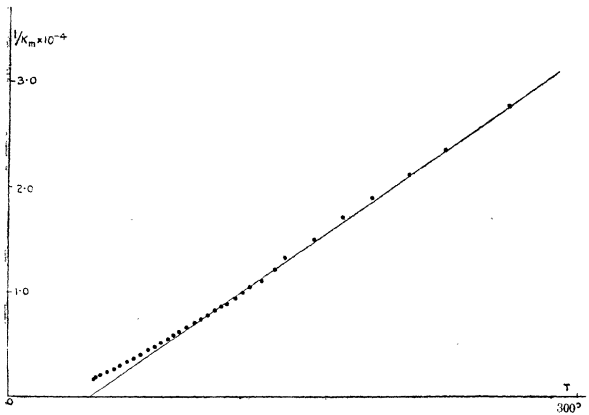

particular, a theory based on the conceptions of wave mechanics has been advanced by Heisenberg (*Zeit. f. Phys.* xlix. p. 619, 1928). This theory has been discussed by Fowler and Kapitza (Proc. Roy. Soc. cxxiv. p. 1, 1929) and extended to account for magnetostriction and the large changes in specific heat which occur at the magnetic critical point. Fowler and Kapitza show that if a ferromagnetic substance contains one magnetizable electron per atom, then the theory requires a "step-down" in the value of the specific heat at constant volume by an amount approximately equal to a little less than 3 calories per gm. mol. as the temperature rises through the magnetic critical

point from below. In support of this view they quote the results for nickel obtained by Weiss and his collaborators. The more recent and more accurate results of Potter and Sucksmith (Proc. Roy. Soc. cxii. p. 157, 1926) also support the conclusions, viz. that the results for nickel fit the theory. The available data for iron and magnetite, however, do not fit, and it is therefore concluded that for these substances a theory based on the presence of two or three magnetizable electrons per atom is required. Such a theory has not been worked out, but Fowler and Kapitza consider that it would differ only from that already given in complication of detail, and would give a "step-down" in specific heat respectively two or three times as great as that given in the single electron theory, and thus be in agreement with the experimental values. This generalization, however, cannot always be permissible, for the writer has shown (Bates, *loc. cit.*) that 1 gm. of the arsenide requires 1·79 calories to enable it to change from the ferromagnetic state at 36° C. to the paramagnetic state at 45° C. The so-called "step-down" in the specific heat at the magnetic critical point is roughly 0·9 cal. per deg. per gm., or 120 cal. per deg. per gm. mol. If the above generalization is correct, the number of magnetizable electrons must be of the order of 40 per molecule, which is very unlikely. Of course the huge heat changes may be brought about by a change in lattice structure, and here the results of an X-ray examination will be of interest. The experimental evidence above the magnetic critical point indicates that 4 Bohr magnetons and not 40 are associated with 1 gm. mol.

When we try to picture the processes which are here in operation, we have to remember that we must explain the disappearance of ferromagnetism at 45° C., the very slight variation of magnetic susceptibility with temperature between 92° and 130° C., and the very pronounced temperature hysteresis. We ought, perhaps, to treat the hysteresis phenomena in two portions, but this seems scarcely necessary in a preliminary discussion without the benefit of X-ray analysis. We may imagine that ferromagnetism arises through the association of atoms in groups as outlined by Stoner, or as a regular distortion of the crystal lattice as viewed by Derflinger and Ewald, or through the forces between electrons which are described as homopolar valency forces by Heitler and London. At the magnetic

critical point the groupings, or distortions, and the forces disappear. The crystal remains intact, of course, because these forces are only a fraction of the total forces which hold the crystal together. It follows that the elastic constants of the crystal should change as one passes through the magnetic critical point, and steps will be taken to investigate this with the arsenide. In the case of the arsenide it is clear that the groupings and the forces are not always re-established when the initial temperature conditions are restored. This means that at least two stable groupings are possible, or that the disappearance of ferromagnetism is accompanied by a change in position of some constituent of the crystal which has two or more stable positions of equilibrium. Now, in the case under discussion, we have, comparatively speaking, tremendous changes, between 36° and 45° C., but above 45° C. the magnitude of the specific heat does not excite comment. Hence any change in grouping is probably almost complete at 45° C., and further changes are likely to be only slight. However, these slight changes are accompanied by hysteresis phenomena. It is suggested here that these are due to the disturbing effects produced by loosely bound particles, each of which may occupy several positions of equilibrium. Let us consider two regularly formed crystal layers of atoms separated by certain loosely bound particles which constitute a crystal boundary, a conception which is based upon that given by Prandtl in his explanation of elasticity hysteresis. We may further consider that these particles themselves contribute little or nothing to the magnetic moment of the specimen, but they are entirely responsible for the occurrence of hysteresis. The loosely bound particles may be taken to come into play when the substance is passing through the magnetic critical point. From the evidence of hysteresis curves taken when the maximum temperature to which the specimen is heated is higher or slightly lower than the critical temperature, it is clear that several equilibrium positions of the loosely bound particles must be possible. When the ferromagnetic groupings have broken down, the loosely bound particles take up positions of great stability, so that the reconstruction of the groupings on cooling is impossible, until conditions are such that the particles are able to move to positions of lower potential energy, where they cannot affect the reconstruction of the groups. This is sufficient

to explain the hysteresis phenomena observed when we heat the substance to slightly over 45° C., and, clearly, little difficulty lies in the way of the extension of this idea to explain the hysteresis phenomena at higher temperatures, for there appears to be no difficulty in the way of extending the number of positions of equilibrium.

The behaviour of the substance between 92° and 130° C., however, calls for further comment. The susceptibility over this range of temperature may be regarded as approximately constant, and we are led to compare its behaviour with that of potassium bichromate in the solid form and in solution (*cf.* Weiss and Mlle Collet, *Comp. Rend.* clxxviii. p. 2146, 1924; and clxxxi. p. 1057, 1925), and of solutions of luteocobaltic chloride. To explain the constancy of these paramagnetic susceptibilities with temperature, Weiss has suggested that in these cases the resultant magnetic moments of all the electron orbits in the molecules are zero, and that constant magnetic susceptibility is due to an orientation of some kind in which only a portion of an atom is involved, and must therefore be regarded as an intra-atomic phenomenon. If we may extend this argument to manganese arsenide, then presumably an internal electron arrangement in the manganese atom would be responsible for the constant paramagnetism. The presence of loosely bound particles places no difficulties in the way of the Weiss explanation.

It remains to consider what constitutes the above-mentioned loosely bound particles. A possible conjecture is that they are atoms of arsenic. The mode of formation of the substance would certainly appear to lend itself to the production of such loosely bound particles of arsenic, which should themselves neither contribute to the magnetic susceptibility nor give rise to appreciable temperature variations.

When we consider the results for manganese phosphide, we have the results of Whitmore (*loc. cit.*), which show that there is no very pronounced change in specific heat at the critical point. We should have expected, according to Fowler and Kapitza's arguments, a much greater change of specific heat, although it may be urged that only one atom in each ferromagnetic grouping possesses a resultant magnetic moment. Since 3·69 Bohr magnetons per gm. mol. are associated with the phosphide, we may perhaps consider that only about one in every two manganese

atoms contributes to the magnetic moment. Even this, however, would require a much more pronounced change of specific heat than is actually observed. The behaviour of the isothermals below 40° C. at first occasioned some surprise, but actually the fact that the isothermals are straight lines before this temperature is reached really means that the magnetic critical point is well below that temperature. Whitmore's curve of magnetic induction with temperature shows that $I.dI/d\mathrm{T}$ is a maximum at 17° C., and the ferromagnetic properties must disappear below 30° C. We are, in fact, dealing with a very weakly ferromagnetic substance which becomes very strongly paramagnetic above the magnetic critical point, and the curve of magnetic induction with temperature, for a given field, is liable to misinterpretation.

Further experiments with these substances are contemplated and are already in hand. Firstly, a complete X-ray examination over a wide range of temperature is to be carried out. Secondly, steps will be taken to obtain a large single crystal of the arsenide, to test its directional properties and the variation of the elastic constants in the neighbourhood of the magnetic critical point.

Summary.

Observations have been made of the magnetic properties of two simple compounds of manganese, a phosphide and an arsenide, at temperatures above their magnetic critical points, where both substances are strongly paramagnetic. In the case of the arsenide the susceptibility is practically constant over a range of temperature from 90° to 130° C., after which the Weiss law is obeyed. The nature of the temperature hysteresis which this substance exhibits is discussed, and an explanation based on the presence of loosely bound particles of arsenic is put forward. In the case of the phosphide the Weiss law is approximately obeyed.

The writer has already acknowledged his indebtedness to Mr. B. G. Whitmore for assistance in the early stages of the work. It remains for him to express his deep appreciation of the kind and helpful interest which Professor E. N. da C. Andrade has taken in these experiments.

Carey Foster Laboratory,
University College, London.

LXXX. *Some Factors governing the Magnitude of Frictional Electric Charges. By* P. A. MAINSTONE, *M.Sc., Lecturer in Physics in the University College of North Wales* *.

IN recent measurements of frictional electricity attempts have been made to control the actual conditions of rubbing, and to reduce the number of unknown factors to a minimum.

Shaw [1] established a frictional series, and investigated the effects of temperature variation, flexure of the rubbing surfaces, changes in the mechanical nature of the surfaces, etc. The effect of the surrounding medium must clearly be an important factor, and the first investigation of this nature was made by J. H. Jones [2], who measured the maximum charge produced on a given specimen in various gaseous and liquid media. He found that in the case of gaseous media the charge generated in air was greater than in any other gas except sulphur dioxide. It appears doubtful, however, whether the gases used in these experiments were entirely free from moisture, and the action of moisture in reducing the magnitude of frictional charges is well known. Vieweg [3] drew up a frictional series including a number of crystalline substances and discussed the order of various elementary substances in the series. When two surfaces are rubbed together, that surface whose atoms or molecules give up electrons more readily becomes positively charged with respect to the other. Thus atoms with low ionization potentials should lie at the positive end of the series, those with high potentials at the negative end. Several metals included in the series conformed to this order. Vieweg also made an exhaustive examination of the effect of water vapour, and found that it produced an additional positive charge on each of the rubbing surfaces. A surface normally negative had its charge reduced when moisture was present, and if the normal charge was small, its sign might even be reversed. This effect might explain some of the apparent anomalies often observed. Macky [4], using various insulators rubbing on polished metal surfaces, examined the effect of the surrounding medium, and was the first to observe the effect of varying the gas pressure. The charge

* Communicated by Prof. E. A. Owen, M.A., D.Sc.

generated by a given rubbing process diminished as the pressure was reduced until at a pressure of 1 or 2 mm. it had dropped almost to zero. This effect was observed in all the gases used, but no appreciable differences between the magnitudes of the charges in the different gases was noted.

The present research was undertaken with a view to measuring the frictional charges produced by a very small amount of mechanical work, and also to investigate the effect of the surrounding medium.

Apparatus.

The first apparatus used consisted of a brass tube about 45 cm. in length and 5 cm. in diameter, along the axis of

Fig. 1.

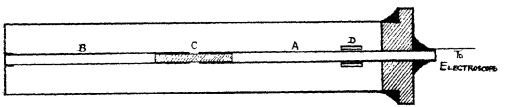

A. Insulated Rail.
B. Earthed Rail.
C Ebonite Bridge.
D Sliding Rubber.

which was fixed either a circular brass rod or a narrow flanged brass strip. The rod or strip was divided into two portions which were bridged by ebonite, one portion being insulated while the other was earthed. Fig. 1 makes the arrangement clear. The tube was arranged to tilt about a horizontal axis at one end so that a rubbing substance could move under gravity along the central rod or strip. A silk-wound bobbin was used in one case, and a small piece of plate glass in the other. The arrangement of the tilting tube was such that the insulated portion of the insulated rod lay uppermost, and this was connected to the measuring electroscope. Starting with the rubber at the end of the insulated portion (see fig. 1), both being at zero potential, and the tube horizontal, sufficient tilt was given to the tube for the rubber to slide down with as little acceleration as possible. When the rubber passed over

from the insulated to the earthed portion of the rod, a deflexion of the electroscope was observed. Contact with the earthed rod was found sufficient to discharge the rubber, and no ionizing agent was necessary.

The tilting tube was connected by rubber pressure tubing or a horizontal glass taper joint to the usual vacuum apparatus. Gas pressures from atmospheric pressure down to about 1 cm. were read by a vertical mercury column, and lower pressures by a McLeod gauge. A hand-worked oil pump served to evacuate down to about 1 mm. and lower pressures were obtained by the use of charcoal and liquid air.

Considerable potentials were developed even when the amount of mechanical work was made extremely small. The mass of the rubber was reduced to a few grammes, and the length of the insulated rod to a few centimetres. The potentials, which were measured on a quadrant electrometer, were generally of the order of 10 to 20 volts.

The effect of water vapour in the apparatus was always very pronounced. Brass, when rubbed by either silk or glass, acquires a negative charge, but the magnitude of the charge increases considerably when the surrounding atmosphere is made perfectly dry. In the present experiments the apparatus always contained phosphorus pentoxide, and the contained gas was always left for a sufficient time for all water vapour to be completely absorbed.

The charge per single rub was generally found to increase with the number of previous rubs until a steady value was reached. This effect has been observed by most other experimenters, and is considered by some to be due to a surface flow of molecules in the rubbed specimens. From the present measurements, however, it would appear probable that the effect is largely due to adsorbed gas films on the rubbing surfaces. This point will be referred to again later.

The effect of varying the gas pressure was not very marked, or was probably masked by other spurious effects. There were indications, however, of a reduction of charge at pressures of a few millimetres, with a subsequent increase at very low pressures.

The brass rod used in these measurements was rubbed with fine glass or emery paper before being fixed in position. The silk-wound bobbin was cleaned in a boiling

solution of powdered soap and common soda, well washed, and dried. On removal from the apparatus after measurements had been made, the silk was always found to be considerably soiled. Such rubbing surfaces are clearly very indefinite. The preparation of a metal surface by distillation *in vacuo* would be a marked improvement in the measurement, but in the present experiments the practical difficulties are considerable. In Macky's work small hand-polished surfaces, approximately plane, were used, and on the publication of this work the apparatus was modified to make the use of polished surfaces possible, while still employing the principle of moving the rubber from an insulated to an earthed surface.

The new friction chamber consisted of a brass cylinder 10 cm. in length and 8 cm. in diameter. This was closed at the ends by overlapping brass disks, and the joints were rendered airtight by picein wax.

The first metal used was brass. Three short lengths were cut from rod 1·8 cm. in diameter. Two were turned down to equal length, while the third was made somewhat shorter, the difference corresponding to the thickness of a small ebonite block on which this particular specimen was intended to rest. When the two longer specimens were fixed directly to a flat metal surface, while the shorter stood on its insulating block which in turn rested on the same flat surface, the upper surfaces of the three specimens could be rubbed down together on emery paper, and then polished accurately in one plane.

The arrangement of the three specimens in the friction chamber is shown in fig. 2, in which two sections at right angles are given. The shorter specimen A and a longer one B were mounted in this way as close together as possible, so that the rubber, usually a glass disk, could move across from one to the other without jolt. The third specimen C was used merely to render easier the polishing process, and played no part in the measurement of charge. In the first measurements the three specimens rested on the base of the chamber itself, B and C being always earthed, while A was insulated and connected to the measuring electroscope. In later measurements, however, the specimens were mounted on a small brass base which rested in a fixed position on the base of the chamber, and which could be removed through a window without opening the entire chamber.

The rubber consisted of a small glass disk of good optical quality. Above this was attached by wax a small block of ebonite. This enabled the rubber to be moved across from A to B by a metal arm operated from outside the chamber by the use of a glass taper joint. Fig. 2 makes the arrangement clear. The amount of travel of the rubber was made definite by attaching to the upper (male) portion of the taper joint a horizontal arm moving between fixed stops. These were arranged so that the rubber moved from a symmetrical position on the specimen A to a corresponding position on B. The distance of

Fig. 2.

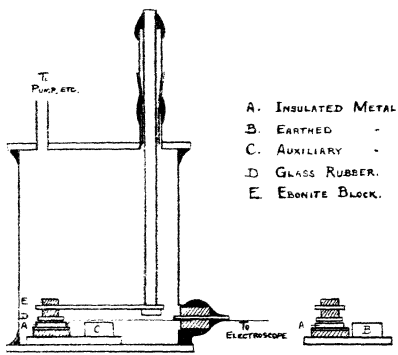

travel was thus about 2 cm. The mass of the entire rubber was 2·5 grams.

The charge was measured on a gold-leaf electroscope used with the leaf system insulated and a potential of about 100 volts on the case. The sensitivity was 1·4 eyepiece divisions per volt. It was generally found necessary to increase the capacity of the apparatus in order to restrict the potentials to suitable values. This was done by the use of cylindrical air condensers. In the case of glass rubbing on metals a total capacity of about 300 cm. restricted the maximum potentials to about 20 or 30 volts.

Results.

The procedure in all the measurements was to fill the apparatus with air or other gas almost to atmospheric pressure, leaving it to dry for a period preferably of several hours. The pressure was then reduced in stages, measurements of the charge per single rub being made at each stage.

The following rubbing substances and gases were used:—

Glass on brass, steel, and silver, each combination in air, hydrogen and nitrogen.

Glass on silver in oxygen.

Ebonite on steel in air.

Fig. 3.

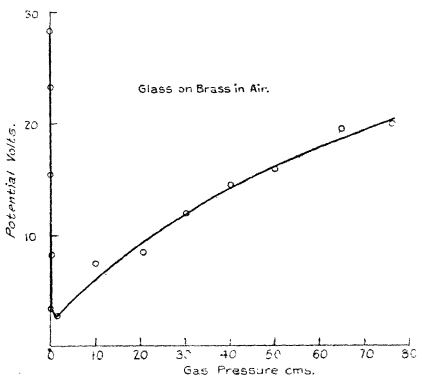

The metal surfaces were polished in the usual way, rouge being used for steel, and diamantine for brass and silver.

Hydrogen was generated by electrolysis, and passed directly into the apparatus. Oxygen was formed by heating potassium chlorate and manganese dioxide and nitrogen was obtained from a commercial cylinder.

The first results for glass on brass in air are shown in fig. 3. As the pressure is reduced a slight decrease in charge is apparent, the decrease becoming more rapid as the pressures approach a value of a few millimetres. A further reduction of pressure maintains a more or less

steady value of the charge, but at a pressure of about 1 mm. a rapid rise commences, and continues to the lowest pressure reached (less than 0·01 mm. as a rule). The slope of the curve in this region is too steep to be shown by the scale of pressures chosen. The same curve, however, as well as a similar one for hydrogen, is shown in fig. 3*a*, where the scale is chosen to show the whole range in centimetres, and also the lowest pressures in millimetres.

In many cases the value of the charge per single rub at a given pressure was quite steady, apart from the initial effect already referred to. At very low pressures, however, the values were less consistent. On reducing the pressure,

Fig. 3*a*.

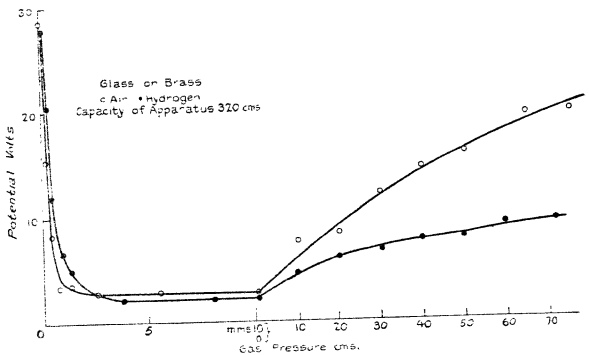

the first rub gave in general a charge which disagreed with those given by subsequent rubs. The usual procedure was to determine the charge per rub after 10, 20, 30, etc., previous to-and-fro rubs had been given. When three or four such readings agreed, the value was taken as definite, but when gradual or irregular changes existed, the rubbing was continued until sufficient values had been obtained for a reasonable average to be accepted. This method sometimes entailed as many as 200 or 250 rubs.

It will be noted that at the higher pressures the charge developed in air is greater than in hydrogen, while at very low pressures it is less. The first effect was obtained in all the cases investigated, but the second was not always apparent.

Other results, each involving the same glass rubber, are shown in figs. 4, 5, and 6. In fig. 4 the brass specimen was

Fig. 4.

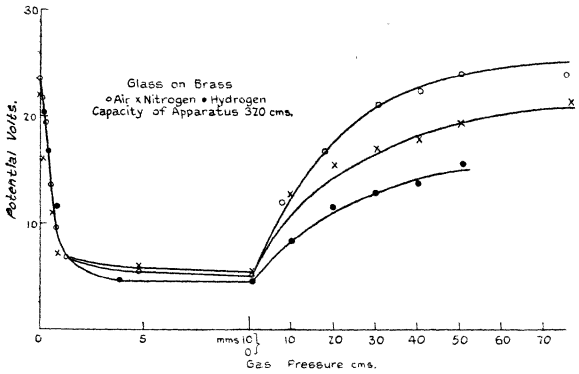

Fig. 5.

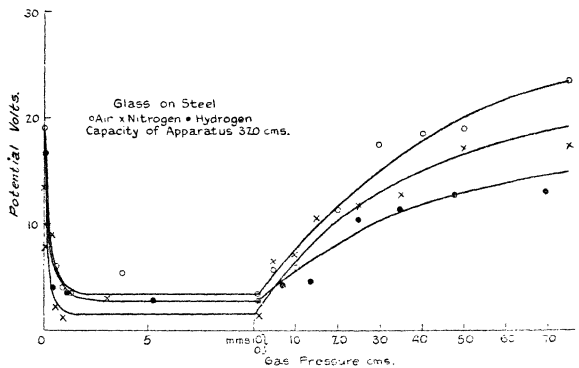

the same as in fig. 3*d*, but an interval of several weeks elapsed between the two sets of measurements, during which an accidental contamination of the metal occurred, re-polishing being subsequently necessary. It will be noted

that in the second series of measurements no difference between the effects of air and hydrogen at very low pressures was apparent.

The general results of these measurements are :—

(1) At the higher pressures the charges for each of the three metals are greatest in air and least in hydrogen.

(2) At these pressures no appreciable difference exists between the charges on the three metals in a given gas at a given pressure.

Fig. 6.

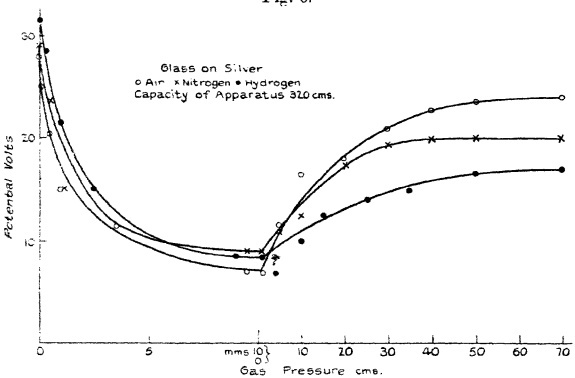

(3) At very low pressures the charges on a given metal are approximately the same in each gas. At the lowest pressure reached the charge varied with the metal, being greatest for silver and least for steel. (The diameters of the silver and steel specimens were, however, slightly less than that of the brass.)

(4) The relative drop in charge at the intermediate pressures was most pronounced in the case of steel, and least pronounced in the case of silver.

Anomalous Results with Silver.

The variation of the charge per single rub with the number of previous rubs has already been referred to. For silver it was found in many cases that the charge per

rub showed a gradual increase up to a point when a sudden decrease was observed. The lower value was generally from one half to three quarters of the higher. On continuing the rubbing, a gradual rise was again observed with the subsequent sudden drop. The effect was found to be liable to exist at all but the very lowest pressures. It would appear to be due to the gradual formation of an adsorbed gas film which at a certain point was wholly or in part removed by the repeated rubbing. Wherever the effect existed, the mean of the highest and lowest potentials was recorded.

Oxygen was used only in the case of glass on silver. It was found necessary to separate the evacuated chamber from the rest of the vacuum apparatus by a closed tap until the oxygen was perfectly dry. The first readings obtained showed no appreciable difference from those in air. At this stage, however, a marked decrease in the charges became apparent. The silver specimens were removed for examination, but no appreciable tarnish of the surfaces was found. As the effect persisted, it appeared probable that it was due to the action of mercury vapour on the polished surfaces. The charges in air were hence measured from day to day. A progressive decrease in the normal negative charge was observed, the sign of the charge ultimately being reversed. This effect persisted after a temporary return to normal conditions when the surfaces were re-polished.

In order to eliminate mercury vapour from the apparatus a Pirani gauge was used to measure the pressures. This gauge [5] consists of a tungsten filament which is heated by an electric current to a temperature somewhat higher than that of the surroundings. Cooling by conduction and convection varies with the gas pressure, and the heating current necessary to maintain a given temperature, and hence also a given resistance, determines the value of the pressure. The filament is included in a Wheatstone bridge with three other resistances with very low temperature coefficients, and the gas pressure is expressed in terms of the potential which must be applied to the ends of the bridge in order to maintain a balance. The gauge is primarily intended for use at very low pressures, but it was found quite easy to use at pressures up to a few millimetres. It was calibrated by means of a McLeod gauge before the latter was shut off from the apparatus. Before

measurements of frictional charges were commenced the apparatus was evacuated and re-opened to air several times in order to sweep out the remaining mercury vapour.

With this modification the silver surfaces were re-polished after a considerable layer had been removed from each. The charge in air at atmospheric pressure was first measured, after which the air was exhausted directly to a pressure of a few millimetres as given by the Pirani gauge. Charges at decreasing pressures down to the lowest attainable were then measured as before. The normal variation of the charge with gas pressure was again obtained. The chamber was left evacuated, and the charge observed at intervals over a period of about a fortnight. A very slight leak existed in the apparatus, and a slight decrease in charge was observed for this reason. No abnormal decrease, however, was noted.

Oxygen was then again admitted to the apparatus after thorough drying. The charge at a pressure of about $\frac{1}{2}$ atmosphere was a little greater than that at the same pressure in air. At low pressures the normal rapid increase of charge was observed, the charge at the lowest pressure being slightly greater than the corresponding charge in air. Observations at very low pressures were made over a further period of ten days, and although due to the slight leakage a rather more rapid decrease of charge than might have been expected was noted. there was no approach to a reversal of charge as in the previous case.

The observed abnormal decrease in the negative charge, with an ultimate reversal to positive charge, may thus be definitely attributed to the presence of mercury vapour.

Measurements with Ebonite on Steel.

Most metals are charged negatively by glass, but steel is positive with respect to ebonite. Use was made of a small ready-to-hand ebonite disk with a moderate state of polish on its surface. The charge in air at atmospheric pressure was much less than in the case of the glass rubber, and it was found necessary to reduce the capacity of the apparatus to about 20 cm. in order to obtain potentials of the same order as before. The measurements were not very consistent on repetition, but the relative diminution in charge at the intermediate pressure was beyond doubt very much less than in the other cases dealt with. The results of one set of measurements are shown in fig. 7.

Effect of varying the Capacity of the Apparatus.

It might be supposed that the variation of charge with gas pressure could be explained by supposing conduction of the gas layer separating the two rubbing surfaces to cause partial neutralization of the two equal and opposite charges. The essential condition for this would be that the potentials generated should be sufficient to cause ionization of the gaseous molecules by collisions. Such ionization would be most efficient when the mean free path of a gaseous ion was of the same order as the thickness of the gas layer, and this condition might be expected at a pressure of a few millimetres. On this supposition the variation of charge with gas pressure should be less pronounced if the capacity of the apparatus were increased,

Fig. 7.

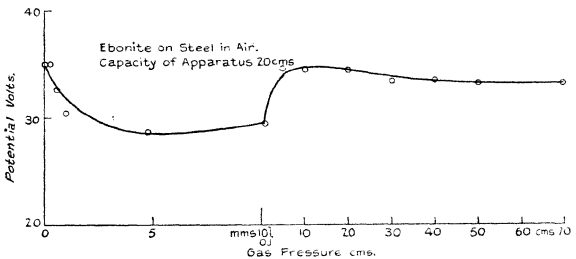

and hence the generated potentials diminished. The first measurements to test this point were made with the brass specimens in their original state of polish corresponding to the curves of fig. 3. The electrical capacity of the main apparatus was 176 cm. and a supplementary capacity of 146 cm. was arranged so that it could be connected to the main apparatus, giving a total capacity of 322 cm., or earthed at will. Each reading could thus be taken with two different capacities. The results are shown in Table I.

Except at the very low pressures the charges measured with the two capacities are almost identical in value. At the lowest pressures the charges with the larger capacity are slightly greater than with the smaller, but the difference is not sufficiently marked to indicate any appreciable effect of varying the capacity.

In these particular measurements the maximum potentials generated with the larger capacity were still considerable, and it was thought desirable to increase the capacity of the apparatus until the maximum potentials did not exceed 1 or 2 volts. Such measurements were made for ebonite on steel and glass on steel, the gas in each case being air. Each reading was, as before, taken with the two different capacities, the higher potentials being read on the gold-leaf electroscope and the lower on a quadrant electrometer used at a sensitivity of 100 mm. per

TABLE 1.

Capacity A 176 cm., B 322 cm.

Gas pressure.	Potential (Volts).		Charge (E.S. Units).	
	A.	B.	A.	B.
70 cm.	34·0	18·5	20·1	19·9
60	34·0	18·5	20·1	19·9
50	31·0	17·0	18·3	18·3
40	25·0	14·0	14·8	15·0
30	20·0	11·0	11·8	11·8
20	17·0	10·0	10·0	10·7
10	11·5	6·5	6·8	7·0
12 mm.	4·5	2·75	2·65	2·95
8	4·5	2·5	2·65	2·70
3·5	4·5	2 5	2·65	2·70
0·8	9·0	5·0	5·3	5·4
0·65	10·5	6·0	6·2	6·4
0·40	12·5	7·5	7·4	8·1
0·175	21·5	12·5	12·7	13·4
0·075	34·0	20·0	20·1	21·5
0·00	Too large to read.	25·5	—	27·4

volt. In the case of ebonite, the usual capacity of 320 cm. was sufficient to reduce the potentials to the requisite lower values, but in the case of glass, plate condensers with sulphur as dielectric were built up to a total value of about 0·01 mfd. The values of the capacities were not known with sufficient accuracy to enable the charges to be calculated, but in the following table, which relates to glass on steel, the ratio of the potentials at each gas pressure is calculated.

Similar results were obtained for ebonite on steel. If the drop in potential at the intermediate pressures is due to gaseous conduction, the effect should be more pronounced with the higher potentials, *i. e.*, with the

smaller capacity. The ratio V_B/V_A might thus be expected to diminish under these conditions. No indication of this was obtained, and it would appear that in these measurements gaseous conduction is not an important factor. There appears to be some evidence, as for example in the work of Kinsley[6] that discharges can take place over very short distances at potentials of the order of 1 volt or less, but it cannot be said that the present experiments afford any confirmation of that result.

Discussion of Results.

If two solid surfaces entirely free from gas films or other contamination are rubbed together, the atoms or molecules

TABLE II.

Gas pressure.	Potentials (Volts).		$V_B - V_A$.
	V_A.	V_B.	
70 cm.	1·20	43·5	36·2
50	1·07	39·5	36·9
40	1·00	37·25	37·2
30	0·90	34·0	37·8
20	0·77	29·5	38·3
10	0·55	22·75	41·3
5	0·45	18·5	41·1
8 mm.	0·35	13·75	39·3
1·5	0·62	24·0	38·7
0·90	0·72	26·5	36·8
0·45	0·82	30·0	36·6
0·04	1·47	55·0	37·4

of each surface are subjected to disruptive influences, and an interchange of electrons between the surfaces takes place. The work required to detach an electron from the parent atom varies with the nature of the atom. Hence with two dissimilar surfaces, that surface whose atoms or molecules give up electrons the more readily becomes positively charged. Vieweg, in the paper referred to, puts forward this view, and suggests that Coehn's rule is an equivalent statement of the same fact. By this rule, substances with high dielectric constants become positively charged when rubbed with substances of lower dielectric constants, the charge being proportional to the difference between the constants for the two given substances. A substance with a high dielectric constant is one in which the binding forces on the outer orbital electrons are small,

hence such electrons could escape more readily than in the case of a substance with a lower constant.

In the present experiments, the charges generated at the lowest gas pressures, when the effect of the gas would be least, were greater for silver than for steel. The ionization potential for silver is 7·5 volts (Foote and Mohler), but reliable values for iron and silicon were not available. The relative magnitudes of the charges, however, agree with the order of glass, iron, and silver in Shaw's frictional series.

The results for pure surfaces will clearly be modified in the presence of a gas, of which the effect may be threefold :—

(1) Conduction across the gas layer separating the two surfaces may take place. This will be a small factor if either the gas pressure or the potential difference between the surfaces is very small. Its bearing on the present measurements has already been discussed, and it is considered to be relatively unimportant.

(2) Each rubbing surface will be covered by an adsorbed gas film, of which the surface density will vary with the gas pressure. The rubbing process would then tend to disrupt gaseous rather than solid molecules.

(3) The metal specimen holds a considerable amount of gas in occlusion. This gas may be assumed to be strongly ionized, and a contact potential between the occluded and the free gaseous ions would be set up due to a difference in concentration. Further the amount of occluded gas is not appreciably reduced on reducing the outside pressure, whilst the number of free gaseous ions is small, whatever the pressure. Hence this factor should depend on the nature of the gas (as well as on the previous history of the metal) but not upon the actual gas pressure at the time of the experiment.

The variation of charge with pressure must thus be explained mainly in terms of the adsorbed gas layers. Each metal surface is certainly covered with a film but in the case of glass at ordinary temperature Langmuir[7] has found that very little adsorption takes place. The glass surface in these experiments may then be taken as moving over a gas layer. Electrons will escape from the solid molecules more easily than from the gaseous, and the gas will become negatively charged, this charge being shared by the metal on which the layer exists. As the

gas pressure is reduced, the surface density of the adsorbed film will also diminish, though probably not in a linear manner. Langmuir (*loc. cit.*) finds in the case of glass and mica at low temperatures a variation of surface density with pressure of the form

$$m = \frac{ap}{1+bp},$$

where a and b are constants characteristic of the surface and of the gas. No reference to a corresponding variation in the case of metals was found, but such a formula might well be fitted to the observed results, assuming the charge produced by a given amount of rubbing to be proportional to the surface density of the adsorbed film.

At very low pressures the amount of gas adsorbed becomes negligibly small, and when this stage is reached the contact between the glass and the metal will become the more important factor. As the gas pressure is reduced to the lowest available limit, the glass-metal contact becomes more perfect, with a coresponding increase of charge.

For a given metal the relative charges in the different gases will depend partly on the respective ionization potentials of the gases, and partly on the relative surface densities of the adsorbed films. The ionization potentials for hydrogen, oxygen, and nitrogen do not differ sufficiently to show any distinction between the charges in these experiments, the available values being :—

Hydrogen	..	16·5 volts (H. D. Smyth).
Oxygen	..	15·5 volts (do.),
Nitrogen	..	16·9 volts (Foote and Mohler).

It is quite possible, however, that the difference between the charges is accounted for by differences in the amounts of the various gases adsorbed.

On this view the positive charge generated by ebonite on steel must be explained by assuming either (*a*) no adsorption on the ebonite, in which case it would be necessary for electrons to escape from molecules within the ebonite less readily than from the gaseous molecules adsorbed on the steel, or (*b*) greater adsorption on the ebonite than on the steel, in which case the conditions approximate to a metal surface rubbing over a gas layer adsorbed on ebonite. The first condition seems very

improbable, but no reference to the amount of adsorption on ebonite was available.

It would thus appear that except at extremely low pressures the true frictional effect is entirely masked by the presence of adsorbed films. Most other experimenters have employed much more vigorous methods of rubbing with the object of breaking through the films. The effect might be expected to be much less marked at higher temperatures, and a form of rubbing chamber suitable for such measurements is in process of construction.

Summary.

(1) In all the cases where a glass surface is rubbed on a metal the charge shows a marked variation with gas pressure, being a minimum over an approximate range from 1 to 10 mm.

(2) At the higher pressures the charge for given rubbing surfaces varies with the gas, but at very low pressures appears to be characteristic of the surfaces rather than of the gas.

(3) The relative variation of charge with gas pressure is independent of the capacity of the insulated system.

(4) The presence of mercury vapour in the friction chamber may lead to entirely false results.

(5) A suggested explanation of the results is based upon the presence of adsorbed gas films on the rubbing surfaces.

The experiments were carried out in the Physics Department of the University College of North Wales, Bangor, and the author is indebted to Professor E. A. Owen for placing at his disposal the necessary apparatus, as well as for much helpful criticism and advice.

References.

(1) Shaw, Proc. Roy. Soc. A. xciv. pp. 16–33, Nov. 1917, and subsequent papers.
(2) J. H. Jones, Phil. Mag. l. pp. 1160–1177, Nov. 1925.
(3) Vieweg, Journ. Phys. Chem. xxx. pp. 865–889, July 1926.
(4) Macky, Proc. Roy. Soc. A. cxix. pp. 107–131, May 1928.
(5) Research Staff, G.E.C., Proc. Phys. Soc. xxxiii. pp. 287–296, May 1921.
(6) Kinsley, Phil. Mag. ix. pp. 692–706, May 1905.
(7) Langmuir, Amer. Chem. Soc. J. xl. pp. 1361–1403, Sept. 1918.

Bangor,
June 1929.

LXXXI. *The Effect of Variation in the Pressure of the Air and Dimensions of the Mouth on the Frequency of an Organ Flue-Pipe.* *By* A. E. BATE, *M.Sc., Northern Polytechnic, London* *.

ABSTRACT.

THE vortex theory of edge tones is shown to apply in the case of the mouth of an organ pipe in that $\frac{V}{nh}$ = a constant, where V is the velocity of the air jet, n is the frequency of the note, and h is the height of the mouth. If V is in feet per second and h is in feet, the constant is 2 for ordinary edge tones; whereas it is large in the case discussed, and is given by $\frac{74}{3}(0{\cdot}3-s)$, where s is the thickness of the jet in inches. An explanation of the deviation is offered, and this indicates that the diameter of the vortices is the same for the three slit-widths used, at all frequencies, for the same value of h, but increases with increase in height of mouth.

§ 1. AN organ pipe is a coupled system, the components being the air jet and the air column. The action resembles that of Melde's experiment, the jet corresponding to the fork, and the air column to the string. It does not appear to be generally known that the resemblance is closer than it seems, for the pipe may be lengthened by a number of half wave-lengths while the same frequency prevails, provided the air pressure be the same throughout.

The writer's attention was first drawn to this fact by Dr. Clay, and led to the research described.

If a pipe of ordinary length be blown and pressure increased, the note is sharpened until it jumps to its first overtone. The reason is that the jet frequency is restrained by the column of air—and consequent change in end-correction—until the column breaks down into two half wave-lengths if open or three quarter wave-lengths if closed.

When a pipe several wave-lengths long is used, increase of air pressure does not cause the note to sharpen to the same extent, but to jump to a higher frequency, say from 256 to 340, depending on the length of the pipe; this is to be expected, since an extra node is more readily formed in a pipe containing 8 (say) nodes than in one containing 1 node, which is the number in the case first cited.

* Communicated by Dr. R. S. Clay.

Hence the jet decides the frequency when the pipe is long, and the pipe decides it when the latter is of normal length. It follows that the mouth conditions—chiefly the air pressure and height (sometimes called the cut-up)—may be varied considerably when a short pipe is used, the natural jet frequency being distorted by lengthening or shortening the pipe as required.

§ 2. The apparatus consists of the organ pipe, air supply and the means of measuring its pressure, and a standard for comparison.

The standards tried were (*a*) a hot-wire microphone; (*b*) a second organ pipe blown at constant pressure; (*c*) a tuning-fork, mounted on a box resonator.

The third was finally adopted. The advantage of (*b*) is that it maintains a constant wave-length whatever the temperature, any change in the frequency being the same in each pipe. It was, however, suspected of interfering with the adjustable pipe, and was therefore rejected.

The organ pipe used in these experiments consists of a brass pipe $2\frac{1}{2}$ in. internal diameter and ·03 in. thick, 6 in. in length, extra lengths of pipe and sleeves of a larger diameter to join them to the first pipe, thereby enabling the length to be increased to any length up to 10 ft. The mouth of the pipe is cut in a plate $\frac{1}{8}$ in. thick fixed on to the end of the pipe and arranged so that the air jet passes across the pipe instead of along it. This allows the mouth to be adjusted without altering the length of the pipe above the lip, which would be the case in an ordinary organ pipe, for the adjustment is made by moving a sharp brass wedge forming the lip across the opening in the end plate. The air was obtained from an air compressor, which delivered it into a tank about 3 ft. in diameter and 6 ft. high; then it passed in succession through two bottles of about $\frac{1}{4}$ ft. and 2 cu. ft. capacity respectively. From the latter it passed directly to the pipe through a short length of wide tubing. The inlet and outlet from this bottle are at opposite ends, and since the consumption of air never exceeds 3 cu. ft. per minute the velocity of the air along the bottle is of the order 2 ft. per minute. The drop in pressure or loss of head, therefore, is negligible, so that the pressure in the bottle, recorded by a water manometer communicating with the middle of the axis, is regarded as the velocity head, the static head being the atmospheric pressure. The pressures rarely exceed 4 in. of water, so that, taking atmospheric pressure as 400 in., the decrease of volume due to pressure

is less than 1 per cent., and is neglected in determining the velocity.

§ 3. Theoretically, the velocity of air at density ρ under an excess pressure P is found from the equation

$$P = \tfrac{1}{2}\rho V^2.$$

If the pressure be H, measured in inches of water, and the velocity V in ft. per sec., this becomes

$$V = 66{\cdot}75\sqrt{H}.$$

(Temperature and pressure effects are neglected, being small.)

Actually the velocity was determined by inserting a tested gas-meter in the air-pipe line between the two bottles and recording the rate of flow and pressure in the second bottle, first with a $\frac{1}{20}$ in. slit $1\frac{1}{2}$ in. wide and then with a $\frac{1}{40}$ in. slit of the same width. The results obtained are:—

	H.....	$\frac{1}{2}$ in.	$\frac{1}{2}$ in.	$\frac{3}{4}$ in.
(*a*)	V.....	24·75	35·07	40·40
	$\frac{V}{\sqrt{H}}$	49·5	49·61	46·66

The values of V were determined by dividing the volume passing per sec. by the area of the slit.

	H.....	$\frac{1}{2}$ in.	1 in.	2 in.	$2\frac{1}{2}$ in.
(*b*)	V.....	36·39	51·88	72·47	80·81
	$\frac{V}{\sqrt{H}}$	51·47	51·58	51·47	51·11

Above the value of H quoted the volume passing was outside the range of the gas-meter, and so the mean value of the first readings in each case are taken. They are 49·6 and 51·5 respectively. Calibration of the slits gave the $\frac{1}{40}$ in. slit correct to within 0·0003 in., $\frac{1}{20}$ in. slit = 0·0482 in. within 0·0003 in. Correcting the latter we get values of $\frac{V}{\sqrt{H}} = 51{\cdot}4$ and 51·5 respectively. The value of the constant, then, is 51·4 nearly, so that $V = 51{\cdot}4\sqrt{H}$.

This discrepancy is probably wholly accounted for by the contraction of the jet after leaving the slit, in which case the value of the vena contracta is 0·77.

§ 4. The process of matching jet and pipe frequencies is known as voicing the pipe, and is accomplished in practice

by expert "Voicers," who adjust the slit and alter the cut-up; but voicing was achieved by the writer as follows: the pipe, about 100 inches in length, was "stopped," *i.e.* the far end was closed by a flat plate. This had the effect of reducing the influence of the mouth upon the frequency of the air column. The air supply was adjusted to give a steady known pressure; then the height of the mouth was adjusted until the pipe gave a note near that required. The length of the pipe was then altered until the note agreed with that of the standard fork. It was usually necessary to readjust the lip to make the pipe speak as well as possible.

On moving the lip towards the slit, maintaining the same pressure, the frequency rises slightly (due, as we shall see later, to a change in the end-correction *), but remains nearly constant down to a certain height, at which the note jumps to a higher frequency; on moving the slit back again, the new frequency prevails to a considerable distance, but finally, at a certain height, resumes its former value. Continuing to open the mouth still more causes the tone to become flat, and again at a certain height a jump occurs, but to a lower frequency; on moving the lip once more to its original position, the initial frequency is suddenly regained. It was noticed that the two transition points at which the frequency returned to its former value were close together, and the position of the lip midway between them was taken as the position of maximum stability for that particular pressure and frequency. The transitions are obviously due to n (say) nodes in the pipe becoming $n+1$ and $n-1$ respectively. In some cases the jump was not back to its original frequency, but beyond it; in fact, in some instances it was impossible to return directly to the original note, so that mean point was selected from a curve connecting frequency and pressure. The curves for a frequency of 256 are shown in fig. 1, and it can be seen that the curve midway between the two inner curves is also midway between the two outer curves. This curve is the curve of maximum of stability. The velocity is proportional to the square root of the pressure, therefore the curves show that the increase above the mean velocity necessary to cause the note to jump to a higher frequency is equal to the decrease in velocity required to make it jump to a lower frequency. The return from these frequencies to the former also requires equal decrease and increase of velocities.

* See "Determination of the End Corrections at the Mouth of a stopped Organ Flue-Pipe," by author, to be published shortly.

The portions of the graph between the two higher curves and between the two lower curves are areas in which the particular frequency (256) is unstable.

§ 5. The explanation of the sudden transition of the note is to be found in the phenomena of "edge-tones," investigated by Wachsmuth and König. These tones are formed

Fig. 1.

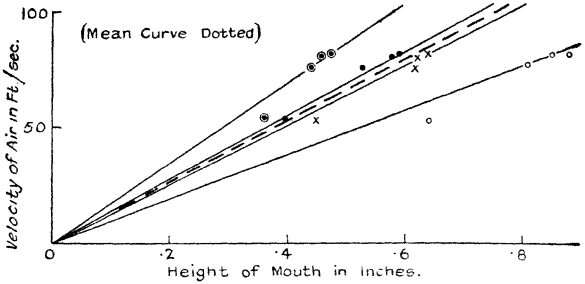

Figs. 2 & 3.

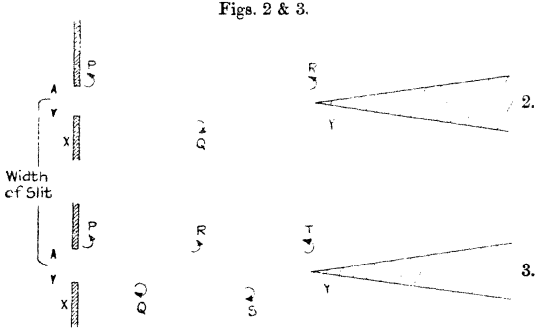

by a stream of air passing from a narrow slit and striking a sharp edge parallel to the slit.

The conditions governing the frequency of the tone are the distance from slit to edge, and the velocity of the air, suitable conditions producing a vortex system as shown in fig. 2. Assuming that air issues from the slit X, and strikes the edge Y, it has been shown that a vortex system is

formed such that when a vortex R passes Y, another, P, is formed on the same side of the air stream at the slit, and a third vortex has been formed the other side midway between P and Q. The frequency of the edge tone is equal to the number of vortices on one side of the jet which pass the edge per second. If U is the velocity of the vortex in the direction XY, and if $XY = h$, as $XY = PR$, $U = nh$.

The air on the outside of the vortex rows is at rest, so the jet must be moving with a velocity 2U, so

$$V = 2U = 2nh$$

or

$$\frac{V}{nh} = 2,$$

where V is the velocity of the jet. This result has been verified by experiment. Increase of jet velocity beyond a certain point causes a rearrangement of the vortex system, as in fig. 3, in which twice the number of vortices pass Y per second. If V be the new velocity, and N the number of vortices passing on one side of the edge per second,

$$\frac{V'}{2Nh} = 2 = \frac{V'}{4nh} = \frac{\frac{V'}{2}}{2nh};$$

i. e. $V' = 2V$; so that double the velocity causes double the frequency, the mouth height h remaining unchanged. This also agrees with experiment. The same spacing of vortices may be obtained by moving the edge opposite to R (fig. 2) without altering the velocity of the air stream; XY will become $\frac{h}{2}$, and

$$\frac{V}{2nh} \text{ becomes } \frac{V}{2 \times 2n \times \frac{h}{2}},$$

and the frequency is $2n$, the octave, as before.

If the system be coupled with a column of air to form an organ pipe, the alternate vortices give rise to compressions which travel up the tube one quarter wave-length and return in time to augment the effect of the next vortex on the other side of the edge, or lip as it now becomes. On increasing the pressure to give rise to the system of fig. 3, the frequency is doubled and the pipe speaks the octave; if, however, the "cut-up" be halved, the octave is again elicited without the increase in pressure and therefore of velocity. *In the former case the octave is obtained by over-blowing; in the latter the pipe is normally blown.*

In the experiments described the jet is arranged to give its natural frequency.

§ 6. The pipe was voiced for different frequencies and pressures according to the method described above. The results, using the slit $\frac{1}{20}$ in. wide, $1\frac{1}{2}$ in. long, and a pipe

Fig. 4.

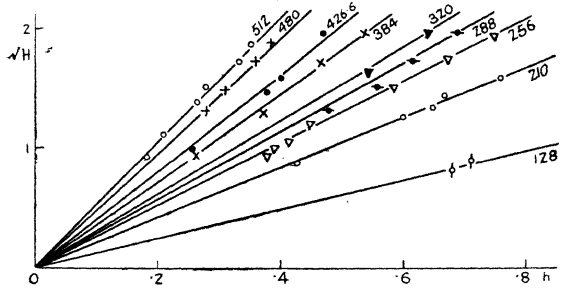

Fig. 5.

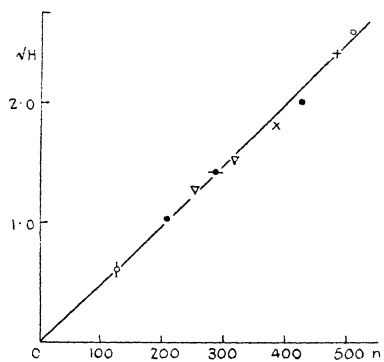

$2\frac{1}{8}$ in. diameter, are shown in figs. 4 and 5. The experiments were conducted at temperatures varying from about 57° F. to 62° F.; fig. 4 gives the curves connecting velocity and height of mouth for various frequencies, and fig. 5 shows the relationship between velocity and frequency for a fixed height of mouth of 0·5 in., the values having been taken

from fig. 4. In each case the curves are straight lines passing through the origin, so that $\frac{V}{k}$ and $\frac{V}{n}$ are constant; therefore $\frac{V}{hn}$ = constant. If P = 1 in., $n = 200$, when $h = \frac{1}{2}$ in., and $\frac{V}{hn} = 6{\cdot}168$ for a slit $\frac{1}{20}$ in. wide.

Fig. 6.

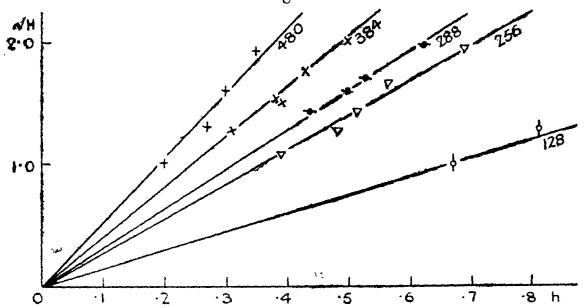

Fig. 7.

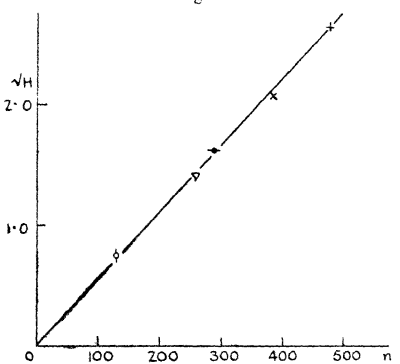

From § 5, $U = hn$, V being the velocity of the vortices; therefore $U = \frac{V}{6{\cdot}168} = 0{\cdot}16\ V$, *i. e.* the velocity of the vortices is ·16 that of the jet. This result is in close agreement with that obtained by Carrière *. He rendered

* Carrière, *Journ. de Phys. et Rad.* p. 61, Fev. 1925.

the vortices visible by a small jet of steam in the main jet and measured their velocity stroboscopically, and found it to be approximately 8 metres per second. He measured the jet velocity with a Pitot tube. It proved to be about 46 m. per second, so that for his experiment V = ·17 V.

Fig. 8.

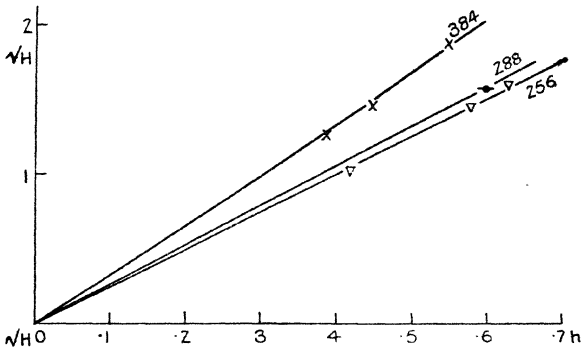

Fig. 9.

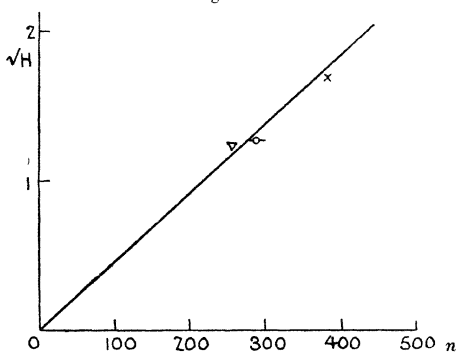

§ 7. Repetition with the $\frac{1}{40}$ in. wide slit, $1\frac{1}{2}$ in. long, and the same pipe, gave the results shown in figs. 6 and 7, which resemble figs. 4 and 5, but in this case $\frac{V}{n\lambda} = 6{\cdot}783$.

§ 8. Further results with a slit $\frac{3}{40}$ in. in width were sought, but the range was limited, only three sets of results being taken (figs. 8 and 9), and

$$\frac{V}{nh} = 5{\cdot}55.$$

§ 9. The variation of $\frac{V}{nh}$ with slit-width is shown in fig. 10. The result is a straight line of which the equation is

$$\frac{V}{nh} = \frac{74}{3}(0{\cdot}3 - s),$$

where s denotes the width of the slit. The minimum value of $\frac{V}{nh}$ is 2, its theoretical value, when the value of s is 0·22.

Fig. 10.

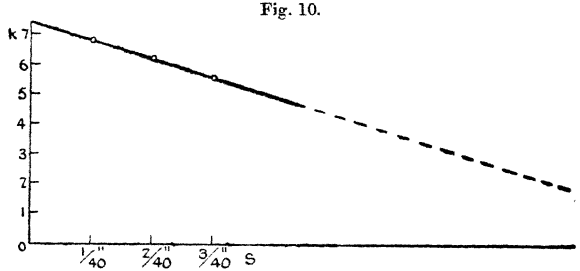

§ 10. From § 3 the area of the vena contracta of the air jet appears to be about 0·77 that of the slit, and we may assume that this contraction is essentially in the thickness, since the ends of the slit are practically in line with the lower part of the pipe, which is connected to the air supply. The widths of the three jets are therefore taken as 0·02, 0·04, and 0·05 inch respectively.

On issuing into the free air, the jet moves with a velocity depending on the pressure in the reservoir, and the free air next to the jet is dragged along, thereby tending to decrease the jet velocity and to form vortices. Vortices are formed, provided the jet velocity is above the critical velocity for turbulent flow.

Consider a vortex P (fig. 11) moving with a linear velocity U, at the side of a jet of velocity V, and parallel to it. The part of P farthest from AB is momentarily at rest, while that nearest AB is moving at a velocity 2U,

the angular velocity and radius of a vortex being constant. From P to AB a viscous drag occurs; if d be the distance from the centre of P to AB (the edge of the jet), the rate of change of velocity $= \frac{V}{r+d}$; hence the centre of the vortex has a velocity of $\frac{V}{r+d} \cdot r$. This we have called U. It follows that

$$r = \frac{U}{V-U} \cdot d = \frac{d}{\frac{V}{U}-1}.$$

Fig. 11.

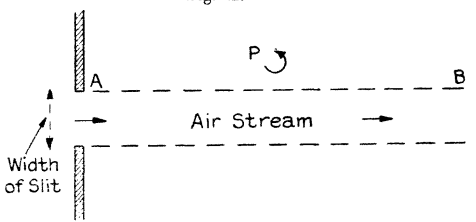

For the narrowest slit,

$$\frac{V}{U} = 6{\cdot}78,$$

and therefore

$$r = \frac{d}{5{\cdot}78}.$$

It has been shown by Karman theoretically and verified by Benton experimentally that the distance between the centres of the avenues on each side of the jet bears a constant ratio to the distance between successive vortices in the same avenue. Karman gives 0·28 as the constant; Benton's value is 0·27. The distance between successive vortices is equal to the distance from slit to lip; hence for a mouth 0·5 in. high the distance between the centres of the avenues $= 0{\cdot}14$ in., taking 0·28 as the constant. If the thickness of the jet from the narrowest slit be taken as 0·02 in., the distance

$$d = \frac{0{\cdot}14 - 0{\cdot}02}{2} = 0{\cdot}06 \text{ in.},$$

so that

$$r = \frac{0{\cdot}06}{5{\cdot}78} = 0{\cdot}01 \text{ in. nearly.}$$

For the slit $\frac{1}{20}$ in. wide,

$$d=\frac{0\cdot14-0\cdot04}{2}=0\cdot05 \text{ in.}$$

and

$$r=\frac{0\cdot05}{5\cdot16}=0\cdot01 \text{ in. nearly.}$$

For the $\frac{3}{40}$ in. slit,

$$d=\frac{0\cdot14-0\cdot06}{2}=0\cdot04 \text{ in.,}$$

so that

$$r=\frac{0\cdot04}{4\cdot55}=0\cdot01 \text{ in. nearly.}$$

If the mouth be 0·75 in. high, the distance between the avenues of vortices =0·21 in., from which the values of d are respectively 0·095 in., 0·085 in., and 0·075 in., which give r=0·0164 in., 0·0164 in., and 0·165 in. for the $\frac{1}{40}$, $\frac{1}{20}$, and $\frac{3}{40}$ in. wide slits respectively. It appears from these results that the vortices have a definite radius for a given height of mouth, and that this radius is independent of the thickness of the jet.

The author desires to acknowledge his indebtedness to Dr. Clay for the interest he has shown in this research.

References.

Sound,' by E. G. Richardson (published by Arnold). This contains an account of the work previously undertaken and copious references to original papers.

'Measurement of Air Flow,' by E. Ower (Chapman & Hall).

LXXXII. *On the Electrification of a Two-dimensional "Ice-pail."* *By* W. B. Morton, *M.A.*, *and* Mary McDonald, *M.Sc.*, *Queen's University, Belfast* *.

THE two-dimensional analogue of Faraday's ice-pail is composed of an infinitely long parallel-sided strip for bottom, with two other strips of equal height to form perpendicular sides. When such an arrangement is freely charged, the electric field in the lower part of the interior becomes very small as the sides are raised. The question of the configuration of the field is here treated as an example of

* Communicated by the Authors.

the general method of Schwarz, applicable to fields bounded by straight conductors. The work follows closely the procedure adopted in an earlier paper * on the electrification of two intersecting planes.

The field in the plane of z is represented on the interior of unit circle in a plane of ζ (fig. 1). To take advantage of the symmetry of the figure we make the points 0 and π on the circle correspond to the mid-points of AA′, CC′ respectively. The differential relation between the complex variables is then

$$dz/d\zeta = C\zeta^{-2}(\zeta - e^{i\alpha})^{\frac{1}{2}}(\zeta - e^{-i\alpha})^{\frac{1}{2}}(\zeta - e^{i\beta})(\zeta - e^{-i\beta})$$
$$(\zeta - e^{i\gamma})^{-\frac{1}{2}}(\zeta - e^{-i\gamma})^{-\frac{1}{2}}$$

where $\alpha\,\beta\,\gamma$ are the arguments of ABC.

Fig. 1.

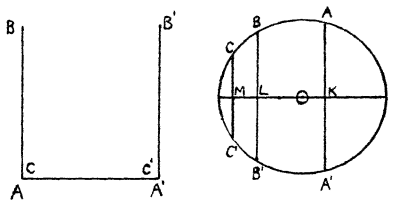

To escape the appearance of a term in ζ^{-1} in the expansion for large values we require the relation

$$\tfrac{1}{2}e^{i\alpha} + \tfrac{1}{2}e^{-i\alpha} + e^{i\beta} + e^{-i\beta} - \tfrac{1}{2}e^{i\gamma} - \tfrac{1}{2}e^{-i\gamma} = 0.$$

or
$$\cos\alpha + 2\cos\beta - \cos\gamma = 0.$$

This implies that β and γ are obtuse angles, and that the points are so placed that $OL = \frac{1}{2}MK$.

There are thus two independent constants, not counting the scale-constant C. One relation connecting these is obtained when we express the condition that the pail shall have a single bottom, *i.e.*, that AB = CB. The second relation is given by the shape of the pail, in the ratio of AB or CB to AA′.

For points on the conductors, which are represented by points on the circumference, we put $\zeta = e^{i\phi}$. The equation then reduces to $dz/d\phi = 2i(\cos\phi - \cos\beta)(\cos\phi - \cos\alpha)^{\frac{1}{2}}(\cos\phi - \cos\gamma)^{-\frac{1}{2}}$.

* Phil Mag. i. p. 337 (1926).

The single-bottom condition is expressed by the vanishing of the integral for z between limits of γ and α for ϕ. As a preliminary to mechanical quadrature, the integral is transformed by the substitution

$$\cos\phi = \cos\gamma \,.\, \cos^2\theta + \cos\alpha \,.\, \sin^2\theta.$$

This does away with the infinite value of the integrand at the lower limit, and makes the range from 0 to $\frac{1}{2}\pi$. To get pairs of corresponding values of the constants, a definite value was given to $\cos\alpha$, and the integrand was then plotted for a number of values of $\cos\gamma$ lying between $-\cos\alpha$ and -1. The positive and negative parts of the areas having been found by planimeter, it was possible to find by interpolation the value of $\cos\gamma$ which made the total area vanish. The shape of the pail could then be found by evaluating the integrals representing the base and the height.

The following values were obtained:—

$\cos\alpha =$	·2	·4	·6
$-\cos\gamma =$	·551	·893	·9943
side/bottom =	·052	·225	·633

From the figures in the last column it will be seen that there is a practical difficulty in the way of getting a form which looks like an ice-pail. If the sides are to be made taller in comparison with the breadth, we shall have to work with values of $\cos\gamma$ lying very close to -1.

The angles of $\alpha\beta\gamma$ give directly the distribution of the total charge between the different parts of the surface, the charge between two points being represented by the arc of the circle between the corresponding points on the ζ-diagram. So each side-plane carries the fraction $(\beta-\alpha)/2\pi$ on its outer, and $(\gamma-\beta)/2\pi$ on its inner surface, while the bottom has α/π on its under surface and $(\pi-\gamma)/\pi$ on its upper surface. The distributions for the three shapes given above are shown on fig. 2, where the fractional charges are represented as segments of the unit vertical height of the figure, plotted against the shape-ratio, of height to diameter of base. The trend of the curves drawn through the points indicates the ultimate transfer of the whole charge to the outsides of the two side-planes as the height of these is increased. It may be noted that the charge borne on the inner surfaces of the side-planes passes through a maximum value.

Fig. 3 shows the forms of the equipotentials and lines of force for the last of the three forms examined. These are the graphs of $\log\rho = \text{const.}$ and $\phi = \text{const.}$, where $\zeta = \rho e^{i\phi}$.

The equipotentials are $\rho = \cdot 9$, $(\cdot 9)^2$, $(\cdot 9)^3$, $(\cdot 9)^4$, and the lines of force correspond to 5° intervals in ϕ. To obtain the former, mechanical quadrature was applied to the expressions

Fig. 2.

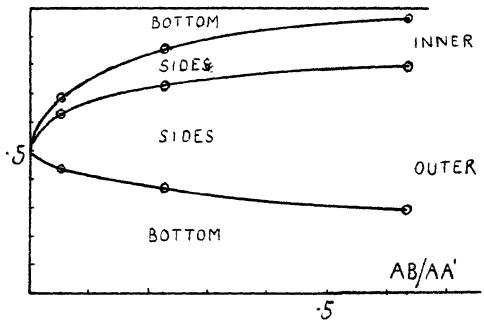

Fig. 3.

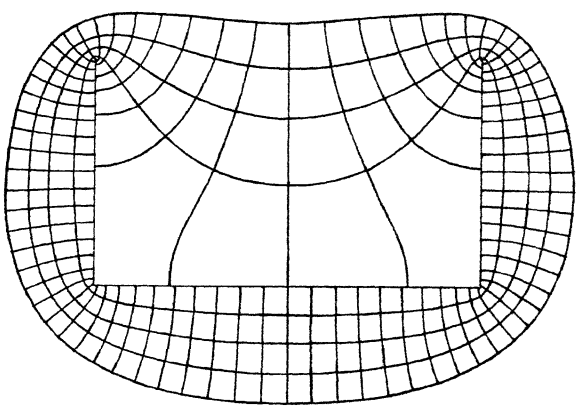

for $\partial x/\partial\phi$, $\partial y/\partial\phi$ given by the fundamental equation. The lines of force were got by joining points with the same ϕ on the different equipotentials.

LXXXIII. *A Method for the Magnetic Analysis of a Spectrum by means of Unresolved Zeeman Patterns, and its Application to Ag II.* By A. G. Shenstone, *M.A., Ph.D., and* H. A. Blair, *M.Sc.**

Abstract.

A method of determining the Landé g-values from unresolved Zeeman patterns is discussed. The method is applied to the spectrum of Ag II., and the cases where the measured values disagree with the theoretical are considered with regard to the usefulness of g-values as compared with intensities as criteria in the indentification of terms.

THE magnetic factors "g" for the terms of a spectrum are known in few cases with any completeness. In general we do not have a complete magnetic analysis because of the fact that it is not possible to obtain patterns of weak lines with the very high resolving power necessary for such work. It should be useful, however, to obtain such complete analyses, even though accuracy is sacrificed for completeness. Such an analysis of the silver spark spectrum is here presented.

The experimental arrangements were very simple. A silver arc was run in air between the poles of a magnet giving about 34,000 gauss. The light was passed through a quartz double-image prism and then through a quartz lens which focussed the two images, one above the other, on the slit of a Hilger E 1 quartz spectrograph. This instrument has shown a resolving power at λ 2500 of approximately 40,000. The exposures varied from a few seconds to about one half-hour.

The Zeeman patterns obtained were all unresolved except two; and it is necessary, therefore, to consider the means of obtaining g-values from such patterns. To do this we can use the theoretical intensity formulæ given by Hönl † in order to calculate the centre of intensity of an unresolved pattern.

The formulæ for the intensities of the Zeeman components for the case of $\Delta J = -1$ are as follows:—

$$A^{M}_{M\pm1} = C\tfrac{1}{2}(J \mp M)(J \mp M - 1) \qquad \sigma\text{-components},$$

$$A^{M}_{M} = C(J^2 - M^2) \qquad \pi\text{-components},$$

* Communicated by the Authors.

† *Z. Physik*, xxxi. p. 340 (1925).

where C represents a factor independent of M. The centre of gravity of the π-components is obviously at the undisplaced position of the line since I_M^M has its maximum for $M=0$. The intensities of successive σ-components are in the ratios

$$(J+J)(J+J-1) : (J+J-1)(J+J-2) : : : \{J-(J-2)\}\{J-(J-2)-1\}$$

i.e. $2J(2J-1) : (2J-1)(2J-2) : : : 3.2 : 2.1.$

If we take the distance between the strongest and weakest components as unity, then, using the principle of moments, the centre of intensity, measured from the weakest component, is given by

$$X=\frac{1}{2J-2}\left\{\frac{1.2.3+2.3.4+\ldots(2J-2)(2J-1)2J}{1.2+2.3\ \ldots\ldots\ (2J-1)2J}\right\}.$$

The two finite series may be summed with the result,

$$X=\frac{1}{2J-2}\left\{\frac{\frac{1}{4}(2J-2)(2J-1)2J(2J+1)}{\frac{1}{3}(2J-1)2J(2J+1)}\right\}=\frac{3}{4},$$

independently of J. The distance of the weakest component from the position of the original line is $(J-1)g_2-(J-2)g_1$, and the distance between the weakest and strongest components is $(g_1-g_2)(2J-2)$. Therefore, the centre of intensity should be at a distance from the undisplaced position equal to

$$(J-1)g_2-(J-2)g_1+\tfrac{3}{4}(g_1-g_2)2(J-1)$$
$$=\tfrac{1}{2}\{g_1(J+1)-g_2(J-1)\}.$$

This simple result may be used in cases of either odd or even multiplicities and $g_1 \lesseqgtr g_2$. It should be noted that J in the formula is the greater of the two J's involved, and that g_1 belongs to the same level as J. The use of this formula depends upon the assumption that the centre of intensity is the point on which the observer sets the cross-hairs of his measuring instrument. In practice it has been found that this assumption is justified if the pattern is sufficiently far from complete resolution, *i.e.*, the method gives the most nearly correct results where g_1-g_2 is not too great.

The formulæ for intensities of Zeeman components in the case of $\Delta J=0$ are :

$$A_{M\pm1}^M = C'\tfrac{1}{2}(J\mp M)(J\pm M+1) \quad \sigma\text{-components},$$
$$A_M^M = C'M^2 \quad \pi\text{-components}.$$

The σ-components have intensities in the ratios,

$$2J.1 : (2J-1)2 : (2J-2)3 : : : 1.2J,$$

i. e., the pattern is symmetrical about its own centre. This centre lies at a distance from the undisplaced line equal to $\frac{1}{2}(g_1+g_2)$ for either odd or even multiplicity. Twice the measured displacement of such a line, therefore, gives directly the sum of the two g's.

The π-components have intensities in the ratios,

(*a*) $1^2 : 2^2 : : : J^2$ for odd multiplicity,

and

(*b*) $1^2 : 3^2 : : : (2J)^2$ for even multiplicity.

In the two cases, taking the distance from the weakest component to the strongest component as unity, the centre of gravity measured from the weakest component is :

$$\text{(a)} \quad y = \frac{1}{J-1} \cdot \frac{1.2^2+2.3^2+\ldots+(J-1)J^2}{1^2+2^2+\ldots+J^2}$$

$$= \frac{1}{J-1} \cdot \frac{\frac{J}{12}(3J+2)(J+1)(J-1)}{\frac{J}{6}(J+1)(2J+1)}$$

$$= \frac{1}{2} \frac{3J+2}{2J+1}$$

$$\text{(b)} \quad y' = \frac{1}{J-\frac{1}{2}} \frac{1.\frac{3^2}{2}+2.\frac{5^2}{2}+\ldots+\left(J-\frac{1}{2}\right)J^2}{\frac{1^2}{2}+\frac{3^2}{2}+\ldots+J^2}$$

$$= \frac{1}{J-\frac{1}{2}} \frac{\frac{1}{192}(2J-1)(2J+1)(12J^2+16J+3)}{\frac{1}{6}(J+1)(2J+1)J}$$

$$= \frac{1}{16} \frac{12J^2+16J+3}{J(J+1)}.$$

The expressions for the centre of intensity measured from the undeviated position are as follows :—

(c) $(g_1-g_2)+y(J-1)(g_1-g_2) = (g_1-g_2)\{1+y(J-1)\}$

for odd multiplicities.

(d) $\frac{1}{2}(g_1-g_2)+y'(J-\frac{1}{2})(g_1-g_2) = (g_1-g_2)\{\frac{1}{2}+y'(J-\frac{1}{2})\}$

for even multiplicities.

As the expressions for the centre of gravity are complicated, it is more useful to tabulate the values of y and y', and use the formulæ c and d.

TABLE I.

Even Multiplicities.		Odd Multiplicities.	
J	y'	J	y
$\frac{1}{2}$	...	1	...
$1\frac{1}{2}$	·90	2	·80
$2\frac{1}{2}$	·84	3	·79
$3\frac{1}{2}$	·82	4	·78
$4\frac{1}{2}$	·80	5	·77
$5\frac{1}{2}$	·79	6	·77
∞	·75	7	·76
		∞	·75

In practice the measurements of the π-components are used only as a check on the more accurate results obtained from the σ-components.

The spark spectrum of silver has been analysed by Majumdar *, McLennan and McLay †, and Shenstone ‡. The second and third analyses are in agreement, but the last is the more complete and is, therefore, used here.

If g-values are to be obtained from unresolved patterns it is obviously necessary to know one of the two g's for each line. In the case of Ag II. the start can be made from the two resolved patterns found, viz.:

$5s^3D_1 - 5p^3P^\circ_1$ (·95) − 1·50 Landé (1·00) ·50, 1·50
$5s^3D_1 - 5p^3P^\circ_2$ ($\overline{0}$ 1·00) − 2·49 „ ($\overline{0}$ 1·00) 1·50, $\overline{2{\cdot}50}$.

The measurements are the average of a large number made on several plates. Dashes indicate components which were present but whose measurements would not add to the accuracy. A number of Cu I. and Cu II. lines were used as standards and were found to be consistent.

It was assumed that the patterns given above differed from the predicted pattern only because of errors of measurement and that, therefore, the g-values for the three terms involved are the Landé values. Knowing these three g's it is then possible, by means of the formulæ developed above, to calculate from the measured unresolved

* Majumdar, Indian Journal of Physics, ii. p. 15 (1928).
† McLennan and McLay, Trans. Roy. Soc. Can. xxii. p. 10 (1928).
‡ Shenstone, Phys. Rev. xxxi. p. 317 (1928).

patterns, the g-values of all the remaining terms. Because of the rather large errors of measurement of the narrow patterns, a method of successive approximation for the g-values was adopted. This involved, first, a calculation of g's from single lines, and afterwards an adjustment of the values to give the best fit to all the lines involving each term. Naturally the values obtained by such a process will have probable errors which will be smaller, the larger the number of lines from which they are calculated. Judging from the range of values obtained for any particular g, the error in those determined from more than five lines should not be higher than three per cent. The variation of the calculated values of g for a single term is illustrated by the following set whose average was used for the g of $5s^1D_2$:

1·00, 1·03, 1·04, 1·04, 1·01, 1·05, 1·07.

Table II. (p. 770) gives the g-values calculated, the Landé g's, the number of lines used in each case, and the g-sums for terms of the same J and configuration.

The following points are important :—

(1) The g-sum rule is fulfilled within the experimental error. The almost exact agreement for the terms of structure $4d^9 5d$ is, of course, fortuitous.

(2) The g-values of most of the terms are reasonably near the Landé values with the following exceptions :—

(*a*) Terms of the structure $4d^9 5p$ and $J=2$.
(*b*) Terms of the structure $4d^9 5d$ and $J=2$ and $J=1$.

The fact that the g-values for the terms just mentioned depart so markedly from the Landé values involves an important theoretical question, viz. : the relative weight which is to be assigned to the g-values and to the intensities of combinations in the designation of the levels of a spectrum. For instance, in the case of the terms of $J=2$ in the structure $4d^9 5p$, the four levels could be named in such a way as to make the individual g's most nearly the Landé values. This would involve a complete sacrifice of the ordinary intensity rules as well as a much greater departure from the interval rule. It would also involve great difficulties in the interpretation of iso-electronic sequences. For example, the term which is now $5p^3D^\circ_2$ in Ag II. would have to be chosen as $5p^3F^\circ_2$, whereas in Pd I. the equivalent term would be chosen as $5p^1D^\circ_2$.

The same theoretical difficulty presents itself in the case of series of terms of two multiplicities converging to the same multiple limit. A case in point is that of the terms

$5s^3$ and ^1D and $6s^3$ and ^1D in the spectrum under discussion. Theoretically, as we proceed to higher series members, the

TABLE II.

Ag II. *g*-values and *g*-sums.

Term.	*g*. Landé.	*g*. Obs.	No. of Lines.	Structure.	J.	*g*-sum. Landé.	*g*-sum. Obs.
$5s^3D_3$	1·33	1·33	4	$4d^9 5s$	1	·50	·50
$5s^3D_2$	1·17	1·13	7		2	2·17	2·16
$5s^3D_1$	·50	·50	7		3	1·33	1·33
$5s^1D_2$	1·00	1·03	7				
				$4d^9 5p$	1	3·00	3·00
$5p^3P^\circ_2$	1·50	1·50	5		2	4·34	4·49
$5p^3F^\circ_3$	1·08	1·08	7		3	3·41	3·43
$5p^3P^\circ_1$	1·50	1·50	7		4	1·25	1·26
$5p^3F^\circ_4$	1·25	1·26	4				
$5p^3D^\circ_2$	1·17	·87	7	$4d^2 6s$	1	·50	·53
$5p^3P^\circ_0$	—	—	3		2	2·17	2·22
$5p^3D^\circ_3$	1·33	1·25	8		3	1·33	1·34
$5p^3F^\circ_2$	·67	·92	7				
$5p^1F^\circ_3$	1·00	1·10	7	$4d^9 5d$	1	5·00	4·99
$5p^1P^\circ_1$	1·00	1·00	8		2	4·34	4·35
$5p^3D^\circ_1$	·50	·52	4		3	4·16	4·23
$5p^1D^\circ_2$	1·00	1·20	5		4	3·30	3·35
					5	1·20	?
$6s^3D_3$	1·33	1·34	3				
$6s^3D_2$	1·17	1·11	4				
$6s^3D_1$	·50	·53	3				
$6s^1D_2$	1·00	1·11	4				
$5d^3S_1$	2·00	1·84	2				
$5d^3G_5$	1·20	?					
$5d^3G_4$	1·05	1·03	2				
$5d^3P$	1·50	1·37	1				
$5d^3P_1$	1·50	·90	2				
$5d^3D_3$	1·33	1·34	2				
$5d^3F_3$	1·08	1·04	3				
$5d^3D_2$	1·17	1·07	3				
$5d^3S_0$	—	—	1				
$5d^3F_4$	1·25	1·26	3				
$5d^1P_1$	1·00	1·51	3				
$5d^3G_3$	·75	·75 ?	2				
$5d^3D_1$	·50	·74	2				
$5d^1G_4$	1·00	1·06	1				
$5d^1D_2$	1·00	1·20	2				
$5d^3F_2$	·67	·71	2				
$5d^1F_3$	1·00	1·10	2				
$5d^1P_0$	—	—	0				

Total No. of Lines=72.

electron couplings change in such a way as to dissolve the identity of the singlet term as it approaches the triplet. The *g*-sum of $^3D_2$ and $^1D_2$ should, therefore, be shared in

some undetermined way and the differentiation of the two levels should decrease, bringing in a relative increase of the intensities of inter-system combinations. In point of fact the g-values do become equal, but the identities of the two levels do not fuse, but become more distinct when intensities are used as the criterion. In other words the naming of these terms by Zeeman effects is impossible, but it can be done uniquely from the intensities of their combinations. To illustrate this point we can compare the relative intensities of the inter-system combinations of the $^1D_2$ with its singlet combinations. Table III. contains these quotients for a number of spectra of the same type as Ag II., and also for the $d^n ns^2$F series terms of Pd II. and Ni II.

TABLE III.

Ratios of Inter-system to Intra-system Intensities.

Spectrum.	Series Member.			1st member. / Last member.
	1	2	3	
Cu II.	2·18	·37		5·4
Ag II.	1·45	·27		5·8
Au II.	1·33	·38		3·5
Ni I.	·54	1·66	0*	∞
Pd I.	1·33	1·73	·33	4·0
Ni II.	·58	·015		Very large.
Pd II.	1·12	·007		Very large.

It is obvious that in every case the intensities of the inter-system combinations fall off much more rapidly for the higher series members than do the intra-system combinations. The apparent increase of the inter-system intensities in the second member for Ni I. and Pd I. is explained by the fact that the second member singlet combinations are in the extreme red, where intensities are quite unreliable.

The method used for the summing of the finite series in this paper is due to Sir Isaac Newton, through Dr. E. U. Condon, who must be Sir Isaac's proxy in the reception of our thanks.

Palmer Physical Laboratory,
Princeton University, N.J.,
6th March, 1929.

* H. N. Russell, Phys. Rev. xxxiv. p. 821 (1929).

LXXXIV. *On the Origin of the Spark Lines in X-ray Spectra.* *By* B. B. Ray, *D.Sc., Calcutta University.*

1. *Introduction.*

BESIDES the characteristic X-ray emission lines of an atom, there are a large number of lines in the X-ray spectra of the elements which do not follow the well-known Moseley law, and are named as "non-diagrammatic" lines. After Kossel's satisfactory explanation of the process for the production of the characteristic emission lines of the atoms, Wentzel suggested that the non-diagrammatic lines might originate from an ionized atom, namely, these lines arise from an excitation process in which more than one electron is removed from the inner levels of the atom. From the close resemblance to conditions necessary for the production of the spark lines in the ordinary optical spectra, Wentzel † suggested the name of spark lines to these lines. The characteristic features of these spark lines are:

(*a*) They accompany a prominent emission line, and generally lie on the shorter wave-length side of the latter. Thus we may have spark lines connected with the lines Kα, Kβ, Lα, Lβ, Mα, and so on.

(*b*) They are broad and diffuse, and Coster (Phil. Mag. xliv. p. 546, 1922) is of opinion that these spark lines may consist of unresolved components.

(*c*) Systematic measurements of the intensity of these lines could not be made with the change in voltage in the X-ray tube, as they are very weak.

Experiments for the proper understanding of the problem of production of these satellites have been made by Bäcklin ‡ for Kα-satellites of Al, and Siegbahn and Larson § for Lα-satellites of Mo, where they have carefully studied the production of these lines, maintaining a constant voltage in the tube, and have shown:

1. That the spark lines are produced at an exciting voltage slightly above, and certainly not much less than twice the critical voltage of, the K- or the L-level, as the case may be

* Communicated by the Author.
† Siegbahn, 'The Spectroscopy of X-rays.'
‡ *Zeit. f. Phys.* xxvii. (1924).
§ *Ark. f. Mat. Astrooch. Fys.* xviii. No. 18 (1924).

2. That all the spark lines appear simultaneously, and that with different voltage the intensity relations of the lines do not change.

3. That at a critical voltage greater than twice the critical voltage necessary to excite the K- or L-lines no new lines appear.

To account for the production of the Kα-satellites, Wentzel assumes that the atom may either lose two electrons from the K-shell, or one from K and others from L- or M-shells, and so on. The transition processes giving rise to the various lines may be illustrated as follows, by making use of the structure diagram :—

K-satellites :

$$\begin{aligned}
\alpha_3 \ldots &\quad 2\mathrm{K}6\mathrm{L}_2 \leftarrow 1\mathrm{K}7\mathrm{L}_2, \\
\alpha_4 \ldots &\quad 1\mathrm{K}5\mathrm{L}_2 \leftarrow 0\mathrm{K}6\mathrm{L}_2, \\
\alpha_5 \ldots &\quad 2\mathrm{K}5\mathrm{L}_2 \leftarrow 1\mathrm{K}6\mathrm{L}_2, \\
\alpha_6 \ldots &\quad 1\mathrm{K}5\mathrm{L}_2 \leftarrow 0\mathrm{K}7\mathrm{L}_2, \\
\alpha' \ldots &\quad 2\mathrm{K}7\mathrm{L}_2 m-1 \leftarrow 1\mathrm{K}8\mathrm{L}_2 m-1.
\end{aligned}$$

In favour of Wentzel's supposition may be cited the fact that his prediction that $\Delta\nu$ values for $\alpha_5-\alpha_3$ should equal that for $\alpha_3-\alpha_1$, and $\alpha_6-\alpha_4$ should be equal to $\alpha_3-\alpha_1$ for the next higher element. These conditions are fulfilled in the measurements of Wetterblad * on the spark lines of Mg, Al, and Si. Following Wentzel, Druyvesteyn † obtained the relation

$$(\mathrm{K}\beta''-\mathrm{K}\beta_1)z=(\mathrm{L}-\mathrm{M})_{z+1}-(\mathrm{L}-\mathrm{M})_z,$$

where $\mathrm{K}\beta''$ is the satellite of the $\mathrm{K}\beta_1$-line, and showed that the relation conforms to experimental results. But the extension of the relation to L-satellites gave less satisfactory results.

Richtmeyer ‡ has recently discussed the whole question of X-ray spark lines, and has shown that neither Wentzel's theory nor Druyvesteyn's suggestion does really explain all the facts known about these lines. He has suggested "the hypothesis that these satellites are produced by two-electron transfers, similar to the primed lines (terms) in optical spectra," and "that the line $\mathrm{K}\alpha_4$ is the result of the simultaneous jump of one electron from the L_{II} level to a vacancy in the K shell, and of another electron from an optical level to a vacancy in the M shell, both transfers cooperating to emit a single quantum," but no suitable choice of combination

* *Zeit. f. Phys.* xlii. (1927).
† Dissertation, Groningen (1928).
‡ Phil. Mag., July 1928.

of frequencies could be made in any atom to get the right result, even qualitatively.

2. *Suggested Interpretation.*

Saha and Ray * have pointed out that, in order to explain the origin of the characteristic emission lines of an atom, the subdivision of L_2, M_2, N_2 into two statically distinct levels such as $L_{21}L_{22}$, $M_{21}M_{22}$, $M_{32}M_{33}$, $N_{21}N_{22}$, ..., and so on, is unwarranted, and such subdivision is opposed to the structure of the outer shells as revealed by the analysis of optical spectra. The division of such sublevels as $L_{21}L_{22}$, $M_{32}M_{33}$, etc., appears by the synthesis of the quantum characteristic of the electrons according to the Pauli-Hund principle, as is usually done in the analysis of the optical spectra.

Thus, in order to explain the $K\alpha_1$ and $K\alpha_2$ radiations, we consider transition of the type $K_1 6L_2 \rightarrow 2K_1 5L_2$, which gives us $K\alpha_1$ and $K\alpha_2$ (K gives ^2S, $6L_2$ gives $^1S_0$, and the resultant is $^2S_1$; similarly $2K_1$ gives $^1S_0$ and $5L_2$ gives $^2P_1$, $^2P_2$ and the resultant is $^2P_1$, $^2P_2$).

During the process of transition from $L_2 \rightarrow K$ we have two lines, $K\alpha_1$, and $K\alpha_2$, corresponding to $^2S_1 \leftarrow 2P_1$, $^2S \leftarrow 2P_2$.

The origin of lines $K\beta_1$, $K\beta_2$ in the K series, and all the lines in L or M series, could be similarly explained.

According to this method, Wentzel's suggestion for the origin of the $K\alpha$ satellites is defective, inasmuch as he neglects the multiplicity of terms arising in such process. Thus, for $K\alpha_3$ Wentzel suggests transition of the type $1K7L \rightarrow 2K6L$. In this process the Pauli-Hund principle demands a larger number of lines than what Wentzel considers. The number of terms arising out of such transition will depend on the actual transference of the electron from L_1 or L_2 level. Moreover, the argument that all the lines arising out of such process will be crowded at $K\alpha_3$ cannot be true, as the separation of the terms in this transition will be more marked than the characteristic emission lines ($K\alpha_1$ and $K\alpha_2$), because of the increase of the net central charge in the ionized atom. Further, according to Wentzel, the intensity relation between the spark lines should change with the change in the existing voltage, but Bäcklin's and Siegbahn and Larson's observations for the $K\alpha$ and $L\alpha$ satellites of Al and Mo respectively are directly opposed to this contention. On the experimental evidences put forward by Siegbahn and Larson † and Bäcklin ‡ that all the spark

* *Phys. Zeits.* xxviii. (1927). ‡ *Loc. cit.*
† *Loc. cit.*

lines are produced simultaneously, we suggest the following scheme *.

Let us suppose that in the process of excitation two electrons are ejected simultaneously—one from K_1, the other from L_1—and that there is now a rearrangement in which one electron passes from L_2 to K_1. The transition is

$$2K_1L_15L_2 \leftarrow K_1L_16L_2,$$
$$K_1 \leftarrow L_2.$$

According to the Pauli-Russel-Hund theory,

the left-hand side gives $^3P_{012}$, $^1P_1$,
the right-hand gives $^3S_1\,^1S_1$.

We now expect a multiplet consisting of 6 lines, as follows :—

$2K_1L_15L_2$ / $K_1L_16L_2$	$^1P_1$	$^3P_0$	$^3P_1$	$^3P_2$
$3S_1$	α_3	α_4	α_6	×
$^1S_0$	α^1		α_5	

In the table of P terms (p. 776) we are arranging the known spark lines on this basis. There are other alternative arrangements possible, but for theoretical reasons we prefer the present one.

In the scheme the line $^3S_1 - {}^2P_2$, which ought to be the strongest, is missing. But this simply means that the difference of $^3P_1 - {}^3P_2$ is very small, and cannot be separated on the plate. Thus α_6 is a composite line which is confirmed by its appearance on the plate as a strong and diffuse line.

There is nothing improbable in such an assumption. We get a similar example in the arc spectrum of He. The combination K_1L_2 gives us $^1P_1\,^3P$, but the ^3P set generally appears as a doublet term. It is only recently that Houston † and Burger‡ have been able to show that the ^3P difference is extremely small. In fact Houston found $\Delta\nu$ for $^3P_0 - {}^3P_1 = -{\cdot}992$, and $^3P_1 - {}^3P_2 = -{\cdot}071$. The terms in He are inverted, *i. e.*, $^3P_0 < {}^3P_1 < {}^3P_2$.

* A further objection against Wentzel's suggestion is that he puts more electrons in the L_2-level than can be allowed by Pauli's principle. For example, Wentzel puts seven electrons in L_2, whereas, according to Pauli, it cannot contain more than six.

† Phys. Rev. xxix. p. 749.

‡ *Zs. f. Phys.* xxxviii. p. 437.

3. *The* $^3S_1 - {}^1S_0$ *Differences.*

The $^3S_1 - {}^1S_0$ terms arise from the coupling K_1L_1, which we obtain in the spectrum of helium. It has been empirically found that the difference $^3S - {}^1S_0$ varies directly as the charge on the nucleus.

TABLE of P terms in ν/R (unit).

		$^3P_0$.	$^3P_1$.	$^3P_2$.	$^1P_1$.	Ordinary doublet, $^2S_{\frac{1}{2}} - {}^2P$.	K-absorption limits in ν/R.
Na	$^3S_1$	77·32		77·98	77·22	Kα	
			77·77		76·99		
	$^1S_0$						
Mg	$^3S_1$	93·14		93·90	92·28	92·34	95·81
			93·66		92·75	$\frac{\Delta\nu}{R} = \cdot02$*	
	$^1S_0$						
Al	$^3S_1$	110·46		111·29	110·25	109·53	114·67
			110·01		109·99	$\frac{\Delta\nu}{R} = \cdot03$*	
	$^1S_0$						
Si	$^3S_1$	128·19		130·13	129·0	128·18	
			129·93		128·66	$\frac{\Delta\nu}{R} = \cdot04$*	
	$^1S_0$						
P						148·4	158·26
						$\frac{\Delta\nu}{R} = \cdot06$*	
S						170·0	181·81
						$\frac{\Delta\nu}{R} = \cdot09$*	
Cl						193·1	207·84
A							235·73
K							265·33

Taking the K_1L_1 coupling in the present case as being perfectly analogous to that of He, the central charge being 11, 12, 13 ... for Na, Mg, and Al ... and assuming that the outer electrons are without effect on the coupling, we find that the $\Delta\nu$ separations $^3S_1 - {}^1S_0$ do actually vary as Z.

* Calculated from Sommerfeld's formula.

	$^3S_1-{}^1S_0$.	$\frac{\Delta\nu}{RZ}$.
He	$\frac{6422}{109765}$	·029
Na	·22	·020
Mg	·24	·020
Al.....	·26	·020

4. *Reasons for assigning the larger difference to the* $L_1 5L_2$ *Coupling.*

We have assigned the larger difference to ^1P-3P differences arising from $L_1 5L_2$ coupling for the following reasons. In the former case, $1Z$, K_1L_1, the electrons were in orbits having different values of the total quantum number n. Hence the effect of coupling is slight. In the present case $n=2$ for both sets, and the effect of coupling will be to produce very large separations in the $^1P-{}^3P$ values. As a matter of fact, this hypothesis is borne out by facts in optical spectra.

The actual values of the separation caused by the coupling $L_1 x L_2 (x=1, \ldots 6)$ in the optical spectra of the group Be ... Na are known only in a few cases. The case parallel to the present one, viz., $L_1 5L_2$ is obtained in the spectra of O, Fl^+ and Ne^{++}. The actual $^1P-{}^3P$ separations here are unknown, but in Fl^+, $^3P_0 < {}^3P_1 < {}^3P_2$. The difference $^1P-{}^3P$ is best known for the coupling L_1L_2, and the figures are given below :—

*$5KL_1L_2$.	Be.	B^+.	C^{++}.
^3P		165343	331939
		44414	58828
^1P		120929	273111

The separation varies as the net charge on the atom.

In other cases as well, for the group $2KL_1XL_2$, the published figures, as far as they are available, support the view that the coupling causes large separation in the value of the terms due to different multiplication, and the value arises roughly as the net nuclear charge.

Element.	Na (11).	Mg (12).	Al (13).	Si (14).	P (15).	S (16).
$\frac{^1P-{}^3P}{R}$	·76	·92	1·04	1·25	—	—
$Z-\sigma$	9	10	11	12	13	14
$\frac{\Delta\nu}{Z-\sigma}$	0·85	·092	·094	·102	—	—

* Phys. Rev. xxvi. pp. 312 & 316.

$Z-\sigma$=net nuclear charge, the two K-electrons being regarded equal to two negative charges and causing a diminution of the central charge by two units.

The mean value of $\Delta\nu=10318$, and the separations observed in the terms of different multiplicity due to the $L_1 x L_2$ coupling amongst the neutral atoms is of this order.

My thanks are due to Prof. M. N. Saha, F.R.S., for many helpful suggestions contained in this paper.

University College of Science,
92 Upper Circular Road, Calcutta,
7th Feb., 1929.

LXXXV. *Proceedings of Learned Societies.*

GEOLOGICAL SOCIETY.

[Continued from p. 272.]

June 26th, 1929.—Prof. J. W. Gregory, LL.D., D.Sc., F.R.S., President, in the Chair.

THE following communications were read:—

1. 'The Geology of the District around Abbey-Cwmhir (Radnorshire).' By Richard Owen Roberts, M.Sc.

This paper deals with an area of about 30 square miles in North-Western Radnorshire, immediately east of the Rhayader district described by Dr. Herbert Lapworth[1]. The rocks belong to the Bala, Valentian, and Wenlock Series.

The Bala rocks have been divided into two groups. The lower group consists of black and blue graptolitic shales and mudstones with grit-bands, which may be correlated with the middle part of the Mydrim Shales of South Wales. A dolerite-sill has been intruded into these black shales. On the west, the upper group consists in the lower part of grey-blue coarsely-mottled mudstones, which yield a few shelly fossils near the base; they are followed by dark-blue rusty-weathering shales and mudstones, while the highest Bala rocks exhibit some lateral variation, and consist of sandy mudstones, shales, and grits. The lithological succession in these Upper Bala rocks resembles that described in other areas in Central Wales. On the east, the Upper Bala rocks consist of grey-blue fossiliferous mudstones.

Only the lowest beds of the Birkhill Stage are exposed, and they are overstepped by the Tarannon Stage, which, over most of the

[1] Q. J. G. S. vol. lvi. (1900) p. 67.

area, rests directly on folded Bala rocks. The succession in the Tarannon is most complete on the north-west; but, eastwards, the upper part of the Tarannon overlaps the lower.

The basal beds of the Wenlock Series consist of mudstones and shales, which are followed by thickly-bedded micaceous grits. In certain localities there appears to be a slight unconformity between the Wenlock and the Tarannon.

The Bala rocks are exposed along the north-eastern extension of the Towy Anticline; but, in this district, the anticlinal axis is partly replaced by an important strike-fault, which hades westwards. Subsidiary folds may be recognized within the Bala rocks. The axes of these folds are parallel to the general strike of the strata, although there is a change in the direction of pitch around Nantmel. The Bala rocks were folded in pre-Tarannon times, but broad shallow folds in the Tarannon and Wenlock rocks indicate that there has been a repetition of folding along the same lines at different periods.

2. 'The Geology of the Country around Bodfean (South-Western Carnarvonshire).' By Charles Alfred Matley, D.Sc., F.G.S., and Albert Heard, Ph.D., M.Sc., F.G.S.

The authors describe the geology of a tract of country, about $3\frac{1}{2}$ miles long by 2 miles wide, between Nevin and Pwllheli, chiefly in the parish of Bodfean. It includes the prominent hill of Garn Bodfean (918 feet above O.D.) and a lesser hill, Moel y Penmaen. Most of the remaining ground is covered by drift.

The country can be divided into two belts with reference to the dominant east-north-easterly strike. The northern belt includes Garn Bodfean and the ground north of Bod-eilan Mill; the southern belt runs from Glan-y-gors to Penprys, through Bodfean Hall and Moel y Penmaen.

In the southern belt there is a volcanic series of submarine lavas and tuffs interbedded with ashy and argillaceous sediments. Fossils found at several horizons indicate a Lower Bala age. Owing to the high dips, mostly nearly vertical, a great thickness (some 3000 feet) of rocks is present in this belt. There is no folding, but there is some strike- and dip-faulting. A zone of tuffs of intermediate composition south of Bodfean Hall is 1000 feet or more thick. The lavas are closely allied to the so-called spilitic suite, and include oligoclase-keratophyres, augite-andesites, and a pyroxene soda-trachyte which may be an albitized augite-andesite.

Garn Bodfean, in the northern belt, has received previous attention from several geologists, and is usually regarded as probably an intrusive boss or neck of andesite. Detailed examination shows that it consists of a great mass of 'felted' and granular keratophyres and some quartz-keratophyres. The 'felted' keratophyres on the southern margin of the hill are seen in a quarry to overlie, at angles of 60° to 70°, a group of bedded tuffs and

agglomerates, the latter resting in turn upon a flow of hypersthene-andesite. Except on this side of the hill, the keratophyres are surrounded everywhere by the Nevin Shales, which have not yielded fossils, but are probably of Llanvirnian age. The curved boundary between the keratophyres and the shales on the western side has been proved by an excavation to be a thrust-plane of low hade, and it is possible that the junction on the northern and eastern flanks may be of the same nature. Keratophyres and quartz-keratophyres, closely akin to those of Garn Bodfean, occur again in the eastern part of the area, north of Bod-eilan Mill, and they are present in force in the country on the north. It seems, therefore, very possible that the whole hill is a transported mass carried over the Nevin Shales by earth-movements.

All the igneous rocks of the area are considered to be extrusive, with the possible exception of a basalt which may be a sill. A detailed account of the petrography is given, with several new chemical analyses.

The paper discusses the tectonics of the area, the Bodfean volcanic series of the southern belt being regarded as part of the volcanic series of Llanbedrog and Madryn brought up as a fold, and the Garn Bodfean Thrust being compared with the Penmorfa Thrust near Criccieth and the deformed thrust of St. Tudwal's Peninsula.

3. 'The Petrography of the Borrowdale Volcanic Series of the Kentmere Area (Westmorland).' By George Hoole Mitchell, Ph.D., M.Sc., F.G.S.

In a previous communication the succession and structure of the Borrowdale Volcanic Series in Troutbeck, Kentmere, and Long Sleddale were described. The present paper forms the sequel, and deals with the petrography of the rocks of that area. The volcanic rocks are composed of both lava-flows and tuffs, and chemical analyses and microscopical examination show them to be of intermediate composition, varying from basic andesites to rhyolites. The rocks are greatly altered, and this has led to difficulty in distinguishing between lava-flows and tuff-deposits, particularly when the former are brecciated owing to flow. The characters of the lava-flows and tuff-deposits are discussed in detail.

The alteration of the rocks, as shown by the changes in mineral composition, together with the materials filling the vesicles, is considered. The conclusion is reached that much of the alteration may be referred to a variety of propylitization.

[*The Editors do not hold themselves responsible for the views expressed by their correspondents.*]

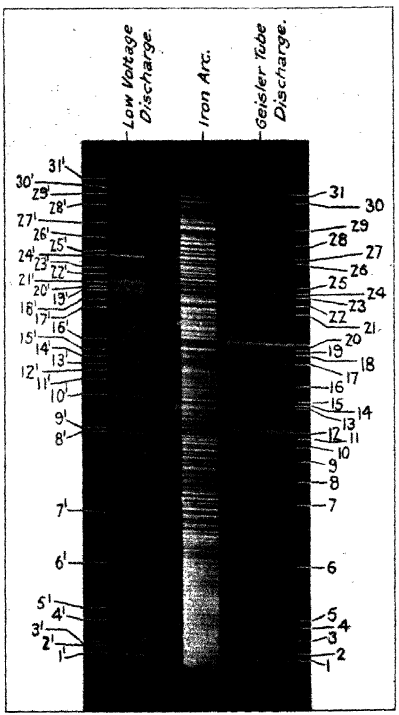
Low Voltage Discharge.
Iron Arc.
Geisler Tube Discharge.
31'
30'
29'
28'
27'
26'
25'
24'
23'
22'
21'
20'
19'
18'
17'
16'
15'
14'
13'
12'
11'
10'
9'
8'
7'
6'
5'
4'
3'
2'
1'
31
30
29
28
27
26
25
24
23
22
21
20
19
18
17
16
15
14
13
12
11
10
9
8
7
6
5
4
3
2
1

THE

LONDON, EDINBURGH, AND DUBLIN

PHILOSOPHICAL MAGAZINE

AND

JOURNAL OF SCIENCE.

[SEVENTH SERIES.]

SUPPLEMENT, DECEMBER 1929.

LXXXVI. *Impact of Spheres of Soft Metals.*

By J. P. ANDREWS, *M.Sc.* *

[Plates XIII. & XIV.]

Abstract.

In the first part of this paper the duration of contact during collision, of two equal spheres of the same material, is investigated with a ballistic pendulum, employing the partial discharge of a condenser to measure the duration. For aluminium, tin, brass, babbitt, and a lead-tin alloy, a law of the form $t = t_0 + a/v^n$ is obtained, where v is the relative velocity at impact, t_0, a, and n are constants. Zinc follows a similar law, but the constants cannot be accurately determined.

In the second part a description of the flattened areas remaining on the spheres after collision is given, and an explanation of the rim which surrounds them is offered. If d is the diameter of these rims, $d = b(v - v_0)^m$, where b, v_0, and m are constants different for different spheres. From v_0 and the elastic moduli of the materials the least pressure required to start flow is calculated in the various cases, and is found to be of the order 10^9 dynes/cm.

* Communicated by Prof. C. H. Lees, F.R.S.

Introduction.

RESEARCH into the process of collision between two solid bodies has followed two main routes, originally laid down by St. Venant and Hertz respectively. Of these, the wave theory of St. Venant has been found to apply to long bars, and bodies whose dimensions are comparatively large. For bodies whose dimensions in the direction of the motion at impact are small, Hertz's theory of perfectly elastic collision is known to be more in harmony with experiment. No precise criterion can be given, but it is known that where the duration of contact is large compared with the time required for a wave of compression to travel across the body and back again Hertz's theory applies *. Thus, in the case of aluminium, where the velocity of sound is $5{\cdot}1 \times 10^5$ cm./sec., $2l/(5{\cdot}1 \times 10^5)$ has to be small compared with the duration of impact, l being the appropriate linear dimension. This paper is concerned with experiments upon spheres small enough for Hertz's theory to apply if the materials are perfectly elastic.

Investigations of the impact of perfectly elastic spheres have, however, already been carried out, and the formulæ deduced by Hertz for the area of compression and the duration of contact have been verified, first by Hertz himself and then by other investigators †. If v is the relative velocity of two equal spheres of the same material at the moment of collision, and t is the duration of their contact, $tv^{1/5}$ = constant, according to Hertz.

When, however, we employ materials other than the hardest steel the assumption of perfect elasticity is no longer justified, and modifications must be introduced. Assuming a resistance to advance proportional to the square of the velocity, from the moment the spheres touch to the moment they begin to recede, T. Pöschl has shown how to modify the theory of Hertz, and has produced an approximate solution of the problem, which shows that tv = constant in this case ‡. It was the original purpose of this research to discover whether or not this law were obeyed.

Method of Investigation.

A good method for investigating this problem was already to hand, and had been used with various modifications by

* *Vide* E. W. Tschudi, Phys. Rev. xviii. p. 423 (1921); J. E. P. Wagstaff, Proc. R. S. cv. p. 544 (1924).

† A. Dinnik, *Jour. d. Russ. Phys. Ges.* xli. p. 57 (1909); W. Müller, *Weiner Ber.* cxxiii. p. 2157 (1914), and others.

‡ T. Pöschl, *Zs. für Phys.* xlvi. p. 142 (1927).

a number of investigators. Only minor improvements have been incorporated here. A condenser is charged, the impact of the metal spheres is allowed to partially discharge it, and the remaining charge is immediately afterwards measured by passing it through a ballistic galvanometer. From a knowledge of the original and final charges and the resistance of the circuit, the time during which the spheres were in contact may be deduced. This method appears to

Fig. 1.

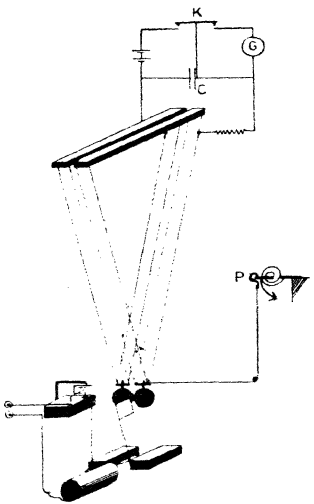

Diagram of Apparatus.

have originated with R. Sabine* in 1876, and has been used, with small differences, by others since, notably by Wagstaff. The chief pitfall to be avoided is the inclusion of appreciable inductance in the circuit, since the formula for calculating the duration of contact then becomes far too complicated. The innovations in the present experiments are the employment of the pendulum suspensions of the spheres as conducting leads and an arrangement enabling the observer to turn the

* R. Sabine, Phil Mag. i. p. 337 (1876)

balls after each collision so as to present a new pair of surfaces at each impact. The spheres were each suspended by four steel wires so as to form pendulums about 180 cm. long, which were so adjusted that the balls were in light contact at points on their equators when at rest. The balls were screwed, as shown, to small bars of brass, to which the suspension wires were soldered. The electrical circuit is represented above. The condenser C is charged by depressing K on the left, while the spheres are separated. This separation is secured by drawing one of the spheres aside by means of a thread passing under a glass rod, and fastened to a hook depending from a platform P. Depressing K to the right then discharges the condenser through the ballistic galvanometer G, producing a throw θ_0. The condenser is charged anew, platform P, which is controlled electro-magnetically, is removed by sudden rotation in the direction of the arrow so as to let the hook and displaced sphere fall perfectly freely, and the spheres collide. Immediately after the collision, the condenser is discharged through G, a deflexion θ being obtained. In order to prevent a further collision, the second sphere, in moving back, actuates a very easily moved switch, and thus causes a flag of mica covered with soft felt to move into the space between the two spheres, insulating them. The masses of the two spheres are adjusted to equality by adding a small weight to one of them if necessary.

Theory of the Method and Preliminary Experiments.

(1) *The Duration of Contact.*

If self-inductance is absent, and the total resistance of the circuit through which the condenser discharges during collision is R, then during this period

$$R\frac{dq}{dt} + q/C = 0,$$

where q is the charge on the condenser. The solution of this equation is

$$q = q_0 e^{-\frac{t}{RC}}, \quad \ldots \ldots \quad (1)$$

C being the capacity of the condenser. If, however, self-inductance is present, but only to a small extent, such that $\frac{L}{C^2R^2}$ is small, then the equation of motion, which is now strictly

$$L\frac{d^2q}{dt^2} + R\frac{dq}{dt} + \frac{q}{C} = 0,$$

may be written approximately

$$R\frac{dq}{dt} + \left(\frac{1}{C} + \frac{1}{C^2R^2}\right)q = 0$$

since from (1)

$$\frac{d^2q}{dt^2} = \frac{1}{C^2R^2}q,$$

and the new solution is

$$\log q = \log q_0 - \frac{1}{R}\left(\frac{1}{C} - \frac{L}{C^2R^2}\right)t. \quad . \quad . \quad . \quad (2)$$

In actual practice q was measured by discharging through a ballistic galvanometer whose deflexions θ were proportional to the quantity discharged, so that (2) may be written

$$\log \theta = \log \theta_0 - \frac{1}{R}\left(\frac{1}{C} + \frac{L}{C^2R^2}\right). \quad . \quad . \quad . \quad (3)$$

Hence, provided self-inductance is zero, and there is no other perturbing quantity, $\frac{1}{R}$ will be a linear function of $\log \theta$, the time t being kept constant.

This matter may be tested by separating the balls to the same distance on each occasion, so that the velocity of approach is always the same, and trying the collision experiment with different values of R in the circuit. But a second consideration enters here. When the spheres first touch, the resistance at their junction must be extremely large, then fall rapidly, reaching a minimum, and finally increase to an infinite value. It may be considered as having an unknown average value r, which may be a not altogether negligible quantity. Equation (3) ought, therefore, to be written approximately

$$\log \theta = \log \theta_0 - \frac{t}{CR\left(1 + \frac{r}{R}\right)\left(1 - \frac{L}{CR^2}\right)}. \quad . \quad . \quad (4)$$

From the form of this equation, provided a wide range of values of R is considered, the two terms in the brackets cannot always compensate one another unless each is separately unity. An experiment was arranged on these lines, the spheres being rotated through a small angle after each collision, using values of R ranging from 113 to 10,000 ohms, and a perfectly rectilinear graph was obtained when $\frac{1}{R}$ was

plotted against $\log \theta$. It follows that $r = 0$ and $L = 0$ very closely. The usual value of R was about 500 ohms. (See fig. 2.)

(2) *The Velocity of Approach.*

When the bob of a pendulum of length l is withdrawn a horizontal distance x, it may be shown that the velocity it

Fig. 2.

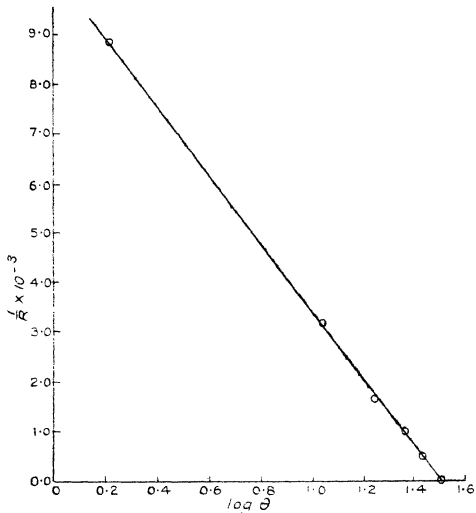

acquires in falling freely to the lowest point of its path is given by

$$v = x\sqrt{\frac{g}{l}}\left\{1 + \frac{x^2}{4l^2}\right\},$$

so long as x is small compared with l. If appreciable damping occurs, and λ is the logarithmic decrement, then the above expression must be multiplied by $\left(1 - \frac{\lambda}{2}\right)$, giving finally

$$v = x\sqrt{\frac{g}{l}}\left\{1 + \frac{x^2}{4l^2} - \frac{\lambda}{2}\right\}.$$

The value of $x^2/4l^2$ never exceeded 1 per cent., and λ varied between 0·012 for aluminium and 0·002 for tin. The corrections were therefore considered negligible.

The Initial Separation of the Spheres.

As it was specially desirable not to contaminate the surfaces of the spheres, the following methods were employed to measure their initial separation. For small separations up to about 20 cm. a large lens was arranged to produce a diminished real image of the spheres, and the horizontal distance between these images was measured in a good travelling microscope. It is estimated that by this means the separation, and therefore the velocity of approach, could be found to about 2 per cent. accuracy, with the exception of the smallest velocities, which were sometimes in error owing to slight draughts. After each set of observations the readings of the microscope were calibrated by observing the apparent length of 10 cm. of a metre scale placed in the position previously occupied by the spheres. For larger distances, where aberration in the lens may have affected the results, the distances were measured directly by a metre scale with stiff paper pointers. For the same degree of accuracy it was only necessary to be certain of the reading to within 4 mm., and it was easy to read it to 1 mm. For simplicity, all the results in this paper are reduced to the microscope scale of the first method.

The Condenser employed.

This was a Siemens Standard 1 mfd., selected because of its small absorption and leakage. In the course of the experiment, as already outlined, the condenser was charged about half a second before the collision, and then discharged about half a second after, so that the chances of any spurious effects due to absorption and leakage were reduced to entirely negligible quantities. The short-circuiting plug of the condenser was inserted for some minutes between collisions. The e.m.f. of the charging battery was carefully watched, and kept at 4 volts.

The Galvanometer.

In the majority of experiments a fluxmeter was employed, this instrument having the advantage of a large periodic time (46 sec.), which enables the ballistic throw to be read off quite accurately. A separate experiment proved that the throw was accurately proportional to the charge suddenly passed through the coil over the whole range employed.

The Spheres.

These were first cast and then turned in the Instrument Shop of East London College. The equatorial zone was turned with special care to a truly spherical figure, since here the collision was to take place; and the whole then polished. In some instances the spheres were subsequently annealed, but this was not possible in the case of zinc and aluminium, as non-conducting films were thereby formed. In all cases the spheres were 4·0 cm. in diameter.

Part I.

Results.

Six substances have so far been examined, viz., aluminium, tin, zinc, an alloy of lead and tin containing 60 per cent. tin, and a babbitt alloy. Typical results follow.

Table I.

Tin. Expt. 2.

Temperature of the air 10°·2 C.

Resistance R, including that of the steel leads = 513·2 ohms.

Length of the pendulum = 184·5 cm.

Capacity of condenser = 1 microfarad.

10 cm. of metre scale = 0·785 cm. on microscope.

$\theta_0 = 32{\cdot}77$ cm.

Separation of spheres, in cm. of microscope. = S.	Throw of galv. θ, cm.	t (sec.) $1{\cdot}18 \log_{10} \frac{\theta_0}{\theta} \times 10^{-3}$,	v $=29{\cdot}40\,S$ cm./sec.	t calc. sec. $\times 10^{-4}$.
0·050	10 35	5·91	1·47	5·91
0·120	12·18	5·09	3·53	5·01
0·177	13 02	4·75	5·20	4·71
0·285	12·95	4·76	8·38	4·38
0·435	14·60	4·15	12·78	4·15
0·900	15·49	3·85	26·5	3·82
1·420	16·15	3·62	41 8	3·65
1·875	16·58	3·50	55·0	3·57
2·63	16·77	3·45	77·3	3·48
0·032	8·85	6·71	0·94	6·49

These results and those in Table II. are represented graphically in fig. 3. Curves representing the results for the other materials are also given in figs. 4 and 5.

TABLE II.

Aluminium. Expt. 3.

Temperature of the air 18° C.
Resistance R, including that of the steel leads, =525 ohms.
Length of pendulum=182·0 cm.
Capacity of condenser=1 microfarad.
10 cm. of metre scale=0·800 on microscope.
θ_0=19·09 cm.

Separation of spheres, in cm. of microscope, =S.	Throw of galv. θ, cm.	Observed t (sec.) $=1{\cdot}212\log_{10}\frac{\theta_0}{\theta}\times10^{-8}$.	v $=29{\cdot}0$ S cm./sec.	t calc. sec. $\times10^{-4}$.
0·085	11·99	2·91	2·46	3·28
0·150	11·53	2·65	4·50	2·47
0·230	13·14	1·96	6·68	2·13
0·335	13·09	1·99	9·73	1·90
0·515	13·66	1·76	14·96	1·71
0·710	14·10	1·60	20·6	1·62
0·935	13·89	1·68	27·2	1·56
1·180	14·73	1·37	34·3	1·51
1·425	14·50	1·44	41·3	1·49
1·700	14·61	1·41	49·2	1·47
0·100	10·20	3·30	2·90	3·04
0·065	8·35	5·34	1·89	3·86
2·000	14·45	1·46	58·0	1·45
1·020	14·00	1·60	29·6	1·54

Fig. 3.

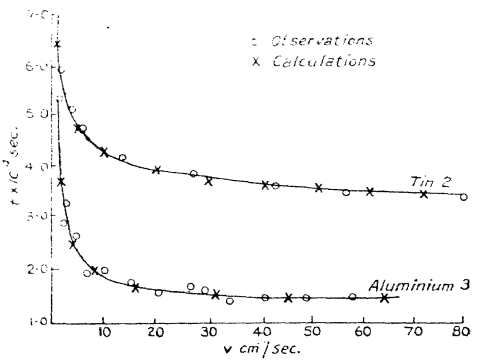

Fig. 4.

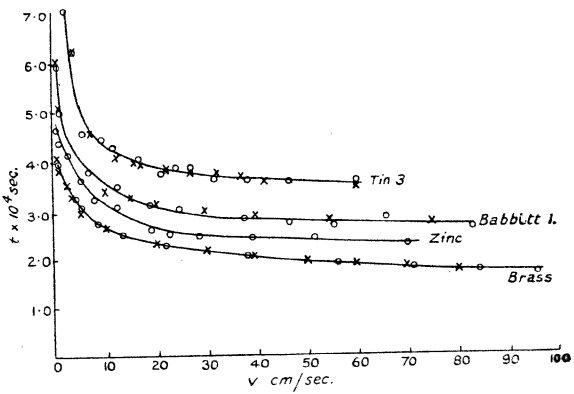
7·0
6·0
5·0
4·0
3·0
2·0
1·0
t × 10⁴ sec.
Tin 3
Babbitt I.
Zinc
Brass
0
10
20
30
40
50
60
70
80
90
100
v cm/sec.

Fig. 5.

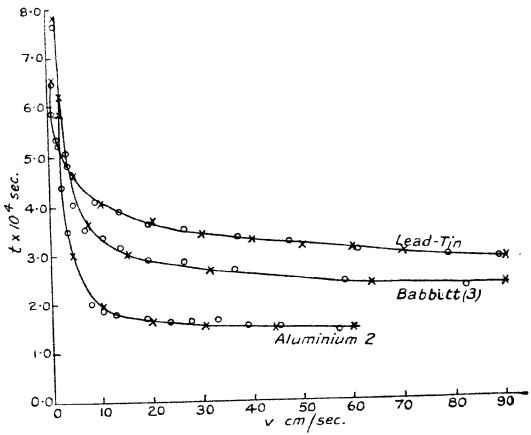
8·0
7·0
6·0
5·0
4·0
3·0
2·0
1·0
0·0
t × 10⁴ sec.
Lead-Tin
Babbitt (3)
Aluminium 2
0
10
20
30
40
50
60
70
80
90
v cm/sec.

The answer to the original question may now be sought, namely, do these results agree with the assumption of a resistance to distortion proportional to the square of the relative velocity? Do they, that is to say, follow a law of the form tv=constant?

In no case is this law obeyed. In some instances a law of the form $(t-t_0)v$=constant would be a first approximation; but after an extensive investigation, the best agreement is found to be with a formula of the type

$$t=t_0+a/v^n,$$

where t_0, a, and n are all constants which differ for the different materials. The values of these constants are

TABLE III.

Substance.	Expt	$t_0\times10^4$ sec.	$a\times10^4$.	n.	Remarks.
Aluminium ...	2	1·38	20·7	1·58	Points scattered.
	3	1·34	4·52	0·92	Re-turned.
Tin	2	2·82	3·58	0·39	
	3	3·40	6·88	0·92	Re-turned.
Babbitt	1	1·89	3·18	0·32	
	2	2·43	6·61	0·98	Re-turned.
	3	1·93	5·88	0·59	Re-turned and annealed.
Brass	1	0·16	3·79	0·19	
Lead–Tin Alloy.	1	1·50	5·00	0·30	
Zinc	No formula found to cover the whole range, but the curve runs in the same general way.				

tabulated in Table III., and the crosses on the curves of figs. 3, 4, and 5 are points calculated from the formula to show how nearly they agree with observations. In one instance, that of zinc, no formula was found to cover the whole range, and repetition gave erratic results, which may have been due to marked differences at different parts of the surface, and to the formation on collision of flattened portions of an unusual character.

In calculating these constants, the usual method (as given, for instance, in Running, 'Empirical Formulas') was found to exaggerate small errors at one end of the range. The following method was therefore employed. The slopes of

tangents drawn at chosen points on a smooth curve through the observations were recorded. Then, since

$$\left(\frac{dt}{dv}\right)^2 = n^2a^2v^{2(1-n)},$$

$$2\log\frac{dt}{dv} = \log(n^2a^2) + 2(1-n)\log v,$$

so that (a) if $\log\frac{dt}{dv}$ is a linear function of $\log v$, the formula $t = t_0 + a/v^n$ follows, and (b) n and a are obtained from the slope and intercept of the straight-line graph indicated. These slopes and intercepts, it should be noted, were definitely calculated by the method recently given by J. H. Awbery*.

Discussion.

According to the formula, the duration of contact tends towards a steady value t_0, which is greater than zero, as the velocity at impact increases. That t_0 would be other than zero is to be anticipated, because at high speeds permanent deformation occurs, and during the process of deformation the spheres must be in contact. It appears that at the highest speeds the diminution of the duration of contact which ought to follow from the larger elastic forces called into play on collision is just counterbalanced by the extension of this period, due to the flow of the metal. A conclusion reached by J. H. Vincent†, after experiments in which a steel ball was dropped upon a lead plate, namely, that the time taken by any one sphere to produce a dent was independent of the velocity of impact, is another example of this compensating action.

At very small speeds $t=a/v^n$ very nearly. This is reminiscent of Hertz's formula $t^{1/5}=$constant. In one instance, that of brass, n is almost exactly 1/5; while in the cases of lead-tin alloy, babbitt, and tin, the value of n in the first experiments, although greater, is not widely different from 1/5, the difference being possibly due to working on the lathe. Of zinc nothing definite can be said in this respect, while aluminium appears to be so susceptible to mechanical working, and so readily forms a non-conducting layer when annealing is attempted, that the results cannot be regarded as evidence on this point. It therefore seems likely that at very small speeds of approach Hertz's law, or a law very similar to it, may apply. Further experiment is required to

* J. H. Awbery, Proc. Phys. Soc. xli. (1929).

† J. H. Vincent, Proc. Camb. Phil. Soc. x. p. 332 (1898–1900).

establish this point, but it may be noted that some experiments by C. V. Raman * upon slow collisions have shown that the coefficients of restitution for lead, brass, and bronze, all approach unity at small speeds of approach. Similar results have been obtained by Ôkubo † for a number of other substances.

The Effect of Mechanical Working and Annealing.

From Table III. it appears, as a rule, that all three constants, t_0, a, and n, increase after the spheres have been re-turned and re-polished; and decrease after annealing. n seems to be the most sensitive in this respect, and t_0 the least. These facts may be understood if t_0 depends upon the properties of the metal in bulk, while n depends on the properties of the outside layer of the material. This is probably the case, for the theory of Hertz assumes that large stresses occur only in the immediate neighbourhood of the area of contact, and the elastic properties of the surface layers are therefore of prime importance in this theory. The present experiments provide a value of n similar to Hertz's when the temporary deformation is confined to the surface and the surface has not been over worked. As soon, however, as comparatively large permanent deformations appear, metal below the surface, and possibly out of the influence of the lathe tool, begins to have a preponderating effect. This is the region in which t_0 is the chief term of the formula.

Finally, these results do not support the view that, after contact is made, the spheres approach one another under a resistance proportional to the square of the velocity.

Part II.

The Permanent Deformation at the Surfaces of the Spheres.

When the speed of approach is fairly high, small flattened portions, circular in shape, are visible on the surfaces of the spheres. To a cursory view they appear planes, as though a small spherical cap had been cut off; but under the microscope they each appear surrounded by a pronounced rim, higher than the flat portion. A magnified section of the sphere through one of these would probably have the appearance of fig. 6 (*a*) in the majority of cases. When light

* C. V. Raman, Phys. Rev. xii. p. 442 (1918).
† J. Ôkubo, Tohôku Univ. Sci. Rep. p. 454 (1922).

is reflected obliquely from the "flat," it is possible to photograph the rim. Pl. XIII. (*a*) shows this. It is not here a question of one harder sphere imposing a concave impression on the other, for as a rule both spheres exhibit the same deformation. To show this clearly, the four photographs, (*b*), (*c*), (*d*), (*e*) of Pl. XIII. are views of the left and right sides respectively of two "flats," one upon each sphere, formed during a single collision. On some occasions the portion usually plane was itself undulating, probably having a section, as in fig. 6 (*b*). This is illustrated in (*f*) and (*g*) of Pls. XIII. & XIV. These remarks apply to all materials, but the case of zinc requires amplification. Whereas in the other cases the rim was perfectly circular, or only slightly distorted, in the case of zinc it was nearly always irregular, and only roughly circular. The flattened portion within the rim, moreover, was traversed by a network of subsidiary

Fig. 6.

ridges which, although readily seen by the eye, were found difficult to record photographically. (*h*), (*i*), and (*j*) of Pl. XIV. are, however, attempts which do show how regions of the "flat" are cast into shadow when viewed by light reflected obliquely. The irregularity of the outline is, in fact, exaggerated in these pictures, the outside rim, although complete, being partly hidden in shadow. The first thought was that the ridges were boundaries of crystals, but in this case the section would have been as in fig. 6 (*c*). stepped on the flattened part. Illumination from the other side ought then to have made the bright lines dark, and shown up other bright lines. In point of fact the same lines were brought out. The conclusion is that the section must have been as in fig. 6 (*d*).

An explanation on the following lines of these rims and ridges suggests itself. During the beginning of the collision, the metal in the neighbourhood of the point of contact is compressed, the pressure being greatest at the centre *. As

* *Vide* Hertz, 'Miscellaneous Papers,' English ed., p. 173.

the centres of the spheres continue to approach, the pressure becomes so great that, if the initial momentum be sufficient, breakdown occurs. The area over which the metal has "fused" will continue to expand until the balls begin to recede. The continued approach of the centres involves the "fusion" of more material at the centre of the compressed area, and this material has to be forced aside. When the spheres cease to approach, and begin to recede, the pressure on this extruded material is relaxed, and it re-sets. The sharply-defined rim suggests that it has been extruded beyond the area of contact, for here it would solidify on emergence, and immediately be covered by more material, thus building up a projecting ring which would be constrained to lie in the plane of contact until the pressure was released. On relaxation the layers first deposited would recover from the strain of subsequent pressure, pulling the projection into a rim.

It may be asked why, if "fusion" occurs over a common area, the spheres do not adhere. This would be easier to explain than the apparent adhesion of the zinc spheres, for the surfaces are covered with exceedingly fine scratches from the lathe tool, each of which provides an air-film to prevent the coalescing of the two parts. But in the case of zinc transitory adhesion does appear to take place, and the ridges within the rim are probably the lines along which the adhesion was most protracted. This offers a ready explanation of the erratic nature of the results for zinc, but its exceptional behaviour remains unexplained.

A very similar phenomenon has been observed by C. V. Raman * when steel balls are dropped upon a glass surface. He hesitates, however, to ascribe the rim to flow of fused material, owing to the time available being so small. When, however, it is recalled that in my experiments the gradient parallel to the surface, of the normal pressure, is of the order 10^{10} dynes per sq. cm. per cm. or more, and the mass of material to be moved of the order 10^{-5} gm., it does not seem at all impossible that the required velocity of flow (less than 1000 cm./sec.) could be acquired in a few ten-thousandths of a second, even allowing for powerful forces due to viscous resistance.

Size of the Permanent Deformation in Relation to the Velocity at Impact.

The diameters of the circular rims were measured microscopically, and the results recorded with the velocities of

* C. V. Raman, J. Opt. Soc. Amer. xii. p. 387 (1926).

approach in Table IV., a typical example. These results are plotted in fig. 7, where d^2 is taken as the ordinate to bring

TABLE IV.

Tin Spheres. Exp. (3).

Diameter of spheres 4·00 cm.
Mass of each sphere 240 gm.

v, cm./sec.	Diameters of rims of deformations. Sphere 1, c.m.	Sphere 2, cm.	Means, cm.	Diameters calculated, cm.
9·2	0·083	0·160	0·095	0·081
11·9	0·110	0·112	0·111	0·106
16·5	0·117	0·129	0·123	0·131
21·0	0·153	0·145	0·149	0·150
23·9	0·162	0·159	0·160	0·162
26·8	0·174	0·176	0·175	0·172
31·8	0·192	0·199		
31·8	0·195	0·187	0·193	0·187
38·6	0·205	0·208	0·206	0 205
46·8	0·230	0·233	0·231	0·225
60·2	0·236	0·235	0·235	0·248

Fig. 7.

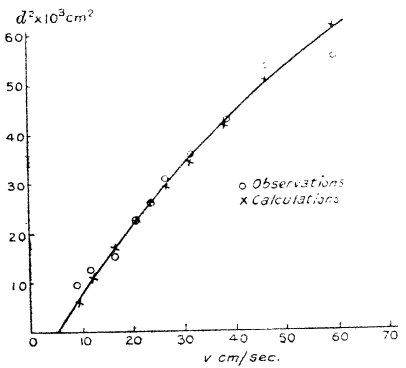

out more clearly the intersection of the curve with the v axis. In some cases the diameters for one sphere of a pair were uniformly a little larger than those for the other, but in all

cases the mean was taken as the most convenient quantity to deal with. The curves for the remaining substances are shown in fig. 8. If the curves may be extrapolated to intersect the axis of v, as has been done in the figures, we learn that no permanent deformation is produced until the velocity of approach reaches a definite value v_0, which is a characteristic of each material. There is nothing new in this idea, but the observation is a justification for it. The values of v_0 are given in Table V. In some instances the diameters could not be measured with sufficient accuracy to

Fig. 8.

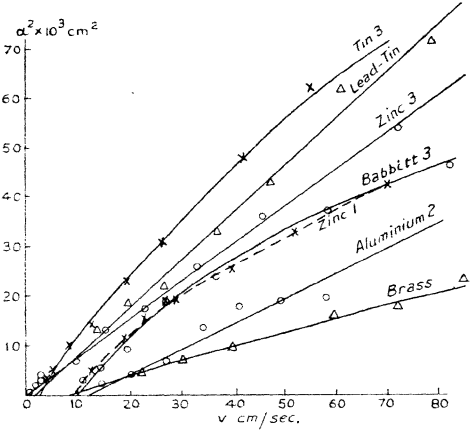

Observations are indicated.

warrant their inclusion here; but, from the reliable sets of observations a formula was sought to represent the results. This was found to be

$$d = b(v - v_0)^m,$$

and Table V. gives the values of the constants b, m, and v_0.

Discussion.

In the cases of aluminium, lead-tin alloy, brass, and zinc after annealing, m is approximately 0·5. Thus d^4 is proportional to a quantity of kinetic energy $k(v-v_0)^2$, which, when v is sufficiently large, differs only a little from the expression

for the kinetic energy of the moving sphere at collision. The volume of the small spherical cap whose diameter is d is $\frac{\pi d^4}{64R}$, R being the radius of the sphere. Hence at high speeds we have the rule, originally given by Vincent for the case of spherical indentations in a lead plate, "the volume of the material apparently removed is proportional to the kinetic energy of the moving sphere at impact."

This is, however, no longer true in general for small values of the kinetic energy, and according to these results it is not a principle applicable to all substances. A similar rule might be made for the other substances, but it would be neither so simple nor so suggestive.

TABLE V.

Substance.	Expt.	b.	v_0, cm./sec.	m.	Remarks.
Aluminium ...	3	0·023	12·0	0·5	Observations rather scattered.
Tin	2	0·048	2·5	0·41	
	3	0·047	5 0	0·42	After re-turning.
Babbitt	3	0·044	10·0	0·375	After re-turning and annealing.
Zinc	1	0·045	9·0	0·37	
	3	0·027	Very small.	0·50	After annealing and then re-turning.
Lead-Tin Alloy.	1	0·098	2·0	0·50	
Extruded Brass.	1	0·020	8·0	0·47	

The Least Pressure Required to initiate Flow.

A knowledge of v_0 enables us to calculate this pressure for the various substances. The calculation is based on the theory of Hertz, and rests on the assumption that the materials may be regarded as perfectly elastic when $v < v_0$. From the first part of this paper, it will be clear that considerable justification exists for this in the cases of brass, lead-tin alloy, babbitt, and perhaps tin; for zinc and aluminium the case is not so good.

Following Love's version of Hertz's work*, we find that the total thrust over the whole area of contact is given by

$$P = \frac{4}{3\pi}\frac{a^3}{R}\frac{4\pi\mu(\lambda+\mu)}{\lambda+2\mu},$$

* Love, "Elasticity," 4th edn. p. 200. The English translation of Hertz's 'Miscellaneous Papers' contains several serious misprints.

where a is the radius of the compressed area, R the radius of the spheres, λ and μ are elastic moduli commonly employed.

The maximum value attained by a is related to the velocity of impact v thus

$$a_{\max.} = \mathrm{R}\left(\frac{v}{c}\right)^{2/5}\left[\frac{5\pi}{16}\frac{(1-\sigma)^2}{1-2\sigma}\right]^{1/5},$$

where c is the velocity of compressional waves in the material of the spheres.

$$c^2 = \frac{\lambda+2\mu}{\rho}; \quad \rho = \text{density of material};$$

$$\sigma = \text{Poisson's Ratio};$$

while the pressure at the centre of the compressed area

TABLE VI.

Substance.	Expt.	$\phi\times10^{-9}$.	$v_0{}^{2/5}$.	P′, dynes/cm.².	Tensile strength. dynes/cm.².
Aluminium ...	3	2·6	2·71	$7{\cdot}1\times10^9$	$5{\cdot}4\times10^9$
Tin	2	2·3	1·45	$3{\cdot}3\times10^9$	$1{\cdot}7\times10^9$
	3	2·3	1·90	$4{\cdot}4\times10^9$	
Babbitt	3	1·7	2·51	$4{\cdot}3\times10^9$	
Zinc.....	1	3·6	2·41	$8{\cdot}7\times10^9$	$1{\cdot}2\times10^9$
	3	3·6	Too small to measure.		
Lead–Tin Alloy.	1	2·3	1·32	$2{\cdot}6\times10^9$	
Extruded Brass.	1	4·1	2·30	$9{\cdot}5\times10^9$	8×10^9

(where it is a maximum), is given when a attains its maximum also by

$$\mathrm{P}' = \frac{3\mathrm{P}}{2\pi a^2}$$

$$= v^{2/5}\left\{\frac{8\lambda(\lambda+\mu)}{\pi(\lambda+2\mu)}\left[\frac{1}{c^2}\frac{5\pi}{16}\frac{(1-\sigma)^2}{1-2\sigma}\right]^{1/5}\right\}$$

$$= v^{2/5}\phi,$$

where the coefficient of $v^{2/5}$ is denoted by ϕ.

If, now, we insert v_0 as the velocity, P′ will be the pressure just capable of starting flow. Table VI. gives the calculated values of these pressures. The necessary elastic constants

for aluminium, zinc, tin, and brass were derived from tables, while those for babbitt and the lead-tin alloy were found from separate experiments on rods of these materials specially cast for the purpose. These pressures may be compared with such quantities as crushing and tensile strengths; but the former are not recorded to any extent except for ferrous metals. The available data on tensile strengths have been added in the last column for comparison. It is interesting to note that these are of the same order as the pressures calculated.

Summary of Results.

Part I.

(*a*) The duration of contact is related to the velocity of approach by the law $t = t_0 + \frac{a}{v^n}$.

(*b*) For the alloys brass, lead-tin, and babbitt n is practically 1/5, as in Hertz's formula $tv^{1/5} = \text{constant}$, provided the surface is not mechanically worked to too great an extent.

(*c*) For the metals tin and aluminium n is definitely greater than 1/5, while for zinc no value can be given.

(*d*) Mechanical working of the surface raises the values of t_0, a, and n, while annealing reduces them again.

Part II.

(*a*) The circular permanent deformations are found to be bounded by a rim.

(*b*) The diameters of these rims are related to the velocity at impact by the law $d = b(v - v_0)^m$.

(*c*) In the cases of aluminium, lead-tin, and brass m is practically 0·5.

(*d*) In the case of zinc the deformations are irregular in outline and intersected by ridges.

(*e*) The pressures necessary to cause the metal to flow are of the order 10^9 or 10^{10} dynes/cm.^{2}, that is, of the order of the tensile strengths.

In conclusion, this is the first paper upon a research, still in progress, carried out at East London College under the encouragement of Prof. C. H. Lees, to whom I am indebted for many helpful suggestions.

LXXXVII. *On the 42-Minute Period in the Frequency of the After-Shocks of Earthquakes.* *By* CHARLES DAVISON, *Sc.D., F.G.S.* *

THE time taken by an earthquake-wave to travel from a focus near the surface to its antipodes is almost exactly 21 minutes. As the crust within and near the focus is for some days in a highly sensitive condition, it is possible that the return-pulsation may affect the frequency of the after-shocks, and my object in this paper is to show that a 42-minute periodicity does govern their occurrence. In two earthquakes, the Mino-Owari earthquake of 1891 and the Kwanto earthquake of 1923, I have applied the same methods in the hope of tracing periods of 21 and 84 minutes, but I have not been able to find any decisive evidence of their existence †.

Let us suppose that the crust is on the point of motion in one direction over a certain area, and that a periodic force of strength sufficient to precipitate motion acts upon it in the same direction. The resulting earthquakes would then be subject to a period of the same duration, and the maximum epoch of the period would coincide approximately with that of the variable force. If the latter force were to act in the direction opposite to that in which the crust is about to move, there might still be the same periodicity in the frequency of earthquakes, but the maximum epoch would coincide with the minimum epoch of the variable force. Thus, if the after-shocks of an earthquake are due mainly to a continued exertion of the forces that give rise to the earthquake, then the maximum epoch of the 42-minute period, if it exists, should coincide with the arrival of the return-movement. On the other hand, if most of the after-shocks are due to the settling of the displaced crust, the maximum epoch of the period should occur about 21 minutes after that return.

The only catalogues of after-shocks at my disposal that are full enough for the purpose are those of five Japanese earthquakes from 1891 to 1927, three European earthquakes from 1894 to 1915, and three others depending on personal observations only.

In the following sections the time of occurrence given is that of the initial epoch of the movement. As, however, the duration of a great earthquake may amount to 4 or 5

* Communicated by the Author.

† On this subject, see H. H. Turner, R. Astro. Soc. Monthly Notices, Geoph. Suppl. vol. i. pp. 31–50, 88–99, and vol. ii. pp. 73–76.

minutes, the epoch of the strongest movement may be a minute or two later. In each earthquake, successive intervals of 42 minutes were divided into 14 minor intervals of 3 minutes each, and 7-interval means were taken of the total numbers of after-shocks occurring in corresponding intervals. In the tables the date of the maximum epoch is the number of minutes after the last complete interval of 42 minutes measured from the initial epoch of the earthquakes. In estimating the amplitude the average number of after-shocks in each 3-minute interval is taken as unity.

Mino-Owari Earthquake of Oct. 28, 1891.

The Mino-Owari earthquake occurred at 6.37 A.M. The seismographs at Gifu and Nagoya were at once put out of action, but the first after-shock was recorded at 1.10 P.M. at Nagoya and 1.55 P.M. at Gifu *. In both records the intervals mentioned range from Oct. 28, 2.0 P.M., to Nov. 2, 1.0 P.M., from that date to Nov. 6, 0.12 P.M., and from the latter to Nov. 10, 11.24 P.M.

Interval.	Gifu.			Nagoya.		
	No. of shocks.	Max. epoch, min.	Ampl.	No. of shocks.	Max. epoch, min.	Ampl.
Oct. 28–Nov. 2 ...	863	18½	·09	507	3½	·11
Nov. 2–6	201	9½	·22	91	9½	·47
Nov. 6–10	177	3½	·22	65	21½	·41

Thus, during the first five days, the minima of the 42-minute period at Gifu, and the maxima at Nagoya, coincided approximately with the return-movements. In the next four days, the series of means were somewhat irregular, and the epochs at both places occupied an intermediate position. In the last four days the epochs were almost reversed, so that the maxima at Gifu and the minima at Nagoya coincided nearly with their return-movements.

The explanation of the opposition in epoch at Gifu and Nagoya is probably to be found in the positions of these places with reference to the great fault-line. Along this fault the crust on the east side was relatively lowered by 10 feet or less, except at one place, Midori, where it was

* F. Omori, Tokyo Imp. Univ. Coll. Sci. Journ. vii. pp. 178–189 (1894).

raised by 20 feet. Gifu lies about 5 miles from the fault-line and 14 miles from Midori. Nagoya lies about 18 miles from the continuation of the fault-line and 34 miles from Midori.

Hokkaido Earthquake of Mar. 22, 1894.

The Hokkaido earthquake occurred at 7.56 P.M., and the after-shocks were recorded at Nemuro (75 miles from the epicentre) without interruption at the start*. The first five days range from Mar. 23, 0.0 A.M., to Mar. 27, 11 P.M., and the next ten days from the latter time to Apr. 6, 9 P.M.

Interval.	No. of shocks.	Max. epoch, min.	Amplitude.
Mar. 23-27	264	$2\frac{1}{2}$	·17
Mar. 27–Apr. 6 ...	55	$23\frac{1}{3}$	·25

Thus, in the first interval, the maxima of the 42-minute period coincided approximately with the return-movements; in the second interval the minimum coincided nearly with those returns.

San-riku Earthquake of June 15, 1896.

The epicentre of this earthquake lay near the foot of the western slope of the Tuscaroora Deep, about 160 miles from the east coast of Japan. It was registered at Tokyo (about 340 miles from the origin) at 7.34 P.M.† During the five days, June 15–19 (36 after-shocks), the maxima of the 42-minute period occurred at $22\frac{1}{2}$ min. after the return-movements (amplitude ·34). After June 19 the recorded shocks are too few in number to determine the existence of the period.

Kwanto Earthquake of Sept. 1, 1923.

The great Kwanto earthquake was recorded at Tokyo at 11 h. 58 m. 44 s., A.M. Most of the seismographs in the central district were overthrown by the shock, but one instrument at Tokyo remained in action throughout. Two lists of after-shocks have been published: one, by A. Imamura and K. Hasegawa, of the after-shocks strong enough to be felt in Tokyo from Sept. 1 to Oct. 1; the other, by T. Yasuda, of all

* F. Omori, Imp. Earthq. Inv. Com. Publ. no. 7, pp. 35–51 (1902).
† Brit. Ass. Rep. 1897, pp. 7–8.

the after-shocks recorded in that city from Sept. 1 to Jan. 31, 1924*. The first after-shocks entered in both lists occurred at 0 h. 1 m. 49 s., P.M. on Sept. 1. For the remainder of Sept. 1, Imamura gives the times of 189 shocks and Yasuda of 225. For the whole of September, the corresponding numbers are 720 and 1303.

Making use first of Inamura's list, the maximum epoch for Sept. 1–6 (463 shocks) occurs at 20½ min. with an amplitude of ·13. During the second and third five days (114 and 45 shocks) the existence of the period becomes uncertain, the series of means being irregular. For Sept. 16–30 (84 shocks) the series of means vary regularly, with the maximum epoch at 32½ min. and the amplitude ·30.

The central district is divided by Imamura and Hasegawa into four regions, to each of which belonged its own series of after-shocks. The region A includes most of Sagami Bay and the land to the north; the region B contains the Boso Peninsula and the sea-bed to the east; the region C lies entirely on land to the north of Tokyo; while the region D includes Tokyo and the surrounding country. Of these regions, A and B are by far the most important; the region C was disturbed by comparatively few after-shocks, and the region D by a larger number, usually of slight intensity.

Nearly 24 hours after the great earthquake, at 11 h. 46 m. 55 s., A.M., on Sept. 2, another violent shock, almost as strong as the first, occurred in region B with its epicentre lying about 41 miles to the east. It is probable that most of the after-shocks in this region were connected with this second earthquake, for only one shock on Sept. 1 is assigned to region B.

Region.	Interval.	No. of shocks.	Max. epoch, min.	Amplitude.
A.....	Sept. 1– 6.	239	16	·13
„	„ 6–11.	30	41½	·83
D	Sept. 1– 6.	89	20½	·47
„	„ 6–11.	48	11½	·33
B.....	Sept. 2– 7.	96	36	·33
„	„ 7–12.	39	23⅓	·36

For regions A and D the first five days are reckoned from noon on Sept. 1, the second five from 11 A.M. on

* A. Imamura and K. Hasegawa, Imp. Earthq. Inv. Com. Bull. ii. pp. 72–93 (1928); T. Yasuda, Imp. Earthq. Inv. Com. Rep. no. 100 A, pp. 261–310 (1925).

Sept. 6, and the maximum epoch from 11.59 A.M. on Sept. 1. For region B the first five days are reckoned from noon on Sept. 2, the second five from 11 A.M. on Sept. 7, and the maximum epoch from 11.47 A.M. on Sept. 2.

Thus, in region D, the minima of the period during the first five days coincided closely, and in region A roughly, with the return-movement; during the second five days the maxima in region A coincided closely with those returns. In region B, during the first and second 5-day intervals, the maxima and minima, respectively, coincided roughly with those returns.

Yasuda's list differs from the other in the inclusion of after-shocks imperceptible to human beings in Tokyo. It is also continued for four additional months. The results are as follows:—

Interval.	No. of shocks.	Max. epoch min.	Amplitude.
Sept. 1– 6	755	$23\frac{1}{2}$	·14
,, 6–11	288	7	·14
,, 11–16	125	13	·11
,, 16–30	133	40	·16
Oct. 1–14	45	$41\frac{1}{2}$	·38
,, 15–31	51	$2\frac{1}{2}$	·22

During the intervals Sept. 6–11 and Sept. 11–16 there is no irregularity in the series of means, and the date of the epoch is probably that of the resultant of two periods with maxima near the middle and end of the 42-minute intervals. During November there is no trace of a 42-minute period in either of the intervals Nov. 1–14 and Nov. 15–30. Thus, after two months the throbbing of the earth due to the original displacement seems to have died away.

Lastly, deducting the number of shocks for each interval in Imamura's list from the corresponding number in Yasuda's list, we obtain the numbers of shocks imperceptible to human beings in Tokyo, with the following results:—

Interval.	No. of shocks.	Max. epoch. min.	Amplitude.
Sept. 1– 6	292	$23\frac{1}{2}$	·28
,, 6–11	174	7	·25
,, 11–16	79	$11\frac{1}{2}$	·30
,, 16–30	49	$2\frac{1}{2}$	·34

Tango Earthquake of Mar. 7, 1927.

The earthquake occurred at 6.27 P.M. It originated along two faults nearly at right angles to one another. Surveys made in May–June, August–September, and October–November of the same year showed that the movements of the crust continued for at least six months of the earthquake, and not always in the same directions. The after-shocks were recorded at three stations, Maiduru, Kinosaki, and Inemura, about 8, 12, and 13 miles, respectively, from the line of the principal fault *. The first after-shock was recorded at Maiduru at 10.12 P.M. on Mar. 11, and at the other stations on the following day. The first interval in the table (see p. 807) ranges from Mar. 12, 3.12 P.M., to Mar. 16, 11 P.M.

A strong after-shock occurred at 6.7 A.M. on Apr. 1, and this was followed by 191 after-shocks on the same day, so slight that only 12 were recorded at all three stations, 20 at one other station besides Maiduru, and 162 at Maiduru only. The list for the latter station gives the following results :—

Interval.	No. of shocks.	Max. epoch, min.	Amplitude.
Apr. 1	191	1½	·23
„ 2–3	58	...	...
„ 4–7	53	22½	·44
„ 8–14 ...	104	...	...

The results given in the above tables seem to depend on the complex origin of the principal earthquake. From Mar. 12 to 31 the maximum epoch is at about 30 min., in April at about 28½ min. Then after about seven weeks the epoch is reversed (to 7½ min.) in May. In June the number of shocks recorded is only 17. The list for July seems to contain misprints, and I am unable to make use of it. In August there is no trace of the period. The epochs for Apr. 1 and Apr. 4–7 are reckoned, as before, from the principal earthquake at 6·27 P.M. on Mar. 7. As the interval between the principal earthquakes and the strong after-shock at 6.7 A.M. on Apr. 1 exceeds a multiple of 42 minutes by 20 minutes, it is at first sight doubtful whether the maxima coincide with the return-movements due to the principal earthquake, or the minima with the return-movements from the after-shock.

* N. Nasu, Tokyo Earthq. Res. Inst. Bull. vi. pp. 300-331 (1929).

Interval.	General.			Maidoru.			Kinosaki.			Inemura.		
	No. of shocks.	Max. epoch, min.	Ampl.	No. of shocks.	Max. epoch, min.	Ampl.	No. of shocks.	Max. epoch, min.	Ampl.	No. of shocks.	Max. epoch, min.	Ampl.
Mar. 12–16...	142	30	·28	140	31½	·30	115	31½	·34	120	28½	·36
16–31...	196	...	...	192	...	...	139	...	...	158	...	...
Apr. 1–14...	409	28½	·09	408	28½	·09	59	28½	·50	57	...	...
15–30...	119	...	...	118	...	...	50	30	·31	56	27	·33
May 1–14...	82	7½	·27	74	7½	·34	53	6	·27	57	7½	·36
15–31...	65	7½	·31	63	7½	·27	33	6	·23	35	...	...
Mar. 12–31...	338	31½	·13	332	31½	·13	254	34½	·19	278	34½	·23
Apr.....	528	28½	·13	526	28½	·13	109	28½	·42	113	25½	·20
May.....	147	7½	·38	137	7½	·31	86	6	·25	92	7½	·34

That the former alternative is the correct one seems clear from the frequency of the after-shocks during the first three 42-minute periods succeeding the strong after-shock. Taking the number of after-shocks in 3-minute intervals and smoothing the curve by taking for each interval the mean of three successive intervals, the maxima of the curve occur close to the beginning of each of the 42-minute periods. Thus, as the first maximum occurs within a few minutes after the strong after-shock, the period must be connected with the return-movements from the principal earthquake rather than with those (if they existed in sufficient strength) from the after-shock. It follows, therefore, that the movement that gave rise to the after-shock was in the opposite direction to the movement that caused the great earthquake.

Locris (N.E. Greece) Earthquakes of Apr. 20 and 27, 1894.

The first earthquake occurred on Apr. 20 at 6.52 P.M., the second and stronger on Apr. 27 at 9.30 P.M. The after-shocks were recorded at Athens (about 60 miles from the epicentre)*. The first interval ranges from April 20, 7.0 P.M., to Apr. 27, 5.36 P.M., the second from Apr. 27, 9.48 P.M., to May 12, 6.48 P.M.

Interval.	No. of shocks.	Max. epoch, min.	Amplitude.
Apr. 20–27.....	21	18	·52
„ 27–May 12 ...	31	9	·23

Thus, for the first interval, the maximum epoch agrees nearly with the return-movements.

Messina Earthquake of Dec. 28, 1908.

The earthquake occurred at 5.20 A.M. The first after-shock was recorded at Mileto at 5.36 A.M. and at Catania at 6.4 A.M.†. In the following table the first interval ranges from Dec. 28, 6.0 AM., to Jan. 2, 5.0 A.M., and the second from the latter time to Jan. 12, 3.0 A.M.

* D. Eginitis, *Athènes Obs. Nat. Ann.* ii. pp. 217–229 (1900).

† *Ital. Sism. Soc. Boll.* xv. pt. 2, pp. 566–639 (1911); xvi. pt. 2, pp. 1–50 (1912).

Record.	Interval.	No. of shocks.	Max epoch, min.	Amplitude.
General ...	Dec. 28–Jan. 2.	107	14½	·28
„	Jan 2–12.	38	35½	·25
Mileto.....	Dec. 28–Jan. 2.	58	11½	·33
„ ...	Jan. 2–12.	34	32½	·45
Catania ...	Dec. 28–Jan. 2.	94	14½	·36

Taking the after-shocks as a whole, the minima of the 42-minute period preceded the return-movements by 6½ min. during the first five days. In the second interval the epoch is reversed. At Mileto the epoch during the first five days preceded the return-movements by 9½ min.; during the next ten days it was reversed. During the months of February and March there is no distinct trace of the period.

Marsica Earthquake of Jan. 13, 1915.

The earthquake occurred at 7.53 A.M. The record of after-shocks at Rocca di Papa (47 miles from the epicentre) is a very full one, the first after-shock being registered at 8.27 A.M. *. The earthquake was unique among those here considered. Though very destructive the area of damage contained only 55 sq. miles and the disturbed area not more than 5700 sq. miles. The first interval of five days (554 after-shocks) gives the maximum epoch at 10 min. and the amplitude as ·06. In succeeding intervals of five, five, and ten days the series of means are somewhat irregular; there is no sign of a reversal of epoch and no certain trace of a 42-minute period after Jan. 18. Making use of shorter intervals, it is clear that the reversal occurred very soon after the earthquake, as follows :—

Interval.	No. of shocks.	Max. epoch, min.	Ampl.
First six hours (6 hr. 18 m.).	177	19	·19
Second „	52	35½	·30
Third „	42	11½	·67
Fourth „	32	2½	·30
Rest of first five days.....	251	40	·09

* A. Cavasino, *Ital. Sism. Soc. Bol.* xix. pp. 236–291 (1915).

Thus, during the first six hours, the minimum epoch coincided nearly with the return-movement; during the next twelve hours the period seems to be the resultant of two periods with different epochs; in the fourth six hours and during the rest of the first five days the maximum epoch coincided nearly with the return-movement. The early reversal of epoch and the brief duration of the 42-minute pulsations are no doubt connected with the small area affected by the earthquake.

Hawaiian Earthquakes of Mar. 28 *and Apr.* 2, 1868.

In these and the remaining earthquakes, the records of after-shocks are non-instrumental. The period considered is, however, too short to be affected materially by the varying conditions of the observers throughout the day.

The first strong earthquake occurred on Mar. 28 at 1.28 P.M., the second and more destructive on Apr. 2 at 3.40 P.M.* The first interval ranges from Mar. 28, 2.6 P.M., to Apr. 1, 6.18 A.M., the second from Apr. 2, 4.12 P.M., to Apr. 7, 4.36 P.M.

Interval.	No. of shocks.	Max. epoch, min.	Amplitude.
Mar. 28–Apr. 1...	118	24½	·23
Apr. 2–7	110	3½	·17

Thus, the minima in the first interval and the maxima in the second interval occurred shortly after the return-movements.

Riviera Earthquake of Feb. 23, 1887.

The principal earthquake occurred at 6.20 A.M. The first interval ranges from Feb. 23, 9.6 A.M., to Feb. 28, 8.6 A.M., and the second from the latter time to Mar. 10, 6.6 A.M. †.

Interval.	No. of shocks.	Max. epoch, min.	Amplitude.
Feb. 23–28	79	20½	·38
Feb. 28–Mar. 10 ...	34	5½	·45

* H. O. Wood, Amer. Seis. Soc. Bull. iv. pp. 178–183 (1914).

† T. Taramelli and G. Mercalli, *Uff. Centr. di Meteor. e Geodin., Annali*, viii. pp. 260–289 (1888).

Thus, in the earlier interval, the maximum epoch occurred at nearly 21 minutes after the return-movements. In the later interval the number of shocks is small, but the epoch tends to agree with those movements. After Mar. 10 there is no trace whatever of the 42-minute period.

Zante Earthquake of Apr. 17, 1893.

The earthquake occurred at 7.4 A.M. The first interval ranges from Apr. 17, 7.0 A.M., to Apr. 22, 6.0 A.M., the second from the latter time to May 2, 4.0 A.M. *

Interval.	No. of shocks.	Max. epoch, min.	Amplitude.
Apr. 17–22	68	21½	·45
Apr. 22–May 2...	46	30½	·34

Thus, for the first five days, the minima of the 42-minute period coincided closely with the return-movements.

Conclusions.

(i.) In each of the series of after-shocks examined, there is evidence of the existence of a 42-minute period, connected more or less closely in point of time with the epoch of the earthquake. As a rule, the maxima at first occur about 21 minutes after the returns of the earthquake-movement. This periodicity lasts for about five days—in one earthquake for a few hours and in two others for three or more weeks—but is continued for several weeks longer with a reversal of epoch.

(ii.) The after-shocks of a great earthquake seem to have two distinct origins. Some, including perhaps the stronger, after-shocks result from repetitions of the original movement, transferred in part to other regions and especially to those bordering the area of displacement. Others are due to the settlement of the displaced mass. At first the latter greatly predominate in number, but after about five days the former begin to assert themselves. The reversal of epoch in the 42-minute period is due, not to any change in the variable force, but to the change in the predominating cause of the after-shocks. The change, however, does not take place abruptly, and there are intervals, lasting it may be for some

* *Athènes Obs. Nat. Ann.* ii. pp. 195–196 (1900).

days, in which neither kind of after-shock distinctly predominates. At such times either the maximum epoch occupies an intermediate position, or the series of means is irregular and leads to no definite period *.

(iii.) Three of the earthquakes here considered were followed, after an interval of from one to seven days, by an earthquake of nearly the same, or even greater, intensity. In the Kwanto earthquakes of 1923 and the Hawaiian earthquakes of 1848 the return-movements coincided nearly with the minima of the 42-minute period in the earlier earthquake and with the maxima of the period in the later. In the Locris earthquake of 1894 the change of epoch was less pronounced, but the number of shocks recorded were small (21 and 31). The evidence, so far as it goes, seems to suggest that, when two principal earthquakes occur in one series, the movement causing the earlier is in the opposite direction to that which gives rise to the first after-shocks, while the movement causing the later is in the same direction.

(iv.) So far as I am aware, the 42-minute period is confined to the after-shocks of great earthquakes. I have examined many records of ordinary earthquakes, both for whole years and for single days, but have failed to find any certain trace of the period, except perhaps for a few of the years of the Philippine earthquakes.

(v.) Next to the existence of the 42-minute period, the most interesting point is the length of time for which it lasts. After the great displacement that gives rise to an earthquake, the earth continues to throb for at least ten days, and, in the Kwanto and Tango earthquakes, for not less than two and three months, respectively. Now, during the latter half of the nineteenth century, Milne chronicles 219 destructive earthquakes of the greatest intensity and 368 of the next degree, or, on an average, 12 a year †. As there are many other earthquakes in uninhabited regions of equal or greater strength, it would thus seem possible that the earth is seldom, if ever, entirely at rest from the quivering that follows great earthquake-producing displacements.

* A similar reversal of epoch occurs in the diurnal periodicity of after-shocks (Phil. Mag. xli. pp. 914–915 (1921). Mr. K. Suda has also noticed that, after three or four days, the frequency of the after-shocks of the Kwanto earthquake of 1923 at various stations was somewhat abruptly reduced (Kobe [Japan] Kup. Mac. Obs. Mem. i. pp. 181–186, 1924).

† Brit. Ass. Rep. 1911, pp. 709–740

LXXXVIII. *The Explosion of Hydrogen-Air Mixtures in a Closed Vessel.*—Part I.

By B. H. THORP, *M.Sc.**

Introduction.

DURING the last twenty years several research workers have been measuring the maximum pressures developed in the explosion of gaseous mixtures in closed vessels. The purpose of this paper is to survey the results obtained for mixtures of hydrogen, oxygen, and nitrogen, and to attempt to account for the extraordinary differences between the figures given by various workers. A new diaphragm indicator will also be described, the development of which has emphasized the importance of certain points that have generally been neglected.

As an example of the disagreement which at present exists, the following results may be quoted for a 29·6 per cent. $H_2 + 14{\cdot}8$ per cent. $O_2 + 55{\cdot}6$ per cent. N_2 mixture exploded at an initial pressure of one atmosphere :—

TABLE I.

According to	Ratio of maximum to initial pressure.	Temperature. Initial t_i° C.	Temperature. Maximum t_m° C.	Apparent mean specific heat of steam $t_i° - t_m°$.
M. Pier†	8·38	19·4	2566	10·9
R. W. Fenning‡	7·78	51·0	2397	13·6
Maxwell and Wheeler§ ..	7·67	15·0	2420	12·5

The pressure ratios are all corrected to an initial temperature of 15° C. to make them comparable (see Appendix C). These figures have been obtained by interpolation ; the different workers have seldom used mixtures of identical composition, and direct comparison of pressure ratios is difficult. The most convenient method seems to be that of comparing the "apparent mean specific heat" of steam

* Communicated by Prof. W. T. David, Sc.D.

† *Zeit. f. Elektrochem*, xv. p. 536 (1909). The original mixture contained 2·2 per cent. H_2O and a small amount of excess H_2 (included in the N_2).

‡ Aer. Res. Comm. Report, No. 902, April 1924. This pressure ratio is 2 per cent. higher than that given by Fenning; in a later paper he says that certain earlier results were 2 per cent. too low, but it is not clear just which.

§ J. C. S. p. 15 (1928). Original mixture contained 1·7 per cent. H_2O (included in the N_2).

between 15° C. and the explosion temperature, calculated from each explosion. The method of obtaining these and the figures used for the specific heats of the diluent gases are shown in Appendix A. Allowance has been made in all cases for heat-loss on the basis of actual measurements by Prof. W. T. David (Appendix B). In calculating the apparent mean specific heats, it has been assumed that there was no dissociation of steam or incomplete combustion at maximum pressure. Hence the extent to which they exceed the true mean specific heat of steam is a measure of the amount of energy existing in the gases at maximum pressure in forms other than that of temperature.

In view of this disagreement, it was decided some three years ago to undertake a comprehensive set of explosions under the direction of Professor David in this laboratory, under the best possible conditions and covering a very wide range of $H_2-O_2-N_2$ mixtures. The full results of these will follow in the second part of this paper; for the present they will only be considered in relation to the results of other workers. With one exception, all the explosions considered in this paper have been made at an initial pressure of one atmosphere.

Description of Apparatus employed.

The explosion vessel is a large cast-steel sphere, 45·4 cm. diameter, with the inner surface silver-plated in order to reduce heat-loss before maximum pressure. It is made in two halves flanged and bolted together; before each explosion it is opened up and the plating polished with rouge. Extreme care is taken in the drying, mixing, and analysing of the explosive mixtures; the calculated and observed chemical contractions usually agree to 1 part in 1000 (except where NO_2 is formed).

At first a Hopkinson indicator was used, but this was not found suitable for rapid explosions. In these it appears to overshoot, owing either to the inertia of its moving parts or to the pocket below the piston. A new diaphragm indicator (fig. 1) was therefore evolved with a view to overcoming these defects.

A flat diaphragm, 2·8 cm. diameter and 0·75 mm. thick with a solid rim, is turned out of Invar. It is clamped down very firmly on to a seating turned in the wall of the explosion vessel, with only a shallow pocket below it; the joint is made with a thin ring of soft copper. The glass mirror is stuck on to a small brass pedestal, which is itself soldered on to

the diaphragm at about half the radius; the mirror and pedestal together weigh only 1 gm. A very long beam of light (0·65 m.) is used to obtain a high magnification, and some months were spent in overcoming the optical difficulties involved. The fine, sharp line now obtained enables the deflexions on the films to be measured with an accuracy of 1 in 500.

At first steel diaphragms were used, but it was found that they were giving misleading results, and a large amount of work had to be thrown away. Although protected from the flame by mica they were heated and consequently distorted

Fig. 1.

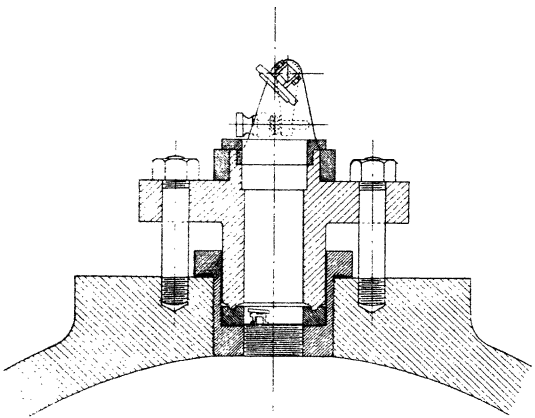

New diaphragm indicator. (Half full size.)

early in the explosion. The distortion due to heating was opposed to that due to increase of pressure inside the vessel, and so the maximum pressure recorded was some 1 per cent. too low. The use of invar has reduced this error to a negligible quantity. Tests on an invar diaphragm in working position showed that a bunsen flame could be held beneath it for at least three seconds before any measurable deflexion took place; whereas with a steel diaphragm a visible deflexion occurred as soon as the flame touched it.

The use of invar had, however, one quite unforeseen effect. While calibrating the indicator it was found that

the temperature of the sphere had a marked influence on the deflexion caused by a given pressure ; a temperature rise of 3° reduced the deflexion 1 per cent. This was at first put down to increase of the modulus of elasticity of invar with temperature, though the data available did not suggest an increase of such magnitude. It was of vital importance to know the cause, as in an average explosion the mean temperature of the diaphragm probably rises some 2° before maximum pressure is reached. If the modulus increases appreciably at the same time, the scale to which the deflexion shall be reckoned is doubtful. The following experiment seemed to show, however, that the modulus does not vary enough to upset the results. During calibration the deflexion produced by a given pressure was determined under the following conditions :—

(*a*) When the diaphragm was at the same temperature as the sphere (15° C.).

(*b*) When some 3 c.c. of half melted snow were dropped on to the diaphragm a couple of seconds before the pressure was applied.

(*c*) When the same was done with water at about 60° C.

No appreciable difference in the deflexions could be measured, and since it can hardly be doubted that the temperature of the diaphragm varied several degrees, it seems clear that it is the temperature of the sphere as a whole whose variations affect the pressure-deflexion scale. It is therefore only necessary to calibrate the indicator over a sufficient range of initial temperatures. The probable explanation is that as the invar diaphragm does not expand thermally along with the sphere as their common temperature rises, but yet is rigidly clamped, it is mechanically stretched and so yields less to the pressure inside the vessel.

Particular care is taken over the calibration of this vessel. The sparking plug is removed from the bottom of the sphere and a tube, passing up through the hole, is screwed into the pocket beneath the diaphragm, the joint being made with a rubber ring. A three-way cock at the bottom of this tube enables the pressure below the diaphragm to be raised suddenly from atmospheric to that of a large tank (170 litres) close by full of compressed air. A record is taken on a film showing the actual jump up of the pressure, the rapidity of which is of the same order as that taking place in an explosion, and the immediate deflexion measured. The

pressure in the tank is measured with a compound mercury gauge to 0·1 per cent., and since it is easy to determine the corrections for such a gauge, the absolute values of the calibration pressures are above suspicion. It is of the utmost importance that the diaphragm should be calibrated in its working position, since the firmness of clamping has a marked effect on the pressure-deflexion scale.

Comparison of Experimental Results with those of other Workers.

Some of the experiments of the following workers have been selected as suitable for comparison with those made here recently :—

M. Pier* (diaphragm indicator ; 40·6 cm. diam. sphere).
R. W. Fenning† (diaphragm indicator ; cylinder 17·8 cm. diam., 20·3 cm. long).
Maxwell and Wheeler‡ (Petavel indicator; 19·7 cm. diam. sphere).
W. Siegel§ (diaphragm indicator ; 40·6 cm. diam. sphere).
W. A. Bone‖ (Petavel indicator ; 7.6 cm. diam. sphere ; 3 atm. initial pressure).

Particulars of these, and the apparent specific heats of steam derived from them, will be found in Table III.

Fig. 2 shows the apparent specific heats plotted against the maximum explosion temperatures for four series of hydrogen-air mixtures—those of Maxwell and Wheeler, Fenning, Bone, and one from this laboratory (Leeds). It is evident that there are considerable differences, and there are good grounds for suggesting that these are chiefly due to the size and shape of vessel used. The Leeds experiments, made in the largest vessel of the four, a sphere 45·4 cm. diameter, give the lowest apparent specific heats—*i. e.* the highest pressure ratios. Maxwell and Wheeler with a sphere 19·7 cm. diameter get intermediate results, while Bone with a very small sphere, only 7·6 cm. diameter, gets the highest apparent specific heat. Fenning, whose results are almost as high as Bone's, used a vessel of about the same size as Maxwell and Wheeler's, but cylindrical in shape. Referring to Table I., it will be seen that Pier with a

* *Loc. cit.* † *Loc. cit.* ‡ *Loc. cit.*
§ *Zeit. f. Phys. Chem.* lxxxvii. p. 641 (1914).
‖ Proc. Roy. Soc. A, cviii. (1925).

40·6 cm. sphere got a much lower apparent specific heat than Maxwell and Wheeler.

Experimental confirmation of this effect of size and shape of vessel on the maximum pressure developed has been obtained in this laboratory. Each mixture was made up in a large tank, drawn off from there to four different vessels (all with rough, black, inner surfaces) and exploded in them under identical conditions. The indicators were calibrated simultaneously, and every precaution taken to ensure strict comparability. Two or more explosions were

Fig. 2.

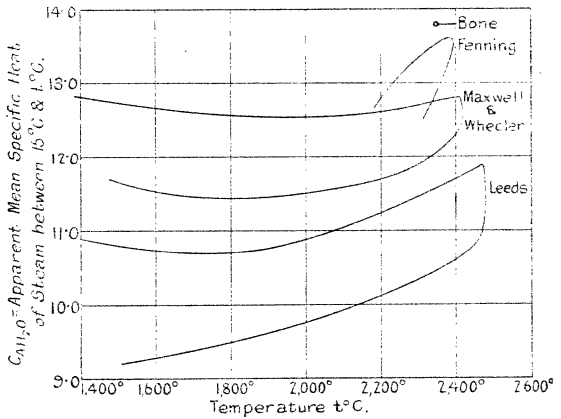

Hydrogen-air mixtures.

made in each vessel for each mixture, and several mixtures were tried. The following results are typical :—

TABLE II.

Mixture.	Maximum pressure developed in 45·4 cm. sphere.	30·3 cm. cylinder.	15·1 cm. sphere.	15·1 cm. cylinder.
23 % CO+3 % H_2+74 % O_2...	7·73	7·60	7·53	7·43
20 % CO+6 % H_2+74 % O_2...	7·69	7·46	7·58	7·36

If it be assumed that the absolute rate of heat-loss for a spherical vessel varies as the area of the inner surface (*i. e.* as the diam.^{2}), then the rate of heat-loss, expressed as a percentage of the heat of combustion (which $\propto$ diam.^{3}), varies inversely as the diameter. On the other hand, the time taken to attain maximum pressure varies roughly as the diameter, so that the total percentage heat-loss up to the moment of maximum pressure is almost independent of the diameter. In a cylinder it will be perhaps 50 per cent. greater than in a sphere. But it is believed (on the strength of Professor David's measurements, see Appendix B) that in these rapid explosions it amounts to less than 1 per cent.

Fig. 3.

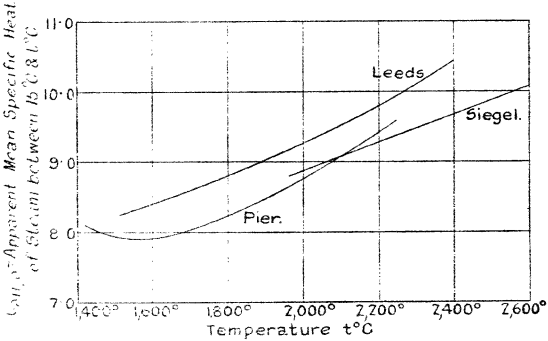

Excess hydrogen-oxygen mixtures.

and that the differences in the pressure ratios must be due to some other far more important factor.

The low pressure ratios recorded by some workers may be partly due to their use of "static" calibration. Pier and Siegel calibrated their indicators by sudden application of compressed air (as is done here), approximating to explosion conditions. The others appear to allow the calibrating pressure to act on the indicator for some time, so that elastic creep may occur before the deflexion is measured. Pier measured this creep and found that it might cause an error of the order of 1 per cent.

Fig. 3 shows apparent specific heat curves derived from

the series of excess hydrogen-oxygen explosions by Pier and Siegel and a third series from this laboratory, all in large spheres of much the same size. It appears that the Leeds experiments are in fair agreement with the others, though they suggest that the maximum pressures recorded by Pier and Siegel are from 1 to 2 per cent. too high. When calibrating they moved their diaphragms to a special vessel (of very small volume, so that it might be filled rapidly to the required pressure with compressed air), and though these may not have been so susceptible to alterations in clamping as the Leeds diaphragms, this throws some doubt on the absolute values of their recorded pressures. They also used steel diaphragms, and our experience has shown (see above) that the distortion of these by heating early in the explosion may cause an error of 1 per cent. either way (depending on the particular diaphragm) in the maximum pressure as calculated from the deflexion. Every care has been taken in this laboratory to obtain very great accuracy in experimenting, and it is believed that the pressures are within $\pm\frac{1}{2}$ per cent. of the true values.

Discussion of Results.

It has been shown how marked an effect the size and shape of the explosion vessel have upon the maximum pressure developed in it for any given mixture of gases, and that this cannot well be explained by heat-loss before maximum pressure. The most likely explanation seems to be that it is due to a time lag in the process of combustion. If the overall reaction $H_2+\frac{1}{2}O_2\longrightarrow H_2O+57{,}290$ cal., after being started in any small volume of gas by the flame travelling through it, takes an appreciable time to complete itself, then the larger the vessel and the more closely it approximates to a sphere with central ignition the more advanced will the reaction be on the average throughout the vessel at the moment of maximum pressure (or at any moment after the flame has reached the walls), and the greater the proportion of the total energy showing itself as temperature and pressure.

There is abundant evidence from other sources to support this theory of "incomplete combustion at maximum pressure," and it will be discussed more fully in the second part of this paper.

TABLE III.

Pier. $x\,°/_{\circ}\,(H_2+\frac{1}{2}O_2)+y\,°/_{\circ}\,H_2+z\,°/_{\circ}\,H_2O$.

No.	x %.	z %.	Max. temp. t_m° C.	C $^{15°,\,t_m°}_{\Delta H_2O}$.
164.....	13·3	2·0	1417	8·1
165.....	15·0	2·0	1592	7·9
166.....	17·7	1·8	1831	8·3
167.....	20·0	1·8	2017	8·8
168.....	23·4	2·0	2250	9·6

Siegel. $x\,°/_{\circ}\,(H_2+\frac{1}{2}O_2)+y\,°/_{\circ}\,H_2$.

No.	x %.	Max. temp. t_m° C.	C $^{15°,\,t_m°}_{\Delta H_2O}$.
78.....	19·2	1963	8·8
75.....	22·2	2205	9·3
76.....	25·2	2428	9·7
79.....	26·8	2535	9·9
77.....	27·8	2593	10·1

Fenning. $x\,°/_{\circ}\,H_2+y\,°/_{\circ}\,O_2+3{\cdot}9\,y\,°/_{\circ}\,N_2$.

No.	x %.	Max. temp. t_m° C.	C $^{15°,\,t_m°}_{\Delta H_2O}$.
179.....	25·2	2188	12·6
175.....	28·0	2306	13·4
171.....	32·3	2330	12·8
169.....	34·6	2314	12·5

Bone, 29·6 °/$_{\circ}$ H_2 + 14·8 °/$_{\circ}$ O_2 + 55·6 °/$_{\circ}$ N_2 at 3 atm. initial pressure, gives

Max. temp. = 2347° C. and C $^{15°,\,t_m°}_{\Delta H_2O}$ = 13·8.

Maxwell and Wheeler. $x\,°/_{\circ}\,H_2+y\,°/_{\circ}\,O_2+3{\cdot}8y\,°/_{\circ}\,N_2$.

x °/$_{\circ}$.	Max. temp. t_m° C.	C $^{15°,\,t_m°}_{\Delta H_2O}$.
14·8	1385	12·8
19·1	1688	12·9
24·1	2090	12·2
28·4	2312	12·8
33·5	2306	12·1
36·6	2258	11·7
38·7	2190	11·7
43·6	2056	11·5
45·0	2010	11·6
53·1	1772	11·4
56·2	1666	11·5
61·2	1477	11·7

Appendix A.

Calculation of Apparent Specific Heat of Steam.

Let Q = heat of formation of 1 gm. mol. of steam = 57,290 cal.;

h = heat-loss before maximum pressure, as fraction of Q;

x = proportion of steam formed;

w, y, z = proportions of steam, H_2 and (N_2+O_2) present as diluents;

t_i, t_m = initial and maximum temperatures of explosion;

C_{VH_2} = true mean specific heat of hydrogen over the range t_i to t_m;

C_{VN_2} = true mean specific heat of N_2 and O_2 over the range t_i to t_m;

C_{AH_2O} = apparent mean specific heat of steam over the range t_i to t_m.

Then

$$x.Q(1-h)=(t_m-t_i)[(w+x).C_{AH_2O}+y.C_{VH_2}+z.C_{VN_2}],$$

$$C_{AH_2O}=\frac{x}{w+x}\left[\frac{Q(1-h)}{t_m-t_i}-\frac{y.C_{VH_2}+z.C_{VN_2}}{x}\right].$$

If the original mixture is dry, $w=0$, and this simplifies to

$$C_{AH_2O}=\frac{Q(1-h)}{t_m-t_i}-\frac{y.C_{VH_2}+z.C_{VN_2}}{x}.$$

The mean specific heats of hydrogen, nitrogen, and oxygen are taken from Partington and Shilling's 'Specific Heats of Gases' (1925), and are as follows:—

0° to	1200°	1600°	2000°	2400°	2800°
C_{VH_2}	5·27	5·41	5·55	5·69	5·83
C_{VN_2, O_2}	5·22	5·37	5·55	5·77	6·02

It should be pointed out that from 1600° upwards these figures have themselves been obtained from explosion experiments. It is, however, improbable that they are so far incorrect (at any rate relatively to each other) as to vitiate the main conclusions reached.

Appendix B.

Heat-loss before Maximum Pressure.

The heat-loss up to the moment of maximum pressure is calculated from the formula constructed by Prof. W. T. David (Proc. Roy. Soc. A, xcviii. p. 308) from his measurements of loss by radiation and conduction during explosion of coal-gas-air mixtures. It has been assumed that the loss from hydrogen-air explosions is appreciably the same, and that the loss per cent. per second from two different vessels varies directly as the ratio of surface to volume. For the 18 in. sphere the formula becomes

$$\text{Per cent. heat-loss} = \frac{5{\cdot}57 \times (\text{max. temp. }^{\circ}\text{C.})^{2{\cdot}5} \times \text{time of explosion in secs.}/1000}{10^9 \times \text{per cent. } H_2O \text{ formed}}.$$

For the hydrogen mixtures that have been exploded in the 45·4 cm. diam. sphere the correction varies from 0·3 per cent. for the fastest explosions to 1·4 per cent. for the slowest. For Pier and Siegel's sphere the constant in the formula becomes 6·23, for Maxwell and Wheeler's sphere it is 12·8, for Fenning's cylinder 16·7, for Bone's sphere 10·8 (at three atmospheres, the per cent. loss is assumed inversely proportional to the initial pressure).

This correction has been applied, in calculating the apparent specific heats, by subtracting it from the heat of combustion, which is the only legitimate method. The maximum temperatures given are those actually reached, as calculated from the maximum pressures.

Appendix C.

Correction of Pressure Ratios for Initial Temperature.

This correction is based on the assumption that two explosions of the same mixture at slightly different initial temperatures, but otherwise under identical conditions, will give the same temperature rise, *i. e.* for two explosions *a* and *b* (if T_i, T_m = initial and maximum temps. abs.),

$$(T_m - T_i)_a = (T_m - T_i)_b,$$

$$\frac{T_{ma}}{T_{ia}} = \frac{T_{mb}}{T_{ib}} \times \frac{T_{ib}}{T_{ia}} + 1 - \frac{T_{ib}}{T_{ia}},$$

and, if P_m, P_i be the maximum and initial pressures and e the contraction ratio,

$$\frac{P_{ma}}{P_{ia}} = \frac{P_{mb}}{P_{ib}} \times \frac{T_{ib}}{T_{ia}} + e\left(1 - \frac{T_{ib}}{T_{ia}}\right).$$

All the pressure ratios are corrected to 15° C., *i. e.*

$$\left[\frac{P_m}{P_i}\right]_{15^\circ} = \left[\frac{P_m}{P_i}\right]_{T_i} \times \frac{T_i}{288} + e\left(1 - \frac{T_i}{288}\right).$$

This correction neglects the effect of the initial temperature on the mechanism of combustion. Higher initial temperatures probably assist the combustion, but within the limits of these experiments (10° and 23° C.) the effect must be negligible.

LXXXIX. *The Explosion of Hydrogen-Air Mixtures in a Closed Vessel.*—Part II. *By* B. H. Thorp, *M.Sc.**

IN the preceding paper (p. 813) it was shown that the maximum pressure developed in a gaseous explosion is greatly affected by the size and shape of the explosion vessel, large spheres with central ignition giving the highest pressures. It was suggested that combustion lags behind inflammation, and that in the large spheres combustion has, on an average through the vessel, reached a more advanced stage at the moment of maximum pressure, and that therefore a larger proportion of the total energy is making itself felt as pressure.

A new diaphragm indicator was also described, and it was shown that the maximum pressures recorded by this for any particular mixtures in a sphere 45·4 cm. diameter were among the highest found by any workers. Pier and Siegel alone give maximum pressures from 1 to 2 per cent. higher, in a sphere of much the same size, but reasons were mentioned for believing that the results obtained in this laboratory are closer to the true absolute values than theirs.

Our results will now be considered in detail. They consist of six series of explosions at an initial pressure of

* Communicated by Prof. W. T. David, Sc.D.

1 atmosphere. In each series the ratio of nitrogen to oxygen was kept constant, and the resulting "air" was mixed with hydrogen over as wide a range as possible. The ratios of nitrogen to oxygen in the six series were 0, 2, 3·9, 4·9, 6·1 and 6·8. The results are given in Table II.

TABLE I.

The Pressures developed in the Explosion of x per cent. H_2+y per cent. O_2+ay per cent. N_2 Mixtures.

% H_2.	% H_2O formed.	$\left[\frac{P_m}{P_i}\right]_{15°}$.	Initial Temp.°C.	Maximum Temp. °C.	$C_{A_{H_2}}$.	Time of Explosion in secs./1000 from Spark.	Rise.
			$N_2/O_2=0$.				
15·0	15·0	5·46	17·6	1430	12·9	51	36
18·9	18·9	6·33	16·0	1742	12·5	34	26
21·1	21·1	6·76	14·1	1903	12·4	25	19
22·7	22·7	7·07	18·5	2027	12·3	15	12
25·3	25·3	7·49	16·9	2200	12·3	13	11
—	—	—	—	—	—	—	—
86·5	26·1	8·13	16·0	2420	10·5	—	6
87·5	24·1	7·84	13·1	2292	10·1	9	7
88·5	22·2	7·52	16·5	2165	9·7	—	8
89·4	20·5	7·22	14·2	2043	9·4	13	10
90·1	19·1	6·91	18·2	1930	9·1	16	12
90·6	18·0	6·71	17·8	1857	8·9	18	14
91·2	16·9	6·45	14·7	1757	8·7	22	16
91·8	15·6	6·11	17·0	1640	8·5	29	21
92·4	14·4	5·79	18·8	1530	8·3	40	28
			$N_2/O_2=2$.				
16·3	16·3	5·95	20·5	1600	11·2	41	30
18·4	18·4	6·44	16·3	1772	11·1	34	24
20·3	20·3	6·82	18·2	1917	11·2	23	16
22·5	22·5	7·22	14·8	2067	11·4	16	12
25·2	25·2	7·63	21·4	2250	11·6	12	9
27·4	27·4	7·94	12·8	2372	11·8	11	8
—	—	—	—	—	—	—	—
59·3	27·3	8·19	17·5	2463	10·9	8	6
61·6	25·8	8·02	16·4	2383	10·6	9	7
63·8	24·3	7·82	15·4	2293	10·4	10	8
65·9	22·9	7·58	13·3	2190	10·1	11	9
67·4	21·8	7·44	14·9	2127	9·9	12	10

TABLE I. (*cont.*).

The Pressures developed in the Explosion of x per cent. H_2+y per cent. O_2+ay per cent. N_2 Mixtures.

% H_2.	% H_2O formed.	$\left[\frac{P_m}{P_i}\right]_{15°}$	Initial Temp.°C.	Maximum Temp.°C.	$C_{A_{H_2C.}}$	Time of Explosion in secs./1000 from Spark.	Rise.
			$N_2/O_2=2$ (*cont.*).				
69·4	20·5	7·17	15·8	2030	9·7	15	12
72·5	18·4	6·72	14·5	1860	9·4	18	14
74·6	17·0	6·38	13·6	1737	9·2	22	18
76·5	15·8	6·10	16·7	1637	9·1	32	22
78·6	14·4	5·77	18·5	1520	8·9	43	30
			$N_2/O_2=3·9$.				
13·6	16·6	6·11	14·2	1644	10·7	51	35
17·4	17·4	6·26	18·6	1710	10·7	44	30
20·3	20·3	6·88	15·6	1938	10·8	29	20
22·3	22·3	7·24	18·7	2083	11·0	22	16
25·0	25·0	7·65	18·9	2250	11·4	19	14
27·6	27·6	8·01	16·0	2407	11·7	15	12
29·8	28·9	8·13	20·2	2473	11·9	14	11
32·5	27·8	8·21	16·6	2476	11·0	12	10
35·6	26·6	8·13	13·1	2427	10·7	12	10
38·0	25·6	7·98	17·0	2364	10·5	12	10
41·0	24·3	7·82	12·3	2290	10·3	12	10
44·3	23·1	7·59	17·5	2204	10·1	13	10
49·9	20·7	7·17	15·3	2030	9·8	16	13
51·8	19·9	7·00	17·9	1972	9·7	18	14
53·8	19·0	6·81	16·8	1900	9·6	21	16
56·7	17·9	6·56	16·8	1808	9·5	23	19
59·8	16·6	6·26	14·6	1694	9·4	30	24
62·1	15·7	6·04	18·5	1620	9·3	34	28
64·8	14·5	5·74	18·2	1516	9·2	42	32
			$N_2/O_2=4·9$.				
12·8	12·8	5·13	15·4	1307	10·9	132	95
15·1	15·1	5·73	20·4	1517	10·8	70	50
17·1	17·1	6·20	17·1	1680	10·7	50	35
19·1	19·1	6·65	17·1	1847	10·7	33	28
21·9	21·9	7·21	18·6	2060	10·9	27	22
24·3	24·3	7·64	13·8	2228	11·0	22	20
25·9	25·1	7·74	16·0	2277	11·1	23	18
27·5	24·6	7·82	15·8	2295	10·4	19	17
28·4	24·2	7·78	14·9	2273	10·3	20	17
31·4	23·2	7·63	16·6	2214	10·1	19	17

TABLE I. (*cont.*).

% H_2.	% H_2O formed.	$\left[\frac{P_m}{P_i}\right]_{15°}$.	Initial Temp.°C.	Maximum Temp.°C.	$C_{A_{H_2O}}$.	Time of Explosion in secs./1000 from Spark.	Rise.
			N_2O_2=4·9 (*cont.*).				
35·8	21·7	7·33	17·7	2097	10·0	21	18
39·7	20·3	7·10	12·9	2003	9·8	23	19
42·5	19·4	6·90	15·4	1926	9·7	24	20
46·0	18·1	6·64	18·1	1833	9·6	27	22
50·9	16·5	6·25	13·3	1685	9·4	44	31
53·7	15·6	6·02	12·3	1605	9·4	—	40
			N_2/O_2=6·1.				
13·3	13·3	5·22	19·4	1343	10·8	123	83
15·7	15·7	5·86	19·9	1564	10·7	72	52
17·8	17·8	6·35	16·3	1737	10·7	54	40
19·9	19·9	6·82	18·0	1910	10·7	42	30
22·4	21·8	7·20	18·9	2057	10·8	32	27
24·9	21·1	7·16	15·7	2035	10·2	30	25
27·5	20·5	7·04	17·8	1990	10·0	29	22
29·8	19·7	6·92	19·8	1948	9·9	29	23
34·9	18·4	6·66	15·2	1842	9·7	32	25
39·9	17·1	6·36	16·7	1734	9·6	34	28
44·6	15·8	6·04	17·1	1618	9·6	43	34
49·6	14·3	5·65	19·0	1485	9·5	58	45
52·7	13·5	5·43	18·1	1407	9·5	75	56
54·5	13·0	5·30	17·3	1364	9·5	86	64
			N_2/O_2=6·8.				
14·0	14·0	5·46	16·2	1420	10·6	107	80
14·8	14·8	5·64	16·5	1485	10·6	96	70
15·7	15·7	5·89	17·4	1570	10·6	72	53
17·2	17·2	6·23	18·0	1696	10·6	62	48
17·9	17·9	6·40	18·5	1757	10·6	59	45
20·2	20·2	6·93	14·4	1943	10·6	43	35
22·3	20·0	6·95	16·9	1957	10·1	39	32
24·6	19·5	6·86	17·8	1920	9·9	38	30
26·2	19·0	6·77	19·4	1890	9·8	36	29
29·0	18·3	6·63	11·0	1827	9·7	35	28
33·1	17·2	6·39	14·5	1740	9·6	37	30
36·4	16·3	6·18	17·6	1667	9·6	42	35
40·2	15·4	5·95	15·4	1584	9·5	55	45
44·4	14·3	5·66	17·8	1487	9·5	75	60

Fig. 1.

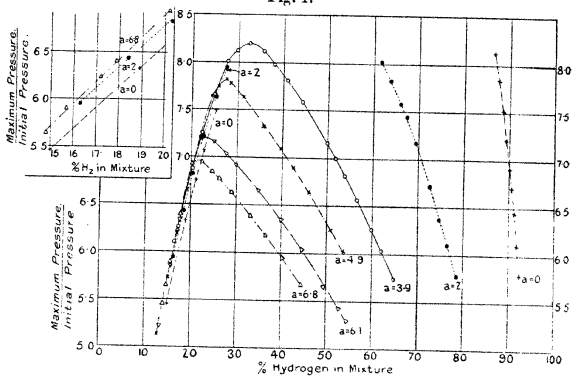

The ratios of maximum to initial pressure (P_m/P_i) are all corrected to an initial temperature of 15°C., and the "apparent mean specific heat" of steam ($C_{A_{H_2O}}$) between

Fig. 2.

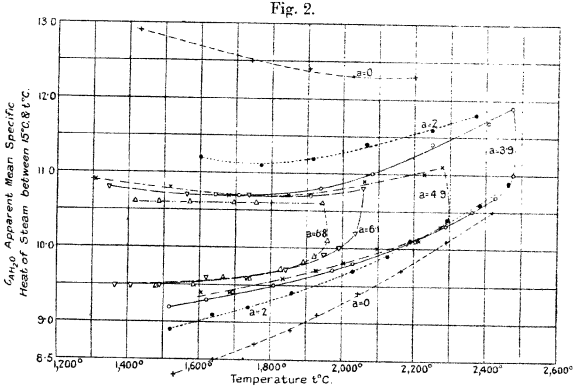

the initial and maximum temperature is calculated for each explosion (see Appendices to previous paper). These apparent specific heats are shown plotted against the

maximum temperatures in fig. 2, curves being drawn through the points belonging to each series. There are three striking features :—

1. It will be noticed that each curve consists of two almost parallel lines, the points on the lower line being obtained from mixtures containing an excess of hydrogen, and those on the upper line from mixtures containing an excess of " air."

2. In the case of mixtures containing excess hydrogen, the replacement of part of that hydrogen by nitrogen causes a great increase in the apparent specific heat of steam, or, in other words, reduces the maximum pressure.

3. In the case of mixtures containing excess oxygen, the replacement of part of that oxygen by nitrogen causes a great decrease in the apparent specific heat of steam, *i. e.* it increases the maximum pressure.

Considering 1, three possible explanations might be put forward :—

(*a*) That there is greater dissociation of steam at maximum pressure in the excess oxygen than in the excess hydrogen mixtures ; or,

(*b*) That the chemical process $H_2+\frac{1}{2}O_2 \rightarrow H_2O+57290$ cals. is further from completion at the moment of maximum pressure in the excess oxygen than in the excess hydrogen mixtures ; or,

(*c*) That, contrary to general belief, the specific heat of oxygen is much higher than that of hydrogen at high temperatures.

As mixtures containing very little excess oxygen or hydrogen differ nearly as much as those containing large excesses (*c*) may be ruled out. For the series in which the nitrogen/oxygen ratio is 6·8 the highest temperatures reached are only about 1950°C., and since " dissociation " in the strict sense of the word is negligibly small at temperatures below 2000°C. this cannot account for the missing energy. It seems probable therefore that there is extensive " incomplete combustion " (defined in the sense

described in (*b*) above) at the moment of maximum pressure in all the mixtures containing excess oxygen, and that at the higher temperatures (over 2000°C.) dissociation occurs as well.

The second feature may be readily explained on the principle of mass action, but the third is directly opposed to that principle, and apparently some process is taking place which completely swamps the mass action effect. Comparing for example the mixtures :—

20 per cent. $(H_2+\frac{1}{2}O_2)+$ 70 per cent. O_2 giving a maximum pressure of 6·55 atm.,

20 per cent. $(H_2+\frac{1}{2}O_2)+13{\cdot}3$ per cent. $O_2+56{\cdot}7$ per cent. N_2 giving a maximum pressure of 6·76 atm.,

20 per cent. $(H_2+\frac{1}{2}O_2)+1{\cdot}3$ per cent. $O_2+68{\cdot}7$ per cent. N_2 giving a maximum pressure of 6·82 atm.,

it is evident that here the presence of nitrogen has a beneficial effect on the overall process of combustion.

It is possible that H_2O_2 is a primary product in those explosions where there is a large excess of O_2; it would reduce the maximum pressure both through having a higher heat of formation than steam, and also through increasing the chemical contraction.

It has been felt that some attempt should be made to find out whether chemical equlibrium is established at the moment of maximum pressure. If the exploded gases could be very rapidly cooled just after maximum pressure has been reached, analysis might show whether chemical reaction is still in progress.

An arrangement has been made whereby a valve in the wall of the explosion vessel may be suddenly opened and closed again at any desired points during the explosion. Through this valve carbon dioxide may be injected in large quantities into the exploded gases, cooling them down suddenly to 200° or 300°C. Alternatively the valve may be opened to allow a large fraction (20 per cent.) of the hot gases to be injected into cool carbon dioxide or any desired reagent. This apparatus is still in the trial stage and no definite results can yet be given.

It is proposed to continue these experiments at higher initial densities, and a start has already been made with explosions at three atmospheres.

Calculation of the Extent of Incomplete Combustion for any mixture.

If several mixtures which develop the same maximum explosion temperature give different values for the apparent mean specific heat of steam between 15°C. and that temperature, it may be supposed that there is least incomplete combustion at the moment of maximum pressure in the mixture which gives the lowest value for the mean specific heat. It is possible to calculate how much more incomplete combustion there is in the other mixtures than in that one, but not to obtain absolute values from the data here available.

Fig. 2 shows that the lowest values for the apparent specific heat of steam come from mixtures containing hydrogen only as diluent. It will be assumed for the present that these are the true values, and on that basis the amount of incomplete combustion in any other mixture may be calculated as follows :—

Let Q = the heat of formation of 1 gm.mol. of H_2O = 57290 cal.,

a = proportion of incomplete combustion at maximum pressure,

x = proportion of H_2O formed by the end of the explosion,

t_i, t_m = initial and maximum temperatures of explosion,

C_{H_2O} = true mean specific heat of steam over the range t_i to t_m,

C_d = true mean specific heat of the diluent N_2, H_2 & O_2 between t_i & t_m.

Then $$x \cdot Q(1-a) = (t_m - t_i)[x \cdot C_{H_2O} + (1-3x/2) \cdot C_d]$$

$$1-a = \frac{t_m - t_i}{Q}\left(C_{H_2O} + \frac{2-3x}{2x} \cdot C_d\right),$$

or $$a = 1 - \frac{t_m - t_i}{Q}\left(C_{H_2O} + \frac{2-3x}{2x} \cdot C_d\right).$$

It must be observed that the calculated maximum temperature

$$t_m = t_i \times \frac{P_m}{P_i} \times \frac{1}{1-\frac{1}{2}(1-a)x}$$

depends on the proportion of incomplete combustion. For the case $x=0{\cdot}2$, t_m will be 0·6 per cent. lower when the incomplete combustion $a=0{\cdot}05$ than when $a=0$, *i. e.* perhaps 12° in 2000°C. This will only be so if "incomplete combustion" means that some of the H_2 and O_2 molecules that should have combined to form H_2O still exist as H_2 and O_2 molecules at maximum pressure, so that chemical contraction is also incomplete. If, however, incomplete combustion is not chemical in nature, or if it means that some intermediate endothermic product such as H_2O_2 is in existence at maximum pressure, the chemical contraction may be complete by this time. It has therefore been considered advisable to neglect the possible effect on the maximum temperature.

TABLE II.

Percentage Incomplete Combustion at Maximum Pressure.

Maximum Temp. °C.	Ratio N_2/O_2 =	0	2	3·9	4·9	6·1	6·8
	Excess Hydrogen Mixtures.						
1600	... ...	0	1·6	2·2	2·7	3·1	3·1
1800	... ...	0	1·8	2·1	2·2	2·7	3·1
2000	... ...	0	0·9	1·6	1·7	2·8	—
2200	... ...	0	0·7	1·2	1·2	—	—
2400	... ...	0	0·7	0·7	—	—	—
	Excess "Air" Mixtures.						
1600	... ...	11·2	7·4	6·6	6·6	6·6	5·8
1800	... ...	11·4	7·2	6·0	6·0	6·0	5·3
2000	... ...	10·6	7·1	5·6	5·4	5·0	—
2200	... ...	9·3	6·6	5·5	4·3	—	—
2400	... ...	—	6·0	5·5	—	—	—

These are minimum figures in that they are based on the assumption that there is no incomplete combustion in mixtures of oxygen with excess hydrogen.

Conclusions.

It has been shown from the experiments carried out in this laboratory on mixtures of hydrogen, oxygen and nitrogen, that :—

(*a*) There seems to be extensive incomplete combustion at the moment of maximum pressure in mixtures containing excess oxygen.

(*b*) Probably the same is true in a lesser degree for mixtures containing excess hydrogen ; hence the specific heat of steam, as calculated from the maximum pressures developed in explosion experiments, must always be rather too high.

(*c*) By taking the lowest apparent specific heat of steam found for a given temperature as the true specific heat, the extent of incomplete combustion at maximum pressure in other mixtures giving that same maximum temperature may be estimated.

(*d*) For mixtures containing excess hydrogen, the gradual replacement of that hydrogen by nitrogen causes a steady decrease in the maximum pressure, *i. e.*, an increase in the amount of incomplete combustion.

(*e*) For mixtures containing excess oxygen, the gradual replacement of that oxygen by nitrogen causes a steady increase in the maximum pressure, *i. e.* a decrease in the amount of incomplete combustion.

I should like to express my indebtedness and gratitude to Professor David for his invaluable direction and advice during the progress of this work, and for permission to use the results of other workers in this laboratory of the Engineering Department, Leeds University (see Part I, Table 2 ; they have also taken a considerable part in the development of the new diaphragm indicator).

I should also like to thank the Department of Scientific and Industrial Research for maintenance grants during the two years 1925-27, which enabled me to begin this work.

XC. *The Characteristic Numbers of the Mathieu Equation with Purely Imaginary Parameter.* *By* H. P. MULHOLLAND *and* S. GOLDSTEIN *.

METHODS are known for calculating the characteristic numbers of integral order of the Mathieu equation

$$\frac{d^2y}{dx^2}+(4a-16q\cos 2x)y=0, \quad . \quad . \quad . \quad . \quad (1)$$

and tables have been given † for real q. We have calculated the first eight characteristic numbers for purely imaginary q, and the results are given in Tables I. *a* and I. *b* (p. 839).

The notation is the usual one ‡. a_n and β_n correspond to the functions ce_n and se_n respectively.

The equation with purely imaginary parameter is of importance in the physical problem of the alternating flow of electricity along conducting elliptic cylinders. In addition, it has considerable theoretical interest.

Numerical Example and Tabular Values.

As an example we shall give the calculation of β_2 (corresponding to the function $se_2(x)$, odd in x and $\frac{1}{2}\pi-x$) for $q=1{\cdot}8i$.

If
$$se_2(x,q)=\sum_{r=1}^{\infty}B_{2r}\sin 2rx, \quad . \quad . \quad . \quad . \quad . \quad (2)$$

$$iB_{2+r2}/B_{2r}=u_r, \quad . \quad . \quad . \quad . \quad . \quad . \quad . \quad . \quad (3)$$

and
$$q=is, \quad . \quad . \quad . \quad . \quad . \quad . \quad . \quad . \quad (4)$$

then the recurrence relations for the B lead to the formula

$$u_{r-1}=\frac{2s}{r^2-a+2su_r} \quad (r>1). \quad . \quad . \quad . \quad (5)$$

and the equation

$$L=1-a+2su_1=0. \quad . \quad . \quad . \quad . \quad . \quad (6)$$

* Communicated by Prof. E. L. Ince.

† Ince, Proc. Roy. Soc. Edin. xlvi. pp. 20–29 (1925); xlvi. pp. 316–322 (1926); xlvii. pp. 294–301 (1927). Goldstein, Trans. Camb. Phil. Soc. xxiii. pp. 303–336 (1927).

‡ See the papers cited above, or Whittaker and Watson's 'Modern Analysis,' Chap. xix. The parameters $a=4a$ and $\theta=8q$ are also employed sometimes

The method of calculation is to take $u_r=0$ for a sufficiently large value of r, and to find the required zero of L by Newton's rule. A first approximation, α, to the zero is found by methods to be given later, and a second approximation is given by $\alpha+\delta\alpha$, where

$$\delta\alpha=-\mathrm{L}/\frac{\partial \mathrm{L}}{\partial\alpha}. \quad . \quad . \quad . \quad . \quad . \quad . \quad (7)$$

To calculate $\partial\mathrm{L}/\partial\alpha$ we first differentiate (5), obtaining

$$\frac{\partial}{\partial\alpha}(2su_{r-1})=u^2_{r-1}\left[1-\frac{\partial}{\partial\alpha}(2su_r)\right], \quad . \quad . \quad . \quad (8)$$

by repeated applications of which we arrive at the convenient formula :

$$-\partial\mathrm{L}/\partial\alpha=1-u_1{}^2+u_1{}^2u_2{}^2-u_1{}^2u_2{}^2u_3{}^2+\ldots \quad . \quad . \quad (9)$$

For q equal to $1{\cdot}8i$, we choose $3{\cdot}6829-3{\cdot}1779i$ as first approximation to β_2 (see p. 838). It is sufficient to take u_8 equal to zero.

Then

$$u_7=\frac{3{\cdot}6}{60{\cdot}3171+3{\cdot}1779i}=0{\cdot}060-0{\cdot}003i,$$

$$u_6=\frac{3{\cdot}6}{45{\cdot}3171+3{\cdot}1779i+3{\cdot}6(0{\cdot}060-0{\cdot}003i)}$$
$$=0{\cdot}0787-0{\cdot}0055i,$$

$$u_5=\frac{3{\cdot}6}{32{\cdot}3171+3{\cdot}1779i+3{\cdot}6(0{\cdot}0787-0{\cdot}00551i)}$$
$$=0{\cdot}10949-0{\cdot}01060i,$$

and so on until we get

$$u_2=0{\cdot}4702\ 3365-0{\cdot}2213\ 5931i,$$

$$u_1=\frac{3{\cdot}6}{0{\cdot}3171+3{\cdot}1779i+3{\cdot}6(0{\cdot}4702\ 3365-0{\cdot}2213\ 5931i)}$$
$$=0{\cdot}7452\ 61814-0{\cdot}8828\ 48342i,$$

and

$$\mathrm{L}\equiv 1-\alpha+2su_1=0{\cdot}0000\ 4253-0{\cdot}0003\ 5403i.$$

Also

$$-\partial L/\partial\alpha = 1 - u_1^2 + u_1^2u_2^2 - u_1^2u_2^2u_3^2 + \ldots = 0{\cdot}9380 + 1{\cdot}1374i,$$

Hence we take

$$\delta\alpha = \frac{0{\cdot}0000\ 4253 - 0{\cdot}0003\ 5403i}{0{\cdot}9380 + 1{\cdot}1374i} = -0{\cdot}000167 - 0{\cdot}000175i.$$

Our next approximation to α is therefore

$$\alpha = 3{\cdot}682733 + 3{\cdot}178075i,$$

and with this value of α we find

$$L = -0{\cdot}0000\ 0002 - 0{\cdot}0000\ 0001i.$$

It is to be noticed that the ratios of the coefficients in the Fourier series are found in the process of finding the characteristic numbers, so that the calculation of the functions themselves is a simple matter.

The series of Mathieu * suffice to show that, for sufficiently small s, α_{2m} and β_{2m} are real. We find that α_0 and α_2 become equal when $s = 0{\cdot}1836\ldots$. For larger values of s, up to $2{\cdot}0$, the tables show α_0 and α_2 as conjugate complex numbers. It will be seen later that a certain asymptotic expansion gives good numerical approximations to α_0 for the larger values of s here considered, and unless this ceases to hold with increasing s, α_0 remains complex, and α_0 and α_2 remain conjugate.

Similar remarks apply to β_2 and β_4.

We have found α_4 and α_6 and β_6 and β_8 to behave in a similar way. The numerical values suggest the theorem that α, as a function of q, has an infinite number of branch-points on the imaginary axis in the q plane.

In the neighbourhood of the point where α_0 and α_2 become equal, Newton's method fails. Hence, having taken u_r as zero for some sufficiently large value of r, we must write out the equation $L = 0$ in full, and use another method for finding the roots in question—say Horner's method for real roots and the root-squaring method of Dandelin, Lobachevsky, and Graeffe for complex ones. [The process was employed to find α_0 and α_2 for $s = 0{\cdot}2$. It was sufficient to solve a quintic, and it was quicker to find the real roots by Horner's method and divide out than to use the root-squaring method.]

α_{2m+1} and β_{2m+1} are conjugate complex numbers.

* *Journ. de Math.* (2) xiii. pp. 137–203 (1868).

Asymptotic Expansions.

Numerical values show that, as s increases, α_0 and α_2 approach α_1 and β_1, and β_2 and β_4 approach α_3 and β_3.

Now α_0 and α_2 being given on the real axis, their values on the imaginary axis beyond the branch-point will depend on the path taken from a point on the real axis (or, alternatively, on the cuts made in the q-plane). A full discussion of the singularities of α as a function of q is beyond the scope of this paper, but for the sake of clarity it is desirable to be able to distinguish between α_0 and α_2. We shall therefore suppose the path in the q-plane so chosen that along the imaginary axis, for the sufficiently large values of s to be considered, α_0 is nearly equal to β_1. Similarly we shall suppose that α_3 is nearly equal to β_4.

Now when q is real and positive,

$$\alpha_m \sim \beta_{m+1} \sim \mathrm{A}_m^*, \quad . \quad . \quad . \quad . \quad . \quad (10)$$

where

$$\mathrm{A}_m \equiv -\tfrac{1}{8}k^2 + \tfrac{1}{4}m'k - \frac{m'^2+1}{2^5} - \frac{m'(m'^2+3)}{2^8 k} - \frac{54m'^4+34m'^2+9}{2^{12}k^2} - \frac{m'(33m'^4+410m'^2+405)}{2^{16}k^3} - \frac{63m'^6+1260m'^4+2943m'^2+486}{2^{18}k^4} - \frac{m'(527m'^6+15617m'^4+69001m'^2+41607)}{2^{22}k^5} - \ldots$$

$$. \quad . \quad . \quad (11)$$

Here $$k = +(32q)^{\frac{1}{2}}, \quad \text{and} \quad m' = 2m+1 \quad . \quad . \quad . \quad (12)$$

Also †

$$\beta_{m+1} - \alpha_m \sim \mathrm{B}_m \quad . \quad . \quad . \quad . \quad . \quad . \quad (13)$$

where

$$\mathrm{B}_m \equiv \tfrac{1}{2}\left(\frac{k}{\pi}\right)^{\frac{1}{2}} \frac{(8k)^{m+1}}{m!}\, e^{-2k}\left(1 + \frac{c_1}{k} + \frac{c_2}{k^2} + \ldots\right), \quad . \quad (14)$$

* Ince, *loc. cit.*; Goldstein, *loc. cit.*

† Goldstein, Proc. Roy. Soc. Edin. xlix. pp. 210–223 (1929). The numerical results given here were obtained about the same time as the above formula, and provided at first a strong incentive to finding the formula, and later a valuable check on its accuracy, since it was obtained by a formal process only.

and it has been found empirically from numerical results for real q that when m is 0, c_1 is $-0{\cdot}45$, and when m is 1, c_1 is $-1{\cdot}698$.

We had not proceeded far with the calculation when we noticed that the following asymptotic expressions would give good numerical approximations when q is a positive imaginary:

$$\alpha_0 \sim \beta_1 \sim A_0 \quad . \quad . \quad . \quad . \quad . \quad . \quad (15)$$

and

$$\alpha_3 \sim \beta_4 \sim A_1, \quad . \quad . \quad . \quad . \quad . \quad . \quad (16)$$

where arg q is given its principal value in interpreting the $q^{\frac{1}{2}}$ involved.

We found similarly that the formulæ

$$\beta_1 - \alpha_0 \sim B_0 \quad . \quad . \quad . \quad . \quad . \quad . \quad (17)$$

and

$$\beta_4 - \alpha_3 \sim B_1 \quad . \quad . \quad . \quad . \quad . \quad . \quad (18)$$

held for the larger values of s considered.

(The obvious extensions of these formulæ are

$$\alpha_{4m} \sim \beta_{4m+1} \sim A_{2m}, \quad \alpha_{4m-1} \sim \beta_{4m} \sim A_{2m-1}, \quad . \quad (19)$$

and

$$\beta_{4m+1} - \alpha_{4m} \sim B_{2m}, \quad \beta_{4m} - \alpha_{4m-1} \sim B_{2m-1}.) \quad . \quad (20)$$

When q is real and positive, A_m is a better approximation to $\frac{1}{2}(\alpha_m + \beta_{m+1})$ than to either α_m or β_{m+1}. Numerical values show similar results for A_0 and A_1 when q is imaginary, so that we have compared A_0 with $\frac{1}{2}(\alpha_0 + \beta_1)$ and A_1 with $\frac{1}{2}(\alpha_3 + \beta_4)$ (see Table II. *a*, p. 840). Also $\beta_1 - \alpha_0$ is compared with B_0, and $\beta_4 - \alpha_3$ with B_1 (Table II. *b*, p. 840). The values of c_1 are the same as for real q for m equal to 0 and 1 respectively.

Finally, we point out how an approximate value of α is found to start the main calculation. First, when s is sufficiently small, we use the series of Mathieu previously mentioned. When s is moderately large, we take $A_0 - \frac{1}{2}B_0$ as an approximation to α_0, and when α_0 has been calculated, take $\alpha_0 + B_0$ as an approximation to β_1. Similarly we take $A_1 - \frac{1}{2}B_1$ as an approximation to α_3, and $\alpha_3 + B_1$ as an approximation to β_4. In this way the approximation to β_2 (which is conjugate to β_4) when s is 1·8, namely $3{\cdot}6829 - 3{\cdot}1779i$, was obtained. As examples we may note that when s is as low as 0·4 we get $0{\cdot}603 - 0{\cdot}990i$ as an approximation to α_0, and $0{\cdot}5286 - 0{\cdot}9395i$ as an approximation to β_1—both very good approximations indeed, with which we have no difficulty in completing the calculation.

TABLE I. *a*.

s.	a_0.	a_2.
0·02	0·003209	0·997324
0·04	0·012947	0·989185
0·06	0·029567	0·975226
0·08	0·053740	0·954772
0·10	0·086618	0·926663
0·12	0·130223	0·888869
0·14	0·188444	0·837489
0·16	0·270636	0·763155
0·18	0·422320	0·620331

TABLE I. *b*.

s.	α_0.	β_1.
0·2	$0{\cdot}526248-0{\cdot}217463\,i$	$0{\cdot}328562-0{\cdot}416728\,i$
0·4	$0{\cdot}599837-0{\cdot}992788\,i$	$0{\cdot}528852-0{\cdot}940749\,i$
0·6	$0{\cdot}705302-1{\cdot}640667\,i$	$0{\cdot}713982-1{\cdot}602207\,i$
0·8	$0{\cdot}821211-2{\cdot}306374\,i$	$0{\cdot}838783-2{\cdot}299441\,i$
1·0	$0{\cdot}931317-2{\cdot}995455\,i$	$0{\cdot}939893-2{\cdot}999885\,i$
1·2	$1{\cdot}030380-3{\cdot}699973\,i$	$1{\cdot}032031-3{\cdot}704884\,i$
1·4	$1{\cdot}119646-4{\cdot}413499\,i$	$1{\cdot}118567-4{\cdot}416182\,i$
1·6	$1{\cdot}201620-5{\cdot}132870\,i$	$1{\cdot}200182-5{\cdot}133715\,i$
1·8	$1{\cdot}278205-5{\cdot}856723\,i$	$1{\cdot}277220-5{\cdot}856638\,i$
2·0	$1{\cdot}350591-6{\cdot}584391\,i$	$1{\cdot}350120-6{\cdot}584019\,i$

s.	α_2.	β_2.	β_3.
0·2	$2{\cdot}211411-0{\cdot}016747\,i$	1·053942	3·978050
0·4	$2{\cdot}130732-0{\cdot}141334\,i$	1·223940	3·903906
0·6	$2{\cdot}143946-0{\cdot}406823\,i$	1·544119	3·742990
0·8	$2{\cdot}294532-0{\cdot}719887\,i$	2·162533	3·346121

		β_4.
1·0	$2{\cdot}541327-1{\cdot}065650\,i$	$2{\cdot}895037-0{\cdot}906426\,i$
1·2	$2{\cdot}852994-1{\cdot}475122\,i$	$3{\cdot}063353-1{\cdot}538181\,i$
1·4	$3{\cdot}181293-1{\cdot}974374\,i$	$3{\cdot}255211-2{\cdot}088545\,i$
1·6	$3{\cdot}472882-2{\cdot}543309\,i$	$3{\cdot}464373-2{\cdot}627919\,i$
1·8	$3{\cdot}718564-3{\cdot}138044\,i$	$3{\cdot}682733-3{\cdot}178075\,i$
2·0	$3{\cdot}935301-3{\cdot}737708\,i$	$3{\cdot}901859-3{\cdot}746215\,i$

NOTE.—β_1 and α_3 are conjugate to α_1 and β_3 respectively, and α_0 and β_4 when complex, are conjugate to α_2 and β_2 respectively.

TABLE II *a*.

s.	$\frac{1}{2}(\alpha_0+\beta_1)$.	A_0.
0·2	$0{\cdot}427405-0{\cdot}317095i$	$0{\cdot}381560-0{\cdot}346229\,i$
0·4	$0{\cdot}564344-0{\cdot}966768\,i$	$0{\cdot}567214-0{\cdot}963367\,i$
0·6	$0{\cdot}709642-1{\cdot}621437\,i$	$0{\cdot}709697-1{\cdot}622127\,i$
0·8	$0{\cdot}829997-2{\cdot}302907\,i$	$0{\cdot}829848-2{\cdot}302867\,i$
1·0	$0{\cdot}935605-2{\cdot}997670i$	$0{\cdot}935618-2{\cdot}997634\,i$
1·2	$1{\cdot}031205-3{\cdot}702428\,i$	$1{\cdot}031215-3{\cdot}702430\,i$
1·4	$1{\cdot}119106-4{\cdot}414840\,i$	$1{\cdot}119107-4{\cdot}414843\,i$
1·6	$1{\cdot}200901-5{\cdot}133292\,i$	$1{\cdot}200900-5{\cdot}133292\,i$
1·8	$1{\cdot}277712-5{\cdot}856680\,i$	$1{\cdot}277712-5{\cdot}856680\,i$
2·0	$1{\cdot}350356-6{\cdot}584205\,i$	$1{\cdot}350356-6{\cdot}584205\,i$
s.	$\frac{1}{2}(\alpha_3+\beta_4)$.	A_1.
1·0	$2{\cdot}7182-0{\cdot}9860\,i$	$2{\cdot}6720-0{\cdot}9759\,i$
1·2	$2{\cdot}9582-1{\cdot}5067\,i$	$2{\cdot}9593-1{\cdot}5014\,i$
1·4	$3{\cdot}2183-2{\cdot}0315\,i$	$3{\cdot}2234-2{\cdot}0309\,i$
1·6	$3{\cdot}4686-2{\cdot}5856\,i$	$3{\cdot}4693-2{\cdot}5874\,i$
1·8	$3{\cdot}7006-3{\cdot}1581\,i$	$3{\cdot}7001-3{\cdot}1585\,i$
2·0	$3{\cdot}9186-3{\cdot}7420\,i$	$3{\cdot}9183-3{\cdot}7418\,i$

TABLE II. *b*.

s.	$\beta_1-\alpha_0$.	B_0.
0·2	$-0{\cdot}20\quad-0{\cdot}20\,i$	$-0{\cdot}14\quad-0{\cdot}17\,i$
0·4	$-0{\cdot}0710\quad+0{\cdot}520\,i$	$-0{\cdot}0712\quad+0{\cdot}0533\,i$
0·6	$+0{\cdot}0087\quad+0{\cdot}0385\,i$	$+0{\cdot}0089\quad+0{\cdot}0382\,i$
0·8	$+0{\cdot}01757\quad+0{\cdot}00693\,i$	$+0{\cdot}01754\quad+0{\cdot}00686\,i$
1·0	$+0{\cdot}008576-0{\cdot}004430\,i$	$+0{\cdot}008542-0{\cdot}004439\,i$
1·2	$+0{\cdot}001651-0{\cdot}004911\,i$	$+0{\cdot}001640-0{\cdot}004902\,i$
1·4	$-0{\cdot}001079-0{\cdot}002683\,i$	$-0{\cdot}001081-0{\cdot}002678\,i$
1·6	$-0{\cdot}001438-0{\cdot}000845\,i$	$-0{\cdot}001436-0{\cdot}000842\,i$
1·8	$-0{\cdot}000985+0{\cdot}000085\,i$	$-0{\cdot}000983+0{\cdot}000085\,i$
2·0	$-0{\cdot}000471+0{\cdot}000372\,i$	$-0{\cdot}000470+0{\cdot}000372\,i$
s.	$\beta_4-\alpha_3$.	B_1.
1·0	$+0{\cdot}35\quad+0{\cdot}16\,i$	$+0{\cdot}33\quad+0{\cdot}18\,i$
1·2	$+0{\cdot}210\quad-0{\cdot}063\,i$	$+0{\cdot}215\quad-0{\cdot}062\,i$
1·4	$+0{\cdot}0739\quad-0{\cdot}1142\,i$	$+0{\cdot}0731\quad-0{\cdot}1149\,i$
1·6	$-0{\cdot}0085\quad-0{\cdot}0846\,i$	$-0{\cdot}0082\quad-0{\cdot}0842\,i$
1·8	$-0{\cdot}03583-0{\cdot}04003\,i$	$-0{\cdot}03568-0\,03988\,i$
2·0	$-0\,03344-0{\cdot}00851\,i$	$-0{\cdot}03336-0{\cdot}00849\,i$

XCI. *Measurement of the Flow of Heat.* *By* A. F. Dufton, *M.A., D.I.C., and* W. G. Marley *.

[Plates XV. & XVI.]

1. THE method recently described † of recording the flow of heat across the surface of a wall is only applicable when the flow of heat is toward the wall. It requires, moreover, the insertion of thermocouples in the surface of the wall, and cannot be used at a glass surface such as a window. Simpler apparatus has now been devised which does not suffer from these limitations and the transfer of heat by radiation and by convection can be recorded as separate items.

2. The instrument shown in Pl. XV. is designed to measure radiation. It comprises 40 sheets of tinfoil (0·5 in. × 0·3 in.) connected in series by wire alternately of 40 s.w.g. constantan $\frac{1}{2}$ in. long and of 46 s.w.g. copper. Alternate sheets are cemented together, with paper insulation in the overlap, to form panels (2 in. × $\frac{1}{2}$ in.) and the terminals are connected to a recording galvanometer. The obverse of one panel and the reverse of the other are sprayed with carbon black.

3. The radiation instrument was calibrated upon a wall, the flow of heat to which was measured by the method referred to above. The heating was contrived so that the temperature of the air was automatically kept equal to that of the wall surface : the heating was purely radiant.

An E.M.F. of 743 microvolts was recorded by the instrument when the flow of heat was 10 B.Th.U. per square foot per hour.

This calibration was checked by exposing the instrument between blackened copper surfaces, one of which was at room temperature. Table I. shows the measured values together with the radiation between surfaces of emissivity 0·92 calculated from Stefan's Law ($\sigma = 5{\cdot}7 \times 10^{-5}$ erg cm.$^{-2}$ sec.$^{-1}$ deg.$^{-4}$).

4. The instrument shown in Pl. XVI. is designed to measure convection. It comprises short lengths of 40 s.w.g. wire, alternately of copper and of constantan, soldered together to form 16 junctions touching the wall surface and 16 junctions 5·0 mm. from the wall. The terminals are connected to a recording galvanometer.

* Communicated by the Authors.

† Journ. of Scientific Inst. iv. p. 446 (1927).

5. The convection instrument was calibrated upon a wall, the convection of heat to which was recorded as the difference

TABLE I.

Temperature difference °C.	Radiation (B.Th.U./sq. ft./hour).	
	Measured.	Calculated.
3·4	5·8	5·6
4·0	6.6	6·6
4·7	8·1	7·8
5·5	9·2	9·2
7·1	11·9	11·9
8·0	13·5	13·5
12·6	21·1	21·7
14·6	24·8	25·4

Fig. 1.

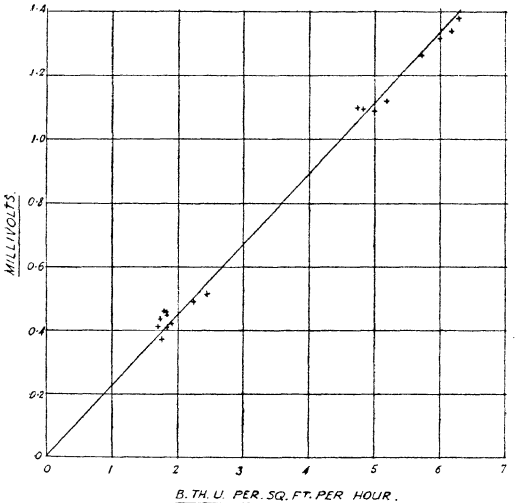

Calibration of convection instrument.

between the total flow and the radiant heat measured as described above.

The measurements show that the convected heat is proportional to the 1·07th power of the E.M.F. recorded by the instrument. Although the relationship is not linear, it is clear from fig. 1 that for the range required the error in "making it so" is negligible.

6. The radiation and convection instruments can be combined to record the total flow of heat. Simultaneous records of the flow from a room to a wall by the original method and by the new instrument are shown in fig. 2. It will be

Fig. 2.

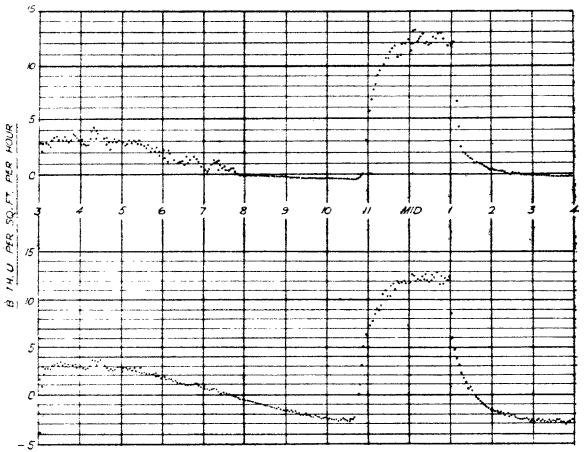

The flow of heat from a room to a wall simultaneously recorded by the original method (above) and by the new instrument.

seen that the original method ceased to measure when the flow became zero and when the uncovered surface of the wall became cooler than the surface covered by the square foot of cork. On resumption the record was inaccurate for a short period until the square foot had regained uniformity with the remainder of the wall.

Note on the Convection of Heat.

In the calibration of the convection instrument the convection of heat to a wall was recorded as the difference

between the total flow of heat and the radiant heat. A record was also made of the temperature difference between the air (at 5·0 cm. from the wall) and the wall surface. Corresponding values are plotted in fig. 3.

Previous experimenters, using small bodies, have found the convection of heat per unit area to be approximately proportional to the 5/4th power of the temperature difference and to be a function of the size of the body.

Fig. 3.

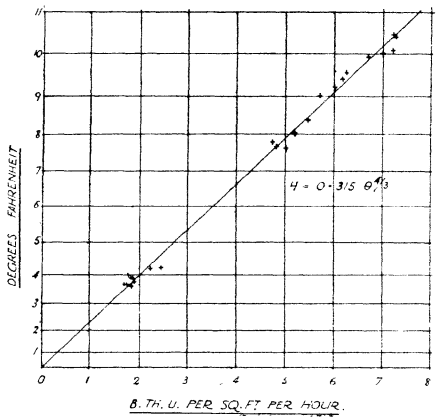

Heat transfer by convection.

Considerations of Similitude * show that if the convection per unit area were independent of the size of the body it would be proportional to the 4/3rd power of the temperature difference.

The present measurements show the convection of heat to a wall to be proportional to the 4/3rd power of the temperature difference and equal to 0·315 B.Th.U. per sq. ft. per hour for a temperature difference of 1° Fahrenheit.

Building Research Station,
Garston, Herts.

* Dict. of Applied Physics, i. p. 477.

XCII. *The K-Absorption Discontinuities of Manganous and Chromate Ions.* *By* Don M. Yost, *Fellow of the National Research Council and International Education Board* *.

IT is known that the wave-length of the X-ray absorption discontinuity of an element is influenced not only by the valence of the element, but also by the nature of the crystal in which the element occurs. Thus the wave-length of the K-absorption discontinuity of chloride ion in crystalline sodium chloride is different from that found in the case of potassium chloride †. It was thought that similar effects might be found when the discontinuity for ions in aqueous solution was compared with that for the same ions present in a crystal.

The solutions of the salts used were placed in fine quartz capillary tubes. The outside diameters of the tubes varied from 0·04 mm. to 0·1 mm., the inside diameter being about six-tenths of the outside diameter. To fill the tubes it was only necessary to dip one end into the solution, the capillary action causing the liquid to rise in them. The longer-filled tubes were cut into sections of about one centimetre in length, and the ends of the latter carefully sealed with a bit of hard wax. The tubes, before being used, were placed in a spectrograph, which was then evacuated. After some fifteen minutes the tubes were examined and the defective ones rejected. They were also examined at the end of an experiment to make sure that no leaks had developed.

In an absorption experiment a tested tube was placed directly in a V-shaped slit in such a way that the walls of the tube were tangent to the walls of the slit. Two small bits of soft wax served to hold the tube securely in place. The vacuum spectrograph used was of the conventional Siegbahn type. A piece of 20-μ red-coloured goldbeater's skin was employed as a window between the body of the spectrograph and the X-ray tube to prevent the light emitted by the filament from fogging the photographic plate. Both filament and anticathode were of tungsten. The tension used was about twice that corresponding to the wave-length of the absorption discontinuity; the electron current varied from 25 to 100 milliamperes, and the length of the exposures from 4 to 8 hours. The analysing crystal was of calcite.

* Communicated by the Author.

† See Siegbahn's 'Spectroscopy of X-rays' Oxford Univ. Press, (1925). Also Otto Stelling, 'Ueber den Zusammenhang zwischen chemischer Konstitution und K-Röntgenabsorptionsspectra.' Thesis from Lund University, Sweden.

Preliminary experiments showed that for the region of longer wave-lengths (3·5 Å and greater) the absorption of the quartz itself was so great that satisfactory photograms could not be obtained in a reasonable length of time. The final experiments were carried out with solutions of manganous chloride and potassium chromate, the ions of interest being manganous ion and chromate ion. The small amount of material actually present in the path of the beam of X-rays made it necessary to use concentrations of at least 0·7 molal, since with lower concentrations the lack of photographic contrast at the absorption edge made it impossible to measure the plates with any accuracy.

In the following table are presented some representative results. The values there given are the distances in millimetres between the absorption edges and a standard reference line photographed on the same plate. The corresponding measurements for the solid salts are also given, and were obtained with the same spectrograph.

Results of the Absorption Measurements.

Radius of spectrograph : 176·27 mm.
Analysing crystal: Calcite.

Substance.	Concentration.	Std. line.	Dist. of edge from std. line.	Distance of white line from std. line.
$MnCl_2$ ...	Solid.	$FeK\alpha_1$	2·58 mm.	—
$MnCl_2$ ...	1·399 m.	,,	2·61 ,,	—
$MnCl_2$ ...	0·699 m.	,,	2·64 ,,	—
K_2CrO_4...	Solid.	,,	7·81 ,,	8·13 mm.
K_2CrO_4...	1·681 m.	,,	7·78 ,,	8·08 ,,

Within the limits of experimental error the absorption discontinuities of manganous and chromate ions in solution have the same wave-lengths as the corresponding ions in crystalline salts. It is possible that differences might be observed in the region of longer wave-lengths, say for the case of chlorides; the experimental difficulties to be overcome are rather formidable, however. It is to be especially noted that the fine structure of the chromate edge (designated as a white line in the table) observed in the case of the solid salts is also observed unchanged in the spectra obtained with solutions. Moreover, it was also found that no observable reduction of the chromate to lower valence forms had taken place. In this case, at least, the fine structure is to be

attributed to the chromate chromium itself, and not to reduced forms arising as a result of the action of the X-radiation.

I wish to express here my appreciation of Prof. M. Siegbahn's kindness in allowing me to make use of the facilities of his laboratory at Uppsala. I am also indebted to him for suggesting and providing the capillary tube.

Uppsala,
June 1929.

XCIII. *The Scattering of Beta-Particles by Light Gases and the Magnetic Moment of the Electron.* *By* MALCOLM C. HENDERSON, *Ph. D., Trinity College, Cambridge* *.

1. *Introduction.*

IN 1925 Uhlenbeck and Goudsmit † showed that the multiplet structure of line spectra could be interpreted if it were postulated that the electron is not merely a point charge of electricity, but possesses also an angular momentum of $\frac{1}{2} \cdot \frac{h}{2\pi}$ due to its own rotation and a magnetic moment equal to one Bohr magneton. This postulate provides a theoretical basis for the fourth quantum number. The problem then arises as to the effect the magnetic moment will have when two electrons collide with one another.

If an electron possesses at all times a magnetic field, such as is necessarily associated with a magnetic moment, the collisions between it and a β-particle, that is, between two electrons, should be profoundly modified. For example, it may be calculated simply from the law of force between magnets in the "end-on" position $(6MM'/r^4 = e^2/r^2$, where $M = M' = 9{\cdot}2 \times 10^{-21}$ Gauss-cms.) that the distance at which the electrostatic force equals the magnetic force is about 5×10^{-11} cm. As usually calculated from the electrostatic force alone, the closest possible approach in a head-on collision between a 344,000 volt β-ray and an electron is about $8{\cdot}3 \times 10^{-13}$ cm.,

* Communicated by Dr. J. Chadwick. The material in this paper formed part of a Thesis submitted for the degree of Doctor of Philosophy at the University of Cambridge.

† Uhlenbeck & Goudsmit, *Naturwiss.*, xiii. p. 953 (1925); 'Nature,' cxvii. p. 264 (1926).

that is, about 1/60 as much. At less than 5×10^{-11} cm. the magnetic force of attraction will exceed the electrostatic force of repulsion, since it varies as a higher negative power of the distance. The deflexion experienced by a β-ray on passing an electron at 60 times the minimum possible distance of approach is about half a degree. All deflexions larger than this amount should be greatly influenced by the magnetic force. The angle through which a particle is deflected for a given nearness of approach should be widely different from the deflexion as calculated from the inverse square law only. Consequently the manner in which the number of particles scattered varies with their deflexion should also be different from the calculated distribution. It may be noted in passing that an inverse fourth power orbit is unstable and under some conditions the electrons might theoretically coalesce.

The other kind of magnetic deflexion, namely, that experienced by a charged particle moving in a magnetic field, is eliminated by the assumption that the particles come at once into the end-on position. The motion is then entirely along the lines of force and the equation $H\rho = mv/e$ no longer applies. If this assumption is not made, a rough calculation shows that the maximum distance at which the two forces may be equal is about 8×10^{-12} cm.

From the theory of single scattering, as developed in detail by Darwin*, it can easily be shown that for small angles the ratio of the nuclear to the electronic scattering is $N^2 : N$, where N is the atomic number of the scattering element. Hence for hydrogen and helium the electronic scattering will be respectively $\frac{1}{2}$ and $\frac{1}{3}$ of the total. For these elements a discrepancy in electronic scattering should therefore be expected to show most markedly. By comparing the scattering of β-rays by these two gases with the scattering by nitrogen and argon it should be possible to determine whether the electrons do in fact possess some field of force in addition to their normal electrostatic field.

Of the solid elements in which the scattering of β-rays has been studied, aluminium is the lowest in atomic number. For small angles the electrons of this element cause, theoretically, about 8 per cent. of the total scattering.

* C. G. Darwin, Phil. Mag. xxvii. p. 499 (1914).

In previous investigations * the interest was in the nuclear scattering and a correction was made for the scattering by the electrons. The agreement between the experimental results when corrected and those expected from theory suggests that the electronic scattering is in fact not very different from 8 per cent. But the correction is too small, compared to the total scattering, for this evidence to be conclusive. From observations of β-ray tracks in a Wilson expansion chamber, Bothe † found the electronic scattering in air to be of about the expected amount, but the small number of collisions observed leaves something to be desired statistically.

Accordingly, some preliminary measurements were made with hydrogen, helium, nitrogen, and argon in a simple form of scattering chamber. Use was made of a familiar principle, namely, the reduction in the number of particles in a beam caused when some of them are deflected through more than a fixed angle. The results suggested an increased scattering in hydrogen and helium. The following more accurate investigation was therefore undertaken.

2. *Apparatus and Method.*

The scattering chamber used was of the "annular ring" type. It was similar to the one used by Rutherford and Chadwick ‡ for measuring the scattering of α-particles in helium.

The dimensions are shown in the figure (see p. 850). The diaphragms were originally of graphite, but the natural effect when the chamber was evacuated was much too high. The diaphragms were therefore backed with 2 mm. of lead (not shown in the figure) and the central disks were joined and supported by a brass rod only slightly smaller in diameter than the disks. The support for the rod was a thin sheet of graphite. The scattering from this support is unavoidable. It amounted, however, together with other residual scattering, to less than $\frac{1}{8}$ of the total current and was deducted from the readings. The average angular limits of the scattering were 9·2 and 29·7 degrees, and the thickness of the scattering layer was 3 cm.

The gases measured were hydrogen, helium, nitrogen, argon, and air. The first four were drawn from cylinders of

* Chadwick and Mercier, Phil. Mag. l. p. 208 (1925); and others.

† Bothe, *Zeit. f. Phys.* xii. p. 117 (1922).

‡ Rutherford and Chadwick, Phil. Mag. iv. p. 605 (1927).

the compressed gas. Every gas passed over phosphorus pentoxide before entering the scattering chamber, and the hydrogen and helium were in addition passed through two charcoal tubes cooled in liquid air. A test experiment showed no difference between hydrogen that was thus purified and that which was taken directly from the cylinders. Nevertheless it was always thus purified. The nitrogen was taken directly from the cylinders. Any impurity was presumably air, and since the ratio of the theoretical scatterings of air and nitrogen is 69·6 : 65·8, an impurity of this kind would be quite negligible. The argon used was about 99·5 per cent. pure.

The source of β-rays was a deposit of radium E on a nickel button 3 mm. in diameter. The deposit was

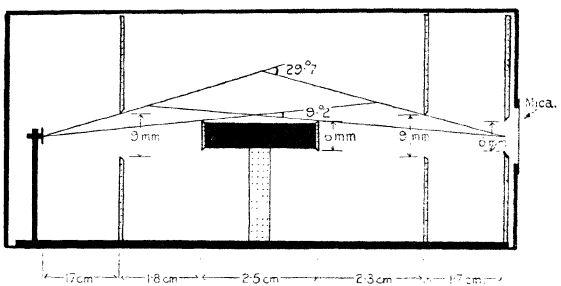

obtained by stirring the button for some time in a hot solution of radium D, E, and F. The initial strength of the source was equivalent to about $\frac{3}{4}$ mg. of radium, as measured on a β-ray electroscope. The amount of radium D on the button was less than 1 per cent.

The β-rays from radium E are heterogeneous and their velocity varies over rather a large range. The average energy is in the neighbourhood of 344,000 volts*, $\beta=0{\cdot}8$. The deflexion which any particle experiences in a given encounter varies inversely as the square of its energy. This fact is not important as long as only the relative scattering by different elements is measured. A possible source of error is that hydrogen may scatter, for example, the low velocity rays relatively more strongly than the

* Ellis and Wooster, Proc. Roy. Soc. A, cxvii. p. 109 (1927).

high velocity rays in comparison with argon. Such a selective effect would mean that the scattering varies with the energy of the rays according to a different law for different atomic numbers. For such a departure from theory there is no experimental evidence.

The measurements were made with a Dolezalek electrometer with a sensitivity of about 3000 mm. per volt. During each experiment the electrometer was held at its zero position by a charge induced on a small condenser forming part of the insulated system. A measure of the ionization current was afforded by the time required for the voltage on the outer casing of the condenser to change by a fixed amount while holding the electrometer stationary. The ionization chamber was cylindrical, 10 cm. in diameter and 14 cm. deep. The outer casing was maintained at 200 volts. Guard rings protected the insulated system from leakage across the insulation of the ionization chamber and condenser.

3. *The Theoretical Scattering Power.*

In the original annular scattering chamber * the scattering substance was in the form of foil. A term $t \sec \phi/2$ entered the integrand of the expression for the scattering because the foil was not perpendicular to the incident beam of particles. In the chamber as modified for gases t is measured along the incident beam and is approximately constant. The expression for the scattering by the nuclei then becomes :

$$\nu_n = \frac{Q n t N^2}{8 r^2}\left(\frac{e^2}{mv^2}\right)^2 \int_{\phi_1}^{\phi_2} \operatorname{cosec}^3\frac{\phi}{2} \cdot \cos\frac{\phi}{2} \cdot d\frac{\phi}{2}$$

$$= \frac{Q n t N^2}{16 r^2}\left(\frac{e^2}{mv^2}\right)^2 \left[-\operatorname{cosec}^2\frac{\phi}{2}\right]_{\phi_1}^{\phi_2}.$$

ν_n is the number of particles received per unit area of the final diaphragm perpendicular to the axis of the chamber. Q is the number of particles in the incident beam, n is the number of atoms of the gas per c.c., N is the atomic number of the scatterer, m is the mass and v the velocity of the β-particle, and r is the average distance from the source to the scattering layer. This expression differs only slightly, in numerical value, from the more complex formula in the original paper.

* Chadwick, Phil. Mag. xl. p. 734 (1920).

If we consider an electron in the atom to be at rest before the encounter and take its mass equal to that of the incident β-particle, then the amount of the electronic scattering will be given by

$$\nu_e = N\frac{Qnt}{4r^2}\left(\frac{e^2}{mv^2}\right)^2\left[-\operatorname{cosec}^2\phi\right]_{\phi_1}^{\phi_2}.$$

The number of electrons projected between the angles ϕ_1 and ϕ_2 will be

$$N\frac{Qnt}{4r^2}\left(\frac{e^2}{mv^2}\right)^2\left[\sec^2\phi\right]_{\phi_1}^{\phi_2}.$$

For the values of ϕ_1 and ϕ_2 used in these experiments the projected electrons are relatively so few in number that they will be neglected in the calculations which follow.

The sum of these expressions gives the total scattering by the gas.

However, as shown by C. G. Darwin *, each of these expressions must be corrected for the change in the orbit caused by the variation of the mass of the β-particle with its velocity, the so-called relativity correction. For the nuclear scattering this takes the form

$$\left[\frac{\beta\operatorname{cosec}\psi}{\cot\frac{\phi}{2}}\right]^2, \quad \text{where} \quad \beta\cot\psi = \tan\left[\pi - \cos\psi\left(\frac{\phi+\pi}{2}\right)\right].$$

The mean value of this correcting factor was calculated to be 1·2 for the conditions of the present experiments.

The corresponding correcting factor for the electronic scattering has not been worked out. However, elementary considerations show that it will have a value less than one, that is, it will serve to reduce the calculated amount of electronic scattering, for in the encounter with an electron the β-particle will be retarded in its motion, not accelerated as in an encounter with the positive nucleus. The correction will in general be small and it has been omitted in the following calculations.

Adding the above expressions for the nuclear and electronic scattering and simplifying :

$$\nu = \frac{Qnt}{4r^2}\left(\frac{e^2}{mv^2}\right)^2\left[\frac{1}{4}N^2\operatorname{cosec}^2\frac{\phi}{2}\cdot\left[\frac{\beta\operatorname{cosec}\psi}{\cot\frac{\phi}{2}}\right]^2 + N\operatorname{cosec}^2\phi\right]_{\phi}^{\phi_1}.$$

* C. G. Darwin, Phil. Mag. xxv. p. 201 (1913).

Substituting the values for the experimental conditions, viz.,

$$\phi_2 = 29°{\cdot}7\,; \quad \phi_1 = 9°{\cdot}2\,; \quad \left[\frac{\beta \operatorname{cosec} \psi}{\cot \frac{\phi}{2}}\right]^2 = 1{\cdot}2$$

$$\nu = k\left[\mathrm{N}^2 \cdot \frac{14{\cdot}3 \cdot 2}{4} \cdot 1{\cdot}2 + 35{\cdot}3\,\mathrm{N}\right],$$

where $k = \frac{Qnt}{4r^2}\left(\frac{e^2}{mv^2}\right)^2$,

or, to a sufficiently exact approximation.

$$\nu = 35{\cdot}8k(1{\cdot}2\,\mathrm{N}^2 + \mathrm{N}).$$

As shown by this formula the number of scattered particles should be proportional to $1{\cdot}2\mathrm{N}^2 + \mathrm{N}$ when there are the same number of atoms present per c.c. The values entered in column 2 of Table II are calculated from this expression.

4. *Experimental Results.*

In each experiment readings of the ionization current were taken for different pressures of the various gases: hydrogen, helium, nitrogen, argon, and air. When the pressure is plotted against the ionization current the points lie approximately on straight lines, indicating the predominance of single scattering, up to a pressure of about 2 cm. for argon, 6 cm. for nitrogen, 50 cm. for helium and 70 cm. for hydrogen. There is a tendency toward upward curvature as plural scattering becomes more prominent *. The observed values of the ionization current in two experiments, corrected for natural effect, with the corresponding pressures are shown in columns 2 and 3 of Table I. The ionization current divided by the pressure gives a constant for each gas, and the ratios of these constants to each other are the ratios of the scattering powers. The quotients of the figures in column 2 divided by those in column 3 are entered in column 4.

Table II. gives the collected results of the last five experiments. In column 2 are the theoretical values of

* It may be noted that the scattering ceases to be single at about the point indicated by Wentzel's criterion. For example, the scattering in nitrogen is single up to a pressure of about 6 cm., for which 4ω under the conditions of these experiments was about 4·8°, while ϕ varies from 9° to 30°. (*Cf.* Wentzel, *Ann. d. Phys.* lxix. p. 335, 1922.)

the relative scattering power of the gas concerned (see section 3), in column 3 are the theoretical percentage

TABLE I.

Showing the pressures and corresponding ionization currents for various gases and the resulting relative scattering powers.

1	2 P.	3 I.	4 I./P.	5 Av.	
N	5·01	23·3	4·65	4·64	
	4·23	20·5	4·84		
	3·23	14·4	4·46		
H_2	73·50	17·2	·234	·234	$\frac{4\cdot64}{\cdot23_4} = \frac{65\cdot8}{3\cdot32} = \frac{N_2}{H_2}$
	55·00	12·9	·235		
He	67·15	19·0	·283	·277	$\frac{4\cdot64}{\cdot27_7} = \frac{65\cdot8}{3\cdot92} = \frac{N_2}{He}$
	37·30	10·1	·271		
A	2·57	48·1	18·7	19·4	
	1·90	37·9	19·9		
	1·21	23·9	19·7		$\frac{19\cdot4}{8\cdot4} = \frac{203}{88} = \frac{A}{Air}$
Air	2·05	16·9	8·25	8·4	
	4·14	35·8	8·65		
	6·12	50·5	8·25		

TABLE II.

Collected Results.

1 Gas.	2 Theoretical scattering power $1{\cdot}2N^2 \div N$	3 Theoretical percentage electronic contribution.	4 Experimental scattering powers. A=203.	5 Ratio experimental to theoretical.
H_2	2·2	45	4·0	1·8
He	3·4	29	4·8	1·4
N_2	65·8	10·6	79	1·2
Air	69·6	10·4	84	1·2
A	203	4·4	203	1

contributions by the electrons to that scattering power, in column 4 are the experimentally determined scatterings all reduced to 203 for argon (the ratio of nitrogen to air is taken as normal, that is, equal to 65·8 : 69·6), in column 5

are the ratios of experimental to theoretical scattering power.

5. *Discussion.*

The results in Table II. show that the lighter gases possess a scattering power for β-rays in excess of that calculated from the expression $1{\cdot}2N^2+N$. This excess scattering may be attributed to the orbital electrons, since it increases with decreasing atomic number in about the same manner as does the theoretical electronic scattering. An attempt was made to fit the expression $1{\cdot}2N^2+kN$ to the observed scatterings by using various values of k. When $k=3{\cdot}3$ the relative values of this expression lie within eight per cent. of the observed scatterings in the gases measured.

In the collisions between nucleus and β-particle it is usually assumed that the magnitude of the velocity of the β-particle is unchanged by the encounter, unless there is radiation. On the other hand its velocity is reduced in an encounter with another electron because of the energy imparted to the latter. Calculation of a special case shows that when a β-particle of velocity $\cdot 8c$ is scattered by an electron through an angle of 11·2 degrees, its velocity is reduced to $\cdot 79c$ and the projected electron moves with a velocity of $\cdot 25c$ in a direction at 76·7° with the incident particle. The loss of velocity suffered by the β-particle is thus small. No correction has therefore been made for this effect in these experiments.

As calculated in section 1. if the magnetic moment of the electron is one Bohr magneton. the maximum distance at which the magnetic and electric forces between two electrons become equal is 5×10^{-11} cm. This is about 60 times the minimum apsidal distance for collisions between the average radium E β-particle and an electron, calculating the apsidal distance in the usual way for a purely electrostatic field. The theoretical deflexion for an impact parameter of 60 times the minimum apsidal distance is about half a degree. For larger angles of scattering the magnetic force should be the more important factor in determining the final path of the particles. It would appear that under the conditions adopted in the present experiments the electronic scattering should be determined almost completely by the magnetic forces. A rough calculation on these lines shows that the amount

of scattering should be very different from that actually found, and it therefore seems unlikely that the electron can have a magnetic moment as large as one Bohr magneton. The fact that an increase in the number of particles was observed, roughly proportional to the relative importance of the electron in the atoms, suggests, however, that there is an additional field of force present in collisions between electrons. Without measurements over other ranges of angle the nature of this field of force cannot be inferred.

From the nature of magnetic force the force between two magnetons must depend both in sign and magnitude upon the orientation of the axes of the particles with respect to each other. The magnetons will also in general exert a torque upon each other tending to bring them into the position of greatest attraction. If, however, the magnetic moment is the result of an actual spin, the two particles will merely precess about the line of centres. The force between them will not then be increased by their rotation toward the end-on position. Calculation of the orbits described under such conditions is difficult. Hicks * and Wessel † have made calculations of this nature for the somewhat simpler conditions of a fixed magneton and a non-magnetic moving particle. Bothe ‡ also has calculated the orbits of a β-particle about a nucleus, using a somewhat different assumption. He considers that the magnetic β-particle is moving in the inhomogeneous magnetic field of the nucleus. In this case there are two possible orientations. The axes of the particles may be either parallel or anti-parallel.

An objection to the conception of an electron as possessing spin and consequent magnetic moment is the relative complexity of this model compared to the point charge. Dirac § has shown how to avoid the necessity for a magnetic electron by a more complete solution of the fundamental equations. The electron according to his theory is still a point charge but it displays a duplex character, in many respects resembling the behaviour of a magneton. Iwanenko and Landau ¶ have shown by an

* Hicks, Proc. Roy. Soc. A, xc. p. 376 (1914).
† Wessel, *Ann. d. Phys.* lxxviii. p. 757 (1925).
‡ Bothe, *Zeit. f. Phys.* xliv. p. 543 (1927).
§ Dirac, Proc. Roy. Soc. A, cxvii. p. 610 (1928); cxviii. p. 351 (1928).
¶ Iwanenko and Landau, *Zeit. f. Phys.* xlviii. p. 340 (1928).

entirely different method that the assumptions of wave mechanics lead to the same result. The problem of the collision of a β-particle with an electron has not yet been examined on the basis of Dirac's equations, and although it seems possible that the duplex character of an electron in an orbit may be interpreted to give a magnetic field effective in collisions, the magnitude of the effect eannot be estimated without a laboured calculation. When such calculations are available it may be possible to give an adequate explanation of the results obtained in the present experiments, without any further hypotheses.

In the experiments performed heretofore on β-ray scattering, additional fields of force, usually magnetic, have often been postulated to explain increased scattering, but they have always been discarded later after more exact investigation. Whether the increased scattering found in the present work must finally be explained by that postulate is a matter for further investigation to decide.

Summary.

The hypothesis of the magnetic electron put forward by Uhlenbeck and Goudsmit in 1925 raises the question as to the effect which the magnetic field of the electron will have upon the collisions between β-particles and electrons in their orbits. Experiments upon the scattering power of light gases for β-particles have therefore been carried out to determine whether there is any such effect.

The experiments with the β-particles from radium E show that hydrogen and helium possess a scattering power, measured between 10° and 30°, about 80 and 40 per cent., respectively, in excess of that to be expected from the usual theory. The variation in scattering power with atomic number (N) is fitted within 8 per cent. by the expression aN^2+kN, where a is the relativity correction and k is 3·3 instead of the theoretical value slightly less than unity. Although this result suggests that the electron possesses a field of force in addition to the normal electrostatic field, it apppears unlikely that it can have a magnetic moment as large as one Bohr magneton.

The author is indebted to Professor Sir Ernest Rutherford and to Dr. J. Chadwick for their advice and interest during this investigation.

XCIV. *The Thermal Expansion of Liquids according to van der Waals.* *By* J. E. VERSCHAFFELT, *Professor in Physics at the University of Ghent* *.

THE Philosophical Magazine has published recently a paper by Mr. V. N. Thatte †, in which the author intended to show that from van der Waals's equation of state,

$$p+\frac{a}{v^2}=\frac{RT}{v-b}, \quad . \quad . \quad . \quad . \quad . \quad . \quad (1)$$

taken at temperatures so low that the vapour pressure p may be neglected against the pressure of cohesion $\frac{a}{v^2}$, a formula may be derived for the relative coefficient of cubical expansion $c=\frac{1}{v}\frac{dv}{dT}$ of the liquid similar to that of Davies. Putting $p=0$ in the equation (1), one finds

$$\frac{1}{c}=\frac{a}{R}-2T, \quad . \quad . \quad . \quad . \quad . \quad . \quad (2)$$

and this relation is indeed similar to the formula of Davies when we suppose, as Mr. Thatte does, that the term $\frac{a}{vR}$ is (at least nearly) a constant proportional to the critical temperature T_c; only the coefficients are different. Determining the coefficient of T_c by using experimental data, Mr. Thatte finds

$$\frac{1}{c}=2{\cdot}5\ T_c-2T.$$

I wish to say that I do not quite agree with this result. I do not see why Mr. Thatte deduces the value of the term $\frac{a}{vR}$ from experiment, instead of deriving it from the equation of state, by which it is completely determined; that seems to me illogical. Now we know that at very low temperatures that equation gives $v=b$, and it is known also that, according to the same equation,

$$\frac{a}{bR}=\frac{27}{8}T_c; \quad . \quad . \quad . \quad . \quad . \quad . \quad (3)$$

* Communicated by the Author.

† V. N. Thatte, "Coefficient of Cubical Expansion of Liquids and Critical Temperature," Phil. Mag. vii. p. 887 (May 1929).

so it results from the equation itself that the term $\frac{a}{v\mathrm{R}}$ is really proportional to T_c, but the coefficient of proportionality is $\frac{27}{8} = 3{\cdot}4$ instead of being 2·5.

But this is only a limit value. One must not overlook the fact that the term $\frac{a}{v\mathrm{R}}$ may not be considered as constant, because v is a function of temperature, and this circumstance modifies also the value of the coefficient of T. In order to find this coefficient, we write equation (2) in the form

$$\frac{1}{c} = \frac{a}{\mathrm{R}}\delta - 2\mathrm{T} = \mathrm{T}_c\left(\frac{a}{3b\mathrm{R}\mathrm{T}_c}\cdot\frac{\delta}{\delta_c} - 2\frac{\mathrm{T}}{\mathrm{T}_c}\right) = \mathrm{T}_c\left(\frac{9}{8}\cdot\frac{\delta}{\delta_c} - 2\frac{\mathrm{T}}{\mathrm{T}_c}\right), \quad . \quad . \quad . \quad . \quad (4)$$

where $\delta = \frac{1}{v}$ is the (molecular) density; for according to van der Waals's equation.

$$\delta_c = \frac{1}{3b}. \quad . \quad . \quad . \quad . \quad . \quad . \quad . \quad . \quad (5)$$

Now values of $\frac{\delta}{\delta_c}$ corresponding to different values of $\frac{\mathrm{T}}{\mathrm{T}_c}$ have been calculated by J. P. Dalton *. From his table and equation (4) we deduce the following one :—

$\frac{\mathrm{T}}{\mathrm{T}_c}$	$\frac{\delta}{\delta_c}$	$\frac{1}{c}$
$=0$	$=3{\cdot}00$	$=3{\cdot}375\,\mathrm{T}_c$.
0·1	2·91	3·07
0·2	2·81	2·76
0·3	2·70	2·44
0·4	2·59	2·11
0·5†	2·46	1·76

and from this it is easily seen that we may put approximately :

$$\frac{1}{c} = 3{\cdot}4\,\mathrm{T}_c - 3{\cdot}2\,\mathrm{T}. \quad . \quad . \quad . \quad . \quad . \quad . \quad (6)$$

But according to van Waals the relation between $\frac{1}{c}$ and T is not really linear, as in Davies's formula, deduced from the

* See J. P. Kuenen, 'Die Zustandsgleichung der Gase und Flüssigkeiten, p. 94 (1907).

† Up to this value of $\frac{\mathrm{T}}{\mathrm{T}_c}$ the vapour pressure remains negligible. See Kuenen, *loc. cit.*

law of the rectilinear diameter. The exact relation is to be found by substitution in (4) of the function $\frac{\delta}{\delta_c}$ determined by the equation :

$$\frac{a}{v^2}=\frac{RT}{v-b} \quad \text{or} \quad a\delta=\frac{RT}{1-b\delta},$$

which may be put in the reduced form :

$$3\frac{\delta}{\delta_c}\left(3-\frac{\delta}{\delta_c}\right)=8\frac{T}{T_c}. \quad . \quad . \quad . \quad . \quad . \quad . \quad (7)$$

The greatest root of this quadratic equation must be taken. By developing it in a series, one finds

$$\delta=3\delta_c(1-x-x^2-2x^3-\ldots\ldots), \quad . \quad . \quad . \quad (8)$$

with

$$x=\frac{8}{27}\frac{T}{T_c}, \quad . \quad . \quad . \quad . \quad . \quad . \quad . \quad . \quad (9)$$

and consequently

$$\frac{1}{c}=\frac{27}{8}T_c\,(1-3x-x^2-2x^3-\ldots\ldots), \quad . \quad . \quad (10)$$

or

$$c=\frac{8}{27T_c}(1+3x+10x^2+35x^3+\ldots\ldots), \quad . \quad . \quad (11)$$

which last relation may be deduced directly from (8) by observing that

$$c=\frac{1}{v}\frac{dv}{dT}=\frac{d\log v}{dT}=-\frac{d\log\delta}{dT}.$$

The relation (11), however, is less useful than (10) on account of its less rapid convergency.

It is obvious that form (6) does not agree well with the experimental data; only Davies's formula does for normal substances at low temperatures (at which the density of the vapour is nearly zero). Even Thatte's formula, partly deduced from experiment, is in disagreement, save for $T=\pm\frac{1}{2}T_c$, at which temperature both the formulæ of Davies and Thatte give $\frac{1}{c}=1{\cdot}5\,T_c$. It may, moreover, be remarked that van der Waals's equation does not give a quite different value.

Natuurkundig Laboratorium,
Ghent, Aug. 1929.

XCV. *On the Operational Solution of Linear Differential Equations and an Investigation of the Properties of these Solutions.* By BALTH. VAN DER POL, *D.Sc.* *

1. *Introduction.*

IN a former paper † the rules for solving operationally linear differential equations with constant coefficients and with an arbitrary second member were considered. Arbitrary given initial conditions could be taken care of. The best-known case is that for which the system is originally fully at rest, while at the instant $t=0$ a unit force is suddenly impressed upon the system.

It is the purpose of the present paper (i.) to consider some general rules in connexion with the operational calculus, (ii.) to outline a method similar to the one used in the former paper for the solution of linear differential equations with variable coefficients, and (iii.) to consider simple operational methods for the investigations of the properties of the functions defined by those equations.

Though the subject matter is relatively new in physics ‡ the idea of fractional differentiation and integration, which forms an important part of the operational calculus, was worked out by Riemann ('Werke,' p. 331), a report of which is to be found in Pincherle's article on "Funktional-operationen und -Gleichungen" in the *Enz. der Math. Wiss.* ii. A. 11, where again, however, no mention is made of Heaviside's important contributions to the subject §.

As in our former paper, we will here again take as a basis of the development the integral equation of Carson ‖, of which Bromwich's well-known integral ¶ is the solution.

* Communicated by the Author.

† Balth. van der Pol, "A Simple Proof and an Extension of Heaviside's Operational Calculus for Invariable Systems," Phil. Mag. vii. p. 1153 (1929).

‡ *E.g.* we do not find any reference to it either in the new edition of Riemann–Weber, 'Die Differential-gleichungen der Physik' (1927) or in Courant–Hilbert, 'Mathematische Physik,' i. (1924).

§ The same is true for the article by A. Voss, "Integralrechnung," *Enz. der Math. Wiss.* ii. A. 2, p. 116, where, also, fractional differentiation is considered.

‖ J. R. Carson, 'Electric Circuit Theory and the Operational Calculus (McGraw-Hill, New York, 1926).

¶ T. J. I'a. Bromwich, Proc. London Math. Soc. xv. p. 401 (1916). In this paper arbitrary initial conditions are already considered in the operational solution of differential equations. See also H. Jeffreys, 'Operational Methods in Mathematical Physics' (Cambridge University Press, London, 1927).

In order to expound our method as clearly as possible we insert various examples, mostly taken from Bessel functions, spherical harmonics, and other functions. It is found to be a relatively simple matter, once the operational representations of these functions have been obtained, to write down, almost at a glance, many relations between those functions, of which several may be new. In particular we refer to the parallelism between the familiar relations which exist between Bessel functions of different order on the one hand and the well-known similar relations between spherical harmonics on the other hand. It will, for instance, be shown that the one set of relations can directly be derived from the other. Further, three new expressions will be derived for the derivative of Bessel functions with respect to their order. In this respect a new function,

$$\mathrm{Ji}(x) = \int_{\infty}^{x} \frac{\mathrm{J}_0(x)}{x} dx, \quad . \quad . \quad . \quad . \quad . \quad (1)$$

which is analogous to

$$\mathrm{Ci}(x) = \int_{\infty}^{x} \frac{\cos x}{x} dx, \quad . \quad . \quad . \quad . \quad . \quad (2)$$

will be shown to play an important part. It looks to the writer as if the shortest way to expound and explore the properties of Bessel functions, for example, is by the powerful method of operators. Finally, at the end of the paper a list is given of the symbolic representations of many functions, of which several may here be given for the first time. Throughout, the notations of the well-known tables of Jahnke–Emde * will be adhered to.

2. *Some General Theorems.*

We assume the symbolic or operational representation $f(p)$ of a function $h(x)$ of x to be defined by Carson's integral:

$$f(p) = p \int_0^{\infty} e^{-px} h(x)\, dx. \quad . \quad . \quad . \quad . \quad . \quad (3)$$

Thus, on the one hand, when the function $h(x)$ is given its operational representation $f(p)$ is found by an integration. On the other hand, when the operational expression $f(p)$ of the unknown function $h(x)$ is given, (3) represents an integral equation for the unknown function $h(x)$. The

* Jahnke-Emde, 'Funktionentafeln' (Teubner, Leipzig und Berlin).

solution of the integral equation is given by the following complex integral, first obtained by Bromwich :—

$$h(x) = \frac{1}{2\pi i}\int_{c-i\infty}^{c+i\infty} e^{px}\frac{f(p)}{p}\,dp, \quad . \quad . \quad . \quad . \quad (4)$$

where $c > 0$; this was pointed out by Lévy * and March †.

Now from the definition (3) of the operational representation $f(p)$ of a function $h(x)$ a set of theorems has been derived by Carson. As we shall make frequent use of these relations, they will here be summarized without proof. The proofs can be found in the above-mentioned treatise of Carson.

Thus, if $f(p) \doteqdot h(x)$ ‡,

then

$$f\left(\frac{p}{s}\right) \doteqdot h(sx) \qquad (s = \text{constant}), \quad . \quad . \quad . \quad (5)$$

$$pf(p) \doteqdot \frac{d}{dx}h(x) \qquad (\text{provided } h(0) = 0), \quad (6)$$

$$\frac{1}{p}f(p) \doteqdot \int_0^x h(x)\,dx, \quad . \quad . \quad . \quad . \quad . \quad . \quad . \quad . \quad (7)$$

$$\frac{p}{p+\alpha}f(p+\alpha) \doteqdot e^{-\alpha x}h(x), \quad . \quad . \quad . \quad . \quad . \quad . \quad . \quad . \quad (8)$$

$$e^{-\lambda p}f(p) \doteqdot \begin{cases} 0 & \text{for } x < \lambda \\ h(x-\lambda) & \text{for } x > \lambda \end{cases} \quad (\lambda > 0), \quad (9)$$

$$e^{+\lambda p}f(p) \doteqdot h(x+\lambda)\ \S, \qquad (\lambda > 0). \quad . \quad (10)$$

when $h(x) = 0$ for $0 < x < \lambda$.

To this list the following relations may be added :—

$$\left(-p\frac{d}{dp}\right)^n f(p) \doteqdot \left(x\frac{d}{dx}\right)^n h(x), \qquad (n > 0), \quad . \quad (11)$$

$$p\left(-\frac{d}{dp}\right)^n \left\{\frac{f(p)}{p}\right\} \doteqdot x^n . h(x), \qquad (n > 0), \quad . \quad (12)$$

$$\int_p^\infty \frac{f(p)}{p}\,dp \doteqdot \int_0^x \frac{h(x)}{x}\,dx, \quad . \quad . \quad . \quad . \quad . \quad . \quad . \quad (13)$$

$$\int_0^p \frac{f(p)}{p}\,dp \doteqdot \int_0^\infty \frac{h(x)}{x}\,dx, \quad . \quad . \quad . \quad . \quad (13\,a)$$

* P. Lévy, 'Le Calcul symbolique de Heaviside' (Gauthier-Villars, Paris, 1926).

† H. W. March, "The Heaviside Operational Calculus," Bull. Am. Math. Soc. xxxiii. p. 311 (1927).

‡ When $f(p)$ is the operational representation of $h(x)$, as defined by (3), we use the symbol $\doteqdot$, and write $f(p) \doteqdot h(x)$.

§ See also Jeffreys, *l. c.* p. 18.

$$\int_0^\infty \frac{f(p)}{p}\,dp = \int_0^\infty \frac{h(x)}{x}\,dx. \quad . \quad . \quad . \quad . \quad . \quad (14)$$

$$\operatorname*{Lim}_{p\to\infty} f(p) = \operatorname*{Lim}_{x\to 0} h(x), \quad . \quad . \quad . \quad . \quad . \quad . \quad (15)$$

$$\operatorname*{Lim}_{p\to 0} f(p) = \operatorname*{Lim}_{x\to\infty} h(x), \quad . \quad . \quad . \quad . \quad . \quad . \quad (15\,a)$$

provided the definite integrals and limits have a meaning, *i.e.* they can be extended to the limits 0 and ∞.

If, further,

$$f_1(p) \doteqdot h_1(x)$$

and

$$f_2(p) \doteqdot h_2(x),$$

then

$$p\left\{h_1\left(-\frac{d}{dp}\right)\right\}\cdot\left[\frac{f_2(p)}{p}\right] = p\left\{h_2\left(-\frac{d}{dp}\right)\right\}\cdot\left[\frac{f_1(p)}{p}\right] \doteqdot h_1(x).h_2(x), \quad . \quad . \quad . \quad (16)$$

provided either $h_1(x)$ or $h_2(x)$ can be expanded in a series of positive powers of x.

Finally, we have the very important theorem

$$f_1(p).f_2(p).\frac{1}{p} \doteqdot \int_0^x h_1(\xi).h_2(x-\xi).d\xi = \int_0^x h_2(\xi).h_1(x-\xi).d\xi. \quad . \quad (17)$$

As the theorems (11)–(16) were not given by Carson, the proof will be indicated here.

To prove (11) differentiate both sides of (5) with respect to s and then put $s=1$. We obtain

$$-p\frac{df(p)}{dp} \doteqdot x\frac{dh(x)}{dx}. \quad . \quad . \quad . \quad . \quad (11\,a)$$

A repeated differentiation with respect to s thus yields (11). When, further, (11a) is multiplied by p^{-1}, which, according to (7), means integration on the right-hand side between zero and x, we obtain

$$-\frac{df(p)}{dp} \doteqdot \int_0^x x.\frac{dh(x)}{dx}dx = xh(x) - \int_0^x h(x)\,dx$$

or

$$-\frac{df(p)}{dp} + \frac{f(p)}{p} = -p\frac{d}{dp}\left(\frac{f(p)}{p}\right) = x.h(x),$$

from which (12) follows.

To demonstrate (13) an integration of both members of (5) can be effected between the limits zero and unity. If the same integration is taken between the limits zero and infinity (14) is obtained, while the subtraction of (13) and (14) yields (13 *a*). Further, (15) follows from (3) when it is remembered that

$$\operatorname*{Lim}_{\substack{x\geqq 0\\ p\to\infty}} p e^{-px} = \delta(x)$$

is a function of the type as used by Dirac* in atomic theory, and called by him a δ function. It has the property

$$\int_{-\infty}^{+\infty} \delta(x)\, dx = 1,$$

and is zero everywhere except at $x=0$, where it is infinite.

These functions have the property

$$\int_{-\infty}^{+\infty} \delta(x) . h(x)\, dx = h(0),$$

and thus (15) follows. It is interesting to remark that these δ-functions were recognized and used extensively by Heaviside † already thirty-five years ago. He called them "impulsive" functions.

Thus
$$1 \doteqdot [1],$$
$$p \doteqdot \delta(x),$$
$$p^2 \doteqdot \delta'(x),$$
$$p^3 \doteqdot \delta''(x),$$
$$\cdot \quad \cdot \quad \cdot \quad \cdot$$

with the general property

$$\int_{-\infty}^{+\infty} f(x) . \overset{(n)}{\delta}(x) . dx = \overset{(n)}{f}(0).$$

Further, (16) can be demonstrated with the aid of (12). When one of the functions $h_1(x)$ or $h_2(x)$ can be expanded as a power series (8) is thus seen to be a special case of (16), because we have

$$f_1(p) = \frac{p}{p+\alpha} \doteqdot e^{-\alpha x} = h_1(x),$$

$$f_2(p) \doteqdot h_2(x),$$

* See, *e.g.*, Proc. Roy. Soc. A, cxiii. p. 625 (1926).
† See, *e.g.*, Heaviside, 'Electromagnetic Theory, ii. p. 92.

and applying (15), we find

$$p e^{\alpha \frac{d}{dp}} \left(\frac{f_2(p)}{p}\right) = p\left(1+\alpha \frac{d}{dp} + \frac{\alpha^2}{2!}\frac{d^2}{dp^2} + \ldots\right)\frac{f_2(p)}{p}$$

$$= \frac{p}{p+\alpha} \cdot f_2(p+\alpha) \doteq e^{-\alpha x} h_2(x).$$

Finally (17), which is the most important theorem of all, is frequently used by Carson. It is of the type of a "produit de composition," as defined by Volterra, and it is on the basis of this theorem that Lévy * builds up the operational calculus. This expression was also at the base of Riemann's investigation †. Further, this theorem was given by Borel ‡, and is closely related to Borel's "associated function" § and his "sommation exponentielle" of divergent series. Moreover, it expresses the well-known Hopkinson–Boltzmann's superposition principle, and it is used and demonstrated in a special case by Lord Rayleigh in his 'Theory of Sound,' i. p. 74. It will be of frequent use further on.

3. *Examples illustrating the General Theorems.*

After having obtained a rather complete set of theorems, or working rules, we will now consider some examples of application of these rules. From the definition of the $\Pi(n)$ functions

$$\Pi(n) = \int_0^\infty e^{-u} . u^n . du,$$

where $\Pi(n) = n!$ for $n =$ positive integer,

i follows at once from (3) that

$$\frac{1}{p^n} = \frac{x^n}{\Pi(n)}, \quad \ldots\ldots \quad (18)$$

which s valid for all values of n for which $n > -1$, fractional values of n included.

Similarly, we have

$$\frac{p}{p+1} \doteq e^{-x}, \quad \ldots\ldots \quad (18a)$$

* *Loc. cit.*

† *Enz. der Math. Wiss.* ii. A. 11, p. 771.

‡ E. Borel, 'Leçons sur les Séries divergentes,' (Gauthier-Villars, Paris, 1928).

§ See, *e. g.*, Whittaker and Watson, 'Modern Analysis,' p. 140.

$$\frac{p}{p^2+1} \doteq \sin x, \quad \ldots\ldots \quad (18\,b)$$

$$\frac{p^2}{p^2+1} \doteq \cos x. \quad \ldots\ldots \quad (18\,c)$$

These expressions can easily be verified by series expansion. *E. g.* :

$$\frac{p^2}{p^2+1} = 1-\frac{1}{p^2}+\frac{1}{p^4}-\ldots \doteq 1-\frac{x^2}{2!}+\frac{x^4}{4!}-\ldots = \cos x.$$

Consider (9). Let again $f(p) \doteq h(x)$. As (3) only considers the values of $h(x)$ in the region 0 to ∞, it cannot give any information as to the behaviour of $h(x)$ in the region $x < 0$. In connexion with (9) it is, therefore, appropriate to consider all our functions to be zero for $x<0$.

This is demonstrated in fig. 1. A factor $e^{-\lambda p}$ therefore shifts $h(x)$ over a distance to the right, while a factor $e^{+\lambda p}$ shifts it over the same distance to the left, but in the last case a part of the function is moved through an imaginary vertical cut along the y-axis and slipped under a rigid cover, which keeps the function equal to zero whenever $x<0$. That this is the only consistent interpretation follows directly from the integral (3). For

$$e^{-\lambda p}.f(p) = p\int_0^\infty e^{-p(x+\lambda)}h(x)\,dx = p\int_A^\infty e^{-ps}.h(s-\lambda)\,ds,$$

or

$$e^{-\lambda p}.f(p) = p\int_\lambda^\infty e^{-px}.h(x-\lambda)\,dx.$$

When λ is positive this would be the representation of $h(x-\lambda)$ if the lower limit of the last integral were zero. This can be obtained if $h(x-\lambda)$ is taken to be zero in the region $0<x<\lambda$, as represented in fig. 1 *b*. Again, if λ is negative and $\lambda=-\lambda'$, the lower limit of the integral can again be made zero if $h(x+\lambda')$ is taken to be zero in the region $x<0$, *i. e.*, if the function starts as indicated in fig. 1 *c*.

That the function $e^{-\lambda p}.f(p)$ is rightly interpreted above can also be proved simply by theorem (17), when $e^{-\lambda p}$ is interpreted as being unity for $x>\lambda$ and zero for $x<\lambda$.

Let us consider an instance.

$h(x)=x$ is represented symbolically by $\frac{1}{p}$, or $\frac{1}{p} \doteq x$ (see

fig. 2*a*); fig. 2*b* represents $e^{-\lambda p}.\frac{1}{p}$; fig. 2*d*, $e^{+\lambda p}.\frac{1}{p}$. If, however, $e^{-\lambda p}.\frac{1}{p}$ were developed as

$$\left(1-\frac{\lambda p}{1!}+\frac{\lambda^2 p^2}{2!}-\ldots\right)\frac{1}{p},$$

Fig. 1*a*.

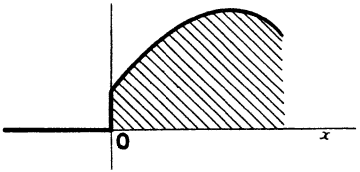

$h(x) \doteq f\ p$

Fig. 1*b*.

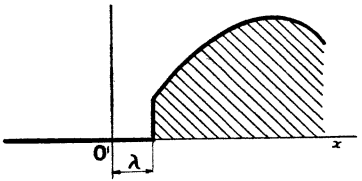

$e^{-\lambda p} f(p)$.

Fig. 1*c*.

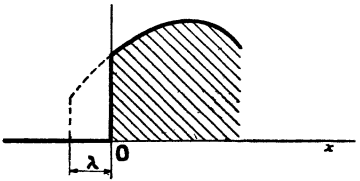

$[e^{+\lambda p} f(p)]$.

and the positive powers of p were rejected, we should obtain

$$\frac{1}{p}-\lambda \doteq x-\lambda,$$

Fig. 2 *a*.

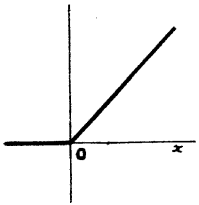

$h(x) \doteqdot \frac{1}{p} \doteqdot x$

Fig. 2 *b*.

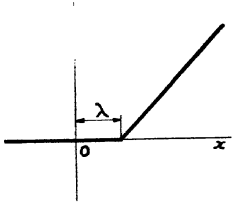

$e^{-\lambda p} \cdot \frac{1}{p}$.

Fig. 2 *c*.

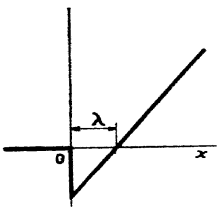

$\left[e^{-\lambda p} \cdot \frac{1}{p}\right] = \frac{1}{p} - \lambda = x - \lambda.$

Fig. 2 *d*.

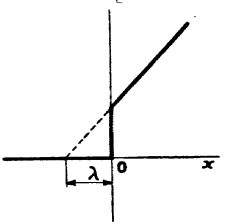

$\left[e^{+\lambda p} \cdot \frac{1}{p}\right] \begin{cases} = x+\lambda & \text{for } x>0, \\ = 0 & \text{for } x<0. \end{cases}$

Fig. 2 *e*.

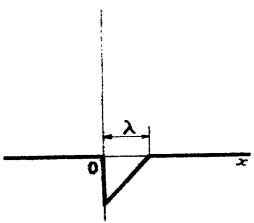

$$-\left[\left[e^{-\lambda p} \cdot \frac{1}{p}\right]\right] = \frac{1}{p}\left\{\frac{\lambda^2 p^2}{2!} - \frac{\lambda^3 p^3}{3!} + \frac{\lambda^4 p^4}{4!} - \cdots\right\}.$$

as represented in fig. 2 *c*, which is erroneous. It is, however, interesting to note that

$$\left[e^{-\lambda p}\frac{\Pi(n)}{p^n}\right] \doteqdot (x-\lambda)^n$$

if n is a positive integer, and when the brackets [ ] are understood to mean the omission of all positive powers of p. Therefore the difference

$$[[e^{-\lambda p}.f(p)]] = e^{-\lambda p}.f(p) - [e^{-\lambda p}.f(p)],$$

(where the double brackets symbolize the retention of the positive powers of p only, the zero'th power excluded) yields (see fig. 2 *e*)

$$[[e^{-\lambda p}.f(p)]] \doteqdot \begin{cases} -h(x-\lambda), & 0<x<\lambda \\ 0, & x<0 \text{ or } x>\lambda \end{cases}. \quad (18\,d)$$

In the same way it follows that

$$[[e^{+\lambda p}.f(p)]] = 0, \qquad 0<x<\infty,$$

for the factor $e^{+\lambda p}$ shifts the function to the left as explained above, there being no positive region at present where the function is continuously zero.

These considerations are obviously only valid when $h(x)$ can be developed as a series of positive powers of x. Later on, in the treatment of the Legendre functions, we shall come back to these properties. The relation of these properties with a Laurent development has not yet been investigated.

Returning to the meaning of $e^{-\lambda p}$, it follows at once from the development of

$$\frac{1}{2}\left\{1+\coth\frac{hp}{2}\right\} = \frac{1}{1-e^{-hp}} = 1+e^{-hp}+e^{-2hp}+e^{-3hp}+\ldots$$

that

$$\frac{1}{2}\left\{1+\coth\frac{hp}{2}\right\}$$

means the "staircase"-function depicted in fig. 3 *, because each following term adds discontinuously unity to the function.

Again

$$\frac{1}{2}\tanh\frac{hp}{2} = \frac{1}{2} - e^{-hp}+e^{-2hp}-e^{-3hp}+\ldots$$

represents the meander-function of fig. 4 †.

* See Heaviside, 'Electromagnetic Theory,' ii. p. 90.
† Heaviside, *loc. cit.* ii. p. 97.

As an instance of (13) we take

$$f(p) = \frac{p}{p^2+1} \doteqdot \sin x = h(x).$$

Applying (13), we find on the one hand

$$\int_p^\infty \frac{f(p)}{p}\,dp = \int_p^\infty \frac{dp}{p^2+1} = \tan^{-1}p\Big|_p = \cot^{-1}p.$$

On the other hand we have

$$\int_0^x \frac{h(x)}{x}\,dx = \int_0^x \frac{\sin x}{x}\,dx = \mathrm{Si}(x),$$

Fig. 3.

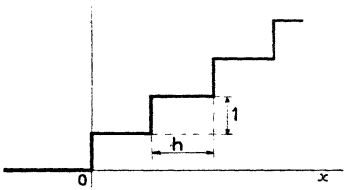

Fig. 4.

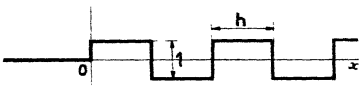

and thus we find, as the operational expression for the integral sine,

$$\cot^{-1}p \doteqdot \mathrm{Si}(x) = \int_0^x \frac{\sin x}{x}\,dx \quad . \quad . \quad . \quad (19)$$

Applying theorem (14) to this result, we find at once

$$\int_0^\infty \frac{\sin x}{x}\,dx = \operatorname*{Lim}_{p\to 0} \cot^{-1}p = \frac{\pi}{2}.$$

Again, let us consider

$$f(p) = \frac{p^2}{p^2+1} \doteqdot \cos x = h(x).$$

The application of (13 *a*) yields, on the one hand,

$$\int_0^p \frac{p\,dp}{p^2+1} = \log\sqrt{p^2+1}.$$

On the other hand, by definition we have

$$\int_x^\infty \frac{\cos x}{x}\,dx = -\mathrm{Ci}(x),$$

and thus we find as the operational expression for the integral cosine

$$\log\frac{1}{\sqrt{1+p^2}} \doteqdot \mathrm{Ci}(x) = \int_\infty^x \frac{\cos x}{x}\,dx \quad . \qquad (20)$$

In the same way we can treat

$$\mathrm{Ei}(x) = \int_\infty^{-x} \frac{e^{-x}}{x}\,dx.$$

For, with (13), (13 *a*), and (14), we find

$$\int_\infty^{-x} \frac{e^{-x}}{x}\,dx = \int_\infty^x \frac{e^{-x}}{x}\,dx + \int_x^0 \frac{e^{-x}}{x}\,dx + \int_0^x \frac{e^{+x}}{x}\,dx$$

$$\doteqdot -\int_0^p \frac{dp}{p+1} - \int_p^\infty \frac{dp}{p+1} + \int_p^\infty \frac{dp}{p-1} = \log\frac{1}{p-1},$$

and thus

$$-\log(p-1) \doteqdot \mathrm{Ei}(x) = \int_\infty^{-x} \frac{e^{-x}}{x}\,dx. \quad . \quad . \quad (21)$$

As another example of the application of (14), we take the Frullani integral *

$$\int_0^\infty \frac{e^{-ax} - b^{-bx}}{x}\,dx.$$

Writing this integral operationally, we obtain

$$\int_0^\infty \left(\frac{1}{p+a} - \frac{1}{p+b}\right)dp = \log\frac{b}{a},$$

and thus we have found operationally

$$\int_0^\infty \frac{e^{-ax} - e^{-bx}}{x}\,dx = \log\frac{b}{a}.$$

Before taking up our main subject, the solution of linear differential equations, attention may first be drawn to the

* Bromwich, 'Infinite Series,' p. 488.

operational representation of $\log x$. Here we first follow Heaviside's example *.

Above we found from (1)

$$\frac{1}{p^n} \doteqdot \frac{x^n}{\Pi(n)}. \quad . \quad . \quad . \quad . \quad . \quad . \quad . \quad (18)$$

Now differentiate both members with respect to n. We thus obtain

$$\frac{1}{p^n}\log\frac{1}{p} \doteqdot \frac{x^n}{\Pi(n)}\{\log x - \psi(n)\}, \quad . \quad . \quad . \quad (18e)$$

where

$$\psi(n) = \frac{d}{dn}\{\log \Pi(n)\}\dagger. \quad . \quad . \quad . \quad . \quad (18f)$$

We therefore have the special cases

$$\left.\begin{aligned}
&\log\frac{1}{p} \doteqdot \log x - \psi(0) = \log x + C,\\
&\frac{1}{p}\log\frac{1}{p} \doteqdot \frac{x}{1!}(\log x + C - 1),\\
&\frac{1}{p^2}\log\frac{1}{p} \doteqdot \frac{x^2}{2!}(\log x + C - 1 - \tfrac{1}{2}),\\
&\quad . \quad . \quad . \quad . \quad . \quad . \quad . \quad . \quad . \quad .\\
&\frac{1}{p^n}\log\frac{1}{p} \doteqdot \frac{x^n}{n!}\left(\log x + C - 1 - \tfrac{1}{2} - \tfrac{1}{3} \ldots - \frac{1}{n}\right),
\end{aligned}\right\} \quad (18g)$$

where $C = 0{\cdot}57722\ldots.$

With the aid of (18g) we can now easily expand, *e.g.*, (20). Thus,

$$\log\frac{1}{\sqrt{1+p^2}} = \log\frac{1}{p} - \frac{1}{2}\log\left(1+\frac{1}{p^2}\right)$$

$$= \log\frac{1}{p} - \frac{1}{2}\left(\frac{1}{p^2} - \frac{1}{2p^4} + \frac{1}{3p^6} - \ldots\right)$$

$$\doteqdot \log x + C - \frac{1}{2}\cdot\frac{x^2}{2!} + \frac{1}{4}\cdot\frac{x^4}{4!} - \frac{1}{6}\cdot\frac{x^6}{6!} + \ldots = \mathrm{Ci}(x).$$

* Heaviside, *loc. cit.* ii. p. 358.

† Here our notation for $\psi(n)$ differs from that of Jahnke-Emde, 'Funktionentafeln,' but agrees with that of Schafheitlin, 'Die Theorie der Besselschen Funktionen' (Teubner, Berlin, 1908). As $\Pi(n)$ coincides with $n!$ for n=integer, we believe that it is advisable to use Π-functions instead of Γ-functions. Thus, instead of defining

$$\psi(n) = \frac{d}{dn}(\log\Gamma(n)),$$

we use the definition (18f).

4. *Linear Differential Equations* : (a) *with Constant Coefficients.*

Suppose the following simple differential equation be given :—

$$\dot{y}+\alpha y=[\cos\omega t],$$

where the sign [ ] bracketing $\cos\omega t$ means that the force as expressed by the right-hand member is zero for $t<0$ and is $\cos\omega t$ for $t>0$. Let the initial condition be $y(0)=0$, from which it follows that $y(0)=\dot{y}(0)=\ddot{y}(0)=\ldots=0$.

To solve our equation operationally we must obtain the expression for

$$f(p)=p\int_0^\infty e^{-pt}y(t)\,dt. \quad . \quad . \quad . \quad . \quad . \quad (3)$$

Hence we proceed as in our former paper*, multiply throughout with e^{-pt}, and integrate between zero and infinity. Integration by parts of the first member yields

$$(p+\alpha)\mathrm{X}(p)=\int_0^\infty e^{-pt}\cos\omega t\,.\,dt=\frac{p}{p^2+\omega^2}, \quad . \quad (22)$$

where $$\mathrm{X}(p)=\int_0 e^{-pt}\,.\,y(t)\,dt.$$

As $$f(p)=p\,.\,\mathrm{X}(p),$$

we can write at once, from (21),

$$f(p)=\frac{p^2}{(p^2+\omega^2)\,.\,(p+\alpha)}\doteqdot y(t). \quad . \quad . \quad . \quad (23)$$

The same result would have been obtained if we had simply replaced $\frac{d}{dt}$ by p and had written the symbolic expression for $\cos\omega t$ for the second member. It may be remarked that the result (23) would also have been obtained if the original differential equation had been symbolically

$$(p^2+\omega^2)\,.f(p)=\frac{p^2}{p+\alpha},$$

or, written in t,

$$\ddot{y}+\omega^2y=\frac{d}{dt}[e^{-\alpha t}].$$

Hence the operational method enables us often easily to write down several differential equations which have the

* Phil. Mag. vii. p. 1153 (1929).

same solution. It also answers the following question: let a right-hand member [1], representing the sudden application of a constant force, be given to the equation

$$\ddot{y}+y=0,$$

what must be done in order to have no transient phenomena? It is easily seen that a second-order impulse, i. e., p^2, must also be impressed on the system; for if

$$(p^2+1)\,.\,f(p)=1+p^2,$$

then $$f(p)=1, \quad \text{or} \quad y(t)=[1].$$

Let us take another example. The solution of

$$\dot{y}+y=0, \quad \text{with} \quad y=y(0) \text{ for } t=0,$$

is easily found to be

$$f(p)=y(0)\,.\,\frac{p}{1+p} \doteq y(0)\,.\,e^{-t}.$$

Now let the equation be multiplied with $(t-a)$, and the solution again be sought for the same initial condition. We have

$$(t-a)(\dot{y}+y)=0, \quad . \quad . \quad . \quad . \quad . \quad (24)$$

or

$$t\dot{y}-a\dot{y}+ty-ay=0. \quad . \quad . \quad . \quad . \quad (24\,a)$$

Again multiply by e^{-pt} and integrate. The first term thus becomes

$$\int_0^\infty e^{-pt}\,.\,t\frac{dy}{dt}\,dt=-\frac{d}{dp}\int_0^\infty e^{-pt}\frac{dy}{dt}dt$$

$$=-\frac{d}{dp}\left\{-y(0)+p\int_0^\infty e^{-pt}\,.\,y(t)\,dt\right\}$$

$$=-\frac{d}{dp}(pX)=-\frac{d}{dp}f(p).$$

A similar reduction of the other terms of $(24\,a)$ yields

$$\frac{df}{dp}+a(f-y(0))+\frac{d}{dp}\left(\frac{f}{p}\right)+a\frac{f}{p}=0,$$

or

$$(p+1)\frac{df}{dp}+\left(ap+1-\frac{1}{p}\right)f=a\,y(0)\,p\,; \quad (24\,a)$$

$$\therefore \quad f(p)=y(0)\frac{p}{p+1}+Ce^{-ap}\,.\,\frac{p}{p+1} \quad . \quad . \quad . \quad (25)$$

The interpretation of the first term is simply

$$y(0) \cdot \frac{p}{p+1} \doteq y(0) \cdot e^{-t},$$

but the second term must be explained with (9) as

$$Ce^{-ap} \cdot \frac{p}{p+1} \doteq \begin{cases} 0 & \text{for } t < a, \\ Ce^{-(t-a)} & \text{for } t > a, \end{cases} \quad \text{or}$$

so that the complete solution is

$$y(t) = \begin{cases} y(0)e^{-t} & \text{for } t < a, \\ y(0)(1+Ce^{a})e^{-t} & \text{for } t > a, \end{cases} \quad \text{or}$$

meaning that in (24), through the multiplication by $t-a$ the initial condition determines the solution up to the time $t=a$. At that moment, however, the multiplier $t-a=0$, and thus leaves the other factor in (24), $\dot{y}+y$, free to take any value ; thus our operational solution shows that at that moment the amplitude may discontinuously be increased by the arbitrary value C, and after that instant the effect of the initial condition is lost. If we had made $a=0$, *i. e.*, if (24) had the multiplier t, instead of $t-a$, the initial conditions would have been lost from the beginning. As the example shows, we could have taken $y(0)=0$ from the start and solved (24 *a*) simply with the second member equal to zero. Later on, in (25), the integration constant C could have been adjusted to the initial conditions, and thus the right solution would have been obtained in a simple way. Obviously the multiplication of the original differential equation by t simply brings in a differentiation $\frac{d}{dp}$ throughout in the operational expression; similarly a factor t^2 causes $\frac{d^2}{dp^2}$, etc. Very often it is, therefore, much simpler to take

$$y(0)=\dot{y}(0)=\ddot{y}(0)=\ldots=0$$

from the beginning.

5. *Linear Differential Equations* : (b) *with Variable Coefficients.*

Our last example brought us already from the domain of equations with constant coefficients to those with variable

coefficients, and to the latter we will now turn our attention. Let us consider the equation for the Bessel functions,

$$\frac{d^2z}{du^2}+\frac{1}{u}\frac{dz}{du}+\left(1-\frac{n^2}{u^2}\right)z=0. \quad . \quad . \quad . \quad (26)$$

Substitute

$$z=u^{-n}y, \quad \text{and} \quad u^2=4x;$$

thus (26) becomes

$$x\frac{d^2y}{dx^2}+(1-n)\frac{dy}{dx}+y=0. \quad . \quad . \quad . \quad . \quad (27)$$

Now multiply (27) again by e^{-px} and integrate between 0 and ∞ in order to find

$$X=\int_0^\infty e^{-px}\,.\,y(x)\,.\,dx,$$

from which

$$f(p)=pX \doteq y(x).$$

As integrations by parts are mostly necessary, we can, beforehand, make a list as follows. Through the integration

$$\left.\begin{array}{lll}
y & \text{becomes} & X, \\
xy & \text{,,} & -\dfrac{dX}{dp}, \\
x^2y & \text{,,} & \dfrac{d^2X}{dp^2}, \\
\cdot\ \cdot\ \cdot\ \cdot\ \cdot\ \cdot\ \cdot\ \cdot\ \cdot & & \\
\dfrac{dy}{dx} & \text{,,} & -y(0)+pX, \\
x\dfrac{dy}{dx} & \text{,,} & -\dfrac{d}{dp}(pX), \\
x^2\dfrac{dy}{dx} & \text{,,} & \dfrac{d^2}{dp^2}(pX), \\
\cdot\ \cdot\ \cdot\ \cdot\ \cdot\ \cdot\ \cdot\ \cdot\ \cdot & & \\
\dfrac{d^2y}{dx^2} & \text{,,} & -y'(0)-py(0)+p^2X, \\
x\dfrac{d^2y}{dx^2} & \text{,,} & y(0)-\dfrac{d}{dp}(p^2X), \\
x^2\dfrac{d^2y}{dx^2} & \text{,,} & \dfrac{d^2}{dp^2}(p^2X), \\
\cdot\ \cdot\ \cdot\ \cdot\ \cdot\ \cdot\ \cdot\ \cdot\ \cdot & &
\end{array}\right\} \quad . \quad . \quad (28)$$

Applying the transformations (28) to (27) we can now at once write down (taking $y(0)=0$)

$$p\cdot\frac{d(pX)}{dp}+\left(n-\frac{1}{p}\right)pX=0,$$

or

$$pX=f(p)=Cp^{-n}\cdot e^{-\frac{1}{p}}.$$

Adjusting C to the ordinary normalization of the Bessel functions, we thus have found

$$x^{\frac{n}{2}}\cdot J_n(2\sqrt{x}) \doteqdot p^{-n}\cdot e^{-\frac{1}{p}}, \quad . \quad . \quad . \quad (29)$$

which is valid for $n>-1$. Thus the development of the second member as a power series in p^{-1} gives us the familiar series for Bessel functions.

Now that the operational representation has been obtained, we can, with the aid of our theorems (5) to (17), write down, almost at a glance, several properties of J_n.

(*a*) Differentiate the left-hand member of (29), *i. e.*, multiply the right-hand member by p. Thus we find

$$\frac{d}{dx}\left(x^{\frac{n}{2}}\cdot J_n(2\sqrt{x})\right) \doteqdot p^{-n+1}\cdot e^{-\frac{1}{p}} \doteqdot x^{\frac{n-1}{2}}\underset{n-1}{J}(2\sqrt{x}),$$

or

$$\frac{n}{x}J_n(x)+J_n'(x)=\underset{n-1}{J}(x), \quad . \quad . \quad . \quad . \quad (30)$$

a familiar relation.

(*b*) Again, multiplication of (29) by p^n yields

$$\frac{d^n}{dx^n}\left(x^{\frac{n}{2}}\cdot J_n(2\sqrt{x})\right) \doteqdot p^n\cdot p^{-n}\cdot e^{-\frac{1}{p}}=e^{-\frac{1}{p}} \doteqdot J_0(2\sqrt{x}),$$

or

$$\left(\frac{d}{x\,dx}\right)^n(x^n\cdot J_n(x))=J_0(x), \quad . \quad . \quad . \quad . \quad (31)$$

which is also a well-known relation. However, operationally it still has a meaning when n is *not* an integer.

(*c*) Now apply (11) in the form

$$-p\frac{df(p)}{dp} \doteqdot x\frac{dh(x)}{dx},$$

which easily gives

$$\frac{n}{x}J_n(x)-J_n'(x)=\underset{n+1}{J}(x), \quad . \quad . \quad . \quad . \quad (32)$$

(*d*) Next apply (12) in the form

$$-p\frac{d}{dp}\left(\frac{f(p)}{p}\right) \doteqdot x\cdot h(x),$$

which yields, after reduction,

$$\underset{n+1}{\mathrm{J}}(x)+\underset{n-1}{\mathrm{J}}(x)=\frac{2n}{x}\cdot \mathrm{J}_n(x). \quad . \quad . \quad . \quad (33)$$

(*e*) If we further apply (9), we obtain

$$e^{-\lambda p}\cdot p^{-n}\cdot e^{-\frac{1}{p}}=(x-\lambda)^{\frac{n}{2}}\cdot \mathrm{J}_n(2\sqrt{x-\lambda}), \quad (x>\lambda),$$

where the development of the first member yields

$$\left(\frac{1}{p^n}-\frac{\lambda}{p^{n-1}}+\frac{\lambda^2}{2!\,p^{n-2}}-\ldots\right)e^{-\frac{1}{p}}.$$

Each term represents a function of the form

$$\frac{\lambda^m}{m!}\cdot x^{\frac{n-m}{2}}\cdot \underset{n-m}{\mathrm{J}}(2\sqrt{x}),$$

and thus, after an obvious transformation, we obtain

$$\sum_{r=0}^{r=\infty}\frac{1}{\Pi(r)}\left(\frac{-a^2}{2x}\right)^r\cdot \underset{n+r}{\mathrm{J}}(x)$$

$$=\left(1-\frac{a^2}{x^2}\right)^{\frac{n}{2}}\cdot \mathrm{J}_n(\sqrt{x^2-a^2}) \qquad (x>a). \quad . \quad (34)$$

(*f*) Next consider

$$e^{-\frac{a}{p}}\cdot p^{-n}\cdot e^{-\frac{1}{p}}=p^{-n}\left(1-\frac{a}{p}+\frac{a^2}{2!\,p^2}-\ldots\right)e^{-\frac{1}{p}}=p^{-n}\cdot e^{-\frac{1+a}{p}},$$

and interpret the series as a series of Bessel functions. This series becomes

$$x^{\frac{n}{2}}\mathrm{J}_n(2\sqrt{x})-ax^{\frac{n+1}{2}}\cdot \underset{n+1}{\mathrm{J}}(2\sqrt{x})+\frac{a^2}{2!}x^{\frac{n+2}{2}}\cdot \underset{n+2}{\mathrm{J}}(2\sqrt{x})-\ldots$$

$$=\frac{1}{(1+a)^n}\{(1+a)\cdot x\}^{\frac{n}{2}}\cdot \mathrm{J}_n(2\sqrt{(1+a)x}),$$

which, with

$$\sqrt{1+a}=y \quad \text{and} \quad 2\sqrt{x}=s,$$

and replacing s again by x, becomes

$$\sum_{r=0}^{r=\infty}\frac{1}{\Pi(r)}\cdot\left\{(1-y^2)\frac{x}{2}\right\}^r\cdot \underset{n+r}{\mathrm{J}}(x)=y^{-n}\mathrm{J}_n(yx), \quad . \quad (35)$$

being the theorem for the multiplication of the argument of a Bessel function.

(*g*) Further, let us apply (14). This theorem gives

$$\int_0^\infty p^{-(n+2)} \cdot e^{-\frac{1}{p}} \cdot dp = \int_0^\infty x^{\frac{n+1}{2}} \cdot \frac{J_{n+1}(2\sqrt{x})}{x}\, dx,$$

or, after the substitution $2\sqrt{x}=s$, and replacing s again by x,

$$\Pi(n) = \frac{1}{2^n}\int_0^\infty x^n \cdot J_{n+1}(x)\, dx \quad (n>-1) \qquad (36)$$

(*h*) Next, with the definition (3), we can at once write down the integral

$$p^{-n} \cdot e^{-\frac{1}{p}} = p\int_0^\infty e^{-px} \cdot x^{\frac{n}{2}} \cdot J_n(2\sqrt{x})\, dx,$$

which, after an obvious transformation, becomes

$$\int_0^\infty e^{-\alpha x} \cdot x^n \cdot J_{n-1}(2\alpha x)\, dx = \frac{1}{2\alpha} \cdot e^{-\alpha} \qquad (\alpha > 0). \qquad (37)$$

(*j*) As

$$e^{\frac{i}{p}} \doteqdot J_0(2\sqrt{-ix}) = \text{ber}\,(2\sqrt{x}) + i\,\text{bei}\,(2\sqrt{x}),$$

and

$$e^{-\frac{i}{p}} \doteqdot J_0(2\sqrt{+ix}) = \text{ber}\,(2\sqrt{x}) - i\,\text{bei}\,(2\sqrt{x}),$$

we obtain at once the operational expressions for Kelvin's "ber" and "bei" functions as

$$\left.\begin{aligned} \text{ber}\,(2\sqrt{x}) &\doteqdot \cos\frac{1}{p}, \\ \text{bei}\,(2\sqrt{x}) &\doteqdot \sin\frac{1}{p}. \end{aligned}\right\} \quad . \quad . \quad . \quad (29\,a)$$

(*k*) Let us finally make use of the very fertile theorem (17) of the "produit de composition." Taking, *e. g.*,

$$f_1(p) = p^{m-n} \doteqdot \frac{x^{n-m}}{\Pi(n-m)}, \qquad (n-m>-1)$$

$$f_2(p) = p^{1-m} \cdot e^{-\frac{1}{p}} \doteqdot x^{\frac{m-1}{2}} \cdot J_{m-1}(2\sqrt{x}), \quad (m>0)$$

we find

$$f_1(p) \cdot f_2(p) \cdot \frac{1}{p} = p^{-n} \cdot e^{-\frac{1}{p}} \doteqdot x^{\frac{n}{2}} \cdot J_n(2\sqrt{x}).$$

The application of (17) thus at once gives

$$\frac{1}{\Pi(n-m)}\int_0^x (x-\xi)^{n-m}\,.\,\xi^{\frac{m-1}{2}}\,.\,\underset{m-1}{\mathrm{J}}(2\sqrt{\xi})\,.\,d\xi = x^{\frac{n}{2}}\,.\,\mathrm{J}_n(2\sqrt{x})$$

or

$$\frac{2^{m-n}}{\Pi(n-m)}\cdot\int_0^x (x^2-\xi^2)^{n-m}\,.\,\xi^m\,.\,\underset{m-1}{\mathrm{J}}(\xi)\,.\,d\xi = x^n\mathrm{J}_n(x) \qquad (38)$$

$$(n-m->1, \quad m>0)$$

Taking in (38),

$$m=\tfrac{1}{2}, \qquad \xi = x\sin\omega,$$

and making use of

$$\xi^{\frac{1}{2}}\mathrm{J}_{-\frac{1}{2}}(\xi) = \sqrt{\frac{2}{\pi}}\cos\xi,$$

(38) becomes

$$\int_0^{\pi/2} (\cos\omega)^{2n}\,.\,\cos(x\sin\omega)\,d\omega = \sqrt{\pi}\,.\,2^{n-1}\,.\,\Pi(n-\tfrac{1}{2})\,.\,x^{-n}\mathrm{J}_n(x)$$

$$(n>-\tfrac{1}{2}),$$

which for $n=0$ gives the familiar integral definition of the zero'th Bessel function

$$\frac{2}{\pi}\int_0^{\pi/2}\cos(x\sin\omega)\,d\omega = \mathrm{J}_0(x). \quad . \quad . \quad . \quad (39)$$

The results (30–39), which could easily be still further extended, were all obtained with the aid of the operational expression for

$$x^{\frac{n}{2}}\mathrm{J}_n(2\sqrt{x}).$$

In order to obtain another operational expression for a Bessel function we return to the differential equation (26). After the substitution $z=u^{-n}y$, and writing x for u, we obtain

$$x\frac{d^2y}{dx^2} + (1-2n)\frac{dy}{dx} + xy = 0. \quad . \quad . \quad . \quad (26\,a)$$

Now we transform (26 a) again operationally by multiplying it with e^{-px} and integrating; this is simplified by the use of table (28). Hence we can write at once

$$(p^2+1)\frac{d\mathrm{X}}{dp} + (2n+1)p\mathrm{X} = 0, \quad . \quad . \quad . \quad (26\,b)$$

where, as explained above, we took $y(0)=0$, and where again

$$\mathrm{X}(p) = \int_0^\infty e^{-px}\,.\,y(x)\,dx.$$

The solution of (26 *b*) is easily found to be

$$f(p)=pX(p)=\frac{Cp}{(p^2+1)^{n+\frac{1}{2}}},$$

and again, after adjustment of the integration constant to the usual normalization of the Bessel function, we find a new operational expression

$$\frac{\Pi(2n)}{2^n\Pi(n)}\cdot\frac{p}{(p^2+1)^{n+\frac{1}{2}}}=\frac{2_n\Pi(n-\frac{1}{2})}{\sqrt{\pi}}\cdot\frac{p}{(p^2+1)^{n+\frac{1}{2}}}\doteqdot x^n\cdot J_n(x), \quad . \quad . \quad . \quad (40)$$

which is valid for $n>-\frac{1}{2}$. As particular instances we note, for $n=0$ and $n=\frac{1}{2}$,

$$\frac{p}{\sqrt{p^2+1}}\doteqdot J_0(x), \quad . \quad . \quad . \quad . \quad . \quad . \quad (41)$$

$$\sqrt{\frac{2}{\pi}}\frac{p}{p^2+1}\doteqdot x^{\frac{1}{2}}\cdot J_{\frac{1}{2}}(x). \quad . \quad . \quad . \quad . \quad . \quad (42)$$

The last relation (42) can be interpreted by (18 *b*), giving the familiar result,

$$x^{\frac{1}{2}}\cdot J_{\frac{1}{2}}(x)=\sqrt{\frac{2}{\pi}}\cdot\sin x. \quad . \quad . \quad . \quad . \quad . \quad (43)$$

Of course (40) can again be developed as a series in p^{-1}, thus yielding the expansion of $J_n(x)$ in a series of positive powers of x. Obviously one could, as in the former case, apply several of the theorems (5)–(17) to (40) again. We will, however, only derive a new relation with the aid of (17), in the following way.

Take

$$f_1(p)=\frac{p}{(p^2+1)^{n+\frac{1}{2}}},$$

$$f_2(p)=\frac{p}{(p^2+1)^{-n+\frac{1}{2}}};$$

then

$$f_1(p)\cdot f_2(p)\cdot\frac{1}{p}=\frac{p}{p^2+1}\doteqdot\sin x.$$

Hence, applying (17), we obtain

$$\frac{2^n\Pi(n)}{\Pi(2n)}\cdot\frac{2^{-n}\Pi(-n)}{\Pi(-2n)}\cdot\int_0^x(x-\xi)^nJ_n(x-\xi)\cdot\xi^{-n}J_{-n}(\xi)\,d\xi=\sin x,$$

which, after simplification and the use of

$$\Pi(n) \cdot \Pi(-n) = \frac{\pi n}{\sin \pi n},$$

becomes

$$\cos n\pi \cdot \int_0^x \left(\frac{x}{\xi} - 1\right)^n \mathrm{J}_n(x-\xi) \cdot \mathrm{J}_{-n}(\xi) \cdot d\xi = \sin x, \quad (44)$$

which is valid for $-\frac{1}{2} < n < +\frac{1}{2}$. Moreover, the expression (40) is well adapted for a derivation (with the aid of (8)) of the asymptotic series for Bessel functions, but we shall not enter into these details.

We now turn our attention to still another symbolic representation of Bessel functions, which will show us the close relation of these functions to spherical harmonics. Consider therefore again the fundamental differential equation (26). This time, however, we write ix instead of x, and $n+\frac{1}{2}$ instead of n:

$$\frac{d^2z}{dx^2} + \frac{1}{x}\frac{dz}{dx} - \left(1 + \frac{(n+\frac{1}{2})^2}{x^2}\right) z = 0.$$

Substitute

$$z = y \cdot \sqrt{x},$$

which gives

$$x^2 \frac{d^2y}{dx^2} + 2x\frac{dy}{dx} - (x^2 + n(n+1))y = 0,$$

We now obtain again, with the aid of table (28), the differential equation for

$$\mathrm{X}(p) = \int_0^\infty e^{-px} y(x)\, dx$$

as

$$(p^2-1)\frac{d^2\mathrm{X}}{dp^2} + 2p\frac{d\mathrm{X}}{dp} - n(n+1)\mathrm{X} = 0,$$

which is the equation of the spherical harmonics.

We thus find, choosing the right harmonic and the right normalization,

$$\sqrt{\frac{2}{\pi}} \cdot p \cdot \mathrm{Q}_n(p) \doteqdot x^{-\frac{1}{2}} \underset{n+\frac{1}{2}}{\mathrm{I}}(x), \quad . \quad . \quad . \quad (45)$$

from which we may conclude at once with (1)

$$\int_0^\infty e^{-px} x^{-\frac{1}{2}} \underset{n+\frac{1}{2}}{\mathrm{I}}(x)\, dx = \sqrt{\frac{2}{\pi}} \cdot \mathrm{Q}_n(p), \quad . \quad (45\,a)$$

where the I-function is as usually defined by:

$$I_m(x) = e^{-\frac{1}{2}m\pi i} J_m(ix) = \sum_{r=0}^{r=\infty} \frac{(\frac{1}{2}x)^{m+2r}}{\Pi(r) \cdot \Pi(m+r)} *.$$

(45) shows the close relation between the Bessel function of imaginary argument and the Legendre functions, the latter being the operational representation of the former. In fact the familiar relations between Legendre functions on the one hand and those between Bessel functions (such as (30), (32), (33)) on the other are easily transformed into each other. *E.g.*:

$$P'_{n+1}(x) - P'_{n-1}(x) = (2n+1) \cdot P_n(x)$$

is transformed, with the aid of theorem (12), into

$$J_{n-1}(x) + J_{n+1}(x) = \frac{2n}{x} \cdot J_n(x),$$

and similarly for the others.

Leaving the spherical harmonics for the present, we now turn our attention to still another operational representation of Bessel functions. We therefore obtain from (26) (taking $u=x$) directly through the usual process the differential equation for

$$X = \int_0^\infty e^{-px} \cdot z(x)\, dx.$$

The result is

$$\frac{d}{dp}\left\{ pX + (p^2+1)\frac{dX}{dp} \right\} - n^2 X = 0,$$

of which the solution is

$$X = \frac{C}{\sqrt{1+p^2}} (\sqrt{1+p^2} - p)^{\pm n}.$$

Choosing the proper solution and the right integration constant, we thus find

$$\frac{p}{\sqrt{1+p^2}} \cdot (\sqrt{1+p^2} - p)^n = \frac{p}{\sqrt{1+p^2}} \cdot e^{-n \sinh^{-1} p} \doteqdot J_n(x), \quad \ldots \quad (46)$$

which expression we will study somewhat closer, as it gives us several properties of the Bessel functions in a very direct way.

* Watson, 'Bessel Functions,' p. 77.

(*a*) Writing $\alpha = \sqrt{1+p^2}-p,$

we have $$\frac{p}{\sqrt{1+p^2}} \cdot \alpha^n \doteq J_n(x).$$

Further

$$\int_0^x J_n(x)\,dx \doteq \frac{\alpha^n}{\sqrt{1+p^2}} = \frac{p}{\sqrt{1+p^2}} \cdot \frac{2\alpha^{n+1}}{1-\alpha^2}$$

$$= \frac{2p}{\sqrt{1+p^2}} \cdot \alpha^{n+1}(1+\alpha^2+\alpha^4+\ldots),$$

and hence

$$\int_0^x J_n(x)\,dx = 2\sum_{r=0}^{r=\infty} J_{n+1+2r}(x). \quad . \quad . \quad . \quad (47)$$

(*b*) Again take the series

$$J_1 - J_3 + J_5 - J_7 + \ldots \doteq \frac{p}{\sqrt{1+p^2}}(\alpha - \alpha^3 + \alpha^5 - \alpha^7 + \ldots)$$

$$= \frac{p}{\sqrt{1+p^2}} \cdot \frac{\alpha}{1+\alpha^2} = \frac{1}{2}\frac{p}{1+p^2} \doteq \frac{1}{2}\sin x. \quad . \quad (48)$$

(*c*) Further, another series,

$$-J_0 + 2(J_0 - J_2 + J_4 - \ldots)$$

$$\doteq \frac{p}{\sqrt{1+p^2}}\{-1 + 2(1-\alpha^2+\alpha^4-\alpha^6\ldots)\}$$

$$= \frac{p}{\sqrt{1+p^2}} \cdot \frac{1-\alpha^2}{1+\alpha^2} = \frac{p^2}{1+p^2} \doteq \cos x. \quad . \quad (49)$$

(*d*) Again, as for integer n

$$J_{-2n}(x) = J_{+2n}(x),$$

we easily find the sum

$$\sum_{n=-\infty}^{n=+\infty} J_n(x) = J_0 + 2J_1 + 2J_2 + 2J_4 + \ldots$$

$$\doteq \frac{p}{\sqrt{1+p^2}}(1 + 2\alpha^2 + 2\alpha^4 + 2\alpha^6 + \ldots)$$

$$= \frac{p}{\sqrt{1+p^2}}\frac{1+\alpha^2}{1-\alpha^2} = \frac{p}{\sqrt{1+p^2}} \cdot \frac{\sqrt{1+p^2}}{p} \doteq 1, \quad (50)$$

as a matter of algebra.

(*e*) Next apply theorem (13) to (46). It follows that

$$\int_p^\infty \frac{\alpha^n}{\sqrt{1+p^2}}\,dp \doteq \int_0^x \frac{J_n(x)}{x}\,dx \qquad (n>0).$$

The left-hand member equals

$$-\frac{1}{n}\Big[\alpha^n\Big]_p = \frac{\alpha^n}{n} \qquad (n>0),$$

and we thus find the meaning of α^n as

$$\alpha^n = (\sqrt{1+p^2}-p)^n \doteq n\int_0^x \frac{J_n(x)}{x}\,dx \quad (n>0), \qquad (51)$$

and further,

$$p\alpha^n = p(\sqrt{1+p^2}-p)^n \doteq \frac{n J_n(x)}{x} \qquad (n>0). \quad (51\,a)$$

(*f*) Further, consider (46) in connexion with (17). Let us take as

$$f_1(p) = \frac{p}{\sqrt{1+p^2}}\cdot\alpha^n \doteq J_n(x),$$

$$f_2(p) = \frac{p}{\sqrt{1+p^2}}\cdot\alpha^{-n} \doteq J_{-n}(x).$$

Hence

$$f_1(p)\cdot f_2(p)\cdot\frac{1}{p} = \frac{p}{1+p^2} \doteq \sin x,$$

and thus we can write down at once the interesting result:

$$\int_0^x J_n(\xi)\cdot J^{-n}(x-\xi)\,d\xi = \sin x, \quad (-1<n<+1). \quad (52)$$

More generally we also have

$$\frac{p}{\sqrt{1+p^2}}\alpha^n\cdot\frac{p}{\sqrt{1+p^2}}\alpha^m\cdot\frac{1}{p} = \frac{p}{1+p^2}p^{n+m}\cdot\frac{1}{p},$$

which, interpreted with the aid of (51*a*), gives us the relation

$$\frac{1}{n+m}\int_0^x J_n(\xi)\cdot J_m(x-\xi)\cdot d\xi = \int_0^x \frac{\sin(x-\xi)}{\xi}\cdot J_{n+m}(\xi)\cdot d\xi$$
$$(n>-1, \quad m>-1, \quad n+m>0). \quad (53)$$

(*g*) Let us further inquire as to the meaning of $h(x)$, where

$$f(p) = \log\frac{1}{\alpha} = \sinh^{-1}p = \log(p+\sqrt{p^2+1}) \doteq h(x).$$

To this end we start again with

$$\frac{p}{\sqrt{1+p^2}} \doteq J_0(x).$$

Next apply (13 *a*), giving us

$$\int_0^p \frac{dp}{\sqrt{1+p^2}} \doteq \int_x^\infty \frac{J_0(x)}{x}\,dx,$$

or
$$\sinh^{-1} p = \log\,(p+\sqrt{p^2+1}) = -\mathrm{Ji}(x), \quad . \quad (54)$$

where, analogous to

$$\mathrm{Ci}(x) = \int_\infty^x \frac{\cos x}{x}\,dx,$$

we define
$$\mathrm{Ji}(x) = \int_\infty^x \frac{J_0(x)}{x}\,dx, \quad . \quad . \quad . \quad . \quad (55)$$

which function could be called integral Bessel function.

This function, which does not seem to have been much studied, will appear again later on.

(*h*) Finally, the application of (17) directly gives us some new and interesting relations, for we can write (46) as

$$\frac{p}{\sqrt{1+p^2}}\alpha^n . p\alpha^m . \frac{1}{p} \doteq J_{n+m}(x),$$

and thus we find, with the aid of (51 *a*), at once

$$m\int_0^x \frac{J_m(\xi)}{\xi} . J_n(x-\xi)\,d\xi = J_{n+m}(x) \quad (m>0, \quad n>-1). \quad (55\,a)$$

A further interesting Frullani integral involving $J_0(x)$, and closely related to our Ji function, can also be easily evaluated by the operator method. Let it be required to find

$$\int_0^\infty \frac{J_0(x)-\cos x}{x}\,dx = \mathrm{Y}.$$

Here the application of our theorem (14) gives us at once the required result, for

$$\mathrm{Y} = \int_0^\infty \left(\frac{1}{\sqrt{p^2+1}} - \frac{p}{p^2+1}\right) dp = \log\left(\frac{p+\sqrt{p^2+1}}{\sqrt{p^2+1}}\right)\Big|_0^\infty = \log 2,$$

and hence

$$\int_0^x \frac{J_0(x)-\cos x}{x}\,dx = \log 2. \quad . \quad . \quad . \quad (53\,a)$$

6. *The Derivation of* $J_n(x)$ *with respect to* n.

In § 5 we obtained, among others, three operational representations of Bessel functions:

$$x^{\frac{n}{2}} . J_n(2\sqrt{x}) \doteqdot \frac{1}{p^n} . e^{-\frac{1}{p}}, \qquad (n>-1) . \quad . \quad . \quad (29)$$

$$x_n . J_n(x) \doteqdot \frac{2^n . \Pi(n-\frac{1}{2})}{\sqrt{\pi}} \cdot \frac{p}{(p^2+1)^{n+\frac{1}{2}}}, \quad (n>-\tfrac{1}{2}). \quad (40)$$

$$J_n(x) \doteqdot \frac{p}{\sqrt{1+p^2}} . e^{-n \sinh^{-1} p}, \qquad (n>-1). \quad . \quad (46)$$

In order to obtain new expressions for $\frac{\partial J_n(x)}{\partial n}$, we differentiate all three expressions with respect to n. We thus obtain, respectively,

$$x^{\frac{n}{2}} \left\{ \frac{1}{2} \log x . J_n(2\sqrt{x}) + \frac{\partial J_n(2\sqrt{x})}{\partial n} \right\} \doteqdot - \log p . p^{-n} . e^{-\frac{1}{p}} .$$

. . . (56)

$$x^n \left\{ \log x . J_n(x) + \frac{\partial J_n(x)}{\partial n} \right\} \doteqdot$$

$$\frac{2^n \Pi(n-\frac{1}{2})}{\sqrt{\pi}} \cdot \frac{p}{(p^2+1)^{n+\frac{1}{2}}} \{\log 2 + \psi(n-\tfrac{1}{2}) - \log(p^2+1)\}$$

. . (57)

$$\frac{\partial J_n(x)}{\partial n} \doteqdot - \sinh^{-1} p . \frac{p}{\sqrt{1+p^2}} . e^{-n \sinh^{-1} p} . \quad . \quad (58)$$

Now above we found already the three functions in (56), (57), and (58), namely,

$$-\log p \doteqdot \log x + C \quad . \quad . \quad . \quad (18\,g)$$

$$-\log \sqrt{1+p^2} \doteqdot \mathrm{Ci}(x), \quad . \quad . \quad . \quad . \quad . \quad (20)$$

$$-\sinh^{-1} p \doteqdot \mathrm{Ji}(x), \quad . \quad . \quad . \quad . \quad . \quad (55)$$

and therefore we are prepared to write the right-hand members of (56), (57), and (58) with theorem (17) as "produits de composition." The three equations thus yield, after some slight transformations, the following interesting relations:

$$\frac{\partial J_n(x)}{\partial n} = \log \frac{\gamma x}{2} . J_n(x) + \int_0^x \log\left(1 - \frac{\xi^2}{x^2}\right) . \left(\frac{\xi}{x}\right)^n J_{n-1}(\xi)\, d\xi,$$

$$(n>-1) \quad . \quad (59)$$

$$\frac{\partial J_n(x)}{\partial n} = \left\{ \psi(n-\tfrac{1}{2}) - \log\frac{x}{2} \right\} \cdot J_n(x) + 2\int_0^x \mathrm{Ci}(x-\xi) \cdot \left(\frac{\xi}{x}\right)^n \cdot J_{n-1}(\xi)\, d\xi, \qquad (n > -\tfrac{1}{2}) \cdot \quad (60)$$

$$\frac{\partial J_n(x)}{\partial n} = \int_0^x \mathrm{Ji}(x-\xi) \cdot J_n'(\xi) \cdot d\xi, \qquad (n>0). \quad . \quad . \quad (61)$$

All three relations are, as far as I know, new, and the ease with which they can be derived with the aid of the operators is remarkable.

7. *Legendre, Laguerre, and Hermite Polynomials.*

The familiar differential equation for the Legendre polynomials is

$$(1-x^2)\frac{d^2y}{dx^2} - 2x\frac{dy}{dx} + n(n+1)y = 0.$$

Substitution of

$$x = s+1$$

yields

$$(s^2+2s)\frac{d^2y}{ds^2} + 2(s+1)\frac{dy}{ds} - n(n+1)y = 0. \quad . \quad (62)$$

Applying the operational transformation on (62) gives us, with the aid of (28),

$$\frac{d^2f}{dp^2} - 2\frac{df}{dp} - \frac{n(n+1)}{p^2}f = 0,$$

where

$$f(p) \doteqdot y(s),$$

or, with the proper normalization, and for integral values of n, we obtain

$$\left.\begin{aligned} P_n(x+1) &\doteqdot (-1)^n \left[\sqrt{\frac{\pi p}{2}} \cdot e^p \, I_{-(n+\frac{1}{2})}(p) \right] \\ &= p^{n+1} \cdot e^p \left(-\frac{1}{p}\frac{d}{dp} \right)^n \left(\frac{e^{-p}}{p} \right) \end{aligned}\right\} \cdot \quad . \quad (63)$$

Hence the operational representation of a Legendre polynomial is given by a Bessel function, in the same way as we found before that the operational representation of a Bessel function was given by a Legendre polynomial (see (45)). Obviously this symmetry is no accident and we will return to it later on. It is interesting to consider (63) in

relation to what has been found before in § 3 in connexion with the operational meaning of $e^{-\lambda p}$. Hence, if we multiply (63) by e^{-p}, we obtain

$$P_n(x) \doteq (-1)^n \left[\sqrt{\frac{\pi p}{2}} \cdot \underset{-(n+\frac{1}{2})}{I}(p)\right] = \left[p^{n+1}\left(-\frac{1}{p}\frac{d}{dp}\right)^n \frac{e^{-p}}{p}\right], \quad . \quad . \quad . \quad . \quad (63\,a)$$

where, as before, by the brackets [ ] is meant the omission of all positive powers of p (the zero'th power excluded).

With the aid of (3) we therefore obtain the interesting integral

$$p\int_0^\infty e^{-px} P_n(x)\,dx = (-1)^n \sqrt{\frac{\pi}{2}}\,[p^{+\frac{1}{2}} \underset{-(n+\frac{1}{2})}{I}(p)], \quad . \quad (64)$$

where in the result the negative powers of p (zero'th power included) are to be retained only.

From (9) and (63) one can also find

$$\int_1^\infty P_n(x) e^{-px}\,dx = p^n\left(-\frac{1}{p}\frac{d}{dp}\right)^n\left(\frac{e^{-p}}{p}\right).$$

We now return to another consideration of the Legendre functions. If we change the independent variable of θ, where

$$x = \cos\theta,$$

we obtain for the differential equation for $P_n(\cos\theta)$, which for short we write $P_n(\theta)$,

$$\sin\theta \cdot \frac{d^2P}{d\theta^2} + \cos\theta \cdot \frac{dP}{d\theta} + n(n+1)\sin\theta \cdot P = 0.$$

A further substitution of

$$\lambda = i\theta$$

yields

$$e^{+\lambda}\left(-\frac{d^2P}{d\lambda^2} - \frac{dP}{d\lambda} + n(n+1)P\right) + e^{-\lambda}\left(\frac{d^2P}{d\lambda^2} - \frac{dP}{d\lambda} - n(n+1)P\right) = 0. \quad . \quad (65)$$

In this case, where the coefficients contain exponentials, the usual transformation leads to a difference equation instead of a differential equation. In fact, we obtain

$$(p+n)(p-n-1)X_n(p-1) = (p-n)(p+n+1)X_n(p+1). \quad (66)$$

where, as before,

$$X_n(p) = \int_0^\infty e^{-p\lambda} \cdot P_n(\lambda)\,d\lambda.$$

From (66) the following solution follows at once

$$\underset{n-1}{\mathrm{X}}(p) \cdot \mathrm{X}_n(p) = \frac{-1}{n^2-p^2}, \quad . \quad . \quad . \quad . \quad (67)$$

and when we now return to the variable θ again, and therefore let p relate to θ, instead of to λ, (67) becomes

$$\underset{n-1}{\mathrm{X}}(p) \cdot \mathrm{X}_n(p) = \frac{1}{p^2+n^2}. \quad . \quad . \quad . \quad . \quad (68)$$

Now, writing

$$p\mathrm{X}_n(p) = \mathrm{Y}_n(p),$$

where, therefore,

$$\mathrm{Y}_n(p) \doteqdot \mathrm{P}_n(\theta),$$

(68) becomes

$$\underset{n-1}{\mathrm{Y}}(p) \cdot \mathrm{Y}_n(p) \cdot \frac{1}{p} = \frac{1}{n} \cdot \frac{pn}{p^2+n^2},$$

which expression can be regarded as a "produit de composition." Hence the application of (17) gives us immediately the interesting and apparently new relation

$$\int_0^\theta \underset{n-1}{\mathrm{P}}(\phi) \cdot \mathrm{P}_n(\theta-\phi)\, d\phi = \frac{\sin n\theta}{n} \quad (n=\text{integer}). \quad (70)$$

The directness with which this result is obtained with the use of the operator is again striking.

Returning to (69), and taking the integration constant of the difference equation (66) or (69), such that

$$\mathrm{P}_0(\theta) = 1,$$

we obtain as the operational expressions for the Legendre functions

$$\left.\begin{aligned}
&\mathrm{P}_0(\theta) \doteqdot 1, \\
&\mathrm{P}_1(\theta) \doteqdot \frac{p^2+0^2}{p^2+1^2} \\
&\mathrm{P}_2(\theta) \doteqdot \frac{p^2+1^2}{p^2+2^2}, \\
&\mathrm{P}_3(\theta) \doteqdot \frac{(p^2+0^2)(p^2+2^2)}{(p^2+1^2)(p^2+3^2)}, \\
&\mathrm{P}_4(\theta) \doteqdot \frac{(p^2+1^2)(p^2+3^2)}{(p^2+2^2)(p^2+4^2)}, \\
&\mathrm{P}_5(\theta) \doteqdot \frac{(p^2+0^2)(p^2+2^2)(p^2+4^2)}{(p^2+1^2)(p^2+3^2)(p^2+5^2)}, \\
&\quad . \quad . \quad . \quad . \quad . \quad . \quad . \quad . \quad . \quad . \quad .
\end{aligned}\right\} \quad . \quad . \quad (71)$$

Letting finally, in (69), $n \to \infty$, this expression becomes

$$\lim_{n\to\infty} Y_n^2(p) = \frac{p^2}{p^2+n^2},$$

or

$$\lim_{n\to\infty} Y_n(p) = \frac{p}{\sqrt{p^2+n^2}},$$

which second member, as we found before (see (41)), represents $J_0(n\theta)$, and hence we found

$$\lim_{n\to\infty} P_n\left(\cos\frac{\theta}{n}\right) = J_0(\theta). \quad . \quad . \quad . \quad . \quad (72)$$

Finally, we consider the differential equation for the Laguerre polynomials L_n:

$$x\frac{d^2L_n}{dx^2} + (1-x)\frac{dL_n}{dx} + nL_n = 0. \quad . \quad . \quad . \quad (73)$$

It transforms into

$$(1-p)\frac{d}{dp} + \frac{n}{p}f = 0,$$

where

$$f(p) \doteq L_n(x).$$

Hence, with the proper normalization, we find

$$L_n(x) \doteq n!\left(1-\frac{1}{p}\right)^n \quad (n=\text{integer}). \quad (74)$$

Similarly we obtain from its differential equation, as the operational expression for the Hermite's polynomials He_n

$$He_n\left(\frac{x}{2}\right) \doteq n!\left[\frac{e^{-p^2}}{p^n}\right] \quad (n=\text{integer}), \quad (75)$$

where [ ] means the retention of negative powers of p only.

It is, further, a quite simple matter to obtain from (74) and (75) the properties of the Laguèrre's and Hermite's polynomials.

8. *Final Considerations.*

From the many examples discussed above of the operational transformation of a differential equation for $y(x)$ into another differential equation for $f(p)$, where $f(p) \doteq y(x)$, and also from a general consideration of the method, it follows that there exists a close analogy between the well-known Laplacian transformation and the transformation discussed above.

In a Laplacian transformation we express as an exponential integral :

$$y(x)=\int_a^b e^{qx}.\phi(q)\,dq, \quad . \quad . \quad . \quad . \quad . \quad (76)$$

while in our case we calculated

$$X(p)=\frac{1}{p}f(p)=\int_0^\infty e^{-px}y(x)\,dx. \quad . \quad . \quad . \quad (77)$$

As was pointed out in connexion with (3) and (4), with a suitable choice of the limits a and b in (76), or with a suitable choice of the path of integration in the complex plane,

$$\phi(s)=f(s), \quad . \quad . \quad . \quad . \quad . \quad . \quad (78)$$

or, in other words, the solution of a Laplace integral, considered as an integral equation, is again a Laplace integral. Hence many of the operational expressions $f(p)$ for functions $y(x)$ obtained above have exactly the same form as the integrand of the Laplace integral expression for $y(x)$. In fact (76), (77), and (78) can probably be considered to constitute a Fourier integral identity.

A very interesting list of Fourier integrals, published recently by G. A. Campbell * can therefore be considered also to be a list of operational representations of the functions examined.

The ultimate identity between the operational solution of a differential equation and the solution in the form of a Laplace integral clearly shows when the operational treatment of a problem has advantages over the normal analytical treatment. When, *e. g.*, functions such as Bessel functions occur, an operational treatment clearly is much simpler and very often much more direct than the normal way.

The above examples, which could easily be considerably extended, where many properties, known and new ones, *e. g.* of Bessel functions, could be derived in a most simple and direct way, were, in fact, intended to prove this statement. If, on the other hand, a physical problem would lead, say, to the function $y(x)$, where

$$y(x)=x^{-n}.e^{-x},$$

the operational method would lead to a Bessel function because this last expression is itself the operational representation of a Bessel function. In such a case the operational method would have no advantages. Hence the

* The Bell System Technical Journal, vii. p. 639 (1928).

operational way of solving physical or technical problems shows its full advantages in those problems where complicated functions occur which cannot be expressed directly by more elementary functions. It often happens that the operational representation of those complicated functions is given by rather elementary functions, as was demonstrated in many of the above examples, and in those cases the directness and simplicity with which the properties of those complicated functions can be studied is most remarkable.

Finally we wish to remark that several formulæ derived above are also valid outside the range mentioned. In fact, negative powers of x (except negative integral powers) can be represented operationally by positive powers of p (except positive integral powers). However, under these circumstances difficulty arises from the integral definition in § 3 of the Π functions. In this case the $\Pi(n)$ functions have to be extended into the domain $n<-1$ (*e. g.*, by means of the Gauss limit of an infinite product).

In conclusion we wish to express our great indebtness in preparing this paper to the writings of Heaviside, especially volume ii. of his 'Electromagnetic Theory,' and to the late Dr. Bromwich of Cambridge and Dr. Le Corbeiller of Paris, and Professor Elias of Delft University, with whom I had the opportunity to discuss several of the questions treated in this paper. My thanks are also due to Dr. K. F. Niessen (of this Laboratory) for verifying most of the formulæ.

List of some Operational Representations derived above and of some other Results obtained.

$$p[1] \doteqdot \delta(x) \quad \text{(Heaviside's "impulsive" function } p[1] = \text{Dirac's } \delta(x)\text{)}.$$

$$\frac{1}{2}\left(1+\coth\frac{hp}{2}\right) \doteqdot \text{"staircase" function of fig. 3.}$$

$$\frac{1}{2}\tanh\frac{hp}{2} \doteqdot \text{"meander" function of fig. 4.}$$

$$\cot^{-1}p \doteqdot \mathrm{Si}(x) \text{ (integral sine).} \quad . \quad . \quad (19)$$

$$-\log\sqrt{1+p^2} \doteqdot \mathrm{Ci}(x) \text{ (integral cosine).} \quad . \quad (20)$$

$$-\log(p-1) \doteqdot \mathrm{Ei}(x). \quad . \quad . \quad . \quad . \quad . \quad . \quad . \quad (21)$$

$$\frac{1}{p^n}\log\frac{1}{p} \doteqdot \frac{x^n}{\Pi(n)}\{\log x - \psi(n)\} \quad . \quad . \quad . \quad (18e)$$

$$\psi(n) = \frac{d}{dn}(\log\Pi(n)) \quad . \quad (18f)$$

$$\frac{1}{p^n}e^{-\frac{1}{p}} \doteqdot x^{\frac{n}{2}} \cdot \mathrm{J}_n(2\sqrt{x}). \quad (n>-1) \quad (29)$$

$$\left.\begin{aligned}\cos\frac{1}{p} &\doteqdot \mathrm{ber}\,(2\sqrt{x})\\ \sin\frac{1}{p} &\doteqdot \mathrm{bei}\,(2\sqrt{x})\end{aligned}\right\} \text{Kelvin's "ber" and "bei" functions.} \quad (29a)$$

$$\frac{2^n}{\sqrt{\pi}}\Pi(n-\tfrac{1}{2})\cdot\frac{p}{(p^2+1)^{n+\frac{1}{2}}} \doteqdot x^n \cdot \mathrm{J}_n(x). \quad (40)$$

$$\sqrt{\frac{2}{\pi}}\cdot p \cdot \mathrm{Q}_n(p) \doteqdot x^{-\frac{1}{2}}\,\mathrm{I}_{n+\frac{1}{2}}(x). \quad (45)$$

$$\frac{p}{\sqrt{1+p^2}}\cdot e^{-n\sinh^{-1}p} \doteqdot \mathrm{J}_n(x). \quad (46)$$

$$p\cdot e^{-n\sinh^{-1}p} \doteqdot \frac{n}{x}\cdot \mathrm{J}_n(x) \quad (n>0). \quad (51a)$$

$$-\sinh^{-1}p \doteqdot \mathrm{Ji}(x) = \int_{\infty}^{x}\frac{\mathrm{J}_0(x)}{x}\,dx \text{ (integral Bessel function).} \quad (54)$$

$$(-1)^n\left[\sqrt{\frac{\pi p}{2}}\cdot \mathrm{I}_{-(n+\frac{1}{2})}(p)\right] \doteqdot \mathrm{P}_n(x) \ (n=\text{integer}). \quad (63a)$$

$$n!\left(1-\frac{1}{p}\right)^n \doteqdot \mathrm{L}\,(x) \text{ (Laguerre's polynomials).} \quad (74)$$

$$n!\left[\frac{1}{p^n}e^{-p^2}\right] \doteqdot \mathrm{He}_n\left(\frac{x}{2}\right) \text{ (Hermite's polynomials).} \quad (75)$$

$$\sum_{r=0}^{r=\infty}\frac{1}{\Pi(r)}\left(\frac{-a^2}{2x}\right)^r\cdot \mathrm{J}_{n-r}(x) = \left(1-\frac{a^2}{x^2}\right)^{\frac{n}{2}}\cdot \mathrm{J}_n(\sqrt{x^2-a^2}) \quad (x>a). \quad (34)$$

$$\sum_{r=0}^{r=\infty}\frac{1}{\Pi(r)}\left\{(1-y^2)\frac{x}{2}\right\}^r\cdot \mathrm{J}_{n+r}(x) = y^{-n}\cdot \mathrm{J}_n(yx) \quad (35)$$

$$\int_0^{\infty} e^{-\alpha x^2}\cdot x^m\cdot \mathrm{J}_{n-1}(2\alpha x)\,dx = \frac{1}{2\alpha}\cdot e^{-\alpha} \quad (\alpha>0). \quad (37)$$

$$\frac{2^{m-n}}{\Pi(n-m)}\cdot\int_0^x (x^2-\xi^2)^{n-m}\cdot\xi^m\cdot \mathrm{J}_{m-1}(\xi)\,d\xi = x^n\cdot \mathrm{J}_n(x) \quad (n-m>-1,\quad m>0). \quad (38)$$

$$\cos n\pi \int_0^x \left(\frac{x}{\xi}-1\right)^n . J_n(x-\xi) . J_{-n}(\xi)\, d\xi = \sin x \qquad (-\tfrac{1}{2} < n < +\tfrac{1}{2}). \quad (44)$$

$$\int_0^x J_n(\xi) . J_{-n}(x-\xi)\, d\xi = \sin x \qquad (-1 < n < +1). \quad (52)$$

$$m \int_0^x \frac{J_m(\xi)}{\xi} . J_n(x-\xi)\, d\xi = J_{n+m}(x) \qquad (m>0). \quad (55\,a)$$

$$\int_0^\infty \frac{J_0(x)-\cos x}{x}\, dx = \log 2. \quad . \quad . \quad . \quad . \quad . \quad (53\,a)$$

$$\frac{\partial J_n(x)}{\partial n} = \log\frac{\gamma x}{2} . J_n(x) + \int_0^x \log\left(1-\frac{\xi^2}{x^2}\right) . \left(\frac{\xi}{x}\right)^n J_{n-1}(\xi)\, d\xi. \qquad (n>-1). \quad (59)$$

$$\frac{\partial J_n(x)}{\partial n} = \left\{ \psi(n-\tfrac{1}{2}) - \log\frac{x}{2} \right\} . J_n(x) + 2\int_0^x \mathrm{Ci}(x-\xi) . \left(\frac{\xi}{x}\right)^n J_{n-1}(\xi)\, d\xi. \quad (60)$$

$$\frac{\partial J_n(x)}{\partial n} = \int_0^x \mathrm{Ji}(x-\xi) . J_n'(\xi) . d\xi. \quad . \quad . \quad . \quad . \quad . \quad . \quad (61)$$

$$\int_0^\infty e^{-sx} . P_n(x)\, dx = (-1)^n \sqrt{\frac{\pi}{2}} . \left[\frac{1}{\sqrt{s}} I_{-(n+\frac{1}{2})}(s)\right] . \qquad (n = \text{integer.}) \quad (64)$$

$$\int_0^\theta P_{n-1}(\cos\phi) . P_n(\cos(\theta-\phi))\, d\phi = \frac{\sin n\theta}{n} \quad . \quad . \quad . \qquad (n = \text{integer.}) \quad (70)$$

$$\lim_{n\to\infty} P_n\left(\cos\frac{\theta}{n}\right) = J_0(\theta) \quad . \quad . \quad . \quad (72)$$

Summary.

§ 1 considers the earlier work on operators by Riemann, Heaviside, Pincherle, Carson, Lévy, and Bromwich. Bromwich's complex integral gives the solution of Carson's integral considered as an integral equation.

In § 2 some general theorems in connexion with the operational method, and formulated by Carson, are considered, and some new theorems are added. Heaviside's "impulsive" function p[1] is shown to be identical with Dirac's $\delta(x)$

function. The very fertile theorem (17) is considered as a "produit de composition" as defined by Volterra, and used by Borel in his "sommation exponentielle" of divergent series. It was known in physics as the Hopkinson–Boltzmann superposition principle for linear systems.

In § 3 some of the general operational theorems are considered in more detail, especially the meaning of $e^{-\lambda p}.f(p)$ by itself, and further, the meaning of the same expression after omission in its series development of all positive powers of p. The results are illustrated by figs. 1 and 2. Further, the "staircase" function of fig. 3 and the "meander" function of fig. 4 are found to be expressible in a very simple way with the aid of operators. Further, with the aid of the above theorems symbolic expressions are derived for $\mathrm{Si}(x)$, $\mathrm{Ci}(x)$, $\mathrm{Ei}(x)$, and $x^n \log x$.

§ 4 considers some examples of the solution of differential equations with constant coefficients, and a simple operational method is considered for finding the conditions for the elimination of transients in switching operations. It is further shown how the factor $(t-a)$ in $(t-a)(\dot{y}+y)=0$ fully destroys the effect of the initial condition after the instant $t=a$, thus leading up to

§ 5, where linear differential equations with variable coefficients are discussed. Starting from the differential equation for Bessel functions, the operational representation

$$p^{-n}.e^{-\frac{1}{p}} \doteqdot x^{\frac{n}{2}} \mathrm{J}_n(2\sqrt{x})$$

is derived. Several of the familiar relations existing between Bessel functions can at once be derived from (29). Similarly, the multiplication theorem of the argument of a Bessel function (35) can easily be found. Further, the operational relations

$$\mathrm{ber}\,(2\sqrt{x}) \doteqdot \cos\frac{1}{p} \quad \text{and} \quad \mathrm{bei}\,(2\sqrt{x}) \doteqdot \sin\frac{1}{p} \quad (29\,a),$$

are obtained, while the application of theorem (17) yields in a straightforward way the solution of some fairly complicated integrals involving Bessel functions. Next, another operational expression for $x^n \mathrm{J}_n(x)$ (40), is derived from the differential equation, which enables us to obtain several other interesting integrals containing a Bessel function. Further, a new operational representation,

$$x^{-\frac{1}{2}}\,\mathrm{I}_{n+\frac{1}{2}}(x) \doteqdot \sqrt{\frac{2}{\pi}}.p.\mathrm{Q}_n(p) \quad (45),$$

involving spherical harmonics is obtained, from which the analogy of the relations existing between the spherical harmonics are shown to be at once derivable from similar relations existing between Bessel functions. A further operational representation,

$$p(1+p^2)^{-\frac{1}{2}}(\sqrt{1+p^2}-p)^n \doteqdot J_n(x)$$

is found to lead easily to the derivation of several series and integrals involving Bessel functions.

Special attention is given to the function

$$\mathrm{Ji}(x)=\int_{\infty}^{x}\frac{J_0(x)}{x}\,dx,$$

which is formed in a similar way to $\mathrm{Ci}(x)$, and which plays an important part in an integral expressing $\frac{\partial J_n(x)}{\partial n}$. Next some Frullani integrals are shown to be easily solved with the aid of operators.

§ 6 discusses three new integral expressions for the derivation of a Bessel function $J_n(x)$ with respect to its order n. These three integrals contain log, Ci, and Ji functions respectively.

In § 7 operational expressions for Legendre, Laguerre, and Hermite's polynomials are obtained. Legendre polynomials, considered as a function of θ, lead to a difference equation for its operational representative, from which an interesting and apparently new integral relation (70) containing Legendre polynomials can at once be derived. Similarly, the asymptotic behaviour of P_n as a Bessel function when $n\to\infty$ is easily demonstrated.

§ 8 contains some general considerations on operators. It is shown that the operational representation of a function is closely related to its representation as a Laplace integral. It is further pointed out when in physical problems the operational solution is to be preferred to the ordinary solution. In those cases, which are many indeed, the operational solution leads to the desired result in a most remarkable and direct way.

At the end of the paper a number of operational expressions derived are summarized, together with some of the integral relations obtained.

Natuurkundig Laboratorium der
N. V. Philips's Gloeilampenfabrieken,
Eindhoven, July 1929.

XCVI. *On the Damping of a Pendulum by Viscous Media.* *By* F. E. Hoare, *B.Sc., A.R.C.S.**

Introduction.

THE following experiments were undertaken in an attempt to develop an alternative method for the measurement of viscosity. The torsional oscillation developed by O. Meyer, in which a horizontal disk, supported by a suspension wire, performs oscillations in its own plane, is well known, and although the theory is not above suspicion, the usual formula gives results for the viscosities of liquids which are in fair agreement with those obtained by other methods. The theory of this method was first developed by Stokes †, and in the same paper he gives the theory of a simple pendulum performing oscillations in a viscous medium.

The equation of motion of a pendulum consisting of a sphere attached to a fine wire and performing oscillations in a vertical plane, the sphere being immersed in a viscous medium of density ρ and coefficient of viscosity η, can be written according to the classical theory ‡,

$$M\frac{d^2x}{dt^2} = -(M-M')\frac{g}{l}.x.$$

$$-M'\left(\frac{1}{2}+\frac{9}{4\beta r}\right)\frac{d^2x}{dt^2}-\frac{9}{4}M'\sigma\left(\frac{1}{\beta r}+\frac{1}{\beta^2r^2}\right)\frac{dx}{dt}, \quad (1)$$

where

x = displacement at time t,

$\beta = \sqrt{\frac{\pi\rho}{\eta T}}$,

$\sigma = \frac{2\pi}{T}$,

r = radius sphere,

T = periodic time,

M = mass of sphere,

M′ = mass of fluid displaced,

l = length of pendulum,

g = acceleration due to gravity.

* Communicated by Prof. F. H. Newman, D.Sc.

† Stokes, Camb. Phil. Soc. ix. p. 8.

‡ Lamb, 'Hydrodynamics,' p. 635.

This equation is formulated without taking into account either the resistance experienced by the wire, which will in general be small compared with that experienced by the sphere, or the finite arc of swing of the pendulum. Thus the equation will apply accurately only to infinitesimally small oscillations.

The solution of equation (1) may be written

$$x = e^{-\frac{M'9\pi k'}{4T(M+kM')}\cdot t} X \cdot \cos(\theta - \gamma), \quad . \quad . \quad . \quad (2)$$

where X and γ are constants dependent upon the initial conditions, and

$$k = \left(\frac{1}{2} + \frac{9}{4\beta r}\right),$$

$$k' = \left(\frac{1}{\beta r} + \frac{1}{\beta^2 r^2}\right),$$

$$\theta = t \cdot \sqrt{\frac{(M-M')g}{(M+kM')l} - \frac{1}{4}\left\{\frac{M'\frac{9}{2}\frac{\pi}{T}k'}{M+kM'}\right\}^2}.$$

The second term under the root sign in the expression for θ is small and can be neglected in comparison with the first term. Hence the time of vibration is given by

$$T = 2\pi\sqrt{\frac{M+kM'}{M-M'}\cdot\frac{l}{g}}.$$

The periodic time, T_1, *in vacuo*, which is not greatly different from that in air, is

$$T_1 = 2\pi\sqrt{\frac{l}{g}},$$

and hence

$$\frac{T}{T_1} = \sqrt{\frac{M+kM'}{M-M'}}.$$

By substituting for k and rearranging the terms, it will be seen that

$$\eta = \frac{1}{9\pi\rho T r^4}\left\{(M-M')\frac{T^2}{T_1^2} - \left(M+\frac{M'}{2}\right)\right\}^2. \quad . \quad (3)$$

If T and T_1 can be measured with sufficient accuracy this affords one method of finding η. The results obtained in this way will be given later.

The logarithmic decrement of the amplitude is, from (2),

$$\lambda = \frac{M' 9\pi k'}{8(M + kM')}. \quad . \quad . \quad . \quad . \quad . \quad (4)$$

The quantities k and k' depend upon the periodic time T, but as this is independent of the amplitude according to the theory given above, λ should be constant and its measurement would thus provide another method for finding the viscosity η.

If, when substituting for k' in (4), $\frac{1}{\beta^2 r^2}$ is neglected in comparison with $\frac{1}{\beta r}$, and 2λ in comparison with π, the expression for λ reduces to the simple form,

$$\lambda = \frac{9\pi M'}{4(2M + M')} \cdot \frac{1}{\beta r}. \quad . \quad . \quad . \quad . \quad . \quad (5)$$

The relative magnitude of the terms $\frac{1}{\beta^2 r^2}$ and $\frac{1}{\beta r}$ can be readily estimated by assuming for water the following values as rough approximations :

$$\eta = \cdot 01 \text{ c.g.s.},$$
$$\rho = 1,$$
$$r = 2 \text{ cm.},$$
$$T = 3 \text{ sec.}$$

With these values, the approximate values of $\frac{1}{\beta^2 r^2}$ and $\frac{1}{\beta r}$ are

$$\frac{1}{\beta r} = \frac{1}{20},$$

$$\frac{1}{\beta^2 r^2} = \frac{1}{400}.$$

Consequently, no serious error for the present purposes will be made by neglecting $\frac{1}{\beta^2 r^2}$. From the results of the experiments performed, the error produced by neglecting 2λ in comparison with π is about 2 per cent., which is equally negligible.

Experimental.

Originally it was proposed to determine the coefficient of viscosity by finding the period of a pendulum in air and then

immersed in water, using equation (3). For this purpose three brass spheres of diameter $1\frac{1}{2}$ inches, $1\frac{3}{4}$ inches, and 2 inches respectively—each accurate to two-thousandths of an inch—were obtained, and a fine german-silver wire of ·027 cm. diameter was fastened to each by drilling a small hole, heating the ball, and then filling the hole with soft solder and immersing a few millimetres of the carefully cleaned wire into the molten solder. It was found that the wires so fastened held very well and the method employed was not at all likely to disturb the sphericity of the balls. A large tank about 3 ft. 6 in. by 1 ft. by 1 ft. was used to contain the water in which the balls oscillated. Each ball was suspended so that when vibrating it was at a mean depth of about 5 inches below the surface of the water. It is necessary to employ a large tank, as in the development of the theory it is assumed that the fluid is of infinite extent and at rest at infinity, and, if a small tank is used wall effects would vitiate the results. By using a tank with the above dimensions it was considered that no correction would be necessary from this cause. Actually, of course, in calculating η a correction should be made for the resistance experienced by the wire, but as the diameter of the wire was so small in comparison with that of the spheres employed, and only a short length was immersed, it was considered negligibly small, and consequently ignored in the calculations.

The chief experimental difficulty in measuring the periodic time of the pendulum when the ball is immersed in water is caused by the rapidity of decay of the oscillations, it being impossible to obtain more than about 70 vibrations. Preliminary experiments using a stop-watch to time the vibrations showed that much greater accuracy in measuring the time would be necessary before this method could be employed for finding η. Accordingly it was decided to use a chronograph capable of measuring 1/100 of a second, the instrument being controlled by a tuning-fork and the order of accuracy 1/100 sec. The results of preliminary experiments with the $1\frac{1}{2}$ inch sphere are given below.

Temp.	Swings taken.	T.	T_1.	η c.g.s.
20° C.	60	2·9153	...	·008
	100	...	2·6595	
16° C.	65	2·8327	...	·014
	100	...	2·5794	

These results were considered too discordant to make the continuance of these particular experiments of any value, either as a test of the theory or as a method for finding the coefficient of viscosity, and it was decided to find η by the measurement of the log. dec.

Logarithmic Decrement Experiments.

In these experiments the log. dec. was measured for each sphere for two different lengths of wire suspending the ball. Errors arise in the log. dec. if forced oscillations are set up in the support, so a means of suspension which was at once rigid and easily adaptable was sought. The method finally adopted was to pass the wire to which the brass ball was attached through a fine drill chuck which could be screwed up tight, so that all four jaws were holding the wire. This drill chuck could be fastened, for the longer periods, into a bracket made of half-inch square brass screwed to a wooden beam in the ceiling, and for the shorter periods it was fitted into a bracket mounted on a solid cylinder of iron 2 in. in diameter which stood on a massive iron foot on a table. In neither case was it at all probable that appreciable forced oscillations would be set up.

The amplitudes were observed on one side only with a telescope containing a scale in the eyepiece situated $2\frac{1}{2}$ metres from the suspending wire. At this distance the image of the wire when properly in focus was fairly fine, and little difficulty was experienced in estimating to a tenth of a division in the eyepiece. The greatest angle through which the wire was displaced from the vertical in any experiment was less than 1·8°, and in every experiment the pendulum made several complete vibrations before any readings were taken.

According to theory the amplitudes should be in decreasing geometrical progression, and this was tested before proceeding further. The ratios of successive observed amplitudes were not sufficiently accurate for this law to be tested owing to the error of observation in each measurement, and it was therefore decided to find $\log \frac{\alpha_0}{\alpha_{11}}$ for a series of observations.

In the following table the amplitudes are given in eyepiece scale divisions and the last column gives $\log \frac{\alpha_n}{\alpha_{n+11}}$, the results being for the 2 in. sphere vibrating with a period of 3·58 sec.

a_n.	a_{n+11}.	$\log \frac{a_n}{a_{n+11}}$.
50·0	26·5	·6349
46·2	25·4	·5982
43·5	24·1	·5906
40·4	22·9	·5677
38·2	21·9	·5564
36·1	21·0	·5418
34·1	20·0	·5336
32·3	19·1	·5254
30·9	18·2	·5293
29·2	17·3	·5235
27·7	16·6	·5120

It will be seen that, except for one value of the logarithm, there is a progressive decrease in the third column showing that the assumption of successive amplitudes being in geometrical progression, and thus that the resistance experienced by the sphere is directly proportional to the velocity, is unjustifiable.

Modified Theory.

To account for the variation of the damping as found by experiment it was assumed that the decay of the amplitude could be resolved into two parts, one proportional to the velocity and the other to the square of the velocity. The differential equation for the variation of the amplitude can then be written

$$\frac{d\alpha}{dt} = = A\alpha - B\alpha^2, \quad . \quad . \quad . \quad . \quad . \quad (6)$$

where α is the amplitude at time t, A and B being constants.

Integrating this equation, and substituting the end conditions,

$$\alpha = \alpha_0 \text{ at } t = 0$$

$$\alpha = \alpha_1 \text{ at } t = t_1,$$

we have

$$t_1 = \frac{1}{A}\log\frac{\alpha_0}{\alpha_1} - \frac{1}{A}\log\frac{A + B\alpha_0}{A + B\alpha_1}.$$

This solution involving constants in the logarithm is inconvenient for calculation, so the following method due to Stokes * was adopted.

Rewriting the equation (6) in the form

$$\frac{d\alpha}{\alpha} = -A\,dt - B\alpha\,dt,$$

we can substitute for α in the last term from the equation

$$\alpha = \alpha_0\left(\frac{\alpha_1}{\alpha_0}\right)^{\frac{t}{t_1}},$$

an approximation in the present case, but accurately true when the amplitudes decrease in geometrical progression.

Substituting, and integrating, we have

$$\log\frac{\alpha_0}{\alpha_1} = At_1 + Bt_1\frac{\alpha_0-\alpha_1}{\log\frac{\alpha_0}{\alpha_1}}.$$

This equation involving two disposable constants will represent the experimental results as was shown by one or two trials, and from it an equation for η can easily be developed by the use of subsidiary hypotheses in the following manner.

The dimensions of the right-hand side must be zero, so assuming $\log\frac{\alpha_0}{\alpha_1}$ to depend only on the four quantities, η, T, r, ρ, where these symbols have the same meaning as before, it follows from a consideration of dimensions that $\log\frac{\alpha_0}{\alpha_1}$ must be of the form

$$\log\frac{\alpha_0}{\alpha_1} = K\left(\frac{\eta T}{r^2\rho}\right)^s$$

where s is some as yet undetermined power. If the theory already given be assumed to hold as a first approximation, we find from equation (5) that

$$s = \tfrac{1}{2}.$$

Consequently, equation (7) becomes

$$\log\frac{\alpha_0}{\alpha_1} = K_1\sqrt{\frac{\eta T}{r^2\rho}} + B_1\eta T\frac{\alpha_0-\alpha_1}{\log\frac{\alpha_0}{\alpha_1}}, \quad . \quad . \quad (8)$$

* Stokes, *loc. cit.*

where $nT = t_1$,

n = complete vibrations between α_0 and α_1.

The quantities α_0 and α_1 in equation (8) are the angular amplitudes. In the term $\log\frac{\alpha_0}{\alpha_1}$ the ratio will be the same if linear amplitudes or angular amplitudes are used, but for the term involving $\alpha_0-\alpha_1$ the angular amplitudes must be obtained. This is easily done by setting up a metre scale in the same place as that in which the pendulum oscillates and reading off the number of centimetres corresponding to 100 scale divisions in the eyepiece. The mean result of several observations showed that 100 scale divisions corresponded with 5·2 cm. ;

$\therefore$ 1 scale div. = ·052 cm. deflexion of wire.

Also the angular amplitude corresponding to one scale division

$$= \frac{\cdot 052}{x},$$

where x is the distance in cm. from the point of support to the point on wire where the amplitude is observed.

Hence, if "a" is the amplitude of an oscillation measured in cm., equation (8) can be written

$$\log\frac{a_0}{a_1} = K_1\sqrt{\frac{\eta T}{r^2\rho}} + \frac{B_2}{x}\frac{a_0-a_1}{\log\frac{a_0}{a_1}}. \quad . \quad . \quad . \quad (9)$$

The method of testing this equation was to substitute in it the values obtained for a_0, a_{10}, and a_{20} from a single experiment, using the 2 in. sphere vibrating with a period of 3·58 sec. and assuming the value ·0110 c.g.s. for the viscosity at 17° C., at which temperature the experiments were performed, and 1 for the density of water. Values were thus obtained for K_1 and B_2. The latter was next assumed to be some function of the periodic time, and the form of this function was obtained by considering the experiments with the same sphere, but vibrating with a shorter period. In this way it was found that B_2 could be written

$$B_2 = B_3 T^2.$$

Finally, a further assumption was made, viz., that B_3 was some function of the radius of the sphere. From the experiments on the $1\frac{3}{4}$ in. sphere vibrating with a period of 3·568 sec. it was found that

$$B_2 = K_2\frac{T^2}{r^{3/2}}.$$

Rewriting equation (9), we now have

$$\log\frac{a_0}{a_1} = K_1\sqrt{\frac{\eta T}{r^2\rho}} + K_2\frac{T^2}{xr^{3/2}}\cdot\frac{a_0-a_1}{\log\dfrac{a_0}{a_1}}. \quad . \quad (10)$$

To verify all the assumptions the value of the viscosity η was calculated from the results obtained with the three spheres, each vibrating with a long and a short period. For this purpose it does not matter if "a" is given in cm. or in scale readings, K_2 alone being affected by a constant factor. In the following table "a" is therefore given in scale deflexions, but the constants utilized in determining the results are in those appropriate units, so that "a" is in cm. to facilitate comparison with future work.

Results.

The mean value of x was taken to the nearest cm. for the long and short pendulums.

For short pendulums..... $x = 84$ cm.

For long pendulums ..... $x = 216$ cm.

Values used for calculating constants in equation (10) :

$\eta = \cdot0110$ c.g.s.
$\rho = 1.$
$T = 3\cdot58$ sec.
$r = 2\cdot54$ cm.
$a_0 = 50\cdot0$ divisions.
$a_{10} = 27\cdot7$,,
$a_{20} = 17\cdot3$,,

1 scale division = $\cdot052$ cm. deflexion of wire.

These values, when substituted, give the following values for the constants :

$K_1 = 3\cdot86.$
$K_2 = 10\cdot04.$

Hence, if "a" is measured in cm.,

$$\log\frac{a_0}{a_1} = 3\cdot86\sqrt{\frac{\eta T}{r^2\rho}} + 10\cdot04\frac{T^2}{r^{3/2}x}\cdot\frac{a_0-a_1}{\log\dfrac{a_0}{a_1}}.$$

The results are divided into Section A and Section B, the former relating to the 2 in. and $1\frac{3}{4}$ in. spheres which were used indirectly in finding the form of equation (10), and the

latter referring to these experiments on the $1\frac{3}{4}$ in. and $1\frac{1}{2}$ in. spheres which have not been used at all in the development of the equation for η.

SECTION A.

Sphere.	T secs.	a_0.	a_{10}.	η c.g.s.	Means.
2 in.	3·58	47·0	26·9	·0097	
,,	,,	49·0	27·1	·0116	·0105
,,	,,	49·5	27·8	·0101	
,,	2·48	48·5	27·1	·0096	
,,	,,	48·2	26·9	·0099	
,,	,,	48·9	27·2	·0098	·0010
,,	,,	43·8	26·3	·0101	
,,	,,	47·9	26·8	·0098	
,,	,,	49·0	27·1	·0103	
$1\frac{3}{4}$ in.	3·568	49·0	25·4	·0098	
,,	,,	47·8	25·0	·0098	
,,	,,	48·4	25·2	·0097	·0101
,,	,,	46·3	24·1	·0106	
,,	,,	46·8	24·2	·0108	

SECTION B.

Sphere.	T secs.	a_0.	a_{10}.	η c.g.s.	Means.
$1\frac{3}{4}$ in.	2·484	44·0	22·9	·0097	
,,	,,	46·0	23·2	·0125	
,,	,,	47·0	23·9	·0115	·0112
,,	,,	49·0	24·0	·0127	
,,	,,	48·2	24·3	·0105	
,,	,,	45·9	23·6	·0102	
$1\frac{1}{2}$ in.	3·553	46·8	21·0	·0125	
,,	,,	49·2	22·1	·0114	
,,	,,	45·9	20·7	·0110	·0116
,,	,,	50·0	22·2	·0118	
,,	,,	48·7	21·9	·0115	
,,	,,	48·7	21·9	·0115	
,,	2·52	47·0	20·9	·0115	
,,	,,	47·5	21·0	·0105	
,,	,,	46·2	20·5	·0110	·0108
,,	,,	46·0	20·6	·0105	
,,	,,	47·1	20·9	·0104	

Conclusion.

The results in Section B show a close approximation to the true result, viz., ·0110 c.g.s. units, and indicate that the theory accounts for the observed phenomena. The mean value of η from the results in this section is ·0112 c.g.s. units, which is in remarkably close agreement with the true result when it is remembered that the accuracy of the constants K_1 and K_2 depends entirely upon the accuracy with which merely three readings of the amplitude have been made in the case of the 2 in. sphere.

It is suggested that the physical meaning of K_1 and K_2 may be found from further experiments with different liquids, and these are about to be undertaken.

XCVII. *On Conditions near the Cathode of a Glow Discharge.* *By* NORA M. CARMICHAEL, *M.Sc., and* K. G. EMELÉUS, *M.A., Ph.D., Department of Physics, The Queen's University of Belfast* *.

THE cathode dark space is not a simple unit of the glow-discharge, but includes, when fully developed, a number of partially distinct sections, there being encountered in turn, on proceeding out from the cathode, the primary dark space, the cathode glow, the cathode dark space proper, and the transition region between the dark space and negative glow. The present communication is a preliminary account of an investigation of the region of the cathode glow and primary dark space with an exploring electrode, for conditions not far removed from those of the normal cathode fall in potential †.

I. *Experimental procedure.*

The form of tube used is shown in fig. 1. The cathode C consisted of a hollow, nickel-ended iron cylinder, with an iron tail T resting in the end-tube E ; with this construc-

* Communicated by the Authors.

† The work described was done early this year. Its completion has been unavoidably delayed, and although we hope to proceed again with it shortly, it is believed that the results already obtained are of sufficient interest to be published at this stage.

tion small changes were readily made in the position of the cathode with a magnet. The anode A was a nickel disk. The exploring electrode was a filament of tungsten, 0·09 mm. in diameter, or molybdenum, 0·107 mm. in diameter, strung across the tube in front of the cathode,

Fig. 1.

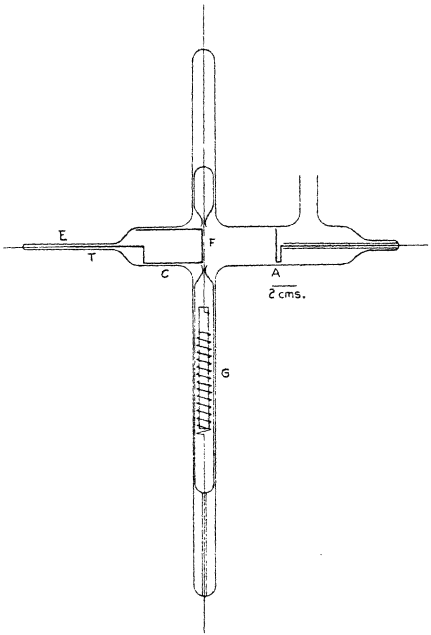

and kept taut by a 10 gm. piece of copper tube G. Care was taken that the glass sheath of F did not touch F for the last 6 mm. of its length on each side of the discharge, and that the filament was parallel to the surface of the cathode, although the latter precaution was found not to be of great significance. The metal parts were degassed in a vacuum furnace before assembly, and before admission

of any specimen of gas, the tube was baked out with a hand-flame at a pressure of less than 10^{-4} mm. Hg. That part of the surface of the cathode which was immediately opposite to the filament was also repeatedly subjected to electron bombardment from the latter. The gases used were oxygen, nitrogen, and neon, prepared as has been described elsewhere *, hydrogen, admitted through a palladium regulator, and technical argon, containing some 20 per cent. of nitrogen. Pressures were recorded by a McLeod gauge, and condensible vapours were kept from the tube by liquid-air traps.

Simultaneous measurements were made of the current to F (i_c); the current through the tube (i_t) as measured by the current to the anode; and the difference in potential between collector and cathode (V), and cathode and anode. The discharge was always allowed to pass for at least an hour before any readings were taken, and was then so steady that it was not necessary to correct i_c for fluctuations in i_t. The potential applied between anode and cathode ranged from 250 volts to 450 volts, and the gas-pressures from 0·2 to 1·5 mm. Hg. The filament was always between 0·3 and 0·9 mm. from the cathode, and no change in its position was noticeable as its potential was varied. The results were not affected in their main features by change of the discharge conditions between these limits.

A typical collector characteristic is shown in fig. 2, in which a current below the axis of voltage is one in which there is a net flow of positive electricity from the gas to the filament. The zero of potentials is that of the cathode. The appearance of the curve is similar to that of the curve obtained when a collector in the negative glow is starting to act as a main cathode for the discharge †, but there are important differences in detail. the curve of fig. 2 exhibiting more or less sharp discontinuities of slope at the points A, B, and C (B is usually sharper than in this particular instance).

We are not sure that the discharge was not seriously disturbed locally when the filament was hot. Very small changes in i_t also probably correspond to the breaks A, B, and C. Discussion of these two points is reserved for

* Emeléus and Beck, Phil. Mag. viii. p. 121 (1929).
† Emeléus and Brown, Phil. Mag. vii. p. 17 (1929).

a later paper. All data given in the present communication were obtained with F cold.

II. *Interpretation of the Characteristic Curves.*

It is of fundamental importance to know if an ionic sheath forms round a collector in the cathode dark space. Theoretically, the problem is indeterminate, since in the usual integration of Poisson's equation it is necessary to know the field either at the surface of the collector or at some point in the sheath, supposed present, or at its

Fig. 2.

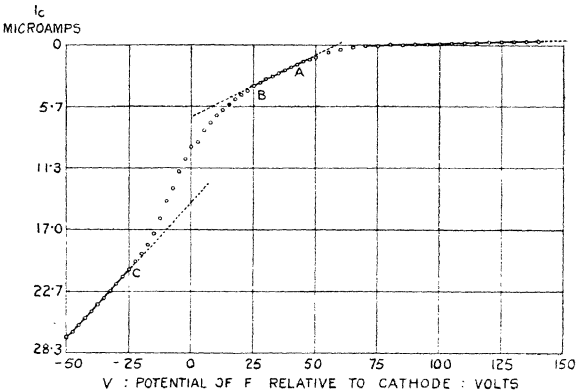

i_c=6·7*m*A. Tube voltage=310. F to cathode=0·6 mm. Gas-nitrogen. Thickness of cathode dark space=7 mms.

outer boundary; to assume a value for the field in the present case is tantamount to assuming the existence of the sheath. The problem can be approached directly in two ways from the experimental side; first, by visual observation, and, secondly, from the shape of the characteristic curves. Visual observation is impossible with the tubes that we have used, but has recently been made the subject of a special study by W. L. Brown and E. E. Thomson in this laboratory *. Their observations,

* See the following paper, p. 918

which are reported upon elsewhere, show that the well-known shadows thrown by obstacles in the cathode dark space can be used to find space-potentials, but are not conclusive as to the existence of sheaths like those formed in plasma-type discharges. We have thus to rely upon the form of the characteristic curves, and this appears to be irreconcilable with the existence of ordinary sheaths. There are several reasons for arriving at this conclusion. First, simultaneous observation of shadows and of collector currents in Brown and Thomson's apparatus, in the part of the cathode dark space in which we are now interested, has shown that the space-potential lies at or close to the break B. There is in this part of the characteristic no sign of the reception of the groups of slow electrons which produce a rise in the characteristic curve in other parts of the discharge at the space-potential, and, in spite of the large electric field in most of the cathode dark space, some of these slow electrons might be expected to be present near the cathode glow. Secondly, the position of the characteristic curve relative to the axis of voltage shows that, when insulated, the collector charges up positively to the surrounding space, as Aston suggested in his explanation of the reputed "Kathodensprung" in potential *. This shows that there are present large numbers of positive ions, or that the collector is emitting electrons, or that both of these effects, the latter of which certainly tends to destroy a sheath, are co-existent. Positive ions are, of course, known to be present in excess of electrons through most of the dark space, although the electrons may preponderate near the cathode. From such considerations we have come to regard the action of a collector in the dark space as more nearly like that of a grid wire in an evacuated thermionic triode, that is, its effect is not confined to a region bounded by a separate ionic sheath, but extends without existence of a definite boundary into the pre-existing space-charges of the cathode dark space, modified by the ionic shadows thrown by the collector.

Conditions appear to be too complicated to make a mathematical formulation of these ideas possible, but we can account for the course of the characteristic curves

* Aston, Proc. Roy. Soc. lxxxiv. p. 526 (1910).

qualitatively on lines indicated by Aston *. Fig. 3 *a*, which is taken from his paper, shows the probable trajectories of positive ions (thick lines) and electrons (thin lines) near a—positive—insulated collector F. We are concerned with what happens when F is made more negative than in this case, and it is evident that this will be accompanied by a gradual straightening of the lines until when F is at the space-potential, they run parallel to each other and perpendicular to the cathode. At this stage the space between the lines tangential to F will be

Fig. 3.

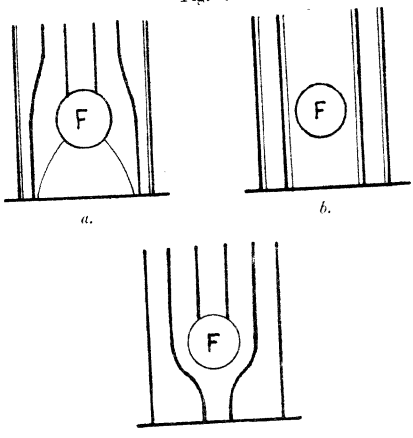

a. *b*. *c*.

shielded from the streams of ions and electrons and will appear as a shadow of these dimensions, this constituting Brown and Thomson's method for finding the space-potential. Meanwhile, only small and essentially steady changes will have been occurring in the current to the collector, so far as these ions and electrons are concerned. After passing the space-potential F will affect the positive ions which have passed it on their way to the cathode, so that their paths are more like the lines in fig. 3 *c*. The

* Aston, Proc. Roy. Soc. lxxxiv. p. 526 (1910).

positive ion current to F will commence to increase rather more rapidly than before, together with any secondary emission of electrons from F, and we might thus expect the net positive current to F from the gas to start to increase more rapidly after F has been made negative to the space, and so to give the discontinuous increase in slope that is observed to the negative side of B (fig. 2). As F is made still more negative, the positive current to F from the gas must increase more and more rapidly as the potential of F approaches nearer to that of the main cathode, whatever the precise nature of the processes which render an electrode capable of maintaining a discharge when cold. It is, of course, unlikely that conditions are quite so simple as this, but some such correlation of figs. 2 and 3 seems reasonable.

We have still to account for the breaks A and C. Of the two, C is the more pronounced, and might conceivably arise in at least three ways.

(i.) The region of the characteristic between B and C might correspond to the transition from a discharge of normal type on the collector to one of abnormal type, these terms being used to denote incomplete and complete utilization of the geometrical surface of the collector F; after the discharge is started, sputtering between F and the main cathode probably rapidly makes the two effectively of the same material, and so the fact that the break C, supposed to mark the onset of the normal discharge, is negative to the potential of the main cathode, could be supposed to be due to the fact that the collector F is a wire of large curvature. Against this view is the fact that a space-charge has already been established for F by the main discharge, and certain regularities in the position of C that are referred to again in section III.

(ii.) The point C might correspond to the closing in of the edges of the shadow behind F towards the main cathode until at this stage it ceased to reach to the main cathode.

(iii). The break at C is of a type which is usually associated with the reception of a group of fast electrons in a retarding field by a collector. Such a group could arise either from the gas, or from the surface of the cathode, being produced in the latter case photoelectrically, or by bombardment with excited atoms, or positive ions, or by some other process of the second kind taking place there. It is, of course, possible that fast electrons could come both

from the electrode and gas, but we should be inclined to favour the former source, particularly on account of the general similarity between our curves and those published by Oliphant for electrons liberated from a metal surface by metastable atoms *. On this interpretation of the curves, whatever the space-potential near F, the maximum energy of emission of the electrons from the cathode will be measured by the potential of C relative to the cathode, and many of the electrons would appear to have one half the maximum energy in the group. This form of apparatus is. however, not suited for study of slow electrons from the cathode, since these, unlike electrons emitted with a considerable initial velocity, will follow fairly closely the lines of the positive ions incident upon the cathode, and since the latter have escaped collection by F, the slow electrons liberated where the positive ions hit the cathode —but not necessarily *by* the positive ions—must likewise largely escape detection. There is, in fact, no upward break in the characteristic near the cathode potential. The break A may be very tentatively attributed to the failure of fast electrons liberated from F by a similar process to reach the main cathode in the field retarding their motion in that direction.

We are unfortunately unable at present to decide definitely between the alternatives II. and III.

Curves similar to that of fig. 2 were obtained by Aston † for a collecting electrode behind a hole in the main cathode, but are even less easy to interpret, both because of the disturbance of the main discharge by the aperture, and because there are rather too few experimental points to be sure of the existence of discontinuities in slope at B and A.

III. *Results of Discussion.*

The interpretation of the characteristic curves remains much less satisfactory than could be desired. We may, however, indicate some of the consequences of assuming that the tentative conclusions of the last section are correct.

(*a*) The break B occurs at a potential consistently closer to that of the cathode than it would be if the fall in

* Oliphant, Proc. Roy. Soc. cxxiv. p. 228 (1929).
† Aston, Proc. Roy. Soc. xcvi. p. 200 (1920).

potential across the whole region between cathode and negative glow followed the parabolic law of Aston *, in general agreement with the results of Brown and Thomson.

(*b*) There are certain regularities in the position of the break C. In each gas there appears to be, on the interpretation iii. of the preceding section, a fairly definite maximum velocity for the electrons emitted from the cathode. In the cases of neon and argon, the break was double, the position of the more negative discontinuity corresponding to the position of the break in nitrogen; in these cases the less negative break has been assumed to be that for the inert gas itself. On the interpretation ii. this could be connected with the shadow reaching to the cathode at one stage, and to the primary dark space at

TABLE I.

Gas.	No. of breaks measured.	Max. energy of electrons : volts.	Corresponding critical potential of gas in volts.
Nitrogen.....	16	22 $\pm$5	28 : dissociation to two singly ionized atoms.
Hydrogen ...	7	25·5$\pm$4	29·7 : process as for nitrogen.
Argon	9	13·5$\pm$3·5	15·5 : ionization of atom.
Neon	6	18·0$\pm$3·5	21·5 : ionization of atom.

another. The data obtained for the maximum energies are collected in Table I., where the errors given against the energies are the root mean square departures from the mean. These errors are large, which points to the need for better control of the purity of the gas and electrodes than we have yet been able to attain. It may be significant, nevertheless, that the averages lie, as shown, a few volts below important critical potentials of the gas in each case †, and it is tempting to suppose that fast electrons are liberated from the cathode by the atomic processes in question taking place there, the electrons losing at least energy measured by the work-function of the cathode—4·4 volts

* Aston, Proc. Roy. Soc. lxxxiv. p. 526 (1910).

† Data from Geiger-Scheele, *Handb. d. Physik*, xxiii. article by Franck and Jordan for Ar, Ne, N_2, from Vencov, *Comptes Rendus*, clxxxix. p. 27 (July 1929), for H_2.

for nickel in vacuum *—in leaving it. The processes may then be identifiable with neutralization of the normal singly charged ions in neon and argon, simultaneous neutralization of two protons, with recombination of the latter to form H_2 in hydrogen, and neutralization of two atoms followed by recombination in nitrogen.

No breaks were found corresponding to C on five characteristics taken in oxygen.

IV. *Summary.*

The characteristic curves for a collector very close to the cathode of a glow-discharge have discontinuities in slope. The most negative of these, which is always negative to the potential of the cathode, may be taken to indicate that there is a group of fast electrons leaving the cathode surface, where it is produced by some process of neutralization and recombination of the ions of the cathode dark space. The second, which is always positive to the cathode potential, is attributed to a change occurring in the mode of reception of the current at the space-potential, which, on this interpretation, is consistently more negative than if Aston's parabolic law held. The origin of the third, more positive break, is most uncertain, but it may indicate that there is an emission of fast electrons from the collector.

XCVIII. *The Potential Distribution across the Cathode Dark Space.* *By* W. L. Brown, *M.Sc., Demonstrator, and* E. E. Thomson, *M.Sc., Musgrave Demonstrator, Physics Department, Queen's University, Belfast* †.

[Plate XVII.]

Introduction.

THE chief contributions to the study of the electrical conditions in the cathode dark space of the glow discharge have been those of Aston ‡, Brose §, and Geddes ‖.

* Marx, *Handb. d. Radiologie.* iv. 3, p. 299.
† Communicated by Dr. K. G. Emeléus, M.A.
‡ Aston, Proc. Roy. Soc. lxxxiv. p. 526 (1911).
§ Brose, *Ann. d. Phys.* lviii. p. 731 (1919).
‖ Geddes, Proc. Roy. Soc. Edinb. xlvi. 2, p. 136 (1925–26).

Aston determined the electric fields at different points along the dark space in a wide tube, by passing across it a beam of cathode rays from a subsidiary tube kept at very low pressure. The deflexion of the beam at different distances from the cathode was used as a basis for the calculation of the electric field. It was not possible to take measurements right up to the cathode, but over the region investigated it was found that the field at any point was proportional to its distance from the negative glow. This means that the space charge is constant throughout that part of the dark space considered. The tube voltages varied between 265 and 610 volts.

Brose, using high voltages, 1000 to 4000 volts, in discharge-tubes of narrow bore, and with gases at low pressures, found the distribution of the field by measurement of the Stark effect. In common with Aston, he found a positive space charge throughout the main part of the dark space, but his results indicate that this is not constant, and also that there is a negative space charge in the region near the cathode.

Geddes applied Aston's method to discharges at high voltages. His results were similar to those obtained by Aston.

Many attempts have been made to measure the potential distribution across the dark space by introducing a third electrode, and measuring by means of an electrometer the potential taken up by it. These methods fail chiefly on account of the differences in mobility and concentration of electrons and positive ions, which prevent the wire from taking up the potential of the surrounding space *.

It was intended, on beginning the work described in the present paper, to take current-voltage characteristics of a collector or third electrode inserted in the cathode dark space of the glow discharge, and to attempt the analysis of these characteristics by some modification of Langmuir's method †. Previous work on the glow discharge has been concerned with the negative glow, Faraday dark space, and positive column, in which the characteristics obtained can be analysed by this method. The form of the characteristics in the cathode dark space is quite different from that obtained in other parts of the discharge, and the

* *Vide*, *e. g.*, Emeléus, 'Conduction of Electricity through Gases,' p. 39.

† Langmuir and Mott-Smith, Gen. Elect. Rev. xxvii. p. 554 (1924).

interpretation of the curves is difficult. The chief difference between the dark space and the rest of the discharge is the high value of the field in the dark space, almost the whole fall of potential applied to the tube taking place across it.

The data obtained were plotted in different ways and the resulting curves examined. The relation V against log (c+const.) gives a straight line with a break at a voltage between that of anode and cathode. This voltage approaches that of the anode as the collector is moved nearer the negative glow. We compared the values of this potential with observations taken by the method to be described later, but although agreement was very close near the cathode, it became less exact as the collector approached the negative glow.

The characteristics proving unsatisfactory, we turned our attention to another phenomenon. That there is a shadow cast towards the cathode by an obstacle placed in the cathode dark space has long been known. However, so far as we are aware, the effect of applying a potential to the obstacle has not been investigated. We carried out a series of observations, using obstacles (or *collectors*), of different shapes. Metals were used for all electrodes.

The effect of using a large circular collector, 8 mm. in diameter, mounted parallel to a cathode 2·5 cm. in diameter was very striking. When the collector was insulated, there was a circular patch cut out of the cathode glow underneath, and of greater area than the collector, while there was a very small circular patch cut out of the negative glow. On reducing the potential of the collector relative to the cathode, the cathode patch diminished while that in the negative glow increased in size, passing through the intermediate stage when both were equal in area to the collector, to the condition in which there was a large patch cut out of the negative glow, while the cathode glow was almost undisturbed.

The results of observations, using as collector a wire, 0·4 mm. in diameter, mounted parallel to the cathode surface, may be summarised as follows :—

(*a*) The potential applied to the collector by an external battery, necessary to maintain the shadow towards the cathode in the same form as when the collector is insulated, is always near the anode potential.

The form of the shadow is shown in Pl. XVII. fig. 1. It will be seen that the shadow is much wider than the wire.

(*b*) If the applied potential is reduced, the width of the shadow decreases. When the shadow to the cathode side has the same width as the wire, another shadow has appeared on the anode side, also of the same width as the wire. This is shown in Pl. XVII. fig. 2.

(*c*) Further reduction of the applied potential leads to the complete disappearance of the shadow to the cathode side, while the shadow on the anode side increases in size.

(*d*) As the potential approaches that of the cathode, a bright layer appears on the cathode side of the wire, while on the anode side the shadow is almost parabolic, with a bright layer round the edges. (Pl. XVII. fig. 3.)

The photographs shown were obtained in argon, with a tube voltage of 470 volts; the potential of the wire relative to the cathode was 228 volts in Pl. XVII. fig. 2 and 62 volts in Pl. XVII. fig. 3. In Pl. XVII. fig. 1 the wire was insulated. The dark space was 1 cm. in width in all cases. The photographs have all been enlarged two diameters, and only a small part of the cathode is shown.

The above facts can be explained qualitatively by considering that the potential of the collector when the shadows thrown to the two sides of it are equal is the potential of the surrounding space. This is reasonable, because the disturbance of the discharge, caused by the presence of the collector, appears to be least at this potential. Apparently positive ions moving towards the cathode, and electrons moving towards the anode, in paths parallel to the axis of the tube, are not deflected. When the potential of the wire is near that of the cathode, *i.e.*, negative to the surrounding space, we should expect electrons moving towards the anode to be deflected away from the collector and positive ions moving towards the cathode to be deflected towards it, so that the discharge would be more concentrated than normal between collector and cathode, and less concentrated on the other side of the

wire. The converse would be true when the potential of the collector was near that of the anode.

From such considerations, we have concluded that the potential of the collector, when the shadows thrown to the two sides of it are equal in width, is the potential of the surrounding space, and we have used this as a basis for measuring the potential distribution across the cathode dark space.

Preliminary Observations.

Before considering the experimental arrangements for carrying out measurements of potential, it is of interest to mention some observations made in connexion with the shadow thrown to the cathode side of the collector. It was found that if the collector were charged to some potential at which a shadow was cast towards the cathode, and the discharge left running for a considerable time, perhaps an hour, the part of the cathode in shadow became sharply defined by a curious bluish marking, bounded by sharp lines. A photograph of markings on an iron cathode surface, obtained in this way, using a molybdenum collector, is shown in Pl. XVII. fig. 4.

The marking obtained was more intense with longer exposure to the discharge, and with higher current densities. If the potential of the wire is changed after a marking has been formed, so that there is no longer a shadow on the cathode side, the marking will disappear after a time.

It is well known that the glass surrounding the cathode of a discharge-tube becomes sputtered after a time depending on the intensity of the discharge, and the cathode material. This is due to atoms of the metal being liberated from the cathode by the impact of positive ions and being deposited on the neighbouring glass surfaces. We may attribute the marking described above to the same cause. Atoms of metal pass temporarily into the discharge, and most of these are returned to the cathode, the remainder depositing on the tube walls. We suggest that those atoms which deposit on that part of the cathode in shadow tarnish the surface, while atoms returning to the bright part of the cathode are prevented from tarnishing it by the continual bombardment of positive ions. This explanation is borne out by the fact that the

marking disappears when the discharge is allowed to fall on it.

We should also point out here that Oliphant * has obtained disintegration of the cathode, due to metastable helium atoms.

The form of the markings produced by using different types of collectors was studied next. In every case the shape of the marking corresponded roughly with that of the collector, small obstacles giving the most sharply defined markings.

The sharp lines on the edges of the markings (Pl. XVII. fig. 4) might possibly be due to a kind of focussing effect. There will be a tendency for positive ions to move across the dark space more or less perpendicularly to the cathode, under the influence of the large electric field. The path will, of course, be zigzag, but the main direction will be normal to the cathode. A positive ion moving in this direction, and passing near the wire when it is charged positively to the space, will be deflected away from the wire. If the number of collisions is fairly large, the path of the ion will rapidly return to a direction parallel to the original direction, and the effect of the wire will be merely to displace the particle sideways. Other positive ions passing the wire at greater distances will be displaced less, and this will tend to lead to a sharp line of demarcation between the shadow and the normal discharge. If the number of collisions is not large, we should expect a more diffuse edge to the marking.

An interesting case studied was that of a wire introduced from a side tube, and bent so that its free end was furthest from the cathode. The marking produced on the cathode surface is shown in Pl. XVII. fig. 5. It will be observed that the marking is not parallel sided, as in Pl. XVII. fig. 4. but has a maximum width, diminishing to a point towards the free end of the wire. We should expect that the point where the marking is the same width as the wire corresponds to that point of the wire which has the same potential as the space surrounding it. Bearing in mind the facts mentioned in the Introduction, it is clear that the part of the wire nearest the negative glow may not cast any shadow at all.

On the cathode of Pl. XVII. fig. 5 the marking was

* Oliphant, Proc. Roy. Soc. cxxiv. p. 228 (1929).

brown, the collector in this case being of copper-clad nickel iron, and the cathode of iron. The potential of the collector relative to the cathode was 240 volts.

Wehnelt * and Villard † found that the cathode became tarnished with a film of oxide on that part of it *exposed* to the discharge. They put this down to the oxidizing action of positive rays. The part of the cathode in shadow remained bright, while the edges of the deposit were not sharp. The differences between their results and those considered above must be due to the fact that they worked

Fig. 1.

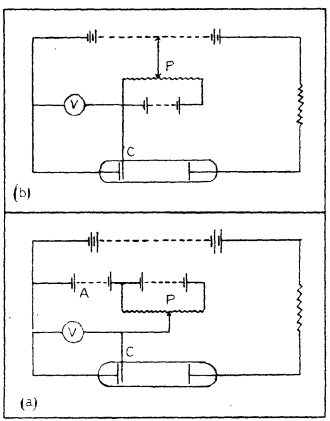

with an induction-coil discharge in air at low pressure, and a copper cathode.

Experimental Arrangements.

The discharge-tube was run off a battery of small accumulators, capable of giving a maximum voltage of 660 volts. The first circuit used is shown in fig. 1. *a*. There was a wire resistance of 1100 ohms in series with the tube, to prevent the glow discharge from passing into an

* Wehnelt, *Ann. d. Phys.* lxvii. p. 421 (1899).
† Villard, *Comptes Rendus*, cxxvi. p. 1564 (1898).

arc. The potential applied to the collector C could be adjusted by varying the voltage of the battery A, and fine control was obtained by means of the potentiometer P, which had a maximum range of 60 volts. Voltages were read on the Weston high range voltmeter V. When taking current-voltage characteristics, Pye mirror galvanometers were brought into the circuit.

With this arrangement there was the difficulty that as the voltage available for the battery A was often less than half that of the main battery, there was a break in the series of readings when the voltage which was required for the collector was nearly half-way between anode and cathode potential. In order to avoid this, in some of the later work the battery A was abandoned, and the lead to it was taken to a plug, which could be connected to any desired point along the main battery (fig. 1, *b*). The potentiometer P was retained, and with this arrangement any voltage between anode and cathode potential could be applied to the collector.

The only possible objection to this arrangement was the fact that the tube and collector circuits were more closely coupled than when the first circuit was used. However, it was found that the results obtained with the two circuits showed no differences.

The discharge-tubes were exhausted by a Gaede steel mercury vapour pump, backed by a Hyvac pump. The tube section of the apparatus was cut off by a tap from the McLeod gauge and the pumps, and arrangements were made to introduce the different gases as required. Argon was purified by running an arc between calcium electrodes in a bulb sealed to the apparatus near the discharge-tube. For neon, this bulb was replaced by a liquid-air trap containing charcoal. The nitrogen used was generated by exploding sodium azide in a side reservoir, and was considered sufficiently pure without treatment. In all cases mercury vapour from the pump and the McLeod gauge, and hydrocarbon vapours from the taps, were kept out of the discharge-tube by means of liquid-air traps. Before making observations the discharge-tube and the glass-work near it were well baked by the gas flame for some hours. While observations were being made a liquid-air trap was always used.

These precautions allowed us to work with the gases in a fairly pure state. In the argon, after the calcium arc had

been running for several hours, no trace of nitrogen could be detected spectroscopically, although the Balmer lines of hydrogen were just visible. Both the neon and the argon showed a well marked primary dark space. The sample of neon used contained 2 per cent. of helium, other impurities being removed by the charcoal tube.

The discharge-tube, of soda glass, was 3 cm. in internal diameter. The cathode was a steel tube 4 cm. long, and fitted it fairly closely. The end of the steel tube was closed by a disk of iron or nickel, which acted as the cathode face. A small hole was drilled through this disk, as near the edge as possible, and through this was passed a thin glass rod, 4 cm. long; this rod carried the anode, which was made of light nickel sheet. The distance between the electrodes was therefore constant. The glass rod was so fine that it did not disturb the discharge appreciably.

The collector was a fine steel wire, 0·4 mm. in diameter, carried by a glass sheath which was introduced through a side tube. Steel was used as it was the only material at hand stiff enough to remain quite straight when supported only at one end.

The discharge-tube was set up with a slight tilt towards the cathode end of the tube. When a set of observations was being made, it was begun with the cathode as close to the collector as possible, so that after each reading had been taken, a slight tap on the tube caused the cathode to move a little farther from the collector. When a series of observations was completed the cathode could be brought back to its original position by means of an electromagnet. The distance between the cathode and the collector was measured with a travelling microscope, adjusted so that its axis was parallel to the collector.

Results.

The observations of the potential at which the shadows on both sides of the wire were equal could be reproduced to within 5 volts throughout the dark space except near its cathode and negative glow boundaries, where the shadow on one side became so short that it was more difficult to determine the point of balance. This represents quite a high degree of accuracy when we consider that a wire 0·4 mm. in diameter placed in a field of 300 volts per cm.,

such as exists in the dark space, will be lying in a region across which there is a fall of potential of 12 volts.

When the collector approached close to the negative glow edge, it was found that not only did the shadows cast by the wire alter in form but the edge of the glow itself became somewhat distorted, as the potential applied to the wire was altered. However, in spite of this, no great difficulty was experienced in obtaining the balancing potential, since the glow assumed its normal outline when the shadows were balanced. By "normal outline," we refer to the contour of the glow before the collector was moved near.

Another point of some importance arises here. If the negative glow is not parallel to the cathode but presents a convex surface towards it, as is often the case at low voltages when the pressure is low, then we must consider that the equipotential surfaces across the section of the tube are curved also. In such cases the shadow cast by the wire will vary in width, and it is of importance to know the point of the wire for which we have balanced the shadows. On one occasion an accidental tap on the tube caused the glass sheath carrying the collector to move, so that its end passed into the path of the discharge. The shadow cast by it towards the cathode (it will be remembered that an insulated obstacle of any description casts a shadow towards the cathode) was wider than that cast by the wire when near the balancing potential. Although on the side of the tube remote from the eye, this shadow could be seen quite well in addition to that thrown by the wire. The shadow thrown by the glass may be seen in Pl. XVII. fig. 6.

In such cases the point of balance becomes rather indefinite, and the shadow of the same width as the wire seems to move along it as the potential is slightly altered; so that the shadows thrown by all parts of the wire influence the observer in deciding the balancing potential. That there is not any great deviation from plane equipotential surfaces in most cases, however, seems to be indicated by the parallelism of the marking on the cathode shown in Pl. XVII. fig. 4.

On completing a series of observations over the dark space by the shadow method, we usually estimated the space potential in the negative glow by moving the collector

into it and increasing the voltage applied until the electron current to the collector began to increase rapidly. Points on the curves which were thus obtained are marked with an L.

Data obtained with different gases under various conditions of pressure and voltage are given in Table I.

Fig. 2

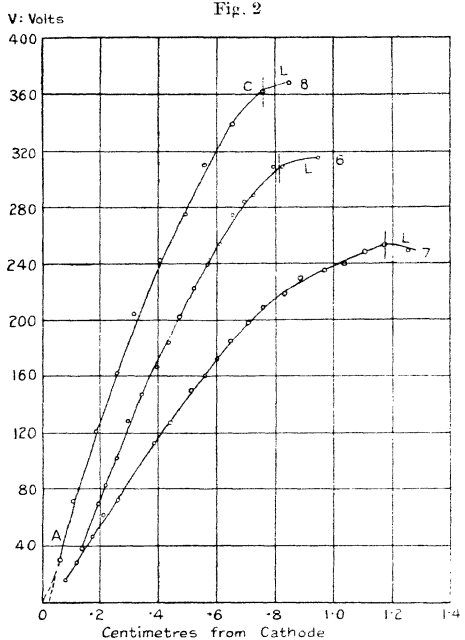

The vertical lines indicate the positions of the negative glow edge. Data for these curves will be found in Table I. Nos. 6, 7, and 8.

Some typical graphs drawn from these data are shown in figs. 2 and 3.

One of the curves in fig. 2 is lettered for the purpose of explanation. It rises smoothly to the point C, where the collector passes into the negative glow. The vertical line

through the curve indicates the position of the cathode edge of the negative glow. There is a break in the curve near its lower end, and the middle part, AC, when extrapolated, does not pass through the origin but cuts the axis at a distance of the order of half a millimetre from it. This initial part of the curve cannot be found accurately by the shadow method, as the cathode shadow here is so short; but the fact that AC does not pass through the

Fig. 3

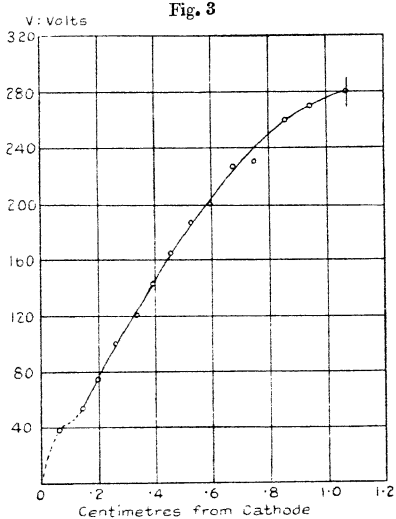

The vertical line indicates the position of the negative glow edge. Data for this curve will be found in Table I. No. 25.

origin confirms the supposition that there is a layer of negative space charge near the cathode surface, as shown by Brose's curves for strongly abnormal cathode fall, and that the effective cathode is the edge of this layer.

P. M. Morse * has recently given a comprehensive theory of the glow discharge, which is the most satisfactory yet proposed, and which it is desirable to test from these

* Morse, Phys. Rev. xxxi. p. 1003 (1928).

Table I. A.

No.	5.		6.		7.		8.		9.		10.		11		12.	
Tube Voltage.	295		314		247·5		373		250		300		360		410	
C.D.S.† width.	·9 cm.		·77		1·16		·74		·98		1·07		1·07		1·04	
	x.	V.	*x*.	V.	*x*.	V.	*x*.	V.	*x*.	V.	*x*.	V.	*x*.	V.	*x*.	V.
	·091	21	·137	38	·077	15	·061	50	·084	18	·066	27	·075	25·5	·100	38
	·122	40	·197	70	·115	28	·106	72	·104	28·5	·090	40	·112	42?	·170	78
	·142	60	·217	83	·172	46·5	·186	121	·139	37·5	·120	47	·160	67·5	·225	116
	·172	71	·257	102	·209	62	·256	162	·189	57	·146	60	·202	91·5	·295	159
	·207	84	·297	128	·259	72·5	·316	204	·244	80·5	·188	76	·240	110 ?	·365	195
	·228	97	·342	147	·385	112·5	·406	242	·304	93	·218	90	·290	142·5	·445	225
	·260	110	·397	166	·442	127	·496	275	·359	125	·244	104	·330	164	·495	249
	·299	128	·437	184	·512	149	·561	310·5	·414	133	·275	117	·380	180	·560	281
	·339	140	·472	202	·559	160	·656	339·5	·479	151·5	·303	129	·435	198	·620	304
	·372	150	·522	222	·602	172	·761	362	·576	179	·338	144	·500	226	·675	313
	·402	167	·567	239	·650	185	·85*	369L	·664	200	·361	150	·567	243	·735	332
	·440	178	·612	254	·712	197·5			·819	228	·390	163	·640	265	·802	351
	·455	190	·657	274	·762	208			·869	235	·433	177	·733	295	·855	369
	·479	197	·697	284	·834	218			·929	243	·475	190	·830	317	·915	374
	·550	220	·727	288	·890	229·5			·989	247·5	·502	201	·932	335	·975	394
	·582	227	·797	309	·972	235			1·027	247·5	·564	215	1·020	353·5	·995	405
	·600	239	·827	309	1·040	240			1·114	250	·625	235	1·400	358L	1·095	406
	·634	244	·955	314L	1·112	248					·665	245				
	·692	261			1·160	253					·730	257				
	·722	263			1·25*	248L					·764	267				
	·782	283									·828	280				
	·826	287									·877	289				
	·882	291									·926	302				
											·975	306				
											1·069	308				
											1·22*	298L				

x is the distance from the cathode in centimetres : V is the space potential in volts.

* These positions are approximate. L indicates that the value was obtained by Langmuir's method.

† The values for the width of the cathode dark space are necessarily approximate. Runs : 5–12 Argon.

TABLE I. B.

No.	17.		18.		19.		20.		21.		24.		25.		27.	
Tube Voltage.	525		460		566		225		270		372		285		314	
C.D.S.† width.	1·40		1·55		1·46		·90		·77		·80		1·05		·93	
	x.	V.	*x*.	V.	*x*.	V.	*x*.	V.	*x*.	V.	*x*.	V.	*x*.	V.	*x*.	V.
	·050	30	·135	37	·065	14	·052	30	·075	60	·070	60	·065	39	·095	60
	·090	45	·190	70	·115	37	·087	48	·150	75	·130	81	·146	54	·165	75
	·130	75	·250	100	·170	67	·142	55	·210	98	·200	120	·201	75	·235	98
	·200	120	·310	128	·240	112	·200	75	·280	127	·257	150	·260	100	·311	135
	·275	157	·380	150	·305	163	·249	90	·360	150	·308	180	·335	120	·386	165
	·350	195	·460	180	·370	195	·332	110	·430	180	·354	202	·390	143	·448	186
	·535	280	·530	200	·450	228	·402	124	·530	200	·437	237	·453	165	·524	210
	·590	300	·630	228	·530	266	·432	135	·620	220	·495	265	·525	187	·575	230
	·675	330	·695	248	·620	295	·490	157	·686	233	·557	288	·595	200	·654	250
	·740	350	·765	270	·740	345	·590	165	·710	246	·620	315	·675	227	·712	270
	·840	380	·860	300	·860	385	·700	180	·775	255	·690	330	·752	230	·781	280
	·900	405	·920	328	·980	420	·780	198	·925	270	·735	345	·860	260	·860	300
	1·025	435	1·010	345	1·110	458	? ·768	210			·801	355	·945	270	·933	305
	1·086	457	1·100	360	1·250	505	1·030	210			·935	370	1·070	280		
	1·135	467	1·175	374	1·375	535										
	1·200	480	1·300	390	1·460	564										
	1·235	488	1·370	400												
	1·270	495	1·470	412												
	?1·331	543														

x is the distance from the cathode in centimetres: V is the space potential in volts.

† The values for the width of the cathode dark space are necessarily approximate.

Runs: 17–19 Nitrogen.
20–27 Neon.

data. Starting from Poisson's equation, and making use of Townsend's relation,

$$a=pNe^{-pNv/E} \quad . \quad . \quad . \quad . \quad . \quad . \quad (1)$$

he arrived at the equation

$$V=4D(1-c)-4D(1-c)e^{-2pNx/3}+8DN(1-c)E_a px/3. \quad (2)$$

for the fall of potential across the cathode dark space.

In the above equations :

a=the number of ions formed per cm. of path by an electron moving under a field E,

p=pressure of gas,

$1/(1-c)$=fraction of total discharge current carried by positive ions.

v=ionization potential of the gas,

V=space potential at any distance x from cathode,

D=diffusion coefficient,

E_a=a constant.

Morse also gives the relation,

$$4D(1-c)=V' \text{ approximately, } . \quad . \quad . \quad . \quad (3)$$

where V′ is the normal cathode fall of potential.

From (2) and (3),

$$V=V'(1-e^{-2pNx/3}+2NE_a px/3).$$

which may be written

$$V=V'(1-e^{-kpx}+Kpx) \quad . \quad . \quad . \quad . \quad . \quad (4)$$

where $k=2N/3$, and $K=kE_a$.

Hence,

$$S/V'=kpe^{-kpx}+Kp \quad . \quad . \quad . \quad . \quad . \quad (5)$$

where $S=dV/dx$.

When $x=0$,

$$S/pV'=k+K=\sigma. \quad . \quad . \quad . \quad . \quad . \quad (6)$$

In the analysis of our curves on this basis, the main part of the experimental curve AC (fig. 2) has been extrapolated to cut the axis, and the point of section taken to be the effective cathode ($x=0$). The slope of the tangent drawn at this point gives a value of S. By substituting this value in equation (6), the value of $k+K$ is found, p and V′ being known.

Putting $V=V'$ in equation (4), we have

$$e^{-kpx}=Kpx.$$

The value of x for $V=V'$ is found from the experimental curve and substituted in this equation. The values of k and K can then be found, either by trial or graphically, by drawing the curve

$$\eta=\xi+e^{-\xi}, \text{ where } \eta=\sigma px \text{ and } \xi=kpx,$$

Fig. 4.

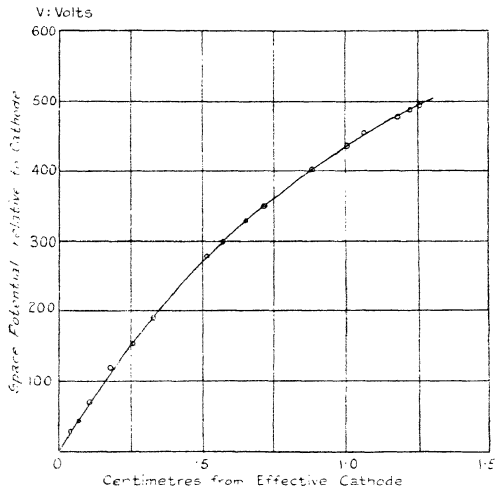

The distance between cathode and effective cathode is 0·02 cm.
The data for this curve will be found in Tables I. and II. No. 17.

$\sigma\ px$ is known, and so from the graph we can get kpx and hence k. The values of k, K, V′, and p are now all known, and are substituted in equation (4), and the curve of V against x computed and drawn.

Owing to the nature of Morse's equation, involving as it does three terms including an exponential, there is some latitude in choosing the value of V′ (see below), and of course k and K vary in consequence. This, taken in conjunction with the difficulty of drawing a tangent at the

effective cathode, rendered it necessary to test the values obtained in each case, by drawing the theoretical and experimental curves. If the agreement was not satisfactory the values were recalculated. In all cases excellent agreement was finally obtained between the calculated curve and the experimental points. One of the curves is shown in fig. 4, where the line is the computed curve, and the dots are the experimental values.

TABLE II.

No.	V′.	*k*.	K.	*p*.	E_a.	Gas.
5	270	15·6	4·5	·107	·288	Argon.
6	290	15·9	4·7	„	·295	
7	227	14·0	3·3	„	·235	
8	340	16·0	4·6	„	·285	
9	230	26·3	7·7	·055	·293	
10	275	28·7	7·0	„	·243	
11	330	34·0	4·5	„	·132	
12	376	33·4	4·46	„	·133	
17	480	48·8	7·3	·026	·149	Nitrogen.
18	385	46·4	7·6	„	·163	
19	515	41·9	8·1	„	·193	
20	206	17·1	1·14	·123	·067	Neon.
21	248	15·9	2·5	„	·156	
24	341	22·5	5·4	·074	·239	
25	261	20·7	4·3	„	·207	
27	288	21·7	4·5	„	·206	

V′ is in volts and p in centimetres of mercury.

The cathode fall of potential can therefore be represented by Morse's equation between the effective cathode and the negative glow. At the cathode edge of the glow the equation breaks down *.

When several of the potential-distance curves for a given pressure and gas are drawn on the same scale, we find that,

* Morse gives the value of the field at the point of breakdown as $V'kp$. This is incorrect, as it involves the assumption that at the end of the dark space e^{-kpx} is negligible, which we know (Table II.) is not the case.

as we should expect, the field at the end of the dark space decreases as the tube voltage decreases, the point of breakdown of the dark space curve on passing into the negative glow becoming less sharp as the cathode fall of potential approaches the normal fall for the material of the cathode (see, for example, fig. 2).

The values found for the quantities in the equation are given in Table II.

In the table the pressure p is in centimetres of mercury and V′ in volts.

V′ is not the normal fall of potential, as it was found that the normal fall was too low to admit of the equation fitting the curves. The value used was 11/12 of the voltage across the tube, which was less than the actual fall across the cathode dark space as shown by Langmuir characteristics taken in the negative glow, but was greater than the normal cathode fall in all cases except those at very low voltage. The fraction 11/12 was found by trial to be a suitable value.

Discussion.

From Table II. it may be seen that k is nearly constant for a given gas at a fixed pressure. Beyond this there is nothing definite, but there are two possibilities. The first is that kp is a constant for a given gas. For runs 5–8, kp has an average value of 1·65, while for runs 9–12 the average value is 1·68. In nitrogen the average value of kp is 1·19. The values of k in neon, however, change very little with pressure.

The second possibility is that k is nearly constant for a given gas, and almost independent of pressure. In this case we should have to assume that some impurity got into the gas when the pressure was changed between runs 8 and 9. It is highly probable that neither of the above suggestions is strictly true, but that, as is indicated below, k is influenced considerably by both pressure and the degree of purity of the gas.

Since k is nearly constant, the value of N ($=3k/2$) is also nearly constant for a given gas at a fixed pressure. According to Townsend, N is the number of ionizing collisions made by an electron per centimetre of path, in a field of 1 volt per cm., the pressure being 1 mm. of mercury. Since it is known that pressure influences the rate of

removal of excited atoms, we might expect some variation from Townsend's values *. N is also dependent on the purity of the gas.

The observed values of N, expressed in Townsend's units, are of the same order of magnitude as those given by him. Values for different gases are given in the following table :—

TABLE III.

Gas.	Argon.	Nitrogen.	Neon.	Helium.
Townsend's value of N ...	13·6	12·4	—	2·8
Observed value of N	3·4	6·8	2·9	—

Observed values of N were obtained from average values of k in Table II.

Townsend does not give a value for neon, but the value he gives for helium is close to that found for neon. Considering also that we measure the density of the gas only indirectly by means of the pressure, the agreement in this table is good evidence in favour of Morse's theory.

The value of K shows little regularity and is not of obvious theoretical significance. Its value is always considerably less than that of k, their ratio being roughly as 1 : 5. E_a therefore does not vary a great deal from 0·21.

The total space charge per sq. cm. between two layers parallel to the cathode surface whose distance apart is $(a-b)$ can be determined from Poisson's equation.

Since

$$\frac{d^2V}{dx^2} = -4\pi\rho,$$

we have

$$\left[\frac{dV}{dx}\right]_b^a = -4\pi\int_b^a \rho.dx = \left(\frac{dV}{dx}\right)_a - \left(\frac{dV}{dx}\right)_b,$$

and therefore

$$\int_b^a \rho.dx = \frac{1}{4\pi}\left[\left(\frac{dV}{dx}\right)_b - \left(\frac{dV}{dx}\right)_a\right].$$

If we measure the slope of the potential-distance curve at two points distant a and b respectively from the cathode,

* Townsend, 'Electricity in Gases,' p. 295 (1915).

we can determine the mean space charge per c.c. between these points. The slope can be determined either from Morse's equation by differentiating and substituting the appropriate constants obtained from our experimental data, or directly by drawing a tangent to the experimental curve.

Referring again to figs. 2 and 3, it is evident that we can do no more than suggest the form of the curve between the cathode and the experimental points. For this reason it is impossible to measure the total space charge between the cathode and the negative glow, although the variation of space charge from the beginning of the experimental curve to the negative glow can be studied.

TABLE IV.

No. 5...	x	·1	·2	·3	·4	·5	·6	·7		
	E.....	510	454	402	362	324	294	270		
	ρ	·169	·143	·121	·102	·087	·073	·062		
No. 11...	x	·1	·2	·3	·4	·5	·6	·7	·8	·9
	E.....	594	508	436	373	323	284	247	221	198
	ρ	·254	·210	·175	·145	·120	·100	·083	·069	·057
No. 17...	x	·1	·3	·5	·7	·9	1·1	1·3		
	E.....	629	509	413	341	283	240	206		
	ρ	·181	·140	·109	·084	·065	·051	·039		
No. 21...	x	·1	·2	·3	·4	·5	·6	·7	·8	·9
	E.....	476	404	347	300	258	226	201	179	161
	ρ	·164	·135	·111	·091	·075	·062	·051	·042	·034

x is in centimetres. E in volts per cm. ρ in e.s.u. per c.c.

From Morse's equation we have, by differentiating,

$$\mathrm{E}=\frac{d\mathrm{V}}{dx}=\mathrm{V}'(kpe^{-kpx}+\mathrm{K}p) \quad . \quad . \quad . \quad . \quad (5)$$

and

$$-4\pi\rho=\frac{d^2\mathrm{V}}{dx^2}=-\mathrm{V}'k^2p^2e^{-kpx}.$$

When the appropriate values of V', k, K, and p are substituted in the above equations, we can draw up a table showing the variation of field and space charge as x is increased. Such a table of values obtained from the data for several of the given curves is shown in Table IV.

Values of field obtained by measuring a series of slopes on the experimental curve for run 17 are plotted against the distance from the cathode in fig. 5 *a*. In the same figure, curve (*b*) shows the corresponding space charge distance curve, the data for which were obtained by measuring the slopes at different points on curve (*a*). Leaving out of consideration the region between cathode and effective cathode, it will be observed that the field has its maximum value a short distance out from the

Fig. 5.

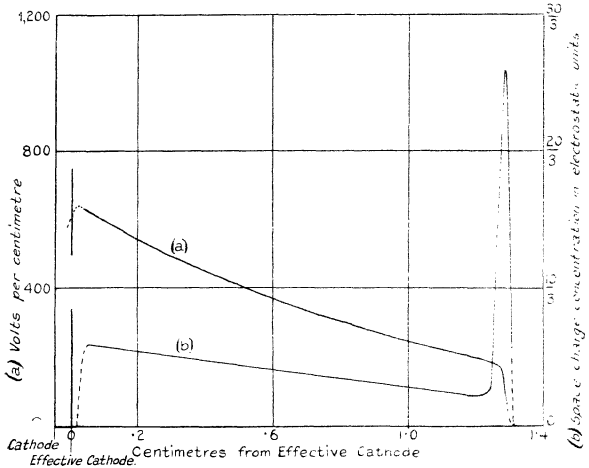

cathode, and falls gradually to less than one-third of this value at the cathode edge of the negative glow, when it drops rapidly to zero in the negative glow. Curve (*b*) indicates that the positive space charge concentration prevailing throughout the greater part of the dark space decreases almost uniformly to less than half its initial value between the effective cathode and the negative glow edge. Between this point and the middle of the negative glow the positive space charge varies rapidly, at first increasing to from 4 to 6 times its average value over the dark space, and then falling to zero.

Regarding the space between the cathode and the effective cathode, it is evident that there must be at least one point of inflexion on the potential distance curve; that is, the space charge curve must pass through zero. This is indicated by the dotted line. There may, of course, be two points of inflexion, giving a positive space charge on the cathode surface, with a negative space charge farther out, and then the main dark space. This is discussed later.

The sudden change in space charge concentration in curve (*b*) marks the point where Morse's equation ceases to hold. It is impossible to mark off the boundaries of this layer of high positive space charge accurately in many cases since the point where the curve turns over to run parallel to the distance axis is not very definite. The average estimated thickness of the layer is 1 mm., while the space charge concentration in it is approximately three times the mean space charge over the region to which the equation is applicable.

Miss N. M. Carmichael * in some recent work in this laboratory, has shown that on the cathode side of the negative glow maximum, and between it and the feeble luminosity in the cathode dark space, there exists a dark layer. This dark space has not yet been observed in any gas other than oxygen. Voltage-current characteristics taken near this dark space show a change in form as the collector is moved through it. It is probable that if a similar dark space should subsequently be found in other gases, it will correspond in position to the breakdown of the cathode dark space potential-distance curve.

Emeléus and Carmichael † have given reasons for supposing that there is a positive space charge on the cathode surface. Now a positive space charge is indicated when the potential distance curve is concave to the distance axis. If this is so, consideration of the curves for argon in fig. 2 shows that the curve between the cathode and the experimental points should have two points of inflexion. All the curves drawn from the observations in neon, of which fig. 3 is an example, show at least one point, that nearest the cathode, which does not lie on the smooth line through the others.

* Carmichael, Phil. Mag. viii. p. 362 (1929).
† Emeléus and Carmichael, Phil. Mag. v. p. 1039 (1928).

The dotted lines in figs. 2 and 3 show the most obvious ways of drawing the curves between the cathode and the experimental points, taking into consideration only the actual distribution of the points themselves. At first sight it would appear that the observations in neon would justify us in drawing the initial parts of the curves in such a way as to be in accord with the idea of a positive space charge immediately in front of the cathode surface. The absence of a corresponding point in argon and nitrogen would, however, be difficult to account for.

Again, when we consider the difficulty of making an observation of balancing potential close up to the cathode surface, a task which, while troublesome in all cases, is especially so in the case of neon, in which a primary dark space is visible (for example, Pl. XVII. fig. 6), we are inclined to attribute the position of the first point to an experimental error. The presence of the primary dark space means that the shadow to the cathode side of the collector is shorter by the width of the dark layer, with the result that the first reliable reading, other things being equal, is somewhat farther from the cathode in cases where a primary dark space is visible. On the other hand, the point always appears on the same side of the main curve, seeming to indicate that any experimental error in determining its position is not of great account.

Taking into account all these facts, we do not think our results in this region afford decisive evidence either for or against the existence of a positive space charge on the cathode surface.

The presence of a layer or layers of space charge near the cathode surface must almost certainly be associated in some way with the production of the Aston or primary dark space. From the fact that the effective cathode had to be taken at some distance out from the cathode in most cases, whether a primary dark space was present or not, we think we are justified in supposing that some, at least, of the conditions necessary for the production of a primary dark space must obtain in all glow discharges. Provided that a similar argument holds in the case of the dark space near the negative glow, it appears that the potential-distance curve can be expressed in the form of the equation given by Morse, if we consider only that part of the cathode dark space proper lying between these two more intensely dark regions. The effective cathode is not, however, at

the cathode potential, and so there must be some modification of the curve in the transition region between the primary dark space and the main dark space.

The sheath surrounding the collector in neon is very interesting, as it is the first indication we have had of anything resembling the ordinary positive ion sheath in the cathode dark space. The characteristic curve affords no evidence either for or against the existence of a positive ion sheath round a collector in the dark space, for, although the curve obtained at potentials negative to that of the surrounding space has a form compatible with the presence of such a sheath, we know that the grid characteristic of a valve, in which the grid is not limited in its influence by a positive ion sheath, has a similar form. A photograph taken in neon, when the collector potential was negative to the surrounding space, is shown in Pl. XVII. fig. 6. A further investigation of sheath formation in the dark space is contemplated.

To summarize our results: by means of the shadow method, a continuous distribution of potential has been found from close upon the cathode to the negative glow. This in itself is important, as we do not have to account for an anomalous distribution of potential of the type of the "Kathodensprung" either near the cathode or at the boundary between the cathode dark space and the negative glow, where our curve passes continuously into the Langmuir curve of potentials for the negative glow itself. Although, as indicated previously, there is some latitude in the choice of the values of V', k, and K in Morse's equation, yet the agreement of the values of N with those obtained by Townsend is strong evidence in support both of the substantial accuracy of Morse's theory of the dark space and of our methods of observation. Nevertheless, owing to the complex nature of the problem of the cathode dark space, we have thought it best to give in detail a large part of the data obtained, so that, should any further theory be worked out, a preliminary test will be available.

Summary.

1. Details are given of some markings observed on the cathode when an obstacle, or collector, is placed in the cathode dark space.

2. A new method of determining space potentials in the cathode dark space is put forward, based on the behaviour of shadows thrown by a wire inserted in it. Values of the potential obtained in the dark space by this method and in the negative glow by Langmuir's method give a continuous curve from near the cathode potential right into the negative glow, for cathode falls in potential between 220 volts and 560 volts.

3. The results obtained conform to a theoretical expression given by P. M. Morse, connecting space-potential and distance from the cathode, provided we measure distance from an " effective cathode," about half a millimetre from the cathode surface, and choose suitable constants.

4. The constants in Morse's equation involve N, the number of ionizing collisions of an electron per centimetre of path under given conditions. Values of N obtained from our data are shown to be of the same order as Townsend's values.

5. Space-charge and electric field conditions over the dark space are discussed.

We are indebted to Dr. K. G. Emeléus for suggestions made during the course of the investigation, and for help in the preparation of this paper.

Key to Plate XVII.

Figs. 1–3 show the form of shadows thrown by a wire inserted in the cathode dark space of the glow discharge and charged to different potentials.

The photographs were obtained with argon, with a tube voltage of 470; the potential of the wire relative to the cathode was 228 volts in fig. 2 and 62 volts in fig. 3. In fig. 1 the wire was insulated. The dark space was 1 cm. in width. The photographs have been enlarged two diameters and only a small part of the cathode is shown.

Figs. 4 and 5 show markings produced on that part of the cathode in shadow. In fig. 4 the molybdenum wire causing the shadow was parallel to the cathode surface and at a distance from it of 0·48 cm. The cathode dark space was 0·7 cm. in width. The wire was charged to a potential 380 volts positive to the cathode, while the tube voltage was 440 volts. The diameter of the wire was 0·01 cm. and the width of the marking 0·11 cm.

In fig. 5 the wire was of copper-clad nickel-iron and was inclined to the cathode surface at an angle of 30°. The potential applied to the wire was 240 volts, while the tube voltage was 490.

Fig. 6 shows a bright sheath round the wire formed when its potential was negative to the surrounding space. The discharge in this case was in neon and shows a well-marked primary dark space.

XCIX. *Problems of determining Initial and Maximum Stresse in Ties and Struts under Elastic or Rigid End Constraints*

By W. H. Brooks, *B.Sc., Ph.D.(Eng.) Lond.**

Introduction.

In practice it may often be very desirable to know the minimum and maximum stresses to which any particular tie or strut may be subjected when forming part of a given structure and consequently stressed by irremovable dead loads.

The stresses taken in designing the tension and compression members of many framed structures are commonly based upon the assumptions of pin-jointed ends and negligible deformation of the configuration of the structure when loaded, but faulty workmanship, coupling adjustment, or a slight alteration or configuration, due to the loads or to the subsidence of a support, may set up stresses only determinate by direct experiment, and in extreme cases of subsidence, even reversals of stresses in certain members may result.

Methods for determining the stresses in thin wires and slight swaged rods—as the bracing wires and raf-wires of aeroplanes—are known [1] to [6], but the application is limited to members whose transverse dimensions are small as compared with their lengths. Instruments are in use [7] to [10] which are applicable to members of larger cross-sectional areas; but these indicate only incremental stresses by the direct measurements of strains in the usual cases where the initial loads cannot be reduced to zero, which fact often appears to be overlooked.

The objects of the author are (*a*) to show how, by using any suitable one of the three methods introduced later, it is possible to find the stress (due to irremovable loading) existing in a tie or strut of uniform cross-section having its ends constrained by hinges or clamps; (*b*) to indicate by Stress Charts how most of the equations established may be readily solved; and (*c*) to experimentally verify some of the cases discussed.

The following methods are confined to the determination of initial direct stress, set up by a longitudinal end load F,

* Communicated by the Author. Section of Thesis approved for the Degree of Doctor of Philosophy in the University of London. (Copies of the complete Thesis are deposited in the University Library, South Kensington.)

to which—at any particular cross-section—would be added any secondary bending stresses due to lateral loading or to eccentricity of end load, both of which may co-exist with P. Methods for calculating such secondary stresses are fully discussed in standard books on materials.

The direct stress f_d at any section $= \frac{P}{A}$, where A is the cross-sectional area, and f_d will have its minimum or maximum values according as P has its initial and lowest value P_a or its highest value when increased by incremental temporary loading ;

$$i.e.,\ f_d \text{ min.} = \frac{P}{A},$$

$$f_d \text{ max.} = (P_a + \text{incremental P})/A.$$

In this latter expression the magnitude of the second term may be determined by the strain gauges in use ; hence, when P_a is known, f_d max. is also known. Alternatively, f_d max. may be found direct by the application of one of the following methods to the member under maximum load conditions.

Principles and Preliminary Argument.

The underlying principles herein involved in the determination of these direct stresses are briefly as follows :—

The member, whether tie or strut, is very slightly flexed by the temporary application of either lateral known forces or known couples of magnitude sufficient to give the smallest deflexions or slopes that can be accurately measured. The test readings taken are then treated as described under "General Procedure."

These deflexion and slope effects are known to be proportional to the disturbing causes in the isolated cases of members having their ends either simply supported or *encastré* with no end load. They are also proportional—as will be seen from the equations established later—when the end load remains of constant magnitude during the flexing of the member. When, however, the end loads are applied through strong end constraints, the process of flexing may be expected to result in altered reactions of the constraints with consequent alteration of the direct stress induced in the member, and, if the initial end load is large (in the case of a tie it may be many multiples of the crippling load for the

same member when used as a strut), this effect may be apparent for comparatively very small deflexions.

Consider a tie A, B under initial tension $= P_a$ (fig. 1), caused by the reaction of elastic end constraints, for which the springs A, C and B, D are simple substitutes. C and D are at a fixed distance apart. When a slight flexing is given to A, B, as shown exaggerated in fig. 2, the effect will be a reduction of the original length to, say, $(l - \delta l)$, so forcing the springs to slightly elongate, and thereby increasing P_a to, say, $P_a + \delta P = P$ in fig. 2.

Thus, in the case of a tie under end loads applied through elastic constraints, the effect of flexing is increased tension. Conversely, in the case of a strut, the effect of flexing is reduction in compression, as may readily be seen by replacing A, C and B, D by compression springs.

Fig. 1.

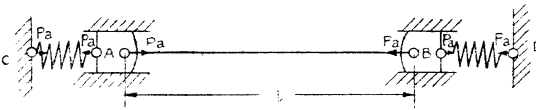

Fig. 2.

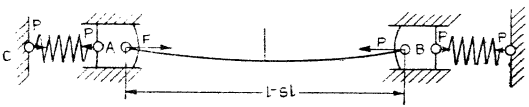

In the case of a tie or strut having its ends fixed by rigid constraints, the flexed axis length is greater than the length (l) of the unflexed axis, and, assuming the yield of the end clamps to be negligible, it may be shown that the longitudinal strain of the flexed axis is *increased* by

$$\frac{1}{2l}\int_0^l \left(\frac{dy}{dx}\right)^2 dx,$$

with consequent *increase* in the *tension*, or *decrease* in *compression*, according to whether the member is a tie or a strut:

$$= \frac{EA}{2l}\int_0^l \left(\frac{dy}{dx}\right)^2 dx,$$

where the symbols have their usual meaning, and the origin is taken at one end of the member.

In all cases it should therefore be assumed at the outset that, directly a member is flexed, the initial end load will be altered in some unknown varying manner, and the problem is to find the magnitude of the initial load that exists before any temporary alteration is induced by flexing.

General Procedure and Further Argument.

The general experimental procedure is as follows:—A few values of either the disturbing force or the disturbing couple are chosen as independent variables "X," and the corresponding values of "Y," either of the deflexion or of the slope at a particular point, are experimentally determined, tabulated, and plotted, as indicated by the curve B, B_1 in fig. 3.

Fig. 3.

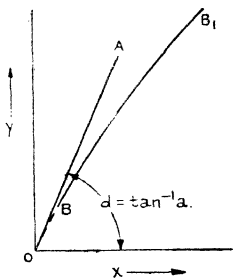

Now the ratio $\frac{Y}{X}$, established in each of the various cases dealt with later, is a function of the end load P (assumed variable with flexure), and holds for all values of P.

When the initial value of $P=P_a$ required, $Y=0$ and $X=0$; or the initial magnitude of the ratio $\frac{Y}{X}=\frac{0}{0}$, and is a definite value $=$"a," say, for each set of conditions.

The value of "a" is given by the slope of the curve B, B_1 when extended backward to the origin, as shown by the broken line in fig. 3; *i.e.*, "a" $=\tan \widehat{AOX}$, and may be calculated from the curve B, B_1 or approximately determined graphically.

Having determined this value of "a"—*which hereinafter*

will for each case treated be referred to as "the initial derivative of the X, Y *graph," or more shortly as "the* X, Y *derivative,"*—it is substituted for $\frac{Y}{X}$ in the equation for the particular method used, and the equation is then solved for l'_a by approximation or by graph. (For graphical solution methods, see Stress Charts later.)

For example, in the case of a tie with pinned ends flexed centrally through distance δ by a central load W (as dealt with in case A and illustrated in fig. 4, *quod vide*), the general equation is

$$Y/X=(L-\tanh nL/n)/2P$$

and "a" $=(L-\frac{1}{n_a}\tanh n_aL_a)/2P_a$. (*Tie equation* A_δ.)

Fig. 4.

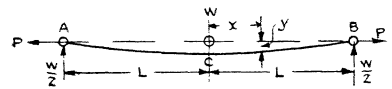

To facilitate its solution by Stress Chart I., this equation is written

$$2Pa=L-\tanh nL/n,$$

the suffix (small a) being suppressed for simplicity.

In the equations, P_a is expressed for simplification in terms of

$$n_a=\sqrt{P_a/EI},$$

where EI is the flexural rigidity of the member at right angles to the plane of flexing, and should be made the smaller possible value if the member be not of circular cross-section.

Thus P_a required $=n^2_aEI$, and during bending $P=n^2EI$, where $P \gtrless P_a$ according as the member is a tie or a strut.

To determine Expressions for Y/X *for Ties flexed by various Methods.*

Method 1 A :—

Consider a straight uniform tie A, B of length $2L_a$ pin-jointed at the ends and strained by an initial end load P_a.

When a concentrated lateral load W is applied at mid-span to produce a small deflexion in a transverse direction, assume P_a to be increased by elastic constraints at A and B to a value P, and the unflexed span to be slightly decreased to 2L, as shown in fig. 4.

Taking an origin O at mid-span on the line of action of P, and considering the deflexion y at $+x$ from O as negative, and therefore the bending moment for the curvature shown as of positive sign [11],

$$M_x = W(L-x)/2 + Py = EI\frac{d^2y}{dx^2}, \quad . \quad . \quad . \quad (1)$$

where the symbols have their usual meaning.

Let $$P/EI = n^2.$$

Then $$d^2y/dx^2 - n^2y = WL/2EI - Wx/2EI. \quad . \quad . \quad (2)$$

The general solution to equation (2) is

$$y = A\cosh nx + B\sinh nx + Wx/2P - WL/2P. \quad . \quad (3)$$

From equation (3) it follows that

$$\delta \text{ max. at } C = W(L - \frac{1}{n}\tanh nL)/2P \text{ as measured} \quad . \quad (4)$$

or $$\delta/W = (L - \frac{1}{n}\tanh nL)/2n^2EI \quad . \quad . \quad . \quad . \quad (5)$$

Here $\delta = Y$ and $W = X$ referred to in the "General Procedure."

Thus initially, when $\delta = 0$ and $W = 0$, equation (5) becomes

$$0/0 = a = L_a - \frac{1}{n_a}\tanh n_aL_a)/2n_a^2EI. \quad (\textit{Tie equation } A_\delta.)$$

(where L_a is the initial unflexed half-length),

or $$2n_a^2EI \,.\, a \,.= L_a - \frac{1}{n_a}\tanh n_aL_a). \quad . \quad . \quad . \quad (6)$$

Equation (6) when solved for n_a by trial or graph yields $P_a = n_aEI$, which is sought.

Graphical equations to equation (6) may be readily obtained from the wide range of "A values" given in Chart I.

To obtain a solution from this chart, the curves plotted from generating equation A are used—which is equation (6), wherein the suffix a is suppressed for simplicity. Having obtained experimentally the "initial derivative a," the corresponding value of EIa is located along the A values up the ordinate through $n^2=0{\cdot}05$ on the abscissæ and the polar ray drawn—preferably on tracing-paper—through the point to the origin. The intersection of this ray with the appropriate L curve, interpolated from the vertical scale on the

CHART I.

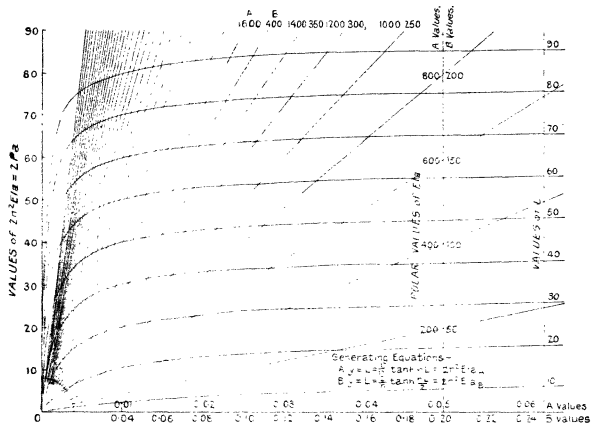

Stress Chart for Ties A and B by deflexion.

extreme right of the chart, locates a point vertically above the value of n_a^2 sought along the abscissæ scale of A values.

The initial direct stress (f_d) is thus found, since

$$f_d = P_a/A = n_a^2 EK^2,$$

where K is the radius of gyration of the cross-section of the member.

A simpler expression which may be used for an approximate solution is obtained by writing equation (6) as

$$2n_a^2 EIa = (L_a - 1/n_a) \quad . \quad . \quad . \quad . \quad . \quad (7)$$

since $\tanh n_a L_a$ rapidly approaches unity for values of $n_a L_a >$ about 4 ; and this value will be easily exceeded in ties of fair length and cross-section under moderate stresses : *e. g.*, for a tie-rod of mild steel 1 inch in diameter in which $f_a = 10{,}000$ lb. per square inch, $E = 30 \times 10$ lb. per square inch, and $L = 60$ inches,

$$nL = 4{\cdot}392.$$

For $\frac{3}{4}$ in. tie-rod of the same length under the above stress,

$$nL = 5{\cdot}850.$$

It should perhaps be here observed that the equations obtained in the foregoing case, and in all the following cases with hinged ends, are based upon the assumption that no friction couples exist about these transverse axes of constraint, and that results arising from this theoretical condition may, of course, be easily obtained in experimental work where friction slipping about the pins occurs, by taking two series of Y values : one series for increasing values of X, the other for decreasing values of X, so that the effect of friction may be neutralized by plotting the series of mean Y values against the one series of X values.

Fig. 5.

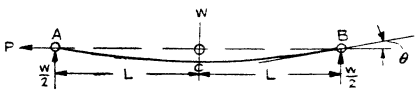

Method 1 A. *Alternative* :—

If, instead of measuring the deflexion at C, the slope (dy/dx) be measured at either end, as shown at B in fig. 5, we shall get

$$dy/dx = \theta(\text{say}) = W(\tanh nL \,.\, \sinh nL - \cosh nL + 1)/2P$$
$$= W(1 - \operatorname{sech} nL)/2P = W(1 - \operatorname{sech} nL)/2n^2EI, \quad (8)$$

or

$$d\theta/dW \text{ (initially)} = a = (1 - \operatorname{sech} n_a L_a)/2n_a{}^2EI.$$

(*Tie equation* A) ;

$$i.e., \; 2n_a{}^2EIa = 1 - \operatorname{sech} n_a L_a. \quad . \quad . \quad . \quad (9)$$

Here "a" is found by treating θ as Y, and W as X, as described in the "General Procedure." A graphical solution for n_a, and hence for P_a, may then be found by the aid of Chart II.

To use this chart, the experimental value of "a" having been found, the polar value of $1000\,EIa/L^2$ is next located up the ordinate through $n^2L^2=20$, or located along the top of the chart where these polar values are extended; then the polar ray is drawn. The point of intersection of this ray with the "A curve," projected on to the abscissa scale, gives the solution to n^2L^2, and thus to the solution of P.

Now, as nL increases, such nL rapidly decreases from

CHART II.

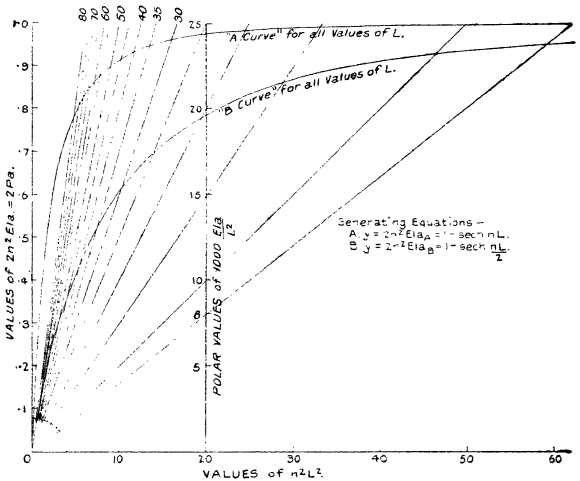

Stress Chart for Ties A and B by slope.

unity to a very small fraction, and, when nL > about 6, equation (9) may be written

$$a \doteqdot 1/2n_a^2EI \doteqdot 1/2P_a, \quad \text{or} \quad P_a \doteqdot 1/2a. \quad . \quad . \quad (10)$$

This is clearly shown by the "A" curve of Chart II.

Method 1 B :—

As in Method 1 A, but with ends constrained by fixing couples M, M in the line of action of P, instead of being pin-jointed. (See fig. 6.)

Using the same sign conventions as in Method 1 A, the bending moment at $+x$ from the origin O=

$$M_x = W(L-x)/2 + P.y - M = EId^2y/dx^2, \quad . \quad (11)$$

or $$d^2y/dx^2 - n^2y = (WL/2 - M)/EI - Wx/2EI. \quad . \quad (12)$$

The general solution to equation (12) is

$$y = A \cosh nx + B \sinh nx + Wx/2P + M/P - WL/2P . \quad (13)$$

Fig. 6.

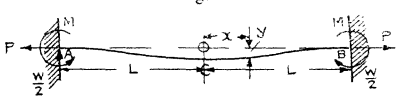

From this it follows that numerically at C, remembering that y is negative,

$$\delta = -y_0 = W(L - 2n . \tanh nL/2)/2n^2EI ; \quad . \quad (14)$$

i. e., initially,

$$\delta/W = 0/0 = a = \frac{1}{2n_a^2EI}\left(L_a - \frac{2}{n_a}\tanh n_aL/2\right). \quad (15)$$

(*Tie equation* B_δ.)

Graphical solutions to this equation are given by the B values of Chart 1. In this case the solution to n^2 is located along the abscissa scale of B values by interpolation from the appropriate polar ray of EIa(B) values, and the curve of L as described for the corresponding Method 1 B.

Fig. 7.

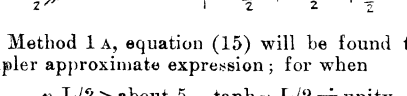

As in Method 1 A, equation (15) will be found to reduce to a simpler approximate expression; for when

$$n_aL/2 > \text{about } 5, \quad \tanh n_aL/2 \doteq \text{unity},$$

and the above equation becomes

$$2n_a^2EIa \doteq (L - 2/n_a). \quad . \quad . \quad . \quad . \quad . \quad (16)$$

Method 1 B. *Alternative*:

By measuring the slope θ at L/2 from the origin, instead of the deflexion δ at the middle. (See fig. 7.)

From equations (11) and (13) we get

$$M_x = W(\tanh\frac{nL}{2}\cosh nx - \sinh nx)/2n \quad . \quad . \quad (17)$$

$$= 0 \text{ when } x = L/2 ;$$

i.e., the point of inflexion and therefore of maximum slope $= \theta$ occurs at $\frac{1}{4}$ span from either end.

Also from equation (13)

$$dy/dx = \frac{W}{2P}(\tanh\frac{nL}{2}\sinh\frac{nL}{2} - \cosh\frac{nL}{2} + 1) = \theta$$

$$= W(1 - \operatorname{sech} nL/2)/2P. \quad . \quad . \quad . \quad . \quad . \quad . \quad (18)$$

Thus "a" here $= d\theta/dW$ (initially) $= (1 - \operatorname{sech} n_a L_a/2)/2n_a^2 EI.$

(*Tie equation* B_θ). . . . . (19)

Graphical solutions to equation (19) may readily be found from the B curve of Chart II., which has been drawn to cover a very wide range. A solution to n^2L^2 is obtained from this chart by the intersection of the "B" curve for all values of L, with the polar ray given by the determined value of "a" in a similar way to that described for Method 1 A. Alternative.

In passing, it may be noted that for values of $nL >$ about 12, $\operatorname{sech} nL/2$ is a very small fraction, and therefore equation (19) becomes

$$a \doteq 1/2P_a \quad \text{or} \quad P_a \doteq 1\ 2a \text{ as in Method 1 A.}$$

It is important to observe that in all cases, only the the smallest possible measurable values of Y and X are necessary for the determination of the XY derivative, so that the range of cases as regards rigidity to which these flexing methods are applicable is controlled by the problem of accurate measurement or magnification.

The complete Thesis contains detailed descriptions of flexing apparatus designed by the author to test the applicability of the theoretical expressions established here, and others of much more general utility established later. The results obtained therefrom show that remarkable agreements exist between the theoretical and the practical results.

Units.

It will be observed that throughout the series of stress charts (there are twelve in the complete series) units of force and of length are suppressed thereon. The reason for this

suppression lies in the fact—as a moment's consideration will show—that the charts hold for any system of consistent units whatsoever, and, since the quantity E is compounded of units of both force and length, the particular units applicable to any experimental determination will be those taken for E. Thus, if E is taken in pounds per square inch, length values (L) must be read off in inches, load values (P) in pounds, stress values (f_d) in pounds per sq. inch, and second moment of area values (I) in inches^4, or radius of gyration values (K) in inches. If E is taken in kilograms per square millimetre, L must be read off in millimetres, P in kilograms, f_d in kilograms per square millimetre, I in millimetres^4, or K in millimetres.

In this way, and by a judicious choice of units—although on some of the charts only a few curves for L have been drawn,—these curves may be used for a number of actually different lengths by the expedient of altering the units of length to suit a chosen curve, thereby considerably extending the range of the chart used.

References.

(1) "Tension Meters.—II." By Dr. A. H. Stuart. 'Model Engineer and Electrician,' p. 245, Feb. 28, 1924.
(2) "An Acoustic Tension Meter." By Dr. A. H. Stuart. Journal of the Royal Aeronautical Society, Feb. 1923, vol xxvii. no. 146.
(3) "Tensiometer for measuring Tautness of Airplane Wires and Cables." Miscellaneous Publications of the Bureau of Standards, no. 26, pp. 38–40, April 1, 1921.
(4) "Mechanical Testing.—I. and II." By Batson & Hyde. D. U. Technical Series. Chapman & Hall.
(5) "Apparatus for measuring the Tension in Taut Wires.—Tautness Meter." Cambridge & Paul Instrument Co. P. 429 in ref. 4 above.
(6) "The Larson Tautness Meter." Developed by L. J. Larson. P. 430 in ref. 4 above.
(7) "The Tudsbery Stress Indicator." C. F. Casella & Co., Ltd., London.
(8) "Bureau of Standards' Telemeter for recording Strains in Bridges." 'World Power,' p. 254, May 1924; and Journal of Soc. of Automotive Engineers, p. 582, June 1924.
(9) "Measurement of Movements and Stresses in Structures," chap. xviii. Bib. 4, above.
(10) "The Fereday-Palmer Stress Recorder." 'Notes on the Analysis and Testing of Bridges.' By Mr. Fereday.
(11) "Sign Conventions applied to Flexing Problems." By the author. Philosophical Magazine, vol. v. April 1928.

(To be continued.)

C. *Oscillations in Low Pressure Discharge-Tubes.* *By* E. W. B. Gill, *B.Sc., M.A., Fellow of Merton College, Oxford* *.

MANY observers have noticed the occurrence of oscillations when direct current discharges pass in gases at low pressures ; but as no systematic investigation appears to have been made of the phenomenon the following experiments leading to a simple theory were carried out.

The discharge-tube T in the figure, contained two small circular electrodes, about 1 cm. in diameter, whose distance

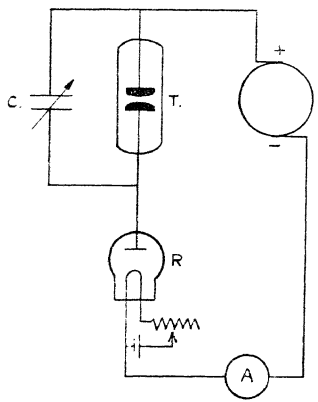

apart could be varied from a fraction of a mm. to about 1 cm. The tube contained air at a low pressure. A standard adjustable air-condenser C was connected externally across the electrodes, and a discharge was passed through the tube from a direct current high voltage dynamo. This current was maintained at any desired value by the insertion in one of the leads to the dynamo of a 2-electrode valve R. The discharge current had to pass across the valve and could therefore be adjusted to any desired value by controlling the temperature of the valve filament.

* Communicated by Prof. J. S. Townsend, F.R.S.

In this arrangement the potential across the discharge-tube is that necessary for the particular current passing, and the remaining potential of the dynamo falls across the valve. It was found that up to a limiting current of the order of 2 or 3 milliamps this discharge, over a very large range of pressures, produced oscillations varying in frequency according to circumstances from a few per second to about 150,000 a second.

The oscillations were detected and their wave-length determined by a single valve self heterodyning wireless receiver graduated in wave-lengths. This receiver was placed a few yards from the discharge-tube, which emitted quite enough energy to produce a loud signal.

The waves emitted were extremely rich in harmonics, and care was necessary not to confuse the fundamental with some of the louder harmonics.

Experimental Results.

In what follows the fundamental wave-length λ was found to depend on the following factors :—

1. The pressure p of the air in the discharge-tube measured in mm. of mercury.
2. The distance d between the electrodes.
3. The current i flowing through the tube.
4. The capacity C of the condenser.

The results of varying one only of these factors keeping the remainder constant were as follows :—

1. *Pressure.*—Oscillations were examined from $p = 85$ to $p=2$. It is difficult to get oscillations below $p=2$, but they can be produced for much higher values than $p=85$. The general effect of a reductionin pressure is a reduction in the wave length but the variation is not large.

2. *Distance between the Electrodes.*—The wave-length λ increases rapidly as the distance is increased: thus for $p=25$, $i=2$ m.a. & C$=110$ cm.; when $d=\cdot7$ mm. $\lambda=2700$ metres; $d=1\cdot1$ mm. $\lambda=4200$; and $d=1\cdot5$ mm. $\lambda=6800$. As the wave-length gets inconveniently large for the larger values of d most of the measurements were made with small gaps.

3. *The Current.*—The current magnitude has a much greater effect upon the wave-length than any of the other factors. Thus for $p=25$ mm. $C=110$ cm., $d=\cdot7$ mm. the corresponding values of i and λ are given below.

i.	λ.	λi.
·5 m.a.	10400	5·2
·75	6850	5·14
1	5250	5·25
1·25	4250	5·31
1·5	3500	5·25
1·75	3000	5·25
2	2700	5·4
2·25	2400	5·4
2·5	2100	5·25

The last column gives the product of i and λ and shows that very approximately $i\lambda=$constant; for small values of i the oscillations are of audible frequency. A large number of sets of observations were made for various values of C and d, and in all cases $i\lambda$ was approximately constant in each set.

4. *The Capacity.*—As the capacity is increased the wave-length increases and the curve giving the relation between C and λ is very accurately a straight line. The line does not pass through the origin and is given by the equation

$$\lambda=k\ (C+c'),$$

where k and c' are constants: c' is small and depends on the current, being larger for the larger currents.

For example, with $p=6\cdot7$ $d=1\cdot1$ mm.; when the current is ·21 m.a. the wave-length increases uniformly, being 8200 metres for $C=15$ cm. and 12,600 metres for $C=40$ cm.; here $c'=30$ cm.

For a current of 1·35 m.a. λ increases from 2500 metres for $C=15$ to 6000 metres for $C=100$: in this case $c'=45$.

The final experimental result is therefore that

$$\lambda=\frac{k(C+c')}{i};$$

k depends only on d and p and increases if either is increased. c' is small and depends chiefly on i and decreases if i is increased.

The following theory appears to be adequate to explain the experimental results :—Suppose that the valve filament is first of all heated to the temperature necessary to allow a current i to pass the valve. At the moment when the external E.M.F. is applied practically all of it falls across the valve owing to its very small capacity. The current i thus commences to flow instantaneously through the valve, and, provided the external E.M.F. is large enough, this current i remains constant whatever happens in the rest of the system.

At the outset the tube insulates, the potential across it being low, and all the current i flows into the condenser, and the potential across it and the tube increases until the sparking potential is reached. At this stage the tube begins to conduct and the current through it begins to grow from zero value ; but as the constant current i is still flowing into the combination a portion of it will still flow into the condenser until the discharge current has grown to the value i. At the instant, therefore, when current ceases to flow into the condenser the potential across it and the discharge-tube *is slightly above the sparking potential*, say v_1.

For air this state of affairs is essentially unstable ; as the sparking potential is higher than that required to maintain a current, the potential cannot remain at v_1, the condenser begins to discharge through the tube, and the current through the tube begins to exceed i.

The relation between E.M.F. and current in a discharge-tube is that for zero current the E.M.F. is the sparking potential, and that as the current is increased the E.M.F. falls till it reaches a certain value v_2 corresponding to a current i_2, after which, however much the current is increased, the E.M.F. remains practically the same.

The superposition of the condenser discharge current upon the current i flowing through the tube runs the potential across the tube down to this value v_2 and the condenser then ceases to discharge, as the P.D across it can fall no further. If i is less than the critical value i_2 the discharge must go out, as the potential v_2 at this instant across the tube will only maintain currents equal to or greater than i_2. If i is equal to or larger than i_2 the

discharge current remains constant, the condenser has no further effect, and no oscillations occur, which explains why no oscillations could be found unless the current was small.

For the small currents the discharge goes out and the current again all flows into the condenser, charging it from v_2 to v_1, at which point it again discharges, after which the process repeats itself indefinitely. The time for the charging is

$$C\frac{(v_1-v_2)}{i},$$

and if the time for discharge is t_0 the total time for one cycle is $C\frac{(v_1-v_2)}{i}+t_0$. But λ is proportional to the total time of one cycle, and since λi was found to be constant if C is fixed, this shows, as might have been expected, that t_0 is indefinitely small; for v_1 and v_2 are constant and independent of i. Thus far, then, it has been proved that

$$\lambda \propto \frac{C}{i}.$$

It remains to account for the constant c'.

At first sight it might appear that stray capacities and the capacity of the electrodes might account for this, but these corrections cannot be more than a few electrostatic units while c' is about 30.

It must be remembered, however, that when the potential across the condenser reaches its maximum value v_1 the gap is discharging, and its capacity is not solely due to the electrodes but is very much increased by the space charges. That this is the correct explanation is borne out by the fact that c' increases if i is increased.

Finally, therefore,

$$\lambda \propto \frac{(v_1-v_2)(c+c')}{i};$$

v_1-v_2 is the difference between the sparking potential and the minimum maintenance potential. This difference is increased if we increase the distance between the electrodes or raise the pressure, which is in accordance with the observed facts.

A simple experiment verified the deduction that t_0 is very small. A hot wire ammeter was placed to read the

current flowing into and out of the condenser. There is no possibility of resonance on the wave-lengths emitted, and the condenser current cannot therefore exceed the current flowing into the system. But when 1 m.a. was flowing through the 2-electrode valve the hot wire ammeter read as much as 30 m.a. This can only occur if the discharge current reaches momentarily a very high value causing the AC instrument to give a reading greater than the DC instrument.

The impurity of the emitted wave is evident from a consideration of the process occurring. The potential across the condenser rises uniformly from v_2 to v_1 and falls instantaneously to v_2 each cycle.

An application of Fourier's analysis indicates that in such a case the amplitude of the nth harmonic is $\frac{1}{n}$ of the amplitude of the fundamental.

The presence of the external condenser is not essential for the production of oscillations, the capacity of the electrodes magnified, as explained by the presence of the space charges, being sufficient to produce oscillations.

It appears, therefore, that any discharge-tube is in a state of oscillation provided that the sparking potential is higher than the maintenance potential and that the current is less than that at which the maintenance potential is independent of the current. At the higher pressures there is a fair range of currents over which oscillations occur, but at pressures of 2 or 3 multimetres they only occur if the current is a very small fraction of a milliampere.

It is scarcely necessary to add that the existence of oscillations in no way depends on the particular method of limiting the current by a valve. If the current is controlled instead by a large resistance oscillations occur equally well, but the calculations are not quite so simple.

Professor Townsend, in whose laboratory the experiments were made, has most kindly given me much advice and assistance.

(*a*)

(*b*)

(*c*)

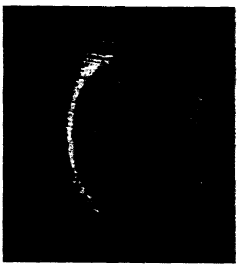

(*d*)

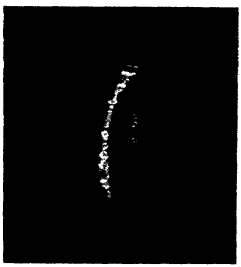

(*e*)

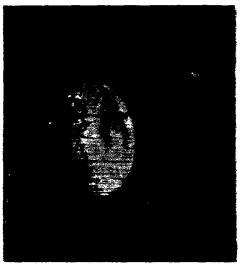

(*f*)

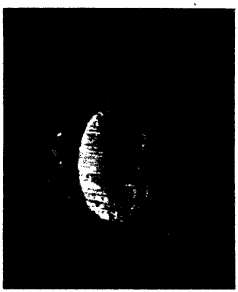

(g)

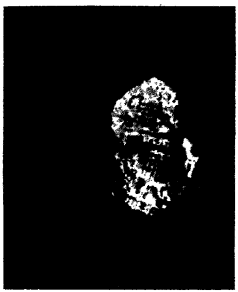

(h)

(i)

(j)

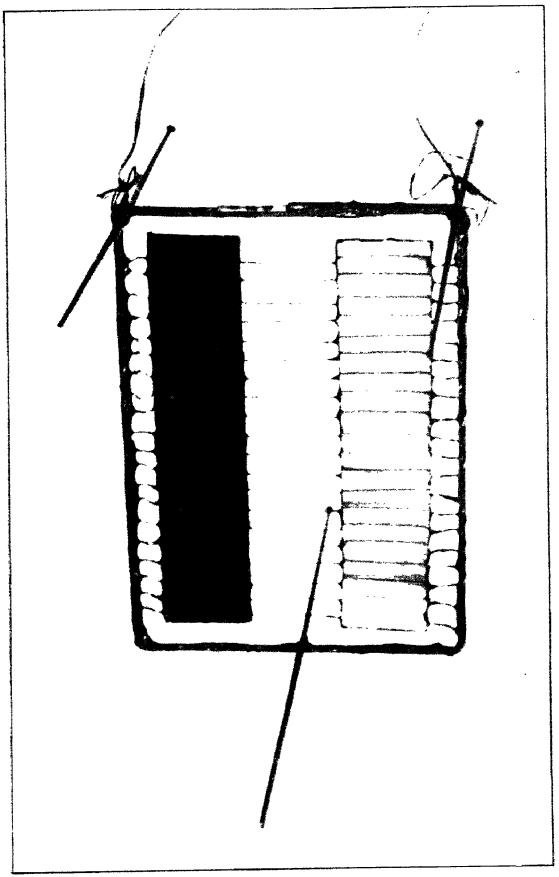

Radiation Instrument.

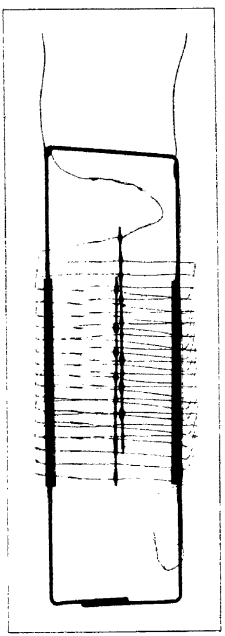

Convection Instrument.

Fig. 1.

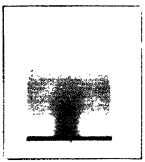

Fig. 2.

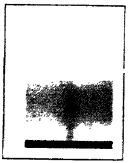

Fig. 3.

Fig. 4.

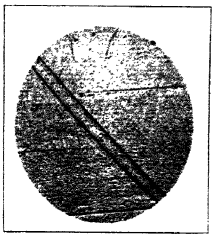

Fig. 5.

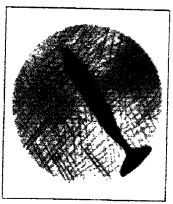

Fig. 6.

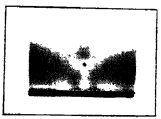

THE

LONDON EDINBURGH, AND DUBLIN

PHILOSOPHICAL MAGAZINE

AND

JOURNAL OF SCIENCE.

[SEVENTH SERIES.]

DECEMBER 1929.

CI. *The Efficiency of Production of Fluorescent X-Rays.*

By ARTHUR H. COMPTON, *Professor of Physics at the University of Chicago* *.

THERE exists a simple theory of the mechanism by which fluorescent X-rays are produced, which gives a definite prediction of the intensity of these rays. According to this theory, when an electron in the K energy level of an atom absorbs a quantum of X-rays, it is ejected as a photoelectron. An electron from the L or outer levels will then fall into the K level, resulting in the emission of a quantum of K series X-rays. For each quantum of energy absorbed by the K electrons there should thus be emitted one quantum of fluorescent X-rays of the K type. The ratio of the absorbed to the emitted rays can thus be directly calculated.

This simple theory has, however, predicted two important results which are inconsistent with experiment. The intensity of the fluorescent X-rays is found not to be as great as this theory indicates ; and the β-rays excited by the X-rays are found to be more plentiful than it predicts. Both of these facts are indicated by the data accumulated

* Communicated by the Author.

by Sadler * and have been emphasized by Barkla † and by Barkla and Dallas ‡.

The Compound Photoelectric Effect and Fluorescent Yield.

A source of difficulty with the theory was made evident by Auger's discovery in 1925 § of the "compound photoelectric effect," *i. e.*, the simultaneous ejection of several β-particles from the same atom. By measuring their ranges ‖ he found that in addition to the photoelectron whose velocity is given by Einstein's equation

$$E_{kin}=h\nu-h\nu_K$$

for absorption by a K electron, there might be emitted from the same atom an electron of energy

$$E=h\nu_K-2h\nu_L$$

and others of a similar type. The total energy of all the β-particles from a single atom was never more than $h\nu$. This observation showed that there are two different processes by which the atom can return to its normal condition. The first process is that in which the energy liberated when the atom returns to its normal state is radiated as a fluorescent ray. In the second process the energy absorbed by the atom is spent in ejecting from the atom one or more electrons. This may be considered either as a kind of internal photelectric absorption, or, as Auger thinks more reasonable, a radiationless energy transfer of the type which Klein and Rosseland describe as an "event of the second kind." Such an event—the transfer of the energy of an excited atom to an electron—has been recognized for some time in optics, and Rosseland had opined ¶ that it should also appear in the X-ray domain. It is clear that the occurrence of events of this second type will result in less intense fluorescent radiation,

* C. A. Sadler, Phil. Mag. xvii. p. 739 (1909); xviii. p. 107 (1909); xix. p. 337 (1910).

† C. G. Barkla, Phil. Trans. ccxvii. p. 315 (1917).

‡ C. G. Barkla and Miss Dallas, Phil. Mag. xlvii. p. 1 (1924).

§ P. Auger, *C. R* clxxx. p. 65 (1925); *J. de Phys. et Radium*, vi. p. 205 (1925).

‖ P. Auger, *Ann. de Physique*, vi. p. 183 (1926).

¶ Rosseland, *Zeits. f. Phys.* xiv. p. 173 (1923). The suggestion that such an event might account for the anomalous ionization and fluorescence by X-rays was suggested by Kossel, *Zeits. f. Phys.* xix. p. 333 (1923), and by Barkla and Dallas, Phil. Mag. xlvii. p. 1 (1924).

and more intense β radiation, which is precisely what is needed to satisfy the demands of Sadler's and Barkla's work.

Auger* has determined the probability that an event involving fluorescence will occur by the direct method of counting the number n of photoelectrons ejected from the K shell of an element (these can be identified for the heavier elements, because the range is shorter than that of a photo-electron ejected from an outer level), and comparing this with the number n_2 of atoms from which go associated tracks of the second kind. The difference $n-n_2$ is the number n_1 of fluorescent quanta emitted. He thus obtains what is known as the "fluorescence yield,"

$$w=n_1/n. \quad . \quad . \quad . \quad . \quad . \quad . \quad . \quad . \quad (1)$$

His results are summarized in the following table:

TABLE I.

Element.	Voltage.	w.
18 A	70 kv	·07
36 Kr	70	·5
	22	·51
54 Xe	43	·71

The experiments on krypton, using two different wave-lengths of primary X-rays, indicate that the fluorescence yield is a property of the atom and is independent of the wave-length of the exciting radiation. It is evident from these results that especially for the lighter elements the compound photoelectric effect is of relatively great importance.

Fluoresence Yield from Measurements of Fluorescence.

It is also possible to determine the fluorescence yield from measurements of the intensity of the fluorescent rays. If the compound photoelectric effect is the sole cause of the difficulty with the simple theory outlined above, the yield thus calculated should be identical with that deter-

* P. Auger, *Ann. de Physique*, vi. p. 183 (1926).

mined by Auger. Kossel * and Bothe † have calculated approximate values of this factor using the fluorescence data given by Sadler and Barkla respectively. Kossel's results are :—

TABLE II.

	24	26	27	29	30
Element	Cr	Fe	Co	Cu	Zn
w	·23	·32	·39	·42	·51

These values are of the same order of magnitude as those of Auger, but vary with atomic number at a surprising rate. Kossel himself evidently does not have much confidence in their reliability, since he remains uncertain whether the experiments really show that w is less than 1. His work is of especial interest, however, in that he was led from these figures to give the first suggestion of atomic transformations of the second kind in order to account for a fluorescence yield less than unity.

The values of w calculated by Bothe, 0·5 for Br and 0·23 for Cr, fit more acceptably than do Kossel's with Auger's data. Jauncey and De Foe ‡ have also made a rough measurement of the ratio of the fluorescent energy from copper to the absorbed rays, leading to a value of the fluorescence yield less than unity.

Since Auger's discovery of the compound photoelectric effect, two measurements of the fluorescence yield have been made, one by Balderston § and one by Harms ‖. Balderston compares the total number of absorbed quanta with the number of fluorescent K quanta, calling the ratio u. Since only about $\frac{7}{8}$ of all the absorbed quanta are absorbed by the K shell, his ratio u must be divided by $\frac{7}{8}$ in order to get the fluorescence yield, w, which is comparable with Auger's data. As thus corrected, his values are :—

* W. Kossel, *Zeits. f. Phys.* xix. p. 333 (1923).
† W. Bothe, *Physik. Zeits.* xxvi. p. 410 (1925).
‡ G. E. M. Jauncey and O. K. De Foe, Proc. Nat. Acad. xi. p. 520 (1925).
§ L. Balderston, Phys. Rev. xxvii. p. 695 (1926).
‖ M. I. Harms, *Ann. d. Phys.* lxxxii. p. 87 (1926).

TABLE III.

	26	28	29	30	42	47
Element ...	Fe	Ni	Cu	Zn	Mo	Ag
w	·38	·45	·50	·57	·95	·86

The experimental error in these determinations is probably large. Balderston calls attention to an uncertainty of 13 per cent. in the solid angle subtended by the window of the ionization chamber. Errors which are probably of the same order of magnitude are introduced also by uncertainty in the absorption in the ethyl bromide vapour, and by the method of calculation, which involves an extrapolation, assuming a linear variation over a range of wave-lengths in some cases more than 3 times the range over which observations were taken. More serious errors of a consistent nature are apparently introduced by the assumption that the ionization of different wave-lengths in air is proportional to the absorption in air, whereas for the shorter wave-lengths a large part of the absorption is due to scattering, and does not result in ionization. Also, since in his experiments the fluorescent rays struck the side walls of the ionization chamber, whereas the primary rays did not, it was not possible to compare the relative intensities, even of the same wave-length, by comparing the ionizations. These values can therefore be assigned but little weight.

Harms* has made a more careful analysis of the problem. In the following table his results are given in columns 2 and 3.

TABLE IV.

Element.		w'.	w.	w (corrected).
26	Fe	·530	·303	·282
29	Cu	·589	·394	·378
30	Zn	·598	·418	·403
34	Se	·647	·530	·517
38	Sr	·598	·590	·615
42	Mo	·754	·754	(·730)

* M. 1. Harms, *loc. cit.*

In calculating w' Harms has made use of Kossel's relation between the wave-length and the ionization current per erg of β-ray energy. As he himself notes, Kulenkampff * and Kircher and Schmitz † have independently reached the conclusion that from ·5A to 1·5A there is a strict proportionality between absorbed energy and ionization. Yet Kossel considers the older work of Lenard and Holthusen more reliable, and Harms has used Kossel's correction factor to calculate the energy from the ionization. The conclusion of Kulenkampff and of Kircher and Schmitz has recently been confirmed by Crowther and Bond ‡, and is supported by the results about to be described. Harms's data should thus not have been corrected by Kossel's factor, and he should have obtained the values of w given in column 4.

There are some minor corrections that should be applied to Harms's results :—(1) The mass scattering coefficient of air for λ ·71 should be, from Hewlett's data on carbon §, not less than 0·20, whereas Harms has used the value 0·17 ; (2) a part of the secondary X-rays is scattered, whereas Harms assumes that it is wholly fluorescent. From my measurements this fraction varies from 4 per cent. in the case of λ ·71 A exciting secondary rays in iron to 0·4 per cent. in selenium ; (3) the value for strontium was obtained using a surface of strontium sulphate instead of the element, and a correction of 5 per cent. must be applied to make it comparable with the values for the other elements ; (4) the value for molybdenum is an extrapolated one, assuming that the variation of w with the atomic number is linear. This assumption probably is not justified. These minor corrections give us the values in the last column.

Harms's measurements are subject to some uncertainty, because the intensity of the primary and fluorescent beams were measured by two ionization chambers of very different design. The measurements thus involved a comparison of the capacities of the two systems, the sensitivity of the two electrometers, and the effective path of the X-rays in the two ionization chambers. Moreover, he used a beam from a molybdenum target, filtered through

* H. Kulenkampff, *Ann. der Phys.* lxxix. p. 97 (1926).
† H. Kircher and W. Schmitz, *Zeits. f. Phys.* xxxvi. p. 484 (1926).
‡ J. C. Crowther and W. N. Bond, Phil. Mag. vi. p. 401 (1928).
§ C. W. Hewlett, Phys. Rev. xvii. p. 284 (1921).

a zirconium screen, and assumed that the effective wavelength of the transmitted rays was that of the K lines. A spectral analysis of the X-rays under these conditions * shows that ordinarily only about 25 per cent. of the filtered beam consists of the Kα lines, and that there is a band of the continuous spectrum in the neighbourhood of 0·5A which has more energy than has the Kα radiation. This heterogeneity makes it impossible to estimate the absorption accurately from tables of absorption coefficients, as Harms found it necessary to do. It would, nevertheless, seem that Harms's values of the fluorescence yield, after applying the corrections noted above, are more reliable than those of the other investigators.

Fig. 1.

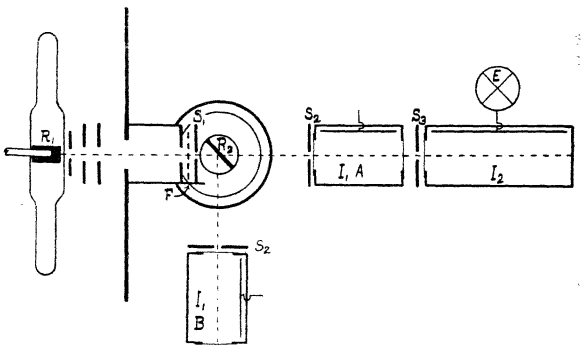

New Measurements of the Fluorescent Yield.

In view of the unsatisfactory status of these fluorescence measurements, I have undertaken some new measurements of the fluorescence yield. These measurements were meant to be of only a preliminary character; but as they have led to results that seem more reliable than those now in the literature, and since it is uncertain when the experiments can be continued, it seems worth while to publish them at this time.

The apparatus used in my experiments is shown in fig. 1, which is drawn approximately to scale.

* A. W. Hull, Phys. Rev. x. p. 666 (1917).

Nearly homogeneous X-rays were obtained by taking the fluorescent rays from plates of various elements placed at R_1, just over the X-ray tube *. These homogeneous rays were limited by a diaphragm S_1, and fell on the radiator R_2 whose fluorescence yield was to be determined. R_2 was a flat thick plate placed at 45 degrees on the crystal table of a Bragg spectrometer, and of area large enough to intercept all the rays coming through the diaphragm S_1. The fluorescent rays from R_2 entered the ionization chamber I_1 at its position B, through a lead diaphragm S_2. The ionization current thus obtained was compared with that observed when the chamber was turned to the position A, with the radiator R_2 removed, and with a second diaphragm at S_1 of opening small enough so that the ionization current was of the same order of magnitude as that found in position B. The water-cooled tungsten target X-ray tube was usually operated at about 40 milliamperes and 53 peak kilovolts.

The ionization chamber was 8 cm. diameter and 11 cm. long, inside. The dimensions of the diaphragm used at S_2 were such that no X-rays reached the side walls in either position A or B. The front and back faces of the chamber were covered with thin celluloid, and the chamber was filled with methyl bromide vapour. The fraction of the X-rays absorbed by the gas in the chamber was measured for each wave-length employed by the use of a second ionization chamber I_2. The absorption by the celluloid windows was corrected for by measuring the direct beam through an equal thickness of celluloid placed at F. For the longer-wave-lengths it was necessary to apply a correction for the absorption in the 11 cm. column of air displaced by the ionization chamber.

Calculation of the Fluorescence Yield.

The intensity of the fluorescent X-rays may be calculated as follows: If μ' is the total absorption coefficient of the primary X-rays in the radiator, we have

$$\mu' = \sigma' + \tau', \quad . \quad . \quad . \quad . \quad . \quad . \quad . \quad (2)$$

* The high degree of homogeneity thus obtained was recognized long ago by Barkla, and has recently been investigated by the writer (Proc. Nat Acad. xiv. p. 549, 1928). In the latter paper I failed to mention the work of Allison and Duane (Proc. Nat. Acad. xi. p. 486, 1925), who also call attention to this remarkable homogeneity.

where τ' is the photoelectric absorption, and σ' is the absorption due to scattering. If, as is the case in these experiments, the primary wave-length λ' is shorter than the critical K absorption wave-length of the radiator λ_K, the greater part of the photoelectric absorption is that due to the electrons in the K shell, τ_K'. Let us suppose that a beam of intensity I' and of cross-section A' traverses a thickness ds of the radiator. The number of quanta absorbed by the K electrons, and hence the number of photoelectrons ejected from the K energy levels of the atoms will then be

$$dn = \mathrm{I'A'}\tau_K' ds \cdot \frac{1}{h\nu'}, \quad . \quad . \quad . \quad . \quad . \quad (3)$$

where ν' is the effective frequency of the primary rays. By equation (1), the number of fluorescent quanta is then $dn_1 = w\,dn$, where w is the fluorescence yield, and the total power in the fluorescent beam will be $h\nu'' dn_1$, where ν'' is the effective frequency of the fluorescent ray. Barkla and Sadler have shown that the intensity of the fluorescent ray is the same in all directions. Thus the power in the fluorescent ray entering the ionization chamber from the thin layer ds (uncorrected for absorption) is

$$d\mathrm{P}'' = h\nu'' dn_1 \frac{\mathrm{A}''}{4\pi r^2} = \frac{w}{4\pi} \mathrm{P'} \frac{\mathrm{A}''}{r^2} \tau_K' \frac{\nu''}{\nu'} ds, \quad . \quad . \quad (4)$$

where A'' is the area of the diaphragm S_2, r is the distance from R_2 to S_2, and $\mathrm{P'} = \mathrm{A'I'}$ is the power in the primary beam striking the radiator.

If the fluorescent ray leaves the surface at the same angle with the normal as that at which the primary beam enters, the paths of the primary beam and of the secondary beam in the radiator are equal, having the value, let us say, s. Writing μ' and μ'' for the absorption coefficients of the two beams *, we thus have for the power in the fluorescent beam from a thick radiator,

$$\left.\begin{aligned} \mathrm{P}'' &= \frac{w}{4\pi} \mathrm{P'} \frac{\mathrm{A}''}{r^2} \tau_K' \frac{\nu''}{\nu'} \int_0^\infty e^{-(\mu'+\mu'')s} ds \\ &= \frac{w}{4\pi} \mathrm{P'} \frac{\mathrm{A}''}{r^2} \frac{\tau_K'}{\mu' + \mu''} \frac{\nu''}{\nu'} \end{aligned}\right\} \quad . \quad . \quad . \quad (5)$$

* Strictly speaking, one should use an absorption coefficient intermediate between μ' and τ', since part of the primary rays scattered in the radiator are reabsorbed before leaving the radiator. However, μ' and τ' are so nearly equal that this difference can be neglected.

Writing instead of ν''/ν' its equivalent λ'/λ'', we obtain for the value of the fluorescence yield,

$$w = 4\pi \frac{r^2}{A''} \frac{\mu' + \mu''}{\tau_K'} \frac{\lambda''}{\lambda'} \frac{P''}{P'}. \quad . \quad . \quad . \quad . \quad . \quad (6)$$

The quantities r and A'' can be measured directly, λ' and λ'' are the weighted mean wave-lengths of the fluorescent radiations from the radiators R_1 and R_2 respectively *, and μ' and μ'' are the absorption coefficients in the radiator of the wave-lengths λ' and λ''. The values of μ' and μ'' have been interpolated from the tables of absorption data compiled by the writer †. According to Richtmyer and Warburton ‡, the coefficient k in Owen's formula for the photoelectric absorption per atom,

$$\tau_a = KZ^4\lambda^3,$$

is 0·0224 on the short wave-length side of the K absorption limit and 0·0033 on the long wave-length side. The fraction $(224-33)/224 = 0{\cdot}85$ of τ is thus due to the K electrons. For absorption in the radiators here considered, the scattering term σ is less than 1 per cent. of μ and may be neglected in the calculation. We thus have,

$$\tau_K' = 0{\cdot}85\mu'. \quad . \quad . \quad . \quad . \quad . \quad . \quad (7)$$

In order to obtain the ratio P''/P' from the experimental data, let us assume in accord with the results of Kulenkampff §, Kircher and Schmitz ‖, and Crowther ¶ that the ionization is proportional to the energy spent in producing β-rays. Of the total energy absorbed in the methyl bromide vapour, the fraction τ/μ is spent in exciting photoelectrons (the part spent in exciting recoil electrons may be neglected). As we have seen, if the frequency is greater than the K limit of bromine, 85 per cent. of this is absorbed in the K shell, and 15 per cent. in the outer shells. If n_a is the total number of absorbed quanta, a number

$$n_f = 0{\cdot}85 w_B \frac{\tau}{\mu} n_a$$

* On the basis of the results of Unnewehr (Phys. Rev. xxii. p. 529, 1923) and the writer (Proc. Nat. Acad. xiv. p. 549, 1928) the ratio of the α lines to the β lines has been taken as 5 : 1 for the elements used.

† A. H. Compton, 'X-Rays and Electrons' (Van Nostrand, 1926), p. 184.

‡ F. K. Richtmyer and F. W. Warburton, Phys. Rev. xxii. p. 539 (1923).

§ H. Kulenkampff, *Ann. der Phys.* lxxix. p. 97 (1926).

‖ H. Kircher and W. Schmitz, *Zeits. f. Phys.* xxxvi. p. 484 (1926).

¶ J. C. Crowther and W. N. Bond, Phil. Mag. vi. p. 401 (1928).

reappears as fluorescent K rays of frequency ν_{Br}''. The energy of the K rays escaping to the walls is thus

$$0{\cdot}85 w_{Br} \frac{\tau}{\mu} n_a h \nu_{Br}'' e^{-\mu'' \bar{x}}, \quad . \quad . \quad . \quad . \quad . \quad (8)$$

where μ'' is the absorption of the bromine K rays in the methyl bromide vapour, and $\bar{x}$ is the effective distance traversed by the rays before reaching the walls. An approximate calculation of $e^{-\mu'' \bar{x}}$ gives 0·937. Noting that the absorbed energy is $n_a h\nu$, and that $\nu''/\nu = \lambda/\lambda''$, this means that the fraction of the absorbed energy lost as K radiation is

$$0{\cdot}85 \times 0{\cdot}937 w_{Br} \frac{\tau_{Br}}{\mu_{Br}} \frac{\lambda}{\lambda_{Br}''} = 0{\cdot}796 \left(w \frac{\tau}{\mu} \frac{\lambda}{\lambda''} \right)_{Br}.$$

Any fluorescent L or M radiation will be absorbed before reaching the walls of the ionization chamber, and hence will appear as β-ray energy. There are, however, also scattered rays from the methyl bromide vapour which escape from the ionization chamber without producing ionization. The number of such scattered quanta is $n_a = n_a \sigma/\mu$, of which a fraction $e^{-\mu'' \bar{x}}$ will escape from the chamber. Thus the total fraction of the absorbed energy which escapes from the ionization chamber is

$$0{\cdot}796 \left(w \frac{\tau}{\mu} \frac{\lambda}{\lambda''} \right)_{Br} + e^{-\mu'' \bar{x}} \frac{\sigma}{\mu}.$$

If we call R the ratio of the energy spent in producing ionization to the absorbed energy, we thus have, for rays shorter than the K limit of bromine,

$$R = 1 - 0{\cdot}796 \left(w \frac{\tau}{\mu} \frac{\lambda}{\lambda''} \right)_{Br} - e^{-\mu'' \bar{x}} \frac{\sigma}{\mu}. \quad . \quad . \quad (9)$$

When λ is greater than λ_{KBr} the second term in this expression becomes negligibly small.

Let i' and i'' be the ionization currents due to the primary and secondary rays respectively, f' and f'' the fractions of the two beams absorbed by the methyl bromide, and S′ and S″ be the areas of the slits S_1 used in the two cases. Then,

$$\frac{i''}{i'} = \frac{P'' f'' S''}{P f' S'} \frac{R''}{R'} \frac{e^{-(\mu_a'' r + x'')}}{e^{-(\mu_a' r + x')}}.$$

Here $\mu a'$ and $\mu a''$ are the absorption coefficients in air o the two beams, r is as before the distance from R_2 to the

ionization chamber, and x' and x'' account for the absorption in the celluloid window. We thus have,

$$\frac{P''}{P'} = \frac{i''}{i'} \frac{f}{f''} \frac{S'}{S''} \frac{R'}{R''} \frac{e^{y''}}{e^{y'}}, \quad \ldots \ldots \quad (10)$$

where $$y = \mu_a r + x.$$

Making use of equations (7) and (10), expression (6) now becomes

$$w = 14{\cdot}78 \frac{r^2}{A''} \frac{\mu' + \mu''}{\mu'} \frac{\lambda''}{\lambda'} \frac{i''}{i'} \frac{S'}{S''} \frac{f'}{f''} \frac{R'}{R''} \frac{e^{y''}}{e^{y'}}. \quad \ldots \quad (11)$$

The Measurement of Relative Intensities for different Wave-lengths.

It will be seen that an expression similar to equation (10) affords a means of comparing the power in two X-ray spectrum lines of different wave-lengths in terms of the ionization resulting from them. The appropriate form of the expression is

$$\frac{P_1}{P_2} = \frac{i_1 f_2 R_2 e^{-y_2}}{i_2 f_1 R_1 e^{-y_1}}, \quad \ldots \ldots \quad (12)$$

where the significance of the various terms is as in equation (10). This expression, of course, does not correct for the difference in reflecting power of the grating for the two wave-lengths.

Evaluation of the Fluorescence Yield.

In the present experiment, referring to equation (11), $r = 15{\cdot}78$ cm., $A'' = 7{\cdot}70$ cm.^{2}, and the other quantities are given in the following table :

TABLE V.

Experiment.	λ'.	λ''.	$\frac{\mu' + \mu''}{\mu'}$.	$\frac{i''}{i'}$.	$\frac{S'}{S''}$.	$\frac{f'}{f''}$.	$e^{(y''-y')}$.	$\frac{R'}{R''}$.	w.
1. Sn→Mo	·482	·696	1·425	·370	·00374	·440	1·016	1·136	**·69**
2. Ag→Mo	·549	·696	1·290	·352	·00374	·588	1·013	1·093	**·67**
3. Sn→Se	·482	1·085	2·24	·727	·000472	·742	1·091	·788	**·53**
4. Mo→Se	·696	1·085	1·427	·866	·000472	1·69	1·073	·694	**·55**
5. Sr →Se	·859	1·085	1·334	·970	·000472	2·33	1·048	·622	**·56**
6. Sn→Ni	·482	1·629	4·69	·261	·000472	·343	1·316	·788	**·33**
7. Mo→Ni	·696	1·629	2·30	·441	·000472	·781	1·299	·694	**·38**
8. Sr →Ni	·859	1·629	1·75	·579	·000472	1·08	1·267	·622	**·37**
9. Se →Ni	1·085	1·629	1·40	1·39	·000472	·463	1·210	1·000	**·37**
10. Zn→Ni	1·410	1·629	1·292	1·42	·000472	·805	1·102	1·000	**·42**

The diaphragm apertures S′ and S″ can be measured directly. The ratios i''/i' are the ratios of ionization currents as read from the electrometer, except that corrections have been applied to take account of the scattered primary rays mixed with the fluorescent rays from R_1 and also for the scattered rays mixed with the fluorescent rays from R_2. These corrections were based on absorption measurements of the mixed rays. Only in the cases of tin rays falling on nickel and of the primary rays falling on zinc were these corrections large—that is, in cases 6 and 10. The absorbed fractions f' and f'' were measured directly by means of the auxiliary ionization chamber I_2. The absorption coefficients $\mu a'$ and $\mu a''$ used in calculating y' and y'' were interpolated from a table given by Siegbahn *.

In order to evaluate R'/R'', it was at first assumed that, since the atomic numbers of selenium and bromine are nearly the same, the fluorescence yield w will be the same for both. Expressing R in terms of w, as in equation (9), equation (11) can thus be solved for w in experiments 3, 4, and 5, giving the mean value $w=0{\cdot}549$. In making this calculation, since under the conditions of these experiments σ was less than 1 per cent. of μ, the last term in equation (9) was neglected. Thus for wave-lengths greater than the K limit of bromine R may be taken to have the value 1. Using this value 0·549 for the fluorescent yield in bromine, provisional values of R for the other cases could be calculated, and provisional values of w determined for molybdenum and nickel. This showed the rate of change of w with atomic number, and indicated that if 0·542 is the mean value of w for bromine and selenium, its value for bromine should be ·565. Using this value for $w_{1,\mathrm{K}}$, and taking $\tau=\mu$, the values of R'/R'' shown in column 9 are calculated from equation (9). From equation (11) we then obtain the values of w given in the last column.

Discussion of Results.

There is no significant variation in the values of the fluorescence yield w with the wave-length of the exciting radiation. The only apparent departure from this statement is for the nickel radiator when excited by rays from

* M. Siegbahn, 'Spectroscopy of X-Rays,' p. 246.

tin and from zinc. As we have noted, however, in these two cases the corrections due to the presence of scattered X-rays were so large as to make the results considerably less reliable than in the other cases. The experiments thus indicate (in support of the conclusions of all previous investigators) that the fluorescent yield is a constant characteristic of the radiator, but independent of the exciting radiation.

Fig. 2.

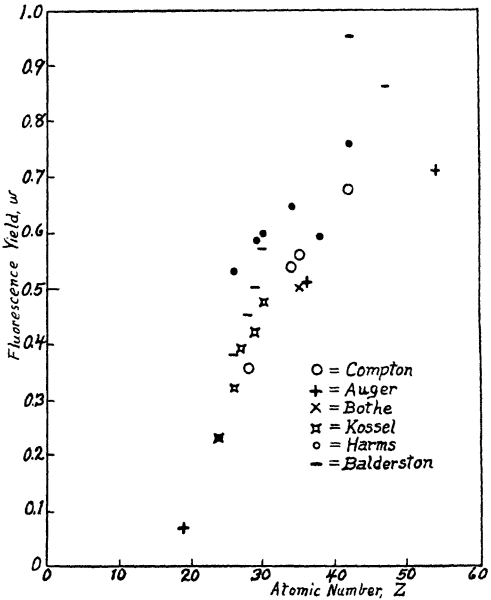

If we had assumed that the number of ions produced per unit energy by the β-rays in the ionization chamber were a function of the wave-length of the incident X-rays, as was assumed by Kossel and Harms, this independence of w of the exciting wave-length would not have appeared. For the efficiency of ion production by the fluorescent rays from any one radiator would have remained constant,

while that due to the exciting rays would on this assumption have varied with their wave-length, resulting in a corresponding variation in w. In so far as the values of w here obtained are constant for a given radiator R_2 therefore, this work supports the conclusions reached by Kulenkampff, Kircher and Schmitz, and Crowther that the ionization by β-rays per unit energy is independent of their energy.

Fig. 3.

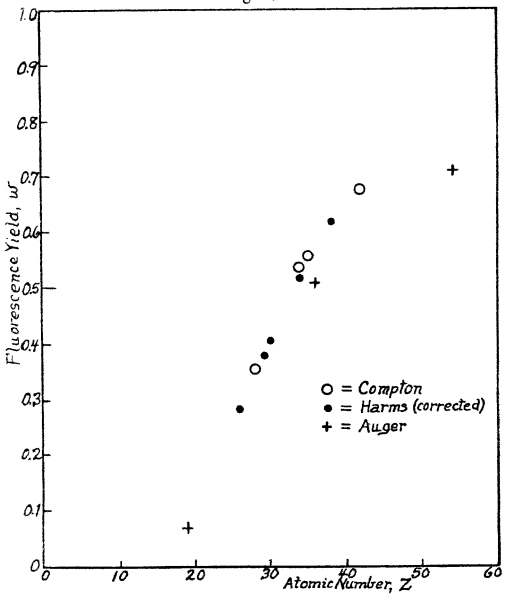

In fig. 2 are plotted the values of the fluorescence yield given by the different investigators. Of these, as we have seen, Auger's values have been obtained by the direct method of comparing the number of single photoelectrons with the number of compound photoelectrons. The results of Bothe, Kossel, and Balderston can be considered only as rough approximations, and Harms's values should

be corrected for certain unjustified assumptions in the calculations. In fig. 3 Harms's values of w as thus corrected are compared with those of Auger and the writer. Their agreement with the writer's results is seen to be good.

If the assumption of Auger and Kossel is correct, that the compound photoelectric effect is the whole explanation of the fact that the fluorescence yield is less than unity, Auger's values should fall on the same curve with those of Harms and the writer. Though this agreement is not exact, it is probably within the limits of experimental error. The present work thus confirms Auger and Kossel's theory that the compound photelectric effect is responsible for the fact that the fluorescence yield is less than unity.

It will be noted that these experiments show a rapid increase of the fluorescence yield with increasing atomic number. For elements as light as aluminium, fluorescence should thus be almost non-existent. On the other hand, for a heavy element such as iodine, a larger portion of the absorbed energy is spent in producing fluorescence and a smaller portion in producing ionization. This gives a lighter element, such as argon, a certain advantage for use in an ionization chamber, though in this case it is, of course, more difficult to secure complete absorption.

Of practical significance is the fact that, having a knowledge of the fluorescence yield, it is now possible to make a reliable calculation of the relative intensity of X-ray beams of different wave-lengths, in terms of the ionization which they produce. The necessary formula is given in equation (10).

Summary.

A review of the published data describing the intensity of fluorescent X-rays shows that the various observers agree that the number of quanta of fluorescent X-rays emitted by a radiator is considerably less than the number of quanta which it absorbs from the primary beam. The values of the efficiency of fluorescence that appear in the literature are for the most part, however, found not to be quantitatively reliable.

New experiments give values of the "fluorescence yield," or ratio of the number of fluorescent K quanta to the number of photoelectrons ejected from the K shell, of 0·68 for a molybdenum radiator, 0·56 for bromine,

0·54 for selenium, and 0·37 for nickel. The values seem to be independent of the wave-length of the exciting rays.

These measurements agree within experimental error with Auger's values of the fluorescent yield, based on his count of the frequency of occurrence of the compound photoelectric effect, and thus indicate that it is this effect which makes the fluorescent yield less than unity.

An expression is derived for calculating the relative intensity of two X-ray beams of different wave-length, in terms of the ionization currents obtained and other factors.

Ryerson Laboratory,
University of Chicago,
December 13, 1928.

CII. *Arc and Spark Radiation from Hydrogen in the Extreme Ultra-Violet.* *By* JOHN THOMSON. *M.A., B.Sc., Ph.D., Lecturer in Physics in the University of Reading* *.

Introductory.

THE purpose of the present communication is to describe certain experiments which reveal the ultimate source of the ionizing radiations emitted by point discharges in hydrogen. The work is a continuation of that described in previous papers †. In the present paper a method is suggested whereby the manner of excitation of the extreme ultra-violet radiations emitted by the gas may be determined, and, as far as the writer is aware, this method is entirely new. It might possibly be applied with success to problems other than the one discussed. The results obtained by it indicate that, under the conditions of the present experiments, by far the greater part of the radiation responsible for the ionization of the gas is emitted by *neutral* molecules or atoms. A small part of the radiation is definitely attributable to *ionized* molecules or atoms, however, and this part is of greater relative importance when the pressure of the gas is large.

* Communicated by Prof. E. Taylor Jones, D.Sc. The writer performed the greater part of this work while a Carnegie Research Fellow in the University of Glasgow.

† J. Thomson, Phil. Mag. v. p. 513; vi. p. 526 (1928); vii. p. 970 (1929).

Theoretical considerations indicate that the new method for determining the source of the radiations has, in these experiments at least, given very plausible results, while the rough test of its basic hypothesis which has been performed is in every way satisfactory.

In the opening paragraphs of the communication some experiments are described concerning the possibility of ionizing radiations being emitted by the metal of the point electrodes themselves.

The Source of the Ionizing Radiations.

In one of the papers by the present writer already mentioned, "On the Ionization of Hydrogen by Its Own Radiations," it was tacitly assumed that the metallic points in a point discharge did not themselves emit ionizing radiations. The justification for this assumption depended upon an experiment performed in earlier work, where it was found that ionizing radiation was certainly

Fig. 1

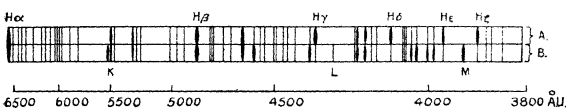

emitted by *the gas in the vicinity of* the points, and also upon the evidence of other workers concerning the *visible* radiations from such a discharge. In all the experiments described in this and preceding papers the current flowing between the points (which were always of platinum) never exceeded 2 milliamp., and the only capacity in the circuit was the small self-capacity of the induction coil itself. But it has been shown by many spectroscopists that under such circumstances, and particularly where the electrodes are of platinum, the spectrum of the discharge is due almost entirely to the gas between the electrodes.

It was thought advisable, however, in view of the peculiar nature of the problem, to make some further investigation, and to this end spectrograms of the visible and near ultra-violet radiation from the discharge were taken. These were then compared with similar spectrograms of a hydrogen vacuum tube: copies of two typical spectra are shown diagrammatically in fig. 1.

Spectrum A was taken from the vacuum tube ; B from the point discharge at atmospheric pressure with about 2 milliamp. flowing. It will be seen that the two spectra are very similar indeed. Out of the sixty or so clear lines present in both spectrograms only the three marked K, L, M in the spectrum of the point discharge are not definitely attributable to hydrogen, and of these three only one can possibly be due to platinum. This one line, M (3923 Å.U.), is the *raie ultime* of that element, and is visible when excited platinum is present as an impurity to the extent of one part in 10^{10}. Consequently, no great significance can be attached to its appearance in this case. In fact, the evidence of the spectrograms is all in favour of the view that the discharge radiations are due almost entirely to the gas.

In passing, an interesting feature of the spectrum of the point discharge may be noted. The spectrum of the vacuum tube consists essentially of the atomic spectrum—the Balmer series. The molecular spectrum in this case is decidedly "secondary." In the discharge at atmospheric pressure, however, the relative intensities of the two spectra are entirely changed. The molecular lines are more intense, while it is difficult to distinguish any of the atomic lines beyond H_γ.

To obtain, if possible, more direct evidence with regard to the source of the ionizing radiations, another experiment was performed.

A discharge-tube similar to that used in a previous investigation was fitted with two pairs of similar points, one pair being of platinum, the other of tin, and the distance between the first pair was made equal to the distance between the second pair. Then the intensity of the ionizing radiations from a discharge between the platinum points carrying 1 milliamp. was compared with the intensity of the radiations from a discharge between the tin points carrying 1 milliamp., the detector of the radiation being at the same distance from the source in both cases. The intensities were found to be equal within the limits of the experimental error, which was about 1 per cent. of the value of either intensity as indirectly measured by an electrometer. Now, if the source of any considerable part of the radiation was the metal of one of the electrodes, one would expect that the greater fusibility of the tin combined with the general

dissimilarity of the metals would cause some distinct difference in the two intensities. That the result of the experiment was negative at least suggests that the radiations emanated from the gas.

The writer has so far been unable to find an *experimentum crucis* to decide conclusively between the two possible sources. All the evidence at present available strongly suggests, however, that the electrodes play no part in the radiation phenomena, and this hypothesis is eminently satisfactory in explaining the results of all the other experiments.

Measurements of the Intensities of the Radiations.

Previous investigations* had shown that there was much to be learned from a quantitative study of the variation in intensity of the radiations as the current flowing in the discharge was varied. The object of the new experiments was to exhaust the possibilites of such a mode of approach by utilising the refinements of technique suggested by previous work. The accuracy of the measurements involved was made the subject of careful investigation, so that accidental variations in readings might not be considered as real phenomena. It is claimed for the results which are to be given later that all the phenomena observed are characteristic of the gas hydrogen.

Experimental Arrangements.

The Gas System.—The experiments consisted essentially in measuring the ionization current in a region Q of a discharge-tube caused by the total radiation emitted by a point discharge in a region P. Maintaining the pressure of the gas at a constant value, this ionization current was measured for different values of the discharge current, the aim of the experiment being to determine the exact relation between the two currents. In a previous investigation it had been found that the value of the ionization current for a given discharge current at a given pressure depended to a very great extent on the purity of the hydrogen. It was therefore necessary to obtain the gas in as pure and dry a state as possible. To this end the hydrogen was generated electrolytically in a specially constructed Hoffmann's apparatus, designed to prevent

* *Loc. cit.* vi. p. 526 (1928).

the passage of oxygen from the anode to the cathode. To reach the discharge-tube the gas passed through a capillary tube, two tubes containing calcium chloride, a tube containing phosphorus pentoxide, and two liquid-air traps. One of the traps was in the discharge-tube system itself (*i. e.*, that part of the system sealed off when experiments were in progress), which also contained a simple pressure gauge, and was connected through a vacuum stop-cock to a Hyvac pump. The entire gas system was glass sealed, thus avoiding any foreign vapours from wax or rubber.

Such a system does not, of course, give pure gas when first used. The glass, the powdered phosphorus pentoxide and calcium chloride, and the glass wool which was also included, all contain much occluded gas and vapour : but, if the system is evacuated and filled with hydrogen a large number of times, sufficient time being allowed after each filling to dry the gas thoroughly over the drying agents, then the moisture disappears from the glass, and the occluded gases are displaced by the hydrogen. In the present experiments it was found to be unnecessary to use liquid air. When the gas was allowed to remain over the drying agents for four or five days, it was found to be fairly dry on entering the tube.

The tests of the purity and dryness of the gas were such as had been suggested by previous investigation. These tests depend upon two properties of the impure gas described in a former paper. If any oxygen is present in the discharge-tube, the ionization current caused by the discharge persists for some time after the latter has been cut off. The magnitude of this residual current is a rough measure of the amount of impurity present in the tube. This test is a very delicate one, as has been shown repeatedly in the course of this and previous experiments. An even finer test, however, is given by the variation of the ionization current when the pressure and discharge current are kept constant, the same sample of gas being used for a number of readings. When the dry gas is introduced into the tube, the ionization current has a comparatively large value. If, however, the tube itself is not dry, successive readings show a diminution in the ionization, indicating that the tube is giving up its moisture to the gas. This test still gave a positive result after the apparatus had been in use for a month. The diminution

in the ionization is a consequence of the fact noted in a previous communication that the drier and purer the gas the greater is the ionization produced. When these tests failed to detect any impurity in the gas, it was assumed that the experiments could be performed with safety.

The Discharge-Tube :—This has already been described in a previous paper. It is shown diagrammatically in fig. 2.

The tube was cylindrical in form with one outlet tube K to connect it to the gas system. E and F were the points

Fig. 2.

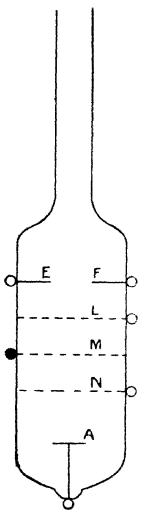

of two platinum electrodes one-half centimetre apart. L, M, N were three circular pieces of wire gauze, while A was a small copper plate coated with copper oxide (CuO). During the experiments L was maintained at a potential of -310 volts. M, which was 1 centimetre below L, was connected to earth, while N, 1 centimetre below M, was maintained at -310 volts. A was about $1\frac{1}{2}$ cm. below N, was connected to the insulated quadrant of a Dolezalek electrometer, and was initially at earth potential.

This arrangement of gauzes effectively screened A from any ions generated in the gap EF. No ions from the space above M could possibly penetrate to A owing to the arrangement of the electric fields. Moreover, owing to the relative distances of N from M and A, it is exceedingly unlikely that any photo-electrons emitted by N could arrive at A. It may therefore be assumed that, when a discharge was passing from E to F, any current passing from N to A was due to ionization of the gas in the vicinity of N or A.

The discharge between E and F was produced by means of an induction-coil used in conjunction with a motor mercury-jet interrupter. Every precaution was taken to render the action of the coil reliable. The mean current (secondary) was measured by means of a delicate meter, reading to about 600 microamperes. The average current between E and F was about 200 microamperes.

The other measurements necessary were of pressure and ionization current. The former was read from an ordinary barometer tube pressure gauge. This was sufficiently accurate for the purpose. The ionization current was measured by means of a Dolezalek electrometer. Since the currents were very large—of the order of 10^{-12} ampere —a phosphor-bronze suspension was used, the sensitivity of which was 10 mm. to the volt with the scale at 1 m. distance. It was necessary that the sensitivity should remain very constant; this was verified on numerous occasions.

Variation of Ionization Current with Discharge Current, the Pressure remaining Constant.

Both the gas and the tube being so dry as to give no indication of impurity when the aforementioned tests were carried out, the discharge-tube was filled with hydrogen to atmospheric pressure. A small current was then passed through the gas, and it was verified that the ionization current remained constant to 1 per cent. of its value over a large number of readings. To avoid any progressive effects due to temperature changes, a 10 minutes' pause was allowed after each reading, and the readings were aken in a definite order. Starting with a discharge current of about 50 microamperes, readings were taken at 50, 100, 150, ..500, 500, ..150, 100, 50. Usually, owing to

temperature variations, and perhaps to a very smal unexamined change in the gas, the readings taken with decreasing discharge current were slightly greater (maximum difference, 2 per cent.) than those taken with the discharge current increasing. Then the pressure of the gas was reduced to about 60 cm. of mercury, and the same series of readings was taken. In general, as the pressure was reduced, it became necessary to reduce the maximum discharge current, since the ionization became too large for accurate measurement. Thus, at about 30 cm. the maximum discharge current was 150 microamperes. In fig. 3 the results of these experiments are shown. The abscissa measures the discharge current ; the ordinate the ionization current. The curves are drawn for different pressures in the same sample of gas.

Discussion of the Results.

The curves shown in fig. 3 are typical of all the samples of gas which were used. The absolute value of the ionization current at a given pressure and for a given discharge current varied slightly from sample to sample ; but the shapes of the curves did not so vary. It is claimed that they are typical of the gas hydrogen.

Suppose that the source of the radiation (the discharge) is at the point A, and the ionization current which was observed takes place in the region B. Then, so long as the pressure of the gas is not varied, the ionization is a measure of the intensity of the radiation at B. Also, so long as the pressure is not varied, the absorption of the radiation between its source A and the point B remains constant, and hence the ionization current at B is a measure of the intensity of the radiation *at its source* A. The only assumption made here is that the quality of the radiations does not vary as the discharge current is varied. Therefore the shape of any particular curve in fig. 3 exhibits the mode of variation of the intensity of the radiation from the discharge as the current in the latter is varied.

It is evident from a casual examination of the curves that, the pressure remaining constant, the radiation intensity increases in a *roughly* linear manner with the discharge current. This had already been observed *.

* *Loc. cit.*

A more careful examination of the curves leads to more definite and more interesting conclusions. The curves, as shown in the figure, have been drawn to pass through the origin, since the radiation intensity must be zero when the discharge current is zero.

Fig 3.

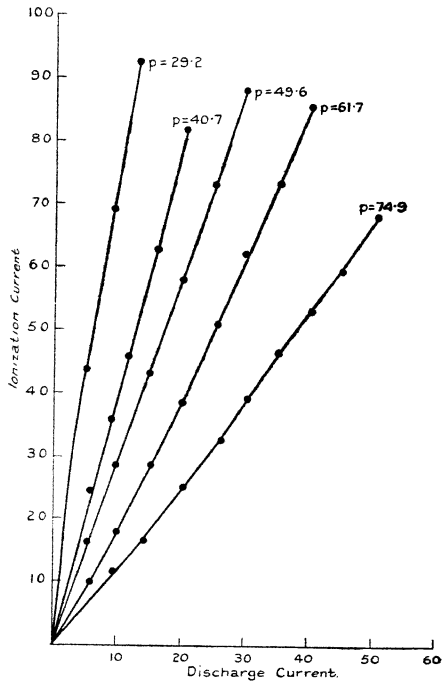

The curves at 74·9 and 61·7 cm. of mercury have a small but definite concavity upwards ; the two curves obtained at 49·6 and 40·7 cm. are almost straight lines ; the curve at 29·2 cm. is slightly convex upwards. Also, in three of the four curves taken at high pressures the point represen-

ting the radiation intensity at lowest discharge current lies above the curve through the origin. These are all real phenomena of the gas; they are shown in all the curves which have been taken.

The results can be reduced to order in a very simple manner. If the origin is taken about two discharge-current units to the left of the origin shown in fig. 3, the curves become very much simplified. The anomalous points now lie on the curves; the curves all show a tendency to concavity upwards; and the concavity, or variation from a straight line, decreases uniformly as the pressure of the gas is reduced. Is there, then, any reason for believing that the true origin of coordinates lies a little to the left of the origin given by the amperemeter?

The current measured by the meter should be the mean current through the secondary of the coil. The current in the coil varies in a periodic fashion; if this current is represented by c, the current measured by the meter should be proportional to $i = \frac{1}{T}\int_0^T c\,dt$, and i should be accurately proportional to c. But even under the best conditions there is always a certain amount of "inverse current" in the secondary circuit. This current is sufficient to produce a very small discharge, and its direction is opposite to that of the current at "break." Hence it is to be *expected* that the current measured by the meter should be less than the true mean current by a small quantity. Under the conditions of the experiment this quantity would seem to have been of the order of two units.

That this inverse current was present was shown by a very interesting experiment. The current flowing in the discharge was reduced by means of a series resistance in the primary circuit. As the current fell to zero, it was observed that the discharge was still just visible in the dark. On increasing the resistance in the primary circuit, the meter actually showed a small negative deflexion due to inverse current. The explanation is to be found in the fact that, while the current at "break" depends upon the current flowing in the primary circuit (which was reduced by adding resistance), the inverse current at "*make*" depends upon the total E.M.F. across the primary circuit (which was not varied by adding resistance). By using a large series resistance in the primary circuit it is possible

to make the inverse current as large as the current at "break."

Fig. 4 shows the corrected curves for the variation of radiation intensity with discharge current. The curves have again been made to pass through the origin. They will now be considered in detail.

Fig. 4.

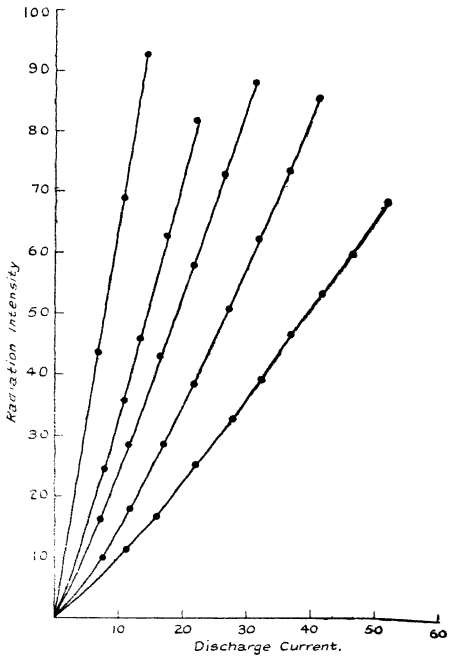

All the curves can be represented by the expression.

$$I = k_1 i + k_2 i^2 \quad . \quad . \quad . \quad . \quad . \quad . \quad . \quad (1)$$

where I is the radiation intensity (ionization current) and i is the discharge current, k_1 and k_2 being constants.

Evaluation of k_1 and k_2 for the curve taken at 74·9 cm. of mercury leads to the expression

$$I = K(200\,i + i^2), \quad \text{or} \quad \frac{k_1}{k_2} = 200.$$

This value is characteristic of the curves taken about atmospheric pressure. The curves obtained at lower pressures are amenable to the same treatment, but, as the pressure is reduced, k_2 tends to zero—the curves become straight lines.

Theoretical Interpretation of the Results.

The use of the corrected values for the secondary current gives a measure of the total current flowing in the discharge, and it has been found that the radiation intensity is proportional to the sum of two quantities proportional to the total current and to the square of the total current. It might be suggested that the two terms in equation (1) represent a second approximation to a function which could be expressed as an infinite series in powers of i. The writer is not inclined to accept this suggestion.

Radiation from a discharge may arise from two principal causes: it may be emitted by the processes following inelastic impact

(i.) between an ion and a neutral molecule, or

(ii.) between two ions.

Assuming that the pressure is constant, and that the field of electric force in the gap is not affected to any extent by variation in the discharge current, then the probability of radiation arising from the impact of ions on neutral molecules will be proportional to the number of ions in the gap, that is

$I = k_1\, i$, where I, k_1, i have their usual meanings.

Making the same assumptions, the probability of radiation arising from the impact of ions with ions will be proportional to the product of the number of ions of either sign in the gap, that is

$I = k_2 i^2$, where k_2 is again a constant.

Hence, if the ionizing radiation is emitted by both processes in the discharge, the intensity will be given by the expression

$$I = k_1\, i + k_2\, i^2, \quad \ldots\ldots\ldots \quad (1)$$

which is the expression already found empirically for the experimental curves.

If the above hypothesis be assumed, it may be concluded that the experiments show that the greater part of the ionizing radiation emitted by the discharge has its source in the impact of ions with neutral molecules. When the pressure is high, a small proportion of the radiation is due to purely ionic impact; but, as the pressure is diminished, these ionic impacts become of smaller relative importance. When the pressure is less than half an atmosphere, it is estimated that less than one-thousandth of the radiation intensity is due to this source.

It is a matter of some difficulty to classify in the category of arc or spark a discharge such as that which has just been discussed. The true arc takes place at a relatively low potential, the true spark at a very much higher potential. The evidence of the rotating mirror has shown that the discharge under consideration is a mixture of both phenomena. A high potential spark is followed by a number of low potential arcs. This is particularly the case at high pressures, where the conductivity of the gas is least. As the pressure diminishes, the arc begins to predominate, until the discharge degenerates into its typical low-pressure form. Thus the evidence of other investigations confirms the result arrived at in the present paper by means of the new hypothesis, since the arc radiation is chiefly emitted by neutral atoms or molecules, while the spark radiation is typical of the interaction of ions.

Experimental Verification of the New Hypothesis.

The hypothesis put forward in the above analysis appears to be sufficiently important to justify exhaustive tests of its validity being made. The writer has carried out a rough test * for a glow discharge.

A neon glow lamp such as is supplied for spectroscopic work was used as the discharge. The current was measured by a milliamperemeter (0–5 milliamp.). The detector of the radiation (visible) was a photoelectric cell supplied by the General Electric Co. (Type KMV6—this is a vacuum cell, the cathode being a monomolecular layer of potassium on copper oxide). The method of

* At the University of Reading.

measuring the photoelectric current was suggested by Professor Crowther, and is certainly worth description. The circuit is shown diagrammatically in fig. 5.

P.E.C. represents the cell, L, M, N are well-insulated keys, C is a capacity of about 1μ F., and G is a ballistic galvanometer. When the cell is exposed to light, the cathode is connected to the capacity which is allowed to charge up for a given time. It is then discharged through the galvanometer and the deflexion noted.

Fig. 5.

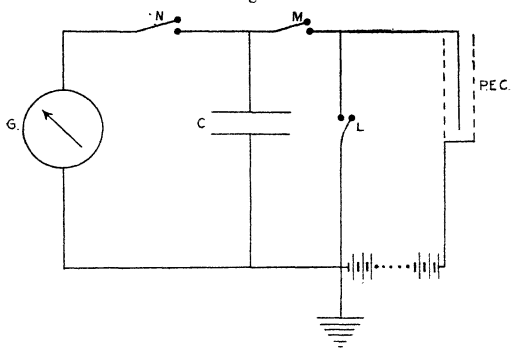

The method has many advantages :—

1. The measuring instrument is a robust galvanometer which need not be particularly sensitive.
2. So long as the insulation of the condenser is good, there is no limit to the sensitivity of the method ; the galvanometer deflexion varies directly as the time of charge.
3. The potential of the cathode, which is also the potential difference across the condenser, need never rise above 0·1 volt.

In the particular experiment carried out by the writer the photoelectric current was of the order 10^{-12} ampere. The galvanometer sensitivity was about 240 mm. per microcoulomb ; the time of charge was 30 sec. and, of course, large deflexions were obtained. This method for

the measurement of reasonably large ionization or photoelectric currents is, in the opinion of the writer, superior to any form of electrometer.

The photoelectric cell was first calibrated. It was found that with 120 volts across the cell the current was accurately proportional to the light intensity. Then the neon lamp was set up in the vicinity of the cell and the p.e. current was measured for discharge currents from 0·5 to 6·0 milliamp. The full line in fig. 6 represents a typical result.

Fig. 6.

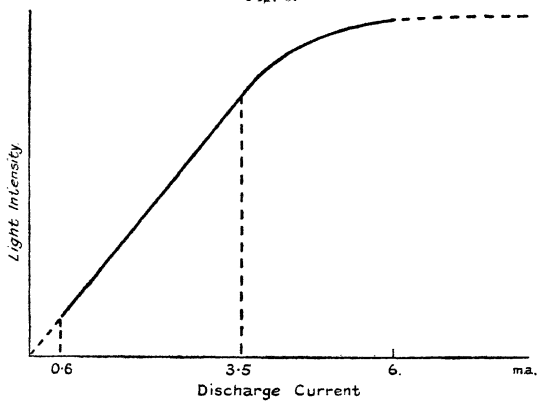

The dotted line is the suggested form of the curve outside the limits of observation.

It will be seen immediately that the curve is in complete agreement with the writer's hypothesis. Practically all the light from such a neon glow is due to the *arc* radiation from the gas. The curve of light intensity against discharge current is a straight line from 0 to 3·5 milliamp. A saturation intensity appears to be reached at about 5 milliamp.

When the current is small, the theory given above is completely verified. When the current is such, however, that the number of ions in the gap is of the same order as the number of gas molecules in the gap, the light intensity will begin to depend also upon the number of the latter.

Ultimately a stage will be reached where the light intensity will be proportional to the number of neutral molecules, and thus a saturation intensity will appear. The value of the discharge current, i, at which the light intensity becomes saturated will be a function only of the pressure of the gas. If it were possible to try the experiment with the same lamp at different gas pressures, i should be found to vary directly as the pressure of the gas.

The writer has not found it possible to pursue the investigation further, or to try the same experiment with a typical "spark" source. If the experiment were performed in the best way, monochromatic light would be used with some form of optical photometer. Should the hypothesis be found to conform to such a test, it might be possible, where the light intensity was sufficiently great, to utilize it to investigate the ultimate source of discharge spectral lines.

Summary.

1. Experiments are described which strongly suggest that the ionizing radiations emitted by point discharges in hydrogen emanate from the gas itself.

2. The mode of variation of the intensities of these radiations with the current flowing in the discharge is set forth.

It is suggested that the intensity of arc radiation from a discharge varies directly as the discharge current, and that the intensity of spark radiation varies as the square of the current.

The results of the present experiments are discussed with reference to this hypothesis.

3. A rough test of the hypothesis is described.

The greater part of the above work was performed in the research laboratories of the Natural Philosophy Department of Glasgow University, and the writer wishes once again to express his gratitude to Professor Taylor Jones for his advice and encouragement. The test of the hypothesis was carried out in the Physics Department of the University of Reading, and the writer's thanks are due to Professor Crowther, who suggested the method of measuring the photoelectric current which is described above.

Reading,
October, 1929.

CIII. *The Effect of Axial Restraint on the Stress in a Rotating Disk.* By WALTER G. GREEN, *Ph.D.**

[Thesis approved for the Degree of Doctor of Philosophy in the University of London.]

§ 1. INTRODUCTION.

THE problem under consideration is that of a rotating disk carried on a shaft. The effect of the presence of the shaft is to check the movements in the direction of the axis, of parts of the disk that are near the axis. The restraint may be effected in various ways. The solution,

Fig. 1.

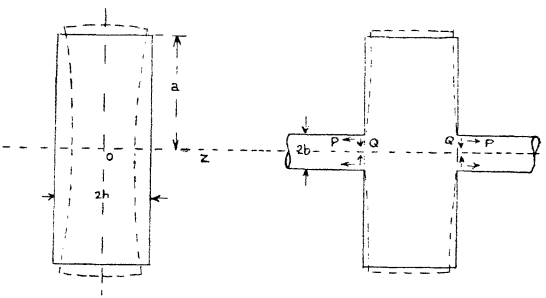

in which a disk of outer radius a, and of thickness $2h$, is restrained by concentrated axial tensions P, induced by rotation, at the centres of the outside faces, has already been given †.

A further development of this analysis can be obtained by representing the shaft as equivalent to symmetrical distributions of normal and tangential surface tractions acting on the outside faces of the disk, and symmetrical about its axis.

Consider, then, a disk of outer radius a and of thickness $2h$, the plane faces being represented by $z = \pm h$. When the

* Communicated by the Author.

† Phil. Mag. i. no. 6, p. 1236 (1926).

disk rotates with angular velocity ω, and is restrained in the manner indicated, two stress-systems will result, viz. :

(A) That due to symmetrical distributions of traction in a complete disk at rest.

(B) That due to rotation ω in a complete disk under no superficial tractions *.

For the first, although it is necessary to regard the radius of the disk as infinite, the results obtained show that the error due to this assumption is negligible.

Before developing the analysis, it will be necessary to glance at the problem of finding the stress-components and displacements produced at the surface of a semi-infinite solid by various distributions of traction applied at the plane boundary. This is Boussinesq's problem †.

The effects of symmetrical distributions of normal and tangential surface tractions will be considered separately.

§ 2. Symmetrical Distribution of Normal Traction about a Point on a Plane Boundary.

For symmetrical strain in a solid of revolution ‡ the results may be expressed in terms of a function χ which satisfies the differential equation $\nabla^4\chi=0$, where

$$\nabla^2\chi\equiv\left(\frac{\partial^2}{\partial r^2}+\frac{1}{r}\frac{\partial}{\partial r}+\frac{\partial^2}{\partial z^2}\right)\equiv\left(\frac{1}{r}\frac{\partial}{\partial r}r\frac{\partial}{\partial r}+\frac{\partial^2}{\partial z^2}\right).$$

The stress-components are then given by

$$\left.\begin{aligned}\widehat{rr}&=\frac{\partial}{\partial z}\left[\sigma\,.\,\nabla^2\chi-\frac{\partial^2\chi}{\partial r^2}\right]\\ \widehat{\theta\theta}&=\frac{\partial}{\partial z}\left[\sigma\,.\,\nabla^2-\frac{1}{r}\,.\,\frac{\partial\chi}{\partial r}\right]\\ \widehat{zz}&=\frac{\partial}{\partial z}\left[(2-\sigma)\nabla^2\chi-\frac{\partial^2\chi}{\partial z^2}\right]\end{aligned}\right\},\quad\ldots\quad(1)$$

$$\widehat{zr}=\frac{\partial}{\partial r}\left[(1-\sigma)\nabla^2\chi-\frac{\partial^2\chi}{\partial z^2}\right],\quad\ldots\quad(2)$$

* For this Chree's solution is taken. See A. E. H. Love, 'Mathematical Theory of Elasticity,' 3rd Ed. § 102, case *b*.

† H. Lamb, Proc. Lond. Math. Soc. xxxiv. p. 276 (1902).

‡ Love, *op. cit.* § 188.

and the displacements by

$$\left.\begin{aligned} u &= -\frac{1+\sigma}{\mathrm{E}}\cdot\frac{\partial^2\chi}{\partial r\partial z}, \\ w &= \frac{1+\sigma}{\mathrm{E}}\cdot\left[(1-2\sigma)\nabla^2\chi+\frac{1}{r}\frac{\partial}{\partial r}r\frac{\partial\chi}{\partial r}\right]. \end{aligned}\right\} \quad . \quad . \quad . \quad (3)$$

Suppose $z=0$ to be the bounding plane, the positive direction of the axis of z to be that which passes into the interior of the body, then, for a normal distribution of traction at the surface, symmetrical about the axis of z, we can write

$$\chi = \int_0^\infty \frac{\phi_1(k)}{k^3}\left[\{(2\sigma+kz)\}\mathrm{J}_0(kr)e^{-kz} - \{2\sigma+kz(1-2\sigma)\}\right]dk, \quad . \quad (4)$$

where

$$\nabla^2\chi = -\int_0^\infty \frac{2\phi_1(k)}{k}\cdot e^{-kz}\mathrm{J}_0(kr)dk. \quad . \quad . \quad . \quad . \quad . \quad (5)$$

The nature of the distribution of normal traction depends on $\phi_1(k)$, a function of k, which is, as yet, arbitrary.

The stress-components then become

$$\left.\begin{aligned} \widehat{rr} &= \int_0^\infty \phi_1(k)e^{-kz}\left[2\sigma\frac{\mathrm{J}_1(kr)}{kr} + \left\{\mathrm{J}_0(kr)-\frac{\mathrm{J}_1(kr)}{kr}\right\}(1-kz)\right]dk, \\ \widehat{\theta\theta} &= \int_0^\infty \phi_1(k)e^{-kz}\left[\frac{\mathrm{J}_1(kr)}{kr}\cdot(1-kz) + 2\sigma\left\{\mathrm{J}_0(kr)-\frac{\mathrm{J}_1(kr)}{kr}\right\}\right]dk, \\ \widehat{zz} &= \int_0^\infty \phi_1(k)\cdot e^{-kz}\cdot(1+kz)\cdot\mathrm{J}_0(kr)dk \end{aligned}\right\} \quad . \quad . \quad (6)$$

$$\widehat{zr} = \int_0^\infty \phi_1(k)\cdot e^{-kz}\cdot kz\mathrm{J}_1kr(dk), \quad . \quad . \quad . \quad . \quad (7)$$

and the displacements are given by

$$\left.\begin{aligned} w &= -\frac{(1+\sigma)}{\mathrm{E}}\int_0^\infty \frac{\phi_1(k)}{k}\cdot e^{-kz}\cdot\{2(1-\sigma)+kz\}\mathrm{J}_0(kr)dk, \\ u &= \frac{(1+\sigma)}{\mathrm{E}}\int_0^\infty \frac{\phi_1(k)}{k}e^{-kz}\cdot\{(1-2\sigma)-kz\}\mathrm{J}_1(kr)dk, \end{aligned}\right\} \quad . \quad . \quad . \quad (8)$$

when $z=0$ we have

$$\left.\begin{aligned} \widehat{zz} &= \int_0^\infty \phi_1(k) \cdot \mathrm{J}_0(kr)dk, \\ \widehat{zr} &= 0, \end{aligned}\right\} \quad . \quad . \quad . \quad . \quad (9)$$

the surface displacements being given by

$$\left.\begin{aligned} w &= \frac{-2(1-\sigma^2)}{\mathrm{E}} \int_0^\infty \frac{\phi_1(k)}{k} \mathrm{J}_0(kr) \cdot dk, \\ u &= \frac{(1-2\sigma)(1+\sigma)}{\mathrm{E}} \int_0^\infty \frac{\phi_1(k)}{k} \mathrm{J}_1(kr)dk \end{aligned}\right\} . \quad . \quad (10)$$

To make equation (9) represent any desired distribution of normal traction, let ρ be the radius vector and b the limiting radius of the area to which traction is applied, then we must write

$$\phi_1(k) = k \int_0^b f(\rho)\mathrm{J}_0(k\rho) \cdot \rho \cdot d\rho, \quad . \quad . \quad . \quad (11)$$

where $f(\rho)$ is the given surface value of $\widehat{zz}$. Some special cases are outlined below :—

(a) *Tension at a Point on a Plane Boundary.*

If the origin is the point at which a total load P is applied then

$$\phi_1(k) = \frac{\mathrm{P} \cdot k}{2\pi}, \quad . \quad . \quad . \quad . \quad . \quad . \quad . \quad (12)$$

where P is positive for tension. The stress-components at the boundary become

$$\left.\begin{aligned} \widehat{rr} &= -\frac{\mathrm{P}}{2\pi r^2} \cdot (1-2\sigma) \\ \widehat{\theta\theta} &= \frac{\mathrm{P}}{2\pi r^2} \cdot (1-2\sigma) \end{aligned}\right\}, \quad . \quad . \quad . \quad . \quad (13)$$

and the surface displacements are

$$\left.\begin{aligned} w &= -\frac{\mathrm{P}}{\pi r} \cdot \frac{(1-\sigma^2)}{\mathrm{E}} \\ u &= \frac{\mathrm{P}}{\pi r} \cdot \frac{(1-2\sigma)(1+\sigma)}{2\mathrm{E}} \end{aligned}\right\} . \quad . \quad . \quad . \quad (14)$$

(b) *Total Load P uniformly distributed round a circumference of radius* b.

Here we may suppose that $f(\rho)$ vanishes at all radii except when $r=b$. Hence,

$$\phi_1(k) = \frac{P \cdot k}{2\pi} J_0(kb), \quad . \quad . \quad . \quad . \quad (15)$$

substituting in equations (6), when $z=0$, and integrating, it can be shown that for values of $r<b$, $\widehat{rr}$ and $\theta\theta$ are both zero. When $r=b$ the integrals become infinite, and finally, for values of $r>b$, the surface values of the stress-components are the same as if P were concentrated at the centre of the circle, and are given by equations (13).

Again, substituting in equations (10), and integrating *, the corresponding surface displacements are given by

$$\left.\begin{aligned} w &= -\frac{P}{\pi E}\frac{(1-\sigma^2)}{b} \cdot {}_2F_1\left(\tfrac{1}{2}, \tfrac{1}{2}; 1; \frac{r^2}{b^2}\right), \\ u &= 0 \end{aligned}\right\} r<b. \quad . \quad (16)$$

$$\left.\begin{aligned} w &= -\frac{P}{\pi E}\frac{(1-\sigma^2)}{r} \cdot {}_2F_1\left(\tfrac{1}{2}, \tfrac{1}{2}; 1; \frac{b^2}{r^2}\right), \\ u &= \frac{P}{\pi E} \cdot \frac{(1-2\sigma)(1+\sigma)}{2r} \end{aligned}\right\} r>b. \quad . \quad (17)$$

Applying Gauss's Theorem for the Hypergeometric Function when $r=b$, w becomes infinite. For values of $r>b$, u is the same as if P were concentrated.

(c) *Symmetrical Distribution of Normal Traction varying as* ρ^{n-1}.

For a total load P we have

$$f(\rho) = (n+1) \cdot \frac{P}{2\pi b^2}\left(\frac{\rho}{b}\right)^{n-1} \cdot \quad . \quad . \quad . \quad (18)$$

* G. N. Watson 'Theory of Bessel Functions'; u comes from Weber's Result, p. 406, Case 8; w from Gubler's Integral. The displacement w, given by equations (16) and (17), is also expressible in the form, $w = -\frac{P}{\pi E} \cdot \frac{1-\sigma^2}{\pi} \cdot \frac{2K}{(r+b)}$, where the modulus of the complete elliptic integral K is $\frac{2\sqrt{rb}}{(r+b)}$.

Hence, from equation (11).

$$\phi_1(k)=\frac{Pk}{2\pi}\cdot\frac{n+1}{b^{n+1}}\int_0^b \rho^n \,.\, J_0(k\rho)\,.\,d\rho. \quad . \quad . \quad (19)$$

Here the surface displacements can be obtained by direct integration of the results given in case b above.

Thus,

$$\left.\begin{aligned} w=&-\frac{(1-\sigma^2)}{E}\frac{P}{\pi}\frac{n+1}{b^{n+1}}\cdot\left[\int_r^b \rho^{n-1}\cdot{}_2F_1\left(\frac{1}{2},\frac{1}{2};1;\frac{r^2}{\rho^2}\right)d\rho\right.\\ &\left.+\int_0^r\frac{\rho^n}{r}\cdot{}_2F_1\left(\frac{1}{2},\frac{1}{2};1;\frac{\rho^2}{r^2}\right)d\rho\right],\\ u=&\frac{(1-2\sigma)(1+\sigma)}{E}\cdot\frac{P}{2\pi b}\cdot\left(\frac{r}{b}\right)^n; \end{aligned}\right\} \quad r<b. \quad . \quad . \quad (20)$$

$$\left.\begin{aligned} w=&-\frac{(1-\sigma^2)}{E}\cdot\frac{P}{\pi}\frac{n+1}{b^{n+1}}\cdot\int_0^b\frac{\rho^n}{r}\cdot{}_2F_1\left(\frac{1}{2},\frac{1}{2};1;\frac{\rho^2}{r^2}\right)d\rho,\\ u=&\frac{(1-2\sigma)(1+\sigma)}{E}\cdot\frac{P}{2\pi r}; \end{aligned}\right\} \quad r>b \quad . \quad . \quad (21)$$

when $r=0$ equation (20) gives

$$w=-\frac{(1-\sigma^2)}{E}\cdot\frac{P}{\pi b}\cdot\frac{n+1}{n}, \quad . \quad . \quad . \quad (22)$$

and the corresponding displacement at the edge of the circle is

$$w=-\frac{(1-\sigma^2)}{E}\cdot\frac{P}{\pi b}\left\{1+\left(\frac{1}{2}\right)^2\frac{n+1}{n+3}+\left(\frac{1.3}{2.4}\right)^2\frac{n+1}{n+5}+\ldots\right\}. \quad . \quad . \quad (23)$$

From equations 6, when $z=0$, the values of the stress-components at the boundary become

$$\left.\begin{aligned} \widehat{rr}&=\frac{P}{2\pi b^2}\cdot(n+2\sigma)\cdot\left(\frac{r}{b}\right)^{n-1},\\ \widehat{\theta\theta}&=\frac{P}{2\pi b^2}(2n\sigma+1)\cdot\left(\frac{r}{b}\right)^{n-1},\\ \widehat{zz}&=\frac{P}{2\pi b^2}\cdot(n+1)\cdot\left(\frac{r}{b}\right)^{n-1}. \end{aligned}\right\}^{*} \quad r<b. \quad . \quad (24)$$

* Equations (6), when $z=0$, involve integrals shown in equations (9) and (10). The stress-components are therefore readily evaluated.

For values of $r>b$ the stress-components are given by equations (13) as before.

(d) *Uniform Distribution of Normal Traction.*

For a total load P, uniformly distributed over the circular area of radius b, put $n=1$ in equation (19). This gives

$$\phi_1(k)=\frac{P}{\pi b}\cdot J_1(kb). \quad . \quad . \quad . \quad . \quad . \quad (25)$$

The surface values of the stress-components are then obtained by putting n equal to unity in equations (24).

For the displacements at the boundary, equations (10) become

$$\left.\begin{aligned} w&=-2\frac{(1-\sigma^2)}{E}\cdot\frac{P}{\pi b}\cdot {}_2F_1\left(\frac{1}{2},-\frac{1}{2};\,1\,;\,\frac{r^2}{b^2}\right),\\ u&=\frac{(1-2\sigma)(1+\sigma)}{E}\cdot\frac{P}{\pi b^2}\cdot\frac{r}{2}; \end{aligned}\right\} r<b. \quad (26)$$

$$\left.\begin{aligned} w&=-\frac{(1-\sigma^2)}{E}\cdot\frac{P}{\pi r}\cdot {}_2F_1\left(\frac{1}{2},\frac{1}{2};\,2\,;\,\frac{b^2}{r^2}\right),\\ u&=\frac{(1-2\sigma)(1+\sigma)}{E}\cdot\frac{P}{2\pi r}. \end{aligned}\right\} r>b. \quad (27)$$

Applying the Gaussian formula for ${}_2F_1(\alpha,\beta,\gamma,1)$, the axial displacement at the edge of the circle is given by

$$w=-\frac{(1-\sigma^2)}{E}\cdot\frac{P}{\pi b}\cdot\frac{4}{\pi}. \quad . \quad . \quad . \quad . \quad . \quad (28)$$

§ 3. Symmetrical Distribution of Tangential Surface Traction about a Point on a Plane Boundary.

Using the notation outlined in the previous article, then, for a distribution of tangential surface traction, symmetrical about the axis of z, we can write

$$\chi=\int_0^\infty\frac{\phi_2(k)}{k^3}\left[\{(1-2\sigma)-kz\}J_0(kr)e^{-kz}\right.$$
$$\left.-\{(1-2\sigma)-2kz(1-\sigma)\}\right]dk, \quad . \quad (29)$$

where

$$\nabla^2\chi=\int_0^\infty\frac{2\phi_2(k)}{k}\cdot e^{-kz}\cdot J_0(kr)dk. \quad . \quad . \quad (30)$$

The nature of the distribution depends on $\phi_2(k)$, a function of k, which is, as yet, arbitrary.

The stress-components may then be written

$$\left.\begin{aligned}
\widehat{rr} &= -\int_0^\infty \phi_2(k)e^{-kz}\left[2\sigma\cdot\frac{\mathrm{J}_1(kr)}{kr}\right.\\
&\qquad\left.+\left\{\mathrm{J}_0(kr)-\frac{\mathrm{J}_1(kr)}{kr}\right\}(2-kz)\right]dk,\\
\widehat{\theta\theta} &= -\int_0^\infty \phi_2(k)e^{-kz}\left[\frac{\mathrm{J}_1(kr)}{kr}(2-kz)\right.\\
&\qquad\left.+2\sigma\left\{\mathrm{J}_0(kr)-\frac{\mathrm{J}_1(kr)}{kr}\right\}\right]dk,\\
\widehat{zz} &= -\int_0^\infty \phi_2(k)e^{-kz}\cdot kz\cdot\mathrm{J}_0(kr)dk.
\end{aligned}\right\} \quad . \quad . \quad . \quad (31)$$

$$\widehat{zr} = \int_0^\infty \phi_2(k)e^{-kz}\cdot(1-kz)\cdot\mathrm{J}_1(kr)dk, \quad . \quad . \quad . \quad . \quad (32)$$

and the displacements become

$$\left.\begin{aligned}
w &= \frac{1+\sigma}{\mathrm{E}}\int_0^\infty \frac{\phi_2(k)}{k}\cdot e^{-kz}\{2(1-\sigma)-(1-kz)\}\mathrm{J}_0(kr)\cdot dk,\\
u &= -\frac{1+\sigma}{\mathrm{E}}\int_0^\infty \frac{\phi_2(k)}{k}\cdot e^{-kz}\{(1-2\sigma)+(1-kz)\}\mathrm{J}_1(kr)dk,
\end{aligned}\right\} \quad . \quad . \quad . \quad (33)$$

when $z=0$ we have

$$\left.\begin{aligned}
\widehat{zz} &= 0,\\
\widehat{zr} &= \int_0^\infty \phi_2(k)\mathrm{J}_1(kr)\cdot dk,
\end{aligned}\right\}, \quad . \quad . \quad . \quad (34)$$

the surface displacements being given by

$$\left.\begin{aligned}
w &= \frac{(1-2\sigma)(1+\sigma)}{\mathrm{E}}\int_0^\infty \frac{\phi_2(k)}{k}\cdot\mathrm{J}_0(kr)dk,\\
u &= -2\frac{(1-\sigma^2)}{\mathrm{E}}\int_0^\infty \frac{\phi_2(k)}{k}\mathrm{J}_1(kr)dk.
\end{aligned}\right\} \quad . \quad . \quad (35)$$

To make equation (34) represent any desired distribution of tangential surface traction we must write

$$\phi_2(k) = k\int_0^b f(\rho)\mathrm{J}_1(k\rho)\cdot\rho\cdot d\rho, \quad . \quad . \quad . \quad (36)$$

where ρ and b have the same meanings as in equation (11), and $f(\rho)$ is the given surface value of $\widehat{zr}$. Some special cases are outlined below.

(a) *Total Tangential Surface Traction Q, uniformly distributed round a Circumference of Radius* b.

Here we may suppose that $f(\rho)$ vanishes at all radii, except when $r=b$. Hence,

$$\phi_2(k) = \frac{k}{2\pi} J_1(kb) \cdot \int_0^b f(\rho) \cdot 2\pi\rho \cdot d\rho,$$

or

$$\phi_2(k) = \frac{Qk}{2\pi} \cdot J_1(kb). \quad . \quad . \quad . \quad . \quad . \quad . \quad . \quad . \quad (37)$$

Substituting in equations (35) the surface displacements are given by *

$$\left.\begin{aligned} w &= \frac{Q}{\pi b} \cdot \frac{(1-2\sigma)(1+\sigma)}{2E}, \\ u &= -\frac{Q}{2\pi} \cdot \frac{r}{b^2} \cdot \frac{(1-\sigma^2)}{E} \cdot {}_2F_1\left(\frac{3}{2}, \frac{1}{2}; 2; \frac{r^2}{b^2}\right); \end{aligned}\right\} r < b, \quad (38)$$

$$\left.\begin{aligned} w &= 0, \\ u &= -\frac{Q}{2\pi} \cdot \frac{b}{r^2} \cdot \frac{(1-\sigma^2)}{E} \cdot {}_2F_1\left(\frac{3}{2}, \frac{1}{2}; 2; \frac{b^2}{r^2}\right), \end{aligned}\right\} r > b. \quad (39)$$

Examining the displacements when $r=b$, as previously indicated, it is seen that u becomes infinite, and w is given by

$$w = \frac{Q}{2\pi b} \cdot \frac{(1-2\sigma)(1+\sigma)}{2E}.$$

(b) *Symmetrical Distribution of Tangential Surface Traction varying as* ρ^n.

Writing $f(\rho) = (n+2)\frac{Q}{2\pi b^2}\left(\frac{\rho}{b}\right)^n$, the surface displacements may be obtained by direct integration of the results given in case a above.

* w comes from Weber's Result, and u from Gubler's Integral. G. N. Watson, *op. cit.* p. 406, Case 8; and p. 410.

Thus

$$\left.\begin{aligned} w = {} & \frac{n+2}{n+1}\cdot\frac{Q}{\pi b}\cdot\frac{(1-2\sigma)(1+\sigma)}{2E}\left\{1-\left(\frac{r}{b}\right)^{n+1}\right\}, \\ u = {} & -\frac{(1-\sigma^2)}{E}\cdot\frac{Q}{2\pi}\cdot\frac{n+2}{b^{n+2}} \\ & \times\left[\int_r^b \rho^{n-1}\cdot {}_2F_1\left(\frac{3}{2},\frac{1}{2};\,2;\,\frac{r}{\rho^2}\right)d\rho,\right. \\ & \left.+\int_0^r \frac{\rho^{n+2}}{r^2}\,{}_2F_1\left(\frac{3}{2},\frac{1}{2};\,2;\,\frac{r^2}{\rho^2}\right)d\rho\right]; \end{aligned}\right\} r<b. \quad (40)$$

$$\left.\begin{aligned} w = {} & 0, \\ u = {} & -\frac{(1-\sigma^2)}{E}\cdot\frac{Q}{2\pi}\cdot\frac{n+2}{b^{n+2}} \\ & \times\int_0^b \frac{\rho^{n+2}}{r^2}\,{}_2F_1\left(\frac{3}{2},\frac{1}{2};\,2;\,\frac{\rho^2}{r^2}\right)d\rho. \end{aligned}\right\} r>b. \quad (41)$$

At the edge of the circle, the radial displacement is then given by

$$u = -\frac{(1-\sigma^2)}{E}\cdot\frac{Q}{2\pi b}\cdot\frac{n+2}{n+3}\left\{1+\frac{3}{2}\left(\frac{1}{2}\right)^2\frac{n+3}{n+5} + \frac{5}{3}\left(\frac{1\cdot 3}{2\cdot 4}\right)^2\frac{n+3}{n+7}+\ldots\right\}. \quad (42)$$

(c) *Symmetrical Distribution of Surface Traction varying as the Radius.*—

For a total tangential surface traction Q we have

$$f(\rho)=\frac{3Q}{2\pi b^2}\cdot\frac{\rho}{b},$$

so that equation (36) becomes

$$\phi_2(k)=\frac{3Q}{2\pi b}\cdot J_2(kb). \quad (43)$$

For the surface displacements we then find

$$\left.\begin{aligned} w = {} & \frac{3Q}{2\pi b}\cdot\frac{(1-2\sigma)(1+\sigma)}{2E}\left\{1-\frac{r^2}{b^2}\right\}^{*}, \\ u = {} & -\frac{3Q}{2\pi b}\cdot\frac{r}{b}\cdot\frac{(1-\sigma^2)}{E}\cdot {}_2F_1\left(\frac{3}{2},-\frac{1}{2};\,2;\,\frac{r^2}{b^2}\right); \end{aligned}\right\} r<b, \quad (44)$$

* These integrals are particular cases of the Weber and Schafheitlin integral (see G. N. Watson, *op. cit.* § 13.41, p. 404, equations (4) and (5)). In deducing the displacement w, it will be noticed that ${}_2F_1\left(1,-1;\,1;\,\frac{r^2}{b^2}\right)=\left(1-\frac{r^2}{b^2}\right)$. Equation (7), p. 404, shows the limiting values of the integrals when $r=b$.

$$\left.\begin{aligned} w &= 0, \\ u &= -\frac{3Q}{2\pi b}\cdot\frac{b^2}{4r^2}\,\frac{(1-\sigma^2)}{E}\cdot {}_2F_1\left(\frac{3}{2},\ \frac{1}{2};\ 3;\ \frac{b^2}{r^2}\right)^{*}. \end{aligned}\right\} r > b. \quad (45)$$

At the edge of the circle, the surface displacements become

$$\left.\begin{aligned} w &= 0, \\ u &= -\frac{Q}{\pi b}\cdot\frac{1-\sigma^2}{E}\cdot\frac{2}{\pi}. \end{aligned}\right\} \quad . \quad . \quad . \quad (46)$$

§ 4. The Stress-System (A), due to a Symmetrical Distribution of Normal Traction, in a Complete Disk at Rest.

(a) This system is made up of three component systems, viz. :

I. That due to symmetrical distributions of traction, acting at the surface of an infinite solid, bounded by the plane $z=-h$, and lying on the side $z>-h$ of this plane.

II. That due to symmetrical distributions of traction, acting at the surface of an infinite solid, bounded by the plane $z=h$, snd lying on the side $z<h$ of this plane.

III. The system in the infinite slab contained between the planes $z=\pm h$, these planes being subject to tractions obtained by reversing the components $\widehat{zz}$ and $\widehat{zr}$ at $z=h$ in I., and $z=-h$ in II.†

Using the notation already given in § 2, the functions χ_1, χ_2, χ_3, representing the systems I., II., and III. respectively, are

$$\left.\begin{aligned} \chi_1 &= \int_0^\infty \frac{\phi_1(k)}{k^3}\left[\{(2\sigma+k(h+z)\}\,J_0(kr)e^{-k(h+z)}\right. \\ &\qquad \left. -\{2\sigma+(1-2\sigma)k(h+z)\}\right]dk, \\ \chi_2 &= -\int_0^\infty \frac{\phi_1(k)}{k^3}\left[\{2\sigma+k(h-z)\}\,J_0(kr)e^{-k(h-z)}\right. \\ &\qquad \left. -\{2\sigma+(1-2\sigma)k(h-z)\}\right]dk, \\ \chi_3 &= \int_0^\infty 2\frac{\phi_1(k)}{k^3}\left[(\alpha\sinh kz-\beta kz\cosh kz)\,J_0(kr)\right. \\ &\qquad \left. -(\alpha-\beta)kz\right]dk, \end{aligned}\right\} \quad (47)$$

* See footnote on preceding page.

† Phil. Mag. *tom. cit.* pp. 1237–1238.

where α and β are given by

$$\left.\begin{aligned}\alpha &= e^{-2hk}\frac{\left[\begin{array}{c}\{2\sigma(1+2hk)+2h^2k^2\}\sinh kh\\ +\{hk(1+2hk)-2hk(1-2\sigma)\cosh kh\end{array}\right]}{2hk+\sinh 2hk},\\ \beta &= e^{-2hk}\frac{[(1+2hk)\sinh kh+2hk\cosh kh]}{2hk+\sinh 2hk}.\end{aligned}\right\} \quad (48)$$

These quantities have been tabulated *, assuming Poisson's Ratio $\sigma=\cdot3$, and are negligible for values of $hk>4$.

(b) *Evaluation of Stress-Components and Displacements.*

For the stress-systems I. and II., of the system (A), equations (6) give the stress-compoaents at any point, by writing $(h+z)$ and $(h-z)$ for z respectively. For the system III. the stress-components become

$$\left.\begin{aligned}\widehat{rr}_3 &= -2\int_0^\infty \phi_1(k)\left[2\beta\sigma\cosh kz\,J_0(kr)-\left\{J_0(kr)-\frac{J_1(kr)}{kr}\right\}\right.\\ &\qquad\left.\times\{(\alpha-\beta)\cosh kz-\beta kz\sinh kz\}\right]dk,\\ \widehat{\theta\theta}_3 &= -2\int_0^\infty \phi_1(k)\left[2\beta\sigma\cosh kz\,J_0(kr)-\frac{J_1(kr)}{kr}\right.\\ &\qquad\left.\times\{(\alpha-\beta)\cosh kz-\beta kz\sinh kz\}\right]dk,\\ \widehat{zz}_3 &= -2\int_0^\infty \phi_1(k)\left[\{\alpha+\beta(1-2\sigma)\}\cosh kz\right.\\ &\qquad\left.-\beta kz\sinh kz\right]J_0(kr)\,dk.\end{aligned}\right\} \quad \ldots \quad (49)$$

The components $\widehat{zr}$ for the three systems are given by

$$\left.\begin{aligned}\widehat{zr}_1 &= \int_0^\infty \phi_1(k)\,e^{-k(h+z)}k(h+z)\,J_1(kr)\,dk,\\ \widehat{zr}_2 &= -\int_0^\infty \phi_1(k)\,e^{-k(h-z)}k(h-z)\,J_1(kr)\,dk,\\ \widehat{zr}_3 &= -2\int_0^\infty \phi_1(k)\,[\beta kz\cosh kz-(\alpha-2\beta\sigma)\sinh kz]\,J_1(kr)\,dk.\end{aligned}\right\} \quad \ldots \quad (50)$$

* Phil. Mag. *tom. cit.* p. 1242.

Expressing the coordinates r, z, in terms of h, these integrals may be evaluated graphically, and the stress-components, in every case, written in the form *

$$\widehat{rr} = \delta_{\widehat{rr}} \cdot \frac{P}{\pi h^2}, \qquad \ldots\ldots\ldots \quad (51)$$

where $\delta_{\widehat{rr}} = \delta_{\widehat{rr}_1} + \delta_{\widehat{rr}_2} + \delta_{\widehat{rr}_3}$, and so on,

the numerical constant $\delta_{\widehat{rr}}$ representing the stress-component $\widehat{rr}$ at the point considered.

In a similar manner, the displacements in the systems I. and II., of the stress-system (A), are obtained from equations (8), while for the system III. the displacements are determed from the function χ_3 given by equation (44).

Putting $z = h$, we have, at the plane face of the disk, for the system (A)

$$\left.\begin{aligned} w_1 &= -\frac{2(1+\sigma)}{E}\int_0^\infty \frac{\phi_1(k)}{k} e^{-2kh}\{(1-\sigma)+kh\}J_0(kr)\,dk, \\ w_2 &= \frac{2(1-\sigma^2)}{E}\int_0^\infty \frac{\phi_1(k)}{k} J_0(kr)\,dk, \\ w_3 &= -\frac{2(1+\sigma)}{E}\int_0^\infty \frac{\phi_1(k)}{k}[\{\alpha+2\beta(1-2\sigma)\}\sinh kh \\ &\qquad -\beta kh\cosh kh]\,J_0(kr)\,dk; \end{aligned}\right\} \quad (52)$$

$$\left.\begin{aligned} u_1 &= \frac{(1+\sigma)}{E}\int_0^\infty \frac{\phi_1(k)}{k}\cdot e^{-2kh} \\ &\qquad \cdot\{(1-2\sigma)-2kh\}\,J_1(kr)\,dk, \\ u_2 &= \frac{(1+\sigma)(1-2\sigma)}{E}\int_0^\infty \frac{\phi_1(k)}{k} J_1(kr)\,dk, \\ u_3 &= \frac{2(1+\sigma)}{E}\int_0^\infty \frac{\phi_1(k)}{k}[(\alpha-\beta)\cosh kh \\ &\qquad -\beta kh\sinh kh]\,J_1(kr)\,dk. \end{aligned}\right\} \quad (53)$$

Expressing these displacements in the form

$$\left.\begin{aligned} w &= \gamma_w \cdot \frac{P}{\pi h E}, \\ u &= \gamma_u \cdot \frac{P}{\pi h E}, \end{aligned}\right\} \quad \ldots\ldots \quad (54)$$

where

$$\gamma_w = \gamma_{w_1} + \gamma_{w_2} + \gamma_{w_3},$$
$$\gamma_u = \gamma_{u_1} + \gamma_{u_2} + \gamma_{u_3},$$

* Phil. Mag. *tom. cit.* p. 1243.

then, when $\phi_1(k)$ is known, the integrations for the systems I. and III. may be performed graphically, and numerical values for γ_w and γ_u obtained.

The strains may be determined directly from the stress-components by writing

$$\lambda\widehat{rr} = \delta\widehat{rr} - \sigma(\delta\widehat{\theta\theta} + \delta\widehat{zz}) \text{ etc.},$$

λ being a constant representing a particular strain in the system (A), such that

$$e_{rr} = \lambda_{rr} \cdot \frac{P}{\pi E h^2}, \text{ etc.} \quad . \quad . \quad . \quad . \quad (55)$$

§ 5. The Stress-System (A) due to a Symmetrical Distribution of Tangential Surface Traction, in a Complete Disk at Rest.

(a) Here the system will be made up of three component systems as in the previous article. The functions χ_1, χ_2, χ_3, representing the systems I., II., and III., respectively, are

$$\left.\begin{aligned}
\chi_1 = & \int_0^\infty \frac{\phi_2(k)}{k^3}\big[\{(1-2\sigma)-k(h+z)\}\,J_0(kr)\,e^{-k(h+z)} \\
& \qquad -\{(1-2\sigma)-2k(h+z)(1-\sigma)\}\big]\,dk, \\
\chi_2 = & -\int_0^\infty \frac{\phi_2(k)}{k^3}\big[\{(1-2\sigma)-k(h-z)\}\,J_0(kr)\,e^{-k(h-z)} \\
& \qquad -\{(1-2\sigma)-2k(h-z)(1-\sigma)\}\big]\,dk, \\
\chi_3 = & \int_0^\infty \frac{2\phi_2(k)}{k^3}\big[(\alpha\sinh kz - \beta\, kz\cosh kz)\,J_0(kr) \\
& \qquad -(\alpha-\beta)\,kz\big]\,dk.
\end{aligned}\right\} \quad (56)$$

The condition for determining the constants α and β is the same as in the previous case. These may be written

$$\left.\begin{aligned}
\alpha = & -e^{-2hk}\,\frac{\big[\{hk(1+2hk)-2hk(1-2\sigma)\}\sinh kh \\ \qquad & +\{(1-2\sigma)(1-2hk)+2h^2k^2\}\cosh kh\big]}{2hk+\sinh 2hk}, \\
\beta = & -e^{-2hk}\,\frac{\big[2hk\sinh kh-(1-2hk)\cosh kh\big]}{2hk+\sinh 2hk}.
\end{aligned}\right\} \quad (57)$$

Assuming Poisson's Ratio $\sigma = \cdot 3$, calculated values of these constants are given in Table I.

TABLE I.

hk.	*α.*	*β.*
0.....	$-\infty$	$+\infty$
·25	−·2137	·2305
·50	−·1482	−·0882
·75	−·1380	−·1156
1·0.....	−·1217	−·0938
1·5.....	−·0723	−·04235
2·0.....	−·0328	−·01509
3·0.....	−·00415	−·00132
4·0.....	−·00038	−·000092
5·0.....	−·0000297	−·0000058
6·0.....	−·00000215	−·00000035

(b) *Evaluation of Stress-Components and Displacements.*

For the stress-systems I. and II., equations (31) give the stress-components at any point, by writing $(h+z)$ and $(h-z)$ for z respectively. For the system III., the corresponding components are given by equations (49), using the values of α and β just determined, and replacing $\phi_1(k)$ by $\phi_2(k)$ in these equations.

The components $\widehat{zr}$ for the three systems are

$$\left.\begin{aligned}
\widehat{zr}_1 &= \int_0^\infty \phi_2(k)\, e^{-k(h+z)}\{1-k(h+z)\}\, \mathrm{J}_1(kr)\, dk,\\
\widehat{zr}_2 &= -\int_0^\infty \phi_2(k)\, e^{-k(h-z)}\{1-k(h-z)\}\, \mathrm{J}_1(kr)\, dk,\\
\widehat{zr}_3 &= -2\int_0^\infty \phi_2(k)\, \{\beta kz \cosh kz - (\alpha - 2\beta\sigma)\sinh kz\}\, \mathrm{J}_1(kr)\, dk.
\end{aligned}\right\} \quad . \quad . \quad . \quad (58)$$

As before, the stress-components at any point may e represented by numerical constants, and written in the form

$$\widehat{rr} = \delta_{\widehat{rr}} \cdot \frac{\mathrm{Q}}{\pi h^2}, \text{ etc., } \quad . \quad . \quad . \quad . \quad . \quad (59)$$

the constants δ to be determined graphically. The displacements for the systems I. and II. are obtained from equations (33), while for the system III. they are given in equations (52) and (53), using the appropriate values of α and β, and replacing $\phi_1(k)$ by $\phi_2(k)$ in these equations.

When $\phi_2(k)$ is known, the displacements may again be written

$$\left.\begin{aligned} w &= \gamma_w \cdot \frac{Q}{\pi h E} \\ u &= \gamma_u \cdot \frac{Q}{\pi h E} \end{aligned}\right\}, \quad \ldots\ldots \quad (60)$$

and numerical values determined as before.

§ 6. The Stress-System (B).

For reference, the results of the solution due to Chree are summarized below. The stress-components are given by

$$\left.\begin{aligned} rr &= \frac{\rho\omega^2}{8}(3+\sigma)(a^2-r^2) + \frac{\rho\omega^2}{6}\sigma\frac{(1+\sigma)}{(1-\sigma)}(h^2-3z^2), \\ \widehat{\theta\theta} &= \frac{\rho\omega^2}{8}\{(3+\sigma)a^2-(1+3\sigma)r^2\} + \frac{\rho\omega^2}{6}\sigma\frac{(1+\sigma)}{(1-\sigma)}\cdot(h^2-3z^2), \\ \widehat{zz} &= \widehat{zr} = 0, \end{aligned}\right\} \quad \ldots \quad (61)^*$$

and the displacements by

$$\left.\begin{aligned} u &= \frac{\rho\omega^2 r}{8E}(1-\sigma)\{(3+\sigma)a^2-(1+\sigma)r^2\} \\ &\qquad + \frac{\rho\omega^2}{6E}\cdot r\sigma(1+\sigma)(h^2-3z^2), \\ w &= -\frac{\rho\omega^2 z}{4E}\sigma\{(3+\sigma)a^2-2(1+\sigma)r^2\} \\ &\qquad - \frac{\rho\omega^2}{3E}\cdot z\cdot\sigma^2\frac{(1+\sigma)}{(1-\sigma)}(h^2-z^2). \end{aligned}\right\} \quad (62)$$

§ 7. Calculated Values of the Stress-Components and Displacements in the System (A). Determination of P and Q.

For any assumed distribution of traction the functions $\phi_1(k)$ and $\phi_2(k)$ may be determined, and the stress-components for the system (A) calculated in terms of P and Q, the total normal and tangential loads applied to the plane faces of the disk at rest. It remains to calculate these quantities P and Q in terms of ω. Three cases are considered.

* ρ being the density in these equations.

Case 1.—*Disk restrained by a Distribution of Normal Traction only.*

Here Q is zero. For the determination of P in terms of ω we may suppose that, for the systems (A) and (B) combined,

(i.) The resultant axial displacement vanishes at $z=\pm h$, $r=0$, or
(ii.) The resultant axial strain vanishes at $z=0$, $r=0$.

TABLE II.

$\frac{\phi_1(k)}{\frac{Pk}{2\pi}\frac{r}{J_0}\frac{(hk)}{4}}$	Plane $z=0$.			Plane $z=\frac{h}{2}$.			Plane $z=h$.	
	$\widehat{rr}$.	$\widehat{\theta\theta}$.	$\widehat{zz}$.	$\widehat{rr}$.	$\widehat{\theta\theta}$.	$\widehat{zz}$.	$\widehat{rr}$.	$\widehat{\theta\theta}$.
$r=0$	−·234	−·234	2·171	−·072	−·072	3·64	− ·475	−·475
$r=\frac{h}{4}$	−·135	−·226	1·899	·058	−·136	3·036	− ·442 −3·642	−·455 2·745
$r=\frac{h}{2}$	·074	−·191	1·283	·424	−·162	1·391	−1·167	·392
$r=\frac{3h}{4}$	·224	−·153	·695	·413	−·135	·470	− ·625	·008
$r=h$	·255	−·115	·296	·257	−·103	·154	− ·372	−·085
$r=\frac{5h}{4}$	·218	−·086	·106	·150	−·084	·048	− ·220	−·099
$r=\frac{3h}{2}$	·164	−·066	·020	·088	−·068	·010	− ·122	−·084
$r=\frac{7h}{4}$	·114	−·052	−·010	·058	−·054	−·007	− ·057	−·062
$r=2h$	·075	−·043	−·019	·042	−·044	−·011	− ·019	−·043

Subcase (a).—*P round a Circumference of Radius* b: § 2 *b*.

$$\phi_1(k)=\frac{Pk}{2\pi}J_0(kb).$$

Values of δ, representing the total stress-components in the system (A), when $b=\frac{h}{4}$, $\frac{h}{2}$, $\frac{3h}{4}$, and h, are shown in Tables II. to V. respectively *. The surface displacements w, corresponding to these distributions, may be obtained from Table VI.

* Calculated values for the case when $b=0$ have already been tabulated. Phil. Mag. *tom. cit.* Table III. p. 1244, and figs. 1, 2, and 3.

TABLE III.

$\frac{\phi_1(k)}{\frac{Pk}{2\pi}J_0\frac{(hk)}{2}}$	Plane $z=0$.			Plane $z=\frac{h}{2}$.			Plane $z=h$.	
	$\widehat{rr}$.	$\widehat{\theta\theta}$.	$\widehat{zz}$.	$\widehat{rr}$.	$\widehat{\theta\theta}$.	$\widehat{zz}$.	$\widehat{rr}$.	$\widehat{\theta\theta}$.
$r=0$	−·056	−·056	1·348	−·206	−·206	1·201	−·401	−·401
$r=\frac{h}{4}$	−·051	−·066	1·283	·090	·172	1·391	−·383	−·390
$r=\frac{h}{2}$	·005	−·080	1·072	·007	·065	1·45	−·334 −1·194	−·363 ·437
$r=\frac{3h}{4}$	·098	−·086	·726	·202	−·035	·770	−·615	·038
$r=h$	·172	−·081	·384	·233	−·073	·280	−·377	−·068
$r=\frac{5h}{4}$	·180	−·070	·166	·161	−·072	·085	−·236	−·088
$r=\frac{3h}{2}$	·149	−·058	·050	·102	−·063	·024	−·137	−·080
$r=\frac{7h}{4}$	·110	−·047	·004	·065	−·052	·002	−·071	−·063
$r=2h$	·074	−·041	−·011	·046	−·043	−·007	−·028	−·046

TABLE IV.

$\frac{\phi_2(k)}{\frac{Pk}{2\pi}J_0\frac{(3hk)}{4}}$	Plane $z=0$.			Plane $z=\frac{h}{2}$.			Plane $z=h$.	
	$\widehat{rr}$.	$\widehat{\theta\theta}$.	$\widehat{zz}$.	$\widehat{rr}$.	$\widehat{\theta\theta}$.	$\widehat{zz}$.	$\widehat{rr}$.	$\widehat{\theta\theta}$.
$r=0$	·051	·051	·668	·146	·146	·381	−·317	−·317
$r=\frac{h}{4}$	·030	·042	·695	·127	·151	·470	−·306	−·311
$r=\frac{h}{2}$	−·008	·022	·726	·019	·148	·770	−·281	−·298
$r=\frac{3h}{4}$	−·003	−·005	·670	−·055	·094	·93	−·235 −·591	−·272 ·084
$r=h$	·057	−·029	·470	·105	−·001	·498	−·378	−·036
$r=\frac{5h}{4}$	·110	−·043	·260	·156	−·043	·184	−·251	−·071
$r=\frac{3h}{2}$	·122	−·044	·116	·114	−·051	·061	−·159	−·070
$r=\frac{7h}{4}$	·107	−·042	·040	·074	−·049	·017	−·094	−·061
$r=2h$	·081	−·037	·003	·048	−·043	·002	−·048	−·050

TABLE V.

$\frac{Pk}{2\pi}J_0(hk)$. $\phi_1(k)$	Plane $z=0$.			Plane $z=\frac{h}{2}$.			Plane $z=h$.	
	$\widehat{rr}$.	$\widehat{\theta\theta}$.	$\widehat{zz}$.	$\widehat{rr}$.	$\widehat{\theta\theta}$.	$\widehat{zz}$.	$\widehat{rr}$.	$\widehat{\theta\theta}$.
$r=0$	·08	·08	·271	·072	·072	·122	−·232	−·232
$r=\frac{h}{4}$	·063	·078	·296	·075	·079	·154	−·228	−·230
$r=\frac{h}{2}$	·022	·071	·334	·066	·094	·280	−·219	−·224
$r=\frac{3h}{4}$	−·023	·052	·470	−·009	·113	·498	−·199	−·211
$r=h$	−·025	·020	·473	−·072	·085	·709	−·172 −·372	−·196 ·004
$r=\frac{5h}{4}$	·019	−·006	·352	·056	·017	·384	−·280	−·047
$r=\frac{3h}{2}$	·066	−·022	·200	·105	−·024	·148	−·188	−·060
$r=\frac{7h}{4}$	·087	−·029	·087	·083	−·035	·046	−·118	−·055
$r=2h$	·079	−·033	·025	·052	−·032	·013	−·070	−·049

TABLE VI.

	$b=0$.		$b=\frac{h}{4}$.		$b=\frac{h}{2}$.		$b=\frac{3h}{4}$.		$b=h$.	
	$\gamma_{w_{1+3}}$.	γ_{w_2}.	$\gamma_{w_{1+3}}$.	γ_{w_2}.	$\gamma_{w_{1+3}}$.	γ_{w_2}.	$\gamma_{w_{1+3}}$.	γ_{w_2}.	$\gamma_{w_{1+3}}$.	γ_{w_2}.
0	−1·059	—	−1·042	3·64	−·982	1·82	−·896	1·213	−·796	·91
$\frac{h}{4}$	−1·042	3·64	−1·021	—	−·965	1·955	−·885	1·25	−·790	·928
$\frac{h}{2}$	−·982	1·82	−·965	1·955	−·920	—	−·854	1·4	−·771	·978
$\frac{3h}{4}$	−·896	1·213	−·885	1·25	−·854	1·4	−·803	—	−·740	1·104
h	−·796	·91	−·790	·928	−·771	·978	−·740	1·104	−·699	—

In this table the values of γ_{w_2}, for the component-system II. of the stress-system (A), are shown separately.

If $w=0$ at $z=\pm h$, $r=0$, condition (i.) above, then from equation (62), if $\sigma=\cdot3$, we must have

$$\frac{P}{\pi h^2}=\cdot2475\,\frac{\rho\omega^2a^2}{\gamma_w}, \quad . \quad . \quad . \quad . \quad . \quad (63)$$

γ_w representing the total displacement w at $z=h$, $r=0$, for the stress-system (A), and for a particular value of b is found from Table VI.

Alternatively, if $\dfrac{\partial w}{\partial z}=0$, at $z=0$, $r=0$, $r=0$, condition (ii.) above, then for P we find

$$\frac{P}{\pi h^2}=\frac{\rho\omega^2a^2}{\lambda_{zz}}\left\{\cdot2475+\cdot0557\frac{h^2}{a^2}\right\}. \quad . \quad . \quad (64)$$

Values of λ_{zz} can be deduced from the stress-components given in Tables II. to V., by means of equation (55). A comparison of these two conditions is shown in Table VII.

TABLE VII.

b/h.	γ_w.	λ_{zz}.
0	—	2·783
$\frac{1}{4}$	2·598	2·311
$\frac{1}{2}$	·838	1·382
$\frac{3}{4}$	·317	·637
1	·114	·223

Subcase (b).—*Where $f(\rho)$ is the given Surface Value of zz.*

This is the general case indicated in equation (11). The stress-components and displacements at any point in the system (A) can be found by direct integration from the results of subcase (a), by writing

$$\left.\begin{aligned}\delta'&=\frac{2\pi}{P}\int_0^b\delta f(\rho).\rho.d\rho,\\ \gamma'&=\frac{2\pi}{P}\int_0^b\gamma f(\rho).\rho.d\rho,\end{aligned}\right\} \quad . \quad . \quad . \quad . \quad (65)$$

the integrations to be performed graphically *.

To illustrate the effect of varying distributions of normal traction on the surface displacements, a distribution varying as ρ^{n-1}, § 2*c*, has been chosen. The components of displacement, for the systems I. and III. of the stress-system

* Where $f(\rho)$ is such that equation (11) may be easily integrated, the stress-components and displacements are determined as outlined in § 4.

(A), have been calculated by means of equations (65) *, and those for the system II. from the results of § 2 *c*.

Table VIII. shows the total displacements in the stress-system (A), at $r = 0$ and $r = b$, for varying values of b and n.

TABLE VIII.

	$b=\frac{h}{2}$.			$b=\frac{3h}{4}$.			$=h$.		
	$r=0$.		$r=b$.	$r=0$.		$r=b$.	$r=0$		$r=b$.
	γ_w.	γ_w.	γ_u.	γ_w.	γ_w.	γ_u.	γ_w.	γ_w.	γ_u.
$n=1$.....	2·618	1·367	·376	1·452	·695	·169	·902	·398	·070
$n=3$.....	1·416	1·633	·380	·669	·881	·179	·340	·554	·085
$n=5$.....	1·180	1·815	·382	·522	1·005	·183	·240	·651	·094
$n=7$.....	1·081	1·952	·383	·461	1·099	·185	·201	·723	·099
$n=9$.....	1·026	2·061	·384	·426	1·174	·187	·181	·780	·101
$n=11$.....	·990	2·156	·385	·404	1·238	·188	·167	·829	·103
$n=21$.....	·918	2·475	·386	·355	1·453	·191	·138	·993	·108
$n=31$.....	·892	2·670	·387	·337	1·584	·192	·128	1·092	·109

Subcase (c).—*Uniform Distribution of Normal Traction* : § 2 *d*.

$$\phi_1(k) = \frac{P}{\pi b} J_1(kb)$$

Values of δ representing the total stress-components in the system (A), for the case when $b=h$, are shown in Table IX. If the conditions (i.) and (ii.) are to be satisfied, the corresponding values of P are given by equations (63) and (64), the appropriate values of γ_w and λ_{zz} being ·902 and ·972 respectively

Case 2.—*Disk restrained by a Distribution of Tangential Traction only.*

Here P is zero. For the determination of Q in terms of ω it may be assumed that the resultant radial displacement vanishes at $z = \pm h$, $r = b$.

* Table VI. is arranged to facilitate these calculations.

TABLE IX.

$\phi_1(k)$ / $\frac{P}{\pi h} J_1(hk)$.	Plane $z=0$.			Plane $z=\frac{h}{2}$.			Plane $z=h$.		
	$\widehat{rr}$.	$\widehat{\theta\theta}$.	$\widehat{zz}$.	$\widehat{rr}$.	$\widehat{\theta\theta}$.	$\widehat{zz}$.	$\widehat{rr}$.	$\widehat{\theta\theta}$.	$\widehat{zz}$.
$r=0$	−·010	−·010	·966	·107	·107	1·018	·457	·457	1
$r=\frac{h}{4}$	−·006	−·015	·927	·101	·095	·999	·472	·466	1
$r=\frac{h}{2}$	·013	−·022	·820	·092	·074	·905	·506	·485	1
$r=\frac{3h}{4}$	·048	−·034	·650	·074	·038	·755	·561	·518	1
$r=h$	·096	−·044	·427	·122	−·016	·440	·624 −·376	·557 −·043	1 0
$r=\frac{5h}{4}$	·125	−·049	·234	·139	−·045	·178	−·248	·075	0
$r=\frac{3h}{2}$	·124	−·046	·103	·106	−·051	·061	−·154	−·072	0
$r=\frac{7h}{4}$	·105	−·042	·034	·071	−·048	·015	−·088	−·061	0
$r=2h$	·079	−·038	·001	·047	−·041	·000	−·044	−·048	0

TABLE X.

$\varphi_2(k)$ / $\frac{3Q}{2\pi h} J_2(hk)$.	Plane $z=0$.		
	$\widehat{rr}$.	$\widehat{\theta\theta}$.	$\widehat{zz}$.
$r=0$	−·116	−·116	−·595
$r=\frac{h}{4}$	−·121	−·111	−·540
$r=\frac{h}{2}$	−·137	−·091	−·385
$r=\frac{3h}{4}$	−·153	−·071	−·200
$r=h$	−·146	−·052	−·017
$r=\frac{5h}{4}$	−·110	·043	·082
$r=\frac{3h}{2}$	−·065	−·036	·082
$r=\frac{7h}{4}$	−·030	−·030	·061
$r=2h$	·000	−·026	·040
$r=3h$	—	—	−·002

Taking the distribution given in § 3 *c*, viz., that in which the surface traction varies as the radius, we have

$$\phi_2(k) = \frac{3Q}{2\pi b} J_2(kb).$$

Values of δ representing the stress-components in the system $(A)_h$ when $b=h$, for the plane $z=0$, are shown in Table X.

If $u=0$ at $z=\pm h$, $r=h$, then from equation (62) it follows that,

$$\frac{Q}{\pi h^2} = -\frac{\rho\omega^2 a^2}{\gamma_u}\left\{\cdot 28875 - \cdot 24375\frac{h^2}{a^2}\right\}, \quad . \quad (66)$$

where $\gamma_u = -\cdot 536$.

Case 3.—*Disk restrained by a Combined Distribution of Normal and Tangential Traction.*

For any assumed distributions two conditions of restraint may be simultaneously satisfied. Take, for example, distributions mentioned in cases 1 and 2, viz.:

$$\phi_1(k) = \frac{P}{\pi b} J_1(kb). \quad \S\ 2\ d,$$

$$\phi_2(k) = \frac{3Q}{2\pi b} J_2(kb). \quad \S\ 3\ c.$$

When $b=h$, the surface displacements, at $r=0$ and $r=h$ for the system (A), are contained in Table XI.

TABLE XI.

	$z=h,\ r=0.$	$z=h,\ r=h.$		$z=0,\ r=0.$
	γ_w.	γ_w.	γ_u.	λ_{zz}.
$\phi_1(k)$	·902	·398	·070	·972
$\phi_2(k)$	−·187	·114	−·536	−·526

If, therefore, $w=0$ at $z=\pm h$, $r=0$, and $u=0$ at $z=\pm h$, $r=b$, we have from equation (61)

$$\cdot 902\frac{P}{\pi h E} - \cdot 187\frac{Q}{\pi h E} = \cdot 2475\frac{\rho\omega^2 a^2}{E}.h,$$

$$\cdot 07\ \frac{P}{\pi h E} - \cdot 536\frac{Q}{\pi h E} = \frac{\rho\omega^2 h}{E}\{\cdot 28875\, a^2 - \cdot 24375\, h^2\},$$

or

$$\left.\begin{aligned}\frac{P}{\pi h^2} &= \rho\omega^2 a^2\left\{\cdot 397-\cdot 097\frac{h^2}{a^2}\right\},\\ \frac{Q}{\pi h^2} &= \rho\omega^2 a^2\left\{\cdot 588-\cdot 468\frac{h^2}{a^2}\right\}.\end{aligned}\right\} \quad . \quad . \quad . \quad (67)$$

With these values it follows that

$$\cdot 398\frac{P}{\pi h E}+\cdot 114\frac{Q}{\pi h E}=\frac{\rho\omega^2 a^2 h}{E}\left\{\cdot 225-\cdot 092\frac{h^2}{a^2}\right\}.$$

If the condition $w=0$, at $z=\pm h$, $r=b$, were satisfied also, then from equations (61) this displacement should be given by

$$\frac{\rho\omega^2 a^2 h}{E}\left\{\cdot 2475-\cdot 195\frac{h^2}{a^2}\right\}.$$

The condition of complete restraint at the surface of the disk is therefore approximately realized by these assumed distributions of traction.

The total stress-components in the system (A), corresponding to these distributions, may be evaluated by combining the results of Tables IX. and X., using the appropriate values P and Q given by equations (67).

§ 8. Summary and Conclusions.

The stresses due to restraint have been taken as those produced in the disk by symmetrical distributions of surface traction, acting on the outside faces of the complete disk at rest, viz., the stress-system (A). The surface displacements arising from these distributions are assumed to neutralize those occurring in a disk rotating under no superficial tractions, viz., the stress-system (B). The total stress-components when rotating under restraint are obtained by combining these two systems.

1. *Disk restrained by Uniform Distributions of Normal Traction.* § 7; Case 1; Subcase (c).

For the stress-system (A) we can now write stress-component $= \delta\cdot\frac{P}{\pi h^2}=\cdot 2475\,.\,\frac{\delta}{\gamma_w}\,.\,\rho\omega^2 a^2$, where $\gamma_w=\cdot 902$, satisfies the condition $w=0$, $z=\pm h$, $r=0$. Values of δ are shown in Table IX. It will be noted that a discontinuous change occurs in these stress-components at the cir-

cumference $r=h$, $z=h$. The maximum values occurring at this point when $r<h$, are as follows :—

$$\left.\begin{aligned} \widehat{rr} &= \cdot 693\,\rho\omega^2a^2, \\ \widehat{\theta\theta} &= \cdot 618\,\rho\omega^2a^2, \\ \widehat{zz} &= 1\cdot 109\,\rho\omega^2a^2. \end{aligned}\right\} \quad . \quad . \quad . \quad . \quad . \quad (68)$$

For the stress-system (B), when $r=h$, $z=h$, equations (61) give

$$\left.\begin{aligned} \widehat{rr} &= \rho\omega^2a^2\left\{\cdot 4125-\cdot 598\frac{h^2}{a^2}\right\}, \\ \widehat{\theta\theta} &= \rho\omega^2a^2\left\{\cdot 4125-\cdot 423\frac{h^2}{a^2}\right\}, \\ \widehat{zz} &= 0. \end{aligned}\right\} \quad . \quad . \quad . \quad (69)$$

From Table VIII., when $n=1$, it will be noticed that γ_w, at $r=h$, is ·398. Comparing this with the value ·902, at $r=0$, it follows that the distribution of normal traction which will produce plane strain over the circular area of radius h must give rise to a greater stress-concentration at the point of discontinuity than is indicated by equations (68). It is probable, however, that the stresses fall more or less rapidly at this point whatever the assumed distribution of normal traction may be.

2. *Disk restrained by a Distribution of Tangential Traction varying at the Radius.* § 7 ; Case 2.

This is of interest, in that the resultant axial pull is everywhere zero. For the stress-system (A) we have, as before,

stress-component =

$$\delta.\frac{Q}{\pi h^2} = -\rho\omega^2a^2.\frac{\delta}{\gamma_u}\left\{\cdot 28875-\cdot 24375\frac{h^2}{a^2}\right\},$$

where $\gamma_u=-\cdot 536$ satisfies the condition $u=0$ at $z=\pm h$, $r=h$. Values of δ. for the plane $z=0$, are shown in Table X. An examination of equations (31) shows that the stress-components, $\widehat{rr}$ and $\widehat{\theta\theta}$, at the circumference $r=h$, $z=h$, are infinite. It will be noted also that on the plane $z=0$ the component $\widehat{zz}$ changes sign at $r=h$ very nearly, so that in a disk carried on a shaft which can withstand no axial pull, radial restraint renders the shaft in a state of compression.

3. *Disk restrained by the Combined Distributions of Normal and Tangential Traction.* § 7 ; Case 3.

For the system (A) the stress-components may be determined from Tables IX. and X., using the appropriate values of P and Q, equations (67). As already mentioned, a uniform distribution of normal traction, combined with a distribution of tangential surface traction varying as the radius, produces an approximate condition of complete restraint over the region of the applied loads.

In conclusion it is interesting to note that radial restraint can only be realized by the application of tangential surface tractions acting on the plane faces of the disk.

Fig. 2.

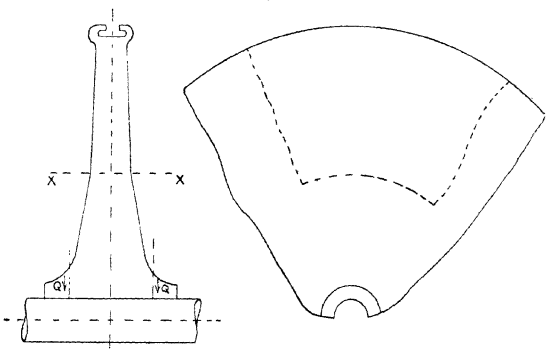

For the purely theoretical case, dealt with in the foregoing analysis, the abrupt change of section at the junction of the disk and the shaft give rises to stress-concentration at this point. In practice, changes of section, although not so abrupt, will produce the same effect. A turbine disk of profile somewhat as shown in fig. 2, having an abrupt change of angle at the section XX, fractured by two opposite pieces flying out.

The nature of the stresses produced might be inferred from the assumption that the central portion is restrained by tangential tractions Q, when, considering the problem from the point of view of case (2) above, it can be seen that the axial component of stress $\widehat{zz}$ will reach its maximum tensile value somewhere in the region XX of the disk.

CIV. *On the Variation with Temperature of Thermal Separation in Gaseous Mixtures.* *By* J. W. H. Lugg, *B.Sc., University of Western Australia* *.

Introduction.

In their development of the kinetic theory of gases, Enskog and Chapman† have shown that the existence of a temperature gradient in a binary gas mixture will in general result in a process of thermal diffusion whereby a composition gradient will ultimately be established. This prediction was verified experimentally by Chapman and Dootson ‡, and the phenomenon has been further studied by Ibbs § and by Elliott and Masson ‖.

Chapman has also shown, by means of calculations based on the use of certain simplified molecular models, that in equilibrium the composition gradient should be proportional to the gradient of the logarithm of the absolute temperature, the proportionality factor, k_T, being a complex function of the composition of the mixture. For a small composition difference, $\Delta\lambda$, an approximate integration is readily effected, and gives the expression :—

$$\Delta\lambda = k_T \ln \frac{T_2}{T_1}, \quad . \quad . \quad . \quad . \quad . \quad . \quad (1)$$

where $\Delta\lambda$ is the (small) composition difference between two portions of the mixture whose absolute temperatures are T_1 and T_2 respectively, and k_T is independent of temperature ; ln denotes the Napierian logarithm.

Ibbs ¶ verified this conclusion by experiments in which the cold portion was at room temperature whilst the temperature of the hot portion was varied between room temperature and 230° C. Nevertheless, Elliott and Masson ** obtained values of k_T for $H_2 - CO_2$ and for $He - CO_2$ mixtures, when the two temperatures were

* Communicated by Prof. S. Chapman, F.R.S.

† D. Enskog, *Phys. Zeit.* xii. p. 538 (1911) ; *Ann. d. Phys.* xxxviii. p. 742 (1912). S. Chapman, Phil. Trans. ccxvi. A, p. 279 (1915), and ccxvii. A, p. 115 (1916).

‡ Phil. Mag. xxxiii. p. 249 (1917).

§ Proc. Roy. Soc. xcix. A, p. 385 (1921), cvii. A, p. 470 (1925), etc.

‖ *Ibid.* cviii. A, p. 378 (1925).

¶ *Ibid.* xcix. A, p. 385 (1921) ; cvii. A, p. 470 (1925), etc.

** *Ibid.* cviii. A, p. 378 (1925).

0° C. and 490° C. respectively, which were considerably greater than Ibbs' corresponding values.

These results suggest that the logarithmic formula may not always be valid at high temperatures, and the present investigation was undertaken with the object of further exploring the region between 230° C. and 490° C., in order to determine whether the observed variation of k_T could be confirmed, and, in the event of it being confirmed, to study the conditions under which the logarithmic formula becomes invalid *.

Experimental.

The arrangement of the diffusion bulbs and the methods of manipulation of the gases were similar to those adopted by Elliott and Masson †.

All the experiments (except one) were carried out with a mixture of hydrogen and carbon dioxide of constant composition. Hydrogen was prepared electrolytically and purified by passage through a silica tube containing metallic copper maintained at a dull red heat. It was finally dried by being slowly led over phosphorus pentoxide. The carbon dioxide was similarly led over phosphorus pentoxide. The carbon dioxide was similarly dried, and it was subsequently tested for purity by absorption with caustic potash; the unabsorbed residue was quite negligible in amount.

The gas mixture was stored in bulk over mercury, and samples were drawn off through a capillary siphon as required. The differences in viscosity between hydrogen and carbon dioxide effected a variation in the composition of the sample which was not greater than ·001 or ·002 in the fraction of a constituent. Manipulation measures were taken to prevent cumulative variation in composition of the supply of mixture.

* Note by S. Chapman.—Since Mr. Lugg first sent me the results here communicated, a paper by T. L. Ibbs, K. E. Grew, and A. A. Hirst has appeared (Proc. Phys. Soc. xli. p. 456, Aug. 1929) in which experiments on thermal diffusion at *low* temperatures are described. They find that as the temperature of liquefaction of one of the constituent gases in their mixtures is approached, k_T decreases. This is in general agreement with Mr. Lugg's result for the H_2-CO_2 mixture (in which one constituent (CO_2) is easily liquefied), that k_T increases at high temperatures; his explanation also is similar to that given by Dr. Ibbs and his collaborators. Mr. C. T. L. Caton is investigating the theoretical variation of k_T, taking account of attractive as well as repulsive forces.

† Proc. Roy. Soc. cviii. A, p. 378 (1925).

Temperature Control and Measurement.

The temperature of the cold bulb was maintained constant at 29° C. or approximately 302° A. The hot-bulb temperature was varied between 100°C. and 470° C.

For most of the diffusions the cold bulb was jacketed in cotton-wool with an accurate thermometer against the side of the bulb. A stone jar which could be gently heated if the room temperature were to fall below 29° C. surrounded this arrangement. Later it was found that a water-jacket for the cold bulb afforded somewhat better temperature control. A water-jacket was therefore employed in the last few diffusions.

Steam at 100° C. was employed to heat the hot bulb for one diffusion. In all other cases an electric furnace, wired and otherwise adjusted so as to eliminate end effects almost completely, was used. A mercury thermometer, nitrogen filled and reading to 560° C., was supported against the bulb in the furnace. The thermometer was carefully calibrated, and the temperature of the hot bulb at any moment could be determined to within a degree or two over the entire range of temperature employed.

In many instances the diffusion was allowed to take place overnight, but variations in the voltage of the mains necessitated completion of each diffusion the following day, with continual observation and adjustment of furnace rheostats so as to maintain the furnace at one temperature for five hours or more. A few of the earlier results were vitiated by failure to observe this precaution, and these are not included in this communication.

Analysis of Contents of the Diffusion Bulbs.

A direct method was employed. A volume of the mixture was measured, and remeasured after absorption of the carbon dioxide. Although in the first cases two samples of each mixture were analysed, it was soon realised that the total volumes from the bulbs would have to be analysed if good accuracy were to be attained.

Correction for Gas contained in Connecting Tubing.

The presence of gas in the small tubing connecting the hot and cold diffusion bulbs necessitated the application of a correction to the observed compositions. It was

considered justifiable to assume that for both hot and cold bulbs this tubing was at the temperature of the cold bulb, viz., 29° C. On this basis a correction was necessary only in the case of the hot-bulb composition.

Results.

The experimental results are summarised in Table I. Here T_1 and T_2 represent the absolute temperatures and λ_1 and λ_2 the compositions, expressed in fractions of hydrogen, of the cold and hot bulbs respectively. Column (7) contains the values for the composition of the hot bulbs obtained after correcting for the amount of cold gas

TABLE I.

Vol. of cold bulb ... 27·451 mils. Vol. of hot bulb... 50·362 mils.
Vol. of leads... ... 1·393 mils. Vol. of leads ... 1·526 mils.

(1) No.	(2) T_1	(3) T_2	(4)	(5) 1	(6) 2	(7) 2 (corr.)	(8) (7)–(5)
1	299	676	0·50890	0·47876	0·54467	0·54919	0·07043
2	302	373·2	·53215	·52200	·53671	·53725	·01525
3	„	477·3	„	·51568	·54708	·54855	·03287
4	„	486·7	„	·51382	·54738	·54893	·03511
5	„	486·7	„	·51374	·54742	·54899	·03527
6	„	531·2	„	·50835	·55231	·55465	·04630
7	„	582·7	„	·50489	·55653	·55945	·05456
8	„	628·7	„	·50177	·56171	·56549	·06372
9	„	680·5	„	·49967	·56721	·57184	·07217
10	„	736·8	„	·49807	·57320	·97850	·08047
11	„	—	„	—	—	—	—

present in the connecting tubes, whilst in column (8) values of the corrected composition difference, $\Delta\lambda$, are given. λ represents the composition of the gas mixture before diffusion.

The first diffusion does not belong to the series 2–11. In diffusion No. 11 the temperature of the hot bulb was in the neighbourhood of 520° C. and the glass gave way, being a softer variety than was anticipated. There is reason to believe that in diffusion No. 10 the amount of separation may be too low in value, since the furnace temperature was rather low overnight.

The total gas pressure during diffusion lay between the limits 0·5 to 1 atmosphere. The fourth and fifth diffusions indicate that the composition difference is most probably independent of the total pressure within these limits. For these two experiments the ratio of the pressures during diffusion was 1·61, other variables being unchanged; the thermal separations, however, were almost identical.

Discussion.

These results have been used to calculate the values of k_T, the "constant" in Chapman's integrated logarithmic formula (Equation (1) above) and also a quantity K defined by the identity $K = \Delta\lambda/(T_2 - T_1)$. The values of these quantities are given in Table II.

TABLE II.

No.	T_2.	k_T.	K.
2	373·2	0·07204 ...	$0{\cdot}0_3 2142$
3	477·3	·07181 ...	$0{\cdot}0_3 1875$
4 and 5	486·7	·07356 ...	$0{\cdot}0_3 1901$
6	531·2	·08218 ...	$0{\cdot}0_3 2020$
7	582·7	·08302 ...	$0{\cdot}0_3 1944$
8	628·7	·08690 ...	$0{\cdot}0_3 1950$
9	680·5	·08844 ...	$0{\cdot}0_3 1907$
10	736·8	·09023 ...	$0{\cdot}0_3 1851$
		Mean ...	$0{\cdot}0_3 195$

The gradual increase of k_T as the temperature T_2 of the hot bulb is raised is unmistakable. It must, however, be borne in mind that, since k_T depends on the composition of the mixture, equation (1) is not strictly applicable, especially at the higher temperature where $\Delta\lambda$ is large. To minimise complications of this nature the composition of the initial mixture was chosen so that for small separations k_T should be near its maximum value, as determined by Ibbs. For this composition the fact that the separation is large will not greatly affect the validity of the present calculations of k_T; moreover, any small error which might be introduced in this way should result in an apparent decrease of k_T at the higher temperatures. The

use of the integrated equation therefore certainly does not diminish the qualitative significance of the results in Table II.

At low temperatures the results check approximately with those of Ibbs for a similar gas-mixture, viz., $k'_T = 0{\cdot}070$, but at higher temperatures K is more nearly a constant than k_T. It may perhaps be noted that over the temperature range used by Ibbs (room temperature to 230° C.) the linear and logarithmic relationships would be difficult to distinguish experimentally.

Using the mean value of K ($\cdot 0_3 195$), $\Delta\lambda$ for a temperature difference of 486° A. would have the value 0·0948. Using the same temperature difference, Elliott and Masson obtained the value 0·1034 for a mixture giving the *maximum* separation.

The theoretical significance of the observed increase of k_T with temperature will not be discussed here, though it may perhaps be pointed out that such an increase might be expected if the character of the intermolecular collisions approximated more closely at the higher temperatures to that of collisions between perfectly elastic spheres.

Summary.

1. The thermal separations for a single mixture of hydrogen and carbon dioxide have been studied with the cold-bulb temperature at 29° C. and the hot bulb at temperatures between 100° C. and 464° C.

2. The results indicate that the separations at the higher temperatures are greater than would be expected on the basis of Chapman's logarithmic formula. The relationship between composition difference and temperature difference is more nearly linear.

In conclusion, the author desires to acknowledge his indebtedness to the founders of the Amy Saw Scholarship and to the Government of Western Australia for pecuniary assistance, and to Dr. G. A. Elliott for suggesting this research and for his advice and instruction during its progress. Thanks are also due to Professor N. T. M. Wilsmore for his advice and for the provision of laboratory facilities, and to Professor S. Chapman for his interest and assistance in publication.

Sept. 23, 1929.

CV. *On the Multiplication of Serial Relations.* *By* D. M. WRINCH, *M.A., D.Sc., Lecturer at Lady Margaret Hall, Oxford* †.

IN this paper we give the relations between the element and gap characters of any series, P and Q, and the series $Q \times P$ obtained by multiplying the two series together.

It will be assumed that a term cannot be the sequent of an ω_m and an ω_n unless $m = n$.

Let ν_1, μ_1 and ν_2, μ_2 be any element character of P and Q respectively, where $\nu_1 \neq \varpi$, $\mu_1 \neq \varpi$, $\nu_2 \neq \varpi$, $\mu_2 \neq \varpi$. And let σ_1, ρ_1 and σ_2, ρ_2 be any gap character of P and Q respectively, where $\sigma_1 \neq \varpi$, $\sigma_2 \neq \varpi$, $\rho_1 \neq \varpi$, $\rho_2 \neq \varpi$. Further, let n_1, ϖ ; ϖ, m_1, and n_2, ϖ; ϖ, m_2 be characters of P and Q respectively ‡. If P has a beginning, n_1, ϖ will be an element character, otherwise it will be a gap character ; if P has an end, ϖ, m_1 will be an element character, otherwise it will be a gap character. In the same way, if Q has a beginning, n_2, ϖ will be an element character, otherwise it will be a gap character ; if Q has an end, ϖ, m_2 will be an element character, otherwise it will be a gap character. It is assumed that ν's, μ's, n's, and m's only have inductive numbers or 0 or -1 as values.

§ 1. The members of the field of $P \times Q$ will be in the form of a couple xy, where x is a member of the field of P, and y is a member of the field of Q ‖. Since P and Q are series, so also is $Q \times P$ ¶. A couple x_1y_1 precedes a couple x_2y_2 in the $Q \times P$ order, if $y_1 Q y_2$ whatever the relation of x_1 to x_2, or if $y_1 = y_2$ and $x_1 P x_2$ There will therefore be stretches of the series $Q \times P$ in which the Q-term remains constant and the P-term runs through the whole of the P-series. Such a stretch is ordinally similar to P. Hence ν_1, μ_1 will be an element character of the stretch. If $n_1, \varpi \in \text{elt}'P$, this stretch will have a first term which is an $^*\omega_n$-predecessor ; if $n_1, \varpi \in \text{gap}'P$, this stretch will be coinitial with an $^*\omega_{n_1}$. If $\varpi_1, m_1 \in \text{elt}'P$, it will have a last term which is an ω_{m_1}-sequent ; and if $\varpi, m_1 \in \text{gap}'P$, it will have an ω_{m_1}-

† Communicated by the Author.

‡ We systematize a term which is the last term of a series, as a ϖ, m_1 element, and a term which is the first term of a series as a n_1, ϖ element.

‖ See 'Principia Mathematica,' *166.

¶ *Op. cit.* *204.55.

confinal with it. Suppose y, the Q-term, has the character ν_2, μ_2. Let

$$r_1 r_2 \dots r_\zeta \dots \qquad \zeta < \omega_{\mu_2}$$

be a series contained in Q, having y as its sequent. If $\mu_2 \neq -1$, if $n_1, \varpi \in \text{elt}^{\text{`}}\text{P}$, and x_0 is the first term of P, $x_0 y$ is the sequent of the series

$$xr_1, xr_2, \dots xr_\zeta \dots \qquad \zeta < \omega_{\mu_2},$$

where x is any P-term ; and this series is an ω_{μ_2} contained in $\text{Q} \times \text{P}$. Consequently, if $\mu_2 \neq -1$ and $n_1, \varpi \in \text{elt}^{\text{`}}\text{P}$, the first term of the stretch is the sequent of an $\omega_{\mu_2}$ and therefore is an $n_1, \mu_2$ element. If $\nu_2 \neq -1$ and $\varpi, m_1 \in \text{elt}^{\text{`}}\text{P}$, the last term of the stretch is the predecessor of the series

$$\dots xs_\xi, \dots xs_2, xs_1 \qquad \xi < \omega_{\nu_2},$$

where

$$\dots \; s_\xi \; \dots \; s_2 \; s_1 \qquad \xi < \omega_{\nu_2}$$

is an ${}^*\omega_{\nu_2}$ having y as its predecessor and contained in Q. The term then is a ν_2, m_1 element. If $\mu_2 = -1$, so that y has an immediate predecessor y', the first term of the stretch $x_0 y$ will be immediately preceded by $x_0 y'$ if P has a last term x_0, and so will be an n_1, μ_2 element as before and will be the sequent of such a series as

$$c_1 y', c_2 y', \dots c_\zeta y' \dots \qquad \zeta < \omega_{m_1},$$

where

$$c_1 \;\; c_2 \;\; \dots c_\zeta \;\; \dots \qquad \zeta < \omega_{m_1}$$

is an ω_{m_1} confinal with P, and therefore will be an n_1, m_1 element if P has no last term. Again, if $\nu_2 = -1$ and $\varpi . m_1 \in \text{elt}^{\text{`}}\text{P}$, the last term of the stretch is a ν_2, m_1 element if P has a first term, and an n_1, m_1 element if P has no first term.

If $n_1, \varpi \in \text{gap}^{\text{`}}\text{P}$, so that P has no first term, the stretch will be coinitial with an ${}^*\omega_{n_1}$

$$\dots d_\xi y, \dots d_2 y, d_1 y \qquad \xi < \omega_{n_1}, \quad . \; . \; . \quad (1)$$

where

$$\dots d_\xi \;\; \dots d_2 \;\; d_1 \qquad \xi < \omega_{n_1}$$

is an ${}^*\omega_{n_1}$ coinitial with P. It is to be remarked that $n_1 \neq -1$, since P has no beginning †. This series, together with the series

$$xr_1 \, xr_2 \dots xr_\zeta \dots \qquad \zeta < \mu_2, \; . \; . \; . \; . \quad (2)$$

† *Cp.* "On the Structure of Serial Relations," Phil. Mag., November 1929.

if $\mu_2 \neq -1$, will give an n_1, μ_2 gap. If $\varpi, m_1 \in$ gap' P, so that P has no last term, the stretch will be confinal with such an ω_{m_1} as

$$c_1 y\ c_2 y \ldots c_\zeta y \ldots \qquad \zeta < \omega_{m_1}. \quad . \quad . \quad . \quad (3)$$

And again it is to be remarked that $m_1 \neq -1$ since P has no end †. This series, together with the series

$$\ldots x s_\xi \ldots x s_2\ x s_1 \qquad \xi < \omega_{\nu_2}, \quad . \quad . \quad . \quad . \quad (4)$$

if $\nu_2 \neq -1$, will give a ν_2, μ_1 gap. But when P has no first term, if $\mu_2 = -1$ so that y has an immediate predecessor y', if P has a last term x_Ω, $x_\Omega y'$ will be the predecessor of such an ω_{m_1} as

$$c_1 y'\ c_2 y' \ldots c_\zeta y' \ldots \qquad \zeta < \omega_{m_1}. \quad . \quad . \quad . \quad (5)$$

It will therefore be an n_1, m_1 element. If P has no last term, (5) and (1) will give together an n_1, m_1 gap. Similarly, if P has no last term, if $\nu_2 = -1$, we shall have an n_1, m_1 element if P has a first term, and otherwise an n_1, m_1 gap.

§ 2. Suppose Q has a first term y_0, and let us consider the character of the stretch of $Q \times P$, for which the Q-term is y_0. If P has a last term x_Ω, the stretch will have a last term $x_\Omega y_0$, which limits the series

$$c_1 y_0,\ c_2 y_0, \ldots c_\zeta y_0 \ldots \qquad \zeta < \omega_{m_1} \quad \text{if } m_1 \neq -1$$

and the series

$$\ldots x f_\xi, \ldots x f_2.\ x f_1 \qquad \xi < \omega_{n_2} \quad \text{if } n_2 \neq -1,$$

where

$$\ldots\ f_\xi \ldots\ f_2\ f_1 \qquad \xi < \omega_{n_2}$$

is an $^*\omega_{n_2}$ coinitial with the Q-series. If $m_1 \neq -1$, $n_2 \neq -1$, $x_\Omega y_0$ will therefore be an n_2, m_1 element. If $m_1 = -1$, so that x_Ω has an immediate predecessor x_Ω', $x_\Omega y_0$ will be immediately preceded by $x_\Omega' y_0$ and will be an $n_2, -1$ element, and so an n_2, m_1 element as before. If $n_2 = -1$, so that y_0 has an immediate successor y_0', if P has a first term x_0, $x_\Omega y_0$ will be immediately followed by $x_0 y_0'$, and so

† *Loc. cit.*

will be an n_2, m_1 element as before. If $n_2 = -1$ and P has no first term, $x_\Omega y_0$ will limit such a series as

$$\dots d_\xi y_0' \dots d_2 y_0' d_1 y_0 \qquad \xi < \omega_{n_1};$$

and so, instead of an n_2, m_1 element, there will be an n_1, m_1 element. If there is no last term in the P-series, there will be no last term in the stretch. Instead, there will be an ω_{m_1} confinal with it,

$$c_1 y_0' c_2 y_0 \dots c_\zeta y_0 \dots \qquad \zeta < \omega_{m_1}, \quad . \quad . \quad . \quad (6)$$

and $m_1 \neq -1$, as P has no last term. This series, together with such a series as

$$\dots x f_\xi \dots x f_2 x f_1 \qquad \xi < \omega_{n_2},$$

if $n_2 \neq -1$, forms an n_2, m_1 gap. If $n_2 = -1$, so that y_0 has an immediate successor y_0', and if P has a first term x_0, $x_0 y_0'$ will limit the series (6) and will be the predecessor of such a series as

$$\dots d_\xi y_0' \dots d_2 y_0' d_1 y_0' \qquad \xi < \omega_{n_1} \; n_1 \neq -1, \quad . \quad (7)$$

or $x_0' y_0'$ if x_0 has an immediate follower x_0'. There will therefore be an n_1, m_1 element instead of an n_2, m_1 gap. If $n = -1$ and P has no first term, instead of the n_2, m_1 gap there will be the n, m_1 gap formed by the series (6) and (7).

The stretch will have a first term if x_0 exists. This term $x_0 y_0$ will be the predecessor of such a series as

$$\dots d_\xi y_0, \dots d_2 y_0, d_1 y_0 \qquad \xi > \omega_{n_1}, \quad . \quad . \quad . \quad (8)$$

and so will be an n_1, ϖ element, since it is the first term of the series $Q \times P$ as well as of the stretch. When x_0 does not exist, the stretch (and the series) will be coinitial with the series (8), and in consequence there will be an n_1, ϖ gap.

We get, therefore, the following characters of the series $Q \times P$, if y_0 exists :—

If x_0 exists, there is an n_1, ϖ element; if it does not, there is an n_1, ϖ gap. If x_Ω exists, there is an n_2, m_1 element which, in the exceptional case when $n_2 = -1$, becomes an n_1, m_1 element if x_0 does not exist. If x_Ω does not exist, there is an n_2, m_1 gap which, in the exceptional case when $n_2 = -1$, becomes an n_1, m_1 element if x_0 exists and an n_1, m_1 gap if x_0 does not exist.

Corresponding results can be obtained by condensing the stretch (if there is one) which has y_Ω as its Q-term.

§ 3. We may sum up the results so far obtained.

1. $\nu_1, \mu_1 \in \text{elt}'\text{P}$.

2. If n_1, ϖ ; $\varpi, m_1 \in \text{elt}'\text{P}$, n_1, μ_2 ; $\nu_2, m_1 \in \text{elt}'\text{Q} \times \text{P}$.

   (*a*) If also $n_2, \varpi \in \text{elt}'\text{Q}$, n_2, m_1 ; $n_1, \varpi \in \text{elt}'\text{Q} \times \text{P}$ in addition.

   (*b*) If also $\varpi, m_2 \in \text{elt}'\text{Q}$, n_1, m_1 ; $\varpi, m_1 \in \text{elt}'\text{Q} \times \text{P}$ in addition.

3. If $n_1, \varpi \in \text{elt}'\text{P}$, $\varpi, m_1 \in \text{gap}'\text{P}$, $n_1, \mu_2 \in \text{elt}'\text{Q} \times \text{P}$, $\nu_2, m_1 \in \text{gap}'\text{Q} \times \text{P}$.

   (*a*) If $n_2, \varpi \in \text{elt}'\text{Q}$, $n_1, \varpi \in \text{elt}'\text{Q} \times \text{P}$, $n_2, m_1 \in \text{gap}'\text{Q} \times \text{P}$ in addition.

   (*b*) If $\varpi, m_2 \in \text{elt}'\text{Q}$, $n_1, m_2 \in \text{elt}'\text{Q} \times \text{P}$, $\varpi, m_1 \in \text{gap}'\text{Q} \times \text{P}$.

4. If $\varpi, m_1 \in \text{elt}'\text{P}$, $n_1, \varpi \in \text{gap}'\text{P}$, $\nu_2, m_1 \in \text{elt}'\text{Q} \times \text{P}$, $n_1, \mu_2 \in \text{gap}'\text{Q} \times \text{P}$.

   (*a*) If $n_2, \varpi \in \text{elt}'\text{Q}$, $n_2, m_1 \in \text{elt}'\text{Q} \times \text{P}$, $n_1, \varpi \in \text{gap}'\text{Q} \times \text{P}$.

   (*b*) If $\varpi, m_1 \in \text{elt}'\text{Q}$, $\varpi, m_1 \in \text{elt}'\text{Q} \times \text{P}$, $n_1, m_2 \in \text{gap}'\text{Q} \times \text{P}$.

5. If n_1, ϖ ; $\varpi, m_1 \in \text{gap}'\text{P}$, ν_2, m_1 ; $n_1, \mu_2 \in \text{gap}'\text{Q} \times \text{P}$.

   (*a*) If $n_2, \varpi \in \text{elt}'\text{Q}$, n_1, ϖ ; $n_2, m_1 \in \text{gap}'\text{Q} \times \text{P}$.

   (*b*) If $\varpi, m_2 \in \text{elt}'\text{Q}$, ϖ, m_1 ; $n_1, m_2 \in \text{gap}'\text{Q} \times \text{P}$.

The conventions with regard to the interpretation of the special cases when the variables take the value -1 are as follows:—In 3 and 4, if μ_2 or ν_2, or m_2 or n_2, is equal to -1, replace the character in which it occurs by the element with m_1 substituted for μ_2 or m_2 and n_1 for ν_2 or n_2. In 5, for ν_2 or n_2, or μ_2 or m_2, if they are equal to -1, put n_1, m_1 respectively.

§ 4. The gaps of P, except those which contain ϖ, are represented in $\text{Q} \times \text{P}$, since $\text{Q} \times \text{P}$ has stretches which are ordinally similar to P. Consider now the gap of Q.

The series

$$xt_1^*, xt_2^*, \dots xt_\zeta \dots \dots \dots \qquad \zeta < \omega_{\rho_2}$$

$$\dots \dots \dots xu_\xi \dots xu_2\, xu_1 \qquad \xi < \omega_{\sigma_2}$$

define a gap in $\text{Q} \times \text{P}$, just as the series

$$t_1\ t_2\ \dots\ t_\zeta \dots \dots \qquad \zeta < \omega_{\rho_2}$$

$$\dots \dots \dots u_\xi\ u_2\ u_1 \qquad \zeta < \omega_{\sigma_2}$$

define a gap in the Q series. And there are no exceptional cases, since ρ_2, σ_2 can neither of them be equal to -1. The gaps of Q therefore occur in $Q \times P$ as well as the gaps of P.

§ 5. The only other question to be considered is the nature of the beginning and end of $Q \times P$. It is plain that only if P and Q have beginnings, $Q \times P$ has a beginning This beginning will be the couple $x_0 y_0$, which is the predecessor of the ${}^*\omega_{n_1}$

$$\dots c_\xi y_0 \dots c_2 y_0 \, c_1 y_0 \qquad \xi < \omega_{n_1}, \quad . \quad . \quad . \quad (9)$$

even if $n_1 = -1$. n_1, ϖ is therefore an element of $Q \times P$. And if x_Ω and y_Ω exist, $x_\Omega y_\Omega$ will be an ϖ, m_1 element even if $m_1 = -1$.

If x_0 does not exist and y_0 exists, there will be no beginning, but the ${}^*\omega_{n_1}$ (9) will be coinitial with $Q \times P$. And $n_1 \neq -1$, since x_0 does not exist. $Q \times P$ therefore has an n_1, ϖ gap.

If y_0 does not exist, the series

$$\dots x e_\xi \dots x e_2, x e_1 \qquad \xi < \omega_{n_2},$$

where

$$\dots \; e_\xi \dots \; e_2 \;\; e_1 \qquad \xi < \omega_{n_2}$$

is an ${}^*\omega_{n_2}$ coinitial with Q, is coinitial with $Q \times P$. $n_2 \neq -1$, since y_0 does not exist. $Q \times P$ therefore contains an n_2, ϖ gap.

Corresponding results may be obtained by considering the nature of the end of $Q \times P$.

The results of this § may be summed up.

If $n_1, \varpi \in \text{elt}'P$, if $n_2, \varpi \in \text{elt}'Q$, $n_1, \varpi \in \text{elt}'Q \times P$,
if $n_2, \varpi \in \text{gap}'Q$, $n_2, \varpi \in \text{gap}'Q \times P$.

If $n_1, \varpi \in \text{gap}'P$, if $n_2, \varpi \in \text{elt}'Q$, $n_1, \varpi \in \text{gap}'Q \times P$,
if $n_2, \varpi \in \text{gap}'Q$, $n_2, \varpi \in \text{gap}'Q \times P$.

If $\varpi, m_1 \in \text{elt}'P$, if $\varpi, m_2 \in \text{elt}'Q$, $\varpi, m_1 \in \text{elt}'Q \times P$,
if $\varpi, m_2 \in \text{gap}'Q$, $\varpi, m_2 \in \text{gap}'Q \times P$.

If $\varpi, m_1 \in \text{gap}'P$, if $\varpi, m_2 \in \text{elt}'Q$, $\varpi, m_1 \in \text{gap}'Q \times P$,
if $\varpi, m_2 \in \text{gap}'Q$, $\varpi, m_2 \in \text{gap}'Q \times P$.

§ 6. The characters of the series $Q \times P$ are therefore as follows:—

In all cases $\nu_1, \mu_1 \in \text{elt}'Q \times P$, σ_1, ρ_1, $\sigma_2, \rho_2 \in \text{gap}'P$. In addition, the series has the characters indicated in the following table. On the left in each are the elements, on the right the gaps.

	Q	ν_2, μ_2 ; σ_2, ρ_2 ϖ, m_2 n_2, ϖ	ν_2, μ_2 ; σ_2, ρ_2 ϖ, m_2 n_2, ϖ	ν_2, μ_2 ; σ_2, ρ_2 ϖ, m_2 n_2, ϖ	ν_2, μ_2 ; σ_2, ρ_2 ϖ, m_2 n_2, ϖ
	P	n_1, μ_2 ; ν_2, m_1 n_1, m_2 n_2, m_1 n_1, ϖ ϖ, m_1	n_1, μ_2 ; ν_2, m_1 n_2, m_1 n_1, ϖ ϖ, m_2	n_1, μ_2 ; ν_2, m_1 n_1, m_2 n_2, ϖ ϖ, m_1	n_1, μ_2 ; ν_2, m_1 n_2, ϖ ϖ, m_2
ν_1, μ_1 ; σ_1, ρ_1 ϖ, m_1 n_1, ϖ		n_1, μ_2 † ; ν_2, m_1 § n_1, m_2 † n_2, m_1 § n_1, ϖ ϖ, m_1	n_1, μ_2 † ; ν_2, m_1 § n_2, m_1 § n_1, ϖ ϖ, m_2	n_1, μ_2 † ; ν_2, m_1 § n_1, m_2 † n_2, ϖ ϖ, m_1	n_1, μ_2 † ; ν_2, m_1 § n_2, ϖ ϖ, m_2
ν_1, μ_1 ; σ_1, ρ_1 ϖ, m_1 n_1, ϖ		n_1, μ_2 † ; ν_2, m_1 * n_1, μ_2 ‡ n_2, m_1 * n_1, ϖ ϖ, m_1	n_1, μ_2 † ; ν_2, m_1 * n_2, m_1 * n_1, ϖ ϖ, m_2	n_1, μ_2 † ; ν_2, m_2 * n_1, μ_2 ‡ n_2, ϖ ϖ, m_1	n_1, μ_2 ‡ ; ν_2, m_1 * n_2, ϖ ϖ, m_2
ν_1, μ_1 ; σ_1, ρ_1 ϖ, m_1 n_1, ϖ		n_1, μ_2 ‡ ; ν_2, m_1 * n_1, m_2 † n_2, m_1 * n_1, ϖ ϖ, m_1	n_1, μ_2 † ; ν_2, m_1 * n_1, ϖ ϖ, m_2	n_1, μ_2 † ; ν_2, m_1 * n_1, m_2 † n_2, ϖ ϖ, m_1	n_1, μ_2 ‡ ; ν_2, m_1 * n_2, ϖ ϖ, m_2

* If ν_2 or n_2 is equal to -1, substitute for it n_1.

† If μ_2 or m_2 is equal to -1, substitute for it m_1.

§ If ν_2 or n_2 is equal to -1, substitute for it n_1 and transfer character to elements.

‡ If μ_2 or m_2 is equal to -1, substitute for it m_1 and transfer character to elements.

§ 7. Our general formula gives interesting results in particular cases. If $P, Q \in \text{Ded}$, P and Q have no gaps ‖, and

‖ See "On the Structure of Serial Relations," *loc. cit.*

therefore $Q \times P$ has no gaps, and so is Dedekindian. Therefore

$$P, Q \in \text{Ded} . \supset . Q \times P \in \text{Ded}.$$

If $Q \times P \in \text{Ded}$, it is clear from the table that $Q, P \in \text{Ded}$. Hence

$$P, Q \in \text{Ded} . \equiv . Q \times P \in \text{Ded}.$$

Suppose $Q \times P \sim \epsilon \text{ Ded}$. $N\nu'(Q \times P + 1) \subset \text{Ded}$, so that $Q \times P$, though not itself Dedekindian, would be Dedekindian with the addition of a last term. Then $Q \times P$ would have no gaps except one with ϖ on the left. Hence P and Q have no gaps except possibly ones with ϖ on the left. And if neither has a gap with ϖ on the left, then $Q \times P$ would be Dedekindian. Hence either P or Q must have a gap with ϖ on the left, and neither may have any other gaps. Therefore either P has no gaps and Q has a gap ϖ, m_2 only, or P has a gap ϖ, m_1 only and $\nu_2 = n_2 = -1$, and Q has no gaps except possibly one with ϖ on the left. Thus, either

$$P \in . \text{Ded} . N\nu'(Q + 1) \subset \text{Ded} . Q \sim \epsilon \text{ Ded},$$

or

$$N\nu'(P + 1) \subset \text{Ded} . P \sim \epsilon \text{ Ded} . Q \in \Omega.$$

The converse is easily verified from the table, and so it is established that

$$N\nu'(Q \times P + 1) \subset \text{Ded} . Q \times P \sim \epsilon \text{ Ded}$$
$$: \equiv : P \in \text{Ded} . N\nu'(Q \times 1) \subset \text{Ded} . Q \sim \epsilon \text{ Ded} . \nu . \quad 7.1\dagger$$
$$N\nu'(P + 1) \subset \text{Ded} . P \sim \epsilon \text{ Ded} . Q \in \Omega.$$

We also have

$$1 + N\nu'(Q \times P) \subset \text{Ded} . Q \times P \sim \epsilon \text{ Ded}$$
$$: \equiv : P \in \text{Ded} . 1 + N\nu'(Q) \subset \text{Ded} . Q \sim \epsilon \text{ Ded} . \nu .$$
$$1 + N\nu'(P) \subset \text{Ded} . P \sim \epsilon \text{ Ded} . Q \in \Omega. \quad . \quad . \quad 7.2\dagger$$

§ 8. If $Q \times P$ is well-ordered ‡, it must have a first term, all its element characters must have -1 on the left, and there must be no gaps except possibly one with ϖ on the left. The existence of the first term of $Q + P$ makes it necessary

† It is clear that this proposition is independent of the assumption made at the beginning of this paper that an element cannot be the sequent of an ω_m and an ω_n unless $m = n$.

‡ See my paper, *loc. cit.*

that P and Q should have first terms, and since $Q \times P$ has no gaps except possibly one with ϖ on the left, P and Q have no gaps except possibly ones with ϖ on the left. Since every element character of $Q \times P$ has -1 on the left,

$$\nu_1 = n_1 = \nu_2 = n_2 = -1.$$

Hence $n_1 = \nu_1 = -1$ and P has no gaps except possibly one with ϖ on the left, and $n_2 = \nu_2 = -1$ and Q has no gaps except possibly one with ϖ on the left. Hence $P, Q \in \Omega$. The converse is easily established, and it follows that

$$P, Q \in \Omega . \equiv . QP \tau \Omega. \quad . \quad . \quad . \quad . \quad . \quad 8.1$$

CVI. *On Levi-Civita's Modification of Einstein's Unified Field Theory.* *By* G. C. McVittie, *M.A.* (*Edin.*), *Christ's College, Cambridge* †.

§ I. *Introduction and Summary.*

PROF. LEVI-CIVITA ‡ has modified Prof. Einstein's Unified Field Theory ‖ of gravitation and electromagnetism by discarding the concept of "parallelism at a distance with respect to 4 orthogonal vectors of reference," which is the basis of the latter's theory, and obtaining a complete description of gravitational and electromagnetic phenomena by means of the Ricci Coefficients of Rotation of 4 orthogonal congruences of lines which, at each point, define 4 orthogonal vectors of reference in a Riemann space.

In the present paper we apply Prof. Levi-Civita's theory to a particular case, *i. e.*, one in which an exact solution of the usual gravitational and electromagnetic equations of the relativity theory is known, and we compare the results so obtained with those arrived at in a previous paper ¶ by the use of Prof. Einstein's theory.

† Communicated by Prof. E. T. Whittaker, F.R.S.

‡ *Berliner Sitzungberichte*, viii.-x. p. 137 (1929).

‖ *Berliner Sitzungberichte*, i. p. 2 (1929).

¶ G. C. McVittie, "On Einstein's Unified Field Theory," Proc. Roy. Soc. A, cxxiv. p. 366.

In § II. we obtain the congruences for this case and show that the 4 orthogonal vectors of reference which these congruences establish at any arbitrary point are substantially the same as those which are obtained by the use of Prof. Einstein's theory.

In § III. we show that the electromagnetic potential vector in the field can be given a geometrical interpretation in Prof. Levi-Civita's theory, which bears a very close analogy to that given to it in Prof. Einstein's theory. In Prof. Levi-Civita's theory, however, this interpretation appears to hold in special cases only, of which ours is one. At any rate, we have not found a general proof that the relation

$$F_{\mu\nu} = \frac{\partial \phi_\mu}{\partial x_\nu} - \frac{\partial \phi_\nu}{\partial x_\mu}$$

between the electric force tensor $F_{\mu\nu}$ and the potential vector ϕ_μ also holds between the geometrical quantities which represent them.

§ II. *Calculation of the Congruences.*

The special case to which we apply Prof. Levi-Civita's theory is that of the gravitational field of an electrostatic field of uniform direction †. The metric and the electromagnetic potential of this field are, respectively,

$$\left.\begin{aligned} ds^2 &= e^{ax_1}dx_4^2 - e^{-2ax_1}dx_1^2 - e^{-ax_1}dx_2^2 - e^{-ax_1}dx_3^2, \\ \phi_4 &= \frac{1}{2\sqrt{\pi}}e^{\frac{1}{2}ax_1}, \quad \phi_1 = 0, \quad \phi_2 = 0, \quad \phi_3 = 0. \end{aligned}\right\} \quad (1)$$

In this field the electromagnetic force which would be measured at an arbitrary point $P(\equiv \tau, a, b, c)$ in the field is an electric force in the direction of the x_1-axis, constant at the point and of amount $\propto e^{aa}/4\sqrt{\pi}$.

Let, then, $\lambda^\nu (\nu = 1, 2, 3, 4)$ denote the contravariant parameters of the sth congruence $(s = 1, 2, 3, 4)$, and let ${}^s\lambda_\nu$ denote the covariant moments of the same congruence ‡. [We have altered the notation for the parameters and moments to bring it into line with that of Prof. Einstein's theory. Indices denoting the congruence are written to the left of the "λ," those denoting the coordinates to the right.]

† G. C. McVittie, *loc. cit.*

‡ Levi-Civita, 'Absolute Differential Calculus,' Chap. x.

If, now, the $g_{\mu\nu}$ define the metric, we have the relations

$$ {}^{i}\lambda_{\nu} = \sum_{\rho=1}^{4} g_{\rho\nu} {}^{i}\lambda^{\rho} $$

and

$$ g_{\mu\nu} = \sum_{i=1}^{4} e_i {}^{i}\lambda_{\mu} {}^{i}\lambda_{\nu}, \quad \ldots\ldots (2) $$

where $e_i = \pm 1$.

In the case of the field given by (1) we have

$$ e_4 = 1, \qquad e_1 = e_2 = e_3 = -1. $$

We now assume that the moments of the congruences are:

$$ \begin{array}{llll} ({}^{4}\lambda_4, & {}^{4}\lambda_1, & 0, & 0) \text{ for the congruence "4,"} \\ ({}^{1}\lambda_4, & {}^{1}\lambda_1, & 0, & 0) \quad " \quad " \quad " \quad "1," \\ (0, & 0, & {}^{2}\lambda_2, & 0) \quad " \quad " \quad " \quad "2," \\ (0, & 0, & 0, & {}^{3}\lambda_3) \quad " \quad " \quad " \quad "3," \end{array} $$

that all these ${}^{s}\lambda_{\nu}$ are functions of x_1 alone, and that

$$ {}^{2}\lambda_2 = {}^{3}\lambda_3. $$

With these values for the moments the ten equations (2) reduce to the five:

$$ \left.\begin{aligned} e^{ax_1} &= {}^{4}\lambda_4{}^{2} - {}^{1}\lambda_4{}^{2}, \\ -e^{-2ax_1} &= {}^{4}\lambda_1{}^{2} - {}^{1}\lambda_1{}^{2}, \\ -e^{-ax_1} &= -{}^{2}\lambda_2{}^{2}, \\ -e^{-ax_1} &= -{}^{2}\lambda_3{}^{2}, \\ 0 &= {}^{4}\lambda_1 {}^{4}\lambda_4 - {}^{1}\lambda_1 {}^{1}\lambda_4. \end{aligned}\right\} \quad \ldots\ldots (2.1) $$

We note that these equations are also the conditions of orthogonality of the four congruences.

The solutions are:

$$ \left.\begin{aligned} {}^{4}\lambda_4 &= e^{\frac{1}{2}ax_1}\cosh v, & {}^{1}\lambda_4 &= e^{\frac{1}{2}ax_1}\sinh v, \\ {}^{4}\lambda_1 &= e^{-ax_1}\sinh v, & {}^{1}\lambda_1 &= e^{-ax_1}\cosh v, \\ {}^{2}\lambda_2 &= e^{-\frac{1}{2}ax_1}, & {}^{3}\lambda_3 &= e^{-\frac{1}{2}ax_1}. \end{aligned}\right\} \quad \ldots\ldots (3) $$

where v is an undetermined function of x_1.

The parameters are, therefore

$$\left.\begin{aligned} {}_4\lambda^4 &= e^{-\frac{1}{2}\alpha x_1}\cosh v, & {}_1\lambda^4 &= e^{-\frac{1}{2}\alpha x_1}\sinh v, \\ {}_4\lambda^1 &= -e^{\alpha x_1}\sinh v, & {}_1\lambda^1 &= -e^{\alpha x_1}\cosh v, \\ {}_2\lambda^2 &= -e^{\frac{1}{2}\alpha x_1}, & {}_3\lambda^3 &= -e^{\frac{1}{2}\alpha x_1}. \end{aligned}\right\} \quad (4)$$

To find v we calculate the geometrical quantities which represent the electromagnetic force tensor and equate them to the known values of the components of this tensor in the field (1). This is done as follows.

The Christoffel symbols for the metric (1) which do not vanish are:

$$\left\{\begin{matrix}12\\2\end{matrix}\right\} = -\frac{\alpha}{2}, \qquad \left\{\begin{matrix}22\\1\end{matrix}\right\} = \frac{\alpha}{2}e^{\alpha x_1},$$

$$\left\{\begin{matrix}13\\3\end{matrix}\right\} = -\frac{\alpha}{2}, \qquad \left\{\begin{matrix}33\\1\end{matrix}\right\} = \frac{\alpha}{2}e^{\alpha x_1},$$

$$\left\{\begin{matrix}14\\4\end{matrix}\right\} = \frac{\alpha}{2}, \qquad \left\{\begin{matrix}44\\1\end{matrix}\right\} = \frac{\alpha}{2}e^{3\alpha x_1},$$

$$\left\{\begin{matrix}11\\1\end{matrix}\right\} = -\alpha.$$

The coefficients of rotation are defined by

$$\gamma_{ikl} = \sum_{\nu,\rho=1}^{4} {}^{i}\lambda_{\nu\rho}\,{}_k\lambda^{\nu}\,{}_l\lambda^{\rho}. \quad \ldots\ldots \quad (5)$$

Hence, to calculate them, we must find the covariant derivatives, ${}^{i}\lambda_{\nu\rho}$, of the moments. The non-zero ones are:

$${}^{4}\lambda_{11} = e^{-\alpha x_1}v'\cosh v, \qquad {}^{4}\lambda_{14} = -\frac{\alpha}{2}e^{\frac{1}{2}\alpha x_1}\cosh v,$$

$${}^{4}\lambda_{41} = e^{\frac{1}{2}\alpha x_1}v'\sinh v, \qquad {}^{4}\lambda_{44} = -\frac{\alpha}{2}e^{2\alpha x}\sinh v,$$

$${}^{4}\lambda_{22} = -\frac{\alpha}{2}\sinh v, \qquad {}^{4}\lambda_{33} = -\frac{\alpha}{2}\sinh v.$$

$${}^{1}\lambda_{41} = e^{\frac{1}{2}\alpha x_1}v'\cosh v, \qquad {}^{1}\lambda_{14} = -\frac{\alpha}{2}e^{\frac{1}{2}\alpha x_1}\sinh v,$$

$${}^{1}\lambda_{11} = e^{-\alpha x_1}v'\sinh v, \qquad {}^{1}\lambda_{44} = -\frac{\alpha}{2}e^{2\alpha x_1}\cosh v,$$

$${}^{1}\lambda_{22} = -\frac{\alpha}{2}\cosh v. \qquad {}^{1}\lambda_{33} = -\frac{\alpha}{2}\cosh v.$$

$$^3\lambda_{13}=\frac{\alpha}{2}e^{-\frac{1}{2}\alpha x_1}, \qquad ^2\lambda_{12}=\frac{\alpha}{2}e^{-\frac{1}{2}\alpha x_1},$$

where

$$v'=\frac{dv}{dx_1}.$$

On substitution into (5) we get that the non-zero coefficients are :

$$\gamma_{414}=-\gamma_{144}=e^{\alpha x_1}\left(v'\sinh v+\frac{\alpha}{2}\cosh v\right),$$

$$\gamma_{411}=-\gamma_{141}=e^{\alpha x_1}\left(v'\cosh v+\frac{\alpha}{2}\sinh v\right),$$

$$\gamma_{422}=-\gamma_{242}=-\frac{\alpha}{2}e^{\alpha x_1}\sinh v,$$

$$\gamma_{433}=-\gamma_{343}=-\frac{\alpha}{2}e^{\alpha x_1}\sinh v,$$

$$\gamma_{133}=-\gamma_{313}=-\frac{\alpha}{2}e^{\alpha x_1}\cosh v,$$

$$\gamma_{122}=-\gamma_{212}=-\frac{\alpha}{2}e^{\alpha x_1}\cosh v.$$

Now it is known that a set of 4 orthogonal congruences in a 4-dimensional Riemann space define 4 unit vectors of reference at each point and that any arbitrary tensor in the space can be defined by of its "invariants" with regard to these 4 unit vectors †. For instance, if A^μ denote the contravariant components of a vector referred to the coordinates, and $^*A^m$ the corresponding "invariant," we have

$$^*A^m=\sum_{\nu=1}^{4}e_m{}^m\lambda_\nu A^\nu,$$

and similarly

$$^*A_m=\sum_{\nu=1}^{4}e_{m\ m}\lambda^\nu A_\nu.$$

Instead of the term "invariants" we shall use the term "lattice-tensor," and denote such lattice-tensors by means of an asterisk.

† Levi-Civita, 'Absolute Differential Calculus,' p. 265.

We now calculate the lattice-tensor

$$\psi^*_{ik}=\sum_{t=1}^{4} e_t\,{}_t\lambda^\rho \frac{\partial \gamma_{ikt}}{\partial x_\rho}=-{}_1\lambda^1\frac{d\gamma_{ik1}}{dx_1}+{}_4\lambda^1\frac{d\gamma_{ik4}}{dx_1}$$

in our case.

We get that the only non-zero components are

$$\psi^*_{41}=-\psi^*_{14}=e^{\alpha x_1}\cosh v\frac{d}{dx_1}\left\{e^{\alpha x_1}(v'\cosh v+\frac{\alpha}{2}\sinh v)\right\}$$
$$-e^{\alpha x_1}\sinh v\frac{d}{dx_1}\left\{e^{\alpha x_1}(v'\sinh v+\frac{\alpha}{2}\cosh v)\right\}. \quad (6)$$

Now Prof. Levi-Civita identifies the lattice-tensor ψ^*_{ik} with the lattice-tensor F^*_{ik}, *i. e.*, with the lattice-tensor corresponding to the electromagnetic force tensor $F_{\mu\nu}$. The relation is

$$F^*_{ik}=a\psi^*_{ik}, \quad . \quad . \quad . \quad . \quad . \quad . \quad (7)$$

where $a=$ constant with the dimensions of an electric charge.

In the case of the field given by (1) we have that

$$F_{41}=-F_{14}=\frac{\alpha}{4\sqrt{\pi}}e^{\frac{1}{2}\alpha x_1},$$

all the other components being zero.

Hence, since

$$F^*_{ik}=\sum_{\mu,\nu=1}^{4} e_i e_k F_{\mu\nu}\,{}_i\lambda^\mu\,{}_k\lambda^\nu,$$

we have

$$F^*_{41}=-F^*_{14}=\frac{\alpha}{4\sqrt{\pi}}e^{\alpha x_1}.$$

Hence, substituting this value into (7), and thence into (6), we get the equation for determining v, viz.,

$$\frac{\alpha}{4a\sqrt{\pi}}=\frac{d}{dx_1}(e^{\alpha x_1}v')+\frac{\alpha}{2}v'e^{\alpha x_1},$$

which gives

$$v=\frac{1}{2a\alpha\sqrt{\pi}}\left(-e^{-\alpha x_1}+\frac{2}{3}e^{-\frac{1}{2}\alpha x_1}+\frac{1}{3}\right), \quad . \quad . \quad (8)$$

the constants of integration being adjusted so that $v=0$ when $\alpha=0$.

Hence, the congruences whose parameters and moments are given by (3), (4), and (8) are completely determined by

the field (1), and conversely, by means of equations (2.1), (5), and (6), the congruences, if known, would exactly determine the field. Also these values of the parameters and moments rigorously satisfy the field equations † given for them by Prof. Levi-Civita (the equations II. being identities and the field (1) having been obtained as a solution of equations I.).

If we compare the solution given by equations (3), (4), and (8) with that obtained by the use of Prof. Einstein's theory ‡, we see that they are identical, except for the presence of the quantity $\sqrt{(-1)}$ in the latter case. This, however, merely arises from the fact that in the present work we have employed the quantities $e_i = \pm 1$ in the calculation, with the result that imaginary quantities do not enter into the final statement of the solution.

We therefore have, finally, *the congruences of Prof. Levi-Civita's theory establish at each point the same four orthogonal unit vectors which are used by Prof. Einstein to define "parallelism at a distance" in the field.*

§ III. *The Geometrical Interpretation of the Electromagnetic Vector Potential.*

This similarity between the solutions on the two theories suggested that the geometrical quantities of the present theory, corresponding to those which defined the electromagnetic potential vector in Einstein's theory, would play the same part in the present one. We therefore calculate the vector

$$\chi_\rho = \sum_{i,\nu=1}^{4} e_i \lambda^\nu ({}^i\lambda_{\rho\nu} - {}^i\lambda_{\nu\rho}) = \sum_{i,\nu=1}^{4} e_i {}^i\lambda^\nu \left(\frac{\partial {}^i\lambda_\rho}{\partial x_\nu} - \frac{\partial {}^i\lambda_\nu}{\partial x_\rho} \right). \quad (9)$$

On substitution into (9) from (3), (4), and (8), we get

$$\left.\begin{aligned} \chi_4 &= \frac{1}{2a\sqrt{\pi}} (e^{\frac{1}{2}x_1} - 1), \\ \chi_1 &= \frac{a}{2}, \\ \chi_2 &= \chi_3 = 0. \end{aligned}\right\} \quad \ldots \quad (10)$$

† Levi-Civita, *Berliner Sitzungberichte*, viii.-x. p. 137 (1929), equations I. and II.

‡ G. C. McVittie, *loc. cit.* equations (2.6), (2.7), and (3.3).

If, now (as had to be done in the case of Einstein's theory when applied to the field (1)), the electromagnetic potential vector in (1) is taken to be

$$\phi_4=\frac{1}{2\sqrt{\pi}}(e^{\frac{1}{2}\alpha x_1}-1), \quad \phi_1=\frac{\alpha}{2a}, \quad \phi_2=0, \quad \phi_3=0,$$

by adding the constants $-1/2\sqrt{\pi}$ and $\alpha/2a$ to ϕ_4 and ϕ_1 respectively, we see that we can make the identification

$$\phi_4=a\chi_4, \quad \phi_1=a\chi_1, \quad \phi_2=a\chi_2, \quad \phi_3=a\chi_3. \quad (11)$$

The vector χ has the following geometrical interpretation:—

By the definition (5) of the γ_{ikt} we have that

$$\gamma_{ikt}-\gamma_{itk}=\sum_{\nu,\rho=1}^{4}{}_k\lambda^\nu{}_i\lambda^\rho\left\{\frac{\partial^t\lambda_\nu}{\partial x_\rho}-\frac{\partial^t\lambda_\rho}{\partial x_\nu}\right\}.$$

Put $i=k$, multiply by e_i and e_t, sum with respect to i, and note that $\gamma_{iit}=0$ for all i. We have

$$\left.\begin{aligned}\sum_{i=1}^{4}e_te_i\gamma_{iti}&=\sum_{i,\nu,\rho=1}^{4}e_te_{it}\lambda^\nu{}_i\lambda^\rho\left\{\frac{\partial^t\lambda_\nu}{\partial x_\rho}-\frac{\partial^t\lambda_\rho}{\partial x_\nu}\right\}\\&=\sum_{\nu,\rho=1}^{4}e_{tt}\lambda^\nu\chi_\nu \qquad [\text{by (9)}]\\&=\chi^*{}_t.\end{aligned}\right\} \quad (12)$$

Now Prof. Levi-Civita calls the lattice-vector

$$c^*{}_t=\sum_{i=1}^{4}e_i\gamma_{iti}$$

the "average curvature of the congruences orthogonal to the tth," *i.e.*, it is the sum of the projections on the direction "t" of the vectors representing the geodesic curvatures of the lines of the three other congruences normal to the tth.

Hence, since $e_tc^*{}_t=\chi^*$, it follows from (11) that, for the field (1), *the lattice tensor $\phi^*{}_t$ corresponding to the electromagnetic potential tensor ϕ_μ is proportional to the average curvature of the congruences.*

In conclusion, I should like to thank Prof. E. T. Whittaker, F.R.S., of Edinburgh University, who was good enough to communicate this paper.

CVII *Investigations on the Effect of Crystalline Structure on Magnetic Susceptibilities by a New Magnetic Balance based on the Principle of Interference of Light.* *By* Prof. S. S. BHATNAGAR, *D.Sc.(Lond.)*, *and* R. N. MATHUR, *M.Sc.**

THE influence of crystalline structure on magnetic susceptibilities has been considerably investigated. Curie † found that red phosphorus is less diamagnetic than yellow, while the diamagnetic susceptibilities of the allotropic forms of sulphur are nearly the same. Honda and Du Bois ‡ investigated the magnetic properties of a large number of elements, some of which had allotropic modifications of different crystalline structures. The method of experimentation did not differ essentially from that of Curie. The magnetic susceptibilities of various allotropic forms of phosphorus, antimony, carbon, and tin showed interesting differences. The ordinary white tetragonal variety of tin was found to be slightly paramagnetic, while grey tin was diamagnetic. Different allotropic forms of carbon gave values which differed considerably. The allotropic modifications of phosphorus and antimony also gave different values. Honda's investigation was continued by Owen §, and he obtained different values for the diamagnetic susceptibilities of rhombic and colloidal sulphur. Oxley ‖ also investigated the influence of molecular constitution on magnetic susceptibilities. According to him the relation between molecular complexity and specific diamagnetic susceptibility χ_D may be written in the form

$$\chi_D = \frac{1}{H}\Sigma n_P \Delta M_P,$$

where ΔM_P is the total diamagnetic moment produced in a complex of type P by the application of an external magnetic field H, n_P is the number of complexes of the type P per gramme, and the summation is extended over all such types. The allotropic forms of an element which possess characteristic crystalline structures will have different molecular distorsions or types of molecular complexes, and consequently different magnetic properties. Oxley (*loc. cit.*)

* Communicated by the Authors.

† *Ann. de Chim. et Phys.* (7) v. pp. 289–405 (1895).

‡ *Ann. der Phys.* xxxii. pp. 1027–1063 (1910); "Versl. Kon. Ak. V. Wetensch," Amsterdam, xii. p. 601 (1910).

§ *Ann. der Phys.* xxxvii. p. 657 (1912).

‖ Phil. Trans. Roy. Soc. A. ccxiv. pp. 108–146 (1914).

also attempted to interpret these changes in magnetic properties in terms of the electron theory of magnetism.

A large number of compounds, besides the elements described above, exist in various isomeric modifications. As for example, the oxide and iodide of mercury exist in yellow and red forms, and there are differences of opinion as to whether the change in their colour is due only to a change in size of the particles or is accompanied by a change in crystalline structure as well. The magnetic susceptibilities of substances are, in general, influenced by their crystalline forms and not by the size of their particles. Wilson * points out that if specimens are reduced to powder by a grinder in the construction of which no magnetic material is used, and then tested for magnetic susceptibilities by his balance, the susceptibilities of the original specimens are obtained. It is therefore obvious that a knowledge of the magnetic properties of isomeric modifications would throw considerable light on their constitution. An attempt was therefore made to determine the magnetic susceptibilities of the red and yellow varieties of mercuric oxide on an apparatus very similar to that described by Wilson (*loc. cit.*). The substance contained in a thin small glass phial, attached to a light aluminium system, is suspended in a non-homogeneous magnetic field by a phosphor-bronze or silver strip. The force exerted by the field is balanced by the torsion of the suspension and read off from a graduated torsion head; but as the differences between the susceptibilities of isomeric modifications are very small, the apparatus was not found sensitive enough to detect them. It was therefore necessary to construct a much more sensitive balance for this investigation.

Nearly all methods commonly used for the measurement of magnetic susceptibilities of solids may be divided into two groups: (1) those in which the specimen is placed in a non-homogeneous magnetic field like Curie's and Oxley's balances, and (2) those in which the specimen is suspended in a homogeneous field as in Gouy's method; but in every case it is the displacement of the substance placed in the magnetic field that is directly or indirectly measured. In Curie's balance the movements of the torsion-rod-pointer over a scale are noted. In Oxley's balance (*loc. cit.*) the movements of a spot of light on a scale, corresponding to the displacements of the substance in the field, are observed; while in some other balances the restoring method is

* Proc. Roy. Soc. A, xcvi. p. 442.

employed, and the amounts of torsion to be given to the suspension wire, to bring back the specimen to its original position, are measured. Now the displacement of a substance in a magnetic field is proportional to its susceptibility, and for substances whose susceptibilities are nearly equal, the displacements for their same mass will also be nearly equal, and may not be differentiated if the apparatus is not sensitive enough. And in order to know accurately the difference between the displacements of such substances, it is necessary that the method of measuring them be very sensitive to small changes. In experiments based upon the principle of interference of light, as for example, formation of Newton's rings, we know that very small changes in the system produce very great changes in the interference rings. It therefore struck us that the displacements of the substance in the magnetic field might be measured in terms of the changes in Newton's rings. A convex lens put on a glass plate gives Newton's rings, and if the plate or lens moves a little a very big change in the position of the rings takes place at once; and either the shift of the rings from their original position can be measured or an appliance can be devised to bring the rings back to their original positions. Accordingly, du Noüy's apparatus for measuring surface tensions was adapted for the purpose of a magnetic balance. Essentially, du Noüy's apparatus is a torsion balance employing a wire to which is clamped a light arm. The torsion is applied to the wire by means of a slow-motion screw, and the angle of torsion is indicated on a graduated dial. The light arm of the balance extends only on one side of the wire. It was therefore replaced by a light aluminium beam extending on both sides of it. To its one end was attached a small convex lens and to the other a small glass tube which could be put in a suitable homogeneous magnetic field. Below the lens was placed a small plane table which could be moved up and down by means of a screw, and on this table was put a plane piece of glass. Above the lens was put a piece of glass plate, inclined at an angle of 45° to reflect light from a sodium flame vertically downwards. A right-angled prism was put above the glass plate, and Newton's rings were observed by means of a microscope. The substance whose susceptibility was to be determined was put in the glass tube. On applying the magnetic field the tube moved up and down in the field, and this produced a shift in the Newton's ring system. Attempts were made to bring the rings back to their original position by applying torsion to the wire. Sometimes the shifts of the rings were also measured b

travelling microscope. The experimental difficulties were, however, so many that they rendered the method much less promising than it at first sight appeared. Attempts were therefore necessary to employ some other device. If two converging beams of light are producing interference fringes and a moving glass plate be placed in the path of one, the shifting of the fringes will depend upon the movements of the plate and can be a measure of it. Moreover, very small movements of the plate will produce very considerable shiftings of the fringes. If, therefore, instead of measuring the movements of a spot of light on a scale, as in Oxley's balance (*loc. cit.*), we measure the shift of the

Fig. 1.

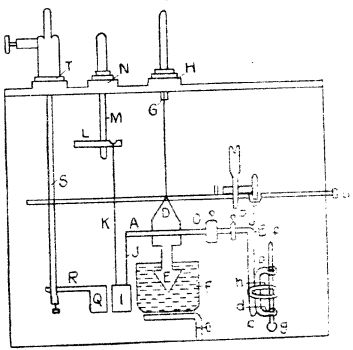

Front Elevation.

fringes produced by the movements of a glass plate, the apparatus will be a very sensitive one. A Rayleigh interferometer provides interference fringes as well as possesses a convenient appliance for measuring the shifting of the fringes. It was therefore adapted for this purpose. The apparatus is represented diagrammatically in figs. 1, 2, 3, and 4.

In fig. 1, ABC is a light aluminium beam bent at right angles at B. The horizontal portion of the beam is fixed to a light aluminium piece D, whose lower end has got cross vanes E. These cross vanes move in a dash pot F containing mixture of paraffin oil and heavy mineral oil to damp the

vibrations of the beam. The aluminium piece D is suspended by a fine silver strip. The other end of the strip is fixed to the rod G which, by a screw, is fixed to the torsion head H. I is a piece of optically plane parallel glass suspended by means of two silk threads J and K. The thread J is attached to the end A of the beam, while the thread K is attached to the end of rod L. The rod L passes through a hole at the end of the rod M, and can be moved forwards

Fig. 2.

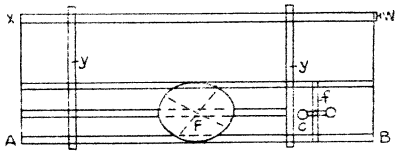

Plan.

Fig. 3.

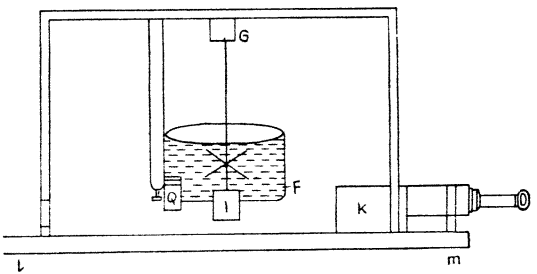

Side Elevation.

and backwards in it. The brass rod M is attached by a screw to the torsion head N. The system LMN is therefore a three-dimensional adjustment appliance. The end of the rod L to which the silk thread is fixed can be moved forwards and backwards by moving L, up and down by moving M up and down, and sideways by twisting M with the torsion head N. O and P are two riders placed over the beam to keep it horizontal. The rider P is much lighter than O (their respective weights being 0·08 and 0·4 gm and is used for fine adjustment. Q is another optic

plane parallel piece of glass of the same thickness as I; it is directly attached to the end of the rod R. The system RST is exactly similar to the system LMN. This is all enclosed inside a box, having a window in front. In order to move the riders O and P over the beam AB, the arrangement of a chemical balance for moving the rider over its beam was fixed in a side of the box. U is the handle and V the hook which holds the rider. In order to rest the torsion arm AB while the phial, containing the substance under

Fig. 4.

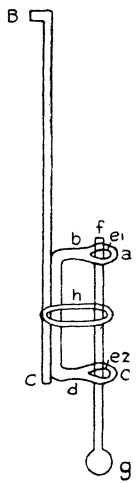

investigation, was being attached to its end C, the rod WX provided with two cranks YY was used (fig. 2). The rod WX passes through a hole in the side of the box, and can be rotated by the handle W. The arrangement for holding the phial is shown in fig. 4. BC is the end of the beam bent at right angles at B. To its end is fixed a piece of aluminium, *abcd*, bent at right angles at *b* and *d*. In the pieces *ab* and *cd* are made two V-shaped holes e_1 and e_2. The phial *gf* is put into them from below. *h* is a thin rubber band passing over the stem of the phial and the end BC of the beam. By means of this rubber band the phial is held tight to the

left in the V-shaped holes. At the top of the stem *f* is made a mark, and whenever the phial is placed in the holes e_1, e_2, this mark is made to coincide with another mark in the plate *ab* near the V end of the hole e_1. By this device the phial is always placed in the same position. Its displacement to the left or right is checked by the V-shaped holes e_1 and e_2 and the rubber band *h*, while its displacement sideways, or up and down, is checked by the marks on the top of the stem *f* and the plate *ab*. Any change in the position of the phial, relative to the pole-pieces of the electromagnet, can now only be due to an alteration in the position of the beam AB, and this could be detected and removed by means of the interference fringes as given afterwards. The phial *g* was placed in a suitable non-homogeneous magnetic field obtained by inclining the pole-pieces of an electromagnet at an angle. The electromagnet was also placed inside the box containing everything else, and this box was fitted over the interferometer in front of its small box containing the movable glass plate and the fixed compensating plate in such a way that the two plates I and Q were in the path of the two parallel beams of light coming from the collimator (fig. 3). *lm* is a part of the heavy base of the interferometer. I and Q are the glass plates of fig. 1 and K is the small box of the interferometer containing the glass plate moved by the micrometer screw and the fixed compensating glass plate. The parallel rays of light coming from the collimator pass through I and Q and then through the two plates in the box. The window for admitting the beams of light into the box is also covered with a piece of optically plane glass. In order to avoid vibrations of the plate I due to air currents, no holes were left open in the sides of the box. A part of the interferometer and the box were also further enclosed in a chamber, with a window, in such a way that only the eyepiece of the interferometer and its micrometer screw were out of it. By using a pointolite lamp the two sets of interference fringes were obtained, and their central black bands were made to coincide. A known weight of the substance whose susceptibility was to be determined was then put in the phial and a constant current of 1·5 amperes, taken from a set of batteries, was passed in the electromagnet. On account of the movements of the phial in the field the glass plate I turns through an angle, and the upper system of fringes shifts to one side. Their central black bands are then again made to coincide by turning the interferometer screw. The number of divisions through which the screw had to be turned are no

Similar readings are taken for the empty phial and phial containing a known weight of water. Let X be the force acting on the substance in the field and let θ be the angle through which the beam is turned due to it. We have now to find the change in the optical path produced by this turning of the plate I through an angle θ. In fig. 5, ABCD represents the original position of the plate and A′B′C′D′ when it has been deflected through an angle θ. SO is the incident ray and OR and OR′ the refracted rays in the two positions of the plate, and ON and ON′ the corresponding

Fig. 5.

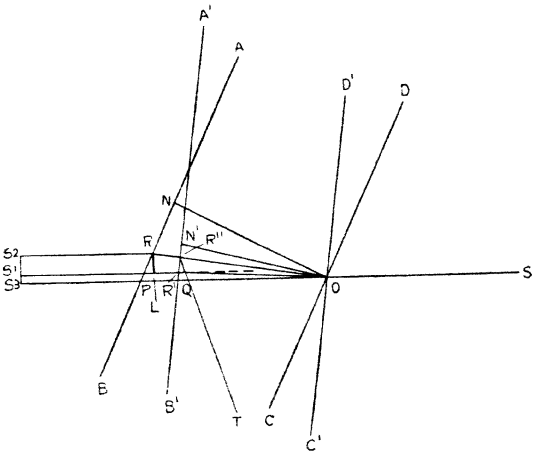

normals drawn from O. The refracted rays coming from out the plate are travelling along RS_2 and $R'S_1$. Produce SO to S_3, cutting AB and A′B′ and P and Q. Let S_1, S_2, and S_3 be in a line. From R″ draw a perpendicular R″T on S_1R' produced, and from R draw a perpendicular RL on $R'S_1$. The optical paths of the rays from S to S_1S_3 are $SO+n\,.\,OR+RS_2$ and $SO+n\,.\,OR'+R'S_1$, where n is the index of refraction of the material of the plate. The change in optical path is therefore given by

$$P = n\,.\,OR - n\,.\,OR' - R'L \qquad (RS_2 = LS_1)$$
$$= n\,.\,OR - n\,.\,OR' - LT + R'T.$$

Let ϕ and ϕ' be the initial angles of incidence and refraction, and let ϕ_1 and ϕ_1' be the corresponding angles when the plate has been turned through an angle θ.

$$\therefore \quad \mathrm{OR} = \frac{h}{\cos\phi'} \qquad (\mathrm{ON} = h \text{ is the thickness of the plate}),$$

$$\mathrm{OR}' = \frac{h}{\cos\phi_1'},$$

$$\mathrm{RR}'' = h\left[\frac{1}{\cos\phi'} - \frac{1}{\cos(\phi'-\theta)}\right],$$

$$\mathrm{LT} = \mathrm{RR}''\cos(\phi-\phi')$$

$$= h\cos(\phi-\phi')\left[\frac{1}{\cos\phi'} - \frac{1}{\cos(\phi'-\theta)}\right],$$

$$\mathrm{R'N'} = h\tan\phi_1',$$

$$\mathrm{R''N'} = h\tan(\phi'-\theta),$$

$$\therefore \quad \mathrm{R'R''} = h[\tan\phi_1' - \tan(\phi'-\theta)],$$

$$\mathrm{R'T} = \mathrm{R'R''}\sin(\phi-\theta)$$

$$= h\sin(\phi-\theta)[\tan\phi_1' - \tan(\phi'-\theta)].$$

Also

$$\sin\phi' = \frac{\sin\phi}{n},$$

$$\cos\phi' = \frac{\sqrt{n^2-\sin^2\phi}}{n},$$

$$\sin\phi_1' = \frac{\sin(\phi-\theta)}{n},$$

$$\cos\phi_1' = \frac{\sqrt{n^2-\sin^2(\phi-\theta)}}{n}.$$

Substituting these values in (1) we have for the change in optical path P

$$\mathrm{P} = h\left\{\frac{n^2}{\sqrt{n^2-\sin^2\phi}} - \frac{n^2}{\sqrt{n^2-\sin^2(\phi-\theta)}}\right.$$

$$-\sin(\phi-\theta)[\tan(\phi'-\theta)-\tan\phi_1']$$

$$\left.-\cos(\phi-\phi')\left[\frac{1}{\cos\phi'} - \frac{1}{\cos(\phi'-\theta)}\right]\right\}$$

$$= h\left\{\sqrt{n^2-\sin^2\phi} - \cos\phi - \sqrt{n^2-\sin^2(\phi-\theta)}\right.$$

$$\left.+\cos\phi\cos\theta + \sin\phi\sin\theta\right\}. \quad . \quad . \quad . \quad . \quad . \quad . \quad . \quad (1)$$

When θ is very small *, $\cos\theta = 1$, and we have to a very close approximation

$$P = h\sin\theta\left\{\sin\phi - \frac{\sin 2\phi}{2\sqrt{n^2-\sin^2\phi}}\right\}. \quad . \quad . \quad (2)$$

As ϕ the initial angle of incidence remains constant, the expression inside the bracket is constant. And as h is also a constant

$$P = K\sin\theta. \quad . \quad . \quad . \quad . \quad . \quad . \quad (3)$$

After putting on the magnetic field, the central black bands of the two systems of interference fringes are again made to coincide. The change in optical path P is then equal in magnitude to the change in optical path produced by the movement of the interferometer plate. And the latter change is directly proportional to r', where †

$$r' = r - Kr^2$$

and r is the number of divisions on the drum through which the micrometer screw is turned to bring back the fringes to their original position, and K is a constant for the instrument. For our interferometer the value of K is 0·000022, and hence

$$r' = r - 0{\cdot}000022\,r^2. \quad . \quad . \quad . \quad . \quad . \quad (4)$$

r' is therefore a number directly proportional to the change in the optical path.

$$\therefore \qquad P = K\sin\theta$$
$$= K_1 r',$$

where K_1 is a constant.

Now, if X is the force acting on the substance in the field,

$$X = K_3\sin\theta$$
$$= K_4 r', \quad . \quad . \quad . \quad . \quad . \quad . \quad . \quad (5)$$

provided the deflexion of the torsion arm is small. K_3 and K_4 are constants.

Now, according to Oxley (*loc. cit.*), if the phial be placed at P with regard to the pole-pieces A and B (fig. 6), the

* An estimate of the magnitude of θ is given under the discussion of possible errors (c).

† Jour. Amer. Chem. Soc. xxxvii. p. 1192 (1915).

mechanical forces acting on the body of specific susceptibility x and mass M are given by

$$X = xM\left(H_x\frac{\partial H_x}{\partial x} + H_y\frac{\partial H_y}{\partial x} + H_z\frac{\partial H_z}{\partial x}\right) \quad . \quad . \quad (6)$$

along OX, with similar expressions for the forces Y and Z along OY and OZ. In practice the forces along OY and OZ are very small, and since the resistance to motion in these directions is very great the disturbance of the equilibrium of the suspended system, due to these forces, may be neglected.

Now let r_1 be the number of divisions through which the micrometer screw is turned when the phial only is placed in

Fig. 6.

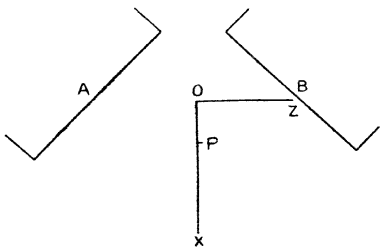

the field, and let r_2 and r be the similar readings when phial containing water and phial containing substance are placed in the field. Then from (5) and (6)

$$K_4(r_2-r_1) = (x_w m_w - x_a m_a)\left(H_x\frac{\partial H_x}{\partial x} + H_y\frac{\partial H_y}{\partial x} + H_z\frac{\partial H_z}{\partial x}\right), \quad . \quad . \quad . \quad (a)$$

$$K_4(r-r_1) = (xM - x_a M_a)\left(H_x\frac{\partial H_x}{\partial x} + H_y\frac{\partial H_y}{\partial x} + H_z\frac{\partial H_z}{\partial x}\right), \quad . \quad . \quad . \quad (b)$$

provided the phial is always placed in the same position relative to the pole-pieces. Here M is the mass of the substance taken, M_a that of air which fills the same volume as the substance, m_w the mass of water taken, and m_a that of air which fills the same volume as occupied by water.

In all the experiments the current was kept constant at 1·5 amperes. The factor involving the field on the right-hand side of (*a*) and (*b*) is constant, and we get

$$x\mathrm{M} = x_a\mathrm{M}_a + (x_w m_w - x_a m_a)\frac{r-r_1}{r_2-r_1}.$$

The specific susceptibilities of water x_w and of air x_a are taken as $-7{\cdot}2\times10^{-7}$ and 210×10^{-7} respectively.

Discussion of Possible Errors.

(*a*) Change in the position of the phial relative to the pole-pieces.—While taking the readings for the empty phial, phial and water, and phial and substance, it is necessary that the phial be placed always in the same position relative to the pole-pieces. As given before, the phial can always be placed in the same position relative to the beam by means of the two V-shaped holes, rubber band, and marks on the top of the stem of the phial and aluminium plate. Any change in its position relative to the pole-pieces could then only be due to a change in the position of the beam, and this could at once be detected by the shifting of the interference fringes. A change in the horizontal position of the beam takes place on account of the varying weights of the contents of the phial. This produces a shift of the interference fringes, and the riders O and P are adjusted to bring them back to their original position. We believe that this is a much more accurate method of bringing the phial always to the same position than those used by others. Slightest changes in the weights of the contents of the phial or very small movements of the rider P over the beam produce appreciable shift of the fringes.

(*b*) Correction due to dissymmetry of phial.—The phial was as nearly spherical as possible. Moreover our measurements are differential ones, and if the phial is placed always in the same position no appreciable error can be introduced from this source.

(*c*) Error due to the assumption in deducing equation (2) that θ is so small that $\cos\theta$ is unity.—In the interferometer used the micrometer screw presses against a steel block at the end of an eight-inch lever. Further, the drum on the screw is divided into 100 equal divisions and the pitch of the screw is 1/2 mm. A rotation corresponding to one division of the drum therefore moves the end of the lever through 0·005 mm., and hence turns the compensating plate through an angle of 5 seconds. A rotation corresponding

to 600 divisions, which is the maximum number of divisions measured in this investigation, will therefore move the plate through 50 mts. Now the plate I is about five times thicker than the interferometer plate. In order to produce the same change in optical path it will therefore only have to move through about 10 mts., and the value of the cosine of this small angle is always taken as unity. The magnitude of θ can also be calculated from equation (1) if we know P. Now, it can readily be shown that for light of wave-length λ the displacement of the central black fringe, measured in fringes, follows the simple relation $N = \frac{P}{\lambda}$, where P is the change in optical path and N is the number of fringes. In the present measurements N never exceeds 10, and taking for λ the wave-length of yellow light, P is of the order $5{\cdot}5 \times 10^{-4}$; and from equation (1), taking the maximum value of ϕ to be 10°, the value of θ comes to be of the same order as before, namely 10 mts.

(*d*) The phial used was slightly paramagnetic. Any variation in temperature during the time readings were being taken will therefore affect the results. But a thermometer placed inside the box practically showed no change in temperature during the interval when the readings for the phial, phial with water, and phial with the substance were being taken.

Experimental Results.

The substances investigated were always prepared as magnetically pure as possible. Rhombic sulphur was prepared by crystallizing Merck's extra pure sulphur from carbon disulphide. Monoclinic sulphur was prepared in the usual way from rhombic sulphur. In order to further test their purity, their melting-points and specific gravities were also determined, as given in the table below.

Substance.	Melting-point.	Melting-point usually given in books of reference.	Specific gravity.	Specific gravity usually given in books of reference.
Rhombic sulphur.	114° C.	115° C.	2·01	2·03
		111–115° C.		
Monoclinic sulphur.	118° C.	117·4° C. (Gernez)	1·981	1·982
		120° C. (Brodie)		1·958 (Deville)

The yellow and red modifications of mercuric iodide were obtained as follows :—Yellow mercuric iodide was prepared

by a method described by Gernez *. Pure red iodide was heated in a long tube. By cooling the liquid and condensing the vapour on the cool sides of the tube the yellow variety was obtained. This easily remained stable for about a day, when it changed into red. In doing the actual experiment the yellow variety was first put in the phial and readings taken. The yellow variety was then left in the phial for a day, when it changed into red and readings were again taken. The results are shown in the table below. r, r_2, and r_1 are the number of divisions on the drum of the micrometer screw after making the correction required by equation (4).

Substances.	r.	r_2.	r_1.	$-x_m \times 10^6$.
Rhombic sulphur	388·2	339·9	531·6	0·487
Monoclinic sulphur	395·5	339·9	531·6	0·462
Mercuric iodide yellow.....	291·6	204·0	345·5	0·272
Mercuric iodide red	291·6	204·0	345·5	0·272

Attempts were also made to determine the magnetic susceptibility of plastic sulphur. This variety of sulphur is usually prepared by pouring molten sulphur into water. But as it was necessary for our purpose that the specimen be absolutely free from water, it was prepared by pouring molten sulphur into a vessel cooled in ice. A small amount of plastic sulphur could be obtained in this way, but it remained stable only for a very short time. No definite readings could therefore be obtained for it, but the trend of readings showed that it is less diamagnetic than rhombic sulphur.

Discussion of Results.

According to Owen (*loc. cit.*) the diamagnetic susceptibility of rhombic sulphur is $-0{\cdot}485 \times 10^{-6}$, and our result is in excellent agreement with his. On account of a change in the crystalline structure it is natural to think that the susceptibility of monoclinic sulphur will be different from that of rhombic, and we find that it is a little less. Again, although no definite results could be obtained the susceptibility of plastic sulphur is less than that of the rhombic form. Foex and Royer † have determined the values of the diamagnetic susceptibilities of some substances which pass into

* *Compt. Rend.* cxxviii. p. 1516 (1899); *Compt. Rend.* cxlviii. p. 1015 (1909).

† "Le Diamagnetisme des Substances nématiques," *C. R.* clxxx. p. 1912 (1925); *Jour. de Phys. Bull.* ccxix. p. 94 (1925).

the nematic state, and they have interpreted the results in terms of diamagnetic orientation. According to them the susceptibility of para azoxy-anisol decreases suddenly by about 17 per cent. when it passes into the nematic state at 116° C. Our results for plastic sulphur therefore seem to be in line with the view of Foex and Royer. As for mercuric iodide, there is difference of opinion as to whether the red and yellow modifications have got the same or different crystalline structures. According to Luczizky * the red iodide crystallizes in tetragonal prisms and pyramids. According to Gernez †, on cooling the liquid iodide or condensing the vapour, the yellow modification is obtained in rhombic prisms. But according to A. Smits ‡, observations made with large crystals of yellow iodide show that the gradual development of the orange colour with rise of temperature is not accompanied by any change in crystalline form. This fact points to the formation of mixed rhombic crystals containing both yellow and red modifications. They are, according to Smits, apparently two isomeric forms of mercuric iodide (α and β) ; the red and yellow modifications being mixed crystals containing the two forms in different proportions. According to all that has been said before a change in crystalline structure must be accompanied by a change in susceptibility. With our sensitive balance § even very small changes in susceptibility can be detected. It therefore appears that magnetic data support Smits' views.

Further work on the magnetic susceptibilities of the other allotropic forms of sulphur and various modifications of mercuric oxides, sulphides, etc., is in progress and will be shortly communicated. Some substances are also being crystallized from different solvents, when they come out with different crystalline structures, and their susceptibilities are being determined.

Finally, we wish to express our thanks to Principal Hem Raj and Mr. K. N. Mathur.

University Chemical Laboratories,
University of the Punjab,
Lahore (India).

* *Zeit. Sch. Kryst. Min.* xlvi. p. 297 (1909).
† *Compt. Rend.* cxxviii. p. 1516 (1899).
‡ *Proc. K. Akad. Wetensch. Amsterdam*, xix. p. 703 (1917).
§ A full account of the sensitivity of the apparatus is given in an extension of this paper shortly to be communicated.

CVIII. *The Thermal Conductivity of a Single Crystal of Bismuth in a Transverse Magnetic Field.* *By* G. W. C. Kaye, *O.B.E., M.A., D.Sc., and* W. F. Higgins, *M.Sc., Physics Department, the National Physical Laboratory, Teddington, Middlesex* *.

THE fact that the thermal conductivity of bismuth in crystalline aggregate is decreased in the presence of a magnetic field was first observed independently in 1887 by Righi † and Leduc ‡. Subsequent investigations by von Ettingshausen §, van Everdingen ‖, and Blyth ¶ confirmed the sign of the change, though their results are not in good agreement. Lownds**, in 1902, examined single crystals of bismuth by the melting-wax method of de Sénarmont ††, and so obtained the effect produced by a field of about 5000 gauss on the ratio of the conductivities parallel and perpendicular to the trigonal axis. His specimens were very small, however, and approximate values only were possible.

It appeared that there was scope for a precise investigation of the effect of a transverse magnetic field on the thermal conductivity of single crystal specimens of bismuth, and the present investigation was undertaken. A "plate" type of apparatus was used similar in design to that recently employed by the authors for the thermal conductivity of solid and liquid sulphur ‡‡, with the exception that the cold block was cooled by a circulation of water instead of being air-cooled. The bismuth crystal, cut in the form of a disk 25 mm. in diameter and 2 mm thick, was sandwiched between the horizontal faces of the hot and cold blocks, the hot block being uppermost. Good thermal contact was effected by using optically flat surfaces, glycerine contact films, and a small load. Above the hot block was a "guard plate" to prevent loss of heat in the upward direction.

The transverse magnetic field was provided by an electromagnet, with pole-pieces measuring 10 cm. by 8·4 cm. The size of the conductivity apparatus necessitated a minimum gap

* Communicated by the Authors.
† Righi, *Mem. Acad. Linc.* (4) iv. p. 433 (1887).
‡ Leduc, *Comptes Rendus*, civ. p. 1783 (1887).
§ von Ettingshausen, Wied. *Ann.* xxxiii. p. 129 (1888).
‖ van Everdingen, Comm. Phys. Lab. Lieden, xlii. p. 4 (1898).
¶ Blyth, Phil. Mag. (6) v. p. 529 (1903).
** Lownds, *Ann. d. Physik*, ix. 3, p. 677 (1902).
†† de Sénarmont, *Comptes Rendus*, xxv. pp. 459, 707 (1847).
‡‡ Kaye and Higgins, Roy. Soc. Proc. A, cxxii. p. 633 (1929).

of 4 cm. between the pole-pieces, which permitted uniform fields up to about 11,000 gauss to be attained.

The change in thermal conductivity was measured for the following orientations of the crystal specimen. In each case the heat-flow was perpendicular to the magnetic field.

(*a*) Heat-flow and magnetic field both perpendicular to the trigonal axis.

(*b*) Heat-flow perpendicular to the trigonal axis; magnetic field parallel to the trigonal axis.

(*c*) Heat-flow parallel to the trigonal axis; magnetic field perpendicular to the trigonal axis.

In the case of specimens cut for investigating the heat-flow perpendicular to the trigonal axis, the value of the conductivity obtained in the absence of a magnetic field agreed closely with that found by Kaye and Roberts* in 1923 for much smaller specimens. The corresponding result for heat-flow parallel to the trigonal axis yielded, however, a figure about 18 per cent. less than the 1923 values. This low figure would be explained by the presence of fissures parallel to the principle cleavage plane (normal to the trigonal axis), an effect which has been observed by other workers using large single crystals of bismuth. It would appear that the constricting effect of the glass mould during the cooling and formation of the crystal may set up strains in the specimen which are relieved by slipping along the cleavage plane. Again, the preparation of the test specimen necessitated a certain amount of mechanical working, and strains set up during cutting and grinding operations might conceivably give rise to cracks along the cleavage planes. Such discontinuities, while having no effect on the thermal resistance parallel to the cleavage planes, might effect an appreciable increase at right-angles to them. In this connexion it may be mentioned that a twenty-fold increase of load (up to 7·5 kilogram per sq. cm.) on the specimen during test caused an increase in conductivity of 2 per cent and a permanent increase of about 1 per cent when the extra load was removed.

Figs. 1 and 2 show the change in conductivity produced by transverse fields up to 11,000 gauss. The accuracy of measurement is within $\pm\frac{1}{2}$ per cent. In the case of heat-flow parallel to the trigonal axis the graph includes results for a second specimen and for the two together.

* Kaye and Roberts, Roy. Soc. Proc. A, civ. p. 98 (1923).

Fig. 1.—Heat-flow ⊥ Trigonal Axis.

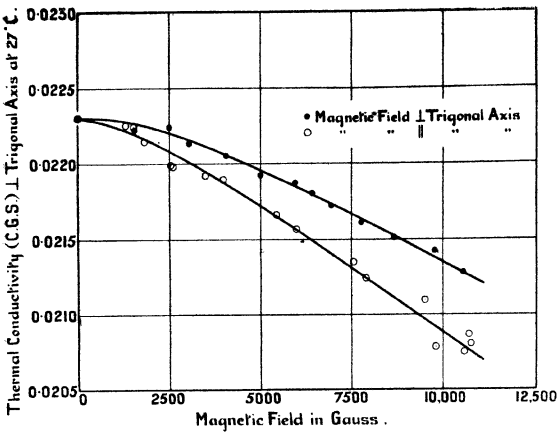

Fig. 2.—Heat-flow ∥ Trigonal Axis.

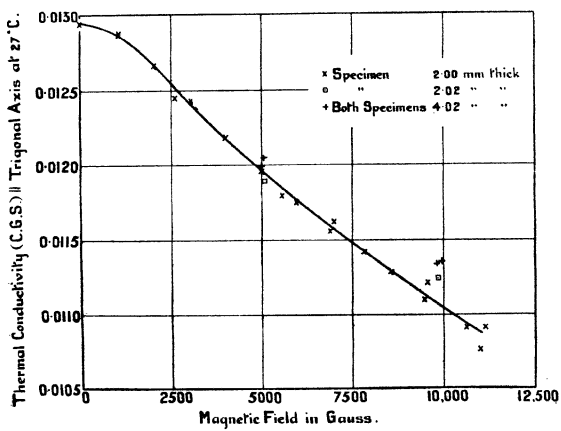

The following are the mean changes in conductivity at 27° C. for the specimens examined to date :—

Direction of heat-flow.	Direction of magnetic field.	Percentage decrease in thermal conductivity in field of 11,000 gauss.
⊥ trigonal axis	⊥ trigonal axis	4·9 %
⊥ „ „	∥ „ „	7·3 „
∥ „ „	⊥ „ „	16·0 „

The work is being continued with certain modifications and greater magnetic fields.

We are again much indebted to Mr. D. E. A. Jones for his very competent assistance.

CIX. *The Rate of Molecular Collisions in Liquid Systems.*

By MAURICE JOWETT, *Ph.D., B.Sc.**

THE rate of molecular collisions in liquid systems is of interest in chemical kinetics, since if the measurable process in a chemical reaction is bimolecular its rate is proportional, other things being equal, to the frequency with which the chemical species concerned collide with one another.

While the rate of molecular collisions in dilute gaseous systems has been satisfactorily treated, collision rates in liquid systems do not appear to have received much serious consideration. Thus, Christiansen [1] considers that the formulæ for collisions in gases may be applied to liquids in point of order of magnitude and in respect of their temperature coefficient. Tolman [2] regards the same formulæ as giving upper limits to the number of collisions between solute molecules in a solution.

Various chemists in discussing chemical kinetics have put forward views concerning the effect of the viscosity of the system on the collision rates between solute molecules in liquids. Thus, Moran and Lewis [3] regarded increased viscosity as hindering collisions, while Scatchard [4] regarded it as being without effect.

* Communicated by Prof. W. C. M. Lewis, F.R.S.

In considering the subject from a physical point of view, it must be remembered that there can be no great difference between the behaviour of solute molecules and solvent molecules. If the rate of collisions between solvent molecules and solute molecules is affected in one direction by a change in the medium, then the rate of collisions between different types of solute molecules must be affected in the same direction. It can now be shown very simply that increase in viscosity is a favouring influence for collisions. Admittedly, an increase in viscosity slows down the rate of diffusion of solute molecules. Now, on the kinetic theory of diffusion, the diffusion coefficient of a substance is given approximately by the relation

$$D = \tfrac{1}{3}\lambda u,$$

where λ is the mean free path of the molecule, and u is its equipartition velocity, this latter quantity being dependent only on the temperature. If therefore the viscosity of the medium be increased by any means at constant temperature, and consequently the diffusion coefficients of dissolved substances are decreased, it follows that the mean free paths of the molecules of the solutes are likewise decreased. The mean free paths being decreased, and the speed of the molecules being unchanged, the number of collisions undergone per second by these molecules must have increased.

A difficulty in appreciating this argument has perhaps been due to an incorrect appreciation of the meaning of Smoluchowski's formula [5] for the rate of rapid coagulation of colloidal particles. This may be applied to the calculation of a special type of collision rate between molecules in liquids, but not to the rate of continuous collisions.

Smoluchowski obtains the expression

$$J\,dt = 4\pi(D_1 + D_2)\nu_1\nu_2(r_1 + r_2)\,dt$$

for the rate at which two types of particles, none of them initially in contact, come into contact with each other for the first time. In this way he obtains a quantity analogous to a collision rate which is of value when we do not require to take into account collisions subsequent to the first collision which two particles may undergo. The particles are regarded as diffusing into contact, and their subsequent history is not of interest for Smoluchowski, since in the case he considers they do not persist as such after first coming into contact. If they do persist, however, it is evident that after coming into contact they may undergo a number of mutual collisions before parting company. With these subsequent collisions Smoluchowski's formula is not concerned.

It is the continuous collision rate of molecules which is of interest to us, since in measurable chemical reactions in liquids only a small fraction of the total number of collisions between the two reactant chemical species concerned leads to chemical change.

An attempt has been made by Norrish and Smith[6] to calculate the rate of collisions between solute molecules in liquids by the use of the formula for collisions in gases modified to allow for the space occupied by solvent molecules. These authors suppose the rate of collision between two types of molecules to be given by the collision rate calculated from gas theory multiplied by a factor $(V/V-s)^2$, V being the volume of the system, and s the actual volume occupied by molecules themselves. The quantity $V/V-s$ is regarded as a free-space term, but this assumption is quite arbitrary. In the deduction of van der Waals's equation it is shown that the "free space" in a dilute gaseous system is equal to the total space less four times the volumes of the molecules, when collisions with a boundary are being considered. The factor will be less than four when the system is no longer dilute, since spheres of twice the molecular radius drawn round the molecules will intersect to a large extent. There is, however, no reason to suppose that the factor can become unity. Apart from this, however, the correction factor of Norrish and Smith is quite empirical, since the free-space term should not be squared. Let us for convenience replace $V-s/V$ by v_F: then the gaseous rate must be divided by v_F, not v_F^2, in order to obtain the collision rate in a liquid, since the average volume swept out by a molecule between two successive collisions is reduced from unity to v_F, not to v_F^2.

The number of collisions taking place in unit time between a single molecule of species 1 and all molecules of species 2 in a liquid system may be represented by the equation

$$_1Z_2 = \frac{1}{v_{F_{12}}} \cdot 2\nu_2 S_{12}^2 \sqrt{2\pi RT(1/M_1+1/M_2)}, \quad . \quad . \quad (1)$$

which relates the collision rate in a liquid with that in a gas by means of a "free-space term" $v_{F_{12}}$ which has yet to be determined. It cannot be assumed *a priori* that in a liquid system containing several species of molecules the free-space term will be the same for all the types of collisions, that is, we cannot assume that

$$v_{F_{12}} = v_{F_{13}} = v_{F_{23}} = \ldots.$$

From a purely steric point of view, for instance, regarding

a liquid as an assembly of elastic spheres, fairly closely packed, we might not unreasonably suggest that a small molecule could penetrate, without collision, interspaces that the centre of a large molecule could enter only after collisions.

Kinetic Theory of Diffusion in Liquids.

An attempt may be made to evaluate v_F through the kinetic theory of diffusion applied to liquids.

The interdiffusion in a liquid system containing two kinds of molecules may be treated analogously to interdiffusion in the gaseous state. Jeans [7] denotes by Γ_1 the rate of increase per unit time and area of the number of molecules of the first kind on the positive side of a plane $z=z_0$, and derives the equation

$$\Gamma_1\nu_2-\Gamma_2\nu_1 = \tfrac{1}{3}\nu_1\lambda_2\bar{c}_2\frac{\partial\nu_2}{\partial z}-\tfrac{1}{3}\nu_2\lambda_1\bar{c}_1\frac{\partial\nu_1}{\partial z},$$

where ν refers to the number of molecules per c.c., λ to their free path, and $\bar{c}$ to their mean velocity.

Introducing the conditions appropriate to the liquid state, and assuming that V_1 and V_2, defined as partial molecular volumes (in the sense of other partial molecular or molar quantities), do not vary with the composition of the system, we have

$$V_1\nu_1+V_2\nu_2 = 1.$$

$$V_1\frac{\partial\nu_1}{\partial z}+V_2\frac{\partial\nu_2}{\partial z} = 0.$$

$$\Gamma_1V_1+\Gamma_2V_2 = 0.$$

Combining the above four equations, we derive

$$-\Gamma_1 = \frac{1}{3}\frac{\partial\nu_1}{\partial z}(V_1\nu_1\lambda_2\bar{c}_2+V_2\nu_2\lambda_1\bar{c}_1),$$

whence

$$D_{12} = \tfrac{1}{3}(V_1\nu_1\lambda_2\bar{c}_2+V_2\nu_2\lambda_1\bar{c}_1), \quad . \quad . \quad . \quad . \quad (2)$$

where D_{12} is the coefficient of interdiffusion for the system (usually called the diffusion coefficient of the more dilute chemical species). For the special case of a dilute solution (of 1 in 2) we may take $\nu_1=0$ and find

$$D = \tfrac{1}{3}\lambda_1\bar{c}_1. \quad . \quad . \quad . \quad . \quad . \quad . \quad . \quad (3)$$

This relation is the same as that found for self-diffusion in gases, and was deduced by Riecke [8] in another manner for diffusion in a dilute solution.

As is shown by Jeans [7], if we consider the molecules to be elastic spheres, and allow for the tendency of velocity to persist after a collision, the above relation becomes

$$D = \frac{1{\cdot}051}{3(1-\theta_1)}\lambda_1\bar{c}_1, \quad \ldots\ldots \quad (4)$$

where θ_1 is the average persistence of velocity of the solute molecule considered, a quantity taken as dependent only on the relative masses of the colliding molecules, and increasing towards unity when the molecule considered is heavy compared with the molecules with which it collides *. In making use of the above expression we are assuming that the molecular force fields are sufficiently uniform for their effects to be neglected, and that ternary collisions do not occur. Equation (4) will be applicable only approximately, and in any case only in dilute solutions.

With the limitations mentioned, the total number of collisions undergone per second by a solute molecule of species 1—these collisions being mainly with solvent molecules of species S—will then be

$$ {}_1Z_S = \bar{c}_1/\lambda_1.$$

or

$$ {}_1Z_S = \frac{1{\cdot}051}{3(1-\theta_1)} \cdot \frac{\bar{c}_1^2}{D_{1S}},$$

or

$$ {}_1Z_S = \frac{8 \times 1{\cdot}051}{3\pi(1-\theta_1)} \cdot \frac{RT}{M_1 D_{1S}}.$$

Hence

$$ {}_1Z_S = \frac{0{\cdot}892}{1-\theta_1} \cdot \frac{RT}{M_1 D_{1S}}. \quad \ldots\ldots \quad (5)$$

This equation allows us to calculate the total collision rate of a molecule in a dilute solution, when we know its diffusion coefficient in the solution, and also the molecular weights of the solute and solvent molecules, the latter weight being required to evaluate θ_1. The existence of an unknown degree of solvation of solutes and of polymerization of solvents may, of course, make our results of doubtful value.

* The value of θ_1 is not very different from that of the ratio M_1/M_1+M_2.

Calculation of Collision Quantities in Aqueous Solutions.

By the use of equations (1) and (5) we shall now calculate values of ${}_1Z_S$, λ_1, and v_{F_1S} for various substances in dilute aqueous solution at 18° C.

The diffusion data used have been taken from the 'International Critical Tables'[9]. The values used, with the exception of that for hydrogen, are considered to have a probable error of less than 7 per cent. When the measurements were made at a slightly different temperature, values for 18° C. have been obtained with the aid of the Sutherland-Einstein equation :

$$D = \frac{RT}{N} \cdot \frac{1}{6\pi\eta r}.$$

Values of θ_1 have been calculated by the methods given by Jeans[7], only approximate values being required and obtained. It was found useful, after some values had been calculated, to obtain the remainder graphically, plotting $\left(\frac{M_1}{M_1+M_S}-\theta_1\right)$ against $\frac{M_1}{M_1+M_S}$. For the purpose of calculating θ_1 and other quantities it has been assumed that the solute molecules are not hydrated. The water molecules have been taken to be present as dihydrol ($M_S=36$). Over the large range of molecular weights in Table I., $(1-\theta_1)$ varies very widely, and the use of the concept of persistence of velocity, as calculated on the basis of elastic collisions, has therefore a very large effect on the nature of the results obtained for ${}_1Z_S$ and v_{F_1S}.

In calculating v_{F_1S} equation (1) is used, which involves the molecular radii. For the calculation of these no exact method is available. As it is desirable that the same basis should be used for obtaining all the values in the table, a method of general applicability has been found in the assumption that at low temperatures the molecules, which are taken to be spherical, are tightly packed (occupying 74 per cent. of the space). The radii are then obtained from the formula

$$r = 6{\cdot}63 \times 10^{-9}.(Mv_0)^{1/3}, \quad . \quad . \quad . \quad . \quad (6)$$

in which v_0 is the volume of 1 gram of the substance. The density data employed for hydrogen, oxygen, and carbon dioxide refer to these substances in the solid state at the lowest temperature for which measurements are available. For the remainder of the substances the density data used

TABLE I.—Collision Quantities for Substances dissolved in Water at 18° C.

Substance.	M_1.	θ_1.	$D_{18} \times 10^5$.	$r_1 \times 10^8$.	${}_1Z_8 \times 10^{-13}$	$\lambda_1 \times 10^{10}$.	$v_{F_{18}}$.
Hydrogen	2	0·050	4·9	1·97	23·0	7·6	0·071
Oxygen	32	·376	1·98	1·87	5·5	8·0	·096
Methyl alcohol	32	·376	1·40	2·28	7·7	5·7	·082
Acetonitrile	41	·437	1·38	2·48	6·8	5·7	·096
Carbon dioxide	44	·454	1·71	1·99	5·3	7·1	·098
Ethyl alcohol	46	·465	1·09	2·57	8·0	4·5	·082
Allyl alcohol	58	·520	0·98	2·70	7·9	4·1	·084
Acetamide	59	·524	0·98	2·46	7·8	4·1	·076
Urea	60	·528	1·12	2·36	6·8	4·7	·084
Propyl alcohol	60	·528	0·95	2·79	8·0	4·0	·085
Butyl alcohol	74	·580	0·84	2·99	8·3	3·5	·086
Pyridine	79	·596	0·63	2·87	10·7	2·6	·063
Isoamyl alcohol	88	·623	0·75	3·15	8·7	3·0	·085
Glycerol	92	·635	0·78	2·77	8·2	3·1	·077
Hydroquinone	110	·678	0·73	2·89	8·3	2·8	·078
Resorcinol	110	·678	0·72	2·92	8·5	2·8	·078
Chlorhydrin	110·5	·679	0·83	2·90	7·3	3·2	·089
O. hydroxy benzyl alcohol	124	·705	0·68	3·15	8·7	2·6	·078
Pyrogallol	126	·708	0·61	2·93	9·6	2·3	·067
Dichlorhydrin	129	·714	0·82	3·03	7·1	3·1	·094
Arabinose	150	·745	0·65	3·01	8·7	2·3	·076
Glucose	180	781	0·57	3·24	9·6	1·9	·073
Mannitol	182	·783	0·55	3·27	9·9	1·8	·072
Lactose	342	·873	0·41	4·03	12·1	1·1	·073
Maltose	342	·873	0·40	4·02	12·4	1·1	·071
Sucrose	342	·873	0·41	3·98	12·1	1.1	·072
Raffinose	504	·911	0·34	4·65	14·2	0·8	·074

refer to temperatures in the neighbourhood of 20° C., some of the substances being solid and others liquid. At this temperature the packing is hardly likely to be close, and therefore the radii obtained may be too large ; on the other hand, if the molecules are not spherical, the assumption of sphericity gives too low a value for the radius, and the two sources of error may to some extent cancel each other.

Since water has been taken as dihydrol, ν_S has the value $1{\cdot}68.10^{22}$, and equation (1) takes the form

$$ {}_1Z_S = \frac{1}{v_{F_{1S}}} . 1{\cdot}31 \times 10^{28} . S_{1S}{}^2 \sqrt{\frac{1}{M_1} + \frac{1}{36}} \quad . \quad . \quad (7) $$

In this S_{1S} is, of course, the sum of the radius of the molecule of species 1 and that of the molecule H_4O_2, which has been calculated as $2{\cdot}19.10^{-8}$ by equation (6), taking v_0 to be 1 c.c.

It is evident from Table I. that the collision rate reaches its highest values when the molecular velocity is high or when the molecular radius is large, and passes through a flat minimum for molecules of medium weight. The collision rate ranges from about 5 to 20×10^{13}, and is hence about 10^4 times as great as in a gas at ordinary temperatures and pressures, due mainly to the higher total molecular concentration (10^3 times as great) in a liquid.

The mean free path decreases as the molecular size increases. This is, of course, due to the definition of free path used, a free path of a large molecule being regarded as terminated by a single collision with a small one, although the molecule continues its motion almost unaffected. The free path ranges from about 8 to 1×10^{-10} cm., about 10^{-4} times the value in a gas.

The free-space term $v_{F_{1S}}$ is, roughly, constant, its mean value being 0·080, and the average deviation from the mean just under 10 per cent. This deviation is of the order that would be expected in view of the probable errors in the diffusion data and molecular radii. It is thus probable that $v_{F_{1S}}$ is really a definitely constant quantity of about 0·080. That is, taking water as dihydrol, the collision rates calculated at 18° C. are about 12·5 times as great as those calculated from the formula for collisions in dilute gases.

Since v_F is a constant when the collisions considered are between water molecules on the one hand, and many and varied types of solute molecules on the other hand, it is only reasonable to suppose that equation (1) will be applicable to

collisions between two solute molecules in water with the same value of v_F.

The value of v_F derived holds, of course, only for one liquid medium at one temperature. The conclusion that v_F has a constant value for collisions between any two molecules in any one liquid medium at any one temperature may reasonably be drawn. There seems no reason to restrict the conclusion to cases where the molecules considered are in dilute solution; where one or both are present in large amounts, it must, however, be recognized that the medium is a different one than is the case when the solution is dilute.

The value of v_F, being specific for each medium, cannot be calculated by the present method without extensive diffusion data, and even if it can be obtained, the numerical value reached is to some extent dependent on the degree of polymerization assumed for the medium. Approximate methods of more general applicability will be discussed in the next section.

It should, perhaps, be emphasized that other definitions of a collision than that employed by Jeans are possible, and these would lead to different collision rates. Neighbouring molecules in a liquid must be undergoing mutual interactions quite continuously. The degree of interaction here regarded as a collision is defined by saying that it is sufficient to alter considerably the motion of the smaller molecule taking part.

Calculation of Collision Quantities in a Pure Liquid.

As it has been shown for the case of one liquid medium, namely, water, that v_F is constant for collision rates of various molecules in solution in that medium, estimation of the "free space" term v_F for collisions between like molecules in a pure liquid should also give us the value of v_F for collisions between any molecules in dilute solution in that liquid.

For the case of auto-diffusion in the pure liquid, the molecules are of equal mass; θ has the value 0·406, and equation (5) becomes

$$Z = \frac{1{\cdot}500\ RT}{MD} \quad . \quad . \quad . \quad . \quad . \quad . \quad . \quad (8)$$

D is obviously not a measurable quantity, and to proceed further it is necessary to evaluate it. We shall do so by assuming the validity of the Sutherland-Einstein diffusion

equation, which, according to Cohen and Bruins [10], reproduces well the variation of the diffusion coefficient with temperature, but gives values of the molecular radii which are only in very moderate agreement with those derived in other ways. Hence the accuracy of the results we shall obtain is limited. Using this equation, equation (8) becomes

$$Z = \frac{9\pi\eta r N}{M}. \quad . \quad . \quad . \quad . \quad . \quad . \quad . \quad (9)$$

Hence in any one liquid there is a linear relation between collision rate and transport of momentum, or viscosity. Since the two molecules concerned in a collision are of the same chemical species, equation (1) takes the form:

$$v_F Z = 16 v r^2 \sqrt{\frac{\pi RT}{M}}.$$

If we now write ν as equal to $\frac{N}{Mv}$, where v is the volume of 1 gram of the liquid, we have

$$v_F Z = \frac{16 N r^2}{Mv} \sqrt{\frac{\pi RT}{M}},$$

which on combination with equation (9) gives

$$v_F = \frac{16r}{9\eta v} \sqrt{\frac{RT}{\pi M}}$$

or

$$v_F = 9150 \times \frac{r T^{1/2}}{\eta v M^{1/2}}. \quad . \quad . \quad . \quad . \quad (10)$$

Equation (10) can be used for evaluating v_F, or we can proceed to obtain an equation which does not explicitly contain the molecular radius.

It is for this purpose desired to replace r by a value in terms of the critical volume. According to Lorenz * the critical volume (v_c) of a substance is very nearly 3·75 times its volume at absolute zero (v_0), and if this estimate is combined with equation (6), equation (10) becomes

$$v_F = 3{\cdot}90 \times 10^{-5} . \frac{v_c^{1/3} T^{1/2}}{\eta v M^{1/6}}. \quad . \quad . \quad . \quad . \quad (11)$$

* Quoted by Herz [11]. The values of Berthelot are similar.

Equations (10) and (11) give a value of v_F which is little dependent on the extent of association which is assumed to exist in the liquid; if the degree of association is n, it can easily be seen that v_F varies proportionately only to $n^{1/6}$.

Now, Batschinski [12] has studied fully an empirical equation for viscosity,

$$\eta = \frac{c}{v-\omega},$$

in which c and ω are specific constants for each liquid. The equation reproduces very well the variation of viscosity with temperature for most liquids, excepting those usually regarded as associated. The constant ω is related to the critical volume. Batschinski showed that on the theory of mechanical similarity the term $\frac{c\mathrm{M}^{1/6}}{\mathrm{T}_c^{1/2}v_c^{1/3}}$ should be constant, and found that for eighteen normal liquids studied by Young it has the value $3{\cdot}58.10^{-6}$, with an average deviation of 3 per cent.

Combining this value with equation (11), we have

$$v_F = 1{\cdot}09\,.\frac{c}{\eta v}\,.\left(\frac{\mathrm{T}}{\mathrm{T}_c}\right)^{1/2},$$

or

$$v_F = 1{\cdot}09\,.\frac{v-\omega}{v}\,.\left(\frac{\mathrm{T}}{\mathrm{T}_c}\right)^{1/2} \quad . \quad . \quad . \quad . \quad (12)$$

Equation (12) relates Batschinski's "free-space term" with that which concerns us. The two terms are very similar, but their ratio is dependent on the temperature.

In Table II. values of v_F have been calculated from equation (12) for a few liquids, some of the numerous data analysed by Batschinski having been used. It should be remembered that the accuracy of the values of v_F, apart from the general accuracy of the diffusion theory, is limited chiefly by the agreement between values of r obtained from the Sutherland-Einstein diffusion equation and from the volume at low temperatures. The liquids are assumed not to be associated.

Evidently v_F can range in liquids at ordinary temperatures over values from about 1/20 to 1/6, though the possible range is, of course, greater.

It is perhaps of interest at this point to collect together some approximate figures showing the relative magnitudes of the various volume terms which have been discussed.

These are given in Table III., relative to the critical volume as unity.

The basis on which v_0 and the next figure are calculated has already been indicated, and the b term is calculated from

TABLE II.

Free Space in Liquids at 20° C.

Substance.	$\frac{v-\omega}{v}$.	T_c (°C.).	v_F.	$\frac{v_F (30° C.)}{v_F (20° C.)}$.
Carbon tetrachloride	0·078	283	0·062	1·160
Benzene	0·079	288·5	0·062	1·157
Chloroform	0·125	262·5	0·101	1·108
Methyl acetate	0·131	234	0·108	1·111
Hexane	0·133	235	0·110	1·107
Acetone	0·148	236	0·123	1·101
Ethyl acetate	0·152	250	0·123	1·088
Pentane	0·165	197	0·142	1·097
Ether	0·174	194	0·150	1·095

TABLE III.

Relative Magnitude of various Volume Terms.

Critical volume (v_c)	1·00
Van der Waals's b	0·77
Volume of liquid at normal boiling-point	0·37
Volume of liquid at normal freezing-point	0·34
Batschinski's ω	0·31
Volume of solid at absolute zero (v_0)	0·26–0·27
Sum of volumes of individual molecules	0·19
The "free space" term v_F	0·02–0·06

them, the value obtained being higher than those usually reached in other ways. Evidently v_F is much smaller than the *actual* free space in a liquid, that is, much less than the difference between the total volume and the sum of the volumes of the individual molecules. To obtain v_F we have to subtract from the total volume about 1·6 times the volume

of the molecules; this factor may be compared with the Norrish and Smith factor 1 and the van der Waals factor 4.

Collision Rate as a Function of Temperature.

It has been shown that the collision rate in liquids is considerably greater than that calculated from gas theory. As the temperature rises the general behaviour of a liquid deviates less from that of a gas; this is true also of collision rates. In other words, with rise of temperature the value of v_F rises towards unity.

It can readily be shown from equations already given (*e. g.* equations (9) and (10)) that, provided the degree of association of the medium does not vary rapidly with temperature, it is very nearly true to write:

$$\frac{d \log v_F}{dT} = \frac{1}{2T} - \frac{d \log \eta}{dT} \quad . \quad . \quad . \quad . \quad *(13)$$

and

$$\frac{d \log Z}{dT} = \frac{d \log \eta}{dT} . \quad . \quad . \quad . \quad . \quad . \quad . \quad . \quad (14)$$

Equation (14) states that the temperature coefficient of collision rates in a liquid system is the same as that of viscosity, for thermal expansion will alter concentrations to an extent usually negligible. (It is naturally assumed that the concentrations of the chemical species considered do not for any other reason change with temperature.)

The temperature coefficient of collision rates is therefore negative, and continues to be so at least until the critical temperature is reached.

For liquids under ordinary conditions the decrease in collision rates is quite considerable for a rise in temperature of 10° C.; whereas $\sqrt{T}$ increases by less than 2 per cent., v_F increases by 10–15 per cent., as shown in Table II.

Previously it has been the custom in calculating temperature coefficients of velocities of bimolecular reactions in liquids to neglect the temperature coefficients of collision rates or to regard them as being the same as in gases.

It now appears that this procedure will lead to erroneous values for energies of activation of reactions, where the

* At two temperatures T_2 and T_1, we have

$$\frac{v_{F_2}}{v_{F_1}} = \frac{\eta_1}{\eta_2} \sqrt{\frac{T_2}{T_1}} .$$

process of which the velocity is measured is actually bimolecular.

The effect of introducing the temperature coefficients of collision rates as calculated here will be to increase the energies of activation derived by some 1500–3000 calories. Such a correction is by no means negligible.

Summary.

An attempt has been made to calculate collision rates in liquids by applying to liquids the kinetic theory of diffusion, with the use of the concept of persistence of velocity. It is found that the collision rates are higher than those calculated by gas formulæ, and higher by a multiple which is probably a constant for each liquid medium at any one temperature. Approximate formulæ are given for the general calculation of this multiple, which is of the order of 10.

The temperature coefficient of collision rates is negative and approximately equal to that of viscosity. It is pointed out that this introduces a correction into calculations of energies of activation for bimolecular reactions in liquid systems.

References.

(1) J. A. Christiansen, *Zeits. f. phys. Chem.* cxiii. p. 35 (1924).
(2) R. C. Tolman, 'Statistical Mechanics with Applications to Physics and Chemistry,' p. 242 (New York, 1927).
(3) T. Moran and W. C. M. Lewis, Journ. Chem. Soc. cxxi. p. 1613 (1922).
(4) G. Scatchard, Journ. Amer. Chem. Soc. xlv. p. 1580 (1923).
(5) M. v. Smoluchowski, *Zeits. f. phys. Chem.* xcii. p. 129 (1917).
(6) R. G. W. Norrish and F. F. P. Smith, Journ. Chem. Soc. p. 129 (1928).
(7) J. H. Jeans, 'Dynamical Theory of Gases,' 4th ed. (Cambridge, 1925).
(8) E. Riecke, *Zeits. f. phys. Chem.* vi. p. 564 (1890).
(9) 'International Critical Tables,' v. (New York, 1929).
(10) E. Cohen and H. R. Bruins, *Zeits. f. phys. Chem.* ciii. p. 404 (1923).
(11) W. Herz, *Zeits. anorg. allg. Chem.* cxlix. p. 230 (1925).
(12) A. J. Batschinski, *Zeits. f. phys. Chem.* lxxxiv. p. 643 (1913).

Muspratt Laboratory of
Physical and Electro-Chemistry,
University of Liverpool.
Sept. 19, 1929.

CX. *Electronic Waves.*

By Sir J. J. Thomson, *O.M., F.R.S.**

Summary.

In a former paper (Phil. Mag., Dec. 1928) I considered the electronic waves accompanying an electron moving uniformly in a straight line. In this paper I consider the waves in the general case, when the electron is under the action of an electric force, so that its velocity and direction of motion are changing. The point of view taken is that the distribution of the sub-electrons in the atmosphere of the electron is affected by the electric force, so that the waves are no longer moving through a uniform medium but one whose properties vary from point to point.

It is shown that in this case both the electric and magnetic forces in the electronic waves are at any point at right-angles to the path a point electron would describe under the action of the electric force. As the direction of propagation of the waves is at right-angles to both the electric and magnetic forces, the waves are always travelling along what would be the path of the point electron.

The electric force E in the electronic wave is shown to be represented to a close approximation by the expression

$$\mathrm{E} = \frac{\mathrm{A}}{q^{1/2}} \cos\Big(pt - \frac{p_0}{c^2}\int q\,ds\Big),$$

and the magnetic force H by

$$\mathrm{H} = \mathrm{A}' q^{1/2} \cos\Big(pt - \frac{p_0}{c^2}\int q\,ds\Big).$$

Here ds is an element of the path of the point electron and q the velocity which such an electron would have when it reached ds; q is not the velocity at the time t of the electron associated with the train of waves. The waves stretch out far in front of this electron, and at any point P there is a definite value of q which does not change as the electron approaches P. When the electron arrives at P its velocity is equal to q.

If the path of the point electron is not a closed curve the existence of electronic waves introduces no new condition, and any such path is a possible path for the electron with its waves. When, however, the path of the point electron is a

* Communicated by the Author.

closed curve the conditions are different. The electric and magnetic forces must recur on a complete circuit of the curve; hence, from the expressions for E and H, if S is the perimeter of this curve,

$$\frac{p_0}{c^2}\int_0^S q\,ds = 2\pi n,$$

where n is an integer. Only curves which satisfy this condition are possible for the electron accompanied by its waves. This condition leads to the same results as those usually deduced by quantum mechanics.

When the path of the point electron is not a closed curve there is radiation of energy, unless the velocity of the electron is uniform; but when the path is a closed curve the energy in the waves moves round and round the curves, none of it gets loose, and there is no radiation. In the latter part of the paper the distribution of electric waves when an electron passes through a crystal is calculated.

IN 'Beyond the Electron' and "Electronic Waves" (Phil. Mag. vi. p. 1254 (1928)) I have supposed that the waves which have been proved to accompany a moving electron are electric waves in an atmosphere surrounding the nucleus of the electron. The atmosphere contains parts—sub-electrons—which can be set in motion by electric forces and which, when moving, produce the effects of electric currents. An atmosphere of this kind would, when light or other electric waves passed through it, behave like a dispersive medium, and have a refractive index depending on the frequency of these waves. The case which is especially important in connexion with electronic waves is when the frequency of the waves passing through the medium is much greater than the frequencies of the individual sub-electrons about their positions of equilibrium. Under these conditions the medium under the influence of electric waves behaves as if the sub-electrons were free, and the connexion between the wave-length and the phase velocity is a very significant one.

An alternating electric field in the region adjacent to the electron will produce, in addition to the usual displacement current proportional to the rate of change of the electric force, convective currents due to the motion of the sub-electrons in the electric field; the effective current is the sum of these currents. The atmosphere around the electron

has a natural period of vibration as a whole, independent of that of the individual sub-electron but depending on the number of sub-electrons per unit volume of the atmosphere. When the atmosphere is oscillating in this period the convective current just balances the displacement one, the effective current vanishes, and with it the magnetic force. As the magnetic force vanishes, and with it the Poynting-vector, there is no transmission of energy and no loss of energy by radiation; the oscillations can persist indefinitely.

In my former papers I showed that when the electron is moving uniformly with velocity u parallel to the axis of x, its atmosphere is traversed by a system of electrical waves represented by

$$Y = A\cos\left(pt - \frac{p_0}{c^2}ux\right), \quad \ldots \quad (1)$$

where p_0 is the natural frequency of the atmosphere of the electron and is given by the equation

$$p_0^2 = N.c^2\frac{e'^2}{4\pi.m'},$$

where N is the number of sub-electrons per unit volume, e' the charge, and m' the mass of a sub-electron.

$$p^2 = p_0^2\left(1+\frac{u^2}{c^2}\right), \quad \text{or, more accurately,} \quad \frac{p_0^2}{1-\frac{u^2}{c^2}}.$$

The waves represented by (1) have a wave-length given by

$$\frac{2\pi}{\lambda} = \frac{p_0 u}{c^2},$$

a phase velocity equal to c^2/u, and a group velocity equal to u; the group velocity is also the velocity with which energy travels through medium. Thus the energy in the wave, since it travels with the same velocity as the electron, does not get dissociated from it, and no free radiant energy arises from the motion of the electron.

The preceding results apply to an electron moving uniformly. We shall now proceed to the consideration of an electron changing its velocity under the action of an electric force.

The wave equations in the atmosphere of the electron are,

if X, Y, Z are the components of the electric and α, β, γ those of the magnetic forces,

$$\left(\frac{d\mathrm{X}}{dt}+p_0^2\int \mathrm{X}\,dt\right)=c^2\left(\frac{d\beta}{dz}-\frac{d\gamma}{dy}\right),$$

where $$p_0^2=4\pi c^2.\mathrm{N}e_1^2/m,$$

when N is the density of the sub-electrons at (x, y, z).

There are similar equations for Y and Z, and three equations of the type

$$\frac{d\mathrm{X}}{dz}-\frac{d\mathrm{Z}}{dx}=\frac{d\beta}{dt}.$$

If the electrical and magnetic quantities vary with the time proportionally to ϵ^{ipt}, the preceding equations may be written

$$(-p^2+p_0^2)\mathrm{X}=c^2ip\left(\frac{d\beta}{dz}-\frac{d\gamma}{dy}\right),$$

$$\frac{d\mathrm{X}}{dz}-\frac{d\mathrm{Z}}{dx}=ip\beta.$$

When the atmosphere of the electron comes under the influence of an external electric force, the distribution of the sub-electrons in it may be affected, and N, their density, may vary from point to point. We assume that the action of the external force is to introduce into the expression for N, and therefore into p_0^2, a term proportional to the potential V of the external force, so that if N_0 is the value of N when the electron is free from force, N, under the action of the force, will be given by the equation

$$\mathrm{N}=\mathrm{N}_0\left(1+\frac{2\mathrm{V}e}{m_0c^2}\right),$$

where e is the charge and m_0 the mass of an electron. The value of V must be chosen so that it vanishes when the charged body which is the source of the force is at an infinite distance from the electron. We have, also, in the equations in which p_0^2 occurs, to write $p_0^2\left(1+\frac{2\mathrm{V}e}{m_0c^2}\right)$ in place of p_0^2; $p_0/2\pi$ is the frequency of the vibrations of the atmosphere of an electron at rest and free from electric force. We shall now apply these equations to some special cases

Electronic Waves associated with an Electron acted upon by a Uniform Electric Force.

Suppose the electric force on the electron acts parallel to x in the positive direction, and that the electron is moving in this direction. Let Y be the electric force in the electronic wave; then in the one-dimensional problem where the electrical quantities depend upon x only, the equations determining the electric waves, if the time factor is ϵ^{ipt} and if γ is the magnetic force, which will be perpendicular to x and y, are

$$\left\{-p^2+p_0^2\left(1+\frac{2\mathrm{V}e}{m_0c^2}\right)\right\}\mathrm{Y}=ipc^2\frac{d\gamma}{dx},$$

$$\frac{d\mathrm{Y}}{dx}=ip\gamma.$$

In the case of a uniform electric force F,

$$\mathrm{V}=-\mathrm{F}x,$$

and the equations give

$$c^2.\frac{d^2\mathrm{Y}}{dx^2}+\left(p^2-p_0^2\left(1-\frac{2\mathrm{F}ex}{m_0c^2}\right)\right)\mathrm{Y}=0. \quad . \quad . \quad (1)$$

Suppose a uniformly moving electron enters the field of force where $x=0$, and that u_0 is its velocity and λ_0 its wave-length; then

$$\frac{p^2-p_0^2}{c^2}=\frac{4\pi^2}{\lambda_0^2}=\frac{u_0^2p_0^2}{c^4}.$$

Equation (1) may be written in the form

$$\frac{d^2\mathrm{Y}}{dx^2}+(a+bx)\mathrm{Y}=0, \quad . \quad . \quad . \quad . \quad (2)$$

where $a=\dfrac{4\pi^2}{\lambda_0^2}$ and $a/b=l$,

where l is the distance through which the force must act to double the initial kinetic energy of the electron

$$\frac{a}{b^{2/3}}=(4\pi^2)^{1/3}\left(\frac{l}{\lambda}\right)^{2/3}.$$

Now λ for ordinary velocities of free electrons is small compared with atomic dimension, while l will be comparable with these dimensions if F is an inter-atomic force and small

compared with them for forces not of this character; hence $a/b^{2/3}$ will generally be an exceedingly small quantity.

If

$$\xi = \frac{a+bx}{b^{2/3}}$$

(2) becomes

$$\frac{d^2Y}{d\xi^2} + \xi Y = 0.$$

Lommel (Gray and Mathews, 'Bessel's Functions,' p. 233) has shown that the solution of this equation is

$$Y = \sqrt{\xi}.\left(AJ_{1/3}\left(\frac{\xi^{3/2}}{\frac{3}{2}}\right) + BJ_{-1/3}\left(\frac{\xi^{3/2}}{\frac{3}{2}}\right)\right).$$

As $a/b^{3/2}$ is very large, ξ will also be very large, and we may use the form of Bessel's Functions suitable for large values of the variable. Doing this, and restoring the time-factor, we find

$$Y = \frac{A}{\xi^{1/4}}\cos\left(pt - \frac{\xi^{3/2}}{\frac{3}{2}} - \alpha\right),$$

where α is a constant. This is equivalent to

$$Y = \frac{A}{(a+bx)^{1/4}}\cos\left(pt - \frac{(a+bx)^{3/2}}{\frac{3}{2}b} - \alpha\right).$$

To get the phase velocity, we notice that if the phase remains unaltered for increments δt and δx in t and x respectively,

$$p\delta t - (a+bx)^{1/2}\delta x = 0;$$

hence the phase velocity is

$$\frac{p}{\sqrt{a+bx}}.$$

The product of the group and phase velocity is equal to c^2; hence the group velocity is $(a+bx)^{1/2}c^2/p$.

From the equations

$$a = \frac{p_0^2u^2}{c^4}, \qquad b = p_0^2\frac{2Fe}{m_0c^4};$$

$$a+bx = \frac{p_0^2}{c^4}\left(u^2 + \frac{2Fex}{m_0}\right)$$

$$= \frac{p_0^2}{c^4}V^2,$$

where V is the velocity which will be attained by the electron when it reaches x, if it starts from $x=0$ with velocity u_0.

Substituting this value, we find that the group velocity of the waves at x equal V and the phase velocity c^2/V. The amplitude of Y is proportional to $(a+bx)^{-1/4}$, *i.e.* to $V^{-1/2}$. What energy there may be in the electronic waves is proportional per unit volume to Y^2, *i. e.*, to V^{-1}; the velocity of the energy is equal to V; hence the energy transmitted across unit area in unit time is constant, so that there is no accumulation of energy in the waves. Since the velocity of the energy at a point in front of the electron is greater than the velocity of the electron, energy will separate from the electron and there will be radiation. In the case of the electron in uniform motion the velocity of the energy is always the same as that of the electron, so that energy does not escape from the electron.

Consider an electron moving in the direction in which the force acts. The wave-lengths of the electronic waves and their group velocity vary from point to point in the atmosphere of the electron. The group velocity is greater in the front of the atmosphere than in the rear. We see from the preceding investigation that when any portion of the atmosphere is passing a point P fixed in space the group velocity of the electronic waves in that portion is equal to the velocity which an electronic charge would possess if it started from $x=0$ with the initial velocity of the electron and fell to P under the action of the electric force. Thus, when the electron arrives at any point the group velocity of the electronic waves in its atmosphere at that point is equal to the velocity of the electron.

We have seen that the solution of the equation

$$\frac{d^2Y}{dx^2}+PY=0,$$

when P is of the form $a+bx$, is approximately

$$Y=\frac{1}{P^{1/4}}\cos\left(\frac{P^{3/2}}{\frac{3}{2}b}+\alpha\right)$$

or

$$Y=\frac{1}{P^{1/4}}\cos\left(\int\sqrt{P}dx+\alpha\right).$$

This form is applicable under the conditions which hold for electronic waves when P is not limited to being a linear function, but has the more general form

$$P=\frac{1}{c^2}\left(p^2-p_0^2-\frac{p_0^2Ve}{m_0c^2}\right),$$

where V is the potential of the forces at the place x.

For, if

$$Y=\frac{1}{P^{1/4}}\cos\left(\int\sqrt{P}.\,dx-\alpha\right),$$

$$\text{say}\qquad =\frac{1}{P^{1/4}}\cos\theta,$$

then

$$\frac{d^2Y}{dx^2}=\frac{5}{16}\frac{1}{P^{9/4}}\left(\frac{dP}{dx}\right)^2\cos\theta-\frac{1}{4}\frac{1}{P^{5/4}}\cos\theta\frac{d^2P}{dx^2}-\frac{P}{P^{1/4}}\cos\theta.$$

For electronic waves the first and second terms on the right-hand side are very small compared with the third. The ratio of the first to the third term is, neglecting the numerical factor,

$$\frac{1}{P}\left(\frac{1}{P}\cdot\frac{dP}{dx}\right)^2.$$

Now

$$P=\frac{p_0^2}{c^2m}(E_0+E),$$

where E_0 is the initial energy and E the fluctuating part due to the action of the electric force,

$$\frac{1}{P}\frac{dP}{dx}=\frac{\frac{dE}{dx}}{E_0+E}.$$

Now suppose ΔE is the maximum value of the fluctuation and d the range in x between a maximum and minimum for E; then dE/dx will be of the order $\Delta E/d$ and

$$\frac{1}{P}\left(\frac{1}{P}\frac{dP}{dx}\right)^2$$

will, since

$$\frac{p^2-p_0^2}{c^2}=\frac{4\pi^2}{\lambda_0^2},$$

be of the order

$$\frac{\lambda^2}{d^2}\left(\frac{\Delta E}{E_0+E}\right)^2,$$

where λ is the wave-length of the electronic waves. Thus, when the wave-length of the electronic waves is small compared with $d(E_0+E)/\Delta E$, the first term in (1) may be neglected in comparison with the third. Similar considerations will show that the same condition makes the second term negligible in comparison with the third.

The approximation ceases to be valid when the fluctuations in P are so great that the minimum value is but a small fraction of the maximum one.

The value

$$\frac{1}{P^{1/4}}\cos\int\sqrt{P}\,dx$$

is the asymptotic one, which, as we have seen under suitable conditions, is a close approximation. As in the case of Bessel's Functions, a still closer approximation can be got by taking as the solution

$$\frac{S_1}{P^{1/4}}\cos\int\sqrt{P}\,.\,dx+\frac{S_2}{P^{1/4}}\sin\int\sqrt{P}\,.\,dx,$$

where S_1 and S_2 are power series of the form

$$1+\Sigma a_n\xi^n;$$

where ξ is a quantity of no dimensions

$$\xi=\frac{dP}{dx}\Big/P^{3/2}$$

satisfies this condition and is small.

The argument of the harmonic term is the same in the more general expression as in the asymptotic one. In many problems on electronic waves the most important factor is the argument of the harmonic terms, and it is immaterial whether the factor by which these terms are multiplied is $1/P^{1/4}$ or a power series.

We shall now consider the general case of an electron moving in a plane under the influence of an electric force whose potential is V. If before the electron enters the field of force the components of its velocity parallel to the axes of x and y are respectively u_0 and v_0, the electric and magnetic forces in the electronic waves are proportional to

$$\cos\Big(pt-\frac{p_0}{c^2}(u_0x+v_0y)\Big),$$

where

$$p^2-p_0^2=\frac{u_0^2+v_0^2}{c^2}p_0^2.$$

We shall suppose that the waves are plane polarized. If the electric force is in the plane xy, the plane in which the electron moves, the magnetic force γ will be at right-angles to this plane, and all the electric and magnetic

quantities can be expressed in terms of γ. If, on the other hand, the electric force Z is at right angles to this plane, they can all be expressed in terms of Z. Let us take the case when the electric force X, Y is in the plane xy.

The wave-equations are

$$\mathrm{X}\left(ip+\frac{{p_0}^2}{ip}\left(1+\frac{2\mathrm{V}e}{m_0c^2}\right)\right)=-c^2\frac{d\gamma}{dy}$$

or

$$\mathrm{X}\left(-p^2+{p_0}^2\left(1+\frac{2\mathrm{V}e}{m_0c^2}\right)\right)=-c^2ip\frac{d\gamma}{dy}$$

or

$$-\frac{\mathrm{X}{p_0}^2}{c^2}\left({u_0}^2+{v_0}^2-\frac{2\mathrm{V}e}{m}\right)=-c^2ip\frac{d\gamma}{dy};$$

but

$${u_0}^2+{v_0}^2-\frac{2\mathrm{V}e}{m}=q^2,$$

where q is the velocity which a point charge starting with the velocity u_0v_0 would attain at the point xy under the influence of a field represented by V. Hence the wave equations are

$$\left.\begin{aligned}\frac{\mathrm{X}{p_0}^2}{c^4}q^2&=ip\cdot\frac{d\gamma}{dy},\\ \frac{\mathrm{Y}{p_0}^2}{c^4}q^2&=-ip\cdot\frac{d\gamma}{dx},\\ \frac{d\mathrm{Y}}{dx}-\frac{d\mathrm{X}}{dy}&=ip\gamma.\end{aligned}\right\}\quad\ldots\quad(3)$$

The equation to determine γ is therefore

$$\frac{{p_0}^2}{c^4}\gamma=-\frac{d}{dx}\cdot\left(\frac{1}{q^2}\frac{d\gamma}{dx}\right)-\frac{d}{dy}\cdot\left(\frac{1}{q^2}\frac{d\gamma}{dy}\right).$$

Now by substitution we can show that

$$\gamma=\mathrm{A}q^{1/2}\cos\left(pt-\frac{p_0}{c^2}\int(u\,dx+v\,dy)\right).\quad\ldots\quad(4)$$

is a close approximation to the solution of this equation provided

$$\frac{\lambda}{d}\left(\frac{q_{\max.}-q_{\min.}}{q_{\max.}+q_{\min.}}\right)$$

is a small quantity. λ is the wave-length of the electronic waves, d the distance an electron would travel between the maximum and minimum values of q; u and v are the components of the velocity at x, y of a point charge with the same energy as the electron and exposed to the same field. The reasoning is the same as that given on page 1080. It must be pointed out that u, v are not the components of the velocity of the electron itself at the time t, but the components of the velocity the electron will have when (it may be after a considerable time) it arrives at the point x, y.

From equations (3) and (4) we see that approximately

$$\frac{\mathrm{X}p_0}{c^2} = \frac{\mathrm{A}}{q^{1/2}} \frac{v}{q} \sin\theta,$$

$$\frac{\mathrm{Y}p_0}{c^2} = -\frac{\mathrm{A}}{q^{1/2}} \frac{u}{q} \sin\theta,$$

when

$$\theta = pt - \frac{p_0}{c^2} \int (u\,dx + v\,dy).$$

Hence

$$\mathrm{X}u + \mathrm{Y}v = 0,$$

so that the electric force is at right angles to the vector u, v, i. e., it is at right angles to the path which a point charge would travel under the influence of the electric field. The direction of propagation of the waves is at right angles to the electric force and also to the magnetic force; hence it will be along the tangent to the path of the charge. The electronic waves will describe curved paths, and these paths will be the paths of a point electron under the electric field. If ds is an element of this path, then

$$u\,dx + v\,dy = q\,ds$$

and

$$\gamma = \mathrm{A}q^{1/2} \cos\left(pt - \frac{p_0}{c^2} \int q\,ds\right).$$

The phase velocity of these waves is c^2/q, and the group velocity q. Thus on this view a series of waves travelling along the path of the electron, but extending in front of the electron, is an integral part of the electron. The group velocity of these waves at any point is equal in magnitude and direction to the velocity which the electron will have when it reaches that point. We may regard the electron with its charge as a kind of hump on the distribution of electric force in the electronic waves, and that this hump is

carried on by these waves with the group velocity of the waves.

When the electron does not describe a closed or re-entrant path, these waves will impose no restriction on the path, and any such path which could be described by a point electron under the influence of the electric field is a possible path of the electron accompanied by its waves. The case is different, however, when the path is re-entrant or closed ; the waves also describe this path, and the electric and magnetic forces in the electronic waves most recur after the circumference has been described.

Thus, as the equation for γ is of the form

$$\gamma = \mathrm{Q} \cos\left(pt - \frac{p_0}{c^2}\int q\, ds\right),$$

where Q is a function of q and the space coordinates, the right-hand side must be the same at the end and the beginning of the circuit. Q will be so automatically, but

$$\cos\left(pt - \frac{p_0}{c^2}\int q\, ds\right)$$

will only be so if

$$\frac{p_0}{c^2}\int_0^{\mathrm{S}} q\, ds = 2n\pi, \quad . \quad . \quad . \quad . \quad . \quad . \quad (5)$$

where n is an integer and S the circumference of the circuit. The only possible closed paths are those which satisfy this condition.

Let us apply this to the case when the path of the point electron under the action of a force at the focus equal to e^2/r^2 is the ellipse

$$\frac{x^2}{a^2} + \frac{y^2}{b^2} = 1.$$

If $\qquad x = a\cos\phi, \qquad y = b\sin\phi,$

$$q\, ds = e\sqrt{\frac{a}{m}}(1 - \epsilon\cos\phi)\, d\phi,$$

where

$$\epsilon^2 = \frac{a^2 - b^2}{a^2},$$

and m is the mass of an electron

$$\int_0^{\mathrm{S}} q\, ds = e\sqrt{\frac{a}{m}}\int_0^{2\pi}(1 - \epsilon\cos\phi)\, d\phi = 2\pi e\sqrt{\frac{a}{m}}.$$

Hence, by (5),

$$\frac{p_0}{c^2} 2\pi e \sqrt{\frac{a}{m}} = 2n \cdot \pi$$

or

$$a = \frac{n^2 \cdot m \cdot c^4}{p_0 c^2}.$$

the same type of expression as that given by the ordinary quantum theory.

When the electron is describing an ellipse under a force directly proportional to the distance if the equation to the ellipse is

$$\frac{x^2}{a^2} + \frac{y^2}{b^2} = 1,$$

and

$$x = a \cos \phi, \quad y = b \sin \phi,$$

then

$$q\, ds = \frac{2\pi}{T} (a^2 \sin^2 \phi + b^2 \cos^2 \phi)\, d\phi,$$

where T is the time the point electron takes to describe an orbit

$$\frac{p_0}{c^2} \int_0^{s} q\, ds = \frac{2\pi p_0}{Tc^2} \int_0^{2\pi} (a^2 \sin^2 \phi + b^2 \cos^2 \phi)\, d\phi = \frac{2\pi^2 p_0}{Tc^2} (a^2 + b^2).$$

This must equal $2n\pi$ where n is an integer; hence

$$\frac{\pi p_0}{c^2 T} (a^2 + b^2) = n.$$

When the orbits of the point charges are nearly circular and q therefore approximately constant, the solution takes a simple form. Use polar coordinates r and θ; if R and T are respectively the radial and tangential components of the electric force in the wave, the wave equations (3) become

$$R \frac{p_0^2}{c^4} q^2 = ip \frac{d\gamma}{r\, d\theta},$$

$$T \frac{p_0^2}{c^4} q^2 = -ip \frac{d\gamma}{dr},$$

$$\frac{dT}{dr} - \frac{dR}{r\, d\theta} = ip\gamma.$$

A solution of these is

$$\gamma = A\cos(pt - k\theta),$$

$$R = \frac{Akpc^4}{rp_0^2q^2}\cos(pt - k\theta),$$

$$T = 0,$$

$$k = \frac{p_0}{c^2}qa,$$

when a is the mean value of r.

Since γ must be unaltered when θ increases by 2π,

$$k2\pi = 2n\pi,$$

where n is an integer.

Thus

$$\frac{p_0qa}{c^2} = n,$$

which is equivalent to the usual quantum relation.

When the orbit of the point electron is a closed curve, the electronic waves of electric and magnetic force flow in closed curves; the energy in these waves travels tangentially round and round these curves, so that there is no radiation and no loss of energy. Thus, the moving electron will only radiate when it escapes from the closed circuit.

By equation (3) we have

$$\left(\frac{dX}{dx} + \frac{dY}{dy}\right)q^2 + \left(X\frac{dq^2}{dx} + Y\frac{dq^2}{dy}\right) = 0.$$

If ρ is the density of the electrification, X_0, Y_0 the components of the applied force,

$$\frac{dX}{dx} + \frac{dY}{dy} = 4\pi\rho; \quad \frac{dq^2}{dx} = \frac{2X_0e}{m}, \quad \frac{dq^2}{dy} = \frac{2Y_0e}{m}.$$

Thus

$$4\pi\rho q^2 + \frac{2e}{m}(XX_0 + YY_0) = 0,$$

now

$$XX_0 + YY_0 = EF\cos\psi,$$

where E is the resultant electric force in the electronic waves F the resultant applied external force, and ψ the angle between E and F. E is at right angles to the path of the point electron under the external force; hence $F\cos\psi$ is

the component of the external force along the normal to the path, so that if S is the radius of curvature of the path,

$$\frac{mq^2}{S} = Fe\cos\psi ;$$

so that

$$2\pi\rho S + E = 0.$$

E is proportional to

$$q^{-\frac{1}{2}}\cos\left(pt - \frac{p_0}{c^2}\int q\,ds\right);$$

hence ρ varies as

$$\frac{1}{S\sqrt{q}}\cos\left(pt - \frac{p_0}{c^2}\int q\,ds\right).$$

The Passage of Electronic Waves through Crystals.

We regard the crystal as a system of atoms arranged in a series of parallel planes at a distance b apart, the arrangement in any one plane being a replica of that in any other. Take the axis of y at right-angles to these planes. Then the properties of the atom are periodic, and can be represented by expressions of the form

$$\alpha_1\cos\frac{2\pi}{b}y + \alpha_2\cos\frac{4\pi}{b}y + \ldots .$$

We shall confine ourselves at first to the case where there is only one harmonic term.

The effect of these atoms on the density of the electronic atmosphere will be to make the quantity which is equal to p_0^2 for the electron in free space become

$$p_0^2\left(1 - \alpha\cos\frac{2\pi}{b}y\right)$$

for the electronic waves inside the crystal. The quantity α will be measured by the work required to drag an electron out of a crystal divided by $mc^2/2$.

Consider now an electron moving in the plane of xy. Let the electronic electric waves be plane polarized and suppose the electric force is in the plane of xy. The magnetic force γ will be at right angles to this plane, and will, if the wave-length is so small that the energy of the electron

only changes by a small fraction in a wave-length, satisfy the equation

$$\frac{d^2\gamma}{dx^2}+\frac{d^2\gamma}{dy^2}+\frac{1}{c^2}\left(p^2-p_0^2+p_0^2\alpha\cos\frac{2\pi}{b}y\right)\gamma=0. \quad . \quad (1)$$

γ is supposed to vary as ϵ^{ipt}.

Let the electronic waves outside the crystal, *i.e.*, where $\alpha=0$, be represented by

$$\gamma=\cos\left(pt-\frac{2\pi}{\lambda}(x\cos i+y\sin i)\right),$$

where i is the angle the incident beam makes with the axis of x.

Substituting this value, we find

$$\frac{4\pi^2}{\lambda^2}=\frac{1}{c^2}(p^2-p_0^2).$$

Put, in equation (1),

$$\gamma=w\epsilon^{\frac{-i2\pi x\cos i}{\lambda}},$$

where w is a function of y only; then (1) becomes

$$\frac{d^2w}{dy^2}+\left(\frac{4\pi^2}{\lambda^2}\sin^2 i+\alpha'\cos\frac{2\pi y}{b}\right)w=0, \quad . \quad . \quad . \quad (2)$$

where

$$\alpha'=\frac{p_0^2}{c^2}\alpha.$$

Putting $\eta=\frac{\pi y}{b}$, (2) becomes

$$\frac{d^2w}{d\eta^2}+(\Theta_0+2\Theta_1\cos 2\eta)w=0, \quad . \quad . \quad . \quad (3)$$

where

$$\Theta_0=\frac{4b^2}{\lambda^2}\sin^2 i, \quad 2\Theta_1=\frac{b^2}{\pi^2}\alpha'=\frac{b^2p_0^2}{c^2\pi^2}\alpha.$$

This is a special case of Hill's equation. Hill's solution is ('Acta Mathematica,' viii. p. 1, 1886)

$$w=\Sigma A_n\epsilon^{ic\eta}\epsilon^{i.2n\eta}\ *,$$

where n is an integer. Thus the only waves possible form a discrete set, such that the wave-length λ is expressed by

$$\frac{2\pi}{\lambda}=(c+2n)\frac{b}{\pi},$$

where n is an integer.

* In what follows c is Hill's constant and not the velocity of light.

The quantity c is given by the equation

$$\frac{1-\cos \pi c}{1-\cos \pi \sqrt{\Theta_0}} = \square(0), \quad \ldots \quad (4)$$

where $\square$ is a determinant with an infinite number of rows. Retaining squares, but neglecting higher powers of Θ_1, Hill proves that

$$\square(0) = 1 + \pi \frac{\cot \frac{1}{2}\pi \sqrt{\Theta_0}}{4\sqrt{\Theta_0}} \times \frac{\Theta_1^2}{1-\Theta_0}, \quad \ldots \quad (5)$$

$$c^2 = 1 + \sqrt{(\Theta_0 - 1)^2 - \Theta_1^2}. \quad \ldots \quad (6)$$

Thus, if we neglect the squares of Θ_1, $\square(0)=1$, and from (4)

$$c = \sqrt{\Theta_0} = \frac{2b \sin i}{\lambda},$$

$$c\eta = \frac{2\pi \sin i \,.\, y}{\lambda}.$$

The term $e^{ic\eta} = \epsilon^{i(2\pi \sin i \,.\, y)/\lambda}$, and thus represents the original wave propagated without change of wave-length. Hence, if we neglect Θ_1^2, there is no change produced by the crystal in the refractive index. Where Θ_1 is large enough to make c differ from $\sqrt{\Theta_0}$, $c\eta$ will no longer be equal to $2\pi \sin i \,.\, y/\lambda$ and the wave-length of the electronic wave in the crystal will differ from that outside. Thus there will be an appreciable refractive index.

Taking the primary wave in the crystal as represented by $\cos c\eta$, and writing equation (8) in the form

$$\frac{d^2w}{d\eta^2} + \Theta_0 w + 2\Theta_1 \cos 2\eta w = 0,$$

and putting $w = \cos c\eta$ in the last term, we have

$$\frac{d^2w}{d\eta^2} + \Theta_0 w + \Theta_1 \cos (c+2)\eta + \Theta_1 \cos (c-2)\eta = 0 ;$$

hence

$$w = \frac{\Theta_1 \cos (c+2)\eta}{(c+2)^2 - \Theta_0} + \frac{\Theta_1 \cos (c-2)\eta}{(c-2)^2 - \Theta_0} + \cos c\eta.$$

Restoring the factors involving x and t, and putting for η its value $\pi y/b$,

$$w = \frac{\Theta_1 \cos\left\{pt - 2\pi\left(\frac{x\cos i}{\lambda} + \frac{(c+2)y}{2b}\right)\right\}}{(c+2)^2-\Theta_0} + \frac{\Theta_1 \cos\left\{pt - 2\pi\cdot\left(\frac{x\cos i}{\lambda} + \frac{(c-2)y}{2b}\right)\right\}}{(c-2)^2-\Theta_0} + \cos\left\{pt - 2\pi\left(\frac{x\cos i}{\lambda} + \frac{c\cdot y}{2b}\right)\right\}, \quad . \quad . \quad (7)$$

the third term representing the primary wave; hence the primary wave is accompanied by two waves, the direction of propagation of the primary one being between the directions of the secondary ones, and its wave-length being also intermediate between those of its secondaries. One or other of these secondaries becomes important when either $(c+2)^2-\Theta_0$ or $(c-2)^2-\Theta_0$ vanish. Θ_0, as we have seen, is equal to $2b\sin i/\lambda$.

We shall leave the general case for the present and consider the very important special case where Θ_1 is so small that its square may be neglected. In this case, as we have seen,

$$c^2 = \Theta_0 = \frac{4b^2\sin^2 i}{\lambda^2}.$$

The primary wave is now

$$\cos\left\{pt - \frac{2\pi}{\lambda}(x\cos i + y\sin i)\right\}.$$

The secondary waves are

$$\left.\begin{aligned} &\frac{\Theta_1 \cos\left\{pt - \frac{2\pi}{\lambda}\left(x\cos i + y\sin i + \frac{\lambda}{b}\right)\right\}}{4c(c+1)} \\ &\frac{\Theta_1 \cos\left\{pt - \frac{2\pi}{\lambda}\left(x\cos i + y\sin i - \frac{\lambda}{b}\right)\right\}}{4c(c-1)} \end{aligned}\right\}. \quad . \quad (8)$$

The second of these increases rapidly as c approaches 1.

We can find the value of $\Theta_1/(c-1)$, $c\to 1$ as follows. By (5),

$$\square(0) = 1 + \pi\frac{\cot\frac{1}{2}\pi\sqrt{\Theta_0}}{4\sqrt{\Theta_0}} \times \frac{\Theta_1^2}{1-\Theta_0}.$$

Let $\Theta_0=1+\epsilon$, where ϵ is small; then

$$\frac{\cot\frac{1}{2}\pi\sqrt{\Theta_0}}{4\sqrt{\Theta_0}}=-\frac{\pi}{16}\epsilon,$$

so that $$\square(0)=1+\frac{\pi^2}{16}\Theta_1^2,$$

and $$\frac{1-\cos\pi c}{1-\cos\pi\sqrt{\Theta_0}}=1+\frac{\pi^2}{16}\Theta_1^2.$$

Let $c=1+\theta$, where θ is small; then, when $\Theta_0=1$,

$$\frac{-\pi^2\theta^2}{4}=\frac{\pi^2}{16}\Theta_1^2 \quad \text{or} \quad \theta=\sqrt{-1}\,\frac{\Theta_1}{2},$$

$$c=1+\sqrt{-1}\,\frac{\Theta_1}{2}.$$

Substituting this value of c in (8), and noticing that, since $\Theta_0=1$, $\lambda/b=2\sin i$, the expression for one of the secondary waves is

$$\tfrac{1}{2}\epsilon^{-\Theta_1\frac{\pi y}{2b}}\sin\left(pt-\frac{2\pi}{\lambda}(x\cos i-y\sin i)\right).$$

This represents a wave travelling in the direction in which the primary wave would travel if reflected by a mirror parallel to $y=0$. There is a change in phase of $\pi/2$. The intensity diminishes slowly as y increases. The maximum value of the amplitude is half that of the primary wave. The expression given in (8) for the primary wave is on the assumption $c=1$. If the next approximation is taken there will be the factor $\epsilon^{-\Theta_1\frac{\pi y}{2b}}$ in the expression for the amplitude of the primary wave. The condition that the secondary wave should be comparable with the primary, viz., $\lambda=2b\sin i$, is the well-known one for diffraction of waves by a crystal.

The preceding investigation is based on the assumption that Θ_1 is small. This, as we have seen, requires the refractive index of the medium to be unity; for large values of Θ_1, c^2 would no longer be equal to Θ_0 and there would be an appreciable refractive index. The primary wave is represented by the term $\epsilon^{i c\eta}$. Now

$$c\eta=\frac{c\pi y}{b}=\frac{c}{\sqrt{\Theta_0}}\,\frac{2\pi y\sin i}{\lambda},$$

so that the primary wave restoring the factors depending on x and t will be

$$\cos\left(pt-\frac{2\pi}{\lambda}\left(x\cos i+\frac{c}{\sqrt{\Theta_0}}\sin i\right)\right).$$

This may be written as

$$\cos\left(pt-\frac{2\pi}{\lambda'}(x\cos i'-y\sin i')\right),$$

if

$$\frac{\cos i}{\lambda}=\frac{\cos i'}{\lambda'},$$

$$\frac{c}{\sqrt{\Theta_0}}\frac{\sin i}{\lambda}=\frac{\sin i'}{\lambda'},$$

or

$$\frac{1}{\lambda_1}=\frac{1}{\lambda}\sqrt{\cos^2 i+\frac{c^2}{\Theta_0}\sin^2 i}.$$

If μ is the refractive index of the medium, $\mu=\lambda/\lambda'$, hence

$$\mu^2=\cos^2 i+\frac{c^2}{\Theta_0}\sin^2 i.$$

$$\cos^2 i+\frac{\lambda^2}{4b^2}(1+\sqrt{(\Theta_0-1)^2-\Theta_1^2})$$

by equation (6).

Thus μ depends upon the angle of incidence and the wave-length.

When $\Theta_0-1<\Theta_1$ there is an imaginary part in the expression for μ^2. When Θ_0-1 is large compared with Θ_1,

$$\mu^2=1-\frac{\lambda^2}{8b^2}\frac{\Theta_1^2}{\Theta_0-1}.$$

We see from equation (7) that for the diffracted wave

$$(c-2)^2=\Theta_0,$$

$$c-2=-\sqrt{\Theta_0};$$

from this and equation (6), $\sqrt{\Theta_0}$, *i.e.*, $2b\sin i/\lambda$ can be found.

The value of Θ_1 can be expressed in terms of the work required to remove an electron from the crystal. If this work is expressed as V-electron volts, then in (1) $\alpha=2Ve/mc^2$. Hence,

$$2\Theta_1=\frac{2Ve\times 10^8\times b^2p_0^2}{c^2\pi^2.mc^2},$$

$$p_0=2\pi.1{\cdot}2\times 10^{10} \quad \text{if} \quad b=10^{-8}.$$

This makes

$$2\Theta_1=\frac{V}{40} \quad \text{or} \quad \Theta_1=\frac{V}{80}.$$

CXI. *Heats of Dissociation and Absorption Spectra of some Complex Molecules.* *By* T. IREDALE, *D.Sc., and* W. N. W. WALLACE, *Laboratory of Physical Chemistry, University of Sydney* *.

ONE of the outstanding problems in photochemistry is the relationship between the thermal energy required to decompose a substance and the minimum of light energy necessary to bring about the same transformation. The one is usually calculated in terms of energy of binding or heat of linking from thermochemical data, or from energy of activation, and the other from certain limits in the absorption spectrum, or from the commencement of certain regions of photoactivity in the spectrum. Such comparisons have invariably been misleading. One was accustomed to think of thermal decomposition in terms of nuclear separations following on considerable changes in the rotational and vibrational energy in the molecule. The photochemical decomposition was related to orbital changes in one or more of the valency electrons, and although such a process must also involve nuclear separations, the relationship between the two was not always clearly perceived. Only the simpler photochemical changes coming within the boundary of Einstein's law of the Photochemical Equivalence could lend themselves to such a study. The majority of photochemical reactions are very complicated, and involve transfers of energy so rapid as to obscure the original, primary process.

Within recent years a great deal seems to have been cleared up with regard to heats of dissociation and photochemical energy in the case of the simpler molecules. From a study of the absorption spectra of the halogen molecules Franck (Trans. Farad. Soc. xxi. p. 536, 1926) was able to conclude that the primary dissociation into atoms began at a certain region of the spectrum. This region was the convergence limit of the series of oscillation bands characteristic of the molecule. Beyond this limit there was a zone of continuous absorption where complete dissociation into atoms occurred (Mecke, *Ann. d. Phys.* lxxi. p. 104, 1924; Dymond, *Z. Physik*, xxxiv, p. 553, 1925;

* Communicated by Prof. F. G. Donnan, F.R.S.

Kuhn, *Z. Physik*, xxxix, p. 77, 1926). The atoms were not necessarily normal atoms, that is, atoms in the lowest quantum state. In order to account for the fact that at the convergence limit the quantum of light-energy was greater than the heat of dissociation, Franck postulated that one of the atoms was in an excited or metastable state. The energy of excitation was calculated from the difference of the two terms 2^2P_2 and 2^2P_1, and satisfactory agreement was found between the experimental and calculated values (Turner, Phys. Rev. xxvii, p. 397, 1926).

The dissociation, of course, involves a separation of the two nuclei of the atoms, and this possibility depends on the magnitude of the oscillational and rotational energy changes which are coupled with the changes in energy of the electron system due to the absorption of light. If the electron jump is very rapid compared with the slow vibration of the nuclei, and a greatly changed strength of binding occurs, the nuclei may acquire such large amounts of potential energy that the new state of vibration set up may actually bring about their separation (Condon, Phys. Rev. xxvii. p. 640, 1926). All molecules, however, do not dissociate as readily as this even after receiving amounts of energy far exceeding the energy of dissociation. They may exist for some time in excited states far removed from the normal and energy may be re-admitted in the form of molecular fluorescence (*e. g.*, I_2, H_2, etc.). Sometimes a collision during the life of an excited molecule may bring about its dissociation. This is the mechanism postulated by Stern and Volmer (*Zeit. für wissen. Photog.* xix. p. 275, 1920).

The majority of bonds or linkages in molecules which interest the photochemist usually belong to either of the two classes, polar or non-polar. It is possible to learn a great deal about the mode of dissociation of molecules having one or other of these linkages from a study of their absorption spectra. Wherever we find a zone of continuous absorption we are led to expect an elementary dissociation process not involving the collision mechanism of Stern and Volmer, and the long-wave length limit of this absorption band will be related to the heat of dissociation of the molecule in two ways, according to the nature of the linkage, polar or non-polar. For a polar bond, as shown by Franck, Kuhn, and Rollefson (*Zeit. Physik*, xliii.

p. 155, 1927), the heat of dissociation *may* be equal to the energy calculated from the long-wave length limit. This is the case for the alkali halides, and dissociation into two normal atoms is to be expected in the first range of the spectrum. For a non-polar bond, *e. g.*, Ag=I, H=I (Franck and Kuhn, *ibid.* p. 164), the long-wave limit corresponds to the heat of dissociation plus an amount of energy necessary to excite one of the atoms.

These observations have been confined to diatomic molecules. With more complicated molecules very great difficulties might be experienced with the treatment of the subject owing to the increase in the number of linkages and the more complex nature of the oscillational and rotational energy changes. In a special case, however, where a zone of continuous absorption was due to electronic activation at some particular linkage in a molecule, it was considered that the dissociation process might be analogous to the disruption of a diatomic molecule. Organic compounds containing carbon and hydrogen and one non-polar carbon-iodine bond might furnish molecules of this kind. The absorption spectra of their vapours are known to be continuous (Pauer, *Ann. der Phys.* lx. p, 363, 1897; Purvis, Jour. Chem. Soc. xcix. p. 2319, 1911), and they appear to dissociate with the liberation of iodine in the long-wave region (Job and Emschwiller, *Compt. Rend.* clxxix. p. 52, 1924; Iredale, Jour. Phys. Chem. xxxiii. p. 290, 1929). Moreover, within the limits of experimental error, the photochemical decomposition, as in the case of hydrogen iodide, agrees with the law of the photochemical equivalence.

Now the absorption spectrum of hydrogen iodide has been shown to be continuous (Bonhoeffer and Steiner, *Zeit. Phys. Chem.* cxxii. p. 287, 1926; Tingey and Gerke, Jour. Amer. Chem. Soc. xlviii. p. 1838, 1926), and the long-wave length limit fairly definitely established. In continuation of the earlier work of Warburg (*Sitz. Akad. Wiss. Berlin*, ccc. p. 1918) Lewis (Jour. Phys. Chem. xxxii, p. 270, 1928) has shown that the photochemical dissociation of HI in the initial stage is independent of collisions, and Bodenstein and Linweig (*Zeit. Physik. Chem.* cxix. p. 123, 1926) have shown that the mechanism is independent of the state of aggregation of the molecules; within the limits of experimental error it seems that the mode of

dissociation is the same in the liquid as in the gaseous state, and the long-wave limit of the absorption appears to be the same. This, however, would not be quite correct. The heat of dissociation in the liquid state differs from that in the gaseous state according to conventional thermochemical calculations by an amount which is of the order of the molecular heat of vaporization of the liquid.

When we come to examine organic compounds containing the C-I bond experimental difficulties are realized owing to the excessively long columns of the vapours which must be used before an absorption limit can be detected. This is practically also the case with HBr and HI (Tingey and Gerke, *loc. cit.*), though a fairly satisfactory limit seems to have been established in the case of HI. Now the thermochemical data for organic iodine compounds which serve as a basis for the calculation of energy of binding or heat of dissociation of the C–I bond are only available to any degree of accuracy for the substances in the liquid state. We have therefore measured the absorption limits in the liquid state also, which may be open to some objections. As, however, we are not studying band spectra, the continuous absorption in the liquid may be considered to be similar to the continuous absorption in the vapour. The difference in the absorption limits, if any, will be related to the difference in the total energy of the molecule in the two states as affects the oscillation energy of the two nuclei at the place of disruption of the molecule. All that can be said is that this difference is of the order of the molecular heat of vaporization. The molecules in the liquid state appear to be simple; there is no polymerization involving the valency electron (Turner, Molecular Association, lxx. p. 101, 1915).

Experimental.

The absorption measurements were carried out with a Hilger medium quartz spectrograph. As sources of light both the quartz mercury vapour lamp and the condensed carbon spark have been employed. A biprism in front of the slit was used in conjunction with a sector photometer. In the measurements of the absorption limits no rotation of the sectors was, of course, actually employed, and these limits were ascertained with a fair degree of accuracy by

comparing the densities of the photographs of the two spectra in the region where the absorption commenced. Layers of the liquids 1 cm. and 4 cm. in length were used in conjunction with an empty comparison tube, and it was assumed that the loss of intensity through reflexion and absorption by the quartz cover plates, etc., would be the same in the two cases. A slight, and in the present case insignificant, error would arise through having a change of medium quartz-air in the one cell and quartz-liquid in the other. The loss of light by scattering was difficult to ascertain, but it was compensated for in the visible, non-absorbable region of the spectrum by adjusting the photometer to give equal photographic densities of the two comparison spectra in the negative. The negatives were examined with the aid of a strong light through a plate of opalized glass, and also with a Moll recording microphotometer.

Great care was taken to purify the iodides, and after the last traces of iodine were removed many careful distillations under diminished pressure were resorted to in order to

TABLE I.

Heats of combustion (in kilogram calories per gram-molecule) (K).

Methane	(gas)	...	211	Methyl iodide	(liquid)	...	195
Ethane	,,	...	368	Ethyl iodide	,,	...	356
Propane	,,	...	526	Iso-propyl iodide	,,	...	509
Propylene	,,	...	490	Allyl iodide	,,	...	478
Benzene	,,	...	787	Iodobenzene	,,	...	771

Heat of combustion	of	carbon	94·38
,,	,,	,, hydrogen (H) ...	34·19
,,	sublimation	,, carbon ...	150*
,,	,,	,, iodine (I) ...	7·5
,,	dissociation	,, hydrogen (H) ...	50·5
,,	,,	,, iodine (I) ...	17·6

* The value for the heat of sublimation of carbon is given in the International Critical Tables as 152 K. Kohn and Guckel (*Zeit. Physik*, xxvii. p. 305, 1924) arrive at a value 139 K. ± 7 per cent. (see also Herbst, *Zeit. Physik*, xxvii. p. 366, 1926). Older values varied from 120 to 200 K. or more. From a consideration of all the available data we take 150 K. as a more probable value.

obtain pure products. Iodine is easily liberated by heat under certain conditions, and slow decomposition often takes place at ordinary temperatures. The addition of silver foil prevents the formation of colour due to liberated iodine.

The heat of linking or binding of carbon and iodine was calculated from the published data on the heats of combustion of organic iodine compounds. (Berthelot, *Ann. Chim. Phys.* (7) xxi. p. 296, 1900; International Critical Tables, vol. v. 1929). In common with other thermochemical data these are not very satisfactory. Other investigators have not always given the fundamental standards on which their calculations of the heats of binding depend, and as these have altered to some extent during the past few years, we include here to avoid ambiguity a list of the data we have used as a foundation for our calculations.

In the table which follows λ in $\mu\mu$ is the long wave-length limit of the absorption band, Q is the heat of binding in kilo-calories calculated from thermochemical data, and D the heat of dissociation calculated from the absorption limit, taking into account the energy (22 K.) necessary to excite the iodine atom.

TABLE II.

	λ.	Q.	D.
Methyl iodide	395	50	50
Ethyl iodide	413	46	47
Iso-amyl iodide	413	—	47
Iso-propyl iodide	—	50	—
Iodobenzene	415	49	46
(Allyl iodide)	(>440)	45	(<42)
(o-Iodotoluene)	(>420)	—	(<46)

The values for allyl iodide and iodotoluene are enclosed in brackets. We were not certain of the purity of these particular liquids, and a minute trace of coloured impurity may modify their optical properties considerably.

It is impossible to believe that the heat of solution of the products of photodecomposition can enter as a term into the equation for the heat of dissociation, as the redistribution of energy in this case would be established

through the agency of molecular collisions which do not affect the primary process. See, however, Franck and Scheibe (*Zeit. Phys. Chem.* cxxxix. p. 22, 1928), who discuss the formation of an atom of iodine from an ion in an aqeuous medium. It is remarkable that these authors do not consider the possibility of chemical action between the iodine atom and a water molecule, which may have a large heat of reaction. This may be the beginning of a series of chain reactions, and it is surely impossible to learn anything of these from a study of the absorption spectrum.

The values of Q show no intelligible variation among themselves. D varies in a way that might be expected if we consider the binding of C and I to be influenced by the binding of adjacent carbon atoms.

We have said that the absorption is continuous for the vapours of these iodides. This matter certainly needs further investigation, and we hope to continue these studies when suitable equipment is available. It is possible that with molecules having large moments of inertia absorption spectra may sometimes have the semblance of continuity. This will depend on the resolving power of the spectrograph.

Taking the data of Pauer (*loc. cit.*) and Purvis (*loc. cit.*) for iodobenzene, and plotting the absorption limits against the pressure of the vapour, it is easily seen that the limit converges to some wave-length beyond 400 $\mu\mu$.

In all these cases the selection of an absolute wave-length limit would be a somewhat arbitrary proceeding. There must be some molecules possessing internal energy greater than the average. A complete theory of the subject should take into account not only the shift, if any, of the absorption band, but also, perhaps, the variation in the heat of dissociation with the temperature.

We have to thank Miss E. Stobo, B.Sc., for some assistance in purifying the iodides, and the Trustees of the Commonwealth Science and Industry Endowment Fund for a grant of money for the purchase of certain apparatus.

The University of Sydney.

CXII. *A New Inertia-less Chronograph.* *By* P. A. Cooper, *Research Department, Woolwich**.

[Plate XVIII.]

MUCH interest has been shown during the last few years in gas-discharge lamps of the G.E.C. "Osglim" type. Their electrical characteristics have been examined in detail, notably by S. O. Pearson and H. St. G. Anson †, M. A. Oschwald and A. G. Tarrant ‡, J. H. Shaxby and J. C. Evans §, and J. Taylor and W. Clarkson ‖.

Pearson and Anson first described how they could be used for the production of relaxation oscillations. Attempts to apply the principle, however, have never been entirely successful because of the uncertain delay which occurs between the instant at which the requisite voltage is applied to the lamp and that at which the discharge strikes. Since the glow surrounding the cathode is the visible counterpart of this discharge, it was to be expected that attempts to use them for photographic recording might be open to the same objection. Fortunately though it is just as easy to record an event by extinguishing a lamp as by energizing it, and in the early experiments that was always the method used. It was done by connecting the lamp across approximately one-half of a non-reactive resistance bridging a 500-volt D.C. circuit. The event was recorded by short-circuiting the lamp and that part of the resistance in parallel with it, the other part acting solely as a current-limiting device. This method worked quite satisfactorily, but has long been superseded by others of more general utility.

The delay to which reference has been made had claimed a considerable amount of attention and various ways in which it might be minimized had been proposed ¶. However, none of these suggested methods involving the use of ultra-violet light, X-rays, or of radioactive compounds were really successful, because the initial ionization which

* Communicated by the Author.
† Proc. Phys. Soc. xxxiv.
‡ *Ibid.* xxxvi.
§ *Ibid.*
‖ *Ibid.*
¶ *Loc. cit.*

it was their function to produce was not sufficiently intense. A far more satisfactory way of dealing with this difficulty, and one by which the lag in lighting up can be reduced to a negligible amount, is by the use of what might be called a pilot circuit, since it plays very much the same part as the pilot jet in an incandescent gas lamp. This principle has been incorporated in all the circuits to be described and it has made it possible to record events by lighting up lamps just as accurately as by putting them out.

The Osglim lamp is not well adapted for photographic recording; in all probability it was never developed for any other purposes than lighting and advertising. The discharge takes place in a mixture of helium and neon giving

Fig. 1.

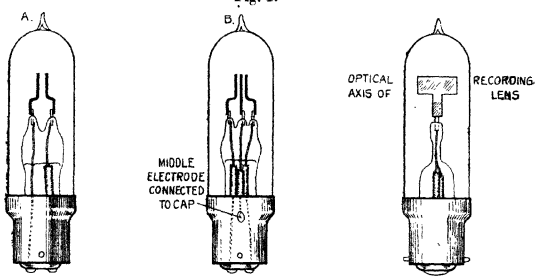

Front view of single cathode lamp. Front view of double cathode lamp. Side view of either lamp.

a light which, for photographic work, would necessitate the use of panchromatic emulsion and this, for routine purposes, has its disadvantages. Because of this it was decided to use lamps having an argon filling, since this gives the blue light to which ordinary emulsion is most sensitive. The first type of lamp specially made by the G.E.C., Ltd., Wembley, to a sketch supplied by this Department, is shown in fig. 1, A. The electrodes, following standard G.E.C. practice, were clean iron plates. They were placed about 1/10 inch apart and were as long as could conveniently be used. This point is important because it is

by looking along the cathode edgeways that one gets the highest intrinsic brightness. Early in 1927 this type was replaced by that shown in fig. 1, B. It comprises a single anode mounted between two separate cathodes, each of which can be made to glow quite independently of the other. The cathodes are connected to the lead contacts in the cap of the lamp, and the anode to the brass cap itself. This arrangement is virtually two lamps in the same glass envelope.

Fig. 2 shows three modifications of the basic circuit which has been developed for time-recording with make and break contacts or with a combination of both. As with all discharge tubes, arc lamps and the like operating from a

Fig. 2.

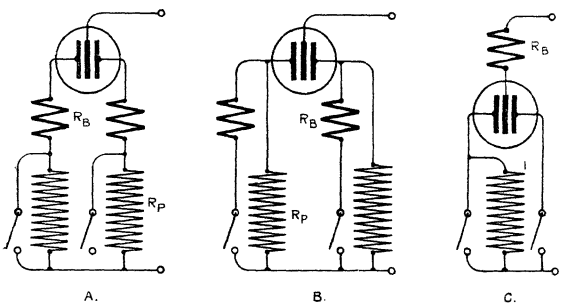

continuous supply, ballast resistances are necessary to limit the magnitude of the discharge currents. These usually take the form of 110-volt 16-c.p. carbon lamps having a reasonably non-inductive resistance of about 400 ohms; they are designated R_B. The pilot circuit principle can easily be traced in each of the three modifications shown. The pilot leak R_P, usually of 50,000 ohms resistance, passes sufficient current to keep the argon filling ionized but not enough to give a photographic record with the film speeds used. The circuit shown in fig. 2, C is unsymmetrical in the sense that only one such pilot leak is used, in association with one of the two

cathodes; as long as the requisite ionization is present within the lamp it does not matter much where it is located.

Fig. 3 shows a bank of double cathode lamps incorporated in a circuit suitable for routine work. For the sake of clearness the leads to the contacts have been kept very short, though actually, as used in a particular piece of experimental work to which this apparatus has been applied, they are air-lines approximately three-quarters of a mile long. O is a milliammeter, calibrated as an ohmmeter, the resistance R_Z being variable in order that the instrument may be used on mains having different voltages (220–250 D.C.).

Fig. 3.

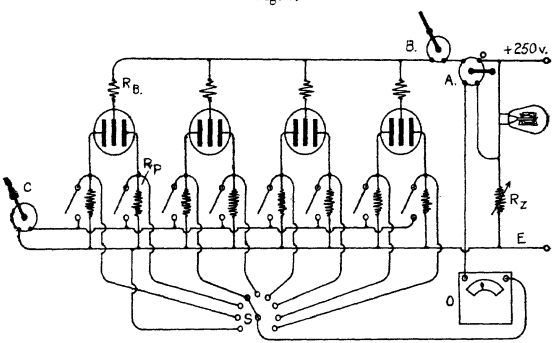

Although the discharge lamps are not excessively overrun it is desirable to conserve them as far as is conveniently possible. This is the function of the switches B and C, the latter being closed just before the records are to be taken, and the former opened immediately afterwards. They are operated by a falling weight, the motion of which is correlated with the opening of the camera shutter; such arrangements have often been used before in work of this nature and do not call for detailed description. Four double lamps only have been shown in the figure, though usually they are assembled in banks of nine behind two slits 1/32-inch wide and $1\frac{3}{4}$ inch apart. The four lamps behind one slit are staggered with respect to the five behind the other in order to keep the

records properly spaced. The lens usually fitted is a kinematograph-taking lens of aperture $1/f$ 1·9 and focal length 2 inches, placed about 15 inches in front of the lamps. For routine work the film speed is 5 metres/second, and the uncertainty with which short time intervals are recorded amounts to less than 1/50,000 second. With picked lamps and a little more care the film speed can be doubled and the uncertainty halved. The developer used is the Maximum Contrast Hydroquinone Developer given in the British Journal Photographic Almanac.

Fig. 4 A.

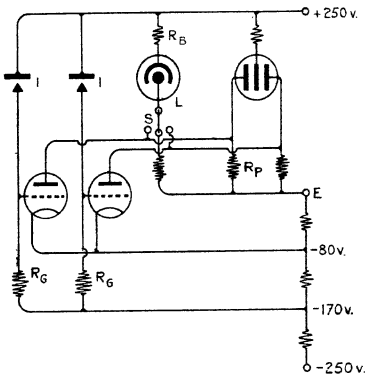

Fig. 4 B.

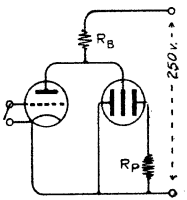

It is not always convenient to use simple make and break contacts and sometimes, even when this can be done, the resistance of the circuit is too high to allow the lamp to light up properly. In cases of this kind it is convenient to use such an arrangement as that shown in fig. 4, A in which each of the cathodes of a double lamp is connected to the plate of a low-impedance thermionic valve. This circuit has been used very successfully for recording the instants at which ionization currents begin to flow. The ionization gaps I are wired in series with high resistances R_G, the common point between them being connected to the grid of the appropriate valve. Until the instant at which

the gas insulation in a particular gap breaks down, the grid of the valve associated with it is strongly negative. When, however, the gap becomes conducting, the potential of the grid becomes more positive and allows current to flow through the valve and that side of the lamp in series with it. A different kind of testing gear has been incorporated in this circuit. It consists of an Osglim lamp L, which can be placed in parallel with either side of the argon lamp used for recording. Since the Osglim lamp strikes at a voltage less than the lower critical voltage of the argon lamp, it takes the whole of the current.

During the actual process of recording, the switch is placed in the neutral position shown in the figure. Pl. XVIII. shows a typical record given by this arrangement. It will readily be appreciated that it can be adapted to many other purposes if the circuit constants are altered to suit the particular conditions.

The one disadvantage attached to the use of the circuit just described lies in the fact that its successful operation necessitates a source of supply of at least 300 volts. Where only one-half of a three-wire D.C. supply system is available it is preferable to use a parallel arrangement of valve and lamp, the essential parts of which are shown in fig. 4 B. The ballast resistance R_B in many cases can with advantage be replaced by an iron-cored choke having the same D.C. resistance and a low value of self capacity.

For all ordinary work the time-trace is provided by a 50 cycles/sec. tuning-fork, and although it is of the vibrating contact type it can be relied upon to give results correct to well within 1 per cent. Where the highest attainable accuracy is required this will be given by a valve-maintained elinvar fork circuit now in course of development.

In conclusion, the writer would like to acknowledge his indebtedness to Dr. G. Rotter, C.B.E., and to Dr. R. Ferguson for their never-failing encouragement, without which this work would not have been possible. He is much indebted, too, to the Director-General of Artillery for permission to offer this paper for publication.

CXIII. *A Quartz Suspension Galvanometer for use in D.C. and A.C. Circuits.*

By D. R. BARBER, *B.Sc., A.Inst.P.*, 1928–29 *Andrew Simon Research Scholar, University College of the South-West of England, Exeter*.*

INSTRUMENTS used in the detection and measurement of very small currents should possess the dual characteristic of high sensitivity combined with inherent stability. The instrument described in the present paper possesses these qualities, and has been developed for measuring either direct or low frequency alternating currents within the range 10^{-3} to 10^{-6} ampere.

The principle utilised is somewhat analogous to that of the quadrant electrometer, since the deflexion is produced by a torsional couple applied to a stretched fibre of quartz, the initial impulse being derived from the motion of two soft-iron armatures symmetrically arranged with respect to the suspension, and floating within two solenoids carrying the current to be detected. The chief advantage of such an arrangement is the high value of torque attainable for weak induction effects—an essential condition if the moving system is to effectively respond at the lower limit of the current range. The suspension fibre is anchored at both ends, and this arrangement is found to give additional mechanical strength to the moving system without unduly lowering the sensitivity of the instrument. The use of quartz in the construction of the rotor assembly ensures a negligible zero error and the elimination of any disturbing temperature effects.

Description of the Instrument.

The instrument is diagrammatically shown in fig. 1 (*a*) representing the plan, and (*b*) the medial section.

A rhomboidal beam of quartz rod, A, 1 mm. diameter, carries at its extremities two soft-iron wires, B, bent into arcs of radius 2·5 cm. and length 1·5 cm. These form the two armatures and are able to move in a horizontal plane within the two solenoids, S_1 and S_2, consisting of a pair of telephone bobbins of which the total resistance is 2000 ohms approximately. A concave mirror, M, is attached to the beam, A, in order that the deflexions of the instrument

* Communicated by Prof. F. H. Newman, D.Sc., F.Inst.P.

may be read by the orthodox lamp and scale method. The whole of the rotating framework is rigidly attached to a quartz fibre, C, diameter 10 μ, length 3·2 cm., stretched vertically between the two extremities of a rectangular quartz frame, D. This latter is mounted on a vertical brass stage, E, which may be adjusted, radially and transversely, so as to facilitate the exact centring of the beam relative to the solenoid coils. These two coils are mounted in stirrups, V, anchored to the brass disk, F, which forms the upper portion of the instrument case, and may be rotated so as to bring varying amounts of the armatures within the solenoids. This movement allows

Fig. 1.

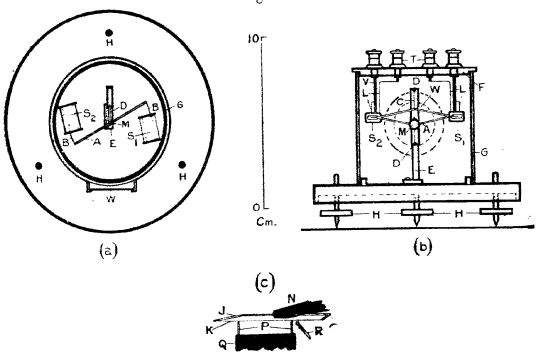

the sensitivity of the galvanometer to be varied over a limited range, and also facilitates vertical adjustment of the solenoid positions when the instrument is initially assembled.

The whole instrument is enclosed within a brass case, G, provided with a circular window, W, and mounted on a cast platform of brass, provided with three levelling screws, H.

The technique of mounting the suspension fibre follows the usual practice employed when dealing with quartz threads of very small diameter. A rectangular stirrup, P, fig. 1 (c), is first made by bending a length of quartz rod, 1 mm. diameter, in the pointed flame of a small hand blowpipe. The ends of the frame are then coated

with fused shellac, and it is then mounted in a rectangular block of ebonite, Q, fig. 1 (*c*). The frame with its support is now placed in a suitable clamp, and the assembly is ready to receive the fibre. A selected quartz thread, K, fig. 1 (*c*), is now taken and stretched on the glass frame, J, fig. 1 (*c*), and its ends attached thereto, care being taken that the length of the fibre is slightly in excess over that required for the completed suspension. This glass frame is now carefully lowered by means of a clamp, N, fig. 1 (*c*), so that the fibre is just in contact with the ends of the quartz frame. While in this position, an additional tension is put on the fibre by slightly flexing the glass frame, and at the same time the shellac is melted with a fragment of heated glass rod, R, fig. 1 (*c*). When the shellac has thoroughly hardened, the excess fibre is carefully detached, leaving the complete suspension on its quartz support. This method of mounting ensures that the suspension shall be stretched as tightly as the tensile strength of the quartz thread will permit—a necessary condition for portability. Suspensions which give the slightest indication of "sagging" have been found to have a short useful life, as the excessive degree of lateral freedom given to the attached beam gives rise to shearing forces at the points of anchorage, and, in consequence, the fibre quickly breaks. The beam, A, fig. 1 (*a*) and (*b*), is attached to the fibre with two small globules, the complete suspension being arranged horizontally for this purpose, while the beam is carefully balanced on the fibre. When the equilibrium position is found the ends of the beam are supported so as to prevent possible movement, and the shellac beads are then fused to the fibre by applying a fragment of heated glass.

The leads, L, from the solenoid coils are joined to four insulated terminals, T, mounted on the disk, F, and this arrangement enables the coils to be joined "in series," or "in parallel," at will.

The period of the complete moving system is 5·5 sec.

Calibration of the Instrument.

The instrument has been calibrated, both with direct and alternating currents, by noting the deflexion produced by a measured current flowing in the solenoid coils, and separate calibration curves have been obtained for "series" and "parallel" coil connexions.

During the initial stages of the calibration considerable "hunting" of the zero was experienced, and in order to remedy this defect it was found necessary to screen the moving iron system from the effects of extraneous magnetic fields, by means of a tinplate cylinder fitted within the case of the instrument. As would be expected in a moving iron instrument, slight hysteresis effects were noticeable throughout the calibration, but there was no permanent zero displacement.

In calibrating the galvanometer it was joined in series with a variable 100,000 ohm standard resistance, a mercury key, and a Ferranti moving coil milliammeter (0–5 m.a.), incorporating a copper oxide rectifying unit for measuring the current in the alternating circuit. The output terminals of a "step-down" transformer ratio 110 : 12 furnished the potential required for the alternating current calibration, the current values being read directly from the milliammeter. Care was taken to insulate the solenoid coils, but, in spite of this precaution, some A.C. leakage took place through the medium of the instrument case, and this effect modified the character of the calibration curves obtained.

For the direct current calibration a 2 v. accumulator was used as the source of potential, the current values in this case being calculated from Ohm's law. Deflexions were measured by the lamp and scale method, the scale being 1 metre from the galvanometer mirror. The results obtained in calibrating the instrument both for direct and alternating currents are given in Tables I. and II.

The calibration curves, reproduced in figs. 2 and 3, were obtained by plotting values of current against deflexion in the calibration for direct current, and values of current against logarithm of deflexion for alternating current. The resulting curves are both linear.

Direct Current Calibration.

It has been found that with direct currents the deflexions of the galvanometer are directly porportional to the current passing through its coils, and for the coils connected "in series"

$$i = kd$$

where i=current in ampères, d=deflexion in millimetres (scale divisions), and K is a constant of the instrument

having a value of $0{\cdot}82 \times 10^{-6}$. This gives a mean sensitivity of 0·82 microamps per mm. scale deflexion.

TABLE I.

Direct Current Calibration.

Series.			Parallel.		
Observed current $\times 10^{-5}$ amp.	Current value from curve $\times 10^{-5}$ amp.	Observed deflexion, mm.	Observed current $\times 10^{-5}$ amp.	Current value from curve $\times 10^{-5}$ amp.	Observed deflexion. mm.
1·96	1·87	24·0	1·99	1·93	12·5
2·17	2·12	26·0	2·21	2·16	14·0
2·43	2·36	29·0	2·48	2·39	15·5
2·77	2·72	33·5	2·84	2·86	18·5
3·22	3·17	39·0	3·30	3·24	21·0
3·88	3·82	47·0	3·96	3·94	25·5
4·75	4·75	58·5	4·94	4·94	32·0
6·23	6·29	77·5	6·55	6·57	42·5

TABLE II.

Alternating Current (50 cycles) Calibration.

Series.				Parallel.			
Observed current $\times 10^{-3}$ amp.	Current value from curve $\times 10^{-3}$ amp.	Observed deflexion D.	Log D.	Observed current $\times 10^{-3}$ amp.	Current value from curve $\times 10^{-3}$ amp.	Observed deflexion D.	Log D.
0·50	0·50	72·0	1·86	0·50	0·49	15·5	1·19
0·55	0·55	96·0	1·98	0·60	0·58	19·5	1·29
0·58	0·58	115·0	2·06	0·70	0·70	28·0	1·45
0·62	0·62	140·0	2·15	0·80	0·80	37·0	1·57
0·67	0·66	184·0	2·26	0·90	0·97	50·5	1·70
0·70	0·71	226·0	2·35	1·00	1·01	67·0	1·83
0·77	0·77	328·0	2·52	1·12	1·12	92·0	1·96
0·80	0·80	386·0	2·59	1·20	1·22	120·0	2·08

When the coils are connected "in parallel" the corresponding value for K is $1{\cdot}55 \times 10^{-6}$, and the sensitivity is 1·55 microamps per mm. scale deflexion. As would be

expected, therefore, the sensitivity is approximately doubled by using the instrument with its coils joined "in series." It may be noted that theory indicates a parabolic relation existing between the values of current

Fig. 2.

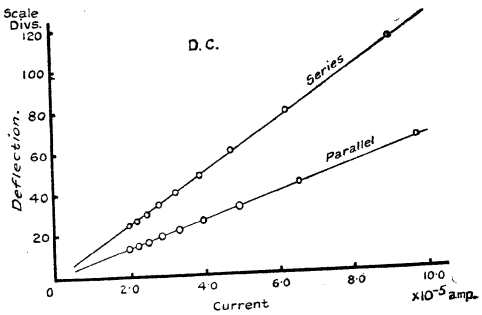

Fig. 3.

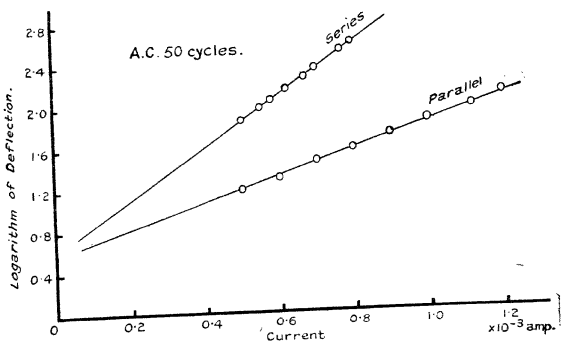

and corresponding deflexion, but this is not applicable to conditions existing during the actual calibration, since the theoretical consideration assumes a constant field value, whereas in practice the value of the permeability μ will vary continuously with the magnetizing current i.

Alternating Current Calibration.

The relation existing between the deflexion d and the virtual current i flowing in the solenoid coils may be represented by the equation

$$i=\beta\ (\log d-\alpha),$$

where β is the constant of the instrument, and α is the "zero-field" correction.

It will be seen from the curves connecting the values of i and $\log d$ that neither curve passes through the origin, and therefore there is a small residual deflexion α when the calibrating current value is zero. This effect may be explained by the presence of eddy currents induced in the solenoid coils, due to leakage through the case of the instrument. Since, however, the magnitude of this effect is practically constant throughout the entire current range, it may be allowed for in the corrected readings.

For values of β equal to $4{\cdot}0\times10^{-4}$ and $8{\cdot}1\times10^{-4}$ respectively for "series" and "parallel" calibration, the values of α are 0·61 and 0·58 respectively.

Summary.

1. A detailed description is given of a new type of galvanometer, employing a quartz fibre suspension, and suitable for use on direct or alternating current circuits.

2. Calibration curves for the instrument are given, and empirical formulæ are obtained giving the value of the current passing through the instrument in terms of the deflexion produced.

In conclusion, the author desires to thank Prof. F. H. Newman, D.Sc., for his kindly interest and helpful advice throughout this investigation.

CXIV. *The Capture of Electrons by Molecules.*

To the Editors of the Philosophical Magazine.

GENTLEMEN,—

IN the issue of your Magazine for last July there appears a communication by Prof. L. B. Loeb which is entirely devoted to attempting "to correct the erroneous impression given by Prof. Bailey's statements," and refers to a paper

by Mr. J. D. McGee and myself which was published in the issue for December 1928. As Prof. Loeb appears to have an "erroneous impression" of our statements on pages 1088 and 1089, and himself makes some erroneous and inconsistent remarks, it seems desirable to comment briefly on his communication.

In a summary of the history of his own investigations he says: "It was shown that, using the *simplifying assumption* of a constant value of the constant of attachment n, a rigorous quantitative test of the theory should be possible by this means." On the next page he gives reasons why a quantitative study was *not possible*, and finds some other justification for regarding his results as being of value, namely, that his (and Wahlin's) estimates of n are correct in order of magnitude, and "still stand today as the only data even in order of magnitude bearing on this important electronic behaviour for any large range of substances." Anyone examining Prof. Loeb's work critically would naturally ask himself the following two questions:

(1) Has the "simplifying assumption" been established in any way?

(2) Would a serious error in the estimated value of n (or its order of magnitude) be likely if this assumption were incorrect?

As the work of Prof. Loeb and his associates (excepting Dr. Cravath) provides little definite information on these points, it is not unreasonable to regard their estimates with some reserve.

The information published in our paper on Ammonia enables us to go even further in our scepticism, for, apart from a large variation in the probability of attachment h $(=1/n)$ in the range 8 to 16 of the ratio X/p, we found our lowest estimate of h to be at least 1000 times larger than that found by Wahlin, which shows (as we stated) that either the "simplifying assumption" involved in Wahlin's estimate is enormously wrong, or else *our* sample of ammonia contained at least 1000 times more impurity than Wahlin's. We have not (as Prof. Loeb states) thrown any doubt on the purity of Wahlin's samples, nor have we said that Wahlin's estimate of 10^{-8} is wrong, since these matters need not be considered in order to conclude that "the results obtained with his (Loeb's) method, and set out in his table, may be quite misleading."

In referring to Cravath's work (by means of an original method), Prof. Loeb says: "Cravath has shown that, contrary to Bailey's belief, n in air also varies with the pressure . . . ."

It is difficult to regard this statement as an expression of Prof. Loeb's real views, for in the same paragraph he accepts my other conclusions, which could not have been reached without making the assumption that n depends *only* on the electronic energy (for a given gas); also it is unnecessary to go to Loeb's own writings to show that, until this latest one, he has held the same "belief"—it is attributed to him by Sir J. J. Thomson on page 13 of the same issue of the Philosophical Magazine. Finally Dr. Cravath himself expresses the following opinion * about the difference between the results of his experiments and mine: "..... the greater consistency of Bailey's data and the simpler conditions in his apparatus justify greater confidence in his results."

I may mention, in conclusion, that we hope soon to have ready for publication new experimental results which strengthen the arguments we have advanced.

Yours truly,

V. A. Bailey.

CXV. *Notices respecting New Books.*

Introduction à la Physique des Rayons X et Gamma. Par MM. Maurice et Louis de Broglie. (Paris: Gauthier Villars et Cie, 55 Quai des Grands-Augustins.)

REFERENCE is made in the Preface of this book to some of the monographs which have appeared in recent years on the subject of X-rays and its many developments. This introduction to the study of X- and γ- rays gives a clear, concise, and up-to-date account of the nature of these rays, their scattering, with and without change of frequency, diffraction by crystals and the modification of Bragg's law, and, above all, the bearing of these discoveries on the structure of matter and radiation. The experiments of G. P. Thomson and others are described, confirming the hypothesis, brought forward some six years ago, of the wave character of a moving electron. In an appendix a brief account is given of the spinning electron of Uhlenbeck and Goudsmit and its application to the anomalous Zeeman effect and other problems.

Ions, Electrons, and Ionizing Radiations. By J. A. Crowther, Sc.D. Fifth edition. (Edward Arnold, Maddox Street, London, W. 1. Price 12*s.* 6*d.* net.)

The publication of the fifth edition of Prof. Crowther's well-known text-book is a sure indication that his work has roused the

* A. M. Cravath, Phys. Rev., April 1929, p. 612.

interest of many students of this branch of physical science and proved to be a useful introduction to the study of its recent developments. The author has submitted his book to a careful revision, and has added new sections describing some of the noteworthy researches carried out during the last few years—in particular, the latest work of Aston, Compton, G. P. Thomson, Millikan and Gerlach and Stern. New photographs of the tracks of ionizing radiations taken by Prof. C. T. R. Wilson replace those which appeared in earlier editions. References to original papers are given at the end of the chapters: a number of these contributions, especially those relating to X-rays and α-rays, have appeared in the pages of this Magazine.

Dynamics. By A. R. Ramsey, M.A. (Cambridge University Press, Fetter Lane, London, E.C. 4. Price 10*s.* 6*d.* net.)

Although this book is claimed to be a text-book of elementary dynamics, it is intended to meet the requirements of pupils in upper forms who are preparing for Honours courses in applied mathematics. The author has drawn on his wide experience as a teacher of this subject, and has written a concise and useful text-book dealing with the ordinary syllabus in dynamics, with some sections of the subject not usually included in an introductory course. Among such may be mentioned motion in a resisting medium, to which the author refers in the Preface, and the problem of orbital motion as modified by the introduction of the small relativity term. Two chapters are devoted to harmonic motion and its applications and to the problem of small oscillations and the stability of motion. In addition to the exercises given at the end of each chapter, a large number of examples, elementary and advanced, are worked out for the guidance of the reader.

Standard Tables of Square Roots. By L. M. Milne-Thomson, M.A. (Geo. Bell & Sons, Ltd., York House, Portugal Street, London, W.C. 2. Price 7*s.* 6*d.* net.)

The author has constructed a very useful and comprehensive table of square roots to eight places of decimals. Square roots of x and $10x$ are set out on the same page with first differences for four-figure values of the argument. Except in the earlier part of the table, linear interpolation is sufficient to give intermediate values of the square root to eight significant figures. A short table is given for the correction of first differences and the division method of computing square roots to fourteen places is explained and illustrated. The Standard Table will be a welcome addition to the equipment of those engaged in computing work, especially in the construction of tables of elliptic and other functions.

INDEX TO VOL. VIII.

END OF THE EIGHTH VOLUME

Printed by TAYLOR and FRANCIS, Red Lion Court, Fleet Street.

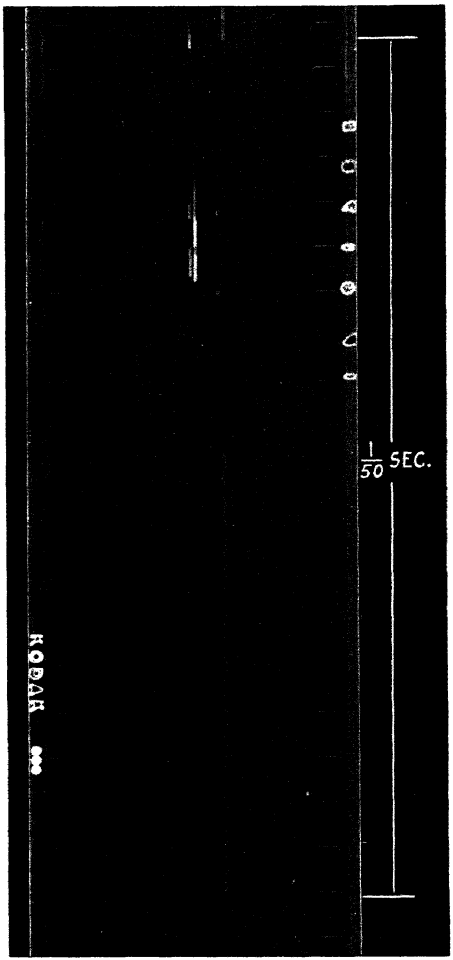
1/50 SEC.
KODAK